INFORMATION TO USERS

This manuscript has been reproduced from the microfilm master. UMI films the text directly from the original or copy submitted. Thus, some thesis and dissertation copies are in typewriter face, while others may be from any type of computer printer.

The quality of this reproduction is dependent upon the quality of the copy submitted. Broken or indistinct print, colored or poor quality illustrations and photographs, print bleedthrough, substandard margins, and improper alignment can adversely affect reproduction.

In the unlikely event that the author did not send UMI a complete manuscript and there are missing pages, these will be noted. Also, if unauthorized copyright material had to be removed, a note will indicate the deletion.

Oversize materials (e.g., maps, drawings, charts) are reproduced by sectioning the original, beginning at the upper left-hand corner and continuing from left to right in equal sections with small overlaps. Each original is also photographed in one exposure and is included in reduced form at the back of the book.

Photographs included in the original manuscript have been reproduced xerographically in this copy. Higher quality 6" x 9" black and white photographic prints are available for any photographs or illustrations appearing in this copy for an additional charge. Contact UMI directly to order.

UMI

A Bell & Howell Information Company
300 North Zeeb Road, Ann Arbor MI 48106-1346 USA
313/761-4700 800/521-0600

The Primary and Secondary Mafic Silicates of Two Alkaline Anorogenic Complexes: Strange Lake (Quebec-Labrador) and Amba Dongar (Gujarat, India).

Jeanette N. Roelofsen

Department of Earth and Planetary Sciences,

McGill University,

Montréal, Québec

January, 1997

A thesis submitted to the Faculty of Graduate Studies

and Research in partial fulfilment of the

requirements of the degree of Doctor of Philosophy.

© Jeanette Roelofsen 1997

National Library of Canada
Acquisitions and Bibliographic Services
395 Wellington Street
Ottawa ON K1A 0N4
Canada

Bibliothèque nationale du Canada
Acquisitions et services bibliographiques
395, rue Wellington
Ottawa ON K1A 0N4
Canada

Your file Votre référence

Our file Notre référence

The author has granted a non-exclusive licence allowing the National Library of Canada to reproduce, loan, distribute or sell copies of this thesis in microform, paper or electronic formats.

L'auteur a accordé une licence non exclusive permettant à la Bibliothèque nationale du Canada de reproduire, prêter, distribuer ou vendre des copies de cette thèse sous la forme de microfiche/film, de reproduction sur papier ou sur format électronique.

The author retains ownership of the copyright in this thesis. Neither the thesis nor substantial extracts from it may be printed or otherwise reproduced without the author's permission.

L'auteur conserve la propriété du droit d'auteur qui protège cette thèse. Ni la thèse ni des extraits substantiels de celle-ci ne doivent être imprimés ou autrement reproduits sans son autorisation.

0-612-30372-1

Canada

ABSTRACT

The primary and secondary mafic silicates from the Amba Dongar carbonatitic-alkaline complex, Gujarat, India and the Strange Lake peralkaline granitic complex, Québec-Labrador, Canada are the subject of this investigation of their origin, evolution and relationship to mineralization. Primary minerals are transformed by a variety of processes related to their crystallization history. The most important of these processes are: magma evolution, magma degassing and metasomatism. These processes are commonly associated with the evolution of peralkaline granitic and carbonatitic-alkaline complexes, and with the formation of associated mineral deposits [e.g., fluorite in the Amba Dongar complex; Zr-, REE- (rare-earth elements), Be-, Nb- and Y-rich deposit in the Strange Lake complex]. Although all minerals in these complexes may be subject to these changes, the mafic silicates amphibole, pyroxene and mica are of particular interest, as they remain poorly studied and may comprise up to 10 vol.% of the rock. Moreover, they can contain significant quantities of high field-strength elements (HFSE), which may be mobilized following interaction with later fluids, and deposited as secondary minerals in the ore zone.

In the Amba Dongar complex, Na-metasomatism followed by K- (or Mg-) metasomatism resulted in the formation of fenites, with mobilization of HFSE, among other trace elements. Vermiculite was formed by a subsequent stage of hydrothermal alteration, which is also responsible for formation of the fluorite deposit. In the Strange Lake complex, enrichment of the primary arfvedsonitic amphibole in HFSE and REE is related to magmatic evolution, whereas later degassing released sufficient amounts of volatiles and Na that the amphibole became more potassic and aegirine crystallized. This amphibole acted as a sink for trace elements such as Li, HFSE and REE. These elements were remobilized during Na-metasomatism through replacement of amphibole by aegirine, and deposited as secondary, generally Ca-rich, minerals (e.g., winchitic amphibole and biopyriboles) during later, lower-temperature Ca-metasomatism. Primary mafic silicates in alkaline complexes can thus undergo metasomatic reactions that result in the mobilization of elements that contribute to formation of related ore deposits. These findings concerning the solid phases involved in both localities correlate very well with indications of mixing of two distinct fluid phases.

RESUMÉ

Les silicates mafiques primaires et secondaires du complexe de carbonatite-alcaline d'Amba Dongar, situé dans la province de Gujarat en Inde, et du complexe granitique hyperalcalin de Strange Lake, Québec-Labrador, Canada, ont été choisis pour l'étude de leur mode de formation, de leur évolution et de leur lien avec les minéralisations économiques. Après leur cristallisation, les minéraux primaires subissent des transformations dues à une variété de processus: réaction avec le magma, dégazage et métasomatose. Ces processus sont très communs durant l'évolution des complexes granitiques hyperalcalins et des complexes alcalins associés aux carbonatites, ainsi que durant la formation des gisements de minéraux qui leurs sont associés (e.g., mine de fluorite du complexe d'Amba Dongar, et gisement de Zr, terres rares, Be, Nb et Y associé au complexe de Strange Lake). Les silicates mafiques de ces complexes sont d'un intérêt fondamental car ils sont rarement étudies et peuvent former jusqu'à 10 % du volume de la roche. De plus, ils peuvent contenir des quantités importantes d'éléments à potentiel ionique élevé, qui peuvent être mobilisés suite à l'interaction avec des fluides tardifs, et précipités sous forme de minéraux secondaires dans la zone minéralisée.

À Amba Dongar, la formation de fénites a été la conséquence d'une métasomatose sodique, suivie d'une métasomatose potassique (ou magnésienne), et de la mobilisation d'éléments à potentiel ionique élevé et des autres éléments traces. De la vermiculite s'est formée subséquemment durant un stade d'altération hydrothermale tardif, au cours duquel la minéralisation en fluorite s'est aussi formée. À Strange Lake, l'amphibole arfvedsonitique primaire montre un enrichissement en éléments à potentiel ionique élevé et en terres rares lié à l'évolution magmatique. Suite à un épisode de dégazage au cours duquel des volatiles et du Na se sont échappés, l'aegyrine et une amphibole plus riche en K ont cristallisé. L'amphibole arfvedsonitique primaire est un minéral concentrateur des éléments rares tel que les éléments à potentiel ionique élevé, les terres rares et le Li. Le remplacement de l'amphibole par l'aegyrine durant un épisode de métasomatose sodique a eu pour effet de mobiliser ces éléments et de les déposer sous forme de minéraux secondaires, généralement riches en Ca (l'amphibole winchitique et les biopyriboles) au cours d'un épisode tardif de métasomatose calcique de basse température. Par

conséquent, l'altération métasomatique des silicates mafiques primaires dans les complexes de roches alcalines a causé la mobilisation et la reconcentration d'éléments qui contribuent à la formation de gisements de minéraux économiques. Les données acquises par l'étude des phase solides provenant des deux localités concordent très bien avec un modèle de mélange de deux fluides distincts.

ACKNOWLEDGEMENTS

I thank my supervisor, Prof. Robert F. Martin, who suggested this thesis topic in response to my interest in the Strange Lake peralkaline complex. Bob was always ready to discuss the implications of my results. He meticulously edited and commented on earlier drafts of this work.

Many thanks to those who provided stimulating discussions and inspiration during the completion of this work: C. Normand, Dr. C. Gammons, Prof. J. Paquette, C. Dalpé, S. Lang, G. Nassif, Dr. S. Salvi, D. Palmer, A. Fournier, Dr. S. Aja, D. Durant, K. Borasov, Dr. K. Livi and Dr. B. Grobéty. Completion of this thesis was aided by access to various computers provided by A.E. Williams-Jones (Willy), Chris Gammons and Dr. M. Nagai. Charles and Bob are thanked for translation of the abstract. Comments on various stages of this work were provided by Willy, Chris and especially Charles. Additional data for comparison purposes on amphibole from the Strange Lake complex were provided by Prof. F.C. Hawthorne and Prof. R. Oberti on amphibole from the Strange Lake complex. Standard mafic glasses for the LAM-ICP-MS analyses were obtained from Prof. N. MacRae and C. Dalpé.

The staff of the Geochemical Laboratories are thanked for the bulk X-ray fluorescence (XRF) data and determinations of F and Cl. Atomic absorption and inductively coupled plasma - mass spectrometry analyses for Li and the REE were performed at Activation Laboratories, Ancaster, Ontario. Amphibole separation was aided by use of a Franz magnetic separator from Prof. N. Machado at the Université de Québec à Montréal.

Electron microprobe analyses and scanning electron microscopy work was completed at McGill University following introductions by G. Poirier, Dr. J. Mungall and H. Campbell. Glenn devised the enormous element tables used for the electron-microprobe analyses. Electron microprobe analyses on the mica were completed at the Department of Earth and Planetary Sciences, the Johns Hopkins University (JHU), under the supervision of Dr. K. Livi.

In the early stages of this project, Prof. A. Dufresne, M. Harrigan and Dr. H. Vali provided access to and training on the Transmission Electron Microscope (TEM) in the Department of Occupational Health. Dr. Vali introduced me to the use of ultramicrotomy

and n-alkylammonium treatment of phyllosilicates. The TEM work presented in this dissertation could not have been completed without unlimited access to the TEM facility provided by Prof. D.R. Veblen from JHU. While there, we had a number of valuable mineralogical and crystallographic discussions. I would also like to thank Ken and B. Grobéty for providing housing during early stages of this study at JHU and introducing me to the TEM. Finally, André Dufresne and Mike Harrigan allowed me access to their darkroom to print all of the TEM photos (except one) that were used in this thesis.

Laser ablation microprobe - inductively coupled plasma - mass spectrometry (LAM-ICP-MS) analyses at the Université de Montréal could not have been completed without the guidance of G. Gauthier. Gilles instructed me on the use of the instrument, set up the analysis procedures, and provided invaluable information on standards, methods of standardization, sample preparation, various errors and instrumental factors. In addition, he allowed me to use a program that was developed by C. Dalpé and him to calculate the concentrations of the elements.

This research was funded by a NSERC grant to Bob and a NSERC Strategic grant, a FCAR team grant and Lithoprobe grant to Bob and Willy. The TEM at JHU is supported by Grant EAR94-18090 to D. Veblen. Financial support to the author was provided by a Fonds pour la Formation de Chercheurs et l'Aide à la Recherche (FCAR) scholarship, and a John Henry Howard award, Reinhardt fellowship and a McGill Major (Reinhardt) award, and a FCAR Stage, which allowed me to spend nine months at JHU. Research awards from the Geological Society of America and Sigma Delta Epsilon (Graduate Women in Science) covered a portion of the TEM costs.

Lastly, I express my thanks to my family and friends, in particular Charles Normand, for their support and advice during completion of this thesis. Many thanks to those who helped with the final preparation of this thesis (C. Normand, S. Mordeau, T. Roelofsen and my parents). The special times with all of them have always provided me with balance with which to approach the rest of my endeavors.

PREFACE

This thesis has been produced with consideration of the following provisions:

> Candidates have the option of including, as part of the thesis, the text of one or more papers submitted or to be submitted for publication, or the clearly-duplicated text of one or more published papers. These texts must be bound as an integral part of the thesis.
>
> If this option is chosen, connecting texts that provide logical bridges between the different papers are mandatory. The thesis must be written in such a way that it is more than a mere collection of manuscripts; in other words, results of a series of papers must be integrated.
>
> The thesis must still conform to all other requirements of the "Guidelines for Thesis Preparation". The thesis must include: A Table of Contents, and abstract in English and French, an introduction which clearly states the rationale and objectives of the study, a review of the literature, a final conclusion and summary, and a thorough bibliography or reference list.
>
> Additional material must be provided where appropriate (e.g. in appendices) and in sufficient detail to allow a clear and precise judgement to be made of the importance and originality of the research reported in the thesis.

In the case of manuscripts co-authored by the candidate and others, the candidate is required to make an explicit statement in the thesis as to who contributed to such work and to what extent. Supervisors must attest to the accuracy of such statements at the doctoral oral defense. Since the task of the examiners is made more difficult in these cases, it is in the candidate's interest to make perfectly clear the responsibilities of all the authors of the co-authored papers.

TABLE OF CONTENTS

	Page
Abstract	i
Résumé	ii-iii
Acknowledgements	iv-v
Preface	vi
Table of Contents	vii-xii
Chapter 1: Introduction	1
Background information	3
Previous work on the Amba Dongar carbonatitic-alkaline complex	5
Previous work on the Strange Lake peralkaline complex	6
Organization of the thesis	9
References	11
Chapter 2: Mineralogical examination of the products of fenitization in the Amba Dongar complex, Gujarat, India *(manuscript)*.	
Abstract	19
Introduction	19
Geological setting	20
Previous investigations of the units	22
Methodology	25
Descriptions of newly recognized units	26
Mineral textures and compositional variation	29
Variation in whole-rock composition	64

Page

Origin of "Ultrafenite" 79

Compositional variation of metasomatic fluid 80

Conclusions 82

Acknowledgements 82

References 84

Chapter 3: Origin of the glimmerite selvage between carbonatite veins and alkaline volcanic and plutonic rocks of the Amba-Dongar carbonatitic-alkaline complex, Gujarat, India *(manuscript)*.

Prologue 93

Abstract 95

Introduction 95

Geological setting 96

Methodology 98

Description of the precusor and glimmerite 99

Compositional variation of the minerals 105

TEM observations 111

Discussion 119

Conclusions 132

Acknowledgements 132

References 134

Prologue to the second portion of the thesis 140

References 142

Chapter 4: The mafic silicates of the Strange Lake peralkaline complex, Quebec-Labrador. I. Primary arfvedsonitic amphibole and aegirine *(manuscript)*.

Abstract 144

Introduction 145

Page

Background information 145
Review of literature on the primary mafic silicates 147
Methodology 148
Results of optical and cathodoluminescence examination 151
Sequence of crystallization 159
Compositional variation of the arfvedsonitic amphibole 159
Compositional variations in aegirine and related minerals 174
Discussion 183
Comparisons with findings on mafic silicates from related complexes 186
Effects of magma degassing and variation of oxygen fugacity 191
Conditions of formation of the Strange Lake suite 192
Conclusions 195
Acknowledgements 196
References 198

Chapter 5: The mafic silicates of the Strange Lake peralkaline complex, Quebec-Labrador. II. Effects of Na-metasomatism *(manuscript)*.

Prologue to Chapters 5 and 6 207
Abstract 209
Introduction 209
Background information 211
Review of the literature on mafic silicates 212
Comparison of analytical methods 213
Methodology 214
Results 216
Discussion 241
Redistribution of elements during Na-metasomatism and the deposit 247
Conclusions 251
Acknowledgements 252
References 253

Page

Chapter 6: The mafic silicates of the Strange Lake peralkaline complex, Quebec-Labrador. III. Effects of Ca-metasomatism *(manuscript)*.

Abstract 263
Introduction 263
Background information 265
Review of the mafic silicates at Strange Lake 266
Application of analytical methods 267
Methodology 268
Results 270
Sequence of Ca-metasomatism 289
Discussion 293
Evolution of the Strange Lake complex 299
Relationship to other complexes 302
Conclusions 303
Acknowledgements 303
References 305
Epilogue 313
References 315

Chapter 7: Conclusions

General conclusions 317
Contributions to knowledge 318
Suggestions for further investigation 319
References 321

Page

Appendices

A. Amba Dongar carbonatitic-alkaline complex

1. Sample descriptions ..... A- 1
2. Electron-microprobe analyses of aegirine ..... A- 4
3. Electron-microprobe analyses of amphibole ..... A- 14
4. Electron-microprobe analyses of mica ..... A- 17
5. Electron-microprobe analyses of feldspar ..... A- 30
6. Electron-microprobe analyses of apatite ..... A- 37
7. Electron-microprobe analyses of titanite ..... A- 42
8. Electron-microprobe analyses of garnet ..... A- 43
9. Electron-microprobe analyses of etc. mineralogy ..... A- 45
10. AEM analyses of mica ..... A- 48
11. Average errors in AEM analyses ..... A- 65
12. XRD data on mica ..... A- 66

B. Strange Lake peralkaline complex

1. Electron-microprobe analyses of arfvedsonitic amphibole ..... B- 1
2. Electron-microprobe analyses of aegirine ..... B- 26
3. Electron-microprobe analyses of selected titanium silicates ..... B- 40
4. Bulk ICP-MS analyses of amphibole ..... B- 51
5. LAM-ICP-MS analyses ..... B- 52
6. Setup conditions for LAM-ICP-MS analysis ..... B- 66
7. Calculated lower limit of detection (LLD) of LAM-ICP-MS analyses ..... B- 67
8. Low Z elemental contents of arfvedsonitic amphibole ..... B- 68
9. X-ray powder diffraction data ..... B- 69
10. AEM analyses of minerals from the hypersolvus granite ..... B- 70
11. AEM analyses of minerals from the subsolvus granite ..... B- 81
12. Relative errors of AEM analyses ..... B- 83
13. Method of calculation of the amount released ..... B- 84

Page

14. Electron-microprobe analyses of winchitic amphibole ..... B- 85
15. Electron-microprobe analyses of phyllosilicates ..... B- 86
16. AEM analyses of winchitic amphibole ..... B- 90
17. AEM analyses of biopyriboles ..... B- 94
18. AEM analyses of related minerals ..... B- 96
19. AEM analyses of phyllosilicates B-102

Chapter 1:

INTRODUCTION

Alkaline and peralkaline plutonic and volcanic rocks (e.g., carbonatite, granite, syenite, nephelinite, phonolite and tephrite) are characteristic of anorogenic complexes (igneous complexes associated with rift environments). Their alkaline nature is exhibited by the possible presence of the alkali mafic silicates aegirine, arfvedsonitic amphibole and alkali iron-titanium silicates, such as aenigmatite and astrophyllite. Fluids exsolved from such intrusive complexes can metasomatize rocks in and around the complex. Although relatively rare, these alkaline complexes are economically important, as they tend to be associated with deposits of high field-strength elements (HFSE; elements with small ionic radius and high charge), the rare-earth elements (REE), and fluorite. In this study of the mafic silicates biotite, amphibole and pyroxene in two anorogenic complexes, I aim to determine the nature of the primary (magmatic) minerals, and to characterize the products of their interaction with aqueous fluid(s) during cooling of the igneous suite. As the primary minerals can sequester important proportions of the HFSE (especially REE) and F, the conversion of primary to secondary minerals may well be associated with important mobilization of these elements. Therefore, this study will touch on important economic issues.

The complexes chosen for examination of the primary and secondary mafic minerals from peralkaline complexes are: the Amba Dongar carbonatitic-alkaline complex, Gujarat, India, and the Strange Lake peralkaline complex, Québec-Labrador border, Canada. The study focuses on aegirine-augite, aegirine, biotite, phlogopite and arfvedsonitic amphibole, as they are the common rock-forming mafic silicates in peralkaline anorogenic complexes. Thus, the results of this in-depth study should find direct applications to other complexes where similar magmatic and metasomatic processes are known to have taken place. The effects of these processes will be investigated through a detailed mineralogical study combining results of electron-microprobe analyses, laser-ablation microprobe - inductively coupled plasma - mass spectrometry (LAM-ICP-MS), and transmission electron microscopy (TEM).

Background Information

The evolution of an igneous complex can best be described by the mineralogical changes that occur during this evolution. However, the conditions of formation of the primary minerals (i.e., temperature, fO_2, depth of crystallization, etc.) must be determined first, if conditions of metasomatism are to be addressed. If the same primary mafic silicate crystallizes throughout the evolution of the complex, its compositional variation can be used to characterize the magma's evolution. The general trend of compositional variation observed, for example, in pyroxene and amphibole is an enrichment in Na and Fe^{3+} relative to that of Ca and Mg, respectively. The incompatible elements and H_2O also are enriched during this evolution, especially in the apical part of the complex. Other effects on these minerals occur through magma degassing, which results in the nucleation and loss of a volatile phase and accompanying mobilization of incompatible elements. Primary mafic silicates can be replaced by the interaction with the migrating fluid phase, commonly in more than one episode.

Fenitization (or alkali metasomatism) involves the addition to, or removal of constituents from, a protolith by fluid related to an alkaline magmatic source to produce new, bulk compositions in equilibrium with the fluid phase. The resultant fenites are classified on the basis of major element(s) added to the protolith; thus, there are sodic and potassic fenites or, more rarely, magnesian or calcic fenites. The resultant mineral assemblages are dependent on the composition of the protolith and of the fenitizing fluid, and the temperature at which reaction occurred (Le Bas, 1981; Woolley, 1982; Rubie & Gunter, 1983).

The existence of a gradient in temperature in the aureole can explain the presence of potassic fenite of low-temperature origin near the surface and in distal parts of the exocontact with the host rocks, and sodic fenite of high-temperature origin at depth and in proximal parts of the aureole in carbonatite-alkaline complexes (Vartiainen & Woolley, 1976; Viladkar, 1980). As an alternative, these fluids could have been emitted from different sources, with K-metasomatism generally attributed to a carbonatitic magma, and Na-metasomatism, to an ijolitic magma (Le Bas, 1977). Na-metasomatism has also been observed related to peralkaline granites (Bowden et al., 1987). Constituents released during

the metasomatic replacement of earlier mineral assemblages associate with those from the metasomatic fluid and, after changes in the physico-chemical properties of the metasomatic fluid, result in deposition of new mineral assemblages characteristic of the fluid composition. Determination of the compositional variation of these minerals by electron-microprobe analysis is difficult, as replacement occurs at a submicroscopic scale. Traditionally, methods of study have been appropriate for coarse-scale observations. However, the best method with which to examine these fine-scale replacements involves the use of transmission electron microscopy (TEM), especially high-resolution TEM (HRTEM), selected-area electron diffraction (SAED) and analytical electron microscopy (AEM or energy- dispersion spectrometry performed with the TEM). The great advantage of AEM over electron-microprobe analysis is that, when combined with HRTEM and SAED, it is easier to ascertain what mineral is being analyzed.

Numerous studies suggest that bioypriboles are produced by retrograde hydration or metasomatism (Veblen & Buseck, 1979, 1981; Grobéty, 1996, and references therein). The term biopyribole was initially used by Johannsen (1911) to describe mica (e.g., biotite), pyroxene and amphibole. Thompson (1978) applied this term to the polysomatic series of these minerals; he suggested that additional phases may contain combinations of the single-chain structure of pyroxene, the double-chain structure of amphibole, and the sheet structure of mica. Veblen & Burnham (1978a, b) were the first to confirm the existence of these intermediate phases in natural samples. The triple-chain structure of chesterite and double- and triple-chain structures of (clino)jimthompsonite were described by Veblen & Buseck (1979, 1980, 1981) from TEM examination. Since that time, numerous ordered and disordered structures of predominantly Ca-, Mg- (or Mn-) and Fe-rich compositions have been documented between amphibole and mica (Schumacher & Czank, 1987; Maresch & Czank, 1988; Grobéty, 1996), and pyroxene and amphibole (Nakajima & Ribbe, 1981). Hydrothermal experiments suggest a limit to the amount of Na that can be incorporated in the structure of a Ca-Mg-rich chesterite-like biopyribole (Akai & Saito, 1985). However, Chisholm (1973) and Ahn & Buseck (1991) observed the presence of rare wide-chain biopyribole defects in asbestiform riebeckite, a sodic amphibole, whose origin they related to the effects of late-stage fluids. One of the aims of this study is to evaluate the possible

formation of Na-Fe^{3+}- (± K) biopyriboles through replacement of arfvedsonitic amphibole by aegirine, or of aegirine-augite by mica.

Ross (1984) suggested that the presence of biopyriboles intermediate to aegirine and arfvedsonitic amphibole explains the nonstoichiometry (apparent excess of ΣNa+K+Si in arfvedsonitic amphibole) commonly observed in this amphibole. However, Hawthorne et al. (1992, 1993) and Czamanske & Dillet (1988) related this enrichment to the presence of elements that are rarely sought (e.g., Zn, Zr and REE), especially those whose concentration cannot be established using the electron microprobe (e.g., Li). Hawthorne et al. (1992, 1993, 1996) observed that arfvedsonitic amphibole may contain significant amounts of Li, and described the new Li-rich alkali amphiboles leakeite and ferro-ferri-leakeite. Therefore, full description of the compositional variation of arfvedsonitic amphibole requires determination of their light- and trace-element content, as well as a TEM examination.

Most analyses of the mafic silicates, arfvedsonitic amphibole, aegirine and mica, from peralkaline complexes have been performed using the electron microprobe (Mitchell, 1980; Lalonde & Martin, 1983; Andersen, 1989; Czamanske & Dillet, 1988). The minor- and trace-element content of arfvedsonitic amphibole has been assessed by ion probe (Hawthorne et al., 1992) and bulk analyses by either X-ray fluorescence spectrometry (XRF) or instrumental neutron activation analyses (INAA) (Pillet et al., 1993; Abdel-Rahman, 1994), but these studies are not numerous. Microbeam methods of analysis are better, because they can be used to examine mineralogical zonation. In this study of mafic minerals from the Amba Dongar carbonatitic-alkaline and Strange Lake peralkaline complex, laser-ablation microprobe - inductively coupled plasma - mass spectrometry (LAM-ICP-MS) has been chosen as the preferred method to perform analyses for trace and minor elements.

Previous work on the Amba Dongar carbonatitic-alkaline complex

The 30-km^2 complex (late Cretaceous to early Tertiary: Deans et al., 1973) is located in the state of Gujarat, India, about 100 km east of Baroda, 6 km north of the Narmada River and associated rift valley. Sukheswala & Udas (1963) were the first to note that the complex contains carbonatite. The latter is composed of calciocarbonatite breccia surrounded by a calciocarbonatite ring dyke and cut by ferrocarbonatite plugs and veins, all

of which were emplaced in Bagh sandstone (and intercalated limestone) of Cretaceous age, and Deccan flood basalt (Sukheswala & Udas, 1964; Viladkar, 1981; Gwalani et al., 1993). Plugs of coeval tinguaite, nephelinite, tephrite, phonotephrite and ijolite occur throughout the region (Viladkar, 1984; Sethna, 1989; Gwalani et al., 1993). The complex contains one of the largest fluorite mines in Asia (11.6 million tonnes at 30% CaF_2; Deans et al., 1973). Ore deposition resulted from mixing of fluid derived from the carbonatite with that derived from the surrounding host-rocks (Simonetti & Bell, 1995; Palmer & Williams-Jones, 1996).

Fenites from this complex were chosen for study, as they represent a commonly quoted type example of fenitization due to the relative purity of the unfenitized quartzite (Viladkar, 1981) and the presence of increasingly sodic fenites with depth (Viladkar, 1986). Other studies of the effects of fenitization on quartzite have examined cation variation, mineralogy and origin of fenites of the Brent Crater and Callander Bay, Ontario (Currie, 1971; Currie & Ferguson, 1971, 1972), and of Mississauga quartzite, near Espanola, Ontario (Siemiatkowska & Martin, 1975), and variation of REE contents due to fenitization of the Borralan Complex, N.W. Scotland (Martin et al., 1978).

A second type of fenite present in the Amba Dongar complex, glimmerite, is composed predominantly of mica that originated at the expense of aegirine-augite. It occurs at the contact of calciocarbonatite veins and sodi-potassic fenite (Viladkar, 1991). Examination of the mafic minerals from the glimmerite will constrain the composition of the metasomatic fluid and the influence of later fluids related to formation of the ore deposit. Similar contact fenites have been described by Gittins et al. (1975), Morbidelli et al. (1986) and Andersen (1989) from other carbonatite-alkaline complexes.

Previous work on the Strange Lake peralkaline complex

The 36-km^2 Strange Lake peralkaline granitic complex (Proterozoic; Pillet et al., 1989; Miller et al., 1997) on the Québec-Labrador border, Canada is considered to have economic potential as a source of Y, Zr, Nb, Be and possibly REE (52 million tonnes of ore; Miller, 1988). Currie (1985) related its origin to the Gardar anorogenic event in Greenland, and to a series of coeval occurrences of anorthosite and A-type granite that extend from Newfoundland to the central United States. The complex was first identified from a Pb and

F anomaly in waters and sediments of Lac Brisson by the Iron Ore company of Canada in 1979.

The complex is surrounded by quartz monzonite and quartzofeldspathic, calc-silicate, graphitic, dioritic, gabbroic, and anorthositic gneisses. Nassif & Martin (1991) subdivided the granites, based on the textural development of alkali feldspar, into early hypersolvus (one feldspar, later unmixed), late subsolvus (two coexisting primary feldspars) or transsolvus (intermediate case). Other units are based on the alteration of the subsolvus granite (fresh versus altered) and the degree of enrichment of ore minerals (Miller, 1986).

The ore mineral content of the rocks ranges from 5 vol.% in hypersolvus granite to 20 vol.% in the ore zone (Zajac et al., 1984). The ore minerals are calcium (gittinsite) and sodium zirconosilicates (elpidite), zircon and REE-rich silicates and fluorides (e.g., pyrochlore, gagarinite and monazite). Recent studies of the ore minerals have concentrated on whether gittinsite is magmatic or metasomatic (Birkett et al., 1992; Salvi & Williams-Jones, 1990, 1995; Miller, 1996). Salvi & Williams-Jones (1990, 1992) determined, through fluid inclusion studies on quartz, that a high-temperature (≥350°C) episode of Na-metasomatism occurred prior to a low temperature (<200°C) episode of Ca-metasomatism. They also determined (Salvi & Williams-Jones, 1990) that the gittinsite was of low temperature origin and formed during this later episode of Ca-metasomatism. Mass-balance calculations (Salvi & Williams-Jones, 1996), bulk-rock analyses (Currie, 1985; Nassif, 1993; Boily & Williams-Jones, 1994) and mineralogical examination (Pillet et al., 1992) provide additional support for the latter origin. Boily & Williams-Jones (1994) also noted the influence of later fluids from a oxygen isotope study of amphibole separates.

During late-stage orthomagmatic processes related to degassing of peralkaline granites, Na-metasomatism resulted in albitization of feldspar (Elliott, 1983; Bowden et al., 1987; Kovalenko et al., 1995), and aegirine replacement of arfvedsonitic amphibole (Bonin, 1986). The HFSE, and the HREE, released during these processes can be mobilized as fluoride complexes (e.g., Wood, 1990; Keppler, 1993). Changes in the intensive parameters and composition (pH, temperature or Ca content) of the fluid destabilize these complexes and result in the deposition of secondary minerals. Examples of potentially economic ore deposits influenced by Ca-metasomatism include: Thor Lake, Northwest Territories

(Pinckston & Smith, 1995), Ghurayyah microgranites, Saudi Arabia (Drysdall et al., 1984) and Khaldzan-Buregtey, Mongolia (Kovalenko et al., 1995).

The Strange Lake complex was chosen for examination because the ore and feldspar minerals are well documented (Pillet, 1989; Salvi & Williams-Jones, 1990, 1995; Pillet et al., 1992; Birkett et al., 1992; Nassif, 1993; Miller, 1996). Minerals from the complex whose structure or origin have been examined in detail are: gittinsite ($CaZrSi_2O_7$; Roelofsen-Ahl & Peterson, 1989), armstrongite ($CaZrSi_6O_{15}$•$2.5H_2O$; Jambor et al., 1987), yttrian milarite [$K(Ca,Y)_2(Be_2Al)Si_{12}O_{30}$; Cerný et al., 1991] and zajacite ($Na_{0.9}REE_{1.1}Ca_{0.9}F_6$; Jambor et al., 1996). Studies on the mafic minerals include general studies by Pillet (1989) and Pillet et al. (1992), and an examination of the titanium silicates by Birkett et al. (1996). The alkaline mafic minerals, arfvedsonitic amphibole and aegirine, as potential hosts and sources of HFSE, REE elements and Li, are the subject of this investigation. The focus is on the contrast between the primary mafic minerals of the primitive rocks and those of the evolved, highly metasomatized ones in and near the ore zone.

This thesis will examine the origin of mafic silicates of primary and secondary origin and discuss their relationship to ore mineralization using results of TEM and electron-microprobe, AEM and LAM-ICP-MS analyses.

Organization of the Thesis

This thesis consists of, first, a brief introduction (the previous portion of this chapter), followed by five manuscripts (Chapters 2 to 6), and conclusions (Chapter 7). It has been subdivided on the basis of specific topics pertaining to the mafic minerals of the two complexes to be examined. The first two papers relate to the primary mafic minerals, their metasomatism and late hydrothermal alteration present in the Amba Dongar carbonatitic-alkaline complex, Gujarat, India. In Chapter 2, the effects of metasomatism are examined through electron-microprobe analyses, bulk-sample analyses, X-ray powder diffraction and textural observations. Chapter 3 is a detailed examination of the origin of glimmerite through transmission electron microscopy (TEM). Chapter 4 describes the origin and evolution of the primary mafic silicates arfvedsonitic amphibole and aegirine from the Strange Lake peralkaline granitic complex, Québec-Labrador, Canada. The effects of Na-metasomatism have been examined in detail in Chapter 5 followed by those of Ca-metasomatism in Chapter 6. All manuscripts are to be submitted to refereed scientific journals for publication.

My supervisor, Prof. R.F. Martin, is the second author on all of the papers. He contributed to this thesis by suggesting the project in response to my interest in the Strange Lake complex, providing advice on the organization of the text, corrections thereof, discussions on the implications of the results, and collection and interpretation of the X-ray powder diffraction data (XRD) on the feldspar and mica from the Amba Dongar complex, as well as arfvedsonitic amphibole from the Strange Lake complex. While at Johns Hopkins University, Prof. D.R. Veblen, who appears as the third author in the manuscripts that comprise Chapters 3, 5 and 6 of the thesis, contributed to this work through providing access to the TEM and discussions of the TEM results, suggestions of additional TEM techniques, and comments on the figures and papers. The final author on the first manuscript is Prof. A.E. Williams-Jones (Willy), who commented on all the manuscripts and made helpful suggestions on the stability of phases. Willy, D. Palmer and I performed the field work at the Amba Dongar carbonatitic-alkaline complex. It was facilitated by the staff of the Gujarat Mineral Development Corporation Fluorspar Mines and Prof. S. Viladkar (St. Xavier's College, in Bombay), who provided an introduction to the complex

and specimens of fenitized sandstone and drill-core. Field work on the Strange Lake peralkaline complex was completed by Willy, Prof. S. Wood, Dr. S. Salvi, R. Marr, G. Nassif and Dr. M. Boily in the summer of 1989. Stefano Salvi obtained the drill-core material from the Iron Ore Company of Canada. The petrographic studies, TEM investigations, electron microprobe and other analyses and interpretations, except where noted, were performed by me.

References

Abdel-Rahman, A.-F. (1994): Alkali amphibole: a potential source of rare earth elements in felsic alkaline rocks. *Exploration and Mining Geology*, 3, 81-94.

Ahn, J.H. & Buseck, P.R. (1991): Microstructures and fiber-formation mechanisms of crocidolite asbestos. *American Mineralogist*, 76, 1467-1478.

Akai, J. & Saito, M. (1985): Ca-Mg triple-chain silicate derived from Na-Mg triple-chain silicate by ion-exchange experiment and its structural model. *Bulletin de Minéralogie*, 108, 21-28.

Andersen, T. (1989): Carbonatite-related contact metasomatism in the Fen complex, Norway: effects and petrogenetic implications. *Mineralogical Magazine*, 53, 395-414.

Birkett, T.C., Miller, R.R., Roberts, A.C. & Mariano, A.N. (1992): Zirconium-bearing minerals of the Strange Lake intrusive complex, Quebec-Labrador. *Canadian Mineralogist*, 30, 191-205.

-------, Trzcienski, W.E., Jr. & Stirling, J.A.R. (1996): Occurrence and compositions of some Ti-bearing minerals in the Strange Lake intrusive complex, Quebec-Labrador boundary. *Canadian Mineralogist*, 34, 779-801.

Boily, M. & Williams-Jones, A.E. (1994): The role of magmatic and hydrothermal processes in the chemical evolution of the Strange Lake plutonic complex (Quebec-Labrador). *Contributions to Mineralogy and Petrology*, 118, 33-47.

Bonin, B. (1986): **Ring complex granites and anorogenic magmatism**. Studies in Geology, North Oxford Academic Publishers Ltd., Great Britain, 188p.

Bowden, P., Black, R., Martin, R.F., Ike, E.C., Kinnaird, J.A. & Batchelor, R.A. (1987): Niger-Nigerian alkaline ring complexes: a classic example of African Phanerozoic anorogenic mid-plate magmatism. *In* **Alkaline Igneous Rocks** (Fitton, J.G. & Upton, B.G.J., eds.). Geological Society Special Publication, 30, 357-379.

Černý, P., Hawthorne, F.C., Jambor, J.L. & Grice, J.D. (1991): Yttrian milarite. *Canadian Mineralogist*, 29, 533-541.

Chisholm, J.E. (1973): Planar defects in fibrous amphiboles. *Journal of Materials Science*, 8, 475-483.

Currie, K.L. (1971): A study of potash fenitization around the Brent Crater, Ontario - A Paleozoic alkaline complex. *Canadian Journal of Earth Sciences*, 8, 481-497.

------- (1985): An unusual peralkaline granite near Lac Brisson, Quebec-Labrador. *Geological Survey of Canada Paper*, 85-1A, 73-90.

------- & Ferguson, J. (1971): A study of fenitization around the alkaline carbonatite complex at Callander Bay, Ontario, Canada. *Canadian Journal of Earth Sciences*, 8, 498-517.

------- & ------- (1972): A study of fenitization in mafic rocks, with special reference to the Callander Bay Complex. *Canadian Journal of Earth Sciences*, 9, 1254-1261.

Czamanske, G.K. & Dillet, B. (1988): Alkali amphibole, tetrasilicic mica and sodic pyroxene in peralkaline siliceous rocks, Questa Caldera, New Mexico. *American Journal of Science*, 288A, 358-392.

Deans, T., Sukheswala, R.N., Sethna, S.F. & Viladkar, S.G. (1973): Metasomatic feldspar rocks (potash fenites) associated with the fluorite deposits and carbonatites of Amba Dongar, Gujarat, India. *Transactions, Institute of Mining and Metallurgy*, 81, B1-9.

Drysdall, A.R., Jackson, N. J., Ramsay, C.R., Douch, C.J. & Hackett, D. (1984): Rare element mineralization related to Precambrian alkali granites in the Arabian Shield. *Economic Geology*, 79, 1366-1377.

Elliott, J.E. (1983): Peralkaline and peraluminous granites and related mineral deposits of the Arabian Shield. *U.S. Geological Survey, Open-File Report* 83-389, 35p.

Gittins, J., Allen, C. & Cooper, A.F. (1975): Phlogopitization of pyroxenite: its bearing on the carbonatite magmas. *Geological Magazine*, 112, 503-507.

Grobéty, B.H. (1996): New short-range biopyribole polysomes from the Lepontine Alps, Switzerland. *American Mineralogist*, 81, 404-417.

Gwalani, L.G., Avasia, R.K., Chang, W.-J., Fernandez, S., Allègre, C.J. & Prinzhofer, A. (1993): Alkaline rocks and carbonatites of Amba Dongar and adjacent areas, Deccan Igneous Province, Gujarat, India: 1. Geology, petrography and petrochemistry. *Mineralogy and Petrology*, 47, 219-253.

Hawthorne, F.C., Oberti, R., Ungaretti, L. & Grice, J. (1992): Leakeite, $NaNa_2(Mg_2Fe^{3+}{}_2Li)Si_8O_{22}(OH)_2$, a new alkali amphibole from the Kajlidongri

manganese mine, Jhabua district, Madhya Pradesh, India. *American Mineralogist*, 77, 1112-1115.

-------, -------, -------., Ottolini, L., Grice, J.D. & Czamanske, G.K. (1996): Fluor-ferro-leakeite, $NaNa_2(Fe^{2+}{}_2Fe^{3+}{}_2Li)\ Si_8O_{22}F_2$, a new alkali amphibole from the Canada Pinabete pluton, Questa, New Mexico, U.S.A. *American Mineralogist*, 81, 226-228.

-------, Ungaretti, L., Oberti, R., Bottazzi, P. & Czamanske, G.K. (1993): Li: an important component in igneous alkali amphiboles. *American Mineralogist*, 78, 733-745.

Jambor, J.L., Roberts, A.C. & Grice, J.D. (1987): Armstrongite from the Strange Lake alkalic complex, on the Quebec-Labrador boundary, Canada. *Powder Diffraction*, 2, 2-4.

-------, -------, Owens, D.R. & Grice, J.D. (1996): Zajacite-(Ce), a new rare-earth fluoride from the Strange Lake deposit, Quebec-Labrador. *Canadian Mineralogist*, 34, 1299-1304.

Johannsen, A. (1911): Petrographic terms for field use. *Journal of Geology*, 19, 317-322.

Keppler, H. (1993): Influence of fluorine on the enrichment of high field strength trace elements in granitic rocks. *Contributions to Mineralogy and Petrology*, 114, 479-488.

Kovalenko, V.I., Tsaryeva, G.M., Goreglyad, A.V., Yarmolyuk, V.V., Troitsky, V.A., Hervig, R.L. & Farmer, G.L. (1995): The peralkaline granite-related Khaldzan-Buregtey rare metal (Zr, Nb, REE) deposit, western Mongolia. *Economic Geology*, 90, 530-547.

Lalonde, A.E. & Martin, R.F. (1983): The Baie-des-Moutons syenitic complex, La Tabatière, Quebec. II. The ferromagnesian minerals. *Canadian Mineralogist*, 21, 81-91.

Le Bas, M. J. (1977): **Carbonatite-Nephelinite Volcanism**. Wiley, New York, 347p.

------- (1981): Carbonatite magmas. *Mineralogical Magazine*, 44, 133-140.

Maresch, W.V. & Czank, M. (1988): Crystal-chemistry, growth-kinetics and phase-relationships of structurally disordered (Mn^{2+},Mg)-amphiboles. *Fortschritte der Mineralogie*, 66, 69-121.

Martin, R.F., Whitley, J.E. & Woolley, A.R. (1978): An investigation of rare-earth mobility: fenitized quartzites, Borralan Complex, N.W. Scotland. *Contributions to Mineralogy and Petrology*, 66, 69-73.

Miller, R.R. (1986): Geology of the Strange Lake alkalic complex and the associated Zr-Y-Be-REE mineralization. *Current Research, Newfoundland Department of Mines and Energy, Mineral Development Division*, Report 86-1, 11-19.

-------- (1988): Yttrium (Y) and other rare metals (Be, Nb, REE, Ta, Zr) in Labrador. *Current Research, Newfoundland Department of Mines and Energy, Mineral Development Division*, Report 88-1, 83-91.

------- (1996): Structural evolution of the Strange Lake peralkaline rare-element (NYF) granitic pegmatite, Quebec-Labrador. *Canadian Mineralogist*, 34, 349-371.

-------, Heaman, L.M. & Birkett, T.C. (1997): U-Pb zircon age of the Strange Lake peralkaline complex: implications for Mesoproterozoic peralkaline magmatism in north-central Labrador. *Precambrian Research*, 81, 67-83.

Mitchell, R.H. (1980): Pyroxenes of the Fen alkaline complex, Norway. *American Mineralogist*, 65, 45-54.

Morbidelli, L., Beccaluva, L., Brotzu, P., Conte, A., Garbarino, C., Gomes, C.B., Macciotta, G., Ruberti, E., Scheibe, L.F. & Traversa, G. (1986): Petrological and geochemical studies of alkaline rocks from continental Brazil. 3. Fenitization of jacupirangite by carbonatite magmas in the Jacupiranga Complex. *Periodico di Mineralogia*, 55, 261-295.

Nakajima, Y. & Ribbe, P.H. (1981): Texture and structural interpretation of the alteration of pyroxene to other biopyriboles. *Contributions to Mineralogy and Petrology*, 78, 230-239.

Nassif, G.J. (1993): The Strange Lake peralkaline complex, Québec-Labrador: The hypersolvus-subsolvus granite transition and feldspar mineralogy. McGill University, M.Sc. thesis, Montréal, Québec, 104p.

------- & Martin, R.F. (1991): The hypersolvus granite-subsolvus granite transition at Strange Lake, Québec-Labrador. *Geological Association of Canada - Mineralogical Association of Canada*, Abstracts with Programs, 16, A89.

Palmer, D. & Williams-Jones, A.E. (1996): Genesis of the carbonatite-hosted fluorite deposit at Amba Dongar, India: evidence from fluid inclusions, stable isotopes, and whole rock-mineral geochemistry. *Economic Geology*, 91, 934-950.

Pillet, D. (1989): Le granite peralcalin du Lac Brisson, Labrador Central (province du Québec, Canada): pétrologie, géochronologie, et relations avec les minéralisations internes à Zr, Y, Nb. Thèse de doctorat, Université Claude Bernard: Lyon I, Lyon, France, 276p.

-------, Bonhomme, M.G., Duthou, J.L. & Chenevoy, M. (1989): Chronologie Rb/Sr et K/Ar du granite peralcalin du lac Brisson, Labrador central, Nouveau-Québec. *Canadian Journal of Earth Sciences*, 26, 328-332.

-------, Chenevoy, M & Bélanger, M. (1992): Pétrologie du granite peralcalin du lac Brisson, Labrador central, Nouveau-Québec. I. Mode de mise en place et évolution chimique. *Canadian Journal of Earth Sciences*, 29, 353-372.

-------, ------- & ------- (1993): Pétrologie du granite peralcalin du lac Brisson, Labrador central, Nouveau-Québec. II. Minéralogie et modalités de cristallisation. *Canadian Journal of Earth Sciences*, 30, 2423-2435.

Pinckston, D.R. & Smith, D.G.W. (1995): Mineralogy of the Lake Zone, Thor Lake rare-metals deposit, N.W.T., Canada. *Canadian Journal of Earth Sciences*, 32, 516-532.

Roelofsen-Ahl, J.N. & Peterson, R.C. (1989): Gittinsite: a modification of the thortveitite structure. *Canadian Mineralogist*, 27, 703-708.

Ross, M. (1984): Ultraalkalic arfvedsonite and associated richterite, acmite, and aegirine-augite in quartz syenite, Magnet Cove alkalic igneous complex, Arkansas. *EOS*, 65, 293.

Rubie, D.C. & Gunter, W.D. (1983): The role of speciation in alkaline fluids during fenite metasomatism. *Contributions to Mineralogy and Petrology*, 82, 165-175.

Salvi, S. & Williams-Jones, A.E. (1990): The role of hydrothermal processes in the granite-hosted Zr, Y, REE deposit at Strange Lake, Quebec/Labrador: evidence from fluid inclusions. *Geochimica et Cosmochimica Acta*, 54, 2403-2418.

------- & ------- (1992): Reduced orthomagmatic C-O-H-NaCl fluids in the Strange Lake rare-metal granitic complex, Quebec/Labrador, Canada. *European Journal of Mineralogy*, 4, 1155-1174.

------- & ------- (1995): Zirconosilicate phase relations in the Strange Lake (Lac Brisson) pluton, Quebec-Labrador. *American Mineralogist*, 80, 1031-1040.

------- & ------- (1996): The role of hydrothermal processes in concentrating HFSE in the Strange Lake peralkaline complex, Northeastern Canada. *Geochimica et Cosmochimica Acta*, 60, 1917-1932.

Schumacher, J.C. & Czank, M. (1987): Mineralogy of triple-and double-chain pyriboles from Orijärvi, southwest Finland. *American Mineralogist*, 72, 345-352.

Sethna, S.F. (1989): Petrology and geochemistry of the acid, intermediate and alkaline rocks associated with the Deccan basalts in Gujarat and Maharashtra. *Geological Society of India, Memoir*, 15, 47-61.

Siemiatkowska, K.M. & Martin, R.F. (1975): Fenitization of Mississauga quartzite, Sudbury area, Ontario. *Geological Society of America Bulletin*, 86, 1109-1112.

Simonetti, A. & Bell, K. (1995): Nd, Pb, and Sr isotope systematics of fluorite at the Amba Dongar carbonatite complex, India: evidence for hydrothermal and crustal fluid mixing. *Economic Geology*, 90, 2018-2027.

Sukheswala, R.N. & Udas, G.R. (1963): Note on the carbonatite of Amba Dongar (Gujarat state) and its economic potentialities. *Science and Culture*, 29, 563-568.

------- & ------- (1964): The carbonatite of Amba Dongar, India - some structural considerations. *22nd International Geological Congress*, Abstract Volume, 7, 1-13.

Thompson, J.B., Jr. (1978): Biopyriboles and polysomatic series. *American Mineralogist*, 63, 239-249.

Vartiainen, H. & Woolley, A.R. (1976): The petrography, mineralogy and chemistry of the fenites of the Sökli carbonatite intrusion, Finland. *Geological Survey of Finland Bulletin*, 280, 1-87.

Veblen, D.R. & Burnham, C.W. (1978a): New biopyriboles from Chester, Vermont: I. Descriptive mineralogy. *American Mineralogist*, 63, 1000-1009.

------- & ------- (1978b): New biopyriboles from Chester, Vermont: II. The crystal chemistry of jimthompsonite, clinojimthompsonite, and chesterite, and the amphibole-mica reaction. *American Mineralogist*, 63, 1053-1073.

------- & Buseck, P.R. (1979): Chain-width order and disorder in biopyriboles. *American Mineralogist*, 64, 687-700.

------- & ------- (1980): Microstructures and reaction mechanisms in biopyriboles. *American Mineralogist*, 65, 599-623.

------- & ------- (1981): Hydrous pyriboles and sheet silicates in pyroxenes and uralites: intergrowth microstructures and reaction mechanisms. *American Mineralogist*, 66, 1107-1134.

Viladkar, S.G. (1980): Fenitized aureole of the Newania carbonatite, Rajasthan. *Geological Magazine*, 117, 285-292.

------- (1981): The carbonatites of Amba Dongar, Gujarat, India. *Geological Society of Finland Bulletin*, 53, 17-28.

------- (1984): Alkaline rocks associated with the carbonatites of Amba Dongar, Chhota Udaipur, Gujarat, India. *Indian Mineralogist*, Sukheswala Volume, 130-135.

------- (1986): Fenitization at the Amba Dongar carbonatite-alkalic complex, India. *Proceedings NEMIRAM (New Minerals and Raw Materials) Symposium* (Gabriel, M., ed.), Karlovy Vary, Czechoslovakia, 170-189.

------- (1991): Phlogopitization at Amba Dongar carbonatite alkalic complex, India. *Neues Jahrbuch für Mineralogie Abhandlungen*, 162, 201-213.

Woolley, A.R. (1982): A discussion of carbonatite evolution and nomenclature, and the generation of sodic and potassic fenites. *Mineralogical Magazine*, 46, 13-17.

Wood, S.A. (1990): The aqueous geochemistry of the rare-earth elements and yttrium. 2. Theoretical predictions of speciation in hydrothermal solutions to 350°C at saturation water vapor pressure. *Chemical Geology*, 88, 99-125.

Zajac, I.S., Miller, R.R., Birkett, T.C. & Nantel, S. (1984): Le gîte de Zr, Y, Nb et Be du complexe alcalin de Strange Lake, Québec-Labrador. *Ministère de l'Énergie et des Ressources du Québec*, DV 84-18, 127-142.

Chapter 2:

MINERALOGICAL EXAMINATION OF THE PRODUCTS OF FENITIZATION IN THE AMBA DONGAR CARBONATITIC-ALKALINE COMPLEX, GUJARAT, INDIA.

Jeanette N. Roelofsen, Robert F. Martin
and Anthony E. Williams-Jones

Department of Earth and Planetary Sciences,
McGill University,
3450 University Street,
Montréal, Québec
H3A 2A7, Canada

Abstract

Previous studies of the process of fenitization generally involved a detailed examination of compositional and textural relationships of minerals in the protolith and its derived fenite to infer the composition of the fenitizing fluids. Sodic and potassic fenitization of sandstone and alkaline volcanic and plutonic rocks has occurred in the Amba Dongar carbonatitic-alkaline complex, Gujarat, India. These rocks are compositionally distinct starting points from which to examine the effects of the fenitizing fluids. The results of this paper establish that the fenites were produced by the interaction of a fluid emitted from the carbonatite with igneous and surrounding sedimentary rocks, whereby the protolith has undergone high-temperature sodic and lower-temperature potassic fenitization. Sodic fenites formed by metasomatism of sandstone were enriched in Na, Ca, Mg, Al and Fe, whereas potassic fenites were enriched in K, Rb and Ba at the expense of Si. Mg-fenitization of alkaline volcanic and plutonic rocks after Na-fenitization resulted in formation of glimmerite (mica-rich regions at the edge of carbonatite veins), whereas extreme Na- (+K) fenitization of the alkaline volcanic and plutonic rocks, following silicification, produced an ultrafenite that is enriched in Na, Ca, Si, Fe, Mg, and, in part, Ba and S. This study shows that the fenitization of both kinds of starting materials was produced by a single metasomatic fluid that was enriched in Na, K, Ca, S, Ba and possibly Al, with convergence in the final product.

Introduction

Fenitization involves the fluid-mediated addition or removal of constituents from a protolith near an alkaline magmatic source to produce new, increasingly alkali-rich minerals. Consequently, the resultant mineralogy is dependent on the composition of the protolith and of the fenitizing fluid, as well as the temperature at which the reaction occurred (Le Bas, 1981; Woolley, 1982; Rubie & Gunter, 1983; Morogan, 1994). Variation in temperature of the fluid may explain the presence of potassic fenite of low-temperature origin near the surface and sodic fenite of high-temperature origin at depth in carbonatite complexes (e.g., Newania: Viladkar, 1980; Sökli: Vartiainen & Woolley, 1976). These

fluids also could have been emitted from different sources: the K-rich fenites have been attributed to a carbonatitic magma, and the sodic ones, to an ijolitic magma (Le Bas, 1977; Morogan, 1994).

Fenites associated with the Amba Dongar carbonatitic-alkaline complex, in India, are ideal to study the processes responsible for fenitization. Unfenitized Bagh sandstone surrounding the complex provides an excellent starting point from which to examine the process of fenitization of a protolith that has a very simple mineralogy (96-98% quartz; Viladkar, 1981). Viladkar (1986) proposed a relationship between the type of fenite developed at the expense of Bagh sandstone and depth. However, the recent recognition of fenitized alkaline volcanic and plutonic rocks (e.g., nephelinite and ijolite) in close proximity to outcrops of Bagh sandstone seems to complicate this simple relationship, as they may also be fenitized and, where extremely fenitized, may resemble those developed at the expense of Bagh sandstone. In this paper, mineralogical observations and petrological relationships are used to infer the temperature(s) and composition(s) of the fluid(s) involved in fenitization of the alkaline volcanic and plutonic rocks and Bagh sandstone in the Amba Dongar carbonatitic-alkaline complex.

Geological Setting

The 30-km^2 Amba Dongar complex (late Cretaceous to early Tertiary: Deans et al., 1972) is located 400 km northeast of Bombay in the state of Gujarat, India, (Crookshank, 1936; Yellur, 1968; Fig. 1A). The complex is composed of a calciocarbonatite breccia surrounded by a calciocarbonatite ring-dyke and both cut by ferrocarbonatite plugs and veins, all of which were emplaced in the Bagh sandstone (and intercalated limestone) of Cretaceous age, and Deccan flood basalt (Sukheswala & Udas, 1964; Viladkar, 1981, 1984; Gwalani et al., 1993; Fig. 1B). Plugs of coeval tinguaite, nephelinite, tephrite, phonotephrite and ijolite occur throughout the region (Sethna & Borges, 1981; Viladkar, 1981, 1984; Sethna, 1989; Gwalani et al., 1993). A late-stage basalt (Viladkar, 1981; Gwalani et al., 1993) is located in the center of the complex. One of the largest fluorite mines in Asia (11.6 million tonnes at 30% CaF_2; Deans et al., 1972) is located in the northeastern part of the complex. The fluorite occurs as veins or as a replacement of calciocarbonatite and

Figure 1A. Location of the Amba Dongar carbonatitic-alkaline complex and associated village in Gujarat, India. Faults associated with the rift zone near the Narmada river, near the complex, are represented by short black lines (after Karkare & Srivistava, 1990).

B. Geological map of the complex (after Viladkar, 1981, 1984).

C. Location of fenites in the upper portion of the complex near the mine site (after Deans et al., 1972; Viladkar, 1986). The numbers refer to the various sample locations.

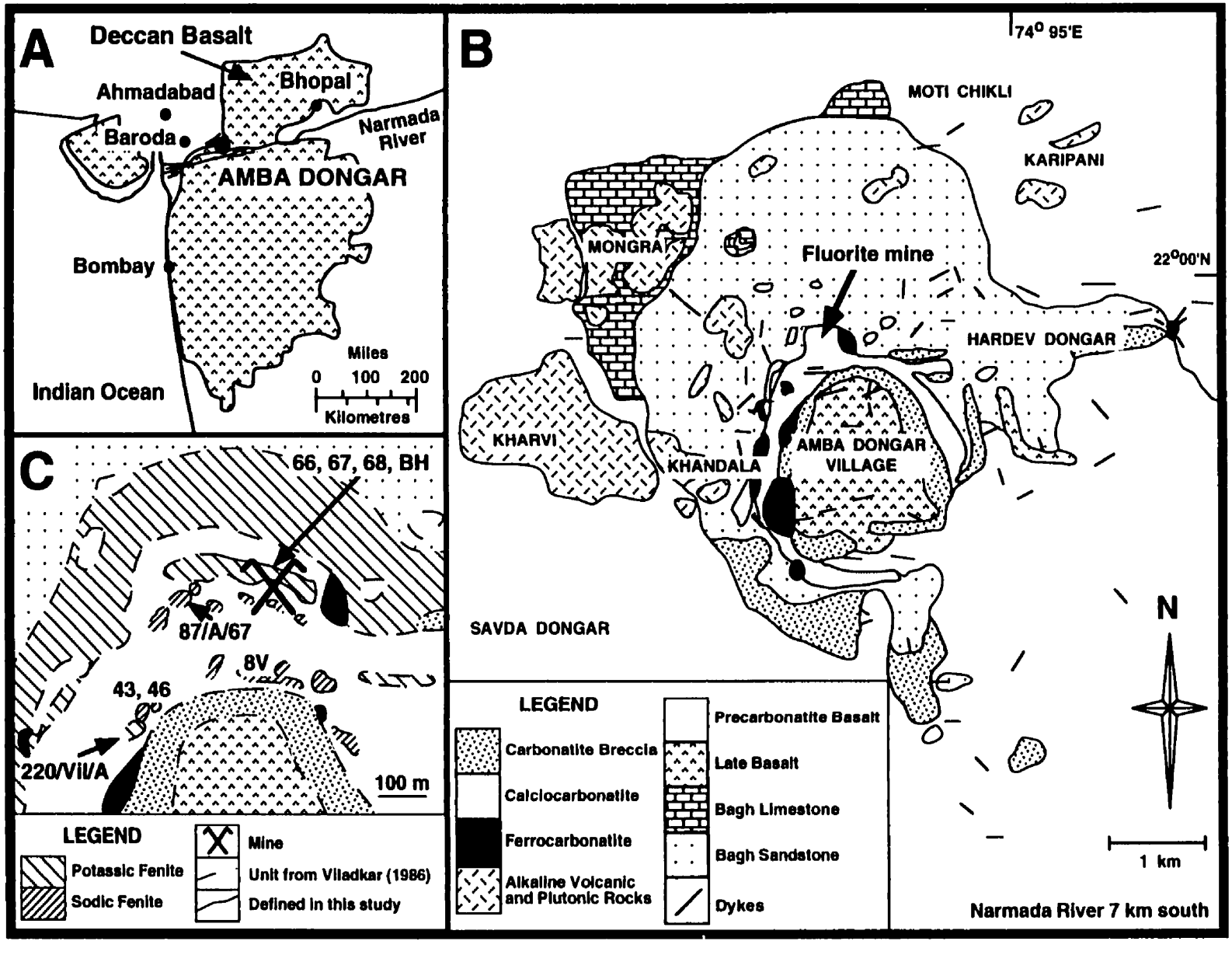
A
Deccan Basalt
Bhopal
Ahmadabad
Baroda
Narmada River
AMBA DONGAR
Bombay
Indian Ocean
Miles
0 100 200
Kilometres
B
74° 95'E
MOTI CHIKLI
KARIPANI
MONGRA
Fluorite mine
22°00'N
HARDEV DONGAR
KHARVI
KHANDALA
AMBA DONGAR VILLAGE
SAVDA DONGAR
N
1 km
Narmada River 7 km south
LEGEND
Carbonatite Breccia
Calciocarbonatite
Ferrocarbonatite
Alkaline Volcanic and Plutonic Rocks
Precarbonatite Basalt
Late Basalt
Bagh Limestone
Bagh Sandstone
Dykes
C
66, 67, 68, BH
87/A/67
8V
43, 46
220/Vil/A
100 m
LEGEND
Potassic Fenite
Sodic Fenite
Mine
Unit from Viladkar (1986)
Defined in this study

ferrocarbonatite (Viladkar, 1981; Palmer & Williams-Jones, 1996). Formation of fluorite resulted from mixing of a fluid derived from the carbonatite with a subalkaline fluid that originated in the surrounding host-rocks (Deans & Powell, 1968; Simonetti & Bell, 1995; Palmer & Williams-Jones, 1996).

Previous Investigations of the Units

Emplacement of the carbonatitic-alkaline complex resulted in uplift, faulting and fenitization of Bagh sandstone within 300 m of the contact (Sukheswala & Udas, 1981; Viladkar, 1981; Avasia et al., 1992; Fig. 1C). Viladkar (1986) documented five types of fenite formed at the expense of Bagh sandstone: a) ultrasodic, composed of monomineralic albite; b) sodic, composed of albite and aegirine-augite; c) sodi-potassic, composed of either: i) microperthite and aegirine-augite with minor orthoclase and albite, or ii) orthoclase, aegirine-augite, apatite and calcite; d) potassic, composed of orthoclase, albite, iron oxides, apatite and calcite ± sanidine and quartz; and e) ultrapotassic, composed of orthoclase or microcline. Potassic fenite developed at the expense of sandstone is dominant in the complex. At the present erosional surface, potassic fenite, which is dominant, was produced by the replacement of quartz grains by microcline or orthoclase (± albite).

A second type of potassic fenite, composed predominantly of mica, occurs at the contact of calciocarbonatite veins and sodi-potassic fenite or nephelinite (Viladkar, 1986, 1991). Viladkar (1991) proposed that this mica originated at the expense of pyroxene. However, as will be discussed in further detail in Chapter 3, there was insufficient pyroxene for this to have been the sole mechanism of formation. Instead, mica crystallized by Mg-metasomatism of K-feldspar from the associated alkaline volcanic and plutonic rocks, and through crystallization, in a topotactic relationship, on earlier mica. A detailed description of the units previously described from the complex is provided below.

Bagh Sandstone and Fenitized Equivalents

The Bagh sandstone and minor intercalated limestone that surround the complex (Fig. 1A) display prominent graded bedding, cross-bedding and asymmetrical ripple marks. The quartzite is white to grey and medium-grained in hand specimen. It is composed of 96-

98% quartz, with traces of feldspar, chlorite and hematite, and may be recrystallized (Avasia et al., 1992; Palmer & Williams-Jones, 1996).

In potassic fenite, the extent of fenitization, as determined from the degree of feldspathization, deformation and brecciation, increases toward the carbonatite. This fenite becomes more pink with an increase in the amount of feldspar and finely disseminated hematite. Rare (to 3 vol.%) fine- to medium-grained muscovite is present in the more strongly K-fenitized sandstones. Optical examination reveals that feldspathization produced microcline (± albite and muscovite) at the expense of quartz. Relict quartz (typically 60-85%) is strained, with undulose extinction, or recrystallized. In sodic and sodi-potassic fenites, albite and hematite are the dominant feldspar and oxide minerals, respectively, although poikilitic pyroxene and rare grains of amphibole are present in a few samples. No quartz-free fenites developed at the expense of Bagh sandstone were observed. Palmer & Williams-Jones (in prep.) are analyzing fluid inclusions and conducting mass-balance calculations of potassic fenitization of Bagh sandstone to determine the exact nature of the fenitizing fluid.

Alkaline Volcanic Rocks

Where unmetasomatized, the green nephelinite or tephrite contains medium- to coarse-grained euhedral phenocrysts of strongly zoned, prismatic aegirine-augite (7-10 vol.%), altered euhedral nepheline (12-15 vol.%) and zoned garnet (dark red-brown core to lighter brown rim; 5-10 vol.%), as well as ubiquitous fine-grained apatite (3 vol.%) and rare twinned titanite (Fig. 2A). One nephelinite contains phenocrysts of phlogopite. The fine-grained altered groundmass consists of hematite, calcite, analcime, orthoclase or sanidine, nepheline, clay minerals and what is possibly devitrified volcanic glass (Sethna, 1989; Gwalani et al., 1993). Rare clots of diopside are also present. Aegirine-augite exhibits a complicated zoning, embayments, and a resorbed appearance. It has a light green to colourless core with an oscillatory zoned, green rim. A detailed description of the zonation of unfenitized aegirine-augite was provided by Rock et al. (1994) and will be provided for the garnet (Gwalani, pers. comm.). Biotite- or phlogopite-rich glimmerite rims to calciocarbonatite veins in nephelinite or sodi-potassic fenite were attributed by Viladkar (1991) to potassic fenitization.

Figure 2. Textures of the nephelinites and ijolites.

A. Typical texture of nephelinite with twinned titanite (tit) and zoned aegirine-augite (aeg) and garnet (gt), and blocky pseudomorphs of nepheline (ne; length of image = 4 mm).

B. Ijolite (ij) cross-cut by a 2 cm syenite (sy) vein, which contains two feldspars and comb-textured aegirine-augite. Note the light (greenish) ijolite near the contact and the darker (red) ijolite at some distance from the vein.

C. Textural and mineralogical zonation in glimmerite (glim) developed at the margins of carbonatite veins (vein) in alkaline volcanic and plutonic rock (ij). Fenitization increases from left to right as the original textures of the alkaline rocks become obscured. This is accompanied by an increase in the relative amount and grain-size of mica until it predominates at the edge of the carbonatite vein (length of image = 5.5 mm).

D. Effects of extreme alteration of the phenocrysts. Relics of altered garnet (gt; hexagons), aegirine-augite or wollastonite (pr; prisms), titanite (wedges) and nepheline (ne; coarse equant grains) (length of image = 4 mm).

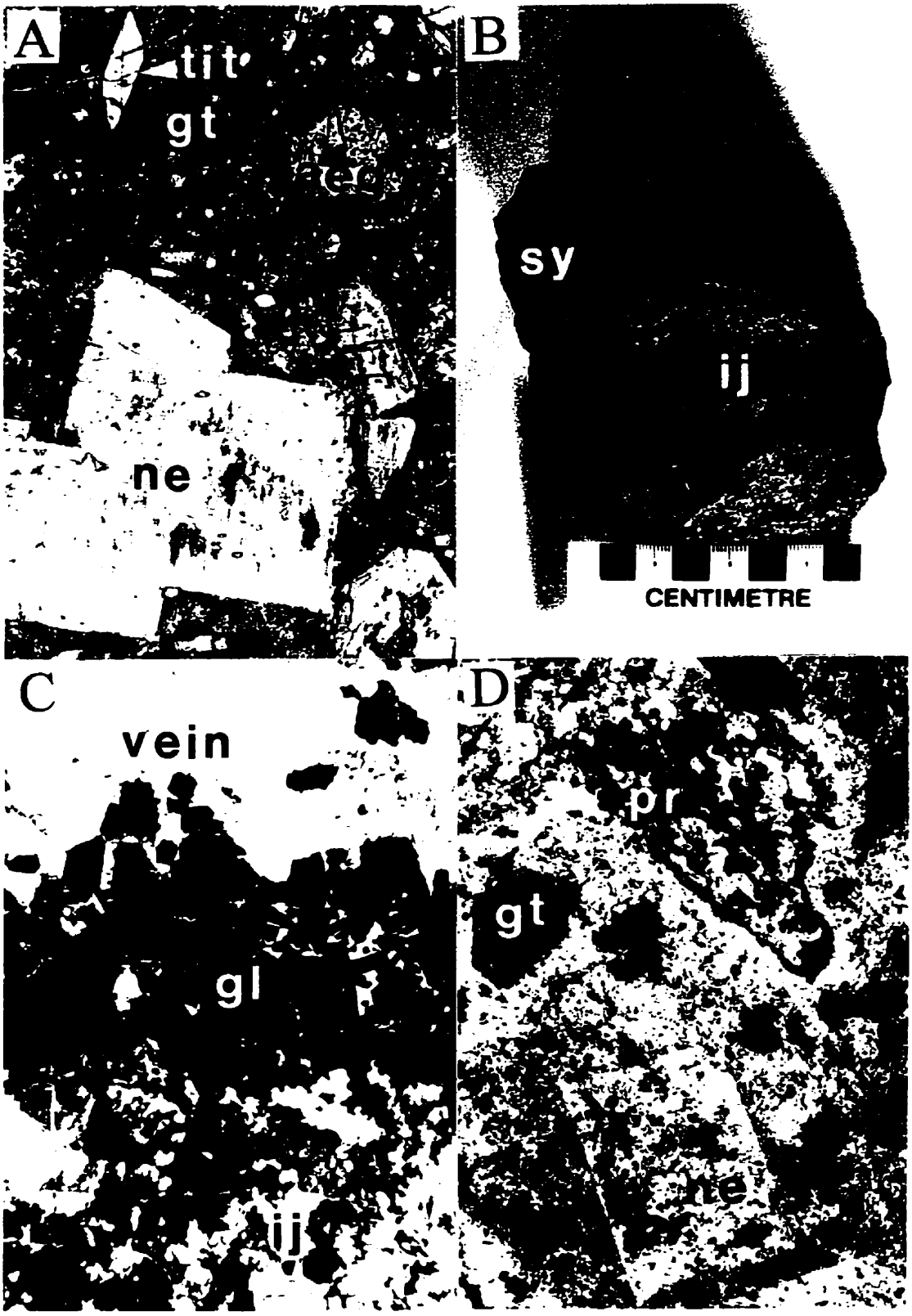
A
tit
gt
ne
B
sy
ij
CENTIMETRE
C
vein
gl
ij
D
pr
gt
ne

Alteration of the volcanic rocks at the present erosional surface resulted in: a) a blue-green or dusty pink appearance to the nepheline caused by alteration to analcime, calcite, kaolinite, cancrinite, and the presence of fine-grained hematite; and b) replacement of aegirine-augite, garnet and titanite by hematite ± calcite and a smectite-group mineral (Fig. 2D), as identified from optical examination, X-ray powder diffraction (XRD) and transmission electron microscopy (TEM) results (Roelofsen, unpub. data). In this study, the mineralogical variations and whole-rock chemistry of each type of fenite, in particular those from the alkaline volcanic and plutonic rocks, were determined.

Methodology

XRD patterns were recorded for feldspar and analcime using a Guinier-Hägg focussing camera and Cu$K\alpha_1$ radiation. Cell parameters were refined using the program of Appleman & Evans (1973), as modified by Garvey (1986). The composition of the feldspar was calculated from the cell volume by application of the equation of Kroll & Ribbe (1983), and the apparent degree of Al-Si order was calculated from the expressions of Blasi (1977).

Cameca Camebax and JEOL JSM-840 wavelength-dispersion spectrometry (WDS) electron microprobes, operated at an accelerating voltage of 15 kV and a beam current of 20 or 40 mA, with a defocussed beam (5, 7 or 10 μm), were used to determine compositions of the aegirine-augite, amphibole, apatite, feldspar, wollastonite, titanite and garnet. Counting times were 25 s for major elements and 50 s for minor elements, with the exception of F and Cl, for which the peaks were counted for 100 s. Standards employed for the silicates were: andradite (Fe, Ca and Si), vanadinite (V and Cl), ilmenite (Mn and Ti) or spessartine (Mn) and titanite (Ti and Ca), diopside (Si, Mg and Ca) or garnet (Mg), orthoclase (K, Al and Si), albite (Na), zircon (Zr), willemite (Zn), chromite (Cr), niobium metal (Nb), barite (Ba), synthetic glass (Sr), apatite (P) and fluorite (F). Durango apatite (P and Ca), orthoclase (Si), albite (Na), fluorapatite or fluorite (F), vanadinite (Cl) and synthetic glasses (La, Ce, Nd and Sr) were used for the analysis of apatite. Analyses of carbonates and oxides by energy-dispersion spectrometry (EDS) were performed with a Link spectrometer attached to a JEOL JSM-840 scanning electron microscope (SEM).

WDS analyses on mica were performed on a JEOL JXA 8600 Superprobe equipped with Tracor Northern software at Johns Hopkins University, Baltimore, Maryland, operated at 15 kV with a defocussed beam (10 μm). The standards used were: albite (Na), orthoclase (K), enstatite (Mg), rhodonite (Mn), fayalite (Fe), chromite (Cr), anatase (Ti), benitoite (Ba), fluorphlogopite (F) and anorthite (Ca, Si and Al). Collection times were 60 s or until 0.5% precision was reached (K and Si), except for counts for F and Ba, which were collected for 120 s.

Whole-rock analyses by X-ray fluorescence (XRF) were conducted on 29 samples at the Geochemical Laboratories, McGill University. The fenites of the alkaline volcanic and plutonic rocks were subdivided based on colour and mineralogical differences. Concentrations of major elements and Ba, Ce, Co, Cr, Ni, Sc, V and Zn were determined on fused beads of samples, whereas concentrations of the rest of the trace elements (Nb, Zr, Y, Sr, Rb, Pb, Th and U) were determined on pressed pellets. The Fe^{3+}/Fe^{2+} ratio of the selected rocks was determined with a solution containing powdered rock sample titrated against potassium permanganate. Concentrations of rare-earth element (REE) and additional trace elements were analyzed by inductively coupled plasma - mass spectrometry (ICP-MS) at Activation Laboratories Ltd (16 samples) or ACME Analytical Laboratories Ltd (13 samples).

Description of Newly Recognized Units

Units not previously described in the literature on the Amba Dongar complex were noted during our field investigations. These are described below, along with their relationship to the units described above. For detailed descriptions of the specific samples, refer to Appendix A-1.

Alkaline Plutonic Rocks

Green ijolite and urtite (classification of Le Maitre, 1989) were observed in the field. They are mineralogically similar to their volcanic equivalents (nephelinite and tephrite) described above, except that they contain anhedral alkali feldspar(s) ± prismatic wollastonite and anhedral nepheline (Fig. 2B). These rocks are cross-cut by syenite veins (1

cm to 0.5 m) and, in one case, a melteigite vein. Both types of veins contain comb-textured aegirine-augite at the margin. The syenite veins contain two distinct orthoclase feldspars at the core and disseminated hematite throughout. The melteigite also contains minor fine-grained titanite, apatite, sulphides and oxides. The contact between the veins and ijolite is pale green (Fig. 2B).

Fenitized Alkaline Volcanic and Plutonic Rocks

Localized potassic fenitization of alkaline rocks near veins of calciocarbonatite produces a green to pink halo (on average 15 cm wide), which grades into glimmerite (>80 vol.% biotite) at the vein margin (Fig. 2C; Chapter 3). Green aegirine-augite varies from euhedral and zoned in the fresh rock to a brighter green, more anhedral and unzoned in the fenitized region, nearer to the vein. This is matched by a steady increase in the proportion and grain-size of the mica toward the vein. Finally, a 0.5- to 1-cm-wide layer of 86 vol.% fine-grained, brown to greenish brown mica, 10 vol.% hematite, 5 vol.% calcite and 7 vol.% apatite is formed. Further increases in the grain size of mica (from 0.5 mm to 0.5 cm), size of the reversely pleochroic core of phlogopite and the proportion of apatite occur toward the calciocarbonatite veins. However, as noted in Chapter 3, there is an insufficient volume of aegirine-augite in unfenitized alkaline rock for all mica to have originated by K-metasomatism of aegirine-augite, as suggested by Viladkar (1991). This difference can be attributed to the replacement of K-feldspar by mica, which forms 5 vol.% of the rock, and, in particular, to the crystallization of normally pleochroic (i.e., more aluminous) biotite in a topotactic relationship onto the reversely pleochroic phlogopite.

"Ultrafenite"

A previously unreported fine-grained, dark green material is present as plugs in the calciocarbonatite and breccia near the basaltic core of the complex (Fig. 1C). The extremely fine-grained (<15 μm) mineral assemblage consists of 45 vol.% anhedral feldspar, where either albite or sanidine predominate, and <10 vol.% quartz (identified by XRD), as well as up to 7 vol.% hematite, 25–40 vol.% weakly zoned and preferentially oriented bright green aegirine-augite or rare pale greenish yellow amphibole, and up to 5 vol.% colourless barite (Fig. 3A). There is a general lack of igneous texture, although banding, swirls and ovoid

Figure 3A. Fine-grained "ultrafenite" contains albite, K-feldspar, aegirine-augite, hematite, richteritic amphibole, minor quartz, and, in some samples, barite. Grains of the mafic minerals are oriented parallel to the dark and light bands. This image also shows feldspathic regions (feld; see C) and is cross-cut by a late aegirine-carbonate vein (aeg). An ovoid-like region (see D) and a relict grain are present in the lower right-hand corner (arrows; length of image = 6 mm).

B. Ovoid regions containing feldspar ± amphibole (ric) in dark, hematite-rich (hem), bands of "ultrafenite". The amphiboles appear to be oriented with their long axes parallel to the banding (length of image = 0.13 mm).

C. Vein-like fine-grained feldspar-rich regions (feld; predominantly orthoclase or albite ± quartz and rare calcite) indicate that recrystallization or feldspathization occurred. These regions are cross-cut by mafic veins composed of aegirine-augite (aeg), hematite and carbonate, and by later veinlets of hematite (hem; length of image = 6 mm).

D. The veins of calcite and hematite contain cores of richteritic amphibole (ric). They are surrounded by zones of richteritic amphibole ± aegirine-augite and aegirine-augite + hematite away from the vein. Late veinlets (<0.5 mm; cannot be observed) of hematite, britholite and calcite cross-cut both the fine-grained material and the veins (length of image = 6 mm).

hem
ric
A
B
aeg
feld
ftc
C
D

regions of feldspar and amphibole are present. The darker bands result from increases in concentrations of hematite (to 15 vol.%) and, in some cases, aegirine-augite and amphibole. Some light bands contain swirls of the dark material at their contact with the dark bands. The fine grain-size of this material, the presence of ovoid agglomerations (Fig. 3B), and absence of igneous texture are indicative of recrystallization or feldspathization. A few samples contain coarser regions of anhedral feldspar, and hematite pseudomorphous after a prismatic mineral, which produce a texture analogous to that described above for the syenite veins. The fine grain-size, mineralogy, banding, relicts and ovoid regions suggest that these samples have been produced at relatively high-temperature by metasomatism of alkaline volcanic or plutonic rocks. The presence of quartz could be due to veining (silicification).

A succession of four types of veins (up to 5 mm in width) cross-cut the ultrafenite: 1) vein-like regions of fine-grained orthoclase or albite ± quartz and rare calcite (Fig. 3C), 2) medium-grained aegirine-augite veins with finer-grained hematite ± calcite oriented approximately 60° to the banding of the host, 3) calcite and hematite veins surrounded by a fine-grained pale green aegirine-augite ± amphibole halo, containing zoned (core versus rim), prismatic greenish yellow amphibole at the core (Fig. 3D), and 4) veinlets (<0.5 mm) of hematite and calcite surrounded by a halo of hematite (Fig. 3C) or of fine-grained britholite (identified by EDS) and hematite (Fig. 3D).

Mineral Textures and Compositional Variation

Aegirine-augite

Back-scatter SEM images and results of electron-microprobe analyses show that the aegirine-augite phenocrysts from alkaline volcanic and plutonic rocks are zoned from a clear, complexly zoned, embayed, more hedenbergite-rich core to a green, aegirine-rich, oscillatory zoned overgrowth (Fig. 4; Rock et al., 1994). Electron-microprobe analyses show that the aegirine-augite (classification of Morimoto, 1989) contains, on average, 0.48 wt.% TiO_2, 0.72 wt.% Al_2O_3, 0.70 wt.% MnO and 0.1 wt.% V_2O_3 and ZrO_2, with minor amounts of Zn, Nb and Cr (Table 1; Appendix A-2). The aegirine-rich rims have higher concentrations of Ti, Mn, Cr and V than the hedenbergite-rich cores. Rock et al. (1994) did not propose an origin for the zonation of the pyroxene from the Amba Dongar complex.

Figure 4. SEM image of zonation in aegirine-augite from a nephelinite. The subhedral, patchy zoned and embayed, Di-rich, light core is surrounded by a lighter green region and then a green, Ae-rich, oscillatory zoned euhedral rim. The brighter inclusions in the pyroxene and surrounding it are grains of andradite, and the wedge-shaped grains are titanite. The darker portion of the image represents the groundmass.

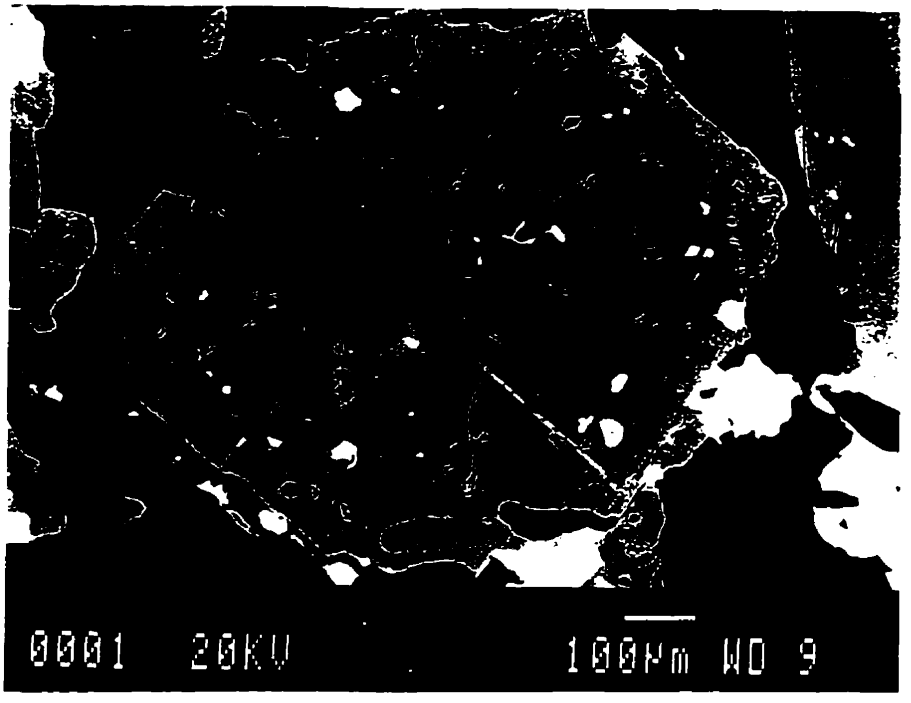
0001 20KV
100µm WD 9

Table 1. Selected aegirine-augite and amphibole electron-microprobe analyses and formulae.

Mineral	**Aegirine-augite**[1]							
Sample #	**37A**	**66D2**		**66J1**	**66J2**		**66A1**	**66B**
Description	**edge**	**lt. mid.**	**lt.ed.**	**dark**	**v.light**			
SiO_2	50.18	50.29	50.34	50.14	50.56	52.41	51.91	52.30
TiO_2	0.38	0.25	0.29	0.43	0.36	0.05	0.43	0.51
Al_2O_3	1.22	0.71	0.84	1.09	0.96	0.32	0.64	1.21
Fe_2O_3	8.63	9.22	9.46	7.93	10.17	8.93	25.65	21.15
FeO	11.14	9.52	9.01	8.86	11.19	6.39	0.31	3.82
MgO	6.20	7.33	7.36	8.95	5.43	9.64	3.86	3.68
MnO	0.88	0.62	0.65	0.56	0.59	0.57	0.54	0.54
ZnO	0.00	0.00	0.02	0.01	0.00	0.00	0.00	0.00
V_2O_3	0.13	0.11	0.07	0.09	0.24	0.08	0.26	0.24
Cr_2O_3	0.01	0.00	0.00	0.01	0.03	0.00	n.d.	n.d.
ZrO_2	n.d.	0.02	0.00	0.10	n.d.	n.d.	0.11	0.03
Nb_2O_5	0.09	0.00	0.01	0.00	0.00	0.02	0.00	0.01
CaO	19.54	19.36	19.47	20.49	17.86	19.96	7.24	7.27
Na_2O	2.66	2.67	2.74	1.89	3.55	2.81	9.81	9.10
K_2O	0.00	0.00	0.00	0.00	0.00	0.00	0.01	0.20
Total	101.04	100.10	100.27	100.53	100.94	101.18	100.89	100.17

Table 1. Selected aegirine-augite and amphibole electron-microprobe analyses and formulae (continued).

Mineral	**Aegirine-augite**[1]							
Sample #	**37A**	**66D2**		**66J1**	**66J2**		**66A1**	**66B**
Description	**edge**	**lt. mid.**	**lt.ed.**	**dark**	**v.light**			
Si	1.931	1.940	1.937	1.916	1.948	1.966	1.960	1.990
Ti	0.011	0.007	0.008	0.012	0.011	0.001	0.012	0.015
^{IV}Al	0.055	0.032	0.038	0.049	0.044	0.014	0.029	0.010
Σ Tetrahedral	1.997	1.980	1.983	1.977	2.003	1.981	2.002	2.014
Fe^{3+}	0.250	0.268	0.274	0.228	0.295	0.252	0.729	0.605
Fe^{2+}	0.359	0.307	0.290	0.283	0.361	0.201	0.010	0.121
Mg	0.355	0.421	0.422	0.510	0.312	0.539	0.218	0.208
Mn	0.029	0.020	0.021	0.018	0.019	0.018	0.017	0.017
Zn	0.000	0.000	0.001	0.000	0.000	0.000	0.000	0.000
^{VI}Al	0.000	0.000	0.000	0.000	0.000	0.000	0.000	0.044
V	0.004	0.003	0.002	0.003	0.008	0.003	0.011	0.011
Cr	0.000	0.000	0.000	0.000	0.001	0.000	0.000	0.000
Zr	0.000	0.000	0.000	0.002	0.000	0.000	0.002	0.001
Nb	0.002	0.000	0.000	0.000	0.000	0.000	0.000	0.000
Σ Octahedral	0.998	1.021	1.010	1.044	0.995	1.013	0.987	1.008
Ca	0.806	0.800	0.803	0.839	0.737	0.802	0.293	0.296
Na	0.199	0.199	0.204	0.140	0.265	0.204	0.718	0.671
K	0.000	0.000	0.000	0.000	0.000	0.000	0.000	0.010
Σ Rest	1.004	1.000	1.007	0.979	1.002	1.006	1.011	0.977
Mol.%								
Aegirine	19.85	19.94	20.43	14.00	26.50	20.40	71.82	60.70
Diopside	35.54	42.15	42.21	50.99	31.17	53.92	21.75	20.85
Hedenbergite	35.86	30.71	29.00	28.31	36.06	20.05	0.98	12.14

[1] Pyroxene formulae calculated based on 4 cations and 6 anions with Fe^{3+}/Fe^{2+} determined by charge balance.

lt. = light; dk. = dark; v. = very; n.d.=not detected.

Table 1. Selected aegirine-augite and amphibole electron-microprobe analyses and formulae (continued).

Mineral	**Aegirine-augite**[1]					**Richteritic Amphibole**[2]		
Sample #	**87/A/67**	**87/A/94**	**41E**			**66I**	**46D**	
Description			**by vein**	**far**	**v. far**	**light**	**mid**	**edge**
SiO_2	52.77	52.85	53.26	53.28	53.65	52.07	55.59	55.37
TiO_2	0.46	0.75	0.39	0.51	0.50	0.62	0.16	0.35
Al_2O_3	0.58	0.30	0.23	0.31	0.36	0.72	0.22	0.09
Fe_2O_3	30.17	13.95	6.06	6.08	6.28	5.57	0.00	0.00
FeO	0.00	4.04	2.86	3.70	2.70	5.55	7.19	9.44
MgO	1.62	7.88	13.03	12.31	12.90	10.60	19.25	17.71
MnO	0.16	0.53	0.58	0.54	0.50	1.40	0.95	1.36
ZnO	0.00	0.00	0.00	0.00	0.00	0.01	0.02	0.02
V_2O_3	0.48	0.10	0.20	0.20	0.17	0.46	0.04	0.16
Cr_2O_3	0.01	0.00	0.02	0.00	0.01	0.03	0.01	0.01
ZrO_2	n.d.	n.d.	n.d.	n.d.	n.d.	0.15	0.00	0.00
Nb_2O_5	0.00	0.01	0.00	0.01	0.02	0.01	n.d.	n.d.
CaO	2.51	14.67	21.24	20.24	20.52	20.17	5.37	2.66
Na_2O	12.70	5.71	2.19	2.60	2.62	2.43	7.02	8.03
K_2O	0.00	0.00	0.00	0.00	0.00	0.00	1.68	2.35
F	n.d.	n.d.	n.d.	n.d.	n.d.	n.d.	2.39	1.33
Cl	n.d.	n.d.	n.d.	n.d.	n.d.	n.d.	0.00	0.00
H_2O	n.a.	n.a.	n.a.	n.a.	n.a.	n.a.	0.96	1.44
Total	101.45	100.79	100.06	99.77	100.23	99.74	99.83	99.77

Table 1. Selected aegirine-augite and amphibole electron-microprobe analyses and formulae (continued).

Mineral	**Aegirine-augite[1]**					**Richteritic Amphibole[2]**		
Sample #	**87/A/67**	**87/A/94**	**41E**			**66I**	**46D**	
Description			**by vein**	**far**	**v. far**	**light**	**mid**	**edge**
Si	1.978	1.981	1.975	1.985	1.982	1.966	7.944	8.008
Ti	0.013	0.021	0.011	0.014	0.014	0.018	0.017	0.038
Al(IV)	0.022	0.013	0.010	0.013	0.016	0.032	0.038	0.000
Σ Tetrahedral	2.013	2.015	1.996	2.012	2.011	2.015	7.999	8.046
Fe^{3+}	0.851	0.394	0.169	0.170	0.175	0.158	0.000	0.000
Fe^{2+}	0.000	0.127	0.089	0.115	0.084	0.174	0.859	1.141
Mg	0.091	0.440	0.720	0.683	0.710	0.597	4.100	3.819
Mn	0.005	0.017	0.018	0.017	0.016	0.045	0.115	0.167
Zn	0.000	0.000	0.000	0.000	0.000	0.000	0.002	0.002
Al(VI)	0.003	0.000	0.000	0.000	0.000	0.000	0.000	0.016
V	0.015	0.003	0.006	0.006	0.005	0.014	0.004	0.019
Cr	0.000	0.000	0.001	0.000	0.000	0.001	0.001	0.001
Zr	0.000	0.000	0.000	0.000	0.000	0.003	0.000	0.000
Nb	0.000	0.000	0.000	0.000	0.000	0.000		
Σ Octahedral	0.964	0.981	1.003	0.992	0.990	0.991	5.080	5.165
Ca	0.101	0.589	0.844	0.808	0.812	0.816	0.821	0.413
Na	0.922	0.415	0.158	0.188	0.187	0.178	1.946	2.252
K	0.000	0.000	0.000	0.000	0.000	0.000	0.306	0.433
Σ Rest	1.023	1.004	1.001	0.996	0.999	0.994	3.073	3.097
F							1.082	0.610
Cl							0.001	0.000
OH							0.916	1.390
Σ Na+K+Si							10.20	10.69
Σ Ca + Al(IV)							0.86	0.41
Mol.%								
Aegirine	84.94	39.48	15.75	16.79	17.73	15.76		
Diopside	9.05	44.02	72.02	68.33	71.03	59.66		
Hedenbergite	0.00	12.65	8.86	11.54	8.35	17.36		

[1] Pyroxene formulae calculated based on 4 cations and 6 anions with Fe^{3+} determined by charge balance.

[2] Amphibole mineral fomulae calculated based on 23 anions and calculation of Fe^{3+}/Fe^{2+} by charge balance.

lt. = light; dk. = dark; v. = very; n.d.=not detected; n.a.=not analyzed.

Moreover, Dawson et al. (1995) attributed the embayed cores and aegirine-rich oscillatory zoned rims of aegirine-augite from xenoliths of ijolite at Oldoinyo Lengai to resorption and Na-metasomatism, respectively. Such a relationship is consistent with the present observations.

On a Ae-Di-Hd plot, the clinopyroxene compositions of igneous or metasomatic origin follow a broken curve from diopside (Di) toward hedenbergite (Hd) and then aegirine (Ae; Fig. 5A). This curve links the compositional variations of four groups of pyroxene defined by the associated rock-type. These are: 1) relatively unzoned aegirine-rich (Ae > 65%) phenocrysts from alkaline rocks that exhibit the effects of fenitization, 2) zoned phenocrysts with a green Ae-rich rim in the same rocks (cores <45% Ae; those from ijolite are more Hd-rich), 3) fine-grained Di-rich pyroxene from "ultrafenites", and 4) a Di-rich pyroxene inclusion (possibly a xenocryst) from the alkaline volcanic rocks. Enrichment in Ae, lack of zonation of aegirine-augite in Group 1, and the presence of an Ae-rich rim on zoned, unaltered aegirine-augite (Group 2) are consistent with an early episode of Na-metasomatism. Texture (grain-size and banding) and composition (relatively Di-rich) indicate a metasomatic origin of aegirine-augite ± amphibole in "ultrafenite" (Group 3). Furthermore, the Ca-rich, Na-poor aegirine-augite from the cores of clinopyroxene in Groups 2, 3 and 4 indicates that crystallization occurred in a magma of low Si content (Larsen, 1978). Clinopyroxene from silica-undersaturated rocks, in general, tends to fall into the Hd-poor portion of the Di-Ae-Hd triangle compared to that from silica-oversaturated rocks (Bonin & Giret, 1985).

The observed compositional trend of aegirine-augite in Figure 5B is similar to that noted by Viladkar (1986) for fenites, and Viladkar & Avasia (1992) and Rock et al. (1994) for alkaline volcanic rocks from the Amba Dongar complex. Viladkar (1986) subdivided this trend into three groups, with the Di-rich, higher-temperature aegirine-augite in Group 1, the more Hd-rich, intermediate-temperature aegirine-augite in Group 2, and the most Ae-rich, lowest-temperature aegirine-augite in Group 3. His subdivisions are comparable to Groups 2 and 3 from the present study, although that of his Group 3 is more Di-rich. Group 1 from the present study is contained in his Group 3, but Group 4 has no equivalent.

The relationship between temperature and composition of aegirine-augite noted by Viladkar (1986) is applicable to the present study. Aegirine-augite from the "ultrafenite"

Figure 5. Compositional variation of aegirine-augite on a Ae-Di-Hd plot.

A. The main trend is from Di-rich to Hd-rich and finally Ae-rich pyroxene. The pyroxene only shows an Ae-enrichment following a compositional break. Aegirine-augite from the various rock types shows a more restricted compositional range. The upper hatched region represents fenitized aegirine-augite, whereas the lower hatched region represents unfenitized, zoned aegirine-augite. The horizontally hatched region represents aegirine-augite from "ultrafenite". The other region represents a pyroxene inclusion in a nephelinite. Arrows represent compositional changes between the cores and rims of individual pyroxene phenocrysts (shaded circles).

B. Comparison between the data of the present study (shaded regions) and the results of Viladkar (1986), Viladkar & Avasia (1992) and Mitchell (1980). The three different types of pyroxene (I, II, III) defined by Viladkar (1986) are comparable to those from this study. The three major trends defined by Mitchell (1980) of aegirine from the Fen complex are represented by the arrows labeled A, B and C. All are equivalent to the pyroxene compositions noted in this study (see text).

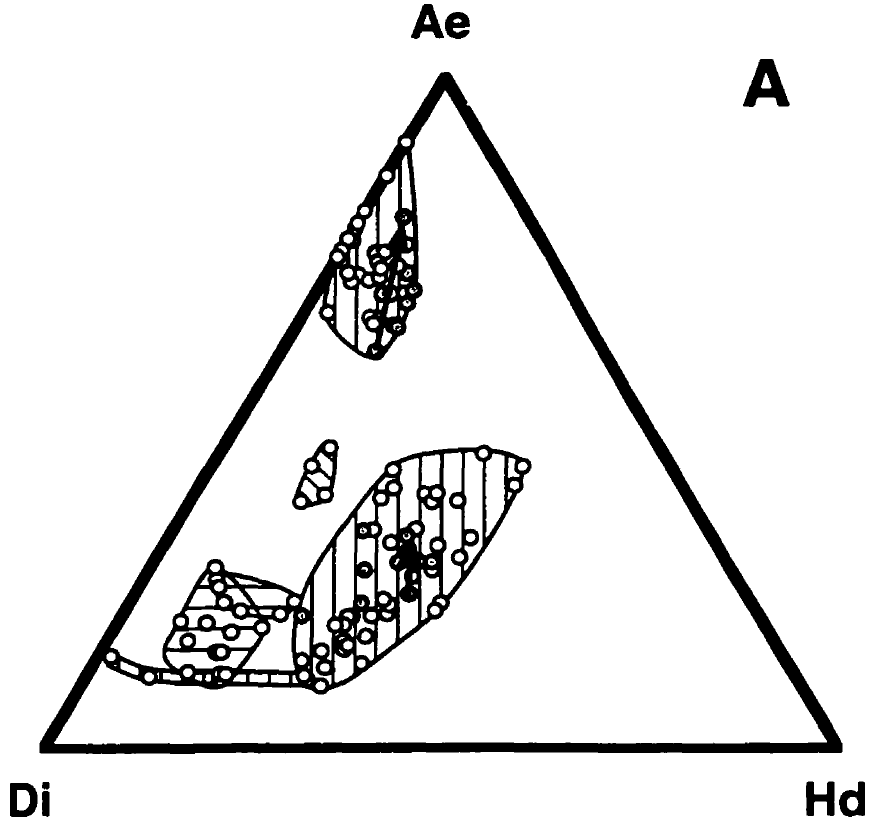
Ae
A
Di
Hd

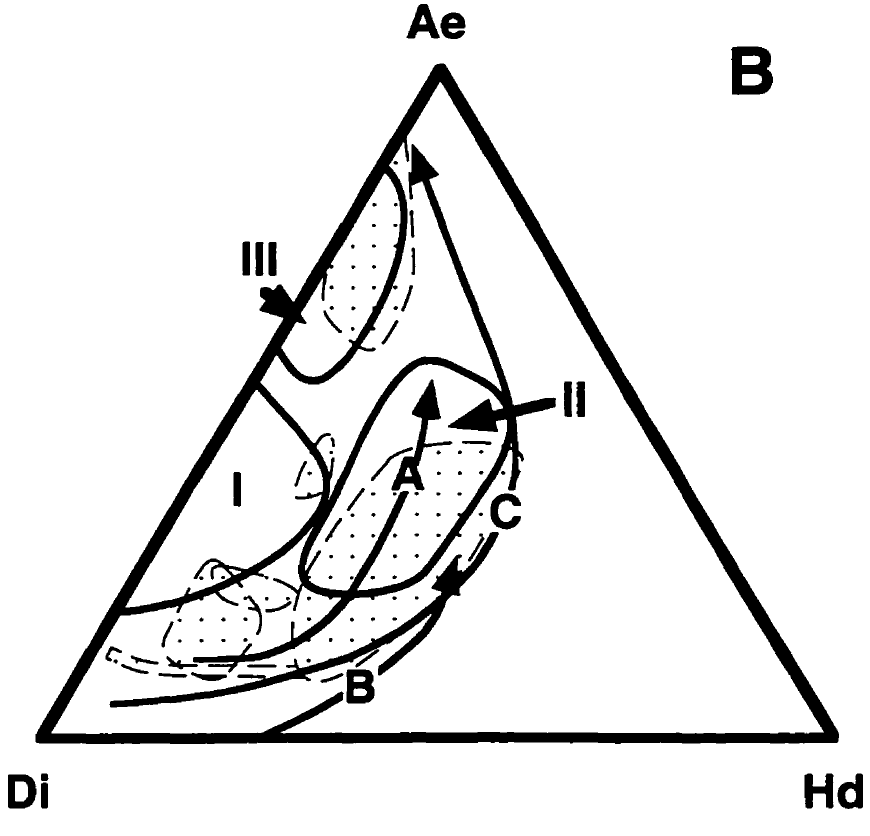
Ae
B
III
II
I
A
C
B
Di
Hd

(Type 3) and the pyroxene inclusions in tephrite are the most Di-rich, which suggests a high-temperature origin when combined with the feldspar data (see below). Na-metasomatism increases the Ae component of the pyroxene, which is thereby indicative of a lower temperature of formation. The compositional variation of pyroxene described by Tyler & King (1967) and Mitchell (1980; A, B, C in Fig. 5B) for alkaline volcanic suites from Uganda and Fen, Norway, respectively, follows the same trend as that from this complex, and thereby are interpreted to have the same trend of evolution for the aegirine originating from alkaline volcanic and plutonic rocks.

The difficulty with most studies of fenites is that they fail to distinguish the aegirine-augite compositions by rock type. Only Kresten & Morogan (1986), Morogan & Woolley (1988) and Morogan (1994) separated their compositional trends into different groups representing a different precursor and type of fenite. They noted the presence of Di-rich aegirine-augite in fenites produced by reaction of the rock with fluids that originated from ijolites that were re-equilibrated with calciocarbonatite, whereas Ae-rich pyroxene developed in the same manner with fluids in equilibrium with carbonatite. Their Di-rich trend is identical to Group 3 ("ultrafenite") of the present study, whereas the Hd-rich trend is identical to that of Group 1 (Na-metasomatized alkaline volcanic or plutonic rock).

Amphibole

Pale greenish yellow amphibole is present as uncommon small anhedral grains in "ultrafenite", especially near the calciocarbonatite veins, or as euhedral grains in the core of these veins. The composition of the amphibole averages (in wt.%): 2.47 F, 1.69 K_2O, 0.82 MnO, 0.25 Al_2O_3, 0.18 TiO_2 and 0.11 V_2O_3, with minor Cr, Cl, Zn and Zr (Table 1; Appendix A-3). It is potassian fluor-richterite with a small component of fluor-magnesio-arfvedsonite or, in a few grains, contains a fluor-magnesio-katophorite component (classification of Hawthorne, 1983; Fig. 6). In the veins, the amphibole is normally zoned, with the rim slightly enriched in Mn, Fe, OH and V, but depleted in F and Mg.

The compositional variation of amphibole reported in the present study is comparable to that from other fenites or carbonatites, as most contain mainly magnesio-richterite or magnesio-arfvedsonite (Sutherland, 1969a; Fabriès, 1978; Hogarth & Lapointe, 1984; Mian & Le Bas, 1986; Hogarth et al., 1987). The amphiboles from the present study

Figure 6. $\Sigma Ca+{}^{IV}Al$ versus $\Sigma K+Na+Si$ plot (after Fabriès, 1978) which depicts the extremely restricted composition of the amphiboles. Most amphiboles are end-member potassian fluor-richterite, with a small proportion of the arfvedsonitic or katophoritic component. The abbreviations used are: Arfvedsonite = Arf; leakeite = Lkt; riebeckite = Rbk; richterite = Ric; winchite = Win; katophorite = Ktp; barrosite = Brt; and taramite = Trm.

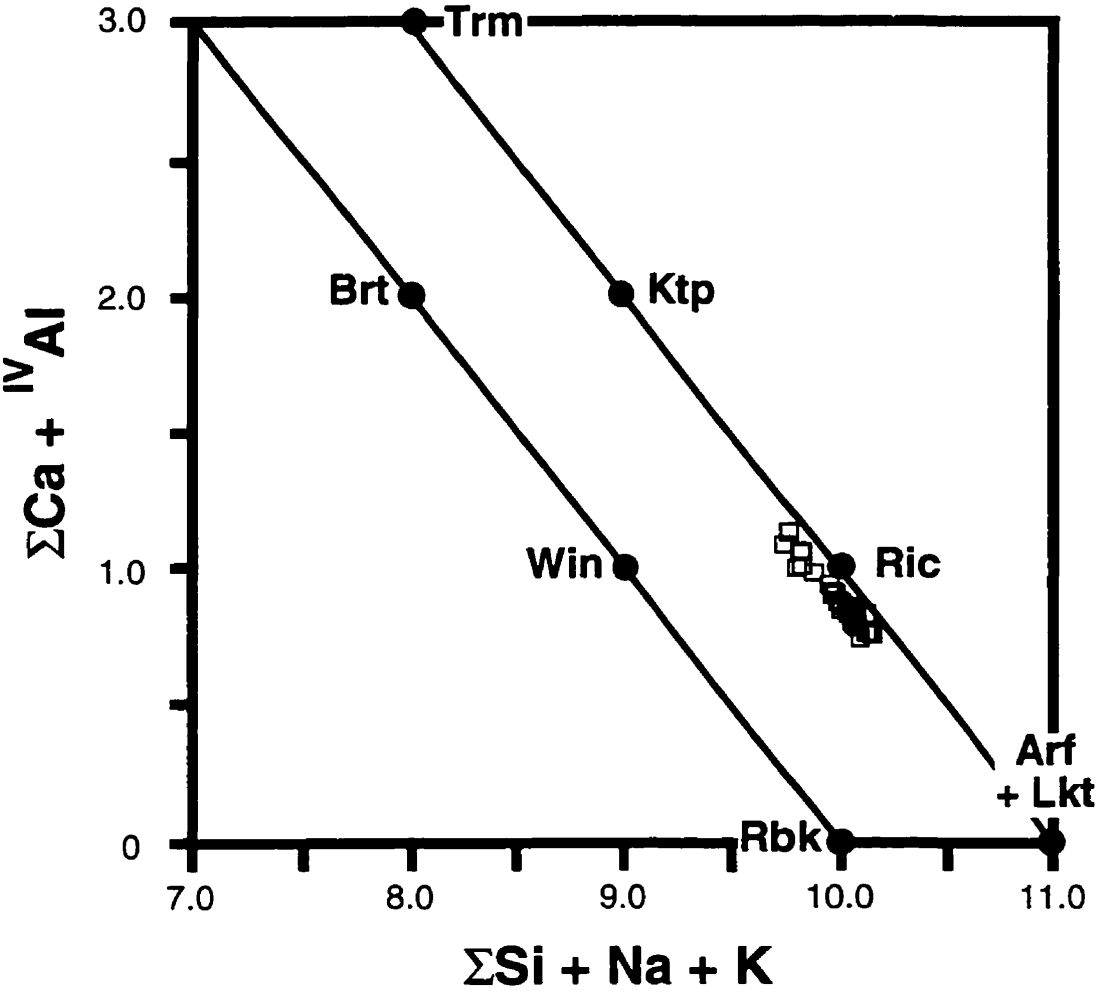
3.0
2.0
1.0
0
Trm
Brt
Ktp
Win
Ric
Arf
+ Lkt
Rbk
7.0
8.0
9.0
10.0
11.0
ΣCa + IVAl
ΣSi + Na + K

have equivalent concentrations of Ti, F, Cl and Cr, but higher Mn and lower Al contents than those described by most of these authors. These compositional differences can be accounted for by a close link with a calciocarbonatitic source (i.e., Mn enrichment; see below) and that the composition of the amphibole may reflect the composition of the protolith and that of the fenitizing fluid (Mian & Le Bas, 1986).

The increase in the proportion of amphibole compared to aegirine near the calciocarbonatite veins implies that the metasomatic fluid likely became more K-, Mg-, Fe^{2+}- and F-rich, and Si- or Na-poor. This relationship offers a small-scale example of early sodic fenitization followed by a more localized potassic fenitization, as observed in the glimmerite. Zonation of amphibole in the vein is indicative of a late enrichment of the metasomatic fluid in Mn, Fe and V, and depletion in Mg and F.

Mica

Phlogopite and biotite, dominant in glimmerite (Chapter 3), also forms rare phenocrysts in unfenitized nephelinite. Although potassic fenite derived from Bagh sandstone contains minor muscovite, this description focuses on mica from glimmerite developed at the margins of calcite carbonatite veins in alkaline volcanic and plutonic rocks. The minor muscovite produced by fenitization at the expense of Bagh sandstone will not be discussed in this paper. In unmetasomatized nephelinite, phlogopite exhibits exfoliation and hematite inclusions, especially along the cleavage at grain margins, respectively. Coarse-grained biotite in glimmerite contains a resorbed, reversely pleochroic (i.e., strongest direction of absorption parallel to the cleavage) orange to red phlogopite core (60-75 vol.%) surrounded by a brown to greenish brown normally pleochroic rim of biotite. Mica flakes vary from coarse-grained near carbonatite veins to more fine-grained and normally pleochroic at some distance from them. Fine-grained hematite is present in reversely pleochroic phlogopite near its contact with the biotite rim and along the cleavages (pseudomorphic after magnetite). This two-stage zonation recalls that previously noted for the aegirine-augite.

The results of electron-microprobe analyses show that biotite and phlogopite are enriched in F, Mn and Ti (to 4.23 wt.% F, 1.41 wt.% MnO and 4.32 wt.% TiO_2), with minor amounts of Na, Ca, Cr, V and Ba (generally <0.5 wt.% oxide; Table 2; Appendix A-

Table 2. Selected electron-microprobe analyses and calculated mineral formulae for mica.*

Sample #	BH/18/2.1				BH/18/2.2	BH/9/1	66B	66E	87/A/67
Description	R	R	N	N	N	N	N	N	N
SiO_2	41.18	41.85	41.00	39.97	41.25	38.84	39.13	40.22	41.38
TiO_2	0.61	0.65	0.94	2.13	1.17	1.80	1.71	1.98	1.01
Al_2O_3	9.32	10.53	10.75	11.41	10.28	10.58	10.77	11.35	10.62
Cr_2O_3	0.02	0.01	0.02	0.02	0.02	0.01	0.02	0.03	0.03
Fe_2O_3	1.81	1.11	0.00	0.00	0.00	0.00	0.00	0.00	0.00
FeO	8.15	7.15	12.66	13.80	13.73	19.70	16.66	13.26	15.12
MnO	0.18	0.16	0.56	0.51	0.50	1.17	1.41	0.63	0.88
MgO	23.23	23.69	19.40	17.90	18.69	14.35	16.05	18.26	16.80
CaO	0.00	0.12	0.10	0.01	0.17	0.02	0.18	0.14	0.11
BaO	0.03	0.04	0.06	0.00	0.00	0.17	0.01	0.05	0.01
Na_2O	0.29	0.19	0.24	0.27	0.18	0.19	0.15	0.15	0.15
K_2O	10.21	9.63	10.10	10.19	9.27	9.96	9.76	9.57	9.20
F	3.21	2.70	3.57	3.07	2.49	2.48	2.32	2.53	2.69
H_2O	2.57	2.88	2.35	2.56	2.85	2.74	2.85	2.82	2.71
Total	100.81	100.70	101.75	101.84	100.60	102.01	101.02	100.99	100.71
F,Cl=O	1.35	1.14	1.50	1.29	1.05	1.04	0.98	1.07	1.13
Total	99.46	99.56	100.25	100.54	99.55	100.97	100.04	99.93	99.58

Table 2. Selected electron-microprobe analyses and calculated mineral formulae for mica (continued).*

Sample #	BH/18/2.1				BH/18/2.2	BH/9/1	66B	66E	87/A/67
Description	R	R	N	N	N	N	N	N	N
Si	3.015	3.020	3.041	2.986	3.071	2.971	2.972	2.997	3.111
^{IV}Al	0.804	0.896	0.94	1.005	0.902	0.954	0.964	0.997	0.889
^{IV}Fe^{3+}	0.100	0.060	0.000	0.000	0.000	0.000	0.000	0.000	0.000
Ti	0.034	0.024	0.018	0.009	0.027	0.076	0.065	0.006	0.000
Σ Tetrahedral	3.953	4.000	4.000	4.000	4.000	4.000	4.000	4.000	4.000
^{VI}Al	0.000	0.000	0.000	0.000	0.000	0.000	0.000	0.000	0.052
Ti	0.000	0.011	0.034	0.111	0.039	0.028	0.033	0.105	0.057
Cr	0.001	0.001	0.001	0.001	0.001	0.001	0.001	0.002	0.002
^{VI}Fe^{3+}	0.000	0.000	0.000	0.000	0.000	0.000	0.000	0.000	0.000
Fe^{2+}	0.499	0.431	0.785	0.862	0.855	1.260	1.058	0.826	0.951
Mn	0.011	0.010	0.035	0.032	0.032	0.076	0.091	0.040	0.056
Mg	2.535	2.548	2.145	1.993	2.074	1.636	1.817	2.028	1.883
Σ Octahedral	3.047	3.001	3.001	3.000	3.001	3.000	3.000	3.001	3.000
Ca	0.000	0.009	0.008	0.001	0.014	0.002	0.015	0.011	0.009
Ba	0.001	0.001	0.002	0.000	0.000	0.005	0.000	0.002	0.000
Na	0.041	0.027	0.035	0.039	0.026	0.028	0.022	0.022	0.022
K	0.954	0.886	0.956	0.971	0.880	0.972	0.946	0.910	0.882
Σ Interlayer	0.996	0.923	1.000	1.011	0.920	1.007	0.983	0.944	0.913
F	0.743	0.616	0.838	0.725	0.586	0.600	0.557	0.596	0.640
OH	1.257	1.384	1.163	1.275	1.414	1.400	1.443	1.404	1.360
Fe/(Fe+Mg)	0.164	0.145	0.268	0.302	0.292	0.435	0.368	0.289	0.336
Σ Cations	7.996	7.923	8.000	8.011	7.920	8.007	7.983	7.944	7.913
Charge Deficiency	0.743	0.616	0.700	0.495	0.477	0.484	0.456	0.426	0.438

N = normally pleochroic; R = reversely pleochroic.

* Cations calculated on the basis of 11 oxygens and 7 cations + Na + K + Ca.

Fe^{3+} was calculated by charge balance assuming full occupancy of the cation sites.

4) and no Cl. Furthermore, the low K content of the mica (as low as 7.61 wt.% K_2O) suggests alteration to vermiculite, as documented in a transmission electron microscopy (TEM) investigation (Chapter 3). The rare normally pleochroic phlogopite phenocrysts in nephelinite feature the highest Ti and ^{IV}Al, but lowest Mn and Si values. The reversely pleochroic cores of phlogopite contain more Na, but less Ti, Mn and ^{IV}Al than the normally pleochroic rim of biotite (Fig. 7; Chapter 3). Moreover, the highest values of Mn and Ti in mica from the glimmerite occur at the contact between the reversely pleochroic cores and the normally pleochroic rims. The low ^{IV}Al content of the reversely pleochroic phlogopite implies the presence of Fe^{3+} in the tetrahedral site, as noted by Faye & Hogarth (1969). Some grains of mica from glimmerite have traces of Ca, elevated Fe, and slightly elevated Si. These variations are the result of the presence of calcite, ankerite, hematite and amorphous silica inclusions and vermiculite, as determined by electron-microprobe analyses and TEM (Chapter 3).

The relative lack of Al and Si in the tetrahedral site of the reversely pleochroic phlogopite from glimmerite indicates crystallization in a relatively Al- and Si-poor environment, such as from a carbonatitic magma (Chapter 3; McCormick & Le Bas, 1996). This was followed by a hiatus in crystallization (insufficient Al in the carbonatite magma for crystallization of phlogopite), resorption of the mica and crystallization of fine-grained, octahedra of magnetite (now hematite pseudomorphs) at the margins. Later, optically continuous rims of Fe- and Al-rich normally pleochroic mica crystallized. The most probable way to produce the biotite rims is through crystallization from more Al-rich fenitizing fluids derived from the interaction with the surrounding alkaline volcanic and plutonic rocks (Chapter 3).

The compositions of normally and reversely pleochroic mica from the present study are similar to the two types of mica noted by Viladkar (1991) from the Amba Dongar complex. He reported that mica from K-fenitized nephelinite is Mg- and Al-rich (16-22 wt.% MgO; 10-16 wt.% Al_2O_3), whereas that from sodi-potassic fenite of unspecified origin is Fe-rich (16-22 wt.% FeO) and Mg- and Al-poor (12.5-16 wt.% MgO; 9-12 wt.% Al_2O_3). The Al contents of Viladkar's micas correspond to that of the normally pleochroic phlogopite and reversely pleochroic biotite, respectively, except that the other elemental variations are the converse. Moreover, he did not associate these compositional differences

Figure 7. Compositional variation of mica.

A. A Fe/(Fe+Mg) (Fe#) versus ^{IV}Al plot depicting the three types of mica: normal pleochroic biotite (dark shading), reversely pleochroic phlogopite (light shading), and a mica phenocryst in nephelinite (vertical lines). Note the difference in the aluminum content of each type of mica.

B. Mica from the present study is in general depleted in ^{IV}Al compared to mica of other carbonatitic-alkaline complexes. Examples of reversely pleochroic mica from other complexes (circled in the figure) are enriched in ^{IV}Al and depleted in Fe# compared to those from the present study. Mica compositions are compiled from: the Fen complex (Andersen, 1989; Andersen & Austrheim, 1991), the Loe Shilman complex (Mian & Le Bas, 1987), the Mud Tank carbonatite (Currie et al., 1992), the Jacupiranga complex (Morbidelli et al., 1986), the Siilinjärvi complex (Puustinen, 1973), carbonatites from Uganda (McCormick & Le Bas, 1996), and the Tapira complex (Brigatti et al., 1996).

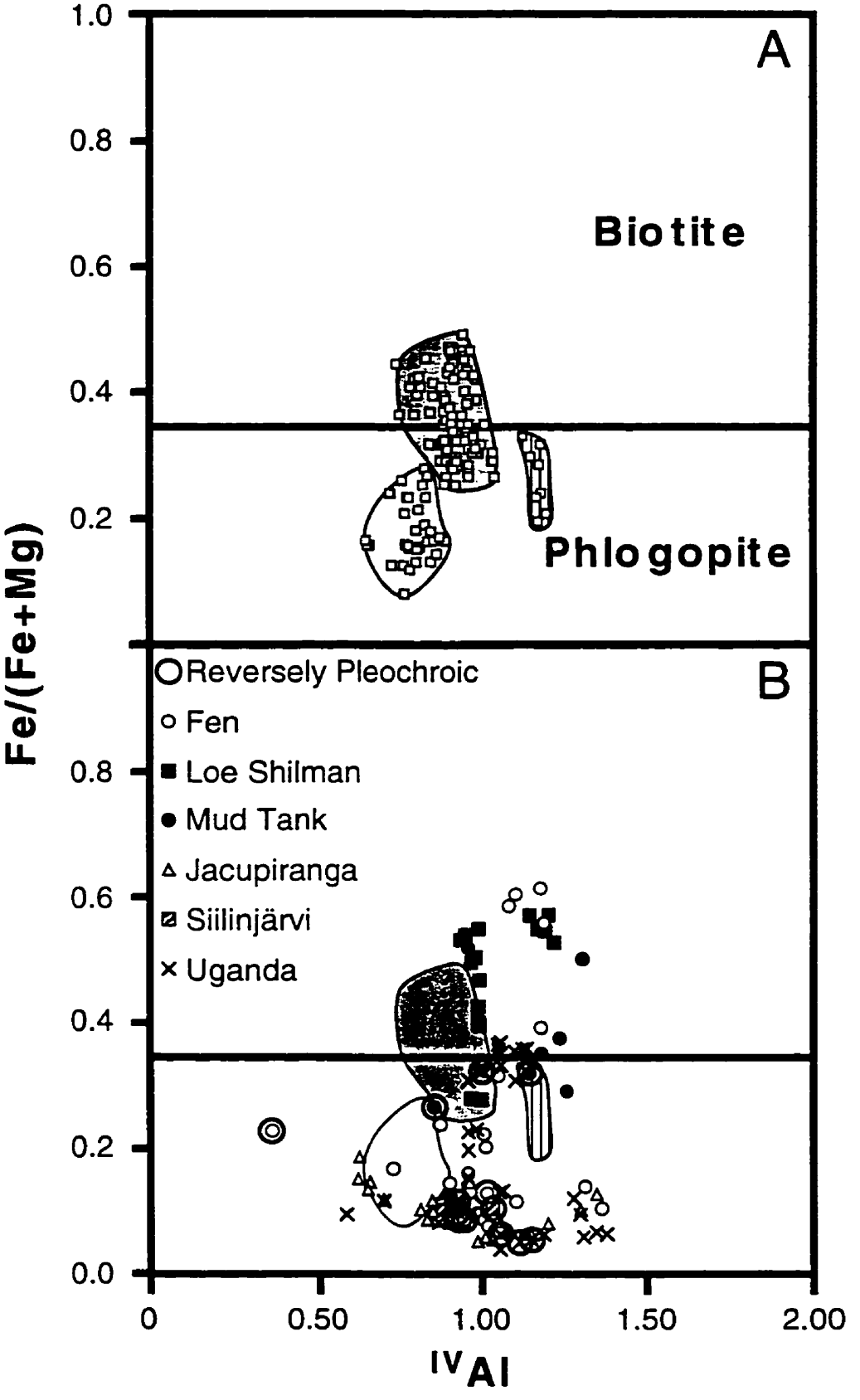
A
Biotite
Phlogopite
B
Reversely Pleochroic
Fen
Loe Shilman
Mud Tank
Jacupiranga
Siilinjärvi
Uganda
Fe/(Fe+Mg)
1.0
0.8
0.6
0.4
0.2
0.8
0.6
0.4
0.2
0.0
0
0.50
1.00
1.50
2.00
IVAl

with pleochroism, although Viladkar & Wimmenauer (1992) noted the presence of reversely pleochroic mica.

In general, mica in glimmerite at Amba Dongar, especially reversely pleochroic phlogopite, contains less ^{IV}Al at an equivalent Fe/(Fe+Mg) (Fe#) than reversely pleochroic phlogopite from other complexes. This difference is only possible if more Fe^{3+} is present in the tetrahedral site. This enrichment in Fe (or apparent depletion in Mg) may result from the presence of minute inclusions of hematite along the cleavage (Chapter 3).

Feldspar

The anhedral feldspar is fine grained in the "ultrafenite" and the groundmass of the alkaline volcanic rocks (fenitized or not), but not in fenites formed at the expense of Bagh sandstone and the alkaline plutonic rocks and related veins. In fenitized sandstone, feldspar occurs as a more potassic or sodic feldspar rim on grains of quartz and earlier formed feldspars. Fenites formed at the expense of Bagh sandstone contain microcline (± minor albite) or, rarely, orthoclase. The presence of microcline and its degree of order (t_1O value of 0.66 to 0.89 inferred from XRD data) indicate partial equilibration at a low temperature (below 450°C; Table 3), and thus, provides a way of distinguishing them from the other fenites.

In the "ultrafenite", fine-grained disordered sanidine and albite (along with <10 vol.% quartz as determined by XRD) are both present in the light bands, whereas only the dominant type of feldspar in the light bands is present in the dark bands. Unfortunately, an increase in Ba in the feldspar structure is accompanied by an increase in Al, which increases the apparent disorder of the Al-Si sites. Consequently, no temperature information can be gleaned from the apparent disorder in the feldspar in cases where the Ba content is above trace levels.

Alkaline volcanic rocks also contain sanidine ($2t_1$=0.31), whereas fenitized tephrite contains relict phenocrysts composed of sanidine rimmed by analcime. In alkaline plutonic rocks, a fine-scale perthitic intergrowth or separate grains of orthoclase ± albite are present. In contrast, albite and two types of orthoclase are present in the syenite veins that cut these rocks (identified by SEM examination). The feldspar assemblage records a rapid quench and incomplete low-temperature recrystallization, whereas the disordered sanidine in the

Table 3. Composition, cell parameters and degree of Al-Si order in feldspar.

Unit	Sample	Description	Felsic Mineralogy	N_{Or} or N_{Ab}	Other Comments
Syenite	66D	Pink felsic	Ab + 2 Or (low sanidine)	0.95; 0.30	Perthite; Sanidine is disordered
				1.00	Presence suggests high temperature
		Wall-rock	Sanidine		More disordered in wall-rock
Fenitized nephelinite	66K	Matrix	Sanidine + Mica	0.96	$t_1O=t_1m=0.31$
	1205/Vil/A	White core	Sanidine	0.92	$t_1O=0.30$
		Pink rim	Sanidine + Analcime		$t_1O=0.30$
Fenitized sandstone	35/Vil/A		Microcline + Or		
	288/Vil/A	Pink	Ab + Microcline		$t_1O=1.00$; $t_1O=0.89$
					Unmixing of a single feldspar
		Grey	Microcline + Qtz ± Ab		$t_1O=0.91$
	397/Vil/A		Or ± Ab		$2t_1=0.66$; more potassic Or
	659/Vil/A	Dark rim	Microcline + Qtz	0.97	
		Light core	Ab + Qtz		
"Ultrafenite"	43B	Dark	Ab + Qtz	0.97	>550°C
		Light	Ab + Qtz ± trace K-feldspar	0.96	>550°C
	66F	Black	Ab + Qtz ± trace K-feldspar	0.99	>550°C
		Green near vein	2 Or + Ab		>550°C; 1 feldspar is sanidine
	66I	Light green	Sanidine + 10% Qtz ± Ab	0.75	$2t_1=0.56$ for sanidine; >550°C
		Dark	Sanidine + 10% Qtz	0.80	$2t_1=0.57$; more potassic; >550°C

N.B. In sanidine: $t_1= 0.25$; in microcline $t_1O=1.00$
Qtz = quartz; Or=orthoclase; Ab= albite

adjacent wall-rock is indicative of a high-temperature fenitization event prior to veining.

Electron-microprobe data show that K-feldspar (Or_{72-95}) may contain significant Ba (up to 5.71 wt.% BaO) and minor Fe, Sr and Ca (up to 1.49 wt.% Fe_2O_3, 0.95 wt.% SrO and 0.14 wt.% CaO; Table 4; Appendix A-5). Albite is almost of end-member composition (Ab_{95-98}), and contains much less Fe, Ca, Ba and Sr than the K-feldspar (Table 4; Appendix A-5; Fig. 8). The highest Ba, Sr, Fe and Al contents are present in fine-grained bright cores or zones in the rim of K-feldspar (as observed in back-scatter SEM mode) from sodic fenites formed at the expense of Bagh sandstone and in the "ultrafenite". Correlation of the high Ba content with Al indicates a significant celsian component. Disseminated hematite in K-feldspar is considered to result from exsolution of Fe from feldspar during recrystallization in the presence of metasomatic fluids. The near end-member composition of the feldspars and enrichment in Ba (Smith, 1975), as well as the presence of hematite are consistent with a metasomatic origin. The XRD and compositional variation of these feldspars will be discussed in detail by Martin et al. (in prep.).

The compositional variation of feldspar in fenites formed at the expense of Bagh sandstone is comparable to that noted by Viladkar (1986), except that this feldspar contains slightly less Ca (Fig. 8). Where Viladkar (1986) observed three compositionally distinct types of K-feldspar (I-III), only end-member Ab and a solid solution of Or toward Ab were distinguished in the present study. Viladkar (1986) related his three types of K-feldspar to the type of aegirine-augite. The high-temperature assemblage contains microperthite (K-feldspar - Or>87) and Di-rich pyroxene, while the low-temperature assemblage contains orthoclase (Or>90; Or>94 in the orthoclase-rich rocks or orthoclasites) and aegirine. The Or content of K-feldspar of his high-temperature fenites, determined by electron microprobe, are the same as those from the alkaline plutonic rocks and "ultrafenite" described in this study.

Experimental studies, especially those that simulate metasomatic processes (at low pressure and relatively high temperature), of ion-exchange equilibria between an alkali feldspar and a solution have shown that alkali feldspar crystallizing from a hydrothermal solution is consistently more potassic than the solution itself, especially at low temperature (Orville, 1963; Fournier, 1976; Lagache & Weisbrod, 1977; Lagache, 1984). At an increased temperature (pressure produces only a slight effect), the alkali feldspar is more

Table 4. Selected electron-microprobe analyses of feldspar and calculated mineral formulae.

Feldspar	Albite	K-feldspar							
Sample #	87/A/94	66L	66I	66J1	1205/Vil/A		66L	66I	
Description	dark	dark		dark	core	light	light	core	light
SiO_2	67.87	68.42	68.25	63.74	64.73	63.53	64.29	63.95	64.06
Al_2O_3	18.89	19.76	19.59	18.65	16.99	16.75	18.39	19.13	19.13
P_2O_5	0.00	0.00	0.00	0.00	0.00	0.00	0.00	0.00	0.00
TiO_2	0.00	0.00	0.00	0.02	0.00	0.07	0.00	0.04	0.06
Fe_2O_3	0.61	0.04	0.05	0.42	0.29	1.45	0.01	0.11	0.08
MnO	0.00	0.00	0.01	0.00	0.00	0.01	0.00	0.02	0.00
CaO	0.05	0.06	0.04	0.00	0.00	0.00	0.00	0.00	0.00
MgO	0.01	0.00	0.00	0.00	0.00	0.00	0.00	0.02	0.00
BaO	0.04	0.02	0.11	1.01	0.23	2.23	0.03	1.37	1.64
SrO	0.23	0.20	0.24	0.28	0.23	0.30	0.22	0.32	0.38
K_2O	0.23	0.10	0.69	13.99	15.70	15.15	14.42	12.01	12.44
Na_2O	11.27	11.56	11.28	1.34	0.86	0.69	1.20	2.68	2.38
Total	99.20	100.18	100.28	100.19	99.86	100.97	99.33	100.28	100.83

Table 4. Selected electron-microprobe analyses of feldspar and calculated mineral formulae (continued).*

Feldspar	Albite	K-feldspar							
Sample #	87/A/94	66L	66I	66J1	1205/Vil/A		66L	66I	
Description	dark	dark		dark	core	light	light	core	light
Si	2.969	2.957	2.957	2.969	3.030	2.993	2.997	2.958	2.958
Al	1.025	1.060	1.053	1.024	0.938	0.930	1.011	1.043	1.042
P	0.000	0.000	0.000	0.000	0.000	0.000	0.000	0.000	0.000
Ti	0.000	0.000	0.000	0.001	0.000	0.002	0.000	0.001	0.002
Fe^{3+}	0.020	0.001	0.002	0.015	0.010	0.051	0.000	0.004	0.003
Mn	0.000	0.000	0.000	0.000	0.000	0.000	0.000	0.001	0.000
Ca	0.002	0.003	0.002	0.000	0.000	0.000	0.000	0.000	0.000
Mg	0.001	0.000	0.000	0.000	0.000	0.000	0.000	0.001	0.000
Ba	0.001	0.000	0.002	0.018	0.004	0.041	0.001	0.025	0.030
Sr	0.006	0.005	0.006	0.008	0.006	0.008	0.006	0.009	0.010
K	0.014	0.006	0.040	0.831	0.938	0.911	0.858	0.709	0.733
Na	0.956	0.968	0.948	0.121	0.078	0.063	0.109	0.240	0.213
Total	4.993	5.000	5.009	4.987	5.004	5.001	4.981	4.991	4.991
Mol.%									
Albite	95.56	96.82	94.76	12.07	7.81	6.31	10.88	24.01	21.32
Orthoclase	1.37	0.57	4.02	83.13	93.75	91.07	85.78	70.89	73.31
Anorthite	0.22	0.29	0.19	0.01	0.00	0.00	0.00	0.00	0.00
Celsian	0.07	0.04	0.18	1.84	0.42	4.12	0.05	2.48	2.97
Sr feldspar	0.59	0.51	0.59	0.76	0.63	0.83	0.60	0.87	1.02

*Mineral formulae calculated based on 8 anions.

Figure 8. Compositional variation in feldspar from the various rock types of the complex. Albite and orthoclase plot near their end-member compositions. Both contain little anorthite component. The larger compositional variation of orthoclase is because it occurs in many more rock types. The orthoclase data from the present study cannot be differentiated into the three distinct groups of K-feldspar (I, II, III) noted by Viladkar (1986) strictly from electron-microprobe analyses.

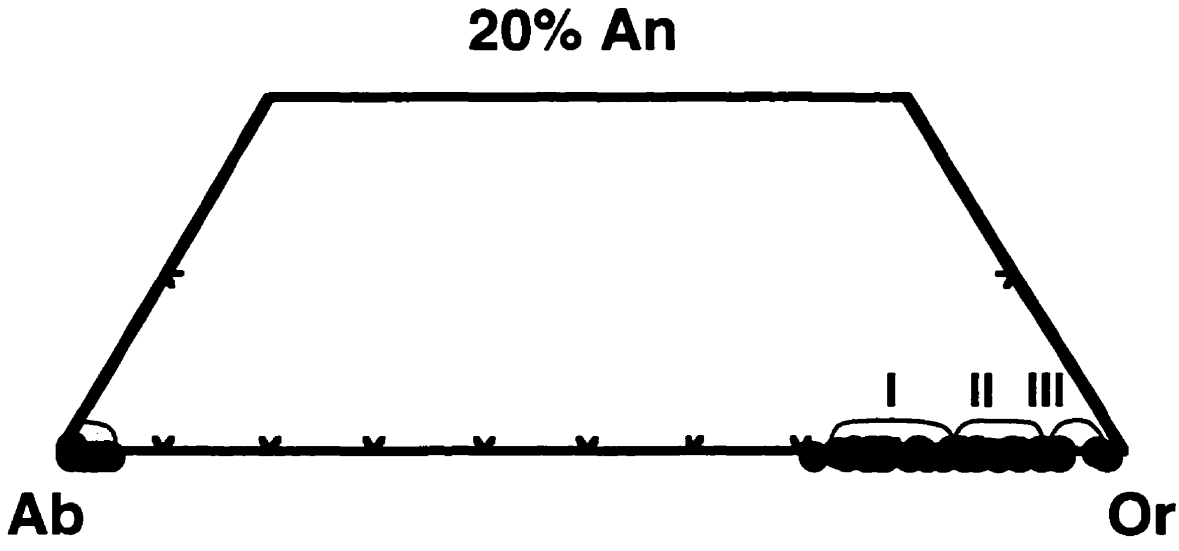
20% An
I
II
III
Ab
Or

sodic. Iiyama (1965) and Lagache (1984) suggested that solutions rich in CO_3^{2-} and F^- produce a more potassic feldspar than those rich in Cl^- owing to the difference in the degree of dissociation of the electrolyte solution. The presence of higher temperature more potassic feldspars and the relative abundance of CO_3^{2-} from the carbonatite would produce more potassic feldspars as observed in this study. In natural systems, a single fluid, at different temperatures, could produce all the compositional variation (both sodic and potassic) resulting from fenitization observed in feldspar from the Amba Dongar complex.

Phosphates

Apatite is present as fine to medium grains in glimmerite, especially near calciocarbonatite veins, and in alkaline volcanic and plutonic rocks and melteigite. Back-scatter electron SEM images show that the fluorapatite grains from alkaline volcanic and plutonic rocks and calciocarbonatite veins consist of a multiply resorbed core surrounded by an unzoned 5-10 μm rim (Fig. 9A). The compositions of the fluorapatite fall in two groups: 1) a relatively Sr- (approx. 0.5 wt.% SrO), REE-, F- and Na-poor core, and 2) a Sr-rich (approx. 0.8 wt.% SrO), and REE-, F- and Na-enriched rim (Table 5; Appendix A-6; Figs. 9B, C). In both groups, minor amounts (<0.5 wt.%) of LREE and Si are present, whereas Mn, S and Cl are below the limit of detection. The LREE contents are the same as those noted by Liu and Comodi (1993) for equivalent rocks. Darker portions of first group (the core) have lower analytical totals, which suggests that they are carbonate-bearing. This two-stage zonation corresponds to that noted above for aegirine-augite and mica, where the core has formed during magmatic crystallization, and the rim, during an episode of metasomatism. Compositionally, the apatite is similar to that described by Viladkar & Wimmenauer (1992), also from Amba Dongar, except that the apatite that they described contains slightly more Ce. Furthermore, no such complex zonation was described. In this study, the inferred presence of carbonate apatite, Sr:Mn > 50:1 and lower F content in the core of the apatite grains imply crystallization of the core from a carbonatitic magma. By implication, therefore, the rim was deposited during fenitization.

This two-stage zonation of apatite is the same as observed in other carbonatite complexes, such as at: Bayan Obo, China (Le Bas et al., 1992), Perry and Conway Counties, Arkansas (McCormick & Heathcote, 1987), near Gatineau, Québec (Hogarth et

Figure 9. Two-stage zonation of apatite from the alkaline volcanic and plutonic rocks.

A. Back-scatter SEM image of apatite from nephelinite showing the complicated zonation in the core (related to resorption) and surrounded by a distinctly brighter approximately 5 μm rim. Lighter regions in this photograph contain elements of higher atomic number. The complicated zonation in the core implies numerous stages of resorption.

B. Compositional variation of apatite in a ΣLa+Ce+Nd versus Sr plot. Two different groups of apatite are observed; the rims are enriched in Sr and REE and the cores are poor in Sr and REE.

C. Na versus Sr plot, showing the same relationship as B.

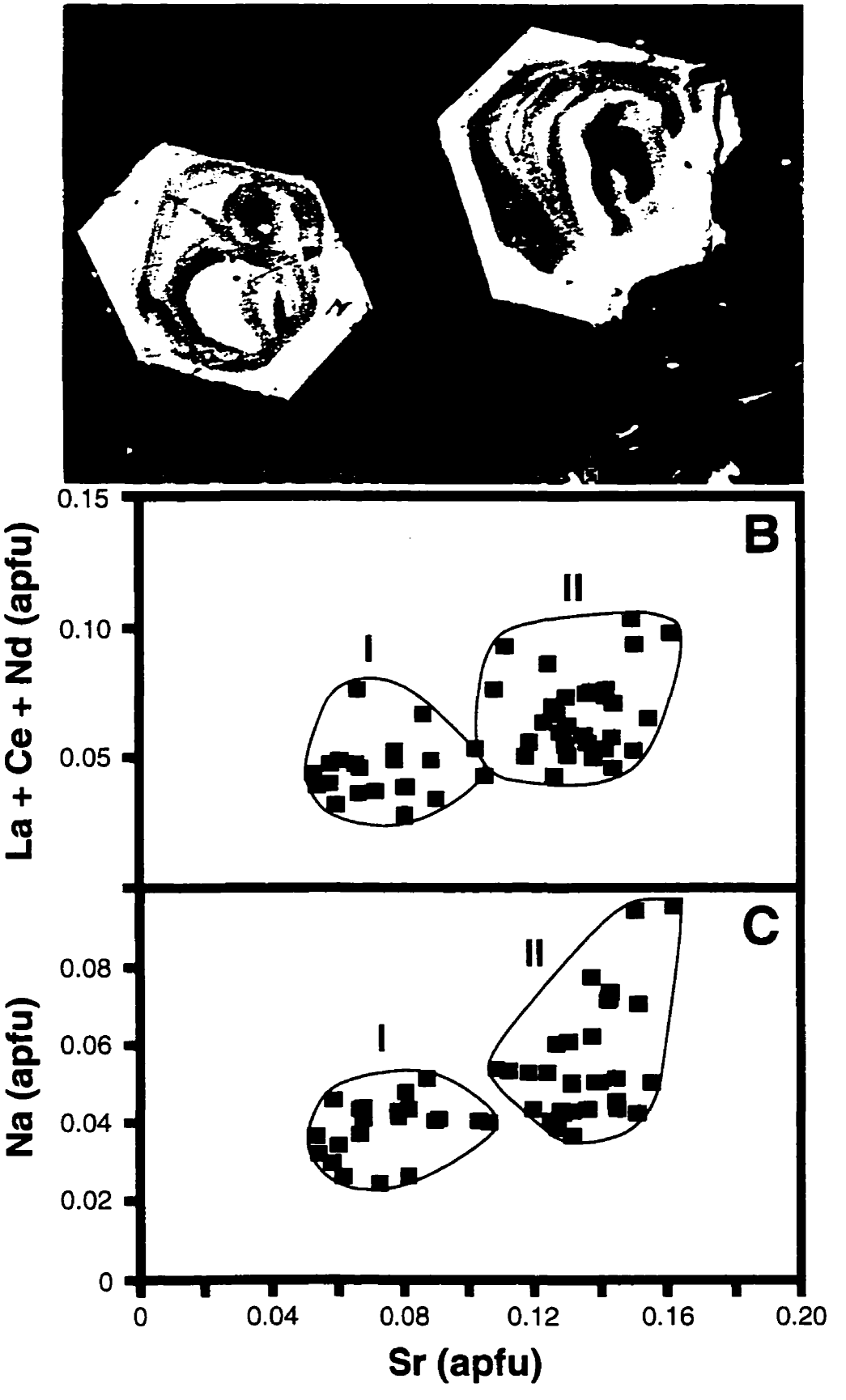
B
C
I
II
I
II
La + Ce + Nd (apfu)
Na (apfu)
Sr (apfu)
0.15
0.10
0.05
0.08
0.06
0.04
0.02
0
0
0.04
0.08
0.12
0.16
0.20

Table 5. Selected apatite and britholite electron-microprobe analyses and calculated formulae.

Mineral	Apatite[1]									Britholite[2]
Sample #	43E	66A1						66B		41E
Description	mid	v.lt	med.	v.dark	mid.	edge	dk	top mid.	mid. lt	
CaO	55.21	54.67	55.14	56.43	55.56	54.43	56.80	56.42	54.44	15.24
Na_2O	0.18	0.12	0.11	0.08	0.12	0.18	0.10	0.13	0.28	n.d.
La_2O_3	0.32	0.41	0.30	0.13	0.13	0.25	0.17	0.14	0.49	17.58
Ce_2O_3	0.60	0.73	0.49	0.22	0.31	0.43	0.31	0.28	0.80	28.97
Nd_2O_3	0.18	0.20	0.15	0.08	0.13	0.18	0.16	0.13	0.27	n.d.
SrO	1.28	1.25	1.32	0.83	0.67	1.30	0.56	0.93	1.63	n.d.
P_2O_5	40.23	40.30	41.40	40.59	41.47	40.44	40.03	40.98	39.79	9.68
SO_4	0.00	0.00	0.00	0.04	0.03	0.02	0.04	0.01	0.03	n.d.
SiO_2	0.23	0.42	0.20	0.25	0.32	0.22	0.32	0.12	0.21	28.53
F	3.76	2.28	2.42	2.37	2.34	2.59	2.33	2.82	3.35	n.d.
Cl	0.01	0.00	0.00	0.00	0.01	0.00	0.01	0.00	0.00	n.d.
H_2O	0.00	0.65	0.59	0.64	0.63	0.49	0.67	0.43	0.15	n.d.
Total	102.00	101.03	102.12	101.66	101.71	100.52	101.48	102.39	101.44	100.00
O=F,Cl	1.59	0.96	1.02	1.00	0.99	1.09	0.98	1.19	1.41	
Total	100.42	100.07	101.10	100.66	100.73	99.43	100.50	101.20	100.03	100.00

Table 5. Selected apatite and britholite electron-microprobe analyses and calculated formulae (continued).*

Mineral	Apatite[1]									Britholite[2]
Sample #	43E	66A1						66B		41E
Description	mid	v.lt	med.	v.dark	mid	edge	dk	top mid	mid lt	
Ca	9.754	9.759	9.781	9.870	9.862	9.764	9.880	9.840	9.659	4.885
Na	0.058	0.039	0.035	0.025	0.040	0.058	0.031	0.039	0.091	
La	0.019	0.025	0.018	0.008	0.008	0.016	0.010	0.009	0.030	1.941
Ce	0.036	0.045	0.030	0.013	0.019	0.026	0.018	0.017	0.048	3.174
Nd	0.011	0.012	0.009	0.005	0.007	0.010	0.009	0.007	0.016	
Sr	0.122	0.121	0.127	0.079	0.065	0.126	0.052	0.088	0.156	
P	5.616	5.684	5.802	5.609	5.817	5.731	5.501	5.647	5.578	2.466
S	0.000	0.000	0.000	0.004	0.003	0.003	0.004	0.001	0.003	
Si	0.038	0.070	0.033	0.041	0.054	0.037	0.052	0.019	0.035	8.533
F	1.961	1.201	1.267	1.224	1.225	1.372	1.196	1.452	1.754	
Cl	0.003	0.000	0.000	0.000	0.002	0.000	0.003	0.000	0.000	
OH	0.000	0.721	0.655	0.697	0.694	0.550	0.722	0.470	0.168	
Σ REE	0.07	0.08	0.06	0.03	0.03	0.05	0.04	0.03	0.09	5.12
XF	0.98	0.60	0.63	0.61	0.61	0.69	0.60	0.73	0.88	
XCl	0.00	0.00	0.00	0.00	0.00	0.00	0.00	0.00	0.00	
XOH	0.00	0.36	0.33	0.35	0.35	0.27	0.36	0.23	0.08	

[1] Apatite analyses determined by WDS.

[2] Determined by EDS analysis, calculated assuming that the sum is 100.00 and based on 10 cations.

*Structural formula calculated based on Ca+Na+La+Ce+Nd+Sr = 10 and assuming F+Cl+OH=2, except for britholite; XF=F/(F+Cl+OH); XCl=Cl/(F+Cl+OH); XOH=OH/(F+Cl+OH)

lt=light; dk=dark; v=very; mid.=middle; n.d.=not detected.

al., 1985), Blackburn, Ontario (Hogarth et al., 1988) and Fen, Norway (Andersen, 1986). Magmatic crystallization followed by metasomatism, also proposed by Le Bas et al. (1992) and McCormick & Heathcote (1987), results in enrichment of the rim in Sr, REE and F. Not all of their compositional variations between the core and rim are identical to those noted in the Amba Dongar complex; for example, no covariance was observed by them among levels of Sr, REE and Na. In addition, F shows a greater variation at the expense of Cl and OH, than that of Sr, REE and Na.

Britholite (identified by EDS with 5.12 apfu LREE, Table 5) is associated with hematite ± calcite in late, <1 mm wide veinlets that cross-cut "ultrafenite" and earlier veins (Fig. 3C). Its presence indicates that the fluid from which it formed appears to have been more enriched in the LREE and Si. The most likely source for this REE and Fe is the late ferrocarbonatite, as it is the carbonatite that is the most enriched in these elements (for discussion of the compositional variation see below; Viladkar & Wimmenauer, 1992).

Other minerals

Titanite phenocrysts (up to 5 vol.%) in the alkaline volcanic and plutonic rocks form uncommon twinned, euhedral grains (Fig. 2A) that are unusually rich in Nb (up to 4.62 wt.% Nb_2O_5), contain major Fe and minor amounts of Al, V, Zr and Na (2.08 wt.% Fe_2O_3, 0.76 wt.% Al_2O_3, 0.36 wt.% V_2O_3, 0.21 wt.% ZrO_2 and 0.13 wt.% Na_2O, on average), but very low K and undetectable F (Table 6; Appendix A-7). In back-scatter SEM images, the brightest regions of the zoned crystals are enriched in Nb, but depleted in Ti and V, as has also been noted for titanite, in general, by Paterson & Stephens (1992).

Andradite is more common than titanite in alkaline volcanic and plutonic rocks (Fig. 2A), as euhedral grains with a dark brown core and a lighter rim. It also forms rare oscillatory zoned grains. Fenites formed at the expense of these rocks contain rare garnet and wollastonite in the Ca-rich cores of the aegirine-augite veins (Fig. 10).

Electron-microprobe analyses show that the garnet varies from titanian andradite to melanite, and nearly to schorlomite (max. 16.8 wt.% TiO_2; classification of Deer et al., 1982; Table 6; Appendix A-8). All varieties contain, on average, 1.5, 0.6, 0.5, 0.4 and 0.3 wt.% of Al_2O_3, MnO, ZrO_2, MgO and V_2O_3, respectively (Table 6). The observed zonation in garnet from the alkaline volcanic and plutonic rocks is the result of an increase in Ti, Zr,

Table 6. Selected garnet and titanite electron-microprobe analyses and calculated mineral formulae.

Mineral	Garnet[1]						Titanite[2]		
Sample #	37A		1205/Vil/A		22B		37A		66J1
Description	middle	edge	darker	lighter	edge	middle	dark	light	
SiO_2	31.54	31.58	34.4	30.44	29.29	27.17	30.75	30.37	30.99
Al_2O_3	1.26	1.27	3.37	1.48	1.62	1.9	0.79	0.71	0.46
TiO_2	8.23	8.32	2.22	5.76	11.86	16.51	34.18	33.19	35.88
ZrO_2	0.48	0.46	0.12	0.23	0.54	0.82	0.32	0.40	0.03
Nb_2O_5	n.d.	n.d.	n.d.	n.d.	n.d.	n.d.	2.52	4.62	1.26
Cr_2O_3	0	0.03	0.02	0	0.01	0.01	n.d.	n.d.	n.d.
V_2O_3	0.32	0.31	0.26	0.17	0.29	0.22	0.40	0.30	0.36
Fe_2O_3	21.89	21.41	25.42	27.56	21.68	16.56	2.81	2.57	2.51
FeO	3.49	3.49	0	0	2.04	3.97	n.d.	n.d.	n.d.
MgO	0.51	0.49	0.46	0.25	0.25	0.27	0.01	0.01	0.00
MnO	0.31	0.32	0.55	0.53	0.97	1.28	0.02	0.01	0.02
CaO	31.87	31.97	33.07	32.78	32.77	32.23	27.88	27.37	28.22
Na_2O	n.d.	n.d.	n.d.	n.d.	n.d.	n.d.	0.11	0.22	0.13
K_2O	n.d.	n.d.	n.d.	n.d.	n.d.	n.d.	0.01	0.02	0.02
F	n.d.	n.d.	n.d.	n.d.	n.d.	n.d.	0.00	0.00	0.00
Total	99.90	99.64	99.89	99.20	101.32	100.94	99.80	99.79	99.88

Table 6. Selected garnet and titanite electron-microprobe analyses and calculated mineral formulae (continued).

Mineral	Garnet[1]						Titanite[2]		
Sample #	37A		1205/Vil/A		22B		37A		66J1
Description	middle	edge	darker	lighter	edge	middle	dark	light	
Si	2.680	2.688	2.864	2.601	2.456	2.291	2.000	2.000	2.000
^{IV}Al	0.126	0.127	0.136	0.149	0.160	0.189	n.a.	n.a.	n.a.
$^{IV}Fe^{3+}$	0.190	0.180	0.000	0.250	0.380	0.520	n.a.	n.a.	n.a.
^{VI}Al	0.000	0.000	0.195	0.000	0.000	0.000	0.060	0.060	0.040
Ti	0.526	0.532	0.139	0.370	0.748	1.047	1.670	1.640	1.740
Zr	0.020	0.019	0.005	0.010	0.022	0.034	0.010	0.010	0.000
Nb	n.d.	n.d.	n.d.	n.d.	n.d.	n.d.	0.070	0.140	0.040
Cr	0.000	0.002	0.001	0.000	0.001	0.001	n.a.	n.a.	n.a.
V	0.022	0.021	0.017	0.012	0.020	0.015	0.020	0.020	0.020
$^{VI}Fe^{3+}$	1.210	1.191	1.592	1.522	0.988	0.531	0.140	0.130	0.120
Fe^{2+}	0.230	0.240	0.000	0.000	0.140	0.280	n.a.	n.a.	n.a.
Mn	n.a.	n.a.	n.a.	n.a.	n.a.	n.a.	0.010	0.000	0.000
Mg	n.a.	n.a.	n.a.	n.a.	n.a.	n.a.	0.000	0.000	0.000
Fe^{2+}	0.020	0.010	0.000	0.000	0.000	0.000	n.a.	n.a.	n.a.
Mn	0.037	0.035	0.032	0.018	0.018	0.019	n.a.	n.a.	n.a.
Mg	0.039	0.041	0.068	0.068	0.121	0.161	n.a.	n.a.	n.a.
Ca	2.902	2.915	2.950	3.001	2.944	2.912	1.940	1.930	1.950
Na	n.a.	n.a.	n.a.	n.a.	n.a.	n.a.	0.010	0.030	0.020
K	n.a.	n.a.	n.a.	n.a.	n.a.	n.a.	0.000	0.000	0.000
F	n.a.	n.a.	n.a.	n.a.	n.a.	n.a.	0.000	0.000	0.000
Charge Deficiency	0.00	0.00	0.04	0.11	0.00	0.00			

[1] Garnet formulae calculated based on 8 cations and 12 anions and assuming only Ti^{4+} is present.

[2] Titanite formulae calculated based on 2 Si and assuming that all Fe is Fe^{3+}.

lt. = light; n.d.=not detected; n.a.=not analyzed.

Figure 10. Titanian andradite (gt) and wollastonite (wo) present in the core of an aegirine-augite rich vein in fenitized nephelinite (width of image = 2 mm).

gt
gt
gt

Al, Fe^{3+} and Mn, and a decrease of V and Fe^{2+} in the dark cores compared to the lighter rims. Their compositions are the same as the garnets defined by Gwalani (pers. comm.) that contain slightly more Al from nephelinite, tephrite and phonotephrite of this complex.

Melanite from the veins consists of a brown, Ti- (up to 5.76 wt.% TiO_2) and Zr-rich (up to 0.5 wt.% ZrO_2) core with a honey yellow titanian andradite rim. This rim exhibits a weak anomalous birefringence, has lower totals and contains less Al and Zr, but more Si and Fe^{3+}. The first two attributes of the titanian andradite indicate the presence of up to 0.60 wt.% H^+.

Titanian andradite, with significantly higher levels of OH, F and Zr than measured in the present study, has been reported from other carbonatitic-alkaline complexes (Deer et al., 1982; Flohr & Ross, 1989). Ulrych et al. (1994) described similar examples of melanite from melilitic rocks (Oseçná complex, Bohemia), which have a dark Zr-rich core of melanite with overgrowths of weakly birefringent, pale yellow, (OH,F)-bearing, Zr-poor and Al-rich titanian andradite. Whereas they attributed the origin of melanite to incipient metasomatism, and the yellow andradite, to an advanced stage of this process, andradite can also be magmatic in origin. The common occurrence of brown, euhedral, zoned melanite garnet in the relatively unmetasomatized volcanic and plutonic rocks noted in the present study indicates a magmatic origin with a fO_2 slightly above NNO (Huggins et al., 1977; Kühberger et al., 1989). Flohr & Ross (1989) described four different types of garnet from ijolite xenoliths from the Diamond Jo quarry, Arkansas. Three of these are primary in origin, while the fourth, the most hydrous and fluorine-enriched, forms a metasomatic overgrowth, produced by F-rich metasomatic fluids, on melanite. In the same manner, the brown to yellow titanian andradite (possibly hydrous), now in association with hematite and wollastonite located at the cores of aegirine-augite veins in fenitized nephelinite at Amba Dongar, are metasomatic in origin. The zonation scheme of the garnets from the veins is the same as that of melilitic rocks documented by Ulrych et al. (1994) from Bohemia, where garnets were suggested to have crystallized from a Si-poor, F-enriched, low-temperature fluid with an initially low, but increasing fO_2. Moreover, the presence of aegirine-augite, garnet and wollastonite in these veins indicates that the metasomatic fluid contained significant Fe^{3+}, Ca, Na and Mg. The results of the study of Huckenholz & Yoder (1969) on the stability of andradite implies that the assemblage hematite - wollastonite is unstable

below approximately 1137°C, thus the assemblage in the Amba Dongar complex does not represent an equilibrium assemblage at the lower temperature assumed for metasomatism.

Hsu (1980) suggested, from experimental work, that the occurrence of hydrogarnet (hydrogrossular or hydroandradite) may be used as a temperature indicator, as its maximum temperature of formation is at or below 420°C. By inference, the presence of hydrous andradite in the Amba Dongar complex implies a temperature of less than 420°C for the final stages of crystallization in the aegirine-augite vein.

Prismatic wollastonite also is common as euhedral to subhedral grains in ijolite, where it coexists with garnet, aegirine-augite and nepheline. Wollastonite is near the end-member in composition, with traces of Fe, Mn, Mg and Na (Table 7; Appendix A-9). Enrichments of Fe and Mn along cleavages and grain boundaries reflect the presence of other pyroxenoids (e.g., bustamite and ferrobustamite), which may have been produced by alteration.

Most of the prismatic and unaltered wollastonite in the alkaline volcanic and plutonic rocks of the Amba Dongar complex is interpreted to be magmatic in origin. Peterson (1989) suggested that the appearance of wollastonite in nephelinite originated by diopside fractionation from a low-Mg nephelinite to produce Mg-depleted, Ca-bearing magma. Dawson et al. (1995) used this interpretation to explain the rare association of pyroxene and wollastonite in igneous xenoliths from Oldoinyo Lengai. Platt & Edgar (1972) proposed that wollastonite phonolite is the product of fractional crystallization of melilite nephelinite and, thus, that wollastonite melilite gives way to wollastonite phonolite. Such an evolution, though possible, is unlikely in the complex, because of the habit of wollastonite and lack of any replacement textures. Its presence in ijolite and urtite from carbonatitic-alkaline complexes has been attributed by Peterson (1989) to Ca-fenitization by a carbonatite. His hypothesis would only be valid, in alkaline rocks from this complex, if Ca-metasomatism occurred prior to intrusion of the alkaline volcanic or plutonic rocks. Only an isotopic investigation of alkaline volcanic and plutonic rocks could resolve this question.

Nepheline forms euhedral phenocrysts or anhedral interstitial grains in alkaline volcanic and plutonic rocks, respectively. The phenocrysts are bluish green owing to replacement, mainly by analcime, but also by calcite, kaolinite, or possibly, cancrinite. A

Table 7A. Selected analcime, wollastonite and carbonate analyses and mineral formulae.

Mineral	Analcime[1]		Wollastonite[2]		Calcite[3]	Ankerite[3]		
Sample #	66J2	22B	1205/Vil/A	66J2	BH/18/2.1	BH/18/2.2		BH/4/2
Description				center	core	fibrous	fibrous	
SiO_2	46.45	46.91	51.46	50.72	0.00	0.00	0.00	0.01
Al_2O_3	29.63	28.84	0.01	0.01	0.14	0.27	0.28	0.36
TiO_2	0.00	0.05	0.00	0.00	0.33	0.00	0.17	0.02
P_2O_5	n.d.	n.d.	0.38	0.40	n.d.	n.d.	n.d.	n.d.
Fe_2O_3	n.d.	n.d.	0.21	0.69	n.d.	n.d.	n.d.	n.d.
FeO	0.31	0.66	0.58	0.00	1.95	8.24	7.12	11.83
Cr_2O_3	n.d.	n.d.	n.d.	n.d.	0.01	0.01	0.00	0.20
MnO	0.01	0.01	0.67	0.60	0.00	1.55	1.62	3.19
MgO	0.03	0.01	0.16	0.05	0.27	37.74	36.96	31.31
CaO	0.34	1.31	46.88	47.44	93.96	52.20	52.53	50.66
BaO	0.01	0.04	0.52	0.26	0.24	n.d.	0.00	0.19
SrO	0.14	0.17	0.01	0.01	3.11	n.d.	1.31	n.d.
Na_2O	14.62	14.64	0.03	0.00	0.00	0.00	0.00	2.24
K_2O	0.07	0.04	0.03	0.02	n.d.	n.d.	n.d.	n.d.
Total	91.61	92.68	100.94	100.20	100.00	100.00	100.00	100.00

Table 7A. Selected analcime, wollastonite and carbonate analyses and mineral formulae (continued).

Mineral	Analcime[1]		Wollastonite[2]		Calcite[3]	Ankerite[3]		
Sample #	66J2	22B	1205/Vil/A	66J2	BH/18/2.1	BH/18/2.2		BH/4/2
Description				center	core	fibrous	fibrous	
Si	1.390	1.810	1.980	1.970	0.000	0.000	0.000	0.000
Al	1.310	1.200	0.000	0.000	0.003	0.005	0.006	0.007
Ti	0.000	0.000	0.000	0.000	0.005	0.000	0.002	0.000
P			0.010	0.010				
Fe^{3+}			0.010	0.020				
Fe^{2+}	0.010	0.020	0.020	0.000	0.031	0.114	0.099	0.167
Cr^{3+}					0.000	0.000	0.000	0.003
Mn	0.000	0.000	0.030	0.020	0.000	0.022	0.023	0.046
Mg	0.000	0.000	0.010	0.000	0.008	0.932	0.919	0.787
Ca	0.010	0.000	1.930	1.970	1.917	0.927	0.939	0.916
Ba	0.000	0.000	0.010	0.010	0.002	0.000	0.000	0.001
Sr	0.000	0.000	0.000	0.000	0.034	0.000	0.013	0.000
Na	1.060	1.010	0.000	0.000	0.000	0.000	0.000	0.073
K	0.000	0.000	0.000	0.000				
Σ Cations	3.790	4.040	4.000	4.000	2.000	2.000	2.000	2.000

[1] Analcime formulae calculated based on 6 anions.

[2] Wollastonite formulae calculated based on 4 cations and 12 charges with Fe^{3+}/Fe^{2+} calculated by charge balance.

[3] Calcite and ankerite analyses determined by EDS averaged to 100%.
The cation units were calculated based on 2 cations so that they could be compared.
n.d.=not detected.

Table 7B. Selected sulphide and oxide analyses from EDS analyses.

Mineral	Pyrite	Chalcopyrite
Sample #	66F	
Fe	40.35	29.45
Cu	0.00	30.01
Ti	0.00	0.50
Mn	0.39	0.21
Cr	0.00	0.00
V	0.17	0.00
Si	n.d.	n.d.
S	59.10	39.83
Total	100.00	100.00

Mineral	Hematite			
Sample #	87/A/94		1205/Vil/A	BH/4/2
FeO	91.05	88.38	96.03	96.29
TiO_2	5.85	4.34	2.50	1.31
MnO	1.15	2.55	0.79	0.00
Cr_2O_3	0.12	0.05	0.22	0.08
V_2O_3	0.00	0.87	n.d.	n.d.
SiO_2	1.83	3.81	0.46	2.33
Total	100.00	100.00	100.00	100.00

n.d.=not detected.

dusty pink appearance may be produced by minute inclusions of hematite. Only analcime was observed in XRD patterns of phenocrystic nepheline from volcanic rocks. In thin section, it forms fine-grained, colourless aggregates at the expense of the feldspathoid. Analyses of analcime show that it contains minor amounts of Ca, Fe, Mg, Ba, Sr, K, Ti and Mn (<0.5 wt.% oxide on average; Table 7; Appendix A-9).

Carbonates are found in carbonatites, as late inclusions in mica of glimmerite, and in late veins (± hematite) that cross-cut the glimmerite and "ultrafenite". In calciocarbonatite, the dominant mineral is calcite (>95%). Inclusions of both calcite and ankerite are present in the cleavages of mica in glimmerite. Whereas inclusions of calcite are visible with the naked eye, ankerite inclusions could only be observed by TEM examination (Chapter 3). EDS analyses of both carbonates show that the calcite is near end-member, but ankerite is enriched in Mn (to 2.4 wt.% MnO) and Sr (to 0.3 wt.% SrO) (Table 7; Appendix A-9). This calcite and hematite in the veins could have originated from the recyrstallization of ferrocarbonatite in the presence of later fluids, as suggested for the Fen complex by Andersen (1984, 1989). The paragenesis of the ankerite inclusions indicates a secondary origin, as they originated by the interaction of Mg and Fe (released from breakdown of biotite) with Ca^{2+} and CO_3^{2-} in solution (Chapter 3).

Hematite, the predominant oxide in all rock types, occurs as a pseudomorph after magnetite, in veins with calcite, in "ultrafenite" with aegirine-augite, and in cleavages of mica. It contains minor (<0.5 wt.% oxide) Ti, Mn and Cr (from EDS). In the ferrocarbonatite, it is the product of the pseudomorphic replacement of magnetite related to an increase in fO_2 (Viladkar, 1981). Other oxides and sulphides (determined by reflected light) make up a maximum of 3 vol.% of melteigite veins, fenitized tephrite and "ultrafenite", in the sequence chalcopyrite to pyrite to magnetite and finally hematite. The chalcopyrite-to-pyrite sequence was inferred from the study of sulphides from this locality by Srivastava & Karkare (1989). This sequence in the alkaline volcanic and plutonic rocks, related fenites, and "ultrafenite", reflects an increase in fO_2 or decrease in fS_2.

Barite is present in ferrocarbonatite (Viladkar, 1980; Palmer & Williams-Jones, 1996) or as fine grains in "ultrafenite". It is stable to a high temperature under oxidizing conditions (Segnit & Gelb, 1970; Chabu & Boulègue, 1992). Under reducing conditions, Ba-rich silicates (e.g., feldspar) are formed. Thus, formation of barite in ferrocarbonatite

may be the result of fractional crystallization, a high fO_2 and the lack of sufficient Si and Al for formation of feldspar. Variation in the celsian component of K-feldspar and formation of barite in "ultrafenite" may be related to changes in fO_2, fS_2 and a_{SiO_2}.

Variation in Whole-Rock Compositions

The major-, minor- and trace-element concentrations of the units from the complex are listed in Table 8. The quartzite averages 96.5 wt.% SiO_2, with minor to trace amounts of Fe, Ti, Ca, Al, Na, K and Ba. On the other hand, all samples of carbonatite are enriched in LREE, Mn, Sr, Ba ± Nb, whereas the other alkaline igneous rocks are enriched in Nb and Zr compared to the averages noted by Woolley & Kempe (1989) and Le Bas et al. (1986). The carbonatites can be classified after Woolley & Kempe (1989), as calciocarbonatite or ferrocarbonatite.

The various units in the complex can be subdivided based on mineralogy, texture and the whole-rock composition. In Figure 11A, carbonatite plots in the lower left corner near the contact between the $Na_2O + K_2O$ and SiO_2 axes. Alkaline volcanic and plutonic rocks plot to the right, and fenites, syenite and melteigite veins with "ultrafenite" plot in between. Samples of Bagh sandstone and related fenites exhibit increasing fenitization by a string of data points from the bottom right corner of the figure. The samples of fenitized Bagh sandstone form sodic, potassic and sodi-potassic "trends" on the plot (Fig. 11B). Weakly fenitized alkaline volcanic and plutonic rocks (e.g., 66F) have the same Na and K contents as their unfenitized equivalents. Potassic fenites formed at the expense of Bagh sandstone show a trend of increasing K towards K-feldspar with fenitization (Fig. 11B), while the alkaline volcanic and plutonic rocks, their mildly fenitized equivalents and that of two samples of "ultrafenite" are located in another vertical region (in the igneous rocks this trend is related to the unit) at approximately equal K and Na contents. The third sample of "ultrafenite" is generally enriched in Na, but depleted in K compared to the other two, as it falls in the region where both the alkaline volcanic rocks and the sodic fenite formed at the expense of Bagh sandstone plot in Figure 11B.

Trace-element and REE contents of the rocks vary in the sequence: carbonatite > sodi-potassic fenites derived from the Bagh sandstone > alkaline volcanic and plutonic

Table 8. Whole-rock analyses from the Amba Dongar carbonatitic-alkaline complex.

Sample #	**9**	**37A**	**66K**	**8V**	**66Agr**	**66Jij**
Rock Type	**Nephelinite**	**Nephelinite**	**Fen. teph.**	**Fen. neph.**	**Ijolite**	**Ijolite**
SiO_2	43.31	44.20	53.53	53.59	45.35	49.01
TiO_2	0.96	0.85	0.62	0.18	1.15	1.11
Al_2O_3	13.37	16.05	10.39	13.51	13.79	15.28
Fe_2O_3	6.82	5.07	2.56	3.95	7.02	3.52
FeO	1.36	2.33	4.02	0.98	1.52	2.90
MnO	0.27	0.29	0.35	0.30	0.33	0.26
MgO	1.19	1.40	5.82	1.61	2.47	1.37
CaO	11.98	11.00	10.14	11.64	10.36	13.89
Na_2O	5.93	7.29	3.52	3.02	3.25	3.81
K_2O	1.83	2.02	4.41	7.35	4.93	4.26
P_2O_5	0.38	0.74	0.16	0.29	0.89	0.78
BaO	0.12	0.11	0.04	0.87	0.37	0.20
LOI	11.88	7.90	3.65	2.70	8.27	3.20
Total	99.40	99.25	99.21	99.98	99.70	99.58

Table 8. Whole-rock analyses from the Amba Dongar carbonatitic-alkaline complex (continued).

Sample #	9	37A	66K	8V	66Agr	66Jij
Rock Type	Nephelinite	Nephelinite	Fen. teph.	Fen. neph.	Ijolite	Ijolite
Sc	n.d.	9	3.4	12	10	4
V	89	510	471	0	368	188
Cr	26	10	177	11	39	11
Co	67.9	25.3	18	0.6	17.3	31.1
Ni	16	2	128	13	0	0
Zn	47	302	n.d.	219	355	79
Rb	253.6	138.2	127	231.5	160.4	145.2
Sr	88.7	1109	977	214.7	942.9	465.2
Y	12	23	22	211	20	9
Zr	68.2	265.9	271	4812.9	145.6	714.3
Nb	22.4	161.1	139	752.1	123.5	170.5
Mo	0.7	4	6	2.6	7.7	1
Cs	1	2.9	28	13.1	3.5	1.7
Hf	2.6	4.8	6	81.2	3.3	14.9
Ta	3.56	1.87	12	56.15	1.6	3.63
W	463.2	98.9	63	13.7	49.2	144.3
Pb	26	21	n.d.	35	13	16
Th	19.46	8.79	18	36.24	15.93	6.31
U	1.81	3.67	3.4	8.22	6.15	1.68
La	49	87.2	150	576.1	106.4	44.9
Ce	67.4	167.3	260	979	195.6	68.9
Pr	4.71	18.59	n.d.	85.19	19.78	5.97
Nd	14.7	66.7	87	265.9	66.8	19.2
Sm	3.1	11	10	43.7	9.4	2.6
Eu	0.81	3.28	3.3	4.07	2.82	0.88
Gd	3.4	7.5	n.d.	35.1	5.6	1.7
Tb	0.5	1.1	1.3	6.6	0.8	0.3
Dy	2.3	5.4	n.d.	38.2	3.8	1.5
Ho	0.4	1	n.d.	8	0.7	0.3
Er	1.3	2.6	n.d.	22.9	1.8	1
Tm	0.21	0.43	n.d.	3.8	0.31	0.21
Yb	1.7	3.7	3.25	22.8	2.7	2.1
Lu	0.29	0.66	0.63	3.14	0.55	0.47

ss=sandstone; fen. = fenitized; nep. = nephelinite; tep. = tephrite; ij. = ijolite; pk = pink; gr = green; pg = pegmatitic vein

Table 8. Whole-rock analyses from the Amba Dongar carbonatitic-alkaline complex (continued).

Sample #	66Apk	66Dpk	66Dpg	66Jgr	43A	66F
Rock Type	**Fen. ij.**	**Fen. ij.**	**Syenite**	**Melteigite**	**Ultrafenite**	**Ultrafenite**
SiO_2	43.75	43.81	57.61	39.71	58.43	46.83
TiO_2	1.14	0.85	0.26	0.84	0.21	1.31
Al_2O_3	14.81	16.41	13.99	5.47	6.81	16.48
Fe_2O_3	5.50	4.66	4.56	6.21	0.97	1.76
FeO	2.10	1.60	1.19	9.20	1.51	4.97
MnO	0.27	0.25	0.21	0.41	0.15	0.30
MgO	1.85	2.50	0.52	3.50	6.22	1.91
CaO	15.18	14.13	5.65	20.27	8.62	9.92
Na_2O	2.80	2.86	3.45	2.85	4.94	4.07
K_2O	3.43	2.98	9.01	1.60	0.51	5.08
P_2O_5	0.85	0.85	0.30	5.90	0.42	0.56
BaO	0.16	0.15	0.20	0.05	0.05	0.47
LOI	7.79	8.79	3.44	1.73	10.66	5.65
Total	99.63	99.84	100.38	97.74	99.51	99.31

Table 8. Whole-rock analyses from the Amba Dongar carbonatitic-alkaline complex (continued).

Sample #	66Apk	66Dpk	66Dpg	66Jgr	43A	66F
Rock Type	Fen. ij.	Fen. ij.	Syenite	Melteigite	Ultrafenite	Ultrafenite
Sc	9	10	1	6	12	n.d.
V	456	461	279	251	373	226
Cr	23	36	32	14	227	0
Co	10.1	46.8	15.4	13.3	9.9	10.3
Ni	5	18	0	7	108	25
Zn	216	282	145	125	99	232
Rb	5.2	42.9	113	94.8	113	5.08
Sr	1004.2	2576.4	1968.1	2217.7	3633.4	2322.4
Y	54	52	35	47	64	44
Zr	32.8	214.3	636.7	239.4	380.7	885.4
Nb	46.9	214.2	356.4	116.5	158.3	553.4
Mo	0.8	2.8	1.1	0.8	1.5	0.7
Cs	0	2.6	3.5	174.2	103.6	3.2
Hf	0.6	2.7	11.7	5.3	8.3	15.9
Ta	0.52	7.34	6.16	4.03	5.8	23.84
W	41.7	19.9	41.1	39.6	20.6	27.4
Pb	24	2	4	3	7	42
Th	39.24	72	16.59	12.34	11.72	73.58
U	2.83	8.14	3.76	3.15	2.56	20.96
La	190.3	603.8	130.8	117.3	128.6	211.5
Ce	263.4	1043.8	217.6	202.2	222.2	356.4
Pr	23.19	92.9	21.48	21.04	24.04	36.15
Nd	73.8	300	74.7	77.7	91.8	121.8
Sm	10.5	37.3	11.4	13.9	17.8	18.3
Eu	2.56	8.07	3.1	3.88	6.15	4.97
Gd	8.1	20.4	8.2	11.4	15.8	12.8
Tb	1.4	2.4	1.2	1.7	2.4	1.9
Dy	8.2	11.1	6.5	8.9	12.4	9.6
Ho	1.7	1.8	1.3	1.8	2.4	1.8
Er	4.8	3.6	3.6	4.6	6.2	4.3
Tm	0.65	0.45	0.55	0.64	0.86	0.63
Yb	3.5	2.5	3.4	4	5.2	4.1
Lu	0.47	0.45	0.53	0.54	0.73	0.61

ss=sandstone; fen. = fenitized; nep. = nephelinite; tep. = tephrite; ij. = ijolite; pk = pink; gr = green; pg = pegmatitic vein

Table 8. Whole-rock analyses from the Amba Dongar carbonatitic-alkaline complex (continued).

Sample #	**66I**	**10A**	**34**	**37C**	**49**	**48B**
Rock Type	**Ultrafenite**	**Fresh ss**	**Fresh ss**	**Fresh ss**	**Fen. ss**	**Fen. ss**
SiO_2	55.10	95.41	97.92	96.05	88.06	83.82
TiO_2	0.49	0.06	0.32	0.16	0.13	0.08
Al_2O_3	10.43	2.58	0.18	1.35	5.51	8.14
Fe_2O_3	2.36	0.20	0.14	0.23	0.22	0.28
FeO	3.22	0.00	0.00	0.00	0.00	0.00
MnO	0.35	0.00	0.00	0.01	0.00	0.00
MgO	6.14	0.00	0.00	0.00	0.00	0.00
CaO	7.67	0.03	0.27	0.07	0.00	0.00
Na_2O	3.42	0.30	0.27	0.29	0.41	0.47
K_2O	5.66	0.66	0.06	0.93	4.79	6.82
P_2O_5	0.35	0.01	0.01	0.03	0.02	0.01
BaO	0.51	0.05	0.01	0.08	0.06	0.08
LOI	3.76	0.66	0.32	0.22	0.18	0.24
Total	99.46	99.96	99.50	99.42	99.38	99.94

Table 8. Whole-rock analyses from the Amba Dongar carbonatitic-alkaline complex (continued).

Sample #	66I	10A	34	37C	49	48B
Rock Type	Ultrafenite	Fresh ss	Fresh ss	Fresh ss	Fen. ss	Fen. ss
Sc	10	0.6	0.8	1.3	0.9	0.6
V	845	18	43	76	25	26
Cr	160	0	49	30	0	0
Co	11.7	120	140	150	94	100
Ni	56	22	24	17	24	31
Zn	206	n.d.	n.d.	n.d.	n.d.	n.d.
Rb	187.4	15	2	23	112	162
Sr	2442	23	9	27	74	67
Y	29	3	3	6	5	0
Zr	489	67	90	206	86	62
Nb	281.5	2	32	49	62	15
Mo	0.8	0	0	0	10	6
Cs	43.7	0	0	0	0	0
Hf	11.9	0	4.7	6	3.7	0
Ta	6.96	3	4	4	3	3
W	46.2	n.d.	n.d.	n.d.	n.d.	n.d.
Pb	30	n.d.	n.d.	n.d.	n.d.	n.d.
Th	10.11	7	5	4	6	10
U	1.62	n.d.	n.d.	n.d.	n.d.	n.d.
La	160.9	11	7	36	21	21
Ce	249.5	26	12	18	31	39
Pr	26.65	n.d.	n.d.	n.d.	n.d.	n.d.
Nd	92.9	11	10	15	15	16
Sm	13.4	1.1	0.4	1.1	1.7	1.9
Eu	3.82	0.3	0.2	0.4	0.6	0.7
Gd	8.8	n.d.	n.d.	n.d.	n.d.	n.d.
Tb	1.3	0	0	0.8	0	0
Dy	6.5	n.d.	n.d.	n.d.	n.d.	n.d.
Ho	1.2	n.d.	n.d.	n.d.	n.d.	n.d.
Er	2.8	n.d.	n.d.	n.d.	n.d.	n.d.
Tm	0.41	n.d.	n.d.	n.d.	n.d.	n.d.
Yb	3	0.7	0.7	1.19	0.9	0.7
Lu	0.63	0	0.1	0.16	0.12	0.1

ss=sandstone; fen. = fenitized; nep. = nephelinite; tep. = tephrite; ij. = ijolite; pk = pink; gr = green; pg = pegmatitic vein

Table 8. Whole-rock analyses from the Amba Dongar carbonatitic-alkaline complex (continued).

Sample #	**47C**	**30C**	**66L**	**68**	**87/A/94**
Rock Type	**Fen. ss**	**Fen. ss**	**Fen. ss**	**Fen. ss**	**Fen. ss**
SiO_2	80.44	74.73	79.34	82.10	66.86
TiO_2	0.12	0.64	0.08	0.07	0.07
Al_2O_3	7.58	10.28	11.09	9.28	17.33
Fe_2O_3	0.88	2.81	0.44	0.69	1.91
FeO	0.00	0.00	0.21	0.22	0.55
MnO	0.01	0.02	0.02	0.02	0.06
MgO	0.00	0.00	0.13	0.00	1.23
CaO	2.03	1.00	0.27	0.24	0.84
Na_2O	0.43	0.42	1.04	1.63	10.15
K_2O	6.46	8.61	6.40	5.28	0.67
P_2O_5	0.05	0.02	0.04	0.18	0.04
BaO	0.15	0.22	0.03	0.07	0.02
LOI	1.82	1.55	1.24	0.60	0.27
Total	99.97	100.30	100.33	100.38	100.00

Table 8. Whole-rock analyses from the Amba Dongar carbonatitic-alkaline complex (continued).

Sample #	47C	30C	66L	68	87/A/94
Rock Type	Fen. ss	Fen. ss	Fen. ss	Fen. ss	Fen. ss
Sc	0.6	n.d.	4	0	2
V	76	323	235	0	10
Cr	0	57	7	15	16
Co	66	n.d.	13.9	0.7	43
Ni	40	52	3	5	0
Zn	n.d.	n.d.	234	2028	38
Rb	129	160	101.5	357.1	10.9
Sr	142	79	1959.7	336.5	316.7
Y	7	9	26	282	3
Zr	99	1878	466.5	5079.6	69.8
Nb	39	55	305.3	1178.9	16.7
Mo	14	n.d.	0.3	7.8	1.1
Cs	0	n.d.	18.1	16.4	0.2
Hf	4.1	n.d.	8.6	76.7	1.6
Ta	2	n.d.	5.4	46.96	1.89
W	n.d.	n.d.	26.6	9.1	238.3
Pb	n.d.	n.d.	45	259	14
Th	13	7	14.38	128.68	2.92
U	n.d.	n.d.	7.12	30.95	1.01
La	46	n.d.	175.9	1227	16.3
Ce	53	n.d.	211	2014.8	22.7
Pr	n.d.	n.d.	17.34	171.38	2.04
Nd	27	n.d.	53	547.3	6.9
Sm	2.3	n.d.	7.8	86	1.1
Eu	1	n.d.	2.13	7.83	0.22
Gd	n.d.	n.d.	5.7	55.6	0.9
Tb	0	n.d.	0.8	9.6	0.1
Dy	n.d.	n.d.	4.4	61.5	0.7
Ho	n.d.	n.d.	0.8	10.5	0.1
Er	n.d.	n.d.	2.2	30.2	0.4
Tm	n.d.	n.d.	0.32	6.04	0.06
Yb	0.9	n.d.	2.1	31.3	0.4
Lu	0.13	n.d.	0.32	4.37	0.08

ss=sandstone; fen. = fenitized; nep. = nephelinite; tep. = tephrite; ij. = ijolite; pk = pink; gr = green; pg = pegmatitic vein

Figure 11A. $Na_2O + K_2O$ versus SiO_2 plot, used to differentiate the various rock types in the complex. Carbonatites plot to the left, alkaline volcanic and plutonic rocks, related fenites, the syenite and melteigite veins and the "ultrafenite" plot in the central portion and Bagh sandstone (ss) and related fenites plot to the right. Increasing fenitization of Bagh sandstone is denoted by the arrow.

B. Cation units of K versus Na to differentiate the different fenites. The most sodic fenites plot at the bottom right of the diagram, whereas the more potassic fenites plot in the upper left. Sodi-potassic fenites, alkaline volcanic and plutonic rocks and the "ultrafenite" plot between these two. Two vertical lines can be drawn between the potassic fenites of Bagh sandstone (with increasing fenitization vertical) and the alkaline volcanic and plutonic rocks and "ultrafenites". The last "ultrafenite" plots in the region where the alkaline volcanic rocks and the sodic fenite of Bagh sandstone are located. The feldspars albite and K-feldspar have been noted on this diagram for purposes of comparison.

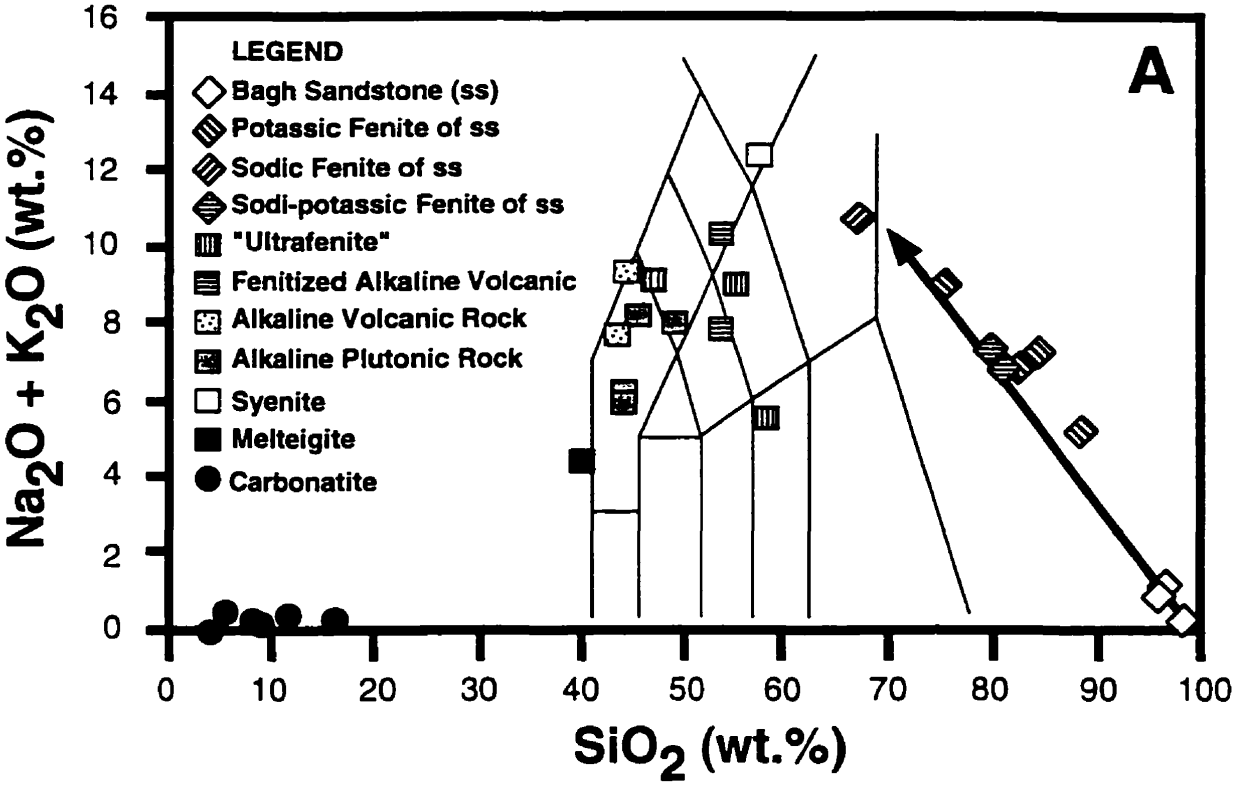
LEGEND
Bagh Sandstone (ss)
Potassic Fenite of ss
Sodic Fenite of ss
Sodi-potassic Fenite of ss
"Ultrafenite"
Fenitized Alkaline Volcanic
Alkaline Volcanic Rock
Alkaline Plutonic Rock
Syenite
Melteigite
Carbonatite
A
Na2O + K2O (wt.%)
SiO2 (wt.%)
0
2
4
6
8
10
12
14
16
0
10
20
30
40
50
60
70
80
90
100

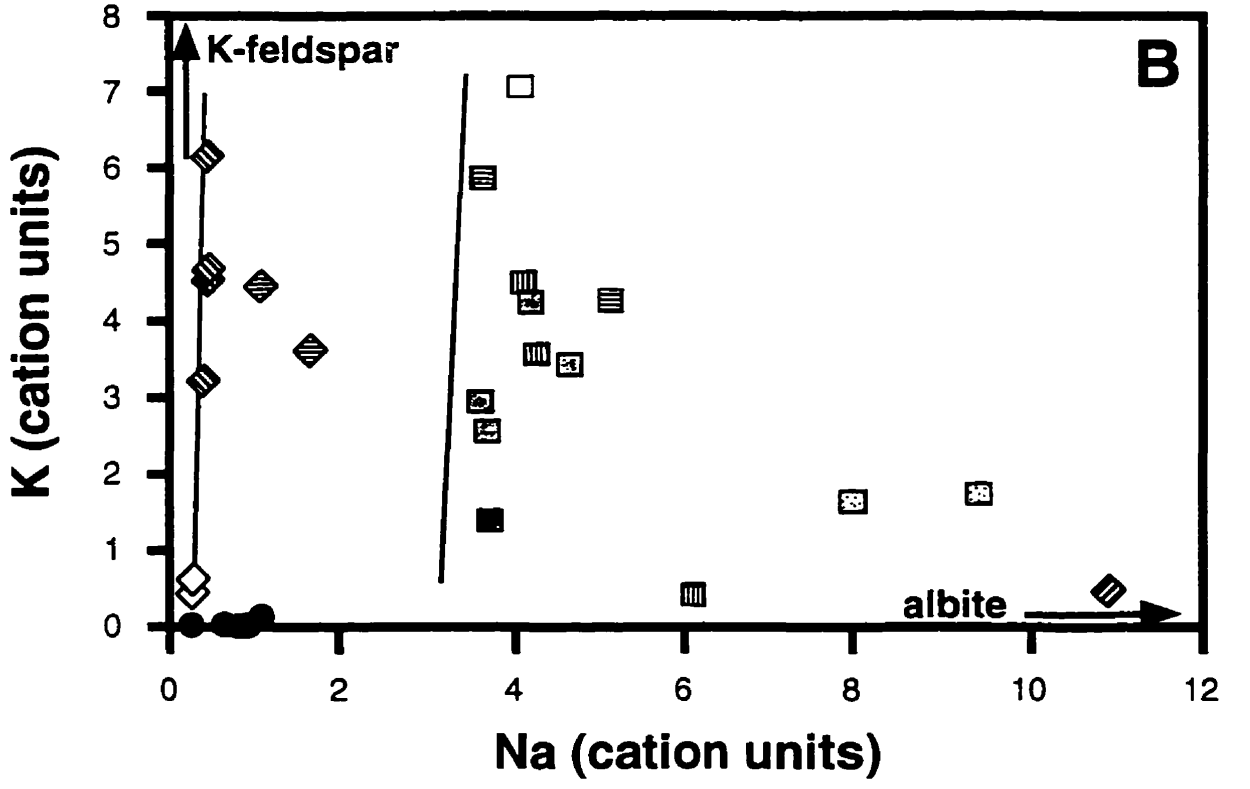
K-feldspar
B
albite
K (cation units)
Na (cation units)
0
1
2
3
4
5
6
7
8
0
2
4
6
8
10
12

rocks, and "ultrafenite" > potassic fenite > sodic fenite >> Bagh sandstone (Fig. 12). The spider and REE diagrams show that "ultrafenite" exhibits enrichments similar to those in the alkaline volcanic and plutonic rocks, but intermediate to those of carbonatite and sandstone (Fig. 12). The difference is that the "ultrafenite" is slightly enriched in the MREE over the HREE compared to the alkaline igneous rocks. Fenitized ijolite is slightly enriched in LREE, but distinctly enriched in MREE to HREE compared to the unfenitized equivalent.

The results presented in this study confirm, within error, those of Viladkar (1981), Viladkar (1986), Viladkar & Dulski (1986), Viladkar & Wimmenauer (1992) and Gwalani et al. (1993) for this complex. However, where Viladkar & Dulski (1986) noted that fenites from this complex show little REE-enrichment, data from the present study suggest that most fenites are as enriched in REE and trace elements as the alkaline volcanic and plutonic rocks. Viladkar (1986) noted that sodic fenites are more depleted than K-fenitized Bagh sandstone in Si, enriched in Fe^{3+}, Fe^{2+}, Mg, Ca, Na and P, but of equivalent Al and Ti content. Comparison of his sodic fenites to those from the present study shows that the latter is more enriched in Fe^{2+}, Mg, Mn and Na, but depleted in Al. The most strongly fenitized potassic fenites from the present study have a higher Ba, Ca and Fe^{3+} content than his. However, the highest Ca, Mg, Ti, Mn, P and Ba contents of all are observed in the "ultrafenite".

Chemical variation in the fenites can be represented in cation % calculated for 100 anions (O, OH and F; after McKie, 1966). Both sodic and potassic fenites of Bagh sandstone show the addition of Al, Fe, Ti, Mn, Ba, K and Na, but the loss of Si (Fig. 13A). K-fenitization resulted in an increase in K, Al, Rb, Ba and Fe^{3+} at the expense of Si (Palmer & Williams-Jones, in prep.). Sodi-potassic fenites exhibit wide variations in Na and K contents, higher levels of Mn and P, and lower levels of Ti and Ba with respect to the potassic ones. These compositional variations reflect the presence of albite and possibly hematite. Sodic fenite is enriched in Al, Na, Fe, Mg and Ca, but depleted in P compared to the potassic fenites. These compositional differences are reflected in the mineralogy of each type of fenite: potassic fenites contain K-feldspar, muscovite and hematite and more sodic fenites contain albite, hematite ± aegirine-augite.

The alkaline volcanic and plutonic rocks are generally homogeneous in

Figure 12. Trace element variation of the units in the complex.

A. Chondrite-normalized (Sun & McDonough, 1989) spider diagram comparing Bagh sandstone, the different carbonatites, and sodic and sodi-potassic fenites of the sandstone.

B. Comparison between "ultrafenite" and the alkaline volcanic or plutonic rocks indicates that they show the same pattern, as both show a distinct depletion of P and Ti. The patterns of the various "ultrafenites" are significantly different than those of the carbonatites and Bagh sandstone depicted in A. One of the two samples of sodic fenite of Bagh sandstone shows a similar enrichment to that of the "ultrafenite"; however, in this fenite is distinctly enriched in REE compared to the "ultrafenite".

C. Chondrite-normalized (Sun & McDonough, 1989) REE diagram of the same samples showing the same relationships as previously noted for the spider plots of A and B.

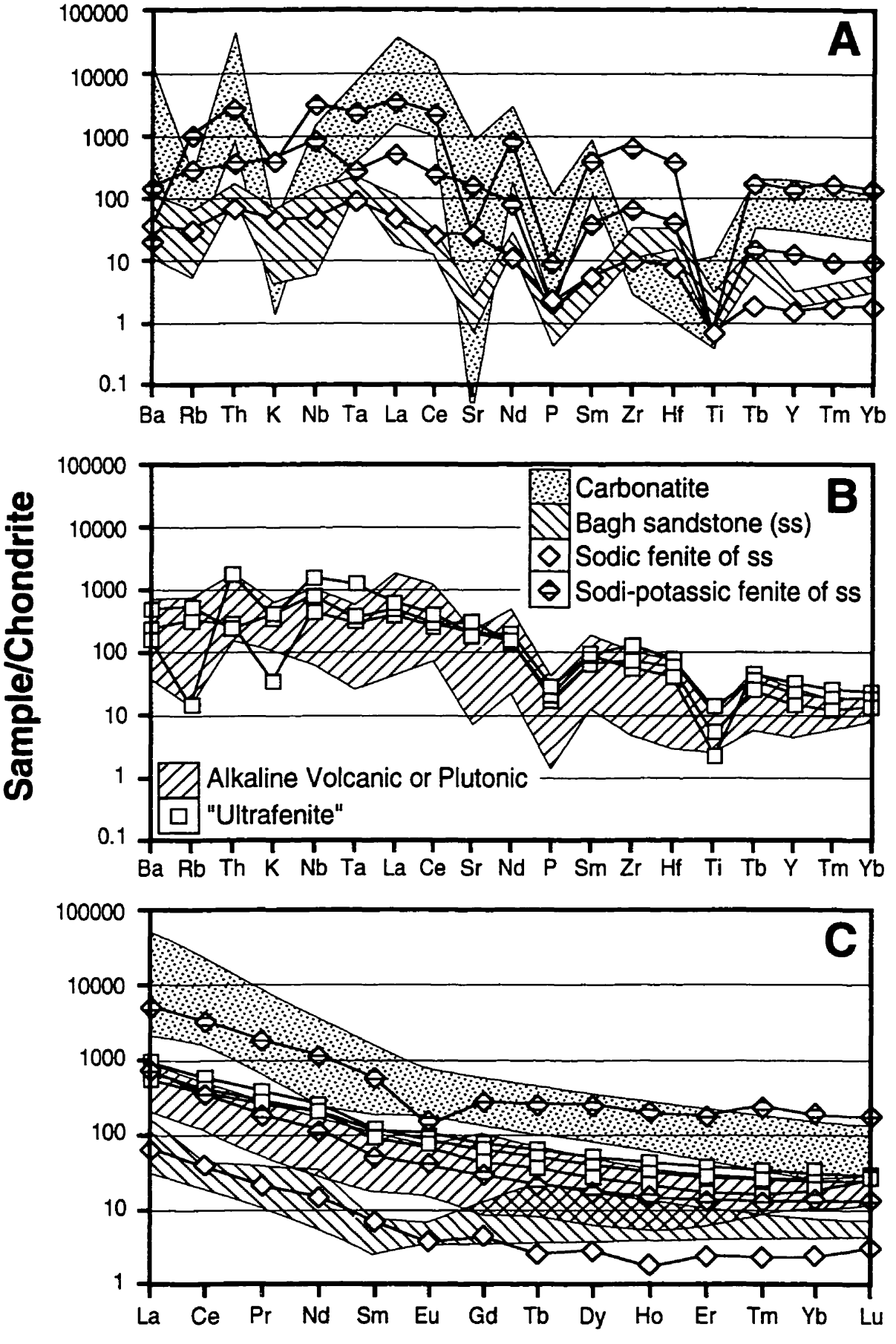
A
B
C
Sample/Chondrite
100000
10000
1000
100
10
1
0.1
Ba Rb Th K Nb Ta La Ce Sr Nd P Sm Zr Hf Ti Tb Y Tm Yb
Carbonatite
Bagh sandstone (ss)
Sodic fenite of ss
Sodi-potassic fenite of ss
Alkaline Volcanic or Plutonic
"Ultrafenite"
La Ce Pr Nd Sm Eu Gd Tb Dy Ho Er Tm Yb Lu

Figure 13. Plot of cation % variation between the various rock types, related fenites and the "ultrafenite".

A. Plot of the cation % of Bagh sandstone compared to its fenitized equivalents arranged in order of increasing fenitization, from unfenitized Bagh sandstone at the center of the diagram. More potassic fenites are plotted on the right, whereas sodic fenite and "ultrafenite" are plotted on the left. Note the distinct enrichment of the potassic fenites in K, Al, Ba at the expense of Si compared to the unfenitized sandstone. Sodi-potassic fenites formed at the expense of Bagh sandstone exhibit a distinct increase in Na and depletion of K. Moreover, sodic fenite contains significantly more Na and Al, but less Si than the sodi-potassic and potassic fenites. This sample also contains more Fe, Mg and, in some cases, Ca than that from the other units. Finally, the "ultrafenites" show distinctly different elemental variations than the Bagh sandstone and fenites in that they are enriched in Al, Na, K, Ca, Mg, Fe, Ti, P, Mn and Ba. Their Si content is, in general, less than that from the fenitized sandstone, although the most enriched sample has approximately the same Si content as that of the sodic fenite of Bagh sandstone.

B. Variation in cation % of selected fenitized and unfenitized alkaline volcanic and plutonic rocks, and "ultrafenite". The compositions of the alkaline volcanic and plutonic rocks are similar with the exception of the amount of Na, Ca, P and, to a lesser extent, Mg and Fe. Fenitized alkaline volcanic and plutonic rocks contain slightly more Si, less Al, Fe^{3+}, Ti and P than either of these. The syenite vein contains more Si, K, but less Ca, Mg, Fe, Na, Ti and P compared to the rest of these alkaline rocks. The Si content of the "ultrafenite" is, for two samples, in the range of that from the alkaline volcanic and plutonic rocks and their fenites. The last sample of "ultrafenite" is slightly enriched in Si. The other elemental variations range from equivalent to that in these other units to less as in Al, Fe^{3+}, Ca and P.

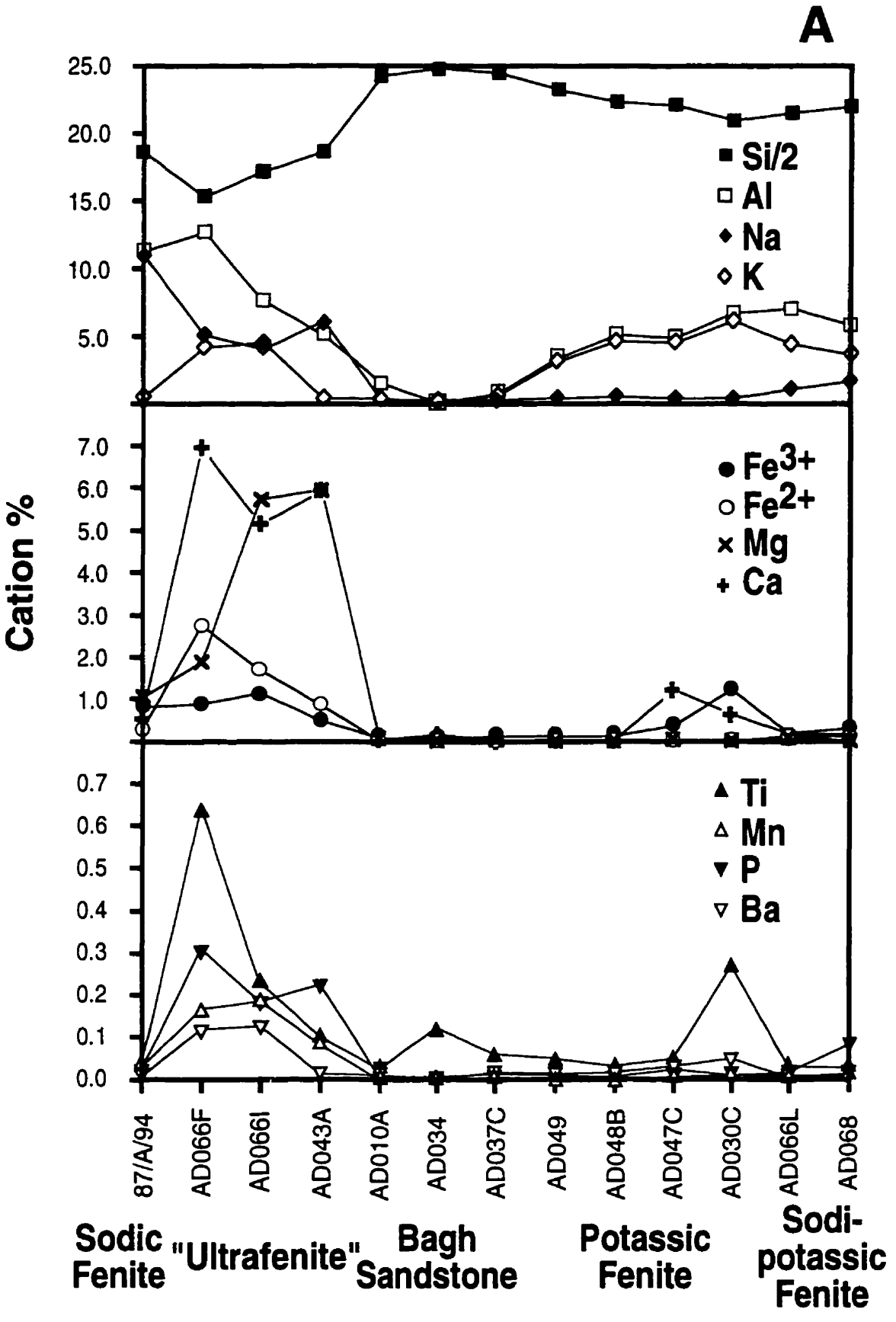
A
Cation %
25.0
20.0
15.0
10.0
5.0
Si/2
Al
Na
K
7.0
6.0
5.0
4.0
3.0
2.0
1.0
Fe3+
Fe2+
Mg
Ca
0.7
0.6
0.5
0.4
0.3
0.2
0.1
0.0
Ti
Mn
P
Ba
87/A/94
AD066F
AD066I
AD043A
AD010A
AD034
AD037C
AD049
AD048B
AD047C
AD030C
AD066L
AD068
Sodic Fenite
"Ultrafenite"
Bagh Sandstone
Potassic Fenite
Sodi-potassic Fenite

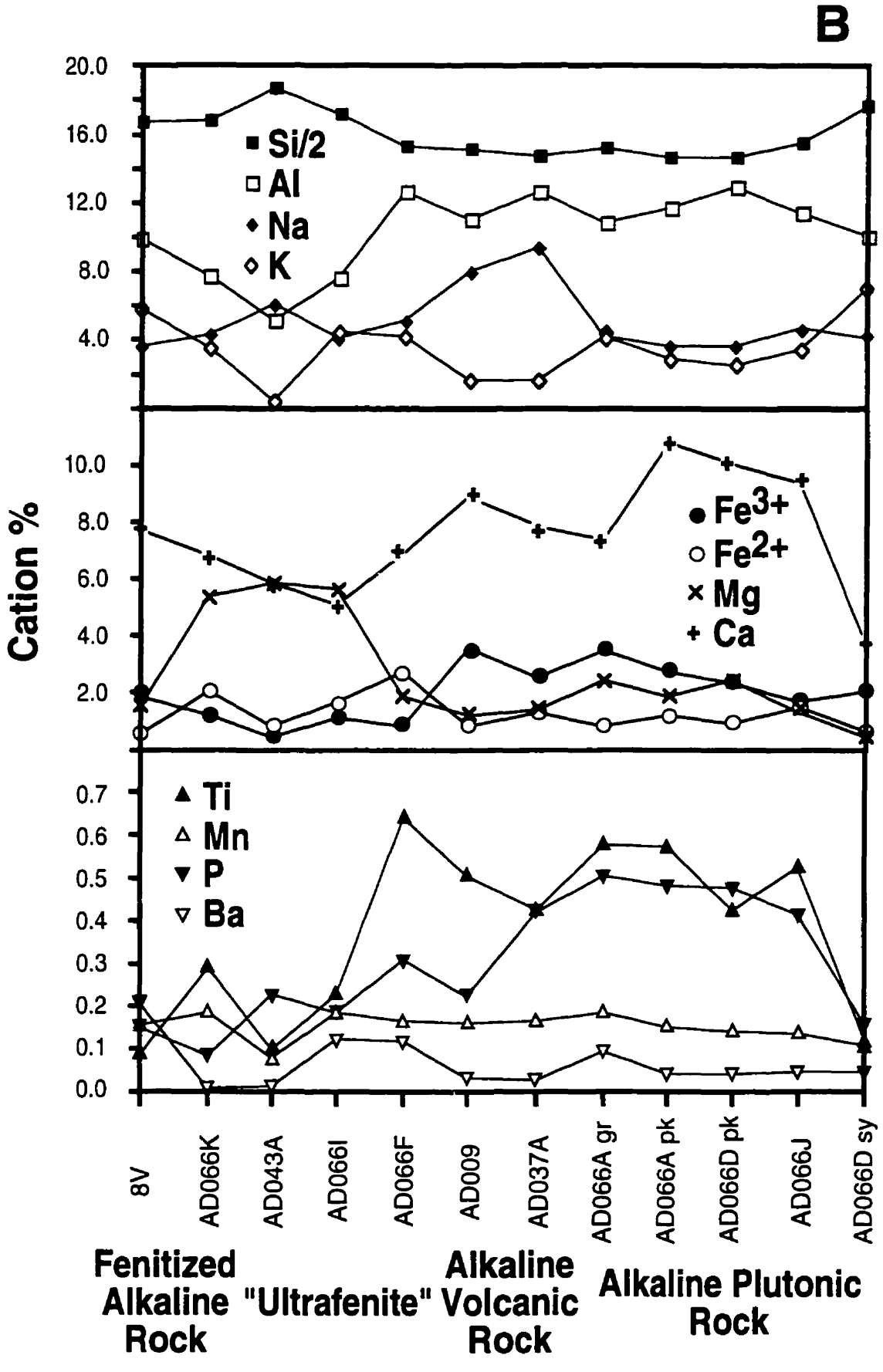
B
Cation %
20.0
16.0
12.0
8.0
4.0
Si/2
Al
Na
K
10.0
8.0
6.0
4.0
2.0
Fe3+
Fe2+
Mg
Ca
0.7
0.6
0.5
0.4
0.3
0.2
0.1
0.0
Ti
Mn
P
Ba
8V
AD066K
AD043A
AD066I
AD066F
AD009
AD037A
AD066A gr
AD066A pk
AD066D pk
AD066J
AD066D sy
Fenitized Alkaline Rock
"Ultrafenite"
Alkaline Volcanic Rock
Alkaline Plutonic Rock

composition, except that the latter contains less Na, but more Ca, P and Mg. Fenites formed at the expense of these rocks contain slightly more Si, but less Al, Fe^{3+}, Ti and P than the unfenitized rocks. The syenite vein contains more Si, K, Ba, Rb, Zr and Nb, but less Ca, Mg, Fe, Na, Ti and P than the rest of these alkaline rocks (owing to their late emplacement). On the other hand, melteigite is enriched in Ti, Mn, Fe, Ca, P, Ce, Y and Sm compared to ijolite (Table 8). Most of the "ultrafenite" samples contain the same proportion of Si as that of the alkaline volcanic and plutonic rocks and their fenites, except for one which shows a slight enrichment in Si. The other elements of the "ultrafenite" are in concentrations equivalent to those in the alkaline volcanic and plutonic rocks and their fenites, except for Al, Fe^{3+}, Ca and P which are lower. Overall, variation in mineral composition and whole-rock chemistry indicates that the metasomatic fluid was enriched in Na, Fe^{3+}, Mn, Ti, Al, Si, Sr, F and REE.

Mineralogical investigation of the sodic fenites formed by alteration of alkaline volcanic and plutonic rocks indicates that they have become enriched in Fe^{3+}, Si, Ca, Na and Mg, with later enrichment in Ti, and possibly F and CO_2 (Fig. 13B). Fenitization also is reflected in a change in the Ba content of K-feldspar and the presence of barite, which indicates that the metasomatic fluid was enriched in Ba. Whole-rock analyses indicate Ba-enrichment of ferrocarbonatite relative to the rest of the units from the complex. Finally, compared to alkaline volcanic and plutonic rocks, samples of "ultrafenite" are enriched in Si (especially 43A) and Mg, but depleted in Al, Ti, P, Fe^{3+} and Ca.

The different units present in the complex can be separated in Ti versus Al and Mg versus Al plots (Fig. 14). In Figure 14A, two of the "ultrafenite" samples (66I and 66K) and a sample of fenitized sandstone (30C) plot between the positions of the fenitized sandstone, carbonatite, syenite, melteigite, and the other alkaline volcanic and plutonic rocks. Fenitized sandstone (30C) contains the same amount of Al and Ti (Fig. 14A), but less Mg than "ultrafenites" (Fig. 14B). Sample 43A contains significantly more Si, but less Al and Ti at constant Mg than the other "ultrafenites". This sample is also enriched in Si, but depleted in Al and Ti. All of these differences suggest a possible difference in origin between it and the other samples of "ultrafenite".

It is interesting to note that by inspection of Figures 11 and 14, samples of fenite of the different units, especially most of the "ultrafenite" samples, in the complex converge to

Figure 14. Comparison between "ultrafenite" with the rest of the units from the Amba Dongar carbonatitic-alkaline complex to suggest its precursor.

A. Ti versus Al plot (in cation units) to differentiate between the units. Two samples of "ultrafenite" plot between the alkaline and volcanic plutonic rocks, carbonatite and sandstone. The other "ultrafenite" (43A) contains significantly less Al and Ti than the others, such that it plots near that of the fenitized sandstone. One sample of fenitized sandstone (30C) contains the same amount of Ti and Al as two of the "ultrafenites". Two samples of carbonatite that contain significant hematite show a significant enrichment in Ti over the other units represented.

B. Mg versus Al plot (in cation units) shows the same separation between the units as in A, except that Sample 30C contains significantly less Mg than all samples of "ultrafenite". In addition, "ultrafenite" plots between the alkaline volcanic and plutonic rocks and carbonatite or the carbonatite and the more fenitized examples of Bagh sandstone.

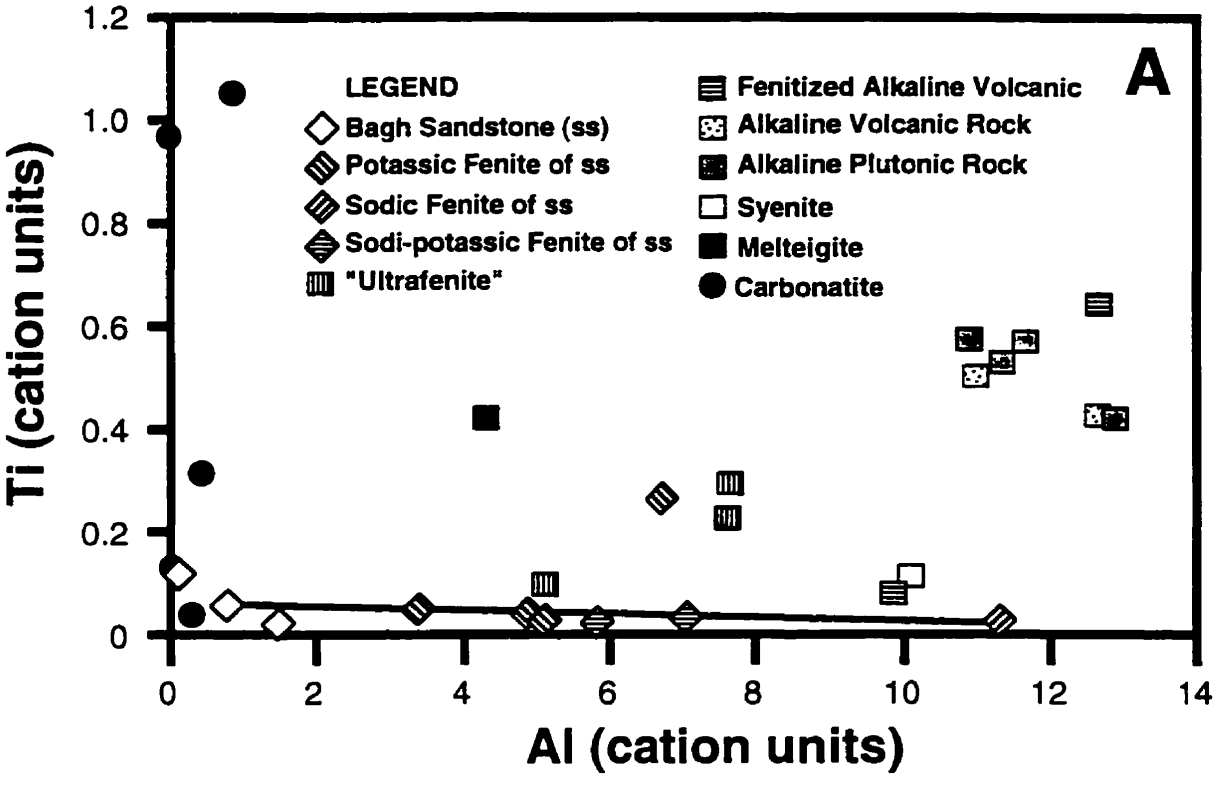
A
LEGEND
Bagh Sandstone (ss)
Potassic Fenite of ss
Sodic Fenite of ss
Sodi-potassic Fenite of ss
"Ultrafenite"
Fenitized Alkaline Volcanic
Alkaline Volcanic Rock
Alkaline Plutonic Rock
Syenite
Melteigite
Carbonatite
Ti (cation units)
Al (cation units)
0
0.2
0.4
0.6
0.8
1.0
1.2
0
2
4
6
8
10
12
14

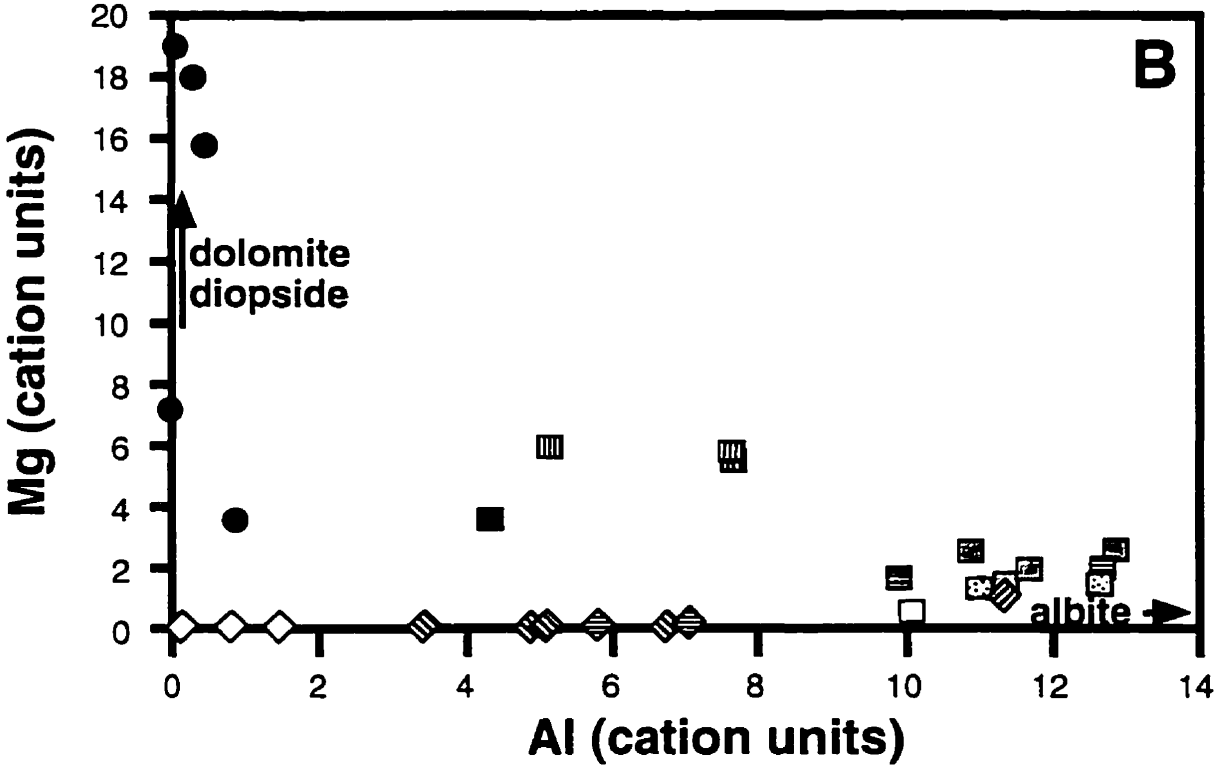
B
dolomite
diopside
albite
Mg (cation units)
Al (cation units)
0
2
4
6
8
10
12
14
16
18
20
0
2
4
6
8
10
12
14

a syenitic composition. These "ultrafenites" show compositional similarities with those of average syenite or nepheline syenite of Le Maitre (1976). This tendency of convergence of fenites developed at the expense of many rock types to one final composition also was noted by Currie & Ferguson (1972). They suggested that fenites from mafic rocks converge to more felsic fenites due to equilibration with the surrounding rocks.

Origin of "Ultrafenite"

"Ultrafenite" from the Amba Dongar complex may have originated in three ways: 1) extreme fenitization of an alkaline volcanic or plutonic rocks, Deccan basalt or sandstone at a temperature near or above its melting point (the latter is a rheomorphic fenite), 2) fenitization of alkaline volcanic or plutonic rock or basalt at a lower temperature than in 1 (i.e., where no melting has occurred), or 3) fenitization of a silicified alkaline volcanic or plutonic rock. The prevalent layering and relict textures of these rocks reflect either original layering of the protolith, such as in sandstone, relics of earlier veining, or were produced during fenitization. Swirls of interfingering light and dark material in the unit are consistent with small-scale rheomorphism. The presence of sanidine and Di-rich pyroxene, and the fine grain-size indicate formation by high-temperature (>550°C) fenitization.

The fine grain-size and relative lack of original textures in the "ultrafenite" makes it difficult to identify the protolith. Deccan basalt is significantly depleted in REE and other trace elements compared to other units from the complex. Much of this basalt, especially the later units (Krishnamurthy & Cox, 1977; Peng et al., 1994), is enriched in Ti compared to "ultrafenite". Furthermore, the "ultrafenite" has a significantly different composition and mineralogy than the mildly fenitized basalt from the complex described by Udas (1971). Finally, the presence of quartz (<10%) suggests that the precursor of the fenites was a sandstone, or that silicification of an alkaline rock occurred prior to fenitization. The latter hypothesis is supported by a slight increase in Si of the fenitized alkaline volcanic and plutonic rocks. In addition, Palmer & Williams-Jones (1996) and Viladkar & Wimmenauer (1992) noted that silicification occurred in the complex before and during fluorite deposition. The similarity in whole-rock composition of samples 66I and 66K with alkaline volcanic and plutonic rocks, respectively, suggests their origin by fenitization of these

protoliths following silicification, although an origin from extremely fenitized Bagh sandstone cannot be ruled out. The Si enrichment of 43A appears to be the result of fenitization of a more silica-rich source such as produced by more silicification prior to fenitization or extreme fenitization of Bagh sandstone.

Compositional Variation of the Metasomatic Fluid

Differences in the type of fenite appear to be due to changes in the temperature of the fluid and the composition of the protolith, as discussed in the mineralogical section above. There is a distinct evolution from an early Na- to a later K-metasomatic event. In glimmerite and "ultrafenite", fenitization is at the decimeter scale along veins, with the initial higher temperature Na-fenitization covering a wider area than the later lower temperature K-fenitization, which is restricted to the margins of the veins. Although the results of the present study show that more sodic fenites at the expense of Bagh sandstone occur at depth, the sampling density used was insufficient to confirm a relationship. Application of the experimental studies discussed above on the origin of alkali feldspars indicates that K-feldspar crystallized at a lower temperature (<400-450°C; Rubie & Gunter, 1983) than albite, as is consistent with the XRD data on the feldspars. Comparison of the data on these feldspars with the composition of the associated aegirine-augite indicates that feldspar of a higher temperature origin exists with Di-rich aegirine-augite, while that of lower temperature origin exists with Ae-rich pyroxene. Identical mafic and felsic mineralogical variations have been described by Garson (1962), Sutherland (1969b), Vartiainen & Woolley (1976) and Rubie & Gunter (1983). Rubie & Gunter (1983) noted that K-fenitization occurs at low (<400-450°C)-temperature, whereas Na-fenitization occurs at a higher temperature from a fluid of the same composition. Na-fenitization in the Amba Dongar complex is associated with increases of Na, Fe^{3+}, Mg and Mn, whereas K-fenitization is associated with increases of K, Al, Ba and Rb and possibly Fe^{3+}, irrespective of the composition of the protolith. In summary, data from the present study suggest that the composition of the metasomatic fluid was more or less constant during the fenitization reactions. Furthermore, it was impossible to determine whether the observed variation in the type of fenite was related to depth in the intrusion. The observed variation with depth

suggested by Viladkar (1986) could be related to local variations in the fenites formed at the expense of Bagh sandstone, as noted developed on a small scale in the glimmerite and "ultrafenite".

The composition of the fluids that produced the fenites in the Amba Dongar complex was probably similar to that estimated by Kresten & Morogan (1986) and Morogan (1994) for fluids emitted from a carbonatitic source. They suggested that these fluids are oxidizing, Ca- and CO_2-rich, Si-poor, with high Fe/Mg and variable, but relatively high Na/K. Kresten (1988) noted from mineralogical observations that fenites produced by carbonatites are Mg-, Fe^{3+}-, P- and, in most cases, Mn-rich. In the present study, the fluid involved in fenitization shows a comparable pattern of enrichment, except for Ca and CO_2, which are likely somewhat less than they predicted. This Ca-enrichment is contrary to the results of fluid inclusion studies by Vard & Williams-Jones (1993) and Samson et al. (1995) on minerals in phonolite and carbonatite, respectively. The fluid inclusion studies of Samson et al. (1995a) and Andersen (1986) to determine the nature of the orthomagmatic fluids in apatite from carbonatite indicate a low CO_2 content, but that Cl and S are elevated, and HCO_3^- and CO_3^{2-} may be high. These same compositional variations may also be true in the hydrothermal fluid (Samson et al., 1995b). Similar variations in the composition (low CO_2, but significant Ca, Al, Na, Cl and S) of the hydrothermal fluid were also indicated in the fluid inclusion study of Palmer & Williams-Jones (1996) on the Amba Dongar complex. These results are consistent with the composition of the fluid implied by the present study.

Kresten (1988) and Andersen (1989) suggested that the composition of their fenites vary with the areal extent of fenitization, composition of the protolith and temperature of fenitization. For example, the extent of fenitization varies between contact (e.g., glimmerite) and aureole fenites. The first are of a higher temperature and produced by dominantly Mg- (but also K-) fenitization (Chapter 3; Kresten, 1988; Andersen, 1989). Aureole fenites of Bagh sandstone cover a large area and show gradual mineralogical and chemical changes. The composition of these fenites is also related to that of the fluid and protolith (Rubie & Gunter, 1983). Consequently, fenites from the Amba Dongar complex originated from a single metasomatic fluid whose evolution was related to variations in the temperature under which fenitization occurred.

Conclusions

The fenites at Amba Dongar formed through interaction of a single fluid, derived from the calciocarbonatite with the host-rocks, which produced sodic fenite at high temperature and potassic fenite at low temperature. The effects of these two types of fenitization can be seen on the cm-scale (glimmerite and "ultrafenite") and to the 100 m-scale (Bagh sandstone). Support for a single wave of fenitizing fluid comes from examination of mineralogical variations in the various fenites, where K-rich minerals (K-feldspar, mica and amphibole) form at lower temperatures than Na-rich minerals (albite and aegirine). In some fenites, the final stage of fenitization includes formation of wollastonite and titanian andradite by Ca-metasomatism. Sodic fenite formed at the expense of Bagh sandstone is enriched in Na, Ca, Mg and Fe at the expense of Si, whereas potassic fenite is enriched in K, Rb and Ba at the expense of Si. Relatively localized Mg-metasomatism of alkaline volcanic and plutonic rocks produced glimmerite, whereas extreme, high-temperature (550°C), Na (+K) fenitization, after a prior episode of silicification, produced an "ultrafenite" enriched in Na, Ca, Si, Fe and Mg.

Acknowledgements

The Gujarat Mining and Development Corporation is thanked for providing access to the locality, along with transportation and accommodation during field work. S. Viladkar furnished an introduction to the locality and arranged logistical support. David Palmer and I had fruitful discussions concerning the locality and also helped with the field work. Dr. L.G. Gwalani provided preprints of his work. G. Poirier and Dr. K. Livi helped set up the procedure for electron-microprobe analyses performed at McGill University and Johns Hopkins University, respectively. Glen Poirier and Prof. D. Baker supplied Figure 9A, which was produced while on a reconnaissance trip to JEOL in Japan. I am grateful for scholarship support from: a) Fonds pour la Formation de Chercheurs et l'Aide à la Recherche (FCAR), who also provided funding for a Stage; b) GSA through a student research award; and c) Sigma Delta Epsilon through a Women in Science award. RFM and

AEW-J acknowledge support for this research from NSERC and FCAR. Earlier versions of this paper were commented on by C. Normand, T. Roelofsen, and K. Currie.

References

Andersen, T. (1984): Secondary processes in carbonatites: petrology of "rödberg" (hematite-calcite-dolomite-carbonatite) in the Fen central complex, Telemark (south Norway). *Lithos*, 17, 227-245.

------- (1986): Magmatic fluids in the Fen carbonatite complex, S.E. Norway: evidence of mid-crustal fractionation from solid and fluid inclusions in apatite. *Contributions to Mineralogy and Petrology*, 93, 491-503.

------- (1989): Carbonatite-related contact metasomatism in the Fen complex, Norway: effects and petrogenetic implications. *Mineralogical Magazine*, 53, 395-414.

------- & Austrheim, H. (1991): Temperature-HF fugacity trends during crystallization of calcite carbonate magma in the Fen complex, Norway. *Mineralogical Magazine*, 55, 81-94.

Appleman, D.E. & Evans, H.T., Jr. (1973): Job 9214: indexing and least-squares refinement of powder diffraction data. U.S. Geological Survey, Computer Contribution 20 (NTIS Doc. PB2-16188).

Avasia, R.K., Chang, W.-J. & Gwalani, L.G. (1992): Textural and structural characteristics of the Cretaceous Bagh sandstones associated with carbonatite-alkaline intrusives of Chhota Udaipur, Gujarat, India. *Gondwana Geological Magazine*, 4-5, 31-39.

Blasi, A. (1977): Calculation of T-site occupancies in alkali feldspar from refined lattice constants. *Mineralogical Magazine*, 41, 525-526.

Bonin, B. & Giret, A. (1985): Clinopyroxene composition trends in oversaturated and undersaturated alkaline ring complexes. *Journal of African Earth Sciences*, 3, 175-182.

Brigatti, M.F., Medici, L., Saccani, E. & Vaccaro, C. (1996): Crystal chemistry and petrologic significance of Fe^{3+}-rich phlogopite from the Tapira carbonatite complex, Brazil. *American Mineralogist*, 81, 913-927.

Chabu, M. & Boulègue, J. (1992): Barian feldspar and muscovite from the Kipushi Zn-Pb-Cu deposit, Shaba, Zaire. *Canadian Mineralogist*, 30, 1143-1152.

Crookshank, H. (1936): Geology of the northern slopes of Satpuras between the Morand and Sher Rivers. *Memoir, Geological Survey of India*, 66(2), 137-381.

Currie, K.L. & Ferguson, J. (1972): A study of fenitization in mafic rocks, with special reference to the Callander Bay complex. *Canadian Journal of Earth Sciences*, 9, 1254-1261.

-------, Knutson, J. & Temby, P.A. (1992): The Mud Tank carbonatite complex, central Australia - an example of metasomatism at mid-crustal levels. *Contributions to Mineralogy and Petrology*, 109, 326-339.

Dawson, J.B., Smith, J.V. & Steele, I.M. (1995): Petrology and mineral chemistry of plutonic igneous xenoliths from the carbonatite volcano, Oldoinyo Lengai, Tanzania. *Journal of Petrology*, 36, 797-826.

Deans, T. & Powell, J. L. (1968): Trace elements and strontium isotopes in carbonatites, fluorites, and limestones from India and Pakistan. *Nature*, 218, 750-752.

-------, Sukheswala, R.N., Sethna, S.F. & Viladkar, S.G. (1972): Metasomatic feldspar rocks (potash fenites) associated with the fluorite deposits and carbonatites of Amba Dongar, Gujarat, India. *Transactions, Institute of Mining and Metallurgy*, 81, B1-9.

Deer, W.A., Howie, R.A. & Zussman, J. (1982): Garnet Group. *In* **Rock-forming minerals. Orthosilicates**. John Wiley & Sons, New York, 1A, 467-698.

Fabriès, J. (1978): Les types paragénétiques des amphiboles sodiques dans les roches magmatiques. *Bulletin de Minéralogie*, 107, 155-165.

Faye, G.H. & Hogarth, D.D. (1969): On the origin of reverse pleochroism of a phlogopite. *Canadian Mineralogist*, 9, 25-34.

Flohr, M.J.K. & Ross, M. (1989): Alkaline igneous rocks of Magnet Cove, Arkansas: metasomatized ijolite xenoliths from Diamond Jo Quarry. *American Mineralogist*, 74, 113-131.

Fournier, R.O., (1976): Exchange of Na^+ and K^+ between water vapor and feldspar phases at high temperature and low vapor pressure. *Geochimica et Cosmochimica Acta*, 40, 1553-1561.

Garson, M.S. (1962): The Tundulu carbonatite ring-complex in southern Nyasaland. *Geological Survey Department, Nyasaland Protectorate*, Zomba, Malawi, 248p.

Garvey, R. (1986): LSUCRIPC, least squares unit-cell refinement with indexing on the personal computer. *Powder Diffraction*, 1, 114.

Gwalani, L.G., Avasia, R.K., Chang, W.-J., Fernandez, S., Allègre, C.J. & Prinzhofer, A. (1993): Alkaline rocks and carbonatites of Amba Dongar and adjacent areas, Deccan Igneous Province, Gujarat, India: 1. Geology, petrography and petrochemistry. *Mineralogy and Petrology*, 47, 219-253.

Hawthorne, F.C. (1983): The crystal chemistry of the amphiboles. *Canadian Mineralogist*, 21, 173-480.

Hogarth, D.D. & Lapointe, P. (1984): Amphibole and pyroxene development in fenite from Cantley, Quebec. *Canadian Mineralogist*, 22, 281-295.

-------, Chao, G.Y. & Townsend, M.G. (1987): Potassium and fluorine-rich amphiboles from the Gatineau area, Quebec. *Canadian Mineralogist*, 25, 739.

-------, Hartree, R., Loop, J. & Solberg, T.N. (1985): Rare-earth element minerals in four carbonatites near Gatineau, Quebec. *American Mineralogist*, 70, 1135-42.

-------, Rushforth, P. & McCorkell, R.H. (1988): The Backburn carbonatites near Ottawa, Ontario: dykes with fluidized emplacement. *Canadian Mineralogist*, 26, 377-390.

Hsu, L.C. (1980): Hydration and phase relations of grossular-spessartine garnets at P_{H2O} = 2 Kb. *Contributions to Mineralogy and Petrology*, 71, 407-415.

Huckenholz, H.G. & Yoder, H.S. (1969): Andradite stability in air at 1 atm, O_2 up to 30 kb, and $H_2O + O_2$ up to 20 kb total pressure. *Carnegie Institution Yearbook*, 69, 182-188.

Huggins, F.E., Virgo, D. & Huckenholz, H.G. (1977) Titanium-containing silicate garnets II. The crystal chemistry of melanites and scholomites. *American Mineralogist*, 62, 646-665.

Iiyama, J.T. (1965): Influence des anions sur les équilibres d'échange d'ions Na-K dans les feldspaths alcalins à 600°C sous une pression de 1000 bars. *Bulletin de Societié Français Minéralogie et Cristallographie*, 88, 618-622.

Karkare, S.G. & Srivistava, R.K. (1990): Regional dyke swarms related to the Deccan Trap Alkaline province, India. *In* **Mafic Dykes and Emplacement Mechanisms** (Parker, A.J., Rickwood, P.C. & Tucker, D.H., eds.). Proceedings of the Second International Dyke Conference, Adelaide, South Australia, September, 1990, 335-347.

Kresten, P. (1988): The chemistry of fenitization: examples from Fen, Norway. *Chemical Geology*, 68, 329-349.

------- & Morogan, V. (1986): Fenitization at the Fen complex, southern Norway. *Lithos*, 19, 27-42.

Krishnamurthy, P. & Cox, K.G. (1977): Picrite basalts and related lavas from the Deccan Traps of Western India. *Contributions to Mineralogy and Petrology*, 62, 53-75.

Kroll, H. & Ribbe, P.H. (1983): Lattice parameters, composition and Al-Si order in alkali feldspars. *In* **Feldspar Mineralogy** (P.H. Ribbe, ed.). Mineralogical Society of America, Reviews in Mineralogy, 2, 57-99.

Kühberger, A., Fehr, T., Huckenholz, H.G. & Amthauer, G. (1989): Crystal chemistry of a natural schorlomite and Ti-andradites synthesized at different oxygen fugacities. *Physics and Chemistry of Minerals*, 16, 741-746.

Lagache, M. (1984): The exchange equilibrium distribution of alkali and alkaline-earth elements between feldspars and hydrothermal solutions. *In* **Feldspars and Feldspathoids** (Brown, W.L., ed.). D. Reidel Publishing Company, 247-279.

------- & Weisbrod, A. (1977): The system: two alkali feldspars-KCl-NaCl-H_2O at moderate to high temperatures and low pressures. *Contributions to Mineralogy and Petrology*, 62, 77-101.

Larsen, M.N. (1978): Clinopyroxenes and coexisting mafic minerals from the alkaline Ilimaussaq intrusion, South Greenland. *Journal of Petrology*, 17, 258-290.

Le Bas, M. J. (1977): **Carbonatite-Nephelinite Volcanism**. Wiley, New York, 347p.

------- (1981): Carbonatite magmas. *Mineralogical Magazine*, 44, 133-140.

-------, Le Maitre, R.W., Streckeisen, A. & Zanettin, B. (1986): A chemical classification of volcanic rocks based on the total alkali-silica diagram. *Journal of Petrology*, 27, 745-750.

-------, Keller, J., Kejie, T., Wall, F., Williams, C.T. & Peishan, Z. (1992): Carbonatite dykes at Bayan Obo, Inner Mongolia, China. *Mineralogy and Petrology*, 46, 195-228.

Le Maitre, R.W. (1976): The chemical variability of some common igneous rocks. *Journal of Petrology*, 17, 589-637.

-------, ed. (1989): **A Classification of Igneous Rocks and Glossary of Terms**. Blackwell Scientific Publications, London, 193p.

Liu, Y. & Comodi, P. (1993): some aspects of the crystal-chemistry of apatites. *Mineralogical Magazine*, 57, 709-719.

McCormick, G.R. & Heathcote, R.C. (1987): Mineral chemistry and petrogenesis of carbonatite intrusions, Perry and Conway Counties, Arkansas. *American Mineralogist*, 72, 59-66.

------- & Le Bas, M.J. (1996): Phlogopite crystallization in carbonatitic magmas from Uganda. *Canadian Mineralogist*, 34, 469-484.

McKie, D. (1966): Fenitization. *In* **Carbonatites** (Tuttle, O.F. & Gittins, J., eds.). John Wiley & Sons, Ltd., London, 261-294.

Mian, J. & Le Bas, M.J. (1986): Sodic amphiboles in fenites from the Loe Shilman carbonatite complex, NW Pakistan. *Mineralogical Magazine*, 50, 187-197.

------- & ------- (1987): The biotite-phlogopite series in fenites from the Loe Shilman carbonatite complex, NW Pakistan. *Mineralogical Magazine*, 51, 397-408.

Mitchell, R.H. (1980): Pyroxenes of the Fen alkaline complex, Norway. *American Mineralogist*, 65, 45-54.

Morbidelli, L., Beccaluva, L., Brotzu, P., Conte, A., Garbarino, C., Gomes, C.B., Macciotta, G., Ruberti, E., Scheibe, L.F. & Traversa, G. (1986): Petrological and geochemical studies of alkaline rocks from continental Brazil. 3. Fenitization of jacupirangite by carbonatite magmas in the Jacupiranga Complex. *Periodico di Mineralogia*, 55, 261-295.

Morimoto, N. (1989): Nomenclature of pyroxenes. *Canadian Mineralogist*, 27, 143-156.

Morogan, V. (1994): Ijolite versus carbonatite as sources of fenitization. *Terra Nova*, 6, 166-176.

------- & Woolley, A.R. (1988): Fenitization in the Alnö complex, Sweden: distribution, mineralogy and genesis. *Contributions to Mineralogy and Petrology*, 100, 169-182.

Orville, P.M. (1963): Alkali ion exchange between vapor and feldspar phases. *American Journal of Science*, 261, 201-237.

Palmer, D. & Williams-Jones, A.E. (1996): Genesis of the carbonatite-hosted fluorite deposit at Amba Dongar, India: evidence from fluid inclusions, stable isotopes, and whole rock-mineral geochemistry. *Economic Geology*, 91, 934-950.

Paterson, B.A. & Stephens, W.E. (1992): Kinetically induced compositional zoning in titanite: implications for accessory-phase/melt partitioning of trace elements. *Contributions to Mineralogy and Petrology*, 109, 373-385.

Peng, Z.X., Mahoney, J., Hooper, P., Harris, C. & Beane, J. (1994): A role for lower continental crust in flood basalt genesis? Isotopic and incompatible element study of the lower six formations of the western Deccan Traps. *Geochimica et Cosmochimica Acta*, 58, 267-288.

Peterson, T.D. (1989): Peralkaline nephelinites. II. Low pressure fractionation and the hypersodic lavas of Oldoinyo L'engai. *Contributions to Mineralogy and Petrology*, 102, 336-346.

Platt, R.G. & Edgar, A.D. (1972): The system nepheline-diopside-sanidine and its significance to the genesis of melilite- and olivine-bearing alkaline rocks. *Journal of Geology*, 80, 223-236.

Puustinen, K. (1973): Tetraferriphlogopite from the Siilinjärvi carbonatite complex, Finland. *Geological Society of Finland, Bulletin*, 45, 35-42.

Rock, N.M.S., Gwalani, L.G. & Griffin, B.J. (1994): Alkaline rocks and carbonatites of Amba Dongar and adjacent areas, Deccan Igneous Province, Gujarat, India. 2) Complexly zoned clinopyroxene phenocrysts. *Mineralogy and Petrology*, 51, 113-135.

Rubie, D.C. & Gunter, W.D. (1983): The role of speciation in alkaline fluids during fenite metasomatism. *Contributions to Mineralogy and Petrology*, 82, 165-175.

Samson, I.M., Liu, W. & Williams-Jones, A.E. (1995a): The nature of orthomagmatic hydrothermal fluids in the Oka carbonatite, Quebec, Canada: evidence from fluid inclusions. *Geochimica et Cosmochimica Acta*, 59, 10, 1963-1977.

-------, Williams-Jones, A.E. & Liu, W. (1995b): The chemistry of hydrothermal fluids in carbonatites: evidence from leachate and SEM-decrepitate analysis of fluid inclusions from Oka, Quebec, Canada. *Geochimica et Cosmochimica Acta*, 59, 1979-1989.

Segnit, E.R. & Gelb, T. (1970): Reactions of kaolinite with barium carbonate and barium sulphate. *Journal of the Australian Ceramic Society*, 6, 12-18.

Sethna, S.F. (1989): Petrology and geochemistry of the acid, intermediate and alkaline rocks associated with the Deccan basalts in Gujarat and Maharashtra. *Memoir, Geological Society of India*, 15, 47-61.

------- & Borges, S.M. (1981): Petrology of the carbonatites and associated alkaline rocks of Siriwasan, Chhota Udaipur. *Journal of the Geological Society of India*, 22, 417-425.

Simonetti, A. & Bell, K. (1995): Nd, Pb, and Sr isotope systematics of fluorite at the Amba Dongar carbonatite complex, India: evidence from hydrothermal and crustal fluid mixing. *Economic Geology*, 90, 2018-2027.

Smith, J.V. (1975): Some chemical properties of feldspars. *In* **Feldspar Mineralogy** (Ribbe, H.P., ed.). Mineralogical Society of America, Reviews in Mineralogy, 2, 281-296.

Srivastava, R.K. & Karkare, S.G. (1989): Sulphide mineralization around Ambadungar, Baroda district, Gujarat. *Current Science*, 58(17), 962-964.

Sukheswala, R.N. & Udas, G.R. (1964): The carbonatite of Amba Dongar, India - some structural considerations. *22nd International Geological Congress*, Abstract Volume, 7, 1-13.

------- & ------- (1981): Fenitized sandstones in Amba Dongar carbonatites, Gujarat, India. *Journal of the Geological Society of India*, 22, 368-374.

Sun, S.-s. & McDonough, W.F. (1989): Chemical and isotopic systematics of oceanic basalts: implications for mantle composition and processes. *In* **Magmatism in the Ocean Basins** (Sunders, A.D. & Norry, M.J., eds.). *Geological Society, Special Publication*, 42, 313-345.

Sutherland, D.S. (1969a): Sodic amphiboles and pyroxenes from fenites in East Africa. *Contributions to Mineralogy and Petrology*, 24, 114-135.

------- (1969b): Potassic-trachytes and ultrapotassic rocks associated with the carbonatite complex of Tororo Hills, Uganda. *Mineralogical Magazine*, 35, 363-378.

Tyler, R.C. & King, B.C. (1967): The pyroxenes of the alkaline igneous complexes of eastern Uganda. *Mineralogical Magazine*, 36, 5-21.

Udas, G.R. (1971): Fenitisation of basalts and associated dolerites in the Amba Dongar carbonatite alkalic complex. **Studies in the Earth Sciences; a volume in honour of W.D.West** (Murty, J.V.V.G.R.K., ed.). Todays and Tomorrow's Publishers, Delhi, India, 617-627.

Ulrych, J., Povondra, P., Pivec, E., Rutšek, J. & Sitek, J. (1994): Compositional evolution of metasomatic garnet in melilitic rocks of the Oseçnà complex, Bohemia. *Canadian Mineralogist*, 32, 637-647.

Vartiainen, H. & Woolley, A.R. (1976): The petrography, mineralogy and chemistry of the fenites of the Sökli carbonatite intrusion, Finland. *Geological Survey of Finland, Bulletin*, 280, 1-87.

Viladkar, S.G. (1980): Fenitized aureole of the Newania carbonatite, Rajasthan. *Geological Magazine*, 117, 285-292.

------- (1981): The carbonatites of Amba Dongar, Gujarat, India. *Geological Society of Finland Bulletin*, 53, 17-28.

------- (1984): Alkaline rocks associated with the carbonatites of Amba Dongar, Chhota Udaipur, Gujarat, India. *Indian Mineralogist*, Sukheswala Volume, 130-135.

------- (1986): Fenitization at the Amba Dongar carbonatite-alkalic complex, India. *Proceedings NEMIRAM (New Minerals and Raw Materials) Symposium* (Gabriel, M., ed.), Czechoslovakia, 170-189.

------- (1991): Phlogopitization at Amba Dongar Carbonatite Alkalic Complex, India. *Neues Jahrbuch für Mineralogie, Abhandlungen*, 162(2), 201-213.

------- & Avasia, R.K. (1992): Pyroxenes from alkaline rocks of the Chhota Udaipur carbonatite-alkalic province, Gujarat, India. *Journal of the Geological Society of India*, 39, 313-319.

------- & Dulski, P. (1986): Rare earth element abundances in carbonatites, alkaline rocks and fenites of the Amba Dongar complex, Gujarat, India. *Neues Jahrbuch für Mineralogie, Montashefte*, 1, 37-48.

------- & Wimmenauer, W. (1992): Geochemical and petrological studies on the Amba Dongar carbonatites (Gujarat, India). *Chemie der Erde*, 52, 277-291.

Woolley, A.R. (1982): A discussion of carbonatite evolution and nomenclature, and the generation of sodic and potassic fenites. *Mineralogical Magazine*, 46, 13-17.

------- & Kempe, D.C. (1989): Carbonatites: nomenclature, average chemical compositions, and element distribution. *In* **Carbonatites: Genesis and Evolution** (Bell, K., ed.). Unwin Hyman, London, 1-14.

Yellur, D.D. (1968): Carbonatite complex as related to the structure of the Narmada valley. *Journal of the Geological Society of India*, 9, 118-123.

Chapter 3:

ORIGIN OF THE GLIMMERITE SELVAGE BETWEEN CARBONATITE VEINS AND ALKALINE VOLCANIC AND PLUTONIC ROCKS OF THE AMBA DONGAR CARBONATITIC-ALKALINE COMPLEX, GUJARAT, INDIA

Jeanette N. Roelofsen, Robert F. Martin[1] and David R. Veblen[2]

[1] Department of Earth and Planetary Sciences,
McGill University,
3450 University Street,
Montreal, Quebec, H3A 2A7

[2] The Morton K. Blaustein Department of Earth and Planetary Sciences,
The Johns Hopkins University,
3300 N. Charles Street,
Baltimore, Maryland 21218

Prologue

In the previous paper, it was noted that sodic fenitization and crystallization of aegirine-augite and albite was followed by potassic fenitization and crystallization of K-feldspar, biotite, and in some samples, fluor-richteritic amphibole. Viladkar (1986, 1991) suggested that the biotite that forms the glimmerite of the Amba Dongar carbonatitic-alkaline complex at the contact between carbonatite veins and sodi-potassic fenite or nephelinite, formed at the expense of aegirine-augite. Previous work on other complexes suggests either a similar mode of formation for the mica in glimmerite (Verschure & Maijer, 1984) or its formation at the expense of K-feldspar (Andersen, 1989). Chapter 3 presents the results of a detailed investigation of glimmerite from the Amba Dongar complex, in order to ascertain the origin of the mica and, at the same time, of the glimmerite, and to determine their relationship to the associated fluorite deposit. Fine-scale examination of the glimmerite mica was performed through transmission electron microscopy, with AEM used to determine the compositions of minute regions that had been identified through HRTEM.

References

Andersen, T. (1989): Carbonatite-related contact metasomatism in the Fen complex, Norway: effects and petrogenetic implications. *Mineralogical Magazine*, 53, 395-414.

Verschure, R.H. & Maijer, C. (1984): Pluri-metasomatic resetting of Rb-Sr whole-rock systems around the Fen peralkaline-carbonatitic ring-complex, Telemark, South Norway. *Terra Cognita*, 4, 191-192.

Viladkar, S.G. (1986): Fenitization at the Amba Dongar carbonatitic-alkalic complex, India. *Proceedings NEMIRAM (New Minerals and Raw Materials) Symposium* (Gabriel, M., ed.), Karlovy Vary, Czechoslovakia, 170-189.

------- (1991): Phlogopitization at Amba Dongar carbonatite alkalic complex, India. *Neues Jharbuch für Mineralogie. Abhandlungen*, 162, 201-203.

Abstract

Glimmerite, a type of contact fenite composed predominantly of mica, forms a rim at the edge of carbonatite veins that cut alkaline volcanic or plutonic rocks in the Amba Dongar carbonatitic-alkaline complex, Gujarat, India. These micaceous regions have been examined at a fine scale with transmission electron microscopy (TEM) to determine the origin and alteration of the mica. The results show that the mica evolved in three stages: 1) igneous, 2) metasomatic, and 3) hydrothermal. The first stage involved crystallization of phlogopite in a Si- and Al-depleted environment (the carbonatitic magma), which led to the incorporation of Fe^{3+} in the tetrahedral site of the mica structure in amounts reaching up to 0.25 atoms per formula unit. Such mica displays reverse pleochroism. A second generation of mica (biotite) was formed through Mg- and, to a lesser extent, K- or Fe-metasomatism of aegirine-augite and K-feldspar, respectively, and as a rim on the earlier phlogopite. Reaction of the metasomatic fluid with the surrounding wall-rocks produced a fluid sufficiently Al- and Si-rich for biotite to crystallize. This event was preceded, at a higher temperature, by an episode of Na-metasomatism or by reaction with the last vestiges of magma, and resulted in the formation of an aegirine-rich rim on aegirine-augite phenocrysts or complete replacement by aegirine-augite near the vein. Later hydrothermal alteration, related to formation of the fluorite deposit, resulted in oxidation, vermiculitization, exfoliation and dissolution of both micas. Inclusions of hematite, silica and ankerite formed from Fe^{3+}, Ti, Si, Mn, Fe^{2+} and Mg released during the alteration of the mica, and from Ca and HCO_3^- which were introduced with the solution. The magmatic and postmagmatic processes involved in formation and evolution of the glimmerite from the Amba Dongar carbonatitic-alkaline complex may by implication be applied to those from other carbonatitic-alkaline complexes.

Introduction

Glimmerite, a mica-dominated metasomatic rock, commonly results by contact fenitization, whereby a host rock is modified by reaction with a fluid phase exsolved from an alkaline magmatic source, such as a carbonatite. The fluid phase acts as a medium

through which constituents are added or removed by reaction with the protolith to form new minerals, with which it is in equilibrium. Biotite formed at the expense of a precursor like pyroxene is an example of such an interaction. The final concentration of each element and resultant mineralogy of the rock are dependent on the composition of the protolith and of the fenitizing fluid, and on temperature of reaction (Le Bas, 1981; Woolley, 1982; Rubie & Gunter, 1983). In this paper, a model is presented for the multistage evolution of glimmerite associated with the Amba Dongar carbonatitic-alkaline complex.

Glimmerite associated with basic and ultrabasic rocks and carbonatite provides an excellent example of localized fenitization. Morbidelli et al. (1986), Gaspar & Wyllie (1987) and Andersen (1989) provided a detailed description of the textures and reported on the compositional variation of glimmerite from the Jacupiranga carbonatite complex, in Brazil, and the Fen carbonatitic-alkaline complex, in Norway, respectively, on the basis of optical examination and results of electron-microprobe analyses. More recently, Brigatti et al. (1996) studied the reversely pleochroic mica from these complexes through single crystal X-ray diffraction and Mössbauer spectroscopy. Mica from glimmerite commonly is of sufficiently fine grain-size, or contains mixed layers or minute inclusions of other minerals, that electron microscopy is the most appropriate technique for investigation (e.g., Gilkes & Suddhiprakarn, 1979; Bisdom et al., 1982; Veblen & Ferry, 1983; Banfield & Eggleton, 1988; Fordham, 1990; Pozzuoli et al., 1992). TEM is applied in this paper to suggest an origin for the mica from the glimmerite.

Geological Setting

The late Cretaceous to early Tertiary (Deans et al., 1973), 30-km^2 Amba Dongar carbonatitic-alkaline complex is located approximately 400 km northeast of Bombay, north of the Narmada River, in Gujarat State, India (Crookshank, 1936; Yellur, 1968; Fig. 1A). It is composed of carbonatite ring-dykes and breccia, and later plugs of calcite to ankerite carbonatite, which all cross-cut the surrounding Bagh sandstone (and intercalated limestone), coeval alkaline volcanic and plutonic rocks, and Deccan flood basalts (Viladkar, 1981, 1984; Gwalani et al., 1993; Fig. 1B). Sethna & Borges (1981), Viladkar (1981) and Gwalani et al. (1993) noted that plugs of tinguaite, nephelinite, tephrite, phonotephrite and

Figure 1A. Geographic location of the Amba Dongar carbonatitic-alkaline complex, Gujarat, India (after Viladkar, 1981).

B. Geological map of the complex showing the various units that comprise it and its environs (after Deans et al., 1973; Viladkar, 1984).

C. Map of the upper portion of the complex (near the fluorite mine) showing the locations of the various samples of glimmerite examined for this study (after Viladkar, 1986).

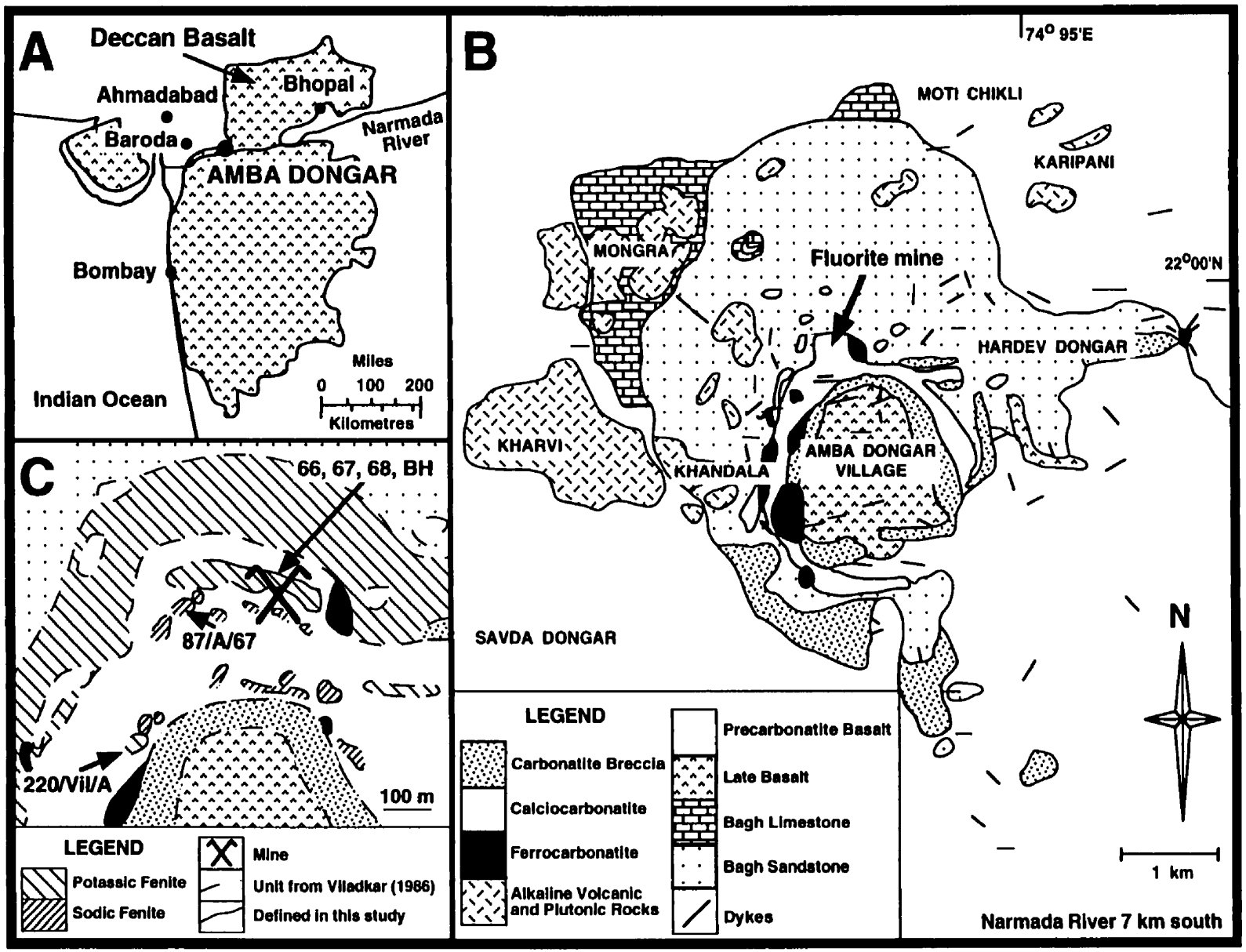
A
Deccan Basalt
Ahmadabad
Bhopal
Baroda
Narmada River
AMBA DONGAR
Bombay
Indian Ocean
Miles
0 100 200
Kilometres
B
74° 95'E
MOTI CHIKLI
KARIPANI
MONGRA
Fluorite mine
22°00'N
HARDEV DONGAR
KHARVI
KHANDALA
AMBA DONGAR VILLAGE
SAVDA DONGAR
N
1 km
Narmada River 7 km south
C
66, 67, 68, BH
87/A/67
220/Vil/A
100 m
LEGEND
Potassic Fenite
Sodic Fenite
Mine
Unit from Viladkar (1986)
Defined in this study
LEGEND
Carbonatite Breccia
Calciocarbonatite
Ferrocarbonatite
Alkaline Volcanic and Plutonic Rocks
Precarbonatite Basalt
Late Basalt
Bagh Limestone
Bagh Sandstone
Dykes

ijolite surround the complex. Furthermore, Viladkar (1981) suggested that basalt at the center of the complex is post-Deccan in origin. The northeastern sector of the complex contains one of the largest fluorite mines in Asia (11.6 million tonnes at 30% CaF_2; Deans et al., 1972). Deans & Powell (1968), Simonetti & Bell (1995) and Palmer & Williams-Jones (1996) suggested that the deposit was produced by mixing of F-rich fluids derived from the carbonatite with Ca-bearing meteoric fluids. Recently, Palmer & Williams-Jones (1996), primarily from a study of fluid inclusions in fluorite, inferred that this fluid was low temperature (<180°C), of low-salinity and acidic (pH<3.5).

This complex is also famous for its potassic (and sodic) fenites developed at the expense of essentially pure quartzite (Deans et al., 1973; Viladkar, 1986), although glimmerite is also present at the contact between calciocarbonatite veins and nephelinite or sodi-potassic fenite (Viladkar, 1991). Viladkar (1991) attributed the origin of the biotite- or phlogopite-rich glimmerite to potassic fenitization of a sodi-potassic fenite or nephelinite, respectively, as it was noted that the Mg:Fe ratio of the mica was dependent on that of the precursor pyroxene.

Methodology

Wavelength-dispersion spectrometry (WDS) analyses of mica were performed on a JEOL JXA 8600 Superprobe electron microprobe operated with Tracor Northern software at the Johns Hopkins University (JHU). The instrument was operated at 15 kV with a defocussed beam (10 μm), and with a CITZAF correction. The following standards were used: albite (Na), orthoclase (K), enstatite (Mg), rhodonite (Mn), fayalite (Fe), chromite (Cr), anatase (Ti), benitoite (Ba), fluorphlogopite (F) and anorthite (Ca, Si and Al). The lack of a suitable Rb standard precluded WDS analyses for this element. Collection times were 60 seconds or until 0.5% precision was attained (K and Si), except for F and Ba, for which counts were collected for 120 seconds. Formulae of the mica were calculated on the basis of 11 anions and seven cations, excluding the interlayer site, with the proportion of Fe^{3+} estimated by charge balance (i.e., the mica is considered to be perfectly trioctahedral; the potential errors of this technique are mentioned in the discussion). Zonation and mineral relationships of the mica were imaged on a JEOL JSM-840 scanning electron microscope

(SEM) at McGill University. Energy-dispersion spectrometry (EDS) analyses of carbonates and hematite were performed with a Link spectrometer attached to this SEM.

TEM samples were prepared by ion-thinning 2.3 mm Cu or 3.0 mm C grids, which had been glued to thin sections prepared with either Crystalbond® or bees' wax and removed by heating on a hot plate. The samples were then ion-thinned on a Gatan dual ion mill (model 600) with Ar guns tilted at 17°. For the final stage of ion-thinning, the mill was operated at 6 keV, 1 mA or 0.5 mA, and a tilt of 12°. The sample was subsequently C-coated.

TEM work was conducted by high resolution TEM (HRTEM), selected area electron diffraction (SAED) and analytical electron microprobe (AEM) with a Philips EM420 at JHU, operated with an accelerating voltage of 120 keV. Standardless AEM analyses were performed with a Li-drifted silicon detector. Independent analyses of standards of known composition (Bayan fayalite or Willsboro diopside) were also obtained to aid in the quantification of the analytical results. Element concentrations were calculated with the program DTSA (Desk-Top Spectral Analysis; Fiori et al., 1994). The estimated error in these analyses is approximately 4% of the measured values. The major drawback of AEM analyses is that an overlap between $F_{K\alpha}$ and Fe_L precludes determination of the F content. Thus, mineral formulae were calculated on the basis of 11(O + OH^-); the Fe^{3+} content could not be calculated in the case of AEM data.

Description of the Precursor and Glimmerite

Glimmerite occurs at the contact between carbonatite and alkaline volcanic (phonolite, nephelinite, phonotephrite and tephrite) and plutonic (ijolite and urtite) rocks of the Amba Dongar complex. It is common in the southern part of the fluorite mine, but also was noted at depth (in drill core).

Unmetasomatized alkaline volcanic rocks are typically dark greenish grey in hand specimen and contain coarse- to medium-grained phenocrysts of strongly zoned prismatic aegirine-augite (7-10 vol.%), altered blocky nepheline (12 to 15 vol.%), and andradite garnet (5 to 10 vol.%) showing oscillatory or, rarely, normal zoning, with ubiquitous fine-grained apatite (3 vol.%) and rare twinned titanite in an aphanitic groundmass. One sample

also contains phlogopite phenocrysts. The aegirine-augite is zoned from an embayed, light green to colourless core to a green rim showing oscillatory zoning (Chapter 2; Rock et al., 1994). This same two-stage zonation is observed in apatite (Chapter 2). The fine-grained altered groundmass contains hematite, calcite, analcime, K-feldspar, nepheline and clay minerals. Remnants of volcanic glass were reported by Sethna (1989) and Gwalani et al. (1993). The related plutonic rocks contain the same minerals, but are coarser grained, and may contain anhedral alkali feldspar, nepheline and prismatic wollastonite (Chapter 2). Their porphyritic nature implies subvolcanic crystallization. Veins of pink syenite (1 cm to 0.5 m in width), and, in one case, a dike of melteigite, were noted to cut these rocks. All such veins contain comb-textured pyroxene at the margin with orthoclase feldspar, hematite, and, in some cases, pyrite and chalcopyrite concentrated at the core (Chapter 2).

At the surface in the complex, the phenocrysts are weathered. This produces a blue-green or dusty pink appearance to the nepheline caused by the presence of analcime, calcite and fine-grained hematite (all identified by XRD), respectively. Pyroxene, wollastonite, garnet and titanite are also replaced by variable proportions of hematite ± calcite and clay minerals.

Fenitization of the alkaline rocks typically produced a 15-cm-wide halo along the calcite carbonatite veins (0.5 to 5 cm wide), which culminated in formation of glimmerite at vein margins (Fig. 2). This halo can be divided, by pyroxene and mica content, into seven successive zones (A to G; Fig. 3). The pyroxene from Zone A, which shows a two-stage zonation from a colourless core to a green rim, becomes uniformly green (increased aegirine component) and unzoned (Zone B) veinward. K-feldspar occurs in the aphanitic groundmass or as interstitial grains. The amount of K-feldspar increases to a maximum of 5 to 7 vol.%, whereas that of nepheline decreases from 12 or 15 vol.% to nil in the interval between Zones A and C. Some of the feldspar appears primary, however it is difficult to ascertain exactly what the precursor of the majority of the feldspar was. It could represent the felsic fraction in the fine-grained groundmass or phenocrysts. Minor, fine-grained mica (<5 vol.%) is associated with aegirine and feldspar in Zone B. Between Zones B to E, there is an increase in the proportion of mica at the expense of the pyroxene and, possibly, of K-feldspar (Fig. 4A). Zone C contains fine-grained mica (biotite) with minor apatite, hematite and rare relict pyroxene. All aegirine and K-feldspar are replaced by mica in Zone D, which

Figure 2. Sample of fenitized nephelinite showing the micaceous glimmerite rims (0.5 cm; dark) adjacent to reddish calcite carbonatite veins. The upper arrow points to an altered phenocrysts of nepheline, while the lower one points to the glimmerite.

CENTIMETRE

Figure 3. Schematic diagram of the halo (15 cm) developed in the protolith near calcite carbonatite veins (0.5 to 5 cm wide). Zones A to E represent increasing degrees of metasomatism based on changes in the mafic mineralogy. These zones are: A) euhedral, zoned aegirine-augite in the protolith, B) green, anhedral aegirine-augite, with minor amounts of biotite and oxides present along the cleavages and rimming the aegirine-augite, C to E), the relative amount of mica increases and that of aegirine-augite decreases. Grain-size of the mica and relative size of the reversely pleochroic mica core increase toward the carbonatite vein, F) coarse-grained mica with a reversely pleochroic core in the vein, and G) calciocarbonatite vein.

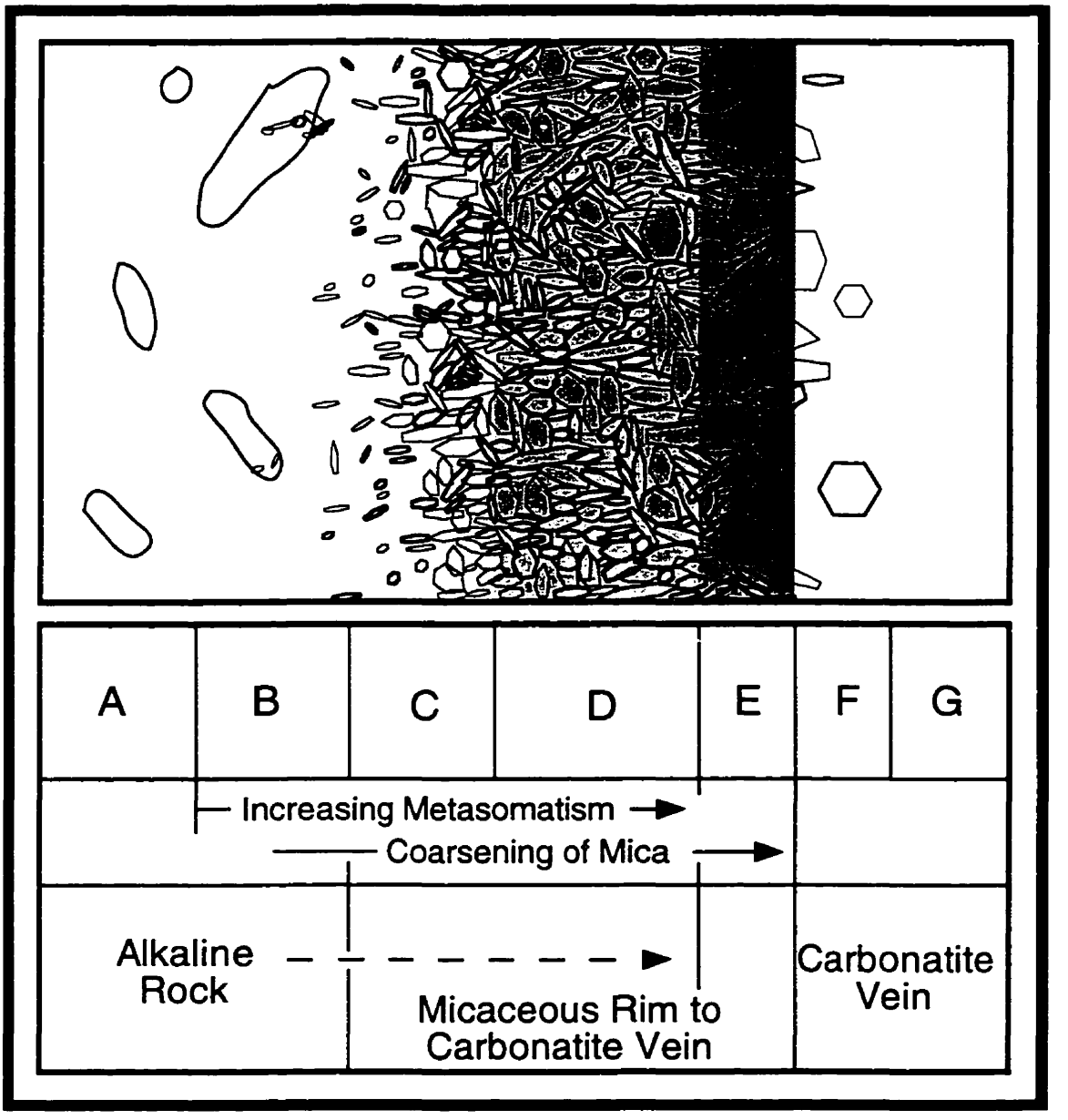
A
B
C
D
E
F
G
Increasing Metasomatism
Coarsening of Mica
Alkaline Rock
Micaceous Rim to Carbonatite Vein
Carbonatite Vein

Figure 4. Examples of the textures in glimmerite.

A. Biotite (bio) replacement of green, anhedral aegirine-augite (aeg) on the margins and along the cleavages. At the bottom of the image is a late calcite vein, another occurs at the contact between calcite from the carbonatite and the mica (width of field of view: 0.5 cm).

B. Photograph of a 4-mm grain of mica from near the calciocarbonatite vein in plane-polarized light. Note the greenish brown normally pleochroic rim (biotite; bio) and the foxy red, reversely pleochroic core (phlogopite; phl) separated by a narrow zone containing more hematite. Colourless regions are also present in the core. "Bullets" of hematite and inclusions of calcite are concentrated along the cleavages of both types of mica. Kinking (at the tip of the white arrow) is evident throughout the crystal, and the whole grain is cross-cut by a vein of calcite.

C. Magnified image of the upper portion of the grain depicted in Figure 4B, with the stage rotated at 90°, which shows the green pleochroism (darker) of the vermiculite-rich regions in the pale orange (light) reversely pleochroic mica. The calcite inclusions (cal) have anhedral cores surrounded by a columnar rims, and the hematite "bullets" are more obvious (width of field of view: 2 mm).

bio
cal
aeg
A
bio
phl
B
cal
C

also contains hematite and apatite. Reversely pleochroic orange-red to pale orange phlogopite cores appear in the mica in Zone D as the mica coarsens. The point at which carbonate is first observed is Zone E. Zone F corresponds to the interval over which the carbonate content is greater than that of the mica and extends to where mica is absent. The glimmerite layer (1/10 the thickness of the halo) occurs between Zones C and F. It consists of 86 vol.% fine- to medium-grained, brown to greenish brown biotite, 10 vol.% hematite, 5 vol.% calcite and 7 vol.% colourless apatite along the veins. Between Zones E and F, the grain-size of mica increases to a maximum of 0.5 cm as the amount of apatite and size of the reversely pleochroic cores increase. The maximum grain-size of the mica and relative proportion of reversely pleochroic cores occurs in Zone F, which is along the calcite carbonatite veins. Veinlets (to 2 mm) of calcite and <0.2 mm colourless phyllosilicate grains cut these last two zones. The calcite carbonatite veins correspond to Zones F and G.

Coarse-grained mica in Zones E and F contains a core of reversely pleochroic phlogopite (60-75 vol.% of the mica) surrounded by a rim of normally pleochroic biotite in a topotactic relationship (Fig. 4B). Here, reverse pleochroism refers to a reversal in the normal pleochroic scheme where the strongest direction of absorption lies parallel to the cleavage. This mica is altered along the cleavage to a phyllosilicate, possibly vermiculite, which exhibits colourless to green pleochroism and normal birefringence (Figs. 4B, C). These composite phyllosilicate grains are kinked through both types of mica. The sharp contact between the core and rim is accentuated by numerous grains of an equant <0.1 mm black oxide (formerly magnetite, now replaced by hematite; Figs. 4B, C). The sharp contact between the two types of mica and presence of hematite at their contact suggests overgrowth after a hiatus in crystallization. Mild kinking followed.

Hematite and calcite form elongate inclusions, generally <0.5 cm in length, that lie parallel to the cleavage of the reversely pleochroic mica (Fig. 4C). These carbonate inclusions contain a core of fine-grained, polygranular, randomly oriented calcite surrounded by a rim of columnar, <0.1 mm Mn-rich calcite (to 2.0 wt.% MnO by EDS) that is oriented perpendicular to the mica's cleavage. Relatively rare, small calcite veins (up to 0.2 mm in width) cross-cut this coarse mica (Fig. 4C).

Compositional Variation of the Minerals

Aegirine-augite

The phenocrysts of aegirine-augite of Zone A in alkaline volcanic and plutonic rock consist of a complexly zoned, embayed, diopside- and hedenbergite-rich core overgrown by a green, more aegirine-rich (up to 45% Ae) pyroxene showing oscillatory zoning (Type-2 aegirine-augite in Chapter 2; Rock et al., 1994). This evidence of two-stage growth is also observed in apatite from this zone, and in mica from the glimmerite. In Zone B, these phenocrysts are no longer zoned (Type-1), but are more aegirine-rich (>65% Ae).

Hematite, Apatite and Carbonates

Apatite in glimmerite displays a two-stage zonation like that from the mica, where the rim is enriched in Sr, REE, F and Na relative to the core. Analyses of the complexly zoned cores show low totals, which suggest a carbonate component. In addition, EDS analysis of hematite and ankerite both indicate an enrichment in Mn (<0.5 and 2.4 wt.% MnO, respectively; Chapter 2; Appendix A-9). Hematite also may contain <0.5 wt.% TiO_2 and Cr_2O_3. Moreover, ankerite is enriched in Sr (to 0.3 wt.% SrO), whereas calcite is near end-member.

Mica

Calculated formulae of mica from Zones C to F, as determined from electron-microprobe results, are presented in Table 1. The compositional data shows that the mica is either biotite or phlogopite. Three populations are delineated: 1) cores of reversely pleochroic phlogopite (Zones E, F and in part in D); 2) rims of normally pleochroic biotite (Zones C to E); and 3) phlogopite phenocrysts from nephelinite (Zone A; Fig. 5). The first two types of mica are F-rich (up to 1.09 apfu F) compared to the last type. None contain detectable Cl. They are enriched in Mn and Ti (up to 0.09 Mn and 0.24 Ti atoms per formula unit, apfu), contain minor Ca, Cr and Ba (<0.02 apfu) and less than 0.08 apfu Na. Some mica grains, generally reversely pleochroic mica in glimmerite, contain higher-than-normal Ca (up to 0.4 wt.% CaO), elevated Fe (1-2 wt.% FeO) and slightly elevated Si (by

Table 1. Selected electron-microprobe analyses and calculated mineral formulae for mica.

Sample #	54B1	66B	87/A/67.1	BH/18/2	BH/18/2	BH/18/2	BH/18/2	BH/18/2	BH/18/2
Description	Normal	Normal	Normal	Normal	Normal	Rev. lt	Rev. dk	Rev. lt	Rev. dk
SiO_2	37.86	39.13	41.38	41.00	39.97	41.18	41.49	41.85	41.51
TiO_2	3.92	1.71	1.01	0.94	2.13	0.61	0.59	0.65	0.73
Al_2O_3	13.57	10.77	10.62	10.75	11.41	9.32	9.15	10.53	10.07
Cr_2O_3	0.13	0.02	0.03	0.02	0.02	0.02	0.03	0.01	0.02
Fe_2O_3	0.00	0.00	0.00	0.00	0.00	1.81	1.94	1.11	1.08
FeO	12.08	16.66	15.12	12.66	13.80	8.15	7.10	7.15	7.19
MnO	0.17	1.41	0.88	0.56	0.51	0.18	0.19	0.16	0.16
MgO	18.40	16.05	16.80	19.40	17.90	23.23	24.01	23.69	23.75
CaO	0.04	0.18	0.11	0.10	0.01	0.00	0.01	0.12	0.05
BaO	0.30	0.01	0.01	0.06	0.00	0.03	0.05	0.04	0.04
Na_2O	0.19	0.15	0.15	0.24	0.27	0.29	0.37	0.19	0.26
K_2O	9.97	9.76	9.20	10.10	10.19	10.21	10.11	9.63	9.88
F	1.10	2.32	2.69	3.57	3.07	3.21	3.29	2.70	2.76
H_2O	3.53	2.85	2.71	2.35	2.56	2.57	2.56	2.88	2.82
Total	101.26	101.02	100.71	101.75	101.84	100.81	100.88	100.70	100.31
F,Cl=O	0.46	0.98	1.13	1.50	1.29	1.35	1.39	1.14	1.16
Total	100.80	100.04	99.58	100.25	100.54	99.46	99.49	99.56	99.15

Table 1. Selected electron-microprobe analyses and calculated mineral formulae for mica (continued).

Sample #	54B1	66B	87/A/67.1	BH/18/2	BH/18/2	BH/18/2	BH/18/2	BH/18/2	BH/18/2
Description	Normal	Normal	Normal	Normal	Normal	Rev. lt	Rev. dk	Rev. lt	Rev. dk
Si	2.802	2.972	3.111	3.041	2.986	3.015	3.023	3.020	3.017
^{IV}Al	1.184	0.964	0.889	0.94	1.005	0.804	0.786	0.896	0.863
$^{IV}Fe^{3+}$	0.000	0.000	0.000	0.000	0.000	0.100	0.106	0.060	0.059
Ti	0.014	0.065	0.000	0.018	0.009	0.034	0.032	0.024	0.040
Σ Tetrahedral	4.000	4.000	4.000	4.000	4.000	3.953	3.947	4.000	3.979
^{VI}Al	0.000	0.000	0.052	0.000	0.000	0.000	0.000	0.000	0.000
Ti	0.204	0.033	0.057	0.034	0.111	0.000	0.000	0.011	0.000
Cr	0.008	0.001	0.002	0.001	0.001	0.001	0.002	0.001	0.001
$^{VI}Fe^{3+}$	0.000	0.000	0.000	0.000	0.000	0.000	0.000	0.000	0.000
Fe^{2+}	0.748	1.058	0.951	0.785	0.862	0.499	0.432	0.431	0.437
Mn	0.011	0.091	0.056	0.035	0.032	0.011	0.012	0.010	0.010
Mg	2.030	1.817	1.883	2.145	1.993	2.535	2.607	2.548	2.573
Σ Octahedral	3.000	3.000	3.000	3.001	3.000	3.047	3.053	3.001	3.021
Ca	0.003	0.015	0.009	0.008	0.001	0.000	0.001	0.009	0.004
Ba	0.009	0.000	0.000	0.002	0.000	0.001	0.001	0.001	0.001
Na	0.027	0.022	0.022	0.035	0.039	0.041	0.052	0.027	0.037
K	0.941	0.946	0.882	0.956	0.971	0.954	0.940	0.886	0.916
Σ Interlayer	0.981	0.983	0.913	1.000	1.011	0.996	0.994	0.923	0.958
F	0.258	0.557	0.640	0.838	0.725	0.743	0.758	0.616	0.635
OH	1.743	1.443	1.360	1.163	1.275	1.257	1.242	1.384	1.366
Fe/(Fe+Mg)	0.269	0.368	0.336	0.268	0.302	0.164	0.142	0.145	0.145
Σ Cations	7.980	7.983	7.913	8.000	8.011	7.996	7.994	7.923	7.958

Rev.=reverse; lt=light; dk=dark.

Figure 5. A plot of Fe/(Fe+Mg) (Fe#) versus ^{IV}Al showing the separation between phlogopite (core) and biotite (rim; classification of Deer et al., 1962). The mica compositions can be divided into three groups: 1) normally pleochroic biotite, predominantly (middle), 2) reversely pleochroic phlogopite, which exhibits both a lower Fe# and a lower level of ^{IV}Al (bottom left), and 3) phlogopite present in mica phenocrysts in nephelinite.

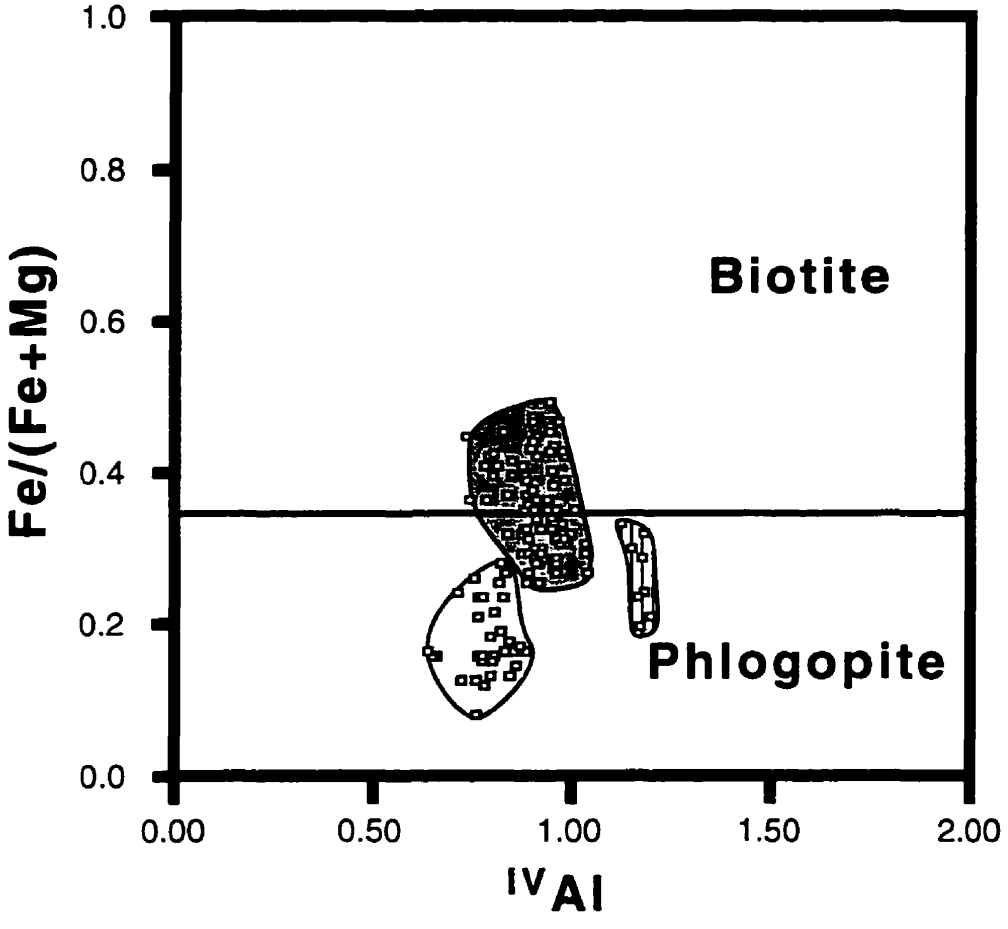
1.0
0.8
0.6
0.4
0.2
0.0
Fe/(Fe+Mg)
Biotite
Phlogopite
0.00
0.50
1.00
1.50
2.00
IVAl

0.5 wt.% SiO_2), suggesting the presence of minute inclusions of calcite, ankerite, hematite and silica.

A reduced occupancy of the interlayer site is reflected in the low K content (0.80 to 0.98 apfu K). The lack of full occupancy can only be partly accounted for by minor Rb (up to 0.02 apfu Rb as determined during reconnaissance EDS analysis), Ca, Na and Ba. In addition, reversely pleochroic mica is enriched in Na relative to normally pleochroic mica (Fig. 6A).

Beside Fe and Mg in the octahedral site, the mica from glimmerite (both the core and rim) contains Mn, Ti, Cr (traces) and Al. It is Mn- (up to 0.09 apfu) and Ti-enriched (up to 0.18 apfu; Fig. 6B), with the highest values occurring at the contact between the core of reversely pleochroic phlogopite and the rim of normally pleochroic biotite. Moreover, the reversely pleochroic phlogopite is depleted in Mn and Ti compared to the normally pleochroic biotite (Fig. 6B). The proportion of ^{IV}Al is generally low (<1.0 apfu), while that of ^{VI}Al is even less (0.00 to 1.01 apfu, with most values in the range of 0.00 to 0.20). Fe-F avoidance is exhibited primarily by reversely pleochroic mica, as F correlates negatively with Fe, but positively with Mg. Only reversely pleochroic phlogopite contains significant Fe^{3+} (up to 0.25 apfu). The inferred Fe^{3+} content of this mica decreases with increasing Ti (or Al) until the Ti content reaches 0.04 apfu (Fig. 6C). However, the highest Ti and Al contents, but lowest Mn and Si contents are restricted to phlogopite from the phenocrysts. Thus, phenocrysts of normally pleochroic phlogopite are compositionally distinct from the mica of glimmerite, which imply a different origin.

When insufficient Si and Al are present in the tetrahedral site of a mica, Fe^{3+} and Ti are assumed to be present in this site (refer to discussion). Thus, the low ^{IV}Al content of the phlogopite core compared the biotite rim and the phlogopite phenocrysts (Fig. 5) implies the presence of $^{IV}Fe^{3+}$ in the phlogopite core.

The elevated Ca, Fe and Si and reduced K contents of some mica from the glimmerite indicates the presence of minute inclusions of other minerals that influence its composition. None of the observed compositional variation of the mica appears to be related to the presence of relict pyroxene, as no replacement textures were observed during examination of the mica grains with scanning electron microscopy to select the regions for

Figure 6. Plots showing the compositional characteristics of normally pleochroic biotite (rim) and reversely pleochroic phlogopite (core) in glimmerite and normally pleochroic phlogopite in nephelinite.

A. A slight increase occurs in the Na content at the same Si content in the reversely pleochroic core compared to that of the normally pleochroic rim. The region to the left represents mica that occurs as a phenocryst phase in nephelinite.

B. Plot of Mn versus Ti concentration. The normally pleochroic rim mica seems to contain slightly more Mn and Ti than the reversely pleochroic core. Mica from the phenocrysts in nephelinite contains significantly more Ti and strikingly less Mn.

C. Plot of Fe^{3+} versus Ti concentration. Fe^{3+} is restricted to the reversely pleochroic mica, as normally pleochroic mica rim contains no detectable Fe^{3+}. The amount of Fe^{3+} in the reversely pleochroic mica decreases as that of Ti increases until 0.04 apfu Ti. The difference in Fe^{3+} and Ti content of the different magmas from which they crystallized (see text).

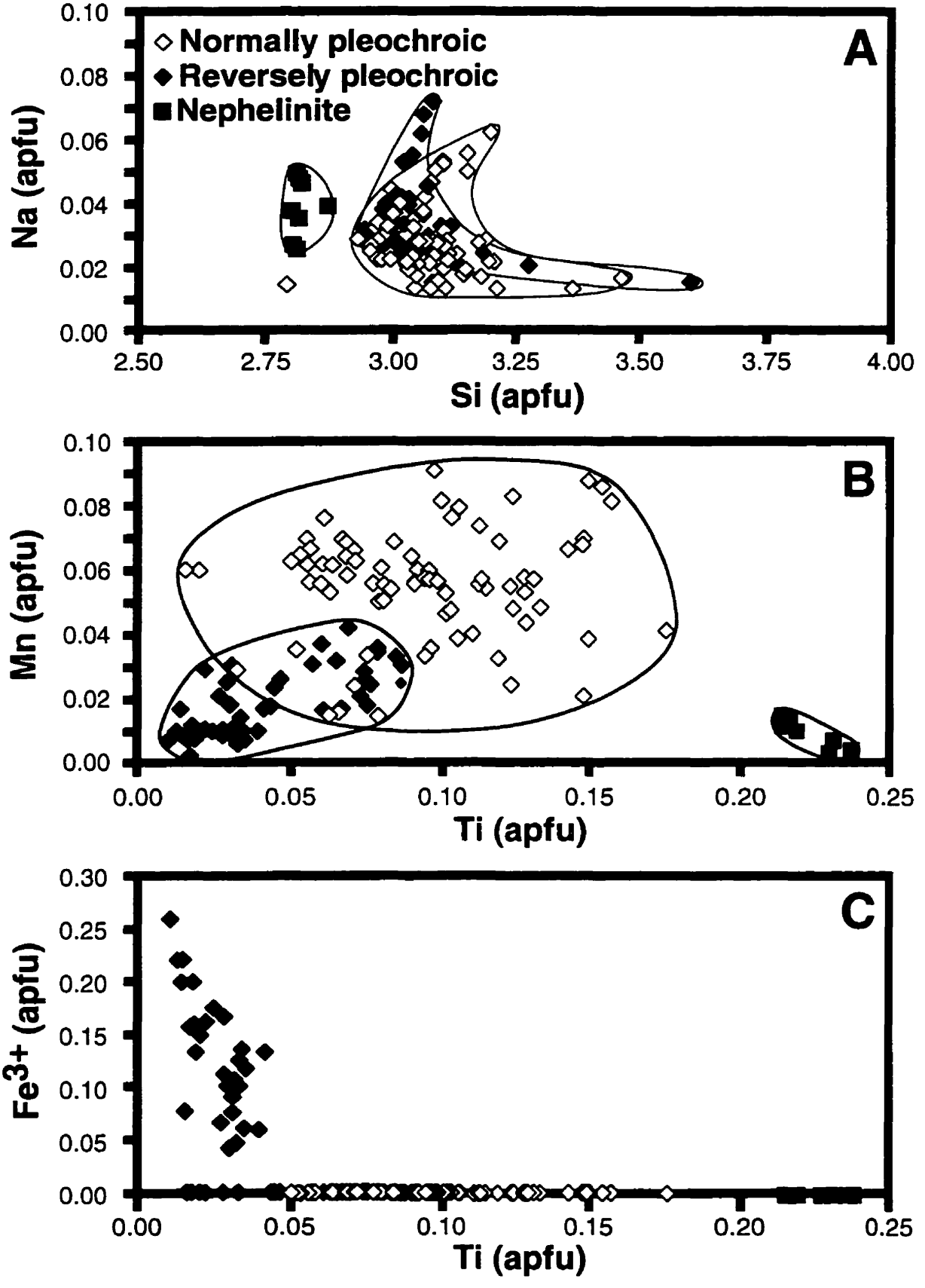
Normally pleochroic
Reversely pleochroic
Nephelinite
A
Na (apfu)
Si (apfu)
B
Mn (apfu)
Ti (apfu)
C
Fe3+ (apfu)
Ti (apfu)

analysis. The possible presence of minute inclusions of other minerals in the mica can only be verified by TEM.

TEM Observations

A HRTEM image of unaltered biotite shows the 10 Å (1 Å = 10^{-10}m) lattice fringe of mica along the *c* axis or (001) of the structure and is represented by the sequence of alternating light and dark lines (Fig. 7). Under the focus conditions used, the distance between consecutive light lines in the image represents the basal-spacing. In the SAED image (bottom of Fig. 7), this fringe is represented by the first spot along the c^* axis.

A direct contact between aegirine and mica could not be found in TEM examination, unlike that noted during optical examination. Juxtaposed aegirine-augite - biotite is commonly separated by K-feldspar, calcite or a clay mineral (Fig. 8). Furthermore, minor replacement of aegirine-augite by hematite and a smectite-group phase occurs along the cleavage. The presence of a clay mineral between the aegirine and biotite suggest that alteration may have obscured the original aegirine-augite - biotite interface.

HRTEM and SAED images reveal the presence of lattice fringes or peaks (in the direction of c^*) that correspond to vermiculite or chlorite (the lighter regions), and biotite (10 Å; Fig. 9A). Vermiculite is the most likely alteration, as the dark and light portions of the HRTEM image are equivalent (Figs. 9B and C; chlorite would produce unequal dark and light portions of the lattice fringes). Further proof for the presence of vermiculite is provided by XRD data, and preliminary examinations of these phyllosilicates after *n*-alkylammonium treatment. The XRD data were obtained with a Guinier-Hägg focussing camera using Cu$K\alpha_1$ radiation, and cell parameters of the phyllosilicate were determined using the program of Appleman & Evans (1973), as modified by Garvey (1986). The pattern obtained has a (060) spacing of 1.541 ± 0.002 Å, which is consistent with a slight increase in (060) relative to that of phlogopite or biotite caused by the presence of vermiculite. TEM examination of ultrathin samples that were pretreated with *n*-alkylammonium, according to the method proposed by Vali & Hesse (1992a, b), showed an expansion typical of that produced by vermiculite (Roelofsen et al., 1993).

Figure 7. HRTEM image of biotite, with arrows to show the regularly repeating 10 Å spacing of the mica along c^* [the (001) direction of the mica] represented by the distance between light lines in the image between tips of the arrows. The inset is a SAED pattern of the same area. Each spot on the pattern represents diffraction from a particular plane in the grain, and so, the 10 Å spacing along c^* is represented by the basal-spacing between the central electron beam and the first spot in the direction of the c^* axis. Also, a^* is approximately perpendicular to the c^* and lies to the bottom right of c^*.

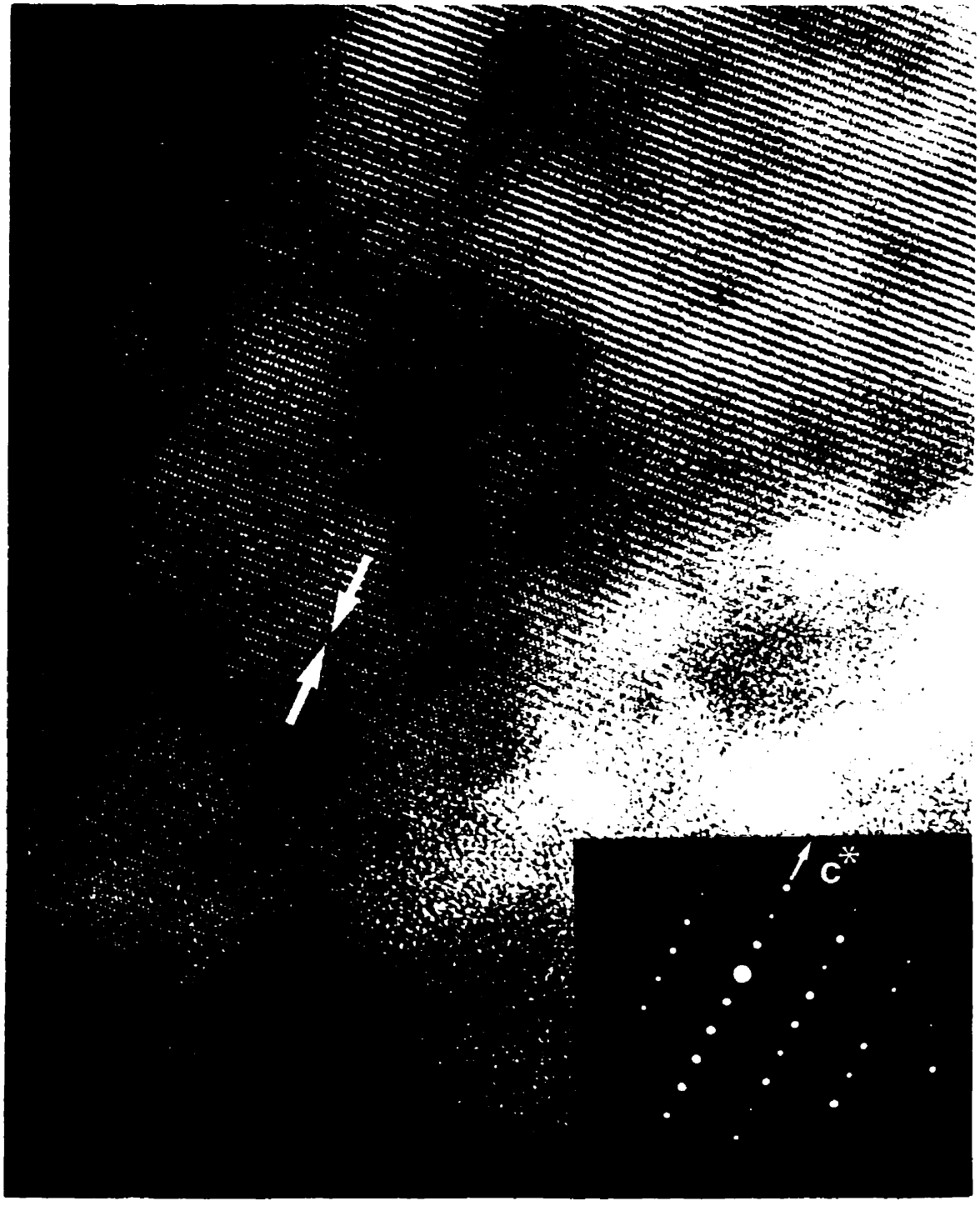
c*

Figure 8. Low-resolution TEM image of the aegirine-augite and biotite interface. The upper region, dominantly made of aegirine, is separated from the lower domain of phyllosilicate (biotite and vermiculite; phyllo) by calcite (cal) and hematite (the dark region; hem). The pyroxene (pyx) consists of a number of grains that show some alteration to smectite ± hematite (scale bar represents 0.5 μm).

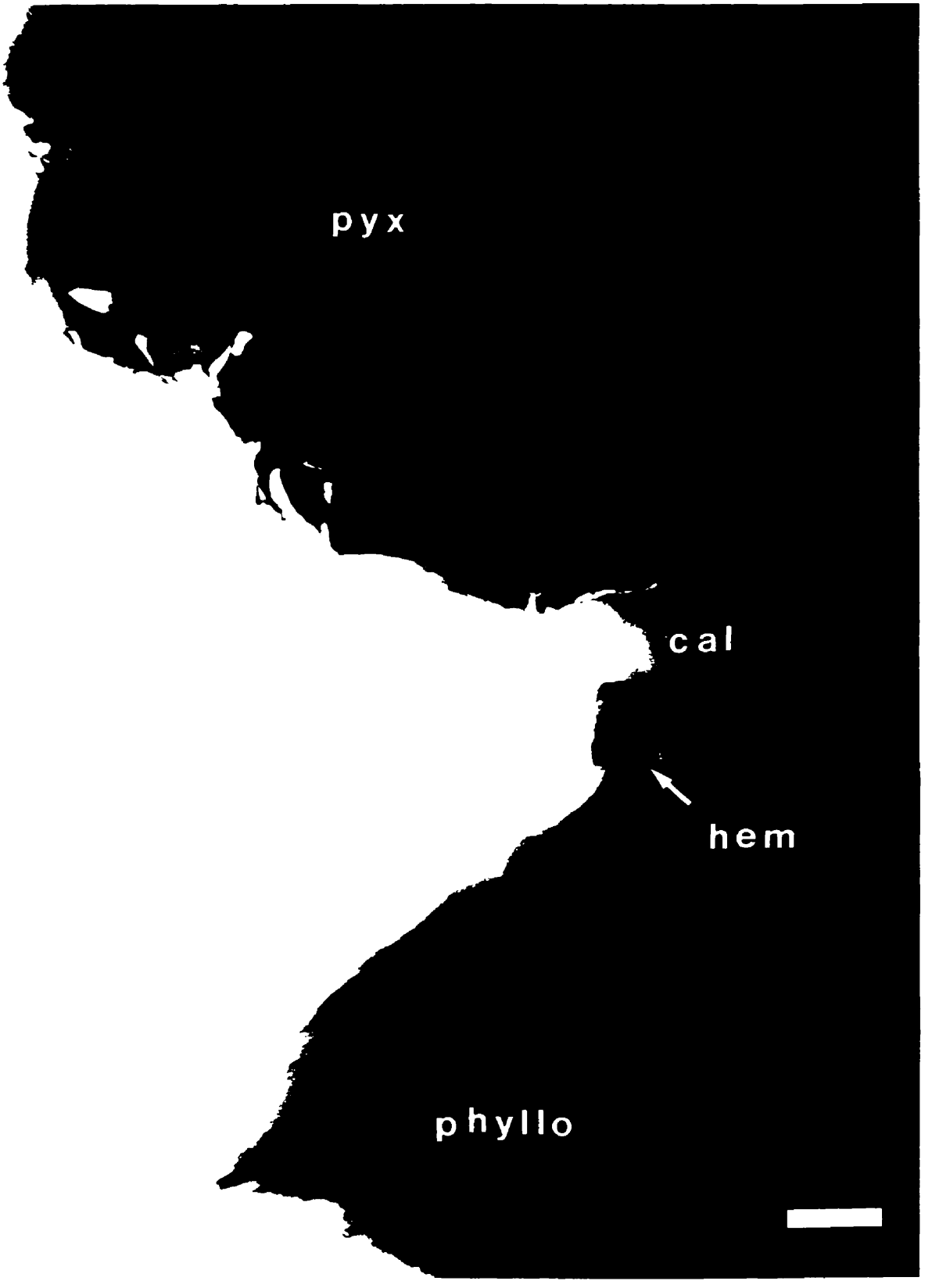
pyx
cal
hem
phyllo

Figure 9. Alteration of biotite to vermiculite.

A. SAED of vermiculitized biotite showing the extra spots in the mica pattern (m) produced by vermiculite (v; along c^*).

B. HRTEM image of the area represented by the SAED image (Fig. 9A). The vermiculite layers appear lighter (whiter; between the arrows) and wider than biotite (at the arrow). This region depicts a regularly repeating intergrowth of vermiculite and biotite (hydrobiotite).

C. Low resolution TEM image of Figure 9A showing numerous lighter layers of vermiculite in mica (scale of the image: 0.1 μm).

D. HRTEM image of one vermiculite layer in mica. Note the deformation of the mica structure to accommodate the termination of the vermiculite.

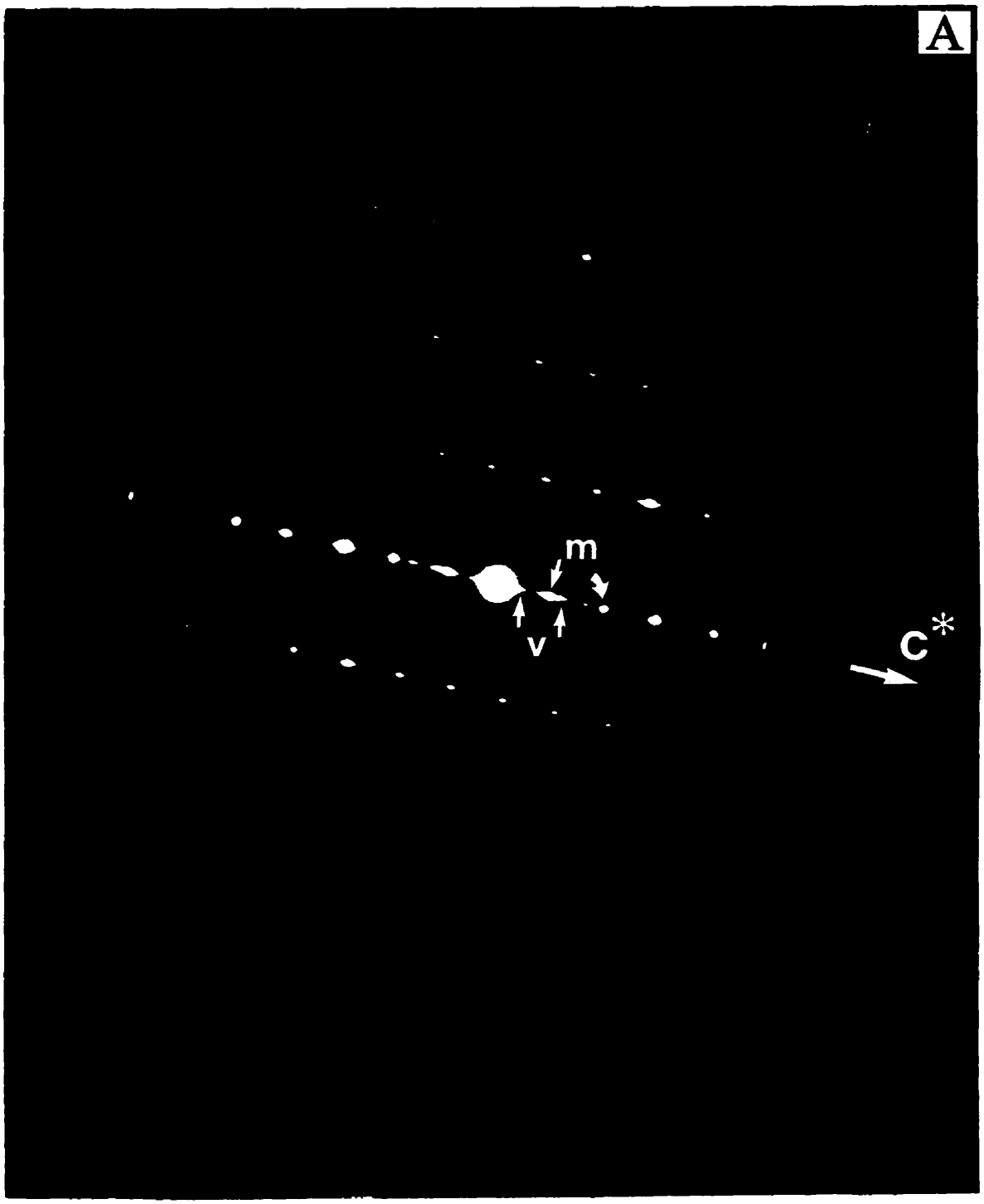
A
m
v
c*

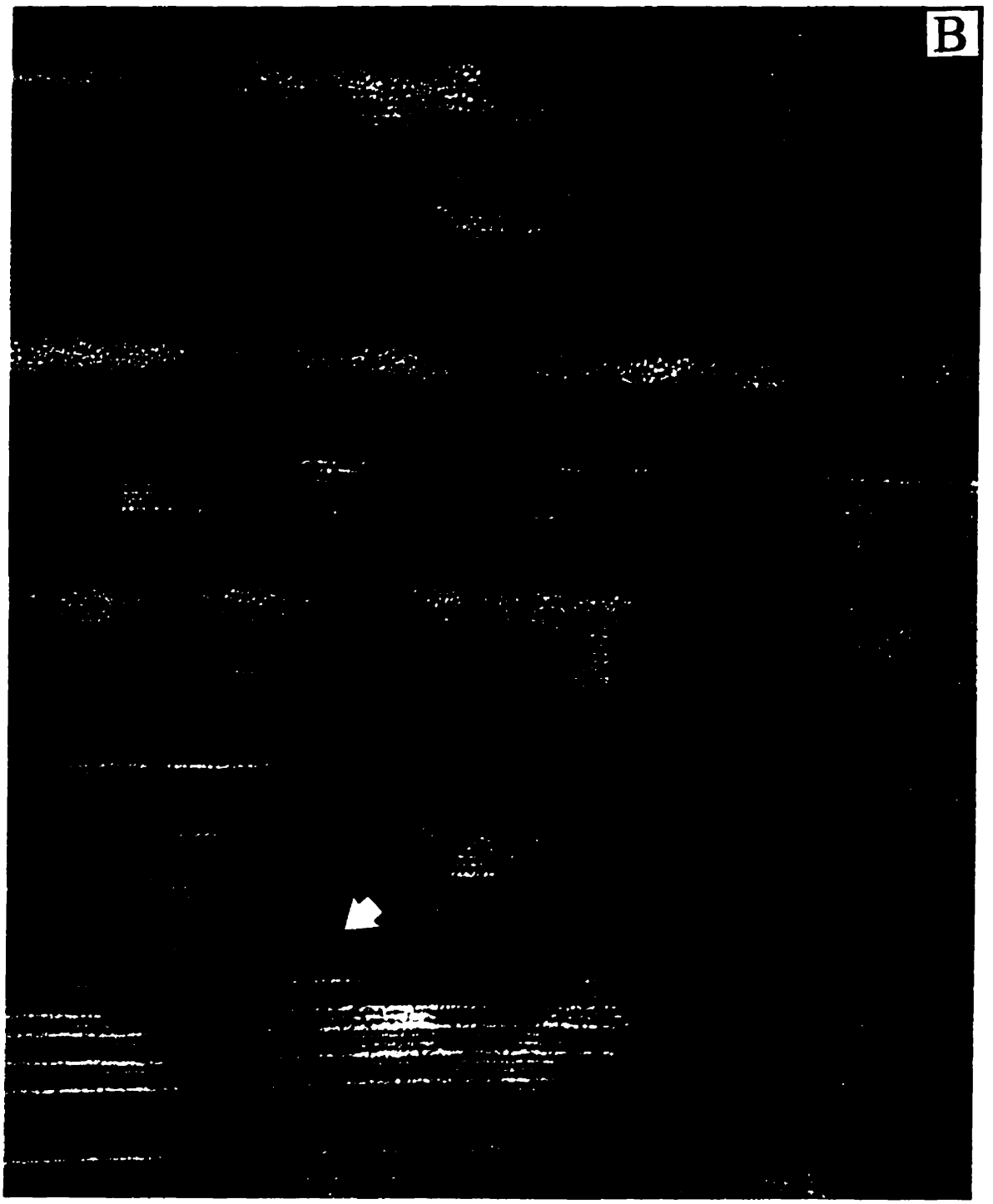
B

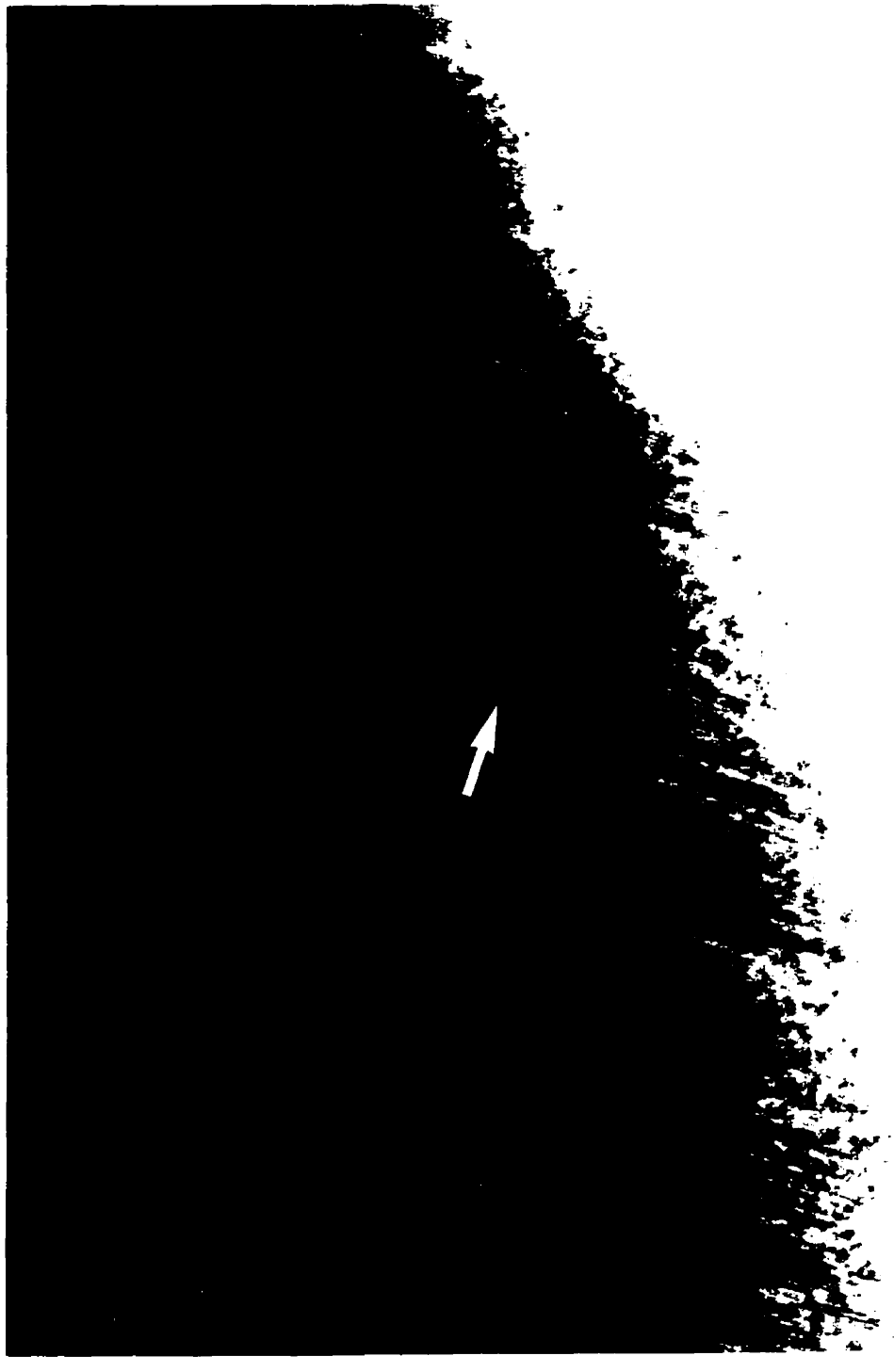

C

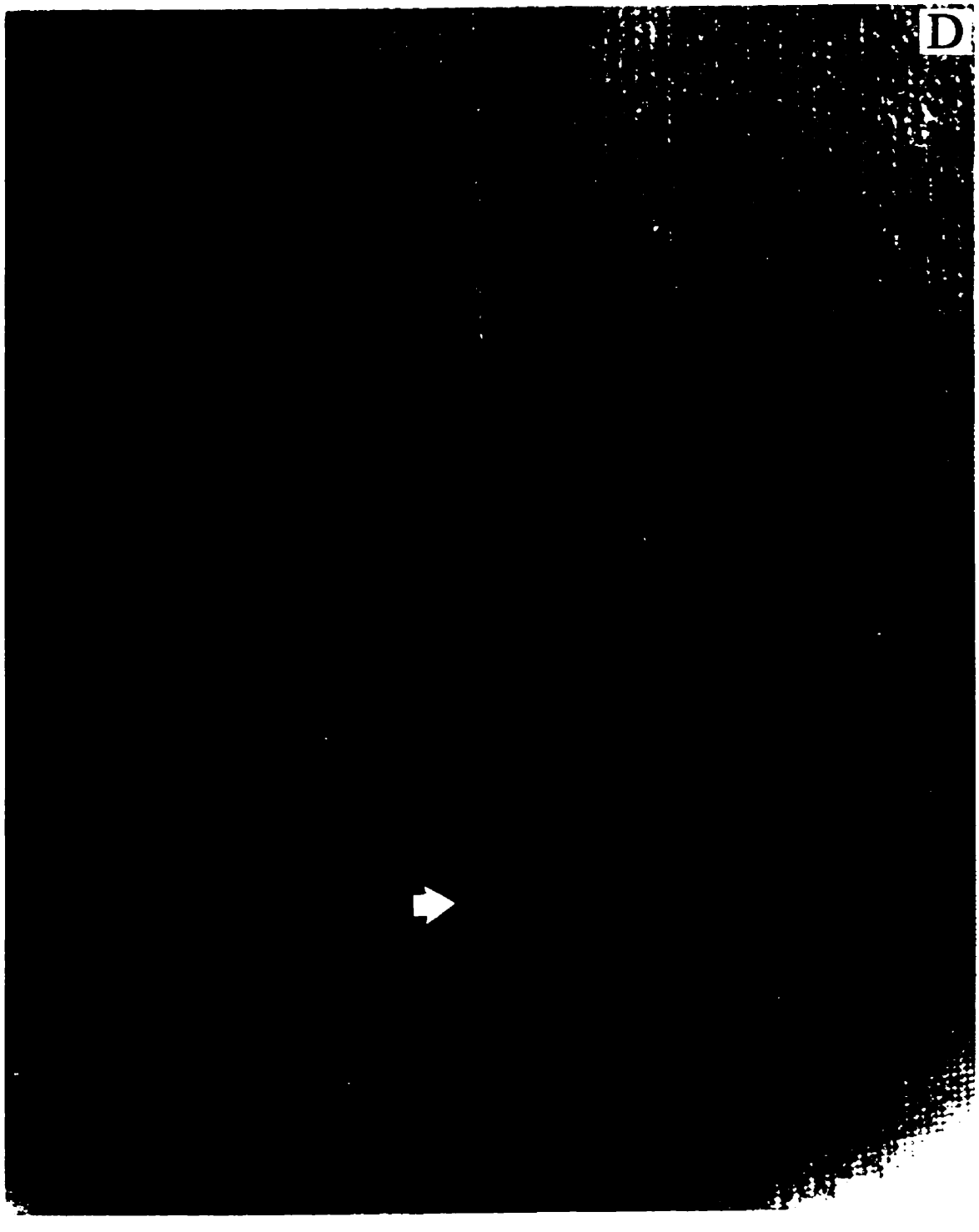
D

Where these vermiculite layers end, lattice fringes of mica deform to fill the remaining space (Fig. 9D). Minor vermiculitization is observed in normally pleochroic biotite from samples from near or at the present erosional surface, although its intensity appears to increase with depth (Fig. 9D). In less altered mica, these layers of vermiculite separate four or five layers of mica, but near grain margins and in reversely pleochroic mica, the frequency increases until the ratio between mica and vermiculite is approximately 1:1 (Fig. 9B). Brindley et al. (1983) termed such intergrowths hydrobiotite.

The compositions of normally and reversely pleochroic mica, as determined from AEM analyses (Table 2), show more compositional variation than that determined from electron-microprobe data (compare Fig. 10 with Fig. 5). However, the compositions of both types of mica obtained from the different methods of analysis are the same, except that those from reversely pleochroic mica have a higher Fe/(Fe+Mg) ratio (Fe#). This difference can be attributed to the problem of differentiating between the normally and reversely pleochroic mica in the TEM and associated images, the influence of grain thickness on AEM analyses of the heavier element Fe (Peacor, 1992), and the number of hematite inclusions nearby. The variation may also be attributed to differences in the method employed to calculate the mineral formulae and the elements analyzed. Finally, these compositions also show a tendency toward decreasing ^{IV}Al (increasing Si) with increasing Fe#, especially in the hydrobiotite and reversely pleochroic mica, which is a further indication of the presence of vermiculite. These compositional variations are consistent with the presence of vermiculite, as the presence of chlorite or smectite would be indicated by an increase in Mg and decrease in Si or an increase in both Si and Al content, respectively.

Other processes (e.g., exfoliation, dissolution and kinking) operated along with vermiculitization. Only minor exfoliation (separation of mica parallel to the cleavage) and dissolution, but no kinking (unlike optical observations) were evident in the TEM images (Fig. 11). Dissolution of mica produced void space, as seen in the upper portion of Figure 10.

The regions of mica that show the most vermiculitization, exfoliation and dissolution contain elongate (<0.5 μm) inclusions of hematite (the most common type), carbonate and amorphous silica (length-to-width ratio approximately 10:1) oriented parallel to the cleavage of mica. The hematite "bullets" are the dominant type of inclusion (as

Table 2. Selected AEM analyses and calculated mineral formulae for mica.

Sample #	66B	87/A/67.1	BH/18/2.1	BH/18/2.1	BH/18/2.1	BH/18/2.1	BH/18/2.1	BH/18/2.1
Type of Mica*	Normal	Normal	Normal	Reverse	Reverse	Reverse	Reverse	Reverse
SiO_2	35.26	36.64	32.21	36.30	39.27	36.98	37.22	35.46
Al_2O_3	9.93	10.29	10.17	11.09	13.01	12.57	11.98	9.35
TiO_2	0.99	1.20	2.02	0.00	0.28	0.52	1.23	0.45
FeO	20.78	18.73	20.26	21.18	17.64	15.07	17.54	12.19
MnO	1.44	0.85	0.47	0.32	0.23	0.23	0.03	0.22
MgO	19.05	19.30	20.82	21.94	16.96	22.22	18.48	29.21
CaO	0.85	0.46	0.45	0.31	0.00	0.22	0.18	0.00
Na_2O	0.00	0.00	0.31	0.26	0.24	0.57	0.53	0.38
K_2O	11.69	12.53	13.29	8.61	12.37	11.62	12.80	12.74
Total	100.00	100.00	100.00	100.00	100.00	100.00	100.00	100.00
Si	3.098	3.155	2.894	3.083	3.264	3.076	3.154	2.981
^{IV}Al	0.902	0.845	0.951	0.917	0.736	0.924	0.846	0.819
^{VI}Al	0.007	0.078	0.000	0.063	0.389	0.164	0.210	0.000
Al	0.908	0.923	0.951	0.980	1.125	1.088	1.057	0.819
Ti	0.051	0.061	0.106	0.000	0.014	0.026	0.061	0.022
Fe	0.919	0.811	0.915	0.905	0.737	0.631	0.747	0.515
Mn	0.065	0.038	0.021	0.014	0.010	0.010	0.001	0.010
Mg	1.934	1.920	2.161	2.152	1.628	2.135	1.809	2.837
Ca	0.053	0.028	0.028	0.018	0.000	0.013	0.010	0.000
Na	0.000	0.000	0.034	0.026	0.024	0.058	0.055	0.039
K	0.738	0.775	0.858	0.525	0.738	0.694	0.779	0.770
Σ Cations	7.766	7.710	7.970	7.703	7.541	7.730	7.674	7.992

* Normal=normally pleochroic mica; Reverse=reversely pleochroic mica as determined by optical examination. Mineral formulae calculated on the basis of 11 oxygen.
The total is set to 100.00 as these are AEM analyses.

Figure 10. Compilation of AEM data for both normally pleochroic and reversely pleochroic mica, in terms a plot of a Fe# versus ^{IV}Al diagram. The data show a wider distribution than that determined from the electron-microprobe analyses, because the formula was calculated from results of AEM analyses, in which F was not determined. The arrow indicates the trend of the compositions toward that of ideal vermiculite.

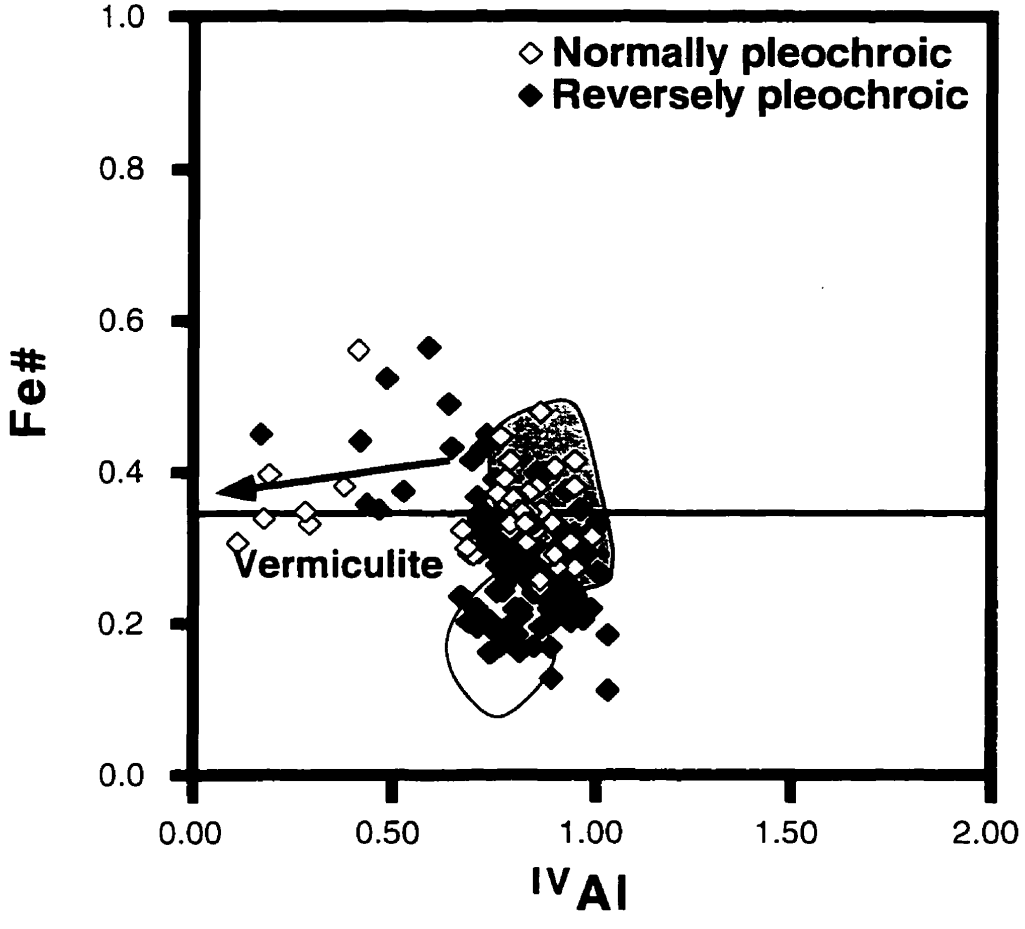
1.0
0.8
0.6
0.4
0.2
0.0
Fe#
◇ Normally pleochroic
◆ Reversely pleochroic
Vermiculite
0.00
0.50
1.00
1.50
2.00
IV Al

Figure 11. HRTEM image that shows exfoliation and dissolution of mica as white regions (indicated by the arrows). During dissolution, the 10 Å layers have been destroyed. Note that vermiculite is not present in these regions; however, such regions of exfoliation provide a pathway for fluids. These regions of exfoliation and dissolution release components into solution.

identified by AEM and SAED; Fig. 12A). Although these bullets lie between cleavages, their structures do not appear to be related to those of mica. Furthermore, the relative concentration of these inclusions increases with the degree of conversion to hydrobiotite, especially in the reversely pleochroic phlogopite. The presence of significant submicroscopic inclusions of hematite may be a cause of some of the reddish appearance of the reversely pleochroic mica. However, this in no way accounts for the majority of the compositional and optical variations observed in the reversely pleochroic phlogopite (ref. discussion). As for the carbonates, calcite forms large aggregates (as was observed optically), but anhedral, fine-grained ankerite surrounded by a rim composed of columnar ankerite is the common inclusion at the TEM scale. These carbonate inclusions contain significant amounts of Mn (to 3.4 wt.% MnO). Silica inclusions have cores and rims identical in appearance to the carbonate inclusions (Fig. 12B), except that they are amorphous, as indicated by the lack of a SAED pattern.

Discussion

Glimmerite associated with alkaline rocks from the Amba Dongar carbonatitic-alkaline complex originated in a three stage process: 1) Early aegirine-augite phenocrysts (Zone A; Fig. 3) crystallized from an alkaline silicate magma (either volcanic or plutonic) and reversely pleochroic mica (Zones D, E and F) crystallized from carbonatitic magma; 2) Aegirine-augite was metasomatized to aegirine, and normally pleochroic biotite formed at the expense of K-feldspar and aegirine, and in optical continuity with the early mica (Zones B and C), and 3) Later alteration resulted in oxidation, exfoliation, vermiculitization and dissolution of mica and formation of hematite, ankerite and silica inclusions.

Primary Aegirine-augite and Phlogopite

The diopside- and hedenbergite-rich cores of pyroxene from the unmetasomatized rocks were likely the product of magmatic crystallization. Aegirine-rich pyroxene grains may well record the influence of an early stage of Na-metasomatism, while the oscillatory rims record the influence of late-stage magmatic to post-magmatic processes (possibly Na-

Figure 12. Low resolution TEM images of late inclusions along mica cleavages.

A. A "bullet" of hematite (hem; 0.5 μm in length) along the mica cleavage. No vermiculite is observed between the phyllosilicate (phyllo) at the point where the hematite inclusion occurs. There is no specific orientation relationship was observed in the SAED between hematite and mica.

B. Inclusion of silica (sil) that exhibits an anhedral core surrounded by a columnar rim. The impossibility to obtain a SAED pattern from the silica suggests that it is amorphous (scale of inclusion: 0.5 μm).

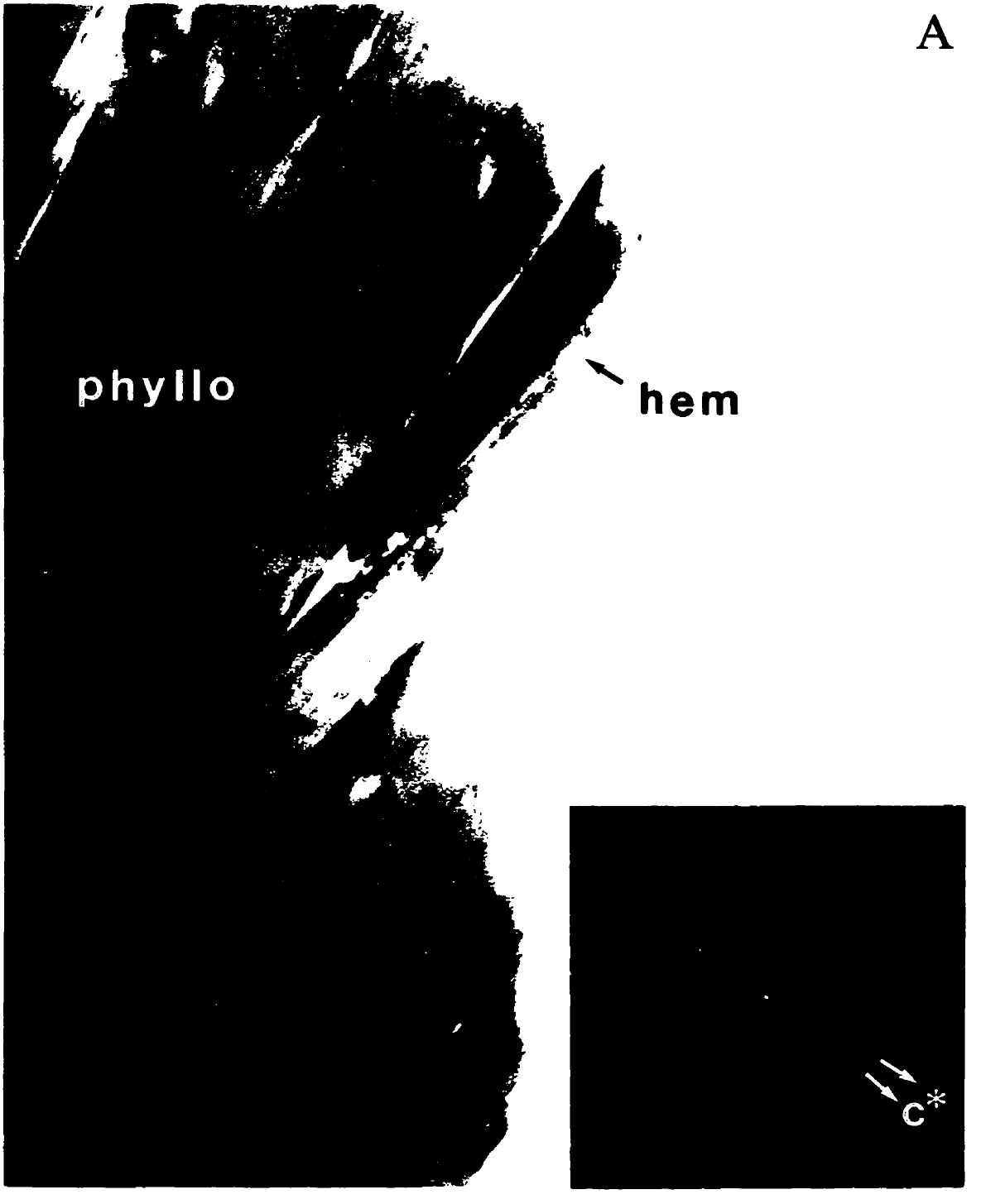
A
phyllo
hem
c*

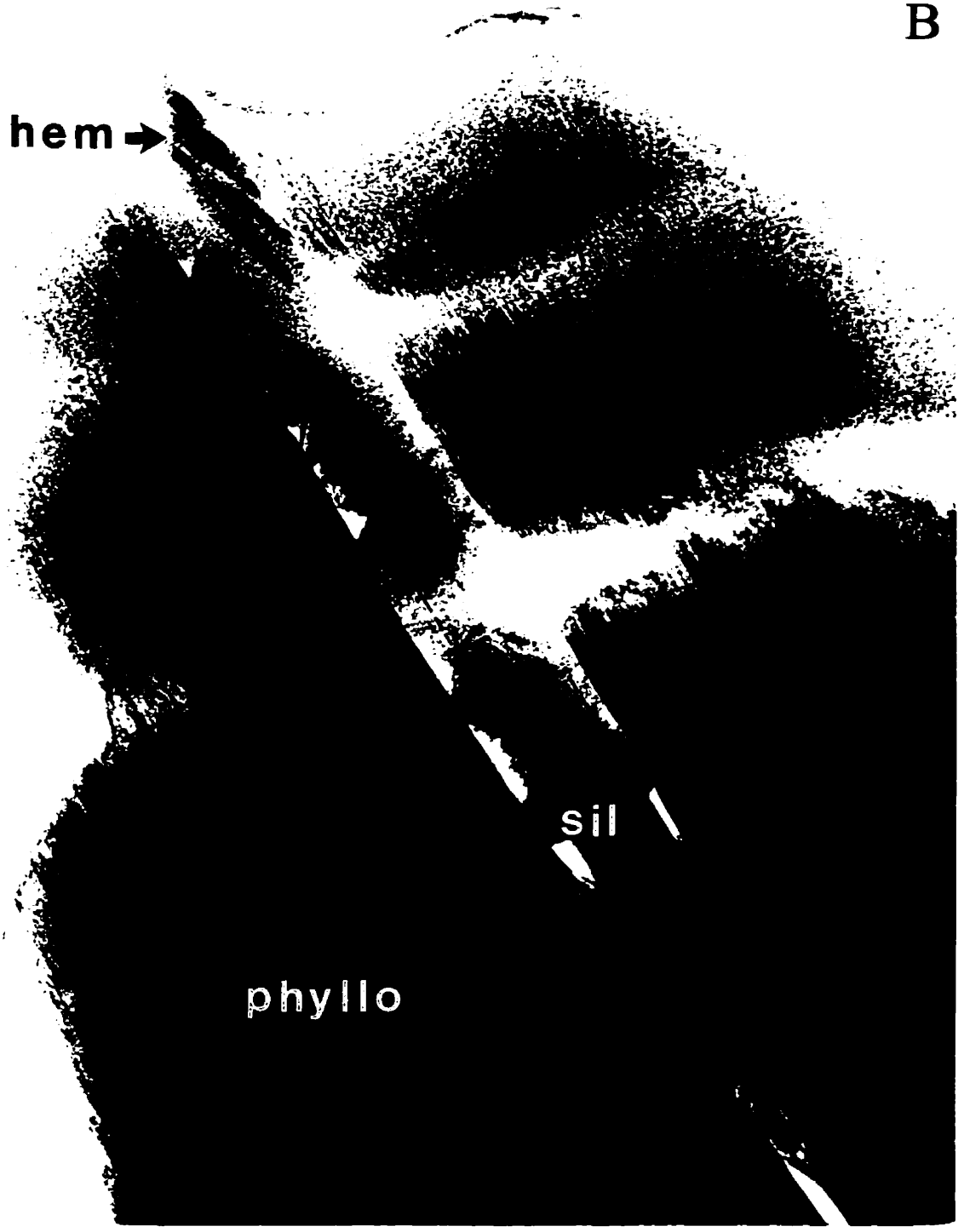
B
hem
sil
phyllo

metasomatism). As the majority of aegirine-augite phenocrysts, even those unrelated to the glimmerite, show this two-stage zonation, it is unlikely that the episode of Na-metasomatism related to formation of the glimmerite influenced these grains. The temperature at which Na-metasomatism occurred was probably the same as that during the formation of aegirine-augite in sodic fenites at the expense of Bagh sandstone (Viladkar, 1986). The compositional and XRD data on the feldspars suggest a relatively high-temperature of fenitization (Viladkar, 1986; Chapter 2).

The presence of Fe^{3+} in the tetrahedral site of the mica has been interpreted by Mössbauer spectrosocopy as the cause of the reverse pleochroism of the mica (Grum-Grzhimailo & Rimskaya-Korsakova, 1964; Faye, 1968; Faye & Hogarth, 1969; Rancourt et al., 1992; Cruciani et al., 1995). The incorporation of Fe^{3+} in the tetrahedral site of the reversely pleochroic phlogopite indicates crystallization in a comparatively Al- and Si-poor, but Fe^{3+}-rich environment, such as would exist in a carbonatitic magma (Puustinen, 1973; Gittins et al., 1975; Andersen & Austrheim, 1991; McCormick & Le Bas, 1996). Thus, the presence of reversely pleochroic mica in glimmerite immediately adjacent to carbonatite veins implies crystallization from a carbonatitic magma. Furthermore, the significant compositional (higher Ti and lower Si content) and optical differences between the reversely pleochroic phlogopite and phlogopite from phenocrysts in nephelinite indicate a separate origin. Crystallization of phlogopite, the first silicate to form, reduced the activity of Al and Si in the carbonatitic magma until there was an insufficient concentration of either for further crystallization of mica. The fine-grained octahedra of magnetite (now replaced by hematite) at the margins of the reversely pleochroic phlogopite may have formed following resorption of the phlogopite in the melt. Such a process was described Brearley (1987) and Peterson & Le Cheminant (1993) for spinel formed during breakdown of biotite.

Scott Smith et al. (1984) suggested that a hiatus in crystallization in kimberlite accounted for mica overgrowths of normally pleochroic mica on reversely pleochroic cores, as observed in the present study. Following this break in crystallization, normally pleochroic mica formed an optically continuous rim on the reversely pleochroic core (Zones D to F), and separate grains (Zones B to E). There are two possible explanations for the formation of normally pleochroic mica; both require activities of Al and Si higher than those prevailing during crystallization of the reversely pleochroic phlogopite. The first explanation involves

enrichment of carbonatitic magma in Al (K and Si) through wall-rock assimilation (McCormick & Le Bas, 1996). The second is equilibration of the metasomatic fluid released from the carbonatite with the Al-rich wallrocks (the alkaline volcanic and plutonic rocks). A metasomatic origin is more likely, because the large compositional difference invoked by the previous explanation would result in rapid crystallization of the magma. This crystallization of the phlogopite from a carbonatitic magma was followed by crystallization of the biotite rim from a later metasomatic fluid. This relationship is supported by the same core and rim relationship in the apatite, where the possible carbonate in the core indicates crystallization from a carbonate-rich source (e.g., carbonatite). The difference in origin between the micas suggests that reversely pleochroic phlogopite is less stable and more likely to be altered than normally pleochroic biotite, although the biotite forms rims around the phlogopite.

Temperatures of formation, calculated from the chemical formulae, of adjacent apatite (Chapter 2; Appendix A-6) and both types of mica from the glimmerite using the apatite-biotite geothermometer of Zhu & Sverjensky (1992), imply temperatures of between 300 and 950°C. The lower temperature portion of this range suggests formation of mica during metasomatism, as already suggested for the rim of normally pleochroic biotite and apatite. On the other hand, the higher temperature portion of this range suggests crystallization from carbonatitic magma. However, the wide variation in calculated temperatures can also be attributed to disequilibrium crystallization conditions between the apatite and mica or modifications produced by later fluids. The strong random zonation of apatite, especially in the core, implies disequilibrium or rapidly changing conditions during crystallization, while the presence of hematite along the cleavage of the mica implies the effects of later fluids. Thus, the estimated temperature range is not considered completely representative of the true values.

Comparison with Other Studies

The chemistry of normally and reversely pleochroic mica in glimmerite from Amba Dongar corresponds well to those from fenitized nephelinite and sodi-potassic fenite described by Viladkar (1991) from this complex. Furthermore, in Chapter 2, it was noted that sodi-potassic fenites described by Viladkar (1991) now seem to be the product of

fenitization of earlier fenitized alkaline volcanic or plutonic rocks. Moreover, mica from fenitized nephelinite is Mg- and Al-rich (16-22 wt.% MgO; 10-16 wt.% Al_2O_3), whereas that from sodi-potassic fenite is Fe-rich (16-22 wt.% FeO), but Mg- and Al-poor (12.5-16 wt.% MgO; 9-12 wt.% Al_2O_3). Even though the Al contents noted by Viladkar (1991) are similar to those of normally pleochroic and reversely pleochroic mica, respectively, from this study, his Mg contents are the reverse of what was found. Viladkar (1991) made no statement with respect to the pleochroism of these two micas. Consequently, it is difficult to draw any further comparisons with the results of the present examination.

Comparison of mica from the Amba Dongar complex with that of the same origin from other carbonatite or carbonatitic-alkaline complexes (Fen, Jacupiranga, Mud Tank, Loe Shilman and Tapira; Andersen, 1989; Andersen & Austrheim, 1991; Morbidelli et al., 1986; Currie et al., 1992; Mian & Le Bas, 1987; Brigatti et al., 1996, respectively) indicates that mica from the Amba Dongar complex contains the same amount of Ti, Fe, Mg, and possibly Ca, less Na, Ba and ^{IV}Al (Fig. 13), but more Mn and F. Furthermore, mica identified as reversely pleochroic in the other studies contains less ^{IV}Al and is of lower Fe# than the normally pleochroic mica (Fig. 13B). The higher Mn content of mica in this study reflects the higher than average Mn content of all units from the complex (Viladkar, 1981). Likewise, the high F content is consistent with the presence of significant F in orthomagmatic fluid derived from the carbonatite (Deans & Powell, 1968; Simonetti & Bell, 1995; Palmer & Williams-Jones, 1996).

A comparison of electron-microprobe data for the normally pleochroic rim and the reversely pleochroic core shows that the former contains more Si, Al, Mn and Ti, but less Na, Ba, Ca, Mg and Fe^{3+} (Figs. 5, 6; Table 1). The same differences between normally and reversely pleochroic micas have been reported by Puustinen (1973), for mica from the Siilinjärvi carbonatite complex in Finland, except that he noted a higher Si and OH, but lower Al and Na content in the reversely pleochroic mica. This slight enrichment of Na in reversely pleochroic mica (Fig. 6B) is of the same magnitude as noted by Velde (1979) for reversely pleochroic mica from melilite-rich volcanic rocks. The present study reveals that much of these compositional variations are generally the result of minute inclusions of ankerite, and, to a lesser extent, coarser inclusions of calcite. TEM observations confirm that variations in Na and Ba content are not due to the presence of inclusions. However, the

Figure 13. Plot of Fe# versus ^{IV}Al comparing the results of the present study with mica compositions from other carbonatite and carbonatitic-alkaline complexes. The complexes chosen for comparison are the Fen carbonatitic-alkaline complex (Andersen, 1989; Andersen & Austrheim, 1991), Jacupiranga carbonatite complex (Morbidelli et al., 1986), Mud Tank carbonatite complex (Currie et al., 1992), carbonatitic complexes from Uganda (McCormick & Le Bas, 1996), Tapira carbonatite complex (Brigatti et al., 1996), and the Loe Shilman carbonatite complex (Mian & Le Bas, 1987). Micas clearly identified as reversely pleochroic in the preceding studies are shown by large open circles. The reversely pleochroic phlogopite from these other studies is enriched in ^{IV}Al or Fe# compared to the reversely pleochroic phlogopite from the present study. Only one analysis of reversely pleochroic mica is from the Mud Tank complex is in the range of that from the present study. The fact that the normally pleochroic mica (generally biotite) from the Amba Dongar complex is somewhat depleted in ^{IV}Al compared to that of the other complexes. This difference is the result of the close relationship between the normally and reversely pleochroic mica. Finally, normally pleochroic phlogopite from the Amba Dongar complex is of significantly higher Fe# than phlogopite or slightly lower Fe# than biotite from the other complexes. Much of these differences can be attributed to differences in the conditions under which the micas crystallized, as discussed for the phlogopite and biotite from the present complex in the text.

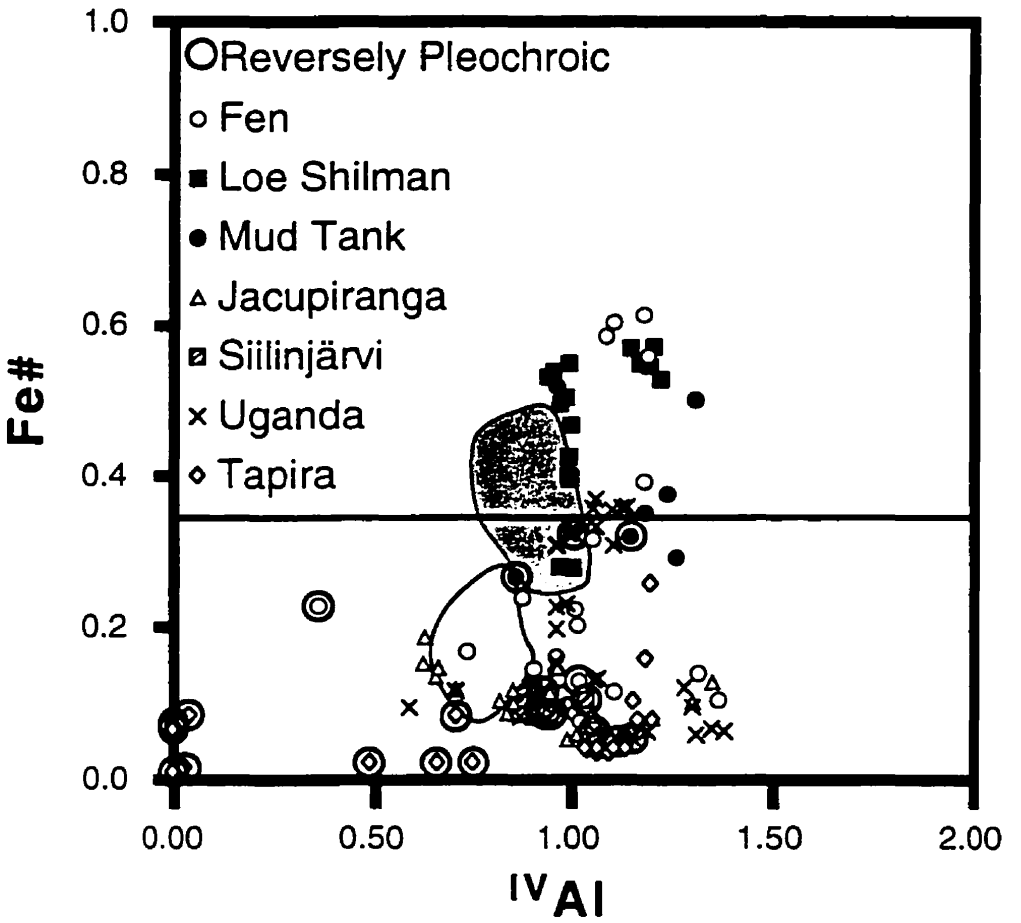
1.0
0.8
0.6
0.4
0.2
0.0
Fe#
OReversely Pleochroic
Fen
Loe Shilman
Mud Tank
Jacupiranga
Siilinjärvi
Uganda
Tapira
0.00
0.50
1.00
1.50
2.00
IVAl

higher Si content of mica from the Siilinjävi complex may, by implication of the data from the present study, be due to the presence of more silica inclusions. In the same manner, the presence of carbonate inclusions in the mica reported by Andersen & Austrheim (1991) could account for the slight enrichment in Ca of mica from the Fen complex.

Metasomatic Reactions

Na-metasomatism of aegirine-augite to aegirine at a relatively high-temperature (see above) in Zone B involved a gain of Na and Fe^{3+} from the fluid and the release of Ca and Mg into the fluid. In Zones B and C, this aegirine-rich pyroxene reacted at a lower temperature with fluid to produce the normally pleochroic biotite. If one assumes a minimal change in volume (9%; as implied by TEM observations) and that the Mg:Fe of the mica is 2:1 (from AEM analyses), the replacement reaction can be represented by the equation:

$$3\text{Aegirine} + K^{+} + 2Mg^{2+} + Al^{3+} + 3.5H_2O \rightarrow \text{Biotite} + 3Na^{+} + \text{Hematite} + 3SiO_{2(aq)} + 5H^{+} + 0.25O_2 \quad (1).$$

This reaction requires the addition of K, Mg and Al in the ratio 1:2:1 from the fluid to form biotite and hematite, while releasing Na, Si and H into solution.

A reaction relationship similar to that between mica and pyroxene was noted by Verschure & Maijer (1984) in the fenite aureole from the Fen carbonatitic-alkaline complex. At Fen, this reaction was also preceded by an earlier episode of Na-metasomatism, where the pyroxene became aegirine-rich and sodic amphibole formed. Later, Mg-metasomatism produced stipnomelane at the expense of this aegirine or sodic amphibole.

The second relationship documented in this examination through TEM observations is the presence of K-feldspar and carbonate between adjacent grains of aegirine and mica (normally pleochroic biotite). The experimental work of Bailey (1966) and Puhan & Johannes (1974) indicates that the reaction of K-feldspar with dolomite can produce phlogopite and calcite. This reaction reaches equilibrium below 600°C depending on the mole fraction of CO_2:H_2O of the fluid and pressure. When this reaction is modified

somewhat to accommodate the mineral assemblage in the Amba Dongar carbonatitic-alkaline complex and is adjusted to be isovolumetric. K-feldspar reacts with ankerite to produce biotite (where Mg:Fe = 2:1) and calcite, while almost conserving K and Al via the reaction:

$$2.5\text{K-feldspar} + \text{Ankerite} + 3.25Mg^{2+} + 1.75Fe^{2+} + 5H_2O + 0.5O_2 \rightarrow 2\text{Biotite} + \text{Calcite} + 0.5K^+ + 0.5Al^{3+} + 1.5SiO_{2(aq)} + 8H^+ + CO_2 \qquad (2).$$

This metasomatic reaction requires the addition of Mg and Fe in a 1.86:1 ratio. Thus, Mg-metasomatism, not K-metasomatism, is the dominant mechanism for conversion of K-feldspar to biotite, as also noted by Andersen (1989) in fenites from Fen, Norway.

Since a feldspar, carbonate or phyllosilicate is present between aegirine and mica, as indicated by the TEM examinations, it is inferred that mica formation may commonly be achieved by metasomatism of early K-feldspar. The problem is that together these reactions account for only approximately 15% of the mica observed in glimmerite, as calculated from the relative amount of each mineral observed during TEM examination and the relative amount of mica in the glimmerite determined by optical examination. Thus, a Mg-metasomatic origin of biotite at the expense of these minerals does not appear to be the sole mechanism of formation of this mica.

The normally pleochroic biotite could also have crystallized from the metasomatic fluid in a topotactic relationship on a template of reversely pleochroic phlogopite that has been resorbed earlier. Near the carbonatite veins, the space produced during resorption and dissolution of carbonate (that forms late carbonate inclusions and calcite veins), was accommodated by normally pleochroic biotite rims. A comparison of each of these processes with the relative amount of mica in each zone and the relative lack of relict grains of pyroxene in the glimmerite suggests that the biotite forms predominantly as a topotactic rim on the phlogopite. However, in the outer margins of the glimmerite (near the alkaline volcanic and plutonic rock), some combination of the other processes noted above is more likely.

Later Alteration

After formation, the micas were later kinked and exhibit the effects of exfoliation, dissolution and vermiculitization (Zones D to F). This kinking cross-cuts both normally and reversely pleochroic mica, but it is cross-cut by later vermiculite. Kinks are important, as they may provide the conduit necessary for the infiltration of solutions required for vermiculitization (Amouric, 1987). The absence of kinking on the TEM scale may be related to the lack of a second coincident layer of vermiculite which, according to Banfield & Eggleton (1988), is a requirement for a kink to form. Currie et al. (1992) also suggested that kinking could result from the application of a slight stress. As exfoliation and dissolution are common in more altered mica, the fact that it was rarely observed in this study indicates that alteration was weak. Exfoliation caused by vermiculitization was documented by Banfield & Eggleton (1988) for mica from granitic rocks in Australia, but was not observed in this study.

Two mechanisms are proposed to explain the late conversion of biotite to vermiculite: 1) direct replacement with little change in the 2:1 layer structure, and 2) conversion of two biotite layers to one vermiculite layer (Iijima & Buseck, 1978; Veblen & Ferry, 1983; Banfield & Eggleton, 1988). Direct replacement results in selective removal of interlayer cations, while leaving the 2:1 layered structure almost intact. The adjacent structural layers bend slightly to compensate for this change in volume. In contrast, the gradual reduction of two sheets of biotite to one of vermiculite results from rearrangement of portions of the biotite structure, and is believed to develop at edge dislocations (Banfield & Eggleton, 1988). Both edge dislocations and interlayer regions provide a pathway for the introduction of water and removal of cations, and thus, a manner to focus the alteration. The 1:1 relationship between vermiculite and biotite and local bending of the mica structure at the termination of the vermiculite in mica at Amba Dongar (Fig. 9D) suggest that the first mechanism dominated.

Vermiculitization results in selective replacement of interlayer cations (e.g., K^+) of the mica by H_3O^+, and a concurrent increase in size of the interlayer, as, in the (001) direction, the unit-cell of vermiculite is 40% greater than that of mica (Norrish, 1973). In artificially weathered mica, replacement of K^+ by H_3O^+ is related to charge reduction due to

oxidation of Fe^{3+} and formation of hematite inclusions (Norrish, 1973; Gilkes, 1973). This oxidation results in the release of octahedrally coordinated cations, such as Fe, Ti and Mn, which are not accommodated in the vermiculite structure in as high a concentrations as in the mica (Gilkes et al., 1972; Fordham, 1990; Acker & Bricker, 1992; Turpault & Trotignon, 1994; Kalinowski & Schweda, 1996).

Throughout vermiculitization, Kalinowski & Schweda (1996) noted that the Mg, Al and Si generally remain fixed in the tetrahedrally and octahedrally coordinated sites. However, a slight variation in the amount of Si is consistent with the experimental results of Acker & Bricker (1992), who noted an increase in the amount of Si in the mica following its reaction with a fluid when the pH changes from 3 to 4 [This range of pH is the region suggested by Palmer & Williams-Jones (1996) for the hydrothermal fluid involved in formation of the fluorite deposit in the present complex]. The observed increase in the Mg content of the layer of octahedra also is consistent with the experimental results of Acker & Bricker (1992), but not that of Kalinowski & Schweda (1996). Finally, the complete breakdown of mica by dissolution releases K, Mg, Fe, Mn, Ti, Si and F into solution.

Some of the elements released were later deposited as inclusions of hematite, carbonate and amorphous silica along the cleavage of the mica. The hematite inclusions are recognizable from electron-microprobe data on mica, as Fe^{3+} may be required to fill the tetrahedral site of the mineral formulae. The presence of hematite "bullets" could explain the variation in Fe content of mica from other carbonatitic-alkaline complexes in the same manner as the submicroscopic inclusions of copper in biotite (identified by HRTEM) were shown by Ilton & Veblen (1988) to contribute to the observed increase in Cu in electron-microprobe data. Furthermore, Mg, Mn and some Fe combined with Ca^{2+} and HCO_3^- derived from the carbonatite to form ankerite. The last two components also combined to form calcite. Both types of carbonate inclusions and minute inclusions of amorphous silica account for the slight enrichment of Ca and Si, respectively, evident in electron-microprobe results.

"Bullets" of hematite and amorphous silica were first noted by Veblen & Ferry (1983) in their TEM study of the formation of chlorite at the expense of biotite. In this study, the inclusions of silica are sufficiently large to be readily identified as amorphous, unlike those of Veblen & Ferry (1983). Banfield & Eggleton (1988) also observed the

presence of "bullets" of hematite in their TEM examination of alteration of mica from granitoids of Australia. In both cases, the inclusions were found to form from the breakdown of mica or replacement by chlorite or vermiculite and the release of cations into solution.

The reaction that represents the effects of late alteration on mica of glimmerite from the Amba Dongar complex, assuming constant Al (due to the lack of Al-bearing inclusions), and an approximately equal volume, while accounting for the TEM and optical observations, is:

$$2\text{Phlogopite} + 2Ca^{2+} + 4HCO^{-}_{3} + 2.5O_2 \rightarrow \text{Vermiculite} + 2\text{Ankerite} + 0.5\text{Hematite} + 4SiO_{2(am.\,aq)} + 2K^{+} + 2OH^{-} \quad (3).$$

Such a reaction would release K^{+} and OH^{-} (and possibly F from the mica) into solution.

The relationship between this later alteration of mica and the fluorite deposit can be inferred from the presence of other phyllosilicates in the complex and fluid inclusions in the fluorite. Both isotopic and fluid inclusion studies indicate that the fluorite deposit formed from the interaction of F-rich fluids from the carbonatite with groundwater from surrounding rocks (Deans & Powell, 1968; Simonetti & Bell, 1995; Palmer & Williams-Jones, 1996). In their fluid inclusion study, Palmer & Williams-Jones (1996) determined that the fluorite formed at less than 180°C and a pH < 3.5. Kaolinite, noted by Palmer (1994) and identified by TEM and AEM (Roelofsen, unpubl. data), occurs as radiating accordion-like inclusions in the white fluorite layer that separates yellow and blue fluorite. As the vermiculite is of late stage origin and the fluorite is the result of hydrothermal alteration, both clay minerals may have the same origin.

Thus, the sequence of events involved in formation of mica in the glimmerite began with the crystallization of reversely pleochroic mica from a carbonatitic magma. After a hiatus, this was superseded by crystallization of metasomatic mica with normal pleochroism after aegirine-augite, K-feldspar and earlier mica, kinking and calcite veining followed by hydrothermal alteration. The latter resulted in vermiculitization, oxidation, exfoliation and dissolution of the mica with subsequent precipitation of hematite, late carbonate and amorphous silica inclusions along the 001 cleavage (Fig. 14).

Figure 14. Schematic representation of the processes affecting mica in glimmerite. Initially, reversely pleochroic mica crystallized from the carbonatitic magma. This was followed by crystallization of normally pleochroic, more aluminous mica, as metasomatism progresses and the temperature decreased. Later, kinking and calcite veining of the mica occurred. This was followed by vermiculitization, oxidation (formation of hematite inclusions), exfoliation and dissolution of the mica and the formation of late inclusions of carbonate and amorphous silica. Lastly, amorphous silica formed a rim on the earlier silica.

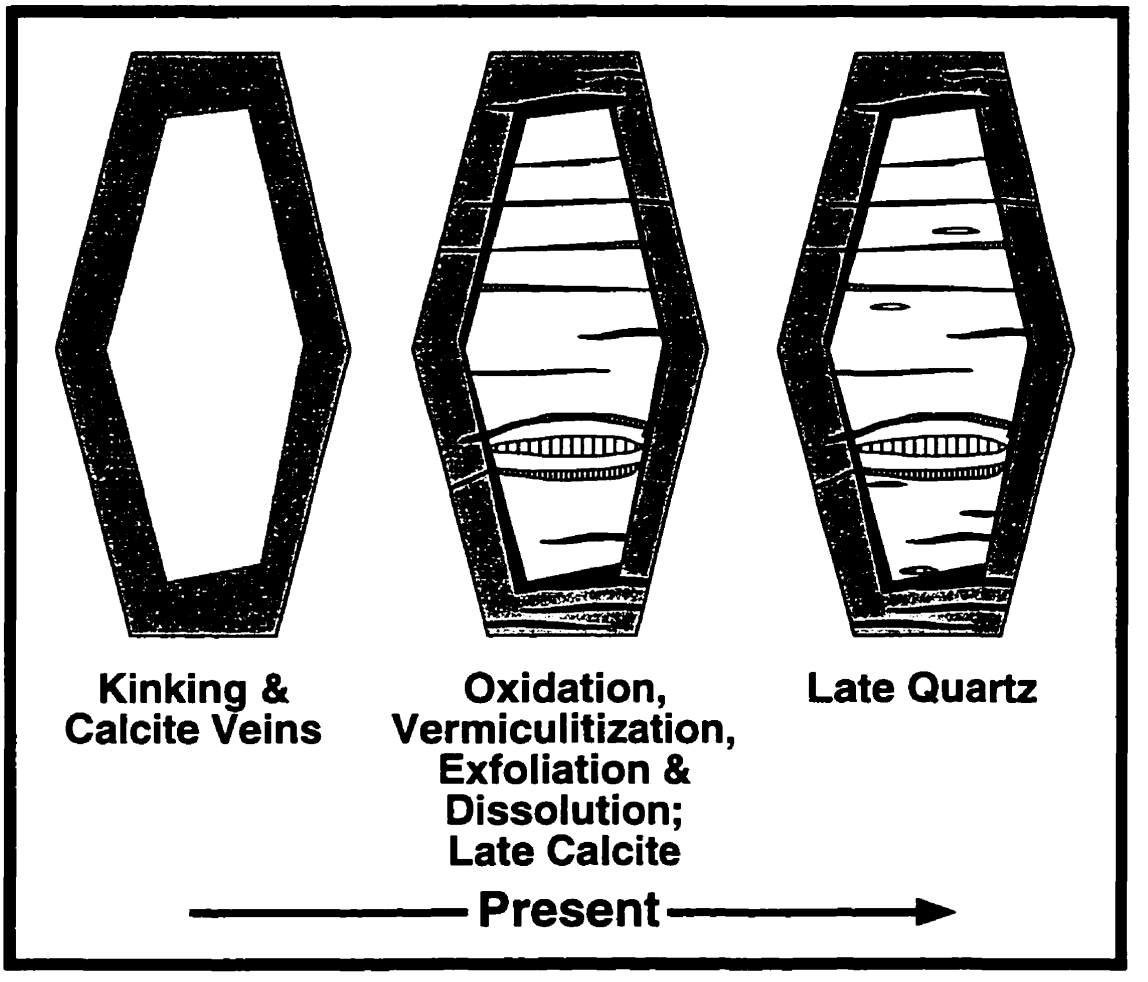
Kinking &
Calcite Veins
Oxidation,
Vermiculitization,
Exfoliation &
Dissolution;
Late Calcite
Late Quartz
Present

Comparison with Previous Studies

Andersen (1989) provided the most detailed account of the petrogenesis of mica from glimmerite of the Fen complex, Norway. He suggested that the mica originated by Mg-metasomatism of K-feldspar. Both he, Gaspar & Wyllie (1987) and Peterson & Le Cheminant (1993) documented phlogopite pseudomorphically replaced by chlorite. In the Amba Dongar complex, vermiculite formed at the expense of phlogopite instead of chlorite. Andersen (1989) suggested that phlogopite and dolomite reacted to form chlorite, quartz and calcite, whereas Peterson & Le Cheminant (1993) suggested that the same products resulted solely from reaction of phlogopite with the fluid. This replacement of phlogopite by chlorite is similar to that of phlogopite by vermiculite produced by hydrothermal alteration at Amba Dongar. Anderson (1989) suggested that the calcite replaced the mica. However, present TEM examinations suggest that crystallization of carbonate was associated with hydrothermal alteration. Peterson & Le Cheminant (1993) also noted the presence of minute (<100 μm), ribbon-like inclusions of quartz between cleavage planes of mica, and suggested that they resulted from its dissolution and subsequent precipitation of Si. In the present study, amorphous silica inclusions are believed to have formed by the precipitation of Si (among other elements) released as a result of the reaction of mica with the hydrothermal fluids. In the last stage of metasomatism, Andersen (1989) suggested that the alteration of ankerite to calcite and hematite was caused by the influence of groundwater derived hydrothermal fluids. Thus, it is believed that fluids involved in the alteration of mica from the Amba Dongar complex produced the same reaction products as hydrothermal fluids in other complexes. These fluids have been related by Simonetti & Bell (1995) and Palmer & Williams-Jones (1996) to the origin of the fluorite deposit in the Amba Dongar complex.

Vermiculitization of mica, which is common in carbonatitic-alkaline complexes, may produce significant vermiculite deposits (Palabora Mining Company Limited Mine Geological and Mineralogical Staff, 1976; Mariano, 1989; Notholt et al., 1990). The results of the present study imply the influence of hydrothermal alteration, rather than weathering (Mariano, 1989; Notholt et al., 1990), in the formation of such deposits. Weathering has been ruled out as the origin for much of the vermiculitization that occurred in the Amba

Dongar carbonatitic-alkaline complex, because it was more extreme at depth and in the reversely pleochroic phlogopite.

Conclusions

The mineral assemblage in glimmerite associated with the alkaline rocks from the Amba Dongar carbonatitic-alkaline complex originated in a three-stage process:

1. Early reversely pleochroic mica crystallized from carbonatitic magma below 950°C. The Fe^{3+} present in the tetrahedral site (up to 0.25 apfu) in this mineral, as inferred from electron-microprobe results, may include a contribution of submicroscopic inclusions of hematite in the structure.

2. Crystallization of biotite with normal pleochroism occurred by Mg-metasomatism (at a relatively high temperature). The most common mechanism involved crystallization of biotite in a topotactic relationship on previously formed mica compared to the replacement of K-feldspar and aegirine-augite by mica during metasomatism. The Al-enrichment of the mica was related to equilibration of the metasomatic fluid with the surrounding, more Al-rich alkaline and volcanic rocks. Locally, this metasomatism was preceded by Na-metasomatism whereby aegirine-augite was converted to aegirine.

3. Later alteration related to formation of the fluorite deposit, at <180°C, resulted in oxidation, vermiculitization, exfoliation and breakdown of the mica, followed by the formation of hematite, ankerite and silica inclusions from the cations released in combination with late carbonate and Ca. These late reactions presumably mobilized Ca and F that contributed to the fluorite mineralization.

Acknowledgements

Drs. K. Livi and B. Grobéty are thanked for guidance with the TEM at JHU. Drill-core samples of glimmerite were supplied by Dr. S. Viladkar (St. Xavier's College, Bombay). This research, especially the TEM portions of it, could not have been completed without the support of a number of awards to the first author: a) Fonds pour la Formation de Chercheurs et l'Aide à la Recherche (FCAR), who also provided funding for a Stage; b)

additional funding for TEM time and analyses through scholarships from the GSA and SDE (Sigma Delta Epsilon) to the first author. Additional support was provided by NSERC grants to the second author. The TEM facility at JHU was run under Grant EAR94-17585 from National Science Foundation to DRV. Dr. H. Vali introduced the first author to the use of *n*-alkylammonium ions for the identification of the presence of vermiculite. Prof. A. Dufresne allowed us to use his TEM facilities to examine these samples. Prof. A.E. Williams-Jones, Dr. C. Gammons and C. Normand are thanked for discussions and comments on earlier versions of this chapter.

References

Acker, J.G. & Bricker, O.P. (1992): The influence of pH on biotite dissolution and alteration kinetics at low temperature. *Geochimica et Cosmochimica Acta*, 56, 3073-3092.

Amouric, M. (1987): Growth and deformation defects in phyllosilicates as seen by HRTEM. *Acta Crystallographica*, B43, 57-63.

Andersen, T. (1989): Carbonatite-related contact metasomatism in the Fen complex, Norway: effects and petrogenetic implications. *Mineralogical Magazine*, 53, 395-414.

------- & Austrheim, H. (1991): Temperature-HF fugacity trends during crystallization of calcite carbonate magma in the Fen complex, Norway. *Mineralogical Magazine*, 55, 81-94.

Appleman, D.E. & Evans, H.T., Jr. (1973): Job 9214: indexing and least-squares refinement of powder diffraction data. U.S. Geological Survey, Computer Contribution 20 (NTIS Doc. PB2-16188).

Bailey, D.K. (1966): Potash feldspar and phlogopite as indices of temperature and partial pressure of CO_2 in carbonatite and kimberlite. *Mineralogical Society of India, International Mineralogical Association*, 5-8.

Banfield, J.F. & Eggleton, R.A. (1988): Transmission electron microscope study of biotite weathering. *Clays and Clay Minerals*, 36, 47-60.

Bisdom, E.B.A., Stoops, G., Delvigne, J., Curmi, P. & Altemuller, H.-J. (1982): Micromorphology of weathering biotite and its secondary products. *Pédologie*, 32(2), 225-252.

Brearley, A.J. (1987): An experimental and kinetic study of the breakdown of aluminous biotite at 800°C: reaction microstructures and mineral chemistry. *Bulletin de Minéralogie*, 110, 513-532.

Brigatti, M.F., Medici, L., Saccani, E. & Vaccaro, C. (1996): Crystal chemistry and petrologic significance of Fe^{3+}-rich phlogopite from the Tapira carbonatite complex, Brazil. *American Mineralogist*, 81, 913-927.

Brindley, G.W., Zalba, P.E. & Bethke, C.M. (1983): Hydrobiotite, a regular 1:1 interstratification of biotite and vermiculite layers. *American Mineralogist*, 68, 420-425.

Crookshank, H. (1936): Geology of the northern slopes of Satpuras between the Morand and Sher Rivers. *Memoir, Geological Survey of India*, 66(2), 137-381.

Cruciani, G., Zanazzi, P.F. & Quartieri, S. (1995): Tetrahedral ferric iron in phlogopite: XANES and Mössbauer compared to single-crystal X-ray data. *European Journal of Mineralogy*, 7, 255-265.

Currie, K.L., Knutson, J. & Temby, P.A. (1992): The Mud Tank carbonatite complex, central Australia - an example of metasomatism at mid-crustal levels. *Contributions to Mineralogy and Petrology*, 109, 326-339.

Deans, T. & Powell, J. L. (1968): Trace elements and strontium isotopes in carbonatites, fluorites, and limestones from India and Pakistan. *Nature*, 218, 750-752.

-------, Sukheswala, R.N., Sethna, S.F. & Viladkar, S.G. (1973): Discussion and contributions on: Metasomatic feldspar rocks (potash fenites) associated with the fluorite deposits and carbonatites of Amba Dongar, Gujarat, India. *Transactions, Institute of Mining Metallurgy*, 82, B 33-40.

Deer, W.A., Howie, R.A. & Zussman, M.A. (1962): **Rock Forming Minerals: Sheet Silicates**. John Wiley & Sons Inc., New York, 3, 270p.

Faye, G.H. (1968): The optical absorption spectra of iron in six-coordinate sites in chlorite, biotite, phlogopite and vivianite. Some aspects of pleochroism in the sheet silicates. *Canadian Mineralogist*, 9, 403-425.

------- & Hogarth, D.D. (1969): On the origin of reverse pleochroism of a phlogopite. *Canadian Mineralogist*, 9, 25-34.

Fiori, C.E., Swyt, C.R. & Myklebust, R.L. (1994): NIST/NIH Desktop spectrum analyzer program, Version 2.0.1. U.S. Department of Commerce.

Fordham, A.W. (1990): Weathering of biotite into dioctahedral clay minerals. *Clay Minerals*, 25, 51-63.

Garvey, R. (1986): LSUCRIPC, least squares unit-cell refinement with indexing on the personal computer. *Powder Diffraction*, 1, 114.

Gaspar, J.C. & Wyllie, P.J. (1987): The phlogopites from the Jacupiranga carbonatite intrusions. *Mineralogy and Petrology*, 36, 121-134.

Gilkes, R.J. (1973): The alteration products of potassium depleted oxybiotite. *Clays and Clay Minerals*, 21, 303-313.

------- & Suddhiprakarn, A. (1979): Biotite alteration in deeply weathered granite. I. Morphological, mineralogical, and chemical properties. *Clays and Clay Minerals*, 27, 349-360.

-------, Young, R.C. & Quirk, J.P. (1972): The oxidation of octahedral iron in biotite. *Clays and Clay Minerals*, 20, 303-315.

Gittins, J., Allen, C. & Cooper, A.F. (1975): Phlogopitization of pyroxenite: its bearing on the carbonatite magmas. *Geological Magazine*, 112, 503-507.

Grum-Grzhimailo, S.V. & Rimskaya-Korsakova, O.M. (1964): Absorption spectra of phlogopite holding trivalent iron in fourfold coordination. *Doklady Akademie Nauk SSSR*, 156, 123-125 (Russian, from Faye & Hogarth, 1969).

Gwalani, L.G. & Avasia, R.K., Chang, W.-J., Fernandez, S., Allègre, C.J., Prinzhofer, A. (1993): Alkaline rocks and carbonatites of Amba Dongar and adjacent areas, Deccan Igneous Province, Gujarat, India: 1. Geology, petrography and petrochemistry. *Mineralogy and Petrology*, 47, 219-253.

Iijima, S. & Buseck, P.R. (1978): Experimental study of disordered mica structures by high-resolution electron microscopy. *Acta Crystallographica*, A34, 709-719.

Ilton, E.S. & Veblen, D.R. (1988): Copper inclusions in sheet silicates from porphyry Cu deposits. *Nature*, 334, 516-518.

Kalinowski, B.E. & Schweda, P. (1996): Kinetics of muscovite, phlogopite, and biotite dissolution and alteration at pH 1-4, room temperature. *Geochimica et Cosmochimica Acta*, 60, 367-385.

Le Bas, M. J. (1981): Carbonatite magmas. *Mineralogical Magazine*, 44, 133-140.

Mariano, A.N. (1989): Nature of economic mineralization in carbonatites and related rocks. *In* **Carbonatites: Genesis and Evolution** (Bell, K., ed.). Unwin Hyman, London, 149-176.

McCormick, G.R. & Le Bas, M.J. (1996): Phlogopite crystallization in carbonatitic magmas from Uganda. *Canadian Mineralogist*, 34, 469-484.

Mian, I. & Le Bas, M.J. (1987): The biotite-phlogopite series in fenites from the Loe Shilman carbonatite complex, NW Pakistan. *Mineralogical Magazine*, 51, 397-408.

Morbidelli, L., Beccaluva, L., Brotzu, P., Conte, A., Garbarino, C., Gomes, C.B., Macciotta, G., Ruberti, E., Scheibe, L.F. & Traversa, G. (1986): Petrological and geochemical studies of alkaline rocks from continental Brazil. 3. Fenitization of jacupirangite by carbonatite magmas in the Jacupiranga Complex. *Periodico di Mineralogia*, 55, 261-295.

Norrish, K. (1973): Factors in the weathering of mica to vermiculite. *In* **Proceedings of the International Clay Conference, Madrid, 1972** (Serratosa, J.M, ed.). Division de Ciencias, CSIC, Madrid, 417-432.

Notholt, A.J.G., Highley, D.E. & Deans, T. (1990): Economic minerals in carbonatites and associated alkaline igneous rocks. *Transactions, Institute of Mining Metallurgy*, 99, B 59-80.

Palabora Mining Company Limited Mine Geological and Mineralogical Staff (1976): The geology and the economic deposits of copper, iron, and vermiculite in the Palabora Igneous Complex: a brief review. *Economic Geology*, 71, 177-192.

Palmer, D. (1994): Geology and geochemistry of the Amba Dongar carbonatite-hosted fluorite deposit, India. Unpublished M.Sc. thesis, McGill University, 109p.

------- & Williams-Jones, A.E. (1996): Genesis of the carbonatite-hosted fluorite deposit at Amba Dongar, India: evidence from fluid inclusions, stable isotopes, and whole rock-mineral geochemistry. *Economic Geology*, 91, 934-950.

Peacor, D.R. (1992): Analytical electron microscopy: x-ray analysis. *In* **Minerals and Reactions at the Atomic Scale: Transmission Electron Microscopy** (Buseck, P.R., ed.). Mineralogical Society of America, Reviews in Mineralogy, 27, 113-140.

Peterson, T.D. & Le Cheminant, A.N. (1993): Glimmerite xenoliths in early Proterozoic ultrapotassic rocks from the Churchill province. *Canadian Mineralogist*, 31, 801-819.

Pozzuoli, A., Vila, A., Franco, E., Ruiz-Amil, A. & de la Calle, C. (1992): Weathering of biotite to vermiculite in quaternary lahars from Monti Ernici, central Italy. *Clay Minerals*, 27, 175-184.

Puhan, D. & Johannes, W. (1974): Experimentelle untersuchung der reaktion dolomit + kalifeldspat + H_2O = phlogopit + calcit + CO_2. *Contributions to Mineralogy and Petrology*, 48, 23-31.

Puustinen, K. (1973): Tetraferriphlogopite from the Siilinjärvi carbonatite complex, Finland. *Bulletin of the Geological Society of Finland*, 45, 35-42.

Rancourt, D.G., Dang, M.-Z. & Lalonde, A.E. (1992): Mössbauer spectroscopy of tetrahedral Fe^{3+} in trioctahedral micas. *American Mineralogist*, 77, 34-43.

Rock, N.M.S., Gwalani, L.G. & Griffin, B.J. (1994): Alkaline rocks and carbonatites of Amba Dongar and adjacent areas, Deccan Alkaline Province, Gujarat, India. 2. Complexly zoned clinopyroxene phenocrysts. *Mineralogy and Petrology*, 51, 113-135.

Roelofsen, J.N., Vali, H. and Martin, R.F. (1993): Application of ultramicrotomy in the investigation of igneous and metasomatic assemblages by HRTEM. *Geological Association of Canada - Mineralogical Association of Canada, Program with Abstracts*, 18, A90.

Rubie, D.C. & Gunter, W.D. (1983): The role of speciation in alkaline fluids during fenite metasomatism. *Contributions to Mineralogy and Petrology*, 82, 165-175.

Scott Smith, B.H., Danchin, R.V., Harris, J.W. & Stracke, K.J. (1984): Kimberlites near Orroroo, South Australia. *In* **Kimberlites: Proceedings of the Third International Kimberlite Conference** (Kornprobst, J., ed.), Elsevier, New York, Developments in Petrology, 11, 121-142.

Sethna, S.F. (1989): Petrology and geochemistry of the acid, intermediate and alkaline rocks associated with the Deccan basalts in Gujarat and Maharashtra. *Geological Society of India, Memoir*, 15, 47-61.

------- & Borges, S.M. (1981): Petrology of the carbonatites and associated alkaline rocks of Siriwasan, Chhota Udaipur. *Journal of the Geological Society of India*, 22, 417-425.

Simonetti, A. & Bell, K. (1995): Nd, Pb, and Sr isotope systematics of fluorite at the Amba Dongar carbonatite complex, India: evidence for hydrothermal and crustal fluid mixing. *Economic Geology*, 90, 2018-2027.

Turpault, M.-P. & Trotignon, L. (1994): The dissolution of biotite single crystals in dilute HNO_3 at 24°C: evidence of an anisotropic corrosion process of micas in acidic solutions. *Geochimica et Cosmochimica Acta*, 58, 2761-2775.

Vali, H. & Hesse, R. (1992a): Arrangement of n-alkylammonium ions in phlogopite and vermiculite: an XRD and TEM study. *Clays and Clay Minerals*, 40, 240-245.

------- & ------- (1992b): Identification of vermiculite by transmission electron microscopy and X-ray diffraction. *Clay Minerals*, 27, 185-192.

Veblen, D.R. & Ferry, J.M. (1983): A TEM study of the biotite-chlorite reaction and comparison with petrologic observations. *American Mineralogist*, 68, 1160-1168.

Velde, D. (1979): Trioctahedral micas in melilite-bearing eruptive rocks. *Carnegie Institute of Washington, Yearbook*, 78, 468-475.

Verschure, R.H. & Maijer, C. (1984): Pluri-metasomatic resetting of Rb-Sr whole-rock systems around the Fen peralkaline-carbonatitic ring-complex, Telemark, South Norway. *Terra Cognita*, 4, 191-192.

Viladkar, S.G. (1981): The carbonatites of Amba Dongar, Gujarat, India. *Bulletin of the Geological Society of Finland*, 53, 17-28.

------- (1984): Alkaline rocks associated with the carbonatites of Amba Dongar, Chhota Udaipur, Gujarat, India. *Indian Mineralogist*, Sukheswala Volume, 130-135.

------- (1986): Fenitization at the Amba Dongar carbonatite-alkalic complex, India. *Proceedings NEMIRAM (New Minerals and Raw Materials) Symposium* (Gabriel, M., ed.), Czechoslovakia, 170-189.

------- (1991): Phlogopitization at Amba Dongar Carbonatite alkalic complex, India. *Neues Jahrbuch für Mineralogie, Abhandlungen*, 162(2), 201-213.

Woolley, A.R. (1982): A discussion of carbonatite evolution and nomenclature, and the generation of sodic and potassic fenites. *Mineralogical Magazine*, 46, 13-17.

Yellur, D.D. (1968): Carbonatite complex as related to the structure of the Narmada valley. *Journal of the Geological Society of India*, 9, 118-123.

Zhu, C. & Sverjensky, D.A. (1992): F-Cl-OH partitioning between biotite and apatite. *Geochimica et Cosmochimica Acta*, 56, 3435-3467.

Prologue to the Second Portion of this Study

In the first portion of this study, the process of fenitization in the Amba Dongar carbonatitic-alkaline complex was investigated through examination of the effects of metasomatism on the primary mineral assemblages of alkaline volcanic and plutonic rocks, and on detrital minerals of the Bagh sandstone. Bulk-rock analyses indicate that metasomatism resulted in enrichment of Na, K, Ca, REE ± Mg, among other elements, in these rocks. Sodic fenites are less common than the potassic fenites. Glimmerite also forms by Mg- and, to a lesser extent, K-metasomatism after an episode of Na-metasomatism at the contact between the carbonatite vein and the alkaline volcanic or plutonic rock. Finally, rare late Ca-metasomatism occurs in the form of central seams of wollastonite and andradite in aegirine-augite veins that cut the alkaline volcanic rocks. Thus, the sequence of metasomatism is from sodic to potassic and, locally, calcic.

Metasomatism in anorogenic complexes is also associated with peralkaline granites, such as at the Strange Lake peralkaline complex, Québec-Labrador, Canada. Salvi & Williams-Jones (1990, 1992) noted, from fluid inclusion studies, that the primary magmatic minerals in the complex are influenced by both Na- and Ca-metasomatism. The primary mafic silicate, arfvedsonitic amphibole, is Na-metasomatized to an aegirine-rich assemblage (Salvi & Williams-Jones, 1990, 1992; Pillet et al., 1993). The main effect of Ca-metasomatism is the replacement of elpidite by gittinsite (Salvi & Williams-Jones, 1990, 1995). Thus, the sequence of metasomatism between the two complexes is similar in that Na-metasomatism is followed by Ca-metasomatism. Nevertheless, the extent of metasomatism varies widely at Strange Lake, with Na-metasomatism more extensive than the Ca-metasomatism.

Ore deposits associated with both complexes have been formed or modified by the circulation of late-stage fluids. Simonetti & Bell (1995) and Palmer & Williams-Jones (1996) determined that the fluorite deposit in the Amba Dongar complex originated by the reaction of F-bearing orthomagmatic fluid derived from the carbonatite with fluids from the surrounding country-rocks. Salvi & Williams-Jones (1990, 1996) noted that Na- and F-rich orthomagmatic fluid mobilized the HFSE that are deposited during subsequent Ca-metasomatism.

The main focus of the next three papers of this study is an investigation of the effects of metasomatism on the primary mafic silicates, in particular arfvedsonitic amphibole, from the Strange Lake complex. As the units of the Strange Lake complex contain significant levels of Zr, Nb, Y and REE, it is necessary to examine the trace-element content of the arfvedsonitic amphibole and aegirine and to determine their relationship to the ore minerals. Furthermore, the Li content of this amphibole also may be significant (Hawthorne et al., 1992, 1993). In the following chapter, the compositional variation of the primary arfvedsonitic amphibole and of the aegirine (both primary and secondary), will be examined in detail using the results of electron-microprobe and laser-ablation microprobe - inductively coupled plasma - mass spectrometry (LAM-ICP-MS) analyses.

References

Hawthorne, F.C., Oberti, R., Ungaretti, L. & Grice, J. (1992): Leakeite, $NaNa_2(Mg_2Fe^{3+}{}_2Li)Si_8O_{22}(OH)_2$, a new alkali amphibole from the Kajlidongri manganese mine, Jhabua district, Madhya Pradesh, India. *American Mineralogist*, 77, 1112-1115.

-------, Ungaretti, L., Oberti, R., Bottazzi, P. & Czamanske, G.K. (1993): Li: An important component in igneous alkali amphiboles. *American Mineralogist*, 78, 733-745.

Palmer, D.A.S. & Williams-Jones, A.E. (1996): Genesis of the carbonatite-hosted fluorite deposit at Amba Dongar, India: evidence from fluid inclusions, stable isotopes, and whole rock-mineral geochemistry. *Economic Geology*, 91, 934-950.

Pillet, D., Chenevoy, M. & Bélanger, M. (1993): Pétrologie du granite peralcalin du lac Brisson, Labrador central, Nouveau-Québec. II. Minéralogie et modalités de cristallisation. *Canadian Journal of Earth Sciences*, 30, 2423-2435.

Salvi, S. & Williams-Jones, A.E. (1990): The role of hydrothermal processes in the granite-hosted Zr, Y, REE deposit at Strange Lake, Quebec/Labrador: evidence from fluid inclusions. *Geochimica et Cosmochimica Acta*, 54, 2403-2418.

------- & ------- (1992): Reduced orthomagmatic C-O-H-NaCl fluids in the Strange Lake rare-metal granitic complex, Quebec/Labrador, Canada. *European Journal of Mineralogy*, 4, 1155-1174.

------- & ------- (1995): Zirconosilicate phase relations in the Strange Lake (Lac Brisson) pluton, Quebec-Labrador. *American Mineralogist*, 80, 1031-1040.

------- & -------- (1996): The role of hydrothermal processes in concentrating HFSE in the Strange Lake peralkaline complex, northeastern Canada. *Geochimica et Cosmochimica Acta*, 60, 1917-1932.

Simonetti, A. & Bell, K. (1995): Nd, Pb, and Sr isotope systematics of fluorite at the Amba Dongar carbonatite complex, India: evidence for hydrothermal and crustal fluid mixing. *Economic Geology*, 90, 2018-2027.

Chapter 4:

THE MAFIC SILICATES OF THE STRANGE LAKE PERALKALINE COMPLEX, QUEBEC-LABRADOR. I. PRIMARY ARFVEDSONITIC AMPHIBOLE AND AEGIRINE.

Jeanette N. Roelofsen and Robert F. Martin
Department of Earth and Planetary Sciences,
McGill University,
3450 University Street,
Montréal, Québec
H3A 2A7

Abstract

Changes in composition of primary mafic minerals coincide with changes in composition of the magma or fluid from which they crystallize, and, in some cases, degassing of the magma. Consequently, compositional changes of arfvedsonitic amphibole and aegirine can be used to reconstruct the evolution of composition, temperature and fO_2 (as Fe^{2+}/Fe^{3+} is recorded by the minerals) of a peralkaline magma or fluid. Primary arfvedsonitic amphibole and aegirine from the Strange Lake peralkaline complex on the Québec-Labrador border reflect such compositional variations. Crystallization from the magma produced three different types of fluor-arfvedsonitic amphibole: 1a) early primary cores present in hypersolvus granite, with inclusions of monazite, zircon, zajacite, yttriofluorite and gagarinite, that is enriched in Na- and Fe, 1b) optically continuous rims on 1a enriched in Ca, Mg, Mn and Al, 2) zoned composite grains (K-, Mn-, Fe^{2+}- and Al-rich) associated with Type-1 (yellow, Ca-, Mn- and Ti-rich) aegirine in altered subsolvus granite, and 3) rare late-stage, fine-grained, acicular K-, Mn-, Li- and Zn-rich amphibole from mafic pods in or near the ore zone. Changes in the crystallization conditions of the mafic minerals resulted in the formation of Type-3 (yellow green), Ca-, Mn- and slightly Ti-enriched aegirine in the ore zone. Late Ti-rich Type-1 (green) aegirine, of late-stage magmatic origin, rims Type-1 and -2 amphibole in hypersolvus and subsolvus granites. Compositional variation or enrichment of K, Mg, Zn, Mn, REE and HFSE (e.g., Zr and Nb) of these primary amphiboles results from magmatic evolution. Furthermore, the presence of Fe^{2+}-dominant Ti silicates (e.g., astrophyllite and aenigmatite) and perthitic feldspar in the earlier hypersolvus granite indicate fractional crystallization at a low fO_2 (at least two log units below FMQ). The dominance of the primary, Fe^{3+}-rich mineral aegirine and two feldspars in altered subsolvus granite indicates crystallization at higher $P(H_2O)$ and fO_2 conditions. Degassing resulted in an increase of the K content of late amphibole and raised fO_2 sufficiently for crystallization of aegirine. As mineralogical successions are observed in other peralkaline granitic complexes, comparable trends and compositional variations of these mafic silicates are expected.

Introduction

The Strange Lake peralkaline A-type granite on the Québec-Labrador border, 150 km west of Nain, Labrador (Fig. 1A), is considered to have economic potential, as it contains a deposit of 52 million tonnes of ore with 2.93% ZrO_2, 0.54% REE, 0.31% Y_2O_3, 0.08% BeO and 0.38% Nb_2O_5 (Miller, 1988). The importance of this granitic pluton has motivated in depth investigations of the mineralogy and geochemistry of magmatic products of crystallization and of the hydrothermally altered rocks near the core of the complex where the ore minerals are concentrated (Salvi & Williams-Jones, 1990; Birkett et al., 1992; Pillet et al., 1993; Miller, 1996). Compositional variation in the primary mafic silicates expresses the degree of geochemical evolution of the magma, and records the effects of degassing. The mafic silicates, as potential hosts of some of these rare elements, are the subject of this investigation of the Strange Lake complex.

Background Information

The 36-km^2 Proterozoic (Pillet et al., 1989; Miller et al., 1997) Strange Lake peralkaline complex is located in the eastern Rae province of the Canadian Shield (Hoffman, 1988). The complex is surrounded to the south and southwest by an Elsonian rapakivi quartz monzonite, and to the north and northeast by Aphebian quartzofeldspathic, calc-silicate, graphitic, dioritic, gabbroic, and anorthositic gneisses (Fig. 1B). Its emplacement has been related by Currie (1985) to the Elsonian Gardar anorogenic event in Greenland (Blaxland et al., 1978), and to a series of coeval anorthosites and A-type granites that extend from Newfoundland to the central United States (Emslie, 1978a, b).

The peralkaline granites that comprise the Strange Lake complex have been subdivided on the basis of textural development of the dominant mineral: alkali feldspar (Nassif & Martin, 1991; Fig. 1B). Field relationships indicate that hypersolvus granite is the earliest unit to be emplaced. This was followed by transsolvus granite and then subsolvus granite. The transsolvus granite occurs as wisps and isolated lenses (to 1 m) in hypersolvus granite in the southeast of the complex and as enclaves in the subsolvus granite (Nassif, 1993). The subsolvus granite was later altered in the northern part of the complex, but

Figure 1. Location and geology of the Strange Lake peralkaline complex, Québec-Labrador, Canada.

A. The complex is located northeast of Schefferville and west of Nain.

B. Unit map of the complex after Bélanger (1984) and Nassif (1993). The core of the complex is composed of hypersolvus granite. It is surrounded by later altered subsolvus granite. The ore zone (to vol. 20% ore minerals) occurs in the most altered subsolvus granite to the north of the hypersolvus granite. Small amounts of transsolvus granite, fresh subsolvus granite and roof pendants are also present. The complex itself is surrounded by quartz monzonite, to the southwest, and various gneisses, metadiorite and metagabbros, etc., to the northeast. The samples locations are represented by circles, squares and diamonds. The sample numbering system for the circles is based on a grid that was superimposed on the complex during sample collection, in which the first number represents the grid number, the letter the location within the grid and the final number (noted in the remainder of the paper and not in this figure) reflects the number of samples collected at each location.

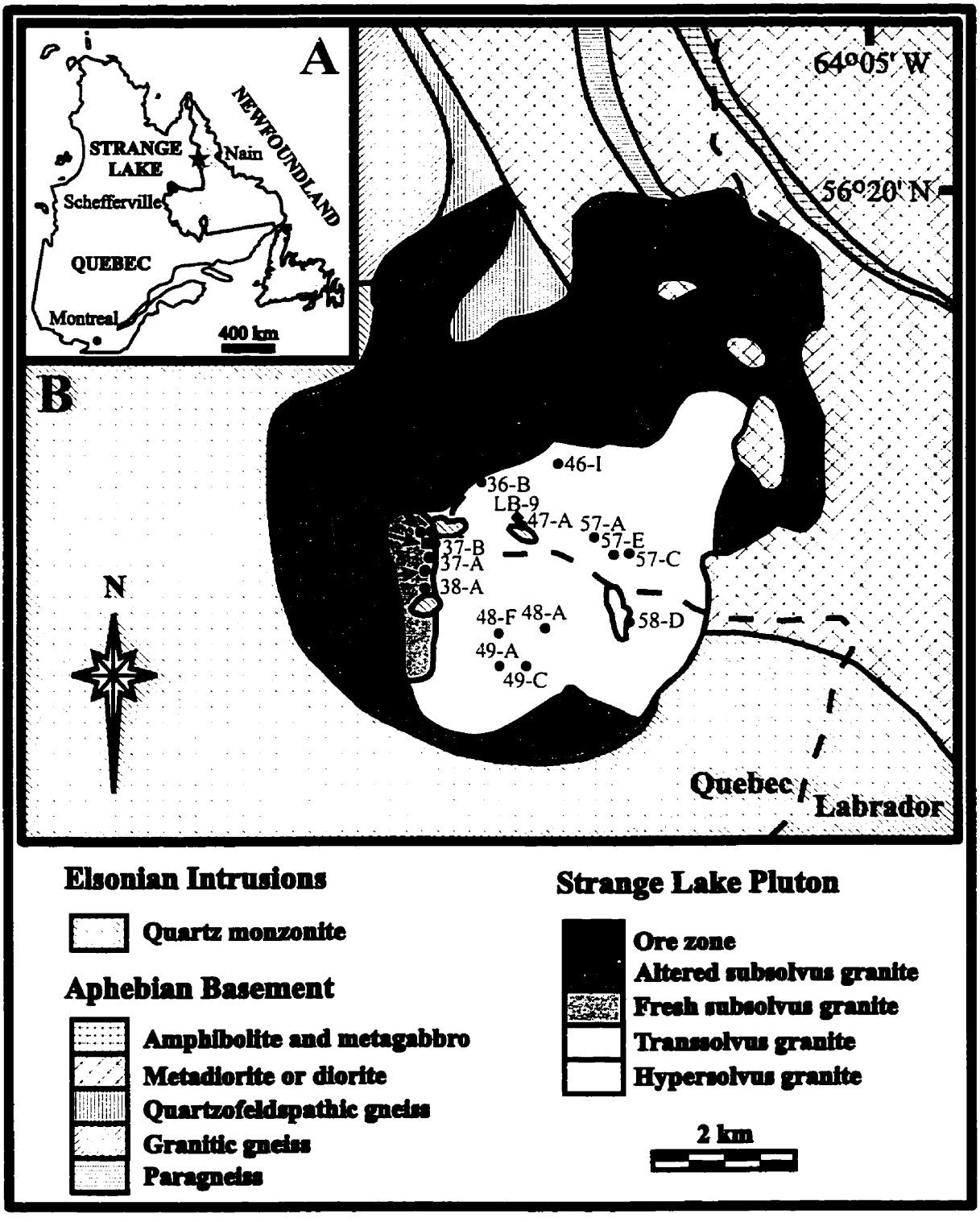
A
STRANGE LAKE
Nain
NEWFOUNDLAND
Schefferville
QUEBEC
Montreal
400 km
B
64°05' W
56°20' N
46-I
36-B
LB-9
47-A
57-A
57-E
57-C
37-B
37-A
38-A
48-F
48-A
58-D
49-A
49-C
N
Quebec
Labrador
Elsonian Intrusions
Quartz monzonite
Aphebian Basement
Amphibolite and metagabbro
Metadiorite or diorite
Quartzofeldspathic gneiss
Granitic gneiss
Paragneiss
Strange Lake Pluton
Ore zone
Altered subsolvus granite
Fresh subsolvus granite
Transsolvus granite
Hypersolvus granite
2 km

remains unaltered in the western portion of the complex (fresh subsolvus granite). Bodies of pegmatite (on average 1-2 m in diameter), both fresh and altered, are present throughout the complex, but they dominate in the altered subsolvus granite, especially, in the ore zone (denoted for that portion of the complex that contains up to 20 vol.% ore minerals, unlike the 5 vol.% present in the some of the other units; Zajac et al., 1984; Miller, 1986). Lastly, a distinct increase in potassium was noted by Nassif (1993) in feldspar from the subsolvus altered granite, ore zone, and especially, pegmatites, which he related to magma degassing and the preferential loss of Na.

Review of the Literature on the Primary Mafic Silicates

Silicates and oxides typical of peralkaline granites, in general, are: arfvedsonitic amphibole, aegirine, astrophyllite [$(Na,K)_3(Fe,Mn)_7Ti_2Si_8O_{24}(O,OH)_7$], aenigmatite [$Na_2Fe_5TiSi_6O_{20}$], neptunite [$KNa_2Li(Fe,Mn)_2Ti_2Si_8O_{24}$], ilmenite and hematite. At Strange Lake, these minerals comprise, on average, 5 to 20 vol.% of the granites. Whereas all occur in the hypersolvus and fresh subsolvus granites, only primary arfvedsonitic amphibole and aegirine are present in the altered subsolvus granite (Pillet et al., 1993; Birkett et al., 1996). Primary aegirine is the dominant mafic silicate in the ore zone, although minor, late, fine-grained arfvedsonitic amphibole also occurs. Ilmenite occurs as rare grains at the core of arfvedsonitic amphibole and, in some cases, the titanium silicates only in the hypersolvus and fresh subsolvus granites.

Pillet (1989), Pillet et al. (1993) and Birkett et al. (1996) documented the textures, compositional variation and paragenesis of arfvedsonitic amphibole, aegirine, astrophyllite, aenigmatite and neptunite. Although the overall compositional variation of these minerals, especially arfvedsonitic amphibole, was documented by Pillet (Pillet, 1989; Pillet et al., 1993), he did not fully explain their differences. Furthermore, the minor- and trace-element data are sketchy. For example, amphibole was not analyzed for Zr, which is commonly present in amphibole from anorogenic complexes (Borley, 1976). Birkett et al. (1996) documented the compositional variation, and substitutions in the Ti-bearing silicates astrophyllite, aenigmatite, neptunite, titanite, narsarsukite [$Na_2(Ti,Fe^{3+})Si_4(O,F)_{11}$] and bafertisite [$Ba(Fe,Mn)_2TiSi_2O_7(O,OH)_2$] in addition to the interrelationships between these

minerals and arfvedsonitic amphibole and aegirine. They also noted the presence of three different generations of arfvedsonitic amphibole and aegirine.

Previous attempts to determine the conditions of formation of arfvedsonitic amphibole and aegirine from various complexes involved determination of their compositional variation using electron-microprobe analysis (Czamanske & Dillet, 1988; Pillet, 1989; Abdel-Rahman, 1994), examination of solid inclusions (Bogoch et al., 1992) and bulk-sample analysis of amphibole [X-ray fluorescence spectroscopy (XRF), atomic absorption spectroscopy (AA) and neutron activation analysis (NAA); Pillet et al., 1993; Abdel-Rahman, 1994]. Hawthorne et al. (1992, 1993) noted that the lack of complete chemical characterization of arfvedsonitic amphibole (i.e., evaluation of the amount of Li), in particular, resulted in an amphibole composition that was distinctly enriched in ΣNa+K+Si (apfu) compared to the ideal. Ross (1984) attributed this variation to the presence of submicroscopic inclusions of aegirine. Consequently, the information currently available is incomplete and inadequate to establish the conditions of primary crystallization of the mafic silicates (arfvedsonitic amphibole and aegirine) from the Strange Lake peralkaline complex, and to better understand the metasomatic changes to be documented in Chapters 5 and 6.

This study examines the evolution of arfvedsonitic amphibole and aegirine of primary to subsolvus origin from the Strange Lake peralkaline complex through their compositional variation. It is the first in a series of papers that explores the compositional (major-, minor- and trace-element) variations of these mafic minerals in the complex by laser-ablation microprobe - inductively coupled plasma - mass spectrometry (LAM-ICP-MS), electron-microprobe analysis and transmission electron microscopy (TEM).

Methodology

Cathodoluminescence

Cathodoluminescence observations were performed on inclusions in amphibole on thin sections using a ELM-3R Luminoscope (Herzog et al., 1970). The operating conditions of the Luminoscope were: a beam voltage of 7 to 11 keV, a beam current of 0.5 mA and a beam diameter of approximately 5 μm.

Electron-microprobe analysis

Cameca Camebax and JEOL 840 electron microprobes were operated in wavelength-dispersion spectrometry mode (WDS) at an accelerating voltage of 15 or 20 kV and a beam current of 20 or 30 nA with a slightly defocussed beam (5 to 7 μm). The counting times used were 25 s for major-elements, 50 s for most minor elements, and 100 s for the rest (including F and Cl). The standards employed were: andradite (Fe), vanadinite (V, Cl), ilmenite (Mn, Ti) or spessartine (Mn) and TiO_2 (Ti), diopside (Si, Mg, Ca), orthoclase (K, Al), albite (Na), zircon (Zr), willemite (Zn), chromite (Cr), niobium metal (Nb), fluorite (F) and, in some cases, synthetic glass (Y, Yb). The chemical formulae resulting from the 554 analyses of amphibole were calculated on the basis of 23 atoms of oxygen, with Fe^{3+}/Fe^{2+} calculated from charge balance (16 cations and assumption of full cation occupancy) after the method of Droop (1987). Chemical formulae resulting from the 146 aegirine analyses were calculated on the basis of 4 cations and 6 atoms of oxygen, with Fe^{3+}/Fe^{2+} calculated as for amphibole.

Bulk analysis of amphibole by ICP-MS

Five representative samples of rock containing amphibole selected for study by bulk ICP-MS analysis were crushed with a BICO jaw crusher and sieved into <100 μm, >100 to <200 μm, and >200 μm fractions. The amphibole was concentrated by passing the selected size-fraction through a Franz magnetic separator, followed by hand picking under a binocular microscope. Each sample was ground with an agate pestle and mortar to produce 0.5 to 1 gram of powder. Bulk analysis by ICP-MS for HFSE (following lithium metaborate fusion) and atomic absorption spectroscopy for Li were performed by Activation Laboratories, Ancaster, Ontario, after a four-acid digestion (HF, $HClO_4$, HCl and HNO_3) and dilution in aqua regia. Whole-rock reference materials were used to calibrate the solutions.

LAM-ICP-MS analysis of amphibole and aegirine

Mounts of oriented grains of amphibole or composite grains of amphibole and aegirine were polished with 1-μm alumina grit followed by cleaning in an ultrasonic bath

with alcohol. The grains were chosen on the basis of the results of reconnaissance electron-microprobe analyses on amphibole from thin sections. An orientation perpendicular to the *c* axis was chosen to establish the extent of compositional zonation. Grains in these mounts were examined by SEM and electron-microprobe analysis prior to LAM-ICP-MS analysis.

The grains were analyzed at the Université de Montréal using a Fisons-VG PQ2+ ICP mass spectrometer and Fisons-VG LaserProbe equipped with a Spectron SL2B2 300 mJ Nd:YAG laser operated at 1064 nm with a 5 ns half-pulse duration. The laser was operated in Q-switched mode at 620 V flash lamp voltage, with a repetition rate of 5 Hz. The laser was focused on the surface of the sample. Specimen ablation was performed inside a quartz-glass sample cell, with the ablated material transferred to a torch by a continuous stream of Ar gas. The sequence of analysis was: gas blank (to establish the background), three standard analyses on NIST glass (external calibration), in-house standard, four analyses of the sample (the unknown). This sequence was performed twice in one cycle, with one minute between each analysis to allow for flushing of the tubing.

The 90 analyses of the amphibole and pyroxene were performed in two stages: first they were analyzed for elements with low atomic number (Z; ^{6}Li, ^{9}Be and ^{11}B), followed by elements with higher Z (^{51}V, ^{52}Cr, ^{66}Zn, ^{85}Rb, ^{88}Sr, ^{89}Y, ^{90}Zr, ^{93}Nb, ^{138}Ba, ^{139}La, ^{140}Ce, ^{141}Pr, ^{146}Nd, ^{147}Sm, ^{151}Eu, ^{157}Gd, ^{159}Tb, ^{162}Dy, ^{165}Ho, ^{166}Er, ^{169}Tm, ^{174}Yb, ^{175}Lu, ^{178}Hf, ^{232}Th and ^{238}U). This procedure was used to increase the counting statistics for each element, as tuning on ^{7}Li for the former or ^{88}Sr for the latter allowed optimum conditions of measurement. The analytical conditions used in the two sets of analyses are listed in Appendix B-10.

Synthetic glass (NIST 610) was used as a standard to determine the content of elements of low Z, whereas NIST 612 glass was used as a standard to determine the content of those of high Z. The trace-element content of NIST 612, reported by Stix et al. (1995), is in the range of that expected in the amphibole. Unfortunately, it was impossible to obtain a matrix-matched dark glass standard for the amphibole, because most such standards are Ca-rich (up to 11 wt.% CaO) and Na-poor (<3 wt.% Na_2O), unlike the amphibole, which contains approximately 9 wt.% Na_2O and only 0.5 wt.% CaO. A dark in-house standard glass made from olivine nephelinite (HF-13; Dalpé et al., 1995) was used to check for variations in matrix effects during analysis of the materials for elements with low Z. Dark glass (JW-87; Whalen, 1985) made from fused amphibole was used to perform the same

checks during analysis for elements with high Z. Variation in the ideal elemental content of the standards and of the dark glasses, treated as unknowns compared to the expected values, was within 1σ. Element concentrations were calculated using the values quoted by Stix et al. (1995) for the NIST standards, by Dalpé et al. (1995) for HF-13, and by Whalen (1985) for JW-87. Although attempts were made to use ^{44}Ca, ^{57}Fe, ^{55}Mn, ^{47}Ti, ^{48}Ti, ^{49}Ti, ^{50}Ti and ^{30}Si as the internal standard to compensate for differential sampling, ^{30}Si provided the most reproducible results with the smallest standard deviation. Standardization with ^{44}Ca produced slightly less reliable results, with an increased standard deviation owing to the low levels of Ca of the amphibole.

Unfortunately, the presence of fine-scale compositional zones (less than the 70-80 μm width of the laser beam) in the amphibole parallel to the *c* axis, and possibly even perpendicular to it, precluded any reasonable determinations of precision. The lower limit of detection (LLD) of each element was calculated from the equation of Bos et al. (1984), as applied by Dalpé et al. (1995). LLD values, in the range of 9 to 113 ppm, with most in the 10 to 15 ppm range (Appendix B-11), are consistent with or greater than those from previous LAM-ICP-MS studies (Jackson et al., 1992; Williams & Jarvis, 1993; Dalpé et al., 1995). Higher values result from the presence of minute inclusions or a short dwell-time on each element. As this is the first attempt to quantify the trace-element variation of the amphibole and, to a lesser extent, aegirine at Strange Lake, the short dwell-time is the result of the choice to examine a wide variety of elements enriched in the deposit, rather than a concern about decreasing the LLD, especially since these elements are generally enriched in the amphibole.

Results of Optical and Cathodoluminescence Examination

As numerous studies have described the units of the complex in detail (Miller, 1986; Salvi & Williams-Jones, 1990; Birkett et al., 1992; Nassif, 1993), only the salient information is summarized in Table 1. The granites vary, according to the nomenclature of Streckeisen (1976), from alkali feldspar granite to granite and leucogranite. A typical granite contains alkali feldspar, quartz, arfvedsonite and aegirine, and ore minerals that comprise 30-55 vol.%, 15-35 vol.%, 7-10 vol.% and 5-20 vol.% of the granite, respectively.

Table 1. Mineralogical and petrological differences between the different peralkaline granites.

Unit	Description	Mineral Content (%)	
Hypersolvus	Pale grey to bluish	Perthitic feldspar	50-70%
	Fine- to medium-grained	Quartz	15-25%
	Hypidiomorphic	Amphibole	7-15%
	Equigranular to porphyritic	Aegirine	0- 5%
		Accessory minerals[1]	5-10%
Transsolvus	Grey to blue gray	Feldspars	50-60%
	Fine-grained	Quartz	20-30%
	Hypidiomorphic	Amphibole	15-20%
	May be porphyritic	Accessory minerals[1]	5- 7%
Subsolvus			
1) Fresh	Buff to greenish blue	Quartz	30-40%
	Medium- to coarse-grained	2 Feldspars	45-55%
	Inequigranular	Amphibole/aegirine	to 10%
	May be porphyritic	Accessory minerals[1]	10-25%
2) Altered	Yellow to red-brown	Quartz	30-40%
	Bright yellow and red spots	2 Feldspars	5-55%
	in ore-rich samples	Amphibole/aegirine	to 10%
	Medium- to coarse-grained	Hematite	3- 5%
	Porphyritic	Accessory minerals[1]	15-25%

[1] The accessory minerals refer to primarily the ore minerals, but also ilmenite and the titanium silicates.

The principal difference, other than the type of feldspar and the content of the ore minerals, between subsolvus and the hypersolvus granites is that the former is quartz-rich (30-40 vol.%).

Textural Development of the Primary Mafic Minerals

Hypersolvus Granite

The areas of the pluton exhibiting distinct textures and assemblages of the mafic minerals are directly related to the areas defined by the map-units (Fig. 2). Primary amphibole from the hypersolvus granite (here called Type-1), is weakly zoned and pleochroic, from dark blue to blue-green. It forms oikocrystic patches, that are thus late-crystallizing, or subhedral to euhedral phenocrysts. This amphibole is zoned parallel to the *c* axis, from an inclusion-bearing euhedral core (Type-1a) to an inclusion-free euhedral overgrowth (Type-1b; Figs. 3A, B). Both generations of amphibole have the same optical appearance, which makes their contact difficult to define, even with the presence of inclusions. Type-1a amphibole contains inclusions (<1.5 mm in diameter) of ilmenite, aenigmatite (or possibly neptunite), zircon, and numerous smaller grains of primary subhedral fluoride minerals [Y-rich gagarinite, REE-rich yttriofluorite, and zajacite have been identified. The formula for gagarinite is $NaCa(LREE,Y)(F,Cl)_6$, while that of zajacite is $Na_{0.90}REE_{1.12}Ca_{0.92}F_6$ (Jambor et al., 1996)] and monazite (identified by EDS). Cathodoluminescence observations show that the fluoride minerals (colourless in thin section) exhibit colours that vary from a purple core to a green rim, whereas monazite has a darker blue-purple colour. These grains comprise up to 10 or 15 vol.% of the area at the core of the amphibole (Type-1a). They occur in two types: coarse- and fine-grained. In three samples, these tiny inclusions of fluoride are aligned parallel to the *c* axis of the amphibole and are particularly dominant at grain boundaries with other minerals. These inclusions are generally present in samples that contain "swapped" margins, which are intergrowths of arfvedsonitic amphibole and subsolvus albite that mantles earlier feldspar. Finally, dark green, rarely zoned, subsolvus (Type-1) aegirine mantles Type-1b arfvedsonitic amphibole in hypersolvus granite. These textures suggest that a transition from hypersolvus crystallization to subsolvus crystallization occurred at a very advanced

Figure 2. Surface distribution of mafic minerals.

A. Distribution of mafic minerals associated with arfvedsonitic amphibole. The margin of the hypersolvus granite is coincident with the limit of astrophyllite (Ast), aenigmatite (Aen), neptunite (Nep) and Type-1 aegirine (g Ae). Amphibole replacement by Type-2 aegirine (y Ae) occurs throughout the complex, but dominates in the altered subsolvus granite. This aegirine may be either hematite-poor (Hem-poor) or hematite-rich (Hem-rich). Moreover, Type-3 aegirine from the ore zone is yellow green.

B. Distribution of arfvedsonitic amphibole. Increased amphibole (Arf) contents are consistent with the contact of the hypersolvus and fresh subsolvus granites (7-10 vol.%) with the altered subsolvus granite. The most amphibole-rich (>10 vol.%) region contains transsolvus granite and the center of the hypersolvus granite. Phenocrysts of mafic minerals dominate in the altered subsolvus granite and the northeastern and eastern portions of the complex. These phenocrysts are commonly associated with fine-grained, interstitial amphibole (two Arf). Rare late-stage, fine-grained acicular arfvedsonitic amphibole is present in pod-like regions in the ore zone and near the upper contact between the altered subsolvus and hypersolvus granites.

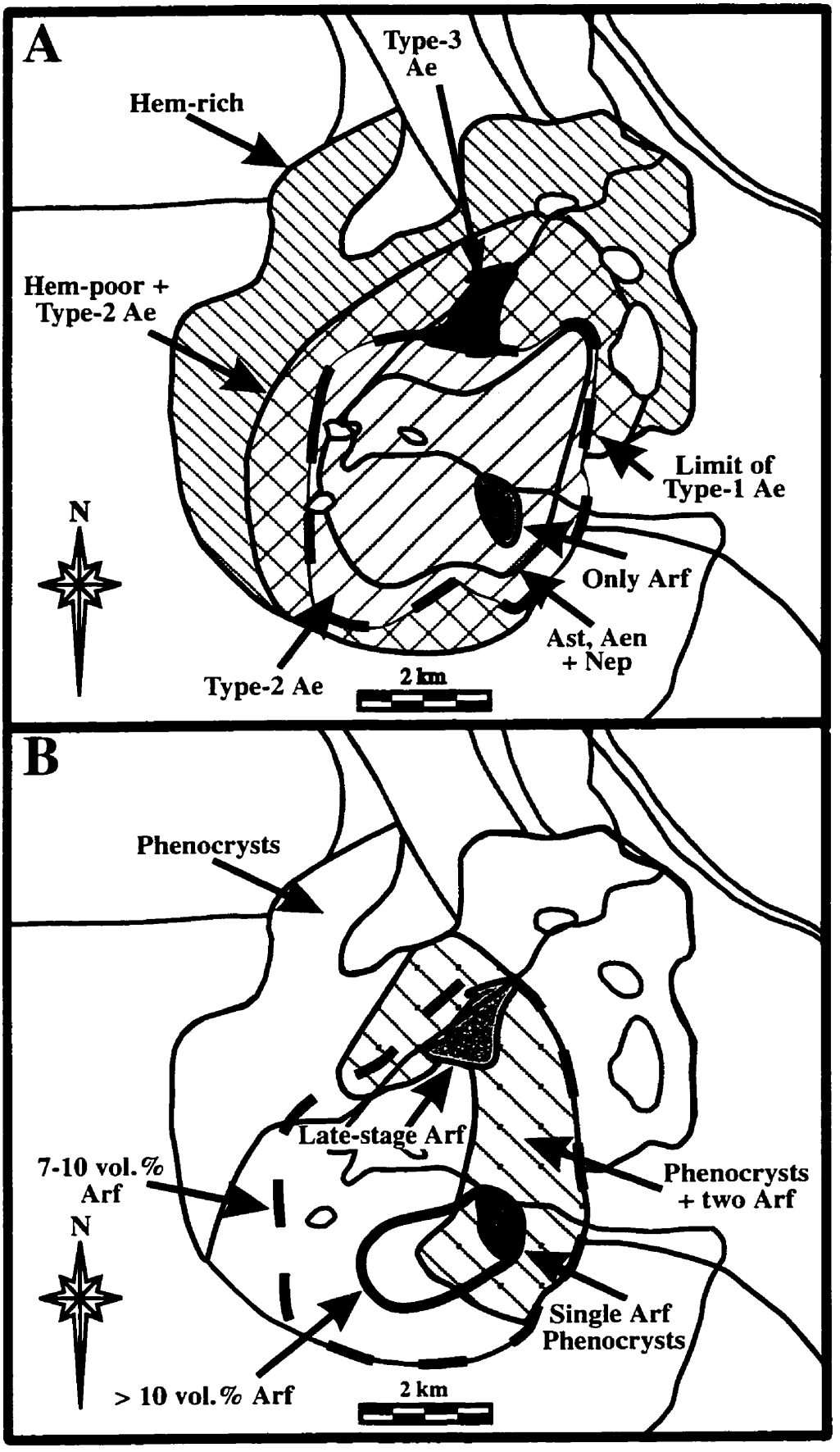
A
Type-3
Ae
Hem-rich
Hem-poor +
Type-2 Ae
Limit of
Type-1 Ae
N
Only Arf
Ast, Aen
+ Nep
Type-2 Ae
2 km
B
Phenocrysts
Late-stage Arf
7-10 vol.%
Arf
Phenocrysts
+ two Arf
N
Single Arf
Phenocrysts
> 10 vol.% Arf
2 km

Figure 3. Photomicrographs of the textures of the arfvedsonitic amphibole from the hypersolvus granite.

A. Amphibole from hypersolvus granite in plane-polarized light. Type-1a arfvedsonitic amphibole (black) containing inclusions of monazite, zajacite, yttriofluorite and gagarinite (white) at the core is surrounded by a rim of inclusion-free Type-1b amphibole. It is surrounded by quartz (qtz) to the left, alkali feldspar (feld) to the right and pyrochlore (prc) at the bottom of the image (width of the image is 2 mm).

B. Cathodoluminescence image of the zonation in the same grains. Numerous inclusions of numerous monazite, zajacite, yttriofluorite and gagarinite inclusions are present in the core. Note the relatively sharp boundary between Type-1a and Type-1b amphibole, which is strongly accentuated by cathodoluminescence and delineated by the dashed line (cf. Fig. 3A; width of the image is 2 mm).

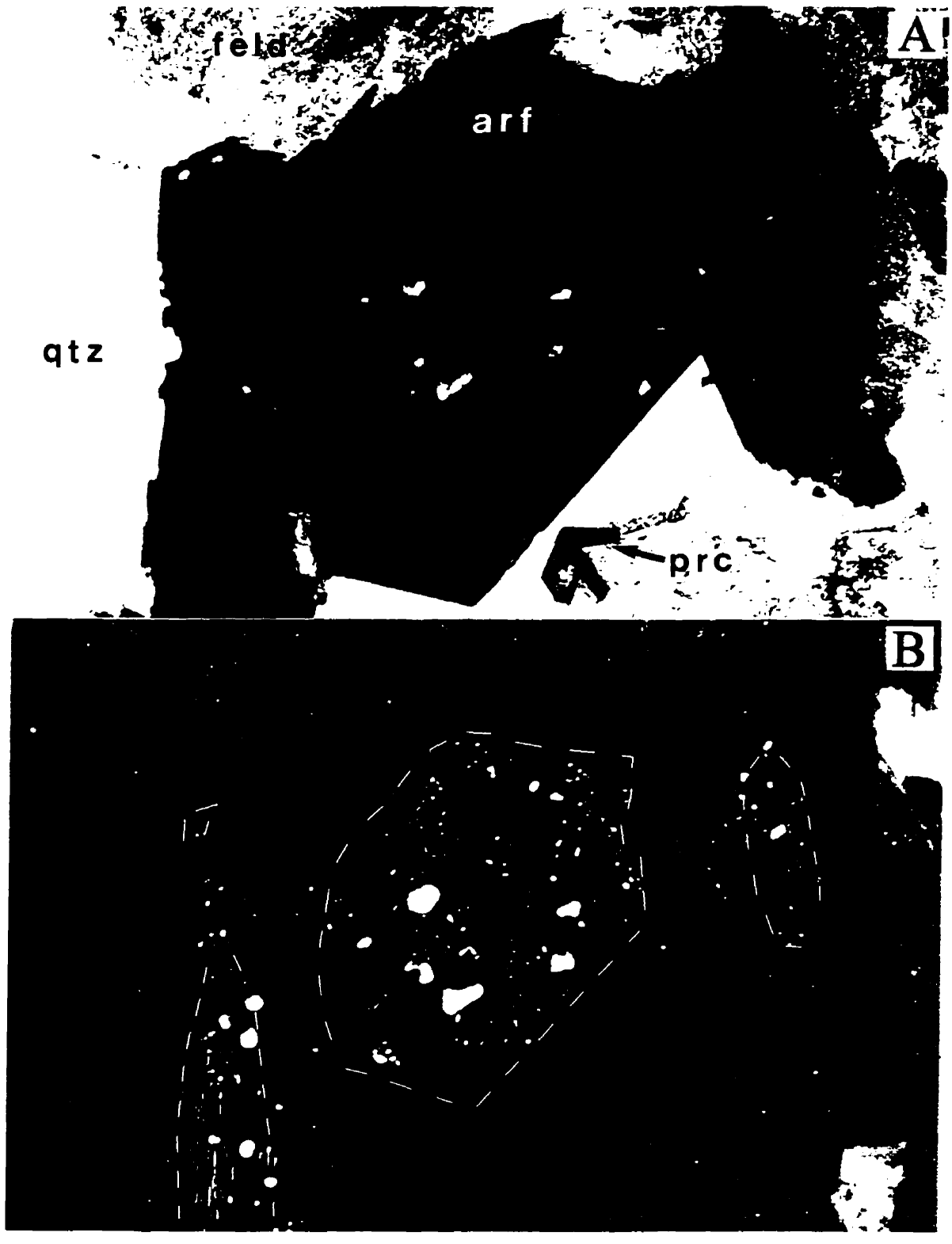
feld
arf
qtz
prc
A
B

stage of magmatic crystallization (>95%) in this unit.

Pale yellow (Type-2) aegirine occurs between Type-1 aegirine (10 vol.%) and Type-1 arfvedsonitic amphibole, especially near the margins of the hypersolvus granite map-unit (Fig. 4A). Type-2 aegirine replaced the amphibole in the core and near the former grain boundary between the amphibole and Type-1 aegirine. The former euhedral grain boundary is now accentuated by a change from Type-1 to Type-2 aegirine. This Type-2 aegirine, which comprises approximately 17 vol.% of the composite grain examined in detail, is composed of a mosaic of subgrains of almost the same orientation that separate relict inclusions of Type-1a and -1b amphibole. The "moth-eaten" appearance of Type-2 aegirine results from the presence of minute, dark brown to black inclusions of amphibole or oxide, and brown fibers of astrophyllite up to 2-mm-long (0.5-5 vol.%). This astrophyllite occurs at the contact between Type-1a amphibole and aenigmatite, neptunite, ilmenite, as inclusions in Type-1 amphibole and perthite, or rimming an earlier bright yellow to orange, interstitial variety.

Other titanium silicates associated with arfvedsonitic amphibole and aegirine in the hypersolvus granite are aenigmatite, neptunite, bafertisite and narsarsukite. Aenigmatite (non-pleochroic bright red) rims ilmenite, is intergrown with neptunite (weakly pleochroic and red), or occurs as euhedral grains in Type-1a amphibole. Neptunite also replaces Type-1 aegirine or is replaced by late fibers of astrophyllite. Rare greenish yellow bafertisite occurs as fibrous intergrowths with the late astrophyllite that rims ilmenite. In addition, narsarsukite is euhedral and acicular, or poikilitic with pale-yellow pleochroism. It rims grains of most of the other Ti-silicates, except for the fibers of bafertisite or astrophyllite, or occurs as interstitial grains.

Transsolvus Granite

Two generations of arfvedsonitic amphibole are present in samples that exhibit the transsolvus feldspar: fine- to medium-grained subhedral amphibole and late fine-grained interstitial amphibole. Aenigmatite and neptunite form euhedral to subhedral inclusions at the core of some grains. Type-2 aegirine is rare, and Type-1 aegirine is volumetrically insignificant (Fig. 2A). This unit and the adjacent samples of hypersolvus granite have the highest content of mafic minerals (≥10 vol.%; Fig. 2B).

Figure 4. The aegirine-arfvedsonitic amphibole relationships.

A. In the hypersolvus granite when oriented perpendicular to the *c* axis, arfvedsonitic amphibole (darkest grey; arf) is mantled on the bottom by Type-1 (dark grey; Ti-aeg) aegirine in plane-polarized light. Amphibole is replaced by Type-2 (light grey; aeg) aegirine near its contact with Type-1 aegirine and an aegirine and astrophyllite assemblage at the core. Note that the remnant of the original grain margin of the amphibole (black) is accentuated by the contact between Type-1 and -2 aegirine (49-C-2; length of image is 2 mm).

B. Zonation of arfvedsonitic amphibole (arf; black), Type-2 aegirine and hematite (aeg; dark grey) in altered subsolvus granite oriented perpendicular to the *c* axis of these silicates (in plane-polarized light). The sequence of zonation is aegirine assemblage at the core surrounded by amphibole and then the aegirine assemblage at the rim (length of image is 4 mm).

C. Arfvedsonitic amphibole - aegirine relationship in a composite grain from an altered pegmatite in the hypersolvus granite. Note the presence of small, angular inclusions of arfvedsonitic amphibole (dark grey; arf) in Type-2 aegirine (light grey; aeg), which indicates replacement of amphibole by aegirine (46-I-3; length of image is 2 mm).

D. Fine-grained, euhedral, aligned acicular arfvedsonitic amphibole (dark grey; arf), which forms late-stage felty pods between prismatic Type-3 aegirine (light grey; aeg). The prismatic aegirine contains late replacements of quartz or fluorite (SL-BS-1; length of the image is 4 mm).

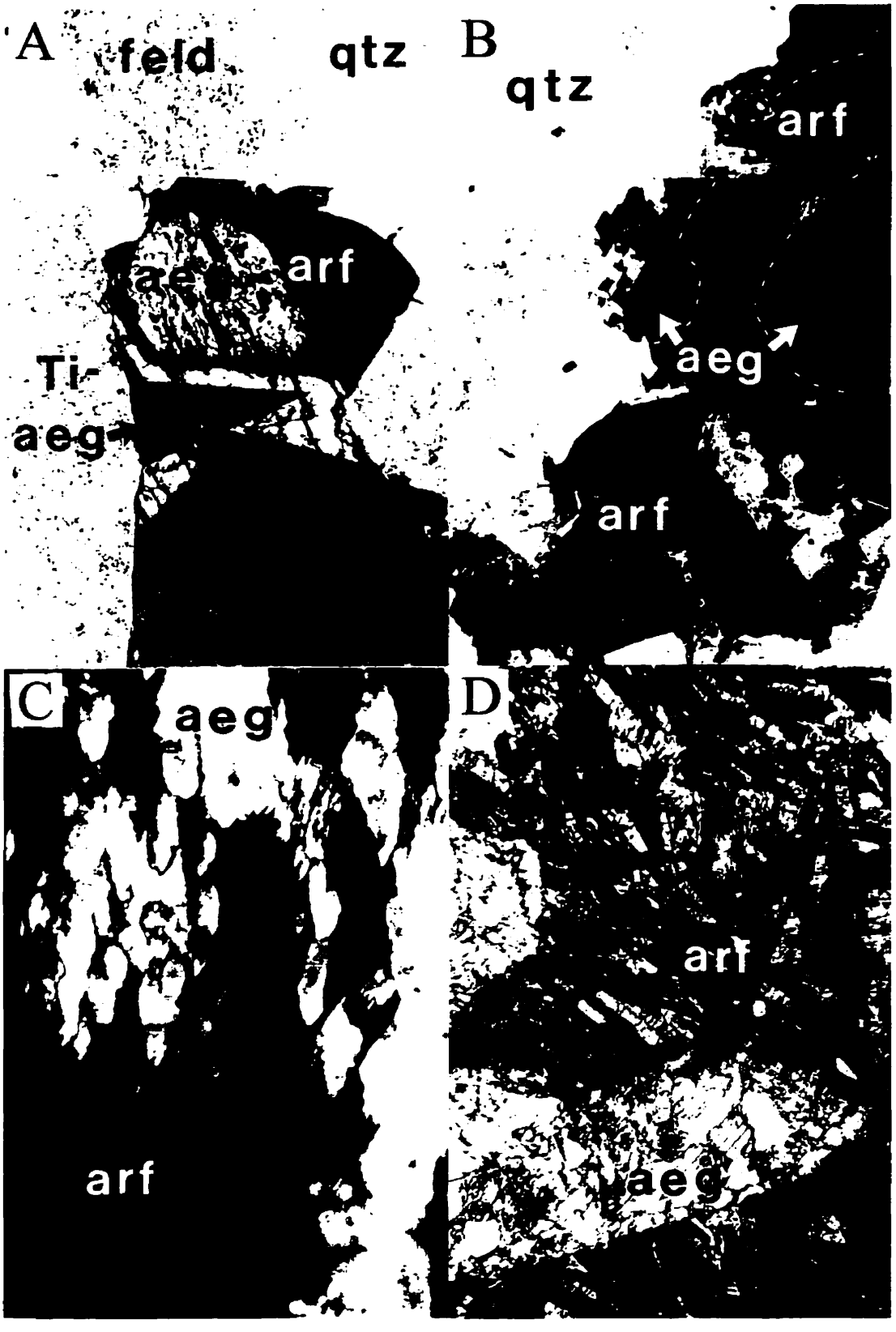
A
feld
qtz
aeg
arf
Ti-
aeg
B
qtz
arf
aeg
arf
C
aeg
arf
D
arf
aeg

Subsolvus Granite

In samples of subsolvus granite, Type-2 amphibole occurs in two textural varieties: subhedral to euhedral porphyritic (1-2 cm) and, less commonly, as anhedral, fine-grained oikocrysts. Where fresh, samples of subsolvus granite contain Type-1 aegirine in some cases intergrown with Ti silicates, arfvedsonitic amphibole and aegirine. In the altered subsolvus granite, the arfvedsonitic amphibole and aegirine form composite, zoned phenocrysts of Type-2 amphibole (10-60 vol.%) alternating with an assemblage of Type-2 aegirine and 0.5 mm grains of hematite ± quartz (Fig. 4B). Both zones contain feldspar inclusions. The amphibole and aegirine zonation and presence of fine-grained hematite and aegirine, and relict amphibole in aegirine near the amphibole-aegirine contact suggest replacement of amphibole by aegirine, as mentioned in descriptions of the hypersolvus samples. In drill core, the amphibole occurs as phenocrysts in the porphyritic granite or interstitial grains in the equigranular granite (these granite types were defined by Salvi & Williams-Jones, 1995). No astrophyllite, aenigmatite or neptunite is present in the altered subsolvus granite (Fig. 2A). This granite only contains the most Fe^{3+}-rich mafic minerals.

Pegmatitic Samples

Isolated grains of amphibole from pegmatite may be fresh, or replaced completely or in part by Type-2 aegirine (e.g. SL-4-15 versus 46-I-3; Fig. 4C). At the surface in the ore zone, medium- to coarse-grained, euhedral, yellow green aegirine (Type-3) with the typical aegirine cross-section is present. No amphibole inclusions indicative of a secondary origin were found in Type-3 aegirine. Altered subsolvus granite contains melanocratic lenses of mafic character intercalated between pegmatitic and aplitic horizons. These lenticular masses, that consist of approximately 60 vol.% Type-3 amphibole, have an igneous texture. The amphibole prisms are fine-grained (0.3 mm) and constitute a matrix to "phenocrysts" of Type-3 aegirine (Fig. 4D) and the ore minerals. K-feldspar and fluorite are intersitital to these amphibole grains that contain minute, pale yellow octahedra of pyrochlore. The acicular nature, fine grain-size and mat-like nature of this amphibole and its occurrence in pods imply late-stage crystallization from an evolved mafic liquid. Such mesocratic amphibole-rich regions were termed "lindinosite" by Lacroix (1922), or "lujavrite" where present in silica-undersaturated complexes (Brögger, 1890).

Sequence of Crystallization

The paragenetic sequence of crystallization of these mafic minerals can be inferred from their textural relationships (Fig. 5). Zircon, elpidite (in some cases), ilmenite, aenigmatite, monazite, gagarinite, yttriofluorite, zajacite and fluorite crystallized before the amphibole. In addition, in the hypersolvus granite feldspar and quartz began to crystallize before Type-1 amphibole. This was followed, in the hypersolvus granite, by the crystallization of amphibole, further crystallization of feldspar and late formation of a "sawtooth" intergrowth between the two minerals (e.g., swapped margins). Type-1 aegirine rims on arfvedsonitic amphibole, in the hypersolvus and transsolvus granite, was the last mafic mineral to crystallize from the melt. Late quartz crystallized in the subsolvus granite after amphibole or Type-3 aegirine. This aegirine formed either by late-stage magmatic processes or from a postmagmatic fluid. In the ore zone, Type-3 aegirine, not amphibole, was the first mafic silicate to crystallize. It was followed, in cases of extreme fractionation, by crystallization of late-stage Type-3 amphibole in mafic pods. Secondary processes that resulted in the replacement of arfvedsonitic amphibole by Type-2 aegirine will be dealt with in Chapter 5.

Compositional Variation of the Arfvedsonitic Amphibole

Amphibole from the complex is predominantly Li-bearing, fluor-arfvedsonite. In a few cases, where the rocks are geochemically more primitive (specific samples of hypersolvus granite), the amphibole may be fluor-richterite (up to 75% richterite). Specific analyses of the amphibole from more altered subsolvus granite may also contain up to 50% richterite. These samples exhibit the effects of Ca-metasomatism (Chapter 6). Type-3 amphibole is Li-bearing potassian-fluor-arfvedsonite (Table 2; Fig. 6A; nomenclature after Leake, 1978). Most amphiboles contain a maximum of: 3.06 wt.% CaO, 3.28 wt.% K_2O, 1.48 wt.% MgO, 1.83 wt.% MnO, 2.67 wt.% ZnO, 0.78 wt.% ZrO_2, 0.24 wt.% Li_2O, 0.18 wt.% ΣREE_2O_3, 2.53 wt.% TiO_2, 2.90 wt.% Al_2O_3 and 3.19 wt.% F (Tables 2, 3). Other elements present in some cases in minor amounts include Nb, Yb, Cr, V and Cl.

Figure 5. Paragenetic sequence of crystallization of the primary mafic minerals in the Strange Lake peralkaline complex. The first minerals to crystallize are zircon followed by magnetite, monazite and fluoride inclusions, and then the titanium silicates (aenigmatite, astrophyllite, neptunite, bafertisite and narsarsukite). Later in the sequence the feldspar and amphibole crystallize. The sequence in which they crystallize in depends on the unit in which they crystallize. The amphibole is generally late in the sequence in the hypersolvus granite, but early in the subsolvus granite. Primary aegirine occurs as late rims on arfvedsonitic amphibole (Type-1 aegirine) or prismatic crystals followed by late acicular Type-3 amphibole (Type-3 aegirine).

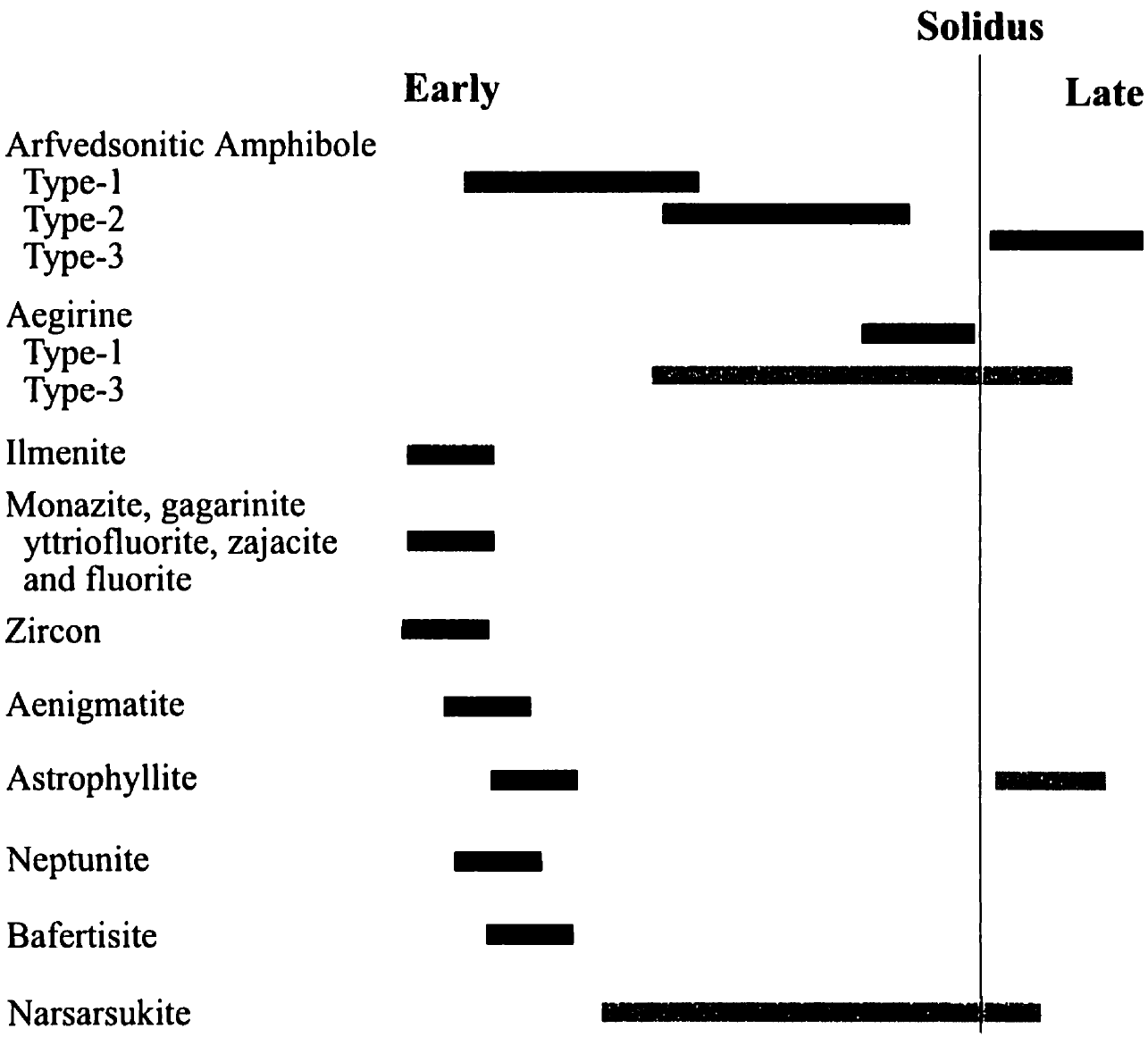
Solidus
Early
Late
Arfvedsonitic Amphibole
Type-1
Type-2
Type-3
Aegirine
Type-1
Type-3
Ilmenite
Monazite, gagarinite
yttriofluorite, zajacite
and fluorite
Zircon
Aenigmatite
Astrophyllite
Neptunite
Bafertisite
Narsarsukite

Table 2. Selected electron-microprobe analyses of amphibole.

Type	Type-1a	Type-1b			Type-2	Type-3
Unit	Hypersolvus		Altered Pegmatite	Fresh Subsolvus	Altered Subsolvus	Mafic Pod
Sample #	49-C-2	49-C-2	46-I-3	38-B-3	25-C-1	SL-BS-1
Description	center	edge	middle	light	away	middle
Na_2O	9.15	9.07	8.96	9.36	8.91	9.34
K_2O	1.07	1.09	2.23	1.58	1.45	2.35
CaO	0.55	0.61	0.21	0.09	0.25	0.04
FeO	28.54	29.36	25.60	27.49	27.75	24.39
Fe_2O_3	6.44	5.18	6.82	4.81	5.86	7.32
MgO	0.18	0.22	0.01	0.02	0.69	0.00
MnO	0.67	0.67	1.44	1.01	0.67	1.90
ZnO	0.19	0.18	0.70	0.48	0.36	0.86
Nb_2O_5	0.00	0.00	0.01	0.00	0.02	0.03
V_2O_3	0.02	0.02	0.00	0.01	0.00	0.00
Cr_2O_3	0.00	0.01	0.00	0.00	0.00	0.00
Yb_2O_3	0.02	0.01	0.00	0.00	0.00	0.00
ZrO_2	0.14	0.12	0.48	0.29	0.10	0.13
TiO_2	1.04	1.03	0.80	1.84	0.73	0.44
Al_2O_3	0.51	0.54	0.16	0.28	0.29	0.16
SiO_2	50.15	50.69	50.45	50.55	50.43	51.79
F	1.99	1.98	1.94	1.23	2.65	1.92
Cl	0.01	0.02	0.00	0.00	0.00	0.00
H_2O	0.94	0.95	0.96	1.30	0.62	0.99
Total	101.60	101.74	100.76	100.32	100.77	101.69
-O=F	0.84	0.84	0.81	0.52	1.12	0.81
-O=Cl	0.00	0.00	0.00	0.00	0.00	0.00
Total	100.76	100.90	99.95	99.80	99.65	100.88

Table 2. Selected electron-microprobe analyses of amphibole (continued).

Type	**Type-1a**	**Type-1b**			**Type-2**	**Type-3**
Unit	**Hypersolvus**		**Altered Pegmatite**	**Fresh Subsolvus**	**Altered Subsolvus**	**Mafic Pod**
Sample #	**49-C-2**	**49-C-2**	**46-I-3**	**38-B-3**	**25-C-1**	**SL-BS-1**
Description	**center**	**edge**	**middle**	**light**	**away**	**middle**
Na	2.810	2.778	2.774	2.889	2.756	2.849
K	0.216	0.219	0.454	0.321	0.295	0.472
Ca	0.093	0.103	0.036	0.016	0.043	0.007
Fe^{2+}	3.781	3.879	3.418	3.660	3.705	3.209
Fe^{3+}	0.768	0.616	0.820	0.576	0.704	0.867
Mg	0.043	0.053	0.002	0.004	0.164	0.001
Mn	0.090	0.089	0.195	0.136	0.091	0.253
Zn	0.022	0.020	0.083	0.056	0.042	0.100
Nb	0.000	0.000	0.000	0.000	0.001	0.001
V	0.002	0.002	0.000	0.001	0.000	0.000
Cr	0.000	0.001	0.000	0.000	0.000	0.000
Yb	0.001	0.001	0.000	0.000	0.000	0.000
Zr	0.011	0.009	0.037	0.023	0.008	0.010
Ti	0.124	0.122	0.096	0.220	0.088	0.053
^{VI}Al	0.040	0.100	0.000	0.000	0.054	0.029
Si	7.945	8.008	8.056	8.048	8.050	8.148
^{IV}Al	0.055	0.000	0.029	0.052	0.000	0.000
F	0.998	0.991	0.977	0.620	1.338	0.955
Cl	0.003	0.005	0.000	0.001	0.000	0.001
OH	0.998	1.004	1.023	1.379	0.662	1.044

Mineral formulae were calculated based on 23 oxygen and 16 cations using the method of Droop (1994) to determine the Fe^{3+}/Fe^{2+} ratio.

Figure 6. Compositional variation of arfvedsonitic amphibole.

A. $\Sigma Ca+^{IV}Al$ versus $\Sigma Na+K+Si$ (apfu) plot after Fabriès (1978) that shows the compositional variation of the amphibole as determined from electron-microprobe analysis. The average amphibole composition plots at approximately 11.40 on the $\Sigma Na+K+Si$ axis and trends from arfvedsonite (Arf) (with a ferro-leakeite component; Lkt) to ferro-richterite (Ric). The other amphiboles are ferri-kataphorite (Kpt) and ferri-winchite (Win).

B. Composition variation of the amphibole with the mineral formulae calculated from a combination of electron-microprobe and LAM-ICP-MS (e.g., Li, REE, Nb and Zr) analysis after removal of analyses not containing Li and those that contain the effects of Ca-metasomatism as discussed further in Chapter 6. The average amphibole contains slightly less Ca content, and $\Sigma Na+K+Si$ shifts to a maximum of 11.25.

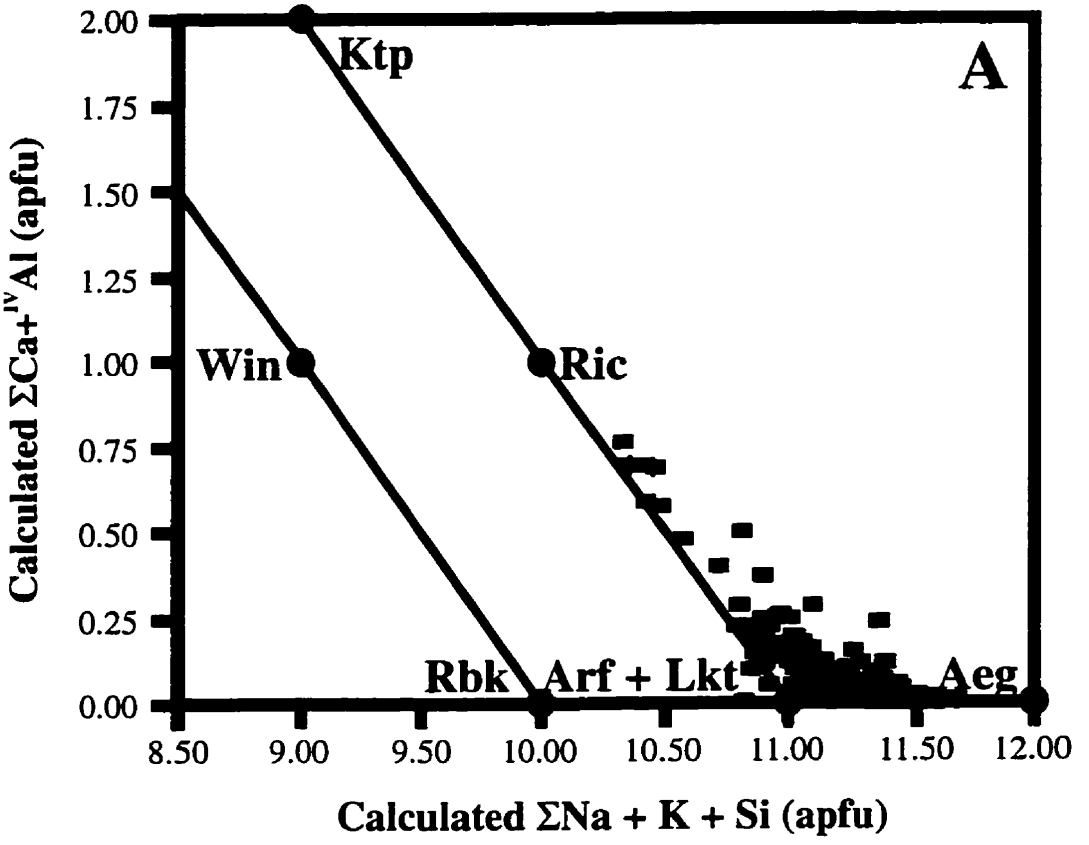
A
Ktp
Win
Ric
Rbk
Arf + Lkt
Aeg
2.00
1.75
1.50
1.25
1.00
0.75
0.50
0.25
0.00
8.50
9.00
9.50
10.00
10.50
11.00
11.50
12.00
Calculated ΣCa+IVAl (apfu)
Calculated ΣNa + K + Si (apfu)

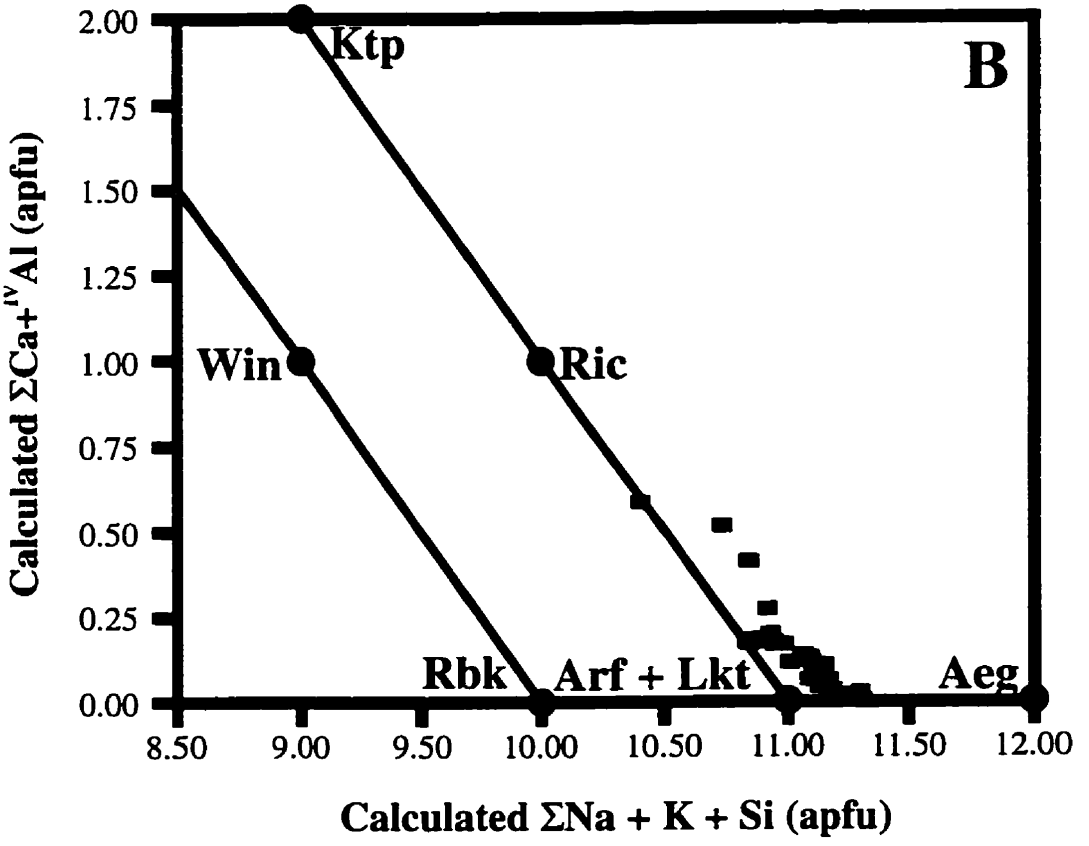
B
Ktp
Win
Ric
Rbk
Arf + Lkt
Aeg
2.00
1.75
1.50
1.25
1.00
0.75
0.50
0.25
0.00
8.50
9.00
9.50
10.00
10.50
11.00
11.50
12.00
Calculated ΣCa+IVAl (apfu)
Calculated ΣNa + K + Si (apfu)

Table 3. Selected LAM-ICP-MS analyses of amphibole.

Unit	Hypersolvus			Altered Pegmatite	Fresh Subsolvus	Altered Subsolvus	Mafic Pod
Sample #	**48-A-7**	**49-C-2**	**57-A-1**	**46-I-3**	**38B3#2**	**63-B-1**	**SL-BS-1**
Na_2O	9.35	8.82	8.94	9.16	9.53	9.34	9.19
K_2O	1.25	1.06	1.40	2.24	1.30	1.51	2.34
CaO	0.63	0.55	0.26	0.19	0.35	0.32	0.06
Fe_2O_3	33.75	34.70	30.60	31.75	33.34	32.82	30.84
MgO	0.20	0.16	0.23	0.00	0.15	0.19	0.03
MnO	0.87	0.66	1.51	1.45	0.66	0.80	1.83
ZnO	0.28	0.24	0.63	0.70	0.19	0.30	0.96
Cr_2O_3	0.00	0.00	0.01	0.00	0.00	0.00	0.00
V_2O_3	0.00	0.00	0.01	0.01	0.02	0.01	0.02
Nb_2O_5	0.00	0.00	0.00	0.01	0.00	0.00	0.04
ZrO_2	0.22	0.12	0.14	0.50	0.16	0.21	0.09
Y_2O_3	0.00	0.00	0.00	0.00	0.00	0.00	0.00
Yb_2O_3	0.01	0.00	0.00	0.02	0.00	0.03	0.00
TiO_2	0.91	1.05	1.29	0.84	1.12	1.61	0.52
Al_2O_3	0.46	0.50	0.47	0.16	0.40	0.30	0.16
SiO_2	50.14	50.13	50.79	50.39	50.57	50.39	51.55
F	1.56	1.97	1.89	1.85	2.04	1.93	1.66
Cl	0.01	0.01	0.01	0.00	0.01	0.01	0.01
Total	98.98	99.14	97.38	98.47	98.97	98.94	98.58

Table 3. Selected LAM-ICP-MS analyses of amphibole (continued).*

Unit	Hypersolvus			Altered Pegmatite	Fresh Subsolvus	Altered Subsolvus	Mafic Pod
Sample #	48-A-7	49-C-2	57-A-1	46-I-3	38B3#2	63-B-1	SL-BS-1
Li	770	1373	n.d.	1692	1301	967	n.d.
Be	60	12	n.d.	15	102	27	n.d.
B	17	2	n.d.	4	22	3	n.d.
V	1	2	4	0	1	0	2
Cr	6	0	1	3	1	1	12
Zn	3159	2755	5109	7242	2334	3712	7143
Rb	16	25	132	70	28	27	75
Sr	88	2	35	2	3	4	10
Y	3012	43	281	63	35	64	186
Zr	644	1007	618	4538	1368	1576	570
Nb	133	64	144	272	75	130	897
Ba	13	1	37	2	1	5	18
La	232	13	3379	2	9	6	56
Ce	619	43	5336	7	25	20	110
Pr	109	7	712	1	4	3	15
Nd	556	28	2448	4	16	11	40
Sm	197	7	254	1	2	3	15
Eu	14	0	8	0	0	0	1
Gd	252	4	204	1	2	2	18
Tb	59	1	16	0	0	1	6
Dy	449	7	72	6	5	9	52
Ho	105	2	11	3	2	4	10
Er	364	13	31	27	13	33	33
Tm	56	4	6	9	4	12	5
Yb	340	48	63	99	48	143	40
Lu	42	12	14	20	12	35	4
Hf	30	32	23	182	51	55	24
Th	21	0	422	0	0	0	34
U	1	0	3	0	0	0	184
Σ REE	3395	189	12555	180	144	282	406

* Concentrations in ppm.
n.d.: Not determined.

Structural formulae of the amphibole calculated solely from results of electron-microprobe analysis, produce an average calculated ΣNa+K+Si of 11.40 (apfu) in the ΣCa+^{IV}Al versus ΣNa+K+Si plot (Fig. 6A), first proposed by Fabriès (1978). The value for ΣNa+K+Si should be 11.0 for ideal arfvedsonite and leakeite, and 12.0 for the equivalent four formula units of aegirine (Fig. 6A). Amphibole formulae calculated from a combination of electron-microprobe and LAM-ICP-MS analysis, after removal of samples that exhibit Ca-metasomatism (Chapter 6) and those for which no analyses were performed for Li, show that the average values of ΣNa+K+Si are decreased to 11.25 (Fig. 6B).

Distinct compositional trends are observed in bar graphs showing calculated formulae of amphibole from a combination of electron-microprobe and LAM-ICP-MS results (Fig. 7). Figure 7A shows a striking increase in the level of K and Mn between the hypersolvus granite and the mafic pods, which is mirrored in Figure 7B by an equivalent increase in the amount of Zn between these same units. These increases coincide with a decrease in Fe^{3+} between the hypersolvus granite and the mafic pods (Fig. 7A), followed by an increase, to a value greater than in the hypersolvus granite, in 46-I-3. Minor variations in K and Mn, or a significant enrichment in Zn occurs in the altered pegmatite from hypersolvus granite (46-I-3). Amphibole from the mafic pod is distinctly enriched in K and Mn compared with that of the other units. Where the Li content of the arfvedsonitic amphibole decreases between the hypersolvus and fresh subsolvus granites, it increases in the altered subsolvus granite and the mafic pods, but then decreases in the altered pegmatite in the hypersolvus granite to slightly less than that from the hypersolvus granite (Fig. 7B). The F content follows the reverse trend. Moreover, the F content of amphibole from the hypersolvus granite is equivalent to F-poor amphibole from the altered subsolvus granite. The ^{VI}Al content of amphibole varies by: increasing between the hypersolvus and subsolvus granites, but decreasing between altered subsolvus granite, mafic pods and altered pegmatite. On average, the Ca content of amphibole from hypersolvus and fresh subsolvus granites are comparable, whereas that from the altered subsolvus granite is on average depleted (Fig. 7B). More primitive samples of amphibole from the hypersolvus granite (Type-1a) that contain Ti silicates also exhibit the same enrichment in Ca (and Mg) as Ca-enriched arfvedsonitic amphibole from the altered subsolvus granite. Amphibole from the mafic pods is extremely depleted in Ca.

Figure 7. Major-element variations in the calculated (from LAM-ICP-MS and electron-microprobe analysis), amphibole formulae. In this figure, H refers to amphibole from hypersolvus granite, S fresh refers to amphibole from fresh subsolvus granite, S alt refers to amphibole from altered subsolvus granite, 46-I-3 refers to amphibole from altered pegmatite and BS refers to amphibole of the mafic pods (sample SL-BS-1). The data represents the averages of analyses, where the average from the hypersolvus granite (H) is based on 29 analyses, that of the fresh subsolvus granite (S fresh) is based on either 14 or 8 analyses (depending on whether elements of high or low Z, respectively, were analyzed), that of the altered subsolvus granite (S alt) is based on either 29 or 23 analyses (with the same stipulations), that of the mafic pods (lindinosite; SL-BS-1) is based on 2 or 1 analyses (as above), and finally, that of altered pegmatite in the hypersolvus granite (46-I-3) is based on 12 analyses. Unfortunately, the fine grain-size of amphibole from the mafic pods precluded analysis for elements of low Z by LAM-ICP-MS, so the Li_2O content was calculated by multiplying that determined from ICP-MS analysis by a factor that accounts for the difference (see below) between it and that from LAM-ICP-MS.

A. F, Fe^{3+}, K and Mn contents of arfvedsonitic amphibole.

B. Li, Ca, Zn and ^{VI}Al contents of the amphibole.

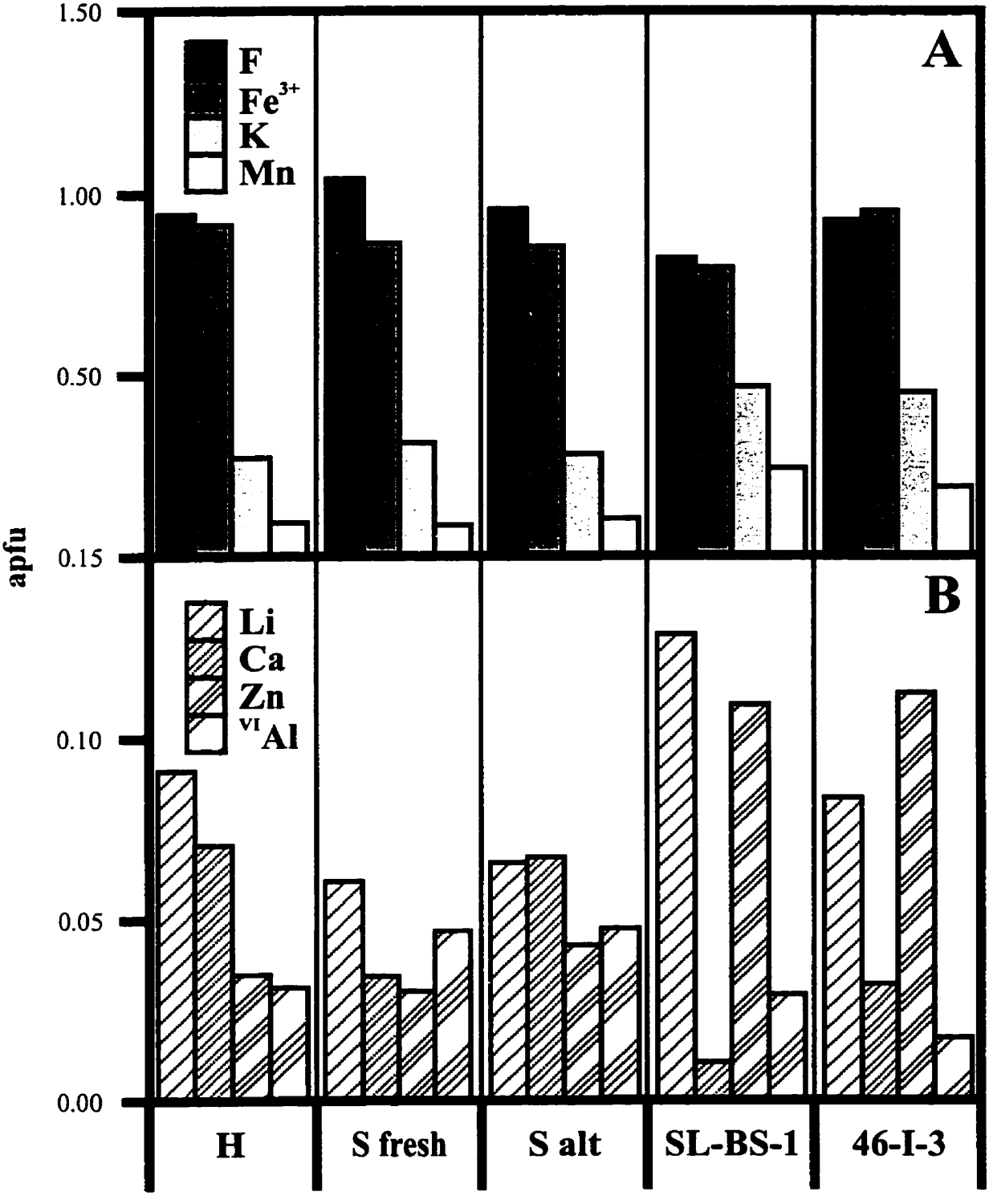
1.50
1.00
0.50
0.15
0.10
0.05
0.00
apfu
A
F
Fe3+
K
Mn
B
Li
Ca
Zn
VIAl
H
S fresh
S alt
SL-BS-1
46-I-3

The compositional variation of amphibole, on the basis of the formulae calculated solely from electron-microprobe analysis, are best depicted in Figures 8 and 9. The sample size used is much larger than that used to construct Figure 7, as the results of electron-microprobe analyses were used (554 analyses). Figure 8A shows a simultaneous increase in Zn and Mn, especially in the altered pegmatite in the hypersolvus granite. Although amphibole from the mafic pods is the most enriched in Zn and Mn, the trend of compositional variation reflects a negative correlation (indicative of a different origin) between Zn and Mn. Amphibole from the few samples of the transsolvus granite have the same low Zn content as amphibole from the hypersolvus granite, which is low in Zn.

The positive correlation also is observed between Zr and Ti, although the Zr shows only a minor increase (Fig. 8B). The Ti and Zr contents of amphibole are the same in the hypersolvus and fresh subsolvus granites, but are slightly enriched compared to that from the altered subsolvus granite. Amphibole from the mafic pods contains slightly less Ti, at an equivalent to lower Zr content, than that from the other granites. The Ti content of the altered pegmatite in the hypersolvus granite is independent of the Zr content, but is intermediate to the Ti content of the other units. Zr-poor compositions of amphibole from the altered pegmatite in hypersolvus granite are of an equivalent Ti content, as the most Zr-rich amphibole from the hypersolvus granite. The few analyses of amphibole from the transsolvus granite fall in the region defined by amphibole from the hypersolvus granite, except those from the transsolvus granite which are slightly enriched in Ti. The Zr, Ti, Mn and Zn content of amphibole from the mafic pods generally seems to follow the same evolutionary trend as amphibole from the other units, although it is always at the compositional extreme. By comparison, amphibole from altered pegmatite in hypersolvus granite shows, for some elements, distinct differences in composition that are the same as those observed in the altered subsolvus granite.

Slightly less K than average occurs in amphibole from the hypersolvus granite compared to that from altered subsolvus granite and, in particular, that from mafic pods and from altered pegmatite in hypersolvus granite (Fig. 9A). Moreover, most amphibole has, in general, a lower Mn/(Mn+Fe) (Mn#) than that from the mafic pods or altered pegmatites in the hypersolvus granite. The lowest values of K and Mn# are present in amphibole from the altered subsolvus granite, although that from the equigranular altered subsolvus granite

Figure 8. Element variation plots of amphibole formulae calculated solely from electron-microprobe analysis. The acronyms used are as in Figure 7, except for those described below which are: H-S alt refers to amphibole from hypersolvus granite near the contact with that of the altered subsolvus granite, S alt peg refers to amphibole from pegmatites present in the altered subsolvus granite, S core refers to amphibole from the subsolvus granite (generally altered subsolvus granite) from drill core, and S core ore refers to the same subsolvus granite from amphibole of the equigranular granite or pegmatites (for classification see Chapter 5) from depth in the ore zone. The lines on these and the following plots are: dark dotted line which represents a combination of amphibole analyses from hypersolvus and transsolvus granites and hypersolvus granite near its contact with the altered subsolvus granite; light dotted line which represents amphibole from altered subsolvus granite; dark dashed line which represents amphibole from altered pegmatites in the altered subsolvus granite; light dashed line which represents amphibole from altered pegmatite in hypersolvus granite near its contact with the altered subsolvus granite (46-I-3); dark line which represents amphibole from the subsolvus granite from the drill core; light line which represents amphibole from the equigranular subsolvus granite from the drill core (Chapter 5) ; dark dashed and dotted line which represents amphibole from the mafic pods (SL-BS-1).

A. Zn versus Mn plot that shows an increase in Zn and Mn due to magmatic evolution of arfvedsonitic amphibole from the hypersolvus and subsolvus granites. Amphibole from altered pegmatite in the hypersolvus granite is slightly more enriched in Mn relative to Zn than that of typical amphibole. The most enriched amphibole is that from the mafic pods.

B. Zr versus Ti plot that shows the same concurrent increase due to magmatic evolution as A, except for the distinct enrichment of amphibole from sample 46-I-3 and some of the amphibole from the hypersolvus granite in Zr.

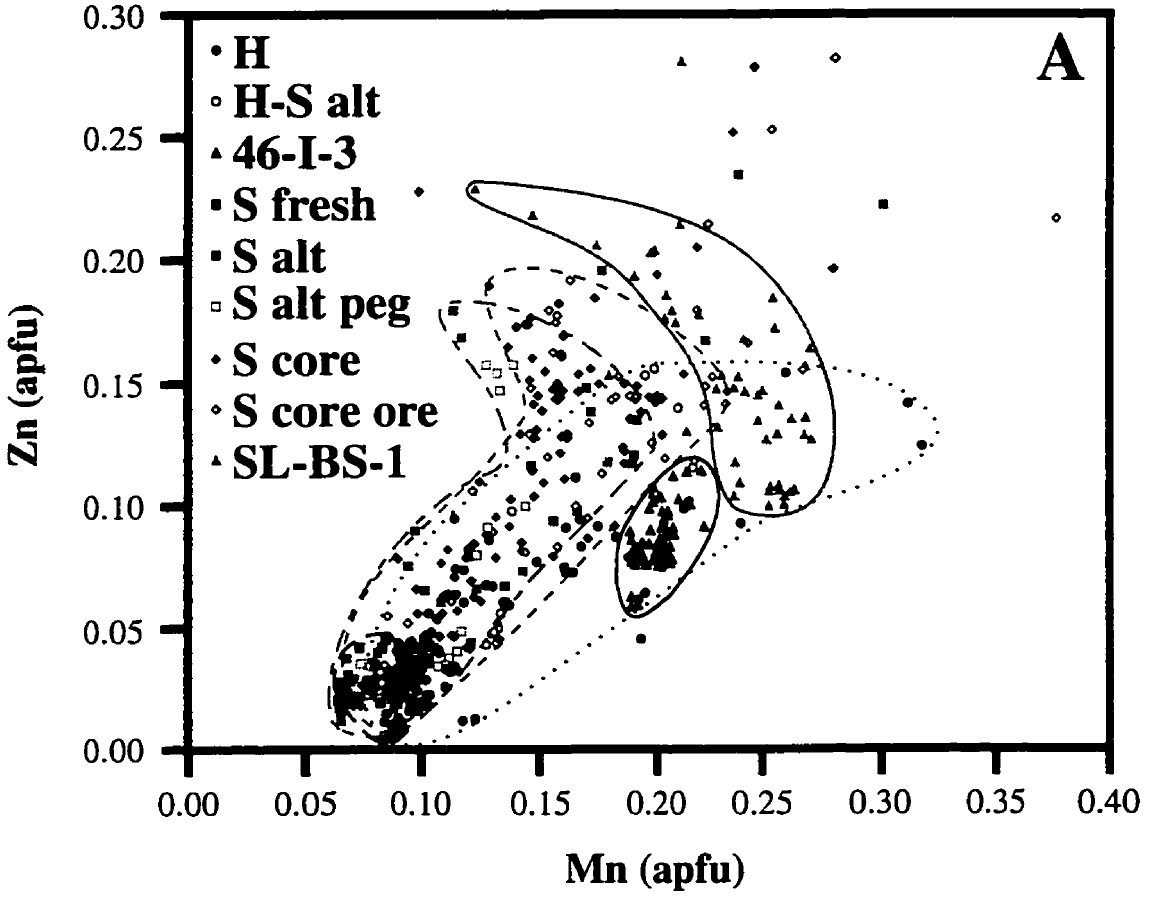
A
H
H-S alt
46-I-3
S fresh
S alt
S alt peg
S core
S core ore
SL-BS-1
Zn (apfu)
Mn (apfu)
0.00
0.05
0.10
0.15
0.20
0.25
0.30
0.35
0.40

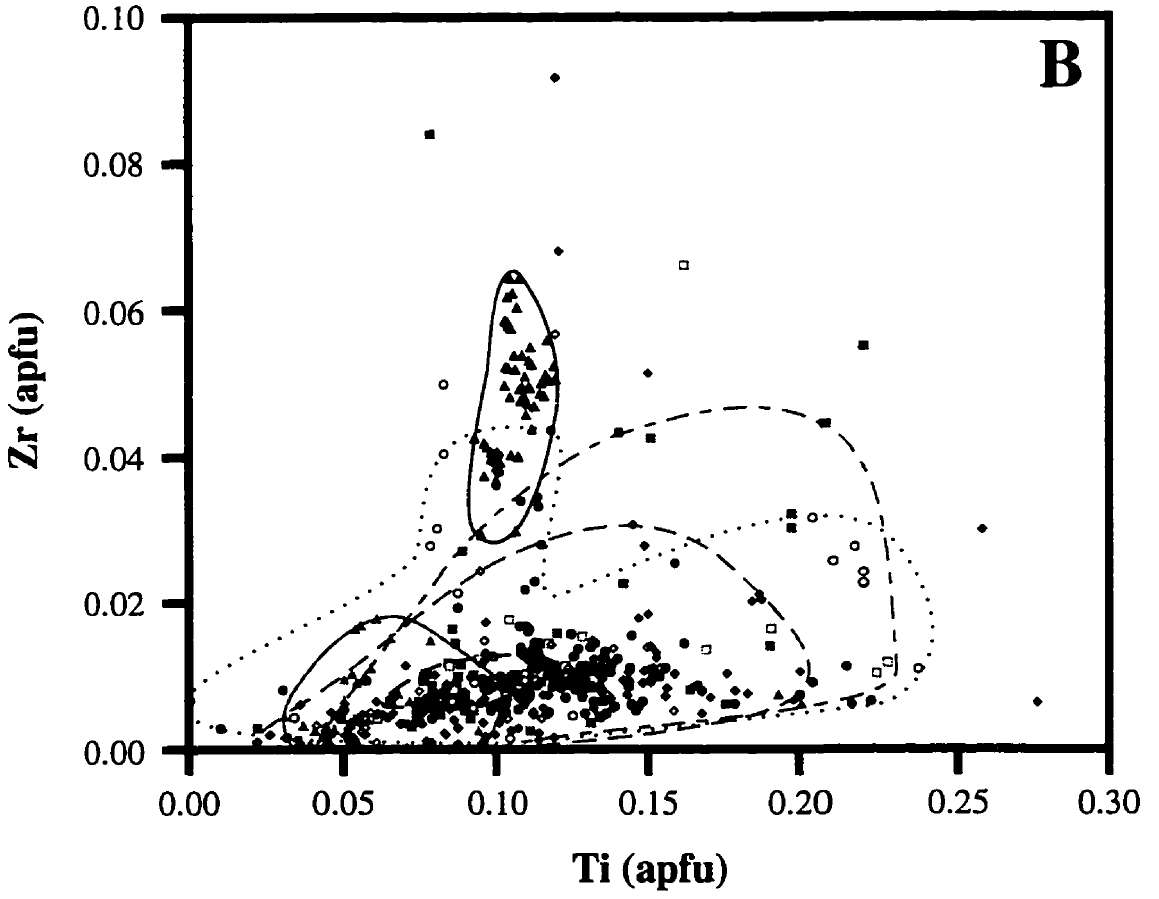
B
Zr (apfu)
Ti (apfu)
0.00
0.02
0.04
0.06
0.08
0.10
0.05
0.15
0.20
0.25
0.30

Figure 9. Additional plots of amphibole formulae. The acronyms, unit subdivisions and symbols used are as defined in Figures 7 and 8.

A. K versus Mn# [Mn/(Mn+Fe)] plot that shows the distinct increase in K (especially in the later units) and Mn# in the different units with magmatic evolution. Note also the difference in amphibole composition in the drill core between that from the ore zone (the equigranular granite) and the remainder of it (the porphyritic granite).

B. Peralkalinity [(Na+K)/Al] versus Mn# plot of the same compositions.

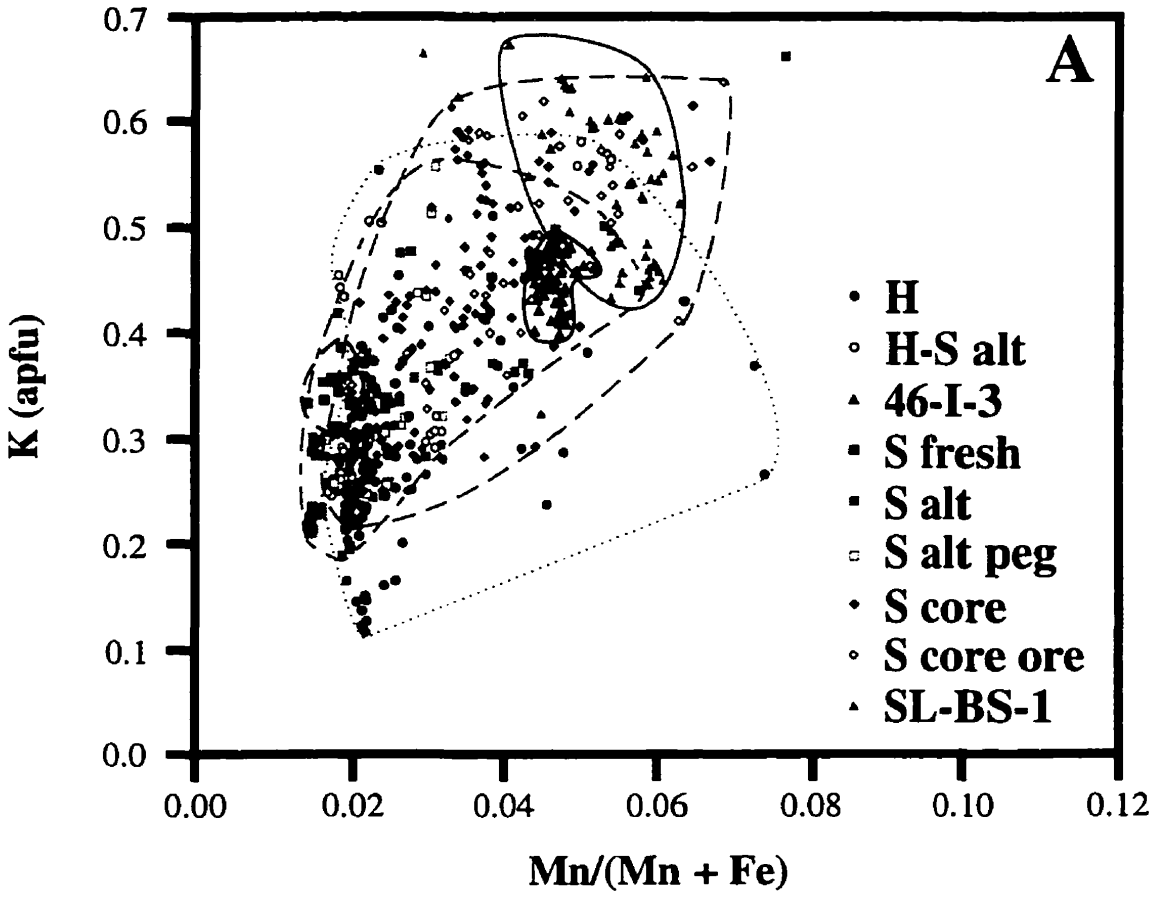
A
K (apfu)
Mn/(Mn + Fe)
0.0
0.1
0.2
0.3
0.4
0.5
0.6
0.7
0.00
0.02
0.04
0.06
0.08
0.10
0.12
H
H-S alt
46-I-3
S fresh
S alt
S alt peg
S core
S core ore
SL-BS-1

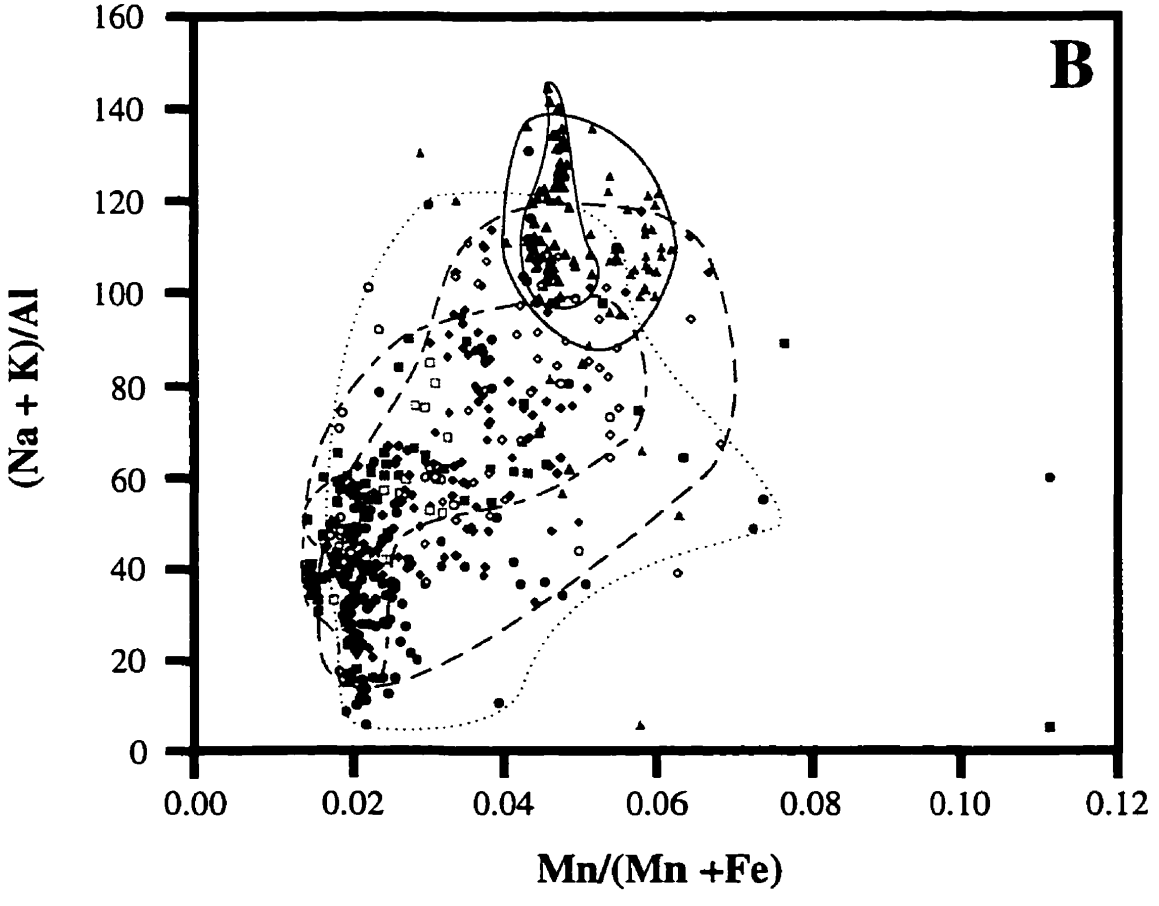
B
(Na + K)/Al
Mn/(Mn +Fe)
0
20
40
60
80
100
120
140
160
0.00
0.02
0.04
0.06
0.08
0.10
0.12

contains more K and shows an increase in Mn# compared to that from the rest of the drill core.

Figure 9B shows that the peralkalinity, (Na+K)/Al, of the amphibole increases with Mn# in the expected sequence: hypersolvus to subsolvus to altered pegmatite in the hypersolvus granites to mafic pods. This variation is concurrent with the decrease in Fe^{3+} content of the amphibole noted above (Fig. 7A) and suggestive of a process related to magmatic evolution. Furthermore, amphibole from the subsolvus granite in the drill core, pegmatites in the altered subsolvus granite, and especially, the equigranular subsolvus granite at depth contains less Fe^{2+}, and more K and Mn than that from the altered subsolvus granite (Fig. 9 and inferred from Fig. 7). These differences are likely due to the interaction of fluids with the amphibole (ref. Chapters 5, 6).

The trace-element variation of the amphiboles is shown in spider and rare-earth element (REE) diagrams (Fig. 10); concentrations have been normalized to either the bulk-rock analysis of one of the most primitive hypersolvus granites from the complex (49-C-1; Table 4) or chondrite (Sun, 1982; Thompson, 1982; Rollinson, 1993). These amphiboles are enriched in HFSE and REE, especially HREE, compared to 49-C-1 and chondrite (Fig. 10). Amphibole acts as a sink for these elements in the rock, as these elements are not as enriched in the other common gangue minerals feldspar and quartz.

The trace-element variation is greater in amphibole from the hypersolvus granite than in any other unit. However, only a few samples (e.g., 48-F-3 and 57-A-1) are significantly enriched in HFSE and REE. The remainder are of the same enrichment as those from the other units (Fig. 10). In addition, the average ΣREE, excluding that of the unusually enriched amphibole, increases from the hypersolvus granite to the altered subsolvus granite. Lastly, the results of the bulk ICP-MS (Table 4) and LAM-ICP-MS analyses are equivalent, except for the slight HREE depletion of amphibole from the hypersolvus granite and the enrichment of REE, especially LREE, from the mafic pods.

Zr and Hf are enriched in amphibole from the fresh subsolvus granite (versus that of the hypersolvus granite) and, in particular, the altered pegmatite from the hypersolvus granite compared to that in the other units. The Nb content of amphibole from the mafic pods also is enriched compared to the other units. Moreover, a wide variation exists in Th and Hf contents, both in amphibole from the same unit and among units. Amphibole from

Figure 10. Trace-element variation of the amphiboles from the same units, as determined predominantly by LAM-ICP-MS.

A. Chondrite-normalized spider diagram (Thompson, 1982; Rb and K values from Sun, 1982; after Rollinson, 1993) of the same data as for Figure 10A to better compare the amphibole analyses from this complex with those from other complexes. Bulk ICP-MS analysis of amphibole from Table 4 are shown as a line within the LAM-ICP-MS regions.

B. Chondrite-normalized REE diagram showing the same results as that from B for comparison with amphibole analysis from other complexes. Bulk ICP-MS analysis of amphibole from Table 4 also are depicted.

C. Spider diagram of sample (in ppm) normalized to the whole-rock data from a primitive hypersolvus A-type granite (49-C-1) that shows a distinct enrichment in HFSE and REE of amphibole compared to granite. Bulk-amphibole analyses are represented by the single line in most units.

D. REE pattern of sample (in ppm) normalized to the whole-rock data from the same hypersolvus granite that shows a distinct enrichment in REE, especially HREE, of amphibole compared to the granite. The bulk-amphibole analyses are represented in the same manner as in A.

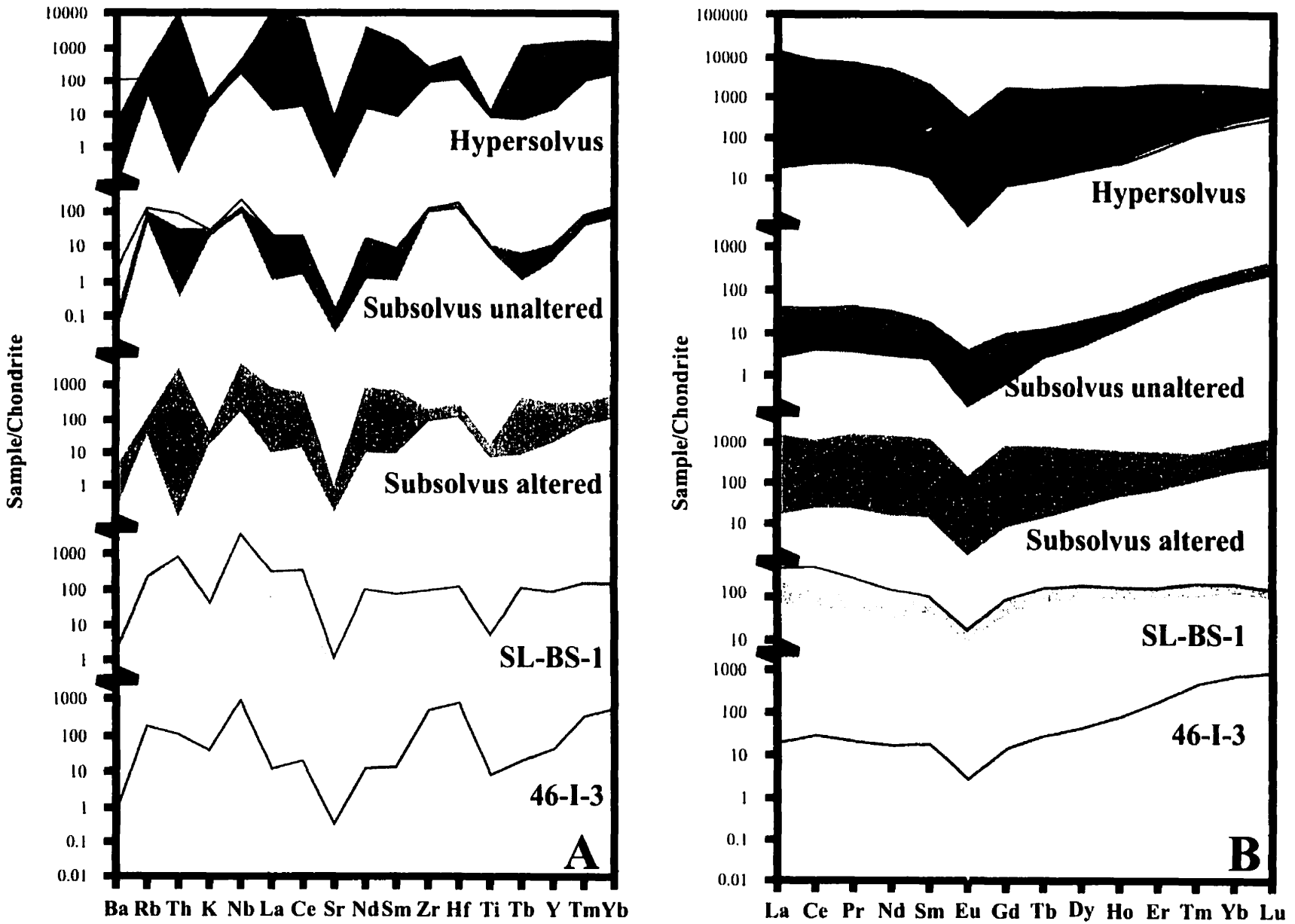
Sample/Chondrite
10000
1000
100
10
1
Hypersolvus
100
10
1
0.1
Subsolvus unaltered
1000
100
10
1
Subsolvus altered
1000
100
10
1
SL-BS-1
1000
100
10
1
0.1
0.01
46-I-3
A
Ba Rb Th K Nb La Ce Sr Nd Sm Zr Hf Ti Tb Y Tm Yb
Sample/Chondrite
100000
10000
1000
100
10
Hypersolvus
1000
100
10
1
Subsolvus unaltered
1000
100
10
Subsolvus altered
100
10
SL-BS-1
1000
100
10
1
0.1
0.01
46-I-3
B
La Ce Pr Nd Sm Eu Gd Tb Dy Ho Er Tm Yb Lu

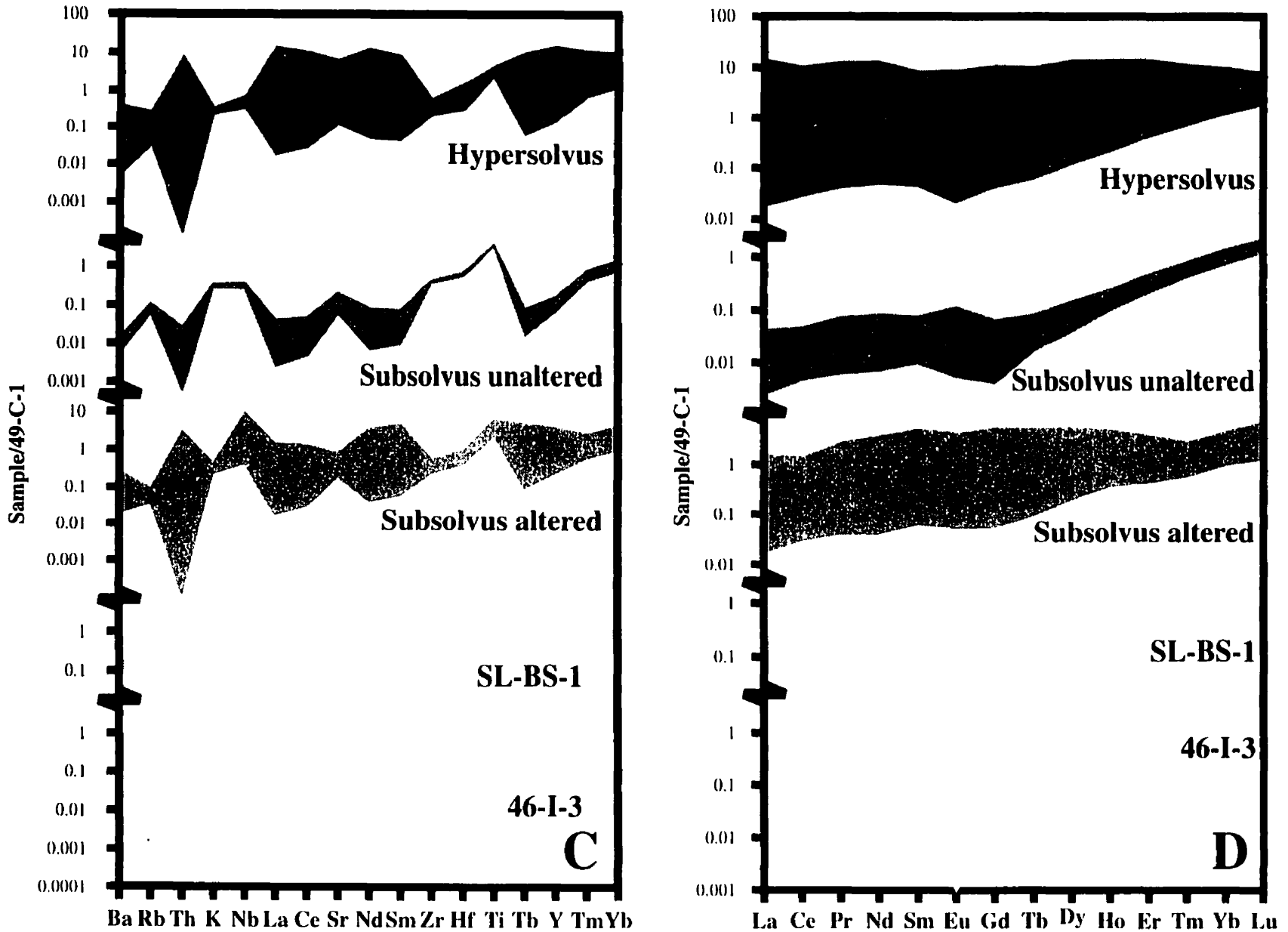
Sample/49-C-1
100
10
1
0.1
0.01
0.001
Hypersolvus
Subsolvus unaltered
Subsolvus altered
SL-BS-1
46-I-3
C
0.0001
Ba Rb Th K Nb La Ce Sr Nd Sm Zr Hf Ti Tb Y Tm Yb
Sample/49-C-1
Hypersolvus
Subsolvus unaltered
Subsolvus altered
SL-BS-1
46-I-3
D
La Ce Pr Nd Sm Eu Gd Tb Dy Ho Er Tm Yb Lu

Table 4. Bulk ICP-MS and whole-rock analyses.*

	Arfvedsonitic amphibole				Bulk-rock
Sample #	**48-A-7**	**46-I-3**	**SL-4-15**	**SL-BS-1**	**49-C-1**
Unit	**Hypersolvus**	**Altered Pegmatite**	**Fresh Subsolvus**	**Mafic Pod**	**Hypersolvus**
Li**	1545	2254	3100	2165	112
Zn	3114	7101	2953	10214	288
Rb	38	63	51	81	447
Sr	7	4	1	16	13
Y	38	85	20	181	180
Zr	1000	3207	903	638	2521
Nb	126	325	91	1369	170
Ba	677	5	13	15	95
La	46	4	8	105	232
Ce	125	17	20	297	503
Pr	10	2	2	26	55
Nd	34	8	6	68	187
Sm	6	3	1	15	38
Eu	0	0	0	1	2
Gd	5	3	1	17	32
Tb	1	1	0	6	6
Dy	5	10	2	44	32
Ho	2	4	1	9	7
Er	11	26	8	26	25
Tm	4	11	3	5	5
Yb	43	119	36	32	34
Lu	10	21	9	4	5
Σ REE	301	230	98	655	1164
Hf	50	163	43	25	70
Ta	2	7	1	75	12
Th	3	4	4	39	56
U	5	2	1	291	10
Pb	75	32	55	75	88
V	0	2	25	0	0
Cr	0	6	0	0	629
Ni	0	8	0	0	8
Co	0	1	1	0	26
Cu	9	9	0	10	19
Ga	10	12	7	12	41
Sn	114	917	175	736	49

* Concentrations in ppm.
** The Li content was determined by AA.

hypersolvus granite, especially sample 48-F-3, is slightly enriched in Y compared to that from the other units.

The two types of zonation observed from electron-microprobe analysis and in back-scatter images with the SEM were: 1) patchy zoning involving Zr and possibly REE perpendicular to the *c* axis, which was inferred from the significant changes in the relative intensity of element peaks during the replicate LAM-ICP-MS analyses, thereby reducing the reproducibility of these analyses, and 2) concentric zoning parallel to the *c* axis, where brighter regions (in SEM back-scatter mode) are enriched in Ca, Fe^{2+}, Mg, ^{IV}Al, OH, LREE, but depleted in K, Na, ^{VI}Al, Si, Li, Ti, Mn, and possibly in Fe^{3+} and HREE (Fig. 11). Where present, patchy zonation is more common in amphibole from subsolvus granite, in particular, altered subsolvus granite, and may actually be related to the replacement of amphibole by aegirine as it is more common near the contact between these minerals. Concentric zoning is common in amphibole from the hypersolvus granite, but rare in other units. Here, the zoning is due to the substitution of significant amounts of Li, Zn, Mn and Ti for Fe^{2+}. The high Li content of the amphiboles indicates that the most relevant scheme of substitution in these amphiboles is the ferro-leakeite substitution [$LiFe^{3+}(Fe^{2+}Fe^{2+})_{-1}$; Hawthorne et al., 1992, 1993, 1996a]. Thus, darker amphibole, when viewed in the SEM, contains more ferro-leakeite. The same type of zoning is observed between amphibole and aegirine of composite grains in altered subsolvus granite (Fig. 3B).

Compositional Variations in Aegirine and Related Minerals

Aegirine varies from 80 to 100% Ae (Fig. 12A; after Morimoto, 1989). It contains, on average, 0.5 wt.% TiO_2 and MnO, and trace amounts of Al, Zn, Nb, Zr and Ca (Tables 5, 6). The relative amounts of Zr, Mn and Ti are covariant, but the other elements are more variable. The aegirine can be separated into three types: 1) green (Ti-rich; up to 4.91 wt.% TiO_2), magmatic to early postmagmatic aegirine that mantles amphibole in the hypersolvus and transsolvus granites, 2) yellow aegirine (slightly Ti-, Mn- and Ca-enriched) that replaces amphibole in hypersolvus and subsolvus granites, and 3) primary yellow green euhedral aegirine (the purest of the three, although it still contains minor Ca, Ti, Mn and Nb) from the ore zone (Fig. 12B; Table 5; Roelofsen et al., 1995). The most Ti-rich, Type-1

Figure 11. Compsitional zonation of arfvedsonitic amphibole.

A. SEM image of the zonation of arfvedsonitic amphibole from the hypersolvus granite oriented perpendicular to the *c* axis. Note that darker regions are particularly obvious to the left side of the grain, which is actually the rim. The core of the amphibole is the lighter portion on the right hand side of the image. The bright 50 to 70 μm inclusions in the amphibole are monazite. The 70 to 80 μm circular regions are the points where LAM-ICP-MS analysis were performed (Grain size is 1.4 mm).

B. Back-scatter-electron map of showing the variations in Ca content of the same grain of amphibole as in A. Darker regions are of lower Ca content than the lighter ones.

C. Plot of the compositional variation from a combination of electron-microprobe analysis and LAM-ICP-MS analysis across the grain from dark on the left (rim) to light on the right (core) that shows the Ca variation of the amphibole. This decrease in Ca content from core to rim is consistent with that of Fe^{2+}, ^{IV}Al, Mg, but the opposite of that of K, Na, ^{VI}Al, Si, Li, Ti, Mn, slightly in Zr and possibly in Fe^{3+}.

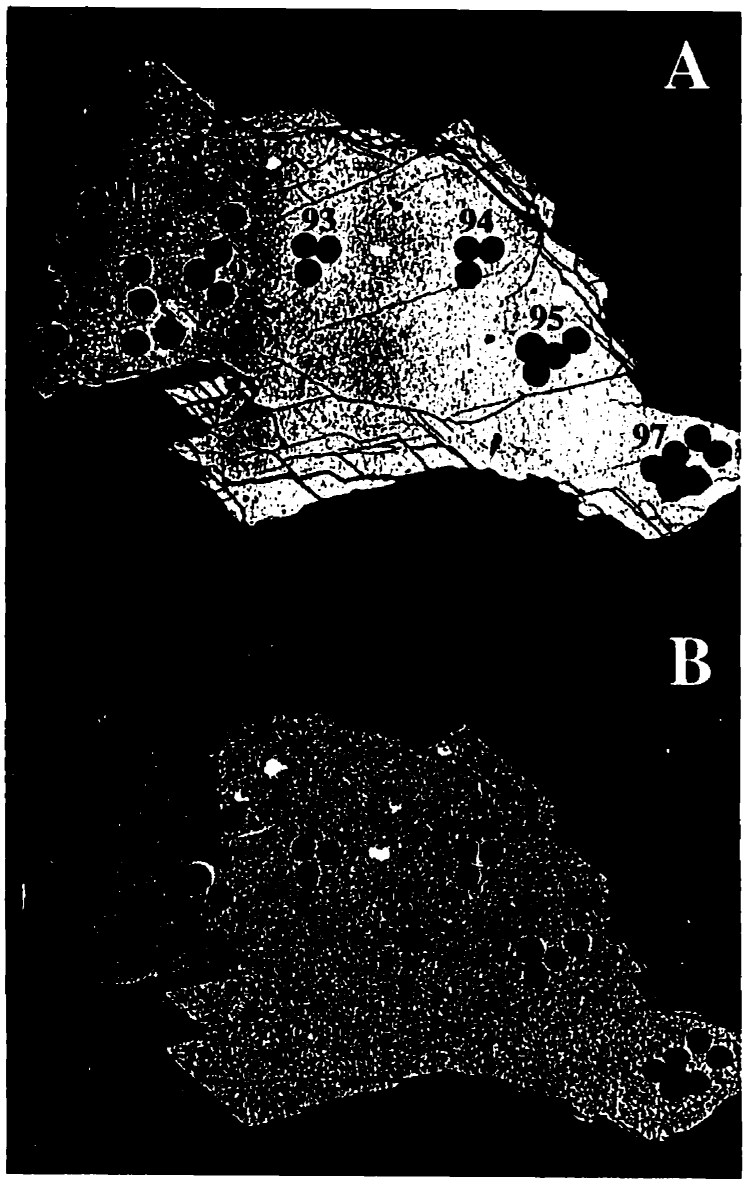
A
93
94
95
97
B

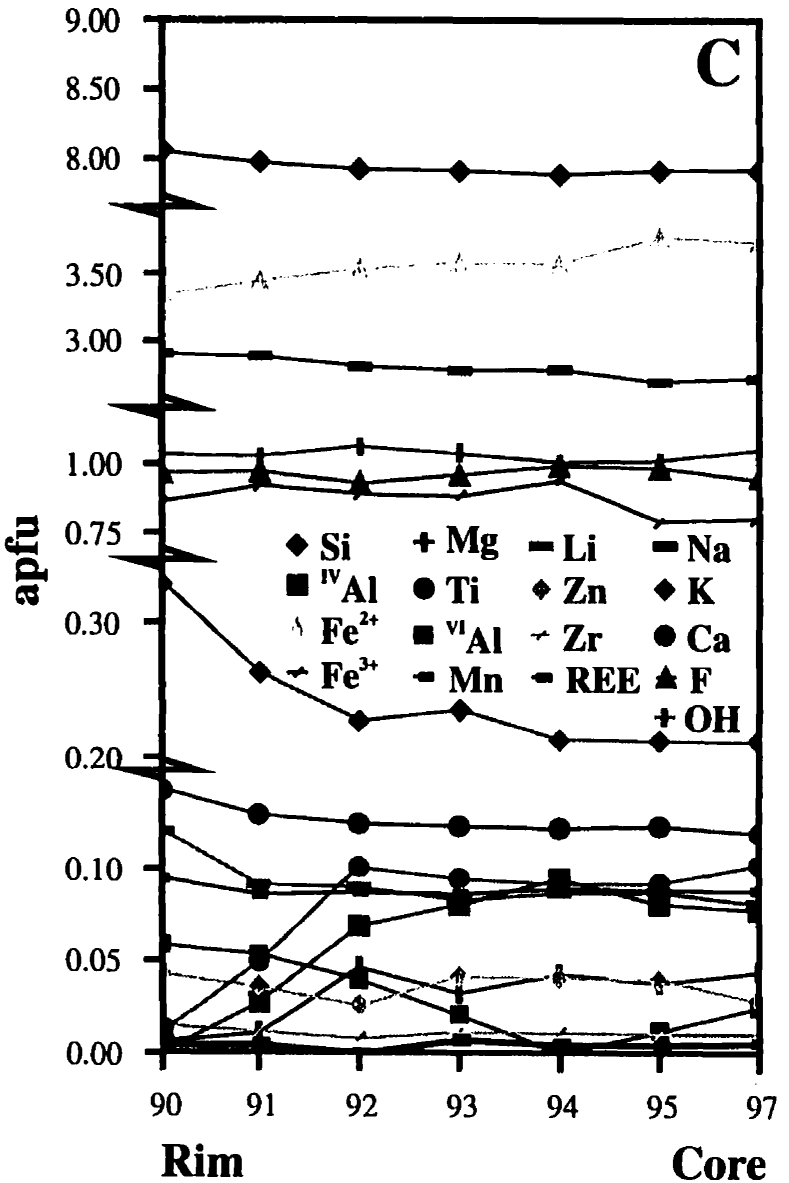
C
9.00
8.50
8.00
3.50
3.00
1.00
0.75
0.30
0.20
0.10
0.05
0.00
apfu
Si
Mg
Li
Na
IVAl
Ti
Zn
K
Fe2+
VIAl
Zr
Ca
Fe3+
Mn
REE
F
OH
90
91
92
93
94
95
97
Rim
Core

Figure 12. Compositional variation of aegirine.

A. Triangular plot (Fe^{3+}-Ca-Fe^{2+} from 80% Fe^{3+}) of the aegirine (80 to 100% Ae). Type-1 aegirine falls on the Fe^{3+} and Fe^{2+} side of the plot, whereas Type-2 aegirine shows less compositional variation toward the Fe^{2+} apex. The Type-3 aegirine from the ore zone is the purest of the three types of aegirine, but contains minor Ca and Fe^{2+}. The numbers in brackets behind each type of aegirine are the number of analyses performed.

B. The compositional variation of the three types of aegirine. Type-1 aegirine is enriched in Ti, Type-2 is slightly enriched in Ti and Mn and Type-3 aegirine is slightly enriched in Mn and Ca.

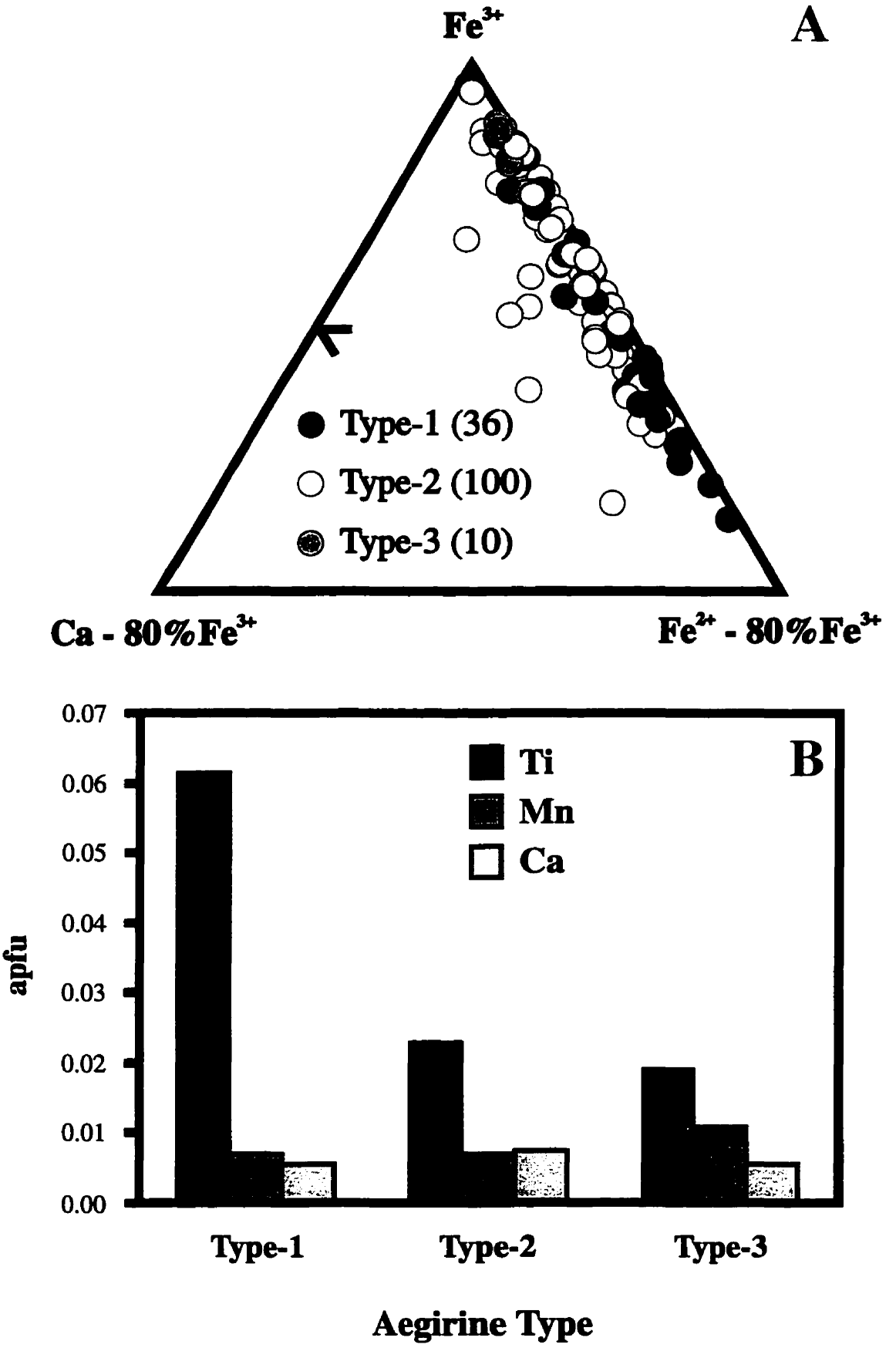
A
Fe^{3+}
Type-1 (36)
Type-2 (100)
Type-3 (10)
Ca - 80%Fe^{3+}
Fe^{2+} - 80%Fe^{3+}
B
Ti
Mn
Ca
apfu
0.07
0.06
0.05
0.04
0.03
0.02
0.01
0.00
Type-1
Type-2
Type-3
Aegirine Type

Table 5. Selected electron-microprobe analyses of aegirine and astrophyllite.

Mineral	Aegirine						Astrophyllite	
Type	Type-1	Type-2				Type-3		
Unit	Hypersolvus			Altered Pegmatite	Altered Subsolvus	Ore	Hypersolvus	
Sample #	57-A-1	49-C-2	49-C-2	46-I-3	27-B-1	SL-1-20	49-A-1	49-C-1
Na_2O	13.92	13.29	13.57	13.11	13.45	13.54	2.32	3.70
K_2O	0.00	0.00	0.00	0.01	0.00	0.00	1.61	2.44
CaO	0.06	0.25	0.21	0.12	0.11	0.11	0.21	1.57
Fe_2O_3	31.76	27.87	30.28	28.53	30.24	31.84	n.d.	n.d.
FeO	0.64	3.41	2.33	3.78	2.66	1.75	30.21	34.45
MgO	0.04	0.02	0.02	0.02	0.12	0.00	0.04	0.02
MnO	0.21	0.24	0.07	0.47	n.d.	0.18	2.89	1.40
ZnO	0.00	0.05	0.03	0.00	0.25	0.03	0.99	0.16
Nb_2O_5	0.00	0.01	0.03	0.02	n.d.	0.06	0.64	0.02
V_2O_3	0.01	0.02	0.00	0.00	0.02	0.03	n.d.	n.d.
ZrO_2	0.27	0.91	0.14	1.02	0.11	0.08	1.59	0.00
SnO_2	n.d.	n.d.	n.d.	n.d.	n.d.	n.d.	0.00	n.d.
PbO	n.d.	n.d.	n.d.	n.d.	n.d.	n.d.	1.30	n.d.
BaO	n.d.	n.d.	n.d.	n.d.	n.d.	n.d.	0.52	n.d.
SrO	n.d.	n.d.	n.d.	n.d.	n.d.	n.d.	0.00	n.d.
TiO_2	1.38	1.62	1.15	0.81	0.65	0.44	9.09	11.47
Al_2O_3	0.30	0.18	0.49	0.16	0.33	0.20	0.64	0.08
SiO_2	51.48	51.60	52.00	51.73	52.36	51.68	36.77	36.19
F	n.d.	n.d.	n.d.	n.d.	0.00	n.d.	1.14	2.80
Cl	n.d.	n.d.	n.d.	n.d.	0.01	n.d.	0.05	0.02
Total	100.07	99.46	100.33	99.77	100.30	99.95	89.50	94.31
-O=F	0.00	0.00	0.00	0.00	0.00	0.00	0.48	1.18
-O=Cl	0.00	0.00	0.00	0.00	0.00	0.00	0.01	0.00
Total	100.07	99.46	100.33	99.77	100.29	99.95	89.01	93.13

Table 5. Selected electron-microprobe analyses of aegirine and astrophyllite (cont'd).

Mineral	Aegirine						Astrophyllite	
Type	Type-1	Type-2				Type-3		
Unit	Hypersolvus			Altered Pegmatite	Altered Subsolvus	Ore	Hypersolvus	
Sample #	57-A-1	49-C-2	49-C-2	46-I-3	27-B-1	SL-1-20	49-A-1	49-C-1
Na	1.031	0.995	1.003	0.981	0.995	1.007	1.113	1.685
K	0.000	0.000	0.000	0.000	0.000	0.000	0.507	0.733
Ca	0.003	0.010	0.009	0.005	0.005	0.005	0.056	0.396
Fe^{3+}	0.913	0.810	0.869	0.828	0.868	0.919	n.d.	n.d.
Fe^{2+}	0.021	0.110	0.074	0.122	0.085	0.056	6.250	6.771
Mg	0.002	0.001	0.001	0.001	0.007	0.000	0.015	0.008
Mn	0.007	0.008	0.002	0.015	0.000	0.006	0.606	0.278
Zn	0.000	0.001	0.001	0.000	0.007	0.001	0.181	0.027
Nb	0.000	0.000	0.000	0.000	0.000	0.001	0.072	0.002
V	0.000	0.000	0.000	0.000	0.001	0.001	0.000	0.000
Zr	0.005	0.017	0.003	0.019	0.002	0.002	0.192	0.000
Sn	n.d.	n.d.	n.d.	n.d.	n.d.	n.d.	0.000	0.000
Pb	n.d.	n.d.	n.d.	n.d.	n.d.	n.d.	0.086	0.000
Ba	n.d.	n.d.	n.d.	n.d.	n.d.	n.d.	0.051	0.000
Sr	n.d.	n.d.	n.d.	n.d.	n.d.	n.d.	0.000	0.000
Ti	0.040	0.047	0.033	0.023	0.019	0.013	1.690	2.028
^{VI}Al							0.185	0.022
Si	1.966	1.992	1.983	1.996	1.998	1.981	9.095	8.504
Al(Total)	0.013	0.008	0.022	0.007	0.015	0.009		
F	0.000	0.000	0.000	0.000	0.000	0.000	0.895	2.080
Cl	0.000	0.000	0.000	0.000	0.000	0.000	0.019	0.007
Σ Cations	4.000	4.000	4.000	4.000	4.000	4.000	20.099	20.454

Mineral formulae calculated based on 6 oxygen and 4 cations for aegirine and 31 oxygens for astrophyllite. Fe^{3+}/Fe^{2+} was used to calculate mineral formulae for aegirine by the method of Droop (1994).
n.d.: Not determined.

Table 6. Selected LAM-ICP-MS analyses of aegirine.

Type	Type-1 or 2	Type-1 or 2	Type-1	Type-2	Type-2	Type-2
Unit	Hypersolvus	Hypersolvus	Fresh Subsolvus	Fresh Subsolvus	Altered Pegmatite	Altered Subsolvus
Sample #	48-A-7	57-A-1	38-B-3	38-B-3	46-I-3	SL-8-1
Na_2O	13.89	13.76	13.64	13.86	13.94	13.58
K_2O	0.00	0.00	0.00	0.00	0.00	0.00
CaO	0.04	0.02	0.16	0.10	0.13	0.03
Fe_2O_3	33.87	32.66	31.23	33.35	34.04	34.01
MgO	0.00	0.01	0.01	0.02	0.00	0.01
MnO	0.09	0.17	0.21	0.09	0.59	0.10
ZnO	0.00	0.00	0.00	0.00	0.04	0.00
Cr_2O_3	0.01	0.00	0.00	0.00	0.00	0.00
V_2O_3	0.01	0.01	0.02	0.00	0.01	0.00
Nb_2O_5	0.00	0.00	0.00	0.00	0.04	0.00
ZrO_2	0.13	0.10	0.30	0.13	0.07	0.11
Y_2O_3	0.00	0.00	0.00	0.00	0.00	0.00
Yb_2O_3	0.02	0.00	0.00	0.00	0.01	0.01
TiO_2	1.07	2.01	3.09	1.15	0.63	0.77
Al_2O_3	0.27	0.36	0.44	0.40	0.17	0.20
SiO_2	52.51	52.87	51.83	52.05	52.14	52.08
Total	101.90	101.96	100.91	101.16	101.82	100.90

Table 6. Selected LAM-ICP-MS analyses of aegirine (continued).*

Type	Type-1 or 2	Type-1 or 2	Type-1	Type-2	Type-2	Type-2
Unit	Hypersolvus	Hypersolvus	Fresh Subsolvus	Fresh Subsolvus	Altered Pegmatite	Altered Subsolvus
Sample #	48-A-7	57-A-1	38-B-3	38-B-3	46-I-3	SL-8-1
Li	1385	614	n.d.	n.d.	18	n.d.
Be	12	12	n.d.	n.d.	36	n.d.
B	4	5	n.d.	n.d.	30	n.d.
V	2	1	0	0	1	0
Cr	3	1	0	0	1	0
Zn	2815	1936	667	246	1728	623
Rb	16	17	2	308	49	31
Sr	25	6	19	4	14	2
Y	2225	120	157	44	187	66
Zr	913	1390	1103	813	4191	1432
Nb	136	107	213	84	1118	238
Ba	14	9	3	9	38	5
La	452	159	10	5	26	6
Ce	804	257	21	11	90	13
Pr	105	27	5	2	7	2
Nd	481	103	25	10	27	12
Sm	133	18	13	4	16	7
Eu	8	1	1	0	1	0
Gd	153	16	17	5	20	7
Tb	30	2	3	1	7	2
Dy	214	16	23	6	53	14
Ho	46	4	5	1	11	3
Er	147	18	17	5	39	11
Tm	22	5	3	1	10	2
Yb	160	60	42	22	113	26
Lu	24	14	12	6	23	6
Hf	39	53	53	34	148	74
Th	52	34	61	17	33	6
U	3	2	16	4	24	2
Σ REE	2778	701	196	80	443	111

* Concentrations in ppm.
n.d.: Not determined.

aegirine, also contains the most V. Type-1 aegirine plots between the Fe^{3+} and Fe^{2+}-80 Fe^{3+} apices of Figure 13A owing to the substitution $Fe^{2+}Ti^{4+}(Fe^{3+}Fe^{3+})_{-1}$. Type-2 aegirine shows an important, but lower enrichment of Ti than noted for Type-1. Its compositional variation is due to the presence of minute inclusions of astrophyllite, amphibole and F-rich minerals (Roelofsen et al., 1995; Chapter 5).

The trace-element contents of aegirine from the complex are depicted in Figure 13 and noted in Table 6. Unfortunately, the width of the laser beam (70 to 80 μm) made it difficult to differentiate between Type-1 and Type-2 aegirine in the grain mount, especially when they occur as intergrowths (Type-3 aegirine was not analyzed). Nevertheless, an attempt has been made to separate Type-1 and -2 aegirine based on their Ti content (Fig. 13). In so doing, it is deduced that Type-2 aegirine is enriched in Nb, Th and Ba, but depleted in REE, Ti, Zn and Zr (Figs. 13A, C, E). Figures 10 and 13 indicate that amphibole from all units is, in general, enriched in minor and trace elements (Mn, Ti, Zn, Zr, REE, Li, etc.) compared to aegirine. The maximum trace element enrichment of aegirine occurs in the hypersolvus granite, especially in 57-A-1, as previously noted for the amphibole. Type-2 aegirine from altered pegmatite in the hypersolvus granite (e.g., 46-I-3) exhibits the widest compositional variation of the aegirine, with the contents of some trace elements almost equivalent to that of amphibole. Such variation is due to the presence of relict amphibole and the effects of Ca-metasomatism (Chapters 5, 6).

All titanium iron silicates and oxides analyzed are enriched in Mn (Table 5). Aenigmatite also contains minor amounts of Al, Zn, Ca and traces of Mg, Zr and Ba. Moreover, the orange-yellow interstitial astrophyllite is Fe- and Ti-rich, whereas the yellow-brown to brown fibrous grains are Mn- (to 2.5 apfu), Zr-, Zn- and Al-rich. Its fibrous nature and the Mn-enrichment are indicative of a secondary origin. Neptunite is near end-member in composition, F-rich, and has low analytical totals that may reflect the presence of Li. Unfortunately, the fine-grain size of and tendency for intergrowths between these minerals and with other minerals made it impossible to perform LAM-ICP-MS analysis.

Figure 13. Trace-element variation of aegirine that shows that the aegirine is, in general, depleted in trace elements compared to the arfvedsonitic amphibole (Fig. 10).

A. Chondrite-normalized spider diagram showing the compositional variation of the aegirine.

B. Chondrite-normalized REE diagram of the compositional variation of the aegirine.

C. A-type-granite-normalized spider diagram calculated in the same manner as that of amphibole (Fig. 11).

D. A-type-granite-normalized REE diagram.

E. Compositional variation in terms of REE between predominantly Type-1 and -2 aegirine. Primary Type-1 aegirine contains more REE, Ti, Zn and Zr than Type-2.

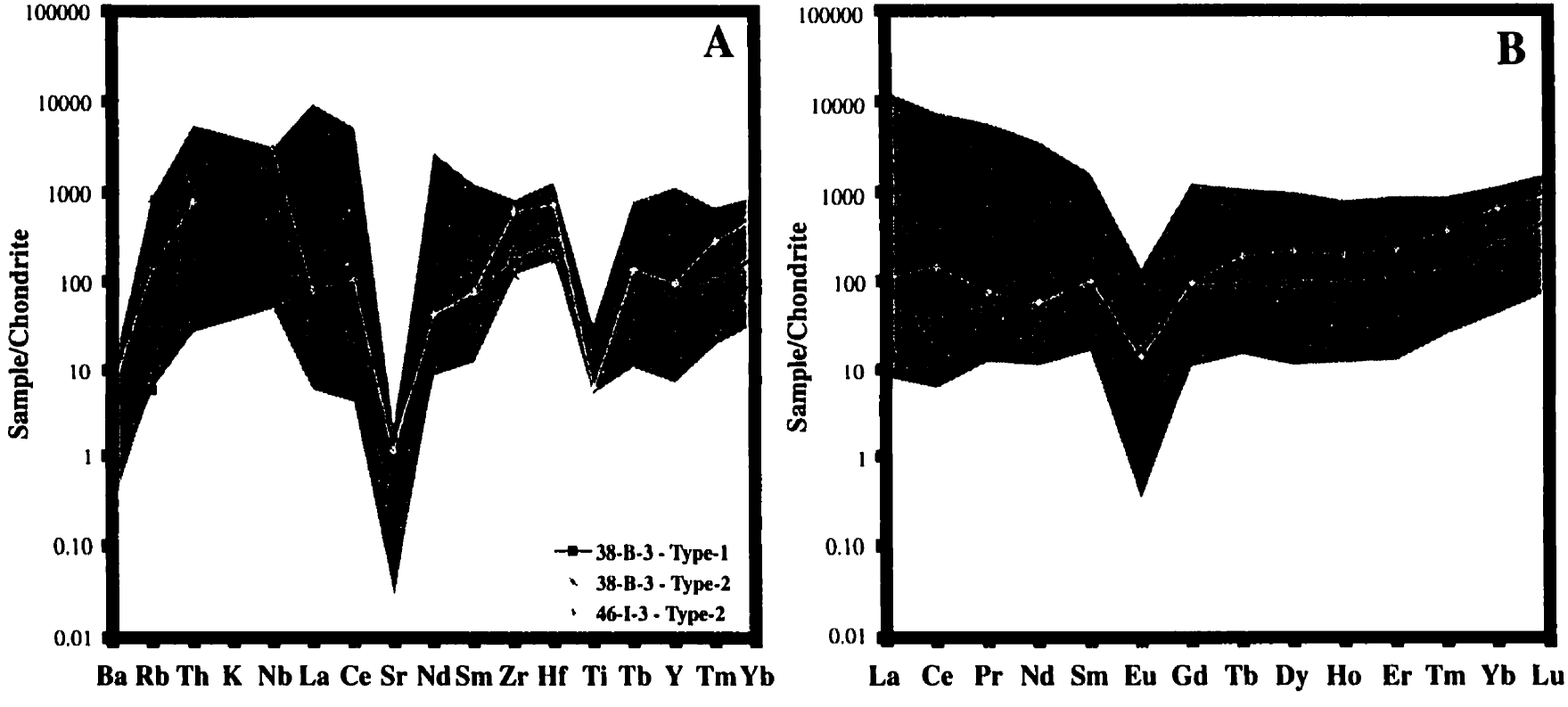
A
B
100000
10000
1000
100
10
1
0.10
0.01
Sample/Chondrite
38-B-3 - Type-1
38-B-3 - Type-2
46-I-3 - Type-2
Ba Rb Th K Nb La Ce Sr Nd Sm Zr Hf Ti Tb Y Tm Yb
La Ce Pr Nd Sm Eu Gd Tb Dy Ho Er Tm Yb Lu

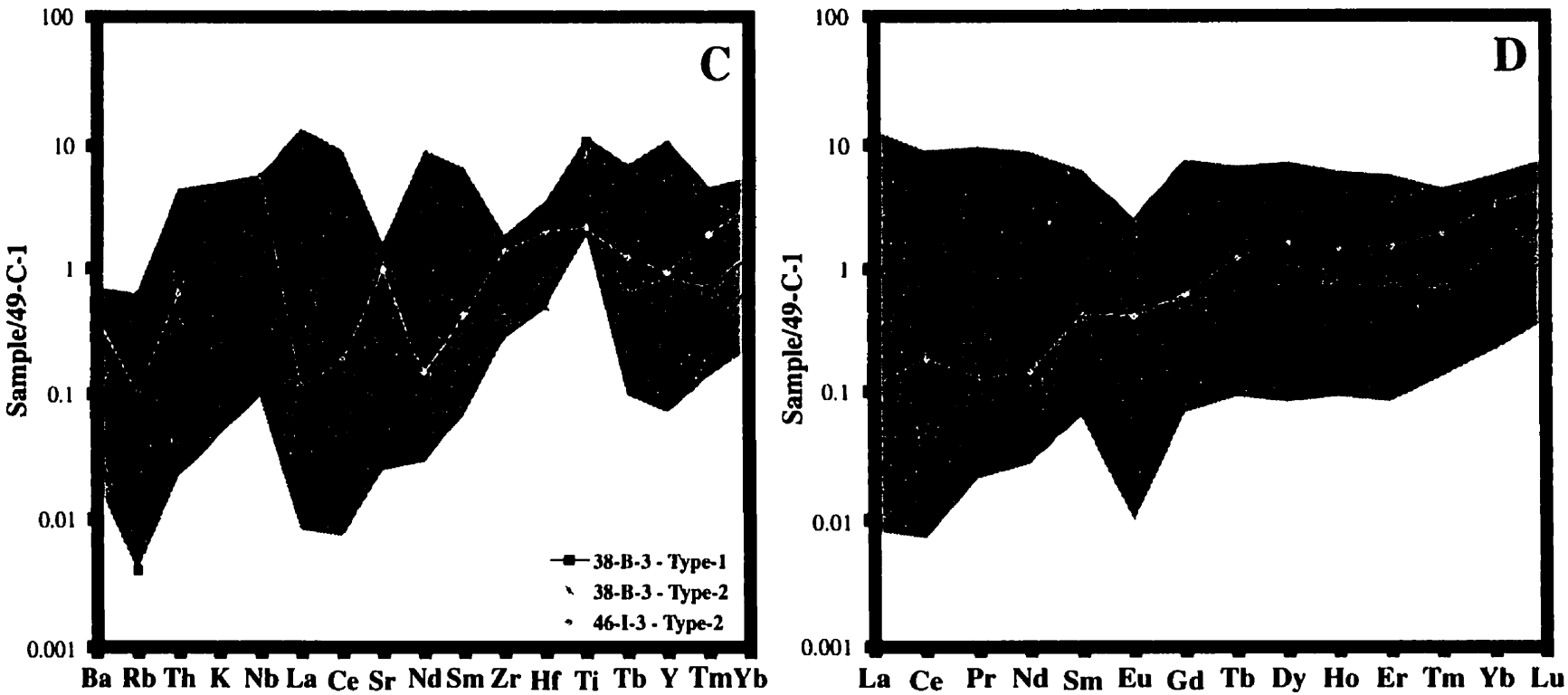
C
D
100
10
1
0.1
0.01
0.001
Sample/49-C-1
Ba Rb Th K Nb La Ce Sr Nd Sm Zr Hf Ti Tb Y Tm Yb
38-B-3 - Type-1
38-B-3 - Type-2
46-I-3 - Type-2
La Ce Pr Nd Sm Eu Gd Tb Dy Ho Er Tm Yb Lu

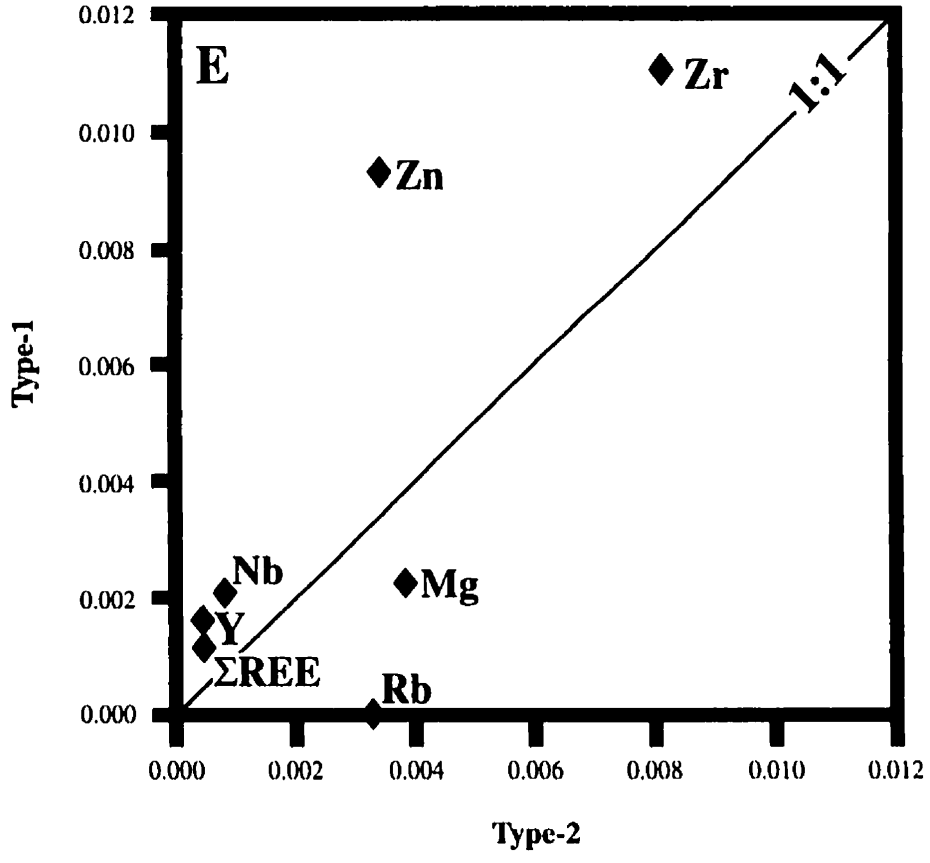
E
Zr
1:1
Zn
Nb
Mg
Y
ΣREE
Rb
0.012
0.010
0.008
0.006
0.004
0.002
0.000
0.000
0.002
0.004
0.006
0.008
0.010
0.012
Type-1
Type-2

Discussion

Three types of primary arfvedsonitic amphibole have been distinguished on the basis of electron-microprobe and LAM-ICP-MS analysis. This amphibole is associated with two types of primary aegirine: Type-1 (green and Ti-rich) and Type-3 (yellow green and Mn and Ca-enriched). Type-1 amphibole in the hypersolvus granite is compositionally zoned in Fe, Mg, Zn, Mn, Ti and Li. Two subtypes (Type-1a and -1b) can be distinguished based on the presence of inclusions or compositional variation where the cores (Type-1a) are Na- and Fe-rich and the rims (Type-1b) contain slightly more Ca, Mn, Mg and Zn. Type-2 amphibole, from the fresh and altered subsolvus granites, is enriched in K, Fe^{2+}, ^{IV}Al, and possibly Mn, but depleted in Fe^{3+}, Li, Ca relative to that of Type-1. Late acicular potassian lithian fluor-arfvedsonitic amphibole from the mafic pods, Type-3, is the most evolved in minor- and trace-element content (e.g., it is K, Mn, Li and F-rich), as the amphibole suite shows a progression from Na-, Zr- and Fe-rich in the hypersolvus granite to K-, Zn-, Mn- and REE-rich in the mafic pods. The positive correlation between K, Mn, Zn, Fe^{2+} and peralkalinity, and a decrease of Ca and Mg and in some cases of Ti, Zr and Al in most units indicate the influence of magma evolution.

The major exceptions to this magmatic trend are the unusual enrichment of amphibole from altered pegmatites in the hypersolvus granite (46-I-3) in Mn and Zn, and the more Ca-rich, and in some cases, Mg- and Mn-rich analyses from selected amphibole in the altered subsolvus granite (ref. Chapter 6). These enrichments of amphibole from altered pegmatite in Zr, Nb, Mg, Zn, Mn and Hf are significantly different than that expected for a hypersolvus granite near the contact with the altered subsolvus granite (ref. Chapter 6). This implies the influence of another process, such as metasomatism.

According to Nassif (1993) and Boily & Williams-Jones (1994), the results of bulk-rock analysis show an increase in Fe^{3+}, Mg, K, Ca, Ti, Zn, Rb, Sr, REE, Y, Zr, Nb, Hf and REE, but a decrease in Na, Al, Na/K and La/Yb in the sequence from the hypersolvus to transsolvus to subsolvus granite to highly K-enriched pegmatites. Whole-rock F content increases between the hypersolvus and fresh subsolvus granites, but decreases in the altered subsolvus granite and pegmatite. These variations in the bulk rock are the same as those

observed in amphibole of each unit, with the exception that: Ti, Zr, Na, Al and F vary, Mn increases, and Ca, Mg and Sr decrease.

Addition of trace elements to the calculated amphibole formulae decreases the excess in ΣNa+K+Si (compare Fig. 6A and 6B). Enrichment of amphibole in ΣNa+K+Si compared to that of ideal amphibole may be an artifact of compositional error, method of formula calculation, the elements analyzed in the samples, uncertainty in the oxidation state of iron, lack of the possibility to determine Li and OH by electron-microprobe analysis (ref. Czamanske & Dillet, 1988; Hawthorne et al., 1993), or the presence of submicroscopic inclusions of aegirine (Ross, 1984). Preliminary results of single crystal X-ray powder diffraction (XRD) work on these amphiboles suggest the possibility of an oxy-amphibole component (Hawthorne et al., in prep.). Confirmation of this requires OH^- and Fe^{3+}/Fe^{2+} determinations and further single-crystal XRD work. The possibility of the presence sub-microscopic inclusions of aegirine in amphibole is examined in Chapter 5.

Variations in the trace-element content of the amphibole or aegirine also can be the result of: 1) fractional crystallization, which leads to an increase in incompatible elements in amphibole in the sequence hypersolvus, fresh subsolvus, altered subsolvus to mafic pods, 2) presence of inclusions, 3) a content near the detection limit, or 4) differences in interaction with the laser beam or in method of standardization. Enrichment in incompatible elements (REE, Zr, Hf and in part Nb, etc.) during the evolution of the complex implies magmatic evolution by fractional crystallization. Comparison of the results of bulk sample ICP-MS analyses and LAM-ICP-MS analyses indicates that amphibole from the mafic pods is enriched in Nb, REE and Sn owing to the presence of minute, inseparable inclusions of pyrochlore. Inclusions of zajacite, yttriofluorite, gagarinite and monazite may account for the high Y and LREE content of amphibole from hypersolvus granite (e.g., especially 48-F-3). Zr enrichment in amphibole from 57-A-1 and some of 49-C-2 of the hypersolvus granite can be attributed to the presence of inclusions of zircon. Early crystallization of zircon, elpidite, monazite, gagarinite, etc. (Fig. 5), slightly decreased the amount of Zr and LREE (and increased the level of HREE) remaining in the magma from which the arfvedsonitic amphibole and later aegirine crystallized. Consequently, they do not represent any unusual compositional extremes. Finally, the wide variation in Th, Hf and U content of the amphibole is a consequence of their values being near the LLD or, in the case of amphibole

from the mafic pods, the presence of inclusions of pyrochlore. The difference in Ba content between ICP-MS and LAM-ICP-MS analyses is likely the product of differences in the method of standardization employed and the fact that the former analyses were performed on a fluid and the latter on a solid (ref. methodology; Moenke-Blankenburg, 1989; Jarvis et al., 1992). In addition, the slightly lower levels of HREE from the bulk ICP-MS analysis compared to those from LAM-ICP-MS can be attributed to absence of inclusions, differences in the method of standardization or the method of analysis. The same discrepancy would be expected for analyses from all units if the second was the case. As it is not, the variation must be representative of that actually present in the sample, in the same manner as the trace element variation in amphibole from the hypersolvus granite.

The definite enrichment of amphibole in HREE indicates that it acts as a sink for HFSE and REE, especially HREE (e.g., Fig. 8B). This HREE enrichment of amphibole is correlated with the late enrichment of the granite in these elements as noted by Nassif (1993), Boily & Williams-Jones (1994) and Salvi & Williams-Jones (1996). Fractional crystallization of plagioclase feldspar and pyroxene before intrusion of the magma and formation of the complex was proposed by Boily & Williams-Jones (1994) to explain the negative Eu anomaly observed in the REE patterns of the granites. In addition, early crystallization of LREE minerals such as monazite and F-rich minerals in the hypersolvus granite removed a portion of these elements from the magma. Later, fractional crystallization (as discussed above) increased the proportion of incompatible elements (e.g., REE) in the remaining magma, as reflected in the composition of the amphibole. The lack of LREE-rich inclusions in amphibole and aegirine from altered subsolvus granite compared to that from the hypersolvus granite suggests their removal by dissolution during the replacement of amphibole by aegirine. Such an enrichment in HREE is also favoured by an increased stability of HREE, compared to LREE, as alkali REE fluoride complexes in the magma (Hermann, 1969; Christiansen et al., 1983). Consequently, the present high REE content of the amphibole is the result of a combination of these processes.

Comparison with Findings on Mafic Silicates from the Strange Lake and Related Complexes

Arfvedsonitic Amphibole

As in this study, most amphibole analyzed by Pillet (1989) and Pillet et al. (1993) from the Strange Lake peralkaline complex is arfvedsonitic amphibole, although his data show a higher richterite component to the arfvedsonitic amphibole from coarse-grained hypersolvus granite (Fig. 14A). Pillet's data also show the highest amounts of Ca, Al, Mg and Ti, but the least Na, K and Si in amphibole from the fine-grained hypersolvus granite. A similar compositional variation with granite evolution was observed in the present study, except that no relationship with grain-size and less richteritic amphibole component was observed, specifically in Type-1 amphibole. Furthermore, amphibole from the equivalent to the altered subsolvus granite was found to contain more Na, K and Si, but less Fe, Ca, Mg and Ti than that from the present study. This study indicates that the amphibole composition is more variable and contains more Li, Zn, Mn and Al, on average, than that examined by Pillet. Moreover, the only Mn enrichment observed by Pillet was noted in amphibole from the border facies, which is equivalent in amount to that from the mafic pods. The main difference between the results of the electron-microprobe analyses of the arfvedsonitic amphibole, astrophyllite and neptunite from this study and those of Pillet is that the F content determined by Pillet is at least 1 wt.% lower. Unfortunately, in neither study does Pillet mention how the electron-microprobe analyses were performed. Thus, it is difficult to explain these differences. Furthermore, the F content of amphibole from the present study is equivalent to that from a bulk-amphibole separate (Salvi, pers. comm.).

The mineral formulae calculated from the data of Pillet (1989) have a ΣNa+K+Si that averages 11.5 (Fig. 14A). The former value is slightly higher than mineral formulae calculated from electron-microprobe analysis in the present study due to a lack of information on various structurally bound elements (e.g., Li, Zn, Nb, Y and Zr) common in peralkaline complexes (Borley, 1976; Bonin, 1986; Hawthorne et al., 1993). Addition of information on Li, Zn and Fe^{3+}/Fe^{2+} to the data by Pillet et al. (1993) and recalculation of the amphibole formulae to 23 atoms of oxygen with 2 OH produced an average ΣNa+K+Si at or below that of ideal arfvedsonite. The results from the present study fall between the

Figure 14. Comparison between the compositional variation of the silicates with that from previous studies.

A. A $\Sigma Ca+{}^{IV}Al$ versus $\Sigma Na+K+Si$ plot of the arfvedsonitic amphibole from the Strange Lake peralkaline complex compared with the compositional variation of that from similar complexes and the earlier study of Pillet (1989) and Pillet et al. (1993). The region represented by all of the chemical formulae from Pillet (1989) indicates a more Ca-rich amphibole (to end-member ferro-richterite). However, the majority of the analyses fall within the inner dashed line near $\Sigma Na+K+Si$ of 11.5 (at the tip of the arrow). This value is greater than the average results of our study (11.4) in which more elements were included. Analyses of alkali amphibole from other peralkaline complexes generally plot in the amphibole quadrilateral represented by the diagonal pattern in the diagram, except for the region near arfvedsonitic amphibole whose significance is discussed in the text.

B. Aegirine (Ae)-Diopside (Di)-Hedenbergite (Hd) plot to compare the results from this study with those from other peralkaline complexes and the results of Pillet (1989). The fields and symbols are identical to those in A. The results of Pillet are diopside- or hedenbergite-poor compared to some of those from our study. The diagonal pattern represents the compositional variation of pyroxene from silica-saturated peralkaline complexes (Bonin & Giret, 1985) modified to account for recent studies (see text).

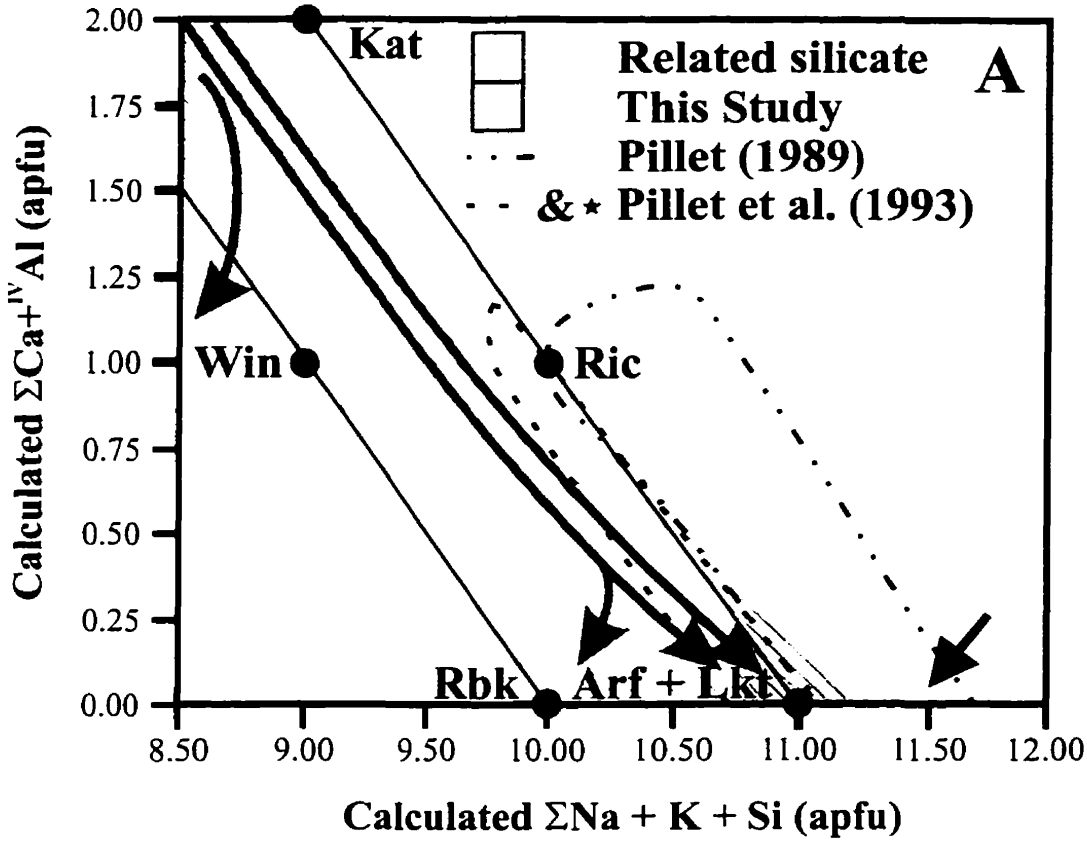
Kat
Related silicate
This Study
Pillet (1989)
& ⋆ Pillet et al. (1993)
A
Win
Ric
Rbk
Arf + Lkt
2.00
1.75
1.50
1.25
1.00
0.75
0.50
0.25
0.00
8.50
9.00
9.50
10.00
10.50
11.00
11.50
12.00
Calculated ΣCa+IVAl (apfu)
Calculated ΣNa + K + Si (apfu)

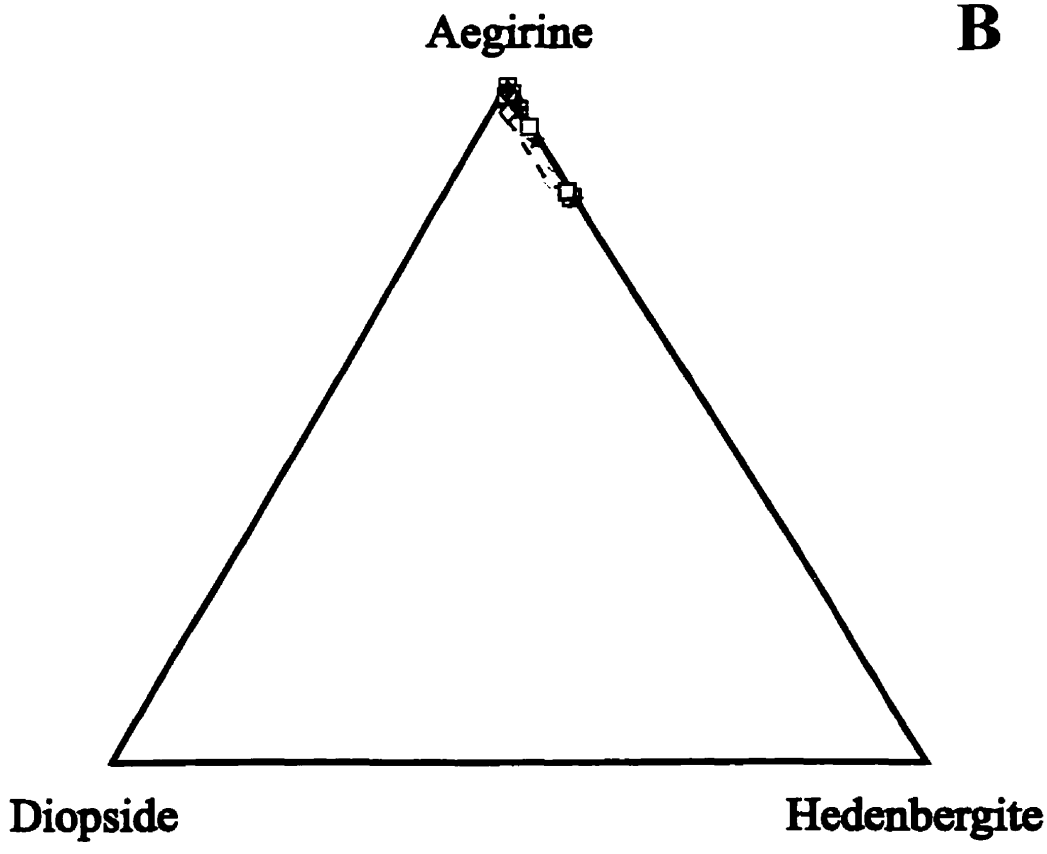
Aegirine
B
Diopside
Hedenbergite

two studies of Pillet, as, although additional trace elements have been included in the calculated mineral formulae, the Fe^{3+}/Fe^{2+} of the amphibole has not been empirically determined.

Arfvedsonitic amphibole from this study (formulae calculated from the results of electron-microprobe analysis), in general, plots in the region of the compositional variation of alkali amphibole represented in numerous studies (diagonal pattern in Fig. 14A). It is particularly interesting to note that many compositions of arfvedsonitic amphibole plot above the upper limit of ΣNa+K+Si in the ideal amphibole quadrilateral. Comparison of the calculated mineral formulae of the arfvedsonitic amphibole for which analyses were conducted solely by electron-microprobe analysis (XRF in Pillet et al., 1993; LAM-ICP-MS in this study) indicates that the amphibole seems closer to being ideal with the addition of these trace and unusual elements. In addition, the compositional evolution observed by Pillet and in this study on the arfvedsonitic amphibole from the Strange Lake peralkaline complex produces identical trends as to those observed by Strong & Taylor (1984) for alkali amphibole of igneous to metasomatic origin from the Topsails and St. Lawrence complexes, Newfoundland (arrows on Fig. 14A).

Strong & Taylor (1984) suggested that variation in the composition of primary alkali and sodic-calcic amphiboles is related to changes in fO_2. Their main trend (the magmatic/subsolidus trend) follows the amphibole quadrilateral down to arfvedsonite, whereas they suggested that under increasing oxidizing conditions, the amphibole will plot to the left of this trend toward riebeckite [$Fe^{3+}/(Fe^{2+} + Fe^{3+})$ of 0.40; Fig. 14B]. However, Hawthorne et al. (1992, 1993) noted that the more oxidized alkali amphibole ferro-leakeite [$Fe^{3+}/(Fe^{2+} + Fe^{3+})$ of 0.50] plots at the same point as arfvedsonite (ratio of 0.20). The results of the present examination indicate that the increase in fO_2 suggested by Strong & Taylor (1984) has validity, but it is tied into the presence of a leakeite component, not a riebeckite component, in the arfvedsonitic amphibole. Consequently, it is impossible to use such a diagram to infer the oxidation state under which the amphibole crystallized, as stated by Hawthorne et al. (1993).

The origin of amphibole-rich "lindinosite" or "lujavrite", is enigmatic, as these mafic pods may be the final stage of fractional crystallization of a granitic or syenitic magma, respectively, a crystal mush, an amphibole-rich cumulate or, perhaps, an

accumulation of hydrothermal origin (Engell, 1973; Ferguson, 1974; Ike et al., 1985; Bonin, 1986). However, the Mn-enrichment of the late amphibole (like astrophyllite), and its pod-like structure indicates a late-stage magmatic origin, which is consistent with textural observations and an expected increase in stability of Mn-rich silicates at a high fO_2 over their Fe-rich equivalents (Bonin & Giret, 1985; Pinckston & Smith, 1995). A late-stage origin for the "lindinosite" in the Strange Lake peralkaline complex is consistent with Bonin's (1986) suggestion, with respect to the observations of Jacobson et al. (1958), that residual liquids from peralkaline granites are Fe-rich. The origin of "lindinosite" and "lujavrite" was related by Engell (1973) to an increase in the amount of H_2O and subsequent decrease in the amount of felsic minerals that crystallized compared to aegirine or arfvedsonite (Bailey, 1969). In addition, the presence of amphibole, and not aegirine, is related to the experimental observations of Ernst (1962, 1968) and Bailey (1969) that alkali amphibole is stable relative to aegirine at a high $P(H_2O)$ and temperature, or at a lower fO_2 and peralkalinity. The occurrence of these pods at the contact between the altered subsolvus granite near the hypersolvus granite in the Strange Lake complex suggests a late-stage magmatic origin.

Trace-element and Li Variation

The results of LAM-ICP-MS analysis for Li are two thirds of the amounts determined by ion probe by Hawthorne et al. (in prep.). In identical samples, LAM-ICP-MS analysis of Li-rich amphibole from this study is bracketed by the other methods, because it contains 0.1 wt.% more Li_2O than that of Hawthorne et al. (in prep.) and 0.1 wt.% less Li_2O than the bulk-AA analysis of the amphibole separates on identical samples. These variations must be attributed to the methodology employed (e.g., standards, interaction of sample with beam, etc.), as zonation of the grains alone cannot account for all of the observed variations.

The decrease in Li content of amphibole through the crystallization sequence, with the exception of that from the mafic pod and 46-I-3, is the same as the trend observed for alkali amphibole from Hurricane Mountain, New Hampshire by Foord et al. (1996) and Hawthorne et al. (1996b). Through the results of XRD and ion-probe analysis, Hawthorne et al. (1996b) emphasized the importance of Li in the fractionation of alkali amphibole from peralkaline granites. They noted an initial increase in Li content followed by a decrease in

the sequence: Li-rich fluor-arfvedsonite, (fluor-ferro-leakeite), Li-bearing arfvedsonite and late-stage riebeckite. The decrease in Li observed by Hawthorne et al. (1996b) is comparable that observed between amphibole from the hypersolvus and fresh subsolvus granites in the present paper. Moreover, the bulk composition of arfvedsonitic amphibole in Foord et al. (1996) is enriched in Fe, Mg, Ca, K, Mn, Sn and H_2O(total), but depleted in Na, Ti, Li, Zr, Nb, F and Zn compared to that of the Li-bearing arfvedsonite (from the same complex). These compositional variations are identical to those of zoned amphibole from the hypersolvus granite in the present study, except that the early-formed arfvedsonitic amphibole from this study is depleted in K, Mn and Si (i.e., is not quite as evolved as in the case they studied).

Abdel-Rahman (1994) carried out the only other detailed study to date on trace-element variation in alkali amphibole through neutron-activation analysis on bulk amphibole separates. He found similar enrichments in REE content of the amphibole, except that those from the present study are distinctly enriched in HREE. Moreover, more variation in the REE content of amphibole was observed in the present study, since point analysis reveals more subtle compositional variations than analysis of the bulk sample.

Aegirine

The only difference between the electron-microprobe data of this study and the information provided by Pillet (1989) is that the data from Pillet shows an enrichment in Ca and Mg (Fig. 14B). Furthermore, Pillet only differentiated the aegirine compositions by rock type and noted its replacement of arfvedsonitic amphibole in the altered subsolvus granite. His results for aegirine from the altered subsolvus granite (Type-2 aegirine) also show a slight enrichment of the aegirine in Fe^{2+} and Ca, but not to the extent observed in my study (85% Ae versus 80% Ae, respectively). His equivalent to Type-1 aegirine contains distinctly less Ti than Type-1 aegirine of the present study (Fig. 14B).

There are very few studies of aegirine from peralkaline complexes with which to compare my findings. As Bonin & Giret (1985) have noted, the general compositional trend of pyroxene from silica-saturated complexes is from near the diopside apex toward the hedenbergite apex and finally to the aegirine apex. In Figure 14B, this region has been expanded to accommodate the findings of Ba et al. (1985) and Platt & Woolley (1986). In

terms of the trace-element content, the HFSE contents here are insignificant compared to those of the arfvedsonitic amphibole (Bailey & Gwozdz, 1994; see above), and show the same enrichment (Rubin et al., 1993).

Effects of Magma Degassing and Variation of Oxygen Fugacity

The composition of arfvedsonitic amphibole in the Strange Lake complex decreases in F and increases in K (the latter at the expense of Na), in the sequence: hypersolvus to altered subsolvus granite to that from the mafic pods. Nassif (1993) noted the presence of primarily K-feldspar in pegmatites. Nassif (Nassif, 1993, Nassif & Martin, 1992) attributed this lack of Na in the feldspar to its preferential loss, along with F and H_2, during degassing. In addition, in a peralkaline melt, the composition of feldspar crystallizing from a melt is always more potassic than the melt (Bailey & Schairer, 1964). Consequently, K-feldspar will then crystallize from the more potassic melt. Thus, this compositional variation of amphibole (i.e., increase in K) provides additional support for degassing. Furthermore, Salvi & Williams-Jones (1996) suggested that degassing was a necessary prelude to Na-metasomatism.

The existence in the subsolvus granite of a free volatile phase (e.g., bubbles) available for degassing is expected as a result of: 1) the presence of two feldspars, which indicate crystallization at high $P(H_2O)$ (Tuttle & Bowen, 1958; Luth, 1976), 2) miarolitic cavities, 3) brecciation, 4) fractionation of anhydrous minerals (e.g. quartz and feldspar), and 5) the presence of pegmatites. Miarolitic cavities form in epizonal granites from boiling after saturation of the magma in H_2O. The fractionation of anhydrous minerals during the initial stages of crystallization results in build-up of volatiles followed by degassing and further crystallization of anhydrous minerals (including aegirine). In the Strange Lake peralkaline complex, Nassif (1993) estimated, from feldspar mineralogy and the presence of miarolitic cavities, that water saturation probably occurred in the subsolvus granite at approximately 575°C. Moreover, build-up of water pressure after saturation resulted in boiling, brecciation, and finally, expulsion of large volumes of H_2O (along with Na and some F) at the surface. This is likely the stage at which many of the pegmatites were formed from an aqueous vapour (Jahns & Burnham, 1969). The presence of aegirine and not

amphibole, as the stable mafic silicate in later stages of formation of the complex is also consistent with an increase in fO_2 owing to degassing. Additional support for degassing comes from the F content of the bulk-rock analysis, which increases from the hypersolvus to transsolvus to fresh subsolvus granites, but decreases, as does the amphibole, in the altered subsolvus granite and pegmatites (Nassif, 1993).

Conditions of Formation of the Strange Lake Suite

Variation of the stability of amphibole with changes in magma composition can interpreted from examination of the amphibole solid solution between arfvedsonite and riebeckite, as represented by the darker shaded region in the experimental hydrous Na-Fe-Si-O system (Fig. 15; after Ernst, 1962). The riebeckite component of the amphibole increases with an increase in fO_2 or decrease in temperature. The maximum temperature of stability of this amphibole solid-solution is 700 or 710°C at $P(H_2O)$ of 2 kbar or 0.7 kbar, respectively. However, an increase in the richterite component in the amphibole, as is the case for Type-1a amphibole, results in an increase in stability of the amphibole to higher temperatures (760°C for end-member ferro-richterite) and fO_2 (Charles, 1975). Thus, in the magmatic sequence, more Ca-rich amphibole crystallizes earlier and at higher temperatures. In addition, an increase in the amount of arfvedsonitic amphibole compared to riebeckitic amphibole occurs as the peralkalinity and content of F and Mn of the amphibole increase and temperature decrease (Ernst, 1962; Charles, 1975). Increased stability of amphibole is the result of the presence of Ti and Mn (Aoki, 1963; Pinckston & Smith, 1995), and substitution of F for OH^-, and Mg for Fe (Ernst, 1960, 1968). Unfortunately, variation in the Na-Fe-Si-O system fails to account for the presence of many other minor and trace elements (e.g., Li and F). The lack of research on the stability of leakeite or Li-rich arfvedsonite precludes further comment on the effect of Li on amphibole stability.

Finally, comparison of the results of XRD work (refer to Appendix B-9 for details) and the results of electron-microprobe analyses on the arfvedsonitic amphibole from the Strange Lake peralkaline complex with maps of silica content and volume of the unit-cell presented by Ernst (1962) shows that ideal arfvedsonitic amphibole would plot in region represented by the diagonal pattern in Figure 15A. However, it should be noted that the

Figure 15. Isobaric log fO_2 versus temperature diagrams of the hydrous Na-Fe-Si-O system Ernst (1962, 1968) depicting the variation in mafic mineralogy from the complex. The arrows indicate the general trends of fO_2 and temperature interpreted from the observed mineral associations. The regions within the amphibole solid solution that contain the hatching represent the approximate fO_2 and temperature, as estimated from the results of XRD and electron-microprobe analyses compared to the data of Ernst (1968).

A. at 700 bars to represent the hypersolvus granite. Riebeckite forms at lower temperatures than arfvedsonite in the region of amphibole solid solution defined by the darker shaded region (Ernst, 1962). Ferro-richterite has a field of stability that exists to higher temperatures and fO_2 than the previous amphiboles (Charles, 1975). Compositional variation of amphibole from the Strange Lake peralkaline complex, as calculated from the X-ray powder diffraction and compositional variation of the amphibole is represented by the diagonal lines in this region. With an increase in fO_2 the composition of the magma passes from the field where amphibole crystallizes into that where aegirine (Ae) and magnetite (Mt) or hematite (H) along with quartz crystallizes. The other abbreviations in the diagram are: Rbk = riebeckite, Arf = arfvedsonite, Aen = aenigmatite, Qtz = quartz, Fa = fayalite, Fe = iron, L = liquid, and F = fluid. The aenigmatite field defined in the diagram from Ernst (1962) is only for Ti-free aenigmatite (likely wilkinsonite). Thus, the approximate region of stability of aenigmatite from Ernst (1962), Carmichael (1962), Nicholls & Carmichael (1969), Lindsley (1971) and Marsh (1975) has been added to define the lighter shaded region.

B. at 2 kbars (after Ernst, 1962, 1968; the shaded regions are the same as for A) to represent the subsolvus granite. As crystallization of the amphibole proceeded from hypersolvus to subsolvus granites, the increase in $P(H_2O)$ likely results in the crystallization of aenigmatite at low $P(H_2O)$ followed by amphibole. Crystallization of aegirine requires a change in fO_2 of the system in either case.

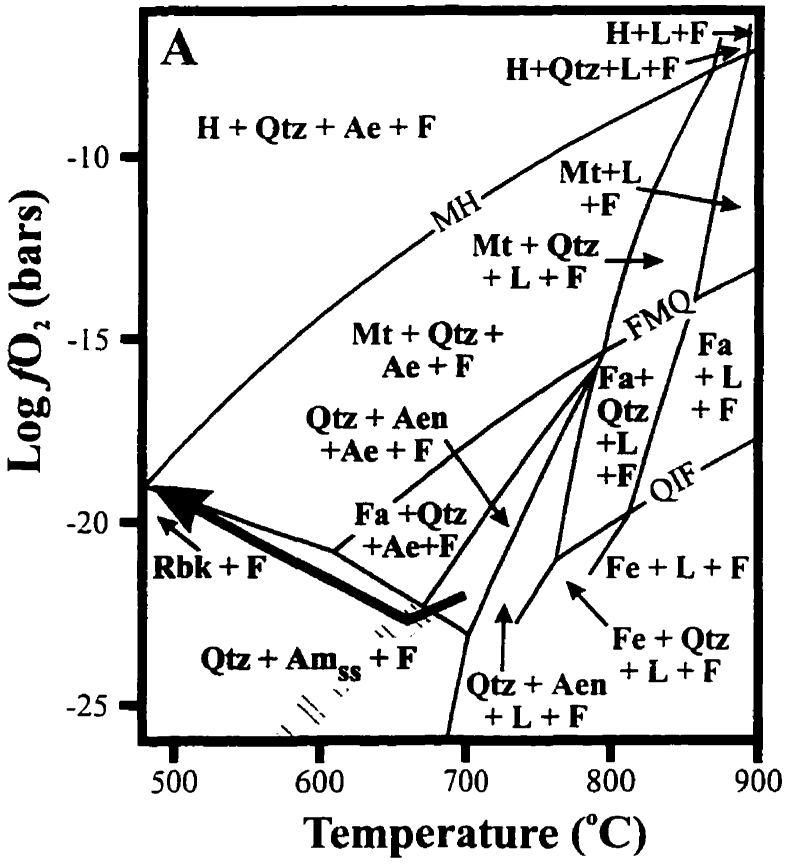
A
H+L+F
H+Qtz+L+F
H + Qtz + Ae + F
Mt+L
+F
MH
Mt + Qtz
+ L + F
FMQ
Mt + Qtz +
Ae + F
Fa
+ L
+ F
Fa+
Qtz
+L
+F
Qtz + Aen
+Ae + F
QIF
Fa +Qtz
+Ae+F
Rbk + F
Fe + L + F
Fe + Qtz
+ L + F
Qtz + Amss + F
Qtz + Aen
+ L + F
-10
-15
-20
-25
500
600
700
800
900
Log fO2 (bars)
Temperature (°C)

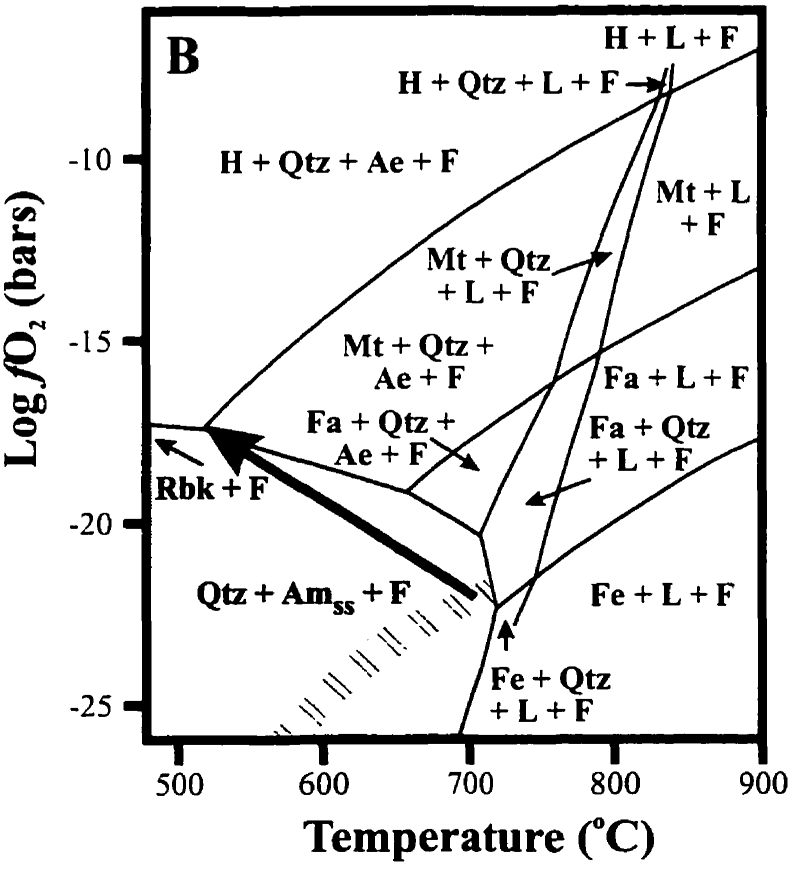
B
H + L + F
H + Qtz + L + F
H + Qtz + Ae + F
Mt + L
+ F
Mt + Qtz
+ L + F
Mt + Qtz +
Ae + F
Fa + L + F
Fa + Qtz +
Ae + F
Fa + Qtz
+ L + F
Rbk + F
Qtz + Amss + F
Fe + L + F
Fe + Qtz
+ L + F
-10
-15
-20
-25
500
600
700
800
900
Log fO2 (bars)
Temperature (°C)

presence of a significant leakeite component to the arfvedsonitic amphibole will decrease its unit-cell volume (Hawthorne et al., 1992, 1993), and consequently, decrease the reliability of such an estimate of temperature and fO_2 at the time of crystallization of the amphibole. Nevertheless, the composition of the early amphibole indicates that it crystallized at relatively low fO_2 (below FMQ) and temperature below 710°C.

A low fO_2 during initial crystallization of the hypersolvus granite also is implied by the presence of ilmenite inclusions in arfvedsonitic amphibole, and aenigmatite (Fig. 15A). In this same granite, grains of ilmenite/aenigmatite indicate a reaction of ilmenite with a Na-rich fluid at a higher fO_2, whereby aenigmatite becomes stable between 550 and 875°C in a "no oxide" field that lies between the FMQ and MH buffers (lighter shaded region in Fig. 15A). According to Ernst (1962), the field of stability of aenigmatite is bound by the stability fields (in the presence of a fluid) of fayalite+quartz+aegirine, fayalite+quartz+liquid and amphibole. The size of the stability field of aenigmatite decreases as $a(Na_2SiO_3)$ increases (Nicholls & Carmichael, 1969). A decrease in temperature during crystallization pushes the magma into the field of stability of aegirine+fayalite+quartz or amphibole (Fig. 15A). Intergrowths involving aenigmatite, aegirine, amphibole, Fe-Ti oxide and amphibole are related to variations in $P(H_2O)$, fO_2 and temperature near the aenigmatite field. A decrease in temperature during crystallization or an increase in $P(H_2O)$ resulted in the crystallization of amphibole or aegirine (Fig. 15B). Late crystallization of the Type-1 aegirine rims on arfvedsonitic amphibole result from an increase in fO_2 likely related to degassing (Flower, 1974). As the $P(H_2O)$ increases, two feldspars are subsequently produced (Martin & Bonin, 1976). In the subsolvus granites and pegmatites, the estimated minimum temperature of crystallization varies from 500°C to 575°C (Nassif, 1993; Pillet et al., 1993). Unfortunately, no experimental data exist on the stability fields of astrophyllite and neptunite, but the dominance of Fe^{2+} implies formation at a low fO_2 as described above for the Ti- and Fe^{2+}-rich mineral aenigmatite.

Alternating zones of the aegirine assemblage and amphibole in composite grains in the altered subsolvus granite are the result of either: 1) variation in the trace-element content of one type of amphibole that results in its preferential replacement, or 2) alternating changes in conditions during crystallization such that aegirine, and not arfvedsonitic amphibole, becomes the stable phase. Support for the first comes from amphibole zonation

in the hypersolvus granite that parallels the *c* axis, which is related to the presence of inclusions and variations in Li, Fe^{3+} and Fe^{2+} content, possibly fO_2, and to subtle changes in composition. As neither Type-2 amphibole from the altered subsolvus granite nor Type-1b from the hypersolvus granite contain inclusions, Type-1a amphibole may have been selectively replaced by aegirine (Fig. 15B). The correspondence between the composition of Type-1b arfvedsonitic amphibole from the hypersolvus granite and that of Type-2 amphibole from the subsolvus granite lends further credence to this hypothesis. The second possibility is that an increase in fO_2, or possibly a_{Na}, pushed the composition of the magma from the amphibole stability field into that of aegirine (Fig. 15). However, an increase in a_{Na} is not supported by the bulk-rock analyses (Nassif, 1993). Thus, variation in fO_2 (likely related to degassing) accounts for crystallization of Type-3 aegirine in the ore zone and in pegmatites of apical portions of the pluton, and amphibole at depth. This is followed by a late increase in the magma or orthomagmatic fluid in Mn and rapid fall of fO_2 that stabilizes the late-stage amphibole at the expense of this aegirine (Nash & Wilkinson, 1970). These variations could also account for the gap in amphibole crystallization (filled by aegirine) in many peralkaline igneous complexes (Giret et al., 1980).

Conclusions

Primary arfvedsonitic amphibole from the Strange Lake peralkaline complex has evolved in the sequence:

1) Na-, Fe-, and inclusion-rich (Type-1a) arfvedsonitic amphibole cores from the hypersolvus granite, surrounded by optically continuous generally more Ca-, Mg-, Mn- and Al-rich, inclusion-free (Type-1b) rims,

2) primary K-, Mn-, Fe^{2+}-, Al- and, in sometimes Ca-rich (Type-2) amphibole present in the subsolvus granite, and

3) late-stage K-, Mn-, Li- and F-rich (Type-3) amphibole.

These amphiboles are associated with green Type-1 subsolvus aegirine present in hypersolvus and transsolvus granites, yellow Type-2 aegirine of replacement origin and yellow green Type-3 aegirine present as the dominant mafic mineral in pegmatites and the

altered subsolvus granite. The differences in mafic mineral content of the complex is related to differences in temperature, $P(H_2O)$ and fO_2 of the different units.

This evolutionary sequence is a combination of:

1) fractional crystallization that increases the concentration of incompatible elements, especially REE, in the magma from which the later amphibole crystallizes. Early crystallization of LREE-rich inclusions explains the relative HREE enrichment of the amphibole,
2) degassing related to an increase in fO_2 and K, and a decrease in Na and F, that produced compositional zonation of amphibole in the hypersolvus granite, and mafic mineral zonation in the subsolvus granite, and
3) Na- and Ca-metasomatism as discussed in Chapters 5 and 6 took over upon liberation of the orthomagmatic fluids and their mixture with extraneous fluids. Thus, the complete evolution of the Strange Lake peralkaline complex can be described through investigation of its primary mafic mineralogy. These results, by implication, may be applied to other peralkaline complexes.

Acknowledgements

I would like to thank G. Poirier for setting up the elemental analysis tables for the electron-microprobe analysis and G. Gauthier is thanked for setup and tuning the LAM-ICP-MS. I also thank G. Gauthier, C. Dalpé, S. Jackson and S. Lang for discussions on sample preparation, standards, standardization and errors. Claude Dalpé and Gilles Gauthier wrote the program to calculate the element contents (in ppm) from the raw LAM-ICP-MS data. Claude and N. MacRae provided the dark glasses HF-13 and JW-87. The field work was performed in 1989 by a field team composed of Dr. S. Salvi, G. Nassif, Prof. A.E. Williams-Jones, Prof. S. Wood, Dr. M. Boily and R. Marr. Stephano also sampled the drill-core. The Iron Ore Company of Canada provided access to the locality and drill-core. This research was supported by NSERC grant, Lithoprobe grant, an FCAR team grant and a NSERC Strategic Grant to R.F. Martin. Additional funding was provided by a FCAR scholarship and stage, a major scholarship from McGill University and a GSA student

research award to me. Comments by C. Normand, A.E. Williams-Jones and G. Gauthier improved this manuscript.

References

Abdel-Rahman, A.-F. (1992): Mineral chemistry and paragenesis of astrophyllite from Egypt. *Mineralogical Magazine*, 56, 17-26.

------- (1994): Alkali amphibole: a potential source of rare earth elements in felsic alkaline rocks. *Exploration and Mining Geology*, 3, 81-94.

Aoki, K. (1963): The kaersutites and oxykaersutites from alkalic rocks of Japan and surrounding areas. *Journal of Petrology*, 4, 198-210.

Ba, H., Black, R., Benziane, B., Diombana, D., Hascoet-Fender, J., Bonin, B., Fabre, J. & Liégeois, J.P. (1985): La province des complexes annulaires alcalins sursaturés de l'adrar des Iforas, Mali. *Journal of African Earth Sciences*, 3, 123-142.

Bailey, D.K. (1969): The stability of acmite in the presence of H_2O. *American Journal of Science*, 267A, 1-16.

------- & Schairer, J.F. (1964): Feldspar-liquid equilibria in peralkaline liquids - The orthoclase effect. *American Journal of Science*, 262, 1198-1206.

Bailey, J.C. & Gwozdz, R. (1994): Li distribution in aegirine lujavrite, Ilímaussaq alkaline intrusion, South Greenland: role of cumulus and post-cumulus processes. *Lithos*, 31, 207-225.

Bélanger, M. (1984): Région du lac Brisson. *Ministère de l'Énergie et des Ressources, Québec*, DP 84-20 (carte annotée, scale 1:50,000).

Birkett, T.C., Miller, R.R., Roberts, A.C. & Mariano, A.N. (1992): Zirconium-bearing minerals of the Strange Lake intrusive complex, Quebec-Labrador. *Canadian Mineralogist*, 30, 191-205.

-------, Trzcienski, W.E., Jr. & Stirling, J.A.R. (1996): Occurrence and compositions of some Ti-bearing minerals in the Strange Lake intrusive complex, Quebec-Labrador boundary. *Canadian Mineralogist*, 34, 779-801.

Blaxland, A.B., Breemen, van, O., Emeleus, C.H. & Anderson, J.G. (1978): Age and origin of the major syenite centers in the Gardar province of South Greenland: Rb-Sr studies. *Geological Society of America Bulletin*, 89, 231-244.

Bogoch, R., Weissbrod, T. & Bar-Matthews, M. (1992): Significance of REE-mineral inclusions in aegirine from an alkali syenite, Negev, Israel. *European Journal of Mineralogy*, 4, 1337-1346.

Boily, M. & Williams-Jones, A.E. (1994): The role of magmatic and hydrothermal processes in the chemical evolution of the Strange Lake plutonic complex (Quebec-Labrador). *Contributions to Mineralogy and Petrology*, 118, 33-47.

Bonin, B. (1972): Le complexe granitique annulaire de la région de Tolla-Cauro (Corse). Thése 3^{e} cycle, Université de Paris VI, France, 127p.

------- (1986): **Ring Complex Granites and Anorogenic Magmatism.** North Oxford Academic Publishers Ltd., Great Britain, 188p.

------- & Giret, A. (1985): Clinopyroxene composition trends in oversaturated and undersaturated alkaline ring complexes. *Journal of African Earth Sciences*, 3, 175-182.

Borley, G.D. (1976): Ferromagnesian mineralogy and temperature of formation of the Younger Granites of Nigeria. *In* **Geology of Nigeria** (Kogbe, C.A., ed.). Elizabethan Press, Lagos, Nigeria, 159-176.

Bos, A.J.J., Vis, R.D., Verheul, H., Prins, M., Davies, S.T., Bowen, D.K., Makjaniç, J. & Valkoviç V. (1984): Experimental comparison of synchrotron radiation with other modes of excitation of X-rays for trace element analysis. *Nuclear Instrumental Methods of Physics Research*, B3, 232-240.

Brögger, W.C. (1890): Die mineralien der syenitpegmatitgänge der südnowegischen augit- und nephelinsyenite. *Zeitschrift für Kristallographie und Mineralogie*, 16, 1-663.

Carmichael, I.S.E. (1962): Pantelleritic liquids and their phenocrysts. *Mineralogical Magazine*, 33, 86.

Charles, R.W. (1975): The phase equilibria of richterite and ferrorichterite. *American Mineralogist*, 60, 367-374.

Christiansen, E.H., Burt, D.M., Sheridan, M.F. & Wilsons, R.T. (1983): The petrogenesis of topaz rhyolites from the Western United States. *Contributions to Mineralogy and Petrology*, 83, 16-30.

Currie, K.L. (1985): An unusual peralkaline granite near Lac Brisson, Quebec-Labrador. *Geological Survey of Canada Paper*, 85-1A, 73-90.

Czamanske, G.K. & Dillet, B. (1988): Alkali amphibole, tetrasilicic mica and sodic pyroxene in peralkaline siliceous rocks, Questa Caldera, New Mexico. *American Journal of Science*, 288A, 358-392.

Dalpé, C., Baker, D.R. & Sutton, S.R. (1995): Synchrotron X-ray-Fluorescence and Laser-Ablation ICP-MS microprobes: useful instruments for analysis of experimental run-products. *Canadian Mineralogist*, 33, 481-498.

Droop, G.T.D. (1987): A general equation for estimating Fe^{3+} concentrations in ferromagnesian silicates and oxides from microprobe analyses, using stoichiometric criteria. *Mineralogical Magazine*, 51, 431-435.

Emslie, R.F. (1978a): Elsonian magmatism in Labrador: age, characteristics and tectonic setting. *Canadian Journal of Earth Sciences*, 15, 438-453.

------- (1978b): Anorthosite massifs, rapakivi granites, and late Proterozoic rifting of North America. *Precambrian Research*, 7, 61-98.

Engell, J. (1973): A closed system crystal-fractionation model for the agpaitic Ilímaussaq intrusion, South Greenland with special reference to the lujavrites. *Bulletin of the Geological Society of Denmark*, 22, 334-362.

Ernst, W.G. (1962): Synthesis, stability relations and occurrence of riebeckite and riebeckite-arfvedsonite solid solutions. *Journal of Geology*, 70, 689-736.

------- (1968): **Amphiboles**. Springer-Verlag, 125p.

Fabriès, J. (1978): Les types paragénétiques des amphiboles sodiques dans les roches magmatiques. *Bulletin de Minéralogie*, 101, 155-165.

Ferguson, J. (1974): The differentiation of agpaitic magmas: the Ilimaussaq intrusion, South Greenland. *Canadian Mineralogist*, 10, 335-349.

Flower, M.F.J. (1974): Phase relations of titan-acmite in the system Na_2O-Fe_2O_3-Al_2O_3-TiO_2-SiO_2 at 1000 bars total water pressure. *American Mineralogist*, 59, 536-548.

Foord, E.E., Erd, R.C., Robie, S.B., Lichte, F.E. & King, V.T. (1996): Li- and F-bearing alkali amphiboles from granitic pegmatites at Hurricane Mountain, Carroll Co., New Hampshire, USA. *Canadian Mineralogist*, 34, 1011-1014.

Giret, A., Bonin, B. & Leger, J.M. (1980): Amphibole compositional trend in oversaturated and undersaturated alkaline plutonic ring complexes. *Canadian Mineralogist*, 18, 481-495.

Hawthorne, F.C., Oberti, R., Ungaretti, L. & Grice, J. (1992): Leakeite, $NaNa_2(Mg_2Fe^{3+}{}_2Li)Si_8O_{22}(OH)_2$, a new alkali amphibole from the Kajlidongri manganese mine, Jhabua district, Madhya Pradesh, India. *American Mineralogist*, 77, 1112-1115.

-------, -------, Ottolini, L. & Foord, E.E. (1996b): Lithium-bearing fluor-arfvedsonite from Hurricane Mountain, New Hampshire: a crystal-chemical study. *Canadian Mineralogist*, 34, 1015-1019.

-------, -------, Ungaretti, L., Ottolini, L., Grice, J.D. & Czamanske, G.K. (1996a): Fluor-ferro-leakeite, $NaNa_2(Fe^{2+}{}_2Fe^{3+}{}_2Li)Si_8O_{22}F_2$. *American Mineralogist*, 81, 226-228.

-------, Ungaretti, L., Oberti, R., Bottazzi, P. & Czamanske, G.K. (1993): Li: An important component in igneous alkali amphiboles. *American Mineralogist*, 78, 733-745.

Hermann, A.G. (1969): Yttrium and lanthanides, Section 39. *In* **Handbook of Geochemistry** (Wedepohl, K.H., ed.), 2, Springer-Verlag, New York.

Herzog, L.F., Marshall, D.J. & Babione, R.F. (1970): The Luminoscope - a new instrument for studying the electron-stimulated luminescence of terrestrial, extraterrestrial and synthetic materials under the microscope. *In* **Space Science Applications of Solid State Luminescence Phenomena** (Weber, J.N. & White, E., eds.). 79-98. MRL publication 70-101, State College, Pennsylvania.

Hoffman, P.F. (1988): United plates of America, the birth of a craton: Early Proterozoic assembly and growth of Proto-Laurentia. *Annual Reviews of Earth and Planetary Sciences*, 16, 543-603.

Ike, E.C., Bowden, P. Martin, R.F. (1985): Amphibole in the porphyries of the Tibchi anorogenic ring-complex, Nigeria: product of deuteric adjustments. *Canadian Mineralogist*, 23, 447-456.

Jackson, S.E., Longerich, H.P., Cunning, G.R. & Fryer, B.J. (1992): The application of laser-ablation microprobe - inductively coupled plasma - mass spectrometry (LAM-ICP-MS) to in situ trace-element determinations in minerals. *Canadian Mineralogist*, 30, 1049-1064.

Jacobson, R.R.E., MacLoed, W.N. & Black, R. (1958): Ring-complexes in the Younger Granites Province of Northern Nigeria. *Geological Society of London, Memoir*, 1, 72p.

Jahns, R.H. & Burnham, C.W. (1969): Experimental studies of pegmatite genesis. I. A model for the derivation and crystallization of granitic pegmatites. *Economic Geology*, 64, 843-864.

Jambor, J.L., Roberts, A.C., Owens, D.R. & Grice, J.D. (1996): Zajacite-(Ce), a new rare-earth fluoride from the Strange Lake deposit, Quebec-Labrador. *Canadian Mineralogist*, 34, 1299-1304.

Jarvis, K.E., Gray, A.L. & Houk, R.S. (1992): **Handbook of Inductively Coupled Plasma Mass Spectrometry**. Blackie, Glasgow, 375p.

Lacroix, A. (1922): Minéralogie de Madagascar. *Challamel*, Paris, 2, 694p.

Leake, B.E. (1978): Nomenclature of amphiboles. *American Mineralogist*, 63, 1023-1052.

Lindsley, D.H. (1971): Synthesis and preliminary results on the stability of aenigmatite ($Na_2Fe^{2+}{}_5TiSi_6O_{20}$). *Carnegie Institute of Washington Yearbook*, 69, 188-190.

Luth, W.C. (1976): Granitic rocks. *In* **The evolution of the crystalline rocks** (Bailey, D.K. & Macdonald, R., eds.). Academic Press, London, 335-417.

Marsh, J.S. (1975): Aenigmatite stability in silica-undersaturated rocks. *Contributions to Mineralogy and Petrology*, 50, 135-144.

Martin, R.F. & Bonin, B. (1976): Water and magma genesis: the association hypersolvus granite - subsolvus granite. *Canadian Mineralogist*, 14, 228-237.

Miller, R.R. (1986): Geology of the Strange Lake alkalic complex and the associated Zr-Y-Be-REE mineralization. Current Research, *Newfoundland Department of Mines and Energy, Mineral Development Division*, Report 86-1, 11-19.

------- (1988): Yttrium (Y) and other rare metals (Be, Nb, REE, Ta, Zr) in Labrador. Current Research, *Newfoundland Department of Mines and Energy, Mineral Development Division*, Report 88-1, 83-91.

------- (1996): Structural evolution of the Strange Lake peralkaline rare-element (NYF) granitic pegmatite, Quebec-Labrador. *Canadian Mineralogist*, 34, 349-371.

-------, Heaman, L.M. & Birkett, T.C. (1997): U-Pb zircon age of the Strange Lake peralkaline complex: implications for Mesoproterozoic peralkaline magmatism in north-central Labrador. *Precambrian Research*, 81, 67-83.

Moenke-Blankenburg, L. (1989): **Laser Microanalysis** (Winefordner, J.D. & Kolthoff, I.M., eds.). Chemical Analysis: a series of monographs on analytical chemistry and its applications, John Wiley & Sons, Ltd., Toronto, 105, 288p.

Morimoto, N. (1989): Nomenclature of pyroxenes. *Canadian Mineralogist*, 27, 143-156.

Nash, W.P. & Wilkinson, J.F.G. (1970): Shonkin Sag laccolith, Montana. I: mafic minerals and estimates of temperature, pressure, oxygen fugacity and silica activity. *Contributions to Mineralogy and Petrology*, 25, 241-269.

Nassif, G.J. (1993): The Strange Lake peralkaline complex, Québec-Labrador: The hypersolvus-subsolvus granite transition and feldspar mineralogy. McGill University, M.Sc. Thesis, Montréal, Québec, 104p.

------- & Martin, R.F. (1991): The hypersolvus granite-subsolvus granite transition at Strange Lake, Québec-Labrador. *Geological Association of Canada - Mineralogical Association of Canada*, Abstracts with Programs, 16, A89.

------- & ------- (1992): Feldspar mineralogy of the Strange Lake peralkaline complex, Québec-Labrador. *Geological Association of Canada - Mineralogical Association of Canada*, Abstracts with Programs, 17, A83.

Nicholls, J. & Carmichael, I.S.E. (1969): Peralkaline acid liquids: a petrological study. *Contributions to Mineralogy and Petrology*, 20, 268-294.

Pillet, D. (1989): Le granite peralcalin du Lac Brisson, Labrador Central (province du Québec, Canada): pétrologie, géochronologie, et relations avec les minéralisations internes à Zr, Y, Nb. Thèse de doctorat, Université Claude Bernard: Lyon I, Lyon, France, 276p.

-------, Bonhomme, M.G., Duthou, J.L. & Chenevoy, M. (1989): Chronologie Rb/Sr et K/Ar du granite peralkalin du lac Brisson, Labrador central, Nouveau-Québec. *Canadian Journal of Earth Sciences*, 26, 328-332.

-------, Chenevoy, M & Bélanger, M. (1992): Pétrologie du granite peralcalin du lac Brisson, Labrador central, Nouveau-Québec. I. Mode de mise en place et évolution chimique. *Canadian Journal of Earth Sciences*, 29, 353-372.

-------, ------- & ------- (1993): Pétrologie du granite peralcalin du lac Brisson, Labrador central, Nouveau-Québec. II. Minéralogie et modalités de cristallisation. *Canadian Journal of Earth Sciences*, 30, 2423-2435.

Pinckston, D.R. & Smith, D.G.W. (1995): Mineralogy of the Lake Zone, Thor Lake rare-metals deposit, N.W.T., Canada. *Canadian Journal of Earth Sciences*, 32, 516-532.

Platt, R.G. & Woolley, A.R. (1986): The mafic mineralogy of the peralkaline syenites and granites of the Mulanje complex, Malawi. *Mineralogical Magazine*, 50, 85-99.

Roelofsen, J.N., Martin, R.F. & Veblen, D.R. (1995): Origin of aegirine in the Strange lake peralkaline complex, Québec-Labrador border: an integrated electron microprobe, HRTEM and AEM study. *Geological Association of Canada - Mineralogical Association of Canada*, Abstracts with Programs, 20, A90.

Rollinson, H. (1993): **Using geochemical data: evaluation, presentation, interpretation.** John Wiley & Sons, Inc., New York, 352p.

Ross, M. (1984): Ultraalkalic arfvedsonite and associated richterite, acmite, and aegirine-augite in quartz syenite, Magnet Cove alkalic igneous complex, Arkansas. *EOS*, 65, 293.

Rubin, J.N., Henry, C.D. & Price, J.G. (1993): The mobility of zirconium and other "immobile" elements during hydrothermal alteration. *Chemical Geology*, 110, 29-47.

Salvi, S. (1990): A fluid inclusion study of calcium metasomatism and Zr-Y-REE-Nb-Be mineralization in peralkaline granite at Strange Lake, Labrador-Quebec, Canada. McGill University, M.Sc. Thesis, Montréal, Québec, 101p.

------- (1995): Magma degassing and wall rock alteration in the rare metal-rich peralkaline granite at Strange Lake, Quebec/Labrador. McGill University, Ph.D. Thesis, Montréal, Québec, 263p.

------- & Williams-Jones, A.E. (1990): The role of hydrothermal processes in the granite-hosted Zr, Y, REE deposit at Strange Lake, Quebec/Labrador: Evidence from fluid inclusions. *Geochimica et Cosmochimica Acta*, 54, 2403-2418.

------- & ------- (1992): Reduced orthomagmatic C-O-H-NaCl fluids in the Strange Lake rare-metal granitic complex, Quebec/Labrador, Canada. *European Journal of Mineralogy*, 4, 1155-1174.

------- & ------- (1995): Zirconosilicate phase relations in the Strange Lake (Lac Brisson) pluton, Quebec-Labrador. *American Mineralogist*, 80, 1031-1040.

------- & ------- (1996): The role of hydrothermal processes in concentrating HFSE in the Strange Lake peralkaline complex, Northeastern Canada. *Geochimica et Cosmochimica Acta*, 60, 1917-1932.

Stix, J., Gauthier, G. & Ludden, J.N. (1995): A critical look at quantitative laser-ablation ICP-MS analysis of natural and synthetic glasses. *Canadian Mineralogist*, 33, 435-444.

Streckeisen, A. (1976): To each plutonic rock its proper name. *Earth Science Reviews*, 12, 1-23.

Strong, D.F. & Taylor, R.P. (1984): Magmatic-subsolidus and oxidation trends in composition of amphiboles from silica-saturated peralkaline igneous rocks. *TMPM Tschermaks Mineralogische und Petrologische Mitteilungen*, 32, 211-222.

Sun, S.S. (1982): Chemical composition and origin of the earth's primitive mantle. *Geochimica et Cosmochimica Acta*, 46, 179-192.

Thompson, R.N. (1982): British Tertiary volcanic province. *Scottish Journal of Geology*, 18, 49-107.

Tuttle, O.G. & Bowen, N.L. (1958): Origin of granite in the light of experimental studies in the system $NaAlSi_3O_8$-$KAlSi_3O_8$-SiO_2-H_2O. *Geological Society of America Memoir*, 74, 153p.

Whalen, J.B. (1985): Geochemistry of an Island-Arc Plutonic Suite: the Uasilau-Yau Intrusive Complex, New Britain, P.N.G. *Journal of Petrology*, 26, 603-632.

Williams, J.G. & Jarvis, K.E. (1993): Preliminary assessment of laser ablation inductively coupled plasma mass spectrometry for quantitative multi-element determination in silicates. *Journal of Analytical and Atomic Spectrometry*, 8, 25-34.

Zajac, I.S., Miller, R.R., Birkett, T.C. & Nantel, S. (1984): Le gîte de Zr, Y, Nb et Be du complexe alcalin de Strange Lake, Québec-Labrador. *Ministère de l'Énergie et des Ressources du Québec*, DV 84-18, 127-142.

Chapter 5:

THE MAFIC SILICATES OF THE STRANGE LAKE PERALKALINE COMPLEX, QUEBEC-LABRADOR. II. EFFECTS OF NA-METASOMATISM

Jeanette N. Roelofsen, Robert F. Martin[1] and David R. Veblen[2]

[1] Department of Earth and Planetary Sciences,
McGill University,
3450 University Street,
Montréal, Québec
H3A 2A7

[2] The Morton K. Blaustein Department of Earth and Planetary Sciences,
The Johns Hopkins University,
3300 North Charles Street,
Baltimore, Maryland 21210

Prologue to Chapters 5 and 6

Now that the compositional variation of the primary arfvedsonitic amphibole and of the aegirine has been examined, the following two chapters will examine the effects of metasomatism on these minerals. Salvi & Williams-Jones (1990, 1992) and Pillet et al. (1992, 1993) determined that the complex was affected by both Na- and Ca-metasomatism. The former authors noted, from fluid inclusion studies, that Na-metasomatism occurred at ≥350°C, and Ca-metasomatism at <200°C. The main effect of Na-metasomatism, in this and other complexes, has been ascribed to the replacement of arfvedsonitic amphibole by the assemblage: aegirine, magnetite and quartz (O'Halloran, 1985; Bonin, 1986; Salvi & Williams-Jones, 1990, 1992). In the Strange Lake complex, Pillet (1989) and Pillet et al. (1993) noted the presence of hematite, and not magnetite, in this replacement assemblage.

Although the effects of Ca-metasomatism are readily apparent in the ore minerals from the complex (Salvi & Williams-Jones, 1990, 1995), these effects have been noted here for the first time in the arfvedsonitic amphibole described in the previous chapter. The only study to suggest the influence of a type of metasomatism other than Na-metasomatism on the mafic silicates is that of Martin (1977), who noted the replacement of arfvedsonitic amphibole by ferro-anthophyllite in fenitized granite from Cape Ann, Massachusetts. The lack of literature discussing the effects of metasomatism on mafic silicates, other than that of Na-metasomatism, may simply be the result of the tendency, noted in the introduction, to examine the felsic minerals and the ore minerals in similar complexes.

In the subsequent chapters, I explore the effects of Na-metasomatism (Chapter 5) and Ca-metasomatism (Chapter 6) on arfvedsonitic amphibole using the Strange Lake peralkaline complex as an example. The cutoff between the two types of metasomatism was arbitrarily set at 200°C, as this is the transition temperature indicated by the fluid inclusion studies of Salvi & Williams-Jones (1990, 1992).

References

Bonin, B. (1986): **Ring Complex Granites and Anorogenic Magmatism**. North Oxford Academic Publishers Ltd., Great Britian, 188p.

Martin, R.F. (1977): The association hypersolvus granite-subsolvus granite-"solvsbergite" at Andrew's Point, Cape Ann, Massachusetts: a case of localized fenitization. *American Journal of Sciences*, 277, 273-287.

O'Halloran, D.A. (1985): Ras ed Dom migrating ring complex: A-type granites and syenites from the Bayuda Desert, Sudan. In Alkaline ring complexes in Africa. *Journal of African Earth Sciences*, 3, 61-75.

Pillet, D. (1989): Le granite peralcalin du Lac Brisson, Labrador Central (province du Québec, Canada): Pétrologie, géochronologie, et relations avec les minéralisations internes à Zr, Y, Nb. Thèse de doctorat, Université Claude Bernard: Lyon I, Lyon, France, 276p.

-------, Chenevoy, M. & Bélanger, M. (1992): Pétrologie du granite peralcalin du lac Brisson, Labrador central, Nouveau-Québec. 1. Mode de mise en place et évolution chimique. *Canadian Journal of Earth Sciences*, 29, 353-372.

-------, ------- & ------- (1993): Pétrologie du granite peralcalin du lac Brisson, Labrador central, Nouveau-Québec. II. Minéralogie et modalités de cristallisation. *Canadian Journal of Earth Sciences*, 30, 2423-2435.

Salvi, S. & Williams-Jones, A.E. (1990): The role of hydrothermal processes in the granite-hosted Zr, Y, REE deposit at Strange Lake, Quebec/Labrador: Evidence from fluid inclusions. *Geochimica et Cosmochimica Acta*, 54, 2403-2418.

------- & ------- (1992): Reduced orthomagmatic C-O-H-NaCl fluids in the Strange Lake rare-metal granitic complex, Quebec/Labrador, Canada. *European Journal of Mineralogy*, 4, 1155-1174.

------- & ------- (1995): Zirconosilicate phase relations in the Strange Lake (Lac Brisson) pluton, Quebec-Labrador. *American Mineralogist*, 80, 1031-1040.

Abstract

During the evolution of peralkaline granites, orthomagmatic fluids may react with the earlier magmatic minerals. One example of such a reaction is the pseudomorphic replacement of arfvedsonitic amphibole by Type-2 (yellow) aegirine during Na-metasomatism (≥350°C) in the Strange Lake peralkaline granitic complex, Québec-Labrador. No NaFe-bearing biopyriboles were formed between arfvedsonitic amphibole and aegirine. The results of this study show that this replacement was accompanied by formation of astrophyllite and a fluoride mineral, or hematite ± quartz and fluorite depending on whether it occurred in the hypersolvus or altered subsolvus granite, respectively. Thus, the Na-metasomatic fluid contained significant Na, minor Ca and Al, and variable Rb, Zn, Ti, Nb and Zr, depending on whether the replacement occurred in the hypersolvus or altered subsolvus granite. This replacement operated either under relatively reducing (in the field of stability of astrophyllite) or oxidizing conditions (in the field of stability of hematite), while K, Ca, Fe, Mg, Li, Mn, REE, F and H_2, or K, Mg, Li, Zn, Zr, Ti, Mn, F and H_2 were released into the fluid in the hypersolvus and altered subsolvus granites, respectively. The amount of hydrogen released during this replacement and the absence of magnetite imply that the Fischer-Tropsch process proposed by Salvi & Williams-Jones (1997) for formation of hydrocarbons, present in fluid inclusions of quartz, may have occurred through reaction of the fluid with hematite or arfvedsonitic amphibole. Comparison of the relative mobility of elements during metasomatism indicates that the REE and, in some cases, Zr, Y and Nb, released by replacement of amphibole by the aegirine-dominant assemblage, could have contributed significantly to the formation of the associated ore deposit. Therefore, the amphibole acted as a sink for HFSE, REE, Mn, Li and Zn during magmatic processes and as a source of these elements during later hydrothermal processes.

Introduction

The Strange Lake peralkaline A-type granite, on the Québec-Labrador border, 250 km northeast of Schefferville, Québec (Fig. 1A), is a potential economic source of Zr, REE,

Figure 1A. Location of the Strange Lake peralkaline complex, Québec-Labrador, Canada.

B. Map units of the complex after Bélanger (1984) and Nassif (1993). The core of the complex, composed of hypersolvus granite, was intruded by subsolvus granite. The ore zone occurs in the most altered subsolvus granite, near its contact with the hypersolvus granite. Small amounts of transsolvus granite, unaltered subsolvus granite and roof pendants also are encountered. The complex is surrounded by quartz monzonite to the southwest and various gneisses, metadiorite and metagabbros to the northeast. Sample locations are denoted by circles, triangles and squares.

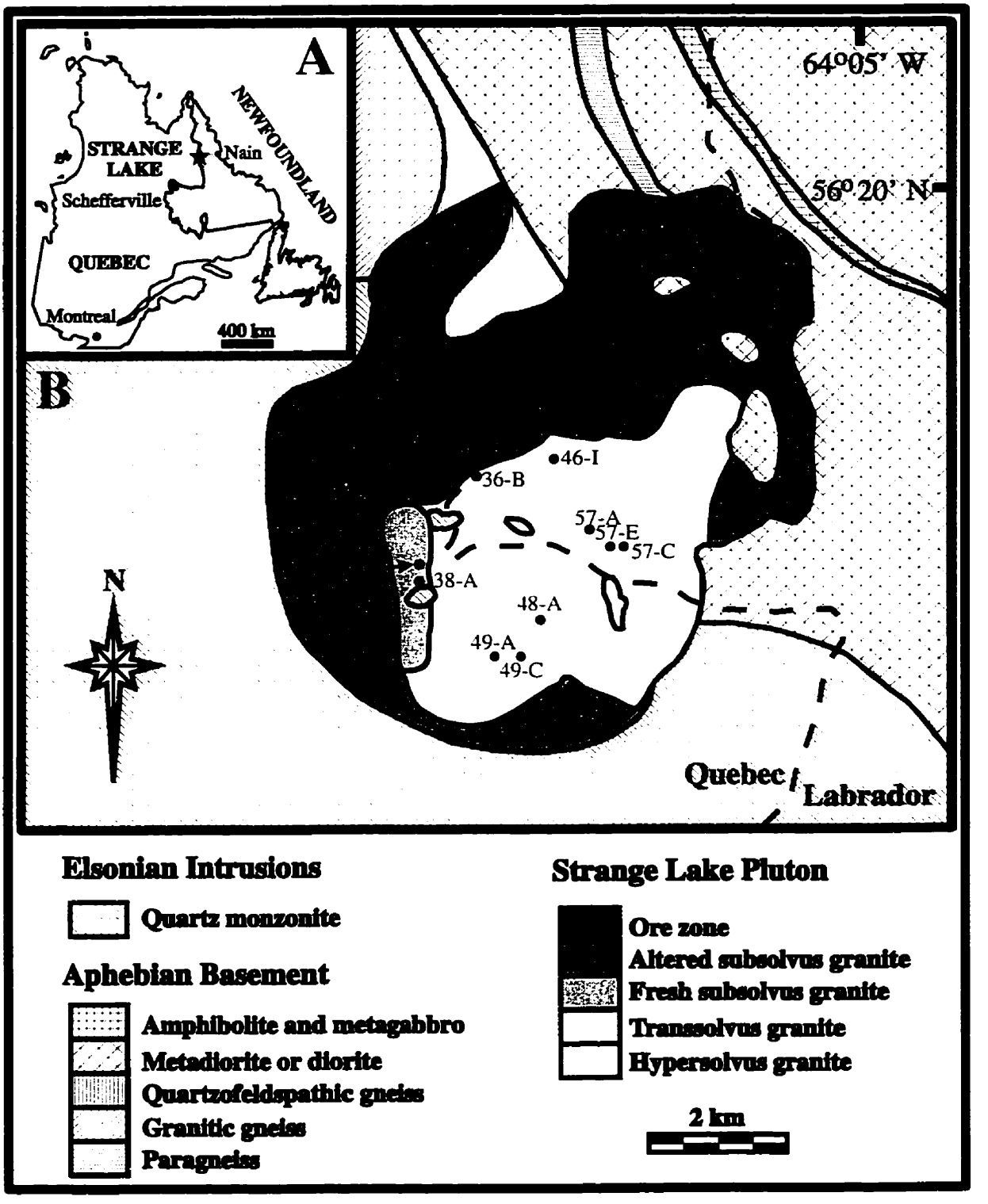
A
NEWFOUNDLAND
STRANGE LAKE
Nain
Schefferville
QUEBEC
Montreal
400 km
B
64°05' W
56°20' N
46-I
36-B
57-A
57-E
57-C
38-A
48-A
49-A
49-C
N
Quebec
Labrador
Elsonian Intrusions
Quartz monzonite
Aphebian Basement
Amphibolite and metagabbro
Metadiorite or diorite
Quartzofeldspathic gneiss
Granitic gneiss
Paragneiss
Strange Lake Pluton
Ore zone
Altered subsolvus granite
Fresh subsolvus granite
Transsolvus granite
Hypersolvus granite
2 km

Y, Be and Nb. Miller (1988) noted that the deposit contains 52 million tonnes of ore with 2.93% ZrO_2, 0.54% REE, 0.31% Y_2O_3, 0.08% BeO and 0.38% Nb_2O_5. The mafic silicates, arfvedsonitic amphibole and aegirine, as potential hosts of these elements, are the subject of this investigation of the Strange Lake complex. The focus of this paper is on the influence of Na-metasomatism on the primary alkaline mafic silicates. Chapter 6 will deal with the effects of Ca-metasomatism on the arfvedsonitic amphibole.

Background Information

The Proterozoic complex (Pillet et al., 1989; Miller et al., 1997) is surrounded to the south and southwest by rapakivi quartz monzonite, and to the north and northeast by a number of gneisses (quartzofeldspathic, calc-silicate, graphitic, dioritic, gabbroic, and anorthositic; Fig. 1B). The peralkaline granites that constitute the Strange Lake complex have been subdivided by Nassif & Martin (1991), on the basis of the textural development of the alkali feldspar, into hypersolvus, transsolvus and subsolvus facies (Fig. 1b). Rocks of the subsolvus facies were altered in the northern part of the complex (altered subsolvus granite), but remain fresh in a small region in the western portion of the pluton.

The ore minerals are calcium and sodium zirconosilicates (e.g., gittinsite, armstrongite and elpidite), zircon, kainosite [$Ca_2(Y,LREE)_2Si_4O_{12}(CO_3)\bullet H_2O$], gadolinite [$(LREE,Y)_2Fe^{2+}Be_2Si_2O_{10}$], gagarinite [$NaCa(LREE,Y)(F,Cl)_6$], bastnäsite, monazite and pyrochlore (Zajac et al., 1984; Miller, 1988; Birkett et al., 1992). The ore mineral content ranges from 5 vol.% in the hypersolvus granite, to 15 vol.% in the altered subsolvus granite, and up to 20 vol.% in the dominantly pegmatitic and aplitic central portion of the complex, where the ore zone is located (Zajac et al., 1984; Miller, 1986, 1996).

There has been a vigorous debate on the origin of the calcium zirconosilicates and, by implication, the other ore minerals. Miller (1986) and Birkett et al. (1992) proposed, in general, a magmatic origin based largely on textural evidence, however the fluid inclusion study of Salvi & Williams-Jones (1990), when combined with textural evidence (Salvi & Williams-Jones, 1990, 1995), suggests the influence of a low-temperature (<200°C) episode of Ca-metasomatism. Pillet et al. (1993) also used textural evidence to suggest that sodium zirconosilicates were pseudomorphed by their calcium equivalents.

An episode of Na-metasomatism at a somewhat higher temperature (≥350°C; Salvi & Williams-Jones, 1992), in which a NaCl-rich fluid caused the replacement of arfvedsonitic amphibole by aegirine (Salvi & Williams-Jones, 1990, 1997) preceded this Ca-metasomatism. This aegirine replacement is dominant in the central portion of the complex and the altered subsolvus granite, unlike the primary green aegirine which rims the early arfvedsonitic amphibole (Pillet et al., 1993; Nassif, 1993). This study will focus on the mineralogical and geochemical effects of this higher-temperature episode of metasomatism of the primary arfvedsonitic amphibole to evaluate its relationship to the evolution of the deposit.

Review of the Literature on Mafic Silicates at Strange Lake

Arfvedsonitic amphibole, aegirine, astrophyllite, aenigmatite, neptunite and rare bafertisite [$Ba(Fe,Mn)_2TiSi_2O_7(O,OH)_2$] comprise, on average, 5 to 20 vol.% of these very evolved granites. All of these contain essential Fe^{2+}, except aegirine and arfvedsonitic amphibole, which also contain Fe^{3+}. Whereas all these minerals occur in the hypersolvus granite and the fresh subsolvus granite, only the first two are present in altered subsolvus granite (Pillet et al., 1993; Birkett et al., 1996). It seems clear that astrophyllite, aenigmatite, neptunite and bafertisite formed only at the low-fO_2 conditions attained during magmatic crystallization. Subtle differences in the mineral assemblages can be attributed to the late increase in fO_2 in the altered subsolvus granite, proposed by Salvi & Williams-Jones (1990, 1996) and Nassif (1993). The chemical composition and paragenesis of these minerals has been documented by Pillet (1989), Pillet et al. (1993), Birkett et al. (1996) and, in detail, in Chapter 4. In their paragenetic sequence of the titanium and related silicates, Birkett et al. (1996) showed three stages of crystallization of amphibole and pyroxene, where each stage of crystallization of amphibole was followed by one of pyroxene. Unfortunately, they did not describe any of these stages. Furthermore, Pillet (1989) and Pillet et al. (1993) did not report important trace-element data (e.g., in the former study Zn and Li) on elements which are enriched in the deposit. For example, Zr was not analyzed despite its common presence in amphibole from anorogenic complexes (Borley, 1976). Such a lack of information makes

it impossible to estimate the role of the mafic silicates on any secondary minerals formed by their replacement.

Neither Pillet or Birkett (and their coworkers) discussed the effects of Na-metasomatism on the mafic silicates, while only Pillet et al. (1993) mentioned the replacement of amphibole by aegirine, hematite and quartz. O'Halloran (1985), Bonin (1986) and Salvi & Williams-Jones (1990, 1996) noted the replacement of arfvedsonitic amphibole by aegirine, magnetite and quartz in peralkaline granite, although crystallization of aegirine after arfvedsonitic amphibole is perhaps contrary to the sequence intuitively expected, and to the variation expected owing to increasing $a(H_2O)$ throughout the evolution of a typical magma (Nicholls & Carmichael, 1969; Ferguson, 1978; Grapes et al., 1979). In this paper, the replacement of arfvedsonitic amphibole by aegirine during Na-metasomatism is examined.

Comparison of Analytical Methods

Previous studies of the composition of arfvedsonitic amphibole and aegirine of anorogenic oversaturated peralkaline complexes, in general, have relied heavily on results of electron-microprobe analyses (Czamanske & Dillet, 1988; Pillet, 1989; Abdel-Rahman, 1994), examination of solid inclusions (Bogoch et al., 1992), bulk-sample analysis (XRF, AA, INAA; Pillet et al., 1993; Abdel-Rahman, 1994) and point analyses with the ion probe (Hawthorne et al., 1992). Hawthorne et al. (1992) and Czamanske & Dillet (1988) noted that the lack of complete analytical information on arfvedsonitic amphibole (specifically, for Li, but also Zn and Zr) results in amphibole formulae that seem to be unrealistically enriched in ΣSi+Na+K (atoms per formula unit; apfu). In the present study, the trace element and Li content of mafic silicates, especially arfvedsonitic amphibole, were determined through the use of laser-ablation - inductively coupled plasma - mass spectrometry (LAM-ICP-MS). This technique simultaneously provides information on a number of minor and trace elements (Moenke-Blankenburg, 1989). The other advantage of LAM-ICP-MS is that it is a technique that requires a relatively small sample size, as samples are analyzed by point analysis.

Ross (1984) suggested that the enrichment of ΣSi+Na+K could reflect the presence of pyriboles (pyroxene, amphibole and intermediate structures) in arfvedsonitic amphibole. The best way to demonstrate this relationship is through transmission electron microscopy (TEM), which permits examination of fine-scale intergrowths between minerals. Biopyriboles (mica, such as biotite, pyriboles and intermediate structures) have been observed in many TEM investigations that focused on silicates of retrograde or metasomatic origin from calc-alkaline or mafic igneous or metamorphic rocks (Veblen & Buseck, 1979, 1980, 1981; Akai, 1982; Akai & Saito, 1985; Yau et al., 1986; Schumacher & Czank, 1987; Droop, 1994; Grobéty, 1996). Where ordered intergrowths of amphibole and mica occur as the biopyriboles jimthompsonite and chesterite (Veblen & Burnham, 1978a, 1978b; Veblen & Buseck, 1979, 1981), few authors (e.g., Akai et al., 1985) have examined the replacement of pyroxene by amphibole. All these studies were performed primarily on Ca-, Mg- and Fe-rich systems. The only investigations of the Na- and Fe-rich amphiboles have focused on asbestiform riebeckite. Chisholm (1973) and Ahn & Buseck (1991), among others, observed the presence of rare triple-chain biopyribole in this mineral. In this study, the replacement of primary arfvedsonitic amphibole by aegirine is examined to evaluate the importance of NaFe-bearing biopyriboles.

Methodology

Electron-microprobe and LAM-ICP-MS analysis

As the methodology employed for electron-microprobe and LAM-ICP-MS analyses is described in detail in Chapter 4, only a brief review will be presented here. For electron-microprobe analysis, Cameca Camebax and JEOL 840 electron microprobes were operated in wavelength-dispersion spectrometry mode (WDS) at an accelerating voltage of 15 or 20 kV and a beam current of 20 or 30 nA with a slightly defocused beam (5 to 7 μm). The counting times used were 25 s for major-elements, 50 s for most minor elements, and 100 s for the rest (including F and Cl). The standards employed are fully noted in Chapter 4. Chemical formulae were calculated on the basis of 23 atoms of oxygen (6 in the case of pyroxene) and 2 OH^-, with Fe^{3+}/Fe^{2+} calculated from charge balance (16 cations or 4 cations and assumption of full cation occupancy) after the method of Droop (1987).

Point analyses were performed on mounts of oriented grains of amphibole or amphibole and aegirine by LAM-ICP-MS at the Université de Montréal using a Fisons-VG PQ2+ ICP mass spectrometer and Fisons-VG LaserProbe equipped with a Spectron SL2B2 300 mJ Nd:YAG laser, operated in Q-switched mode, at 1064 nm with a 5 ns half-pulse duration. The analyses were performed in two stages: first they were analyzed for elements with low atomic number (Z: ^{6}Li, ^{9}Be and ^{11}B), followed by those elements of higher Z (^{51}V, ^{52}Cr, ^{66}Zn, ^{85}Rb, ^{88}Sr, ^{89}Y, ^{90}Zr, ^{93}Nb, ^{138}Ba, ^{139}La, ^{140}Ce, ^{141}Pr, ^{146}Nd, ^{147}Sm, ^{151}Eu, ^{157}Gd, ^{159}Tb, ^{162}Dy, ^{165}Ho, ^{166}Er, ^{169}Tm, ^{174}Yb, ^{175}Lu, ^{178}Hf, ^{232}Th and ^{238}U). For a detailed description of the methodology employed and the resultant errors refer to Chapter 4, and Appendices B-5, B-6 and B-7.

TEM

Selected regions of samples were prepared for TEM examination by ion-thinning samples on 2.3 mm Cu grids after mild heating (<100 °C) and removal from thin sections (the grids were glued with either Crystalbond® or bee's wax instead of epoxy). Ion-thinning was performed with a Gatan dual ion mill (model 600), with Ar guns operated at 6 keV, 1 mA or 0.5 mA and tilted initially at 17°, followed by 12°. The sample was coated with carbon to prevent charging.

TEM work was conducted by high-resolution TEM (HRTEM), with selected-area electron diffraction (SAED) and analytical electron microscopy (AEM). A Philips EM420ST TEM was operated at an accelerating voltage of 120 keV. AEM analyses were performed with a Li-drifted silicon detector. The computer program DTSA [Desk-Top Spectrum Analyzer; Fiori et al. (1994)] was used to calculate concentrations of elements. The estimated error in these analyses is approximately 4%. The main drawback of AEM analyses on arfvedsonitic amphibole is the overlap between $F_{K\alpha}$ and $Fe_{L\alpha}$ peaks, which precludes determination of F. Mineral formulae of amphibole were calculated based on 23 atoms of oxygen, excluding F, as suggested by Peacor (1992). The proportion of Fe^{3+} thus is uncalculated and the mineral formula may contain a slight excess of cations. Formulae of the other minerals were calculated on the basis of 6 atoms of oxygen for pyroxene and 31 atoms of oxygen for astrophyllite (after Woodrow, 1967). The mineral formulae for hematite were calculated based on 3 atoms of oxygen.

Finally, "composite" mineral formulae were calculated from results of electron-microprobe, LAM-ICP-MS and AEM analyses. Although most of the combined formulae were derived from the electron microprobe analyses, those derived from LAM-ICP-MS analyses were used for much of the trace and minor elements contents.

Results

Summary of Findings Concerning the Primary Assemblages

Three types of arfvedsonitic amphibole were documented in Chapter 4: 1) early, Na- and Fe-rich arfvedsonitic amphibole from hypersolvus granite (Type-1a) that contains numerous inclusions of monazite, zircon, gagarinite, yttriofluorite and zajacite ($Na_{0.90}REE_{1.12}Ca_{0.92}F_6$; Jambor et al., in press) rimmed by inclusion-absent amphibole that is slightly enriched in Ca, Mg, Mn and Zn (Type-1b), 2) amphibole from grains composed of amphibole and Type-2 aegirine from subsolvus granite, and 3) fine-grained, prismatic, euhedral and strongly oriented amphibole from late mafic pods or mat-like regions in or near the ore zone or in the altered subsolvus granite near its contact with the hypersolvus granite. The arfvedsonitic amphibole suite varies from Na- and Fe-rich in Type-1 to K-, Zn-, Mn-rich in Type-3 potassian lithian fluor-arfvedsonite. Furthermore, Zr decreases and ΣREE increases in the sequence from Type-1 to -3, although Type-1 amphibole contains more HREE than the others. The trends represented by Type-1, -2 and much of Type-3 reflect magma evolution (ref. Chapter 4).

The three types of aegirine (80-100% Ae) associated with the arfvedsonitic amphibole, as described in Chapter 4, are: 1) Type-1, bright green, primary Ti-rich (to 4.91 wt.% TiO_2), topotactic rims on amphibole from hypersolvus and fresh subsolvus granites, 2) Type-2, topotactic yellow to colourless slightly Ti-, Mn- and Ca-enriched aegirine that replaces Type-1 and -2 amphibole in all units, except the transsolvus granite, and 3) Type-3 yellow green, euhedral, primary or secondary almost pure aegirine from pegmatitic samples in and near the ore zone or in extremely altered subsolvus granite from the erosional surface, which is slightly Ca- and Mn-enriched and contains traces of Ti.

Textural Relationships of Mafic Silicates Associated with Na-Metasomatism

Composite grains of arfvedsonitic amphibole and aegirine from the hypersolvus granite oriented perpendicular to the *c* axis of both mafic silicates show that primary arfvedsonitic amphibole (Types 1a and b) is rimmed in a topotactic relationship by primary Type-1 aegirine (approx. 10 vol.%). Pale yellow, secondary Type-2 aegirine (approx. 17 vol.%) is located between them (Fig. 2). Relics of arfvedsonitic amphibole occur in Type-2 aegirine near the interface with the amphibole. The relict grain boundary of the formerly euhedral grain of primary (Type-1) amphibole is accentuated by a change from Type-1 to -2 aegirine. Type-2 aegirine has a "moth-eaten" appearance produced by numerous, fine-grained dark brown to black fibers of astrophyllite (0.5-5 vol.%) aligned perpendicular to the amphibole grain boundary. This secondary astrophyllite coarsens (to 0.2 mm) near the boundary with the primary amphibole (Fig. 2B). It is of the same habit as that observed in specific zones of feldspar grains, and at the contact between amphibole and feldspar, aenigmatite, astrophyllite, neptunite or ilmenite (Chapter 4). This aegirine-for-amphibole replacement relationship occurs in the outermost part of the hypersolvus granite near the altered subsolvus granite (ref. Fig. 2A in Chapter 4).

The same relationship between primary arfvedsonitic amphibole and aegirine was observed in an altered pegmatite near the ore zone and in the hypersolvus granite near its contact with the altered subsolvus granite (sample 46-I-3; Fig. 3). Although Type-1 aegirine is present, it is a minor (<5 vol.%) phase compared with Type-2 aegirine (30 to 40 vol.%). Numerous small, angular relics of amphibole occur in Type-2 aegirine, especially near the edge of the main amphibole, which indicates replacement of amphibole by aegirine (Fig. 3).

In the altered subsolvus granite, the arfvedsonitic amphibole - aegirine relationship shows similarities to that from the hypersolvus granite, although only yellow, Type-2 aegirine occurs. The other difference between this aegirine assemblage and that from the hypersolvus granite is the presence of fine-grained (0.5 μm) inclusions of hematite, and rare quartz and fluorite along with aegirine in zones of composite grains that alternate with amphibole (Fig. 4). The proportion of hematite in this replacement assemblage varies throughout the altered subsolvus granite, as more hematite is present in the replacement assemblage near the margin of the complex (ref. Fig. 2A in Chapter 4). The relationship

Figure 2. Transmitted-light photomicrographs showing the relationship between aegirine and arfvedsonitic amphibole (oriented perpendicular to the *c* axis of the silicates) from the hypersolvus granite.

A. Arfvedsonitic amphibole (arf) at the core is rimmed by Type-1 aegirine (aeg) and replaced by Type-2 aegirine (the lighter pyroxene between the amphibole and aegirine denoted by aeg) in a topotactic relationship. These mafic silicates are surrounded by alkali feldspar (feld). The former grain margin of the amphibole is accentuated by the contact between the two types of aegirine on the left side of the image (width of image is 4 mm).

B. Higher-magnification image of Type-1 and -2 aegirine (aeg) from A showing the former grain boundary between arfvedsonitic amphibole (arf) and Type-1 aegirine. Type-2 aegirine (aeg) has a "moth-eaten" appearance (Fig. 2A) due to the presence of small dark inclusions of brown astrophyllite (to 0.2 mm at the tips of the arrows), which are particularly evident near the contact with aegirine (width of image is 2 mm).

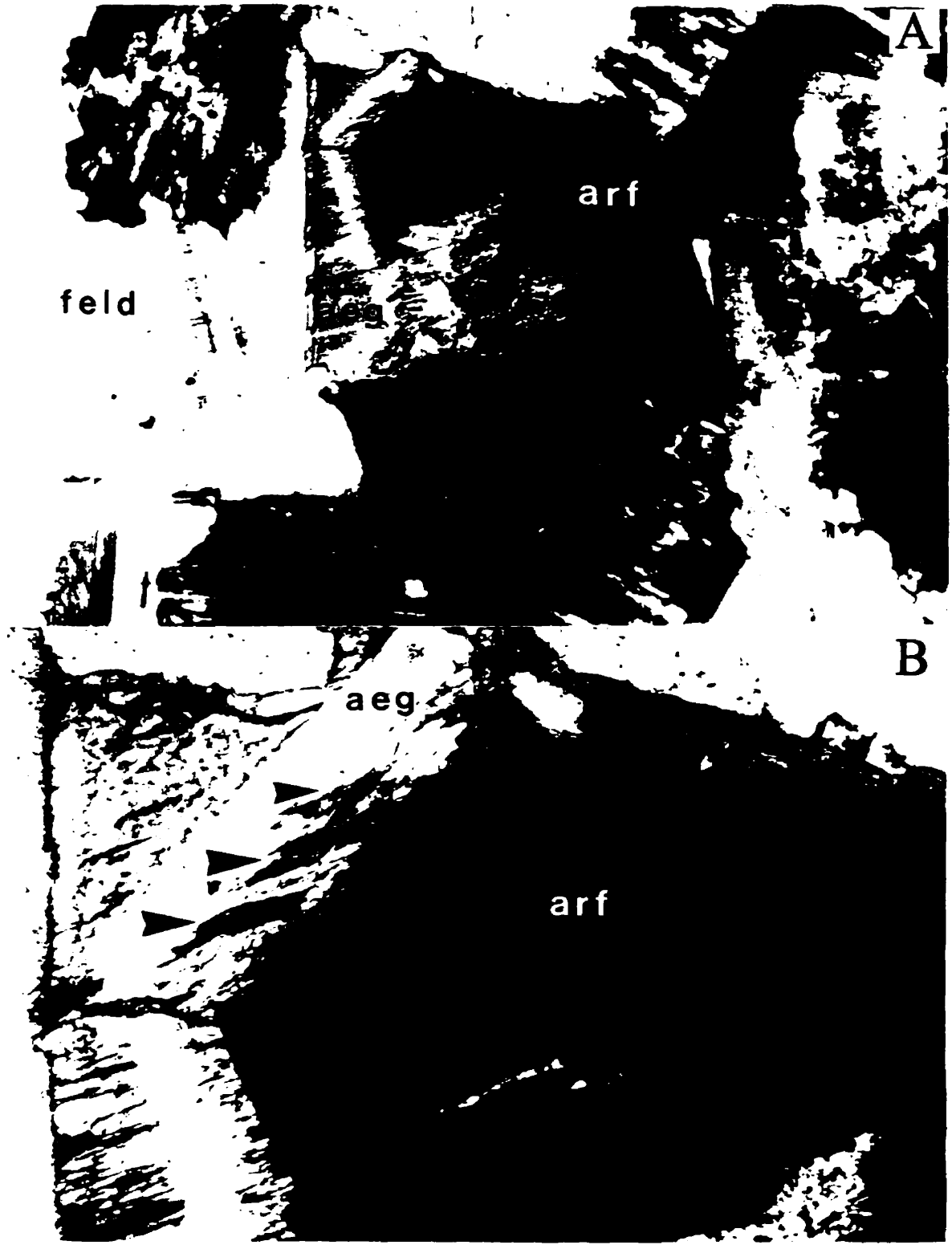
A
arf
feld
aeg
B
aeg
arf

Figure 3. Photomicrograph (transmitted light) showing the arfvedsonitic amphibole (arf) - aegirine (aeg) relationship in a pegmatite in hypersolvus granite near the contact with altered subsolvus granite and the ore zone (46-I-3). Small, angular relics of primary amphibole (dark) in the aegirine (light) are suggestive of replacement. Note the lack of iron oxide inclusions and of Type-1 aegirine (width of image is 4 mm).

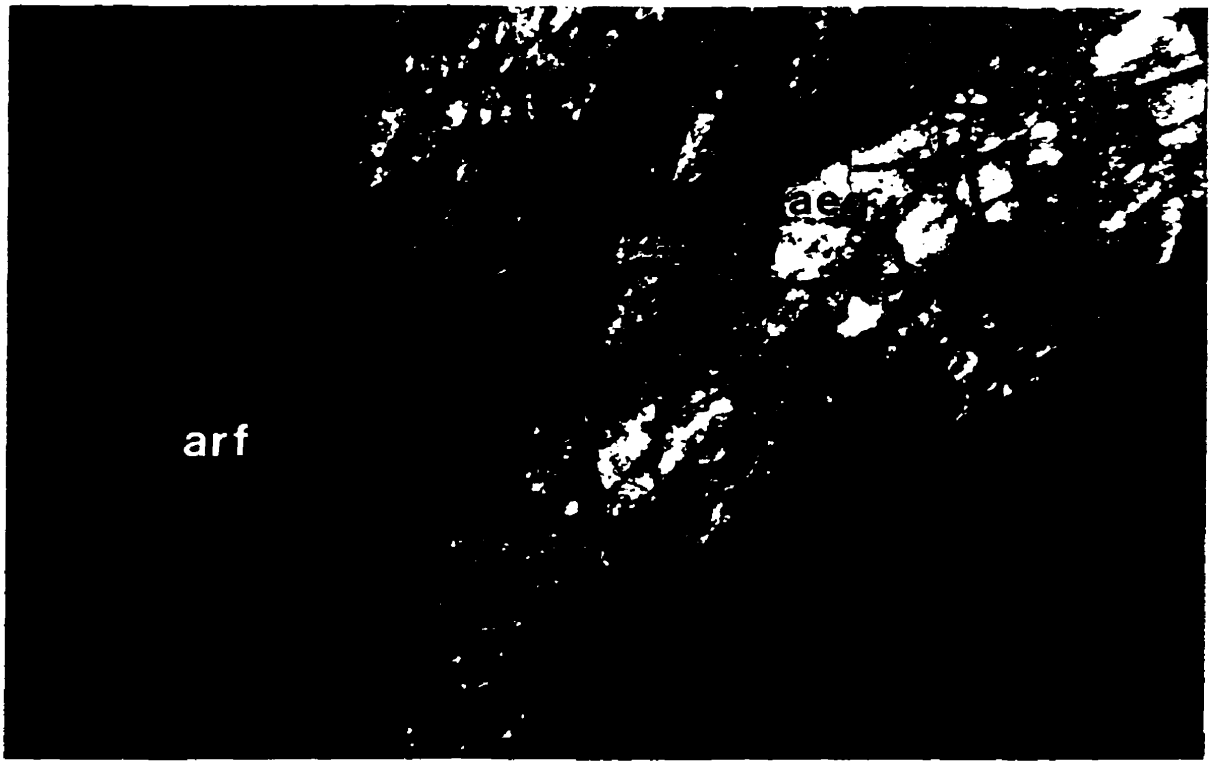
ae
arf

Figure 4. Photomicrograph (transmitted light) depicting the relationship between arfvedsonitic amphibole (arf) and the aegirine (aeg) assemblage in the altered subsolvus granite as depicted in transmitted light. The mineralogical sequence is Type-2 aegirine + hematite ± quartz and rare fluorite surrounding amphibole, which is subsequently repeated in the outer margin (the grain on the left). This Type-2 aegirine contains significantly more hematite than that in Figures 2 and 3. The proportion of quartz and hematite observed in the replacement assemblage varies in different portions of the complex, but quartz is generally minor (width of image is 7 mm).

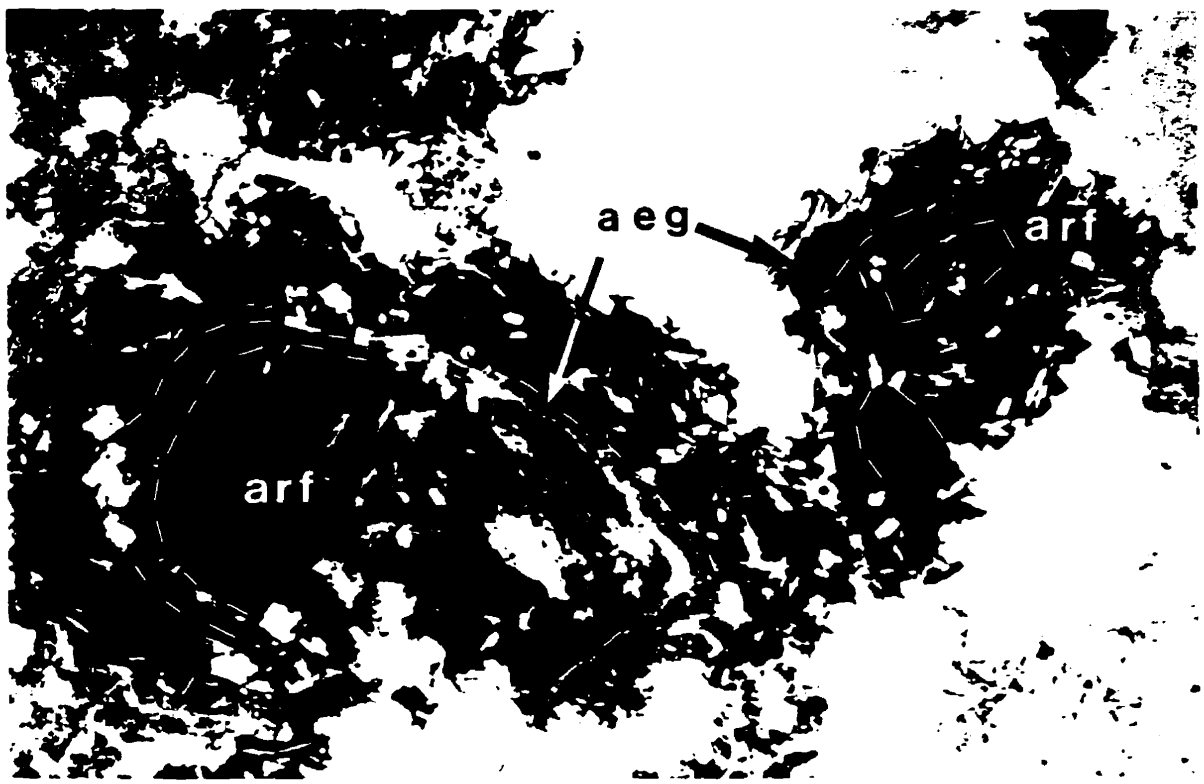
aeg
arf
arf

between zonation of amphibole and aegirine in the altered subsolvus granite, the compositional zoning of the primary amphibole from the hypersolvus granite, and the presence of angular inclusions of amphibole in aegirine, all indicate replacement of amphibole by aegirine. This aegirine replacement assemblage of amphibole is more common than that in which astrophyllite is present. The hematite content of the assemblage is highly variable, as, in some samples, it is nonexistent (as in sample 46-I-3; Chapter 4).

In the ore zone and highly metasomatized samples of the altered subsolvus granite, arfvedsonitic amphibole and both Type-2 and -3 aegirine are present, except that the latter dominates in pegmatites at the surface (Fig. 5A). When cut perpendicular to the *c* axis, Type-3 aegirine displays the typical cross-section of pyroxene and lacks amphibole inclusions. This indicates a primary magmatic origin or, possibly, deposition as a hydrothermal phase in an open space. Prismatic euhedral Type-3 amphibole with pyrochlore inclusions forms mats of aligned grains (2 mm) in rare mafic amphibole-rich pods with minor Type-3 aegirine (Fig. 5B; Chapter 4). These pods occur in the ore zone and near the contact between hypersolvus and altered subsolvus granites.

The relationship between aegirine and amphibole changes with depth and type of subsolvus granite present (Fig. 6). Type-3 aegirine is present, without Type-2 arfvedsonitic amphibole, in pegmatites located near the erosional surface (Figs. 6A & B). However, at depth, Type-2 arfvedsonitic amphibole and, to a lesser extent, Type-2 aegirine are present (Fig. 6C). This difference in type of mafic silicate is related to the texture of the subsolvus granite present [as defined by Salvi & Williams-Jones (1995)]. Primary amphibole, occurring as interstitial grains, appears to be more readily altered to aegirine. The arfvedsonitic amphibole, in the center of this region, may be altered to a brown amphibole or pale green chlorite (refer to Chapter 6; Figs. 6A & B). It is interesting to note that in diamond drill hole SL-182 (Fig. 6C), the region of the hole where brown amphibole occurs is at the center of that where Type-2 aegirine also occurs. However, they are mutually exclusive as both replacements of arfvedsonitic amphibole are never present in the same sample. These mafic silicates appear to be loosely related to the type of zirconosilicate present, as the alteration of arfvedsonitic amphibole to brown amphibole and Type-2 aegirine occurs at the bottom of the portion of the hole that contains elpidite, armstrongite

Figure 5. Photomicrograph of Type-3 aegirine (in transmitted light) surrounded by aligned prismatic grains of late arfvedsonitic amphibole (arf) from the mafic pod near the contact of the hypersolvus and altered subsolvus granites, and the ore zone. The light region in the top left and bottom right corners are K-feldspar, which contains inclusions of amphibole, while coarser prismatic aegirine also is present (aeg; width of image is 6 mm).

arf
aeg

Figure 6. Distinctions between the mafic silicates on logs of selected drill holes. The granite units applied here are as defined by Salvi & Williams-Jones (1995) based primarily on the type of zirconosilicate present in the subsolvus granite. Thin wavy lines represent the transitional contacts between the different types of granite. The textures denoted in the legend are those of amphibole.

A. Drill core LB-30. Arfvedsonitic amphibole is absent in the pegmatite body at the surface, as only Type-3 aegirine is present. The habit of the amphibole changes from phenocrysts immediately adjacent to this pegmatite to phenocrysts and interstitial, and finally to interstitial. In this hole, only a trace of Type-2 aegirine occurs. Both brown amphibole and chlorite alteration of arfvedsonitic amphibole occur at approximately 17.5 m. However, these alterations are not present in the same sample, and chlorite is rare compared to the brown amphibole (Chapter 6).

B. Drill core LB-60. The pegmatite body at the surface contains Type-3 aegirine, while, at depth, the mafic silicates are Type-2 aegirine and interstitial arfvedsonitic amphibole.

C. Drill core SL-182. Here one can compare the habit of amphibole with the type of zirconosilicate, as determined by Salvi & Williams-Jones (1995), present. The thick wavy lines in the image represent changes in the type of zirconosilicate present, where the upper portion of the log contains gittinsite and quartz, the middle portion contains elpidite, armstrongite and gittinsite and the lowest portion contains elpidite. Changes in the habit of amphibole are coincident with a change in texture of the granite. Where amphibole occurs as phenocrysts or a combination of phenocrysts and interstitial grains in the porphyritic granite (anhedral elpidite) in the upper portion of the hole, it occurs as interstitial grains in the equigranular granite (euhedral elpidite) in the central portion of the hole. More aegirine replaces arfvedsonitic amphibole in the equigranular granite then in the rest of this drill core. Arfvedsonitic amphibole, at the core of this region, shows evidence of replacement by brown amphibole, both in inclusions and the equigranular granite.

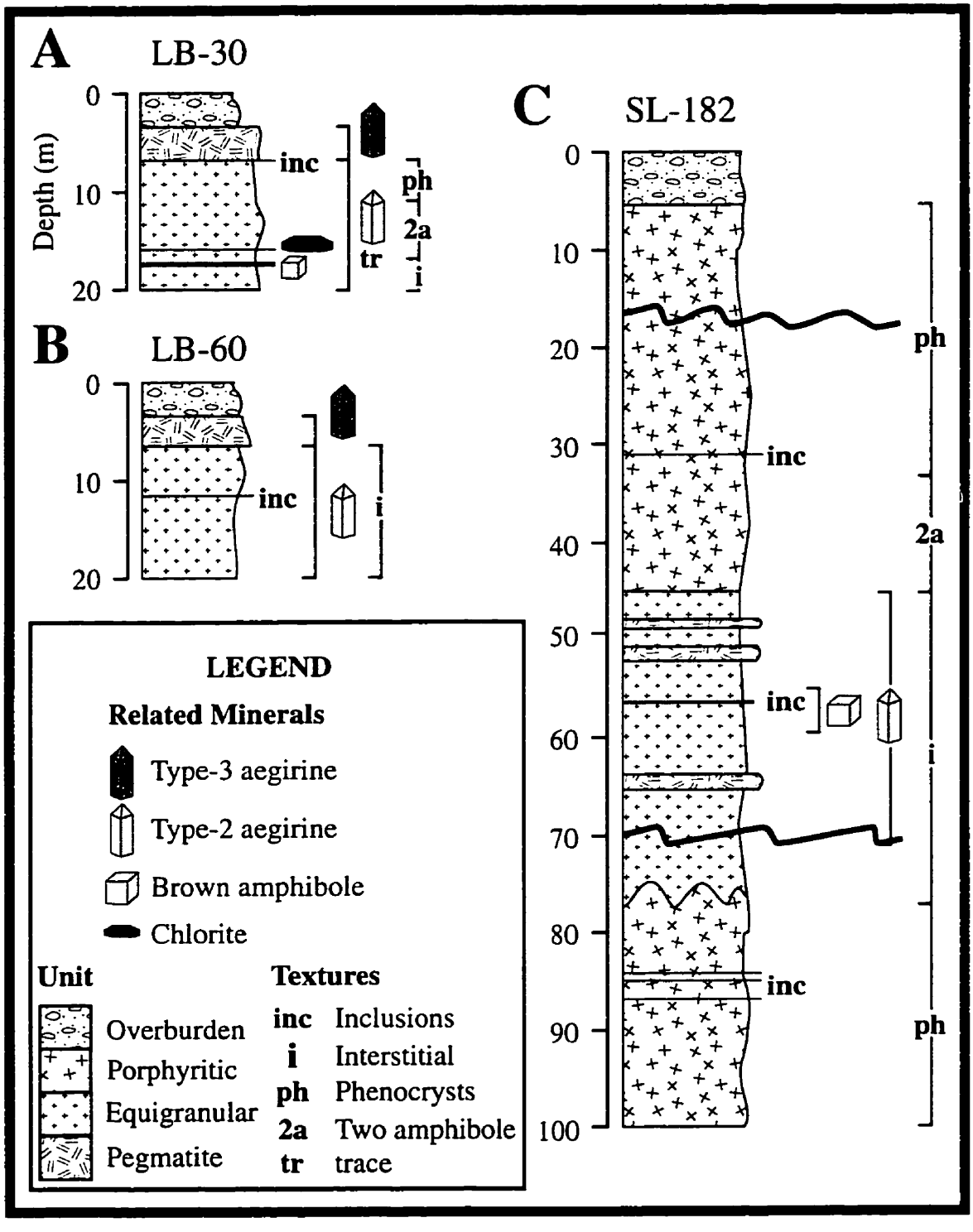
A
LB-30
Depth (m)
0
10
20
inc
ph
2a
tr
i
B
LB-60
0
10
20
inc
i
C
SL-182
0
10
20
30
40
50
60
70
80
90
100
ph
inc
2a
inc
i
inc
ph
LEGEND
Related Minerals
Type-3 aegirine
Type-2 aegirine
Brown amphibole
Chlorite
Unit
Overburden
Porphyritic
Equigranular
Pegmatite
Textures
inc Inclusions
i Interstitial
ph Phenocrysts
2a Two amphibole
tr trace

and gittinsite. These alterations of arfvedsonitic amphibole do not extend into the zone of elpidite.

The paragenetic sequence of the mafic silicates, from magmatic (Chapter 4) to Na-metasomatic conditions, is depicted in Figure 7. Magmatic crystallization of the minerals may well have occurred down to 450°C (Chapter 4; Nassif, 1993). During late stage crystallization (after Chapter 4), arfvedsonitic amphibole, Type-3 aegirine, neptunite and narsarsukite crystallized. This was likely preceded by the formation of Type-1 aegirine rims on arfvedsonitic amphibole and intergrowths between amphibole and albite. One of the early effects of Na-metasomatism on specific samples of amphibole in the hypersolvus granite was the mobilization of REE from inclusions and their later deposition along cleavages (noted in Chapter 4). No similar relationship was observed in amphibole from the subsolvus granite. As the temperature decreased between 450 and 350°C during Na-metasomatism, Type-2 aegirine replaced arfvedsonitic amphibole. This low temperature limit is set based on the fluid inclusion data of Salvi & Williams-Jones (1992). This was accompanied, depending on the type of the granite, by crystallization of either hematite ± quartz and fluorite, or astrophyllite and a F-rich mineral.

Compositional Variation of Mafic Silicates Related to Na-Metasomatism

Selected electron-microprobe and LAM-ICP-MS analyses of arfvedsonitic amphibole, aegirine and astrophyllite are presented in Table 1 (Appendices B-1, B-2, B-3 and B-5) and a detailed description of their compositional variation can be found in Chapter 4 and above. It is important, however, to note that the width of the laser beam used for the LAM-ICP-MS analyses was 70-80 µm. Consequently, the large volume of sample used for these analyses compared to that from the electron microprobe implies that minute inclusions of other minerals (e.g., astrophyllite, hematite and fluorides) also were analyzed along with the amphibole and pyroxene. The influence of the REE-rich fluorides can be readily identified in the analysis, however that of astrophyllite cannot. In addition, the small size of these inclusions precluded their analysis by LAM-ICP-MS.

Type-2 aegirine has been further differentiated, in this chapter, based on the unit of the granite (hypersolvus, altered pegmatite or altered subsolvus granite) in which it occurs

Figure 7. Diagram showing the paragenetic sequence of crystallization of the mafic silicates (and related minerals) resulting from magmatic crystallization and Na-metasomatism. The solid black lines represent minerals or assemblages whose origin is known, while the shaded lines are those whose origin is not strictly defined.

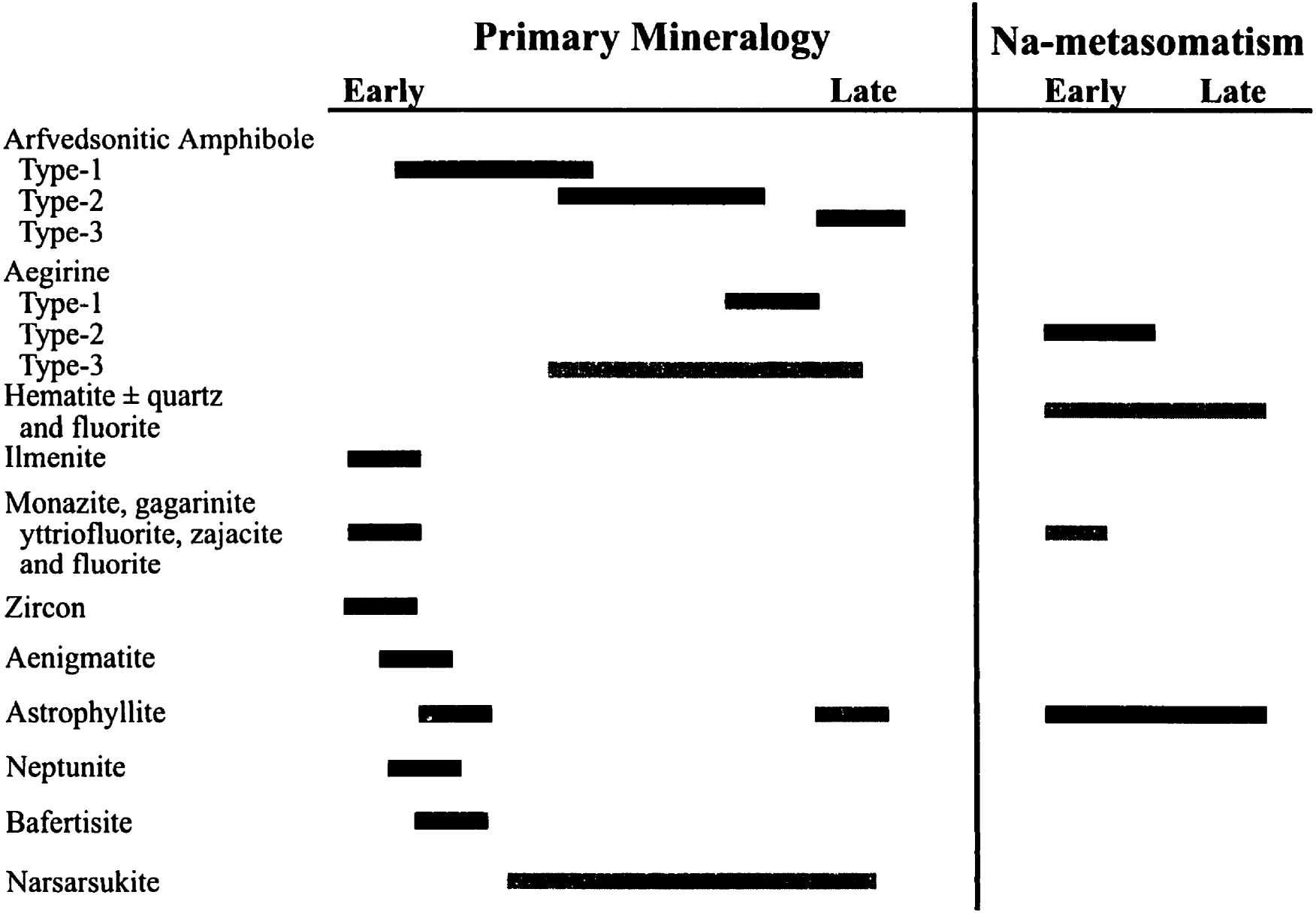
Primary Mineralogy
Early
Late
Na-metasomatism
Early
Late
Arfvedsonitic Amphibole
Type-1
Type-2
Type-3
Aegirine
Type-1
Type-2
Type-3
Hematite ± quartz
and fluorite
Ilmenite
Monazite, gagarinite
yttriofluorite, zajacite
and fluorite
Zircon
Aenigmatite
Astrophyllite
Neptunite
Bafertisite
Narsarsukite

Table 1A. Selected electron-microprobe analyses of mafic silicates.

Mineral	**Arfvedsonitic amphibole**			**Astrophyllite**	
Type	**Type-1b**	**Type-2**	**Type-3**		
Unit	**Hypersolvus**	**Altered Subsolvus**	**Mafic Pod**	**Hypersolvus**	
Sample #	**49-C-2**	**25-C-1**	**SL-BS-1**	**49-A-1**	**49-C-1**
Na_2O	9.07	8.91	9.34	2.32	3.70
K_2O	1.09	1.45	2.35	1.61	2.44
CaO	0.61	0.25	0.04	0.21	1.57
Fe_2O_3	5.18	5.86	7.32	n.d.	n.d.
FeO	29.36	27.75	24.39	30.21	34.45
MgO	0.22	0.69	0.00	0.04	0.02
MnO	0.67	0.67	1.90	2.89	1.40
ZnO	0.18	0.36	0.86	0.99	0.16
Nb_2O_5	0.00	0.02	0.03	0.64	0.02
V_2O_3	0.02	0.00	0.00	n.d.	n.d.
Cr_2O_3	0.01	0.00	0.00	n.d.	n.d.
Yb_2O_3	0.01	0.00	0.00	n.d.	n.d.
ZrO_2	0.12	0.10	0.13	1.59	0.00
Y_2O_3	0.00	0.00	0.00	0.00	n.d.
SnO_2	n.d.	n.d.	n.d.	0.00	n.d.
PbO	n.d.	n.d.	n.d.	1.30	n.d.
BaO	n.d.	n.d.	n.d.	0.52	n.d.
SrO	n.d.	n.d.	n.d.	0.00	n.d.
TiO_2	1.03	0.73	0.44	9.09	11.47
Al_2O_3	0.54	0.29	0.16	0.64	0.08
SiO_2	50.69	50.43	51.79	36.77	36.19
F	1.98	2.65	1.92	1.14	2.80
Cl	0.02	0.00	0.00	0.05	0.02
H_2O	0.95	0.62	0.99	n.d.	n.d.
Total	101.74	100.77	101.69	89.50	94.31
-O=F	0.84	1.12	0.81	0.48	1.18
-O=Cl	0.00	0.00	0.00	0.01	0.00
Total	100.90	99.65	100.88	89.01	93.13

Table 1A. Selected electron-microprobe analyses of mafic silicates (continued).

Mineral	Arfvedsonitic amphibole			Astrophyllite	
Type	Type-1b	Type-2	Type-3		
Unit	Hypersolvus	Altered Subsolvus	Mafic Pod	Hypersolvus	
Sample #	49-C-2	25-C-1	SL-BS-1	49-A-1	49-C-1
Na	2.778	2.756	2.849	1.113	1.685
K	0.219	0.295	0.472	0.507	0.733
Ca	0.103	0.043	0.007	0.056	0.396
Fe^{3+}	0.616	0.704	0.867	n.d.	n.d.
Fe^{2+}	3.879	3.705	3.209	6.250	6.771
Mg	0.053	0.164	0.001	0.015	0.008
Mn	0.089	0.091	0.253	0.606	0.278
Zn	0.020	0.042	0.100	0.181	0.027
Nb	0.000	0.001	0.001	0.072	0.002
V	0.002	0.000	0.000	0.000	0.000
Cr	0.001	0.000	0.000	n.d.	n.d.
Yb	0.001	0.000	0.000	n.d.	n.d.
Zr	0.009	0.008	0.010	0.192	0.000
Y	0.000	0.000	0.000	0.000	0.000
Sn	n.d.	n.d.	n.d.	0.000	0.000
Pb	n.d.	n.d.	n.d.	0.086	0.000
Ba	n.d.	n.d.	n.d.	0.051	0.000
Sr	n.d.	n.d.	n.d.	0.000	0.000
Ti	0.122	0.088	0.053	1.690	2.028
^{VI}Al	0.100	0.054	0.029	0.185	0.022
Si	8.008	8.050	8.148	9.095	8.504
^{IV}Al	0.000	0.000	0.000	n.d.	n.d.
F	0.991	1.338	0.955	0.895	2.080
Cl	0.005	0.000	0.001	0.019	0.007
OH	1.004	0.662	1.044	n.d.	n.d.
ΣCations	16.000	16.000	16.000	20.099	20.454

Mineral formulae calculated based on 23 oxygen and 16 cations for arfvedsonitic amphibole and 31 oxygen for astrophyllite.
The Fe^{3+}/Fe^{2+} ratio was calculated for the amphibole according to the method of Droop (1987).
n.d.: Not determined.

Table 1A. Selected electron-microprobe analyses of mafic silicates (continued).

Mineral			**Aegirine**		
Type	**Type-1**	**Type-2**			**Type-3**
Unit	**Hypersolvus**		**Altered Pegmatite**	**Altered Subsolvus**	**Ore**
Sample #	**49-C-2**	**49-C-2**	**46-I-3**	**SL-8-1**	**SL-1-20**
Na_2O	13.58	13.26	13.32	13.67	13.68
K_2O	0.00	0.01	0.00	0.00	0.01
CaO	0.02	0.09	0.31	0.10	0.18
Fe_2O_3	28.20	28.67	29.47	32.10	31.55
FeO	3.27	4.34	3.39	1.70	1.21
MgO	0.01	0.01	0.04	0.02	0.00
MnO	0.19	0.08	n.d.	0.07	0.54
ZnO	0.00	0.00	0.21	0.00	0.20
Nb_2O_5	0.00	0.00	n.d.	0.00	0.08
V_2O_3	0.03	0.02	0.00	0.01	0.00
Cr_2O_3	n.d.	n.d.	0.01	n.d.	n.d.
Yb_2O_3	n.d.	n.d.	n.d.	n.d.	n.d.
ZrO_2	0.12	0.12	0.56	0.04	0.40
Y_2O_3	n.d.	n.d.	n.d.	n.d.	n.d.
TiO_2	2.44	0.81	0.86	0.29	0.71
Al_2O_3	0.48	0.31	0.23	0.37	0.27
SiO_2	52.06	52.86	52.27	52.17	51.94
Total	100.40	100.57	100.66	100.53	100.77

Table 1A. Selected electron-microprobe analyses of mafic silicates (continued).

Mineral			**Aegirine**		
Type	**Type-1**	**Type-2**			**Type-3**
Unit	**Hypersolvus**		**Altered Pegmatite**	**Altered Subsolvus**	**Ore**
Sample #	**49-C-2**	**49-C-2**	**46-I-3**	**SL-8-1**	**SL-1-20**
Na	1.003	0.979	0.985	1.008	1.009
K	0.000	0.001	0.000	0.000	0.000
Ca	0.001	0.004	0.013	0.004	0.007
Fe^{3+}	0.808	0.822	0.846	0.919	0.904
Fe^{2+}	0.104	0.138	0.108	0.054	0.038
Mg	0.000	0.000	0.002	0.001	0.000
Mn	0.006	0.003	0.000	0.002	0.018
Zn	0.000	0.000	0.006	0.000	0.006
Nb	0.000	0.000	0.000	0.000	0.001
V	0.001	0.000	0.000	0.000	0.000
Cr	0.000	0.000	0.000	0.000	0.000
Yb	0.000	0.000	0.000	0.000	0.000
Zr	0.002	0.002	0.010	0.001	0.007
Ti	0.070	0.023	0.025	0.008	0.020
Si	1.983	2.014	1.994	1.985	1.977
Al	0.022	0.014	0.010	0.017	0.012

Mineral formulae calculated based on 6 atoms of oxygen and 4 cations
The method of Droop (1987) was used to calculate Fe^{3+}/Fe^{2+}.
n.d.: Not determined.

Table 1B. Selected LAM-ICP-MS analyses of mafic silicates.

Mineral	**Arvedonitic amphibole**				
Type	**Type-1**	**Type-2**	**Type-2**	**Type-3**	**Type-1 or 2**
Unit	**Hypersolvus**	**Altered Pegmatite**	**Altered Subsolvus**	**Mafic Pod**	**Hypersolvus**
Sample#	**49-C-2**	**46-I-3**	**63-B-1**	**SL-BS-1**	**48-A-7**
Na_2O	9.15	8.94	9.38	9.19	13.89
K_2O	1.07	2.20	1.55	2.34	0.00
CaO	0.55	0.20	0.29	0.06	0.04
Fe_2O_3	34.33	31.82	32.86	30.84	33.87
MgO	0.18	0.00	0.09	0.03	0.00
MnO	0.67	1.45	0.87	1.83	0.09
ZnO	0.19	0.50	0.35	0.96	0.00
Cr_2O_3	0.00	0.00	0.00	0.00	0.01
V_2O_3	0.02	0.01	0.00	0.02	0.01
Nb_2O_5	0.00	0.02	0.00	0.04	0.00
ZrO_2	0.14	0.56	0.15	0.09	0.13
Y_2O_3	0.00	0.00	0.00	0.00	0.00
Yb_2O_3	0.02	0.01	0.01	0.00	0.02
TiO_2	1.04	0.94	1.92	0.52	1.07
Al_2O_3	0.51	0.15	0.30	0.16	0.27
SiO_2	50.15	50.87	50.55	51.55	52.51
F	1.99	1.74	1.96	1.66	n.d.
Cl	0.01	0.00	0.00	0.01	n.d.
Total	99.17	98.67	99.46	98.58	101.90

Table 1B. Selected LAM-ICP-MS analyses of mafic silicates (continued).*

Mineral	Arvedonitic amphibole				
Type	**Type-1**	**Type-2**	**Type-2**	**Type-3**	**Type-1 or 2**
Unit	**Hypersolvus**	**Altered Pegmatite**	**Altered Subsolvus**	**Mafic Pod**	**Hypersolvus**
Sample#	**49-C-2**	**46-I-3**	**63-B-1**	**SL-BS-1**	**48-A-7**
Li	1371	1955	1086	n.d.	1385
Be	10	18	26	n.d.	12
B	2	8	4	n.d.	4
V	2	0	0	2	2
Cr	0	1	1	15	3
Zn	2847	7209	4858	8028	2815
Rb	25	56	28	90	16
Sr	2	2	3	5	25
Y	41	89	58	82	2225
Zr	1062	5770	1299	458	913
Nb	63	350	152	531	136
Ba	1	2	5	10	14
La	15	2	5	17	452
Ce	45	8	17	36	804
Pr	7	1	3	5	105
Nd	30	6	10	15	481
Sm	6	2	3	7	133
Eu	0	0	0	1	8
Gd	5	2	2	8	153
Tb	1	1	1	3	30
Dy	7	8	8	22	214
Ho	2	5	4	5	46
Er	12	41	32	16	147
Tm	4	15	12	3	22
Yb	44	172	148	21	160
Lu	11	35	35	2	24
Hf	47	220	45	17	39
Th	1	0	0	36	52
U	0	0	0	128	3
ΣREE	188	298	278	161	2778

* Concentrations in ppm.
n.d.: Not determined.

Table 1B. Selected LAM-ICP-MS analyses of mafic silicates (continued).

Mineral		**Aegirine**	
Type	**Type-1 or 2**	**Type-1**	**Type-2**
Unit	**Hypersolvus**	**Fresh Subsolvus**	**Fresh Subsolvus**
Sample#	**57-A-1**	**38-B-3**	**38-B-3**
Na_2O	13.76	13.64	13.86
K_2O	0.00	0.00	0.00
CaO	0.02	0.16	0.10
FeO	32.66	31.23	33.35
MgO	0.01	0.01	0.02
MnO	0.17	0.21	0.09
ZnO	0.00	0.00	0.00
Cr_2O_3	0.00	0.00	0.00
V_2O_3	0.01	0.02	0.00
Nb_2O_5	0.00	0.00	0.00
ZrO_2	0.10	0.30	0.13
Y_2O_3	0.00	0.00	0.00
Yb_2O_3	0.00	0.00	0.00
TiO_2	2.01	3.09	1.15
Al_2O_3	0.36	0.44	0.40
SiO_2	52.87	51.83	52.05
Total	101.96	100.91	101.16

Table 1B. Selected LAM-ICP-MS analyses of mafic silicates (continued).*

Mineral		**Aegirine**	
Type	**Type-1 or 2**	**Type-1**	**Type-2**
Unit	**Hypersolvus**	**Fresh Subsolvus**	**Fresh Subsolvus**
Sample#	**57-A-1**	**38-B-3**	**38-B-3**
Li	614	n.d.	n.d.
Be	12	n.d.	n.d.
B	5	n.d.	n.d.
V	1	0	0
Cr	1	0	0
Zn	1936	667	246
Rb	17	2	308
Sr	6	19	4
Y	120	157	44
Zr	1390	1103	813
Nb	107	213	84
Ba	9	3	9
La	159	10	5
Ce	257	21	11
Pr	27	5	2
Nd	103	25	10
Sm	18	13	4
Eu	1	1	0
Gd	16	17	5
Tb	2	3	1
Dy	16	23	6
Ho	4	5	1
Er	18	17	5
Tm	5	3	1
Yb	60	42	22
Lu	14	12	6
Hf	53	53	34
Th	34	61	17
U	2	16	4
ΣREE	701	196	80

* Concentrations in ppm.
n.d.: Not determined.

(Fig. 8). The composition of Type-2 aegirine is, in most cases, intermediate to that of Type-1 and -3 aegirine. Type-1 aegirine contains the most Ti, while Type-3 contains the most Mn. Ti is enriched in Type-2 aegirine from the hypersolvus granite, although it is more limited than in Type-1. The Ti content of Type-2 aegirine decreases systematically in the sequence: hypersolvus granite, altered pegmatite and altered subsolvus granite. This variation in the amount of Ti correlates positively with that of Fe^{2+}, but negatively with of that of Fe^{3+}, as noted in Chapter 4 (for explanation see below). Moreover, Type-2 aegirine from the altered pegmatite and, in particular, the altered subsolvus granite is the most Ca-enriched of the different types of aegirine. As Type-2 aegirine replaced arfvedsonitic amphibole, the relative concentrations of the minor (and trace) elements in the aegirine were inherited from the arfvedsonitic amphibole (Table 2), although the aegirine is depleted in Mn, Zn, HFSE, REE (especially HREE), Li, K and F compared to the adjacent amphibole. Some of the observed variations (e.g., in Ti and Mn content) can be attributed to the presence of minor astrophyllite, hematite and fluorite in the alteration assemblage (as discussed above and below), but most is due to the compositional difference between arfvedsonitic amphibole and aegirine.

TEM Examination of Aegirine Replacement of Arfvedsonitic Amphibole

Selected AEM analyses of arfvedsonitic amphibole, aegirine, astrophyllite and hematite are presented in Table 3 and Appendices B-10 and B-11. The range of the relative errors of the AEM analyses are listed in Appendix B-12.

Replacement of Amphibole in the Hypersolvus Granite

Figure 9 contains a low resolution TEM image (Fig. 9A) and a combination of HRTEM and SAED (bottom left corner) images (Fig. 9B) of aegirine replacement of amphibole. The low resolution image allows one to examine the relationships between the minerals (i.e., the minute inclusion of amphibole in the aegirine in the selected region). A HRTEM image of Figure 9A (Fig. 9B) reveals the 4.5 Å (.45 nm) spacing of the aegirine between both the vertical and horizontal planes in the image and the corresponding 9.0 Å spacing of the arfvedsonitic amphibole along b^*. For the pyroxene, this spacing is

Figure 8. Variation of the composition of the three types of aegirine (the average is plotted) on a bar graph using Ti, Mn and Ca (in apfu). The acronyms are H for amphibole in the hypersolvus granite, 46-I-3 for altered pegmatite (sample 46-I-3), and S alt for altered subsolvus granite. Type-1 aegirine contains the most Ti of all, while Type-3 contains the most Mn. Ti is also enriched in Type-2 aegirine from the hypersolvus granite. Type-2 aegirine is generally intermediate to the other two, except that in the altered pegmatite and altered granite it is enriched in Ca.

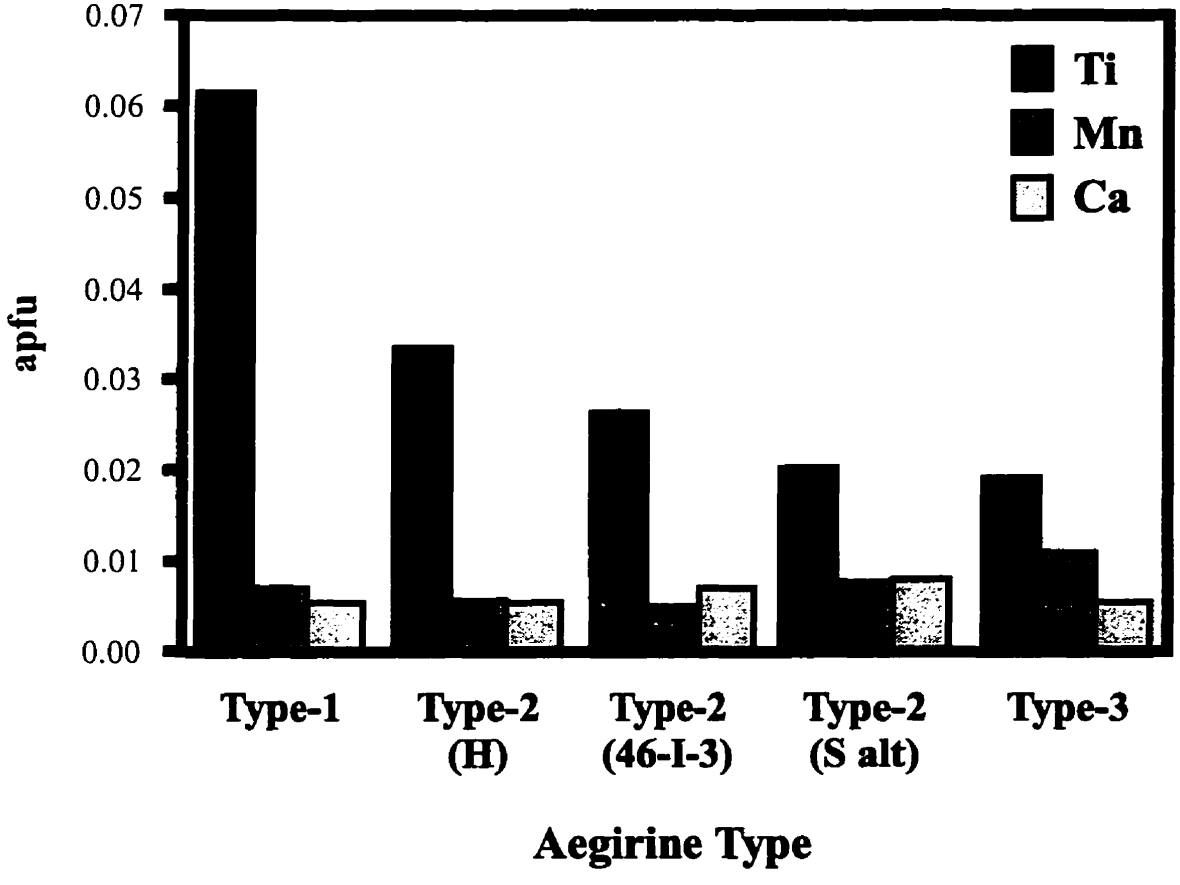
0.07
0.06
0.05
0.04
0.03
0.02
0.01
0.00
apfu
Ti
Mn
Ca
Type-1
Type-2 (H)
Type-2 (46-I-3)
Type-2 (S alt)
Type-3
Aegirine Type

Table 2: Elemental mobility between arfvedsonitic amphibole and aegirine pairs.*

Unit	Hypersolvus	Hypersolvus	Altered Pegmatite	Altered Subsolvus
Sample#	**48-A-7**	**57-A-1**	**46-I-3**	**SL-8-1**
Si	8.576	7.597	4.497	11.587
Al	1.953	3.316	0.175	-0.450
Ti	-0.298	0.549	0.158	0.691
Fe^{2+}	18.336	12.561	9.111	6.514
Mg	0.826	1.041	-0.020	-0.012
Mn	2.733	6.190	4.741	4.724
Li	0.000	0.000	1.572	0.000
Zn	0.205	1.761	4.478	5.015
Rb	0.007	-0.165	0.010	0.022
Y	-0.308	-1.008	-0.137	0.065
Nb	-0.065	-0.079	-0.864	0.209
Zr	0.138	-2.760	-0.247	-0.253
Hf	0.005	-0.109	-0.006	-0.015
Th	-0.023	0.108	-0.010	0.004
ΣREE	3.848	2.227	-0.289	0.238
Na	-36.411	-36.843	-41.767	-40.207
K	15.010	13.529	22.355	21.147
Ca	1.695	-0.151	0.259	0.497
F	9.416	9.141	9.300	8.357
Cl	0.047	0.063	0.012	0.014
La	0.723	0.494	-0.024	0.017
Ce	1.378	1.052	-0.081	0.026
Pr	0.210	0.211	-0.005	0.011
Nd	1.002	0.928	-0.019	0.060
Sm	0.209	0.021	-0.012	0.024
Eu	0.011	0.003	-0.001	0.001
Gd	0.227	-0.042	-0.016	0.023
Tb	0.027	-0.025	-0.006	0.005
Dy	0.097	-0.174	-0.039	0.027
Ho	0.013	-0.035	-0.007	0.005
Er	0.006	-0.099	-0.013	0.016
Tm	-0.004	-0.013	-0.003	0.003
Yb	-0.045	-0.079	-0.049	0.019
Lu	-0.005	-0.014	-0.013	0.003

* Calculated from the difference between their elemental content in apfu. Negative values refer to that gained from solution during replacement. Positive values refer to that lost to the solution.

Figure 9. TEM images showing the relationship between arfvedsonitic amphibole and aegirine.

A. Low-magnification TEM image of the contact between Type-2 aegirine (aeg) and arfvedsonitic amphibole (amp) perpendicular to their *c* axes, that shows the presence of small (<0.1 μm) relics of amphibole in the aegirine (scale bar is 0.1 μm).

B. HRTEM and SAED image (bottom corner) of the area outlined in Figure 9A that clearly shows the structural relationship between aegirine (aeg) and arfvedsonitic amphibole (arf). Comparison of the orientation of the lattice fringes (alternating light and dark lines in the HRTEM image) indicates that the relict grain of amphibole is of identical orientation as the primary amphibole located in the bottom of the image. All of these structural relationships between the aegirine and arfvedsonitic amphibole indicate that the replacement of amphibole was in bulk. In the SAED image, the predominant pattern is that of aegirine (see text). Additional spots produced by the amphibole are located at the tips of the arrows. The lattice fringes in the amphibole inclusion (60 nm) are directly aligned with those of the main amphibole at the bottom of the image, which indicates that this aegirine replaced the amphibole in bulk (scale bar is 20 nm).

A

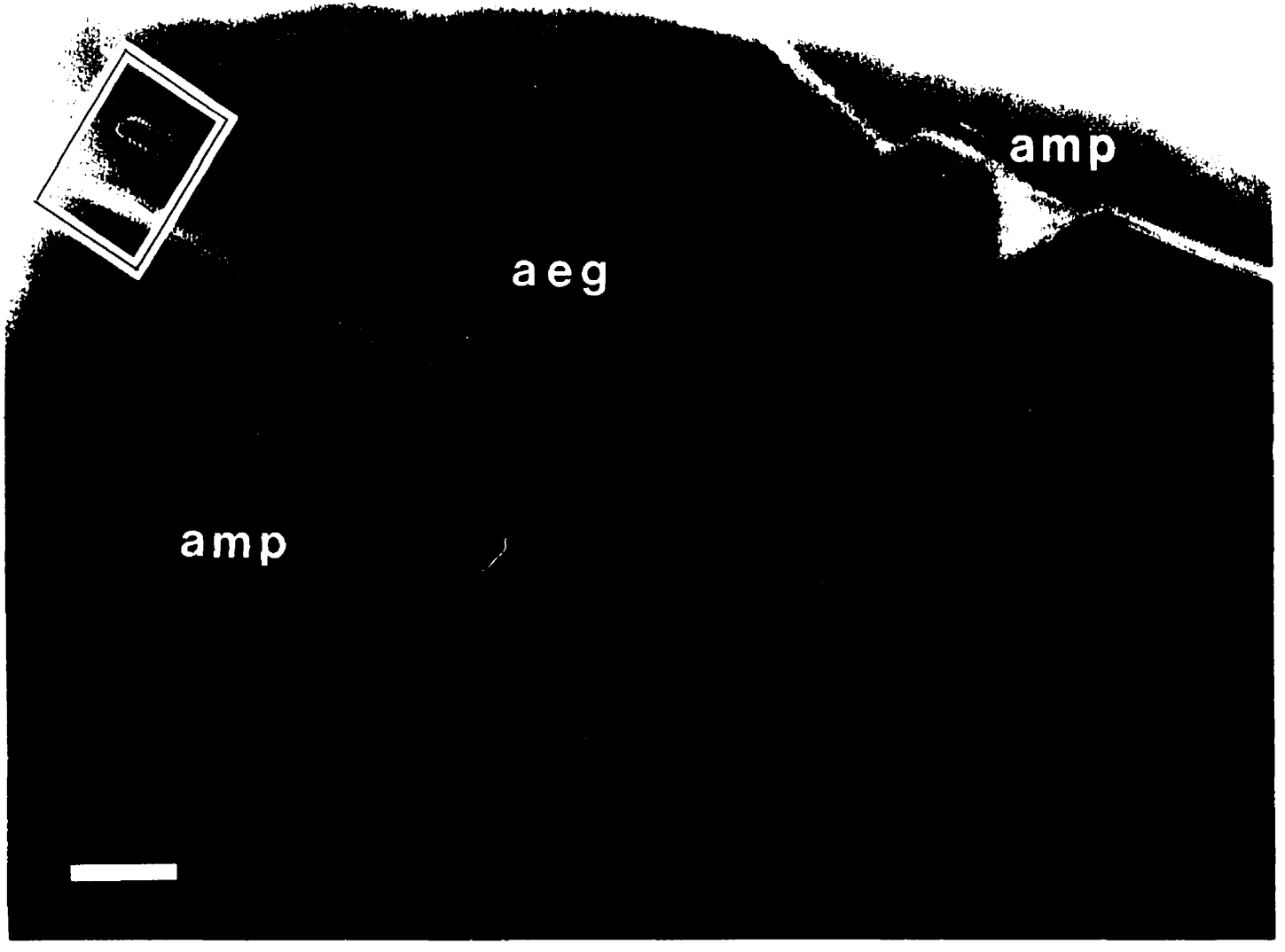

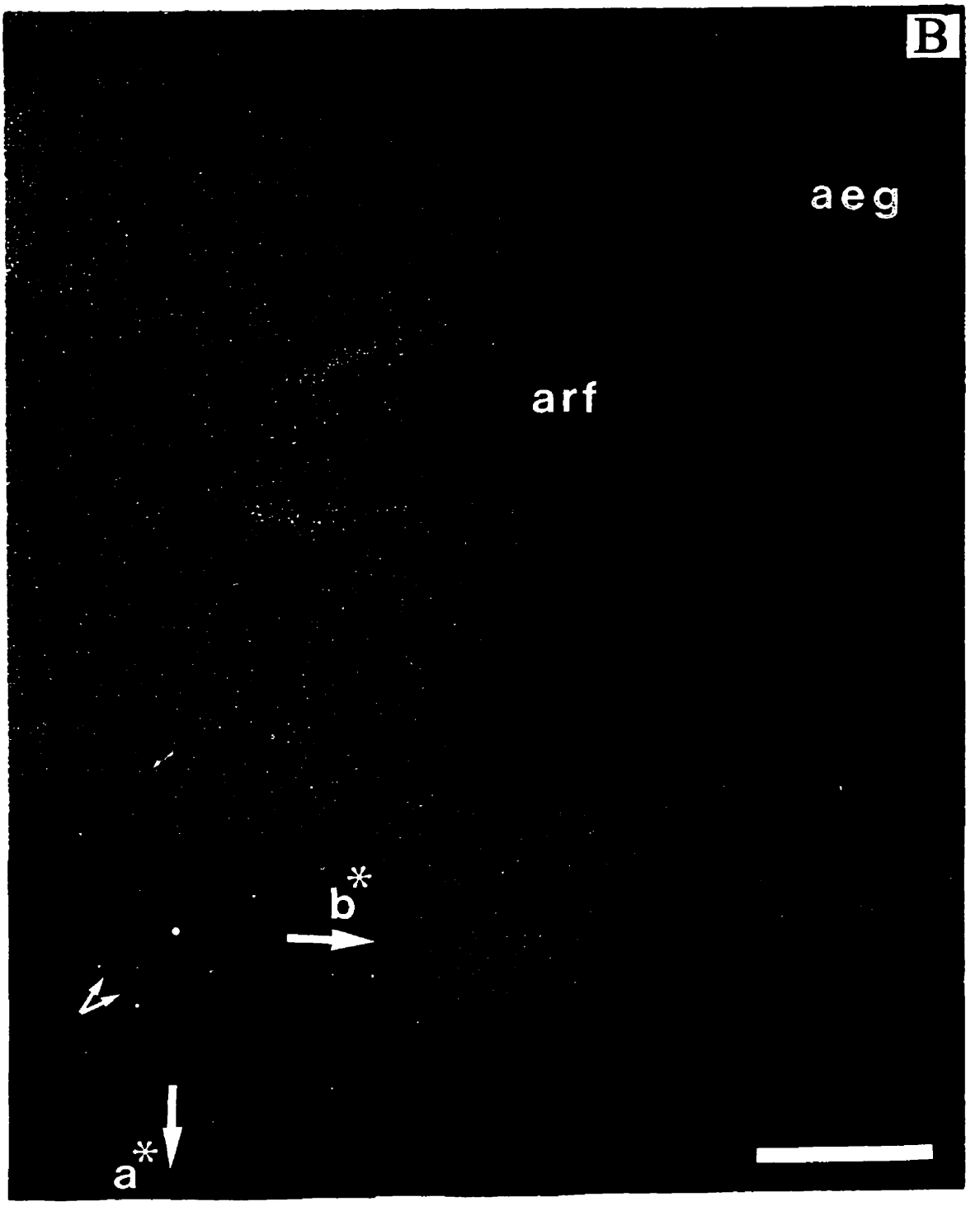
B
aeg
arf
b*
a*

represented by the sequence of alternating light and dark subvertical lines. In the SAED image (bottom left of Fig. 9B), this fringe is represented by the first spot along the b^* axis. The spacing of the arfvedsonitic amphibole is represented by the weaker spots in the SAED image of aegirine (the two arrows; Fig. 9B).

In the hypersolvus granite, Type-2 aegirine contains small arfvedsonitic amphibole inclusions in a topotactic relationship. The angle between their *c* axes is small (4°), while the angle between the a* axes of the two minerals is also 4° (Fig. 9B). Lattice fringes and SAED images indicate that the orientation of the inclusions of amphibole are identical to that of the primary arfvedsonitic amphibole (bottom of Fig. 9B). In addition, AEM analyses indicate that the two are of identical composition. Thus, these grains are the result of bulk replacement by aegirine of amphibole, as it is unlikely that a late-stage of amphibole would occur in a topotactic relationship. These interpretations are consistent with those of Banfield & Barker (1995), who suggested that the presence of oriented inclusions of relict amphibole inclusions in a secondary phyllosilicate resulted from bulk conversion. This bulk conversion of arfvedsonitic amphibole to aegirine indicates the lack of NaFe-bearing biopyriboles intermediate in composition to that of arfvedsonitic amphibole and aegirine. The compositional difference, from AEM analyses, between aegirine and arfvedsonitic amphibole (Table 3) suggests a release of Mn, Mg, Zn, Zr, Ti, Rb, F, K and, possibly, Ca during this replacement.

Astrophyllite and mottled fluorite or gagarinite are also present in this aegirine replacement of arfvedsonitic amphibole (Fig. 10A; Table 3). The ratio of astrophyllite to aegirine is in the range of 1:10, whereas that of fluorite to aegirine is much greater and, as such, cannot be accurately determined by TEM examination. SAED images of the interfaces between the aegirine and fluorite or astrophyllite show a crystallographic relationship with aegirine, and thus, the primary arfvedsonitic amphibole (Figs. 10B, C). These crystallographic relationships indicate co-crystallization of these minerals during the replacement process and disprove a primary origin. The astrophyllite is as enriched in K, Mn, Zn, Rb and Zr, as the fibrous secondary astrophyllite described in Chapter 4. This suggests that some of the elements released during the replacement of amphibole by aegirine (e.g., Ti, Mn, Zn and Rb) are fixed in the astrophyllite.

Table 3: Selected AEM analyses of the mafic silicates and oxides.

Mineral	Arfvedsonitic Amphibole	Aegirine	Aegirine	Astrophyllite	Aegirine and Hematite
K_2O	1.59	0.08	0.34	2.37	0.52
Rb_2O	0.00	0.00	3.82	2.33	4.18
Na_2O	9.75	13.35	12.73	5.30	0.54
CaO	0.33	0.22	0.40	0.64	0.00
MgO	0.71	0.63	0.40	0.27	0.00
FeO	44.49	43.41	41.35	33.78	70.44
MnO	1.30	0.18	0.58	9.99	1.79
ZnO	0.00	0.00	3.52	4.75	10.45
ZrO_2	0.89	0.00	3.62	1.53	2.83
TiO_2	1.01	0.70	0.00	9.42	1.27
Al_2O_3	0.12	1.05	0.00	0.71	0.21
SiO_2	39.81	40.38	33.22	28.92	7.77
Total*	100.00	100.00	100.00	100.00	100.00
ΣOxygen	23	6	6	31	3
K	0.235	0.003	0.015	0.526	0.018
Rb	0.000	0.000	0.075	0.237	0.068
Na	2.448	0.857	0.933	2.004	0.033
Ca	0.047	0.008	0.017	0.138	0.000
Mg	0.170	0.038	0.028	0.098	0.000
Fe^{2+}	4.599	1.147	1.247	5.255	1.744
Mn	0.137	0.005	0.018	1.580	0.045
Zn	0.000	0.000	0.091	0.631	0.221
Zr	0.056	0.000	0.067	0.145	0.043
Ti	0.122	0.022	0.000	1.708	0.037
Al	0.025	0.058	0.000	0.228	0.011
Si	8.184	2.121	1.992	8.947	0.382
ΣCations	16.023	4.258	4.482	21.496	2.601

* The total is set to 100.00 due to the fact that the analyses were performed by EDS, assuming that all Fe present was as Fe^{2+}.

Figure 10. Aegirine replacement of arfvedsonitic amphibole.

A. Low-resolution TEM image of Type-2 aegirine (aeg) that contains inclusions of brown astrophyllite (ast) and mottled fluorite (fl; scale bar is 0.5 μm).

B. SAED image of the contact between aegirine (aeg) and fluorite (fl) that shows the orientation of the fluorite with respect to that of the aegirine. Here, a* of the aegirine is parallel to the 1bar10 direction of the fluorite.

C. SAED image of the contact between aegirine (aeg) and astrophyllite (ast) that shows a relationship between the two minerals. In this case, c* axis of astrophyllite is at a angle of 36° angle to b* axis of the aegirine.

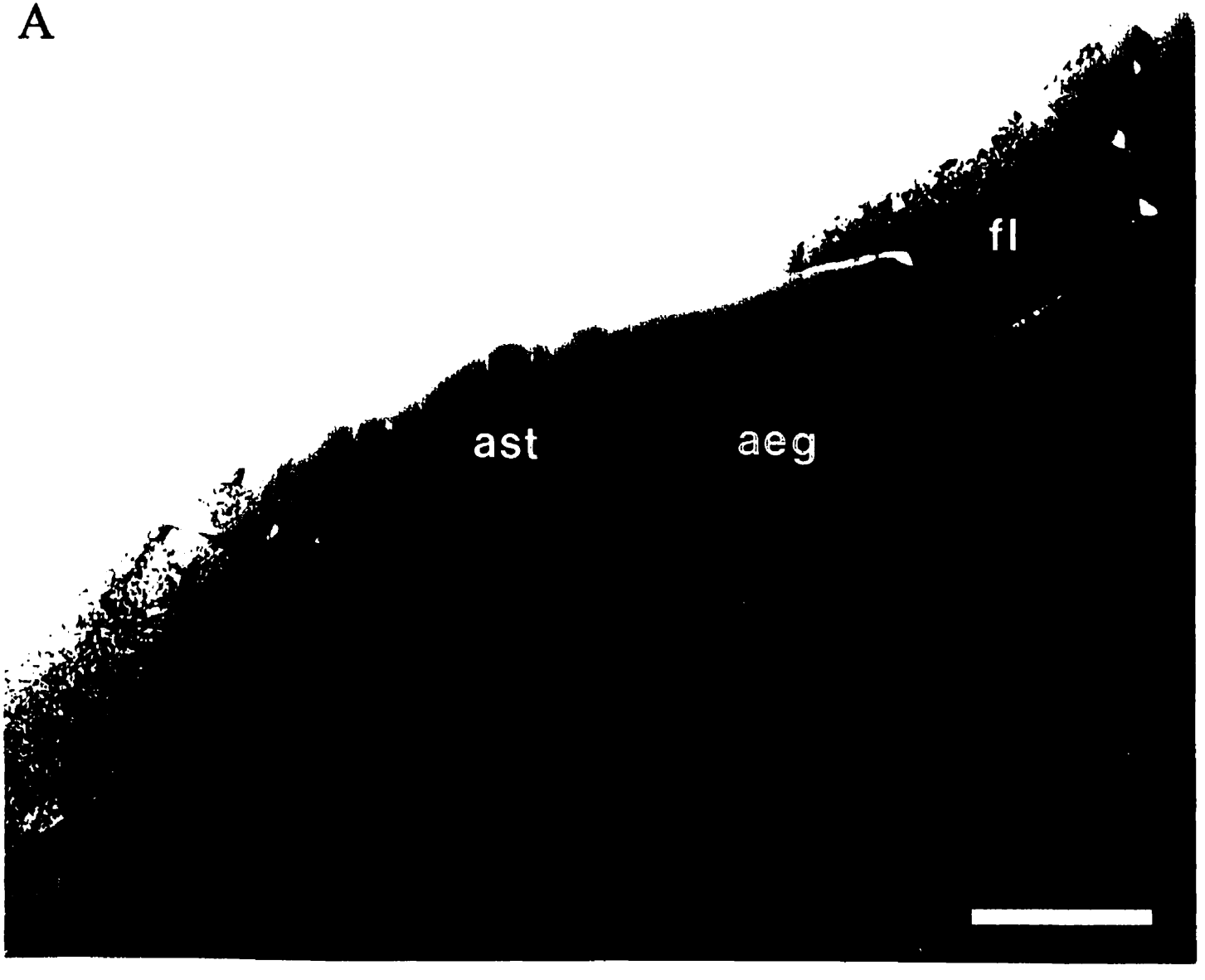
A
fl
ast
aeg

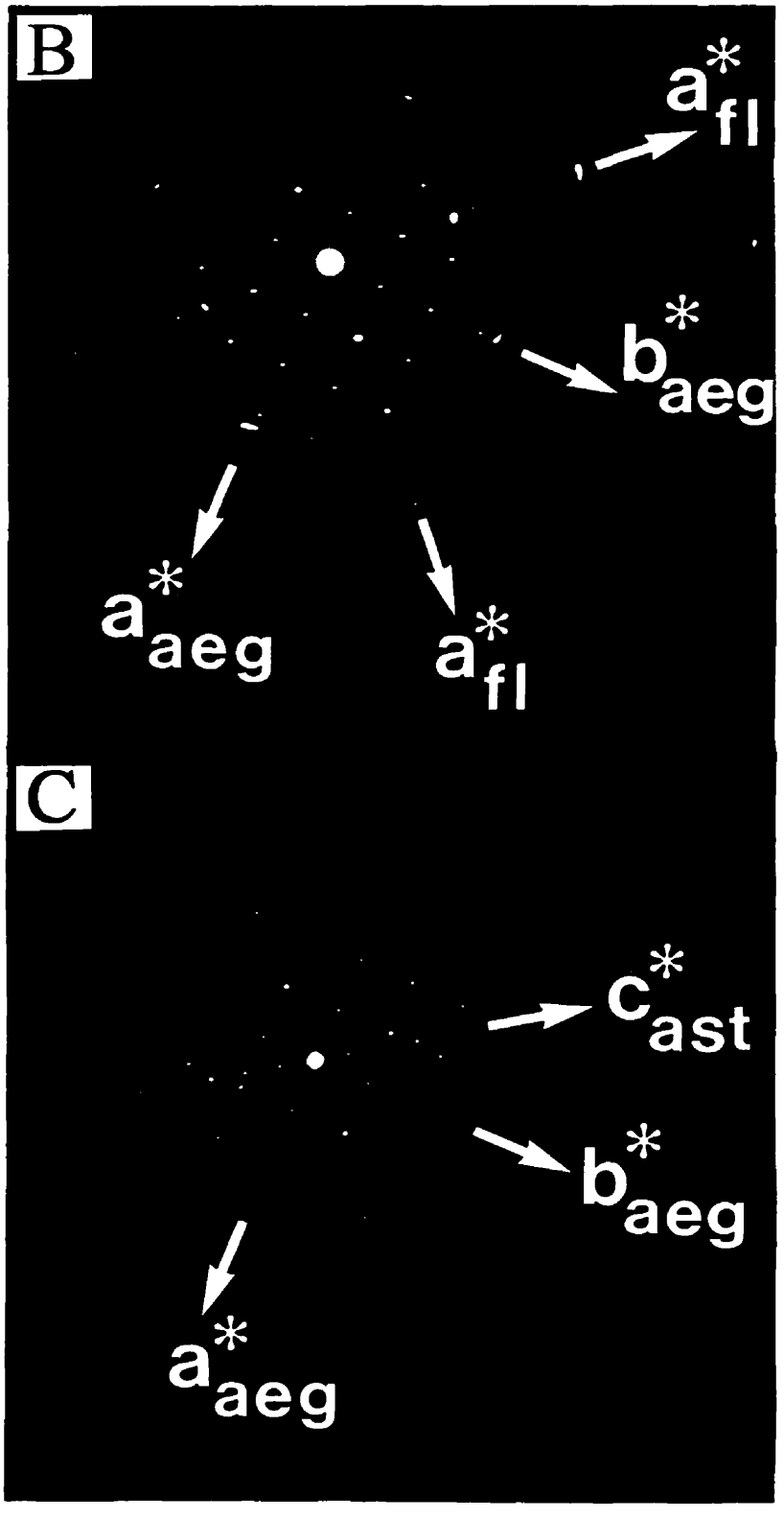
B
a^*_{fl}
b^*_{aeg}
a^*_{aeg}
a^*_{fl}
C
c^*_{ast}
b^*_{aeg}
a^*_{aeg}

Replacement of Arfvedsonitic Amphibole in Altered Pegmatite

The arfvedsonitic amphibole-aegirine relationship in altered pegmatite (sample 46-I-3) is the same as that in the hypersolvus granite, except that: 1) only inclusions of amphibole were observed in the pyroxene, and 2) AEM analyses indicate that the main amphibole and pyroxene are all enriched in Ca, Mg, Zn and Mn (due to Ca-metasomatism; ref. Chapter 6).

Replacement of Arfvedsonitic Amphibole in Altered Subsolvus Granite

Arfvedsonitic amphibole is replaced in bulk by Type-2 aegirine in the same manner as in the hypersolvus granite (Fig. 11). HRTEM and SAED examination, and AEM analyses show that this aegirine contains a clay mineral (Chapter 6) and numerous (10 vol.%) fine-grained (approx. 0.5 μm) inclusions of slightly Mn- and Ti-enriched (approximately 0.03 and 0.04 apfu, respectively) hematite. Fluorite was not found during TEM examination, even though it was rarely observed during optical examination. No evidence was found from grain morphology or SAED of the hematite to indicate that it originated by replacement of magnetite. Hematite, not magnetite, and minor quartz (<5%) were observed in X-ray powder diffraction (XRD) patterns, produced with a Guinier-Hägg focusing camera and Cu$K\alpha_1$ radiation, of this amphibole-pyroxene assemblage. Contamination from the surrounding granite could have introduced the quartz, as none was observed during TEM examination and little during optical examination.

The compositional variation of the minerals of all replacements, as determined from AEM analysis, are identical to those of the combined electron-microprobe and LAM-ICP-MS analyses, except where noted. The overall average of the combined mineral formulae are listed in Table 4.

Discussion

Replacement of Arfvedsonitic Amphibole in the Hypersolvus Granite

Comparison of the combined mineral formulae show that replacement of arfvedsonitic amphibole solely by aegirine during Na-metasomatism releases K, Mn, Ti,

Figure 11. Low-resolution TEM image of Type-2 aegirine (the dark mineral that contains the inclusions) and hematite (hem) that replaced arfvedsonitic amphibole in altered subsolvus granite. This aegirine replacement of arfvedsonitic amphibole contains fine-grained (<0.25 μm) anhedral inclusions of hematite and a late phyllosilicate (phyllo; i.e., clay mineral), but no quartz (scale bar is 2 μm).

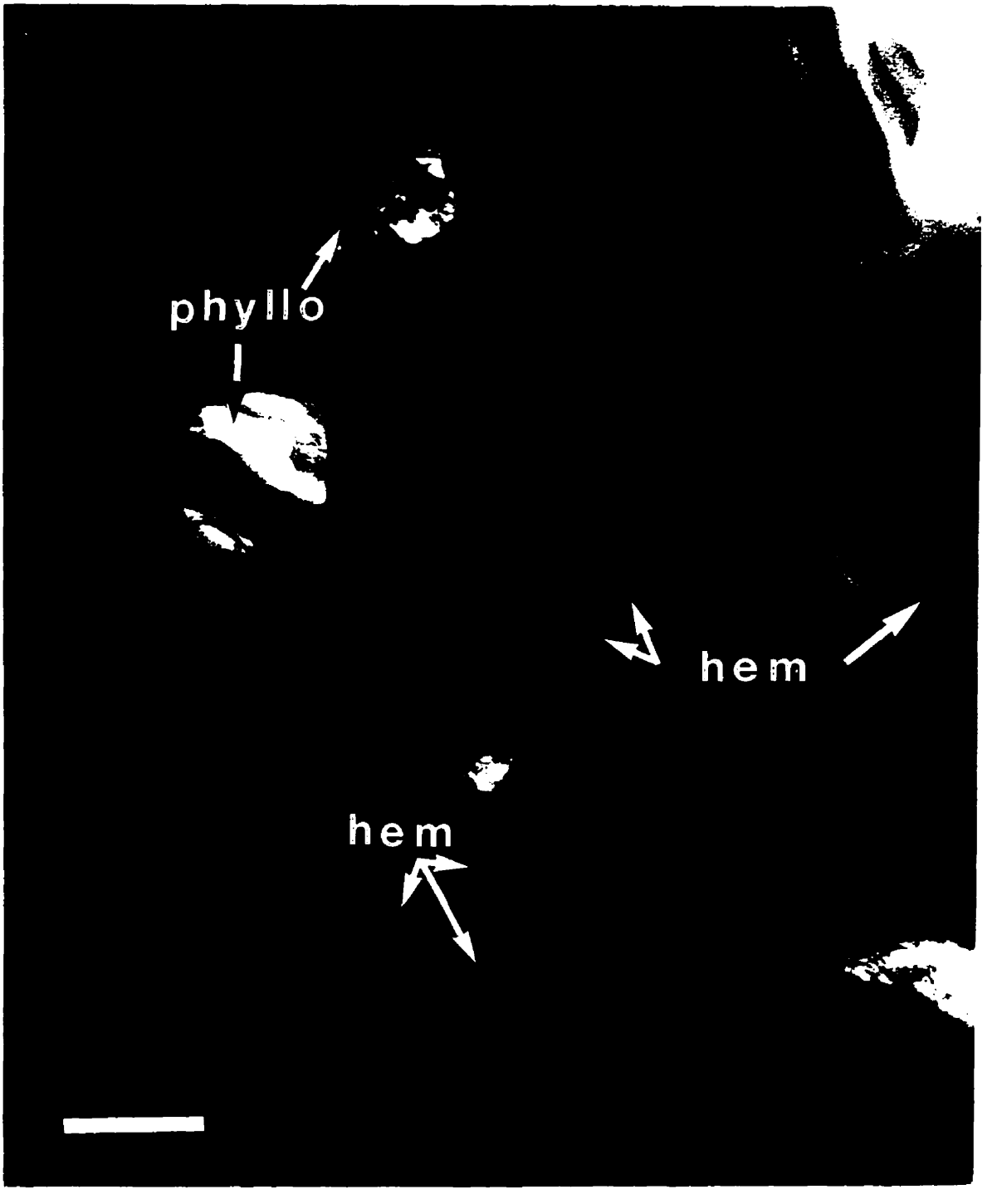
phyllo
hem
hem

Table 4: Combined mineral formulae.*

Mineral	Arfvedsonitic amphibole		Aegirine		Astrophyllite	Hematite
Unit	Hypersolvus	Altered Subsolvus	Hypersolvus	Altered Subsolvus	Hypersolvus	Altered Subsolvus
Na	2.65	2.72	1.00	0.98	1.65	0.00
K	0.32	0.25	0.00	0.00	1.20	0.00
Ca	0.03	0.03	0.00	0.02	0.05	0.00
Rb	0.00	0.00	0.00	0.00	0.10	n.d.
Fe^{2+}	3.96	3.60	0.10	0.02	5.90	0.00
Fe^{3+}	0.50	0.85	0.85	0.93		1.93
Mg	0.04	0.09	0.00	0.01	0.15	0.00
Mn	0.13	0.15	0.01	0.02	1.28	0.03
Li	0.10	0.07	0.01	0.00	n.d.	n.d.
Zn	0.04	0.06	0.01	0.00	0.70	
Nb	0.00	0.00	0.00	0.00	0.05	n.d.
Zr	0.01	0.01	0.01	0.00	0.23	n.d.
ΣREE	0.01	0.00	0.00	0.00	n.d.	n.d.
Ti	0.14	0.12	0.02	0.02	1.72	0.04
^{VI}Al	0.07	0.05	0.00	0.00		n.d.
^{IV}Al	0.00	0.00	0.02	0.00	0.10	n.d.
Si	8.00	8.00	1.98	2.00	7.90	0.00
F	1.00	1.00	n.d.	n.d.	6.10	n.d.
OH	1.00	1.00	n.d.	n.d.	0.90	n.d.
ΣCations	16.00	16.00	4.01	4.00	21.03	2.00

* As determined from electron-microprobe, LAM-ICP-MS and AEM data.
n.d.: Not determined.

Rb, Zn, Zr, Nb, Y, REE, Li, Mg, F and Ca into solution. Replacement aegirine likely inherited a small amount of Mn, Li, Zn, Zr, Ti and Si from the amphibole. The reaction to represent the replacement reaction in this granite, when balanced on the basis of Si, using the typical ratio of aegirine to amphibole of 4:1 (based on the difference between their unit-cell volumes and the number of formula units in the unit-cell) and the average composition of amphibole, pyroxene and astrophyllite (respectively in the reaction) from Table 4 is:

arfvedsonitic amphibole

$$Na_{2.65}K_{0.32}Ca_{0.03}Fe^{2+}_{3.96}Fe^{3+}_{0.50}Mg_{0.04}Mn_{0.13}Li_{0.10}REE_{0.01}Zn_{0.04}Zr_{0.01}Al_{0.07}Ti_{0.14}Si_8O_{22}OH_1F_1 + 1.249Na^+ + 0.006Rb^+ + 0.04Zn^{2+} + 0.0392Ti^{4+} + 0.003Nb^{5+} + 0.0418Zr^{4+} + 0.012Al^{3+} + 1.606H_2O \rightarrow$$

astrophyllite

$$0.06Na_{1.65}K_{1.20}Ca_{0.05}Rb_{0.10}Fe^{2+}_{5.90}Mg_{0.15}Mn_{1.28}Zn_{0.70}Ti_{1.72}Zr_{0.23}Nb_{0.05}Si_{7.9}Al_{0.1}O_{24}OH_{6.10}F_{0.90}$$

aegirine

$$+ 3.8Na_{1.00}Fe^{3+}_{0.85}Fe^{2+}_{0.10}Li_{0.01}Mn_{0.01}Zn_{0.01}Zr_{0.01}Ti_{0.02}Al_{0.02}Si_{1.98}O_6 + 0.248K^+ + 0.027Ca^{2+} + 0.496Fe^{3+} + 0.031Mg^{2+} + 0.062Li^+ + 0.0152Mn^{2+} + 0.01REE^{3+} + 0.946F^- + 0.6816H^+ + 1.5822H_2 \quad (1).$$

This reaction released K, Ca, Fe, Mg, Li, Mn, REE and F into solution. All but F form fluoride, chloride or hydroxy complexes. Some of the Li and REE released during the replacement process may have been accommodated in the astrophyllite or may later have crystallized as other secondary minerals, such as bastnäsite, polylithionite, etc. The F reacted with Ca from the fluid or from breakdown of the amphibole to produce fluorite. Oxidation of Fe^{2+} during this reaction resulted in the release of H_2.

The presence of astrophyllite and absence of hematite in this aegirine-dominant replacement assemblage is a reflection of the presence of significant K, Mn and Ti and the fact that fO_2 was sufficiently low that hematite was not stable (i.e., by analogy with aenigmatite, the assemblage originated in the no oxide field; Chapter 4). Unfortunately, it is impossible to compare this aegirine-dominant replacement assemblage with that from other complexes, as authors who mention aegirine replacement of arfvedsonitic amphibole commonly note the presence of only an iron oxide (e.g., O'Halloran, 1985).

Bulk conversion of arfvedsonitic amphibole to aegirine implies the lack of formation of NaFe-bearing biopyriboles of a structure intermediate to that of arfvedsonitic amphibole and aegirine in these samples. Thus, changes in composition of arfvedsonitic amphibole may be the product of the presence of minute inclusions of secondary aegirine in the primary amphibole or the lack of analysis of certain elements (as supported by data in Chapter 4). Hawthorne et al. (1993) determined that the addition of Li to the analysis of arfvedsonitic amphibole produced a more ideal amphibole formula, as supported by the data in Chapter 4. Furthermore, Hawthorne et al. (1994) observed, through TEM examination, no submicroscopic inclusions in pure Li-rich alkali amphiboles.

Replacement of Arfvedsonitic Amphibole in Altered Subsolvus Granite

Aegirine, hematite, quartz and fluorite are present in the aegirine-dominant replacement assemblage in altered subsolvus granite. Variation in the proportion of hematite and quartz associated with the aegirine that replaces arfvedsonitic amphibole can be accounted for by the following reactions:

$$NaNa_2Fe^{2+}{}_4Fe^{3+}Si_8O_{22}OH_1F_1 + 2Na^+ + 2SiO_2 + 3H_2O \rightarrow 5NaFeSi_2O_6 + F^- + 3H^+ + 2H_2 \quad (2),$$

$$NaNa_2Fe^{2+}{}_4Fe^{3+}Si_8O_{22}OH_1F_1 + Na^+ + 2.5H_2O \rightarrow 4NaFeSi_2O_6 + 0.5Fe_2O_3 + F^- + 2H^+ + 2H_2 \quad (3),$$

and

$$NaNa_2Fe^{2+}{}_4Fe^{3+}Si_8O_{22}OH_1F_1 + 2H_2O \rightarrow 3NaFeSi_2O_6 + Fe_2O_3 + 2SiO_2 + F^- + H^+ + 2H_2 \quad (4).$$

Reaction 2 is based on conservation of Fe, but requires both the addition of Na^+ and the presence of quartz. The addition of Na^+ also is required when Si is conserved (Reaction 3) and hematite and aegirine are produced. If Na is conserved (Reaction 4), the replacement of arfvedsonitic amphibole by aegirine produces excess Fe and Si, which form hematite and quartz, respectively. All three reactions proceed to the right at high fO_2, but only Reactions 2 and 3 imply Na-metasomatism. In all cases, F released by replacement of amphibole

reacts with Ca from both the fluid and the amphibole to form fluorite. Despite this, fluorite was rarely observed during optical investigation and not observed in TEM examination.

When Reactions 2, 3 and 4 proceed to the right, H_2 is released. Substantial amounts of H_2 may have been produced if the system remained open (e.g., during degassing). In fact, this has probably been the case, because a build up of H_2, if the system was closed, would have resulted in a decrease in fO_2 until a buffering assemblage, such as riebeckite-hematite-aegirine or hematite-magnetite was formed. However, no magnetite or riebeckite have been observed in this study, although Birkett et al. (1996) noted the presence of a small amount of titanomagnetite.

The relative lack of quartz in the replacement and the variable, but ubiquitous distribution of hematite (see results above) indicates that Reaction 3 is the most likely of the three possibilities. This reaction, duly modified for the mineral formulae calculated from electron-microprobe, LAM-ICP-MS and AEM analysis, becomes:

arfvedsonitic amphibole

$$Na_{2.72}K_{0.25}Ca_{0.03}Fe^{2+}_{3.60}Fe^{3+}_{0.85}Mg_{0.09}Mn_{0.15}Li_{0.07}Zn_{0.06}Zr_{0.01}Ti_{0.12}Al_{0.05}Si_{8.00}O_{22}OH_1F_1$$
$$+ 1.24Na^+ + 0.01Ca^{2+} + 0.03Al^{3+} + 2.268H_2O$$

aegirine hematite

$$\rightarrow 4Na_{0.99}Ca_{0.01}Fe^{3+}_{0.93}Fe^{2+}_{0.03}Mg_{0.01}Mn_{0.01}Ti_{0.02}Al_{0.02}Si_{1.98}O_6 + 0.316Fe_{1.93}Ti_{0.04}Mn_{0.03}O_3 +$$
$$0.25K^+ + 0.05Mg^{2+} + 0.10Mn^{2+} + 0.07Li^+ + 0.06Zn^{2+} + 0.01Zr^{4+} + 0.027Ti^{4+} + F^- +$$
$$0.08H_4SiO_4^0 + 1.462H^- + 1.877H_2 \qquad (5).$$

This reaction suggests that replacement of arfvedsonite released significant amounts of K, F and H, and minor amounts of Mg, Mn, Li, Zn, Zr and Ti into solution, which complex in the same manner as in Reaction 1. A small amount of Si is released if one uses the ideal mineral formulae of Table 4 and assumes that the proportion of amphibole to aegirine is 1:4. An increase in this proportion to 1:4.04 would result in complete conservation of Si. Furthermore, in the composite grains, zonation of this aegirine-dominant assemblage with arfvedsonitic amphibole was caused by a slight compositional difference between Type-1a and 1b primary amphibole, which results in differential reaction of amphibole to the metasomatic fluid (Chapter 4).

Optical examination of approximately 200 thin sections and, with the TEM, on 20 grids suggest that hematite is by far the dominant oxide in the Strange Lake complex, as supported by the observations of Pillet et al. (1993). The assemblage aegirine-magnetite-quartz proposed by Salvi & Williams-Jones (1990, 1996) from the complex has not been encountered. Moreover, only an insignificant amount of ilmenite is present as an inclusion in arfvedsonitic amphibole from the hypersolvus granite. In addition, it was impossible to determine from the TEM observations if the hematite resulted from the complete replacement of magnetite. The presence of hematite and relative lack of quartz as determined in the present study contrasts with the magnetite and quartz observed by Bonin (1986) in the aegirine replacement of arfvedsonitic amphibole in peralkaline granite from Corsica. The difference in the iron oxide present can be attributed to replacement of arfvedsonitic amphibole by aegirine at a higher fO_2.

Reactions 1 to 5 imply that the replacement of arfvedsonitic amphibole by aegirine is effective in producing a H_2-rich environment favorable for Fischer-Tropsch reaction and the production of the hydrocarbons noted by Salvi & Williams-Jones (1997). Moreover, Gutteridge et al. (1983), White & Yee (1985), Zalma et al. (1987a, 1987b), Shatos et al. (1987), Ghio et al. (1990) and Lund & Aust (1991) suggested that Fe^{2+} at an amphibole (generally fibrous) surface is a more effective for Fischer-Tropsch than that in an aqueous solution or on the surface of magnetite. Despite this, equant amphibole grains have a lower net negative surface-charge than fibrous grains (Schiller et al., 1980), and thus, are less effective catalysts (as in the case of arfvedsonitic amphibole from the Strange Lake complex) than asbestiform riebeckite. These reactions proposed for the replacement of amphibole imply that the Fischer-Tropsch process involved reaction of the fluid with the surface of the arfvedsonitic amphibole or hematite instead of magnetite.

Redistribution of Elements during Na-Metasomatism and Formation of the Deposit

Comparison of the chemical composition of arfvedsonitic amphibole and the replacement aegirine indicates that K, REE, Li, Mg, Mn, F, and, in some cases, Zn, Zr, Nb, Ti and Al are released. K, F and, to a lesser extent, Li, REE, Mn, Zn, Zr and Ti are not accommodated in the aegirine structure to the extent that they were in the arfvedsonitic

amphibole. Some Ti, Mn, Zn, Zr, Nb, Rb and F is accommodated in astrophyllite, and Mn and Ti in hematite. The fine grains of LREE- and Y-rich fluoride mineral observed parallel to the cleavage of amphibole in the hypersolvus granite (Chapter 4) imply minor Na-metasomatism and the mobility of REE, especially LREE, and Y mobilized from the amphibole or earlier LREE and Y-rich inclusions. Estimation of the amount of Zr, Nb, Y and REE released during replacement of arfvedsonitic amphibole by aegirine calculated from amphibole-aegirine mineral pairs (Table 5; method of calculation in Appendix B-13) indicates that, although the REE content of the entire deposit could be produced as a result of this replacement, the proportion of other elements, in particular Nb, may not necessarily be. Consequently, arfvedsonitic amphibole acts as a sink for HFSE, REE, etc.

Most elements released (e.g., REE, Ti, Zr and Nb) during Na-metasomatism (≥350°C and F-rich fluid: Salvi & Williams-Jones, 1992) preferentially form fluoride complexes rather than chloride or hydroxy complexes (Keppler, 1993). In addition, Smith & Martell (1976), Ruaya & Seward (1986) and Gammons & Seward (1996) concluded (the last two experimentally) that mono or difluoride or chloride complexes of Mn and Zn are mobile in solution above 350°C. Haas et al. (1995) calculated that, at 300°C, REE dominantly form fluoride complexes in slightly acidic to neutral solutions. Mineyev (1963) and Taylor et al. (1981) suggested that, as REE form increasingly stable fluoride complexes from La to Lu (Bandurkin, 1961; Bilal et al., 1979; Wood, 1990), Na-metasomatism will produce a strong HREE fractionation. Furthermore, the experimental results of Barsukova et al. (1979) and Bright & Readey (1987) imply the presence of TiF_2^{6-} in F-rich hydrothermal solutions. Lastly, Zr is also soluble as a fluoride complex in a F-rich solution (Norén, 1967, 1969; Ayers & Watson, 1991; Keppler, 1993; Aja et al., 1995). The presence of such F- and Cl-rich solutions in the Strange Lake complex has also been suggested by Salvi & Williams-Jones (1990) and Nassif (1993).

Experimental investigations on the transport of HFSE or REE as fluoride complexes are consistent with observations on natural systems, many of which involve transport via a hydrothermal fluid (Gieré, 1986, 1990; Salvi & Williams-Jones, 1990; Flohr, 1991; Gieré & Williams, 1992). Previous investigations of natural systems include studies of fluid inclusions, bulk-rock analyses and secondary mineral assemblages. Fluid inclusions may contain significant REE (Banks et al., 1994; Campbell et al., 1995) or REE- and Zr-rich

Table 5: Calculated maximum elemental releases from the replacement process.[1]

	Released (g)		Gained (g)[3]	
% conversion[2]	20	40	20	40
Y	1.52E+13	3.04E+13	2.37E+14	1.45E+14
Nb	4.92E+13	9.84E+13	1.86E+13	4.06E+14
Zr	3.24E+13	6.48E+13	6.49E+14	1.30E+15
REE	9.05E+14	1.81E+15	0.00E+00	0.00E+00

[1] Excluding that of 46-I-3 (see text). The assumptions made in this calculation are: a cone-shaped complex of radius 3.385 km that extends to 10 km depth, the density of the rock is 2.8 g/cm^3, the complex is half hypersolvus and half subsolvus granite and the volume of amphibole in the complex is 7%.
For a detailed description of the method of calculation refer to Appendix B-13.

[2] Percentage of arfvedsonitic amphibole converted to aegirine.

[3] The maximum amount of each element that can be gained by the aegirine during its replacement of amphibole is denoted by the heading Gained.

daughter minerals (Kwak & Abeysinghe, 1987; Salvi & Williams-Jones, 1990; Vard & Williams-Jones, 1993). Other indications of a late REE-enriched fluid are the REE- and Y-rich milarite observed in miarolitic cavities in the Strange Lake peralkaline complex by Cerný et al. (1991). The best example of elemental mobility in this complex inferred from bulk-rock analyses, is that of Salvi & Williams-Jones (1996), who determined using mass-balance techniques that Zr, Y and HREE were mobilized during Na-metasomatism. In terms of mineral assemblages produced by hydrothermal processes, Flohr (1991) and Flohr & Ross (1990) suggested that F was an important complexing agent of Ti, V, Nb, Li and, in part, REE, Mn, Ti, V and Zr in the Magnet Cove igneous complex, Arkansas. Lastly, Gieré (1986, 1990; Gieré & Williams, 1992) discussed the mobility of Zr, Ti and REE in the formation of hydrothermal zirconolite, allanite, titanite, rutile, geikielite and högbomite and through the compositional zonation in zirconolite from marble. Cathelineau (1987) noted that U, Th and REE were mobilized from monazite, uraninite, xenotime, apatite and, in part, zircon during albitization (at 350 to 450°C with a high fO_2 and a_F) of granites in the French Massif Central. The results of these studies can be used to suggest the mode of transport of the elements released by the replacement of arfvedsonitic amphibole by the aegirine-assemblage.

In peralkaline granites, Na-metasomatism is reflected in the albitization of feldspar (Elliott, 1983; Bowden et al., 1987; Kovalenko et al., 1995) and replacement of arfvedsonitic amphibole by aegirine (O'Halloran, 1985; Bonin, 1986). Nassif (1993), Nassif & Martin (1992) and the habits of the mafic minerals described in Chapter 4, all suggest that this process led to the formation of albite rims on alkali feldspar and late intergrowths of arfvedsonitic amphibole and albite in the Strange Lake complex. Albitization or Na-metasomatism has been described from other peralkaline complexes by Bowden et al. (1987), Taylor et al. (1981) and Pinckston & Smith (1995). In peralkaline complexes, the mobility of HFSE, REE, and Zn as fluoride complexes has been related by Mineyev (1963), Taylor et al. (1981), Strong et al. (1984) and Bowden (1985) to Na-metasomatism. The results of the calculations presented in this study indicate that arfvedsonitic amphibole may contribute to a portion of the ore in economic deposits, as it acts as a sink for Zr, Zn, REE and Li (Borley, 1976; Hawthorne, 1976, 1983; Hawthorne et al., 1992; Rubin et al., 1993; Abdel-Rahman, 1994). This Na-metasomatism also has been related by Strong et al. (1984)

and Pinckston & Smith (1995) and Salvi & Williams-Jones (1996) to degassing. Degassing in the Strange Lake complex is supported by the presence of solely or dominantly microcline (Nassif, 1993) in the pegmatitic bodies, and the late-stage enrichment in the K content of amphibole (Chapter 4).

The introduction of a subsequent Ca-rich metasomatic fluid from the surrounding country rocks changed the pH or temperature of the system sufficiently to destabilize these fluoride-based complexes and cause their precipitation as secondary minerals (e.g., fluorite, pyrochlore, milarite; Salvi & Williams-Jones, 1996).

Conclusions

Na-metasomatism at (≥350°C; Salvi & Williams-Jones, 1992) resulted in the replacement of arfvedsonitic amphibole by aegirine. In the hypersolvus granite, limited Na-metasomatism of the amphibole resulted in the remobilization of the REE from the amphibole and from the earlier REE-rich fluoride inclusions, to form new grains. However, the major effect of Na-metasomatism is the bulk replacement of arfvedsonitic amphibole by Type-2 aegirine, as observed predominantly through TEM examination. Thus, NaFe-bearing biopyriboles were not observed in this instance.

Replacement of arfvedsonitic amphibole by aegirine released K, Li, Mg, Mn, F and, in some cases, REE, Zn, Zr and Ti into solution. In hypersolvus granite, some of this Li, Mn, Zn, Zr, Ti and Al is accommodated in aegirine, K, Ca, Rb, Mg, Mn, Zn, Ti, Zr, Nb, F and Al in astrophyllite, and F combines with Ca released from the amphibole or from the fluid to produce fluorite. This reaction requires significant Na, but minor Rb, Zn, Ti, Nb, Zr and Al in the metasomatic fluid. In altered subsolvus granite, the replacement process produced hematite ± quartz and fluorite. Some of the Ca, Mg, Mn, Al and Ti, and Ti and Mn, from the amphibole is present in the aegirine and hematite, respectively. This fluid contained significant Na, but minor Ca and Al. It appears that aegirine replacement of arfvedsonitic amphibole was related to an increase in the amount of Na in the fluid in addition to changes in temperature or fO_2 conditions. K, Ca, Fe, Mg, Li, Mn, REE, Zn, Zr, Ti, F and H_2 were released from the amphibole during the replacement process. Consequently, arfvedsonitic amphibole acted as a sink for all these elements. Hydrogen

released during this process could have promoted the formation of hydrocarbons through the Fischer-Tropsch process (Salvi & Williams-Jones, 1997). Calculations of the amount of elements released (Table 5) suggest that significant proportions of HFSE and REE, and possibly Zr, Y and Nb, were released during replacement of arfvedsonitic amphibole by aegirine, and that these contributed in a significant way to the formation of the ore deposit.

The relative lack of quartz and presence of hematite in the aegirine replacement assemblage of arfvedsonitic amphibole suggests different physico-chemical properties of the fluid (possibly to a higher fO_2) compared to those suggested by Bonin (1986). Lastly, this is the first description of astrophyllite in the replacement assemblage. The presence of astrophyllite and not an oxide may reflect formation at a lower fO_2.

Acknowledgements

Glenn Poirier is thanked for setting up elemental analysis tables for electron-microprobe analyses and Gilles Gauthier for setup and tuning the LAM-ICP-MS. Discussions on sample preparation, standards, standardization and errors for the LAM-ICP-MS analyses with G. Gauthier, C. Dalpé, S. Jackson and S. Lang were most helpful. The first two wrote the program used to calculate the elemental contents from raw LAM-ICP-MS data. C. Dalpé and N. MacRae provided the dark glasses HF-13 and JW-87, respectively. Drs. K. Livi and B. Grobéty introduced me to the TEM at JHU. K. Livi also showed the first author how to modify the program to calculate the elemental concentrations to calculate the concentrations of Zn, Zr and Rb. This research was supported by an NSERC, Lithoprobe, FCAR team and NSERC Strategic grants to the second author, as well as a EAR94-17585 from the National Science Foundation grant for support of the TEM facilities to the third author. This research could not have been completed without a FCAR scholarship and stage award, a major scholarship from McGill University, GSA student research award and SDE Women in Science award to me. Many thanks to C. Normand, A.E. Williams-Jones and K. Currie for comments on earlier versions of this manuscript.

References

Abdel-Rahman, A.M. (1994): Alkali amphibole: a potential source of rare earth elements in felsic alkaline rocks. *Exploration and Mining Geology*, 3, 81-94.

Ahn, J.H. & Buseck, P.R. (1991): Microstructures and fiber-formation mechanisms of crocidolite asbestos. *American Mineralogist*, 76, 1467-1478.

Aja, S.U., Wood, S.A. & Williams-Jones, A.E. (1995): The aqueous geochemistry of Zr and the solubility of some Zr-bearing minerals. *Applied Geochemistry*, 10, 603-620.

Akai, J. (1982): Polymerization process of biopyribole in metasomatism at the Akatani ore deposit, Japan. *Contributions to Mineralogy and Petrology*, 80, 117-131.

------- & Saito, M. (1985): Ca-Mg triple-chain silicate derived from Na-Mg triple-chain silicate by ion-exchange experiment and its structural model. *Bulletin de Minéralogie*, 108, 21-28.

-------, Tomita, K. & Yamaguchi, Y. (1985): High resolution electron microscopic observation of pyroxene lamellae in oxyhornblende. *Earth Science*, 38, 334-345.

Ayers, J.C. & Watson, E.B. (1991): Solubility of apatite, monazite, zircon, and rutile in supercritical aqueous fluids with implications for subduction zone geochemistry. *Philosophical Transactions of the Royal Society of London*, A, 335, 365-375.

Bandurkin, G.A. (1961): Behaviour of the rare earths in a fluorine-bearing media. *Geochemistry*, 1961, 159-167.

Banfield, J.F. & Barker, W.W. (1995): Direct observation of reactant-product interfaces formed in natural weathering of exsolved defective amphibole to smectite: evidence for episodic, isovolumetric reactions involving structural inheritance. *Geochimica et Cosmochimica Acta*, 58, 1419-1429.

Banks, D.A., Yardley, B.W.D., Campbell, A.R. & Jarvis, K.E. (1994): REE composition of an aqueous magmatic fluid: a fluid inclusion study from the Capitan Pluton, New Mexico, U.S.A. *Chemical Geology*, 113, 259-272.

Barsukova, M.L., Kuznetsov, V.A., Dorofeyva, V.A. & Khodakovskiy, L.I. (1979): Measurement of the solubility of rutile TiO_2 in fluoride solutions at elevated temperatures. *Geochemistry International*, 7, 41-49.

Bélanger, M. (1984): Région du lac Brisson. *Ministère de l'Énergie et des Ressources*, Québec, DP 84-20 (carte annotée, scale 1:50,000).

Bilal, B.A., Herrmann, F. & Fleisher, W. (1979): Complex formation of trace elements in geochemical systems. 1. Potentiometric study of fluoro-complexes of rare earth elements in fluorite-bearing model systems. *Journal of Inorganic Nuclear Chemistry*, 41, 347-350.

Birkett, T.C., Miller, R.R., Roberts, A.C. & Mariano, A.N. (1992): Zirconium-bearing minerals of the Strange Lake intrusive complex, Quebec-Labrador. *Canadian Mineralogist*, 30, 191-205.

-------, Trzcienski, W.E., Jr., Stirling, J.A.R. (1996): Occurrence and compositions of some Ti-bearing minerals in the Strange Lake intrusive complex, Quebec-Labrador boundary. *Canadian Mineralogist*, 34, 779-801.

Bogoch, R., Weissbrod, T. & Bar-Matthews, M. (1992): Significance of REE-mineral inclusions in aegirine from an alkali syenite, Negev, Israel. *European Journal of Mineralogy*, 4, 1337-1346.

Bonin, B. (1986): **Ring Complex Granites and Anorogenic Magmatism**. Studies in Geology, North Oxford Academic Publishers Ltd., Great Britain, 188p.

Borley, G. (1976): Ferromagnesian mineralogy and temperatures of formation of the Younger Granites of Nigeria. *In* **Geology of Nigeria** (Kogbe, C.A., ed.). Elizabethan Press, Lagos, 159-176.

Bowden, P. (1985): The geochemistry and mineralization of alkaline ring complexes in Africa (a review). *Journal of African Earth Sciences*, 3, 41-49.

-------, Black, R., Martin, R.F., Ike, E.C., Kinnaird, J.A. & Batchelor, R.A. (1987): Niger-Nigerian alkaline ring complexes: a classic example of African Phanerozoic anorogenic mid-plate magmatism. *In* **Alkaline Igneous Rocks** (Fitton, J.G. & Upton, B.G.J., eds.). Geological Society Special Publication, 30, 357-379.

Bright, E. & Readey, D.W. (1987): Dissolution kinetics of TiO_2 in HF-HCl solutions. *Journal of the American Chemical Society*, 70, 900-906.

Campbell, A.R., Banks, D.A. & Yardley, B.W.D. (1995): Geochemistry of Th-U-REE mineralizing magmatic fluids, Captian Mountains, New Mexico. *Economic Geology*, 90, 1271-1287.

Cathelineau, M. (1987): U-Th-REE mobility during albitization and quartz dissolution in granitoids: evidence from south-east French Massif Central. *Bulletin de Minéralogie*, 110, 249-259.

Cerný, P., Hawthorne, F.D., Jambor, J.L. & Grice, J.D. (1991): Yttrian milarite. *Canadian Mineralogist*, 29, 533-541.

Chisholm, J.E. (1973): Planar defects in fibrous amphiboles. *Journal of Material Science*, 8, 475-483.

Czamanske, G.K. & Dillet, B. (1988): Alkali amphibole, tetrasilicic mica and sodic pyroxene in peralkaline siliceous rocks, Questa Caldera, New Mexico. *American Journal of Science*, 288A, 358-392.

Droop, G.T.D. (1987): A general equation for estimating Fe^{3+} concentrations in ferromagnesian silicates and oxides from microprobe analyses, using stoichiometric criteria. *Mineralogical Magazine*, 51, 431-435.

------- (1994): Triple-chain pyriboles in Lewisian ultramafic rocks. *Mineralogical Magazine*, 58, 1-20.

Elliott, J.E. (1983): Peralkaline and peraluminous granites and related mineral deposits of the Arabian Shield. *U.S. Geological Survey Open-File Report* 83-389, 35p.

Ferguson, A.K. (1978): The crystallization of pyroxenes and amphiboles in some alkaline rocks and the presence of a pyroxene compositional gap. *Contributions to Mineralogy and Petrology*, 67, 11-15.

Fiori, C.E., Swyt, C.R. & Myklebust, R.L. (1994): NIST/NIH Desktop spectrum analyzer program, Version 2.0.1. United States Department of Commerce.

Flohr, M.J.K. (1991): Titanium-, vanadium-, and niobium mineralization at the Christy deposit, Magnet Cove alkaline igneous complex, Arkansas. *Geological Society of America*, Abstracts with Program, 23, A292.

------- & Ross, M. (1990): Alkaline igneous rocks of Magnet Cove, Arkansas: mineralogy and geochemistry of syenites. *Lithos*, 26, 67-98.

Gammons, C.H. & Seward, T.M. (1996): Stability of Mn(II) chloride complexes from 25 to 300°C. *Geochimica et Cosmochimica Acta*, 60, 4295-4311.

Ghio, A.J., Kennedy, T.P., Schapira, R.M., Crumbliss, A.L. & Hoidal, J.R. (1990): Hypothesis: is lung disease after silicate inhalation caused by oxidant generation? *Lancet*, 336, 967-969.

Gieré, R. (1986): Zirconolite, allanite and hoegbomite in a marble skarn from the Bergell contact aureole: Implication for mobility of Ti, Zr and REE. *Contributions to Mineralogy and Petrology*, 65, 459-470.

------- (1990): Hydrothermal mobility of Ti, Zr, and REE: examples from the Bergell and Adamello contact aureoles (Italy). *Terra Nova*, 2, 60-67.

------- & Williams, C.T. (1992): REE-bearing minerals in a Ti-rich vein from the Adamello contact aureole (Italy). *Contributions to Mineralogy and Petrology*, 112, 83-110.

Grapes, R., Yagi, K. & Okumura, K. (1979): Aenigmatite, sodic pyroxene, arfvedsonite and associated minerals in syenites from Morotu, Sakhalin. *Contributions to Mineralogy and Petrology*, 69, 97-103.

Grobéty, B.H. (1996): New short-range biopyribole polysomes from the Lepontine Alps, Switzerland. *American Mineralogist*, 81, 404-417.

Gutteridge, J.M.C., Beard, A.P.C. & Quinlan, G.J. (1983): Superoxide-dependent lipid peroxidation. Problems with the use of catalase as a specific probe for Fenton-derived hydroxyl radicals. *Biochemical and Biophysical Research Communications*, 117, 901-907.

Haas, J.R., Shock, E.L. & Sassani, D.C. (1995): Rare earth elements in hydrothermal systems: estimates of standard partial molal thermodynamic properties of aqueous complexes of the rare earth elements at high pressures and temperatures. *Geochimica et Cosmochimica Acta*, 59, 4329-4350.

Hawthorne, F.C. (1976): The crystal chemistry of the amphiboles. V. The structure and chemistry of arfvedsonite. *Canadian Mineralogist*, 14, 346-356.

------- (1983): The crystal chemistry of the amphiboles. *Canadian Mineralogist*, 21, 173-480.

-------, Oberti, R., Ungaretti, L. & Grice, J. (1992): Leakeite, $NaNa_2(Mg_2Fe^{3+}{}_2Li)Si_8O_{22}(OH)_2$, a new alkali amphibole from the Kajlidongri manganese mine, Jhabua district, Madhya Pradesh, India. *American Mineralogist*, 77, 1112-1115.

-------, Ungaretti, L., Oberti, R., Bottazzi, P. & Czamanske, G.K. (1993): Li: an important component in igneous alkali amphiboles. *American Mineralogist*, 78, 733-745.

-------, -------, -------, Cannillo, E. & Smelik, E.A. (1994): The mechanism of $^{[6]}$Li incorporation in amphiboles. *American Mineralogist*, 79, 443-451.

Jambor, J.L., Roberts, A.C., Owens, D.R. & Grice, J.D. (1996): Zajacite-(Ce), a new rare-earth fluoride from the Strange Lake deposit, Quebec-Labrador. *Canadian Mineralogist*, 34, 1299-1304.

Keppler, H. (1993): Influence of fluorine on the enrichment of high field strength trace elements in granitic rocks. *Contributions to Mineralogy and Petrology*, 114, 479-488.

Kovalenko, V.I., Tsaryeva, G.M., Goreclyad, A.V., Yarmolyuk, V.V., Troitsky, V.A., Hervig, R.L. & Farmer, G.L. (1995): The peralkaline granite-related Khaldzan-Buregtey rare metal (Zr, Nb, REE) deposit, Western Mongolia. *Economic Geology*, 90, 530-547.

Kwak, T.A.P. & Abeysinghe, P.B. (1987): Rare earth and uranium minerals present as daughter crystals in fluid inclusions, Mary Kathleen U-REE skarn, Queensland, Australia. *Mineralogical Magazine*, 51, 665-670.

Lund, L.G. & Aust, A.E. (1991): Mobilization of iron from crocidolite asbestos by certain chelators results in enhanced crocidolite-dependent oxygen consumption. *Archives of Biochemistry and Biophysics*, 287, 91-96.

Miller, R.R. (1986): Geology of the Strange Lake alkalic complex and the associated Zr-Y-Be-REE mineralization. Current Research, *Newfoundland Department of Mines and Energy, Mineral Development Division*, Report, 86-1, 11-19.

-------- (1988): Yttrium (Y) and other rare metals (Be, Nb, REE, Ta, Zr) in Labrador. Current Research, *Newfoundland Department of Mines and Energy, Mineral Development Division*, Report 88-1, 83-91.

------- (1996): Structural evolution of the Strange Lake peralkaline rare-element (NYF) granitic pegmatite, Quebec-Labrador. *Canadian Mineralogist*, 34, 349-371.

-------, Heaman, L.M. & Birkett, T.C. (1997): U-Pb zircon age of the Strange Lake peralkaline complex: implications for Mesoproterozoic peralkaline magmatism in north-central Labrador. *Precambrian Research*, 81, 67-83.

Mineyev, D.A. (1963): Geochemical differentiation of the rare earths. *Geochemistry International*, 12, 1129-1149 (*Geokhimiya*, 12, 1082-1100).

Moenke-Blankenburg, L. (1989): **Laser Micro Analysis**. Wiley-Interscience, New York, New York, 288p.

Nassif, G.J. (1993): The Strange Lake peralkaline complex, Québec-Labrador: The hypersolvus-subsolvus granite transition and feldspar mineralogy. McGill University, M.Sc. Thesis, Montreal, Québec, 104p.

------- & Martin, R.F. (1991): The hypersolvus granite-subsolvus granite transition at Strange Lake, Quebec-Labrador. *Geological Association of Canada - Mineralogical Association of Canada*, Abstracts with Programs, 16, A89.

------- & Martin, R.F. (1992): Feldspar mineralogy of the Strange Lake peralkaline complex, Quebec-Labrador. *Geological Association of Canada - Mineralogical Association of Canada*, Abstracts with Programs, 17, A83.

Nicholls, J. & Carmichael, J.S.E. (1969): Peralkaline acid liquids: a petrological study. *Contributions to Mineralogy and Petrology*, 20, 268-294.

Norén, B. (1967): The F complexes of Zr (IV). *Acta Chemica Scandinavica*, 21, 2457-2462.

------- (1969): Solvent extraction studies of the formation of F and sulphate complexes of Zr(IV). *Acta Chemica Scandinavica*, 23, 379-387.

O'Halloran, D.A. (1985): Ras ed Dom migrating ring complex: A-type granites and syenites from the Bayuda Desert, Sudan. *Journal of African Earth Sciences*, 3, 61-75.

Peacor, D.R. (1992): Analytical electron microscopy: x-ray analysis. *In* **Minerals and Reactions at the Atomic Scale: Transmission Electron Microscopy** (Buseck, P.R., ed.). Mineralogical Society of America, Reviews in Mineralogy, 27, 113-140.

Pillet, D. (1989): Le granite peralcalin du Lac Brisson, Labrador Central (province du Québec, Canada): pétrologie, géochronologie, et relations avec les minéralisations internes à Zr, Y, Nb. Thèse de doctorat, Université Claude Bernard: Lyon I, Lyon, France, 276p.

-------, Bonhomme, M.G., Duthou, J.L. & Chenevoy, M. (1989): Chronologie Rb/Sr et K/Ar du granite peralkalin du lac Brisson, Labrador central, Nouveau-Québec. *Canadian Journal of Earth Sciences*, 26, 328-332.

-------, Chenevoy, M. & Bélanger, M. (1993): Pétrologie du granite peralcalin du lac Brisson, Labrador central, Nouveau-Québec. II. Minéralogie et modalités de cristallisation. *Canadian Journal of Earth Sciences*, 30, 2423-2435.

Pinckston, D.R. & Smith, D.G.W. (1995): Mineralogy of the Lake Zone, Thor Lake rare-metals deposit, N.W.T., Canada. *Canadian Journal of Earth Sciences*, 32, 516-532.

Ross, M. (1984): Ultraalkalic arfvedsonite and associated richterite, acmite, and aegirine-augite in quartz syenite, Magnet Cove alkalic igneous complex, Arkansas. *EOS*, 65, 293.

Ruaya, J.R. & Seward, T.M. (1986): The stability of chloro-zinc (II) complexes in hydrothermal solutions up to 350°C. *Geochimica et Cosmochimica Acta*, 50, 651-661.

Rubin, J.N., Henry, C.D. & Price, J.G. (1993): The mobility of zirconium and other "immobile" elements during hydrothermal alteration. *Chemical Geology*, 110, 29-47.

Salvi, S. & Williams-Jones, A.E. (1990): The role of hydrothermal processes in the granite-hosted Zr, Y, REE deposit at Strange Lake, Quebec/Labrador: Evidence from fluid inclusions. *Geochimica et Cosmochimica Acta*, 54, 2403-2418.

------- & ------- (1992): Reduced orthomagmatic C-O-H-NaCl fluids in the Strange Lake rare-metal granitic complex, Quebec/Labrador, Canada. *European Journal of Mineralogy*, 4, 1155-1174.

------- & ------- (1995): Zirconosilicate phase relations in the Strange Lake (Lac Brisson) pluton, Quebec-Labrador. *American Mineralogist*, 80, 1031-1040.

------- & ------- (1996): The role of hydrothermal processes in concentrating HFSE in the Strange Lake peralkaline complex, northeastern Canada. *Geochimica et Cosmochimica Acta*, 60, 1917-1932.

------- & ------- (1997): Fischer-Tropsch synthesis of hydrocarbons during sub-solidus alteration of the Strange Lake peralkaline granite, Quebec/Labrador. *Geochimica et Cosmochimica Acta*, 61, 83-99.

Schiller, J.E., Payne, S.L. & Khalafalla, S.E. (1980): Surface charge heterogeneity in amphibole cleavage fragments and asbestos fibers. *Science*, 209, 1530-1532.

Schumacher, J.D. & Czank, M. (1987): Mineralogy of triple-and double-chain pyriboles from Orijärvi, southwest Finland. *American Mineralogist*, 72, 345-352.

Shatos, M.A., Doherty, J.M., Marsh, J.P. & Mossman, B.T. (1987): Prevention of asbestos-induced cell death in rat lung fibroblasts and alveolar macrophages by scavengers of active oxygen species. *Environmental Research*, 44, 103-116.

Smith, R.M. & Martell, A.E. (1976): **Critical stability constants. Volume 4: Inorganic complexes**. Plenum Press, New York, 257p.

Strong, D.F., Fryer, B.J. & Kerrich, R. (1984): Genesis of the St. Lawrence fluorspar deposits as indicated by fluid inclusion, rare earth element, and isotopic data. *Economic Geology*, 79, 1142-1158.

Taylor, R.P., Strong, D.F. & Fryer, B.J. (1981): Volatile control of contrasting trace element distributions in peralkaline granitic and volcanic rocks. *Contributions to Mineralogy and Petrology*, 77, 267-271.

Vard, E. & Williams-Jones, A.E. (1993): A fluid inclusion study of vug minerals in dawsonite phonolite sills, Montréal, Quebec: implications for HFSE mobility. *Contributions to Mineralogy and Petrology*, 113, 410-423.

Veblen, D.R. & Buseck, P.R. (1979): Chain-width order and disorder in biopyriboles. *American Mineralogist*, 64, 687-700.

------- & ------- (1980): Microstructures and reaction mechanisms in biopyriboles. *American Mineralogist*, 65, 599-623.

------- & ------- (1981): Hydrous pyriboles and sheet silicates in pyroxenes and uralites: intergrowth microstructures and reaction mechanisms. *American Mineralogist*, 66, 1107-1134.

------- & Burnham, C.W. (1978a): New biopyriboles from Chester, Vermont: I. Descriptive mineralogy. *American Mineralogist*, 63, 1000-1009.

------- & ------- (1978b): New biopyriboles from Chester, Vermont: II. The crystal chemistry of jimthompsonite, clinojimthompsonite, and chesterite, and the amphibole-mica reaction. *American Mineralogist*, 63, 1053-1073.

White, A.F. & Yee, A. (1985): Aqueous oxidation-reduction kinetics associated with coupled electron-cation transfer from iron-containing silicates at 25°C. *Geochimica et Cosmochimica Acta*, 49, 1263-1275.

Wood, S.A. (1990): The aqueous geochemistry of the rare-earth elements and yttrium. 1. Review of available low temperature data for inorganic complexes and the inorganic REE speciation of natural waters. *Chemical Geology*, 82, 159-186.

Woodrow, P.J. (1967): The crystal structure of astrophyllite. *Acta Crystallographica*, 22, 673-678.

Yau, Y.-C., Peacor, D.R. & Essene, E.J. (1986): Occurrence of wide-chain Ca-pyriboles as primary crystals in the Salton Sea Geothermal Field, California, USA. *Contributions to Mineralogy and Petrology*, 94, 127-134.

Zajac, I.S., Miller, R.R., Birkett, T.C. & Nantel, S. (1984): Le gîte de Zr, Y, Nb et Be du complexe alcalin de Strange Lake, Québec-Labrador. *Ministère de l'Énergie et des Ressources du Québec*, DV 84-18, 127-142.

Zalma, R., Bonneau, L, Guignard, J. & Pezerat, H. (1987a): Formation of oxy radicals by oxygen reduction arising from the surface activity of asbestos. *Canadian Journal of Chemistry*, 65, 2338-2341.

-------, -------, ------- & ------- (1987b): Production of hydroxyl radicals by iron solid compounds. *Toxicology and Environmental Chemistry*, 13, 171-187.

Chapter 6:

THE MAFIC SILICATES OF THE STRANGE LAKE PERALKALINE COMPLEX, QUEBEC-LABRADOR. III. EFFECTS OF CA-METASOMATISM.

Jeanette N. Roelofsen, Robert F. Martin[1] and David R. Veblen[2]

[1] Department of Earth and Planetary Sciences,
McGill University,
3450 University Street,
Montréal, Québec
H3A 2A7

[2] The Morton K. Blaustein Department of Earth and Planetary Sciences,
The Johns Hopkins University,
3300 North Charles Street,
Baltimore, Maryland 21210

Abstract

The effects of late-stage, metasomatic fluids on peralkaline granites can be investigated through examination of the mafic minerals, principally of arfvedsonitic amphibole. Ca-metasomatism of arfvedsonitic amphibole from the Strange Lake peralkaline complex, Québec-Labrador border, is exhibited in the altered subsolvus granite and pegmatitic bodies, especially in the ore zone. At the surface, this is expressed by the enrichment of arfvedsonitic amphibole from these units in Ca, Mg, Mn, Zn, REE and Al. In altered pegmatites, disordered, Na-, Ca-, Mg- and Fe-rich wide-chain biopyriboles are the result of metasomatism of relics of arfvedsonitic amphibole, formed by aegirine replacement of the arfvedsonitic amphibole. At depth, this metasomatism is expressed by the formation of brown winchitic amphibole at the expense of the arfvedsonitic amphibole. Transmission electron microscope examination indicates that this "amphibole" is actually manganese, zinc or manganoan zincian winchitic amphibole, which forms a rim to titanite, fluorite, quartz ± hematite veinlets. Rare chlorite-smectite intergrowths also replace this arfvedsonitic amphibole at depth. The compositional variation during these local reactions indicates that the metasomatic fluid was enriched in K, Ca, Mg, Al, Mn and Zn. Furthermore, the applications of experimental studies on the stability of chlorite-smectite intergrowths and Ca-rich biopyribole suggest formation from approximately 450°C to 150°C. The low-temperature portion of this range is in the range of the temperature of Ca-metasomatism inferred by Salvi & Williams-Jones (1990).

Introduction

The Strange Lake peralkaline A-type granite, located in Canada on the Québec-Labrador border (Fig. 1A), is considered to have economic potential as a source of Y, Zr, Nb, Be and possibly REE (Zajac et al., 1984; Miller, 1988). Recognition of this potential has led to an in depth investigation of the mineralogy and geochemistry of the products of magmatic crystallization and of the products of their hydrothermal alteration near the mineralized core of the complex. The mafic minerals, as potential hosts of some of these elements, are the subject of this investigation of the Strange Lake complex. The focus is

Figure 1A. Location of the Strange Lake peralkaline complex. It is located on the Québec-Labrador border in Canada, NE of Schefferville and W of Nain.

B. The intrusive units of the complex after Bélanger (1984) and Nassif (1993). The hypersolvus granite core of the complex is surrounded by altered subsolvus granite. The ore zone (up to 20 vol.% ore minerals) occurs in the most altered subsolvus granite. Small amounts of transsolvus granite, unaltered subsolvus granite and roof pendants also are present in the complex. The complex is surrounded by a quartz monzonite to the southwest and various gneisses, metadiorite and metagabbros to the northeast. Sample locations are indicated on the map by the various symbols.

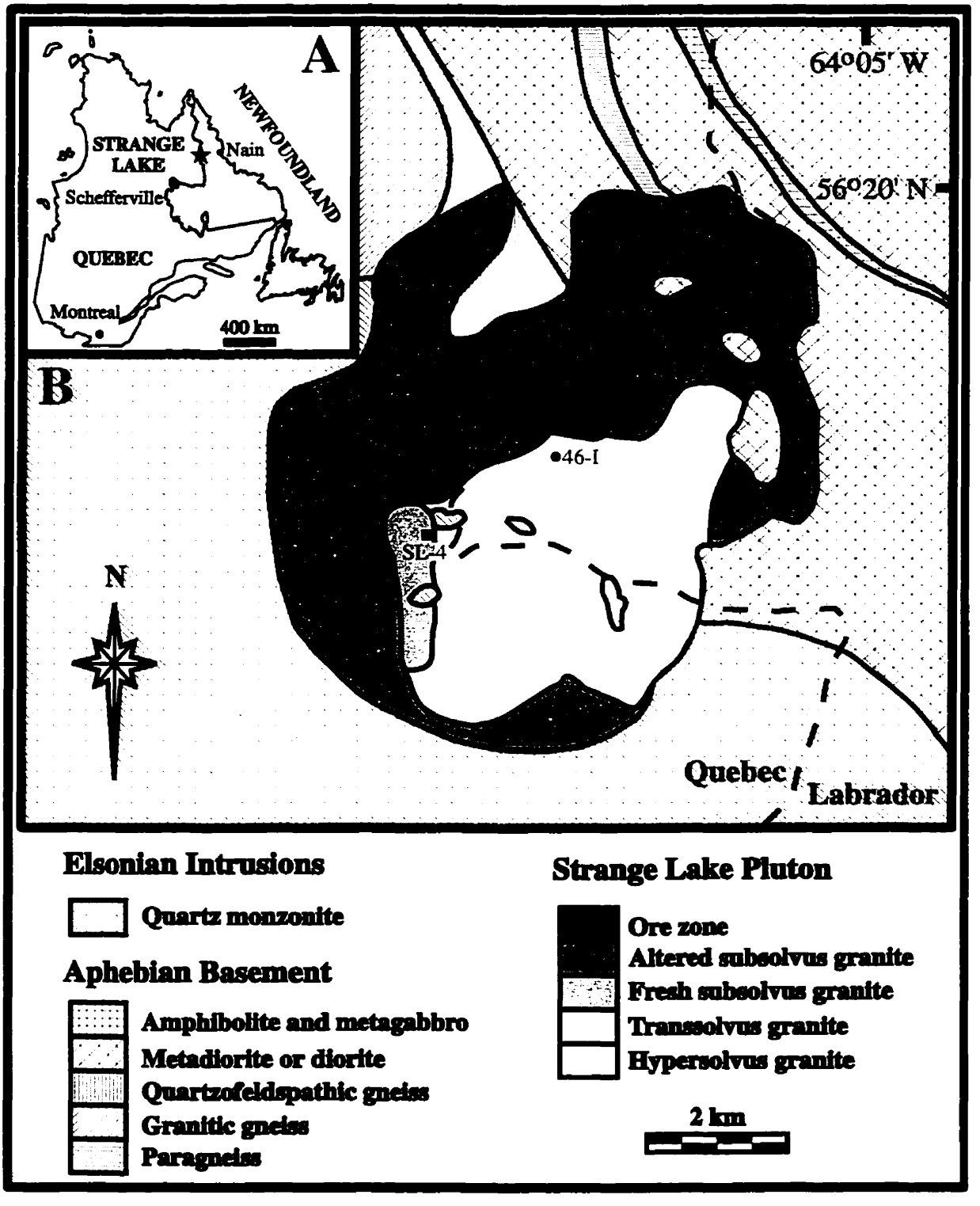
A
STRANGE LAKE
Nain
NEWFOUNDLAND
Schefferville
QUEBEC
Montreal
400 km
B
64°05' W
56°20' N
46-I
SE-4
N
Quebec
Labrador
Elsonian Intrusions
Quartz monzonite
Aphebian Basement
Amphibolite and metagabbro
Metadiorite or diorite
Quartzofeldspathic gneiss
Granitic gneiss
Paragneiss
Strange Lake Pluton
Ore zone
Altered subsolvus granite
Fresh subsolvus granite
Transsolvus granite
Hypersolvus granite
2 km

on the contrast between the primary alkaline mafic minerals in the most primitive rocks of the granitic complex, and those in the most evolved, highly metasomatized parts in and near the ore zone. In particular, the effects of Ca-metasomatism on the arfvedsonitic amphibole will be documented through results obtained largely from an investigation of samples from the more metasomatized portions of the complex by electron-microprobe and laser ablation microprobe - inductively coupled plasma - mass spectroscopy (LAM-ICP-MS) analyses and transmission electron microscopy (TEM).

Background Information

As the geology and mineralogy of the Strange Lake peralkaline complex have been described in detail in Chapter 4, only a few salient points will be noted here. The 36-km^2 Proterozoic complex is surrounded to the south and southwest by an Elsonian rapakivi quartz monzonite, and to the north and northeast by Aphebian quartzofeldspathic, calc-silicate, graphitic, dioritic, gabbroic, and anorthositic gneisses (Fig. 1B).

The peralkaline granites that comprise the Strange Lake complex have been subdivided on the basis of textural development of the dominant mineral, alkali feldspar (Nassif & Martin, 1991; Fig. 1B). Field relationships indicate that hypersolvus granite is the oldest unit. Transsolvus granite and subsolvus granite form successively younger units. The transsolvus granite occurs as wisps and isolated lenses (to 1 m) in the hypersolvus granite in the southeastern part of the complex and as enclaves in the subsolvus granite (Nassif, 1993). The younger subsolvus granite surrounds the hypersolvus granite. This subsolvus granite was later altered in the northern part of the complex, although it remained unaltered in a small region in the western portion. Pegmatite bodies (on average 1-2 m), both fresh and altered, are present throughout the complex, but mostly in the altered subsolvus granite, especially in and near the ore zone (Nassif, 1993).

The ore mineral content ranges from 5 vol.% in the hypersolvus granite, to 15 vol.% in altered subsolvus granite, and up to 20 vol.% in the ore zone (Zajac et al., 1984; Miller, 1986). The complex contains a deposit of 52 million tonnes of ore, with 2.93 wt.% ZrO_2, 0.54 wt.% REE_2O_3, 0.31 wt.% Y_2O_3, 0.08 wt.% BeO and 0.38 wt.% Nb_2O_5, present as calcium and sodium zirconosilicates (e.g., elpidite, gittinsite and armstrongite), zircon,

kainosite [$Ca_2(Y,LREE)_2Si_4O_{12}(CO_3)\bullet H_2O$], gadolinite [$(LREE,Y)_2Fe^{2+}Be_2Si_2O_{10}$], gagarinite [$NaCa(LREE,Y)(F,Cl)_6$], bastnäsite, monazite and pyrochlore (Miller, 1988; Birkett et al., 1992).

Miller (1996) and Birkett et al. (1992) proposed a magmatic origin for the calcium zirconosilicates (and by implication, the other ore minerals) based largely on textural evidence, whereas Salvi & Williams-Jones (1990, 1995) and, to a lesser extent, Pillet et al. (1992, 1993), suggested formation following a low-temperature episode (<200°C) of Ca-metasomatism. Birkett et al. (1992) proposed that the euhedral nature of the hydrous sodic zirconosilicate elpidite and the hydrous calcic zirconosilicate armstrongite are indicative of a magmatic origin. Their textural observations imply that the anhydrous calcic zirconosilicate gittinsite replaced armstrongite. A fluid inclusion study by Salvi & Williams-Jones (1990) of quartz associated with gittinsite as a replacement of an earlier zirconosilicate in and near the ore zone, indicated that the fluid was trapped at low temperature. Salvi & Williams-Jones (1990) also pointed out, as did Pillet et al. (1993), that bulk-rock analyses of material from the altered granite, especially in the ore zone, indicates a unusual enrichment in Ca that is difficult to explain solely by magmatic evolution. In their model for the transformation of elpidite to calcium zirconosilicates, Salvi & Williams-Jones (1995) indicated that both armstrongite and gittinsite are of secondary origin. The net addition of Ca to specific units of the complex was confirmed quantitatively by Salvi & Williams-Jones (1996). This Ca-metasomatic event followed a high-temperature (>350°C; Salvi & Williams-Jones, 1992) Na-metasomatic event during which aegirine replaced arfvedsonitic amphibole (Chapter 5). In the present study, the effects of Ca-metasomatism on the arfvedsonitic amphibole are examined.

Review of the Mafic Silicates at Strange Lake

The mafic silicates, arfvedsonitic amphibole, aegirine, astrophyllite, aenigmatite and neptunite, comprise, on average, 5 to 20 vol.% of the granites. Where all occur in the hypersolvus and fresh subsolvus granites, only those that contain the most Fe^{3+} (arfvedsonitic amphibole and aegirine) are present in the altered subsolvus granite (Pillet et al., 1993; Birkett et al., 1996). This suggests that astrophyllite, aenigmatite, neptunite and

bafertisite formed under low fO_2 conditions, unlike those that prevailed in the altered subsolvus granite. The mafic silicate assemblages are correlated with the type of oxide present in the granite. In the hypersolvus granite, ilmenite occurs as rare inclusions in arfvedsonitic amphibole and alkali Ti silicates, whereas in the altered subsolvus granite and the ore zone, fine-grained, disseminated hematite (max. 5-10 vol.%) results in a reddish hue to the granite, in which aegirine is the dominant mafic silicate. These mineralogical differences between the units can be attributed to a late increase in fO_2, as noted by Salvi & Williams-Jones (1990, 1996) and Nassif (1993).

Pillet et al. (1993) and Birkett et al. (1996) documented the paragenesis of these mafic silicates. However, the data of Pillet et al. (1993) do not include information on some elements (e.g., Zr), which are enriched in the deposit and commonly present in mafic silicates, such as amphibole, from anorogenic complexes (Borley, 1976). This situation makes it difficult to evaluate the role played by alteration of the mafic silicate in the formation of the associated ore deposit at Strange Lake.

Pillet et al. (1993) classified the amphibole from the complex based on the unit of the granite within which it was present and showed some of the compositional variation of the amphibole present. Furthermore, Birkett et al. (1996) observed that both the arfvedsonitic amphibole and aegirine crystallized in three stages. In each case, the amphibole crystallized before the pyroxene. Unfortunately, they did not report the compositional variation of these minerals. These three stages of crystallization and compositional variation, as noted by Birkett et al. (1996) and Pillet et al. (1993), respectively, are concurrent with that observed in Chapter 4. Furthermore, the influence of Na-metasomatism (aegirine replacement of arfvedsonitic amphibole) noted by Pillet et al. (1993) was documented in detail in Chapter 5. However, in none of the studies were the effects of Ca-metasomatism recognized on the mafic silicates.

Application of Analytical Methods

The compositional variation of arfvedsonitic amphibole can best be studied by electron-microprobe and LAM-ICP-MS analyses, in combination with TEM examination. Transmission electron microscopy offers the best method with which to examine the fine-

scale modifications of these mafic silicates produced by metasomatism. The LAM-ICP-MS approach is important, as it allows simultaneous point analysis of a sample for many elements, which are commonly present only in minor and trace concentrations in the amphibole. These elements are significant in that they are major constituents of the ore deposit.

Most TEM studies, to date, concerned the investigation on silicates of retrograde or metasomatic origin from calc-alkaline or mafic igneous and metamorphic rocks (Veblen & Buseck, 1979, 1980, 1981; Akai, 1982; Akai et al., 1985; Yau et al., 1986; Schumacher & Czank, 1987; Droop, 1994). Ordered intergrowths of amphibole and mica occur in the Ca-, Mg- and Fe-rich wide-chain biopyriboles jimthompsonite and chesterite (Veblen & Burnham, 1978a, 1978b; Veblen & Buseck, 1979, 1981). CaMg, MnMg and NaMg variants of chesterite were synthesized by Tateyama et al. (1978), Maresch & Czank (1983), Akai & Saito (1985), Graham et al. (1989) and Welch et al. (1992). Akai & Saito (1985) also suggested that there is a limit to the amount of Na that can be incorporated in a CaMg wide-chain biopyribole, and consequently, Na-rich biopyriboles are rare. TEM studies also have identified minor biopyribole defects in the natural, asbestiform Na- and Fe-rich amphibole riebeckite (e.g., Chisholm, 1973; Ahn & Buseck, 1991). Another aim of the present study is to determine whether an $NaFe^{3+}$- and CaMg-enriched wide-chain biopyribole occurs in arfvedsonitic amphibole from the Strange Lake complex.

In this study, the effects of Ca-metasomatism on the arfvedsonitic amphibole will be examined. For reasons of convenience, the cutoff between the early Na- and later Ca-metasomatism was arbitrarily set at 200°C, as this is the upper temperature limit of Ca-metasomatism determined by Salvi & Williams-Jones (1990) on the basis of results of their fluid inclusion study.

Methodology

Electron-microprobe analysis

The amphibole, aegirine and phyllosilicates were analyzed using both Cameca Camebax and JEOL 840 electron microprobes operated in wavelength-dispersion spectrometry mode (WDS). The instruments were operated at an accelerating voltage of 15

or 20 kV and a beam current of 20 or 30 nA with a slightly defocused beam (5 to 7 μm). Collection times were 25 s for major elements, 50 s for most minor elements, and 100 s for the rest (including F and Cl). A full description of the standards employed is provided in Chapter 4. The structural formulae of amphibole were calculated based on 23 atoms of oxygen, with the proportion of Fe^{3+} estimated by charge balance (16 cations and assumption of full occupancy of the sites) after the method of Droop (1987). Chemical formulae of aegirine were calculated based on 4 cations and 6 atoms of oxygen, with the proportion of Fe^{3+} estimated in the same manner as for the amphibole.

LAM-ICP-MS

Point analyses were performed on mounts of oriented grains by LAM-ICP-MS. The LAM-ICP-MS analyses were performed in two stages: first, samples were analyzed for elements with low atomic number (Z; ^{6}Li, ^{9}Be and ^{11}B), followed by those of higher Z (e.g., ^{85}Rb, ^{88}Sr, ^{89}Y, ^{90}Zr, ^{93}Nb, ^{138}Ba, ^{139}La, ^{140}Ce, ^{141}Pr, ^{146}Nd, ^{147}Sm, ^{151}Eu, ^{157}Gd, ^{159}Tb, ^{162}Dy, ^{165}Ho, ^{166}Er, ^{169}Tm, ^{174}Yb, ^{175}Lu, ^{178}Hf, ^{232}Th and ^{238}U). Further description of sample-preparation techniques, standards used, analytical conditions and comparison with analyses of bulk samples by ICP-MS can be found in Chapter 4 and Appendices B-4, B-5, B-6 and B-7.

TEM

Selected regions of samples were prepared for TEM examination by ion-thinning samples on 2.3 mm Cu grids, which had been glued to thin sections prepared with either Crystalbond® or bees' wax, and removed by heating at a low temperature (<100°C) on a hot plate. The samples were then ion-thinned on a Gatan dual ion mill (model 600) with Ar guns operated at 6 keV, 1 mA or 0.5 mA and tilted at 17°. For the final stage of ion-thinning, the mill was operated at 6 keV or 0.5 mA at a tilt angle of 12°. To prevent charging by the beam, the sample was coated with carbon.

TEM work involved high-resolution TEM (HRTEM), selected-area electron diffraction (SAED) and analytical electron microscopy (AEM) with a Philips EM420ST, operated at an accelerating voltage of 120 keV. Standardless AEM analyses were performed with a Li-drifted silicon detector. Element concentrations were calculated with the program

DTSA [Desk-Top Spectrum Analyzer; Fiori et al. (1994)]. The estimated error in these analyses is approximately 4% of the measured values. The main drawback of AEM analyses on arfvedsonitic amphibole is the overlap between $F_{K\alpha}$ and Fe_L peaks precludes determination of the F content. Mineral formulae of amphibole derived from AEM data were calculated on the basis of 23 atoms of oxygen, excluding F, and thus the proportion of Fe^{3+} was not calculated. The other mineral formulae were calculated on the basis of 6 atoms of oxygen for pyroxene, 28 atoms of oxygen for chlorite, and 22 atoms of oxygen for the other phyllosilicates. Mineral formulae for titanite and hematite were calculated on the basis of 5 and 3 atoms of oxygen, respectively.

Results

Summary of Findings Concerning the Primary Assemblages

Three types of primary arfvedsonitic amphibole were described in Chapter 4. They are: 1) early, inclusion-bearing Na- and Fe-rich amphibole from the hypersolvus granite (Type-1a) with inclusion-free rims that are slightly enriched in Ca, Mg, Mn and Zn (Type-1b); 2) amphibole of grains composed of zones of amphibole and an assemblage of yellow aegirine, hematite±quartz from the subsolvus granite that is even more enriched in Ca, Mg, Mn and Zn than Type-1; 3) fine-grained, acicular, euhedral amphibole grains that are all oriented with their *c* axes parallel. Type-3 amphibole is the dominant mineral of late mafic pods or mat-like regions in or near the ore zone or in the altered subsolvus granite near the contact with the hypersolvus granite. The arfvedsonitic amphibole suite varies from Na- and Fe-rich in Type-1 to Zn-, and Mn-rich Type-3 Li-bearing potassian-fluor-arfvedsonite. Furthermore, the concentration of Zr decreases and that of ΣREE increases in these amphiboles in the sequence from Type-1 to -3, although Type-1 amphibole contains more HREE than the others. The trends represented by Type-1, -3 and much of that of Type-2 amphibole are a reflection of magma evolution. In Chapter 4, I suggested that the enrichment of some of the Type-2 amphibole from the altered subsolvus granite in Ca, Mg, Mn, Zn, Al, REE and HFSE was a consequence of Ca-metasomatism.

Three types of aegirine are associated with these arfvedsonitic amphiboles. They are: 1) bright green, primary Ti-rich (up to 4.91 wt.% TiO_2) topotactic rims on amphibole

from the hypersolvus and fresh subsolvus granites; 2) topotactic yellow to colourless, slightly Ti-, Mn- and Ca-enriched aegirine that replaced Type-1 and -2 amphibole in all units except the transsolvus granite; and 3) yellow green, euhedral, primary or secondary, almost pure aegirine, which is slightly enriched in Ca and Mn and contains minor Ti. Type-3 aegirine is the dominant mafic silicate in pegmatite bodies in and near the ore zone or locally in the altered subsolvus granite at the erosional surface.

Textural Relationship of the Mafic Silicates Subjected to Ca-metasomatism

The textures described below pertain to samples upon which the effects of Ca-metasomatism were identified from electron-microprobe analyses, as they cannot, in general, be discerned solely by optical examination.

Amphibole from pegmatites varies from fresh to that which has been replaced by aegirine (e.g., SL-4-15 or 46-I-3, respectively; location in Fig. 1B) during Na-metasomatism. Composite grains of arfvedsonitic amphibole (60 vol.%) and aegirine (approx. 40 vol.%) are present in altered pegmatites in the hypersolvus granite near its contact with the altered subsolvus granite and near the ore zone (46-I-3; Fig. 2). The amphibole is replaced in a topotactic relationship (parallel to the *c* axes) by pale yellow Type-2 aegirine (30 to 40 vol.%). Angular relics of arfvedsonitic amphibole are present in this aegirine, especially near the amphibole - aegirine contact. Finally, minor (<5 vol.%) primary green Type-1 aegirine rims both the Type-2 aegirine and amphibole.

In the ore zone or extremely altered subsolvus granite, arfvedsonitic amphibole and Types-2 and -3 aegirine are present. Type-3 aegirine is the dominant mafic silicate in pegmatites at the erosional surface. The proportion of Type-2 aegirine that replaced arfvedsonitic amphibole increases with depth in the core of the equigranular subsolvus granite (classification after Salvi & Williams-Jones, 1995; Chapter 5). Outside this region, arfvedsonitic amphibole occurs as phenocrysts or as both phenocrysts and interstitial grains. In the center of this portion of the equigranular subsolvus granite, arfvedsonitic amphibole is replaced along the cleavage by purplish brown amphibole (hereafter termed brown or Type-4 amphibole) associated with rare hematite (Fig. 3).

Rare fine- to medium-grained pale green pleochroic chlorite that exhibits prussian blue birefringence occurs in veins along with quartz that crosscut arfvedsonitic amphibole

Figure 2. Arfvedsonitic amphibole - aegirine relationship in the altered pegmatite (sample 46-I-3), as depicted in a transmitted-light photomicrograph. Small, angular relics of Type-2 aegirine (aeg) are present in Type-1 arfvedsonitic amphibole (arf). This region near the contact between the aegirine and main amphibole suggests that the amphibole has been replaced by aegirine (width of field of view is 4 mm).

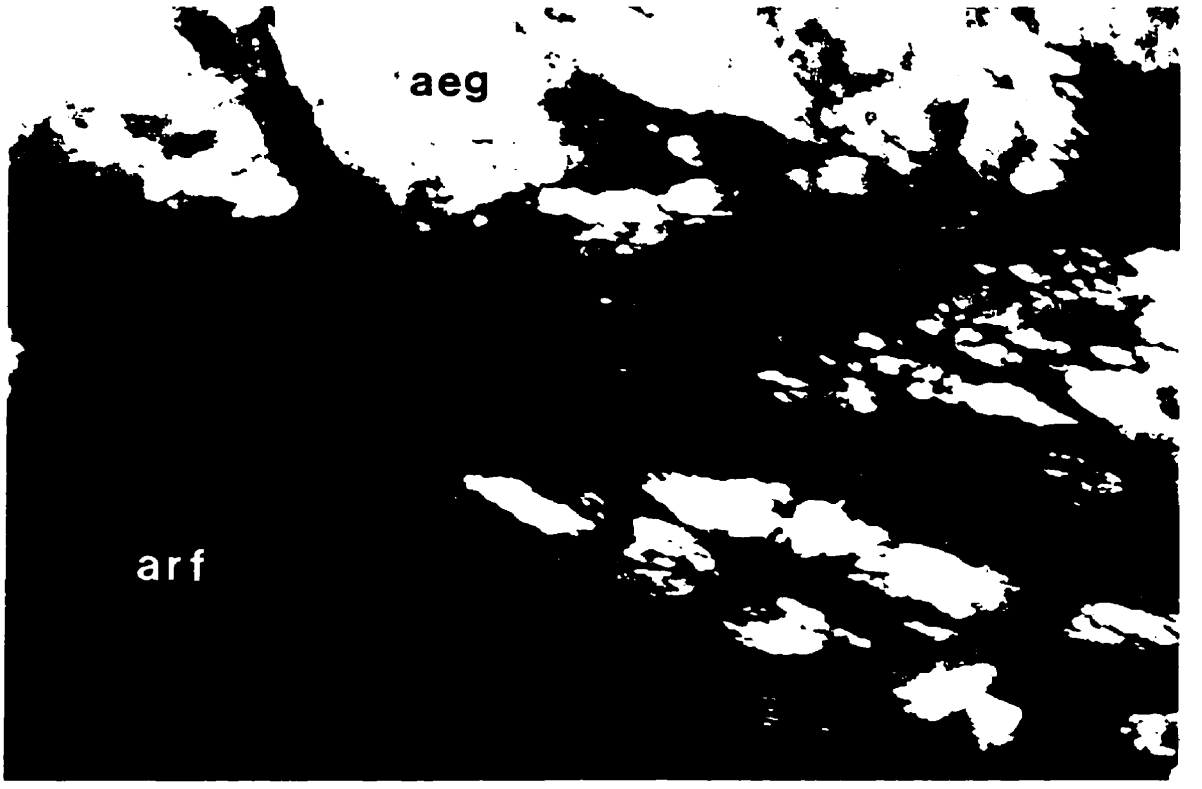
aeg
arf

Figure 3. Transmitted-light photomicrograph of arfvedsonitic amphibole (arf), surrounded by quartz (qtz), that has been replaced along the cleavages by a light purple brown amphibole (br) from drill core SL-182 (at a depth of 54.7 m) in the ore zone (width of field of view is 4 mm).

qtz
arf
br

in this region (Chapter 5; Fig. 4). Its occurrence, and close association with regions of the drill-core that contain Type-4 amphibole and Type-2 aegirine, suggest a metasomatic origin. As this mineral was not dealt with in Chapter 5, its origin will be discussed in greater detail in this chapter. The chlorite and Type-4 amphibole are the only minerals in which the effects of Ca-metasomatism can be readily identified by thin-section examination.

Compositional Variation

Representative electron-microprobe and LAM-ICP-MS analyses of the arfvedsonitic amphibole are listed in Table 1, Appendices B-1 and B-5 and in Chapter 4. An assessment of the relative errors of LAM-ICP-MS analyses can be found in Appendix B-7 and in Chapter 4.

Arfvedsonitic amphibole from altered pegmatite (e.g., 46-I-3) and some analyses of amphibole in the altered subsolvus granite are more enriched in Ca, Mg, Mn, Zn, Al, REE and HFSE (Zr and Nb), but depleted in Li, compared to that from the other units (Table 1; Appendices B-1 and B-5). Concentrations of the pairs Ca and Sr and Zr and Y in these examples of Type-2 arfvedsonitic amphibole appear to be correlated. Other correlations are between Mn and the elements: Rb, Zr, Nb and HREE. However, the amphibole most enriched in the majority of these elements is the brown, Type-4 replacement amphibole. It is enriched in Zr, Al and Zn and varies from manganoan to manganese (ferro-ferri-) winchite to ferro-richterite. Moreover, Type-2 arfvedsonitic amphibole from altered pegmatites (46-I-3) in hypersolvus granite is distinctly enriched in Mn (Fig. 5), Zr and Nb, but depleted in REE compared to that from the altered subsolvus granite. Figure 5A also shows that Ca-enriched arfvedsonitic amphibole in the altered subsolvus granite shows that the increase in La parallels that of CaO. On the other hand, the hypersolvus granite exhibits no variation at all between La and CaO. Although the enrichment in Mn (and to a lesser extent REE) in the altered pegmatites is comparable to that from the mafic pods (ref. Chapter 4), amphibole from these pods is depleted in Zr and likely Nb (the presence of numerous tiny pyrochlore inclusions makes this difficult to ascertain). As amphibole from the mafic pods (SL-BS-1) represents the cumulation of the magmatic evolution of the complex, the elemental enrichments are unrelated to those observed during Ca-metasomatism. Thus, although some of the compositional variation of arfvedsonitic amphibole may be attributed to magmatic

Figure 4. Rare alteration of arfvedsonitic amphibole (arf) to chlorite (at the tip of the arrow) is only present in quartz veins in the drill core LB-30 (depth of 15.80 m), as depicted in this photomicrograph (transmitted light). The large, darker grain in the center of the image is elpidite (elp). These grains are surrounded by quartz (qtz; width of field of view is 4 mm).

elp
qtz

Table 1: Selected combined analyses of arfvedsonitic amphibole and aegirine.

Mineral	**Amph.**	**Amph.**	**Aeg.**	**Amph.**	**Amph.**	**Amph.**
Unit	**Hyper.**	**Fresh Sub.**	**Altered Peg.**		**Altered Sub.**	
Type	**Type 1**	**Type 2**	**Type 2**	**Type 2**	**Type 2**	**Type 2**
Sample#	**48-A-7**	**38-B-3**	**46-I-3**	**46-I-3**	**63-B-1**	**SL-1-17**
SiO_2	50.53	50.57	52.14	50.87	50.39	49.31
Al_2O_3	0.41	0.40	0.17	0.15	0.30	1.07
TiO_2	0.93	1.12	0.63	0.94	1.61	1.14
FeO	33.84	33.34	30.63	31.82	32.82	32.70
MgO	0.01	0.15	0.00	0.00	0.19	0.31
MnO	0.60	0.66	0.59	1.45	0.80	0.65
ZnO	0.22	0.19	0.04	0.50	0.30	0.18
Cr_2O_3	0.00	0.00	0.00	0.00	0.00	0.00
V_2O_3	0.00	0.02	0.01	0.01	0.01	0.00
Nb_2O_5	0.00	0.00	0.04	0.02	0.00	0.00
ZrO_2	0.21	0.16	0.07	0.56	0.21	0.09
Y_2O_3	0.00	0.00	0.00	0.00	0.00	0.00
Yb_2O_3	0.01	0.00	0.01	0.01	0.03	0.00
Na_2O	9.59	9.53	13.94	8.94	9.34	8.91
K_2O	1.24	1.30	0.00	2.20	1.51	1.24
CaO	0.18	0.35	0.13	0.20	0.32	1.91
F	2.09	2.04	0.00	1.74	1.93	2.66
Cl	0.01	0.01	0.01	0.00	0.01	0.01
Total	98.98	98.97	98.41	98.67	98.94	99.05

Table 1: Selected combined analyses of arfvedsonitic amphibole and aegirine (continued).*

Mineral	Amph.	Amph.	Aeg.	Amph.	Amph.	Amph.
Unit	Hyper.	Fresh Sub.	Altered Peg.		Altered Sub.	
Type	Type 1	Type 2	Type 2	Type 2	Type 2	Type 2
Sample#	48-A-7	38-B-3	46-I-3	46-I-3	63-B-1	SL-1-17
Li	1468	1301	18	1955	967	1189
Be	10	102	36	18	27	26
B	3	22	30	8	3	4
V	0	1	1	0	0	2
Cr	2	1	1	1	1	0
Zn	2579	2334	1728	7209	3712	1999
Rb	32	28	49	56	27	17
Sr	2	3	14	2	4	6
Y	29	35	187	89	64	65
Zr	1831	1368	4191	5770	1576	942
Nb	78	75	1118	350	130	1893
Ba	1	1	38	2	5	25
La	4	9	26	2	6	30
Ce	15	25	90	8	20	96
Pr	2	4	7	1	3	14
Nd	9	16	27	6	11	55
Sm	2	2	16	2	3	14
Eu	0	0	1	0	0	1
Gd	1	2	20	2	2	11
Tb	0	0	7	1	1	2
Dy	4	5	53	8	9	15
Ho	2	2	11	5	4	4
Er	11	13	39	41	33	19
Tm	4	4	10	15	12	5
Yb	45	48	113	172	143	61
Lu	11	12	23	35	35	15
Hf	94	51	148	220	55	32
Th	0	0	33	0	0	165
U	0	0	24	0	0	46
Σ REE	111	144	443	298	282	342

* Concentrations in ppm.
Hyp.=hypersolvus; Sub.=subsolvus; Peg.=pegmatite
Amph.=amphibole; Aeg.=aegirine.

Figure 5. Plots showing the relationship between La and CaO or La and MnO in the arfvedsonitic amphibole from the hypersolvus granite (H), altered pegmatite from the hypersolvus granite (46-I-3), fresh subsolvus granite (S fresh), altered subsolvus granite (S alt) and ultramafic pods (SL-BS-1). The CaO and MnO contents were determined through electron-microprobe analysis, while that of La was determined by LAM-ICP-MS analysis. In most cases, the amphibole seems to be mildly enriched in Ca, Mn and La.

A. La (in ppm) versus CaO (in wt.%) plot. These elements show a weak positive correlation in some of the points analyzed. Analyses which show the highest La values cannot be correlated with a specific sample or unit. This is not true of amphibole in the hypersolvus granite, as it shows very little variation. The distinct enrichment of some amphibole data in La is likely the result of the presence of minute REE-rich inclusions (see text; Chapter 4). The more Ca-rich amphibole in the altered subsolvus granite shows either a slight concurrent increase or a larger increase in La content with that of CaO.

B. La (in ppm) versus MnO (in wt.%) plot, where no distinct correlation is observed between the La and MnO. However, amphiboles from the mafic pods and altered pegmatites in the hypersolvus granite are distinctly enriched in Mn compared to that from the other units (refer to text).

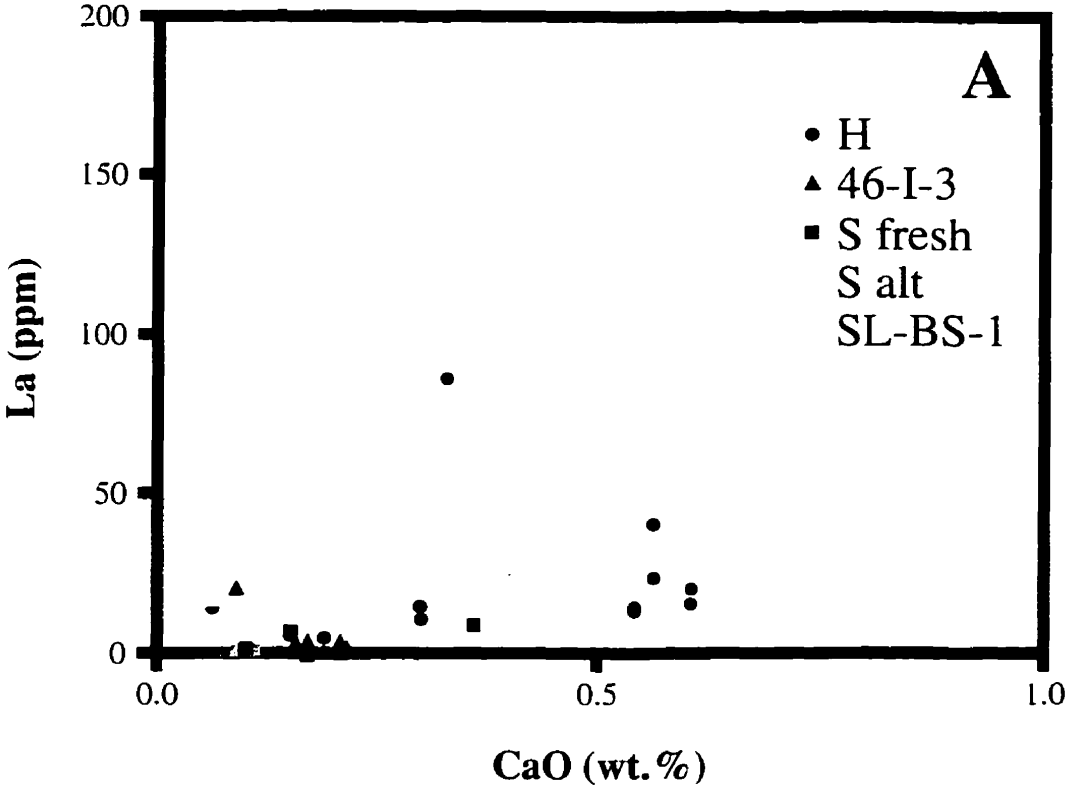
A
• H
▲ 46-I-3
■ S fresh
S alt
SL-BS-1
La (ppm)
200
150
100
50
0
0.0
0.5
1.0
CaO (wt.%)

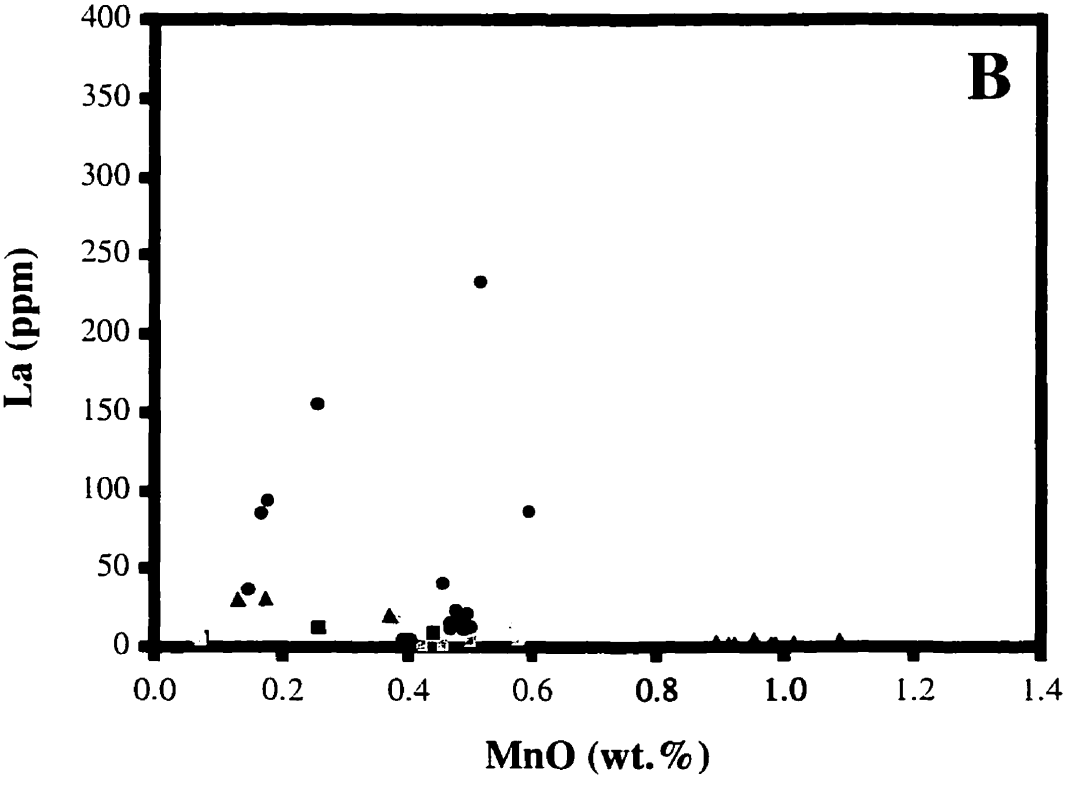
B
La (ppm)
400
350
300
250
200
150
100
50
0
0.0
0.2
0.4
0.6
0.8
1.0
1.2
1.4
MnO (wt.%)

evolution, the distinct enrichment in Ca, Mn, Zr, Al, Mn and possibly in Mg of the amphibole from the altered pegmatites in the hypersolvus granite (sample 46-I-3) and some samples of altered subsolvus granite corresponds to that observed in Type-4 amphibole, which is clearly of Ca-metasomatic origin.

In diamond drill hole SL-182, the average composition of the arfvedsonitic amphibole is approximately constant above and below the portion of the drill core that contains equigranular subsolvus granite (Fig. 6). This is the same portion of the drill core that contains the zirconosilicates elpidite, armstrongite and gittinsite documented by Salvi & Williams-Jones (1995). It is also in this region that the composition of the arfvedsonitic amphibole shows increases in the amount of Mn and F, but depletions in Ca (in general) and Mg. Wide variations exist in the contents of Zn, K and Zr of these amphiboles. These compositional variations may be related to a change in the texture of the amphibole from blocky phenocrysts to interstitial grains, or may result from the presence of minute intergrowths with Type-4 amphibole and Type-2 aegirine. Both Na- and Ca-metasomatism are reflected by the presence of Type-2 aegirine and Type-4 amphibole, respectively. The influence of Ca-metasomatism can only be tested through examination with the TEM even though the compositional variation of the arfvedsonitic amphibole is consistent with the influence of a Ca-metasomatic fluid.

Finally, chlorite varies from Si-, Mn- and Zn-rich (e.g., MnO 3.66 wt.%, ZnO 7.06 wt.%) clinochlore to chamosite (Table 2; Appendix B-15). Although it was not observed at depth in the drill hole illustrated in Figure 6, it has been observed in drill hole LB-30 (ref. Fig. 6 in Chapter 5).

Signs of Ca-metasomatism in the Mafic Silicates at the TEM Scale

Arfvedsonitic Amphibole from Altered Pegmatite

A low-resolution TEM image (Fig. 7A) of the margin between the arfvedsonitic amphibole and aegirine, taken perpendicular to the *c* axis of the silicates from sample 46-I-3, shows that the relict grain of what appears, on thin-section examination, to be arfvedsonitic amphibole (the center of the image) is composed of a number of grains. The

Figure 6. Compositional variation of arfvedsonitic amphibole with depth in drill hole SL-182, and relationship of composition of the arfvedsonitic amphibole to the textural development of the mafic silicates and zirconosilicates. The drill core depicted at the center of the figure is identical to that from Figure 6 of Chapter 5. The units are in sequence from the surface: a) overburden, b) porphyritic granite, c) equigranular granite and pegmatite, and d) porphyritic granite as defined by Salvi & Williams-Jones (1995). The other acronyms in the figure refer to the presence or absence of inclusions or the texture of the amphibole (after Chapter 5): inc for mafic inclusion, ph for phenocrysts, 2a for two different types of amphibole (phenocrysts and interstitial), and i for interstitial. The shaded square represents brown amphibole, while the shaded prism represents Type-2 (yellow) aegirine. The thick wavy lines represent the separation between zones having distinct types of zirconosilicate, as denoted by Salvi & Williams-Jones (1995). The upper portion of the drill core contains gittinsite and quartz, the middle portion contains elpidite, armstrongite and gittinsite, and the lower portion contains elpidite only. Note that the transition to elpidite only corresponds to the termination of the Type-2 aegirine zone. Finally, the thin wavy lines represent a transitional contact between the different types of granite.

A. Variation in Na, K, Fe^{2+} and F content (in apfu) of arfvedsonitic amphibole. All of these elements show minor variations in the equigranular granite compared to the porphyritic granite

B. Variation in Mg, Mn, Zn, Zr and Ca content (in apfu) of arfvedsonitic amphibole. All of these elements show distinct variations within 10 m of edge of the equigranular granite.

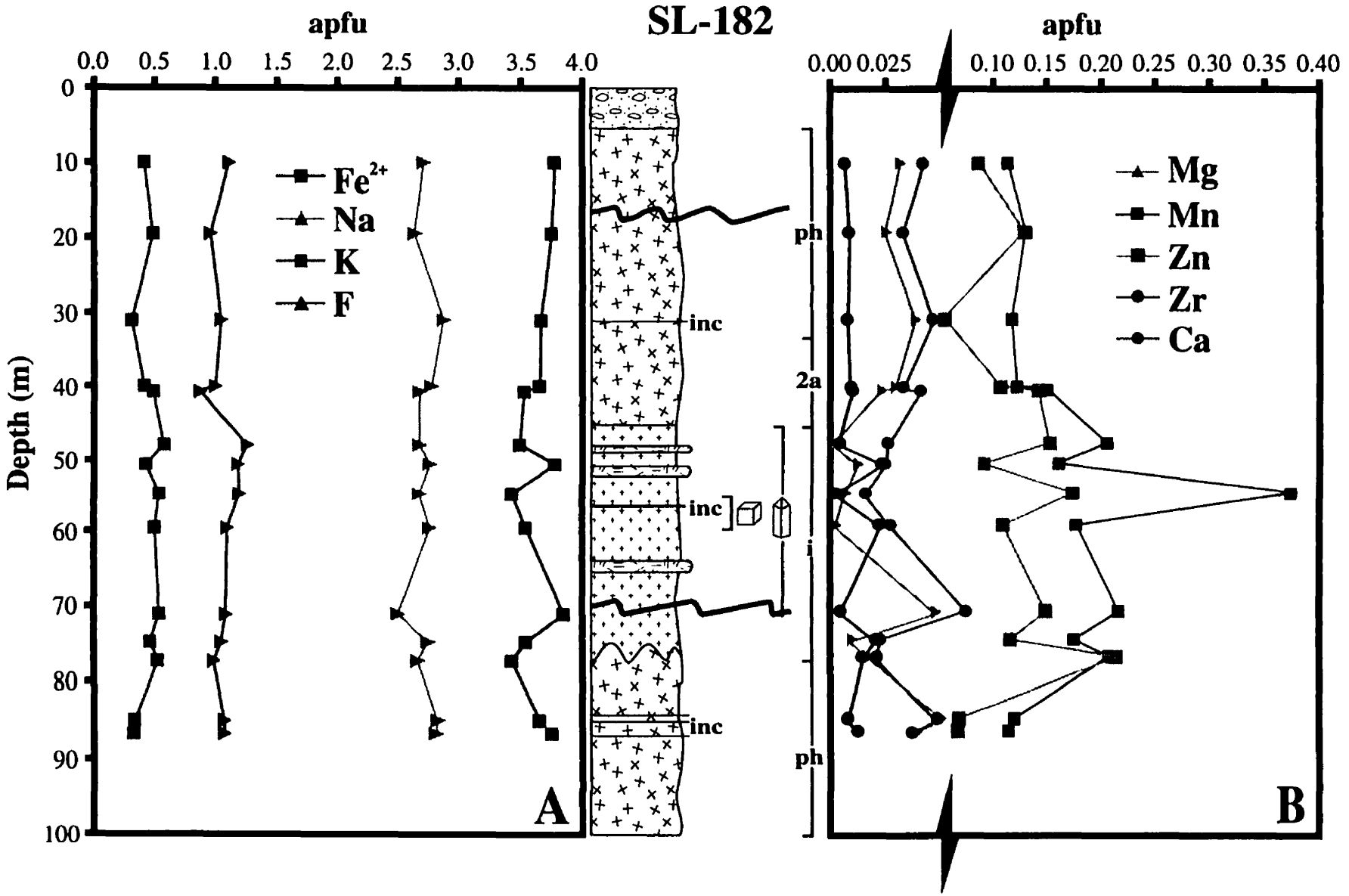
SL-182
apfu
0.0 0.5 1.0 1.5 2.0 2.5 3.0 3.5 4.0
Depth (m)
0 10 20 30 40 50 60 70 80 90 100
Fe2+
Na
K
F
A
inc
inc
inc
ph
2a
i
ph
apfu
0.00 0.025 0.10 0.15 0.20 0.25 0.30 0.35 0.40
Mg
Mn
Zn
Zr
Ca
B

Table 2: Representative electron-microprobe analyses of specific replacements.*

Mineral	Amphibole		Aegirine	
Unit	Altered Pegmatite	Altered Pegmatite	Altered Pegmatite	Altered Pegmatite
Type	Type-2	Type-2	Type-2	Type-2
Description	bleb in pyx	near pyx		
Sample #	46-I-3	46-I-3	46-I-3	46-I-3
Na_2O	13.86	9.10	13.33	13.67
K_2O	0.00	2.13	0.00	0.00
CaO	0.09	0.21	0.14	0.00
MgO	0.01	0.00	0.00	0.03
Fe_2O_3	n.d.	n.d.	29.62	32.18
FeO	29.64	31.40	3.44	1.24
MnO	0.60	1.43	n.d.	0.37
ZnO	0.00	0.50	0.10	0.00
Nb_2O_5	0.00	0.01	n.d.	0.00
V_2O_3	0.00	0.01	0.01	0.00
Cr_2O_3	0.01	0.00	0.01	0.00
Yb_2O_3	0.00	0.02	n.d.	0.00
ZrO_2	0.63	0.60	0.37	0.07
TiO_2	0.14	0.15	0.77	0.59
Al_2O_3	0.94	0.95	0.18	0.35
SiO_2	51.68	51.20	52.16	51.72
F	0.00	1.80	0.00	0.00
Cl	0.01	0.00	0.00	0.00
Total	97.60	98.74	100.13	100.23

Fe_2O_3 for aegirine calculated from charge balance
n.d. not determined
pyx=aegirine; bleb=small region of amphibole

Table 2: Representative electron-microprobe analyses of specific replacements (continued).

Mineral	**Type-4 Amphibole**		**Chlorite**	
Unit	**Altered Subsolvus**	**Altered Subsolvus**	**Subsolvus**	**Subsolvus**
Type				
Description	**bram**	**alt**		**dkalt**
Sample #	**SL-8-1**	**SL-8-1**	**LB-30-15.8**	**LB-30-11.7**
Na_2O	7.97	7.09	0.26	0.13
K_2O	2.89	2.21	0.03	0.77
CaO	0.07	0.11	0.78	1.40
MgO	0.11	0.33	16.07	16.66
Fe_2O_3	n.d.	n.d.	n.d.	n.d.
FeO	27.30	29.08	16.95	12.89
MnO	3.38	1.55	3.61	0.55
ZnO	3.43	1.64	7.06	2.36
Nb_2O_5	0.01	0.00	0.00	0.03
V_2O_3	n.d.	n.d.	n.d.	n.d.
Cr_2O_3	n.d.	n.d.	n.d.	n.d.
Yb_2O_3	n.d.	n.d.	n.d.	n.d.
ZrO_2	0.05	0.05	0.02	0.00
TiO_2	0.60	0.63	0.02	0.07
Al_2O_3	3.05	0.41	8.05	10.21
SiO_2	46.93	51.71	33.14	43.67
F	1.50	1.83	0.02	0.41
Cl	n.d.	n.d.	n.d.	n.d.
Total	97.29	96.63	86.00	89.15

n.d. not determined
bram=brown amphibole; alt=alteration; dkalt=dark alteration

Figure 7. Relict amphibole in Type-2 aegirine, oriented perpendicular to their *c* axes, from altered pegmatite (sample 46-I-3).

A. Low-resolution TEM image of one relict inclusion of amphibole (bpb) in Type-2 aegirine (aeg). Above the dashed white line, the pyroxene is lighter in colour, whereas beneath it, the pyroxene is darker (scale bar is 0.1 mm).

B. HRTEM image of the amphibole replacement of pyroxene (aeg) in Figure 7A. A couple of chains of amphibole replace those of the aegirine (at the two arrows pointing to the right). The amphibole is represented by chains that are double the width, along the b axis, of those of the aegirine. Larger regions of amphibole contain a single chain of a triple-chain (wider) silicate in their center (arrow pointing to the right; scale bar is 20 nm). The SAED image in the upper right hand corner of the image also shows this relationship.

C. HRTEM image of disordered wide-chain biopyribole (bpb) in inclusions of relict amphibole in aegirine (aeg; the center of Figure 7A). The wide-chain biopyribole occurs in the centers of the small grains of amphibole. The white regions at the contact between the different biopyriboles, amphibole and pyroxene represent the effects of rapid beam-induced damage and imply a hydrous nature (scale bar is 20 nm).

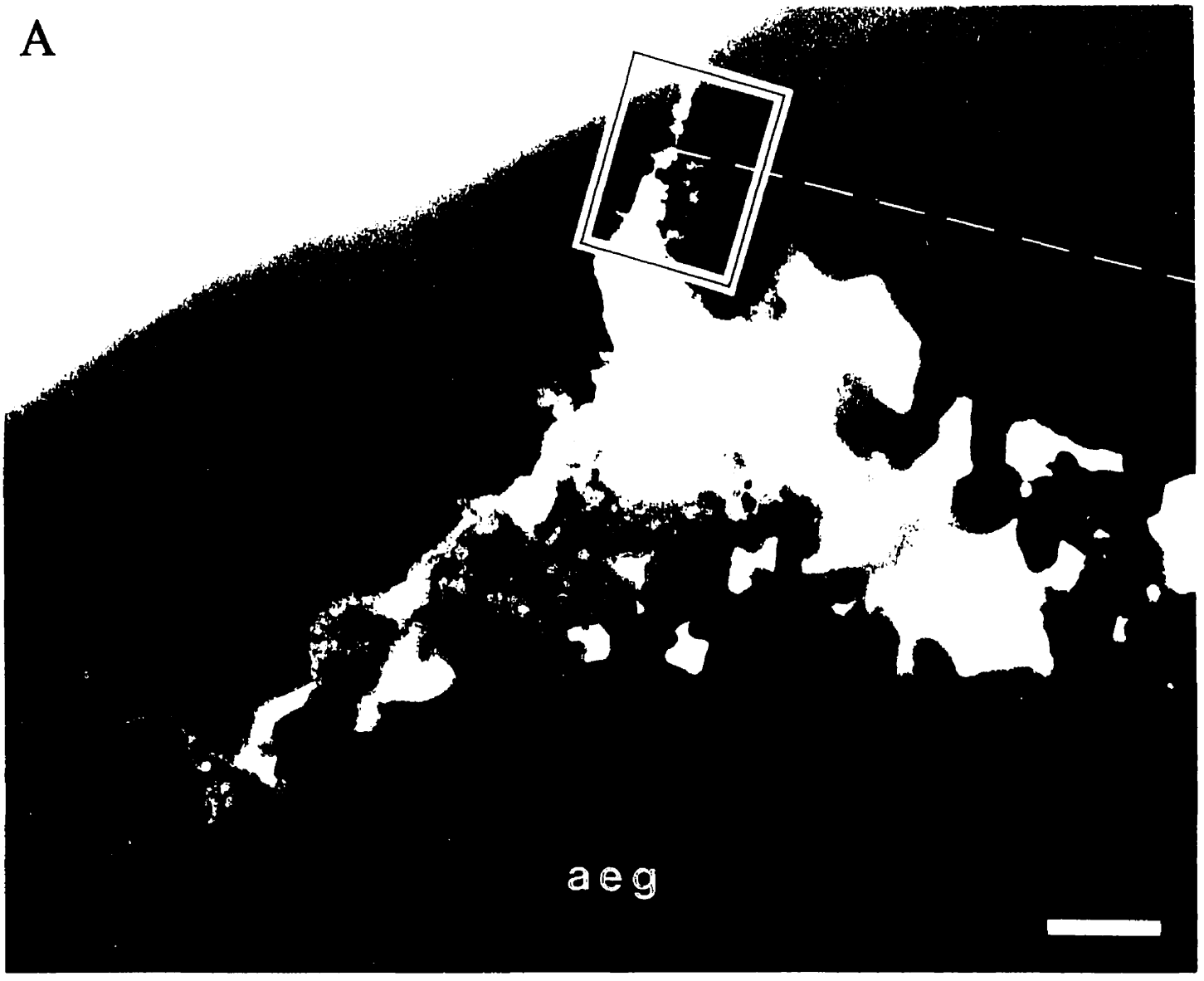
A
aeg

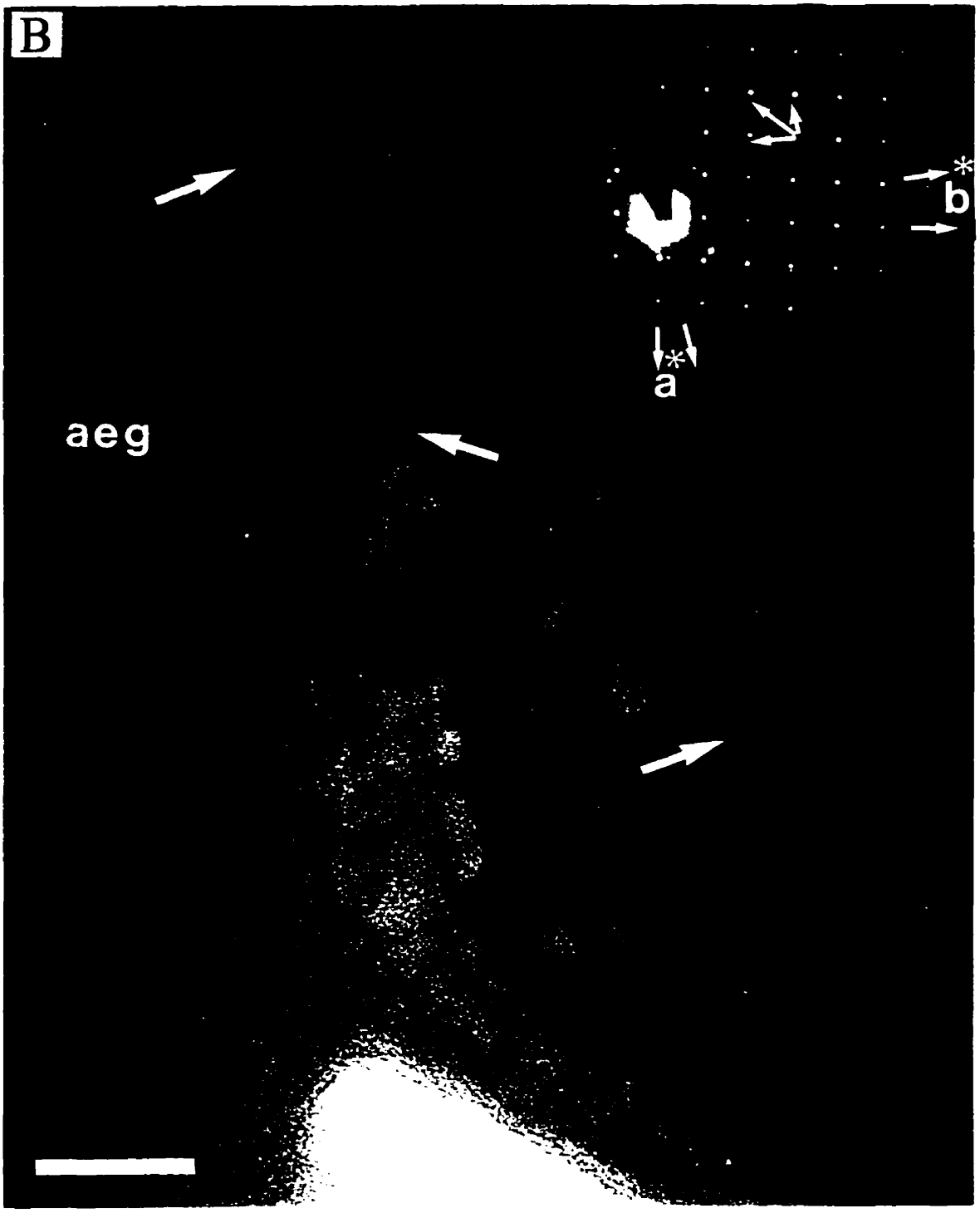
B
b*
a*
aeg

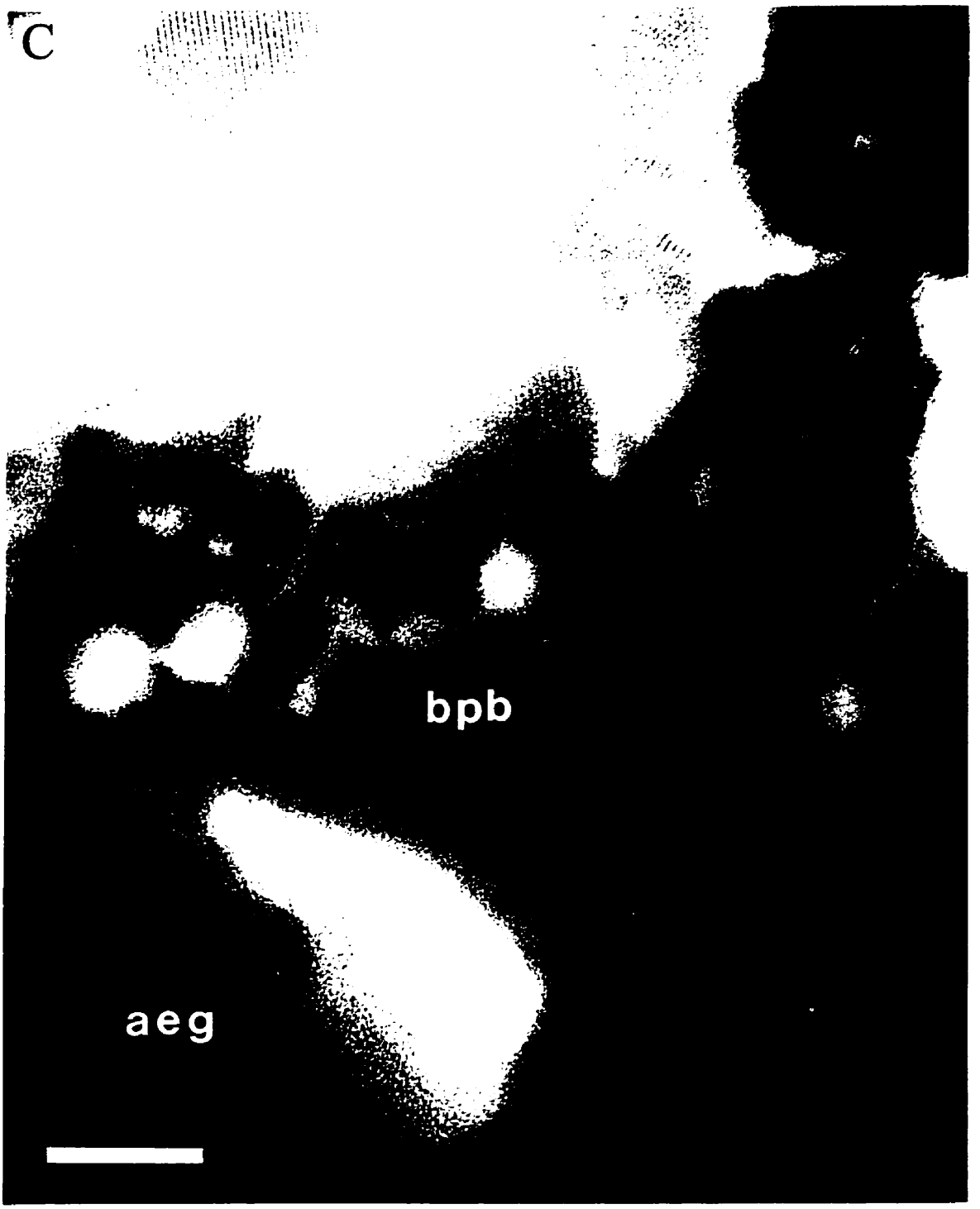
C
bpb
aeg

aegirine surrounding this region is darker in the upper right portion of the image (below the dashed line) than the surrounding pristine aegirine.

A HRTEM image of the selected region in Figure 7A (Fig. 7B) reveals that the darker aegirine is the result of the presence of double-chain defects (refers to the fact that the width between alternating identical light lines in the amphibole of the image are twice those of the aegirine in the direction of the *b* axis) in a topotactic relationship. In other words, one chain of amphibole replaces two chains of aegirine. This replacement of aegirine by amphibole contrasts with the replacement of arfvedsonitic amphibole by aegirine during Na-metasomatism (discussed in Chapter 5). Cores of larger regions of amphibole replacement of aegirine may contain a single unit of triple-chain silicate (Fig. 7B). The relationship of the amphibole to aegirine also can be seen in the SAED image, where the distance between the brightest spots along the main axes represent the shortest distance between two identical lines in the image oriented in the same direction as those in the pattern. The amphibole is represented by the darker spots in the image, such as those to which the three adjacent arrows point in Figure 7B.

AEM analysis indicates that the region of the aegirine that contains this chain-width disorder (between the amphibole and pyroxene) is enriched in Ca, Mg, Mn and Zn, with Mg possibly greater than Fe relative to the pristine aegirine (Table 3; Appendix B-16; the relative errors involved are summarized in Appendix B-12). Ca appears to be enriched by about ten fold and that of the other elements by a factor of two over the amount present in aegirine which doesnot contain these intergrowths. Consequently, the resultant amphibole is ferro-ferri-winchite or, possibly, tremolite.

The inclusions of relict amphibole present in the aegirine contain a disordered intergrowth, in the same orientation as the aegirine, ranging from a few chains of pyroxene to triple-chain and quintuple-chain structures (Fig. 7C). Wider-chain structures occur near the core of these relict grains. AEM analysis of these regions indicate that they are even more enriched in Na, Ca, Mg, Fe, Mn and Zn than the pyroxene which contained the amphibole (Table 3; Appendix B-16).

The presence of wide-chain biopyriboles whose structure is intermediate between those of arfvedsonitic amphibole and mica in the relict amphibole, and their composition implies that they were produced by the same event which produced the winchitic amphibole

Table 3: Representative AEM analyses of the various minerals observed by TEM.

Mineral	**Arfvedsonitic amphibole**		**Biopyribole**		**Aegirine**	
Sample#	**46-I-3**					
Description	**amph**	**near area**			**with win.**	**none**
Na_2O	6.89	3.79	6.19	5.99	11.31	13.38
K_2O	3.06	3.30	0.06	0.08	0.02	0.00
CaO	0.28	0.37	4.29	7.98	2.19	0.20
MgO	0.04	0.00	0.49	0.42	0.13	0.08
FeO	45.47	53.92	54.99	51.73	43.27	43.44
MnO	2.05	2.49	1.47	2.26	0.25	0.65
ZnO	2.71	3.32	4.41	0.85	1.30	0.47
ZrO_2	1.67	2.00	0.44	1.62	1.64	0.88
Rb_2O	0.05	0.00	0.00	0.00	0.10	0.00
TiO_2	0.96	1.01	0.27	0.51	0.57	1.03
Al_2O_3	0.04	0.06	0.36	0.00	0.46	0.05
SiO_2	36.77	29.74	27.05	28.56	38.76	39.83
Total*	100.00	100.00	100.00	100.00	100.00	100.00
# oxygen	23	23	34	34	6	6
Na	1.830	1.121	2.770	2.605	0.750	0.876
K	0.477	0.573	0.015	0.020	0.001	0.000
Ca	0.042	0.063	1.101	1.990	0.083	0.008
Mg	0.010	0.000	0.209	0.173	0.008	0.005
Fe	4.967	6.569	10.134	9.260	1.182	1.171
Mn	0.228	0.309	0.275	0.411	0.007	0.018
Zn	0.253	0.345	0.694	0.130	0.030	0.011
Zr	0.112	0.149	0.049	0.177	0.027	0.014
Rb	0.004	0.000	0.000	0.000	0.002	0.000
Ti	0.122	0.143	0.058	0.107	0.018	0.032
Al	0.009	0.016	0.136	0.000	0.026	0.003
Si	7.986	7.204	9.912	10.166	2.105	2.134
ΣCations	16.040	16.492	25.354	25.039	4.240	4.270

* These results are AEM analyses so all the totals are 100%.

oxygen = number of atoms of oxygen; win.=winchitic amphibole.

Table 3: Representative AEM analyses of the various minerals observed by TEM (continued).

Mineral	**Winchitic amphibole**		**Arfvedson. amphibole**	**Titanite**	**Hematite**	**Chlorite-Smectite**
Sample#[1]	**10.70**	**15.70**	**15.70**	**15.70**	**15.70**	**SL-8-1**
Description				**In vein**	**In vein**	
Na_2O	2.90	2.61	10.10	0.52	4.64	1.50
K_2O	0.00	1.12	2.70	0.01	0.11	1.59
CaO	15.50	4.85	1.04	36.05	1.27	0.50
MgO	12.20	25.49	0.00	0.00	0.39	29.57
FeO	18.30	2.33	36.43	4.08	84.91	11.81
MnO	7.80	0.62	2.97	0.23	0.19	0.35
ZnO	0.00	0.00	7.92	0.33	1.46	5.24
ZrO_2	0.00	4.97	0.00	0.00	0.00	0.00
Rb_2O	0.00	2.39	0.00	0.00	0.00	1.63
TiO_2	0.10	0.03	1.88	32.25	0.79	0.13
Al_2O_3	0.10	4.42	0.05	1.68	1.41	11.40
SiO_2	43.00	51.16	36.91	24.83	4.84	36.29
Total*	100.00	100.00	100.00	100.00	100.00	100.00
# oxygen	23	23	23	5	3	25
Na	0.887	0.708	2.647	0.027	0.281	0.339
K	0.000	0.199	0.416	0.000	0.004	0.211
Ca	2.619	0.726	0.156	1.070	0.044	0.064
Mg	2.867	5.304	0.000	0.000	0.022	6.305
Fe	2.414	0.273	3.931	0.087	2.120	1.096
Mn	1.042	0.074	0.326	0.005	0.005	0.033
Zn	0.000	0.000	0.730	0.006	0.031	0.416
Zr	0.000	0.338	0.000	0.000	0.000	0.000
Rb	0.000	0.214	0.000	0.000	0.000	0.099
Ti	0.012	0.003	0.236	0.801	0.023	0.014
Al	0.019	0.728	0.011	0.074	0.073	2.190
Si	6.781	7.144	7.919	1.052	0.240	6.700
ΣCations	16.641	15.711	16.372	3.123	2.843	17.466

* These results are AEM analyses so all the totals are 100%.

[1]All sample numbers except for that of the chlorite-smectite are for LB-30.

oxygen = number of atoms of oxygen; Arfvedson.=arfvedsonitic.

defects in aegirine. The rapid beam-induced damage of these regions containing wide-chain biopyribole imply a hydrous nature. Unfortunately, this hydrous nature and resultant beam-induced damage, especially at their contacts (zipper terminations), makes them difficult to image. The composition and hydrous nature of these biopyriboles suggest that the amphibole in the relics has been converted to wide-chain biopyriboles. Moreover, the fine-scale disorder in the biopyribole prohibits identification of minerals according to the criteria of Allen (1992) and Veblen (1992).

Arfvedsonitic Amphibole at Depth

TEM examination of the replacement of arfvedsonitic amphibole by Type-4 amphibole (drill core LB-30) shows that, what appears in thin section to be a homogeneous amphibole, is actually arfvedsonitic amphibole rimmed by a second amphibole (of the same orientation) at the margins of titanite + fluorite + quartz ± hematite veinlets (Fig. 8; Table 3). The ratio between the winchitic amphibole and the assemblage in the veinlets is approximately 1:1. It was difficult to estimate the proportion of titanite, fluorite, quartz and hematite from TEM examination, but the best approximation is 4:2:1:1.

AEM analysis shows that the arfvedsonitic amphibole corresponds to that from other units in the complex. Type-4 amphibole contains the most Mn, Mg, Ca, Al and Zn (to a maximum of 18.20 wt.% MnO, 27.20 wt.% MgO, 17.80 wt.% CaO, 18.63 wt.% ZnO and 14.41 wt.% Al_2O_3) of all the types of amphibole identified from the complex (Table 3; Appendix B-17). The composition of the amphibole varies widely, but is consistent with that of manganese, zinc or manganoan zincian winchite. The amphibole domains analyzed by AEM contain less Ti, Ca, Mn, Zn, Mg and F, but an equivalent amount of K, as when this amphibole analyzed with an electron microprobe. Consequently, the compositional variation of these regions is greater than that indicated by the results of the electron-microprobe analyses. These TEM results, when combined with observations on thin sections, suggest that the colouration of Type-4 amphibole can be attributed to the presence of titanite, purple fluorite, traces of hematite and the Mn-rich composition of the amphibole [as in manganoan tremolite (Koenig, 1876)].

Figure 8. TEM images showing the brown winchitic amphibole rim between arfvedsonitic amphibole and the titanite, fluorite, quartz ± hematite veins. This sample was taken from drill core LB-30 (at a depth of 17.22 m).

A. Low-resolution TEM image of an amphibole (amph) rim between arfvedsonitic amphibole and a veinlet of titanite, fluorite, quartz ± hematite (vein; scale bar is 1 μm).

B. With increased magnification, the HRTEM image (of the region on which the lettering amph was placed in Figure 8A) shows that the amphibole immediately adjacent to the vein is composed of arfvedsonitic amphibole (arf) and winchitic amphibole (win; scale bar is 0.1 μm).

A

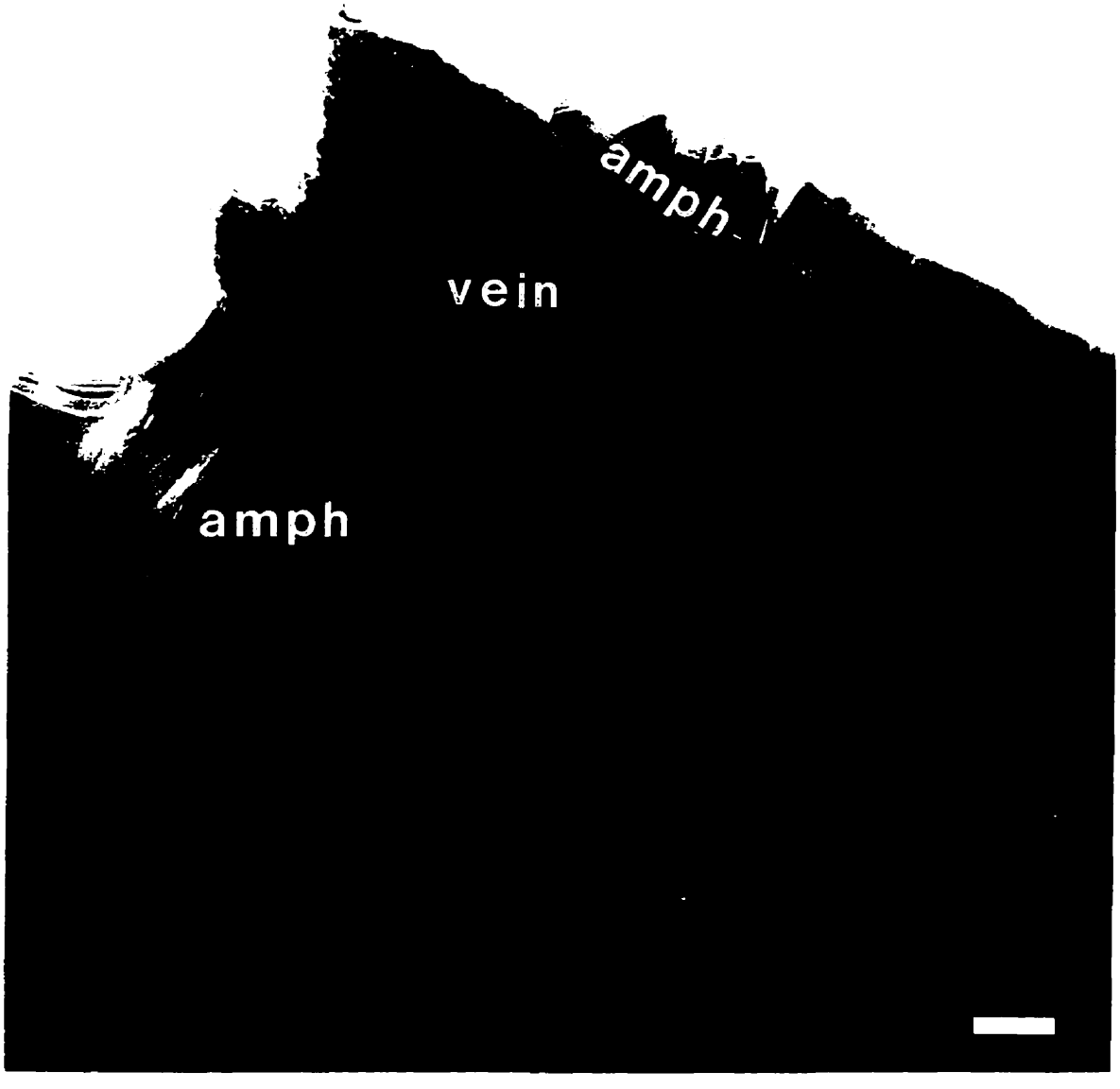

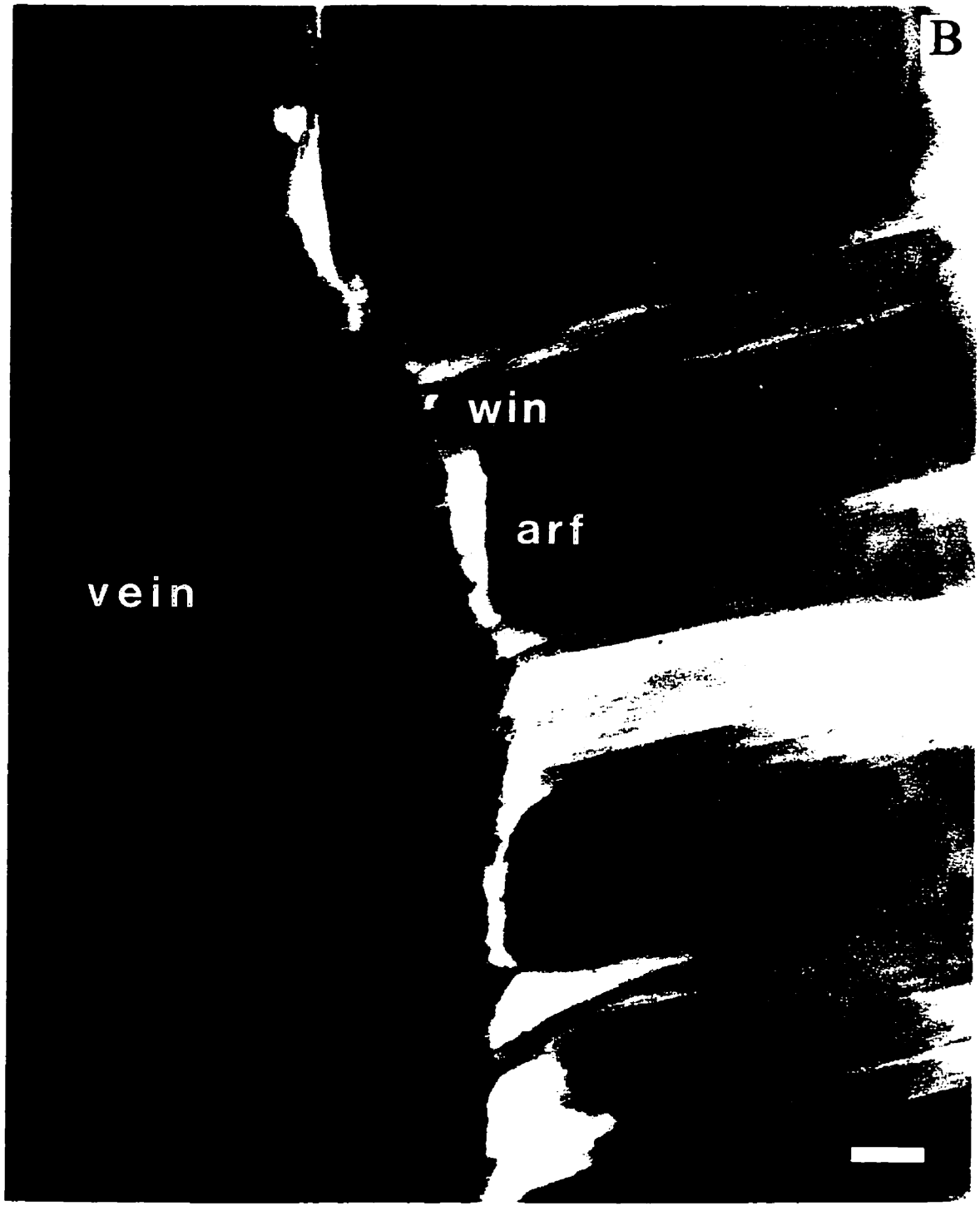
B
win
arf
vein

Phyllosilicates

The phyllosilicate in the veinlet associated with amphibole (Fig. 4) has a 31 Å (3.1 nm) basal-spacing, which is consistent with a regular 1:1 intergrowth of chlorite and a smectite if there has been no collapse of the structure under the effects of the electron beam. As this is highly unlikely, it is more likely that its reaction under the beam is influenced by its unusual composition (see below). Such intergrowths can be termed either tosudite or corrensite, depending on whether the chlorite is trioctahedral or dioctahedral, respectively (Fig. 9; Table 3). A smectite-group mineral (identified by d-value and AEM) succeeded aegirine replacement of arfvedsonitic amphibole in the altered subsolvus granite at or near the erosional surface (ref. Fig. 10 in Chapter 5). In both of these phyllosilicates, it was impossible to determine the relationship between the phyllosilicate and amphibole or aegirine owing to rapid beam-induced damage of the phyllosilicate. AEM analyses of the intergrowth shows that it is somewhat variable, but contains a maximum of 5.9 wt.% ZnO, 4.9 wt.% CaO, 1.1 wt.% MnO, 2.8 wt.% ZrO_2 and 1.6 wt.% K_2O. The enrichment of this phyllosilicate in Mg, Ca and Mn is consistent with the compositional variation noted from the electron microprobe. These same elements also are enriched in the other replacement products of the arfvedsonitic amphibole that can be attributed to the effects of Ca-metasomatism.

In addition, the composition of the chlorite portion of the intergrowth is between clinochlore and chamosite. The smectite portion shows some similarities to nontronite, except that it contains more Fe than is typical for this mineral. Thus, HRTEM and AEM evidence suggest that this intergrowth is tosudite. Unfortunately, the fine grain-size and rarity of this phyllosilicate precluded a X-ray powder-diffraction examination. The average chemical formulae for all of the mafic silicates and their alterations are listed in Table 4.

Sequence of Ca-Metasomatism

The Ca-metasomatic event followed a high-temperature Na-metasomatic event, where reaction with a Na-Cl-rich fluid (Salvi & Williams-Jones, 1992) was conducive to efficient replacement of arfvedsonitic amphibole by aegirine (Chapter 5; Fig. 10). The paragenetic sequence depicted in Figure 10 shows that this replacement was accompanied

Figure 9. HRTEM image of the phyllosilicate alteration of arfvedsonitic amphibole from a depth of 15.80 m in drill core LB-30. The basal spacing of this phyllosilicate, 31 Å (3.1 nm; the distance between the large arrows), indicates the presence of a possible chlorite-smectite intergrowth. This intergrowth is represented by brighter and less bright lines. Changes in this intergrowth can be seen as changes in the widths of the basal spacing and the termination of lattice fringes (one layer of this intergrowth as represented by triangular regions in the image such as the one at the tip of the small arrow).

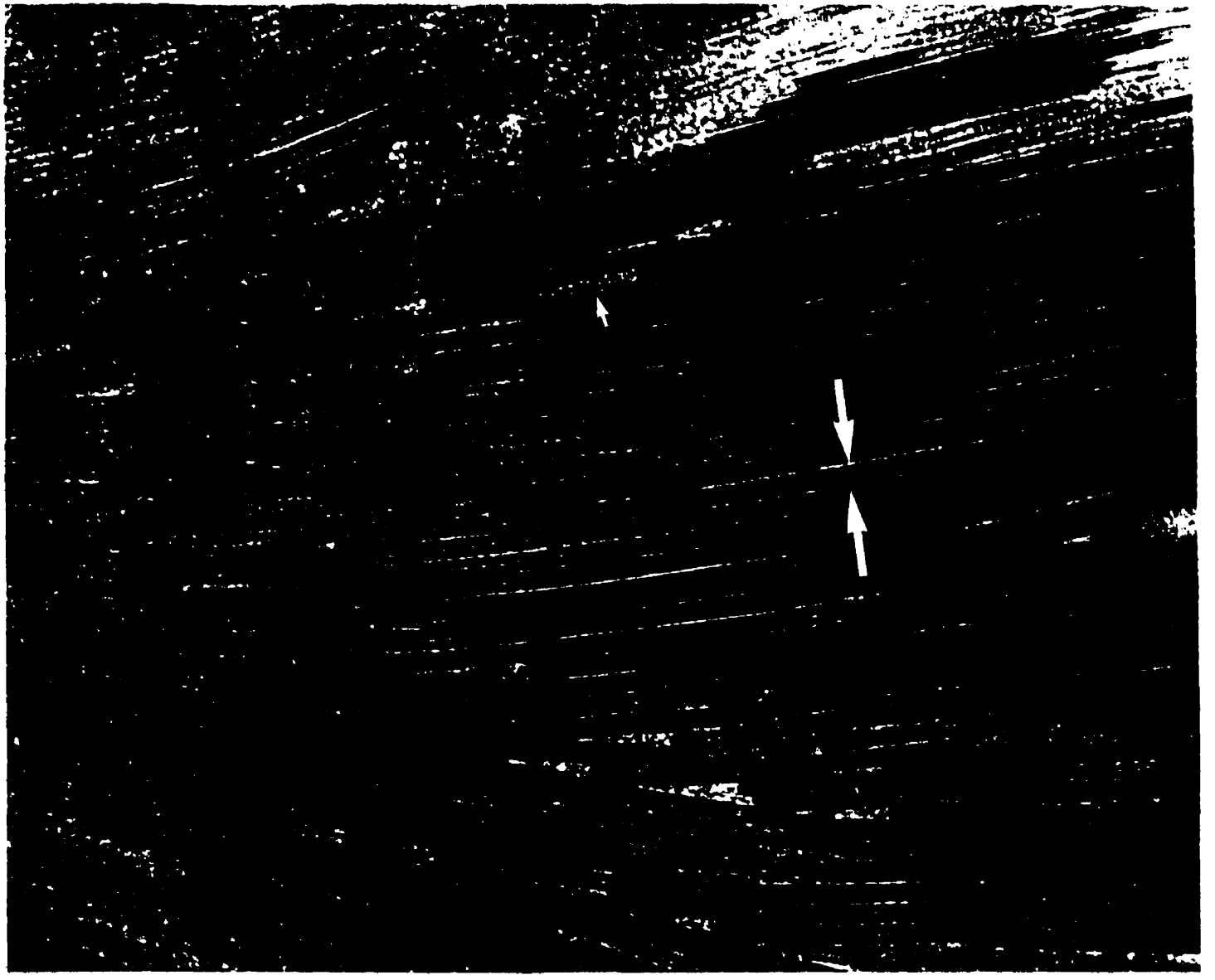

Table 4: Mineral formulae used in the reactions.

Mineral	Aegirine	Winchitic amphibole	Biopyribole	Arfvedsonitic amphibole	Ferro-ferri-winchite	Chlorite-smectite
Cation Units						
Na	0.99	1.13		2.30	0.70	0.09
K				0.44	0.14	0.01
Ca	0.01	0.86	2.00	0.10	1.64	0.15
Mg	0.01	0.08	1.00		2.12	4.40
Fe(Total)	0.96	4.52	7.00	4.10	2.98	2.30
Mn	0.01	0.20		0.23	1.56	0.49
Zn		0.06		0.20	0.10	0.81
Zr		0.08		0.19		
Ti	0.02	0.05		0.19	0.05	
Al	0.02			0.01	0.46	1.50
Si	1.98	8.00	12.00	8.00	7.56	6.50
O	6.00	22.00	32.00	22.00	22.00	20.00
OH		2.00	4.00	2.00	2.00	5.00

* Mineral formulae based on an average of AEM analyses of each mineral, except for aegirine where the values where calculated from a combination of electron-microprobe analyses and AEM analyses.

Figure 10. Diagram depicting the paragenetic sequence of crystallization of minerals related to Na- and Ca-metasomatism. Light lines represent minerals whose origin is more conjectural than those represented by the black lines. Earlier Na-metasomatism involved aegirine (Type-2) replacement of arfvedsonitic amphibole. This may be accompanied by or followed by hematite ± quartz and fluorite. The chlorite-smectite intergrowth may have begun to form during Na-metasomatism, but continued during the Ca-metasomatic event. Replacement of arfvedsonitic amphibole or aegirine by winchitic amphibole began during Ca-metasomatism. The size of the regions of amphibole replacement increased until they could be observed in thin section. At depth, this replacement is accompanied by veinlets of titanite, quartz, fluorite ± hematite. However, at the present erosional surface where aegirine is replaced by winchitic amphibole, relict amphibole (the result of Na-metasomatism) also is replaced by various wide-chain biopyriboles.

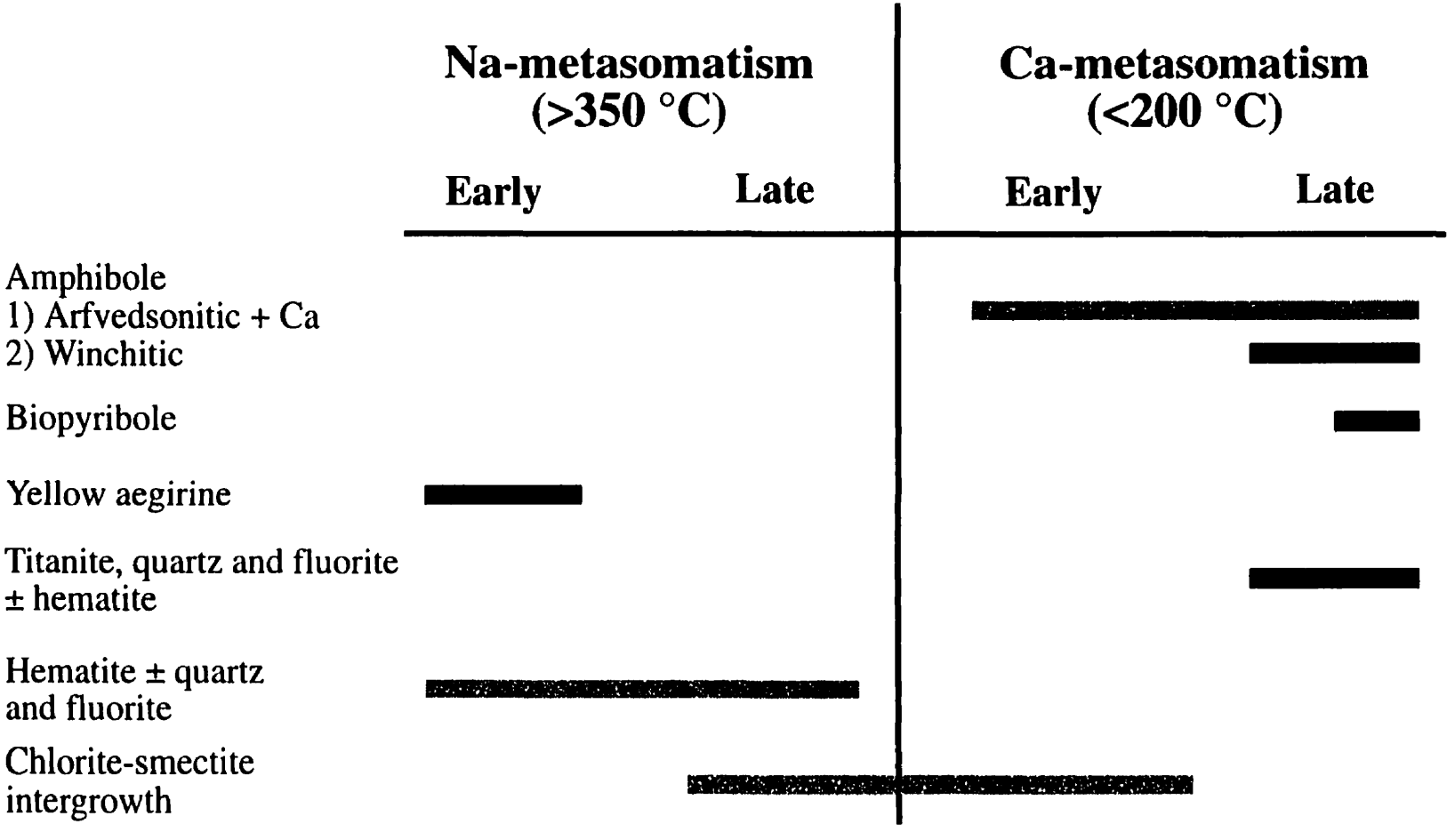
Na-metasomatism
(>350 °C)
Ca-metasomatism
(<200 °C)
Early
Late
Early
Late
Amphibole
1) Arfvedsonitic + Ca
2) Winchitic
Biopyribole
Yellow aegirine
Titanite, quartz and fluorite
± hematite
Hematite ± quartz
and fluorite
Chlorite-smectite
intergrowth

by hematite ± quartz and fluorite. At the same time, it was accompanied by the chlorite-smectite intergrowth, which continued to crystallize during the Ca-metasomatic event. Disordered biopyribole also replaced the arfvedsonitic amphibole. Ca-metasomatism was accompanied by the replacement of arfvedsonitic amphibole or aegirine by winchitic amphibole. The difference between these two types of replacement is that, where aegirine occurred at the present erosional surface along with relics of arfvedsonitic amphibole, arfvedsonitic amphibole occurred at depth as rims to veinlets of titanite, quartz, fluorite ± hematite.

Discussion

Amphibole Replacement of Aegirine in Altered Pegmatite

If one assumes that the amphibole which replaced aegirine is winchite, and if one takes into account the amount of amphibole produced per unit of aegirine and the lack of associated quartz and hematite (in the immediate vicinity), the isovolumetric reaction to represent the replacement is:

aegirine

$$4Na_{0.99}Ca_{0.01}(Fe_{0.96}Mn_{0.01}Mg_{0.01}Ti_{0.02})(Si_{1.98}Al_{0.02})O_6 + 0.82Ca^{2+} + 0.68Fe^{2+} + 0.04Mg^{2+} + 0.16Mn^{2+} + 0.06Zn^{2+} + 0.08Zr^{4+} + 0.08H_4SiO_4^{\circ} + 1.485H_2$$

winchitic amphibole

$$\rightarrow (Na_{1.13}Ca_{0.86})(Fe_{4.52}Mg_{0.08}Mn_{0.20}Zn_{0.06}Zr_{0.08}Ti_{0.05})Si_8O_{22}(OH)_2 + 2.83Na^{+} + 0.08Al^{3+} + 0.03Ti^{4+} + 0.65H^{+} + 0.32H_2O \quad (1).$$

The formula used for the aegirine is that of the average aegirine calculated from a combination of electron-microprobe, AEM and LAM-ICP-MS analyses (Table 4). That of the amphibole was determined solely from the AEM analyses (Table 3) of amphibole-rich regions, as the amphibole was too minute for the results of electron-microprobe analyses to be of any significance. The 4:1 ratio between aegirine and amphibole used in the equation reflects the fact that two chains of aegirine are replaced by one of the amphibole (ref. Fig. 8B), and that a unit cell of aegirine contains half the formula units present in a unit cell of

the amphibole. Thus, during the pseudomorphic transformation of the single-chain pyroxene to the double-chain amphibole, Si is essentially conserved. In Reaction 1, the interaction of Ca-metasomatic fluid containing Mn, Zn, Mg and Fe with aegirine to produce amphibole releases Na and a small amount of Al and Ti that subsequently form complexes in solution.

Biopyriboles

Unfortunately, the disordered nature of the wide-chain biopyriboles does not allow the determination of a representative composition by AEM analysis. Consequently, the mineral formulae have been simplified to account only for the presence of a triple-chain silicate; an estimation has been made of the composition of this triple-chain silicate from AEM analyses of these regions, such that it can be assumed that no Na is present, and the wide-chain biopyribole is Ca- and Fe-rich. As no hematite or quartz is present in the assemblage, the reaction can be balanced on Si. Thus, complete conversion of amphibole to triple-chain silicate is interpreted to have occurred via the idealized reaction:

winchitic amphibole

$$3(Na_{1.13}Ca_{0.86})(Fe_{4.52}Mg_{0.08}Mn_{0.20}Zn_{0.06}Zr_{0.08}Ti_{0.05})Si_8O_{22}(OH)_2 + 1.42Ca^{2-} + 0.44Fe^{2+} + 1.76Mg^{2+} + 1.365H_2$$

triple-chain silicate

$$\rightarrow 2Ca_2Fe_7MgSi_{12}O_{32}(OH)_4 + 3.39Na^{+} + 0.60Mn^{2+} + 0.18Zn^{2+} + 0.24Zr^{4+} + 0.15Ti^{4+} + 0.73H^{+} \quad (2).$$

I have assumed that the ratio between the amphibole and triple-chain silicate is 3:2 to make the reaction isovolumetric (for the same reason as between the amphibole and pyroxene noted above), although a 3:4 ratio was used by Welch et al. (1992) in a study of the conversion of NaMg amphibole to triple-chain silicate. Reaction 2 involves reaction of the fluid containing Ca, Fe and Mg with the amphibole (the product of Reaction 1) to produce the triple-chain silicate while releasing significant Na, but only minor amounts of Mn, Zn, Zr and Ti into solution. The minor amount of Mn and Zn that appears to be released into solution is more likely just a function of the simplification of the formula for the triple-chain

silicate, especially since it was present in the same fluid that formed the associated amphibole. The rest of the elements form chloride and fluoride complexes in solution. A simple modification of the reaction can be made if slightly less Fe is assumed to be present in the triple-chain silicate, which would require less Fe, but more Mg from the fluid. Comparison between Reactions 1 and 2 indicates that in both cases, Ca is added and Na is released. If the same fluid produced both reactions, it is likely that the triple-chain silicate is more Fe-rich and Mg-poor than that estimated above.

This is the first detailed TEM examination of the effects of hydrothermal alteration on arfvedsonitic amphibole to date, although minor biopyribole was noted in fibrous riebeckite by Hutchinson et al. (1976), Alario-Franco et al. (1977), Crawford (1980), Whittaker et al. (1981), Cressey et al. (1982) and Ahn & Buseck (1991). Hawthorne et al. (1993) did not observe any evidence of exsolution or chain-width defects in their TEM examination of Li-rich arfvedsonitic amphibole. Moreover, fibrous riebeckite contains more chain-width defects (to 25% of the fibrils) than the massive variety (Chisholm, 1973; Hutchison et al., 1975; Veblen et al., 1977; Ahn & Buseck, 1991). The formation of these defects has been attributed to a chance occurrence during growth, the presence of dislocations or the result of reaction of amphibole with hydrothermal fluids (Crawford, 1980; Veblen & Buseck, 1980; Whittaker et al., 1981; Cressey et al., 1982; Ahn & Buseck, 1991). When one considers the coincidence of these Ca-rich defects in minerals associated with assemblages formed during Ca-metasomatism in the Strange Lake complex (Salvi & Williams-Jones, 1990, 1996), the third hypothesis seems the most likely.

The disordered biopyriboles from relics of amphibole examined in this study may, if sufficient Na is present, be the most Na- and Fe-rich of all natural wide-chain biopyriboles examined to date. In their metasomatic synthesis of Ca-Mg triple-chain silicates from Na-Mg ones, Akai & Saito (1985) noted that the maximum substitution of Ca by Na is 1:2 between 350 and 650°C at a $P(H_2O)$ of 600 bars. Their work has shown that the biopyriboles have a wide field of stability, which should decrease in the presence of Fe.

Variation with Depth

Replacement of primary arfvedsonitic amphibole by manganese, zinc or manganoan zincian ferro-winchite to ferro-ferri-winchite at depth within the drill core material is

represented by the reaction:

arfvedsonitic amphibole

$(Na_{2.30}K_{0.44}Ca_{0.10})(Fe_{4.10}Mn_{0.23}Zn_{0.20}Zr_{0.19}Ti_{0.19}Al_{0.01})Si_8O_{22}(OH)_2 + 1.54Ca^{2+} + 2.12Mg^{2+} + 1.33Mn^{2+} + 0.45Al^{3+} + 1.76H_2O + 1.955H_2$

$\rightarrow (Ca_{1.64}Na_{0.70}K_{0.14})(Fe_{2.98}Mg_{2.12}Mn_{1.56}Zn_{0.10}Ti_{0.05})(Si_{7.56}Al_{0.46})O_{22}(OH)_2 + 1.60Na^+ +$

ferro-ferri-winchite

$0.30K^+ + 1.12Fe^{2+} + 0.10Zn^{2+} + 0.19Zr^{4+} + 0.14Ti^{4+} + 0.44H_4SiO_4^o + 5.67H^+$ (3).

The average amphibole compositions listed in Table 4 were used in this reaction. The 1:1 ratio used between the amphiboles is due to the fact that, during TEM examination, it was noted that the two amphiboles are isostructural (their contact can only be identified from a change in composition). Interaction of the Ca-metasomatic fluid containing significant Mg, Mn and Al with the arfvedsonitic amphibole produced the winchitic amphibole, while releasing Na, Fe, Si, K, Zr, Ti and Zn. The Fe, Ti and Si released during this replacement likely added to the amount of hematite, titanite and quartz present in the veinlets. In comparison with the composition of the Ca-bearing fluid inferred to be involved in the other reactions, that involved in Reaction 3 is significantly different, except for its Ca content and the resultant release of Na and Ti. The remainder of the elements form fluoride and chloride complexes in solution. Much of this difference can be attributed to the estimated mineral formulae used in the other reactions.

Reaction 3 produced a rim of amphibole adjacent to titanite + fluorite + quartz ± hematite veinlets, where the compositions and relative proportions of these minerals indicate that the fluid in the veinlets may have contained Ca, and minor Ti, Si, Fe, F and even some Al. The presence of Al is reflected in the composition of the titanite, which accommodates a maximum of 0.11 apfu Al. However, this amount is insignificant compared to the maximum amount of Al that can occur in titanite, especially at a high a_F, suggested by Janeczek (1994) and Oberti et al. (1991),

The effects of Ca-metasomatism on arfvedsonitic amphibole described in the present study are similar in some respects to the metasomatic replacement of arfvedsonitic amphibole by ferro-anthophyllite noted by Martin (1977). To my knowledge, no other study

has reported observations of the type described here or by Martin (1977).

There seems to be a large difference between the type of replacement of arfvedsonitic amphibole that occurs at the surface and at depth in the Strange Lake peralkaline complex. Aegirine replaced arfvedsonitic amphibole at and near the surface (apex of the intrusion) and at depth above or surrounding the more pegmatitic portions of the ore zone (Chapter 5). Pure winchitic amphibole, as observed in the equigranular granite from the ore zone at depth, was not observed at the surface, although specific samples may be slightly enriched in Ca and Mg. This suggests that the earlier Na-metasomatism was followed by a later, more localized, subtle episode of Ca-metasomatism in the central portions of the complex (e.g., the altered subsolvus granite).

This TEM examination of the Type-4 amphibole provides an excellent example of the importance of this method to what appears, on thin section examination and with scanning electron microscopy, as a homogeneous mineral. The slight deviation from stoichiometry of the mineral formulae and the anomalous optical properties are useful indicators of the presence of fine-scale intergrowths.

Origin of the Chlorite-Smectite Intergrowth

Alteration of arfvedsonitic amphibole to a 1:1 chlorite-smectite mixed layer phase took place by the reaction:

arfvedsonitic amphibole

$$(Na_{2.30}K_{0.44}Ca_{0.10})(Fe^{2+}_{4.10}Mn_{0.23}Zn_{0.20}Zr_{0.19}Ti_{0.19}Al_{0.01})Si_8O_{22}(OH)_2 + 4.40Mg^{2+} + 1.49Al^{3+} + 0.61Zn^{2+} + 0.26Mn^{2+} + 0.05Ca^{2+} + 7H_2O + 1.175H_2$$

chlorite-smectite

$$\rightarrow (Na_{0.09}K_{0.01}Ca_{0.15})(Mg_{4.40}Fe_{2.30}Zn_{0.81}Mn_{0.49})(Si_{6.50}Al_{1.50})O_{20}(OH)_5 + 2.21Na^+ + 0.43K^+ + 1.5H_4SiO_4^o + 1.8Fe^{2+} + 0.19Zr^{4+} + 0.19Ti^{4+} + 7.35H^+ \quad (4).$$

The mineral formulae used in the reaction were determined in the same manner as above. The Si and Fe released during this reaction formed quartz and hematite, while the other elements form fluoride and chloride complexes in solution. Reaction 4 is similar to that suggested by Abdel-Rahman (1995) for the replacement of alkali amphibole by

chlorite-smectite, except that the metasomatic fluid introduced Mg, Al, Zn, Mn and Ca, but removed Fe and Na.

Insights on whether the chlorite-smectite intergrowth is corrensite or tosudite can be obtained by comparison with other geological settings in which they form. Corrensite usually occurs as a result of hydrothermal alteration of intermediate to basic volcanic rocks (Evarts & Schiffman, 1983; Bettison & Schiffman, 1988), in contact-metamorphic zones (Vergo & April, 1982), and, as a product of burial diagenesis, in sedimentary sequences (Chang et al., 1986). In contrast, tosudite generally occurs in intermediate to felsic igneous rocks or in sandstones (Shimoda, 1969; Nishiyama et al., 1975; Morrison & Parry, 1986; Cho & Kim, 1994). In peralkaline granitic settings in Egypt, Abdel-Rahman (1995) suggested, from electron-microprobe analyses and X-ray powder diffraction (XRD), that the main phyllosilicate alteration of arfvedsonitic amphibole is corrensite. In the present study, the chlorite-smectite alteration of arfvedsonitic amphibole is related to metasomatism. However, it was difficult to determine, from the TEM data gathered, whether the phyllosilicate intergrowth in the Strange Lake complex was corrensite or tosudite.

Further insights on whether the chlorite-smectite intergrowth is corrensite or tosudite can be implied from the chemical conditions under which they form. Tosudite forms at high activities of Si, K ± Al and Li, and low pH above 360°C (Ichikawa & Shimoda, 1976; Eberl, 1978; Maksimovic & Brindley, 1980; Dudoignon et al., 1988; Cho & Kim, 1994). Corrensite crystallizes at lower temperatures (below 200°C; Chang et al., 1986; Dudoignon et al., 1988), as the product of the interaction between high pH, Mg-rich fluids and a phyllosilicate (Grim et al., 1960; April, 1981a, b; Bodine, 1985). These temperatures of crystallization imply that, in the Strange Lake complex, the chlorite-smectite intergrowth may have started to form during Na-metasomatism and may have extended down to lower temperatures during Ca-metasomatism.

Ferrow & Ripa (1991) and Smelik (1995) suggested, from TEM examination of chlorite-smectite alteration of magnesian amphiboles, that the formation of the alteration was a reflection of the composition of its precursor and components introduced by the fluid. The more Fe-rich composition of the chlorite-smectite intergrowth formed by alteration of arfvedsonitic amphibole from the Strange Lake peralkaline complex compared to that noted by Ferrow & Ripa (1991) and Smelik (1995) implies a significant contribution of the

precursor. This is consistent with the electron-microprobe analyses of correnside of Abdel-Rahman (1995), which show an enrichment in Na, K and, in some cases, Ca, and a higher Fe/(Fe+Mg). This variation in electron-microprobe data can be attributed to the presence of relics of amphibole in the phyllosilicate. Furthermore, the distinct enrichment of the phyllosilicate in Ca, Mn and Zn is the result of the metasomatic fluid.

Evolution of the Strange Lake Complex

A summary of the evolution of the Strange Lake complex based primarily on the paragenesis of the mafic silicates (arfvedsonitic amphibole and aegirine) of primary origin (Chapter 4), and of secondary origin (Chapter 5 and the present chapter) is depicted in Figure 11.

The magmatic zirconosilicates, elpidite and zircon, occur as euhedral, early-crystallized grains. Crystallization of arfvedsonitic amphibole, quartz, feldspar, and Type-1 aegirine followed. The temperature of crystallization of the magmatic mafic silicates was below approximately 675°C at the inferred conditions of fO_2 during crystallization of the amphibole as determined from both XRD data and the results of electron-microprobe analysis (Chapter 4). However, Nassif (1993) suggested that this temperature may have been as low as 450°C (determined by the effect of significant F on the granite minimum) in the altered subsolvus granite. A drop in temperature of the system to subsolidus conditions resulted in crystallization of rims of primary Type-1 aegirine on amphibole and crystallization of later Type-1b arfvedsonitic amphibole. Crystallization of the feldspars and zirconosilicates increases the relative concentrations of HFSE, REE, Na and F in localized pockets of residual magma (Chapter 4). Some of these elements, in particular Na and F, are accommodated in the arfvedsonitic amphibole and aegirine, but not all of them.

Later degassing (Chapter 4; Nassif, 1993; Salvi & Williams-Jones, 1996) increased the K content of the melt, as a result of the loss of Na and H_2 from the complex. This is reflected by an increase in K content of the late amphibole (Chapter 4) and the crystallization of microcline (Nassif, 1993) in the altered subsolvus granite, especially in the pegmatites. Retrograde boiling, that accompanied this degassing, was proposed by Salvi & Williams-Jones (1996) as a process that further concentrated the HFSE, beyond that

Figure 11. Schematic representation of the evolution of the Strange Lake peralkaline complex, modified after Salvi & Williams-Jones (1996). The arrows in the diagram represent the approximate directions of the final stages of fluid flow in the complex. The dashed line represents the current erosion level of the pluton, therefore the question marks refer to possible methods whereby degassing occurred. The intrusion of the complex (hypersolvus granite followed by subsolvus granite) is followed by metasomatism, wherein an orthomagmatic fluid that produces the Na-metasomatism reacts with a fluid derived from the country rocks and then is recirculated in the pluton to produce the Ca-metasomatism. Initial Na-metasomatism affects the apex of the pluton and the equigranular granite from the subsolvus granite at depth. The occurrence of later Ca-metasomatism is spatially more restricted at the surface, but seems to become more prominent at depth especially in the equigranular granite (ref. Chapter 5). Consequently, signs of both episodes of metasomatism are particularly obvious in the altered subsolvus granite.

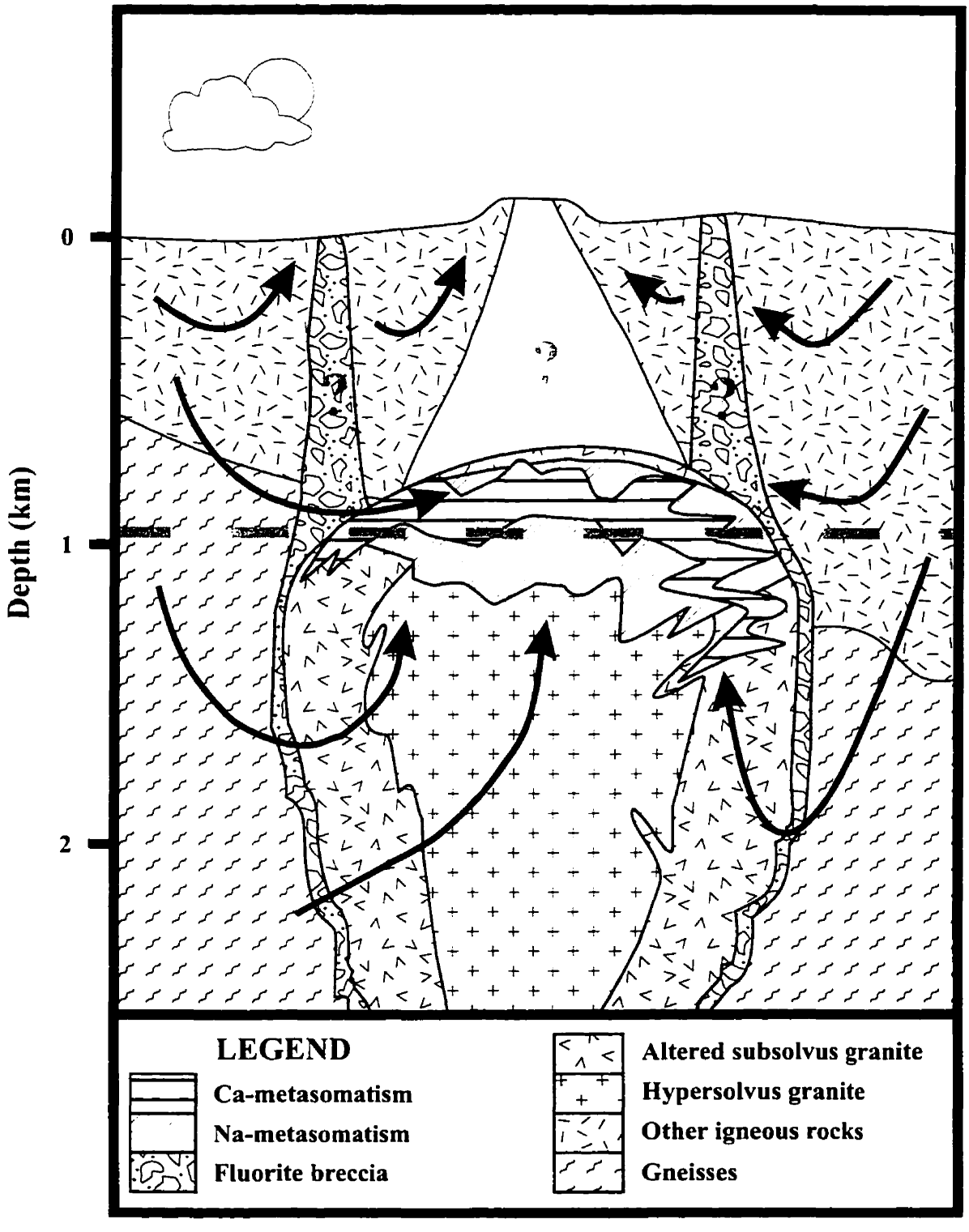
Depth (km)
0
1
2
LEGEND
Ca-metasomatism
Na-metasomatism
Fluorite breccia
Altered subsolvus granite
Hypersolvus granite
Other igneous rocks
Gneisses

produced by fractional crystallization. They also suggested that, during retrograde boiling, a high-temperature (>350°C; Salvi & Williams-Jones, 1992), Na-rich orthomagmatic fluid was exsolved that produced the Na-metasomatism.

Aegirine produced by replacement of arfvedsonitic amphibole was the dominant product of Na-metasomatism (Salvi & Williams-Jones, 1992; Chapter 5). In Chapter 5, it was noted that this aegirine was accompanied by crystallization of either hematite ± fluorite and quartz in the altered subsolvus granite, or astrophyllite and fluoride minerals in the hypersolvus granite. In both cases, replacement of arfvedsonitic amphibole by aegirine released HFSE, REE, K, Li, Ti, F, Zr, Zn and Mn into solution, since these elements were not accommodated in as high a concentration in the aegirine (Chapter 5).

The HFSE, REE, Mn and Zn released during metasomatism formed fluoride and chloride complexes in the fluid (Smith & Martell, 1974; Bright & Readey, 1987; Wood, 1990; Keppler, 1993). The influx of Ca by mixing of the orthomagmatic fluid with a fluid phase derived from an extraneous source, the change in pH and the cooling of the system to <200°C (Salvi & Williams-Jones, 1990) resulted in fluorite precipitation, thereby destabilizing the HFSE and other fluoride complexes (Taylor et al., 1981; Kovalenko et al., 1995). The ultimate source of Ca in the fluid likely was the Ca-rich calc-silicate gneisses and gabbros, with which the Na-rich orthomagmatic fluids reacted (Salvi & Williams-Jones, 1996). Such a Ca-rich fluid could also have originated from deep circulating Ca- and Cl-rich brines, such as those commonly encountered in the Canadian Shield (Kamineni, 1987).

Arfvedsonitic amphibole exposed to such late fluids shows compositional variation toward winchite. The late fluid introduced Ca, Mg, Mn, REE ± Al and Fe into the system (as depicted, in part, in Figure 5 and in the reactions above). The increase in Mn content of the secondary minerals (e.g., the winchitic amphibole and the chlorite-smectite intergrowth) produced by Ca-metasomatism and the presence of hematite is mirrored in the main ore mineral, gittinsite, which is commonly associated with hematite and contains Mn in its structure (Salvi & Williams-Jones, 1995; Roelofsen, unpubl. TEM data). Lastly, the increase in Zr, Mn and REE content of the whole rocks and fluid inclusions has also been related to Ca-metasomatism by Salvi & Williams-Jones (1990, 1996).

The presence of hematite along with titanite, fluorite and quartz (below the surface)

in the veinlets rimmed by winchitic amphibole indicate that these minerals are coeval and related to Ca-metasomatism. Furthermore, the lack of a common correlation between hematite formation and aegirine replacement of arfvedsonitic amphibole during Na-metasomatism (the relative amount of hematite increases in secondary aegirine near the margins of the altered subsolvus granite; Chapter 4) indicates that hematite may have crystallized during both the Na- and Ca-metasomatic events. Salvi & Williams-Jones (1996) suggested that precipitation of hematite followed Na-metasomatism, but was closely associated with the final stages of Ca-metasomatism. This model is derived from the observation that rocks immediately adjacent to the ore zone, where Ca-metasomatism is common, exhibit more intense reddening (hematization).

Relationship to Other Complexes

Na-metasomatism is a late-magmatic to postmagmatic process commonly associated with peralkaline complexes. In peralkaline granites, it is associated with the formation of albite (albitization: Elliott, 1983; Bowden et al., 1987; Pollard, 1989; Kovalenko et al., 1995), and aegirine replacement of arfvedsonitic amphibole (O'Halloran, 1985; Bonin, 1986). The HFSE and HREE released during Na-metasomatism are mobilized as fluoride complexes (Bright & Readey, 1987; Wood, 1990; Keppler, 1993). Other examples of mobilization of HFSE include the studies of Gieré (1990) and Willis et al. (1990), who documented the mobility of Ti in natural systems under hydrothermal conditions. The mobility of Zr under hydrothermal conditions was confirmed by Gieré (1986, 1990), Gieré & Williams (1992), Salvi & Williams-Jones (1990, 1996), Vard & Williams-Jones (1993) and Boily & Williams-Jones (1994). In addition, Rubin et al. (1993) noted that the majority of the Zr in the peralkaline rhyolites and trachytes of the Christmas Mountains, Texas, was hosted by arfvedsonitic amphibole and aegirine. They suggest that zircon in the replacement deposits in limestone near its contact with the volcanic rocks was formed from Zr released by breakdown of arfvedsonitic amphibole and aegirine. These effects produced by the replacement of the amphibole and aegirine are analogous to those produced by the replacement of arfvedsonitic amphibole by aegirine during Na-metasomatism (Chapter 5).

Examples of other peralkaline complexes that exhibit the effects of late Ca-metasomatism are: Thor Lake, Northwest Territories, Canada (Pinckston & Smith, 1995), Ghurayyah microgranites, Saudi Arabia (Drysdall et al., 1984) and Khaldzan-Buregtey deposit, western Mongolia (Kovalenko et al., 1995). Each of these contain potentially economic HFSE deposits. Salvi & Williams-Jones (1996), through mass-balance calculations, determined that Ca-metasomatism influenced ore mineralization in the Strange Lake peralkaline complex and suggested that rare peralkaline complexes that have been affected by Ca-metasomatism are generally associated with potentially economic ore deposits. Thus, the sequence of events, from magmatic to Na- to Ca-metasomatic, strongly influenced the development of the ore minerals in the Strange Lake complex and may also influence those in other peralkaline complexes.

Conclusions

A complex series of events has taken place during the evolution of the Strange Lake peralkaline complex. Initial Na-metasomatism (Chapter 5) was overprinted by later Ca-metasomatism in specific regions of the pluton, such as in the ore zone and the altered subsolvus granite. The fluid responsible for Ca-metasomatism was Ca, K-, Mg-, Mn-, Zn- ± Al-enriched. This metasomatism resulted in the replacement of primary arfvedsonitic amphibole by winchite, wide-chain biopyriboles and tosudite, aegirine by winchite, and in the precipitation of the ore minerals, most of which are Ca-bearing. These silicates may have formed between about 100 and 350°C, which is consistent with the temperatures of Ca-metasomatism determined by Salvi & Williams-Jones (1990). Thus, the evolution of the Strange Lake peralkaline complex can be monitored through investigation of the mafic silicates. As these mafic silicates are common in peralkaline complexes, in general, these results can be applied to other peralkaline felsic complexes.

Acknowledgements

I thank G. Poirier for setting up the tables for elemental analysis for electron-microprobe analyses, and G. Gauthier, for setup and tuning of the LAM-ICP-MS.

Discussions on sample preparation, standards, standardization and errors for the LAM-ICP-MS analyses with G. Gauthier, C. Dalpé, Prof. S. Jackson and S. Lang were most helpful. The first two wrote the program used to calculate the elemental contents from raw LAM-ICP-MS data. C. Dalpé and Prof. N. MacRae provided the dark glasses HF-13 and JW-87, respectively. Drs. K. Livi and B. Grobéty introduced me to the TEM facilities at JHU. The bulk sample ICP-MS analyses were performed by Activation Laboratories, Ancaster, Ontario. This research was supported by NSERC, Lithoprobe, FCAR team and NSERC strategic grants to the second author. The TEM facility at JHU was run under Grant EAR94-17585 from National Science Foundation to DRV. This research could not have been completed without a FCAR scholarship and "stage" award, a major scholarship from McGill University, GSA student research award and SDE Women in Science award to me. This paper profited from reviews by A.E. Williams-Jones, K. Currie and C. Normand.

References

Abdel-Rahman, A.M. (1995): Chlorite in a spectrum of igneous rocks: mineral chemistry and paragenesis. *Mineralogical Magazine*, 59, 129-141.

Ahn, J.H. & Buseck, P.R. (1991): Microstructures and fiber-formation mechanisms of crocidolite asbestos. *American Mineralogist*, 76, 1467-1478.

Akai, J. (1982): Polymerization process of biopyribole in metasomatism at the Akatani ore deposit, Japan. *Contributions to Mineralogy and Petrology*, 80, 117-131.

------- & Saito, M. (1985): Ca-Mg triple-chain silicate derived from Na-Mg triple-chain silicate by ion-exchange experiment and its structural model. *Bulletin de Minéralogie*, 108, 21-28.

-------, Tomita, K. & Yamaguchi, Y. (1985): High resolution electron microscopic observation of pyroxene lamallae in oxyhornblende. *Earth Science*, 38, 334-345.

Alario-Franco, M., Hutchison, J.L., Jefferson, D.A. & Thomas, J.M. (1977): Structural imperfection and morphology of crocidolite-blue asbestos. *Nature*, 266, 520.

Allen, F. (1992): Mineral definition by HRTEM: problems and opportunities. *In* **Minerals and reactions at the atomic scale: Transmission Electron Microscopy** (Buseck, P.R., ed.). Mineralogical Society of America, Reviews in Mineralogy, 27, 289-333.

April, R. H. (1981a): Clay petrology of the upper Triassic/lower Jurassic terrestrial strata of the Newark Supergroup, Connecticut Valley, U.S.A. *Sedimentary Geology*, 29, 283-307.

------- (1981b): Trioctahedral smectite and interstratified chlorite/smectite in Jurassic strata of the Connecticut Valley. *Clays and Clay Minerals*, 29, 31-39.

Bélanger, M. (1984): Région du lac Brisson. *Ministère de l'Énergie et des Ressources*, Québec, DP 84-20 (carte annotée, scale 1:50,000).

Bettison, L.A. & Schiffman, P. (1988): Compositional and structural variations of phyllosilicates from the Point Sal Ophiolite, California. *American Mineralogist*, 73, 62-76.

Birkett, T.C., Miller, R.R., Roberts, A.C. & Mariano, A.N. (1992): Zirconium-bearing minerals of the Strange Lake intrusive complex, Quebec-Labrador. *Canadian Mineralogist*, 30, 191-205.

-------, Trzcienski, W.E., Jr. & Stirling, J.A.R. (1996): Occurrence and compositions of some Ti-bearing minerals in the Strange Lake intrusive complex, Quebec-Labrador boundary. *Canadian Mineralogist*, 34, 779-801.

Bodine, M.W. (1985): Clay mineralogy of insoluble residues in marine evaporites. *In* **Mineralogy - Applications to the Minerals Industry** (Hausen, D.M. & Kopp, O.C., eds.). American Institute of Mining, Metallurgical Petroleum Engineers, New York, 133-156.

Boily, M. & Williams-Jones, A.E. (1994): The role of magmatic and hydrothermal processes in the chemical evolution of the Strange Lake plutonic complex (Quebec-Labrador). *Contributions to Mineralogy and Petrology*, 118, 33-47.

Bonin, B. (1986): **Ring complex granites and anorogenic magmatism**. Studies in Geology, North Oxford Academic Publishers Ltd., Great Britian, 188p.

Borley, G.D. (1976): Ferromagnesian mineralogy and temperature of formation of the Younger Granites of Nigeria. *In* **Geology of Nigeria** (Kogbe, C.A., ed.). Elizabethan Press, Lagos, Nigeria, 159-176.

Bowden, P., Black, R., Martin, R.F., Ike, E.C., Kinnaird, J.A. & Batchelor, R.A. (1987): Niger-Nigerian alkaline ring complexes: a classic example of African Phanerozoic anorogenic mid-plate magmatism. *In* **Alkaline Igneous Rocks** (Fitton, J.G. & Upton, B.G.J., eds.). Geological Society Special Publication, 30, 357-379.

Bright, E. & Readey, D.W. (1987): Dissolution kinetics of TiO_2 in HF-HCl solutions. *Journal of the American Chemical Society*, 70, 900-906.

Chang, H.K., Mackenzie, F.T. & Schoonmaker, J. (1986): Comparisons between the diagenesis of dioctahedral and trioctahedral smectite, Brazilian offshore basins. *Clays and Clay Minerals*, 34, 407-423.

Chisholm, J.E. (1973): Planar defects in fibrous amphiboles. *Journal of Material Science*, 8, 475-483.

Cho, H.G. & Kim, S.J. (1994): Li-bearing tosudite from the Bubsoo mine, Korea. *Neues Jahrbuch für Mineralogie Montashefte*, 20, 130-137.

Crawford, D. (1980): Electron microscopy applied to studies of the biological significance of defects in crocidolite asbestos. *Journal of Microscopy*, 120, 181-192.

Cressey, B.A., Whittaker, E.J.W. & Hutchinson, J. L. (1982): Morphology and alteration of asbestiform grunerite and anthophyllite. *Mineralogical Magazine*, 46, 77-87.

Droop, G.T.R. (1994): Triple-chain pyriboles in Lewisian ultramafic rocks. *Mineralogical Magazine*, 58, 1-20.

------- (1987): A general equation for estimating Fe^{3+} concentrations in ferromagnesian silicates and oxides from microprobe analyses, using stoichiometric criteria. *Mineralogical Magazine*, 51, 431-435.

Drysdall, A.R., Jackson, N. J., Ramsay, C.R., Douch, C.J. & Hackett, D. (1984): Rare element mineralization related to Precambrian alkali granites in the Arabian Shield. *Economic Geology*, 79, 1366-1377.

Dudoignon, P., Beaufort, D. & Meunier, A. (1988): Hydrothermal alteration and supergene alterations in the granitic cupola of Montebras, Creuse, France. *Clays and Clay Minerals*, 36, 505-520.

Eberl, D. (1978): Reaction series for dioctahedral smectites. *Clays and Clay Minerals*, 26, 327-340.

Elliott, J.E. (1983): Peralkaline and peraluminous granites and related mineral deposits of the Arabian Shield. *U.S. Geological Survey, Open-File Report* 83-389, 35p.

Evarts, R.C. & Schiffman, P. (1983): Submarine hydrothermal metamorphism of the Del Puerto ophiolite, California. *American Journal of Science*, 283, 289-340.

Ferrow, E.A & Ripa, M. (1991): Chemistry, reaction mechanisms and micro-structures during retrograde metamorphism of gedrite-biotite-plagioclase bearing rocks from Bergslagen, south-central Sweden. *Lithos*, 26, 271-285.

Fiori, C.E., Swyt, C.R. & Myklebust, R.L. (1994): NIST/NIH Desktop spectrum analyzer program, Version 2.0.1. United States Department of Commerce.

Gieré, R (1986): Zirconolite, allanite and hoegbomite in a marble skarn from the Bergell contact aureole: implication for mobility of Ti, Zr and REE. *Contributions to Mineralogy and Petrology*, 65, 459-470.

------- (1990): Hydrothermal mobility of Ti, Zr, and REE: examples from the Bergell and Adamello contact aureoles (Italy). *Terra Nova*, 2, 60-67.

------- & Williams, C.T. (1992): REE-bearing minerals in a Ti-rich vein from the Adamello contact aureole (Italy). *Contributions to Mineralogy and Petrology*, 112, 83-110.

Graham, C.M., Maresch, W.V., Welch, M.D. & Pawley, A.R. (1989): Experimental studies on amphiboles: a review with thermodynamic perspectives. *European Journal of Mineralogy*, 1, 535-555.

Grim, R.E., Droste, J.B. & Bradley, W.F. (1960): A mixed-layer clay mineral associated with an evaporite. *Clays and Clay Minerals*, 8, 228-236.

Hawthorne, F.C., Ungaretti, L., Oberti, R., Cannillo, E. & Smelik, E.A. (1993): The mechanism of $^{[6]}$Li incorporation in amphiboles. *American Mineralogist*, 79, 443-451.

Hutchinson, J.L., Irusteta, M.C. & Whittaker, E.J.W. (1975): High-resolution electron microscopy and diffraction studies of fibrous amphiboles. *Acta Crystallographica*, A31, 794-801.

-------, ------- & ------- (1976): High resolution electron microscopy of amphiboles. *In* **Developments in Electron Microscopy and Analysis** (Venables, J.A., ed.). Academic Press, London, 497p.

Ichikawa, A. & Shimoda, S. (1976): Tosudite from the Hokuno mine, Hokuno, Gifu prefecture, Japan. *Clays and Clay Minerals*, 24, 142-148.

Janeczek, J. (1994): The effect of aluminous titanite on the biotite-chlorite and amphibole-chlorite reactions. *European Journal of Mineralogy*, 6, 623-625.

Kamineni, D.C. (1987): Halogen-bearing minerals in plutonic rocks: a possible source of chlorine in saline groundwater in the Canadian Shield. *In* **Saline water and gases in crystalline rocks** (Fritz, P. & Frape, S.K., eds.). Geological Association of Canada, Special Paper, 33, 69-79.

Keppler, H. (1993): Influence of fluorine on the enrichment of high field strength trace elements in granitic rocks. *Contributions to Mineralogy and Petrology*, 114, 479-488.

Koenig, G.A. (1876): Hexagonite, Goldsmith, a variety of tremolite. *Proceedings of the Academy of Natural Sciences of Philadelphia*, 1876, 180-181.

Kovalenko, V.I., Tsaryeva, G.M., Goreglyad, A.V., Yarmolyuk, V.V. Troitsky, V.A., Hervig, R.L. & Farmer, G.L. (1995): The peralkaline granite-related Khaldzan-Buregtey rare metal (Zr, Nb, REE) deposit, western Mongolia. *Economic Geology*, 90, 530-547.

Maksimovic, Z. & Brindley, G.W. (1980): Hydrothermal alteration of a serpentinite near Takovo, Yugoslavia to chromium-bearing illite/smectite, kaolinite, tosudite, and halloysite. *Clays and Clay Minerals*, 28, 295-302.

Maresch, W.V. & Czank, M. (1983): Problems of compositional and structural uncertainty in synthetic hydroxyl-amphiboles; with an annotated atlas of the realbau. *Peridico di Mineralogia*, 52, 463-542.

Martin, R.F. (1977): The association hypersolvus granite-subsolvus granite-"solvsbergite" at Andrew's Point, Cape Ann, Massachusetts: a case of localized fenitization. *American Journal of Sciences*, 277, 273-287.

Miller, R.R. (1986): Geology of the Strange Lake alkalic complex and the associated Zr-Y-Be-REE mineralization. Current Research, *Newfoundland Department of Mines and Energy, Mineral Development Division*, Report 86-1, 11-19.

-------- (1988): Yttrium (Y) and other rare metals (Be, Nb, REE, Ta, Zr) in Labrador. Current Research, *Newfoundland Department of Mines and Energy, Mineral Development Division*, Report 88-1, 229-245.

------- (1996): Structural and textural evolution of the Strange Lake peralkaline rare-element (NYF) granitic pegmatite, Quebec-Labrador. *Canadian Mineralogist*, 34, 349-371.

Morrison, S.J. & Parry, W.T. (1986): Dioctahedral corrensite from Permian red beds, Lisbon Valley, Utah. *Clays and Clay Minerals*, 34, 613-624.

Nassif, G.J. (1993): The Strange Lake peralkaline complex, Québec-Labrador: The hypersolvus-subsolvus granite transition and feldspar mineralogy. McGill University, M.Sc. Thesis, Montreal, Québec, 104p.

------- & Martin, R.F. (1991): The hypersolvus granite-subsolvus granite transition at Strange Lake, Quebec-Labrador. *Geological Association of Canada - Mineralogical Association of Canada*, Abstracts with Programs, 16, A89.

Nishiyama, T., Shimoda, S., Shimosaka, K. & Kanaoka, S. (1975): Lithium-bearing tosudite. *Clays and Clay Minerals*, 23, 337-342.

O'Halloran, D.A. (1985): Ras ed Dom migrating ring complex: A-type granites and syenites from the Dayuda Desert, Sudan. *Journal of African Earth Sciences*, 3, 61-75.

Oberti, R., Smith, D.C., Rossi, G. & Caucia, F. (1991): The crystal-chemistry of high-aluminium titanites. *European Journal of Mineralogy*, 3, 777-792.

Pillet, D., Chenevoy, M. & Bélanger, M. (1992): Pétrologie du granite peralcalin du lac Brisson, Labrador central, Nouveau-Québec. I. Mode de mise en place et évolution chimique. *Canadian Journal of Earth Sciences*, 29, 353-372.

-------, ------- & ------- (1993): Pétrologie du granite peralcalin du lac Brisson, Labrador central, Nouveau-Québec. II. Minéralogie et modalités de cristallisation. *Canadian Journal of Earth Sciences*, 30, 2423-2435.

Pinckston, D.R. & Smith, D.G.W. (1995): Mineralogy of the Lake zone, Thor Lake rare-metals deposit, N.W.T., Canada. *Canadian Journal of Earth Sciences*, 32, 516-532.

Pollard, P.J. (1989): Lanthanides, tantalum and niobium: mineralogy, geochemistry, characteristics of primary ore deposits, processing and applications. *In* **Proceedings of a workshop, Berlin, November 1986** (Möller, P., Saupé, F. & Cerný, P., eds.). The Society for Geology Applied to Mineral Deposits, Special Publication 7, Springer-Verlag, New York.

Rubin, J.N., Henry, C.D. & Price, J.G. (1993): The mobility of zirconium and other "immobile" elements during hydrothermal alteration. *Chemical Geology*, 110, 29-47.

Salvi, S. & Williams-Jones, A.E. (1990): The role of hydrothermal processes in the granite-hosted Zr, Y, REE deposit at Strange Lake, Quebec/Labrador: Evidence from fluid inclusions. *Geochimica et Cosmochimica Acta*, 54, 2403-2418.

------- & ------- (1992): Reduced orthomagmatic C-O-H-NaCl fluids in the Strange Lake rare-metal granitic complex, Quebec/Labrador, Canada. *European Journal of Mineralogy*, 4, 1155-1174.

------- & ------- (1995): Zirconosilicate phase relations in the Strange Lake (Lac Brisson) pluton, Quebec-Labrador. *American Mineralogist*, 80, 1031-1040.

------- & -------- (1996): The role of hydrothermal processes in concentrating HFSE in the Strange Lake peralkaline complex, northeastern Canada. *Geochimica et Cosmochimica Acta*, 60, 1917-1932.

Schumacher, J.D. & Czank, M. (1987): Mineralogy of triple-and double-chain pyriboles from Orijärvi, southwest Finland. *American Mineralogist*, 72, 345-352.

Shimoda, S. (1969): New data for tosudite. *Clays and Clay Minerals*, 17, 179-183.

Smelik, E.A. (1995): Fluid channelization at the submicroscopic scale in exsolved orthoamphiboles. *European Journal of Mineralogy*, 7, 825-834.

Smith, R.M. & Martell, A.E. (1974): **Critical stability constants. Volume 4: Inorganic complexes**. Plenum Press, New York, 257p.

Tateyama, H., Shimoda, S. & Sudo, T. (1978): Synthesis and crystal structure of a triple-chain silicates, $Na_2Mg_4Si_6O_{16}(OH)_2$. *Contributions to Mineralogy and Petrology*, 66, 149-156.

Taylor, R.P., Strong, D.F. & Fryer, B.J. (1981): Volatile control of contrasting trace element distributions in peralkaline granitic and volcanic rocks. *Contributions to Mineralogy and Petrology*, 77, 267-271.

Vard, E. & Williams-Jones, A.E. (1993): A fluid inclusion study of vug minerals in dawsonite-altered phonolite sills, Montreal, Quebec: implications for HFSE mobility. *Contributions to Mineralogy and Petrology*, 113, 410-423.

Veblen, D.R. (1992): Electron microscopy applied to nonstoichiometry, polysomatism, and replacement reactions in minerals. *In* **Minerals and reactions at the atomic scale: Transmission Electron Microscopy** (Buseck, P.R., ed.). Mineralogical Society of America, Reviews in Mineralogy, 27, 181-229.

------- & Burnham, C.W. (1978a): New biopyriboles from Chester, Vermont: I. Descriptive mineralogy. *American Mineralogist*, 63, 1000-1009.

------- & ------- (1978b): New biopyriboles from Chester, Vermont: II. The crystal chemistry of jimthompsonite, clinojimthompsonite, and chesterite, and the amphibole-mica reaction. *American Mineralogist*, 63, 1053-1073.

------- & Buseck, P.R. (1979): Chain-width order and disorder in biopyriboles. *American Mineralogist*, 64, 687-700.

------- & ------- (1980): Microstructures and reaction mechanisms in biopyriboles. *American Mineralogist*, 65, 599-623.

------- & ------- (1981): Hydrous pyriboles and sheet silicates in pyroxenes and uralites: intergrowth microstructures and reaction mechanisms. *American Mineralogist*, 66, 1107-1134.

-------, ------- & Burnham, C.W. (1977): Asbestiform chain silicates; new minerals and structural groups. *Science*, 198, 359-365.

Vergo, N. & April, R.H. (1982): Interstratified clay minerals in contact aureoles, West Rock, Connecticut. *Clays and Clay Minerals*, 30, 237-240.

Welch, M.D., Rocha, J. & Klinowski, J. (1992): Characterization of polysomatism in biopyriboles: double-chain/triple-chain lamellar intergrowths. *Physics and Chemistry of Minerals*, 18, 460-468.

Whittaker, E.J.W., Cressey, B.A. & Hutchison, J.L. (1981): Terminations of multiple-chain lamellae in grunerite asbestos. *Mineralogical Magazine*, 44, 27-35.

Willis, M.A., Pasteris, J.D. & Shock, E.L. (1990): Hydrothermal transport of titanium as exemplified by quartz-titanium dioxide veins near Magnet Cove, Arkansas. *Geological Society of America*, Abstracts with Programs, A363.

Wood, S.A. (1990): The aqueous geochemistry of the rare-earth elements and yttrium 2. Theoretical predictions of speciation in hydrothermal solutions to 350°C at saturation water vapor pressure. *Chemical Geology*, 88, 99-125.

Yau, Y.-C., Peacor, D.R. & Essene, E.J. (1986): Occurrence of wide-chain Ca-pyriboles as primary crystals in the Salton Sea Geothermal Field, California, USA. *Contributions to Mineralogy and Petrology*, 94, 127-134.

Zajac, I.S., Miller, R.R., Birkett, T.C. & Nantel, S. (1984): Le gîte de Zr, Y, Nb et Be du complexe alcalin de Strange Lake, Québec-Labrador. *Ministère de l'Énergie et des Ressources du Québec*, DV 84-18, 127-142.

Epilogue

Comparison between the Mafic Silicates from the Two Complexes

A brief comparison of the results from the present study on the Amba Dongar carbonatitic-alkaline complex and the Strange Lake peralkaline complex highlights the effects of fenitization on the mafic silicates amphibole, pyroxene and mica. It is interesting to note, that although each complex contains very different units (e.g., silica-undersaturated in the case of Amba Dongar and silica-oversaturated in the case of Strange Lake) the mineralogy, types of metasomatism and related ore deposits show distinct similarities.

Amphibole from the Strange Lake complex is fluor-arfvedsonitic amphibole (approximately $Arf_{0.80}Lkt_{0.15}Rbk_{0.05}$). It is Mn-, Zn-, Li- and HFSE-rich, but Ca-, Mg-, Al- and K-poor compared to the fluor-richteritic amphibole (on average $Ric_{0.88}Arf_{0.12}$) from the Amba Dongar complex. However, arfvedsonitic amphibole from the Strange Lake complex also may be Ca-rich, when it contains minute inclusions of F-rich minerals or has been affected by Ca-metasomatism. An extreme case of the effects of Ca-metasomatism on the amphibole is that of the winchitic amphibole or wide-chain biopyribole replacement of arfvedsonitic amphibole. Fabriès (1978) noted that amphibole associated with carbonatite is generally K-rich richterite; amphibole from the Amba Dongar complex conforms, as it is more Mg- and K-rich, but Fe-poor compared to that from the Strange Lake complex. Amphibole from the Amba Dongar complex is solely of metasomatic origin, whereas that of the Strange Lake complex is dominantly of primary origin and more plentiful, but also may exhibit the effects of metasomatism.

Pyroxene from the Strange Lake complex is on average $Ae_{0.87}Hd_{0.12}Di_{0.01}$, whereas that from the Amba Dongar complex varies widely from approximately $Di_{0.85}Ae_{0.10}Hd_{0.05}$ to $Ae_{0.95}Di_{0.05}$. Aegirine from the Strange Lake complex is, as already noted for the amphibole, more enriched in Mn, Zn, Ti and HFSE compared to the aegirine-augite from the Amba Dongar complex, which is enriched in Cr and V. For pyroxene from the Strange Lake complex, the composition of the secondary pyroxene is tied to the composition of the amphibole that it has replaced and minute inclusions of either hematite, or astrophyllite and F-rich minerals (Chapter 5). The subsolvus origin of Type-1 aegirine from the Strange Lake

complex is at the same late-stage in the sequence of crystallization as the aegirine-rich rims to aegirine-augite from the Amba Dongar carbonatitic-alkaline complex. Thus, this variation in composition of pyroxene from both complexes is related to both their magmatic and metasomatic origins.

Disordered wide-chain biopyriboles with a Na:Ca of up to 1:1 were observed in arfvedsonitic and winchitic amphibole, but no biopyriboles were observed whose structure was intermediate to that of the arfvedsonitic amphibole and aegirine or aegirine-augite and mica. These observations concur with previous suggestions on a limit to the amount of Na that can be accommodated in the biopyribole (Akai & Saito, 1985). The bulk replacement of arfvedsonitic amphibole by aegirine observed in this study provides further support for this relationship. Likewise, no K-Na biopyriboles were observed between aegirine-augite and mica, so intermediate biopyriboles may not exist.

Biotite is a common product of contact metasomatism (e.g., glimmerite) in the Amba Dongar complex, while rare chlorite-smectite intergrowths replace amphibole in the Strange Lake complex. In the Amba Dongar complex, I determined that metasomatic biotite crystallized in the glimmerite at the expense of phlogopite, and to a lesser extent, feldspar and aegirine-augite. Later hydrothermal alteration of mica from the glimmerite produces hydrobiotite. In Chapter 3, I suggest that formation of this vermiculite is contemporaneous with precipitation of the clay mineral noted by Palmer (1994) in the white fluorite layer of the fluorite deposit (Chapter 3). The phyllosilicate intergrowths between chlorite and smectite are indicative of formation following the interaction of arfvedsonitic amphibole with fluids during Ca-metasomatism (Chapter 6).

References

Akai, J. & Saito, M. (1985): Ca-Mg triple-chain silicate derived from Na-Mg triple-chain silicate by ion-exchange experiment and its structural model. *Bulletin de Minéralogie*, 108, 21-28.

Fabriès, J. (1978): Les types paragénétiques des amphiboles sodiques dans les roches magmatiques. *Bulletin de Minéralogie*, 107, 155-165.

Palmer, D. (1994): Geology and geochemistry of the Amba Dongar carbonatite-hosted fluorite deposit, India. Unpublished M.Sc. thesis, McGill University, Montréal, Québec, 109p.

Chapter 7:

CONCLUSIONS

General Conclusions

The influences of magma degassing and magma evolution followed by later metasomatism have been documented in the two complexes. The enrichment in incompatible elements (e.g., HFSE and REE) of later amphibole in the Strange Lake complex is the result of magma evolution. The effects of degassing also are observed in the composition of the last arfvedsonitic amphibole (Type-3 amphibole) to crystallize contains distinctly more K than either Type-1 or -2 amphibole. Furthermore, the zonation between amphibole and the aegirine assemblage in composite mafic grains from the altered subsolvus granite indicates the possibility of a a variation in fO_2 such that crystallization of the mafic mineral may switch from within the field where arfvedsonitic amphibole is stable to that in which the aegirine assemblage is stable. Thus, the results of this study provide additional support for the process of degassing in the Strange Lake complex. Subsolidus reactions involved the crystallization of Type-1 aegirine as rims on the arfvedsonitic amphibole. In the Amba Dongar complex, the influence of magma evolution is reflected in the slight change in composition of the mica from the reversely pleochroic phlogopite, while the subsolidus reactions result in the formation of late-stage subsolidus rims of aegirine on aegirine-augite grains.

Both complexes exhibit Na- to Ca-metasomatism; Mg- and K-fenitization also occur at the expense of alkaline volcanic or plutonic rocks, or at the expense of Bagh sandstone, respectively, in the Amba Dongar complex. In these complexes, metasomatism varies from widespread to localized (e.g., K or Ca - glimmerite or secondary amphibole). Later Ca-metasomatism is extremely localized, but it occurs in sodic fenites in the Amba Dongar complex. In this complex, the difference between the Na- and K-fenites, as interpreted from their mineralogy, is related to a change in the temperature of the metasomatic fluid (determined from XRD data on the K-feldspar) such that, at high temperatures, it produced Na-rich fenites and, at lower temperatures, it produced K-rich fenites. Fenites from the Amba Dongar complex show that the metasomatic fluid was enriched in Na, K, Ca, S, Ba and Al. Furthermore, formation of glimmerite involved a metasomatic fluid enriched in K, Mg, Al and Fe. Finally, later hydrothermal alteration, related to formation of the associated fluorite deposit, caused vermiculitization of the micas.

In the Strange Lake complex, Na-metasomatism resulted in aegirine replacement of arfvedsonitic amphibole, thereby releasing HFSE, REE, Mn, Zn, K, Li and F (Chapter 5) into solution. Subsequently, more localized Ca-metasomatism destabilized these aqueous complexes, resulting in the precipitation of fluorite and Ca-rich secondary minerals. In Chapter 6, it was shown that this metasomatic fluid must have contained sufficient Ca, Mn, Zn, Al, K and Mg to allow winchitic amphibole and CaMg-enriched wide-chain biopyriboles and chlorite-smectite to crystallize. Thus, the composition of the initial rock and fluid, and the temperature at which metasomatism occurred, explain the difference between metasomatized rocks of both complexes and their relationship to formation of the associated ore deposits. Consequently, primary mafic silicates can undergo metasomatic reactions which result in mobilization of elements that contribute to formation of the associated ore deposits.

Contributions to Knowledge

The most important original contributions to knowledge provided by this thesis are:

1. Arfvedsonitic amphibole may act as a sink for Li, REE and a number of other trace-elements. In particular, release of HFSE and REE from breakdown of amphibole and its inclusions may have a significant effect on the formation of such element-enriched deposits.
2. In both complexes, metasomatism of the mafic silicates is associated with ore mineralization. In the Amba Dongar complex, this is reflected by the vermiculitization of biotite, while in the Strange Lake complex, it is reflected by aegirine replacement of arfvedsonitic amphibole, formation of wide-chain biopyriboles, winchitic amphibole replacement of aegirine and arfvedsonitic amphibole and replacement of arfvedsonitic amphibole by a phyllosilicate. Thus, examination of the commonly overlooked mafic silicates can round out the overall description of the fluid evolution in a complex, as their patterns of alteration provide indications of the fluid evolution in the complex.
3. This thesis provides a detailed mineralogical, petrological, and, in part, a chemical explanation for fenitization of a number of units from the Amba Dongar carbonatitic-alkaline complex, and therefore, expands on the previous studies of fenitization as these variations are described from one complex and of dominantly one origin. Before this could

be accomplished, the nature of the variation in composition of the mineral produced by magmatic processes (magma evolution and degassing) was ascertained.

4. The observed compositional variation of arfvedsonitic amphibole to higher ΣNa+K+Si is related to variation in the trace-element content and an estimated Fe^{3+}/Fe^{2+} ratio, than to the presence of biopyriboles.

5. The most common oxide mineral in the complex is hematite, not magnetite. In the mafic minerals, hematite occurs in the aegirine replacement assemblage of arfvedsonitic amphibole, but only in the altered subsolvus granite. In the hypersolvus granite, aegirine replacement by arfvedsonitic amphibole is accompanied by the previously undescribed presence of astrophyllite and fluorite.

6. The compositional variation of amphibole (e.g., K enrichment), and late crystallization of aegirine in the Strange Lake complex provides additional support for the occurrence of late degassing.

7. This study is one of a growing number on biopyriboles, but it is unusual in that it examined the presence of alkali biopyriboles between Na- and Fe-rich pyroxene and amphibole and K-Na silicates. The results imply the influence of the presence of Ca to the formation of, in particular, wide-chain biopyriboles. This is one of a relatively small number of studies that examine the formation of alkali biopyriboles, but the first to examine those from peralkaline complexes in detail.

Suggestions for Further Investigation

A number of findings of this study that warrant further investigation. They are:

1. Portions of the two complexes require further mapping. Detailed remapping of the Amba Dongar complex is required, as it has not been mapped since the area was deforested. The main aim would be to evaluate the full extent of the "ultrafenite" at Amba Dongar complex and at Strange Lake the effects of metasomatism on the country-rocks remains to be examined. These reactions are critical to a full understanding of the formation of the Ca-rich fluid that selectively infiltrated parts of the complex late in its evolution.

2. A more detailed hydrogen isotope study needs to be conducted on minerals from the hypersolvus granite and mafic pods to evaluate the importance of degassing in the evolution

of the complex. This would be arrived at by comparison the results of such a study with the results of Boily & Williams-Jones (1994). What would be best is to perform this study with the aid of a method of point analysis whereby one could perform analyses for H such as by ion probe.

3. In this study, I did not conclusively resolve the differences in alteration between normal and reversely pleochroic mica. TEM results suggest that the presence of Fe^{3+} in the tetrahedral site, and coloration of the latter mica may be related, in part, to the presence of minute hematite inclusions. A study combining TEM examination with Mössbauer spectroscopy of less altered mica from related complexes should resolve whether these inclusions contribute to this variation.

4. Further examination of phyllosilicates formed by hydrothermal alteration or weathering in peralkaline complexes with the TEM is necessary as, to date, only XRD data (Abdel-Rahman, 1995) and the little TEM data noted in this study exist on this alteration.

5. Cathodoluminescence can be used to resolve the fine-scale zonation in apatite from the Amba Dongar complex, as well as to provide a correlation between zonation of the amphibole with the composition of the feldspar and the type of fluoride present as inclusions in amphibole from the Strange Lake complex. Finally, WDS analyses are required of the composite REE- and Y-rich fluoride grains to correlate the variations observed in the CL images with the different types of F-rich minerals.

6. Detailed LAM-ICP-MS and electron-microprobe analyses of the swapped margins present between arfvedsonitic amphibole and albite (Chapter 4) will best describe the process involved in the formation of this texture.

7. Electron-microprobe analyses and optical examinations suggest that some of the compositional variation noted for the alkali Ti-silicates (e.g., astrophyllite, aenigmatite and neptunite) may be related to fine-scale intergrowths. Further support for this variation comes from the structural similarities of these Ti-silicates to each other, and aegirine or magnetite (Kelsey & McKie, 1964; Woodrow, 1967; Zoltai & Stout, 1984; Barbier & Hyde, 1988). Detailed TEM examination of these minerals from a number of localities can be used to examine their presence.

References

Abdel-Rahman, A.M. (1995): Chlorite in a spectrum of igneous rocks: mineral chemistry and paragenesis. *Mineralogical Magazine*, 59, 129-141.

Barbier, J. & Hyde, B.G. (1988): Structure of sapphirine: its relation to the spinel, clinopyroxene and beta-gallia structures. *Acta Crystallographica*, B44, 373-377.

Boily, M. & Williams-Jones, A.E. (1994): The role of magmatic and hydrothermal processes in the chemical evolution of the Strange Lake plutonic complex (Quebec-Labrador). *Contributions to Mineralogy and Petrology*, 118, 33-47.

Kelsey, D.H. & McKie, D. (1964): The unit cell of aenigmatite. *Mineralogical Magazine*, 33, 986-1001.

Woodrow, P.J. (1967): The crystal structure of astrophyllite. *Acta Crystallographica*, 22, 673-678.

Zoltai, T. & Stout, J.H. (1984): **Mineralogy Concepts & Principles**. Burgess Publishing Company, Minneapolis, Minnesota, 505p.

Appendix A:

Amba Dongar carbonatitic-alkaline complex

Appendix A-1: Description of Fenites and Related Rocks

Bagh sandstone (10A and 34). At the outcrop scale, this pure quartzite sandstone show cross bedding. In hand sample, it is white or grey and medium-grained. In thin section, it is composed of 96-98 vol.% quartz, which may exhibit textures indicative of recrystallization, with traces of feldspar, chlorite and hematite.

Potassic fenite of Bagh sandstone (30C, 37C, 47C, 48B and 49). This fenite, which is readily altered to clay minerals, is pink, buff or red owing to the presence of feldspar (to 30 vol.%) and hematite (3-5 vol.%). Feldspathization produces microcline or orthoclase (± albite and traces of muscovite) at the expense of quartz, whereas the remaining relict quartz is strained (shows undulose extinction) and finer grained, and thus, recrystallized.

Sodic fenite of Bagh sandstone (87/A/94 and 7/A/114.8). Both feldspathization and recrystallization also occurred in these fenites. Thus, this fenite is identical to potassic fenite, except for the nature of the dominant feldspar (albite). The more sodic composition is also reflected in the presence of poikilitic pyroxene (to 10 vol.%) and rare amphibole (to 5 vol.%) in some samples.

Sodi-potassic fenite of Bagh Sandstone (66L, 68 and 8V). The fenite exhibits both the textures and mineralogy described for the potassic and sodic fenite, although the only mafic mineral is hematite. The feldspars are a combination of albite and K-feldspar and comprise up to 40 vol.% of the rock.

"Ultrafenite" (43A, 66I and 66K) is extremely fine-grained (<15 mm) green to dark green and banded. It consists of 45 vol.% anhedral feldspar (albite or sanidine dominant), and <10 vol.% quartz, as well as up to 7-15 vol.% hematite (produces a brownish colour in more enriched samples), 25-40 vol.% weakly zoned and preferentially oriented green pyroxene or rare pale green yellow amphibole, with up to 5 vol.% barite. Dark bands that parallel this orientation result from variations in the hematite, pyroxene and amphibole content. There is a lack of igneous texture, although banding, swirls and ovoid regions (feldspar and amphibole) are present. Four types of veins (to 5 mm), which contain variable amounts of carbonate, amphibole, aegirine, hematite and britholite, cross-cut the samples.

Nephelinite or Tephrite

Unfenitized (9, 22B and 37A) volcanic rock is green and contains medium- to coarse-grained euhedral phenocrysts of complicated and strongly zoned, resorbed green prismatic pyroxene (7-10 vol.%), altered rectangular nepheline (12-15 vol.%) and normally or oscillatory zoned garnet (dark red-brown core to lighter brown rim; 5-10 vol.%), as well as ubiquitous fine-grained apatite (3 vol.%) and rare twinned titanite. The fine-grained altered groundmass contains hematite, calcite, analcime, orthoclase or sanidine, nepheline and clay minerals.

Appendix A-1: Description of Fenites and Related Rocks

Fenitized (66B, 66F and 1205/Vil/A). Potassic fenites form a halo (to 15 cm) of increasing metasomatism at the edge of the calciocarbonatite vein, which cumulates in a 0.5 to 1 cm glimmerite (86 vol.% brown to green brown biotite, 10 vol.% hematite, 5 vol.% calcite and 7 vol.% apatite is formed) at the vein margin. These rocks are zoned from green, fresh rock to pink near the vein. In the halo, pyroxene varies from euhedral and zoned to green and unzoned between fresh and fenitized rock, respectively. The relative amount of feldspar (mostly orthoclase) increases toward the vein. Both are concurrent with a steady increase in the amount of mica at the expense of pyroxene and K-feldspar. Immediately adjacent to the vein, the amount of apatite and size of reversely pleochroic mica cores increase. Weathered sodi-potassic fenite (1205/Vil/A) is composed of predominantly of zoned feldspars and minor amphibole and hematite ± barite. These feldspars have been weathered to clay minerals associated with hematite.

Ijolite or Urtite

Unfenitized (66J). Both are green in colour and mineralogically equivalent to the volcanic rocks, except that they contain anhedral alkali feldspar(s) ± prismatic wollastonite and anhedral nepheline. The difference between the ijolite and urtite is the amount of aegirine present.

Fenitized (66A and 66D). Fenitized examples of these plutonic rocks are comparable to that from the volcanic rocks described above in terms of mineralogy and zonations. However, as the habits of minerals in the original plutonic rock are distinct from those in the volcanic rocks, those of the fenites vary in the same manner.

Veins or dykes (66D - syenite and 66J - melteigite). The 1 cm to 0.5 m veins contain comb-textured pyroxene at the margin, but the syenite vein contains two orthoclase feldspars at the core and disseminated hematite throughout. On the other hand, the melteigite vein also contains significant nepheline and is distinctly enriched in comb-textured pyroxene. Apatite is present at the cores of the felsic minerals (to 3 or 5 vol.%). Trace amounts of fine-grained wedges of titanite are also present. Composite anhedral sulphide-oxide grains (3-7 vol.%), containing chalcopyrite at the core, pyrite and finally magnetite, or more commonly, hematite at the rim, occur between the pyroxene grains.

Appendix A-1: Description of Fenites and Related Rocks

Carbonatite (8C, 10A, 13D and 15A). In the field, the carbonatites vary from a brecciated to coarse-grained or fine-grained and brecciated or plugs, which may contain significant hematite (pseudomorphous after magnetite), apatite and barite. The relative amount of iron oxide changes the hand sample coloration from a pale yellow to yellow brown to brown to red brown. The samples selected for analysis are closely associated with the rocks examined in this study, and are predominantly calciocarbonatite. These calciocarbonatites are composed predominantly of calcite with small amounts of ankerite present in some samples (especially in the veins). Traces of hematite and REE carbonates, as well as rare phlogopite, apatite, fluorite, pyrochlore, barite and thorite were observed.

Samples provided by Dr. S. Viladkar

Sample #	Depth	Description
1205/Vil/A	Surface	Sodic fenite of Bagh sandstone
7/A/114	Surface	Sodic fenite of Bagh sandstone
BH/3/1	103 m	Fenitized nephelinite
BH/4/2	18.8 m	Fenitized nephelinite
BH/6/1	100 m	Fenitized nephelinite
BH/8/1	98 m	Fenitized nephelinite
BH/9/1	91.5 m	Fenitized nephelinite
BH/16/9	99 m	Glimmerite
BH/18/1	84 m	Glimmerite
BH/18/2	82 m	Glimmerite
BH/21/1	39.92 m	Glimmerite

Appendix A-2: Results of electron-microprobe analyses of aegirine-augite*

Sample #	AD037A											AD054B1
Description	40 edge	41	42	43	44	45	46	47 edge	48	49	50	68 lt.ed.
SiO_2	50.18	50.62	50.71	50.59	50.19	49.86	49.52	49.61	49.71	49.96	49.97	52.38
TiO_2	0.38	0.45	0.40	0.45	0.72	0.75	0.61	0.46	0.60	0.51	0.42	0.13
Al_2O_3	1.22	1.46	1.24	1.70	2.33	1.65	2.08	1.82	1.45	1.69	1.08	0.32
Fe_2O_3	8.63	7.30	10.56	11.12	8.07	10.75	8.73	9.99	9.81	9.22	8.33	8.93
FeO	11.14	9.29	9.58	8.30	6.85	9.93	8.17	10.05	9.51	8.38	10.97	3.69
MgO	6.20	8.28	6.22	6.59	9.17	5.80	7.94	5.86	6.35	7.67	6.30	11.37
MnO	0.88	0.66	0.76	0.64	0.47	0.72	0.58	0.66	0.91	0.64	1.02	0.38
ZnO	0.00	0.00	0.00	0.00	0.00	0.00	0.00	0.00	0.00	0.00	0.00	0.00
V_2O_3	0.13	0.11	0.14	0.16	0.18	0.17	0.15	0.15	0.22	0.17	0.17	0.02
Cr_2O_3	0.01	0.01	0.00	0.02	0.03	0.00	0.00	0.02	0.00	0.01	0.00	0.00
ZrO_2	n.d.	n.d.	n.d.	n.d.	n.d.	n.d.	n.d.	n.d.	n.d.	n.d.	n.d.	0.09
Nb_2O_5	0.09	0.00	0.03	0.00	0.04	0.00	0.01	0.05	0.03	0.00	0.00	0.00
CaO	19.54	20.58	18.28	17.52	20.01	18.32	20.07	18.47	18.71	19.74	19.62	19.55
Na_2O	2.66	2.12	3.49	3.83	2.46	3.41	2.41	3.23	3.08	2.63	2.54	2.89
K_2O	0.00	0.00	0.00	0.00	0.00	0.00	0.00	0.00	0.00	0.00	0.00	0.00
Total	101.04	100.88	101.42	100.91	100.52	101.37	100.26	100.36	100.37	100.61	100.41	99.74
Si	1.931	1.926	1.935	1.928	1.899	1.910	1.897	1.917	1.918	1.910	1.934	1.967
Ti	0.011	0.013	0.012	0.013	0.021	0.022	0.018	0.013	0.017	0.015	0.012	0.004
^{IV}Al	0.055	0.066	0.056	0.072	0.101	0.074	0.094	0.083	0.066	0.076	0.049	0.014
ΣTet	1.997	2.005	2.003	2.013	2.020	2.006	2.008	2.013	2.002	2.000	1.996	1.984
Fe^{3+}	0.250	0.209	0.303	0.319	0.230	0.310	0.252	0.291	0.285	0.265	0.243	0.252
Fe^{2+}	0.359	0.296	0.306	0.265	0.217	0.318	0.262	0.325	0.307	0.268	0.355	0.116
Mg	0.355	0.470	0.354	0.374	0.517	0.331	0.453	0.337	0.366	0.437	0.364	0.636
Mn	0.029	0.021	0.025	0.021	0.015	0.023	0.019	0.022	0.030	0.021	0.033	0.012
Zn	0.000	0.000	0.000	0.000	0.000	0.000	0.000	0.000	0.000	0.000	0.000	0.000
^{VI}Al	0.000	0.000	0.000	0.005	0.003	0.000	0.000	0.000	0.000	0.000	0.000	0.000
V	0.004	0.003	0.004	0.005	0.006	0.005	0.005	0.005	0.007	0.005	0.005	0.001
Cr	0.000	0.000	0.000	0.001	0.001	0.000	0.000	0.001	0.000	0.000	0.000	0.000
Zr	0.000	0.000	0.000	0.000	0.000	0.000	0.000	0.000	0.000	0.000	0.000	0.002
Nb	0.002	0.000	0.001	0.000	0.001	0.000	0.000	0.001	0.000	0.000	0.000	0.000
ΣOct.	0.998	1.000	0.992	0.989	0.988	0.988	0.990	0.980	0.994	0.997	1.000	1.019
Ca	0.806	0.839	0.747	0.715	0.811	0.752	0.824	0.765	0.774	0.809	0.814	0.787
Na	0.199	0.157	0.258	0.283	0.181	0.253	0.179	0.242	0.230	0.195	0.191	0.211
K	0.000	0.000	0.000	0.000	0.000	0.000	0.000	0.000	0.000	0.000	0.000	0.000
ΣOct.	1.004	0.996	1.005	0.998	0.991	1.006	1.002	1.007	1.004	1.003	1.004	0.997
Mol.%												
Aegirine	19.85	15.67	25.80	27.81	17.75	25.34	17.86	24.18	23.03	19.48	19.05	21.06
Diopside	35.54	46.98	35.40	37.44	51.67	33.13	45.30	33.74	36.55	43.72	36.36	63.63
Hedenbergite	35.86	29.56	30.58	26.46	21.68	31.82	26.18	32.46	30.70	26.78	35.50	11.58
Jadeite	0.00	0.00	0.00	0.50	0.30	0.00	0.00	0.00	0.00	0.00	0.00	0.00
Pyroxmangite	1.43	1.07	1.23	1.04	0.75	1.17	0.94	1.08	1.49	1.04	1.67	0.60
$CaFeAlSiO_6$	4.39	5.24	4.51	4.07	5.23	5.66	7.29	4.88	4.46	6.05	3.23	1.18
$CaTiAl_2O_6$	1.09	1.28	1.15	1.29	2.05	2.16	1.75	1.33	1.74	1.45	1.22	0.36
$CaCrAlSiO_6$	0.02	0.04	0.00	0.05	0.10	0.01	0.00	0.05	0.00	0.04	0.00	0.00

* Mineral formulae calculated based on 4 cations and 6 oxygens, with Fe^{3+} determined by charge balance

Acronyms: fi. = fine; med. = medium; v. = very; mid. = middle; lt. = light; ed. = edge

Appendix A-2: Results of electron-microprobe analyses of aegirine-augite*

Sample #	AD054B1			AD054B2								
Description	69 med.	71 nr.ed.	72 cs	51 cs	52	53	54 fl.gr.	55	56 dkr	57 other	58	59 fl.dkr
SiO_2	50.42	49.45	51.27	50.88	51.12	51.42	51.62	52.67	51.51	51.37	51.14	52.77
TiO_2	1.34	0.33	0.17	0.53	0.49	0.23	0.31	0.18	0.28	0.28	0.30	0.13
Al_2O_3	1.18	1.05	0.46	0.47	0.65	0.97	0.83	0.37	0.48	0.56	0.45	0.48
Fe_2O_3	4.73	10.36	9.39	8.75	9.30	7.12	8.32	5.84	7.04	6.90	9.75	1.80
FeO	1.36	3.92	5.85	5.39	6.70	7.07	10.39	12.21	6.32	5.68	3.70	13.93
MgO	15.39	9.92	9.97	5.39	6.70	7.07	10.39	12.22	6.32	5.68	3.70	13.93
MnO	0.13	0.42	0.43	0.51	0.69	0.78	0.54	0.43	0.78	0.87	0.93	0.32
ZnO	0.12	0.02	0.01	0.00	0.00	0.00	0.00	0.00	0.00	0.00	0.00	0.00
V_2O_3	0.07	0.09	0.06	0.24	0.29	0.27	0.08	0.42	0.19	0.20	0.19	0.09
Cr_2O_3	0.01	0.01	0.00	0.01	0.00	0.01	0.02	0.02	0.02	0.03	0.00	0.00
ZrO_2	0.04	0.09	0.00	n.d.	n.d.	n.d.	n.d.	n.d.	n.d.	n.d.	n.d.	n.d.
Nb_2O_5	0.00	0.01	0.00	0.04	0.06	0.03	0.01	0.00	0.00	0.04	0.01	0.00
CaO	23.67	20.26	19.90	15.72	18.15	17.26	21.93	22.06	16.13	15.30	14.61	22.34
Na_2O	0.47	2.48	2.57	4.82	3.54	4.12	1.41	1.47	4.76	5.22	5.48	1.65
K_2O	0.00	0.00	0.00	0.00	0.00	0.00	0.00	0.00	0.00	0.00	0.00	0.00
Total	98.92	98.39	100.08	100.43	100.85	101.10	100.22	99.79	100.88	100.93	101.73	99.61
Si	1.885	1.944	1.934	1.960	1.955	1.950	1.955	1.976	1.962	1.960	1.963	1.959
Ti	0.038	0.005	0.008	0.015	0.014	0.007	0.009	0.005	0.008	0.008	0.009	0.004
^{IV}Al	0.052	0.048	0.021	0.021	0.029	0.043	0.037	0.016	0.022	0.025	0.020	0.021
ΣTet	1.974	1.970	1.959	1.996	1.998	1.999	2.001	1.997	1.992	1.993	1.992	1.983
Fe^{3+}	0.133	0.268	0.317	0.379	0.284	0.337	0.135	0.116	0.384	0.416	0.438	0.171
Fe^{2+}	0.043	0.186	0.095	0.282	0.297	0.226	0.264	0.183	0.224	0.220	0.313	0.056
Mg	0.858	0.564	0.604	0.309	0.382	0.399	0.586	0.683	0.359	0.323	0.212	0.770
Mn	0.004	0.014	0.013	0.017	0.022	0.025	0.017	0.014	0.025	0.028	0.030	0.010
Zn	0.003	0.000	0.000	0.000	0.000	0.000	0.000	0.000	0.000	0.000	0.000	0.000
^{VI}Al	0.000	0.000	0.000	0.000	0.000	0.000	0.000	0.000	0.000	0.000	0.000	0.000
V	0.002	0.002	0.002	0.007	0.009	0.008	0.003	0.013	0.006	0.006	0.006	0.003
Cr	0.000	0.000	0.001	0.000	0.000	0.000	0.001	0.001	0.001	0.001	0.000	0.000
Zr	0.001	0.000	0.000	0.000	0.000	0.000	0.000	0.000	0.000	0.000	0.000	0.000
Nb	0.000	0.000	0.000	0.001	0.001	0.001	0.000	0.000	0.000	0.001	0.000	0.000
ΣOct.	1.044	1.033	1.031	0.995	0.996	0.996	1.006	1.009	0.998	0.995	0.999	1.010
Ca	0.948	0.808	0.788	0.649	0.744	0.701	0.890	0.887	0.658	0.625	0.601	0.889
Na	0.034	0.189	0.221	0.360	0.263	0.303	0.104	0.107	0.352	0.387	0.408	0.119
K	0.000	0.000	0.000	0.000	0.000	0.000	0.000	0.000	0.000	0.000	0.000	0.000
ΣOct.	0.982	0.997	1.009	1.009	1.006	1.004	0.993	0.994	1.010	1.012	1.009	1.007
Mol.%												
Aegirine	3.38	18.87	22.14	35.99	26.26	30.29	10.35	10.71	35.19	38.65	40.78	11.86
Diopside	85.78	56.36	60.43	30.92	38.21	39.93	58.63	68.29	35.89	32.29	21.19	77.04
Hedenbergite	4.26	18.57	9.46	28.20	29.73	22.59	26.36	18.31	22.42	22.01	31.31	5.59
Jadeite	0.00	0.00	0.00	0.00	0.00	0.00	0.00	0.00	0.00	0.00	0.00	0.00
Pyroxmangite	0.20	0.70	0.64	0.83	1.12	1.25	0.86	0.69	1.25	1.41	1.52	0.51
$CaFeAlSiO_6$	0.93	3.94	1.54	0.93	1.14	3.42	3.19	0.91	1.17	1.97	1.02	2.22
$CaTiAl_2O_6$	3.76	0.48	0.82	1.53	1.40	0.66	0.87	0.51	0.79	0.80	0.88	0.36
$CaCrAlSiO_6$	0.02	0.01	0.08	0.03	0.00	0.03	0.07	0.06	0.06	0.10	0.00	0.00

* Mineral formulae calculated based on 4 cations and 6 oxygens, with Fe^{3+} determined by charge balance

Acronyms: fi. = fine; med. = medium; v. = very; mid. = middle; lt. = light; ed. = edge

Appendix A-2: Results of electron-microprobe analyses of aegirine-augite*

Sample #	AD054B2	AD066D2									AD066J2	
Description	60 fi.	35 lt.ed.	36 dkr	37 mid.	38 mid.	39 med.ed.	40 lt.mid.	41 dk mid.	42 lt.ed.	43 dk nr ed.	4 #2	5
SiO_2	53.17	51.54	51.35	51.15	50.44	51.18	50.29	50.80	50.34	51.01	51.31	51.66
TiO_2	0.09	0.21	0.28	0.38	0.44	0.36	0.25	0.12	0.29	0.36	0.37	0.33
Al_2O_3	0.37	0.56	0.59	0.69	1.52	0.76	0.71	0.77	0.84	0.82	0.72	0.78
Fe_2O_3	0.59	10.31	7.22	6.99	8.21	7.85	9.22	9.08	9.46	8.04	5.43	5.68
FeO	14.98	9.73	8.67	8.19	8.16	8.48	9.52	6.56	9.01	8.13	10.10	8.75
MgO	14.98	6.64	9.10	9.64	8.42	8.81	7.33	9.23	7.36	8.96	8.89	9.77
MnO	0.34	0.72	0.59	0.55	0.54	0.54	0.62	0.56	0.65	0.54	0.64	0.55
ZnO	0.00	0.00	0.03	0.01	0.03	0.07	0.00	0.02	0.02	0.01	0.00	0.00
V_2O_3	0.05	0.07	0.08	0.05	0.18	0.11	0.11	0.05	0.07	0.11	0.08	0.07
Cr_2O_3	0.01	0.00	0.01	0.02	0.02	0.01	0.00	0.00	0.00	0.00	0.00	0.00
ZrO_2	n.d.	0.05	0.01	0.04	0.00	0.04	0.02	0.03	0.00	0.02	n.d.	n.d.
Nb_2O_5	0.00	0.00	0.00	0.01	0.02	0.00	0.00	0.01	0.01	0.01	0.00	0.02
CaO	20.63	17.77	20.80	21.09	19.86	20.13	19.36	20.02	19.47	20.04	21.54	21.86
Na_2O	1.93	3.62	2.05	1.85	2.49	2.37	2.67	2.51	2.74	2.38	1.62	1.59
K_2O	0.22	0.00	0.00	0.00	0.00	0.00	0.00	0.00	0.00	0.00	0.00	0.00
Total	99.10	101.23	100.78	100.65	100.33	100.70	100.10	99.76	100.27	100.42	100.69	101.05
Si	1.969	1.965	1.950	1.940	1.924	1.945	1.940	1.940	1.937	1.942	1.954	1.949
Ti	0.002	0.006	0.008	0.011	0.013	0.010	0.007	0.003	0.008	0.010	0.011	0.009
^{IV}Al	0.016	0.025	0.026	0.031	0.068	0.034	0.032	0.035	0.038	0.037	0.032	0.035
ΣTet	1.987	1.997	1.984	1.982	2.000	1.989	1.980	1.978	1.983	1.989	1.997	1.994
Fe^{3+}	0.188	0.296	0.206	0.199	0.236	0.224	0.268	0.261	0.274	0.230	0.156	0.161
Fe^{2+}	0.018	0.310	0.275	0.260	0.260	0.270	0.307	0.210	0.290	0.259	0.322	0.276
Mg	0.827	0.377	0.515	0.545	0.479	0.499	0.421	0.525	0.422	0.508	0.504	0.550
Mn	0.011	0.023	0.019	0.018	0.018	0.017	0.020	0.018	0.021	0.017	0.021	0.018
Zn	0.000	0.000	0.001	0.000	0.001	0.002	0.000	0.001	0.001	0.000	0.000	0.000
^{VI}Al	0.000	0.000	0.000	0.000	0.000	0.000	0.000	0.000	0.000	0.000	0.000	0.000
V	0.001	0.002	0.002	0.001	0.006	0.003	0.003	0.002	0.002	0.003	0.003	0.002
Cr	0.000	0.000	0.000	0.001	0.001	0.000	0.000	0.000	0.000	0.000	0.000	0.000
Zr	0.000	0.001	0.000	0.001	0.000	0.001	0.000	0.001	0.000	0.000	0.000	0.000
Nb	0.000	0.000	0.000	0.000	0.000	0.000	0.000	0.000	0.000	0.000	0.000	0.000
ΣOct.	1.045	1.010	1.019	1.025	1.005	1.017	1.021	1.017	1.010	1.019	1.005	1.007
Ca	0.819	0.726	0.846	0.857	0.811	0.820	0.800	0.819	0.803	0.817	0.879	0.884
Na	0.138	0.268	0.151	0.136	0.184	0.174	0.199	0.186	0.204	0.175	0.120	0.116
K	0.010	0.000	0.000	0.000	0.000	0.000	0.000	0.000	0.000	0.000	0.000	0.000
ΣOct.	0.967	0.994	0.997	0.993	0.995	0.994	1.000	1.005	1.007	0.993	0.999	1.000
Mol.%												
Aegirine	13.84	26.79	15.12	13.61	18.39	17.43	19.94	18.59	20.43	17.54	11.96	11.62
Diopside	82.68	37.71	51.47	54.50	47.89	49.91	42.15	52.53	42.21	50.83	50.44	54.95
Hedenbergite	1.82	31.02	27.51	25.98	26.05	26.95	30.71	20.95	29.00	25.87	32.17	27.60
Jadeite	0.00	0.00	0.00	0.00	0.00	0.00	0.00	0.00	0.00	0.00	0.00	0.00
Pyroxmangite	0.54	1.16	0.95	0.89	0.88	0.87	1.01	0.91	1.07	0.87	1.03	0.88
$CaFeAlSiO_6$	0.00	1.81	1.51	2.33	5.18	2.02	2.82	3.51	2.95	2.48	2.59	2.50
$CaTiAl_2O_6$	0.24	0.59	0.80	1.09	1.27	1.03	0.73	0.35	0.84	1.02	1.06	0.93
$CaCrAlSiO_6$	0.04	0.01	0.04	0.06	0.06	0.02	0.01	0.00	0.01	0.00	0.00	0.00

* Mineral formulae calculated based on 4 cations and 6 oxygens, with Fe^{3+} determined by charge balance
Acronyms: fi. = fine; med. = medium; v. = very; mid. = middle; lt. = light; ed. = edge

Appendix A-2: Results of electron-microprobe analyses of aegirine-augite*

Sample #	AD066J2											
Description	6 dk	7 lt	8 v.lt	9 mid.med.	10 lt	11 dkr	12	13 ed.lt.	14	15	16	17
SiO_2	51.15	51.35	50.56	51.01	50.66	51.09	50.89	50.56	52.41	51.45	49.63	50.97
TiO_2	0.39	0.37	0.36	0.29	0.46	0.29	0.30	0.24	0.05	0.13	0.30	0.40
Al_2O_3	1.00	0.86	0.96	1.08	1.32	0.72	0.69	0.72	0.32	0.49	1.19	1.08
Fe_2O_3	5.35	4.79	10.17	10.33	7.93	9.18	14.02	13.12	8.93	12.54	11.53	6.40
FeO	8.38	9.06	11.19	9.27	9.20	10.15	11.37	11.36	6.39	7.40	10.73	7.66
MgO	10.18	10.04	5.43	6.35	7.83	6.88	3.01	3.40	9.64	6.82	4.77	9.88
MnO	0.49	0.52	0.59	0.65	0.50	0.66	0.77	0.77	0.57	0.61	0.55	0.46
ZnO	0.00	0.00	0.00	0.00	0.00	0.00	0.00	0.00	0.00	0.00	0.00	0.00
V_2O_3	0.12	0.11	0.24	0.15	0.19	0.14	0.23	0.20	0.08	0.13	0.21	0.12
Cr_2O_3	0.01	0.01	0.03	0.01	0.00	0.00	0.01	0.00	0.00	0.04	0.01	0.00
ZrO_2	n.d.	n.d.	n.d.	n.d.	n.d.	n.d.	n.d.	n.d.	n.d.	n.d.	n.d.	n.d.
Nb_2O_5	0.01	0.00	0.00	0.00	0.00	0.00	0.00	0.00	0.02	0.00	0.00	0.00
CaO	22.05	22.27	17.86	17.77	20.20	19.26	15.28	15.68	19.96	17.53	17.43	21.84
Na_2O	1.35	1.24	3.55	3.72	2.47	2.93	5.18	4.83	2.81	4.10	3.78	1.64
K_2O	0.00	0.00	0.00	0.00	0.00	0.00	0.00	0.00	0.00	0.00	0.00	0.00
Total	100.47	100.60	100.94	100.62	100.76	101.28	101.75	100.88	101.18	101.23	100.12	100.46
Si	1.938	1.946	1.948	1.954	1.932	1.950	1.962	1.964	1.966	1.955	1.934	1.931
Ti	0.011	0.010	0.011	0.008	0.013	0.008	0.009	0.007	0.001	0.004	0.009	0.012
^{IV}Al	0.045	0.038	0.044	0.046	0.059	0.032	0.031	0.033	0.014	0.022	0.055	0.048
ΣTet	1.994	1.994	2.003	2.008	2.004	1.991	2.002	2.004	1.981	1.980	1.998	1.991
Fe^{3+}	0.153	0.137	0.295	0.298	0.228	0.264	0.407	0.383	0.252	0.358	0.338	0.183
Fe^{2+}	0.266	0.287	0.361	0.297	0.293	0.324	0.367	0.369	0.201	0.235	0.350	0.243
Mg	0.575	0.567	0.312	0.363	0.445	0.391	0.173	0.197	0.539	0.386	0.277	0.558
Mn	0.016	0.017	0.019	0.021	0.016	0.021	0.025	0.025	0.018	0.020	0.018	0.015
Zn	0.000	0.000	0.000	0.000	0.000	0.000	0.000	0.000	0.000	0.000	0.000	0.000
^{VI}Al	0.000	0.000	0.000	0.003	0.000	0.000	0.000	0.000	0.000	0.000	0.000	0.000
V	0.004	0.003	0.008	0.005	0.006	0.004	0.007	0.006	0.003	0.004	0.007	0.004
Cr	0.000	0.000	0.001	0.000	0.000	0.000	0.000	0.000	0.000	0.001	0.000	0.000
Zr	0.000	0.000	0.000	0.000	0.000	0.000	0.000	0.000	0.000	0.000	0.000	0.000
Nb	0.000	0.000	0.000	0.000	0.000	0.000	0.000	0.000	0.000	0.000	0.000	0.000
ΣOct.	1.013	1.011	0.995	0.986	0.988	1.005	0.979	0.981	1.013	1.005	0.989	1.002
Ca	0.895	0.904	0.737	0.729	0.825	0.788	0.631	0.652	0.802	0.714	0.728	0.887
Na	0.099	0.091	0.265	0.276	0.183	0.217	0.387	0.364	0.204	0.302	0.285	0.120
K	0.000	0.000	0.000	0.000	0.000	0.000	0.000	0.000	0.000	0.000	0.000	0.000
ΣOct.	0.994	0.995	1.002	1.006	1.008	1.005	1.019	1.016	1.006	1.015	1.013	1.007
Mol.%												
Aegirine	9.91	9.07	26.50	27.32	18.25	21.70	38.73	36.37	20.40	30.17	28.52	12.03
Diopside	57.47	56.68	31.17	36.26	44.52	39.14	17.32	19.66	53.92	38.62	27.69	55.82
Hedenbergite	26.56	28.71	36.06	29.70	29.34	32.39	36.67	36.89	20.05	23.52	34.96	24.27
Jadeite	0.00	0.00	0.00	0.30	0.00	0.00	0.00	0.00	0.00	0.00	0.00	0.00
Pyroxmangite	0.79	0.84	0.97	1.06	0.80	1.06	1.26	1.27	0.91	0.99	0.90	0.75
$CaFeAlSiO_6$	3.34	2.59	3.00	2.45	4.51	2.68	1.96	1.97	0.79	1.67	4.29	3.22
$CaTiAl_2O_6$	1.12	1.04	1.05	0.84	1.32	0.83	0.87	0.70	0.14	0.37	0.89	1.15
$CaCrAlSiO_6$	0.04	0.03	0.09	0.03	0.00	0.00	0.02	0.01	0.00	0.11	0.02	0.01

* Mineral formulae calculated based on 4 cations and 6 oxygens, with Fe^{3+} determined by charge balance

Acronyms: fi. = fine; med. = medium; v. = very; mid. = middle; lt. = light; ed. = edge

Appendix A-2: Results of electron-microprobe analyses of aegirine-augite*

Sample #	AD066J2	BH/9/1										
Description	18	1 edge	2 mid.	3 ed.	4 ed.	5 ed.	6 mid.lt.	7 ed.	8 ed.	9 mid.dk	10 mid.lt.	11 v.mid.
SiO_2	50.79	50.89	50.98	50.81	51.14	51.14	50.40	50.59	51.81	52.58	52.65	52.41
TiO_2	0.28	0.18	0.22	0.24	0.20	0.20	0.26	0.32	0.57	0.41	0.24	0.36
Al_2O_3	0.83	0.73	1.18	0.68	1.10	0.62	0.75	0.99	0.75	0.63	0.75	0.65
Fe_2O_3	7.87	11.84	11.52	13.84	11.67	12.86	11.48	14.22	23.38	25.67	24.53	23.31
FeO	9.70	8.58	8.91	8.61	8.65	9.89	9.89	7.12	1.31	0.23	0.27	1.17
MgO	7.59	5.23	6.04	5.13	6.31	4.90	5.72	5.91	4.22	3.75	4.35	4.47
MnO	0.61	1.04	0.80	0.81	0.90	0.78	0.69	0.72	0.56	0.54	0.70	0.58
ZnO	0.00	0.06	0.08	0.04	0.05	0.00	0.00	0.04	0.00	0.00	0.00	0.01
V_2O_3	0.10	0.10	0.09	0.17	0.02	0.13	0.14	0.20	0.56	0.36	0.43	0.36
Cr_2O_3	0.02	0.01	0.00	0.02	0.00	0.00	0.02	0.03	0.02	0.01	0.02	0.02
ZrO_2	n.d.	0.07	0.18	0.11	0.10	0.10	0.05	0.16	0.28	0.53	0.29	0.13
Nb_2O_5	0.00	0.01	0.00	0.00	0.01	0.00	0.00	0.04	0.00	0.00	0.00	0.01
CaO	19.87	16.40	16.88	15.88	17.15	15.59	17.34	15.42	8.18	6.41	8.46	8.72
Na_2O	2.52	4.54	4.11	4.76	4.01	4.75	3.78	4.91	9.22	10.32	9.44	9.10
K_2O	0.00	0.00	0.00	0.00	0.00	0.00	0.00	0.00	0.00	0.00	0.00	0.00
Total	100.19	99.67	101.00	101.10	101.29	100.95	100.51	100.65	100.85	101.43	102.13	101.28
Si	1.951	1.973	1.949	1.950	1.948	1.967	1.947	1.938	1.959	1.973	1.962	1.969
Ti	0.008	0.005	0.006	0.007	0.006	0.006	0.008	0.009	0.016	0.012	0.007	0.010
^{IV}Al	0.038	0.027	0.057	0.031	0.049	0.028	0.034	0.045	0.033	0.027	0.033	0.029
ΣTet	1.997	2.000	2.000	1.988	2.000	2.000	1.988	1.992	2.000	2.000	2.000	2.000
Fe^{3+}	0.228	0.346	0.331	0.400	0.335	0.372	0.334	0.410	0.665	0.725	0.688	0.659
Fe^{2+}	0.312	0.278	0.285	0.277	0.276	0.318	0.320	0.228	0.041	0.007	0.008	0.037
Mg	0.435	0.302	0.344	0.293	0.358	0.281	0.329	0.338	0.238	0.210	0.242	0.250
Mn	0.020	0.034	0.026	0.026	0.029	0.025	0.023	0.023	0.018	0.017	0.022	0.018
Zn	0.000	0.002	0.002	0.001	0.001	0.000	0.000	0.001	0.000	0.000	0.000	0.000
^{VI}Al	0.000	0.006	0.002	0.000	0.000	0.000	0.000	0.000	0.000	0.000	0.001	0.000
V	0.003	0.003	0.003	0.005	0.001	0.004	0.004	0.006	0.017	0.011	0.013	0.011
Cr	0.001	0.000	0.000	0.001	0.000	0.000	0.001	0.001	0.001	0.000	0.001	0.000
Zr	0.000	0.001	0.003	0.002	0.002	0.002	0.001	0.003	0.005	0.010	0.005	0.002
Nb	0.000	0.000	0.000	0.000	0.000	0.000	0.000	0.001	0.000	0.000	0.000	0.000
ΣOct.	0.997	0.978	1.003	1.005	1.004	1.004	1.011	1.011	0.993	0.991	0.980	0.987
Ca	0.818	0.681	0.692	0.653	0.700	0.642	0.718	0.633	0.331	0.258	0.338	0.351
Na	0.188	0.341	0.305	0.354	0.296	0.354	0.283	0.364	0.676	0.751	0.682	0.663
K	0.000	0.000	0.000	0.000	0.000	0.000	0.000	0.000	0.000	0.000	0.000	0.000
ΣOct.	1.006	1.022	0.997	1.007	0.996	0.996	1.001	0.997	1.007	1.009	1.020	1.013
Mol.%												
Aegirine	18.77	33.51	30.29	35.44	29.60	35.41	28.33	36.44	66.59	72.10	68.06	66.27
Diopside	43.47	30.24	34.43	29.32	35.80	28.09	32.91	33.75	23.75	20.95	24.16	25.02
Hedenbergite	31.16	27.81	28.50	27.65	27.55	31.81	31.95	22.80	4.13	0.73	0.85	3.68
Jadeite	0.00	0.60	0.20	0.00	0.00	0.00	0.00	0.00	0.00	0.00	0.14	0.00
Pyroxmangite	0.99	1.71	1.29	1.32	1.46	1.26	1.13	1.17	0.90	0.86	1.11	0.92
$CaFeAlSiO_6$	2.98	1.04	2.86	2.52	3.86	1.80	3.05	3.54	0.00	0.37	0.72	0.00
$CaTiAl_2O_6$	0.82	0.53	0.63	0.68	0.56	0.59	0.75	0.92	1.61	1.15	0.68	1.00
$CaCrAlSiO_6$	0.06	0.02	0.00	0.06	0.00	0.01	0.06	0.09	0.07	0.02	0.05	0.05

* Mineral formulae calculated based on 4 cations and 6 oxygens, with Fe^{3+} determined by charge balance

Acronyms: fi. = fine; med. = medium; v. = very; mid. = middle; lt. = light; ed. = edge

Appendix A-2: Results of electron-microprobe analyses of aegirine-augite*

Sample #	BH/9/1	AD066J1				AD066A1						
Description	12	58 dkr	63 lt.	66 mid.med.	67 med.	1	3	4	6	7	8	9 ed.
SiO_2	51.93	50.14	49.70	50.30	50.56	52.54	52.44	52.47	52.13	52.49	52.34	52.54
TiO_2	0.33	0.43	0.30	0.35	0.38	0.33	0.69	0.38	0.48	0.49	0.40	0.44
Al_2O_3	0.70	1.09	0.71	0.91	0.91	0.66	0.62	0.58	0.65	0.65	0.84	0.65
Fe_2O_3	24.17	7.93	11.06	7.82	6.75	22.40	21.13	21.39	23.48	23.44	21.61	22.21
FeO	0.74	8.86	7.59	8.55	8.99	3.21	2.80	3.51	1.72	2.85	2.80	1.82
MgO	4.34	8.95	7.15	8.74	8.87	3.31	4.43	3.60	3.67	2.97	4.06	4.19
MnO	0.54	0.56	0.65	0.55	0.56	0.51	0.62	0.53	0.51	0.45	0.50	0.63
ZnO	0.00	0.01	0.05	0.02	0.00	0.00	0.01	0.00	0.00	0.00	0.00	0.00
V_2O_3	0.39	0.09	0.11	0.09	0.08	0.53	0.26	0.24	0.29	0.25	0.24	0.20
Cr_2O_3	0.02	0.01	0.02	0.01	0.00	n.d.	n.d.	n.d.	n.d.	n.d.	n.d.	n.d.
ZrO_2	0.12	0.10	0.06	0.03	0.05	0.25	0.09	0.15	0.09	0.22	0.25	0.12
Nb_2O_5	0.01	0.00	0.01	0.00	0.00	0.01	0.01	0.00	0.00	0.01	0.00	0.00
CaO	8.46	20.49	18.49	20.63	20.71	6.66	8.89	7.27	7.53	5.59	7.50	7.84
Na_2O	9.19	1.89	3.24	2.02	1.92	9.72	8.76	9.35	9.57	10.24	9.26	9.34
K_2O	0.00	0.00	0.00	0.00	0.00	0.01	0.02	0.01	0.02	0.03	0.01	0.01
Total	100.91	100.53	99.14	100.00	99.79	100.39	100.88	99.59	100.26	99.79	99.90	100.07
Si	1.960	1.916	1.932	1.929	1.940	1.997	1.980	2.007	1.980	2.005	1.992	1.993
Ti	0.009	0.012	0.009	0.010	0.011	0.009	0.020	0.011	0.014	0.014	0.011	0.012
^{IV}Al	0.031	0.049	0.032	0.041	0.041	0.003	0.020	0.000	0.020	0.000	0.008	0.007
ΣTet	2.000	1.977	1.973	1.981	1.992	2.010	2.019	2.018	2.014	2.019	2.011	2.012
Fe^{3+}	0.686	0.228	0.324	0.226	0.195	0.641	0.600	0.616	0.671	0.674	0.619	0.634
Fe^{2+}	0.023	0.283	0.247	0.274	0.289	0.102	0.088	0.112	0.055	0.091	0.089	0.058
Mg	0.244	0.510	0.414	0.500	0.508	0.188	0.249	0.205	0.208	0.169	0.230	0.237
Mn	0.017	0.018	0.021	0.018	0.018	0.017	0.020	0.017	0.016	0.015	0.016	0.020
Zn	0.000	0.000	0.001	0.001	0.000	0.000	0.000	0.000	0.000	0.000	0.000	0.000
^{VI}Al	0.000	0.000	0.000	0.000	0.000	0.027	0.007	0.026	0.010	0.029	0.030	0.022
V	0.012	0.003	0.003	0.003	0.002	0.024	0.012	0.011	0.013	0.011	0.011	0.009
Cr	0.001	0.000	0.000	0.000	0.000	0.000	0.000	0.000	0.000	0.000	0.000	0.000
Zr	0.002	0.002	0.001	0.001	0.001	0.005	0.002	0.003	0.002	0.004	0.005	0.002
Nb	0.000	0.000	0.000	0.000	0.000	0.000	0.000	0.000	0.000	0.000	0.000	0.000
ΣOct.	0.986	1.044	1.013	1.022	1.013	1.003	0.978	0.990	0.975	0.993	1.000	0.982
Ca	0.342	0.839	0.770	0.848	0.852	0.271	0.360	0.298	0.307	0.229	0.306	0.319
Na	0.672	0.140	0.244	0.150	0.143	0.716	0.641	0.694	0.705	0.758	0.683	0.687
K	0.000	0.000	0.000	0.000	0.000	0.001	0.001	0.000	0.001	0.001	0.001	0.000
ΣOct.	1.014	0.979	1.014	0.998	0.995	0.988	1.002	0.992	1.012	0.989	0.989	1.006
Mol.%												
Aegirine	67.23	14.00	24.40	15.00	14.32	63.92	60.41	61.77	67.46	66.95	62.30	63.49
Diopside	24.43	50.99	41.45	49.96	50.75	18.77	24.94	20.52	20.77	16.89	23.01	23.68
Hedenbergite	2.34	28.31	24.69	27.43	28.86	10.21	8.84	11.22	5.46	9.11	8.92	5.78
Jadeite	0.00	0.00	0.00	0.00	0.00	2.70	0.70	2.60	1.00	2.90	3.00	2.20
Pyroxmangite	0.86	0.90	1.06	0.90	0.92	0.83	0.99	0.86	0.81	0.73	0.80	1.00
$CaFeAlSiO_6$	1.41	3.81	1.96	2.59	3.18	0.17	0.00	0.00	0.00	0.43	0.00	0.00
$CaTiAl_2O_6$	0.93	1.25	0.86	1.00	1.09	0.00	1.95	0.00	1.38	0.00	1.13	0.00
$CaCrAlSiO_6$	0.05	0.02	0.05	0.02	0.01	0.00	0.00	0.00	0.00	0.00	0.00	0.00

* Mineral formulae calculated based on 4 cations and 6 oxygens, with Fe^{3+} determined by charge balance

Acronyms: fi. = fine; med. = medium; v. = very; mid. = middle; lt = light; ed. = edge

Appendix A-2: Results of electron-microprobe analyses of aegirine-augite*

Sample #	AD066A1				AD066B1							
Description	10	11 brwn	12	13	1	2 dk	3 dk	4 brwn	5	6	7	8 ed.
SiO_2	52.42	51.91	51.98	52.29	51.93	52.13	52.06	52.77	52.24	52.30	51.81	51.98
TiO_2	0.51	0.43	0.26	0.26	0.35	0.32	0.30	0.33	0.62	0.51	0.46	0.36
Al_2O_3	0.59	0.64	0.63	0.62	0.69	0.67	0.62	0.63	0.61	1.21	0.92	0.54
Fe_2O_3	24.05	25.65	19.34	19.73	21.25	22.00	19.73	20.17	24.00	21.15	22.94	18.39
FeO	1.46	0.31	3.02	3.08	3.09	3.00	4.01	3.80	2.55	3.82	2.00	3.72
MgO	3.68	3.86	4.37	4.40	4.17	3.81	4.18	4.31	3.41	3.68	3.68	5.02
MnO	0.56	0.54	0.53	0.59	0.64	0.45	0.53	0.55	0.44	0.54	0.52	0.61
ZnO	0.01	0.00	0.01	0.00	0.01	0.00	0.00	0.00	0.00	0.00	0.00	0.00
V_2O_3	0.22	0.26	0.48	0.60	0.47	0.47	0.44	0.35	0.21	0.24	0.61	0.33
Cr_2O_3	n.d.	n.d.	n.d.	n.d.	n.d.	n.d.	n.d.	n.d.	n.d.	n.d.	n.d.	n.d.
ZrO_2	0.18	0.11	0.28	0.21	0.17	0.21	0.34	0.20	0.01	0.03	0.17	0.20
Nb_2O_5	0.01	0.00	0.00	0.00	0.00	0.00	0.00	0.02	0.00	0.01	0.00	0.01
CaO	7.05	7.24	9.16	9.27	9.02	8.07	8.75	9.05	6.65	7.27	7.91	9.95
Na_2O	9.83	9.81	8.51	8.50	8.57	9.09	8.52	8.59	9.80	9.10	9.32	7.87
K_2O	0.02	0.01	0.01	0.02	0.01	0.01	0.00	0.02	0.00	0.20	0.01	0.03
Total	100.69	100.89	98.81	99.85	100.60	100.45	99.69	100.95	100.64	100.17	100.64	99.19
Si	1.983	1.960	1.999	1.993	1.973	1.982	1.993	1.993	1.982	1.990	1.965	1.994
Ti	0.014	0.012	0.007	0.007	0.010	0.009	0.009	0.009	0.018	0.015	0.013	0.011
^{IV}Al	0.017	0.029	0.001	0.007	0.027	0.018	0.007	0.007	0.018	0.010	0.035	0.006
ΣTet	2.014	2.002	2.008	2.007	2.010	2.009	2.009	2.010	2.017	2.014	2.013	2.010
Fe^{3+}	0.684	0.729	0.560	0.566	0.608	0.629	0.569	0.573	0.685	0.605	0.655	0.531
Fe^{2+}	0.046	0.010	0.097	0.098	0.098	0.095	0.129	0.120	0.081	0.121	0.064	0.119
Mg	0.207	0.218	0.251	0.250	0.236	0.216	0.238	0.243	0.193	0.208	0.208	0.287
Mn	0.018	0.017	0.017	0.019	0.021	0.015	0.017	0.018	0.014	0.017	0.017	0.020
Zn	0.000	0.000	0.000	0.000	0.000	0.000	0.000	0.000	0.000	0.000	0.000	0.000
^{VI}Al	0.009	0.000	0.028	0.021	0.004	0.012	0.021	0.021	0.009	0.044	0.006	0.018
V	0.010	0.011	0.022	0.027	0.021	0.021	0.020	0.016	0.009	0.011	0.027	0.015
Cr	0.000	0.000	0.000	0.000	0.000	0.000	0.000	0.000	0.000	0.000	0.000	0.000
Zr	0.003	0.002	0.005	0.004	0.003	0.004	0.006	0.004	0.000	0.001	0.003	0.004
Nb	0.000	0.000	0.000	0.000	0.000	0.000	0.000	0.000	0.000	0.000	0.000	0.000
ΣOct.	0.979	0.987	0.980	0.985	0.991	0.992	1.000	0.994	0.991	1.008	0.980	0.994
Ca	0.286	0.293	0.377	0.379	0.367	0.328	0.359	0.366	0.270	0.296	0.321	0.409
Na	0.720	0.718	0.634	0.628	0.631	0.670	0.633	0.629	0.721	0.671	0.685	0.585
K	0.001	0.000	0.000	0.001	0.000	0.000	0.000	0.001	0.000	0.010	0.000	0.002
ΣOct.	1.007	1.011	1.012	1.008	0.999	0.999	0.991	0.996	0.991	0.977	1.007	0.996
Mol.%												
Aegirine	68.14	71.82	55.64	56.74	60.73	62.78	57.15	57.82	68.16	60.70	65.94	52.70
Diopside	20.73	21.75	25.05	24.99	23.64	21.60	23.84	24.28	19.29	20.85	20.81	28.67
Hedenbergite	4.63	0.98	9.72	9.81	9.83	9.55	12.85	11.99	8.08	12.14	6.36	11.95
Jadeite	0.90	0.00	2.80	2.10	0.40	1.20	2.10	2.10	0.90	4.40	0.60	1.80
Pyroxmangite	0.90	0.87	0.87	0.95	1.03	0.73	0.86	0.88	0.71	0.87	0.84	0.99
$CaFeAlSiO_6$	0.30	1.09	0.34	0.00	0.03	0.15	0.00	0.00	0.35	0.00	0.00	0.39
$CaTiAl_2O_6$	1.45	1.23	0.00	0.74	1.01	0.92	0.88	0.94	1.78	1.47	1.32	1.05
$CaCrAlSiO_6$	0.00	0.00	0.00	0.00	0.00	0.00	0.00	0.00	0.00	0.00	0.00	0.00

* Mineral formulae calculated based on 4 cations and 6 oxygens, with Fe^{3+} determined by charge balance

Acronyms: fi. = fine; med. = medium; v. = very; mid. = middle; lt. = light; ed. = edge

Appendix A-2 Results of electron-microprobe analyses of aegirine-augite*

Sample #	AD066B1					87/A/67.1						
Description	9	10 ed.	11 nr vein	12 mid.	13	29	30	31	32	33 mid.	34	35
SiO_2	52.32	51.92	51.95	51.91	52.20	52.25	52.52	52.66	52.85	52.72	52.44	52.77
TiO_2	0.65	0.34	0.35	0.43	0.36	0.22	0.31	0.63	0.27	0.33	0.36	0.46
Al_2O_3	0.67	0.65	0.76	0.64	0.71	0.56	0.73	0.93	0.71	0.67	0.71	0.58
Fe_2O_3	24.52	23.29	22.44	23.93	21.58	21.58	24.92	27.74	24.96	25.63	24.37	30.17
FeO	1.69	1.73	2.20	1.81	3.89	1.39	0.33	0.00	0.57	0.00	0.52	0.00
MgO	2.68	3.65	3.76	3.40	3.41	5.23	3.99	2.52	3.96	3.63	4.31	1.62
MnO	0.28	0.52	0.55	0.60	0.47	0.69	0.48	0.49	0.49	0.45	0.48	0.16
ZnO	0.00	0.01	0.00	0.00	0.01	0.00	0.00	0.00	0.00	0.00	0.00	0.00
V_2O_3	0.65	0.53	0.53	0.40	0.62	0.64	0.65	0.34	0.86	0.96	0.52	0.48
Cr_2O_3	n.d.	n.d.	n.d.	n.d.	n.d.	0.02	0.02	0.01	0.02	0.04	0.03	0.01
ZrO_2	0.28	0.22	0.14	0.26	0.26	n.d.	n.d.	n.d.	n.d.	n.d.	n.d.	n.d.
Nb_2O_5	0.00	0.01	0.02	0.00	0.02	0.00	0.00	0.00	0.00	0.01	0.00	0.00
CaO	4.89	7.89	8.04	6.98	7.02	10.48	7.83	4.35	7.98	7.15	8.67	2.51
Na_2O	10.84	9.41	9.23	9.74	9.36	8.16	9.73	12.02	9.73	10.26	9.33	12.70
K_2O	0.01	0.01	0.00	0.01	0.02	0.00	0.00	0.00	0.00	0.00	0.00	0.00
Total	99.78	100.41	100.21	100.30	100.21	101.23	101.50	101.69	102.39	101.84	101.73	101.45
Si	1.996	1.974	1.977	1.976	1.992	1.964	1.967	1.959	1.965	1.967	1.961	1.978
Ti	0.019	0.010	0.010	0.012	0.010	0.006	0.009	0.018	0.008	0.009	0.010	0.013
^{IV}Al	0.004	0.026	0.023	0.024	0.008	0.025	0.032	0.041	0.031	0.030	0.031	0.022
ΣTet	2.018	2.009	2.010	2.013	2.010	1.995	2.008	2.018	2.004	2.007	2.002	2.013
Fe^{3+}	0.704	0.666	0.643	0.686	0.620	0.610	0.702	0.777	0.698	0.720	0.686	0.851
Fe^{2+}	0.054	0.055	0.070	0.058	0.124	0.044	0.010	0.000	0.018	0.000	0.016	0.000
Mg	0.152	0.207	0.213	0.193	0.194	0.293	0.223	0.140	0.219	0.202	0.240	0.091
Mn	0.009	0.017	0.018	0.019	0.015	0.022	0.015	0.015	0.015	0.014	0.015	0.005
Zn	0.000	0.000	0.000	0.000	0.000	0.000	0.000	0.000	0.000	0.000	0.000	0.000
^{VI}Al	0.026	0.003	0.011	0.005	0.023	0.000	0.000	0.000	0.000	0.000	0.000	0.003
V	0.029	0.024	0.024	0.018	0.028	0.019	0.020	0.010	0.026	0.029	0.016	0.015
Cr	0.000	0.000	0.000	0.000	0.000	0.001	0.001	0.000	0.001	0.001	0.001	0.000
Zr	0.005	0.004	0.003	0.005	0.005	0.000	0.000	0.000	0.000	0.000	0.000	0.000
Nb	0.000	0.000	0.000	0.000	0.000	0.000	0.000	0.000	0.000	0.000	0.000	0.000
ΣOct.	0.980	0.976	0.981	0.983	1.009	0.989	0.971	0.942	0.977	0.966	0.974	0.964
Ca	0.200	0.321	0.328	0.285	0.287	0.422	0.314	0.174	0.318	0.286	0.347	0.101
Na	0.801	0.694	0.681	0.719	0.693	0.595	0.707	0.867	0.701	0.742	0.676	0.922
K	0.001	0.000	0.000	0.000	0.001	0.000	0.000	0.000	0.000	0.000	0.000	0.000
ΣOct.	1.002	1.015	1.009	1.004	0.980	1.016	1.021	1.041	1.019	1.028	1.024	1.023
Mol.%												
Aegirine	70.54	67.05	63.97	68.42	61.97	59.45	70.69	77.70	70.13	72.20	67.62	84.94
Diopside	15.24	20.66	21.31	19.29	19.39	29.32	22.28	13.96	21.92	20.19	24.04	9.05
Hedenbergite	5.41	5.50	7.02	5.77	12.43	4.38	1.02	0.00	1.76	0.00	1.61	0.00
Jadeite	2.60	0.30	1.10	0.50	2.30	0.00	0.00	0.00	0.00	0.00	0.00	0.30
Pyroxmangite	0.45	0.84	0.89	0.96	0.76	1.10	0.76	0.77	0.77	0.71	0.76	0.25
$CaFeAlSiO_6$	0.00	0.00	0.30	0.16	0.00	1.58	0.00	0.00	0.00	0.00	0.97	0.13
$CaTiAl_2O_6$	0.85	0.97	1.00	1.24	1.02	0.63	0.88	1.77	0.76	0.93	1.02	1.29
$CaCrAlSiO_6$	0.00	0.00	0.00	0.00	0.00	0.07	0.05	0.04	0.05	0.10	0.07	0.03

* Mineral formulae calculated based on 4 cations and 6 oxygens, with Fe^{3+} determined by charge balance

Acronyms: fi. = fine; med. = medium; v. = very; mid. = middle; lt. = light; ed. = edge

Appendix A-2. Results of electron-microprobe analyses of aegirine-augite*

Sample #	87/A/67.1			87/A/94				A1041E				
Description	36	37	38	20 ed.	21	22	23	61 ed.	65 nr vein	66 farther	67 far	68 v.far
SiO_2	52.96	52.77	52.48	53.08	52.85	52.49	52.68	53.40	53.26	53.60	53.28	53.65
TiO_2	0.36	0.37	0.33	0.64	0.75	0.44	0.54	0.19	0.39	0.34	0.51	0.50
Al_2O_3	0.60	0.72	0.76	0.32	0.30	0.21	0.27	0.38	0.23	0.27	0.31	0.36
Fe_2O_3	23.84	25.54	25.45	14.79	13.95	13.08	12.49	4.70	6.06	4.07	6.08	6.28
FeO	0.88	0.56	0.11	4.23	4.04	4.29	5.20	2.67	2.86	4.39	3.70	2.70
MgO	4.15	3.27	3.65	7.26	7.88	8.52	8.04	14.31	13.03	13.31	12.31	12.90
MnO	0.56	0.40	0.55	0.49	0.53	0.53	0.60	0.27	0.58	0.56	0.54	0.50
ZnO	0.00	0.00	0.00	0.00	0.00	0.00	0.00	0.00	0.00	0.00	0.00	0.00
V_2O_3	0.95	1.19	1.02	0.08	0.10	0.05	0.06	0.11	0.20	0.18	0.20	0.17
Cr_2O_3	0.02	0.04	0.02	0.00	0.00	0.01	0.02	0.00	0.02	0.03	0.00	0.01
ZrO_2	n.d.	n.d.	n.d.	n.d.	n.d.	n.d.	n.d	n.d.	n.d.	n.d.	n.d.	n.d.
Nb_2O_5	0.00	0.00	0.00	0.01	0.01	0.01	0.01	0.00	0.00	0.08	0.01	0.02
CaO	8.15	6.62	7.35	13.82	14.67	16.01	15.34	22.30	21.24	22.35	20.24	20.52
Na_2O	9.57	10.39	10.02	6.19	5.71	4.88	5.11	1.51	2.19	1.54	2.60	2.62
K_2O	0.00	0.00	0.00	0.00	0.00	0.00	0.00	0.00	0.00	0.00	0.00	0.00
Total	102.03	101.86	101.72	100.89	100.79	100.53	100.37	99.84	100.06	100.73	99.77	100.23
Si	1.974	1.973	1.964	1.990	1.981	1.975	1.987	1.974	1.975	1.978	1.985	1.982
Ti	0.010	0.010	0.009	0.018	0.021	0.013	0.015	0.005	0.011	0.009	0.014	0.014
^{IV}Al	0.026	0.027	0.033	0.010	0.013	0.009	0.012	0.017	0.010	0.012	0.013	0.016
ΣTet	2.010	2.010	2.006	2.018	2.015	1.996	2.014	1.996	1.996	2.000	2.012	2.011
Fe^{3+}	0.669	0.718	0.717	0.417	0.394	0.370	0.354	0.131	0.169	0.113	0.170	0.175
Fe^{2+}	0.027	0.017	0.004	0.133	0.127	0.135	0.164	0.083	0.089	0.136	0.115	0.084
Mg	0.231	0.182	0.204	0.405	0.440	0.478	0.452	0.789	0.720	0.733	0.683	0.710
Mn	0.018	0.013	0.017	0.015	0.017	0.017	0.019	0.009	0.018	0.018	0.017	0.016
Zn	0.000	0.000	0.000	0.000	0.000	0.000	0.000	0.000	0.000	0.000	0.000	0.000
^{VI}Al	0.000	0.004	0.000	0.004	0.000	0.000	0.000	0.000	0.000	0.000	0.000	0.000
V	0.028	0.036	0.031	0.002	0.003	0.002	0.002	0.003	0.006	0.005	0.006	0.005
Cr	0.001	0.001	0.001	0.000	0.000	0.000	0.001	0.000	0.001	0.001	0.000	0.000
Zr	0.000	0.000	0.000	0.000	0.000	0.000	0.000	0.000	0.000	0.000	0.000	0.000
Nb	0.000	0.000	0.000	0.000	0.000	0.000	0.000	0.000	0.000	0.001	0.000	0.000
ΣOct.	0.973	0.972	0.972	0.977	0.981	1.002	0.993	1.014	1.003	1.006	0.992	0.990
Ca	0.326	0.265	0.295	0.555	0.589	0.645	0.620	0.883	0.844	0.884	0.808	0.812
Na	0.691	0.753	0.727	0.450	0.415	0.356	0.374	0.108	0.158	0.111	0.188	0.187
K	0.000	0.000	0.000	0.000	0.000	0.000	0.000	0.000	0.000	0.000	0.000	0.000
ΣOct.	1.017	1.018	1.022	1.005	1.004	1.002	0.993	0.991	1.001	0.994	0.996	0.999
Mol.%												
Aegirine	67.13	71.89	71.71	41.58	39.48	34.62	35.35	10.80	15.75	11.05	16.79	17.73
Diopside	23.05	18.21	20.36	40.54	44.02	47.77	45.22	78.85	72.02	73.25	68.33	71.03
Hedenbergite	2.73	1.74	0.35	13.26	12.65	13.51	16.39	8.25	8.86	13.56	11.54	8.35
Jadeite	0.00	0.40	0.00	0.40	0.00	0.00	0.00	0.00	0.00	0.00	0.00	0.00
Pyroxmangite	0.88	0.64	0.87	0.77	0.85	0.85	0.97	0.43	0.91	0.88	0.85	0.79
$CaFeAlSiO_6$	0.00	0.00	0.00	0.14	0.00	0.41	0.09	1.27	0.16	0.26	0.25	0.00
$CaTiAl_2O_6$	1.01	1.03	0.93	0.81	1.12	1.25	1.53	0.51	1.08	0.93	1.44	1.39
$CaCrAlSiO_6$	0.07	0.12	0.06	0.00	0.00	0.02	0.07	0.00	0.06	0.10	0.00	0.04

* Mineral formulae calculated based on 4 cations and 6 oxygens, with Fe^{3+} determined by charge balance

Acronyms: fi. = fine; med. = medium; v. = very; mid. = middle; lt. = light; ed. = edge

Appendix A-2. Results of electron-microprobe analyses of aegirine-augite*

Sample #	AD041E	AD066I								AD046D
Description	69 furthest	14 lt.ed.	15 dk mid.	16 dk ed.	18	20 lt.	27 lt.ed.	28 lt.	30 vein	75
SiO_2	53.88	51.85	51.44	52.01	52.73	52.07	51.44	52.59	51.28	52.52
TiO_2	0.21	0.18	0.35	0.40	0.23	0.62	0.18	0.47	0.23	0.33
Al_2O_3	1.12	0.66	0.69	0.65	0.59	0.72	0.59	0.92	0.65	0.44
Fe_2O_3	1.87	6.66	10.32	5.89	5.55	5.57	5.21	5.35	6.75	8.74
FeO	5.52	3.02	2.40	4.49	4.47	5.55	5.13	2.72	4.36	2.78
MgO	12.84	12.03	10.58	11.26	12.20	10.60	11.78	13.06	11.51	11.05
MnO	0.54	0.90	0.95	1.08	0.77	1.40	0.69	0.77	0.70	0.83
ZnO	0.00	0.00	0.04	0.01	0.05	0.01	0.11	0.05	0.06	0.00
V_2O_3	0.19	0.34	0.29	0.31	0.17	0.46	0.18	0.13	0.24	0.36
Cr_2O_3	0.02	0.05	0.04	0.06	0.02	0.03	0.05	0.04	0.07	0.03
ZrO_2	n.d.	0.07	0.07	0.15	0.12	0.15	0.06	0.07	0.03	0.04
Nb_2O_5	0.00	0.00	0.02	0.00	0.00	0.01	0.00	0.00	0.02	0.02
CaO	21.46	21.24	18.41	20.85	21.33	20.17	22.54	21.66	21.46	19.05
Na_2O	1.62	2.07	3.46	2.22	1.93	2.43	1.27	1.89	1.82	3.33
K_2O	0.21	0.00	0.00	0.00	0.00	0.00	0.00	0.00	0.00	0.00
Total	99.48	99.09	99.05	99.37	100.15	99.74	99.23	99.71	99.19	99.51
Si	2.004	1.954	1.948	1.963	1.968	1.966	1.950	1.956	1.944	1.971
Ti	0.006	0.005	0.010	0.011	0.007	0.018	0.005	0.013	0.007	0.009
^{IV}Al	0.000	0.029	0.031	0.029	0.026	0.032	0.026	0.040	0.029	0.019
ΣTet	2.010	1.988	1.989	2.004	2.000	2.015	1.981	2.010	1.979	2.000
Fe^{3+}	0.052	0.189	0.294	0.167	0.156	0.158	0.149	0.150	0.192	0.247
Fe^{2+}	0.172	0.095	0.076	0.142	0.140	0.174	0.163	0.085	0.138	0.087
Mg	0.712	0.676	0.597	0.634	0.679	0.597	0.666	0.724	0.650	0.618
Mn	0.017	0.029	0.030	0.035	0.024	0.045	0.022	0.024	0.023	0.026
Zn	0.000	0.000	0.001	0.000	0.001	0.000	0.003	0.001	0.002	0.000
^{VI}Al	0.049	0.000	0.000	0.003	0.000	0.000	0.000	0.000	0.000	0.000
V	0.006	0.010	0.009	0.009	0.005	0.014	0.005	0.004	0.007	0.011
Cr	0.000	0.001	0.001	0.002	0.001	0.001	0.001	0.001	0.002	0.001
Zr	0.000	0.001	0.001	0.003	0.002	0.003	0.001	0.001	0.001	0.001
Nb	0.000	0.000	0.000	0.000	0.000	0.000	0.000	0.000	0.000	0.000
ΣOct.	1.008	1.002	1.010	0.995	1.007	0.991	1.010	0.990	1.015	0.991
Ca	0.855	0.858	0.747	0.843	0.853	0.816	0.915	0.863	0.872	0.766
Na	0.117	0.151	0.254	0.162	0.140	0.178	0.094	0.136	0.134	0.242
K	0.010	0.000	0.000	0.000	0.000	0.000	0.000	0.000	0.000	0.000
ΣOct.	0.982	1.009	1.001	1.005	0.993	0.994	1.009	1.000	1.005	1.008
Mol.%										
Aegirine	4.81	15.15	25.40	15.88	13.97	15.76	9.36	13.65	13.38	24.23
Diopside	71.17	67.58	59.71	63.35	67.87	59.66	66.57	72.40	65.01	61.80
Hedenbergite	17.18	9.53	7.59	14.16	13.96	17.36	16.27	8.48	13.83	8.72
Jadeite	4.90	0.00	0.00	0.34	0.01	0.00	0.00	0.00	0.00	0.00
Pyroxmangite	0.85	1.44	1.52	1.73	1.21	2.24	1.10	1.22	1.13	1.31
$CaFeAlSiO_6$	0.41	1.75	2.00	0.86	1.61	0.07	1.51	1.32	1.87	0.46
$CaTiAl_2O_6$	0.00	0.52	0.99	1.12	0.65	1.77	0.51	1.32	0.65	0.93
$CaCrAlSiO_6$	0.04	0.14	0.13	0.18	0.05	0.08	0.14	0.11	0.20	0.09

* Mineral formulae calculated based on 4 cations and 6 oxygens, with Fe^{3+} determined by charge balance

Acronyms: fi. = fine; med. = medium; v. = very; mid. = middle; lt. = light; ed. = edge

Appendix A-3. Electron-microprobe analyses of amphibole

Sample	87/a/94					AD041E							AD043B			AD046D
Description	5 dk ed.	mid.lt.	ed.dk	mid.lt.	ed.dk	2 ed.	dk.mid.	ed.		mid.	1 mid.	ed.	4 dkr		5	3 ed.
SiO_2	55.35	54.51	55.43	53.37	54.50	54.98	55.90	55.50	55.94	55.28	54.93	56.22	56.71	56.68	57.13	55.48
Al_2O_3	0.10	0.86	0.08	0.94	0.09	0.85	0.70	0.76	0.11	0.05	0.05	0.04	0.06	0.04	0.05	0.06
TiO_2	0.13	0.39	0.13	0.45	0.14	0.25	0.23	0.40	0.16	0.10	0.13	0.11	0.17	0.20	0.19	0.18
FeO	7.86	7.97	8.00	7.89	7.85	4.16	3.11	4.76	4.65	6.28	5.96	6.16	5.25	4.76	4.66	10.69
MgO	19.10	18.74	19.16	19.00	19.07	20.90	21.82	20.37	21.06	19.99	20.14	20.09	20.84	20.79	20.89	17.32
MnO	0.46	0.46	0.41	0.49	0.44	0.32	0.23	0.49	0.47	0.70	0.60	0.60	0.39	0.45	0.41	0.99
ZnO	0.04	0.00	0.00	0.01	0.00	0.03	0.02	0.03	0.04	0.01	0.04	0.00	0.06	0.03	0.00	0.01
ZrO_2	0.00	0.00	0.01	0.00	0.05	0.01	0.02	0.00	0.04	0.02	0.01	0.00	0.00	0.00	0.00	0.02
V_2O_3	0.00	0.00	0.00	0.00	0.01	0.50	0.59	0.74	0.06	0.06	0.02	0.03	0.23	0.29	0.26	0.14
Cr_2O_3	0.00	0.00	0.00	0.01	0.01	0.12	0.12	0.07	0.02	0.01	0.00	0.00	0.06	0.08	0.07	0.01
Na_2O	7.13	6.68	7.19	6.77	7.33	6.54	6.68	6.83	6.51	6.97	6.84	6.91	7.07	6.93	6.76	9.02
K_2O	1.53	1.35	1.47	1.33	1.44	1.52	1.51	1.45	1.47	1.82	1.60	1.87	1.62	1.50	1.57	2.15
CaO	4.79	5.76	4.98	5.87	4.80	6.53	6.33	5.99	6.46	5.49	5.78	5.44	5.49	5.88	6.05	1.32
F	3.00	3.01	3.15	3.03	2.95	2.63	2.88	2.32	2.59	2.47	2.46	2.50	2.69	2.79	2.73	1.96
Cl	0.00	0.01	0.00	0.00	0.00	0.00	0.00	0.01	0.01	0.00	0.00	0.00	0.00	0.00	0.00	0.00
H_2O^*	0.92	0.84	1.07	0.95	0.98	0.97	0.98	0.73	0.72	0.67	0.70	0.73	1.19	1.11	1.16	1.15
Total	100.40	100.59	101.07	100.11	99.64	100.32	101.13	100.44	100.30	99.92	99.26	100.70	101.82	101.53	101.94	100.49
-O=F,Cl	1.26	1.27	1.33	1.27	1.24	1.11	1.21	0.97	1.09	1.04	1.04	1.05	1.13	1.17	1.15	0.82
Total	99.14	99.32	99.75	98.84	98.40	99.22	99.92	99.47	99.21	98.88	98.22	99.65	100.69	100.36	100.79	99.66
						Mineral formulae calculated based on 23 atoms of oxygen										
Si	7.71	7.59	7.69	7.50	7.67	7.59	7.61	7.65	7.70	7.71	7.70	7.76	7.73	7.73	7.76	7.86
^{IV}Al	0.02	0.14	0.01	0.16	0.01	0.14	0.11	0.12	0.02	0.01	0.01	0.01	0.01	0.01	0.01	0.01
ΣTet	7.73	7.73	7.70	7.66	7.69	7.73	7.72	7.77	7.72	7.72	7.71	7.77	7.74	7.74	7.76	7.87
^{VI}Al	0.00	0.00	0.00	0.00	0.00	0.00	0.00	0.00	0.00	0.00	0.00	0.00	0.00	0.00	0.00	0.00
Ti	0.01	0.04	0.01	0.05	0.01	0.03	0.02	0.04	0.02	0.01	0.01	0.01	0.02	0.02	0.02	0.02
Fe^{3+}	0.92	0.93	0.93	0.93	0.92	0.48	0.35	0.55	0.54	0.73	0.70	0.71	0.60	0.54	0.53	1.27
Mg	3.97	3.89	3.96	3.98	4.00	4.30	4.42	4.18	4.32	4.16	4.21	4.13	4.24	4.23	4.23	3.66
Mn	0.05	0.05	0.05	0.06	0.05	0.04	0.03	0.06	0.05	0.08	0.07	0.07	0.05	0.05	0.05	0.12
Zn	0.00	0.00	0.00	0.00	0.00	0.00	0.00	0.00	0.00	0.00	0.00	0.00	0.01	0.00	0.00	0.00
Zr	0.00	0.00	0.00	0.00	0.00	0.00	0.00	0.00	0.00	0.00	0.00	0.00	0.00	0.00	0.00	0.00
V	0.00	0.00	0.00	0.00	0.00	0.06	0.06	0.08	0.01	0.01	0.00	0.00	0.02	0.03	0.03	0.02
Cr	0.00	0.00	0.00	0.00	0.00	0.01	0.01	0.00	0.00	0.00	0.00	0.00	0.00	0.01	0.00	0.00
ΣOct	4.95	4.91	4.95	5.01	5.00	4.91	4.90	4.92	4.94	4.99	5.00	4.93	4.93	4.88	4.86	5.08
Na	1.93	1.80	1.93	1.85	2.00	1.75	1.76	1.82	1.74	1.89	1.86	1.85	1.87	1.83	1.78	2.48
K	0.27	0.24	0.26	0.24	0.26	0.27	0.26	0.26	0.26	0.32	0.29	0.33	0.28	0.26	0.27	0.39
Ca	0.71	0.86	0.74	0.88	0.72	0.97	0.92	0.88	0.95	0.82	0.87	0.80	0.80	0.86	0.88	0.20
ΣM4	2.91	2.90	2.93	2.97	2.99	2.99	2.95	2.96	2.95	3.03	3.01	2.98	2.95	2.95	2.93	3.07
F	1.32	1.33	1.38	1.34	1.31	1.15	1.24	1.01	1.13	1.09	1.09	1.09	1.16	1.20	1.17	0.88
Cl	0.00	0.00	0.00	0.00	0.00	0.00	0.00	0.00	0.00	0.00	0.00	0.00	0.00	0.00	0.00	0.00
OH*	0.68	0.67	0.62	0.65	0.69	0.85	0.76	0.99	0.87	0.91	0.91	0.91	0.84	0.80	0.83	1.12
ΣCations	15.60	15.55	15.59	15.64	15.67	15.63	15.57	15.66	15.61	15.74	15.72	15.68	15.63	15.58	15.55	16.03
Mg/(Mg+Fe)*100	81.25	80.72	81.01	81.10	81.24	89.96	92.59	88.40	88.97	85.01	85.77	85.32	87.62	88.62	88.87	74.27
ΣSi+Na+K	9.91	9.63	9.88	9.58	9.94	9.61	9.63	9.73	9.70	9.92	9.84	9.94	9.89	9.83	9.81	10.73
ΣCa+^{IV}Al	0.73	1.00	0.75	1.04	0.74	1.10	1.04	1.01	0.97	0.83	0.88	0.81	0.81	0.87	0.89	0.21

* H_2O calculated from the OH content which was calculated based on 2(O, OH, F)

The acronyms are: lt=light; dk=dark; dker=darker; med=medium; ed.=edge; mid=middle, 2nd=second, elong.=elongated, rx=rim

Appendix A-3. Electron-microprobe analyses of amphibole

Sample	AD046D															
Description	mkd.	ed.	2nd ed.	mkd.	mkd.	side	mid.side	ed.	2 ed.	mkd.	mkd.	elong.	lt.line	lt.nr.ed.	1 mkd.	lt.nr ed.
SiO_2	55 50	55 18	55.32	55 04	54 80	55 43	55 31	55.72	55 42	55 45	55 54	55 43	55 63	55 47	55.59	55.37
Al_2O_3	0 11	0 10	0 09	0 17	0 09	0 12	0 25	0 98	0 13	0 13	0 11	0 38	0 13	0 15	0 22	0 10
TiO_2	0 11	0 31	0 16	0 30	0 14	0 13	0 09	0 10	0 11	0 09	0 15	0 12	0 11	0 13	0 16	0 35
FeO	7 70	11 23	9 17	9.52	8 53	8 24	7 25	6 52	8 08	7 40	8 42	7 29	7 79	7 91	7.19	9 44
MgO	19 09	17 34	17 95	17.40	18 39	18 61	19 27	19 18	18 86	19 17	18 66	19 38	18 90	19 00	19 25	17.71
MnO	0 95	0 57	1 00	1 17	1 01	0 96	0 95	0 83	0 99	0 92	1 08	0 91	0 98	1 07	0 95	1 37
ZnO	0 06	0 01	0 03	0 02	0 01	0 02	0 02	0 02	0 03	0 02	0 03	0 02	0 03	0 04	0 02	0 02
ZrO_2	0 01	0 06	0 00	0 09	0 00	0 01	0 02	0 03	0 02	0 01	0 03	0 03	0 02	0 00	0 00	0 00
V_2O_3	0 04	0 12	0 05	0 10	0 06	0 03	0 02	0 04	0 05	0 01	0 04	0 07	0 04	0 08	0 04	0 16
Cr_2O_3	0 01	0 02	0 00	0 01	0 00	0 02	0 01	0 01	0 00	0 00	0 00	0 00	0 02	0 00	0 01	0 01
Na_2O	7 05	9 73	7 21	7 30	6 98	6 97	6 94	6 55	7 07	6 91	6 95	6 91	6 73	6 88	7 02	8 03
K_2O	1 72	2 22	1 76	1 60	1 81	1 73	1 68	2 10	1 73	1 76	1 79	1 73	1 89	1 78	1 68	2 35
CaO	5 41	0 52	4 81	4 92	5 13	5 08	5 45	5 66	5 22	5 47	5 31	5 58	5 45	5 46	5 37	2 66
F	2 19	2 00	2 08	2 51	2 23	2 19	2 22	2 23	2 24	2 56	2 25	2 32	2 20	2 21	2 40	1 33
Cl	0 00	0 00	0 00	0 01	0 00	0 00	0 00	0 01	0 00	0 00	0 00	0 00	0 01	0 00	0 01	0 00
H_2O^*	0 94	1 07	1 10	1 09	1 10	1 08	0 94	1 09	1 06	1 10	1 10	1 02	1 47	0 91	1 07	0 83
Total	100 89	100 47	100 72	101 22	100 30	100 62	100 41	101 05	101 01	101 01	101 47	101 19	101 39	101 09	100 95	99.72
-O=F,Cl	0 92	0 84	0 87	1 06	0 94	0 92	0 93	0 94	0 94	1 08	0 95	0 97	0 92	0 93	1 01	0 56
Total	99.97	99 63	99 85	100 16	99.36	99 70	99 48	100 11	100 07	99 93	100 52	100 22	100 47	100 16	99.94	99 15
							Mineral formulae calculated based on 23 atoms of oxygen									
Si	7 74	7 83	7 78	7 72	7 73	7 77	7 73	7 72	7 74	7 72	7 74	7 70	7 76	7 73	7 73	7 88
^{IV}Al	0 02	0 02	0 01	0 03	0 02	0 02	0 04	0 16	0 02	0 02	0 02	0 06	0 02	0 02	0 04	0 02
ΣTet	7 76	7 85	7 80	7 75	7 75	7 79	7 77	7 88	7 76	7 74	7 76	7 76	7 78	7 75	7 77	7 89
^{VI}Al	0 00	0 00	0 00	0 00	0 00	0 00	0 00	0 00	0 00	0 00	0 00	0 00	0 00	0 00	0 00	0 00
Ti	0 01	0 03	0 02	0 03	0 02	0 01	0 01	0 01	0 01	0 01	0 02	0 01	0 01	0 01	0 02	0 04
Fe^{2+}	0 90	1 33	1 08	1 12	1 01	0 97	0 85	0 76	0 94	0 86	0 98	0 85	0 91	0 92	0 84	1 12
Mg	3 97	3 67	3 76	3 64	3 87	3 89	4 01	3 96	3 92	3 98	3 88	4 01	3 93	3 94	3 99	3 76
Mn	0 11	0 07	0 12	0 14	0 12	0 11	0 11	0 10	0 12	0 11	0 13	0 11	0 12	0 13	0 11	0 16
Zn	0 01	0 00	0 00	0 00	0 00	0 00	0 00	0 00	0 00	0 00	0 00	0 00	0 00	0 00	0 00	0 00
Zr	0 00	0 00	0 00	0 01	0 00	0 00	0 00	0 00	0 00	0 00	0 00	0 00	0 00	0 00	0 00	0 00
V	0 00	0 01	0 01	0 01	0 01	0 00	0 00	0 00	0 01	0 00	0 00	0 01	0 00	0 01	0 00	0 02
Cr	0 00	0 00	0 00	0 00	0 00	0 00	0 00	0 00	0 00	0 00	0 00	0 00	0 00	0 00	0 00	0 00
ΣOct	5 00	5 12	4 99	4 95	5 02	4 99	4 99	4 83	5 01	4 96	5 01	4 99	4 98	5 02	4 96	5.10
Na	1 91	2 68	1 97	1 99	1 91	1 89	1 88	1 76	1 92	1 87	1 88	1 86	1 82	1 86	1 89	2 22
K	0 31	0 40	0 32	0 29	0 33	0 31	0 30	0 37	0 31	0 31	0 32	0 31	0 34	0 32	0 30	0 43
Ca	0 81	0 08	0 73	0 74	0 78	0 76	0 82	0 84	0 78	0 82	0 79	0 83	0 82	0 81	0 80	0 41
ΣM4	3 02	3 16	3 01	3 01	3 01	2 97	3 00	2 97	3 00	2 99	2 99	3 00	2 97	2 99	2 99	3 05
F	0 96	0 90	0 92	1 11	0 99	0 97	0 98	0 98	0 99	1 13	0 99	1 02	0 97	0 97	1 05	0 60
Cl	0 00	0 00	0 00	0 00	0 00	0 00	0 00	0 00	0 00	0 00	0 00	0 00	0 00	0 00	0 00	0 00
OH*	1 04	1 10	1 08	0 88	1 01	1 03	1 02	1 02	1 01	0 87	1 01	0 98	1 03	1 03	0 95	1 40
ΣCations	15 78	16 13	15 80	15.71	15.78	15 74	15 76	15 68	15 77	15 70	15.76	15 75	15 73	15.76	15.72	16 04
Mg/(Mg+Fe)*100	81 54	73 35	77.72	76.50	79.34	80 10	82 57	83 98	80 61	82 19	79.79	82.56	81 23	81.05	82 67	76 99
ΣSi+Na+K	9 96	10 91	10 07	10.00	9 97	9 97	9 91	9 85	9 96	9 90	9 94	9 87	9 92	9 91	9 92	10.52
ΣCa+^{IV}Al	0 83	0 10	0 74	0 77	0 79	0 78	0 86	1 00	0 80	0 84	0 81	0 89	0 84	0 84	0 84	0 42

* H_2O calculated from the OH content which was calculated based on 2(O, OH, F)

The acronyms are: lt=light, dk=dark; dker=darker; med=medium; ed =edge, mid=middle, 2nd=second, elong =elongated, nr=near

Appendix A-3 Electron-microprobe analyses of amphibole

Sample	AD046D											AD066I		
Description	lt.nr ed.	dk	dk	dkr	mkl.dkr	mkl.	lt.mkl.	mkl.lt.	nr brith	2 nr.ed.	oed	3dk rim	lt.mkl.	core
SiO_2	55.58	55.72	55.39	55.83	55.19	55.53	55.49	54.06	55.63	54.72	55.83	55.86	55.44	55.76
Al_2O_3	0.13	0.15	0.10	0.10	0.11	0.07	0.11	0.17	0.08	0.36	0.09	0.32	0.41	0.32
TiO_2	0.09	0.07	0.12	0.07	0.11	0.12	0.07	0.24	0.11	0.11	0.12	0.09	0.25	0.07
FeO	7.88	7.45	8.91	7.27	7.37	8.12	8.84	9.67	7.45	7.17	9.27	7.91	7.96	6.69
MgO	18.66	19.10	18.36	19.04	18.86	18.29	18.14	16.42	19.13	18.96	17.98	18.59	18.05	19.11
MnO	0.96	0.96	0.96	0.98	0.96	0.98	1.17	1.66	1.01	0.97	0.98	1.56	1.69	1.69
ZnO	0.05	0.01	0.02	0.04	0.00	0.01	0.02	0.02	0.00	0.03	0.03	0.01	0.03	0.03
ZrO_2	0.03	0.00	0.00	0.00	0.00	0.00	0.00	0.02	0.00	0.00	0.00	0.04	0.04	0.02
V_2O_3	0.05	0.04	0.02	0.02	0.06	0.01	0.06	0.08	0.04	0.03	0.03	0.05	0.04	0.02
Cr_2O_3	0.02	0.01	0.00	0.00	0.00	0.00	0.00	0.00	0.00	0.02	0.00	0.00	0.01	0.03
Na_2O	7.21	7.14	6.71	6.59	6.59	6.68	6.60	6.40	6.62	6.48	6.88	7.04	6.89	6.72
K_2O	1.72	1.63	1.74	1.63	1.61	1.71	1.52	1.41	1.70	1.67	1.63	1.67	1.69	1.86
CaO	5.33	5.34	4.98	5.47	5.40	4.95	4.81	5.96	5.60	5.78	4.84	5.07	5.36	5.47
F	2.63	2.29	2.57	2.45	2.30	2.25	2.46	2.21	2.33	2.27	2.14	2.83	2.61	2.74
Cl	0.00	0.00	0.00	0.00	0.00	0.00	0.00	0.00	0.00	0.00	0.00	0.00	0.00	0.00
H_2O^*	0.92	0.87	0.92	0.88	0.91	0.92	0.99	1.04	1.06	0.97	1.04	1.04	1.05	1.12
Total	101.26	100.76	100.80	100.35	99.46	99.64	100.27	99.36	100.75	99.52	100.86	102.08	101.51	101.64
-O=F,Cl	1.11	0.96	1.08	1.03	0.97	0.95	1.03	0.93	0.98	0.95	0.90	1.19	1.10	1.15
Total	100.15	99.80	99.71	99.32	98.50	98.70	99.24	98.42	99.77	98.56	99.96	100.89	100.42	100.49
						Mineral formulae calculated based on 23 atoms of oxygen								
Si	7.72	7.76	7.75	7.78	7.77	7.82	7.79	7.75	7.76	7.72	7.82	7.71	7.71	7.71
^{IV}Al	0.02	0.02	0.02	0.02	0.02	0.01	0.02	0.03	0.01	0.06	0.01	0.05	0.07	0.05
ΣTet	7.75	7.78	7.76	7.80	7.79	7.83	7.81	7.78	7.77	7.78	7.83	7.76	7.78	7.76
^{VI}Al	0.00	0.00	0.00	0.00	0.00	0.00	0.00	0.00	0.00	0.00	0.00	0.00	0.00	0.00
Ti	0.01	0.01	0.01	0.01	0.01	0.01	0.01	0.03	0.01	0.01	0.01	0.01	0.03	0.01
Fe^{2+}	0.92	0.87	1.04	0.85	0.87	0.96	1.04	1.16	0.87	0.85	1.09	0.91	0.93	0.77
Mg	3.87	3.96	3.83	3.95	3.96	3.84	3.80	3.51	3.97	3.98	3.75	3.82	3.74	3.94
Mn	0.11	0.11	0.11	0.12	0.12	0.12	0.14	0.20	0.12	0.12	0.12	0.18	0.20	0.20
Zn	0.01	0.00	0.00	0.00	0.00	0.00	0.00	0.00	0.00	0.00	0.00	0.00	0.00	0.00
Zr	0.00	0.00	0.00	0.00	0.00	0.00	0.00	0.00	0.00	0.00	0.00	0.00	0.00	0.00
V	0.01	0.00	0.00	0.00	0.01	0.00	0.01	0.01	0.00	0.00	0.00	0.01	0.00	0.00
Cr	0.00	0.00	0.00	0.00	0.00	0.00	0.00	0.00	0.00	0.00	0.00	0.00	0.00	0.00
ΣOct	4.92	4.96	5.00	4.93	4.96	4.93	4.99	4.91	4.98	4.97	4.97	4.94	4.90	4.92
Na	1.94	1.93	1.82	1.78	1.80	1.83	1.80	1.78	1.79	1.77	1.87	1.88	1.86	1.80
K	0.30	0.29	0.31	0.29	0.29	0.31	0.27	0.26	0.30	0.30	0.29	0.29	0.30	0.33
Ca	0.79	0.80	0.75	0.82	0.82	0.75	0.72	0.91	0.84	0.87	0.73	0.75	0.80	0.81
ΣM4	3.04	3.01	2.88	2.89	2.91	2.88	2.79	2.95	2.93	2.95	2.89	2.93	2.96	2.94
F	1.16	1.01	1.14	1.08	1.02	1.00	1.09	1.00	1.03	1.01	0.95	1.24	1.15	1.20
Cl	0.00	0.00	0.00	0.00	0.00	0.00	0.00	0.00	0.00	0.00	0.00	0.00	0.00	0.00
OH*	0.84	0.99	0.86	0.92	0.98	1.00	0.91	1.00	0.97	0.99	1.05	0.76	0.85	0.80
ΣCations	15.70	15.75	15.64	15.61	15.66	15.64	15.59	15.64	15.67	15.69	15.69	15.62	15.64	15.62
Mg/(Mg+Fe)*100	80.84	82.05	78.59	82.36	82.01	80.05	78.52	75.16	82.06	82.50	77.55	80.72	80.17	83.58
ΣSi+Na+K	9.97	9.97	9.88	9.85	9.86	9.96	9.86	9.79	9.85	9.79	9.98	9.88	9.87	9.84
ΣCa+^{IV}Al	0.81	0.82	0.76	0.83	0.83	0.76	0.74	0.94	0.85	0.93	0.74	0.80	0.87	0.86

* H_2O calculated from the OH content which was calculated based on 2(O, OH, F)

The acronyms are: lt=light; dk=dark; dkr=darker; med=medium; ed.=edge; mid=middle; 2nd=second; elong.=elongated; nr=near

Appendix A-4 Electron-microprobe analyses of mica

Sample #	AD054B1								BH/9/1		
Description	1.38 N	1.39 N	1.4 N	1.41 N	1.42 N	1.62 N	1.63 N	1.64 N	1.43 N	1.44 N	1.45 N
SiO_2	37.86	37.86	38.25	38.63	38.22	38.50	38.36	38.32	38.87	41.91	38.84
TiO_2	3.88	3.92	4.20	4.32	3.87	4.17	4.11	3.80	1.97	0.91	1.80
Al_2O_3	13.68	13.57	13.81	13.63	13.37	13.59	13.64	13.57	10.64	10.24	10.58
Cr_2O_3	0.08	0.13	0.12	0.15	0.11	0.16	0.18	0.16	0.02	0.02	0.01
Fe_2O_3	0.00	0.00	0.00	0.00	0.00	0.00	0.00	0.00	0.00	0.00	0.00
FeO	13.29	12.08	10.03	9.66	12.64	8.19	8.08	13.44	20.39	11.06	19.70
MnO	0.22	0.17	0.12	0.06	0.17	0.05	0.02	0.23	1.14	1.00	1.17
MgO	17.52	18.40	19.74	19.96	18.40	20.92	20.87	16.59	14.00	19.97	14.35
CaO	0.16	0.04	0.02	0.01	0.05	0.01	0.00	0.05	0.01	0.07	0.02
BaO	0.26	0.30	0.29	0.32	0.29	0.30	0.28	0.26	0.08	0.03	0.17
Na_2O	0.18	0.19	0.27	0.33	0.25	0.34	0.35	0.27	0.22	0.37	0.19
K_2O	10.00	9.97	9.92	9.87	9.91	9.84	9.77	9.70	9.75	10.38	9.96
F	1.01	1.10	1.43	1.44	1.16	1.64	1.65	1.16	2.31	4.17	2.48
H_2O	3.56	3.53	3.42	3.43	3.52	3.33	3.31	3.45	2.84	2.07	2.74
Total	101.70	101.26	101.62	101.81	101.96	101.04	100.62	101.00	102.24	102.20	102.01
F,Cl=O	0.43	0.46	0.60	0.61	0.49	0.69	0.69	0.49	0.97	1.76	1.04
Total	101.28	100.80	101.02	101.20	101.48	100.35	99.93	100.51	101.26	100.45	100.97
Si	2.808	2.802	2.798	2.819	2.813	2.812	2.810	2.870	2.964	3.103	2.971
^{IV}Al	1.192	1.184	1.191	1.172	1.16	1.17	1.178	1.13	0.956	0.894	0.954
$^{IV}Fe^{3+}$	0.000	0.000	0.000	0.000	0.000	0.000	0.000	0.000	0.000	0.000	0.000
Ti	0.000	0.014	0.011	0.009	0.027	0.018	0.011	0.000	0.080	0.004	0.076
ΣTetrahedral	4.000	4.000	4.000	4.000	4.000	4.000	4.000	4.000	4.000	4.001	4.000
^{VI}Al	0.004	0.000	0.000	0.000	0.000	0.000	0.000	0.068	0.000	0.000	0.000
Ti	0.216	0.204	0.220	0.228	0.187	0.211	0.215	0.214	0.033	0.047	0.028
Cr	0.005	0.008	0.007	0.009	0.006	0.009	0.010	0.010	0.001	0.001	0.001
$^{VI}Fe^{3+}$	0.000	0.000	0.000	0.000	0.000	0.000	0.000	0.000	0.000	0.000	0.000
Fe^{2+}	0.824	0.748	0.614	0.589	0.778	0.500	0.495	0.842	1.300	0.685	1.260
Mn	0.014	0.011	0.007	0.004	0.011	0.003	0.001	0.015	0.074	0.063	0.076
Mg	1.937	2.030	2.152	2.171	2.018	2.277	2.279	1.852	1.591	2.204	1.636
ΣOctahedral	3.000	3.000	3.000	3.000	3.000	3.001	3.001	3.000	3.000	3.000	3.000
Ca	0.013	0.003	0.002	0.001	0.004	0.001	0.000	0.004	0.001	0.006	0.002
Ba	0.008	0.009	0.008	0.009	0.008	0.009	0.008	0.008	0.002	0.001	0.005
Na	0.026	0.027	0.038	0.047	0.036	0.048	0.050	0.039	0.033	0.053	0.028
K	0.946	0.941	0.926	0.919	0.930	0.917	0.913	0.927	0.949	0.980	0.972
ΣInterlayer	0.992	0.981	0.974	0.975	0.978	0.974	0.971	0.978	0.984	1.040	1.007
F	0.237	0.258	0.331	0.332	0.270	0.379	0.382	0.275	0.557	0.977	0.600
OH	1.763	1.743	1.669	1.668	1.730	1.621	1.618	1.725	1.443	1.024	1.400
Fe/(Fe+Mg)	0.299	0.269	0.222	0.214	0.278	0.180	0.178	0.312	0.450	0.237	0.435
# Cations	7.992	7.980	7.974	7.975	7.978	7.974	7.971	7.978	7.984	8.040	8.007
Charge Def.	-0.025	0.033	0.091	0.055	0.059	0.135	0.142	-0.090	0.458	0.728	0.484

* N = normal; R = reverse; 1 or 2 before the decimal refer to the file, the rest is the analysis #
Structural formulae calculated based on 11 oxygens (assuming OH + F = 2) and 7 cations - (Na + K + Ca)

Appendix A-4 Electron-microprobe analyses of mica

Sample #	BH/9/1		AD066B								
Description	1.46 N	1.47 N	1.85 N	1.86 N	1.87 N	1.88 N	1.89 N	1.9 N	1.91 N	1.92 N	1.93 N
SiO_2	39.53	39.00	39.58	39.25	39.74	39.11	39.13	39.59	39.45	38.98	39.89
TiO_2	2.18	1.75	2.75	2.69	1.85	2.61	1.71	1.35	1.75	1.77	1.37
Al_2O_3	10.28	10.71	11.01	11.16	11.30	11.00	10.77	10.08	10.44	10.64	10.49
Cr_2O_3	0.03	0.03	0.01	0.01	0.04	0.01	0.02	0.05	0.01	0.03	0.05
Fe_2O_3	0.00	0.00	0.00	0.00	0.00	0.00	0.00	0.00	0.00	0.00	0.00
FeO	20.28	18.88	16.01	15.94	16.17	17.48	16.66	18.70	19.69	19.84	19.98
MnO	1.28	1.26	1.25	1.32	1.22	1.35	1.41	0.86	0.80	0.72	0.76
MgO	13.75	14.80	15.07	15.04	15.22	14.57	16.05	15.18	13.60	13.52	13.26
CaO	0.01	0.00	0.15	0.13	0.27	0.06	0.18	0.13	0.13	0.13	0.11
BaO	0.03	0.08	0.04	0.08	0.04	0.09	0.01	0.00	0.04	0.02	0.02
Na_2O	0.27	0.23	0.20	0.18	0.22	0.22	0.15	0.19	0.18	0.16	0.18
K_2O	9.85	9.94	9.27	9.24	8.90	9.59	9.76	9.07	9.00	8.91	8.84
F	2.51	2.61	2.09	2.10	2.26	1.82	2.32	2.47	1.91	1.88	1.83
H_2O	2.74	2.70	2.93	2.91	2.86	3.06	2.85	2.75	2.97	2.97	3.01
Total	102.74	101.99	100.36	100.05	100.09	100.97	101.02	100.42	99.97	99.57	99.79
F,Cl=O	1.06	1.10	0.88	0.88	0.95	0.77	0.98	1.04	0.80	0.79	0.77
Total	101.69	100.89	99.48	99.17	99.14	100.20	100.04	99.38	99.17	98.78	99.02
Si	3.013	2.971	3.027	3.009	3.033	2.991	2.972	3.028	3.052	3.024	3.088
^{IV}Al	0.923	0.962	0.973	0.991	0.967	0.992	0.964	0.909	0.948	0.973	0.913
$^{IV}Fe^{3+}$	0.000	0.000	0.000	0.000	0.000	0.000	0.000	0.000	0.000	0.000	0.000
Ti	0.064	0.066	0.000	0.000	0.000	0.017	0.065	0.063	0.000	0.003	0.000
ΣTetrahedral	4.000	4.000	4.000	4.000	4.000	4.000	4.000	4.000	4.000	4.000	4.001
^{VI}Al	0.000	0.000	0.019	0.018	0.049	0.000	0.000	0.000	0.003	0.000	0.044
Ti	0.061	0.034	0.158	0.155	0.106	0.133	0.033	0.015	0.102	0.100	0.080
Cr	0.002	0.002	0.001	0.001	0.002	0.001	0.001	0.003	0.001	0.002	0.003
$^{VI}Fe^{3+}$	0.000	0.000	0.000	0.000	0.000	0.000	0.000	0.000	0.000	0.000	0.000
Fe^{2+}	1.293	1.203	1.024	1.022	1.032	1.118	1.058	1.196	1.274	1.287	1.293
Mn	0.083	0.081	0.081	0.086	0.079	0.088	0.091	0.056	0.052	0.047	0.050
Mg	1.562	1.681	1.718	1.719	1.731	1.661	1.817	1.731	1.568	1.563	1.530
ΣOctahedral	3.000	3.001	3.000	3.000	3.000	3.000	3.000	3.001	3.000	3.000	3.000
Ca	0.001	0.000	0.012	0.011	0.022	0.005	0.015	0.011	0.011	0.011	0.009
Ba	0.001	0.002	0.001	0.002	0.001	0.003	0.000	0.000	0.001	0.001	0.001
Na	0.040	0.034	0.030	0.027	0.033	0.033	0.022	0.028	0.027	0.024	0.027
K	0.958	0.966	0.904	0.904	0.866	0.936	0.946	0.885	0.888	0.882	0.873
ΣInterlayer	0.999	1.002	0.947	0.944	0.922	0.976	0.983	0.924	0.927	0.917	0.910
F	0.605	0.629	0.505	0.509	0.546	0.440	0.557	0.598	0.467	0.461	0.448
OH	1.395	1.371	1.495	1.491	1.455	1.560	1.443	1.403	1.533	1.539	1.552
Fe/(Fe+Mg)	0.453	0.417	0.373	0.373	0.373	0.402	0.368	0.409	0.448	0.452	0.458
# Cations	7.999	8.002	7.947	7.944	7.922	7.976	7.983	7.924	7.927	7.917	7.910
Charge Def.	0.404	0.517	0.182	0.215	0.303	0.182	0.456	0.540	0.269	0.303	0.234

* N = normal; R = reverse; 1 or 2 before the decimal refer to the file; the rest is the analysis #
Structural formulae calculated based on 11 oxygens (assuming OH + F = 2) and 7 cations - (Na + K + Ca)

Appendix A-4 Electron-microprobe analyses of mica

Sample #	AD066B					AD066E					
Description	1.94 N	1.95 N	1.96 N	1.97 N	1.98 N	2.34 N cs.	2.35 N	2.36 N	2.37 N fl.	2.38 N fl.	2.39 N
SiO_2	40 70	38 97	39 69	39 39	39 21	40 71	40 75	40 22	39 76	39 31	40 12
TiO_2	1.11	1.56	1.58	1.93	1.92	1 73	2 32	1 98	1 44	1.78	1 59
Al_2O_3	10 44	10 37	10 35	10 89	10.37	11 45	11 20	11.35	11 12	11 02	11.19
Cr_2O_3	0 02	0 01	0 01	0 03	0 03	0 01	0 02	0 03	0 02	0 02	0 01
Fe_2O_3	0 00	0 00	0 00	0 00	0 00	0 00	0 00	0 00	0 00	0 00	0 00
FeO	15 78	19 37	18 74	18 47	19.20	14 27	13 43	13 26	13 48	13 17	14 20
MnO	0 83	0 84	0 91	0 86	0 83	0 56	0 69	0 63	0 79	0.72	1 00
MgO	16 69	13 78	13 89	13 13	13 07	17 58	17 86	18 26	18 48	17 81	17 02
CaO	0 05	0 13	0 16	0 15	0 16	0 14	0 19	0 14	0 12	0 05	0 02
BaO	0 00	0 04	0 05	0 02	0 07	0 08	0 01	0 05	0 08	0 05	0 09
Na_2O	0 14	0 18	0 18	0 19	0 18	0 15	0 14	0 15	0 15	0 15	0 13
K_2O	9 38	8 60	8 69	8 50	8 56	9 11	9 48	9 57	9 68	9.61	9 77
F	2 14	2 05	1.96	1 89	1 89	2 59	2 49	2 53	2 53	2 40	2 40
H_2O	2.95	2.88	2.94	2.94	2.92	2.80	2.85	2.82	2.80	2.80	2.83
Total	100 23	98 78	99.15	98 39	98 41	101 18	101 43	100 99	100 45	98 89	100.37
F,Cl=O	0 90	0 86	0 83	0 80	0 80	1 09	1.05	1.07	1 07	1 01	1 01
Total	99.33	97.91	98.32	97.59	97.62	100.09	100.38	99.93	99.39	97.87	99.36
Si	3 076	3 037	3 079	3 083	3 079	3 028	3 030	2 997	2 978	2 997	3 033
^{IV}Al	0 924	0 952	0 921	0 917	0 921	0 972	0 97	0 997	0 982	0 99	0 967
$^{IV}Fe^{3+}$	0 000	0 000	0 000	0 000	0 000	0 000	0 000	0 000	0 000	0 000	0 000
Ti	0 000	0 011	0 000	0 000	0 000	0 000	0 000	0 006	0 040	0 013	0 000
ΣTetrahedral	4 000	4 000	4 000	4 000	4 000	4 000	4 000	4 000	4 000	4 000	4 000
^{VI}Al	0 005	0 000	0 025	0 087	0 039	0 031	0 011	0 000	0 000	0 000	0 030
Ti	0 063	0 080	0 092	0 114	0 113	0 097	0 130	0 105	0 041	0 089	0 090
Cr	0 001	0 001	0 001	0 002	0 002	0 001	0 001	0 002	0 001	0 001	0 001
$^{VI}Fe^{3+}$	0 000	0 000	0 000	0 000	0 000	0 000	0 000	0 000	0 000	0 000	0 000
Fe^{2+}	0 997	1 262	1 216	1 209	1 261	0 888	0 835	0 826	0 844	0 840	0 898
Mn	0 053	0 055	0 060	0 057	0 055	0 035	0 044	0 040	0 050	0 047	0 064
Mg	1 880	1 601	1 606	1 532	1 530	1 949	1 979	2 028	2 063	2 024	1 918
ΣOctahedral	3 000	2 999	3 000	3 000	3 000	3 000	3 000	3 001	3 000	3 000	3 000
Ca	0 004	0 011	0 013	0 013	0 014	0 011	0 015	0 011	0 010	0 004	0 002
Ba	0 000	0 001	0 002	0 001	0 002	0 002	0 000	0 002	0 002	0 002	0 003
Na	0 021	0 027	0 027	0 029	0 027	0 022	0 020	0 022	0 022	0 022	0 019
K	0 904	0 855	0 860	0 849	0 858	0 864	0 899	0 910	0 925	0 935	0 942
ΣInterlayer	0 929	0 894	0 902	0 891	0 901	0 899	0 935	0 944	0 959	0 962	0 966
F	0 511	0 505	0 481	0 468	0 469	0 609	0 586	0 596	0 599	0 579	0 574
OH	1 489	1 495	1 519	1 532	1 531	1 391	1 415	1 404	1 401	1 421	1 426
Fe(Fe+Mg)	0 347	0 441	0 431	0 441	0 452	0 313	0 297	0 289	0 290	0 293	0 319
# Cations	7 929	7 894	7 902	7 891	7 901	7 899	7 935	7 944	7 959	7 962	7 965
Charge Def.	0 370	0 389	0 275	0.165	0.207	0.444	0 334	0 426	0 527	0.422	0 360

* N = normal, R = reverse; 1 or 2 before the decimal refer to the file; the rest is the analysis #
Structural formulae calculated based on 11 oxygens (assuming OH + F = 2) and 7 cations - (Na + K + Ca)

Appendix A-4 Electron-microprobe analyses of mica

Sample #	AD066E							87/A/67.1			
Description	2.41 N	2.42 N	2.43 N	2.44 N	2.45 N	2.46 N	2.47 N	1.48 N	1.49 N	1.50 N	1.51 N
SiO_2	40.60	40.02	39.98	40.88	41.35	41.74	40.86	39.09	40.95	40.49	40.32
TiO_2	1.40	1.07	1.00	1.20	0.37	0.29	2.04	1.34	1.26	1.49	1.06
Al_2O_3	10.77	10.78	10.71	10.21	11.00	9.92	11.06	9.23	11.06	10.73	9.84
Cr_2O_3	0.04	0.03	0.00	0.02	0.02	0.01	0.01	0.03	0.04	0.02	0.01
Fe_2O_3	0.00	0.00	0.00	0.00	0.00	0.00	0.00	0.00	0.00	0.00	0.00
FeO	14.85	14.64	14.48	13.79	12.46	13.65	14.08	16.79	15.47	15.72	16.94
MnO	0.94	1.18	1.03	0.99	0.95	0.94	0.85	0.81	0.97	1.07	0.95
MgO	16.49	17.07	17.21	17.38	18.91	18.05	16.73	14.32	15.86	16.50	15.76
CaO	0.16	0.05	0.11	0.12	0.06	0.06	0.07	0.47	0.11	0.11	0.38
BaO	0.05	0.00	0.01	0.03	0.01	0.00	0.03	0.02	0.00	0.05	0.03
Na_2O	0.10	0.13	0.18	0.19	0.09	0.13	0.16	0.11	0.18	0.19	0.22
K_2O	9.00	9.58	9.67	9.27	9.63	9.43	9.57	8.07	9.43	9.66	8.08
F	2.84	2.63	2.74	3.01	2.86	2.83	2.41	2.19	2.58	2.90	2.29
H_2O	2.60	2.70	2.64	2.52	2.67	2.63	2.84	2.69	2.73	2.61	2.82
Total	99.84	99.88	99.76	99.61	100.38	99.68	100.71	95.16	100.64	101.54	98.70
$F_2Cl=O$	1.20	1.11	1.15	1.27	1.20	1.19	1.01	0.92	1.09	1.22	0.96
Total	98.65	98.78	98.61	98.34	99.18	98.49	99.69	94.24	99.56	100.31	97.74
Si	3.083	3.037	3.042	3.107	3.079	3.149	3.080	3.143	3.104	3.050	3.095
^{IV}Al	0.917	0.963	0.958	0.893	0.921	0.851	0.92	0.857	0.896	0.95	0.89
$^{IV}Fe^{3+}$	0.000	0.000	0.000	0.000	0.000	0.000	0.000	0.000	0.000	0.000	0.000
Ti	0.000	0.000	0.000	0.000	0.000	0.000	0.000	0.000	0.000	0.000	0.014
ΣTetrahedral	4.000	4.000	4.000	4.000	4.000	4.000	4.000	4.000	4.000	4.000	4.000
^{VI}Al	0.047	0.001	0.003	0.021	0.044	0.032	0.062	0.017	0.091	0.003	0.000
Ti	0.080	0.061	0.057	0.069	0.021	0.017	0.116	0.081	0.072	0.084	0.047
Cr	0.002	0.002	0.000	0.001	0.001	0.001	0.001	0.002	0.002	0.001	0.001
$^{VI}Fe^{3+}$	0.000	0.000	0.000	0.000	0.000	0.000	0.000	0.000	0.000	0.000	0.000
Fe^{2+}	0.943	0.929	0.922	0.876	0.776	0.861	0.888	1.129	0.981	0.990	1.088
Mn	0.061	0.076	0.066	0.064	0.060	0.060	0.054	0.055	0.062	0.068	0.062
Mg	1.867	1.931	1.952	1.969	2.099	2.030	1.880	1.716	1.792	1.853	1.803
ΣOctahedral	3.000	3.000	3.000	3.000	3.000	3.001	3.000	3.000	3.000	3.000	3.000
Ca	0.013	0.004	0.009	0.010	0.005	0.005	0.006	0.041	0.009	0.009	0.031
Ba	0.002	0.000	0.000	0.001	0.000	0.000	0.001	0.001	0.000	0.002	0.001
Na	0.015	0.019	0.027	0.028	0.013	0.019	0.023	0.017	0.026	0.028	0.033
K	0.872	0.927	0.939	0.899	0.915	0.908	0.920	0.828	0.912	0.928	0.791
ΣInterlayer	0.901	0.951	0.975	0.937	0.933	0.932	0.950	0.886	0.947	0.967	0.856
F	0.682	0.631	0.659	0.724	0.673	0.675	0.575	0.557	0.618	0.691	0.556
OH	1.318	1.369	1.341	1.277	1.327	1.325	1.426	1.443	1.382	1.309	1.444
Fe/(Fe+Mg)	0.336	0.325	0.321	0.308	0.270	0.298	0.321	0.397	0.354	0.348	0.376
# Cations	7.901	7.951	7.975	7.937	7.933	7.932	7.950	7.886	7.947	7.966	7.856
Charge Def.	0.473	0.514	0.516	0.509	0.571	0.524	0.244	0.306	0.321	0.491	0.464

* N = normal; R = reverse; 1 or 2 before the decimal refer to the file; the rest is the analysis #
Structural formulae calculated based on 11 oxygens (assuming OH + F = 2) and 7 cations - (Na + K + Ca)

Appendix A-4 Electron-microprobe analyses of mica

Sample #	87/A/67.1							AMDO105C			
Description	1.52 N	1.54 N	1.55 N	1.56 N	1.57 N	1.58 N	1.59 N	2.49 N	2.50 N	2.51 N	2.52 N dk
SiO_2	40.69	41.38	40.61	39.71	40.80	40.83	40.50	39.21	39.65	39.32	40.20
TiO_2	0.99	1.01	1.20	1.64	1.45	1.21	0.94	2.46	2.05	2.15	1.51
Al_2O_3	10.09	10.62	10.19	10.27	10.08	10.20	10.25	10.43	10.62	11.22	12.89
Cr_2O_3	0.03	0.03	0.02	0.04	0.03	0.02	0.03	0.01	0.01	0.02	0.02
Fe_2O_3	0.00	0.00	0.00	0.00	0.00	0.00	0.00	0.00	0.00	0.00	0.00
FeO	16.57	15.12	16.49	17.84	17.42	15.52	16.56	18.88	17.18	20.18	15.19
MnO	0.96	0.88	0.90	0.88	0.83	1.07	1.01	1.00	1.04	0.73	0.47
MgO	16.76	16.80	15.75	15.03	15.22	17.17	16.48	13.53	14.21	12.55	9.34
CaO	0.06	0.11	0.11	0.13	0.07	0.09	0.05	0.25	0.24	0.19	0.21
BaO	0.04	0.01	0.03	0.04	0.10	0.05	0.01	0.12	0.07	0.04	0.04
Na_2O	0.25	0.15	0.13	0.16	0.16	0.19	0.17	0.16	0.10	0.09	0.08
K_2O	9.66	9.20	8.98	8.99	9.13	9.49	9.82	8.12	8.31	8.16	7.90
F	2.98	2.69	2.43	2.49	2.84	3.00	3.02	2.25	2.80	2.37	1.79
H_2O	2.57	2.71	2.77	2.72	2.58	2.57	2.53	2.80	2.53	2.75	2.73
Total	101.65	100.71	99.61	99.94	100.71	101.41	101.37	99.22	98.81	99.77	92.37
F,Cl=O	1.25	1.13	1.02	1.05	1.20	1.26	1.27	0.95	1.18	1.00	0.75
Total	100.40	99.58	98.59	98.89	99.52	100.15	100.10	98.27	97.63	98.77	91.62
Si	3.063	3.111	3.105	3.050	3.113	3.065	3.062	3.044	3.079	3.046	3.367
^{IV}Al	0.895	0.889	0.895	0.93	0.887	0.902	0.913	0.954	0.921	0.955	0.633
$^{IV}Fe^{3+}$	0.000	0.000	0.000	0.000	0.000	0.000	0.000	0.000	0.000	0.000	0.000
Ti	0.042	0.000	0.000	0.021	0.000	0.033	0.024	0.002	0.000	0.000	0.000
ΣTetrahedral	4.000	4.000	4.000	4.000	4.000	4.000	4.000	4.000	4.000	4.001	4.000
^{VI}Al	0.000	0.052	0.023	0.000	0.019	0.000	0.000	0.000	0.051	0.070	0.640
Ti	0.014	0.057	0.069	0.074	0.083	0.035	0.029	0.142	0.120	0.125	0.095
Cr	0.002	0.002	0.001	0.002	0.002	0.001	0.002	0.001	0.001	0.001	0.001
$^{VI}Fe^{3+}$	0.000	0.000	0.000	0.000	0.000	0.000	0.000	0.000	0.000	0.000	0.000
Fe^{2+}	1.043	0.951	1.054	1.146	1.112	0.974	1.047	1.226	1.116	1.307	1.064
Mn	0.061	0.056	0.058	0.057	0.054	0.068	0.065	0.066	0.068	0.048	0.033
Mg	1.880	1.883	1.795	1.721	1.731	1.921	1.857	1.566	1.645	1.449	1.166
ΣOctahedral	3.000	3.000	3.000	3.000	3.000	3.000	3.000	3.000	3.000	3.000	3.000
Ca	0.005	0.009	0.009	0.011	0.006	0.007	0.004	0.021	0.020	0.016	0.019
Ba	0.001	0.000	0.001	0.001	0.003	0.002	0.000	0.004	0.002	0.001	0.001
Na	0.037	0.022	0.019	0.024	0.024	0.028	0.025	0.024	0.015	0.014	0.013
K	0.928	0.882	0.876	0.881	0.889	0.909	0.947	0.804	0.823	0.806	0.844
ΣInterlayer	0.970	0.913	0.905	0.916	0.921	0.945	0.977	0.853	0.860	0.837	0.877
F	0.709	0.640	0.588	0.605	0.685	0.712	0.722	0.553	0.688	0.581	0.474
OH	1.291	1.360	1.413	1.395	1.315	1.288	1.278	1.448	1.312	1.420	1.526
Fe/(Fe+Mg)	0.357	0.336	0.370	0.400	0.391	0.337	0.361	0.439	0.404	0.474	0.477
# Cations	7.970	7.913	7.905	7.916	7.921	7.945	7.976	7.853	7.860	7.837	7.877
Charge Def.	0.599	0.438	0.406	0.456	0.456	0.589	0.595	0.345	0.435	0.360	-0.622

* N = normal, R = reverse; 1 or 2 before the decimal refer to the file, the rest is the analysis #
Structural formulae calculated based on 11 oxygens (assuming OH + F = 2) and 7 cations - (Na + K + Ca)

Appendix A-4 Electron-microprobe analyses of mica

Sample #	AMDO105C										
Description	2.53 N lt.	2.54 N	2.55 N	2.56 N	2.57 N	2.59 N	2.60 N	2.61 N	2.62 N	2.63 N	2.64 N
SiO_2	40.66	40.40	40.98	44.74	39.06	40.69	38.75	38.39	39.10	39.71	40.92
TiO_2	2.57	2.22	2.13	1.30	1.71	2.18	2.95	2.49	2.26	2.23	1.73
Al_2O_3	10.43	11.05	10.14	14.80	11.84	9.70	9.97	10.58	9.94	10.79	11.33
Cr_2O_3	0.02	0.03	0.04	0.01	0.02	0.04	0.03	0.01	0.01	0.02	0.03
Fe_2O_3	0.00	0.00	0.00	0.00	0.00	0.00	0.00	0.00	0.00	0.00	0.00
FeO	16.03	15.82	16.80	13.91	19.42	15.94	18.71	17.07	18.04	14.54	13.30
MnO	0.58	0.85	0.83	0.51	0.55	0.79	0.61	1.03	0.72	0.88	0.87
MgO	13.98	13.02	13.98	10.08	9.38	14.09	12.73	13.60	13.65	16.13	16.61
CaO	0.28	0.21	0.19	0.14	0.22	0.16	0.18	0.18	0.15	0.07	0.06
BaO	0.07	0.07	0.08	0.05	0.07	0.01	0.06	0.07	0.05	0.00	0.04
Na_2O	0.18	0.14	0.11	0.11	0.08	0.14	0.15	0.11	0.10	0.14	0.09
K_2O	8.56	8.45	8.81	8.70	7.61	8.81	8.28	8.85	8.61	9.43	9.74
F	2.36	2.29	2.74	2.79	2.29	3.12	2.57	2.46	2.68	2.91	3.31
H_2O	2.72	2.70	2.56	2.54	2.56	2.32	2.55	2.61	2.52	2.52	2.38
Total	98.44	97.25	99.39	99.68	94.81	97.99	97.54	97.45	97.83	99.37	100.41
F,Cl=O	0.99	0.96	1.15	1.17	0.96	1.31	1.08	1.04	1.13	1.23	1.39
Total	97.45	96.29	98.24	98.51	93.84	96.68	96.45	96.41	96.70	98.15	99.02
Si	3.175	3.196	3.182	3.470	3.217	3.208	3.087	3.048	3.090	3.052	3.106
^{IV}Al	0.825	0.804	0.818	0.53	0.783	0.792	0.913	0.952	0.91	0.948	0.894
$^{IV}Fe^{3+}$	0.000	0.000	0.000	0.000	0.000	0.000	0.000	0.000	0.000	0.000	0.000
Ti	0.000	0.000	0.000	0.000	0.000	0.000	0.000	0.000	0.000	0.000	0.000
ΣTetrahedral	4.000	4.000	4.000	4.000	4.000	4.000	4.000	4.000	4.000	4.000	4.000
^{VI}Al	0.135	0.227	0.110	0.823	0.366	0.109	0.023	0.038	0.016	0.030	0.120
Ti	0.151	0.132	0.124	0.076	0.106	0.129	0.177	0.149	0.134	0.129	0.099
Cr	0.001	0.002	0.003	0.001	0.001	0.003	0.002	0.001	0.001	0.001	0.002
$^{VI}Fe^{3+}$	0.000	0.000	0.000	0.000	0.000	0.000	0.000	0.000	0.000	0.000	0.000
Fe^{2+}	1.047	1.047	1.091	0.902	1.337	1.051	1.246	1.134	1.192	0.935	0.844
Mn	0.038	0.057	0.055	0.034	0.038	0.053	0.041	0.069	0.048	0.057	0.056
Mg	1.627	1.535	1.618	1.165	1.151	1.656	1.511	1.610	1.608	1.848	1.879
ΣOctahedral	3.000	3.000	3.000	3.000	3.000	3.000	3.001	3.000	3.000	3.000	3.000
Ca	0.023	0.018	0.016	0.012	0.019	0.014	0.015	0.015	0.013	0.006	0.005
Ba	0.002	0.002	0.002	0.002	0.002	0.000	0.002	0.002	0.002	0.000	0.001
Na	0.027	0.022	0.017	0.017	0.013	0.021	0.023	0.017	0.015	0.021	0.013
K	0.853	0.853	0.873	0.861	0.799	0.886	0.841	0.896	0.868	0.925	0.943
ΣInterlayer	0.906	0.894	0.907	0.890	0.834	0.921	0.882	0.931	0.898	0.951	0.963
F	0.583	0.573	0.673	0.684	0.596	0.778	0.647	0.618	0.670	0.707	0.795
OH	1.417	1.427	1.327	1.316	1.404	1.222	1.353	1.382	1.330	1.293	1.205
Fe/(Fe+Mg)	0.391	0.405	0.403	0.436	0.537	0.388	0.452	0.413	0.426	0.336	0.310
# Cations	7.906	7.894	7.907	7.890	7.834	7.921	7.882	7.931	7.898	7.951	7.962
Charge Def.	0.038	-0.031	0.204	-0.664	-0.054	0.265	0.284	0.285	0.382	0.409	0.401

* N = normal; R = reverse; 1 or 2 before the decimal refer to the file, the rest is the analysis #
Structural formulae calculated based on 11 oxygens (assuming OH + F = 2) and 7 cations - (Na + K + Ca)

Appendix A-4 Electron-microprobe analyses of mica

Sample #	AMDO105C	BH/16/9									
Description	2.65 N	1.70 N lt.	1.72 N lt.	1.74 N	1.75 N	1.76 N-R	1.77 N-R lt.	1.80 N lt.	1.81 N lt.	1.82 N	1.83 N
SiO_2	37.02	41.71	41.63	42.16	41.25	41.06	40.85	40.57	40.83	41.82	41.35
TiO_2	2.47	1.59	1.25	1.12	1.05	1.31	1.51	1.16	0.98	1.73	1.64
Al_2O_3	10.47	9.78	9.73	8.40	8.89	10.33	10.32	9.23	9.61	10.18	10.25
Cr_2O_3	0.04	0.05	0.04	0.02	0.03	0.02	0.02	0.04	0.02	0.02	0.01
Fe_2O_3	0.00	0.00	0.00	0.00	0.00	0.00	0.00	0.00	0.00	0.00	0.00
FeO	17.51	16.88	15.80	15.96	16.81	13.55	13.00	19.67	17.48	12.80	12.62
MnO	1.00	1.00	1.02	0.95	0.85	0.44	0.52	1.06	1.08	0.90	0.89
MgO	14.03	15.58	16.28	16.83	15.60	17.63	18.54	14.14	16.08	18.94	18.83
CaO	0.18	0.07	0.03	0.02	0.05	0.03	0.02	0.04	0.08	0.00	0.00
BaO	0.04	0.03	0.03	0.02	0.01	0.00	0.00	0.02	0.06	0.01	0.01
Na_2O	0.17	0.38	0.34	0.42	0.19	0.22	0.31	0.16	0.20	0.35	0.32
K_2O	8.28	9.91	9.95	9.99	9.31	9.28	9.86	9.42	9.78	10.04	10.02
F	2.09	3.74	4.09	4.53	3.80	3.21	3.38	3.48	3.92	4.23	4.01
H_2O	2.76	2.20	2.02	1.80	2.08	2.43	2.39	2.24	2.10	2.06	2.13
Total	96.06	102.92	102.21	102.22	99.92	99.51	100.72	101.23	102.22	103.08	102.08
F,Cl=O	0.88	1.57	1.72	1.91	1.60	1.35	1.42	1.47	1.65	1.78	1.69
Total	95.18	101.34	100.49	100.31	98.32	98.16	99.29	99.76	100.57	101.30	100.39
Si	2.957	3.151	3.153	3.202	3.188	3.117	3.071	3.129	3.093	3.087	3.078
^{IV}Al	0.985	0.849	0.847	0.752	0.81	0.883	0.914	0.839	0.858	0.886	0.899
$^{IV}Fe^{3+}$	0.000	0.000	0.000	0.000	0.000	0.000	0.000	0.000	0.000	0.000	0.000
Ti	0.058	0.000	0.000	0.046	0.002	0.000	0.014	0.032	0.049	0.027	0.023
ΣTetrahedral	4.000	4.000	4.000	4.000	4.000	4.000	4.000	4.000	4.000	4.000	4.000
^{VI}Al	0.000	0.022	0.022	0.000	0.000	0.041	0.000	0.000	0.000	0.000	0.000
Ti	0.090	0.090	0.071	0.018	0.059	0.075	0.071	0.035	0.007	0.069	0.069
Cr	0.003	0.003	0.002	0.001	0.002	0.001	0.001	0.002	0.001	0.001	0.001
$^{VI}Fe^{3+}$	0.000	0.000	0.000	0.000	0.000	0.000	0.000	0.000	0.000	0.000	0.000
Fe^{2+}	1.170	1.067	1.001	1.014	1.087	0.860	0.817	1.269	1.107	0.790	0.786
Mn	0.068	0.064	0.065	0.061	0.056	0.028	0.033	0.069	0.069	0.056	0.056
Mg	1.670	1.754	1.838	1.906	1.797	1.995	2.078	1.625	1.816	2.084	2.089
ΣOctahedral	3.000	3.000	3.000	3.000	3.000	3.000	3.000	3.000	3.000	3.001	3.000
Ca	0.015	0.006	0.002	0.002	0.004	0.002	0.002	0.003	0.007	0.000	0.000
Ba	0.001	0.001	0.001	0.001	0.000	0.000	0.000	0.001	0.002	0.000	0.000
Na	0.026	0.056	0.050	0.062	0.029	0.032	0.045	0.024	0.029	0.050	0.046
K	0.844	0.955	0.961	0.968	0.918	0.899	0.946	0.927	0.945	0.945	0.951
ΣInterlayer	0.887	1.017	1.015	1.032	0.951	0.933	0.992	0.954	0.983	0.996	0.998
F	0.528	0.894	0.980	1.088	0.929	0.771	0.804	0.849	0.939	0.988	0.944
OH	1.472	1.106	1.020	0.912	1.071	1.229	1.196	1.151	1.061	1.013	1.056
Fe/(Fe+Mg)	0.412	0.378	0.353	0.347	0.377	0.301	0.282	0.438	0.379	0.275	0.273
# Cations	7.887	8.017	8.015	8.032	7.951	7.933	7.992	7.954	7.983	7.996	7.998
Charge Def.	0.427	0.513	0.642	0.768	0.664	0.526	0.581	0.658	0.792	0.739	0.707

* N = normal, R = reverse; 1 or 2 before the decimal refer to the file; the rest is the analysis #
Structural formulae calculated based on 11 oxygens (assuming OH + F = 2) and 7 cations - (Na + K + Ca)

Appendix A-4 Electron-microprobe analyses of mica

Sample #	BH/16/9	BH/18/2.1									
Description	1.84 N	1.1 R mkl.	1.2 R lt.	1.3 R dk.	1.4 R	1.5 R lt.	1.6 R dk.	1.7 R	1.8 R dk	1.9 R lt.	1.10 R lt.
SiO_2	41 59	41 82	41 08	41 36	41.10	41 18	41 63	41.97	41.49	42 46	41.56
TiO_2	1 71	0 58	0 82	1.34	0 27	0 61	0.46	0.35	0 59	0.36	0 50
Al_2O_3	10 37	9 05	10 65	11 27	9 00	9 32	9 25	7.77	9.15	7 70	9.08
Cr_2O_3	0 02	0 03	0 04	0 03	0 01	0 02	0.00	0 03	0 03	0 03	0 02
Fe_2O_3	0 00	1 66	0 00	0.00	3 61	1 81	3 21	2.90	1.94	2.42	1 18
FeO	12 57	7 07	11 43	11 94	10 70	8 15	6 57	6 89	7.10	7.17	10.72
MnO	0 94	0 16	0 37	0.39	0 27	0 18	0.16	0.15	0 19	0 12	0 33
MgO	18 42	24 18	20 60	19.72	21 32	23 23	24 21	24 44	24 01	24 64	21 66
CaO	0 00	0 02	0 01	0 01	0 01	0 00	0 03	0 00	0 01	0 02	0 02
BaO	0 00	0 04	0 05	0 00	0 09	0 03	0 04	0 00	0 05	0 03	0 01
Na_2O	0 36	0 39	0 18	0 29	0.25	0 29	0.30	0 48	0.37	0 51	0 26
K_2O	10 16	10 00	9 92	10 11	9 98	10 21	10 13	10.08	10 11	10 05	9 89
F	4 07	3 17	2 78	3 20	3 07	3 21	3 04	3 48	3 29	3 23	3 21
H_2O	2.09	2.62	2.74	2.57	2.64	2.57	2.71	2.46	2.56	2.60	2.55
Total	102 30	100.79	100 67	102 23	102.32	100 81	101.75	101 00	100 88	101 34	100 99
F,Cl=O	1 71	1 33	1 17	1 35	1 29	1 35	1 28	1.47	1 39	1 36	1 35
Total	100 59	99.45	99.50	100.88	101.03	99.46	100.47	99.53	99.49	99.98	99.64
Si	3.101	3 041	3 032	3 035	3 010	3 015	3 004	3 063	3 023	3 081	3 060
^{IV}Al	0 899	0 775	0 926	0 965	0 777	0 804	0 787	0 668	0 786	0 658	0 788
$^{IV}Fe^{3+}$	0 000	0 091	0 000	0 000	0 199	0 100	0 174	0 159	0 106	0 132	0 066
Ti	0 000	0 032	0 043	0 000	0 015	0 034	0 025	0 019	0 032	0 020	0 028
ΣTetrahedral	4 000	3 938	4 000	4 000	4 001	3 953	3 990	3 909	3 947	3 891	3 941
^{VI}Al	0 013	0 000	0 000	0 010	0 000	0 000	0 000	0 000	0 000	0 000	0 000
Ti	0 096	0 000	0 003	0 074	0 000	0 000	0 000	0 000	0 000	0 000	0 000
Cr	0 001	0 002	0 002	0 002	0 001	0 001	0 000	0 002	0 002	0 002	0 001
$^{VI}Fe^{3+}$	0 000	0 000	0 000	0 000	0 000	0 000	0 000	0 000	0 000	0 000	0 000
Fe^{2+}	0 784	0 430	0 705	0 733	0 655	0 499	0 397	0 421	0 432	0 435	0 660
Mn	0 059	0 010	0 023	0 024	0 017	0 011	0 010	0 009	0 012	0 007	0 021
Mg	2 047	2 620	2 266	2 157	2 327	2 535	2 604	2 659	2 607	2 665	2 377
ΣOctahedral	3 001	3 062	3 000	3 000	3 000	3 047	3 010	3 090	3 053	3 109	3 059
Ca	0 000	0 002	0 001	0 001	0 001	0 000	0 002	0 000	0 001	0 002	0 002
Ba	0 000	0 001	0 001	0 000	0 003	0 001	0 001	0 000	0 001	0 001	0 000
Na	0 052	0 055	0 026	0 041	0 036	0 041	0 042	0 068	0 052	0 072	0 037
K	0 966	0 927	0 934	0 947	0 932	0 954	0 932	0 938	0 940	0 930	0 929
ΣInterlayer	1 018	0 985	0 962	0 989	0 971	0 996	0 978	1 006	0 994	1 004	0 968
F	0 960	0 729	0 649	0 743	0 711	0 743	0 694	0 803	0 758	0 741	0 748
OH	1 040	1 271	1 351	1 257	1 289	1 257	1 306	1 197	1 242	1 259	1 253
Fe(Fe+Mg)	0 277	0 141	0 237	0 254	0 220	0 164	0 132	0 137	0 142	0 140	0 217
# Cations	8 018	7 985	7 962	7 989	7 971	7 996	7 978	8 006	7 994	8 004	7 968
Charge Def.	0 635	0 729	0 602	0 558	0 711	0 743	0 694	0 803	0 758	0 741	0 747

* N = normal, R = reverse; 1 or 2 before the decimal refer to the file; the rest is the analysis #
Structural formulae calculated based on 11 oxygens (assuming OH + F = 2) and 7 cations - (Na + K + Ca)

Appendix A-4 Electron-microprobe analyses of mica

Sample #	BH/18/2.1										
Description	1.11 R lt.	1.12 R	1.13 R	1.14 N-R mid.	1.15 N	1.16 N-R lt.	1.17 N	1.18 N	1.19 N	1.20 N-R	1.21 R
SiO_2	40 86	40 91	40 72	40 40	39 79	40 52	40 93	40 37	41 00	40 24	40 77
TiO_2	0 57	1 03	1 56	1 41	1 40	1 20	0 62	0 60	0 94	1 36	1.31
Al_2O_3	9 53	11 01	11 24	10 63	10 56	12 51	9 66	9 64	10 75	10 94	11 06
Cr_2O_3	0 03	0 04	0 04	0 00	0 01	0 02	0 01	0 03	0 02	0 01	0 02
Fe_2O_3	1 34	0 00	0 00	0 00	0 00	0 00	2 24	2 26	0 00	0 00	0 00
FeO	12 61	11 87	12 17	13 29	14 45	13 50	8 50	11 87	12 66	12 33	11 60
MnO	0 48	0 48	0 48	0 56	0 54	0 26	0 23	0 46	0 56	0 38	0 35
MgO	20 16	18 94	19 02	19 15	18 53	17 74	22 63	20 30	19 40	19 11	19 76
CaO	0 01	0 05	0 05	0 03	0 14	0 04	0 01	0 02	0 10	0 00	0 00
BaO	0 08	0 00	0 04	0 02	0 00	0 06	0 05	0 03	0 06	0 00	0 01
Na_2O	0 25	0 20	0 19	0 23	0 18	0 16	0 31	0 24	0 24	0 25	0 27
K_2O	9 92	9 82	9 63	9 82	9 44	9 51	9 89	9 97	10 10	10 21	10 32
F	3 35	3 24	3 00	3 42	3 09	2 24	3 36	3 20	3 57	3 12	3 04
H_2O	2.46	2.46	2.61	2.41	2.54	2.97	2.50	2.53	2.35	2.52	2.60
Total	101 66	100 05	100 75	101 37	100 67	100 73	100 93	101 52	101 75	100 47	101 11
$F_2Cl=O$	1 41	1 36	1 26	1 44	1 30	0 94	1 41	1 35	1 50	1 31	1 28
Total	100.25	98.68	99.49	99.93	99.37	99.79	99.52	100.17	100.25	99.15	99.83
Si	3 025	3 071	3 029	3 005	2 980	3 013	3 000	2 991	3 041	3 020	3 028
^{IV}Al	0 831	0 929	0 971	0 932	0 932	0 987	0 834	0 842	0 94	0 968	0 968
$^{IV}Fe^{3+}$	0 075	0 000	0 000	0 000	0 000	0 000	0 123	0 126	0 000	0 000	0 000
Ti	0 032	0 000	0 000	0 063	0 079	0 000	0 034	0 033	0 018	0 013	0 004
ΣTetrahedral	3 962	4 000	4 000	4 000	3 991	4 000	3 992	3 992	4 000	4 000	4 000
^{VI}Al	0 000	0 045	0 014	0 000	0 000	0 110	0 000	0 000	0 000	0 000	0 000
Ti	0 000	0 058	0 087	0 016	0 000	0 067	0 000	0 000	0 034	0 064	0 069
Cr	0 002	0 002	0 002	0 000	0 001	0 001	0 001	0 002	0 001	0 001	0 001
$^{VI}Fe^{3+}$	0 000	0 000	0 000	0 000	0 000	0 000	0 000	0 000	0 000	0 000	0 000
Fe^{2+}	0 781	0 745	0 757	0 827	0 905	0 840	0 521	0 736	0 785	0 774	0.721
Mn	0.030	0 031	0 030	0 035	0 034	0 016	0 014	0 029	0 035	0 024	0.022
Mg	2.225	2 119	2 109	2 123	2 069	1 966	2 472	2 242	2 145	2 138	2 187
ΣOctahedral	3 037	3 000	3 000	3 001	3 009	3 001	3 008	3 008	3 001	3 000	3 000
Ca	0 001	0 004	0 004	0 002	0 011	0 003	0 001	0 002	0 008	0 000	0 000
Ba	0 002	0 000	0 001	0 001	0 000	0 002	0 001	0 001	0 002	0 000	0 000
Na	0 036	0 029	0 027	0 033	0 026	0 023	0 044	0 035	0 035	0 036	0 039
K	0 937	0 940	0 914	0 932	0 902	0 902	0 925	0 942	0 956	0 977	0 978
ΣInterlayer	0.976	0 973	0 946	0.968	0 939	0 930	0 971	0 979	1.000	1 014	1 017
F	0 784	0 769	0 706	0 804	0 732	0 527	0 779	0 750	0 838	0 741	0 714
OH	1 216	1.231	1 294	1 196	1 268	1 473	1 221	1 250	1.163	1 260	1 286
Fe/(Fe+Mg)	0 260	0 260	0 264	0 280	0 304	0 299	0 174	0 247	0 268	0 266	0 248
# Cations	7 976	7 973	7 946	7 968	7 939	7 930	7 971	7 979	8 000	8 014	8 017
Charge Def.	0 784	0 557	0 534	0.735	0 730	0 334	0 779	0 750	0 700	0 566	0 526

* N = normal, R = reverse; 1 or 2 before the decimal refer to the file; the rest is the analysis #
Structural formulae calculated based on 11 oxygens (assuming OH + F = 2) and 7 cations - (Na + K + Ca)

Appendix A-4 Electron-microprobe analyses of mica

Sample #	BH/18/2.1										
Description	1.22 R	1.23 R	1.24 R	1.25 R	1.26 R	1.27 R lt.	1.30 R lt.	1.31 R lt.	1.32 R	1.33 N	1.34 N
SiO_2	39.97	40.32	42.34	41.53	41.23	40.80	42.32	41.57	41.53	39.97	39.78
TiO_2	1.36	0.76	0.34	0.28	0.20	0.54	0.53	0.86	0.66	2.13	1.29
Al_2O_3	12.03	9.52	7.62	8.56	9.05	9.63	9.69	10.43	9.90	11.41	11.98
Cr_2O_3	0.01	0.02	0.02	0.01	0.02	0.01	0.02	0.02	0.02	0.02	0.02
Fe_2O_3	0.00	2.39	3.66	4.01	4.73	1.81	2.07	0.00	2.13	0.00	0.00
FeO	11.66	11.44	7.45	5.41	3.06	10.51	7.05	12.21	7.38	13.80	13.02
MnO	0.28	0.27	0.19	0.14	0.11	0.40	0.16	0.42	0.12	0.51	0.38
MgO	19.87	20.83	24.29	24.85	25.91	21.32	24.29	20.48	23.74	17.90	19.35
CaO	0.00	0.00	0.00	0.00	0.00	0.02	0.00	0.02	0.00	0.01	0.00
BaO	0.07	0.05	0.01	0.00	0.03	0.01	0.03	0.05	0.02	0.00	0.07
Na_2O	0.21	0.24	0.44	0.30	0.19	0.18	0.27	0.23	0.28	0.27	0.20
K_2O	10.30	10.18	10.18	10.31	10.46	10.07	10.16	10.04	10.13	10.19	10.36
F	2.62	2.86	3.27	3.13	3.11	3.21	2.83	2.59	2.74	3.07	3.17
H_2O	2.82	2.70	2.60	2.65	2.68	2.54	2.85	2.87	2.85	2.56	2.56
Total	101.20	101.58	102.41	101.18	100.78	101.05	102.27	101.79	101.50	101.84	102.18
$F_2Cl=O$	1.10	1.20	1.38	1.32	1.31	1.35	1.19	1.09	1.15	1.29	1.33
Total	100.09	100.38	101.03	99.86	99.47	99.70	101.08	100.70	100.34	100.54	100.85
Si	2.952	2.978	3.057	3.011	2.979	3.012	3.025	3.043	2.998	2.986	2.933
^{IV}Al	1.047	0.829	0.649	0.732	0.771	0.838	0.816	0.9	0.842	1.005	1.041
$^{IV}Fe^{3+}$	0.000	0.133	0.199	0.219	0.250	0.101	0.111	0.000	0.116	0.000	0.000
Ti	0.002	0.042	0.019	0.015	0.000	0.030	0.029	0.047	0.036	0.009	0.026
ΣTetrahedral	4.000	3.982	3.924	3.978	4.000	3.980	3.980	3.991	3.992	4.000	4.000
^{VI}Al	0.000	0.000	0.000	0.000	0.000	0.000	0.000	0.000	0.000	0.000	0.000
Ti	0.074	0.000	0.000	0.000	0.011	0.000	0.000	0.000	0.000	0.111	0.046
Cr	0.001	0.001	0.001	0.001	0.001	0.001	0.001	0.001	0.001	0.001	0.001
$^{VI}Fe^{3+}$	0.000	0.000	0.000	0.000	0.007	0.000	0.000	0.000	0.000	0.000	0.000
Fe^{2+}	0.720	0.707	0.450	0.328	0.185	0.649	0.421	0.748	0.445	0.862	0.803
Mn	0.018	0.017	0.012	0.009	0.007	0.025	0.010	0.026	0.007	0.032	0.024
Mg	2.187	2.293	2.614	2.686	2.790	2.346	2.588	2.235	2.554	1.993	2.127
ΣOctahedral	2.999	3.018	3.077	3.023	3.001	3.020	3.020	3.009	3.008	3.000	3.000
Ca	0.000	0.000	0.000	0.000	0.000	0.002	0.000	0.002	0.000	0.001	0.000
Ba	0.002	0.001	0.000	0.000	0.001	0.000	0.001	0.001	0.001	0.000	0.002
Na	0.030	0.034	0.062	0.042	0.027	0.026	0.037	0.033	0.039	0.039	0.029
K	0.970	0.959	0.938	0.954	0.964	0.948	0.926	0.938	0.933	0.971	0.974
ΣInterlayer	1.003	0.995	1.000	0.996	0.991	0.976	0.965	0.973	0.973	1.011	1.005
F	0.612	0.668	0.747	0.718	0.711	0.749	0.640	0.600	0.626	0.725	0.739
OH	1.388	1.332	1.253	1.282	1.289	1.251	1.360	1.400	1.374	1.275	1.261
Fe/(Fe+Mg)	0.248	0.236	0.147	0.109	0.062	0.217	0.140	0.251	0.148	0.302	0.274
# Cations	8.002	7.995	8.000	7.996	7.991	7.976	7.965	7.973	7.973	8.011	8.005
Charge Def.	0.505	0.668	0.747	0.718	0.711	0.749	0.640	0.541	0.626	0.495	0.681

* N = normal, R = reverse, 1 or 2 before the decimal refer to the file, the rest is the analysis #
Structural formulae calculated based on 11 oxygens (assuming OH + F = 2) and 7 cations - (Na + K + Ca)

Appendix A-4 Electron-microprobe analyses of mica

Sample #	BH/18/2.1			BH/18/2.2								
Description	1.35 N-R	1.36 N-R	1.37 R	2.67 N-R lt.	2.70 R lt.	2.71 R dk.	2.72 R	2.73 N	2.74 R lt.	2.75 R lt.	2.76 R
SiO_2	40.89	41.55	41.96	40.41	46.90	43.38	41.94	39.84	41.85	39.77	41.51
TiO_2	0.41	0.24	0.39	1.09	0.31	0.53	0.32	1.32	0.65	1.21	0.73
Al_2O_3	8.78	9.03	9.50	11.07	15.46	10.04	9.28	11.97	10.53	8.81	10.07
Cr_2O_3	0.02	0.01	0.00	0.03	0.02	0.02	0.00	0.02	0.01	0.03	0.02
Fe_2O_3	2.88	4.04	2.74	0.00	0.00	0.00	2.86	0.00	1.11	0.00	1.08
FeO	11.86	5.44	5.76	14.98	10.64	8.01	5.12	13.57	7.15	16.64	7.19
MnO	0.46	0.16	0.15	0.59	0.03	0.17	0.11	0.33	0.16	0.65	0.16
MgO	20.66	24.79	24.65	18.33	11.21	23.27	24.83	18.85	23.69	17.42	23.75
CaO	0.01	0.02	0.00	0.10	0.18	0.03	0.05	0.01	0.12	0.03	0.05
BaO	0.02	0.07	0.03	0.01	0.00	0.01	0.04	0.07	0.04	0.00	0.04
Na_2O	0.23	0.27	0.24	0.24	0.10	0.15	0.22	0.22	0.19	0.21	0.26
K_2O	10.17	10.31	10.06	9.70	8.32	9.26	9.76	10.09	9.63	9.84	9.88
F	3.30	3.37	3.01	2.73	1.77	2.34	2.69	3.01	2.70	2.92	2.76
H_2O	2.50	2.56	2.74	2.76	3.06	3.05	2.86	2.63	2.88	2.54	2.82
Total	102.20	101.86	101.23	102.04	98.00	100.26	100.09	101.93	100.70	100.07	100.31
F,Cl=O	1.39	1.42	1.27	1.15	0.75	0.99	1.13	1.27	1.14	1.23	1.16
Total	100.81	100.45	99.96	100.89	97.25	99.28	98.96	100.66	99.56	98.84	99.15
Si	3.018	2.997	3.022	2.989	3.608	3.126	3.037	2.946	3.020	3.042	3.017
^{IV}Al	0.764	0.768	0.806	0.965	0.392	0.853	0.792	1.043	0.896	0.794	0.863
$^{IV}Fe^{3+}$	0.160	0.219	0.149	0.000	0.000	0.000	0.156	0.000	0.060	0.000	0.059
Ti	0.023	0.013	0.021	0.047	0.000	0.022	0.014	0.011	0.024	0.070	0.040
ΣTetrahedral	3.965	3.997	3.997	4.000	4.000	4.000	4.000	4.000	4.000	3.906	3.979
^{VI}Al	0.000	0.000	0.000	0.000	1.009	0.000	0.000	0.000	0.000	0.000	0.000
Ti	0.000	0.000	0.000	0.014	0.018	0.007	0.003	0.062	0.011	0.000	0.000
Cr	0.001	0.001	0.000	0.002	0.001	0.001	0.000	0.001	0.001	0.002	0.001
$^{VI}Fe^{3+}$	0.000	0.000	0.000	0.000	0.000	0.000	0.000	0.000	0.000	0.000	0.000
Fe^{2+}	0.732	0.328	0.347	0.927	0.685	0.483	0.310	0.839	0.431	1.064	0.437
Mn	0.029	0.010	0.009	0.037	0.002	0.010	0.007	0.021	0.010	0.042	0.010
Mg	2.273	2.665	2.646	2.021	1.285	2.499	2.680	2.077	2.548	1.986	2.573
ΣOctahedral	3.035	3.004	3.002	3.000	3.000	3.000	3.000	3.000	3.001	3.094	3.021
Ca	0.001	0.002	0.000	0.008	0.015	0.002	0.004	0.001	0.009	0.003	0.004
Ba	0.001	0.002	0.001	0.000	0.000	0.000	0.001	0.002	0.001	0.000	0.001
Na	0.033	0.038	0.034	0.034	0.015	0.021	0.031	0.032	0.027	0.031	0.037
K	0.958	0.949	0.924	0.915	0.816	0.851	0.902	0.952	0.886	0.960	0.916
ΣInterlayer	0.992	0.990	0.959	0.958	0.846	0.875	0.938	0.986	0.923	0.994	0.958
F	0.770	0.769	0.686	0.639	0.431	0.533	0.616	0.704	0.616	0.706	0.635
OH	1.230	1.231	1.314	1.362	1.569	1.467	1.384	1.296	1.384	1.294	1.366
Fe/(Fe+Mg)	0.244	0.110	0.116	0.314	0.347	0.162	0.104	0.288	0.145	0.349	0.145
# Cations	7.992	7.990	7.959	7.958	7.846	7.875	7.938	7.986	7.923	7.994	7.958
Charge Def.	0.770	0.769	0.686	0.607	-1.084	0.494	0.616	0.633	0.616	0.691	0.634

* N = normal; R = reverse; 1 or 2 before the decimal refer to the file; the rest is the analysis #
Structural formulae calculated based on 11 oxygens (assuming OH + F = 2) and 7 cations - (Na + K + Ca)

Appendix A-4 Electron-microprobe analyses of mica

Sample #	BH/18/2.2										
Description	2.77 N	2.78 N rim	2.79 N	2.81 R	2.82 R	2.83 R lt.	2.84 R lt.	2.85 R	2.86 R lt.	2.87 R	2.88 R lt.
SiO_2	41.25	39.81	40.71	43.51	44.26	41.43	42.53	41.29	40.84	41.49	41.04
TiO_2	1.17	2.65	1.41	0.41	0.60	1.11	0.56	0.60	1.55	0.53	0.80
Al_2O_3	10.28	11.57	11.18	9.78	10.34	10.50	9.03	10.24	11.40	10.08	10.60
Cr_2O_3	0.02	0.02	0.02	0.02	0.01	0.00	0.01	0.02	0.02	0.02	0.02
Fe_2O_3	0.00	0.00	0.00	0.00	0.00	0.00	0.76	0.86	0.00	3.06	0.00
FeO	13.73	15.23	14.08	9.47	10.04	13.03	9.58	7.40	14.17	5.60	12.60
MnO	0.50	0.33	0.23	0.17	0.09	0.26	0.16	0.12	0.39	0.14	0.28
MgO	18.69	16.97	18.09	21.65	19.56	19.68	22.67	23.65	17.70	24.55	20.04
CaO	0.17	0.06	0.08	0.01	0.05	0.05	0.07	0.01	0.01	0.01	0.05
BaO	0.00	0.03	0.01	0.01	0.04	0.03	0.00	0.05	0.04	0.02	0.01
Na_2O	0.18	0.22	0.18	0.17	0.14	0.17	0.23	0.26	0.18	0.27	0.20
K_2O	9.27	9.63	9.09	8.93	8.77	9.39	9.50	10.15	10.13	10.09	9.62
F	2.49	2.11	2.55	2.74	2.61	2.28	2.80	2.59	2.34	2.51	2.57
H_2O	2.85	3.02	2.81	2.80	2.81	3.00	2.79	2.88	2.92	2.99	2.84
Total	100.60	101.65	100.44	99.67	99.32	101.02	100.68	100.12	101.69	101.35	100.67
F,Cl=O	1.05	0.89	1.07	1.15	1.10	0.96	1.18	1.09	0.99	1.06	1.08
Total	99.55	100.76	99.37	98.52	98.22	100.06	99.51	99.03	100.70	100.29	99.59
Si	3.071	2.972	3.035	3.183	3.277	3.046	3.098	3.010	3.041	2.979	3.031
^{IV}Al	0.902	1.018	0.965	0.817	0.723	0.918	0.775	0.88	0.959	0.853	0.923
$^{IV}Fe^{3+}$	0.000	0.000	0.000	0.000	0.000	0.000	0.042	0.047	0.000	0.165	0.000
Ti	0.027	0.000	0.000	0.000	0.000	0.035	0.031	0.033	0.000	0.002	0.044
ΣTetrahedral	4.000	3.990	4.000	4.000	4.000	4.000	3.945	3.971	4.000	4.000	3.998
^{VI}Al	0.000	0.000	0.017	0.026	0.180	0.000	0.000	0.000	0.041	0.000	0.000
Ti	0.039	0.149	0.079	0.023	0.033	0.026	0.000	0.000	0.087	0.027	0.000
Cr	0.001	0.001	0.001	0.001	0.001	0.000	0.001	0.001	0.001	0.001	0.001
$^{VI}Fe^{3+}$	0.000	0.000	0.000	0.000	0.000	0.000	0.000	0.000	0.000	0.000	0.000
Fe^{2+}	0.855	0.951	0.878	0.579	0.622	0.801	0.583	0.451	0.882	0.336	0.778
Mn	0.032	0.021	0.015	0.011	0.006	0.016	0.010	0.007	0.025	0.009	0.018
Mg	2.074	1.888	2.010	2.361	2.159	2.157	2.461	2.570	1.964	2.628	2.206
ΣOctahedral	3.001	3.010	3.000	3.000	3.000	3.000	3.055	3.030	3.000	3.000	3.003
Ca	0.014	0.005	0.006	0.001	0.004	0.004	0.006	0.001	0.001	0.001	0.004
Ba	0.000	0.001	0.000	0.000	0.001	0.001	0.000	0.001	0.001	0.001	0.000
Na	0.026	0.032	0.026	0.024	0.020	0.024	0.033	0.037	0.026	0.038	0.029
K	0.880	0.917	0.865	0.833	0.828	0.881	0.883	0.944	0.962	0.924	0.906
ΣInterlayer	0.920	0.955	0.897	0.859	0.854	0.910	0.921	0.983	0.990	0.963	0.939
F	0.586	0.498	0.601	0.634	0.611	0.530	0.645	0.597	0.551	0.570	0.600
OH	1.414	1.502	1.399	1.366	1.389	1.470	1.355	1.403	1.449	1.430	1.400
Fe/(Fe+Mg)	0.292	0.335	0.304	0.197	0.224	0.271	0.192	0.149	0.310	0.113	0.261
# Cations	7.920	7.955	7.897	7.858	7.854	7.910	7.921	7.983	7.990	7.963	7.939
Charge Def.	0.477	0.277	0.486	0.519	0.228	0.482	0.645	0.597	0.303	0.570	0.583

* N = normal, R = reverse; 1 or 2 before the decimal refer to the file, the rest is the analysis #
Structural formulae calculated based on 11 oxygens (assuming OH + F = 2) and 7 cations - (Na + K + Ca)

Appendix A-4. Electron-microprobe analyses of mica

Sample #	BH/18/2.2					
Description	2.89 R	2.90 N rim	2.91 N	2.92 N	2.93 R	2.94 N
SiO_2	41.51	40.13	41.55	39.80	43.03	38.08
TiO_2	0.63	2.21	1.20	1.13	0.29	0.56
Al_2O_3	10.19	11.20	11.02	11.90	9.58	14.95
Cr_2O_3	0.01	0.03	0.03	0.02	0.03	0.04
Fe_2O_3	2.46	0.00	0.00	0.00	1.41	1.38
FeO	6.11	14.29	12.76	13.02	6.45	8.60
MnO	0.15	0.38	0.25	0.23	0.14	0.29
MgO	23.97	17.66	19.11	19.09	24.15	20.66
CaO	0.02	0.01	0.00	0.05	0.01	0.00
BaO	0.00	0.04	0.00	0.03	0.01	0.28
Na_2O	0.21	0.25	0.29	0.17	0.22	0.10
K_2O	9.69	10.07	9.96	9.61	9.16	10.15
F	2.76	2.46	2.87	2.26	2.91	2.26
H_2O	2.84	2.84	2.70	2.96	2.78	3.02
Total	100.54	101.57	101.74	100.27	100.17	100.36
F,Cl=O	1.16	1.04	1.21	0.95	1.23	0.95
Total	99.38	100.54	100.53	99.32	98.95	99.41
Si	3.001	3.001	3.067	2.957	3.101	2.794
^{IV}Al	0.868	0.987	0.933	1.042	0.814	1.206
$^{IV}Fe^{3+}$	0.131	0.000	0.000	0.000	0.076	0.000
Ti	0.000	0.012	0.000	0.001	0.000	0.000
ΣTetrahedral	4.000	4.000	4.000	4.000	3.991	4.000
^{VI}Al	0.000	0.000	0.026	0.000	0.000	0.086
Ti	0.034	0.112	0.067	0.062	0.016	0.031
Cr	0.001	0.002	0.002	0.001	0.002	0.002
$^{VI}Fe^{3+}$	0.003	0.000	0.000	0.000	0.000	0.076
Fe^{2+}	0.369	0.894	0.788	0.809	0.389	0.528
Mn	0.009	0.024	0.016	0.015	0.009	0.018
Mg	2.583	1.968	2.103	2.114	2.594	2.259
ΣOctahedral	3.000	3.000	3.000	3.001	3.009	3.000
Ca	0.002	0.001	0.000	0.004	0.001	0.000
Ba	0.000	0.001	0.000	0.001	0.000	0.008
Na	0.029	0.036	0.042	0.025	0.031	0.014
K	0.894	0.961	0.938	0.911	0.842	0.950
ΣInterlayer	0.925	0.999	0.979	0.940	0.874	0.972
F	0.631	0.582	0.670	0.531	0.663	0.524
OH	1.369	1.418	1.330	1.469	1.337	1.476
Fe/(Fe+Mg)	0.125	0.312	0.273	0.277	0.130	0.189
# Cations	7.925	7.999	7.979	7.940	7.874	7.972
Charge Def.	0.631	0.342	0.463	0.503	0.663	0.524

* N = normal; 2 before the decimal refer to the file, the rest is the analysis #

Appendix A-5: Electron-microprobe analyses of feldspar

Mineral	Albite										
Sample #	AD066D1				1205/VII/A	87/A/94			AD066L	AD041C	
Description	73 dk lam.	75 dk	77 dk	78 lt.	26 dk	66 dk	68 dk	71 dk	59 dk	51	52
SiO_2	68.36	68.61	68.79	68.54	69.19	67.87	68.40	67.59	68.42	68.48	68.68
Al_2O_3	19.20	19.40	19.51	19.42	18.30	18.89	18.41	19.47	19.76	19.48	19.71
P_2O_5	0.00	0.00	0.00	0.00	0.00	0.00	0.00	0.00	0.00	0.00	0.00
TiO_2	0.00	0.00	0.00	0.00	0.00	0.00	0.00	0.00	0.00	0.00	0.01
Fe_2O_3	0.31	0.25	0.15	0.29	0.14	0.61	0.67	0.37	0.04	0.16	0.18
MnO	0.00	0.00	0.00	0.00	0.01	0.00	0.02	0.00	0.00	0.01	0.00
CaO	0.02	0.01	0.02	0.02	0.03	0.05	0.04	0.14	0.06	0.00	0.03
MgO	0.00	0.00	0.01	0.00	0.00	0.01	0.01	0.01	0.00	0.01	0.00
BaO	0.03	0.00	0.03	0.01	0.10	0.04	0.00	0.07	0.02	0.00	0.03
SrO	0.22	0.21	0.22	0.23	0.23	0.23	0.22	0.41	0.20	0.20	0.20
K_2O	0.32	0.26	0.33	0.26	1.37	0.23	0.10	0.14	0.10	0.27	0.24
Na_2O	11.45	11.69	11.61	11.70	10.74	11.27	11.01	11.32	11.56	11.51	11.57
Total	99.92	100.44	100.68	100.48	100.18	99.20	98.89	99.53	100.18	100.13	100.67
	Mineral formulae calculated based on 8 atoms of oxygen										
Si	2.968	2.963	2.963	2.960	3.006	2.969	2.994	2.949	2.957	2.963	2.957
Al	1.034	1.040	1.043	1.041	0.987	1.025	1.000	1.054	1.060	1.046	1.053
P	0.000	0.000	0.000	0.000	0.000	0.000	0.000	0.000	0.000	0.000	0.000
Ti	0.000	0.000	0.000	0.000	0.000	0.000	0.000	0.000	0.000	0.000	0.000
Fe^{3+}	0.010	0.008	0.005	0.009	0.004	0.020	0.022	0.012	0.001	0.005	0.006
Mn	0.000	0.000	0.000	0.000	0.000	0.000	0.001	0.000	0.000	0.000	0.000
Ca	0.001	0.000	0.001	0.001	0.001	0.002	0.002	0.007	0.003	0.000	0.001
Mg	0.000	0.000	0.000	0.000	0.000	0.001	0.001	0.001	0.000	0.001	0.000
Ba	0.001	0.000	0.000	0.000	0.002	0.001	0.000	0.001	0.000	0.000	0.000
Sr	0.005	0.005	0.005	0.006	0.006	0.006	0.006	0.010	0.005	0.005	0.005
K	0.019	0.015	0.019	0.015	0.080	0.014	0.006	0.008	0.006	0.015	0.014
Na	0.964	0.979	0.970	0.980	0.905	0.956	0.934	0.958	0.968	0.966	0.966
ΣCations	5.001	5.010	5.007	5.012	4.991	4.993	4.965	5.001	5.000	5.002	5.003
Mol.%											
Albite	96.38	97.87	97.01	97.97	90.49	95.56	93.44	95.80	96.82	96.56	96.60
Orthoclase	1.87	1.53	1.91	1.53	7.96	1.37	0.61	0.82	0.57	1.54	1.40
Anorthite	0.09	0.04	0.09	0.08	0.12	0.22	0.17	0.66	0.29	0.00	0.14
Celsian	0.05	0.00	0.04	0.01	0.17	0.07	0.00	0.13	0.04	0.00	0.05
Sr feldspar	0.54	0.53	0.54	0.58	0.59	0.59	0.56	1.04	0.51	0.50	0.50

v.fi.gr. = very fine grained; fi.gr. = fine grained; br. = bright; dk = dark; lam.= lamellae

Appendix A-5: Electron-microprobe analyses of feldspar

Mineral	Albite			
Sample #	AD0661			
Description	104	105	109	110
SiO_2	68.26	68.30	68.25	68.49
Al_2O_3	19.61	19.69	19.59	19.67
P_2O_5	0.00	0.00	0.00	0.00
TiO_2	0.00	0.00	0.00	0.00
Fe_2O_3	0.06	0.05	0.05	0.05
MnO	0.00	0.00	0.01	0.01
CaO	0.03	0.02	0.04	0.04
MgO	0.00	0.00	0.00	0.00
BaO	0.10	0.09	0.11	0.08
SrO	0.22	0.24	0.24	0.25
K_2O	0.49	0.46	0.69	0.67
Na_2O	11.45	11.60	11.28	11.40
Total	100.25	100.49	100.28	100.71
	Mineral formulae calculated based on 8 atoms of oxygen			
Si	2.956	2.952	2.957	2.955
Al	1.054	1.056	1.053	1.053
P	0.000	0.000	0.000	0.000
Ti	0.000	0.000	0.000	0.000
Fe^{3+}	0.002	0.002	0.002	0.002
Mn	0.000	0.000	0.000	0.000
Ca	0.001	0.001	0.002	0.002
Mg	0.000	0.000	0.000	0.000
Ba	0.002	0.002	0.002	0.001
Sr	0.006	0.006	0.006	0.006
K	0.029	0.027	0.040	0.039
Na	0.962	0.972	0.948	0.954
ΣCations	5.011	5.018	5.009	5.014
Mol.%				
Albite	96.16	97.23	94.76	95.42
Orthoclase	2.87	2.68	4.02	3.90
Anorthite	0.13	0.08	0.19	0.20
Celsian	0.17	0.15	0.18	0.14
Sr feldspar	0.55	0.61	0.59	0.63

Appendix A-5: Electron-microprobe analyses of feldspar

Mineral	K-feldspar										
Sample #	AD066J1									AD066D1	
Description	83	84	85	86	87	92	93 lt.	94 dk	99	74 lt.	76 lt.
SiO_2	64.58	64.48	64.15	64.39	62.50	64.64	63.46	63.74	64.41	65.39	64.87
Al_2O_3	18.44	18.59	18.66	18.54	19.66	18.53	18.76	18.65	18.70	18.50	18.62
P_2O_5	0.00	0.00	0.00	0.00	0.00	0.00	0.00	0.00	0.00	0.00	0.00
TiO_2	0.01	0.03	0.01	0.01	0.02	0.01	0.05	0.02	0.03	0.00	0.00
Fe_2O_3	0.32	0.25	0.26	0.31	0.26	0.32	0.35	0.42	0.34	0.31	0.13
MnO	0.00	0.00	0.00	0.00	0.00	0.00	0.00	0.00	0.00	0.00	0.01
CaO	0.00	0.00	0.00	0.00	0.01	0.00	0.00	0.00	0.00	0.00	0.00
MgO	0.01	0.00	0.00	0.00	0.00	0.00	0.00	0.00	0.00	0.00	0.00
BaO	0.45	0.43	0.46	0.42	0.53	0.46	1.10	1.01	1.06	0.10	0.41
SrO	0.27	0.27	0.27	0.27	0.25	0.27	0.30	0.28	0.30	0.27	0.25
K_2O	14.19	14.21	14.54	14.37	14.42	14.13	13.84	13.99	13.83	13.43	15.27
Na_2O	1.29	1.30	0.97	1.22	0.93	1.42	1.41	1.34	1.43	2.07	0.66
Total	100.31	100.30	100.09	100.28	99.32	100.51	99.99	100.19	100.84	100.79	101.02
	Mineral formulae calculated based on 8 atoms of oxygen										
Si	2.990	2.985	2.981	2.984	2.932	2.987	2.962	2.969	2.976	2.996	2.991
Al	1.006	1.015	1.022	1.013	1.087	1.009	1.033	1.024	1.019	0.999	1.012
P	0.000	0.000	0.000	0.000	0.000	0.000	0.000	0.000	0.000	0.000	0.000
Ti	0.000	0.001	0.000	0.000	0.001	0.000	0.002	0.001	0.001	0.000	0.000
Fe^{3+}	0.011	0.009	0.009	0.011	0.009	0.011	0.012	0.015	0.012	0.011	0.005
Mn	0.000	0.000	0.000	0.000	0.000	0.000	0.000	0.000	0.000	0.000	0.000
Ca	0.000	0.000	0.000	0.000	0.000	0.000	0.000	0.000	0.000	0.000	0.000
Mg	0.001	0.000	0.000	0.000	0.000	0.000	0.000	0.000	0.000	0.000	0.000
Ba	0.008	0.008	0.008	0.008	0.010	0.008	0.020	0.018	0.019	0.002	0.007
Sr	0.007	0.007	0.007	0.007	0.007	0.007	0.008	0.008	0.008	0.007	0.007
K	0.838	0.840	0.862	0.850	0.863	0.833	0.824	0.831	0.815	0.785	0.898
Na	0.116	0.117	0.087	0.110	0.084	0.127	0.128	0.121	0.128	0.184	0.059
ΣCations	4.978	4.980	4.978	4.983	4.993	4.983	4.989	4.987	4.979	4.984	4.979
Mol.%											
Albite	11.57	11.65	8.72	10.96	8.44	12.70	12.77	12.07	12.85	18.36	5.86
Orthoclase	83.82	83.96	86.18	84.98	86.30	83.28	82.43	83.13	81.55	78.51	89.84
Anorthite	0.00	0.00	0.00	0.00	0.04	0.00	0.00	0.01	0.00	0.00	0.00
Celsian	0.81	0.77	0.83	0.76	0.97	0.83	2.01	1.84	1.92	0.19	0.74
Sr feldspar	0.71	0.73	0.72	0.72	0.67	0.72	0.81	0.76	0.79	0.72	0.66

v.fi.gr. = very fine grained; fi.gr. = fine grained; br. = bright; dk = dark; lam.= lamellae

Appendix A-5: Electron-microprobe analyses of feldspar

Mineral	K-feldspar										
Sample #	AD066D1			AD066K							
Description	79 lt.	80 dk	81 dk	25 ltr	27 ltr	28 fi.gr.	29 fi.gr.	38 fi.gr.	39 cs	45 fi.gr.	46 fi.gr.
SiO_2	65.24	65.06	65.07	65.62	65.88	65.16	65.55	64.91	64.91	64.10	64.93
Al_2O_3	18.61	18.75	18.61	17.78	17.86	17.66	17.79	17.83	17.86	18.93	18.76
P_2O_5	0.00	0.00	0.00	0.00	0.00	0.00	0.00	0.00	0.00	0.00	0.00
TiO_2	0.00	0.02	0.00	0.01	0.02	0.01	0.02	0.02	0.02	0.04	0.03
Fe_2O_3	0.22	0.36	0.19	0.23	0.21	0.09	0.11	0.13	0.18	0.12	0.14
MnO	0.00	0.02	0.00	0.00	0.00	0.00	0.02	0.01	0.01	0.00	0.00
CaO	0.00	0.00	0.00	0.01	0.04	0.00	0.00	0.01	0.02	0.01	0.00
MgO	0.00	0.00	0.00	0.00	0.00	0.01	0.00	0.00	0.01	0.00	0.01
BaO	0.27	0.83	0.31	0.79	0.67	0.94	0.94	0.86	0.86	0.90	0.78
SrO	0.26	0.29	0.24	0.32	0.29	0.29	0.35	0.30	0.31	0.30	0.31
K_2O	14.92	12.41	13.33	12.65	12.04	14.13	13.15	13.45	12.97	12.67	12.74
Na_2O	0.88	2.60	2.11	2.76	3.27	1.64	2.51	2.22	2.53	2.36	2.41
Total	101.18	100.98	100.56	100.83	100.91	100.68	101.14	100.45	100.35	100.09	100.78
	Mineral formulae calculated based on 8 atoms of oxygen										
Si	2.995	2.980	2.991	3.013	3.013	3.016	3.011	3.005	3.003	2.968	2.982
Al	1.007	1.012	1.008	0.963	0.963	0.964	0.964	0.973	0.974	1.033	1.016
P	0.000	0.000	0.000	0.000	0.000	0.000	0.000	0.000	0.000	0.000	0.000
Ti	0.000	0.001	0.000	0.000	0.001	0.000	0.001	0.001	0.001	0.001	0.001
Fe^{3+}	0.008	0.013	0.006	0.008	0.007	0.003	0.004	0.005	0.006	0.004	0.005
Mn	0.000	0.001	0.000	0.000	0.000	0.000	0.001	0.000	0.000	0.000	0.000
Ca	0.000	0.000	0.000	0.000	0.002	0.000	0.000	0.000	0.001	0.000	0.000
Mg	0.000	0.000	0.000	0.000	0.000	0.001	0.000	0.000	0.001	0.000	0.001
Ba	0.005	0.015	0.006	0.014	0.012	0.017	0.017	0.016	0.016	0.016	0.014
Sr	0.007	0.008	0.006	0.008	0.008	0.008	0.009	0.008	0.008	0.008	0.008
K	0.874	0.725	0.782	0.741	0.703	0.835	0.771	0.794	0.765	0.749	0.746
Na	0.079	0.230	0.188	0.246	0.290	0.148	0.224	0.199	0.227	0.212	0.214
ΣCations	4.974	4.985	4.987	4.994	4.998	4.991	5.001	5.002	5.002	4.992	4.987
Mol.%											
Albite	7.86	23.05	18.82	24.56	29.00	14.75	22.37	19.95	22.68	21.22	21.43
Orthoclase	87.39	72.53	78.16	74.09	70.27	83.47	77.11	79.42	76.53	74.87	74.65
Anorthite	0.00	0.00	0.00	0.04	0.17	0.01	0.00	0.03	0.11	0.02	0.00
Celsian	0.48	1.48	0.55	1.43	1.19	1.70	1.70	1.56	1.55	1.64	1.40
Sr feldspar	0.69	0.76	0.64	0.84	0.78	0.76	0.94	0.81	0.82	0.81	0.83

v.fi.gr. = very fine grained; fi.gr. = fine grained; br. = bright; dk = dark; lam.= lamellae

Appendix A-5: Electron-microprobe analyses of feldspar

Mineral	K-feldspar										
Sample #	1205/VII/A					87/A/94				AD066L	
Description	7 core	8 core	9 core	10 lt.	11 lt.	67 lt.	69 lt.	70 lt.	72 br.fl.gr.	60 lt.	61 lt.
SiO_2	64.73	65.38	65.30	63.53	63.77	66.54	66.59	66.47	59.20	64.29	65.06
Al_2O_3	16.99	17.27	17.06	16.75	16.83	18.36	18.15	18.58	20.14	18.39	18.55
P_2O_5	0.00	0.00	0.00	0.00	0.00	0.00	0.00	0.00	0.00	0.00	0.00
TiO_2	0.00	0.02	0.02	0.07	0.08	0.00	0.02	0.00	0.19	0.00	0.00
Fe_2O_3	0.29	0.32	0.35	1.45	1.49	0.69	0.76	0.52	0.38	0.01	0.00
MnO	0.00	0.00	0.00	0.01	0.01	0.00	0.00	0.01	0.01	0.00	0.00
CaO	0.00	0.00	0.00	0.00	0.00	0.00	0.00	0.01	0.04	0.00	0.00
MgO	0.00	0.00	0.00	0.00	0.00	0.00	0.01	0.01	0.06	0.00	0.00
BaO	0.23	0.42	0.34	2.23	2.18	0.08	0.02	0.14	5.71	0.03	0.04
SrO	0.23	0.28	0.26	0.30	0.31	0.25	0.23	0.24	0.95	0.22	0.21
K_2O	15.70	15.36	15.74	15.15	14.93	5.52	5.46	5.37	12.93	14.42	14.17
Na_2O	0.86	1.09	0.91	0.69	0.84	7.57	7.58	7.71	0.24	1.20	1.49
Total	99.86	100.93	100.80	100.97	101.21	99.31	99.10	99.33	100.53	99.33	100.28
	Mineral formulae calculated based on 8 atoms of oxygen										
Si	3.030	3.026	3.030	2.993	2.993	3.001	3.007	2.996	2.850	2.997	2.999
Al	0.938	0.942	0.933	0.930	0.931	0.976	0.967	0.987	1.143	1.011	1.008
P	0.000	0.000	0.000	0.000	0.000	0.000	0.000	0.000	0.000	0.000	0.000
Ti	0.000	0.001	0.001	0.002	0.003	0.000	0.001	0.000	0.007	0.000	0.000
Fe^{3+}	0.010	0.011	0.012	0.051	0.052	0.023	0.026	0.018	0.014	0.000	0.000
Mn	0.000	0.000	0.000	0.000	0.000	0.000	0.000	0.000	0.000	0.000	0.000
Ca	0.000	0.000	0.000	0.000	0.000	0.000	0.000	0.000	0.002	0.000	0.000
Mg	0.000	0.000	0.000	0.000	0.000	0.000	0.001	0.000	0.004	0.000	0.000
Ba	0.004	0.008	0.006	0.041	0.040	0.001	0.000	0.002	0.108	0.001	0.001
Sr	0.006	0.007	0.007	0.008	0.008	0.006	0.006	0.006	0.027	0.006	0.006
K	0.938	0.907	0.932	0.911	0.894	0.318	0.315	0.309	0.795	0.858	0.834
Na	0.078	0.098	0.082	0.063	0.077	0.662	0.663	0.674	0.023	0.109	0.133
ΣCations	5.004	4.999	5.003	5.001	4.998	4.989	4.985	4.993	4.973	4.981	4.980
Mol.%											
Albite	7.81	9.78	8.15	6.31	7.65	66.19	66.35	67.39	2.28	10.88	13.34
Orthoclase	93.75	90.68	93.16	91.07	89.39	31.76	31.47	30.90	79.45	85.78	83.36
Anorthite	0.00	0.00	0.00	0.00	0.00	0.00	0.00	0.03	0.19	0.00	0.00
Celsian	0.42	0.75	0.62	4.12	4.01	0.14	0.04	0.24	10.77	0.05	0.08
Sr feldspar	0.63	0.75	0.69	0.83	0.84	0.65	0.60	0.61	2.66	0.60	0.56

v.fi.gr. = very fine grained; fi.gr. = fine grained; br. = bright; dk = dark; lam.= lamellae

Appendix A-5: Electron-microprobe analyses of feldspar

Mineral	K-feldspar										
Sample #	AD066L				AD041C						
Description	62	63	64	65	47 lt.	49 lt.	50 dk	53 dk	54 lt.	55 lam.	56 lt.
SiO_2	64.98	65.03	64.87	64.64	65.13	61.51	64.38	64.86	64.54	65.49	64.79
Al_2O_3	18.58	18.60	18.60	18.41	18.15	17.48	18.69	18.45	18.49	18.84	18.59
P_2O_5	0.00	0.00	0.00	0.00	0.00	2.73	3.94	0.00	0.00	0.00	0.00
TiO_2	0.00	0.01	0.00	0.00	0.00	0.00	0.00	0.00	0.01	0.01	0.02
Fe_2O_3	0.00	0.02	0.00	0.08	0.20	0.14	0.23	0.19	0.40	0.24	0.30
MnO	0.00	0.00	0.00	0.00	0.00	0.01	0.00	0.01	0.00	0.00	0.00
CaO	0.00	0.00	0.00	0.00	0.00	1.89	2.63	0.00	0.00	0.01	0.00
MgO	0.00	0.00	0.00	0.01	0.07	0.01	0.02	0.00	0.00	0.01	0.01
BaO	0.06	0.05	0.02	0.00	0.14	0.17	0.05	0.51	0.78	0.55	0.47
SrO	0.22	0.21	0.23	0.25	0.24	0.27	0.24	0.24	0.26	0.24	0.24
K_2O	14.64	14.57	14.82	15.85	13.81	13.68	2.59	14.23	13.45	12.21	13.47
Na_2O	1.15	1.14	1.06	0.20	1.66	1.25	9.01	1.28	1.71	2.92	2.00
Total	100.40	100.41	100.39	100.28	100.12	99.85	101.89	100.51	100.35	101.15	100.60
	Mineral formulae calculated based on 8 atoms of oxygen										
Si	2.998	2.998	2.995	3.000	3.007	2.860	2.803	2.995	2.986	2.984	2.984
Al	1.010	1.011	1.013	1.007	0.988	0.958	0.959	1.005	1.008	1.012	1.009
P	0.000	0.000	0.000	0.000	0.000	0.107	0.145	0.000	0.000	0.000	0.000
Ti	0.000	0.000	0.000	0.000	0.000	0.000	0.000	0.000	0.000	0.000	0.001
Fe^{3+}	0.000	0.001	0.000	0.003	0.007	0.005	0.007	0.007	0.014	0.008	0.011
Mn	0.000	0.000	0.000	0.000	0.000	0.000	0.000	0.000	0.000	0.000	0.000
Ca	0.000	0.000	0.000	0.000	0.000	0.094	0.122	0.000	0.000	0.000	0.000
Mg	0.000	0.000	0.000	0.001	0.005	0.000	0.001	0.000	0.000	0.000	0.001
Ba	0.001	0.001	0.000	0.000	0.002	0.003	0.001	0.009	0.014	0.010	0.009
Sr	0.006	0.006	0.006	0.007	0.006	0.007	0.006	0.006	0.007	0.006	0.006
K	0.862	0.857	0.873	0.938	0.814	0.811	0.144	0.838	0.794	0.710	0.791
Na	0.103	0.102	0.095	0.018	0.149	0.113	0.761	0.114	0.153	0.258	0.178
ΣCations	4.980	4.975	4.982	4.973	4.977	4.960	4.949	4.975	4.976	4.990	4.990
Mol.%											
Albite	10.29	10.18	9.45	1.79	14.87	11.30	76.05	11.43	15.30	25.82	17.83
Orthoclase	86.17	85.71	87.28	93.84	81.36	81.12	14.37	83.81	79.39	70.99	79.13
Anorthite	0.00	0.00	0.00	0.00	0.00	9.40	12.24	0.00	0.00	0.04	0.00
Celsian	0.10	0.10	0.04	0.00	0.24	0.30	0.08	0.92	1.42	0.97	0.86
Sr feldspar	0.58	0.56	0.62	0.67	0.64	0.74	0.61	0.63	0.70	0.63	0.64

v.fi.gr. = very fine grained; fi.gr. = fine grained; br. = bright; dk = dark; lam.= lamellae

Appendix A-5: Electron-microprobe analyses of feldspar

Mineral	K-feldspar								
Sample #	AD041C		AD066I						
Description	57 lt.	58 lt.	106 core	107 lt.	108 v.fi.gr.	111	112 fi.gr.	113 dk	114 mid.
SiO_2	64.66	65.21	63.95	64.06	63.79	63.76	63.83	63.68	63.75
Al_2O_3	18.66	18.45	19.13	19.13	20.14	19.59	19.33	19.37	18.86
P_2O_5	0.00	0.00	0.00	0.00	0.00	0.00	0.00	0.00	0.01
TiO_2	0.00	0.00	0.04	0.06	0.03	0.03	0.06	0.05	0.07
Fe_2O_3	0.25	0.25	0.11	0.08	0.38	0.08	0.08	0.10	0.10
MnO	0.01	0.01	0.02	0.00	0.00	0.00	0.01	0.00	0.01
CaO	0.00	0.00	0.00	0.00	0.05	0.03	0.00	0.00	0.00
MgO	0.00	0.00	0.02	0.00	0.29	0.00	0.00	0.00	0.01
BaO	0.58	0.07	1.37	1.64	0.89	1.52	1.96	2.25	0.15
SrO	0.25	0.23	0.32	0.38	0.38	0.37	0.36	0.34	0.46
K_2O	13.86	13.78	12.01	12.44	9.99	11.71	12.16	12.07	12.07
Na_2O	1.62	1.85	2.68	2.38	3.77	2.72	2.46	2.33	2.52
Total	100.59	100.56	100.28	100.83	100.24	100.43	100.88	100.81	98.66
	Mineral formulae calculated based on 8 atoms of oxygen								
Si	2.984	2.997	2.958	2.958	2.920	2.944	2.949	2.948	2.972
Al	1.015	1.000	1.043	1.042	1.087	1.067	1.053	1.057	1.037
P	0.000	0.000	0.000	0.000	0.000	0.000	0.000	0.000	0.001
Ti	0.000	0.000	0.001	0.002	0.001	0.001	0.002	0.002	0.002
Fe^{3+}	0.009	0.009	0.004	0.003	0.013	0.003	0.003	0.003	0.003
Mn	0.000	0.000	0.001	0.000	0.000	0.000	0.000	0.000	0.000
Ca	0.000	0.000	0.000	0.000	0.003	0.001	0.000	0.000	0.000
Mg	0.000	0.000	0.001	0.000	0.020	0.000	0.000	0.000	0.000
Ba	0.010	0.001	0.025	0.030	0.016	0.027	0.035	0.041	0.003
Sr	0.007	0.006	0.009	0.010	0.010	0.010	0.010	0.009	0.013
K	0.816	0.808	0.709	0.733	0.584	0.690	0.717	0.713	0.718
Na	0.145	0.165	0.240	0.213	0.334	0.244	0.220	0.209	0.228
ΣCations	4.985	4.985	4.991	4.991	4.988	4.987	4.989	4.981	4.977
Mol.%									
Albite	14.45	16.47	24.01	21.32	33.45	24.39	21.99	20.90	22.77
Orthoclase	81.62	80.78	70.89	73.31	58.36	69.01	71.70	71.26	71.82
Anorthite	0.00	0.00	0.00	0.00	0.25	0.14	0.00	0.01	0.00
Celsian	1.04	0.12	2.48	2.97	1.60	2.75	3.54	4.08	0.28
Sr feldspar	0.66	0.60	0.87	1.02	1.01	0.98	0.97	0.91	1.25

v.fi.gr. = very fine grained; fi.gr. = fine grained; br. = bright; dk = dark; lam.= lamellae

Appendix A-6: Electron-microprobe analyses of apatite

Sample #	AD043E					AD066A1						AD066A1		
Description	13	15 - mid	16 - mid	17-#6wl	18 - mid	'19	20	22 - edge	23	24 - bottom	26	27	28	29
CaO	55.23	55.04	55.21	56.50	55.13	55.51	56.14	55.30	55.67	55.17	54.68	54.67	56.15	55.19
Na_2O	0.13	0.16	0.18	0.09	0.13	0.13	0.11	0.13	0.16	0.16	0.15	0.12	0.16	0.13
La_2O_3	0.33	0.33	0.32	0.15	0.18	0.35	0.16	0.31	0.33	0.46	0.32	0.41	0.26	0.26
Ce_2O_3	0.62	0.64	0.60	0.33	0.36	0.63	0.38	0.46	0.48	0.75	0.55	0.73	0.39	0.43
Nd_2O_3	0.17	0.23	0.18	0.16	0.18	0.23	0.16	0.15	0.21	0.27	0.15	0.22	0.16	0.19
SrO	1.46	1.09	1.28	0.59	0.67	0.67	0.54	1.37	1.26	1.13	1.55	1.25	1.21	1.20
P_2O_5	39.75	40.05	40.23	41.05	39.96	39.81	39.71	37.44	37.14	37.55	40.90	40.26	39.48	37.70
SO_4	0.00	0.09	0.00	0.00	0.03	0.00	0.03	0.00	0.00	0.00	0.00	0.00	0.00	0.00
SiO_2	0.19	0.36	0.23	0.31	0.26	0.39	0.34	0.13	0.11	0.41	0.14	0.42	0.10	0.16
F	3.77	3.62	3.76	2.47	3.74	3.64	3.52	2.43	2.29	2.42	2.55	2.28	2.25	2.54
Cl	0.01	0.00	0.01	0.00	0.00	0.00	0.00	0.00	0.01	0.00	0.00	0.00	0.00	0.00
H_2O^*	0.00	0.02	0.00	0.59	0.00	0.02	0.09	0.59	0.67	0.60	0.52	0.65	0.70	0.54
Total	101.66	101.63	102.00	102.24	100.64	101.38	101.17	98 31	98.33	98.91	101.51	101.01	100.86	98.33
O=F,Cl	1.59	1.52	1.59	1.04	1.57	1.53	1.48	1.02	0.97	1.02	1.07	0.96	0.95	1.07
Total	100.07	100.11	100.42	101.20	99.07	99.85	99.69	97.29	97.37	97.90	100.44	100.05	99.91	97.27
Structural formula calculated based on Ca+Na+La+Ce+Nd+Sr = 10 and assuming F+Cl+OH=2														
Ca	9.752	9.771	9.754	9.878	9.849	9.821	9.872	9.77	9.77	9.75	9.74	9.76	9.79	9.79
Na	0.042	0.051	0.058	0.028	0.042	0.042	0.035	0.04	0.05	0.05	0.05	0.04	0.05	0.04
La	0.020	0.020	0.019	0.009	0.011	0.021	0.010	0.02	0.02	0.03	0.02	0.03	0.02	0.02
Ce	0.037	0.039	0.036	0.020	0.022	0.038	0.023	0.03	0.03	0.05	0.03	0.04	0.02	0.03
Nd	0.010	0.014	0.011	0.009	0.011	0.014	0.009	0.01	0.01	0.02	0.01	0.01	0.01	0.01
Sr	0.139	0.105	0.122	0.056	0.065	0.064	0.051	0.13	0.12	0.11	0.15	0.12	0.11	0.12
P	5.546	5.618	5.616	5.670	5.642	5.565	5.517	5.23	5.15	5.24	5.76	5.68	5.44	5.28
S	0.000	0.009	0.000	0.000	0.003	0.000	0.003	0.00	0.00	0.00	0.00	0.00	0.00	0.00
Si	0.031	0.060	0.038	0.051	0.043	0.064	0.056	0.02	0.02	0.07	0.02	0.07	0.02	0.03
F	1.965	1.897	1.961	1.275	1.972	1.901	1.827	1.27	1.19	1.26	1.34	1.20	1.16	1.33
Cl	0.003	0.000	0.003	0.000	0.000	0.000	0.000	0.00	0.00	0.00	0.00	0.00	0.00	0.00
OH	0.000	0.025	0.000	0.646	0.000	0.021	0.094	0.65	0.73	0.66	0.58	0.72	0.76	0.59
ΣREE	0.067	0.073	0.066	0.038	0.044	0.073	0.042	0.06	0.06	0.09	0.06	0.08	0.05	0.05
XF	0.982	0.948	0.980	0.637	0.986	0.950	0.913	0.63	0.59	0.63	0.67	0.60	0.58	0.66
XCl	0.001	0.000	0.001	0.000	0.000	0.000	0.000	0.00	0.00	0.00	0.00	0.00	0.00	0.00
XOH	0.000	0.012	0.000	0.323	0.000	0.010	0.047	0.33	0.37	0.33	0.29	0.36	0.38	0.30

lt = light; v. = very; mid = middle; av. = average

Appendix A-6: Electron-microprobe analyses of apatite

Sample #	AD066A1													
Description	30	31	32	33 - #10mid	34	41 - v.light	42 - light	43 - medium	44 - medium	46 - dark	47 - v.dark	48 - v.dark		
CaO	55.14	56.43	56.15	55.14	54.98	54.67	54.68	55.19	55.14	56.15	56.43	56.15	54.91	55.11
Na_2O	0.11	0.08	0.08	0.11	0.12	0.12	0.15	0.13	0.11	0.16	0.08	0.08	0.14	0.13
La_2O_3	0.30	0.13	0.19	0.21	0.24	0.41	0.32	0.26	0.30	0.26	0.13	0.19	0.29	0.27
Ce_2O_3	0.49	0.24	0.40	0.38	0.41	0.73	0.55	0.43	0.49	0.39	0.22	0.40	0.47	0.44
Nd_2O_3	0.15	0.08	0.19	0.15	0.19	0.20	0.15	0.19	0.15	0.16	0.08	0.19	0.15	0.13
SrO	1.32	0.83	0.62	0.66	1.03	1.25	1.55	1.20	1.32	1.21	0.83	0.62	1.45	1.51
P_2O_5	38.20	40.54	39.12	41.17	41.15	40.30	40.56	40.80	41.40	39.53	40.59	39.12	40.41	40.50
SO_4	0.00	0.03	0.00	0.04	0.04	0.00	0.00	0.00	0.00	0.00	0.04	0.00	0.01	0.02
SiO_2	0.20	0.25	0.27	0.37	0.28	0.42	0.14	0.16	0.20	0.10	0.25	0.27	0.23	0.24
F	2.42	2.37	2.44	2.91	3.36	2.28	2.55	2.54	2.42	2.25	2.37	2.44	2.26	2.42
Cl	0.00	0.00	0.00	0.01	0.00	0.00	0.00	0.00	0.00	0.00	0.00	0.00	0.00	0.01
H_2O^*	0.59	0.64	0.60	0.34	0.14	0.65	0.52	0.54	0.59	0.70	0.64	0.60	0.66	0.59
Total	98.92	101.62	100.06	101.49	101.93	101.03	101.17	101.44	102.12	100.91	101.66	100.06	100.97	101.37
O=F,Cl	1.02	1.00	1.03	1.23	1.41	0.96	1.07	1.07	1.02	0.95	1.00	1.03	0.95	1.02
Total	97.90	100.62	99.03	100.27	100.51	100.07	100.10	100.37	101.10	99.97	100.66	99.03	100.02	100.35
	Structural formula calculated based on Ca+Na+La+Ce+Nd+Sr = 10 and assuming F+Cl+OH=2													
Ca	9.78	9.87	9.87	9.86	9.81	9.76	9.74	9.79	9.78	9.79	9.87	9.87	9.76	9.76
Na	0.04	0.03	0.03	0.04	0.04	0.04	0.05	0.04	0.04	0.05	0.03	0.03	0.04	0.04
La	0.02	0.01	0.01	0.01	0.01	0.03	0.02	0.02	0.02	0.02	0.01	0.01	0.02	0.02
Ce	0.03	0.01	0.02	0.02	0.02	0.04	0.03	0.03	0.03	0.02	0.01	0.02	0.03	0.03
Nd	0.01	0.00	0.01	0.01	0.01	0.01	0.01	0.01	0.01	0.01	0.00	0.01	0.01	0.01
Sr	0.13	0.08	0.06	0.06	0.10	0.12	0.15	0.12	0.13	0.11	0.08	0.06	0.14	0.15
P	5.35	5.60	5.43	5.81	5.80	5.68	5.71	5.72	5.80	5.44	5.61	5.43	5.68	5.67
S	0.00	0.00	0.00	0.00	0.00	0.00	0.00	0.00	0.00	0.00	0.00	0.00	0.00	0.00
Si	0.03	0.04	0.04	0.06	0.05	0.07	0.02	0.03	0.03	0.02	0.04	0.04	0.04	0.04
F	1.27	1.22	1.27	1.54	1.77	1.20	1.34	1.33	1.27	1.16	1.22	1.27	1.19	1.27
Cl	0.00	0.00	0.00	0.00	0.00	0.00	0.00	0.00	0.00	0.00	0.00	0.00	0.00	0.00
OH	0.65	0.70	0.66	0.38	0.15	0.72	0.58	0.59	0.65	0.76	0.70	0.66	0.73	0.65
ΣREE	0.06	0.03	0.05	0.05	0.05	0.08	0.06	0.05	0.06	0.05	0.03	0.05	0.06	0.05
XF	0.63	0.61	0.63	0.77	0.88	0.60	0.67	0.66	0.63	0.58	0.61	0.63	0.59	0.63
XCl	0.00	0.00	0.00	0.00	0.00	0.00	0.00	0.00	0.00	0.00	0.00	0.00	0.00	0.00
XOH	0.33	0.35	0.33	0.19	0.08	0.36	0.29	0.30	0.33	0.38	0.35	0.33	0.37	0.33

lt = light; v. = very; mid = middle; av. = average

Appendix A-6: Electron-microprobe analyses of apatite

Sample #	AD066A1								AD066B					
Description	mid	near	mid	#3 edge	mid	#10 edge	mid	edge	3	4-#5	5-#6	6-#7	7-#8	8-#9
CaO	54.59	55.05	55.60	55.26	54.85	55.46	55.56	54.43	55.63	56.62	55.85	55.72	55.20	54.48
Na_2O	0.13	0.12	0.10	0.12	0.15	0.14	0.12	0.18	0.15	0.14	0.13	0.13	0.15	0.21
La_2O_3	0.30	0.25	0.13	0.23	0.31	0.18	0.13	0.25	0.27	0.19	0.21	0.15	0.24	0.46
Ce_2O_3	0.53	0.37	0.25	0.42	0.53	0.30	0.31	0.43	0.41	0.41	0.41	0.35	0.43	0.79
Nd_2O_3	0.20	0.15	0.12	0.17	0.20	0.13	0.13	0.18	0.13	0.16	0.16	0.11	0.11	0.23
SrO	1.28	0.90	0.60	0.78	0.87	0.81	0.67	1.30	1.33	0.60	0.79	0.82	1.40	1.51
P_2O_5	40.86	41.12	40.93	40.68	40.80	41.20	41.47	40.44	41.38	41.75	40.79	41.40	40.66	39.64
SO_4	0.01	0.02	0.01	0.01	0.00	0.01	0.03	0.02	0.06	0.03	0.00	0.00	0.00	0.03
SiO_2	0.25	0.27	0.18	0.29	0.52	0.28	0.32	0.22	0.11	0.22	0.23	0.15	0.10	0.21
F	2.21	2.75	3.09	2.24	2.68	2.31	2.34	2.59	3.39	2.91	3.10	3.52	3.73	3.16
Cl	0.00	0.00	0.00	0.01	0.02	0.00	0.01	0.00	0.02	0.01	0.00	0.00	0.00	0.01
H_2O^*	0.68	0.42	0.27	0.67	0.45	0.64	0.63	0.49	0.14	0.39	0.28	0.08	0.00	0.23
Total	101.04	101.42	101.29	100.88	101.39	101.47	101.71	100.52	103.02	103.43	101.95	102.42	102.02	100.96
O=F,Cl	0.93	1.16	1.30	0.94	1.13	0.97	0.99	1.09	1.43	1.23	1.31	1.48	1.57	1.33
Total	100.11	100.26	99.99	99.94	100.26	100.49	100.73	99.43	101.59	102.20	100.65	100.94	100.45	99.63
	Structural formula calculated based on Ca+Na+La+Ce+Nd+Sr = 10 and assuming F+Cl+OH=2													
Ca	9.77	9.83	9.88	9.83	9.80	9.84	9.86	9.76	9.78	9.85	9.84	9.84	9.77	9.70
Na	0.04	0.04	0.03	0.04	0.05	0.05	0.04	0.06	0.05	0.04	0.04	0.04	0.05	0.07
La	0.02	0.02	0.01	0.01	0.02	0.01	0.01	0.02	0.02	0.01	0.01	0.01	0.01	0.03
Ce	0.03	0.02	0.01	0.03	0.03	0.02	0.02	0.03	0.02	0.02	0.02	0.02	0.03	0.05
Nd	0.01	0.01	0.01	0.01	0.01	0.01	0.01	0.01	0.01	0.01	0.01	0.01	0.01	0.01
Sr	0.12	0.09	0.06	0.08	0.08	0.08	0.06	0.13	0.13	0.06	0.08	0.08	0.13	0.15
P	5.78	5.80	5.75	5.72	5.76	5.78	5.82	5.73	5.75	5.74	5.68	5.78	5.69	5.57
S	0.00	0.00	0.00	0.00	0.00	0.00	0.00	0.00	0.01	0.00	0.00	0.00	0.00	0.00
Si	0.04	0.05	0.03	0.05	0.09	0.05	0.05	0.04	0.02	0.04	0.04	0.02	0.02	0.03
F	1.17	1.45	1.62	1.17	1.41	1.21	1.23	1.37	1.76	1.49	1.61	1.84	1.95	1.66
Cl	0.00	0.00	0.00	0.00	0.01	0.00	0.00	0.00	0.01	0.00	0.00	0.00	0.00	0.00
OH	0.76	0.47	0.30	0.75	0.50	0.71	0.69	0.55	0.16	0.42	0.31	0.09	0.00	0.26
ΣREE	0.06	0.05	0.03	0.05	0.06	0.04	0.03	0.05	0.05	0.05	0.05	0.04	0.05	0.09
XF	0.58	0.72	0.81	0.59	0.71	0.60	0.61	0.69	0.88	0.75	0.81	0.92	0.97	0.83
XCl	0.00	0.00	0.00	0.00	0.00	0.00	0.00	0.00	0.00	0.00	0.00	0.00	0.00	0.00
XOH	0.38	0.24	0.15	0.37	0.25	0.36	0.35	0.27	0.08	0.21	0.15	0.04	0.00	0.13

lt = light; v. = very; mid = middle; av. = average

Appendix A-6: Electron-microprobe analyses of apatite

Sample #	AD066B													
Description	9-#10	10-#11	12-#13		#2	#3	#4 dark	top middle	middle light		#6	#7 SI		edge
CaO	54.72	54.70	54.19	55.78	55.80	54.49	56.80	56.42	54.44	55.83	55.50	55.36	55.34	55.64
Na_2O	0.15	0.15	0.28	0.24	0.22	0.22	0.10	0.13	0.28	0.12	0.13	0.19	0.13	0.12
La_2O_3	0.34	0.37	0.50	0.37	0.39	0.38	0.17	0.14	0.49	0.21	0.31	0.29	0.31	0.21
Ce_2O_3	0.62	0.61	0.88	0.68	0.61	0.60	0.31	0.28	0.80	0.32	0.48	0.45	0.51	0.37
Nd_2O_3	0.19	0.20	0.24	0.15	0.19	0.22	0.16	0.13	0.27	0.16	0.20	0.15	0.14	0.10
SrO	1.31	1.38	1.50	1.40	1.45	1.43	0.56	0.93	1.63	1.29	1.33	1.39	1.30	1.07
P_2O_5	40.08	40.24	39.39	39.70	39.94	39.36	40.03	40.98	39.79	40.61	40.42	40.71	41.03	40.47
SO_4	0.03	0.00	0.03	0.02	0.03	0.02	0.04	0.01	0.03	0.03	0.01	0.02	0.00	0.02
SiO_2	0.23	0.19	0.28	0.22	0.22	0.20	0.32	0.12	0.21	0.11	0.19	0.16	0.24	0.17
F	3.18	3.00	3.49	2.83	3.02	2.70	2.33	2.82	3.35	3.44	2.07	2.37	2.22	2.88
Cl	0.00	0.00	0.00	0.00	0.00	0.00	0.01	0.00	0.00	0.00	0.00	0.00	0.00	0.00
H_2O^*	0.22	0.31	0.08	0.43	0.34	0.45	0.67	0.43	0.15	0.13	0.77	0.63	0.69	0.38
Total	101.07	101.15	100.86	101.80	102.19	100.05	101.48	102.39	101.44	102.24	101.40	101.71	101.90	101.43
O=F,Cl	1.34	1.26	1.47	1.19	1.27	1.14	0.98	1.19	1.41	1.45	0.87	1.00	0.93	1.21
Total	99.73	99.89	99.39	100.61	100.92	98.92	100.50	101.20	100.03	100.79	100.53	100.71	100.97	100.22
	Structural formula calculated based on Ca+Na+La+Ce+Nd+Sr = 10 and assuming F+Cl+OH=2													
Ca	9.76	9.75	9.67	9.72	9.72	9.72	9.88	9.84	9.66	9.80	9.77	9.76	9.78	9.82
Na	0.05	0.05	0.09	0.07	0.07	0.07	0.03	0.04	0.09	0.04	0.04	0.06	0.04	0.04
La	0.02	0.02	0.03	0.02	0.02	0.02	0.01	0.01	0.03	0.01	0.02	0.02	0.02	0.01
Ce	0.04	0.04	0.05	0.04	0.04	0.04	0.02	0.02	0.05	0.02	0.03	0.03	0.03	0.02
Nd	0.01	0.01	0.01	0.01	0.01	0.01	0.01	0.01	0.02	0.01	0.01	0.01	0.01	0.01
Sr	0.13	0.13	0.14	0.13	0.14	0.14	0.05	0.09	0.16	0.12	0.13	0.13	0.12	0.10
P	5.65	5.67	5.55	5.47	5.50	5.55	5.50	5.65	5.58	5.63	5.62	5.67	5.73	5.64
S	0.00	0.00	0.00	0.00	0.00	0.00	0.00	0.00	0.00	0.00	0.00	0.00	0.00	0.00
Si	0.04	0.03	0.05	0.04	0.04	0.03	0.05	0.02	0.04	0.02	0.03	0.03	0.04	0.03
F	1.67	1.58	1.84	1.46	1.55	1.42	1.20	1.45	1.75	1.78	1.08	1.23	1.16	1.50
Cl	0.00	0.00	0.00	0.00	0.00	0.00	0.00	0.00	0.00	0.00	0.00	0.00	0.00	0.00
OH	0.25	0.34	0.09	0.47	0.37	0.50	0.72	0.47	0.17	0.14	0.85	0.69	0.76	0.42
ΣREE	0.07	0.07	0.10	0.07	0.07	0.07	0.04	0.03	0.09	0.04	0.06	0.05	0.06	0.04
XF	0.84	0.79	0.92	0.73	0.78	0.71	0.60	0.73	0.88	0.89	0.54	0.62	0.58	0.75
XCl	0.00	0.00	0.00	0.00	0.00	0.00	0.00	0.00	0.00	0.00	0.00	0.00	0.00	0.00
XOH	0.12	0.17	0.04	0.23	0.18	0.25	0.36	0.23	0.08	0.07	0.42	0.34	0.38	0.21

lt = light; v. = very; mid = middle; av. = average

Appendix A-6: Electron-microprobe analyses of apatite

Sample #	AD066B					
Description				49 - v.lt.av.	45 - med.av.	50 - lt.av.
CaO	55.52	54.92	56.05	56.29	55.16	54.67
Na_2O	0.15	0.21	0.07	0.08	0.12	0.13
La_2O_3	0.24	0.26	0.20	0.16	0.28	0.36
Ce_2O_3	0.35	0.42	0.30	0.32	0.46	0.64
Nd_2O_3	0.14	0.17	0.09	0.14	0.17	0.18
SrO	1.46	1.43	0.73	0.72	1.26	1.40
P_2O_5	40.42	40.77	40.92	39.88	37.95	37.24
SO_4	0.01	0.02	0.01	0.00	0.00	0.00
SiO_2	0.13	0.15	0.24	0.26	0.18	0.28
F	2.72	2.70	2.91	2.41	2.48	2.41
Cl	0.00	0.01	0.00	0.00	0.00	0.00
H_2O^+	0.47	0.46	0.37	0.62	0.56	0.59
Total	101.61	101.51	101.90	100.88	98.63	97.90
O=F,Cl	1.14	1.14	1.22	1.01	1.04	1.01
Total	100.46	100.37	100.67	99.86	97.58	96.88
	Structural formula calculated based on Ca+Na+La+Ce+Nd+Sr = 10 and assuming F+Cl+OH=2					
Ca	9.77	9.74	9.87	9.87	9.79	9.75
Na	0.05	0.07	0.02	0.03	0.04	0.04
La	0.01	0.02	0.01	0.01	0.02	0.02
Ce	0.02	0.03	0.02	0.02	0.03	0.04
Nd	0.01	0.01	0.01	0.01	0.01	0.01
Sr	0.14	0.14	0.07	0.07	0.12	0.14
P	5.62	5.72	5.70	5.52	5.32	5.25
S	0.00	0.00	0.00	0.00	0.00	0.00
Si	0.02	0.02	0.04	0.04	0.03	0.05
F	1.41	1.41	1.51	1.25	1.30	1.27
Cl	0.00	0.00	0.00	0.00	0.00	0.00
OH	0.51	0.51	0.41	0.67	0.62	0.65
ΣREE	0.04	0.05	0.04	0.04	0.06	0.07
XF	0.71	0.71	0.76	0.62	0.65	0.63
XCl	0.00	0.00	0.00	0.00	0.00	0.00
XOH	0.25	0.25	0.20	0.34	0.31	0.33

lt = light; v. = very; mid = middle; av. = average

Appendix A-7: Electron-microprobe analyses of titanite

Sample #	AD037A						AD066J1					AD066B
Description	1 light	2 dark	3 dark	4 lighter	5 dark	6 light	9	10	13	14	15	16
SiO_2	30.29	30.14	30.46	30.84	30.75	30.37	31.24	31.38	30.54	30.79	30.99	39.49
TiO_2	33.65	34.32	34.51	34.16	34.18	33.19	37.66	37.90	36.04	35.47	35.88	2.92
ZrO_2	0.37	0.44	0.33	0.37	0.32	0.40	0.00	0.00	0.01	0.17	0.03	0.13
Nb_2O_5	3.90	2.46	2.38	3.17	2.52	4.62	0.02	0.03	1.77	2.25	1.26	0.07
V_2O_3	0.28	0.37	0.36	0.36	0.40	0.30	0.37	0.35	0.42	0.39	0.36	0.31
Al_2O_3	0.74	0.74	0.76	0.72	0.79	0.71	1.21	1.23	0.43	0.54	0.46	7.43
Fe_2O_3	2.40	2.80	2.39	2.12	2.81	2.57	0.71	0.74	2.01	1.86	2.51	9.57
MnO	0.02	0.03	0.03	0.03	0.02	0.01	0.06	0.03	0.00	0.01	0.02	0.22
MgO	0.01	0.01	0.00	0.01	0.01	0.01	0.00	0.00	0.00	0.01	0.00	0.57
CaO	27.27	27.60	27.70	27.53	27.88	27.37	28.88	28.85	28.15	27.97	28.22	33.74
Na_2O	0.20	0.15	0.11	0.19	0.11	0.22	0.01	0.00	0.16	0.14	0.13	1.65
K_2O	0.02	0.02	0.02	0.02	0.01	0.02	0.02	0.02	0.03	0.02	0.02	0.72
F	0.00	0.00	0.00	0.00	0.00	0.00	0.00	0.00	0.00	0.00	0.00	0.00
Total	99.15	99.08	99.05	99.52	99.80	99.79	100.18	100.53	99.56	99.62	99.88	96.82
	Formulae calculated based on 2 Si and all Fe is Fe^{3+}											
Si	2.000	2.000	2.000	2.000	2.000	2.000	2.000	2.000	2.000	2.000	2.000	2.000
Ti	1.671	1.713	1.704	1.666	1.672	1.644	1.813	1.817	1.775	1.733	1.742	0.110
Zr	0.012	0.014	0.011	0.012	0.010	0.013	0.000	0.000	0.000	0.006	0.001	0.032
Nb	0.117	0.074	0.071	0.093	0.074	0.138	0.001	0.001	0.052	0.066	0.038	0.002
V	0.015	0.020	0.019	0.019	0.021	0.016	0.019	0.018	0.022	0.020	0.019	0.015
Al	0.058	0.058	0.059	0.055	0.061	0.055	0.091	0.092	0.033	0.041	0.035	0.444
Fe^{3+}	0.119	0.140	0.118	0.103	0.138	0.127	0.034	0.036	0.099	0.091	0.122	0.365
Mn	0.001	0.002	0.002	0.002	0.011	0.001	0.003	0.002	0.000	0.001	0.001	0.009
Mg	0.001	0.001	0.000	0.001	0.001	0.000	0.000	0.000	0.000	0.001	0.000	0.043
ΣOctahedra	1.994	2.020	1.983	1.950	1.988	1.993	1.962	1.965	1.982	1.958	1.957	1.020
Ca	1.929	1.963	1.949	1.913	1.943	1.931	1.981	1.970	1.975	1.947	1.952	1.831
Na	0.025	0.019	0.014	0.024	0.014	0.028	0.001	0.000	0.020	0.018	0.016	0.162
K	0.002	0.002	0.002	0.002	0.001	0.001	0.002	0.002	0.003	0.002	0.002	0.077
Σ8-fold	1.956	1.983	1.964	1.939	1.958	1.960	1.984	1.972	1.998	1.966	1.969	2.070
F	0.000	0.000	0.000	0.000	0.000	0.000	0.000	0.000	0.000	0.000	0.000	0.000
ΣCations	5.950	6.003	5.947	5.889	5.945	5.954	5.946	5.937	5.980	5.924	5.927	5.089

Appendix A-8: Electron-microprobe analyses of garnet

Sample #	AD037A								1205/VII/A		
Description	2 mid	3 ed	4 2nd ed	5 mid.	6	7 mid.	8 center	9 center	10 bright	11 darker	12 lighter
SiO_2	31.54	31.84	31.58	32.10	31.02	30.95	31.19	31.08	33.18	34.40	30.44
Al_2O_3	1.26	1.33	1.27	1.18	1.30	1.34	1.25	1.26	0.72	3.37	1.48
TiO_2	8.23	7.76	8.32	7.18	9.27	9.29	9.03	9.04	2.81	2.22	5.76
ZrO_2	0.48	0.38	0.46	0.51	0.51	0.52	0.53	0.56	0.39	0.12	0.23
Cr_2O_3	0.00	0.04	0.03	0.02	0.01	0.02	0.01	0.02	0.00	0.02	0.00
V_2O_3	0.32	0.37	0.31	0.22	0.33	0.30	0.35	0.34	0.35	0.26	0.17
Fe_2O_3	21.89	21.35	21.41	23.83	20.22	20.60	20.49	20.48	28.05	25.42	27.56
FeO	3.49	3.51	3.49	1.45	3.96	3.51	4.03	3.98	0.00	0.00	0.00
MgO	0.51	0.52	0.49	0.50	0.50	0.46	0.47	0.47	0.43	0.46	0.25
MnO	0.31	0.30	0.32	0.27	0.31	0.34	0.31	0.31	0.39	0.55	0.53
CaO	31.87	31.77	31.97	32.30	31.77	32.07	31.74	31.70	32.68	33.07	32.78
Total	99.90	99.17	99.64	98.47	99.21	99.39	99.40	99.24	99.00	99.89	99.20
	Cation units calculated based on 8 cations and 12 atoms of oxygen										
Si	2.680	2.719	2.688	2.672	2.654	2.642	2.664	2.660	2.833	2.864	2.601
^{IV}Al	0.126	0.134	0.127	0.120	0.131	0.135	0.126	0.127	0.072	0.136	0.149
Fe^{3+}	0.190	0.150	0.180	0.210	0.210	0.220	0.210	0.210	0.090	0.000	0.250
^{IV}Al	0.000	0.000	0.000	0.000	0.000	0.000	0.000	0.000	0.000	0.195	0.000
Ti	0.526	0.498	0.532	0.465	0.596	0.596	0.580	0.582	0.180	0.139	0.370
Zr	0.020	0.016	0.019	0.021	0.021	0.022	0.022	0.023	0.016	0.005	0.010
Cr	0.000	0.003	0.002	0.001	0.001	0.001	0.001	0.001	0.000	0.001	0.000
V	0.022	0.025	0.021	0.015	0.023	0.021	0.024	0.023	0.024	0.017	0.012
Fe^{3+}	1.210	1.222	1.191	1.336	1.092	1.103	1.107	1.109	1.713	1.592	1.522
Fe^{2+}	0.230	0.230	0.240	0.100	0.230	0.250	0.270	0.260	0.000	0.000	0.000
Fe^{2+}	0.020	0.020	0.010	0.000	0.050	0.000	0.020	0.020	0.000	0.000	0.000
Mn	0.037	0.038	0.035	0.037	0.036	0.033	0.034	0.034	0.031	0.032	0.018
Mg	0.039	0.038	0.041	0.035	0.040	0.043	0.039	0.040	0.050	0.068	0.068
Ca	2.902	2.907	2.915	2.983	2.912	2.933	2.905	2.906	2.990	2.950	3.001
Charge Def.	0.00	0.00	0.00	0.00	0.00	0.00	0.00	0.00	0.04	0.04	0.11

* Site assignments after Kuhberger et al. (1989), Locock et al. (1995) and Deer et al. (1982) and assuming only Ti^{4+} is present.
Acronyms are: mid = middle; ed = edge; bes = best; l = light

Kuhberger, A., Fehr, T., Huckenholz & Amthauer, G. (1989): Physics and Chemistry of Minerals, 16, 734-740.
Locock, A., Luth, R.W., Cavell, R.G., Smith, D.G.W. & Duke, M.J.M. (1995): American Mineralogist, 80, 27-38.

Appendix A-8: Electron-microprobe analyses of garnet

Sample #	1205/VII/A			AD022B							
Description	13 mid	14 2nd	15 3rd	20 ed	21 mid	22 ed2	23 best	24 best	25 mid.	26 edge	27 mid.
SiO_2	31.77	33.81	34.48	28.98	27.28	29.29	29.36	27.21	27.17	30.01	27.47
Al_2O_3	0.84	1.02	1.35	1.58	1.88	1.62	1.71	1.88	1.90	1.68	1.93
TiO_2	5.56	2.33	0.95	12.16	15.74	11.86	12.17	16.79	16.51	10.67	16.03
ZrO_2	0.50	0.20	0.11	0.59	0.81	0.54	0.54	0.83	0.82	0.49	0.77
Cr_2O_3	0.01	0.00	0.01	0.02	0.00	0.01	0.01	0.00	0.01	0.01	0.00
V_2O_3	0.22	0.29	0.38	0.28	0.21	0.29	0.26	0.17	0.22	0.32	0.23
Fe_2O_3	26.99	29.12	29.11	21.85	17.89	21.68	20.96	16.05	16.56	22.22	16.92
FeO	0.49	0.00	0.00	1.81	3.34	2.04	2.29	4.39	3.97	1.90	3.79
MgO	0.56	0.52	0.45	0.23	0.26	0.25	0.24	0.27	0.27	0.25	0.26
MnO	0.65	0.44	0.28	0.99	1.26	0.97	1.01	1.27	1.28	0.87	1.29
CaO	32.05	32.57	32.76	32.88	32.31	32.77	32.81	32.15	32.23	32.83	32.28
Total	99.64	100.30	99.88	101.37	100.98	101.32	101.36	101.01	100.94	101.25	100.98
	Cation units calculated based on 8 cations and 12 atoms of oxygen										
Si	2.707	2.847	2.905	2.431	2.300	2.456	2.458	2.294	2.291	2.514	2.313
^{IV}Al	0.084	0.101	0.095	0.156	0.187	0.160	0.169	0.187	0.189	0.166	0.192
Fe^{3+}	0.210	0.050	0.000	0.410	0.510	0.380	0.370	0.520	0.520	0.320	0.500
^{IV}Al	0.000	0.000	0.039	0.000	0.000	0.000	0.000	0.000	0.000	0.000	0.000
Ti	0.356	0.148	0.060	0.767	0.998	0.748	0.766	1.064	1.047	0.672	1.015
Zr	0.021	0.008	0.005	0.024	0.033	0.022	0.022	0.034	0.034	0.020	0.032
Cr	0.001	0.000	0.001	0.001	0.000	0.001	0.001	0.000	0.001	0.001	0.000
V	0.015	0.020	0.026	0.019	0.014	0.020	0.017	0.011	0.015	0.021	0.016
Fe^{3+}	1.521	1.795	1.845	0.969	0.625	0.988	0.951	0.498	0.531	1.080	0.572
Fe^{2+}	0.040	0.000	0.000	0.130	0.240	0.140	0.160	0.310	0.280	0.130	0.270
Fe^{2+}	0.000	0.000	0.000	0.000	0.000	0.000	0.000	0.000	0.000	0.000	0.000
Mn	0.040	0.037	0.032	0.016	0.019	0.018	0.017	0.019	0.019	0.018	0.019
Mg	0.083	0.055	0.035	0.124	0.158	0.121	0.126	0.160	0.161	0.109	0.162
Ca	2.926	2.939	2.957	2.955	2.919	2.944	2.943	2.904	2.912	2.946	2.913
Charge Def.	0.00	0.03	0.05	0.00	0.00	0.00	0.00	0.00	0.00	0.00	0.00

* Site assignments after Kuhberger et al. (1989), Locock et al. (1995) and Deer et al. (1982) and assuming only Ti^{4+} is present.
Acronyms are: mid = middle; ed = edge; bes = best; l = light

Kuhberger, A., Fehr, T., Huckenholz & Amthauer, G. (1989): Physics and Chemistry of Minerals, 16, 734-740.
Locock, A., Luth, R.W., Cavell, R.G., Smith, D.G.W. & Duke, M.J.M. (1995): American Mineralogist, 80, 27-38.

Appendix A-9: Additional analyses

Sulphides* Sample #	AD066F	
Description	pyrite	chalcopyrite
Fe	40.35	29.45
Cu	0.00	30.01
Mn	0.39	0.21
Cr	0.00	0.00
V	0.17	0.00
Ti	0.00	0.50
S	59.10	39.83
Total	100.00	100.00

Hematite* Sample #	87/A/94			1205/Vil/A	BH/4/2
Description	#1 dkoxide	#2 oxide	#5 oxide	#1 oxide	#3 oxide
FeO	91.05	88.38	90.84	96.03	96.29
MnO	1.15	2.55	n.d.	0.79	0.00
Cr_2O_3	0.12	0.05	0.41	0.22	0.08
V_2O_3	0.00	0.87	0.80	n.d.	n.d.
TiO_2	5.85	4.34	4.55	2.50	1.31
SiO_2	1.83	3.81	3.40	0.46	2.33
Total	100.00	100.00	100.00	100.00	100.00

Britholite* Sample #	AD041E
Description	
CaO	15.04
MgO	0.24
FeO	1.08
La_2O_3	17.35
Ce_2O_3	28.59
SiO_2	28.15
P_2O_5	9.55
Total	100.00

* Analyses performed by energy dispersive spectrometry (EDS)

Appendix A-9: Additional analyses

Analcime** Sample # Description	AD066J1 821	AD066J2 88 dark	AD022B 100	101	102
SiO_2	33.07	51.66	46.06	46.45	46.91
Al_2O_3	34.22	26.56	29.18	29.63	28.84
TiO_2	0.02	0.04	0.01	0	0.05
FeO	19.35	0.41	0.19	0.31	0.66
MnO	0.12	0.01	0	0.01	0.01
MgO	0.42	0.15	0.61	0.03	0.01
CaO	0.2	1.94	0.03	0.34	1.31
BaO	0.07	0.07	0.05	0.01	0.04
SrO	0.23	0.25	0.16	0.14	0.17
Na_2O	0.89	11.53	11.53	14.62	14.64
K_2O	7.22	0.78	0.06	0.07	0.04
Total	95.81	93.4	87.88	91.61	92.68
	Formulae calculated based on 6 atoms of oxygen				
Si	1.328	1.881	1.739	1.390	1.806
Al	1.619	1.140	1.298	1.307	1.204
Ti	0.001	0.001	0.000	0.000	0.001
Fe^{2+}	0.650	0.012	0.007	0.010	0.020
Mn	0.004	0.000	0.000	0.000	0.000
Mg	0.025	0.008	0.002	0.002	0.001
Ca	0.009	0.076	0.025	0.014	0.001
Ba	0.001	0.001	0.001	0.000	0.001
Sr	0.005	0.005	0.003	0.003	0.003
Na	1.479	0.814	1.072	1.061	1.006
K	0.278	0.036	0.003	0.003	0.002
ΣCations	5.399	3.974	4.150	3.790	4.044

** Analyses performed by wavelength dispersive spectrometry (WDS)

[1] Composite of analcime + hematite + K-feldspar

Mixed with K-feldspar

Appendix A-9: Additional analyses

Mineral	Calcite*	Ankerite*			Wollastonite	
Sample #	BH/18/2.1			BH/4/2	1205/VII/A	
Description	core	#1rim	rim	#3	lt.	dk ed.
CaO	93.96	52.20	52.53	50.66	45.37	32.79
Na_2O	0.00	0.00	0.00	2.24	0.20	10.14
SrO	3.11	n.d.	1.31	n.d.	n.d.	n.d.
BaO	0.24	n.d.	0.00	0.19	0.00	0.00
MgO	0.27	37.74	36.96	31.31	0.19	0.33
MnO	0.00	1.55	1.62	3.19	0.39	0.60
FeO	1.95	8.24	7.12	11.83	0.85	0.39
Cr_2O_3	0.01	0.01	0.00	0.20	0.39	0.31
V_2O_3	0.00	n.d.	n.d.	n.d.	n.d.	n.d.
TiO_2	0.33	0.00	0.17	0.02	0.08	0.54
Al_2O_3	0.14	0.27	0.28	0.36	0.00	0.00
SiO_2	0.00	0.00	0.00	0.01	52.52	54.90
Total	100.00	100.00	100.00	100.00	100.00	100.00

n.d. not determined; dk=dark; lt.=light; ed.=edge

* Analyses performed by energy dispersive spectrometry (EDS)

** Analyses performed by wavelength dispersive spectrometry (WDS)

Appendix A-10: AEM analyses of mica

Sample #	AD066B		AD066a1		87/A/67.2						87/A/67.2
File Name	Aeg spect.		ad066a1(s4)		ADd8new						ADd8
Type of Mica*	N	N	N	N	N	N	N	N	N	N	N
Description[1]	65	67(2470-71)	3(5583-4)	5(5591)	1	2	3 wide beam	4	5	6	4
SiO_2	33.99	33.49	47.37	31.67	54.99	52.87	52.77	35.26	34.59	34.27	35.59
Al_2O_3	10.02	10.16	19.51	8.09	23.00	24.58	23.52	9.93	8.93	8.73	9.94
TiO_2	1.51	1.64	0.47	0.45	0.31	0.24	0.17	0.99	1.43	1.00	1.08
FeO	22.53	21.72	18.38	25.62	5.20	5.20	6.26	20.78	19.65	21.73	20.32
MnO	1.82	1.92	0.39	2.51	0.01	0.00	0.00	1.44	1.20	1.47	1.38
MgO	15.11	16.04	6.58	18.57	4.56	4.74	5.31	19.05	17.84	18.53	17.15
CaO	0.62	0.48	1.39	0.57	0.75	0.92	1.39	0.85	0.65	0.66	0.54
Na_2O	1.12	1.06	0.11	0.79	0.33	0.34	0.58	0.00	0.33	0.49	0.14
K_2O	13.28	13.49	5.79	11.73	10.86	11.10	10.01	11.69	15.38	13.13	13.87
Total[2]	100.00	100.00	100.00	100.00	100.00	100.00	100.00	100.00	100.00	100.00	100.00
	Mineral formulae calculated based on 11 atoms of oxygen										
Si	3.090	3.044	3.571	2.972	3.810	3.696	3.705	3.098	3.116	3.092	3.153
^{IV}Al	0.910	0.956	0.429	0.790	0.190	0.304	0.295	0.902	0.838	0.820	0.847
^{VI}Al	0.038	0.005	1.102	0.000	1.469	1.485	1.424	0.007	0.000	0.000	0.070
Al	0.948	0.961	1.531	0.790	1.659	1.789	1.719	0.908	0.838	0.820	0.917
Ti	0.081	0.087	0.021	0.025	0.013	0.010	0.007	0.051	0.076	0.053	0.056
Fe	1.030	0.993	0.697	1.209	0.181	0.183	0.221	0.919	0.891	0.986	0.905
Mn	0.085	0.089	0.015	0.120	0.000	0.000	0.000	0.065	0.055	0.068	0.062
Mg	1.587	1.684	0.573	2.013	0.365	0.383	0.430	1.934	1.857	1.932	1.756
Ca	0.039	0.030	0.074	0.038	0.036	0.045	0.068	0.053	0.041	0.042	0.033
Na	0.124	0.118	0.010	0.091	0.028	0.029	0.049	0.000	0.036	0.054	0.015
K	0.867	0.881	0.313	0.791	0.540	0.557	0.505	0.738	0.995	0.851	0.883
ΣCations	7.851	7.888	6.805	8.049	6.632	6.693	6.705	7.766	7.905	7.897	7.781
^{IV}Al	0.910	0.956	0.429	0.790	0.190	0.304	0.295	0.902	0.838	0.820	0.847
Fe/(Fe+Mg)	0.394	0.371	0.549	0.375	0.332	0.323	0.339	0.322	0.324	0.338	0.340

* N=normally pleochroic mica; R=reversely pleochroic mica as estimated by earlier optical examination

[1] Numbers here refer first to the point # in the file and the set in brackets corresponding to the TEM image(s)

[2] Total is set to 100.00 due to the fact that the analyses are EDS ones

Appendix A-10: AEM analyses of mica

Sample #	87/A/67.2					87/A/67.1		87/A/67.1	87/A/67.1		87/A/67.1
File Name	ADd8					ADn1		ADn1	87a671 n2		87a671 n3
Type of Mica*	N	N	N	N	N	N	N	N	N	N	N
Description[1]	5	9	10(3990)	11	12	8 Clay-like	9 Clay-like	10 Clay-like	6(6353-55)	8 by ox	6 by calcite
SiO_2	34.72	35.27	35.31	34.00	34.12	55.78	57.84	31.24	36.64	36.33	36.42
Al_2O_3	8.85	9.22	9.53	8.86	9.23	22.61	21.51	9.63	10.29	9.80	10.90
TiO_2	0.99	1.28	1.14	0.99	1.05	0.51	0.03	1.21	1.20	1.03	1.05
FeO	21.39	20.23	21.27	22.45	19.79	8.22	6.59	23.15	18.73	25.87	19.53
MnO	1.36	1.34	1.50	1.41	1.39	0.00	0.13	2.52	0.85	1.02	1.12
MgO	18.08	18.84	18.46	17.44	18.63	5.60	6.95	14.95	19.30	14.45	17.74
CaO	0.53	0.92	1.05	0.48	1.10	1.22	1.82	0.00	0.46	1.40	1.48
Na_2O	0.27	0.20	0.20	0.63	0.90	1.30	0.94	0.00	0.00	0.05	0.14
K_2O	13.80	12.70	11.54	13.74	13.79	4.76	4.20	17.29	12.53	10.04	11.61
Total[2]	100.00	100.00	100.00	100.00	100.00	100.00	100.00	100.00	100.00	100.00	100.00
	Mineral formulae calculated based on 11 atoms of oxygen										
Si	3.124	3.119	3.116	3.096	3.068	3.801	3.878	2.979	3.155	3.222	3.148
^{IV}Al	0.829	0.849	0.876	0.840	0.864	0.199	0.122	0.956	0.845	0.778	0.852
^{VI}Al	0.000	0.000	0.000	0.000	0.000	1.405	1.380	0.000	0.078	0.127	0.128
Al	0.829	0.849	0.876	0.840	0.864	1.604	1.502	0.956	0.923	0.905	0.981
Ti	0.052	0.066	0.059	0.053	0.055	0.020	0.001	0.068	0.061	0.054	0.053
Fe	0.968	0.899	0.944	1.028	0.895	0.282	0.222	1.110	0.811	1.154	0.849
Mn	0.063	0.061	0.068	0.065	0.064	0.000	0.004	0.123	0.038	0.046	0.049
Mg	1.879	1.925	1.882	1.834	1.935	0.441	0.538	1.647	1.920	1.480	1.771
Ca	0.033	0.057	0.065	0.031	0.069	0.058	0.085	0.000	0.028	0.087	0.090
Na	0.030	0.022	0.021	0.070	0.099	0.108	0.077	0.000	0.000	0.005	0.015
K	0.892	0.807	0.731	0.899	0.891	0.233	0.202	1.184	0.775	0.639	0.721
ΣCations	7.871	7.805	7.763	7.916	7.940	6.547	6.510	8.067	7.710	7.594	7.677
^{IV}Al	0.829	0.849	0.876	0.840	0.864	0.199	0.122	0.956	0.845	0.778	0.852
Fe/(Fe+Mg)	0.340	0.318	0.334	0.359	0.316	0.390	0.292	0.403	0.297	0.438	0.324

* N=normally pleochroic mica; R=reversely pleochroic mica as estimated by earlier optical examination

[1] Numbers here refer first to the point # in the file and the set in brackets corresponding to the TEM image(s)

[2] Total is set to 100.00 due to the fact that the analyses are EDS ones

Appendix A-10: AEM analyses of mica

Sample #	87/A/67.1						87/A/67.1		BII/18/2.1		
File Name	87a671 n3						87a671 n1		nbh182.1		
Type of Mica*	N	N	N	N	N	N	N	N	N	N	N
Description[1]	7 by calcite	13 by silica	14 by silica	15	16	17	24 by edge	25 by edge	17(6203-7)	18(6198-201)	19
SiO_2	35.10	50.23	37.30	34.76	34.98	36.20	33.51	34.59	33.85	33.38	34.60
Al_2O_3	9.65	21.69	10.93	8.59	8.14	9.17	8.32	9.26	9.60	9.76	9.76
TiO_2	1.52	0.36	0.95	0.69	0.97	0.76	1.41	1.66	1.30	1.21	1.13
FeO	17.33	11.03	18.42	22.57	22.86	21.46	26.00	22.75	18.20	18.66	18.04
MnO	1.29	0.25	1.35	1.36	1.26	1.02	1.19	1.27	0.75	0.65	0.53
MgO	19.39	8.16	17.97	17.74	17.62	17.40	16.60	16.96	20.69	20.60	21.45
CaO	1.09	0.69	0.28	0.41	0.26	0.10	0.19	0.35	0.00	0.08	0.18
Na_2O	0.11	0.42	0.00	0.37	0.01	0.21	0.55	0.00	0.07	0.28	0.10
K_2O	14.51	7.17	12.80	13.51	13.91	13.68	12.23	13.16	15.54	15.38	14.21
Total[2]	100.00	100.00	100.00	100.00	100.00	100.00	100.00	100.00	100.00	100.00	100.00
				Mineral formulae calculated based on 11 atoms of oxygen							
Si	3.092	3.607	3.198	3.143	3.168	3.208	3.087	3.112	3.021	2.993	3.041
^{IV}Al	0.885	0.393	0.802	0.808	0.767	0.792	0.798	0.867	0.892	0.911	0.893
^{VI}Al	0.000	1.229	0.174	0.000	0.000	0.054	0.000	0.000	0.000	0.000	0.000
Al	0.885	1.622	0.976	0.808	0.767	0.846	0.798	0.867	0.892	0.911	0.893
Ti	0.079	0.015	0.048	0.037	0.051	0.039	0.076	0.088	0.068	0.064	0.058
Fe	0.768	0.398	0.794	1.026	1.041	0.956	1.205	1.030	0.817	0.841	0.797
Mn	0.058	0.009	0.059	0.063	0.058	0.046	0.056	0.059	0.034	0.030	0.024
Mg	1.974	0.677	1.780	1.853	1.843	1.781	1.766	1.763	2.133	2.134	2.178
Ca	0.067	0.035	0.017	0.026	0.016	0.006	0.012	0.022	0.000	0.005	0.011
Na	0.012	0.037	0.000	0.041	0.001	0.022	0.062	0.000	0.008	0.031	0.011
K	0.918	0.370	0.788	0.877	0.905	0.871	0.809	0.851	0.996	0.990	0.897
ΣCations	7.852	6.770	7.660	7.875	7.850	7.777	7.873	7.791	7.967	7.999	7.909
^{IV}Al	0.885	0.393	0.802	0.808	0.767	0.792	0.798	0.867	0.892	0.911	0.893
Fe/(Fe+Mg)	0.280	0.370	0.308	0.356	0.361	0.349	0.405	0.369	0.277	0.283	0.268

* N=normally pleochroic mica; R=reversely pleochroic mica as estimated by earlier optical examination

[1] Numbers here refer first to the point # in the file and the set in brackets corresponding to the TEM image(s)

[2] Total is set to 100.00 due to the fact that the analyses are EDS ones

Appendix A-10. AEM analyses of mica

Sample #	BH/18/2.1						BH/18/2.1				BH/18/2.1
File Name	nbh182.1						nbh182.1				bh182.1decb
Type of Mica*	N	N	N	N	N	N	N	N	N	N	N
Description[1]	20(6193-6)	21(6223-4)	22(6221-2)	23(6213-9)	26 by ox.	28(6226-6232)	31 by hump	38(6809-10)	39(6809-10)	40 away	1(6457-61)
SiO_2	32.21	33.30	32.66	33.46	33.24	29.79	32.57	32.78	32.77	32.06	36.73
Al_2O_3	10.17	9.69	10.09	10.81	8.42	8.58	8.48	7.13	7.30	7.41	10.20
TiO_2	2.02	2.28	2.18	1.82	0.80	0.72	0.40	0.67	0.91	0.65	1.10
FeO	20.26	20.49	19.70	19.79	22.34	31.41	24.57	22.92	20.07	21.01	15.73
MnO	0.47	0.87	0.71	0.76	0.68	0.43	0.34	0.47	0.16	0.45	0.93
MgO	20.82	18.93	20.06	19.61	20.26	15.38	19.28	21.82	21.90	23.28	21.92
CaO	0.45	0.16	0.14	0.36	0.21	0.27	0.18	0.10	0.22	0.12	0.11
Na_2O	0.31	0.00	0.10	0.07	0.08	0.07	0.05	0.09	0.01	0.14	0.12
K_2O	13.29	14.27	14.35	13.31	13.97	13.37	14.13	14.03	16.65	14.87	13.16
Total[2]	100.00	100.00	100.00	100.00	100.00	100.00	100.00	100.00	100.00	100.00	100.00
	Mineral formulae calculated based on 11 atoms of oxygen										
Si	2.894	2.996	2.935	2.968	3.027	2.909	3.014	3.014	3.013	2.947	3.126
^{IV}Al	0.951	0.908	0.944	0.999	0.799	0.872	0.817	0.683	0.699	0.709	0.874
^{VI}Al	0.000	0.000	0.000	0.000	0.000	0.000	0.000	0.000	0.000	0.000	0.029
Al	0.951	0.908	0.944	0.999	0.799	0.872	0.817	0.683	0.699	0.709	0.904
Ti	0.106	0.120	0.115	0.095	0.043	0.041	0.022	0.036	0.049	0.035	0.055
Fe	0.915	0.927	0.891	0.883	1.023	1.543	1.143	1.060	0.928	0.971	0.673
Mn	0.021	0.040	0.033	0.035	0.032	0.022	0.016	0.022	0.008	0.021	0.041
Mg	2.161	1.967	2.083	2.010	2.132	1.735	2.061	2.318	2.327	2.472	2.155
Ca	0.028	0.010	0.009	0.023	0.013	0.018	0.012	0.006	0.014	0.008	0.006
Na	0.034	0.000	0.011	0.007	0.009	0.008	0.005	0.010	0.002	0.016	0.012
K	0.858	0.922	0.926	0.848	0.914	0.938	0.939	0.927	1.100	0.982	0.804
ΣCations	7.970	7.891	7.946	7.866	7.992	8.086	8.028	8.077	8.139	8.162	7.776
^{IV}Al	0.951	0.908	0.944	0.999	0.799	0.872	0.817	0.683	0.699	0.709	0.874
Fe/(Fe+Mg)	0.297	0.320	0.299	0.305	0.324	0.471	0.357	0.314	0.285	0.282	0.238

* N=normally pleochroic mica; R=reversely pleochroic mica as estimated by earlier optical examination

[1] Numbers here refer first to the point # in the file and the set in brackets corresponding to the TEM image(s)

[2] Total is set to 100.00 due to the fact that the analyses are EDS ones

Appendix A-10: AEM analyses of mica

Sample #	BH/18/2.1		BH/18/2.1		BH/18/2.1			BH/18/2.2			
File Name	bh182.1decb		bh182.1decc		BH182.1chl			BH182.1chl3			
Type of Mica*	N	N	N	N	N?	N?	N?	N?	N?	N?	N?
Description[1]	2 by prev.	3 opp.side	1(6479-80)	2by(6479-80)	5(6584-9)	6(6590-2)	9(6599-602)	4(6615)	5(6617-20)	7bottom	8top(6626-9)
SiO_2	36.17	34.65	34.37	34.89	44.84	44.04	37.24	38.66	36.10	37.88	37.34
Al_2O_3	9.68	10.56	9.87	10.07	12.20	13.28	10.24	8.42	8.62	8.75	9.64
TiO_2	1.21	1.32	1.30	1.47	0.64	0.81	0.76	3.06	0.47	0.48	0.74
FeO	16.31	17.20	18.27	16.81	9.82	11.51	13.98	27.81	11.84	12.19	13.05
MnO	0.52	0.70	0.50	0.56	0.46	0.40	0.12	0.00	0.53	0.21	0.26
MgO	21.29	21.39	19.93	20.87	19.12	19.08	24.82	14.23	27.06	27.01	26.63
CaO	0.11	0.00	0.09	0.27	0.00	0.32	0.19	2.36	0.33	0.31	0.18
Na_2O	0.17	0.00	0.28	0.11	0.09	0.64	0.33	0.73	0.27	0.19	0.33
K_2O	14.54	14.17	15.39	14.97	12.82	9.93	12.32	4.74	14.78	12.98	11.82
Total[2]	100.00	100.00	100.00	100.00	100.00	100.00	100.00	100.00	100.00	100.00	100.00
				Mineral formulae calculated based on 11 atoms of oxygen							
Si	3.125	3.021	3.051	3.053	3.488	3.412	3.106	3.315	3.069	3.146	3.097
^{IV}Al	0.870	0.958	0.912	0.917	0.512	0.588	0.889	0.685	0.762	0.757	0.832
^{VI}Al	0.000	0.000	0.000	0.000	0.476	0.483	0.000	0.067	0.000	0.000	0.000
Al	0.870	0.958	0.912	0.917	0.988	1.071	0.889	0.752	0.762	0.757	0.832
Ti	0.061	0.068	0.068	0.075	0.029	0.037	0.037	0.154	0.024	0.023	0.036
Fe	0.708	0.754	0.815	0.740	0.384	0.449	0.586	1.199	0.506	0.509	0.544
Mn	0.023	0.031	0.023	0.025	0.018	0.016	0.005	0.000	0.023	0.009	0.011
Mg	2.125	2.155	2.044	2.110	1.719	1.708	2.391	1.409	2.657	2.592	2.551
Ca	0.007	0.000	0.006	0.016	0.000	0.017	0.011	0.142	0.020	0.018	0.010
Na	0.018	0.000	0.030	0.011	0.008	0.060	0.033	0.076	0.028	0.019	0.033
K	0.902	0.888	0.981	0.941	0.716	0.552	0.738	0.292	0.903	0.774	0.704
ΣCations	7.840	7.876	7.930	7.889	7.351	7.322	7.798	7.339	7.992	7.849	7.820
^{IV}Al	0.870	0.958	0.912	0.917	0.512	0.588	0.889	0.685	0.762	0.757	0.832
Fe/(Fe+Mg)	0.250	0.259	0.285	0.260	0.183	0.208	0.197	0.460	0.160	0.164	0.176

* N=normally pleochroic mica; R=reversely pleochroic mica as estimated by earlier optical examination

[1] Numbers here refer first to the point # in the file and the set in brackets corresponding to the TEM image(s)

[2] Total is set to 100.00 due to the fact that the analyses are EDS ones

Appendix A-10: AEM analyses of mica

Sample #	BH/18/2.1									BH/18/2.1	
File Name	BH182.1									BH182.1	
Type of Mica*	R?	R?	R?	R?	R?	R?	R?	R?	R?	R?	R?
Description[1]	1-31/05 #4	2-31/05 #1	3 -#2 ed.	4 - #3	5-#4 packet	-#5ed packet	9	11 nr carb.	13 by carb.	18 opp. side	23 by ox.
SiO_2	39.62	35.83	34.11	38.72	35.26	37.90	35.87	49.20	50.23	34.50	41.04
Al_2O_3	11.59	9.02	8.84	11.20	10.15	10.33	10.92	25.76	26.58	10.90	15.52
TiO_2	0.80	0.37	1.48	0.33	0.91	0.84	0.60	0.16	0.28	1.01	1.53
FeO	15.32	14.18	13.96	15.58	18.41	13.81	14.35	5.36	6.98	17.08	19.43
MnO	0.28	0.00	0.35	0.00	0.56	0.12	0.46	0.51	0.00	0.59	0.32
MgO	21.80	27.43	31.49	21.35	21.88	25.38	26.17	4.33	4.01	19.37	11.34
CaO	0.16	0.00	0.00	0.00	0.16	0.00	0.23	0.07	0.00	0.00	0.00
Na_2O	0.54	0.54	1.78	0.15	0.47	0.00	0.19	0.79	0.00	0.77	0.00
K_2O	9.90	12.62	7.98	12.68	12.20	11.62	11.21	13.83	11.92	15.79	10.82
Total[2]	100.00	100.00	100.00	100.00	100.00	100.00	100.00	100.00	100.00	100.00	100.00
	Mineral formulae calculated based on 11 atoms of oxygen										
Si	3.221	3.035	2.858	3.216	3.053	3.125	3.001	3.555	3.571	3.045	3.343
^{IV}Al	0.779	0.795	0.771	0.784	0.915	0.875	0.951	0.445	0.429	0.955	0.657
^{VI}Al	0.202	0.000	0.000	0.184	0.000	0.012	0.000	1.492	1.539	0.047	0.659
Al	0.981	0.795	0.771	0.968	0.915	0.887	0.951	1.937	1.967	1.001	1.316
Ti	0.038	0.018	0.073	0.016	0.046	0.040	0.029	0.007	0.012	0.052	0.073
Fe	0.626	0.604	0.588	0.651	0.802	0.573	0.604	0.195	0.249	0.758	0.796
Mn	0.012	0.000	0.015	0.000	0.025	0.005	0.019	0.019	0.000	0.027	0.013
Mg	2.048	2.684	3.048	2.048	2.189	2.417	2.529	0.361	0.329	1.976	1.067
Ca	0.009	0.000	0.000	0.000	0.010	0.000	0.013	0.003	0.000	0.000	0.000
Na	0.053	0.056	0.182	0.015	0.050	0.000	0.020	0.070	0.000	0.083	0.000
K	0.578	0.768	0.480	0.756	0.759	0.688	0.674	0.718	0.609	1.001	0.633
ΣCations	7.566	7.961	8.015	7.670	7.848	7.735	7.841	6.864	6.738	7.944	7.242
^{IV}Al	0.779	0.795	0.771	0.784	0.915	0.875	0.951	0.445	0.429	0.955	0.657
Fe/(Fe+Mg)	0.234	0.184	0.162	0.241	0.268	0.192	0.193	0.351	0.431	0.277	0.427

* N=normally pleochroic mica; R=reversely pleochroic mica as estimated by earlier optical examination

[1] Numbers here refer first to the point # in the file and the set in brackets corresponding to the TEM image(s)

[2] Total is set to 100.00 due to the fact that the analyses are EDS ones

Appendix A-10: AEM analyses of mica

Sample #	BH/18/2.1	BH/18/2.1									
File Name	BH182.1	BH182.1chl2									
Type of Mica*	R?	R?	R?	R?	R?	R?	R?	R?	R?	R?	R
Description[1]	24 further	9 by prev.	12(6630-2)	13 by prev.	15	16 by silica	17(6638-42)	18(6643-5)	19 by 6639	20 further	25(3590-3)
SiO_2	39.27	36.55	37.35	36.66	36.85	36.18	35.23	35.73	33.21	34.30	36.87
Al_2O_3	14.37	9.12	8.70	9.30	8.48	9.16	10.38	10.23	10.18	10.13	11.66
TiO_2	0.00	0.81	0.60	0.00	0.38	0.48	1.10	1.00	1.15	1.10	0.75
FeO	20.72	13.26	11.67	12.08	11.66	11.72	17.31	15.63	21.76	15.65	17.41
MnO	0.73	0.27	0.10	0.00	0.29	0.35	0.33	0.32	0.45	0.46	0.29
MgO	12.99	25.79	27.28	27.46	27.12	26.88	22.24	22.00	20.90	21.71	19.89
CaO	0.04	0.52	0.58	0.34	0.22	0.67	1.18	1.13	1.51	1.39	0.22
Na_2O	0.18	0.12	0.10	0.07	0.05	0.01	0.10	0.09	0.15	0.25	0.00
K_2O	11.69	13.57	13.62	14.10	14.97	14.56	12.12	13.88	10.70	15.01	12.91
Total[2]	100.00	100.00	100.00	100.00	100.00	100.00	100.00	100.00	100.00	100.00	100.00
				Mineral formulae calculated based on 11 atoms of oxygen							
Si	3.294	3.088	3.117	3.079	3.111	3.060	3.033	3.074	2.947	3.009	3.132
^{IV}Al	0.706	0.802	0.756	0.813	0.745	0.806	0.930	0.916	0.940	0.924	0.868
^{VI}Al	0.550	0.000	0.000	0.000	0.000	0.000	0.000	0.000	0.000	0.000	0.163
Al	1.255	0.802	0.756	0.813	0.745	0.806	0.930	0.916	0.940	0.924	1.031
Ti	0.000	0.040	0.029	0.000	0.019	0.024	0.056	0.050	0.060	0.056	0.037
Fe	0.874	0.563	0.490	0.510	0.495	0.499	0.749	0.676	0.971	0.690	0.744
Mn	0.031	0.012	0.004	0.000	0.012	0.015	0.015	0.014	0.020	0.020	0.012
Mg	1.259	2.517	2.630	2.664	2.645	2.627	2.212	2.186	2.143	2.200	1.952
Ca	0.003	0.031	0.034	0.020	0.013	0.040	0.071	0.068	0.094	0.085	0.013
Na	0.019	0.012	0.010	0.007	0.006	0.001	0.011	0.009	0.016	0.027	0.000
K	0.704	0.824	0.816	0.850	0.908	0.884	0.749	0.857	0.682	0.946	0.787
ΣCations	7.439	7.889	7.888	7.943	7.954	7.956	7.826	7.851	7.872	7.959	7.709
^{IV}Al	0.706	0.802	0.756	0.813	0.745	0.806	0.930	0.916	0.940	0.924	0.868
Fe/(Fe+Mg)	0.410	0.183	0.157	0.161	0.158	0.160	0.253	0.236	0.312	0.239	0.276

* N=normally pleochroic mica; R=reversely pleochroic mica as estimated by earlier optical examination

[1] Numbers here refer first to the point # in the file and the set in brackets corresponding to the TEM image(s)

[2] Total is set to 100.00 due to the fact that the analyses are EDS ones

Appendix A-10: AEM analyses of mica

Sample #	BH/18/2.1						BH/18/2.1				
File Name	BH182.1chl2						BH182.1new				
Type of Mica*	R	R	R	R	R	R	R	R	R	R	R
Description[1]	26(3607-9)	27(3602-6)	28(3597-600)	29(3618-22)	30(3623-8)	31(3615-7)	1 #4	2 up a bit	3 down bit	4 nr carb	8 opp.side
SiO_2	39.56	36.90	38.89	36.76	35.83	36.30	39.27	38.31	40.61	37.35	38.02
Al_2O_3	10.26	9.46	9.38	10.68	10.68	11.09	13.01	13.42	13.91	10.98	13.14
TiO_2	0.52	0.36	0.30	0.51	0.22	0.00	0.28	0.33	0.22	0.34	0.34
FeO	15.81	18.83	16.37	19.16	16.19	21.18	17.64	17.04	17.48	18.91	17.63
MnO	0.28	0.13	0.06	0.12	0.47	0.32	0.23	0.01	0.17	0.22	0.02
MgO	25.75	22.36	23.43	20.34	26.24	21.94	16.96	18.37	16.48	18.14	18.26
CaO	0.08	0.22	0.21	0.39	0.49	0.31	0.00	0.16	0.52	0.00	0.07
Na_2O	0.00	0.00	0.00	0.33	0.10	0.26	0.24	0.17	0.33	0.45	1.09
K_2O	7.73	11.75	11.36	11.71	9.78	8.61	12.37	12.19	10.28	13.60	11.42
Total[2]	100.00	100.00	100.00	100.00	100.00	100.00	100.00	100.00	100.00	100.00	100.00
	Mineral formulae calculated based on 11 atoms of oxygen										
Si	3.190	3.153	3.233	3.143	3.004	3.083	3.264	3.184	3.300	3.210	3.174
^{IV}Al	0.810	0.841	0.767	0.857	0.932	0.917	0.736	0.816	0.700	0.790	0.826
^{VI}Al	0.051	0.000	0.044	0.093	0.000	0.063	0.389	0.345	0.476	0.193	0.316
Al	0.861	0.841	0.812	0.950	0.932	0.980	1.125	1.161	1.177	0.983	1.142
Ti	0.025	0.018	0.015	0.025	0.011	0.000	0.014	0.016	0.011	0.017	0.017
Fe	0.641	0.809	0.684	0.824	0.683	0.905	0.737	0.712	0.714	0.818	0.740
Mn	0.012	0.005	0.003	0.005	0.020	0.014	0.010	0.000	0.007	0.010	0.001
Mg	2.399	2.207	2.250	2.009	2.542	2.152	1.628	1.764	1.547	1.801	1.762
Ca	0.004	0.013	0.012	0.023	0.029	0.018	0.000	0.009	0.030	0.000	0.004
Na	0.000	0.000	0.000	0.034	0.010	0.026	0.024	0.018	0.032	0.047	0.111
K	0.448	0.721	0.678	0.719	0.589	0.525	0.738	0.728	0.600	0.840	0.685
ΣCations	7.579	7.769	7.686	7.733	7.819	7.703	7.541	7.592	7.418	7.725	7.636
^{IV}Al	0.810	0.841	0.767	0.857	0.932	0.917	0.736	0.816	0.700	0.790	0.826
Fe/(Fe+Mg)	0.211	0.268	0.233	0.291	0.212	0.296	0.312	0.288	0.316	0.312	0.296

* N=normally pleochroic mica; R=reversely pleochroic mica as estimated by earlier optical examination

[1] Numbers here refer first to the point # in the file and the set in brackets corresponding to the TEM image(s)

[2] Total is set to 100.00 due to the fact that the analyses are EDS ones

Appendix A-10: AEM analyses of mica

Sample #	BH/18/2.1										
File Name	new18										
Type of Mica*	R	R	R	R	R	R	R	R	R	R	R
Description[1]	1	2 more	3 by 1& 2	4 by 1& 2	5	6	7	8	9	10 at hump	11 at top
SiO_2	37.02	37.02	36.08	45.17	35.24	34.66	34.31	34.60	34.62	35.58	36.22
Al_2O_3	10.06	10.06	10.46	19.74	10.15	10.70	11.39	11.35	9.97	12.20	11.73
TiO_2	0.55	0.55	0.37	0.23	0.66	1.03	0.77	1.12	0.25	0.42	0.57
FeO	13.55	13.55	9.05	15.44	11.94	17.66	18.22	19.00	18.58	7.99	14.47
MnO	0.20	0.20	0.22	0.00	0.26	0.88	0.68	0.78	0.68	0.40	0.30
MgO	25.21	25.21	29.29	6.42	26.51	20.21	20.11	18.53	20.65	29.36	24.48
CaO	0.23	0.23	0.17	0.53	0.15	0.45	0.31	0.16	0.56	0.25	0.16
Na_2O	0.11	0.11	0.07	0.99	0.16	0.25	0.42	0.00	0.61	0.42	0.83
K_2O	13.07	13.07	14.30	11.47	14.93	14.17	13.80	14.48	14.08	13.39	11.23
Total[2]	100.00	100.00	100.00	100.00	100.00	100.00	100.00	100.00	100.00	100.00	100.00
				Mineral formulae calculated based on 11 atoms of oxygen							
Si	3.100	3.100	2.990	3.506	2.995	3.039	3.008	3.047	3.060	2.919	3.023
^{IV}Al	0.877	0.877	0.902	0.494	0.898	0.961	0.992	0.953	0.917	1.042	0.977
^{VI}Al	0.000	0.000	0.000	1.101	0.000	0.015	0.047	0.088	0.000	0.000	0.043
Al	0.877	0.877	0.902	1.595	0.898	0.976	1.039	1.040	0.917	1.042	1.020
Ti	0.027	0.027	0.018	0.011	0.033	0.053	0.039	0.058	0.013	0.020	0.028
Fe	0.571	0.571	0.377	0.603	0.510	0.779	0.803	0.841	0.826	0.330	0.607
Mn	0.009	0.009	0.009	0.000	0.011	0.039	0.031	0.035	0.031	0.017	0.013
Mg	2.439	2.439	2.805	0.576	2.603	2.047	2.036	1.885	2.108	2.783	2.360
Ca	0.014	0.014	0.010	0.029	0.009	0.028	0.019	0.010	0.035	0.015	0.009
Na	0.011	0.011	0.007	0.094	0.017	0.027	0.045	0.000	0.066	0.042	0.084
K	0.786	0.786	0.851	0.639	0.911	0.892	0.869	0.916	0.894	0.789	0.673
ΣCations	7.833	7.833	7.970	7.052	7.987	7.880	7.890	7.833	7.949	7.955	7.818
^{IV}Al	0.877	0.877	0.902	0.494	0.898	0.961	0.992	0.953	0.917	1.042	0.977
Fe/(Fe+Mg)	0.190	0.190	0.119	0.511	0.164	0.276	0.283	0.309	0.281	0.106	0.205

* N=normally pleochroic mica; R=reversely pleochroic mica as estimated by earlier optical examination

[1] Numbers here refer first to the point # in the file and the set in brackets corresponding to the TEM image(s)

[2] Total is set to 100.00 due to the fact that the analyses are EDS ones

Appendix A-10. AEM analyses of mica

Sample #	BII/18/2.1										
File Name	new18										
Type of Mica*	R	R	R	R	R	R	R	R	R	R	R
Description[1]	12 packet	13 mid.	14 by bump	15	16	17	18	19	20	21	22
SiO_2	36.27	36.51	38.02	35.68	36.93	36.99	37.07	36.98	34.92	37.55	35.80
Al_2O_3	11.20	11.56	12.09	10.87	10.84	10.54	10.46	12.57	11.97	12.75	11.51
TiO_2	0.95	0.59	0.51	0.77	0.56	0.40	0.46	0.52	0.33	0.30	0.56
FeO	15.99	15.64	18.31	16.08	16.82	15.50	14.60	15.07	13.67	14.52	15.25
MnO	0.30	0.27	0.27	0.29	0.31	0.05	0.32	0.23	0.51	0.37	0.34
MgO	23.06	22.11	17.18	22.85	21.10	23.72	23.95	22.22	27.11	22.67	25.04
CaO	0.12	0.37	0.12	0.00	0.17	0.00	0.10	0.22	0.20	0.41	0.45
Na_2O	0.55	0.63	0.97	0.97	0.39	0.67	1.12	0.57	0.35	0.39	0.11
K_2O	11.56	12.32	12.54	12.50	12.88	12.13	11.92	11.62	10.94	11.05	10.94
Total[2]	100.00	100.00	100.00	100.00	100.00	100.00	100.00	100.00	100.00	100.00	100.00
	Mineral formulae calculated based on 11 atoms of oxygen										
Si	3.056	3.080	3.220	3.044	3.139	3.108	3.108	3.076	2.918	3.093	2.999
^{IV}Al	0.944	0.920	0.780	0.956	0.861	0.892	0.892	0.924	1.041	0.907	1.001
^{VI}Al	0.039	0.096	0.286	0.009	0.098	0.031	0.020	0.164	0.000	0.187	0.003
Al	0.983	1.016	1.066	0.965	0.959	0.922	0.913	1.088	1.041	1.093	1.004
Ti	0.047	0.029	0.025	0.039	0.028	0.020	0.023	0.026	0.016	0.014	0.027
Fe	0.677	0.663	0.780	0.690	0.719	0.655	0.615	0.631	0.575	0.601	0.643
Mn	0.013	0.012	0.012	0.012	0.013	0.002	0.014	0.010	0.022	0.015	0.015
Mg	2.245	2.155	1.681	2.252	2.072	2.303	2.319	2.135	2.617	2.157	2.423
Ca	0.007	0.022	0.007	0.000	0.010	0.000	0.006	0.013	0.012	0.024	0.026
Na	0.056	0.065	0.100	0.101	0.041	0.069	0.115	0.058	0.035	0.039	0.012
K	0.700	0.746	0.763	0.766	0.786	0.732	0.718	0.694	0.656	0.654	0.658
ΣCations	7.784	7.788	7.654	7.869	7.767	7.811	7.830	7.730	7.891	7.692	7.807
^{IV}Al	0.944	0.920	0.780	0.956	0.861	0.892	0.892	0.924	1.041	0.907	1.001
Fe/(Fe+Mg)	0.232	0.235	0.317	0.235	0.258	0.221	0.210	0.228	0.180	0.218	0.210

* N=normally pleochroic mica; R=reversely pleochroic mica as estimated by earlier optical examination

[1] Numbers here refer first to the point # in the file and the set in brackets corresponding to the TEM image(s)

[2] Total is set to 100.00 due to the fact that the analyses are EDS ones

Appendix A-10: AEM analyses of mica

Sample #	BH/18/2.1										
File Name	new18										
Type of Mica*	R	R	R	R	R	R	R	R	R	R	R
Description[1]	23	24	25	26	27	28	29	30	31	32	33
SiO_2	36.22	35.96	37.34	37.52	37.42	37.22	36.63	38.61	39.70	36.15	38.18
Al_2O_3	11.27	10.58	11.29	11.29	10.76	11.98	10.51	12.62	14.32	11.34	12.30
TiO_2	0.33	0.37	0.27	0.34	0.41	1.23	0.92	0.72	0.57	0.66	0.36
FeO	14.09	15.15	15.36	17.35	17.52	17.54	17.99	17.87	17.05	15.90	17.80
MnO	0.31	0.21	0.28	0.17	0.12	0.03	0.22	0.17	0.00	0.21	0.16
MgO	25.45	24.81	23.12	20.12	20.01	18.48	19.32	16.16	14.99	24.32	16.25
CaO	0.21	0.19	0.15	0.32	0.08	0.18	0.03	0.19	0.21	0.05	0.23
Na_2O	0.92	0.30	0.53	0.52	0.64	0.53	0.74	0.83	0.49	0.20	0.31
K_2O	11.20	12.43	11.67	12.35	13.04	12.80	13.63	12.83	12.67	11.17	14.42
Total[2]	100.00	100.00	100.00	100.00	100.00	100.00	100.00	100.00	100.00	100.00	100.00
	Mineral formulae calculated based on 11 atoms of oxygen										
Si	3.023	3.042	3.116	3.172	3.185	3.154	3.158	3.248	3.276	3.032	3.247
^{IV}Al	0.977	0.932	0.884	0.828	0.815	0.846	0.842	0.752	0.724	0.968	0.753
^{VI}Al	0.002	0.000	0.097	0.166	0.138	0.210	0.101	0.353	0.506	0.022	0.337
Al	0.979	0.932	0.981	0.994	0.953	1.057	0.943	1.105	1.230	0.990	1.089
Ti	0.016	0.018	0.013	0.017	0.020	0.061	0.047	0.036	0.027	0.032	0.018
Fe	0.591	0.645	0.645	0.738	0.750	0.747	0.780	0.756	0.708	0.671	0.761
Mn	0.013	0.009	0.012	0.008	0.005	0.001	0.010	0.007	0.000	0.009	0.007
Mg	2.454	2.424	2.229	1.965	1.968	1.809	1.924	1.571	1.429	2.356	1.597
Ca	0.012	0.011	0.009	0.019	0.005	0.010	0.002	0.011	0.012	0.003	0.014
Na	0.094	0.031	0.054	0.054	0.067	0.055	0.078	0.085	0.049	0.021	0.032
K	0.671	0.755	0.700	0.750	0.797	0.779	0.844	0.775	0.751	0.673	0.881
ΣCations	7.854	7.867	7.757	7.716	7.750	7.674	7.785	7.594	7.482	7.787	7.646
^{IV}Al	0.977	0.932	0.884	0.828	0.815	0.846	0.842	0.752	0.724	0.968	0.753
Fe/(Fe+Mg)	0.194	0.210	0.224	0.273	0.276	0.292	0.288	0.325	0.331	0.222	0.323

* N=normally pleochroic mica; R=reversely pleochroic mica as estimated by earlier optical examination

[1] Numbers here refer first to the point # in the file and the set in brackets corresponding to the TEM image(s)

[2] Total is set to 100.00 due to the fact that the analyses are EDS ones

Appendix A-10: AEM analyses of mica

Sample #	BH/18/2.1										
File Name	new18										
Type of Mica*	R	R	R	R	R	R	R	R	R	R	R
Description[1]	34	35	36 v. top	37	38	39	40	41	42	43	50
SiO_2	38.52	35.29	35.52	36.19	36.29	34.77	37.19	34.45	36.79	37.12	35.46
Al_2O_3	11.76	10.78	10.16	10.46	11.33	11.52	11.38	9.46	9.68	10.58	9.35
TiO_2	0.31	0.40	0.66	0.71	0.43	6.03	0.68	4.66	0.80	1.02	0.45
FeO	17.00	16.05	14.21	16.93	19.45	18.04	21.78	15.55	15.57	16.18	12.19
MnO	0.11	0.13	0.01	0.30	0.26	0.18	0.16	0.45	0.30	0.27	0.22
MgO	17.47	23.60	24.82	20.59	17.10	14.83	12.99	20.87	22.16	19.97	29.21
CaO	0.16	0.00	0.39	0.25	0.28	0.26	0.37	0.57	0.19	0.35	0.00
Na_2O	0.37	0.46	0.26	0.72	0.93	0.90	0.80	0.92	0.46	0.69	0.38
K_2O	14.31	13.29	13.97	13.85	13.93	13.47	14.64	13.05	14.05	13.83	12.74
Total[2]	100.00	100.00	100.00	100.00	100.00	100.00	100.00	100.00	100.00	100.00	100.00
	Mineral formulae calculated based on 11 atoms of oxygen										
Si	3.259	3.025	3.030	3.120	3.163	3.024	3.273	2.985	3.145	3.167	2.981
^{IV}Al	0.741	0.962	0.902	0.880	0.837	0.976	0.727	0.853	0.855	0.833	0.819
^{VI}Al	0.294	0.000	0.000	0.059	0.191	0.068	0.316	0.000	0.007	0.107	0.000
Al	1.035	0.962	0.902	0.939	1.028	1.043	1.043	0.853	0.862	0.940	0.819
Ti	0.015	0.020	0.033	0.036	0.022	0.307	0.035	0.237	0.040	0.051	0.022
Fe	0.723	0.692	0.610	0.734	0.852	0.789	0.964	0.678	0.669	0.694	0.515
Mn	0.005	0.006	0.000	0.013	0.012	0.008	0.007	0.020	0.013	0.012	0.010
Mg	1.708	2.337	2.446	2.051	1.721	1.490	1.320	2.089	2.188	1.968	2.837
Ca	0.009	0.000	0.023	0.015	0.017	0.016	0.023	0.035	0.012	0.021	0.000
Na	0.038	0.048	0.027	0.076	0.099	0.096	0.086	0.098	0.048	0.072	0.039
K	0.869	0.818	0.856	0.858	0.872	0.841	0.926	0.812	0.862	0.848	0.770
ΣCations	7.662	7.907	7.927	7.841	7.787	7.615	7.676	7.806	7.839	7.772	7.992
^{IV}Al	0.741	0.962	0.902	0.880	0.837	0.976	0.727	0.853	0.855	0.833	0.819
Fe/(Fe+Mg)	0.297	0.228	0.200	0.264	0.331	0.346	0.422	0.245	0.234	0.261	0.154

* N=normally pleochroic mica; R=reversely pleochroic mica as estimated by earlier optical examination

[1] Numbers here refer first to the point # in the file and the set in brackets corresponding to the TEM image(s)

[2] Total is set to 100.00 due to the fact that the analyses are EDS ones

Appendix A-10: AEM analyses of mica

Sample #	BII/18/2.1				BII/18/2.2					BII/18/2.1	
File Name	new18				18last					nbh182.1	
Type of Mica*	R	R	R	R	R	R	R	R	R	R	R
Description[1]	51	52	53 fl.gr.	54 by prev.	20 bump	21 bump	22 next dip	23	24	4 by ox.	6 by ox.
SiO_2	36.09	37.87	39.68	36.33	26.44	28.77	28.41	30.10	31.18	35.46	33.25
Al_2O_3	10.75	5.81	15.10	11.69	7.13	7.61	7.44	7.83	8.22	8.65	9.17
TiO_2	0.96	0.26	1.20	0.67	1.00	0.58	0.67	0.53	0.56	0.38	0.48
FeO	16.09	25.06	16.20	16.13	26.41	22.19	22.34	21.33	18.30	19.27	20.34
MnO	0.94	0.18	0.71	0.78	0.75	0.88	0.70	0.55	0.54	0.80	0.49
MgO	19.39	18.60	13.67	19.72	18.74	22.11	22.19	21.88	23.64	20.33	21.36
CaO	0.06	0.59	0.16	0.17	0.77	0.61	0.78	0.45	0.68	0.04	0.09
Na_2O	0.67	0.79	0.00	0.30	0.00	0.08	0.28	0.00	0.10	0.41	0.06
K_2O	15.04	10.84	13.27	14.22	18.76	17.17	17.20	17.33	16.77	14.66	14.76
Total[2]	100.00	100.00	100.00	100.00	100.00	100.00	100.00	100.00	100.00	100.00	100.00
	Mineral formulae calculated based on 11 atoms of oxygen										
Si	3.128	3.357	3.269	3.112	2.699	2.778	2.757	2.857	2.877	3.146	3.000
^{IV}Al	0.872	0.536	0.731	0.888	0.758	0.765	0.751	0.774	0.789	0.798	0.861
^{VI}Al	0.098	0.000	0.564	0.155	0.000	0.000	0.000	0.000	0.000	0.000	0.000
Al	0.970	0.536	1.295	1.043	0.758	0.765	0.751	0.774	0.789	0.798	0.861
Ti	0.049	0.013	0.058	0.034	0.060	0.033	0.038	0.030	0.030	0.020	0.025
Fe	0.701	1.117	0.671	0.695	1.355	1.078	1.090	1.018	0.849	0.860	0.923
Mn	0.042	0.008	0.030	0.034	0.039	0.043	0.035	0.027	0.026	0.036	0.023
Mg	1.942	1.905	1.301	1.952	2.210	2.467	2.488	2.399	2.520	2.083	2.226
Ca	0.004	0.036	0.009	0.010	0.055	0.041	0.053	0.030	0.044	0.002	0.005
Na	0.071	0.086	0.000	0.032	0.000	0.009	0.034	0.000	0.012	0.045	0.006
K	0.936	0.690	0.785	0.875	1.375	1.191	1.199	1.182	1.112	0.934	0.956
ΣCations	7.842	7.749	7.418	7.786	8.550	8.406	8.445	8.317	8.259	7.925	8.026
^{IV}Al	0.872	0.536	0.731	0.888	0.758	0.765	0.751	0.774	0.789	0.798	0.861
Fe/(Fe+Mg)	0.265	0.370	0.340	0.263	0.380	0.304	0.305	0.298	0.252	0.292	0.293

* N=normally pleochroic mica; R=reversely pleochroic mica as estimated by earlier optical examination

[1] Numbers here refer first to the point # in the file and the set in brackets corresponding to the TEM image(s)

[2] Total is set to 100.00 due to the fact that the analyses are EDS ones

Appendix A-10: AEM analyses of mica

Sample #	BH/18/2.1								BH/18/2.1		
File Name	nbh182.1								nbh182.1		
Type of Mica*	R	R	R	R	R	R	R	R	R	R	R
Description[1]	8 by ox.	10(6137-39)	11(6137-39)	12 hole(74)	13 bot(71-3)	14 opp.side	15(6203-7)	16(6203-7)	33(6232-5)	34(6237-40)	35 by prev.
SiO_2	33.48	30.82	33.13	37.10	33.93	34.80	33.93	33.77	29.06	34.80	33.12
Al_2O_3	9.00	8.98	9.26	7.87	7.80	8.34	11.17	9.55	7.05	9.13	8.10
TiO_2	0.00	0.65	0.57	0.00	0.46	0.50	0.43	1.36	0.83	0.58	0.75
FeO	24.85	27.46	19.07	14.80	14.46	14.34	18.53	18.13	25.75	14.18	15.35
MnO	1.59	0.04	0.13	0.54	0.42	0.37	1.37	0.79	0.61	0.05	0.44
MgO	16.97	18.61	21.78	26.31	26.69	26.90	22.36	20.68	19.82	27.74	26.94
CaO	0.14	0.31	0.30	0.00	0.09	0.18	0.38	0.11	0.18	0.16	0.09
Na_2O	0.26	0.00	0.25	0.00	0.09	0.06	0.01	0.11	0.02	0.02	0.20
K_2O	13.71	13.13	15.51	13.37	16.07	14.50	11.81	15.49	16.69	13.34	15.00
Total[2]	100.00	100.00	100.00	100.00	100.00	100.00	100.00	100.00	100.00	100.00	100.00
				Mineral formulae calculated based on 11 atoms of oxygen							
Si	3.092	2.905	2.984	3.153	2.991	3.013	2.958	3.016	2.844	2.975	2.928
^{IV}Al	0.865	0.881	0.868	0.697	0.715	0.752	1.014	0.888	0.718	0.812	0.746
^{VI}Al	0.000	0.000	0.000	0.000	0.000	0.000	0.000	0.000	0.000	0.000	0.000
Al	0.865	0.881	0.868	0.697	0.715	0.752	1.014	0.888	0.718	0.812	0.746
Ti	0.000	0.036	0.030	0.000	0.024	0.025	0.022	0.071	0.048	0.029	0.039
Fe	1.154	1.302	0.864	0.633	0.641	0.624	0.812	0.814	1.267	0.610	0.683
Mn	0.075	0.002	0.006	0.023	0.019	0.017	0.061	0.036	0.030	0.002	0.020
Mg	1.810	2.026	2.266	2.584	2.718	2.691	2.252	2.134	2.241	2.740	2.752
Ca	0.009	0.021	0.019	0.000	0.005	0.011	0.023	0.007	0.012	0.009	0.006
Na	0.029	0.000	0.028	0.000	0.010	0.006	0.001	0.012	0.002	0.002	0.022
K	0.910	0.889	1.003	0.816	1.018	0.902	0.740	0.994	1.173	0.820	0.953
ΣCations	7.945	8.063	8.068	7.907	8.141	8.040	7.883	7.972	8.337	8.000	8.148
^{IV}Al	0.865	0.881	0.868	0.697	0.715	0.752	1.014	0.888	0.718	0.812	0.746
Fe/(Fe+Mg)	0.389	0.391	0.276	0.197	0.191	0.188	0.265	0.276	0.361	0.182	0.199

* N=normally pleochroic mica; R=reversely pleochroic mica as estimated by earlier optical examination

[1] Numbers here refer first to the point # in the file and the set in brackets corresponding to the TEM image(s)

[2] Total is set to 100.00 due to the fact that the analyses are EDS ones

Appendix A-10. AEM analyses of mica

Sample #	BH/18/2.1					BH/18/2.1					
File Name	nbh182.1					bh182.1dec					
Type of Mica*	R	R	R	R	R	R	R	R	R	R	R
Description[1]	36 by prev.	37(6809-10)	41	42(6302)	43	1 by crack	2(6419-22)	3(6413-8)	4(6423-7)	5(6428-32)	6 by prev.
SiO_2	33.97	34.64	34.69	31.64	32.52	33.77	33.31	33.96	37.13	34.94	33.57
Al_2O_3	9.12	7.55	9.33	8.09	7.94	10.68	9.92	11.33	10.87	10.36	11.29
TiO_2	0.61	0.89	0.90	1.12	0.59	1.52	1.11	0.94	0.92	0.00	1.43
FeO	15.71	21.52	18.70	19.78	20.69	18.59	23.37	21.06	18.28	21.35	20.89
MnO	0.68	0.27	0.21	0.32	0.50	0.18	0.45	0.31	0.51	0.69	0.31
MgO	26.33	23.37	24.53	22.82	22.02	22.38	17.63	19.53	18.45	20.50	18.65
CaO	0.00	0.21	0.16	0.05	0.09	0.53	0.00	0.17	0.00	0.09	0.29
Na_2O	0.17	0.06	0.07	0.08	0.17	0.00	0.16	0.09	0.00	0.01	0.25
K_2O	13.41	11.49	11.41	16.10	15.48	12.36	14.05	12.60	13.85	12.06	13.32
Total[2]	100.00	100.00	100.00	100.00	100.00	100.00	100.00	100.00	100.00	100.00	100.00
	Mineral formulae calculated based on 11 atoms of oxygen										
Si	2.954	3.064	3.002	2.911	2.982	2.946	3.031	2.995	3.190	3.069	2.983
^{IV}Al	0.826	0.695	0.840	0.775	0.758	0.970	0.939	1.005	0.810	0.931	1.017
^{VI}Al	0.000	0.000	0.000	0.000	0.000	0.000	0.000	0.035	0.162	0.016	0.027
Al	0.826	0.695	0.840	0.775	0.758	0.970	0.939	1.040	0.972	0.947	1.044
Ti	0.031	0.046	0.046	0.060	0.032	0.078	0.059	0.049	0.046	0.000	0.074
Fe	0.687	0.957	0.814	0.915	0.954	0.816	1.070	0.934	0.790	0.943	0.934
Mn	0.030	0.012	0.009	0.015	0.023	0.008	0.021	0.014	0.022	0.031	0.014
Mg	2.646	2.388	2.453	2.425	2.332	2.255	1.853	1.990	1.831	2.080	1.915
Ca	0.000	0.013	0.010	0.003	0.006	0.032	0.000	0.011	0.000	0.006	0.018
Na	0.018	0.006	0.007	0.009	0.019	0.000	0.017	0.010	0.000	0.001	0.027
K	0.837	0.730	0.710	1.064	1.020	0.774	0.918	0.798	0.854	0.761	0.850
ΣCations	8.029	7.911	7.891	8.177	8.127	7.879	7.908	7.840	7.705	7.838	7.859
^{IV}Al	0.826	0.695	0.840	0.775	0.758	0.970	0.939	1.005	0.810	0.931	1.017
Fe/(Fe+Mg)	0.206	0.286	0.249	0.274	0.290	0.266	0.366	0.319	0.301	0.312	0.328

* N=normally pleochroic mica; R=reversely pleochroic mica as estimated by earlier optical examination

[1] Numbers here refer first to the point # in the file and the set in brackets corresponding to the TEM image(s)

[2] Total is set to 100.00 due to the fact that the analyses are EDS ones

Appendix A-10: AEM analyses of mica

Sample #	BH/18/2.1				BH/18/2.1						
File Name	bh182.1dec				bh182.1decb						
Type of Mica*	R	R	R	R	R	R	R	R	R	R	R
Description[1]	7 few defects	8 defects	9(8441-4)	10 further	4	5 by prev.	6 by ox.	7 by ox.	8by(6445-8)	9(6453-6)	10by(6453-6)
SiO_2	33.60	41.00	36.15	35.08	38.04	35.47	35.57	31.53	27.81	29.96	33.57
Al_2O_3	10.33	12.70	8.22	8.94	11.62	8.37	7.82	6.23	5.41	7.13	8.14
TiO_2	1.79	0.18	0.34	0.59	0.50	0.38	0.45	0.61	0.86	0.62	0.43
FeO	20.10	13.09	20.15	19.40	16.36	18.68	19.37	28.05	32.50	27.61	21.96
MnO	0.13	0.02	0.00	0.37	0.19	0.38	0.44	0.47	0.00	0.42	0.61
MgO	21.43	21.32	21.37	21.81	18.40	22.36	20.73	13.12	11.47	15.28	19.24
CaO	0.05	0.00	0.04	0.08	0.17	0.00	0.14	0.35	0.61	0.17	0.20
Na_2O	0.02	0.04	0.20	0.12	0.04	0.11	0.16	0.02	0.00	0.00	0.01
K_2O	12.55	11.64	13.54	13.61	14.69	14.25	15.33	19.62	21.34	18.81	15.85
Total[2]	100.00	100.00	100.00	100.00	100.00	100.00	100.00	100.00	100.00	100.00	100.00
	Mineral formulae calculated based on 11 atoms of oxygen										
Si	2.959	3.281	3.172	3.088	3.223	3.120	3.169	3.144	2.977	2.985	3.083
^{IV}Al	0.947	0.719	0.751	0.819	0.777	0.766	0.725	0.646	0.603	0.740	0.778
^{VI}Al	0.000	0.339	0.000	0.000	0.249	0.000	0.000	0.000	0.000	0.000	0.000
Al	0.947	1.058	0.751	0.819	1.025	0.766	0.725	0.646	0.603	0.740	0.778
Ti	0.092	0.009	0.017	0.030	0.025	0.020	0.023	0.036	0.054	0.037	0.023
Fe	0.890	0.527	0.889	0.859	0.697	0.827	0.868	1.407	1.750	1.383	1.014
Mn	0.006	0.001	0.000	0.017	0.008	0.017	0.020	0.024	0.000	0.021	0.029
Mg	2.180	1.970	2.166	2.218	1.801	2.272	2.134	1.511	1.419	1.759	2.042
Ca	0.003	0.000	0.003	0.005	0.010	0.000	0.009	0.025	0.046	0.012	0.013
Na	0.002	0.004	0.021	0.013	0.004	0.012	0.017	0.002	0.000	0.000	0.001
K	0.794	0.669	0.853	0.861	0.894	0.900	0.981	1.405	1.641	1.346	1.046
ΣCations	7.873	7.518	7.873	7.909	7.688	7.933	7.945	8.200	8.489	8.282	8.028
^{IV}Al	0.947	0.719	0.751	0.819	0.777	0.766	0.725	0.646	0.603	0.740	0.778
Fe/(Fe+Mg)	0.290	0.211	0.291	0.279	0.279	0.267	0.289	0.482	0.552	0.440	0.332

* N=normally pleochroic mica; R=reversely pleochroic mica as estimated by earlier optical examination

[1] Numbers here refer first to the point # in the file and the set in brackets corresponding to the TEM image(s)

[2] Total is set to 100.00 due to the fact that the analyses are EDS ones

Appendix A-10: AEM analyses of mica

Sample #	BH/18/2.1					BH/18/2.1			
File Name	bh182.1decc					BH182.1chl			
Type of Mica*	R	R	R	R	R	R	R	R	R
Description[1]	3(6467-71)	4(6472-5)	5(6461-7)	6 up prev.	7 below	3	10(6603-6)	11 by silica	12(6608-9)
SiO_2	34.80	35.26	36.94	34.04	35.67	51.89	37.44	42.43	41.32
Al_2O_3	10.29	10.13	10.55	10.17	10.00	18.28	10.11	7.44	10.00
TiO_2	1.46	1.30	0.00	1.72	1.43	0.03	0.74	0.57	0.79
FeO	17.68	17.32	12.91	16.88	17.59	10.44	12.58	21.17	15.24
MnO	0.33	0.41	2.32	0.51	0.56	0.17	0.41	0.26	0.26
MgO	20.34	19.41	20.60	21.44	19.72	5.80	28.34	17.91	22.52
CaO	0.41	0.32	0.39	0.13	0.22	0.07	0.15	0.74	0.91
Na_2O	0.00	0.29	0.13	0.09	0.18	0.41	0.02	0.07	0.02
K_2O	14.69	15.56	16.15	15.02	14.63	12.91	10.21	9.41	8.95
Total[2]	100.00	100.00	100.00	100.00	100.00	100.00	100.00	100.00	100.00
	Mineral formulae calculated based on 11 atoms of oxygen								
Si	3.050	3.098	3.175	2.994	3.112	3.822	3.060	3.521	3.321
^{IV}Al	0.939	0.902	0.825	0.931	0.888	0.178	0.860	0.479	0.679
^{VI}Al	0.000	0.025	0.119	0.000	0.020	1.224	0.000	0.164	0.158
Al	0.939	0.926	0.944	0.931	0.908	1.402	0.860	0.643	0.837
Ti	0.075	0.067	0.000	0.089	0.073	0.001	0.035	0.028	0.037
Fe	0.779	0.765	0.558	0.747	0.772	0.387	0.517	0.883	0.616
Mn	0.015	0.018	0.102	0.023	0.025	0.006	0.017	0.011	0.011
Mg	2.059	1.970	2.045	2.179	1.988	0.493	2.675	1.717	2.091
Ca	0.025	0.020	0.024	0.008	0.013	0.004	0.009	0.043	0.051
Na	0.000	0.031	0.014	0.010	0.019	0.037	0.002	0.007	0.002
K	0.925	0.982	0.997	0.949	0.917	0.683	0.599	0.561	0.517
ΣCations	7.868	7.878	7.859	7.931	7.828	6.836	7.775	7.414	7.482
^{IV}Al	0.939	0.902	0.825	0.931	0.888	0.178	0.860	0.479	0.679
Fe/(Fe+Mg)	0.275	0.280	0.214	0.255	0.280	0.439	0.162	0.340	0.228

* N=normally pleochroic mica; R=reversely pleochroic mica as estimated by earlier optical examination

[1] Numbers here refer first to the point # in the file and the set in brackets corresponding to the TEM image(s)

[2] Total is set to 100.00 due to the fact that the analyses are EDS ones

Appendix A-11: Range of relative errors of AEM analyses

Oxide	Average range of the Relative Errors*
K_2O	0.01-0.03
Na_2O	0.04-0.20
CaO	0.03-0.20
MgO	0.01-0.03
FeO	0.01-0.03
MnO	0.05-0.29
TiO_2	0.04-0.12
Al_2O_3	0.01-0.03
SiO_2	0.01-0.03

* Relative errors were calculated from the peak intensity.

Appendix A-12: XRD data of mica from glimmerite.

Sample #	**BH/18/2**
a (Å)	5.353
b (Å)	9.250
c (Å)	20.17
α (°)	90.00
β (°)	94.72
γ (°)	90.00
Volume (Å^3)	995.44
Errors	
a (Å)	0.002
b (Å)	0.002
c (Å)	0.01
α (°)	0.00
β (°)	0.05
γ (°)	0.00
Volume (Å^3)	0.50
d(060)	1.541

Appendix B:

Strange Lake peralkaline complex

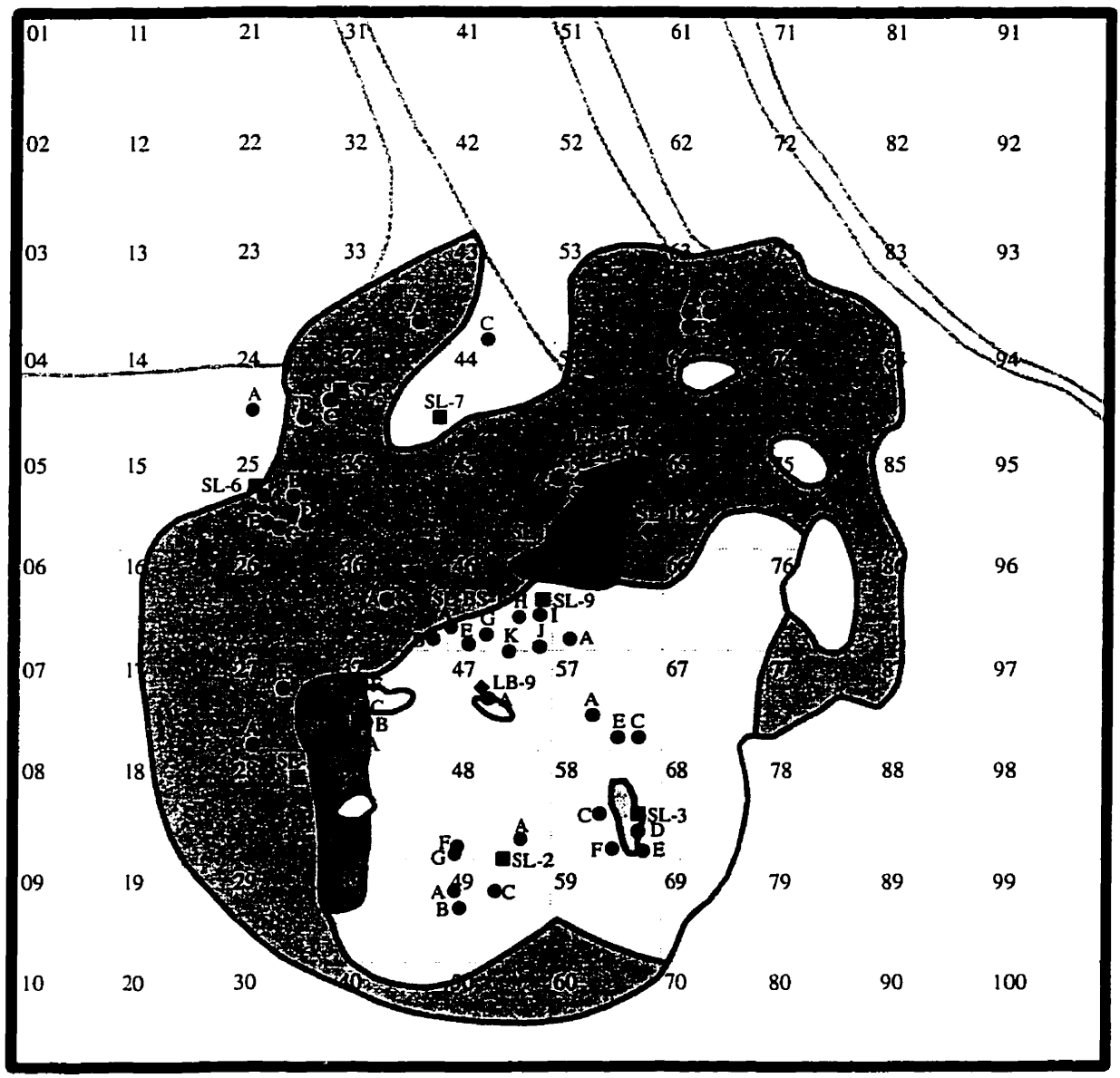

Unit map of the complex showing the locations of the samples.
The coding sequence for the samples is:

circle - surface sample, square - surface sample collected at a different time.

The sample numbering system for the circular code is based on a grid that was superimposed on the complex during sample collection.

The first number represents the grid number, and the letter is the location within the grid.

The final number is based on the number of samples collected at each sample location.

Appendix B-1. Electron microprobe analyses of arfvedsonitic amphibole

Unit	Hypersolvus																						
Sample #	48-A-1		48-A-2									7				48a2		48-A-7					
Description	48a1		48d2ed															48A7ed	mid	center	dker	lter	ared	dk
File	1/1/95	1/1/95	am92	am92	am92	am92	am92	am92	am92	am92	am92	am92	am92	am92	am92	am92	am92	kp	kp	kp	kp	kp	kp	kp
Analysis #	23	25	114	115	118	119	120	121	123	124	125	128	130	131	132	1	2	154	155	156	157	158	159	160
Na_2O	8.93	9.21	8.71	8.75	8.29	8.83	8.71	8.80	8.98	8.49	8.59	8.84	8.83	8.92	9.17	8.98	8.45	9.35	9.65	9.59	9.43	9.42	9.58	9.61
K_2O	1.40	0.81	2.20	1.78	2.66	1.48	1.24	1.35	1.07	1.18	1.37	1.35	1.42	1.27	1.21	0.96	1.94	1.24	1.23	1.24	1.29	1.33	1.39	1.28
CaO	0.24	0.33	0.12	0.52	0.12	0.48	0.78	0.42	0.41	0.70	0.48	0.48	0.37	0.67	0.30	0.39	0.19	0.18	0.16	0.18	0.18	0.17	0.16	0.18
FeO	27.02	28.14	26.21	26.48	27.42	27.36	27.22	27.37	27.79	29.07	29.09	27.71	28.34	27.55	26.69	28.24	28.98	27.90	26.70	27.19	28.02	27.91	26.99	27.08
Fe_2O_3	9.57	8.51	6.51	5.05	4.75	5.45	5.04	5.69	4.91	2.39	2.46	3.73	3.72	4.65	5.48	3.24	2.08	6.39	7.63	7.39	6.23	6.52	7.39	6.89
MgO	0.00	0.00	0.03	0.01	0.01	0.03	0.05	0.03	0.01	0.01	0.01	0.01	0.01	0.03	0.00	0.01	0.02	0.01	0.01	0.01	0.00	0.01	0.01	0.00
MnO	0.88	0.92	0.84	0.83	0.75	0.71	0.68	0.93	0.69	0.64	0.79	0.80	0.88	0.87	0.88	0.83	0.94	0.59	0.60	0.60	0.59	0.62	0.60	0.58
ZnO	0.10	0.11	0.62	0.53	0.46	0.30	0.26	0.57	0.37	0.33	0.51	0.53	0.69	0.62	0.66	0.78	0.71	0.23	0.18	0.22	0.22	0.21	0.22	0.21
Cr_2O_3	0.00	0.02	0.00	0.00	0.00	0.00	0.00	0.00	0.00	0.00	0.00	0.00	0.00	0.00	0.00	0.00	0.00	0.00	0.00	0.00	0.01	0.00	0.00	0.00
V_2O_3	0.00	0.00	0.00	0.00	0.00	0.00	0.00	0.00	0.00	0.00	0.00	0.00	0.00	0.00	0.00	0.00	0.00	0.00	0.00	0.00	0.00	0.02	0.01	0.00
ZrO_2	0.09	0.10	0.08	0.13	0.06	0.15	0.11	0.08	0.11	0.15	0.07	0.09	0.17	0.13	0.08	0.12	0.05	0.16	0.17	0.21	0.17	0.19	0.15	0.22
Nb_2O_5	0.00	0.00	0.05	0.02	0.00	0.00	0.00	0.03	0.01	0.00	0.01	0.00	0.00	0.01	0.00	0.00	0.00	0.00	0.00	0.00	0.00	0.00	0.00	0.00
Y_2O_3	0.00	0.00	0.00	0.00	0.00	0.00	0.00	0.00	0.00	0.00	0.00	0.00	0.00	0.00	0.00	0.00	0.00	0.00	0.00	0.00	0.00	0.00	0.00	0.00
Yb_2O_3	0.00	0.00	0.00	0.00	0.00	0.00	0.00	0.00	0.00	0.00	0.00	0.00	0.00	0.00	0.00	0.00	0.00	0.01	0.00	0.01	0.01	0.00	0.00	0.01
TiO_2	0.00	0.26	0.85	0.87	0.95	0.95	0.68	0.78	0.78	0.91	1.12	0.99	1.08	0.83	0.90	0.91	0.64	0.96	0.96	0.93	0.96	0.95	0.97	0.92
SiO_2	49.24	49.65	49.63	49.38	49.97	49.23	48.68	49.22	49.24	49.02	49.67	49.52	50.03	49.78	49.51	49.63	50.80	50.30	50.32	50.53	50.73	50.71	50.67	50.61
Al_2O_3	1.29	0.99	0.31	0.51	0.21	0.52	1.02	0.80	0.69	0.59	0.46	0.45	0.38	0.59	0.77	0.67	0.13	0.41	0.40	0.41	0.44	0.42	0.42	0.41
F	1.09	1.19	1.90	2.24	2.16	1.83	2.12	1.92	2.13	3.41	2.11	2.24	1.77	2.17	1.80	2.10	2.10	2.12	2.09	2.09	1.70	1.93	1.76	2.15
Cl	0.01	0.02	0.00	0.00	0.00	0.00	0.00	0.00	0.00	0.00	0.00	0.00	0.00	0.00	0.00	0.00	0.00	0.01	0.01	0.01	0.00	0.01	0.01	0.01
H_2O	1.37	1.32	0.95	0.76	0.81	0.97	0.81	0.93	0.82	0.19	0.82	0.76	1.01	0.82	0.99	0.83	0.83	0.87	0.90	0.90	1.08	0.98	1.06	0.87
Total	101.24	101.58	98.98	97.86	98.63	98.27	97.39	98.92	97.98	97.08	97.57	97.49	98.69	98.87	98.44	97.67	97.87	100.72	101.01	101.51	101.05	101.39	101.38	101.02
=O=F	0.46	0.50	0.80	0.94	0.91	0.77	0.89	0.81	0.89	1.43	0.89	0.94	0.75	0.91	0.76	0.88	0.89	0.89	0.88	0.88	0.72	0.81	0.74	0.91
=O=Cl	0.00	0.00	0.00	0.00	0.00	0.00	0.00	0.00	0.00	0.00	0.00	0.00	0.00	0.00	0.00	0.00	0.00	0.00	0.00	0.00	0.00	0.00	0.00	0.00
Total	100.78	101.07	98.18	96.92	97.72	97.50	96.50	98.11	97.09	95.64	96.68	96.54	97.95	97.96	97.68	96.79	96.98	99.83	100.13	100.62	100.34	100.58	100.64	100.12
Si	7.816	7.857	8.059	8.098	8.154	8.038	8.018	7.998	8.064	8.161	8.172	8.146	8.129	8.082	8.046	8.141	8.321	8.022	7.988	7.991	8.039	8.024	8.002	8.031
^{IV}Al	0.184	0.143	0.000	0.000	0.000	0.000	0.000	0.002	0.000	0.000	0.000	0.000	0.000	0.000	0.000	0.000	0.000	0.000	0.012	0.009	0.000	0.000	0.000	0.000
ΣTetrahedral	8.000	8.000	8.059	8.098	8.154	8.038	8.018	8.000	8.064	8.161	8.172	8.146	8.129	8.082	8.046	8.141	8.321	8.022	8.000	8.000	8.039	8.024	8.002	8.031
^{VI}Al	0.058	0.040	0.059	0.099	0.041	0.100	0.197	0.152	0.132	0.116	0.090	0.087	0.074	0.112	0.147	0.129	0.026	0.077	0.064	0.067	0.082	0.078	0.079	0.076
Ti	0.000	0.030	0.103	0.107	0.117	0.117	0.084	0.095	0.096	0.114	0.139	0.123	0.131	0.102	0.110	0.112	0.078	0.115	0.114	0.110	0.114	0.113	0.115	0.110
Fe^{2+}	1.144	1.014	0.796	0.623	0.584	0.670	0.625	0.696	0.606	0.300	0.305	0.462	0.455	0.568	0.670	0.400	0.256	0.767	0.912	0.879	0.743	0.777	0.878	0.823
Fe^{3+}	3.587	3.724	3.559	3.633	3.742	3.736	3.750	3.719	3.806	4.048	4.002	3.812	3.851	3.741	3.627	3.874	3.971	3.722	3.545	3.597	3.714	3.693	3.566	3.594
Mg	0.001	0.000	0.007	0.003	0.003	0.007	0.012	0.008	0.001	0.003	0.002	0.003	0.002	0.007	0.000	0.002	0.004	0.002	0.003	0.003	0.000	0.003	0.002	0.001
Mn	0.119	0.124	0.115	0.115	0.103	0.098	0.095	0.128	0.095	0.090	0.110	0.112	0.121	0.119	0.122	0.115	0.130	0.080	0.081	0.080	0.079	0.083	0.081	0.078
Zn	0.012	0.013	0.074	0.064	0.056	0.036	0.031	0.068	0.044	0.040	0.062	0.064	0.082	0.074	0.079	0.095	0.086	0.027	0.021	0.026	0.026	0.025	0.026	0.024
Cr	0.000	0.002	0.000	0.000	0.000	0.000	0.000	0.000	0.000	0.000	0.000	0.000	0.000	0.000	0.000	0.000	0.000	0.000	0.000	0.000	0.001	0.000	0.000	0.000
V	0.000	0.000	0.000	0.000	0.000	0.000	0.000	0.000	0.000	0.000	0.000	0.000	0.000	0.000	0.000	0.000	0.000	0.000	0.000	0.000	0.000	0.002	0.001	0.000
Zr	0.007	0.008	0.006	0.010	0.005	0.012	0.008	0.006	0.008	0.012	0.006	0.007	0.014	0.010	0.006	0.010	0.004	0.012	0.013	0.016	0.013	0.015	0.011	0.017
Nb	0.000	0.000	0.002	0.001	0.000	0.000	0.000	0.001	0.000	0.000	0.000	0.000	0.000	0.001	0.000	0.000	0.000	0.000	0.000	0.000	0.000	0.000	0.000	0.000
Y	0.000	0.000	0.000	0.000	0.000	0.000	0.000	0.000	0.000	0.000	0.000	0.000	0.000	0.000	0.000	0.000	0.000	0.000	0.000	0.000	0.000	0.000	0.000	0.000
Yb	0.000	0.000	0.000	0.000	0.000	0.000	0.000	0.000	0.000	0.000	0.000	0.000	0.000	0.000	0.000	0.000	0.000	0.000	0.000	0.000	0.000	0.000	0.000	0.000
ΣOctahedral	4.927	4.955	4.722	4.655	4.650	4.775	4.802	4.874	4.790	4.724	4.716	4.669	4.730	4.733	4.761	4.736	4.556	4.803	4.753	4.779	4.771	4.787	4.758	4.724
Na	2.747	2.825	2.743	2.782	2.622	2.794	2.782	2.773	2.851	2.740	2.741	2.818	2.782	2.807	2.889	2.855	2.683	2.892	2.969	2.940	2.898	2.890	2.933	2.956
K	0.284	0.164	0.455	0.373	0.554	0.309	0.260	0.280	0.224	0.251	0.287	0.283	0.295	0.262	0.252	0.200	0.406	0.251	0.250	0.250	0.261	0.269	0.281	0.259
Ca	0.041	0.055	0.021	0.092	0.021	0.083	0.138	0.073	0.071	0.125	0.084	0.084	0.065	0.116	0.052	0.068	0.034	0.031	0.028	0.031	0.030	0.029	0.027	0.031
ΣAlkalis	3.073	3.045	3.219	3.247	3.196	3.187	3.180	3.126	3.146	3.116	3.112	3.185	3.141	3.185	3.193	3.123	3.123	3.175	3.247	3.221	3.189	3.189	3.240	3.246
F	0.548	0.596	0.974	1.163	1.117	0.945	1.104	0.989	1.101	1.794	1.096	1.167	0.910	1.114	0.923	1.088	1.090	1.068	1.047	1.047	0.852	0.964	0.878	1.080
Cl	0.002	0.006	0.000	0.000	0.000	0.000	0.000	0.000	0.000	0.000	0.000	0.000	0.000	0.000	0.000	0.000	0.000	0.002	0.001	0.002	0.001	0.001	0.002	0.001
OH	1.450	1.398	1.026	0.837	0.883	1.055	0.896	1.011	0.899	0.206	0.904	0.833	1.090	0.886	1.077	0.912	0.910	0.930	0.951	0.952	1.147	1.035	1.120	0.919
ΣOH,F,Cl	2.000	2.000	2.000	2.000	2.000	2.000	2.000	2.000	2.000	2.000	2.000	2.000	2.000	2.000	2.000	2.000	2.000	2.000	2.000	2.000	2.000	2.000	2.000	2.000

Acronyms used are: ed=edge; lt=light; lter=lighter; dker=darker; dk=dark; nr=near; mid=middle; 2nd=second; gr=grain
Mineral formulae were calculated based on 23 atoms of oxygen and 16 cations, with Fe3+ calculated by the method of Droop (1987)

Appendix B-1 Electron microprobe analyses of arfvedsonitic amphibole

Unit	Hypersolv													48-F-3					49-C-2					
Sample #	48-A-7																							
Description	lter	48a7ed	near ed	mid	mid	center	opped	ed	2nded	center	center	ed	ed	48f3ed	middk	dk	med	edmed	49c2	2	3			ed
File	kp	kp	kp	kp	kp	kp	kp	kp	kp	kp	kp	kp	kp	kp	kp	kp	kp	kp	am92	am92	am92	am92	am92	am92
Analysis #	161	1.2	2.2	3.2	4.2	5.2	6.2	8.2	9.2	10.2	11.2	12.2	13.2	199	200	201	202	203	72	7.3	74	75	76	79
Na_2O	9.55	9.67	9.60	9.23	8.97	9.23	9.16	9.29	9.24	9.15	9.31	9.38	9.17	9.62	9.35	9.25	9.21	9.23	8.70	8.30	8.31	8.25	8.20	8.81
K_2O	1.25	1.47	1.23	1.22	1.27	1.31	1.41	1.34	1.29	1.31	1.75	1.39	1.62	0.80	1.25	2.10	2.02	1.65	2.49	1.48	1.48	1.44	1.47	1.65
CaO	0.18	0.19	0.34	0.60	0.53	0.40	0.51	0.51	0.45	0.70	0.08	0.41	0.40	0.68	0.63	0.17	0.19	0.33	0.04	0.65	0.58	0.56	0.52	0.19
FeO	27.39	26.82	27.48	28.24	29.53	28.99	28.60	28.59	28.39	28.23	28.02	27.46	28.36	26.20	26.58	25.86	26.46	26.31	25.87	30.32	29.35	28.49	30.92	27.73
Fe_2O_3	7.03	5.49	6.57	6.17	4.47	4.50	4.80	5.37	5.14	4.75	4.76	4.91	4.80	7.83	7.96	7.75	7.48	7.84	6.01	4.03	5.16	6.19	3.95	3.16
MgO	0.01	0.08	0.21	0.25	0.30	0.28	0.35	0.18	0.25	0.25	0.12	0.10	0.18	0.19	0.20	0.16	0.21	0.18	0.03	0.18	0.21	0.23	0.27	0.07
MnO	0.60	1.03	0.65	0.67	0.65	0.66	0.63	0.66	0.77	0.73	0.83	1.04	0.67	0.80	0.87	0.83	0.86	0.84	1.23	0.72	0.65	0.70	0.68	1.09
ZnO	0.27	0.52	0.05	0.16	0.06	0.07	0.13	0.04	0.25	0.15	0.28	0.51	0.11	0.35	0.28	0.23	0.29	0.27	0.94	0.30	0.34	0.26	0.24	0.64
Cr_2O_3	0.00	0.00	0.00	0.00	0.00	0.00	0.00	0.01	0.00	0.00	0.00	0.00	0.00	0.00	0.00	0.01	0.00	0.00	0.00	0.00	0.00	0.00	0.00	0.00
V_2O_3	0.00	0.00	0.00	0.00	0.01	0.01	0.00	0.00	0.01	0.00	0.00	0.01	0.00	0.01	0.00	0.00	0.01	0.01	0.00	0.00	0.00	0.00	0.00	0.00
ZrO_2	0.21	0.11	0.12	0.14	0.13	0.19	0.11	0.15	0.15	0.06	0.09	0.14	0.12	0.06	0.22	0.07	0.06	0.02	0.07	0.16	0.15	0.12	0.08	0.11
Nb_2O_5	0.00	0.00	0.00	0.00	0.00	0.00	0.00	0.00	0.00	0.00	0.00	0.00	0.00	0.00	0.00	0.00	0.00	0.00	0.04	0.04	0.00	0.05	0.00	0.02
Y_2O_3	0.00	0.00	0.00	0.00	0.00	0.00	0.00	0.00	0.00	0.00	0.00	0.00	0.00	0.00	0.00	0.00	0.00	0.00	0.00	0.00	0.00	0.00	0.00	0.00
Yb_2O_3	0.00	0.01	0.00	0.00	0.01	0.01	0.00	0.00	0.01	0.01	0.01	0.00	0.00	0.00	0.01	0.01	0.03	0.02	0.00	0.00	0.00	0.00	0.00	0.00
TiO_2	0.93	1.01	0.88	0.95	1.07	1.12	0.96	1.01	1.08	1.13	1.08	1.03	0.95	1.09	0.91	1.23	1.15	0.81	0.41	1.12	1.15	1.24	1.22	0.92
SiO_2	50.63	51.73	51.17	50.75	50.84	51.24	51.26	51.24	50.98	50.81	51.64	51.26	51.33	49.69	50.14	50.50	50.83	50.29	50.75	49.76	49.00	47.99	49.71	50.27
Al_2O_3	0.41	0.38	0.42	0.55	0.60	0.46	0.61	0.42	0.61	0.59	0.32	0.42	0.47	1.05	0.46	0.61	0.33	0.46	0.19	0.46	0.47	0.46	0.46	0.40
F	2.16	1.91	1.83	1.83	1.67	1.77	1.98	2.07	1.81	2.32	2.09	2.13	2.03	1.65	1.56	1.71	1.56	1.59	2.26	2.26	2.34	2.34	2.30	2.43
Cl	0.01	0.01	0.01	0.01	0.01	0.01	0.01	0.01	0.02	0.01	0.00	0.01	0.01	0.03	0.01	0.00	0.00	0.01	0.00	0.00	0.00	0.00	0.00	0.00
H_2O	0.87	1.00	1.03	1.03	1.10	1.06	0.96	0.92	1.04	0.79	0.91	0.88	0.93	1.10	1.15	1.09	1.17	1.13	0.79	0.79	0.74	0.72	0.77	0.69
Total	101.51	101.42	101.60	101.80	101.22	101.29	101.48	101.81	101.47	100.98	101.29	101.06	101.15	101.16	101.59	101.59	101.86	100.97	99.82	100.59	99.93	99.02	100.79	98.18
=O=F	0.91	0.80	0.77	0.77	0.70	0.75	0.83	0.87	0.76	0.98	0.88	0.90	0.85	0.70	0.66	0.72	0.66	0.67	0.95	0.95	0.99	0.99	0.97	1.02
=O=Cl	0.00	0.00	0.00	0.00	0.00	0.00	0.00	0.00	0.00	0.00	0.00	0.00	0.00	0.01	0.00	0.00	0.00	0.00	0.00	0.00	0.00	0.00	0.00	0.00
Total	100.60	100.61	100.83	101.03	100.51	100.54	100.64	100.94	100.70	100.00	100.41	100.16	100.29	100.45	100.93	100.87	101.20	100.30	98.87	99.64	98.94	98.04	99.83	97.16
Si	8.008	8.134	8.046	7.992	8.045	8.087	8.077	8.063	8.040	8.062	8.153	8.115	8.117	7.856	7.917	7.956	7.991	7.976	8.173	8.008	7.946	7.869	7.991	8.211
^{IV}Al	0.000	0.000	0.000	0.008	0.000	0.000	0.000	0.000	0.000	0.000	0.000	0.000	0.000	0.144	0.083	0.044	0.009	0.024	0.000	0.000	0.054	0.131	0.009	0.000
ΣTetrahedral	8.008	8.134	8.046	8.000	8.045	8.087	8.077	8.063	8.040	8.062	8.153	8.115	8.117	8.000	8.000	8.000	8.000	8.000	8.173	8.008	8.000	8.000	8.000	8.211
^{VI}Al	0.077	0.071	0.078	0.094	0.111	0.086	0.114	0.078	0.113	0.111	0.059	0.079	0.087	0.052	0.002	0.068	0.052	0.061	0.036	0.087	0.037	0.042	0.078	0.078
Ti	0.111	0.119	0.104	0.112	0.127	0.133	0.114	0.120	0.128	0.134	0.129	0.122	0.113	0.129	0.108	0.146	0.136	0.096	0.050	0.136	0.140	0.153	0.148	0.113
Fe^{3+}	0.837	0.649	0.777	0.731	0.532	0.535	0.569	0.637	0.610	0.567	0.565	0.585	0.571	0.932	0.946	0.919	0.885	0.936	0.729	0.488	0.629	0.764	0.478	0.389
Fe^{2+}	3.623	3.527	3.614	3.719	3.909	3.827	3.769	3.763	3.745	3.746	3.700	3.636	3.751	3.464	3.510	3.407	3.479	3.490	3.484	4.081	3.982	3.907	4.157	3.788
Mg	0.003	0.019	0.050	0.059	0.070	0.065	0.081	0.043	0.060	0.059	0.028	0.024	0.042	0.045	0.046	0.039	0.048	0.042	0.008	0.043	0.052	0.056	0.065	0.017
Mn	0.081	0.137	0.086	0.089	0.087	0.088	0.084	0.087	0.102	0.097	0.111	0.139	0.090	0.108	0.116	0.110	0.115	0.113	0.168	0.099	0.089	0.097	0.092	0.151
Zn	0.032	0.061	0.006	0.018	0.007	0.008	0.015	0.005	0.029	0.018	0.033	0.059	0.013	0.041	0.033	0.026	0.034	0.032	0.111	0.036	0.040	0.031	0.028	0.077
Cr	0.000	0.000	0.000	0.000	0.000	0.000	0.000	0.001	0.000	0.000	0.000	0.000	0.000	0.000	0.000	0.001	0.000	0.000	0.000	0.000	0.000	0.000	0.000	0.000
V	0.000	0.000	0.000	0.000	0.001	0.001	0.000	0.000	0.001	0.000	0.000	0.001	0.000	0.001	0.000	0.000	0.001	0.001	0.000	0.000	0.000	0.000	0.000	0.000
Zr	0.016	0.008	0.010	0.011	0.010	0.014	0.009	0.011	0.011	0.004	0.007	0.011	0.009	0.005	0.017	0.005	0.005	0.002	0.005	0.012	0.012	0.010	0.006	0.009
Nb	0.000	0.000	0.000	0.000	0.000	0.000	0.000	0.000	0.000	0.000	0.000	0.000	0.000	0.000	0.000	0.000	0.000	0.000	0.002	0.002	0.000	0.002	0.000	0.001
Y	0.000	0.000	0.000	0.000	0.000	0.000	0.000	0.000	0.000	0.000	0.000	0.000	0.000	0.000	0.000	0.000	0.000	0.000	0.000	0.000	0.000	0.000	0.000	0.000
Yb	0.000	0.000	0.000	0.000	0.001	0.000	0.000	0.000	0.000	0.000	0.000	0.000	0.000	0.000	0.001	0.001	0.002	0.001	0.000	0.000	0.000	0.000	0.000	0.000
ΣOctahedral	4.779	4.591	4.724	4.835	4.855	4.757	4.755	4.745	4.801	4.739	4.633	4.655	4.677	4.776	4.778	4.723	4.756	4.774	4.593	4.985	4.982	4.978	5.053	4.623
Na	2.930	2.949	2.927	2.819	2.754	2.826	2.798	2.836	2.825	2.816	2.850	2.881	2.810	2.949	2.863	2.826	2.807	2.837	2.716	2.591	2.612	2.622	2.556	2.790
K	0.253	0.294	0.247	0.245	0.256	0.264	0.284	0.269	0.259	0.265	0.352	0.280	0.326	0.161	0.252	0.422	0.405	0.334	0.511	0.304	0.306	0.301	0.301	0.345
Ca	0.031	0.012	0.057	0.101	0.091	0.067	0.085	0.086	0.076	0.118	0.013	0.069	0.068	0.114	0.107	0.029	0.032	0.055	0.007	0.112	0.101	0.098	0.090	0.013
ΣAlkalis	3.214	3.275	3.230	3.165	3.100	3.156	3.168	3.191	3.159	3.199	3.214	3.230	3.205	3.224	3.222	3.277	3.244	3.226	3.234	3.007	3.018	3.022	2.947	3.167
F	1.079	0.950	0.911	0.912	0.837	0.886	0.985	1.028	0.902	1.162	1.046	1.067	1.015	0.826	0.780	0.852	0.774	0.798	1.153	1.151	1.202	1.215	1.170	1.253
Cl	0.001	0.002	0.004	0.004	0.003	0.002	0.002	0.002	0.004	0.002	0.000	0.002	0.003	0.009	0.002	0.000	0.001	0.002	0.000	0.000	0.000	0.000	0.000	0.000
OH	0.920	1.048	1.085	1.084	1.160	1.113	1.013	0.970	1.094	0.835	0.954	0.931	0.982	1.166	1.217	1.147	1.225	1.200	0.847	0.849	0.798	0.785	0.830	0.747
ΣOH,F,Cl	2.000	2.000	2.000	2.000	2.000	2.000	2.000	2.000	2.000	2.000	2.000	2.000	2.000	2.000	2.000	2.000	2.000	2.000	2.000	2.000	2.000	2.000	2.000	2.000

Acronyms used are: ed=edge; lt=light; lter=lighter; dk=darker; dkest=darkest; nr=near; mid=middle; 2nd=second; gr=grain

Mineral formulae were calculated based on 23 atoms of oxygen and 16 cations, with Fe3+ calculated by the method of Droop (1987)

Appendix B-1. Electron microprobe analyses of arfvedsonitic amphibole

Unit	Hypersolv																							
Sample #	49-C-2																							
Description	2	3	4	6	49c2 ed	mid	mid	center	center	mid	mid	ed	49c2 ed	mid	center	mid	mid	ed	49 midk	mid	mid	aldehole	axthole	further
File	am92	am92	am92	am92	kp	kp	kp	kp	kp	kp	kp	kp	kp	kp	kp	kp	kp	kp	kp	kp	kp	kp	kp	kp
Analysis #	80	81	82	84	90	91	92	93	94	95	96	97	101	102	103	104	105	106	99.2	100.2	101.2	102.2	103.2	104.2
Na_2O	8.77	9.22	8.69	8.66	9.56	9.51	9.25	9.17	9.15	8.82	9.00	8.96	9.13	9.17	9.33	9.30	9.20	9.07	9.39	9.31	9.10	8.19	8.94	8.90
K_2O	1.46	1.18	1.50	2.19	1.65	1.32	1.14	1.18	1.07	1.06	1.05	1.06	1.15	1.15	1.00	1.09	1.11	1.09	1.57	1.29	1.25	1.22	1.29	1.22
CaO	0.35	0.41	0.37	0.05	0.06	0.30	0.60	0.56	0.55	0.55	0.59	0.61	0.61	0.60	0.59	0.59	0.60	0.61	0.08	0.27	0.31	0.31	0.27	0.29
FeO	28.90	27.00	29.00	26.72	27.21	27.66	28.24	28.62	28.54	29.97	28.72	29.64	27.88	28.39	28.26	28.00	28.24	29.36	27.01	27.37	28.03	32.54	29.19	29.26
Fe_2O_3	3.53	4.11	2.72	5.28	5.44	6.36	6.14	6.08	6.44	5.25	6.59	5.50	6.56	6.33	6.15	6.24	6.77	5.18	6.55	7.11	6.55	1.98	5.44	5.40
MgO	0.11	0.13	0.13	0.07	0.03	0.05	0.20	0.14	0.18	0.16	0.16	0.19	0.19	0.15	0.16	0.15	0.16	0.22	0.05	0.05	0.04	0.05	0.04	0.04
MnO	0.71	0.75	0.77	1.24	0.72	0.65	0.66	0.65	0.67	0.66	0.67	0.66	0.67	0.67	0.66	0.64	0.69	0.67	0.70	0.63	0.64	0.66	0.66	0.65
ZnO	0.27	0.36	0.45	0.79	0.33	0.25	0.22	0.21	0.19	0.24	0.19	0.20	0.21	0.20	0.15	0.21	0.19	0.18	0.14	0.13	0.09	0.25	0.09	0.09
Cr_2O_3	0.00	0.00	0.00	0.00	0.00	0.00	0.00	0.00	0.00	0.00	0.00	0.00	0.00	0.00	0.00	0.00	0.00	0.01	0.00	0.01	0.00	0.00	0.00	0.00
V_2O_3	0.00	0.00	0.00	0.00	0.00	0.01	0.01	0.01	0.02	0.00	0.00	0.01	0.00	0.00	0.01	0.01	0.01	0.02	0.00	0.00	0.00	0.00	0.00	0.01
ZrO_2	0.20	0.32	0.55	0.00	0.08	0.14	0.11	0.13	0.14	0.12	0.11	0.13	0.11	0.14	0.11	0.11	0.11	0.12	0.15	0.14	0.15	0.12	0.13	0.17
Nb_2O_5	0.00	0.02	0.03	0.00	0.00	0.00	0.00	0.00	0.00	0.00	0.00	0.00	0.00	0.00	0.00	0.00	0.00	0.00	0.00	0.00	0.00	0.00	0.00	0.00
Y_2O_3	0.00	0.00	0.00	0.00	0.00	0.00	0.00	0.00	0.00	0.00	0.00	0.00	0.00	0.00	0.00	0.00	0.00	0.00	0.00	0.00	0.00	0.00	0.00	0.00
Yb_2O_3	0.00	0.00	0.00	0.00	0.00	0.00	0.00	0.02	0.02	0.00	0.01	0.01	0.01	0.01	0.01	0.00	0.00	0.01	0.03	0.01	0.01	0.03	0.01	0.01
TiO_2	1.18	1.30	0.97	0.62	1.24	1.10	1.06	1.05	1.04	1.05	1.06	1.02	1.07	1.09	1.10	1.05	1.02	1.03	1.12	1.09	1.14	1.18	1.14	1.12
SiO_2	49.94	49.48	50.03	50.48	51.40	50.91	50.53	50.50	50.15	50.13	49.75	50.38	49.89	50.27	50.40	50.35	50.24	50.69	50.44	49.85	49.54	49.96	49.93	49.72
Al_2O_3	0.39	0.58	0.47	0.21	0.32	0.44	0.59	0.55	0.51	0.50	0.54	0.55	0.58	0.61	0.54	0.56	0.55	0.54	0.32	0.44	0.43	0.46	0.42	0.44
F	2.43	2.57	2.44	2.58	1.95	1.96	1.88	1.94	1.99	1.97	1.89	1.90	1.88	1.95	1.91	2.04	1.89	1.98	1.91	1.84	1.75	2.11	1.68	1.69
Cl	0.00	0.00	0.00	0.00	0.01	0.01	0.01	0.01	0.01	0.01	0.01	0.02	0.01	0.01	0.01	0.01	0.01	0.02	0.00	0.01	0.01	0.00	0.01	0.01
H_2O	0.69	0.61	0.68	0.63	0.97	0.97	1.00	0.98	0.94	0.95	0.98	0.99	0.99	0.97	0.98	0.92	1.00	0.95	0.97	1.00	1.03	0.85	1.07	1.06
Total	98.93	98.05	98.77	99.52	100.96	101.65	101.64	101.80	101.60	101.44	101.32	101.82	100.94	101.71	101.38	101.27	101.79	101.74	100.44	100.54	100.06	99.91	100.30	100.09
=O=F	1.02	1.08	1.03	1.08	0.82	0.83	0.79	0.82	0.84	0.83	0.80	0.80	0.79	0.82	0.81	0.86	0.80	0.84	0.80	0.77	0.74	0.89	0.71	0.71
=O=Cl	0.00	0.00	0.00	0.00	0.00	0.00	0.00	0.00	0.00	0.00	0.00	0.00	0.00	0.00	0.00	0.00	0.00	0.00	0.00	0.00	0.00	0.00	0.00	0.00
Total	97.91	96.97	97.75	98.44	100.14	100.82	100.85	100.99	100.76	100.61	100.53	101.01	100.15	100.88	100.57	100.41	100.99	100.90	99.64	99.77	99.32	99.02	99.59	99.38
Si	8.119	8.088	8.152	8.168	8.126	8.025	7.975	7.973	7.945	7.972	7.914	7.969	7.941	7.947	7.976	7.981	7.937	8.008	8.043	7.961	7.960	8.095	8.005	7.994
^{IV}Al	0.000	0.000	0.000	0.000	0.000	0.000	0.025	0.027	0.055	0.028	0.086	0.031	0.059	0.053	0.024	0.019	0.063	0.000	0.000	0.039	0.040	0.000	0.000	0.006
ΣTetrahedral	8.119	8.088	8.152	8.168	8.126	8.025	8.000	8.000	8.000	8.000	8.000	8.000	8.000	8.000	8.000	8.000	8.000	8.008	8.043	8.000	8.000	8.095	8.005	8.000
^{VI}Al	0.075	0.112	0.090	0.040	0.060	0.082	0.086	0.075	0.040	0.065	0.014	0.072	0.051	0.061	0.077	0.086	0.039	0.100	0.061	0.044	0.040	0.087	0.079	0.077
Ti	0.145	0.159	0.118	0.075	0.147	0.131	0.126	0.126	0.124	0.125	0.126	0.121	0.128	0.129	0.131	0.125	0.121	0.122	0.134	0.131	0.138	0.144	0.138	0.136
Fe^{3+}	0.432	0.506	0.333	0.643	0.647	0.755	0.729	0.723	0.768	0.628	0.789	0.655	0.785	0.753	0.732	0.744	0.805	0.616	0.785	0.855	0.792	0.242	0.657	0.653
Fe^{2+}	3.929	3.691	3.951	3.616	3.598	3.647	3.727	3.779	3.781	3.987	3.820	3.921	3.711	3.753	3.740	3.712	3.731	3.879	3.603	3.656	3.767	4.409	3.914	3.934
Mg	0.027	0.032	0.031	0.016	0.006	0.011	0.047	0.033	0.043	0.039	0.039	0.045	0.045	0.036	0.039	0.036	0.038	0.053	0.012	0.011	0.009	0.012	0.008	0.010
Mn	0.098	0.104	0.107	0.170	0.096	0.087	0.088	0.087	0.090	0.089	0.090	0.088	0.090	0.090	0.088	0.086	0.092	0.089	0.095	0.085	0.087	0.091	0.089	0.089
Zn	0.032	0.043	0.054	0.094	0.038	0.029	0.026	0.025	0.022	0.028	0.023	0.023	0.025	0.023	0.017	0.024	0.022	0.020	0.016	0.015	0.010	0.030	0.010	0.011
Cr	0.000	0.000	0.000	0.000	0.000	0.000	0.000	0.000	0.000	0.000	0.000	0.000	0.000	0.000	0.000	0.000	0.000	0.001	0.000	0.001	0.000	0.000	0.000	0.000
V	0.000	0.000	0.000	0.000	0.000	0.001	0.001	0.001	0.002	0.000	0.000	0.001	0.000	0.000	0.001	0.001	0.001	0.002	0.000	0.000	0.000	0.000	0.000	0.001
Zr	0.015	0.025	0.044	0.000	0.006	0.011	0.008	0.010	0.011	0.009	0.008	0.010	0.008	0.011	0.009	0.009	0.009	0.009	0.012	0.011	0.011	0.009	0.010	0.013
Nb	0.000	0.001	0.001	0.000	0.000	0.000	0.000	0.000	0.000	0.000	0.000	0.000	0.000	0.000	0.000	0.000	0.000	0.000	0.000	0.000	0.000	0.000	0.000	0.000
Y	0.000	0.000	0.000	0.000	0.000	0.000	0.000	0.000	0.000	0.000	0.000	0.000	0.000	0.000	0.000	0.000	0.000	0.000	0.000	0.000	0.000	0.000	0.000	0.000
Yb	0.000	0.000	0.000	0.000	0.000	0.000	0.000	0.001	0.001	0.000	0.000	0.001	0.000	0.000	0.000	0.000	0.000	0.001	0.001	0.001	0.000	0.001	0.000	0.001
ΣOctahedral	4.753	4.674	4.729	4.654	4.599	4.753	4.838	4.860	4.882	4.971	4.911	4.937	4.845	4.856	4.835	4.822	4.858	4.892	4.719	4.809	4.855	5.026	4.906	4.925
Na	2.764	2.920	2.744	2.717	2.931	2.906	2.831	2.807	2.810	2.721	2.774	2.747	2.818	2.810	2.864	2.857	2.816	2.778	2.904	2.882	2.836	2.574	2.778	2.774
K	0.302	0.245	0.311	0.452	0.333	0.265	0.229	0.238	0.216	0.215	0.213	0.213	0.233	0.233	0.203	0.221	0.225	0.219	0.320	0.262	0.256	0.252	0.264	0.251
Ca	0.062	0.072	0.064	0.008	0.011	0.050	0.102	0.095	0.093	0.093	0.101	0.103	0.105	0.101	0.099	0.100	0.101	0.103	0.014	0.042	0.053	0.053	0.047	0.050
ΣAlkalis	3.127	3.238	3.119	3.178	3.275	3.222	3.162	3.140	3.118	3.029	3.089	3.063	3.155	3.144	3.165	3.178	3.142	3.100	3.238	3.191	3.145	2.879	3.089	3.075
F	1.247	1.330	1.256	1.318	0.976	0.979	0.938	0.967	0.998	0.991	0.952	0.950	0.947	0.977	0.957	1.024	0.946	0.991	0.964	0.928	0.888	1.080	0.852	0.861
Cl	0.000	0.000	0.000	0.000	0.001	0.002	0.003	0.003	0.003	0.004	0.003	0.005	0.003	0.003	0.003	0.003	0.005	0.001	0.001	0.002	0.001	0.002	0.001	0.002
OH	0.753	0.670	0.744	0.682	1.023	1.019	1.059	1.030	0.998	1.005	1.045	1.045	1.050	1.020	1.040	0.973	1.051	1.004	1.015	1.071	1.110	0.920	1.146	1.136
ΣOH,F,Cl	2.000	2.000	2.000	2.000	2.000	2.000	2.000	2.000	2.000	2.000	2.000	2.000	2.000	2.000	2.000	2.000	2.000	2.000	2.000	2.000	2.000	2.000	2.000	2.000

Acronyms used are: ed=edge; lt=light; ltr=lighter; dke=darker; dk=dark; nr=near; mid=middle; 2nd=second; gr=grain

Mineral formulae were calculated based on 23 atoms of oxygen and 16 cations, with Fe3+ calculated by the method of Droop (1987)

Appendix B-1. Electron microprobe analyses of arfvedsonitic amphibole

Unit	Hypersol																					
Sample #	49-C-2												57-A-1									
Description	half	arnext	arother	further	further	further	arhole	away	away	heated	away	away	a 49c2	57ahed	#2	#3	#4	#5	#6	#7	ed	#9	mkbl	ed
File	kp	kp	kp	kp	kp	kp	kp	kp	kp	kp	kp	kp	kp	am92	am92	am92	am92	am92	am92	am92	am92	am92	am92	am92
Analysis #	105.2	106.2	107.2	108.2	109.2	110.2	111.2	112.2	113.2	114.2	115.2	116.2	18.2	27	28	29	30	31	32	33	34	35	38	47
Na_2O	9.17	9.22	8.38	8.60	8.63	8.58	7.96	8.61	8.59	8.72	8.45	8.49	8.93	8.38	8.27	8.71	8.51	8.59	8.94	8.87	8.89	8.56	8.61	8.18
K_2O	1.28	1.36	1.14	1.13	1.10	1.16	2.29	2.28	2.27	2.22	2.26	2.26	2.40	1.88	1.78	1.85	1.80	1.64	1.63	1.56	1.77	2.06	1.70	2.00
CaO	0.28	0.17	0.53	0.54	0.56	0.57	0.22	0.18	0.18	0.17	0.20	0.19	0.05	0.16	0.18	0.14	0.14	0.16	0.13	0.23	0.13	0.05	0.11	0.05
FeO	28.45	28.25	30.92	30.19	30.61	30.70	30.19	27.15	26.90	27.35	28.45	28.33	25.75	26.94	27.97	26.97	28.70	29.43	28.46	28.37	27.19	27.48	28.71	28.87
Fe_2O_3	6.19	6.41	4.18	5.08	4.80	4.48	1.94	5.43	5.67	5.18	4.09	4.22	6.09	3.71	3.79	4.56	4.21	4.88	4.18	3.46	2.48	0.54	3.54	2.20
MgO	0.04	0.06	0.16	0.16	0.16	0.14	0.00	0.00	0.00	0.00	0.01	0.00	0.06	0.27	0.18	0.17	0.20	0.20	0.23	0.17	0.13	0.10	0.19	0.24
MnO	0.66	0.62	0.67	0.67	0.66	0.67	1.42	1.43	1.44	1.41	1.46	1.45	1.79	1.23	0.68	0.67	0.66	0.68	0.67	0.87	1.18	1.87	0.72	1.56
ZnO	0.10	0.10	0.07	0.19	0.08	0.06	0.66	0.52	0.69	0.67	0.54	0.38	0.79	0.69	0.27	0.32	0.26	0.31	0.36	0.51	0.75	1.27	0.31	0.82
Cr_2O_3	0.00	0.00	0.01	0.00	0.01	0.00	0.00	0.00	0.00	0.00	0.01	0.01	0.00	0.00	0.00	0.00	0.00	0.00	0.00	0.00	0.00	0.00	0.00	0.00
V_2O_3	0.01	0.00	0.02	0.01	0.00	0.01	0.01	0.02	0.00	0.01	0.01	0.01	0.00	0.00	0.00	0.00	0.00	0.00	0.00	0.00	0.00	0.00	0.00	0.00
ZrO_2	0.14	0.12	0.13	0.12	0.11	0.11	0.48	0.50	0.48	0.52	0.51	0.46	0.02	0.17	0.27	0.42	0.17	0.29	0.36	0.16	0.13	0.09	0.42	0.12
Nb_2O_5	0.00	0.00	0.00	0.00	0.00	0.00	0.00	0.03	0.00	0.02	0.00	0.01	0.01	0.01	0.00	0.00	0.00	0.02	0.02	0.02	0.00	0.00	0.03	0.04
Y_2O_3	0.00	0.00	0.00	0.00	0.00	0.00	0.00	0.00	0.00	0.00	0.00	0.00	0.00	0.00	0.00	0.00	0.00	0.00	0.00	0.00	0.00	0.00	0.00	0.00
Yb_2O_3	0.01	0.02	0.00	0.00	0.03	0.00	0.00	0.00	0.02	0.01	0.00	0.00	0.00	0.00	0.00	0.00	0.00	0.00	0.00	0.00	0.00	0.00	0.00	0.00
TiO_2	1.11	0.92	1.04	0.99	1.06	1.01	0.83	0.82	0.84	0.83	0.84	0.83	0.27	0.88	0.89	0.88	0.92	0.94	0.96	1.03	0.96	1.04	0.93	0.46
SiO_2	50.17	50.39	49.44	49.70	49.93	50.02	50.70	50.38	50.22	50.80	50.83	50.77	51.71	49.01	48.20	49.21	49.75	50.04	50.57	50.47	50.63	51.12	49.79	50.65
Al_2O_3	0.43	0.39	0.49	0.51	0.52	0.53	0.15	0.13	0.15	0.16	0.15	0.14	0.16	1.49	2.62	0.59	0.46	0.50	0.34	0.40	0.32	0.25	0.50	0.20
F	1.78	1.69	1.89	1.76	1.95	1.89	1.57	1.76	1.82	1.77	1.85	1.82	1.69	1.94	1.91	2.18	2.02	2.06	2.26	2.06	2.11	2.24	2.10	2.19
Cl	0.01	0.00	0.01	0.01	0.01	0.02	0.00	0.00	0.01	0.00	0.00	0.00	0.00	0.00	0.00	0.00	0.00	0.00	0.00	0.00	0.00	0.00	0.00	0.00
H_2O	1.04	1.08	0.96	1.03	0.95	0.98	1.10	1.03	1.00	1.04	0.99	1.00	1.09	0.91	0.93	0.79	0.88	0.89	0.79	0.88	0.83	0.77	0.84	0.79
Total	100.87	100.80	100.01	100.65	101.18	100.92	99.53	100.27	100.27	100.87	100.65	100.37	100.81	97.67	97.94	97.75	98.68	100.64	99.90	99.05	97.52	97.43	98.49	98.36
=O=F	0.75	0.71	0.79	0.74	0.82	0.79	0.66	0.74	0.77	0.75	0.78	0.77	0.71	0.82	0.80	0.92	0.85	0.87	0.95	0.87	0.89	0.94	0.88	0.92
=O=Cl	0.00	0.00	0.00	0.00	0.00	0.00	0.00	0.00	0.00	0.00	0.00	0.00	0.00	0.00	0.00	0.00	0.00	0.00	0.00	0.00	0.00	0.00	0.00	0.00
Total	100.12	100.09	99.21	99.91	100.35	100.12	98.86	99.53	99.50	100.12	99.87	99.60	100.10	96.85	97.14	96.83	97.83	99.77	98.95	98.19	96.63	96.48	97.60	97.44
Si	7.991	8.020	7.991	7.969	7.972	7.998	8.216	8.093	8.075	8.107	8.141	8.146	8.204	8.033	7.879	8.081	8.103	8.024	8.129	8.163	8.283	8.382	8.125	8.283
^{IV}Al	0.009	0.000	0.009	0.031	0.028	0.002	0.000	0.000	0.000	0.000	0.000	0.000	0.000	0.000	0.121	0.000	0.000	0.000	0.000	0.000	0.000	0.000	0.000	0.000
ΣTetrahedral	8.000	8.020	8.000	8.000	8.000	8.000	8.216	8.093	8.075	8.107	8.141	8.146	8.204	8.033	8.000	8.081	8.103	8.024	8.129	8.163	8.283	8.382	8.125	8.283
^{VI}Al	0.071	0.073	0.085	0.064	0.070	0.098	0.029	0.024	0.028	0.030	0.028	0.027	0.029	0.288	0.384	0.113	0.089	0.094	0.065	0.077	0.062	0.049	0.095	0.038
Ti	0.133	0.110	0.126	0.120	0.128	0.122	0.101	0.099	0.101	0.100	0.101	0.100	0.032	0.109	0.110	0.109	0.112	0.113	0.115	0.126	0.119	0.128	0.114	0.057
Fe^{3+}	0.742	0.767	0.508	0.613	0.577	0.540	0.237	0.657	0.686	0.623	0.493	0.510	0.727	0.457	0.466	0.601	0.516	0.589	0.506	0.421	0.305	0.066	0.434	0.271
Fe^{2+}	3.790	3.760	4.179	4.048	4.088	4.106	4.091	3.647	3.618	3.650	3.810	3.801	3.416	3.693	3.824	3.705	3.909	3.947	3.825	3.838	3.721	3.768	3.919	3.949
Mg	0.009	0.015	0.037	0.037	0.038	0.033	0.000	0.000	0.000	0.000	0.001	0.000	0.013	0.066	0.044	0.041	0.049	0.048	0.054	0.040	0.032	0.024	0.045	0.057
Mn	0.089	0.084	0.092	0.090	0.089	0.091	0.195	0.195	0.196	0.191	0.198	0.197	0.241	0.170	0.094	0.093	0.091	0.093	0.091	0.119	0.164	0.260	0.099	0.216
Zn	0.012	0.012	0.008	0.022	0.009	0.007	0.079	0.062	0.082	0.079	0.064	0.045	0.093	0.083	0.032	0.039	0.032	0.036	0.043	0.061	0.091	0.154	0.038	0.099
Cr	0.000	0.000	0.001	0.000	0.001	0.000	0.000	0.000	0.001	0.000	0.001	0.001	0.000	0.000	0.000	0.000	0.000	0.000	0.000	0.000	0.000	0.000	0.000	0.000
V	0.001	0.000	0.002	0.001	0.000	0.001	0.001	0.002	0.000	0.001	0.001	0.001	0.000	0.000	0.000	0.000	0.000	0.000	0.000	0.000	0.000	0.000	0.000	0.000
Zr	0.011	0.009	0.010	0.009	0.009	0.008	0.038	0.039	0.038	0.040	0.040	0.036	0.002	0.014	0.022	0.034	0.014	0.023	0.028	0.013	0.010	0.007	0.033	0.009
Nb	0.000	0.000	0.000	0.000	0.000	0.000	0.000	0.001	0.000	0.001	0.000	0.001	0.000	0.000	0.000	0.000	0.000	0.001	0.001	0.001	0.000	0.000	0.001	0.002
Y	0.000	0.000	0.000	0.000	0.000	0.000	0.000	0.000	0.000	0.000	0.000	0.000	0.000	0.000	0.000	0.000	0.000	0.000	0.000	0.000	0.000	0.000	0.000	0.000
Yb	0.001	0.001	0.000	0.000	0.001	0.000	0.000	0.000	0.001	0.000	0.000	0.000	0.000	0.000	0.000	0.000	0.000	0.000	0.000	0.000	0.000	0.000	0.000	0.000
ΣOctahedral	4.858	4.831	5.049	5.005	5.009	5.006	4.771	4.727	4.751	4.715	4.738	4.718	4.554	4.881	4.976	4.734	4.811	4.943	4.729	4.695	4.501	4.457	4.779	4.697
Na	2.833	2.844	2.625	2.673	2.671	2.661	2.502	2.683	2.677	2.698	2.625	2.642	2.747	2.665	2.621	2.773	2.689	2.670	2.785	2.782	2.821	2.721	2.723	2.594
K	0.260	0.277	0.234	0.230	0.223	0.236	0.473	0.467	0.466	0.452	0.461	0.462	0.486	0.394	0.371	0.388	0.373	0.335	0.334	0.321	0.370	0.430	0.355	0.418
Ca	0.048	0.029	0.092	0.092	0.096	0.097	0.038	0.011	0.031	0.029	0.035	0.032	0.009	0.028	0.031	0.024	0.024	0.028	0.023	0.039	0.022	0.009	0.018	0.008
ΣAlkali	3.142	3.149	2.951	2.995	2.991	2.994	3.013	3.180	3.174	3.179	3.121	3.136	3.242	3.086	3.024	3.185	3.086	3.033	3.142	3.142	3.213	3.160	3.096	3.020
F	0.896	0.850	0.964	0.892	0.985	0.953	0.805	0.894	0.927	0.895	0.937	0.926	0.849	1.006	0.985	1.131	1.041	1.043	1.150	1.052	1.093	1.160	1.084	1.133
Cl	0.002	0.001	0.004	0.003	0.004	0.004	0.000	0.001	0.001	0.000	0.001	0.001	0.001	0.000	0.000	0.000	0.000	0.000	0.000	0.000	0.000	0.000	0.000	0.000
OH	1.102	1.149	1.032	1.105	1.012	1.043	1.195	1.105	1.072	1.105	1.063	1.073	1.150	0.994	1.015	0.869	0.959	0.957	0.850	0.948	0.907	0.840	0.916	0.867
ΣOH,F,Cl	2.000	2.000	2.000	2.000	2.000	2.000	2.000	2.000	2.000	2.000	2.000	2.000	2.000	2.000	2.000	2.000	2.000	2.000	2.000	2.000	2.000	2.000	2.000	2.000

Acronyms used are: edmedge, ltxlight; lterxlighter; dkerxdarker; dkxdark; nr=near; mxdxmiddle; 2ndxsecond; grxgrain

Mineral formulae were calculated based on 23 atoms of oxygen and 16 cations, with Fe3+ calculated by the method of Droop (1987).

Appendix B-1: Electron microprobe analyses of arfvedsonitic amphibole

Unit	Hypersol																							
Sample #	57-A-1																							
Description	ed	mid	mid#	mid	area	2	clear		by z	zone	zone	green			ed	#3	spot						ed	57A1
File	am92	am92	am92	am92	am92	am92	am92	am92	am92	am92	am92	am92	am92	am92	am92	am92	am92	am92	am92	am92	am92	am92	am92	am93
Analysis #	48	49	50	51	52	53	54	55	56	57	58	59	60	61	62	63	64	65	66	67	68	69	70	75
Na_2O	8.47	8.36	8.73	8.63	8.52	8.63	8.59	8.50	8.51	8.76	8.69	8.46	8.63	8.50	8.66	8.58	8.57	8.41	8.18	7.99	8.16	8.23	8.42	9.08
K_2O	1.39	1.58	1.31	1.45	1.45	1.44	1.45	1.53	1.17	1.18	1.25	1.46	1.12	1.13	1.11	1.28	1.23	1.39	1.94	1.76	1.83	1.13	1.26	1.62
CaO	0.13	0.09	0.38	0.12	0.25	0.13	0.10	0.11	0.12	0.10	0.17	0.08	0.12	0.21	0.13	0.23	0.22	0.09	0.01	0.04	0.13	0.15	0.08	0.24
FeO	30.62	29.97	29.32	29.17	29.66	29.38	29.42	29.74	30.45	29.42	29.91	30.84	30.12	30.80	30.46	29.78	30.44	29.96	25.80	29.28	29.72	30.62	28.50	26.58
Fe_2O_3	1.17	2.53	3.55	3.55	2.33	3.20	3.56	3.11	2.91	3.85	2.66	1.81	2.82	2.06	1.98	2.08	1.17	0.61	0.88	0.30	0.00	0.00	0.00	4.45
MgO	0.22	0.21	0.23	0.20	0.27	0.16	0.17	0.16	0.16	0.13	0.11	0.15	0.14	0.16	0.20	0.20	0.25	0.27	0.76	0.32	0.22	0.16	0.16	0.32
MnO	0.78	0.73	0.70	0.68	0.71	0.65	0.72	0.65	0.67	0.67	0.71	0.69	0.71	0.69	0.70	0.95	0.73	1.33	3.29	2.28	1.57	1.44	2.23	0.76
ZnO	0.33	0.29	0.33	0.34	0.35	0.36	0.28	0.31	0.33	0.28	0.34	0.35	0.28	0.34	0.34	0.56	0.38	0.72	1.72	1.02	0.84	0.88	1.16	0.40
Cr_2O_3	0.00	0.00	0.00	0.00	0.00	0.00	0.00	0.00	0.00	0.00	0.00	0.00	0.00	0.00	0.00	0.00	0.00	0.00	0.00	0.00	0.00	0.00	0.00	0.00
V_2O_3	0.00	0.00	0.00	0.00	0.00	0.00	0.00	0.00	0.00	0.00	0.00	0.00	0.00	0.00	0.00	0.00	0.00	0.00	0.00	0.00	0.00	0.00	0.00	0.00
ZrO_2	0.13	0.43	0.18	0.10	0.11	0.14	0.18	0.20	0.11	0.17	0.15	0.11	0.20	0.08	0.07	0.12	0.13	0.10	0.04	0.08	0.14	0.06	0.11	0.16
Nb_2O_5	0.01	0.02	0.01	0.04	0.00	0.00	0.01	0.01	0.00	0.00	0.01	0.00	0.00	0.03	0.01	0.05	0.02	0.00	0.02	0.00	0.00	0.02	0.00	0.00
Y_2O_3	0.00	0.00	0.00	0.00	0.00	0.00	0.00	0.00	0.00	0.00	0.00	0.00	0.00	0.00	0.00	0.00	0.00	0.00	0.00	0.00	0.00	0.00	0.00	0.00
Yb_2O_3	0.00	0.00	0.00	0.00	0.00	0.00	0.00	0.00	0.00	0.00	0.00	0.00	0.00	0.00	0.00	0.00	0.00	0.00	0.00	0.00	0.00	0.00	0.00	0.00
TiO_2	0.87	0.92	1.33	0.91	1.17	1.08	0.93	1.02	0.92	0.88	0.90	0.90	0.90	1.07	1.18	1.04	1.03	1.09	0.09	0.61	1.17	0.95	0.87	0.89
SiO_2	50.43	49.65	49.85	49.81	49.93	49.80	49.76	49.79	49.70	49.70	50.09	50.50	49.72	49.83	50.02	50.09	50.30	50.31	51.18	50.52	50.84	50.58	50.97	50.21
Al_2O_3	0.56	0.30	0.40	0.32	0.36	0.34	0.31	0.28	0.27	0.30	0.36	0.29	0.30	0.37	0.32	0.42	0.38	0.42	0.26	0.31	0.42	0.40	0.28	0.36
F	2.12	2.31	2.22	2.31	2.02	2.32	2.38	2.27	2.04	2.51	2.59	2.16	2.33	2.21	2.38	2.46	2.29	2.39	3.24	2.42	2.29	2.25	2.42	2.41
Cl	0.00	0.00	0.00	0.00	0.00	0.00	0.00	0.00	0.00	0.00	0.00	0.00	0.00	0.00	0.00	0.00	0.00	0.00	0.00	0.00	0.00	0.00	0.00	0.00
H_2O	0.83	0.73	0.80	0.74	0.88	0.73	0.71	0.76	0.86	0.64	0.61	0.81	0.72	0.78	0.70	0.67	0.74	0.69	0.29	0.67	0.74	0.75	0.67	0.70
Total	98.05	98.10	99.34	98.35	98.00	98.36	98.56	98.43	98.22	98.59	98.54	98.63	98.13	98.26	98.27	98.50	97.90	97.79	97.67	97.58	98.08	97.60	97.13	98.18
=O=F	0.89	0.97	0.94	0.97	0.85	0.98	1.00	0.95	0.86	1.06	1.09	0.91	0.98	0.93	1.00	1.03	0.97	1.01	1.36	1.02	0.97	0.95	1.02	1.01
=O=Cl	0.00	0.00	0.00	0.00	0.00	0.00	0.00	0.00	0.00	0.00	0.00	0.00	0.00	0.00	0.00	0.00	0.00	0.00	0.00	0.00	0.00	0.00	0.00	0.00
Total	97.16	97.13	98.40	97.38	97.15	97.38	97.56	97.48	97.36	97.54	97.45	97.72	97.15	97.33	97.27	97.46	96.93	96.78	96.30	96.56	97.11	96.65	96.11	97.17
Si	8.245	8.163	8.074	8.148	8.173	8.146	8.134	8.148	8.149	8.125	8.185	8.231	8.160	8.164	8.185	8.183	8.243	8.263	8.413	8.332	8.325	8.338	8.421	8.172
^{IV}Al	0.000	0.000	0.000	0.000	0.000	0.000	0.000	0.000	0.000	0.000	0.000	0.000	0.000	0.000	0.000	0.000	0.000	0.000	0.000	0.000	0.000	0.000	0.000	0.000
ΣTetrahedral	8.245	8.163	8.074	8.148	8.173	8.146	8.134	8.148	8.149	8.125	8.185	8.231	8.160	8.164	8.185	8.183	8.243	8.263	8.413	8.332	8.325	8.338	8.421	8.172
^{VI}Al	0.107	0.057	0.077	0.062	0.069	0.066	0.059	0.054	0.051	0.057	0.069	0.055	0.058	0.072	0.061	0.081	0.074	0.082	0.051	0.060	0.081	0.078	0.054	0.069
Ti	0.107	0.114	0.162	0.112	0.144	0.132	0.115	0.125	0.113	0.108	0.110	0.111	0.111	0.132	0.145	0.127	0.127	0.135	0.011	0.076	0.144	0.118	0.108	0.109
Fe^{3+}	0.144	0.313	0.432	0.437	0.287	0.394	0.438	0.383	0.358	0.473	0.327	0.222	0.348	0.254	0.244	0.256	0.144	0.075	0.108	0.037	0.000	0.000	0.000	0.545
Fe^{2+}	4.186	4.110	3.972	3.990	4.060	4.019	4.022	4.071	4.175	4.022	4.088	4.205	4.134	4.220	4.169	4.069	4.172	4.115	3.547	4.039	4.064	4.209	3.924	3.617
Mg	0.054	0.050	0.056	0.048	0.066	0.039	0.041	0.039	0.040	0.031	0.027	0.037	0.035	0.039	0.050	0.049	0.060	0.065	0.185	0.078	0.055	0.040	0.040	0.078
Mn	0.108	0.101	0.096	0.094	0.099	0.090	0.100	0.091	0.093	0.093	0.098	0.095	0.099	0.096	0.097	0.131	0.101	0.185	0.458	0.318	0.218	0.201	0.312	0.105
Zn	0.040	0.036	0.040	0.041	0.042	0.044	0.033	0.038	0.040	0.034	0.042	0.042	0.034	0.041	0.042	0.067	0.046	0.087	0.208	0.124	0.101	0.107	0.141	0.048
Cr	0.000	0.000	0.000	0.000	0.000	0.000	0.000	0.000	0.000	0.000	0.000	0.000	0.000	0.000	0.000	0.000	0.000	0.000	0.000	0.000	0.000	0.000	0.000	0.000
V	0.000	0.000	0.000	0.000	0.000	0.000	0.000	0.000	0.000	0.000	0.000	0.000	0.000	0.000	0.000	0.000	0.000	0.000	0.000	0.000	0.000	0.000	0.000	0.000
Zr	0.010	0.034	0.014	0.008	0.009	0.011	0.014	0.016	0.009	0.013	0.012	0.009	0.016	0.007	0.006	0.009	0.010	0.008	0.003	0.006	0.011	0.005	0.009	0.013
Nb	0.000	0.001	0.000	0.002	0.000	0.000	0.000	0.000	0.000	0.000	0.001	0.000	0.000	0.001	0.000	0.002	0.001	0.000	0.001	0.000	0.000	0.001	0.000	0.000
Y	0.000	0.000	0.000	0.000	0.000	0.000	0.000	0.000	0.000	0.000	0.000	0.000	0.000	0.000	0.000	0.000	0.000	0.000	0.000	0.000	0.000	0.000	0.000	0.000
Yb	0.000	0.000	0.000	0.000	0.000	0.000	0.000	0.000	0.000	0.000	0.000	0.000	0.000	0.000	0.000	0.000	0.000	0.000	0.000	0.000	0.000	0.000	0.000	0.000
ΣOctahedral	4.757	4.827	4.850	4.793	4.776	4.794	4.822	4.816	4.880	4.833	4.773	4.776	4.837	4.863	4.814	4.793	4.736	4.753	4.572	4.738	4.674	4.757	4.588	4.585
Na	2.685	2.663	2.741	2.736	2.705	2.737	2.722	2.697	2.706	2.777	2.752	2.675	2.747	2.700	2.747	2.717	2.724	2.677	2.606	2.555	2.589	2.629	2.698	2.864
K	0.291	0.332	0.270	0.303	0.302	0.300	0.303	0.320	0.245	0.246	0.261	0.304	0.234	0.236	0.232	0.266	0.258	0.291	0.407	0.369	0.382	0.237	0.266	0.337
Ca	0.022	0.015	0.066	0.020	0.044	0.023	0.018	0.019	0.020	0.018	0.030	0.014	0.022	0.036	0.023	0.041	0.039	0.017	0.002	0.006	0.023	0.026	0.014	0.043
ΣAlkalis	2.998	3.010	3.077	3.059	3.051	3.060	3.043	3.036	2.971	3.042	3.042	2.993	3.003	2.973	3.001	3.024	3.021	2.985	3.015	2.930	2.995	2.892	2.977	3.244
F	1.095	1.198	1.138	1.197	1.043	1.201	1.230	1.172	1.056	1.297	1.339	1.115	1.208	1.144	1.230	1.268	1.188	1.242	1.683	1.262	1.188	1.171	1.266	1.238
Cl	0.000	0.000	0.000	0.000	0.000	0.000	0.000	0.000	0.000	0.000	0.000	0.000	0.000	0.000	0.000	0.000	0.000	0.000	0.000	0.000	0.000	0.000	0.000	0.000
OH	0.905	0.802	0.862	0.803	0.957	0.799	0.770	0.828	0.944	0.703	0.661	0.885	0.792	0.856	0.770	0.732	0.812	0.758	0.317	0.738	0.812	0.829	0.734	0.762
ΣOH,F,Cl	2.000	2.000	2.000	2.000	2.000	2.000	2.000	2.000	2.000	2.000	2.000	2.000	2.000	2.000	2.000	2.000	2.000	2.000	2.000	2.000	2.000	2.000	2.000	2.000

Acronyms used are: ed=edge; lt=light; lter=lighter; dker=darker; dk=dark; nr=near; mid=middle; 2nd=second; gr=grain
Mineral formulas were calculated based on 23 atoms of oxygen and 16 cations, with Fe3+ calculated by the method of Droop (1987)

Appendix B-1. Electron microprobe analyses of arfvedsonitic amphibole

Unit	Hypersolvus	Hypersolvus - Drill Core																						
Sample #	57-A-1	57-A-3			58-D-1					LB-9-2.12												LB-9-5.33		
Description	57a1	57A3 #2		#1	58d1 ed					side mid	mid	ed	mided	lt	dk	lt	dkered	4 lt	middk	lt	mid	ed	mid	ed
File	kp	am93	am93	am93	1/1/95	1/1/95	1/1/95	1/1/95	1/1/95	1/1/95	1/1/95	1/1/95	kp	kp	kp	kp	kp	kp	kp	kp	kp	kp	kp	kp
Analysis #	89.2	65	66	67	2	4	5	7	8	11	14	15	175	176	177	178	179	180	181	182	183	184	185	186
Na_2O	8.94	8.76	9.01	8.96	9.47	9.60	9.56	9.46	9.55	9.34	9.58	9.58	8.55	8.29	8.43	8.19	8.50	8.03	8.65	8.10	8.42	8.88	9.12	9.12
K_2O	1.40	2.02	1.70	1.70	1.86	1.47	1.80	1.36	1.37	1.40	1.43	1.51	1.02	0.67	0.82	0.63	0.60	0.74	0.71	0.72	0.57	2.02	2.05	2.04
CaO	0.26	0.32	0.29	0.44	0.09	0.26	0.12	0.32	0.38	0.29	0.32	0.26	1.37	2.73	1.80	3.07	2.66	2.67	1.34	2.28	2.23	0.16	0.17	0.15
FeO	28.30	26.94	27.37	26.34	27.12	27.35	27.83	27.44	26.92	28.72	27.56	26.82	29.56	28.39	29.25	28.29	27.81	29.03	28.35	29.84	29.02	27.13	26.61	26.71
Fe_2O_3	2.56	4.98	4.51	4.65	5.38	5.33	3.91	5.29	5.81	4.39	5.22	6.12	5.30	6.88	5.62	7.08	7.26	6.38	6.93	5.82	6.76	5.31	5.81	5.60
MgO	0.23	0.42	0.36	0.26	0.20	0.22	0.19	0.20	0.22	0.20	0.22	0.24	0.12	0.29	0.39	0.29	0.25	0.27	0.27	0.34	0.22	0.00	0.01	0.00
MnO	1.51	0.76	0.73	1.30	0.74	0.71	0.68	0.74	0.71	0.66	0.69	0.78	0.72	0.74	0.66	0.76	0.73	0.75	0.71	0.77	0.76	1.23	1.21	1.22
ZnO	0.63	0.31	0.30	0.77	0.24	0.24	0.26	0.27	0.29	0.23	0.24	0.30	0.22	0.17	0.16	0.16	0.21	0.17	0.18	0.19	0.20	0.61	0.64	0.62
Cr_2O_3	0.01	0.00	0.00	0.00	0.00	0.00	0.01	0.01	0.00	0.00	0.00	0.00	0.00	0.00	0.00	0.00	0.00	0.00	0.00	0.00	0.00	0.00	0.00	0.00
V_2O_3	0.01	0.00	0.00	0.00	0.02	0.03	0.00	0.01	0.01	0.01	0.01	0.00	0.01	0.00	0.01	0.01	0.00	0.00	0.00	0.00	0.02	0.01	0.00	0.01
ZrO_2	0.14	0.17	0.10	0.11	0.08	0.15	0.07	0.08	0.10	0.09	0.12	0.13	0.25	0.07	0.08	0.06	0.07	0.07	0.10	0.11	0.08	0.11	0.12	0.15
Nb_2O_5	0.00	0.00	0.03	0.00	0.00	0.00	0.00	0.00	0.00	0.00	0.00	0.00	0.01	0.00	0.00	0.00	0.00	0.00	0.00	0.00	0.00	0.02	0.00	0.02
Y_2O_3	0.00	0.00	0.00	0.00	0.00	0.00	0.00	0.00	0.00	0.00	0.00	0.00	0.00	0.00	0.00	0.00	0.00	0.00	0.00	0.00	0.00	0.00	0.00	0.00
Yb_2O_3	0.00	0.00	0.00	0.00	0.00	0.00	0.00	0.00	0.00	0.00	0.00	0.00	0.04	0.00	0.00	0.01	0.00	0.00	0.00	0.00	0.02	0.01	0.01	0.01
TiO_2	1.29	1.05	1.39	1.38	1.51	1.81	3.00	1.82	1.68	1.88	1.73	1.30	0.73	0.82	1.22	0.86	0.82	0.89	0.81	0.81	0.76	0.80	0.80	0.80
SiO_2	50.79	50.21	50.30	50.15	51.45	51.05	51.06	50.55	50.65	50.97	51.19	51.18	49.70	48.50	48.83	48.22	48.50	48.15	48.45	48.72	48.71	50.80	51.30	51.28
Al_2O_3	0.47	0.46	0.50	0.40	0.28	0.44	0.44	0.45	0.43	0.48	0.46	0.38	0.60	1.20	1.70	1.26	1.25	1.24	1.50	1.04	1.04	0.20	0.20	0.20
F	1.89	2.57	2.60	2.45	2.44	2.40	1.85	2.12	2.34	1.90	2.13	2.23	1.44	2.10	1.44	2.04	2.25	1.55	1.60	1.48	1.71	1.80	1.80	1.82
Cl	0.01	0.00	0.00	0.00	0.00	0.01	0.01	0.01	0.01	0.01	0.01	0.01	0.02	0.04	0.04	0.03	0.03	0.03	0.02	0.03	0.04	0.01	0.00	0.01
H_2O	0.96	0.64	0.63	0.70	0.75	0.76	1.03	0.88	0.78	1.00	0.90	0.85	1.19	0.88	1.20	0.91	0.81	1.13	1.11	1.17	1.06	1.02	1.04	1.02
Total	99.40	99.63	99.83	99.61	101.62	101.83	101.80	101.00	101.25	101.55	101.79	101.68	100.82	101.78	101.65	101.85	101.76	101.11	100.71	101.41	101.60	100.11	100.88	100.77
=O=F	0.80	1.08	1.09	1.03	1.03	1.01	0.78	0.89	0.99	0.80	0.90	0.94	0.61	0.88	0.61	0.86	0.95	0.65	0.67	0.62	0.72	0.76	0.76	0.77
=O=Cl	0.00	0.00	0.00	0.00	0.00	0.00	0.00	0.00	0.00	0.00	0.00	0.00	0.00	0.01	0.01	0.01	0.01	0.01	0.00	0.01	0.01	0.00	0.00	0.00
Total	98.60	98.54	98.74	98.58	100.59	100.81	101.02	100.10	100.26	100.74	100.90	100.74	100.21	100.89	101.04	100.98	100.80	100.45	100.04	100.78	100.87	99.35	100.13	100.00
Si	8.170	8.089	8.079	8.080	8.101	8.027	8.002	8.011	8.010	8.033	8.037	8.051	7.945	7.718	7.731	7.675	7.715	7.708	7.749	7.773	7.757	8.140	8.141	8.149
^{IV}Al	0.000	0.000	0.000	0.000	0.000	0.000	0.000	0.000	0.000	0.000	0.000	0.000	0.055	0.225	0.269	0.237	0.235	0.234	0.251	0.195	0.196	0.000	0.000	0.000
ΣTetrahedral	8.170	8.089	8.079	8.080	8.101	8.027	8.002	8.011	8.010	8.033	8.037	8.051	8.000	7.944	8.000	7.912	7.950	7.942	8.000	7.968	7.953	8.140	8.141	8.149
^{VI}Al	0.090	0.087	0.096	0.076	0.052	0.081	0.081	0.084	0.080	0.088	0.085	0.070	0.058	0.000	0.048	0.000	0.000	0.000	0.032	0.000	0.000	0.037	0.037	0.037
Ti	0.156	0.127	0.168	0.167	0.179	0.214	0.354	0.216	0.200	0.222	0.205	0.154	0.087	0.098	0.145	0.103	0.098	0.107	0.097	0.097	0.091	0.096	0.096	0.095
Fe^{3+}	0.310	0.604	0.545	0.563	0.638	0.631	0.461	0.631	0.691	0.521	0.617	0.724	0.638	0.824	0.670	0.848	0.870	0.769	0.834	0.699	0.810	0.641	0.693	0.670
Fe^{2+}	3.806	3.630	3.677	3.549	3.571	3.597	3.648	3.637	3.560	3.785	3.619	3.528	3.951	3.779	3.872	3.766	3.700	3.886	3.792	3.982	3.865	3.636	3.532	3.550
Mg	0.055	0.100	0.087	0.062	0.047	0.051	0.043	0.047	0.051	0.047	0.051	0.056	0.027	0.069	0.093	0.068	0.059	0.065	0.065	0.080	0.053	0.000	0.002	0.000
Mn	0.206	0.103	0.099	0.178	0.098	0.094	0.090	0.099	0.095	0.088	0.092	0.104	0.097	0.100	0.089	0.102	0.098	0.102	0.096	0.104	0.103	0.167	0.163	0.164
Zn	0.075	0.037	0.036	0.092	0.028	0.028	0.030	0.031	0.034	0.026	0.027	0.035	0.025	0.020	0.019	0.018	0.024	0.020	0.021	0.023	0.023	0.072	0.075	0.073
Cr	0.001	0.000	0.000	0.000	0.000	0.000	0.001	0.001	0.000	0.000	0.000	0.000	0.000	0.001	0.000	0.000	0.000	0.000	0.000	0.001	0.000	0.000	0.001	0.000
V	0.001	0.000	0.000	0.000	0.002	0.003	0.000	0.001	0.001	0.001	0.001	0.000	0.001	0.000	0.001	0.001	0.000	0.000	0.000	0.000	0.002	0.001	0.000	0.001
Zr	0.011	0.014	0.008	0.009	0.006	0.011	0.005	0.006	0.007	0.007	0.009	0.010	0.019	0.006	0.006	0.005	0.005	0.005	0.008	0.008	0.006	0.009	0.010	0.012
Nb	0.000	0.000	0.001	0.000	0.000	0.000	0.000	0.000	0.000	0.000	0.000	0.000	0.001	0.000	0.000	0.000	0.000	0.000	0.000	0.000	0.000	0.001	0.000	0.001
Y	0.000	0.000	0.000	0.000	0.000	0.000	0.000	0.000	0.000	0.000	0.000	0.000	0.000	0.000	0.000	0.000	0.000	0.000	0.000	0.000	0.000	0.000	0.000	0.000
Yb	0.000	0.000	0.000	0.000	0.000	0.000	0.000	0.000	0.000	0.000	0.000	0.000	0.002	0.000	0.000	0.000	0.000	0.000	0.000	0.000	0.001	0.001	0.000	0.000
ΣOctahedral	4.710	4.703	4.716	4.695	4.621	4.710	4.713	4.753	4.719	4.785	4.705	4.681	4.907	4.896	4.943	4.912	4.855	4.956	4.945	4.992	4.952	4.661	4.609	4.602
Na	2.788	2.737	2.807	2.800	2.890	2.925	2.905	2.907	2.929	2.853	2.917	2.921	2.650	2.558	2.586	2.526	2.620	2.494	2.681	2.504	2.599	2.759	2.808	2.809
K	0.287	0.414	0.348	0.350	0.374	0.294	0.360	0.275	0.277	0.280	0.287	0.304	0.208	0.136	0.165	0.127	0.122	0.151	0.144	0.146	0.116	0.413	0.415	0.414
Ca	0.045	0.056	0.049	0.076	0.014	0.043	0.020	0.054	0.065	0.048	0.054	0.043	0.235	0.466	0.305	0.523	0.453	0.457	0.229	0.350	0.380	0.028	0.029	0.026
ΣAlkali	3.120	3.207	3.204	3.225	3.278	3.263	3.284	3.237	3.271	3.182	3.258	3.268	3.093	3.160	3.057	3.176	3.195	3.102	3.055	3.040	3.095	3.199	3.251	3.249
F	0.962	1.311	1.321	1.248	1.214	1.195	0.919	1.062	1.170	0.945	1.056	1.109	0.729	1.056	0.720	1.029	1.131	0.784	0.807	0.749	0.862	0.910	0.902	0.915
Cl	0.004	0.000	0.000	0.000	0.000	0.003	0.002	0.004	0.003	0.004	0.003	0.003	0.004	0.011	0.011	0.009	0.009	0.009	0.004	0.009	0.011	0.001	0.000	0.002
OH	1.034	0.689	0.679	0.752	0.786	0.801	1.080	0.934	0.827	1.051	0.941	0.888	1.267	0.932	1.269	0.962	0.860	1.207	1.189	1.242	1.128	1.088	1.098	1.083
ΣOH,F,Cl	2.000	2.000	2.000	2.000	2.000	2.000	2.000	2.000	2.000	2.000	2.000	2.000	2.000	2.000	2.000	2.000	2.000	2.000	2.000	2.000	2.000	2.000	2.000	2.000

Acronyms used are: ed=edge; lt=light; dk=darker; dk=dark; mid=middle; gr=gran

Appendix B-1: Electron microprobe analyses of arfvedsonitic amphibole

Unit	Near Hypersolvus-Altered Subsolvus Contact																							
Sample #	46-A-3					46-I-3																		
Description	46A3	lt		42		46I3	labrpyx1	lapyx	mix	in	in	withpyx	3		inclinpyx					46I3				
File	am93	am93	am93	am93	am93	1/1/95	1/1/95	1/1/95	1/1/95	1/1/95	1/1/95	1/1/95	1/1/95	1/1/95	1/1/95	1/1/95	1/1/95	1/1/95	1/1/95	am92	am92	am92	am92	am92
Analysis #	67	68	69	70	72	137	138	140	142	143	144	146	151	154	156	158	159	160	161	20	21	22	23	24
Na_2O	8.78	8.41	8.28	8.30	8.46	8.82	8.76	9.01	9.76	9.10	8.70	8.63	8.92	8.85	8.69	8.93	8.72	8.75	8.71	8.31	8.68	8.41	8.64	8.77
K_2O	1.86	2.86	2.35	2.75	2.76	2.18	2.24	2.08	1.61	1.98	2.09	2.01	2.12	2.22	2.20	2.21	2.15	2.25	2.26	2.32	2.32	2.20	2.31	2.32
CaO	0.21	0.01	0.16	0.02	0.00	0.22	0.24	0.22	0.46	0.21	0.19	0.23	0.19	0.20	0.24	0.22	0.24	0.18	0.20	0.20	0.21	0.36	0.25	0.21
FeO	29.76	25.51	28.50	27.50	28.14	27.26	26.91	26.60	24.17	26.35	26.82	27.77	27.56	26.65	27.29	26.03	27.24	26.73	27.17	25.82	25.34	26.92	25.42	25.07
Fe_2O_3	0.42	3.87	1.12	3.56	0.73	4.87	5.26	5.47	7.52	5.81	5.66	4.44	3.63	5.68	5.04	6.23	4.78	5.15	4.82	5.71	6.78	5.05	5.88	6.81
MgO	0.13	0.98	0.46	0.29	0.23	0.00	0.01	0.00	0.02	0.00	0.00	0.02	0.00	0.01	0.00	0.01	0.01	0.01	0.00	0.00	0.00	0.02	0.01	0.01
MnO	1.03	1.51	1.46	1.58	1.62	1.52	1.55	1.45	1.44	1.43	1.54	1.51	1.52	1.51	1.53	1.53	1.56	1.61	1.61	1.48	1.52	1.50	1.53	1.47
ZnO	0.83	1.33	1.29	1.19	0.98	0.73	0.65	0.68	0.74	0.70	0.70	0.69	0.74	0.68	0.71	0.67	0.75	0.86	0.97	0.74	0.80	0.82	0.94	0.85
Cr_2O_3	0.00	0.00	0.00	0.00	0.00	0.00	0.00	0.00	0.01	0.00	0.00	0.00	0.00	0.00	0.00	0.00	0.01	0.01	0.01	0.00	0.00	0.00	0.00	0.00
V_2O_3	0.00	0.00	0.00	0.00	0.00	0.02	0.00	0.01	0.00	0.00	0.01	0.01	0.00	0.01	0.00	0.00	0.00	0.01	0.00	0.00	0.00	0.00	0.00	0.00
ZrO_2	0.14	0.00	0.07	0.06	0.02	0.71	0.69	0.63	0.67	0.69	0.38	0.37	0.72	0.62	0.61	0.59	0.65	0.67	0.62	0.63	0.62	0.62	0.63	0.61
Nb_2O_5	0.01	0.01	0.00	0.03	0.00	0.00	0.00	0.00	0.00	0.00	0.00	0.00	0.00	0.00	0.00	0.00	0.00	0.00	0.00	0.03	0.07	0.04	0.08	0.05
Y_2O_3	0.00	0.00	0.00	0.00	0.00	0.00	0.00	0.00	0.00	0.00	0.00	0.00	0.00	0.00	0.00	0.00	0.00	0.00	0.00	0.00	0.00	0.00	0.00	0.00
Yb_2O_3	0.00	0.00	0.00	0.00	0.00	0.00	0.00	0.00	0.00	0.00	0.00	0.00	0.00	0.00	0.00	0.00	0.00	0.00	0.00	0.00	0.00	0.00	0.00	0.00
TiO_2	1.98	0.36	0.76	0.29	0.87	0.93	0.89	0.93	0.88	0.91	0.88	0.79	0.98	0.92	0.90	0.92	0.91	0.86	0.88	0.96	0.95	0.89	0.84	0.96
SiO_2	51.52	52.09	51.95	52.06	52.66	50.98	50.74	50.89	50.80	50.74	50.25	50.63	51.44	50.71	50.69	50.57	50.72	50.73	51.02	48.60	49.49	49.69	49.64	49.58
Al_2O_3	0.30	0.39	0.20	0.17	0.23	0.16	0.14	0.16	0.18	0.14	0.16	0.17	0.17	0.16	0.16	0.14	0.13	0.16	0.16	0.15	0.13	0.11	0.13	0.14
F	2.44	2.94	2.26	2.64	2.86	2.13	2.09	1.93	1.40	2.00	2.05	1.92	1.95	2.15	2.17	2.09	2.07	2.01	2.09	2.03	2.16	2.13	2.17	2.21
Cl	0.00	0.00	0.00	0.00	0.00	0.00	0.00	0.01	0.00	0.00	0.00	0.01	0.00	0.00	0.00	0.00	0.00	0.00	0.00	0.00	0.00	0.00	0.00	0.00
H_2O	0.72	0.50	0.79	0.63	0.52	0.88	0.89	0.97	1.23	0.93	0.89	0.95	0.96	0.86	0.85	0.89	0.89	0.92	0.89	0.85	0.83	0.84	0.81	0.81
Total	100.13	100.75	99.67	101.05	100.09	101.39	101.06	101.03	100.87	101.00	100.32	100.12	100.89	101.22	101.08	101.01	100.84	100.90	101.41	97.83	99.90	99.59	99.27	99.86
=O=F	1.03	1.24	0.95	1.11	1.21	0.89	0.88	0.81	0.59	0.84	0.86	0.81	0.82	0.91	0.91	0.88	0.87	0.85	0.88	0.85	0.91	0.89	0.91	0.93
=O=Cl	0.00	0.00	0.00	0.00	0.00	0.00	0.00	0.00	0.00	0.00	0.00	0.00	0.00	0.00	0.00	0.00	0.00	0.00	0.00	0.00	0.00	0.00	0.00	0.00
Total	99.10	99.52	98.72	99.94	98.89	100.50	100.18	100.22	100.28	100.15	99.46	99.31	100.07	100.31	100.17	100.13	99.97	100.05	100.53	96.98	98.99	98.69	98.35	98.93
Si	8.248	8.273	8.347	8.292	8.421	8.106	8.094	8.097	8.038	8.081	8.076	8.141	8.185	8.078	8.095	8.063	8.111	8.103	8.116	8.033	8.009	8.071	8.072	8.018
^{IV}Al	0.000	0.000	0.000	0.000	0.000	0.000	0.000	0.000	0.000	0.000	0.000	0.000	0.000	0.000	0.000	0.000	0.000	0.000	0.000	0.000	0.000	0.000	0.000	0.000
ΣTetrahedral	8.248	8.273	8.347	8.292	8.421	8.106	8.094	8.097	8.038	8.081	8.076	8.141	8.185	8.078	8.095	8.063	8.111	8.103	8.116	8.033	8.009	8.071	8.072	8.018
^{VI}Al	0.057	0.072	0.038	0.032	0.044	0.030	0.026	0.030	0.034	0.027	0.030	0.032	0.032	0.031	0.029	0.026	0.024	0.030	0.029	0.030	0.024	0.021	0.024	0.026
Ti	0.238	0.043	0.092	0.034	0.105	0.111	0.106	0.111	0.104	0.109	0.106	0.095	0.117	0.110	0.108	0.110	0.110	0.103	0.105	0.120	0.115	0.109	0.103	0.116
Fe^{3+}	0.050	0.462	0.136	0.426	0.088	0.582	0.632	0.655	0.895	0.696	0.685	0.537	0.435	0.680	0.606	0.747	0.576	0.619	0.577	0.710	0.826	0.617	0.720	0.829
Fe^{2+}	3.985	3.388	3.810	3.664	3.763	3.625	3.591	3.541	3.198	3.510	3.606	3.734	3.667	3.550	3.645	3.471	3.643	3.571	3.614	3.570	3.429	3.657	3.457	3.391
Mg	0.032	0.231	0.110	0.069	0.056	0.000	0.003	0.000	0.004	0.001	0.000	0.004	0.000	0.002	0.000	0.001	0.001	0.001	0.000	0.000	0.000	0.005	0.001	0.003
Mn	0.140	0.203	0.198	0.213	0.220	0.205	0.210	0.196	0.192	0.193	0.210	0.206	0.205	0.204	0.207	0.207	0.212	0.218	0.217	0.207	0.208	0.206	0.211	0.202
Zn	0.098	0.156	0.153	0.140	0.115	0.085	0.077	0.080	0.086	0.082	0.083	0.081	0.087	0.080	0.084	0.078	0.088	0.101	0.114	0.091	0.096	0.098	0.112	0.101
Cr	0.000	0.000	0.000	0.000	0.000	0.000	0.000	0.000	0.001	0.000	0.000	0.000	0.001	0.000	0.000	0.000	0.001	0.001	0.001	0.000	0.000	0.000	0.000	0.000
V	0.000	0.000	0.000	0.000	0.000	0.002	0.000	0.001	0.000	0.000	0.001	0.001	0.000	0.001	0.000	0.000	0.000	0.001	0.000	0.000	0.000	0.000	0.000	0.000
Zr	0.011	0.000	0.006	0.004	0.001	0.055	0.054	0.049	0.052	0.054	0.030	0.029	0.056	0.048	0.048	0.046	0.051	0.052	0.048	0.050	0.049	0.049	0.050	0.048
Nb	0.001	0.000	0.000	0.001	0.000	0.000	0.000	0.000	0.000	0.000	0.000	0.000	0.000	0.000	0.000	0.000	0.000	0.000	0.000	0.001	0.003	0.002	0.003	0.002
Y	0.000	0.000	0.000	0.000	0.000	0.000	0.000	0.000	0.000	0.000	0.000	0.000	0.000	0.000	0.000	0.000	0.000	0.000	0.000	0.000	0.000	0.000	0.000	0.000
Yb	0.000	0.000	0.000	0.000	0.000	0.000	0.000	0.000	0.000	0.000	0.000	0.000	0.000	0.000	0.000	0.000	0.000	0.000	0.000	0.000	0.000	0.000	0.000	0.000
ΣOctahedral	4.612	4.555	4.563	4.583	4.393	4.697	4.699	4.663	4.565	4.673	4.750	4.719	4.599	4.706	4.726	4.687	4.705	4.698	4.705	4.780	4.751	4.764	4.682	4.719
Na	2.725	2.589	2.581	2.564	2.623	2.718	2.710	2.780	2.995	2.809	2.712	2.689	2.753	2.732	2.689	2.762	2.703	2.710	2.687	2.663	2.725	2.647	2.723	2.748
K	0.379	0.580	0.482	0.558	0.564	0.442	0.457	0.422	0.324	0.402	0.429	0.411	0.430	0.451	0.448	0.450	0.439	0.458	0.458	0.488	0.480	0.455	0.480	0.478
Ca	0.036	0.002	0.027	0.003	0.001	0.017	0.040	0.018	0.078	0.036	0.032	0.040	0.032	0.034	0.041	0.037	0.042	0.030	0.035	0.036	0.036	0.063	0.043	0.036
ΣAlkalis	3.140	3.171	3.091	3.125	3.187	3.197	3.207	3.240	3.397	3.246	3.173	3.140	3.215	3.216	3.179	3.249	3.185	3.199	3.179	3.187	3.241	3.165	3.246	3.263
F	1.233	1.475	1.149	1.330	1.448	1.069	1.055	0.970	0.702	1.008	1.040	0.978	0.981	1.084	1.094	1.052	1.046	1.017	1.053	1.061	1.103	1.092	1.116	1.128
Cl	0.000	0.000	0.000	0.000	0.000	0.001	0.000	0.001	0.000	0.000	0.001	0.002	0.001	0.001	0.001	0.000	0.000	0.000	0.000	0.000	0.000	0.000	0.000	0.000
OH	0.767	0.525	0.851	0.670	0.552	0.931	0.945	1.029	1.298	0.992	0.960	1.020	1.018	0.916	0.906	0.948	0.954	0.982	0.947	0.939	0.897	0.908	0.884	0.872
ΣOH,F,Cl	2.000	2.000	2.000	2.000	2.000	2.000	2.000	2.000	2.000	2.000	2.000	2.000	2.000	2.000	2.000	2.000	2.000	2.000	2.000	2.000	2.000	2.000	2.000	2.000

Acronyms used are: edsedge; ltslight; lter=lighter; dkeradarker; dksdark; nrsnear; midsmiddle; 2ndsesecond; grsgrain

Mineral formulae were calculated based on 23 atoms of oxygen and 16 cations, with Fe3+ calculated by the method of Droop (1987)

Appendix B-1 Electron microprobe analyses of arfvedsonitic amphibole

Unit	Near Hyp																						
Sample #	46-1-3																						
Description											dk s	mid	edge	46l3 1ed	center	mid	ed	mid	3 ed	mid	center	ed l6l3 1 mid	ed
File	am92	am92	am92	am92	am92	am92	am92	am92	am92	am92	am92	am92	am92	kp	kp	kp	kp	kp	kp	kp	kp	kp	kp
Analysis #	25	26	27	28	29	30	31	32	33	34	38	39	40	11	12	13	14	15	16	17	18	19	29	30
Na_2O	8.89	8.13	8.19	8.65	8.85	8.92	8.57	8.29	8.33	7.94	8.81	8.90	9.05	9.41	9.54	9.35	9.18	9.51	9.57	9.52	9.26	9.31	9.35	9.07
K_2O	2.29	2.29	2.24	2.29	2.31	2.37	2.36	2.32	2.36	2.31	2.26	2.24	2.37	2.07	2.08	2.14	2.07	2.06	2.05	1.99	2.06	2.08	2.03	2.15
CaO	0.24	0.20	0.20	0.22	0.23	0.23	0.23	0.24	0.22	0.26	0.17	0.18	0.22	0.17	0.17	0.17	0.17	0.18	0.18	0.18	0.17	0.18	0.16	0.16
FeO	25.47	29.50	28.86	25.07	24.39	24.05	26.02	27.55	26.97	29.11	24.91	25.21	22.83	25.61	24.94	25.09	26.11	25.39	25.81	25.47	25.83	25.03	25.34	24.63
Fe_2O_3	5.71	0.42	2.82	7.32	7.64	7.90	5.21	3.59	4.64	2.47	6.99	5.83	9.08	6.13	6.75	6.79	5.41	6.44	5.60	6.44	5.86	6.72	6.53	7.15
MgO	0.00	0.00	0.01	0.00	0.00	0.01	0.00	0.00	0.00	0.02	0.00	0.00	0.01	0.00	0.00	0.00	0.00	0.00	0.00	0.01	0.00	0.00	0.01	0.00
MnO	1.47	1.49	1.49	1.49	1.56	1.54	1.51	1.46	1.51	1.58	1.63	1.64	1.52	1.53	1.52	1.53	1.52	1.52	1.51	1.53	1.52	1.53	1.56	1.54
ZnO	0.83	0.78	0.76	0.86	0.86	0.76	0.73	0.87	0.81	0.84	0.96	0.77	0.74	0.65	0.70	0.72	0.68	0.67	0.73	0.72	0.72	0.66	0.69	0.66
Cr_2O_3	0.00	0.00	0.00	0.00	0.00	0.00	0.00	0.00	0.00	0.00	0.00	0.00	0.00	0.00	0.00	0.01	0.00	0.00	0.00	0.00	0.00	0.00	0.00	0.00
V_2O_3	0.00	0.00	0.00	0.00	0.00	0.00	0.00	0.00	0.00	0.00	0.00	0.00	0.00	0.00	0.00	0.01	0.00	0.00	0.01	0.01	0.02	0.02	0.00	0.04
ZrO_2	0.67	0.63	0.64	0.63	0.67	0.67	0.64	0.64	0.62	0.60	0.09	0.08	0.66	0.75	0.76	0.81	0.78	0.75	0.77	0.76	0.83	0.80	0.75	0.82
Nb_2O_5	0.02	0.01	0.03	0.07	0.04	0.08	0.01	0.05	0.05	0.04	0.07	0.06	0.05	0.03	0.01	0.03	0.04	0.02	0.04	0.01	0.03	0.03	0.02	0.03
Y_2O_3	0.00	0.00	0.00	0.00	0.00	0.00	0.00	0.00	0.00	0.00	0.00	0.00	0.00	0.00	0.00	0.00	0.00	0.00	0.00	0.00	0.00	0.00	0.00	0.00
Yb_2O_3	0.00	0.00	0.00	0.00	0.00	0.00	0.00	0.00	0.00	0.00	0.00	0.00	0.00	0.01	0.02	0.01	0.01	0.01	0.02	0.00	0.01	0.02	0.01	0.02
TiO_2	0.98	0.94	0.97	0.91	0.91	0.92	0.95	0.95	0.88	0.89	1.59	1.65	0.88	0.89	0.88	0.89	0.90	0.89	0.87	0.88	0.88	0.87	0.88	0.89
SiO_2	50.23	50.85	50.28	49.12	49.41	49.42	49.74	49.95	49.73	50.07	49.34	49.75	48.96	51.42	51.39	50.98	51.05	51.57	52.09	51.54	51.09	50.68	50.99	49.75
Al_2O_3	0.12	0.15	0.16	0.15	0.14	0.13	0.12	0.15	0.15	0.25	0.20	0.16	0.17	0.14	0.15	0.14	0.14	0.14	0.14	0.14	0.13	0.14	0.13	0.14
F	2.30	2.43	2.32	2.21	2.20	2.20	2.30	2.34	2.45	2.26	2.12	2.10	2.15	1.77	1.96	1.82	1.94	1.84	1.75	1.71	1.68	1.61	1.71	1.88
Cl	0.00	0.00	0.00	0.00	0.00	0.00	0.00	0.00	0.00	0.00	0.00	0.00	0.00	0.00	0.00	0.00	0.01	0.00	0.01	0.00	0.00	0.01	0.00	0.01
H_2O	0.77	0.68	0.75	0.80	0.81	0.81	0.75	0.73	0.68	0.77	0.85	0.86	0.83	1.06	0.98	1.03	0.97	1.03	1.08	1.10	1.09	1.12	1.08	0.97
Total	100.00	98.48	99.69	99.78	100.03	100.00	99.13	99.13	99.39	99.40	99.99	99.41	99.50	101.63	101.84	101.50	100.96	102.03	102.23	102.01	101.19	100.78	101.24	99.90
=O=F	0.97	1.02	0.98	0.93	0.92	0.93	0.97	0.98	1.03	0.95	0.89	0.88	0.91	0.74	0.82	0.76	0.82	0.78	0.74	0.72	0.71	0.68	0.72	0.79
=O=Cl	0.00	0.00	0.00	0.00	0.00	0.00	0.00	0.00	0.00	0.00	0.00	0.00	0.00	0.00	0.00	0.00	0.00	0.00	0.00	0.00	0.00	0.00	0.00	0.00
Total	99.03	97.46	98.72	98.85	99.10	99.08	98.16	98.15	98.36	98.45	99.10	98.53	98.59	100.89	101.01	100.74	100.15	101.25	101.49	101.29	100.48	100.10	100.52	99.11
Si	8.093	8.323	8.161	7.971	7.980	7.978	8.099	8.147	8.103	8.161	7.961	8.044	7.935	8.105	8.087	8.061	8.119	8.097	8.148	8.091	8.098	8.063	8.076	8.015
^{IV}Al	0.000	0.000	0.000	0.028	0.020	0.022	0.000	0.000	0.000	0.000	0.038	0.000	0.032	0.000	0.000	0.000	0.000	0.000	0.000	0.000	0.000	0.000	0.000	0.000
ΣTetrahedral	8.093	8.323	8.163	7.999	8.000	8.000	8.099	8.147	8.103	8.161	7.999	8.044	7.968	8.105	8.087	8.061	8.119	8.097	8.148	8.091	8.098	8.063	8.076	8.015
^{VI}Al	0.023	0.028	0.030	0.000	0.006	0.002	0.023	0.030	0.028	0.049	0.000	0.031	0.000	0.027	0.027	0.027	0.025	0.025	0.026	0.026	0.024	0.026	0.025	0.027
Ti	0.119	0.115	0.118	0.111	0.111	0.112	0.116	0.117	0.108	0.108	0.193	0.201	0.107	0.105	0.104	0.106	0.107	0.105	0.103	0.104	0.105	0.104	0.104	0.108
Fe^{3+}	0.693	0.051	0.344	0.894	0.929	0.959	0.639	0.441	0.569	0.303	0.849	0.709	1.107	0.727	0.800	0.808	0.647	0.762	0.659	0.760	0.699	0.804	0.778	0.867
Fe^{2+}	3.432	4.038	3.918	3.402	3.295	3.247	3.543	3.758	3.675	3.969	3.361	3.409	3.094	3.375	3.283	3.319	3.473	3.334	3.376	3.344	3.425	3.330	3.356	3.319
Mg	0.000	0.000	0.003	0.000	0.000	0.002	0.000	0.000	0.000	0.004	0.000	0.000	0.001	0.001	0.000	0.000	0.000	0.000	0.000	0.001	0.000	0.000	0.002	0.000
Mn	0.200	0.207	0.205	0.205	0.213	0.211	0.208	0.202	0.209	0.219	0.223	0.225	0.209	0.204	0.203	0.205	0.205	0.202	0.200	0.204	0.204	0.206	0.209	0.210
Zn	0.099	0.094	0.091	0.103	0.103	0.091	0.088	0.105	0.098	0.101	0.114	0.091	0.088	0.075	0.081	0.084	0.080	0.078	0.084	0.083	0.085	0.077	0.080	0.078
Cr	0.000	0.000	0.000	0.000	0.000	0.000	0.000	0.000	0.000	0.000	0.000	0.000	0.000	0.000	0.000	0.001	0.001	0.000	0.000	0.000	0.000	0.000	0.000	0.000
V	0.000	0.000	0.000	0.000	0.000	0.000	0.000	0.000	0.000	0.000	0.000	0.000	0.000	0.000	0.000	0.001	0.000	0.000	0.001	0.001	0.002	0.002	0.000	0.005
Zr	0.052	0.050	0.050	0.050	0.053	0.053	0.051	0.051	0.049	0.047	0.007	0.006	0.052	0.058	0.058	0.062	0.060	0.057	0.058	0.058	0.064	0.062	0.058	0.064
Nb	0.001	0.001	0.001	0.003	0.002	0.004	0.000	0.002	0.002	0.002	0.003	0.003	0.002	0.001	0.000	0.001	0.002	0.001	0.002	0.001	0.001	0.001	0.001	0.001
Y	0.000	0.000	0.000	0.000	0.000	0.000	0.000	0.000	0.000	0.000	0.000	0.000	0.000	0.000	0.000	0.000	0.000	0.000	0.000	0.000	0.000	0.000	0.000	0.000
Yb	0.000	0.000	0.000	0.000	0.000	0.000	0.000	0.000	0.000	0.000	0.000	0.000	0.000	0.000	0.001	0.000	0.001	0.001	0.001	0.000	0.001	0.001	0.001	0.001
ΣOctahedral	4.619	4.585	4.761	4.768	4.712	4.680	4.667	4.705	4.737	4.802	4.752	4.675	4.660	4.574	4.557	4.613	4.602	4.564	4.511	4.582	4.609	4.613	4.614	4.680
Na	2.777	2.580	2.577	2.720	2.773	2.792	2.704	2.623	2.631	2.511	2.756	2.789	2.844	2.876	2.910	2.867	2.832	2.896	2.902	2.897	2.846	2.872	2.872	2.835
K	0.470	0.477	0.464	0.474	0.476	0.488	0.489	0.483	0.491	0.481	0.464	0.461	0.490	0.417	0.417	0.431	0.420	0.413	0.408	0.399	0.417	0.422	0.410	0.443
Ca	0.041	0.036	0.035	0.019	0.039	0.040	0.040	0.041	0.038	0.045	0.029	0.030	0.038	0.029	0.028	0.029	0.028	0.029	0.031	0.031	0.029	0.030	0.028	0.027
ΣAlkalis	3.289	3.093	3.076	3.233	3.288	3.320	3.234	3.148	3.160	3.037	3.249	3.281	3.372	3.321	3.355	3.327	3.280	3.339	3.341	3.326	3.292	3.324	3.310	3.305
F	1.173	1.259	1.189	1.134	1.121	1.122	1.183	1.206	1.264	1.166	1.081	1.073	1.104	0.881	0.974	0.908	0.974	0.916	0.866	0.847	0.841	0.809	0.855	0.956
Cl	0.000	0.000	0.000	0.000	0.000	0.000	0.000	0.000	0.000	0.000	0.000	0.000	0.000	0.000	0.000	0.000	0.001	0.001	0.001	0.001	0.001	0.001	0.001	0.002
OH	0.827	0.741	0.811	0.866	0.879	0.878	0.817	0.794	0.736	0.834	0.919	0.927	0.896	1.119	1.026	1.092	1.025	1.083	1.132	1.152	1.158	1.190	1.145	1.042
ΣOH,F,Cl	2.000	2.000	2.000	2.000	2.000	2.000	2.000	2.000	2.000	2.000	2.000	2.000	2.000	2.000	2.000	2.000	2.000	2.000	2.000	2.000	2.000	2.000	2.000	2.000

Acronyms used are: e=edge; lt=light; ltr=lighter; dkr=darker; dk=dark; nr=near; mid=middle; 2nd=second; gr=grain
Mineral formulae were calculated based on 23 atoms of oxygen and 16 cations, with Fe3+ calculated by the method of Droop (1987)

Appendix B-1: Electron microprobe analyses of arfvedsonitic amphibole

Unit	Near Hypersolvus-Altered Subsolvus Contact																	
Sample #	46-1-3																	
Description	3 ed	mid	ed	4ed	mid	center	46l3 ed	mid	mid	center	mid	mid	nred	ed	46l3			
File	kp	kp	kp	kp	kp	kp	kp	kp	kp	kp	kp	kp	kp	kp	kp	kp	kp	kp
Analysis #	31	32	33	34	35	36	146	147	148	149	150	151	152	153	23.2	24.2	25.2
Na_2O	9.25	9.27	8.76	9.53	9.26	9.24	8.94	8.96	9.12	9.03	9.14	8.94	8.87	9.16	9.10	8.94	9.01
K_2O	2.16	2.20	2.19	2.20	2.21	2.23	2.26	2.23	2.29	2.27	2.33	2.29	2.24	2.24	2.13	2.20	2.14
CaO	0.27	0.17	0.35	0.19	0.18	0.19	0.18	0.21	0.19	0.17	0.17	0.18	0.24	0.19	0.21	0.20	0.20
FeO	26.00	25.68	25.93	25.75	26.22	25.52	25.78	25.60	24.97	26.05	25.14	26.11	26.51	24.69	26.65	26.73	27.02
Fe_2O_3	6.03	6.52	6.33	6.07	5.77	6.91	6.53	6.82	7.59	6.23	7.29	6.32	5.74	7.84	5.28	5.65	5.48
MgO	0.01	0.00	0.01	0.00	0.00	0.00	0.00	0.01	0.00	0.00	0.00	0.00	0.00	0.00	0.00	0.00	0.00
MnO	1.44	1.45	1.48	1.46	1.50	1.48	1.44	1.44	1.47	1.43	1.47	1.46	1.46	1.45	1.43	1.45	1.44
ZnO	0.77	0.65	0.76	0.71	0.66	0.73	0.66	0.70	0.66	0.66	0.68	0.69	0.68	0.70	0.50	0.50	0.54
Cr_2O_3	0.01	0.00	0.00	0.00	0.00	0.00	0.00	0.00	0.01	0.00	0.00	0.00	0.00	0.00	0.00	0.00	0.01
V_2O_3	0.03	0.04	0.01	0.02	0.03	0.01	0.00	0.00	0.00	0.00	0.00	0.01	0.00	0.01	0.01	0.01	0.00
ZrO_2	0.51	0.52	0.51	0.56	0.54	0.54	0.47	0.48	0.51	0.51	0.53	0.52	0.52	0.50	0.60	0.56	0.61
Nb_2O_5	0.01	0.02	0.01	0.03	0.02	0.01	0.02	0.01	0.00	0.00	0.01	0.03	0.02	0.01	0.01	0.02	0.00
Y_2O_3	0.00	0.00	0.00	0.00	0.00	0.00	0.00	0.00	0.00	0.00	0.00	0.00	0.00	0.00	0.00	0.00	0.00
Yb_2O_3	0.02	0.01	0.01	0.01	0.02	0.01	0.01	0.00	0.00	0.01	0.01	0.01	0.01	0.02	0.02	0.01	0.03
TiO_2	0.86	0.89	0.89	0.79	0.81	0.82	0.83	0.80	0.83	0.83	0.82	0.83	0.84	0.84	0.95	0.94	0.93
SiO_2	51.59	51.29	50.08	52.34	51.79	51.26	50.51	50.45	50.56	51.01	50.83	50.81	50.82	50.39	51.20	50.87	51.20
Al_2O_3	0.18	0.15	0.17	0.17	0.15	0.16	0.16	0.16	0.16	0.16	0.14	0.16	0.16	0.16	0.15	0.15	0.15
F	1.66	1.76	1.64	2.05	1.80	1.93	1.81	1.94	1.83	1.89	1.93	1.90	1.89	1.85	1.80	1.74	1.90
Cl	0.01	0.00	0.01	0.01	0.00	0.00	0.00	0.00	0.00	0.00	0.00	0.01	0.00	0.00	0.00	0.00	0.00
H_2O	1.12	1.07	1.09	0.95	1.05	0.99	1.02	0.96	1.02	0.99	0.98	0.99	0.99	1.01	1.03	1.06	0.99
Total	101.90	101.69	100.21	102.83	102.00	102.01	100.62	100.76	101.20	101.26	101.47	101.24	100.97	101.04	101.07	101.03	101.67
=O=F	0.70	0.74	0.69	0.86	0.76	0.81	0.76	0.81	0.77	0.80	0.81	0.80	0.79	0.78	0.76	0.73	0.80
=O=Cl	0.00	0.00	0.00	0.00	0.00	0.00	0.00	0.00	0.00	0.00	0.00	0.00	0.00	0.00	0.00	0.00	0.00
Total	101.20	100.95	99.52	101.96	101.24	101.20	99.86	99.95	100.43	100.46	100.66	100.45	100.18	100.26	100.31	100.30	100.87
Si	8.109	8.087	8.042	8.147	8.136	8.070	8.069	8.056	8.029	8.093	8.051	8.074	8.096	8.016	8.125	8.091	8.098
^{IV}Al	0.000	0.000	0.000	0.000	0.000	0.000	0.000	0.000	0.000	0.000	0.000	0.000	0.000	0.000	0.000	0.000	0.000
ΣTetrahedral	8.109	8.087	8.042	8.147	8.136	8.070	8.069	8.056	8.029	8.093	8.051	8.074	8.096	8.016	8.125	8.091	8.098
^{VI}Al	0.033	0.027	0.031	0.031	0.027	0.029	0.030	0.029	0.029	0.030	0.027	0.031	0.030	0.029	0.028	0.029	0.029
Ti	0.102	0.105	0.107	0.093	0.096	0.097	0.100	0.096	0.100	0.098	0.098	0.099	0.101	0.100	0.113	0.112	0.111
Fe^{2+}	0.713	0.774	0.765	0.712	0.682	0.819	0.785	0.820	0.907	0.744	0.869	0.756	0.688	0.939	0.630	0.677	0.652
Fe^{3+}	3.418	3.387	3.482	3.352	3.445	3.360	3.445	3.418	3.316	3.457	3.331	3.471	3.532	3.285	3.538	3.555	3.575
Mg	0.003	0.000	0.003	0.000	0.000	0.000	0.000	0.002	0.000	0.000	0.000	0.000	0.000	0.000	0.000	0.001	0.000
Mn	0.192	0.194	0.201	0.193	0.199	0.197	0.195	0.195	0.197	0.192	0.197	0.196	0.197	0.195	0.192	0.195	0.192
Zn	0.089	0.076	0.090	0.081	0.076	0.085	0.078	0.083	0.077	0.077	0.079	0.081	0.080	0.082	0.059	0.059	0.063
Cr	0.001	0.000	0.000	0.000	0.000	0.000	0.000	0.000	0.001	0.000	0.000	0.000	0.000	0.000	0.000	0.000	0.001
V	0.003	0.004	0.001	0.002	0.003	0.001	0.000	0.000	0.000	0.000	0.000	0.001	0.000	0.001	0.001	0.001	0.000
Zr	0.039	0.040	0.040	0.043	0.042	0.041	0.037	0.037	0.040	0.040	0.041	0.040	0.041	0.038	0.047	0.044	0.047
Nb	0.000	0.001	0.000	0.001	0.001	0.000	0.001	0.000	0.000	0.000	0.000	0.001	0.001	0.000	0.000	0.001	0.000
Y	0.000	0.000	0.000	0.000	0.000	0.000	0.000	0.000	0.000	0.000	0.000	0.000	0.000	0.000	0.000	0.000	0.000
Yb	0.001	0.001	0.000	0.000	0.001	0.000	0.000	0.000	0.000	0.001	0.000	0.001	0.000	0.001	0.001	0.000	0.001
ΣOctahedral	4.593	4.609	4.721	4.508	4.572	4.631	4.670	4.681	4.667	4.639	4.642	4.676	4.669	4.672	4.609	4.673	4.672
Na	2.820	2.833	2.729	2.878	2.819	2.820	2.768	2.774	2.808	2.778	2.807	2.754	2.759	2.825	2.800	2.755	2.763
K	0.432	0.442	0.448	0.436	0.444	0.448	0.461	0.454	0.465	0.459	0.470	0.465	0.456	0.455	0.431	0.447	0.432
Ca	0.045	0.029	0.060	0.031	0.030	0.031	0.031	0.036	0.032	0.030	0.030	0.031	0.041	0.032	0.035	0.034	0.034
ΣAlkalis	3.297	3.304	3.237	3.345	3.292	3.299	3.261	3.264	3.305	3.267	3.307	3.250	3.235	3.313	3.266	3.236	3.230
F	0.825	0.878	0.834	1.007	0.893	0.963	0.912	0.977	0.918	0.950	0.967	0.952	0.950	0.929	0.903	0.874	0.951
Cl	0.002	0.001	0.002	0.002	0.001	0.000	0.001	0.000	0.000	0.001	0.001	0.001	0.000	0.001	0.001	0.000	0.001
OH	1.173	1.121	1.164	0.991	1.106	1.037	1.087	1.023	1.082	1.049	1.032	1.046	1.050	1.070	1.096	1.125	1.048
ΣOH,F,Cl	2.000	2.000	2.000	2.000	2.000	2.000	2.000	2.000	2.000	2.000	2.000	2.000	2.000	2.000	2.000	2.000	2.000

Acronyms used are: ed=edge; nr=near; mid=middle

Appendix B-1 Electron microprobe analyses of arfvedsonitic amphibole

Unit	Fresh Subsolvus																						
Sample #	37-D-1			37-E-4			38-B-3																
Description	37D1	mid	ed	37E4	#2		bestdk	lt	dk	lt	dker	bltdk	3802 ed	lt	dker	med	lt	dk	dker	dker	lter	ed		lt
File	am93	am93	am93	am93	am93	am93	kp	kp	kp	kp	kp	kp	kp	kp	kp	kp	kp	kp	kp	kp	kp	kp	kp	kp
Analysis #	50	52	54	56	57	60	162	163	164	165	166	167	107	108	109	110	111	112	113	114	115	116	117	118
Na_2O	9.02	9.26	9.04	7.10	9.32	9.33	9.66	9.41	9.82	9.36	9.43	9.38	8.75	8.80	9.50	9.53	9.49	9.19	9.56	9.82	9.68	9.51	9.28	9.05
K_2O	1.64	1.63	1.89	0.90	1.61	1.51	1.52	1.47	1.44	1.58	1.50	1.51	2.49	2.50	1.30	1.30	1.30	2.26	1.26	1.22	1.26	1.23	2.13	2.16
CaO	0.10	0.11	0.09	0.05	0.10	0.13	0.07	0.08	0.08	0.09	0.09	0.08	0.17	0.14	0.32	0.35	0.30	0.07	0.13	0.13	0.14	0.13	0.03	0.04
FeO	28.13	26.54	27.30	34.53	26.23	26.25	27.62	28.56	26.77	27.49	28.01	28.11	27.68	27.59	27.20	27.00	27.29	26.70	27.91	26.85	26.05	27.38	25.75	25.76
Fe_2O_3	5.36	7.62	6.30	0.00	5.11	6.35	3.86	3.78	4.99	4.81	4.32	3.87	5.13	5.52	6.57	7.05	7.00	6.06	5.72	6.91	8.82	6.57	7.25	7.80
MgO	0.05	0.06	0.01	0.43	0.22	0.11	0.02	0.01	0.00	0.02	0.00	0.01	0.15	0.13	0.13	0.15	0.10	0.10	0.09	0.08	0.09	0.10	0.13	0.11
MnO	0.54	0.47	0.61	0.29	0.61	0.58	1.00	0.96	0.98	1.01	0.98	0.99	0.77	0.72	0.63	0.66	0.64	0.59	0.61	0.57	0.57	0.55	0.61	0.60
ZnO	0.35	0.23	0.36	0.55	0.38	0.29	0.43	0.37	0.41	0.48	0.41	0.37	0.34	0.34	0.24	0.19	0.25	0.20	0.20	0.21	0.19	0.19	0.27	0.22
Cr_2O_3	0.00	0.00	0.00	0.00	0.00	0.00	0.00	0.00	0.00	0.00	0.00	0.00	0.00	0.00	0.00	0.00	0.00	0.00	0.00	0.00	0.01	0.00	0.00	0.00
V_2O_3	0.00	0.00	0.00	0.00	0.00	0.00	0.01	0.02	0.00	0.01	0.01	0.01	0.00	0.02	0.02	0.02	0.01	0.02	0.01	0.01	0.01	0.01	0.00	0.01
ZrO_2	0.09	0.12	0.10	0.21	0.13	0.08	0.29	0.31	0.36	0.29	0.33	0.41	0.06	0.14	0.13	0.16	0.12	0.08	0.13	0.12	0.16	0.12	0.36	0.38
Nb_2O_5	0.00	0.03	0.03	0.06	0.04	0.02	0.00	0.00	0.00	0.00	0.00	0.00	0.00	0.00	0.00	0.00	0.00	0.00	0.00	0.00	0.00	0.00	0.00	0.00
Y_2O_3	0.00	0.00	0.00	0.00	0.00	0.00	0.00	0.00	0.00	0.00	0.00	0.00	0.00	0.00	0.00	0.00	0.00	0.00	0.00	0.00	0.00	0.00	0.00	0.00
Yb_2O_3	0.00	0.00	0.00	0.00	0.00	0.00	0.00	0.01	0.02	0.00	0.02	0.02	0.01	0.00	0.01	0.00	0.00	0.00	0.00	0.01	0.00	0.00	0.01	0.01
TiO_2	0.64	0.63	0.87	0.82	0.63	0.53	1.85	1.85	1.83	1.84	1.77	1.71	1.05	1.08	1.12	1.12	0.95	0.72	0.92	0.93	0.83	0.88	0.65	0.66
SiO_2	50.60	50.02	50.40	50.33	50.51	50.21	51.51	51.12	51.15	50.55	50.95	50.89	51.31	51.28	50.61	50.57	50.69	51.32	51.16	51.11	50.11	50.53	50.70	49.92
Al_2O_3	0.35	0.33	0.29	0.19	0.35	0.39	0.30	0.29	0.30	0.28	0.28	0.28	0.19	0.17	0.41	0.40	0.41	0.99	0.38	0.37	0.37	0.36	0.24	0.24
F	3.02	3.19	3.01	0.51	2.78	2.93	2.03	1.30	2.16	1.23	1.49	1.48	1.51	1.52	1.64	2.04	1.65	1.88	1.79	2.10	1.74	1.98	2.02	1.86
Cl	0.00	0.00	0.00	0.00	0.00	0.00	0.00	0.00	0.00	0.00	0.00	0.00	0.00	0.01	0.01	0.01	0.01	0.00	0.01	0.01	0.01	0.01	0.01	0.00
H_2O	0.43	0.36	0.44	1.56	0.53	0.46	0.93	1.28	0.88	1.30	1.18	1.18	1.17	1.17	1.11	0.93	1.11	1.01	1.04	0.90	1.06	0.94	0.92	0.98
Total	100.33	100.59	100.75	97.54	98.53	99.19	101.11	100.81	101.18	100.32	100.77	100.28	100.77	101.12	100.96	101.46	101.34	101.18	100.93	101.35	101.09	100.46	100.35	99.82
=O=F	1.27	1.34	1.27	0.21	1.17	1.23	0.85	0.55	0.91	0.52	0.63	0.62	0.64	0.64	0.69	0.86	0.70	0.79	0.75	0.89	0.73	0.83	0.85	0.78
=O=Cl	0.00	0.00	0.00	0.00	0.00	0.00	0.00	0.00	0.00	0.00	0.00	0.00	0.00	0.00	0.00	0.00	0.00	0.00	0.00	0.00	0.00	0.00	0.00	0.00
Total	99.05	99.25	99.48	97.33	97.36	97.95	100.25	100.27	100.27	99.80	100.14	99.66	100.13	100.48	100.27	100.60	100.64	100.39	100.18	100.46	100.36	99.63	99.50	99.04
Si	8.131	8.028	8.075	8.351	8.197	8.124	8.132	8.095	8.080	8.048	8.080	8.106	8.144	8.119	8.015	7.988	8.006	8.087	8.096	8.060	7.941	8.051	8.088	8.027
^{IV}Al	0.000	0.000	0.000	0.000	0.000	0.000	0.000	0.000	0.000	0.000	0.000	0.000	0.000	0.000	0.000	0.012	0.000	0.000	0.000	0.000	0.059	0.000	0.000	0.000
ΣTetrahedral	8.131	8.028	8.075	8.351	8.197	8.124	8.132	8.095	8.080	8.048	8.080	8.106	8.144	8.119	8.015	8.000	8.006	8.087	8.096	8.060	8.000	8.051	8.088	8.027
^{VI}Al	0.067	0.063	0.054	0.038	0.067	0.075	0.055	0.053	0.055	0.052	0.052	0.053	0.035	0.032	0.076	0.061	0.077	0.185	0.071	0.069	0.009	0.068	0.045	0.046
Ti	0.078	0.076	0.105	0.103	0.077	0.065	0.220	0.220	0.217	0.220	0.211	0.204	0.125	0.128	0.134	0.133	0.113	0.086	0.110	0.110	0.099	0.106	0.078	0.080
Fe^{3+}	0.648	0.921	0.760	0.000	0.624	0.773	0.459	0.451	0.593	0.576	0.515	0.464	0.613	0.657	0.783	0.838	0.832	0.718	0.681	0.820	1.053	0.787	0.871	0.944
Fe^{2+}	3.780	3.562	3.658	4.739	3.560	3.553	3.647	3.783	3.537	3.660	3.715	3.744	3.675	3.654	3.602	3.567	3.605	3.519	3.694	3.542	3.453	3.649	3.435	3.464
Mg	0.012	0.015	0.003	0.106	0.052	0.027	0.004	0.001	0.001	0.004	0.000	0.001	0.035	0.031	0.031	0.036	0.023	0.024	0.022	0.019	0.021	0.023	0.030	0.026
Mn	0.073	0.064	0.083	0.041	0.084	0.080	0.134	0.129	0.131	0.136	0.132	0.133	0.103	0.097	0.085	0.089	0.085	0.078	0.081	0.076	0.077	0.075	0.082	0.082
Zn	0.042	0.028	0.042	0.068	0.045	0.035	0.050	0.043	0.047	0.056	0.048	0.044	0.039	0.040	0.028	0.022	0.029	0.023	0.023	0.024	0.023	0.022	0.032	0.026
Cr	0.000	0.000	0.000	0.000	0.000	0.000	0.000	0.000	0.000	0.000	0.000	0.000	0.000	0.000	0.000	0.000	0.000	0.000	0.000	0.000	0.001	0.000	0.000	0.000
V	0.000	0.000	0.000	0.000	0.000	0.000	0.001	0.002	0.000	0.001	0.001	0.000	0.002	0.002	0.002	0.001	0.002	0.001	0.001	0.001	0.001	0.001	0.000	0.001
Zr	0.007	0.009	0.008	0.017	0.010	0.006	0.022	0.024	0.027	0.023	0.026	0.031	0.004	0.011	0.010	0.012	0.009	0.006	0.010	0.009	0.013	0.009	0.028	0.030
Nb	0.000	0.001	0.001	0.003	0.002	0.001	0.000	0.000	0.000	0.000	0.000	0.000	0.000	0.000	0.000	0.000	0.000	0.000	0.000	0.000	0.000	0.000	0.000	0.000
Y	0.000	0.000	0.000	0.000	0.000	0.000	0.000	0.000	0.000	0.000	0.000	0.000	0.000	0.000	0.000	0.000	0.000	0.000	0.000	0.000	0.000	0.000	0.000	0.000
Yb	0.000	0.000	0.000	0.000	0.000	0.000	0.000	0.001	0.001	0.000	0.001	0.001	0.001	0.000	0.000	0.000	0.000	0.000	0.000	0.001	0.000	0.000	0.000	0.000
ΣOctahedral	4.707	4.739	4.715	5.114	4.522	4.614	4.591	4.707	4.610	4.727	4.702	4.678	4.631	4.651	4.751	4.761	4.775	4.641	4.694	4.670	4.748	4.739	4.602	4.700
Na	2.809	2.881	2.809	2.283	2.931	2.928	2.957	2.888	3.007	2.889	2.898	2.897	2.692	2.701	2.917	2.918	2.905	2.808	2.932	3.002	2.974	2.939	2.870	2.822
K	0.336	0.333	0.386	0.190	0.333	0.312	0.307	0.297	0.291	0.321	0.304	0.306	0.504	0.505	0.263	0.262	0.263	0.454	0.255	0.245	0.254	0.249	0.434	0.444
Ca	0.017	0.018	0.015	0.009	0.017	0.022	0.012	0.013	0.013	0.016	0.016	0.013	0.030	0.024	0.055	0.060	0.050	0.011	0.022	0.023	0.023	0.022	0.006	0.007
ΣAlkalis	3.162	3.233	3.210	2.482	3.281	3.262	3.276	3.198	3.311	3.225	3.218	3.216	3.225	3.230	3.234	3.239	3.218	3.273	3.209	3.270	3.252	3.210	3.310	3.273
F	1.536	1.619	1.526	0.267	1.427	1.499	1.014	0.650	1.076	0.620	0.749	0.745	0.760	0.763	0.820	1.017	0.826	0.935	0.894	1.049	0.874	0.997	1.017	0.946
Cl	0.000	0.000	0.000	0.000	0.000	0.000	0.001	0.001	0.001	0.001	0.001	0.001	0.001	0.001	0.003	0.002	0.003	0.001	0.003	0.002	0.002	0.002	0.002	0.001
OH	0.464	0.381	0.474	1.733	0.573	0.501	0.985	1.349	0.923	1.379	1.250	1.254	1.239	1.236	1.176	0.981	1.171	1.064	1.102	0.949	1.124	1.001	0.981	1.053
ΣOH,F,Cl	2.000	2.000	2.000	2.000	2.000	2.000	2.000	2.000	2.000	2.000	2.000	2.000	2.000	2.000	2.000	2.000	2.000	2.000	2.000	2.000	2.000	2.000	2.000	2.000

Acronyms used are: edsedge; ltslight; lterslighter; dkersdarker; dksdark; nrnear; midsmiddle; 2ndsecond; grngrain

Mineral formulae were calculated based on 23 atoms of oxygen and 16 cations, with Fe3+ calculated by the method of Droop (1987)

Appendix B-1. Electron microprobe analyses of arfvedsonitic amphiboles

Unit	Fresh Subaolvus						
Sample #	38-B-3			SL-4-15			
Description	dker	middk	lt	ltsl415 gr1		ed	ed
File	kcp	kcp	kcp	kcp	kcp	kcp	kcp
Analysis #	119	120	121	122	68.2	69.2	70.2
Na_2O	9.53	9.57	9.73	9.77	9.01	8.94	8.98
K_2O	1.44	1.42	1.32	1.30	1.76	1.79	1.71
CaO	0.16	0.15	0.11	0.11	0.09	0.08	0.10
FeO	26.39	26.50	26.51	26.42	28.93	28.88	28.83
Fe_2O_3	7.44	6.97	7.15	7.12	4.96	4.83	5.36
MgO	0.14	0.17	0.14	0.14	0.09	0.09	0.11
MnO	0.62	0.62	0.61	0.61	0.62	0.67	0.61
ZnO	0.24	0.23	0.21	0.19	0.04	0.10	0.17
Cr_2O_3	0.00	0.00	0.00	0.00	0.00	0.01	0.00
V_2O_3	0.00	0.00	0.01	0.00	0.01	0.01	0.00
ZrO_2	0.12	0.27	0.52	0.65	0.14	0.14	0.14
Nb_2O_5	0.00	0.00	0.00	0.00	0.00	0.00	0.00
Y_2O_3	0.00	0.00	0.00	0.00	0.00	0.00	0.00
Yb_2O_3	0.00	0.00	0.00	0.00	0.02	0.01	0.00
TiO_2	0.78	0.73	0.70	0.69	0.98	0.99	0.95
SiO_2	50.54	50.74	50.84	50.81	51.02	50.88	50.82
Al_2O_3	0.37	0.36	0.36	0.34	0.29	0.29	0.31
F	1.75	1.84	1.87	1.74	2.38	2.18	2.34
Cl	0.01	0.01	0.01	0.01	0.01	0.00	0.00
H_2O	1.05	1.01	1.01	1.06	0.76	0.85	0.78
Total	100.57	100.59	101.09	100.97	101.09	100.73	101.20
-O=F	0.74	0.77	0.79	0.73	1.00	0.92	0.98
-O=Cl	0.00	0.00	0.00	0.00	0.00	0.00	0.00
Total	99.83	99.82	100.30	100.24	100.09	99.81	100.21
Si	8.033	8.060	8.042	8.042	8.114	8.115	8.083
^{IV}Al	0.000	0.000	0.000	0.000	0.000	0.000	0.000
ΣTetrahedral	8.033	8.060	8.042	8.042	8.114	8.115	8.083
^{VI}Al	0.069	0.066	0.068	0.064	0.055	0.055	0.057
Ti	0.093	0.087	0.083	0.083	0.117	0.119	0.114
Fe^{3+}	0.890	0.834	0.851	0.848	0.594	0.580	0.641
Fe^{2+}	3.507	3.520	3.507	3.498	3.848	3.853	3.835
Mg	0.034	0.040	0.033	0.033	0.022	0.020	0.025
Mn	0.083	0.083	0.082	0.081	0.084	0.091	0.082
Zn	0.028	0.027	0.025	0.022	0.004	0.012	0.020
Cr	0.000	0.000	0.000	0.000	0.000	0.001	0.000
V	0.000	0.000	0.001	0.000	0.001	0.001	0.000
Zr	0.009	0.021	0.040	0.050	0.011	0.011	0.011
Nb	0.000	0.000	0.000	0.000	0.000	0.000	0.000
Y	0.000	0.000	0.000	0.000	0.000	0.000	0.000
Yb	0.000	0.000	0.000	0.000	0.001	0.000	0.000
ΣOctahedral	4.713	4.679	4.690	4.679	4.736	4.743	4.785
Na	2.935	2.949	2.983	2.999	2.778	2.764	2.768
K	0.292	0.288	0.267	0.262	0.357	0.364	0.346
Ca	0.028	0.025	0.018	0.018	0.015	0.014	0.018
ΣAlkalis	3.255	3.262	3.268	3.279	3.150	3.142	3.132
F	0.881	0.923	0.933	0.873	1.195	1.098	1.175
Cl	0.002	0.002	0.002	0.003	0.002	0.001	0.001
OH	1.116	1.075	1.065	1.124	0.803	0.901	0.824
ΣOH,F,Cl	2.000	2.000	2.000	2.000	2.000	2.000	2.000

Acronyms used are: edsedge; grgrain

Appendix B-1. Electron microprobe analyses of arfvedsonitic amphibole

Unit	Altered Subsolvus																						
Sample #	25-C-1									27-A-2					34-C-1					54-A-1				
Description	25C1					away	near	amph	spot	27A2			ed	#4ed	#3ed	34c1	alt 1	ared	2nded	arak	54A1				
File	am92	am92	am92	am92	am92	am92	am92	am92	am92	am93	am93	am93	am93	am93	am93	1/1/95	1/1/95	1/1/95	1/1/95	1/1/95	am92	am92	am92	am92	am92
Analysis #	1	3	4	5	11	12	13	16	17	70	71	72	73	74	82	83	85	86	87	41	43	44	45	47
Na_2O	9.15	9.01	9.16	9.60	9.67	8.91	8.99	8.32	8.08	8.63	9.01	8.96	8.92	8.36	8.95	9.73	8.80	9.27	9.14	8.37	9.26	9.33	9.41	9.25
K_2O	1.86	1.68	1.70	1.42	0.97	1.45	1.68	2.30	2.33	2.41	2.04	2.41	2.18	3.18	1.82	1.40	2.16	1.80	1.77	1.44	1.44	1.45	1.46	1.43
CaO	0.09	0.15	0.09	0.11	1.04	0.25	0.08	0.18	0.31	0.07	0.11	0.08	0.06	0.09	0.07	0.71	0.09	0.05	0.05	0.26	0.30	0.24	0.26	0.23
FeO	27.21	28.27	27.86	26.98	17.24	27.75	28.80	27.49	27.84	25.42	26.60	25.09	26.23	23.39	27.33	25.29	26.02	27.26	28.39	30.18	25.99	25.32	25.58	27.85
Fe_2O_3	5.34	4.30	4.23	6.54	17.66	5.86	4.64	4.75	3.72	4.62	6.32	4.32	2.77	3.68	3.16	6.13	3.66	3.37	4.12	2.64	7.77	8.49	9.11	5.65
MgO	0.00	0.19	0.01	0.03	3.75	0.69	0.01	0.02	0.76	0.01	0.07	0.03	0.01	0.24	0.11	0.17	0.14	0.13	0.14	0.18	0.14	0.18	0.10	0.07
MnO	0.70	0.75	0.72	0.68	0.62	0.67	0.60	0.83	0.87	1.64	0.58	1.40	1.27	2.18	1.33	0.93	1.77	1.29	0.91	0.49	0.51	0.51	0.50	0.50
ZnO	0.64	0.56	0.76	0.34	0.24	0.36	0.34	1.50	1.42	1.40	0.23	0.98	1.15	1.85	1.66	0.56	1.98	1.27	0.37	0.31	0.16	0.24	0.20	0.23
Cr_2O_3	0.00	0.00	0.00	0.00	0.00	0.00	0.00	0.00	0.00	0.00	0.00	0.00	0.00	0.00	0.00	0.00	0.00	0.00	0.02	0.00	0.00	0.00	0.00	0.00
V_2O_3	0.00	0.00	0.00	0.00	0.00	0.00	0.00	0.00	0.00	0.00	0.00	0.00	0.00	0.00	0.00	0.00	0.02	0.03	0.01	0.00	0.00	0.00	0.00	0.00
ZrO_2	0.20	0.15	0.21	0.00	0.14	0.10	0.13	0.00	0.05	0.05	0.34	1.06	0.00	0.04	0.07	0.11	0.04	0.08	0.03	0.07	0.09	0.08	0.10	0.08
Nb_2O_5	0.03	0.03	0.00	0.00	0.08	0.02	0.00	0.13	0.09	0.06	0.02	0.05	0.03	0.01	0.00	0.00	0.00	0.00	0.00	0.01	0.04	0.00	0.01	0.07
Y_2O_3	0.00	0.00	0.00	0.00	0.00	0.00	0.00	0.00	0.00	0.00	0.00	0.00	0.00	0.00	0.00	0.00	0.00	0.00	0.00	0.00	0.00	0.00	0.00	0.00
Yb_2O_3	0.00	0.00	0.00	0.00	0.00	0.00	0.00	0.00	0.00	0.00	0.00	0.00	0.00	0.00	0.00	0.00	0.00	0.00	0.00	0.00	0.00	0.00	0.00	0.00
TiO_2	1.00	0.70	0.71	0.83	0.80	0.73	0.72	0.50	0.45	0.40	0.73	0.64	0.78	0.18	0.84	0.87	0.43	1.13	0.93	0.73	0.69	0.72	0.68	0.73
SiO_2	50.77	51.22	51.31	51.15	48.02	50.43	50.99	50.37	50.95	50.75	50.16	50.57	51.21	51.34	51.65	51.32	51.79	52.08	51.68	49.78	49.44	49.24	49.54	50.64
Al_2O_3	0.31	0.30	0.28	0.30	0.45	0.29	0.28	0.19	0.18	0.17	0.26	0.18	0.22	0.19	0.25	0.27	0.23	0.28	0.26	0.45	0.51	0.55	0.49	0.47
F	2.75	2.75	3.00	2.72	1.45	2.65	2.74	1.75	1.64	2.34	2.82	2.61	2.63	3.00	2.04	2.09	1.99	2.74	2.83	2.79	2.55	2.69	2.71	2.94
Cl	0.00	0.00	0.00	0.00	0.00	0.00	0.00	0.00	0.00	0.00	0.00	0.00	0.00	0.00	0.00	0.01	0.00	0.01	0.01	0.00	0.00	0.00	0.00	0.00
H_2O	0.57	0.57	0.45	0.60	1.27	0.62	0.57	1.02	1.09	0.73	0.52	0.61	0.59	0.41	0.91	0.90	0.93	0.59	0.54	0.50	0.65	0.58	0.59	0.48
Total	100.61	100.63	100.48	101.28	103.38	100.77	100.57	99.36	99.76	98.69	99.82	98.98	98.05	98.15	100.20	100.48	100.04	101.40	101.20	98.18	99.52	99.64	100.74	100.62
=O=F	1.16	1.16	1.26	1.14	0.61	1.12	1.15	0.74	0.69	0.99	1.19	1.10	1.11	1.26	0.86	0.88	0.84	1.15	1.19	1.17	1.07	1.13	1.14	1.24
=O=Cl	0.00	0.00	0.00	0.00	0.00	0.00	0.00	0.00	0.00	0.00	0.00	0.00	0.00	0.00	0.00	0.00	0.00	0.00	0.00	0.00	0.00	0.00	0.00	0.00
Total	99.46	99.47	99.22	100.14	102.77	99.65	99.42	98.62	99.07	97.71	98.63	97.88	96.94	96.89	99.34	99.60	99.20	100.24	100.01	97.01	98.45	98.50	99.60	99.38
Si	8.121	8.182	8.212	8.102	7.365	8.050	8.164	8.167	8.192	8.256	8.094	8.214	8.348	8.383	8.254	8.133	8.286	8.233	8.200	8.181	7.985	7.948	7.924	8.097
^{IV}Al	0.000	0.000	0.000	0.000	0.081	0.000	0.000	0.000	0.000	0.000	0.000	0.000	0.000	0.000	0.000	0.000	0.000	0.000	0.000	0.000	0.015	0.052	0.076	0.000
Σ Tetrahedral	8.121	8.182	8.212	8.102	7.446	8.050	8.164	8.167	8.192	8.256	8.094	8.214	8.348	8.383	8.254	8.133	8.286	8.233	8.200	8.181	8.000	8.000	8.000	8.097
^{VI}Al	0.058	0.057	0.052	0.056	0.000	0.054	0.053	0.037	0.033	0.033	0.050	0.034	0.043	0.037	0.047	0.050	0.043	0.052	0.048	0.048	0.082	0.053	0.016	0.088
Ti	0.120	0.084	0.085	0.098	0.092	0.088	0.087	0.061	0.054	0.049	0.089	0.078	0.095	0.023	0.101	0.103	0.052	0.135	0.111	0.090	0.084	0.087	0.082	0.088
Fe^{3+}	0.642	0.517	0.509	0.779	2.038	0.704	0.559	0.580	0.450	0.566	0.767	0.528	0.339	0.453	0.380	0.731	0.441	0.401	0.492	0.326	0.944	1.031	1.097	0.680
Fe^{2+}	3.639	3.776	3.729	3.574	2.211	3.705	3.856	3.728	3.744	3.459	3.590	3.409	3.575	3.194	3.653	3.352	3.481	3.604	3.766	4.148	3.510	3.418	3.421	3.725
Mg	0.000	0.045	0.002	0.007	0.857	0.164	0.003	0.004	0.183	0.002	0.017	0.006	0.002	0.059	0.026	0.041	0.033	0.031	0.033	0.044	0.033	0.044	0.025	0.018
Mn	0.094	0.101	0.097	0.091	0.080	0.091	0.081	0.114	0.118	0.226	0.080	0.193	0.175	0.301	0.179	0.124	0.240	0.173	0.122	0.068	0.070	0.070	0.068	0.067
Zn	0.076	0.065	0.090	0.040	0.027	0.042	0.040	0.179	0.168	0.168	0.028	0.117	0.138	0.223	0.196	0.066	0.234	0.148	0.044	0.038	0.019	0.028	0.024	0.027
Cr	0.000	0.000	0.000	0.000	0.000	0.000	0.000	0.000	0.000	0.000	0.000	0.000	0.000	0.000	0.000	0.000	0.000	0.000	0.002	0.000	0.000	0.000	0.000	0.000
V	0.000	0.000	0.000	0.000	0.000	0.000	0.000	0.000	0.000	0.000	0.000	0.000	0.000	0.000	0.000	0.000	0.002	0.003	0.001	0.000	0.000	0.000	0.000	0.000
Zr	0.016	0.012	0.016	0.000	0.010	0.008	0.010	0.000	0.004	0.004	0.027	0.084	0.000	0.003	0.006	0.009	0.003	0.006	0.003	0.005	0.007	0.006	0.008	0.006
Nb	0.001	0.001	0.000	0.000	0.003	0.001	0.000	0.006	0.004	0.003	0.001	0.002	0.001	0.001	0.000	0.000	0.000	0.000	0.000	0.001	0.002	0.000	0.000	0.003
Y	0.000	0.000	0.000	0.000	0.000	0.000	0.000	0.000	0.000	0.000	0.000	0.000	0.000	0.000	0.000	0.000	0.000	0.000	0.000	0.000	0.000	0.000	0.000	0.000
Yb	0.000	0.000	0.000	0.000	0.000	0.000	0.000	0.000	0.000	0.000	0.000	0.000	0.000	0.000	0.000	0.000	0.000	0.000	0.000	0.000	0.000	0.000	0.000	0.000
Σ Octahedral	4.647	4.659	4.582	4.644	5.320	4.857	4.689	4.710	4.759	4.509	4.648	4.451	4.370	4.293	4.587	4.477	4.530	4.554	4.621	4.807	4.751	4.738	4.740	4.702
Na	2.838	2.791	2.842	2.948	2.874	2.756	2.790	2.616	2.519	2.724	2.819	2.822	2.819	2.648	2.776	2.989	2.729	2.842	2.811	2.665	2.901	2.921	2.917	2.869
K	0.380	0.343	0.348	0.287	0.189	0.295	0.344	0.475	0.477	0.501	0.419	0.499	0.453	0.661	0.372	0.282	0.440	0.363	0.358	0.301	0.297	0.299	0.298	0.292
Ca	0.015	0.025	0.016	0.019	0.171	0.043	0.014	0.032	0.053	0.011	0.019	0.014	0.010	0.015	0.012	0.120	0.015	0.008	0.009	0.046	0.052	0.042	0.045	0.040
Σ Alkalis	3.232	3.159	3.205	3.254	3.235	3.094	3.147	3.123	3.049	3.236	3.258	3.335	3.283	3.324	3.159	3.391	3.184	3.213	3.179	3.012	3.249	3.262	3.260	3.200
F	1.388	1.390	1.517	1.362	0.701	1.338	1.388	0.898	0.835	1.206	1.438	1.340	1.358	1.548	1.031	1.045	1.005	1.371	1.421	1.450	1.300	1.375	1.371	1.487
Cl	0.000	0.000	0.000	0.000	0.000	0.000	0.000	0.000	0.000	0.000	0.000	0.000	0.000	0.000	0.001	0.003	0.001	0.001	0.003	0.000	0.000	0.000	0.000	0.000
OH	0.612	0.610	0.483	0.638	1.299	0.662	0.612	1.102	1.165	0.794	0.562	0.660	0.642	0.452	0.968	0.952	0.994	0.627	0.576	0.550	0.700	0.625	0.629	0.513
Σ OH,F,Cl	2.000	2.000	2.000	2.000	2.000	2.000	2.000	2.000	2.000	2.000	2.000	2.000	2.000	2.000	2.000	2.000	2.000	2.000	2.000	2.000	2.000	2.000	2.000	2.000

Acronyms used are: ed=edge; lt=light; lter=lighter; dker=darker; dk=dark; nr=near; mid=middle; 2nd=second; gr=grain; alt=altered

Mineral formulae were calculated based on 23 atoms of oxygen and 16 cations, with Fe^{3+} calculated by the method of Droop (1987)

Appendix B-1. Electron microprobe analyses of arfvedsonitic amphibole

Unit	Altered Subsolvus																						
Sample #	54-A-1																						
Description	54a1	#2mid	#3ed	mid	54 edmid	middker	centerlt	dkcore	mid	ltered 54a1	1 ed	mid	center	ed	2 ed	mid	center	mid	v ed	3 ed	cter	ed	4 mid	ed
File	am92	am92	am92	am92	kp	kp	kp	kp	kp	kp	kp	kp	kp	kp	kp	kp	kp	kp	kp	kp	kp	kp	kp	kp
Analysis #	49	50	53	54	193	194	195	196	197	198	37	38	39	40	41	42	43	44	45	46	47	48	49	50
Na_2O	8.69	8.83	7.97	9.08	9.50	9.47	9.42	9.68	9.69	9.46	9.67	9.66	9.83	10.00	9.96	9.75	9.75	9.86	9.99	9.72	9.73	9.90	9.81	9.84
K_2O	1.38	1.37	1.44	1.41	1.17	1.17	1.16	1.13	1.14	1.15	1.07	1.08	1.11	1.06	1.05	1.30	1.10	1.07	1.07	1.05	1.09	1.05	1.13	1.13
CaO	0.23	0.25	0.25	0.25	0.22	0.22	0.09	0.23	0.24	0.23	0.22	0.22	0.22	0.23	0.22	0.17	0.21	0.23	0.23	0.24	0.25	0.25	0.22	0.22
FeO	30.04	28.27	32.32	26.68	27.57	28.07	27.22	27.22	27.24	27.34	27.38	27.39	26.25	26.67	27.04	26.64	27.35	27.12	26.96	27.20	26.95	26.60	27.24	27.13
Fe_2O_3	2.49	5.79	1.01	7.18	6.35	5.81	6.69	6.55	7.04	7.09	7.27	7.37	8.47	7.87	7.33	6.92	7.28	7.31	7.08	7.12	7.35	7.99	7.55	7.54
MgO	0.11	0.08	0.09	0.07	0.19	0.29	0.19	0.32	0.26	0.23	0.06	0.06	0.07	0.06	0.11	0.14	0.07	0.08	0.16	0.25	0.27	0.25	0.05	0.05
MnO	0.47	0.51	0.55	0.50	0.49	0.53	0.54	0.53	0.50	0.51	0.49	0.50	0.48	0.49	0.48	0.82	0.48	0.49	0.50	0.49	0.49	0.50	0.49	0.49
ZnO	0.21	0.24	0.23	0.26	0.18	0.17	0.19	0.17	0.16	0.20	0.12	0.17	0.15	0.18	0.18	0.52	0.17	0.10	0.18	0.15	0.17	0.18	0.15	0.14
Cr_2O_3	0.00	0.00	0.00	0.00	0.00	0.00	0.00	0.00	0.00	0.00	0.01	0.00	0.01	0.00	0.00	0.00	0.01	0.00	0.00	0.01	0.01	0.00	0.00	0.01
V_2O_3	0.00	0.00	0.00	0.00	0.02	0.00	0.01	0.01	0.00	0.01	0.00	0.01	0.00	0.02	0.00	0.00	0.00	0.00	0.04	0.00	0.06	0.00	0.00	0.00
ZrO_2	0.05	0.06	0.08	0.11	0.08	0.09	0.12	0.09	0.10	0.10	0.09	0.09	0.08	0.07	0.08	0.09	0.07	0.07	0.07	0.08	0.08	0.09	0.07	0.05
Nb_2O_5	0.03	0.01	0.04	0.00	0.00	0.00	0.00	0.00	0.00	0.00	0.00	0.00	0.00	0.00	0.00	0.00	0.00	0.00	0.00	0.00	0.00	0.00	0.00	0.00
Y_2O_3	0.00	0.00	0.00	0.00	0.00	0.00	0.00	0.00	0.00	0.00	0.00	0.00	0.00	0.00	0.00	0.00	0.00	0.00	0.00	0.00	0.00	0.00	0.00	0.00
Yb_2O_3	0.00	0.00	0.00	0.00	0.00	0.00	0.01	0.00	0.01	0.02	0.01	0.01	0.02	0.02	0.00	0.00	0.00	0.01	0.00	0.00	0.01	0.01	0.00	0.01
TiO_2	0.75	0.67	0.68	0.71	0.68	0.74	0.97	0.76	0.72	0.68	0.65	0.63	0.62	0.66	0.63	0.56	0.63	0.66	0.69	0.65	0.65	0.67	0.63	0.63
SiO_2	50.43	49.56	49.92	49.22	51.09	51.18	51.27	51.19	51.13	50.50	50.79	50.83	50.58	51.34	51.55	51.65	51.14	51.24	51.69	51.07	51.01	51.16	51.26	51.30
Al_2O_3	0.46	0.46	0.39	0.40	0.47	0.45	0.29	0.45	0.47	0.49	0.45	0.46	0.44	0.45	0.43	0.37	0.47	0.46	0.47	0.46	0.45	0.46	0.44	0.45
F	2.83	2.69	2.72	2.61	1.95	2.04	1.99	1.90	1.83	1.97	2.17	2.12	2.17	2.19	2.23	2.27	2.37	2.31	2.29	2.31	2.35	2.44	2.09	2.37
Cl	0.00	0.00	0.00	0.00	0.01	0.01	0.00	0.01	0.01	0.02	0.01	0.01	0.01	0.01	0.02	0.01	0.01	0.01	0.02	0.01	0.01	0.01	0.01	0.01
H_2O	0.49	0.57	0.53	0.61	0.97	0.93	0.96	1.00	1.03	0.95	0.87	0.89	0.86	0.87	0.86	0.83	0.78	0.81	0.83	0.80	0.79	0.75	0.92	0.79
Total	98.66	99.37	98.19	99.08	101.01	101.16	101.73	101.23	101.58	100.93	101.32	101.50	101.37	102.19	102.16	102.04	101.91	101.85	102.25	101.63	101.71	102.31	102.06	102.14
=O=F	1.19	1.13	1.15	1.10	0.82	0.86	0.84	0.80	0.77	0.83	0.91	0.89	0.91	0.92	0.94	0.96	1.00	0.97	0.96	0.97	0.99	1.03	0.88	1.00
=O=Cl	0.00	0.00	0.00	0.00	0.00	0.00	0.00	0.00	0.00	0.00	0.00	0.00	0.00	0.00	0.00	0.00	0.00	0.00	0.00	0.00	0.00	0.00	0.00	0.00
Total	97.46	98.24	97.05	97.99	100.18	100.30	100.89	100.43	100.80	100.10	100.41	100.60	100.46	101.26	101.22	101.08	100.91	100.88	101.29	100.65	100.72	101.28	101.17	101.14
Si	8.223	8.048	8.232	8.004	8.079	8.087	8.066	8.065	8.037	8.014	8.032	8.026	7.991	8.032	8.063	8.096	8.042	8.050	8.072	8.042	8.029	8.007	8.038	8.043
^{IV}Al	0.000	0.000	0.000	0.000	0.000	0.000	0.000	0.000	0.000	0.000	0.000	0.000	0.009	0.000	0.000	0.000	0.000	0.000	0.000	0.000	0.000	0.000	0.000	0.000
Σ Tetrahedral	8.223	8.048	8.232	8.004	8.079	8.087	8.066	8.065	8.037	8.014	8.032	8.026	8.000	8.032	8.063	8.096	8.042	8.050	8.072	8.042	8.029	8.007	8.038	8.043
^{VI}Al	0.087	0.088	0.075	0.077	0.087	0.083	0.054	0.084	0.087	0.092	0.084	0.086	0.073	0.083	0.079	0.068	0.087	0.085	0.086	0.085	0.084	0.086	0.082	0.082
Ti	0.091	0.081	0.084	0.087	0.081	0.087	0.115	0.090	0.086	0.081	0.077	0.075	0.074	0.078	0.074	0.066	0.075	0.078	0.080	0.077	0.077	0.079	0.074	0.075
Fe^{3+}	0.306	0.708	0.125	0.879	0.755	0.691	0.792	0.777	0.833	0.846	0.865	0.875	1.007	0.926	0.863	0.816	0.862	0.865	0.832	0.844	0.871	0.941	0.891	0.890
Fe^{2+}	4.097	3.839	4.457	3.628	3.646	3.710	3.581	3.587	3.581	3.628	3.622	3.617	3.468	3.490	3.538	3.493	3.597	3.563	3.520	3.583	3.548	3.481	3.572	3.558
Mg	0.026	0.020	0.021	0.017	0.044	0.067	0.045	0.075	0.060	0.054	0.014	0.014	0.016	0.014	0.025	0.033	0.017	0.019	0.037	0.059	0.063	0.059	0.013	0.012
Mn	0.065	0.070	0.076	0.068	0.066	0.071	0.072	0.071	0.066	0.068	0.065	0.067	0.065	0.065	0.064	0.108	0.064	0.065	0.066	0.065	0.065	0.066	0.066	0.065
Zn	0.025	0.029	0.028	0.031	0.021	0.020	0.022	0.019	0.019	0.023	0.014	0.020	0.018	0.020	0.021	0.061	0.020	0.012	0.020	0.018	0.019	0.020	0.017	0.016
Cr	0.000	0.000	0.000	0.000	0.000	0.000	0.000	0.000	0.000	0.000	0.001	0.000	0.001	0.000	0.000	0.000	0.001	0.000	0.000	0.001	0.001	0.000	0.000	0.001
V	0.000	0.000	0.000	0.000	0.002	0.000	0.001	0.001	0.000	0.001	0.000	0.001	0.000	0.002	0.000	0.000	0.000	0.000	0.005	0.000	0.006	0.000	0.000	0.000
Zr	0.004	0.005	0.006	0.009	0.006	0.007	0.009	0.007	0.007	0.007	0.007	0.007	0.006	0.005	0.006	0.007	0.006	0.006	0.005	0.006	0.006	0.007	0.005	0.004
Nb	0.001	0.000	0.002	0.000	0.000	0.000	0.000	0.000	0.000	0.000	0.000	0.000	0.000	0.000	0.000	0.000	0.000	0.000	0.000	0.000	0.000	0.000	0.000	0.000
Y	0.000	0.000	0.000	0.000	0.000	0.000	0.000	0.000	0.000	0.000	0.000	0.000	0.000	0.000	0.000	0.000	0.000	0.000	0.000	0.000	0.000	0.000	0.000	0.000
Yb	0.000	0.000	0.000	0.000	0.000	0.000	0.001	0.000	0.000	0.001	0.001	0.001	0.001	0.001	0.000	0.000	0.000	0.000	0.000	0.000	0.000	0.000	0.000	0.000
Σ Octahedral	4.703	4.841	4.875	4.798	4.708	4.738	4.692	4.710	4.741	4.802	4.749	4.761	4.729	4.686	4.671	4.652	4.728	4.694	4.652	4.737	4.741	4.739	4.720	4.703
Na	2.746	2.781	2.547	2.863	2.941	2.902	2.874	2.958	2.953	2.912	2.965	2.958	3.010	3.013	3.020	2.964	2.973	3.002	3.025	2.969	2.969	3.003	2.981	2.991
K	0.287	0.285	0.302	0.293	0.235	0.235	0.353	0.228	0.229	0.233	0.217	0.218	0.224	0.211	0.209	0.259	0.221	0.215	0.213	0.211	0.219	0.210	0.225	0.226
Ca	0.041	0.044	0.044	0.043	0.037	0.038	0.015	0.039	0.040	0.039	0.037	0.037	0.037	0.038	0.037	0.029	0.036	0.039	0.038	0.041	0.042	0.041	0.037	0.036
Σ Alkalis	3.074	3.110	2.893	3.199	3.213	3.175	3.242	3.225	3.222	3.184	3.218	3.213	3.271	3.282	3.266	3.252	3.230	3.256	3.276	3.221	3.230	3.254	3.243	3.254
F	1.462	1.383	1.420	1.340	0.975	1.020	0.992	0.949	0.910	0.989	1.083	1.059	1.086	1.085	1.102	1.127	1.178	1.146	1.130	1.151	1.171	1.210	1.038	1.173
Cl	0.000	0.000	0.000	0.000	0.003	0.002	0.001	0.003	0.003	0.004	0.004	0.002	0.002	0.003	0.004	0.001	0.003	0.003	0.005	0.003	0.003	0.003	0.003	0.003
OH	0.538	0.617	0.580	0.660	1.022	0.979	1.008	1.049	1.086	1.006	0.913	0.939	0.912	0.912	0.894	0.871	0.819	0.851	0.865	0.845	0.826	0.787	0.958	0.824
Σ OH,F,Cl	2.000	2.000	2.000	2.000	2.000	2.000	2.000	2.000	2.000	2.000	2.000	2.000	2.000	2.000	2.000	2.000	2.000	2.000	2.000	2.000	2.000	2.000	2.000	2.000

Acronyms used are: edsedge; ltslight; ltersslighter; dkersdarker; dkedark; nrnear; middmiddle; 2ndsecond; grsgrain; altsaltered

Mineral formulae were calculated based on 23 atoms of oxygen and 16 cations, with Fe^{3+} calculated by the method of Droop (1987)

Appendix B-1: Electron microprobe analyses of arfvedsonitic amphibole

Unit	Altered Suhoivrus																							
Sample #	54-A-1	63-B-1						63-B-2										SL-1-17						
Description	mkd	63b1 ed	mkd	ed	2 ed	mkd	ed	63b2										Sl117	2	3	#2	3	#3	#2	#3
File	kp	kp	kp	kp	kp	kp	kp	am92	am92	am92	am92	am92	am92	am92	am92	am92	am92	am92	am92	am92	am92	am92	am92	am92	am92
Analysis #	51	187	188	189	190	191	192	133	134	135	142	144	152	153	154	156	85	86	87	100	101	105	106	107
Na_2O	9.75	9.13	9.10	9.13	9.34	9.38	9.34	8.63	8.67	7.91	8.81	9.06	8.04	8.45	8.32	8.71	8.82	8.75	8.66	8.05	8.31	8.17	8.86	8.68
K_2O	1.11	1.22	1.27	1.21	1.51	1.55	1.58	1.76	1.53	2.65	1.42	1.24	2.43	2.07	2.10	1.81	1.79	1.77	1.66	2.23	2.26	2.16	1.76	1.78
CaO	0.22	0.39	0.47	0.51	0.32	0.29	0.24	0.12	0.13	0.12	0.19	0.22	0.13	0.25	0.19	0.15	0.12	0.09	0.11	1.63	0.12	0.09	0.09	0.10
FeO	27.53	28.53	28.07	27.86	27.18	27.51	27.50	27.94	27.67	28.43	28.18	28.23	27.23	27.66	28.67	27.29	29.05	28.62	29.10	25.59	27.25	29.00	27.62	28.75
Fe_2O_3	7.08	5.75	6.59	6.80	6.27	5.94	5.57	2.69	3.84	2.41	4.30	4.26	4.46	3.72	3.06	4.98	0.00	1.53	0.00	4.09	3.34	1.96	4.18	3.16
MgO	0.07	0.20	0.19	0.19	0.19	0.09	0.16	0.05	0.02	0.02	0.17	0.18	0.04	0.04	0.07	0.05	0.00	0.02	0.01	0.05	0.01	0.02	0.02	0.02
MnO	0.48	0.73	0.84	0.82	0.80	0.87	0.88	0.93	1.01	0.96	0.53	0.57	0.96	0.93	0.90	1.06	1.15	0.99	1.04	1.38	1.40	1.21	0.99	1.00
ZnO	0.15	0.24	0.32	0.30	0.30	0.35	0.42	1.30	1.30	1.27	0.29	0.29	1.21	0.75	0.66	0.83	0.78	0.50	0.60	0.99	1.11	0.81	0.49	0.56
Cr_2O_3	0.00	0.00	0.00	0.00	0.00	0.00	0.00	0.00	0.00	0.00	0.00	0.00	0.00	0.00	0.00	0.00	0.00	0.00	0.00	0.00	0.00	0.00	0.00	0.00
V_2O_3	0.03	0.00	0.00	0.01	0.01	0.00	0.01	0.00	0.00	0.00	0.00	0.00	0.00	0.00	0.00	0.00	0.00	0.00	0.00	0.00	0.00	0.00	0.00	0.00
ZrO_2	0.07	0.17	0.20	0.15	0.21	0.15	0.13	0.14	0.10	0.18	0.14	0.83	0.05	0.09	0.15	0.22	0.77	0.69	0.70	0.54	0.53	0.40	0.38	0.56
Nb_2O_5	0.00	0.00	0.00	0.00	0.00	0.00	0.00	0.00	0.02	0.03	0.00	0.03	0.05	0.06	0.04	0.04	0.02	0.04	0.03	0.06	0.01	0.00	0.00	0.03
Y_2O_3	0.00	0.00	0.00	0.00	0.00	0.00	0.00	0.00	0.00	0.00	0.00	0.00	0.00	0.00	0.00	0.00	0.00	0.00	0.00	0.00	0.00	0.00	0.00	0.00
Yb_2O_3	0.01	0.00	0.01	0.00	0.03	0.01	0.02	0.00	0.00	0.00	0.00	0.00	0.00	0.00	0.00	0.00	0.00	0.00	0.00	0.00	0.00	0.00	0.00	0.00
TiO_2	0.64	1.42	1.08	1.03	1.61	1.92	1.89	0.69	0.70	0.95	0.97	1.33	0.49	0.84	0.77	0.85	2.01	1.78	1.96	1.13	1.22	1.60	1.61	1.70
SiO_2	51.27	50.16	50.21	50.10	50.39	50.55	50.64	50.49	49.87	50.13	49.49	49.34	49.51	49.97	50.24	49.89	50.69	49.83	50.24	48.79	49.57	49.61	49.58	49.77
Al_2O_3	0.44	0.39	0.39	0.39	0.30	0.30	0.29	0.31	0.31	0.20	0.35	0.49	0.19	0.22	0.21	0.24	0.30	0.27	0.29	0.25	0.23	0.26	0.28	0.27
F	2.18	1.84	1.84	1.87	1.93	1.96	1.93	2.03	1.74	1.74	2.75	2.67	2.07	2.49	2.05	1.74	2.09	2.23	2.32	3.03	1.70	1.63	2.47	2.42
Cl	0.02	0.01	0.00	0.01	0.01	0.00	0.01	0.00	0.00	0.00	0.00	0.00	0.00	0.00	0.00	0.00	0.00	0.00	0.00	0.00	0.00	0.00	0.00	0.00
H_2O	0.87	1.01	1.02	1.00	0.98	0.97	0.98	0.87	1.01	1.00	0.52	0.58	0.83	0.65	0.86	1.02	0.85	0.77	0.72	0.38	1.02	1.05	0.67	0.70
Total	101.91	101.21	101.59	101.37	101.36	101.85	101.59	97.96	97.91	98.01	98.12	99.31	97.68	98.18	98.28	98.88	98.43	97.87	97.44	98.19	98.09	97.96	99.00	99.50
=O=F	0.92	0.77	0.78	0.79	0.81	0.82	0.81	0.85	0.73	0.73	1.16	1.12	0.87	1.05	0.86	0.73	0.88	0.94	0.98	1.27	0.72	0.68	1.04	1.02
=O=Cl	0.00	0.00	0.00	0.00	0.00	0.00	0.00	0.00	0.00	0.00	0.00	0.00	0.00	0.00	0.00	0.00	0.00	0.00	0.00	0.00	0.00	0.00	0.00	0.00
Total	100.99	100.43	100.81	100.59	100.55	101.03	100.77	97.10	97.18	97.27	96.96	98.18	96.80	97.13	97.42	98.15	97.55	96.93	96.47	96.91	97.37	97.28	97.96	98.48
Si	8.054	7.966	7.953	7.950	7.976	7.968	7.996	8.262	8.177	8.235	8.119	8.017	8.180	8.196	8.220	8.108	8.252	8.180	8.278	8.059	8.137	8.152	8.070	8.078
^{IV}Al	0.000	0.034	0.047	0.050	0.024	0.032	0.004	0.000	0.000	0.000	0.000	0.000	0.000	0.000	0.000	0.000	0.000	0.000	0.000	0.000	0.000	0.000	0.000	0.000
Σ Tetrahedral	8.054	8.000	8.000	8.000	8.000	8.000	8.000	8.262	8.177	8.235	8.119	8.017	8.180	8.196	8.220	8.108	8.252	8.180	8.278	8.059	8.137	8.152	8.070	8.078
^{VI}Al	0.081	0.038	0.026	0.023	0.032	0.025	0.049	0.059	0.059	0.038	0.068	0.094	0.036	0.042	0.041	0.045	0.058	0.051	0.057	0.049	0.045	0.049	0.053	0.051
Ti	0.075	0.170	0.128	0.123	0.191	0.228	0.224	0.085	0.086	0.117	0.119	0.162	0.061	0.103	0.094	0.104	0.245	0.220	0.243	0.140	0.151	0.198	0.197	0.208
Fe^{3+}	0.836	0.687	0.786	0.812	0.747	0.704	0.662	0.332	0.474	0.299	0.531	0.521	0.554	0.459	0.377	0.609	0.000	0.190	0.000	0.509	0.412	0.243	0.512	0.386
Fe^{2+}	3.616	3.790	3.718	3.698	3.599	3.627	3.631	3.824	3.793	3.906	3.866	3.836	3.762	3.794	3.924	3.710	3.955	3.929	4.009	3.535	3.741	3.986	3.759	3.903
Mg	0.016	0.048	0.045	0.044	0.044	0.021	0.037	0.013	0.005	0.005	0.043	0.043	0.010	0.010	0.017	0.011	0.000	0.004	0.002	0.013	0.002	0.004	0.005	0.005
Mn	0.064	0.099	0.113	0.111	0.107	0.116	0.118	0.129	0.141	0.133	0.074	0.078	0.135	0.129	0.125	0.146	0.158	0.137	0.145	0.193	0.194	0.169	0.137	0.137
Zn	0.017	0.029	0.038	0.035	0.034	0.041	0.049	0.158	0.157	0.154	0.035	0.034	0.147	0.091	0.080	0.100	0.094	0.060	0.073	0.120	0.135	0.098	0.059	0.067
Cr	0.000	0.001	0.000	0.000	0.001	0.000	0.000	0.000	0.000	0.000	0.000	0.000	0.000	0.000	0.000	0.000	0.000	0.000	0.000	0.000	0.000	0.000	0.000	0.000
V	0.003	0.000	0.000	0.001	0.001	0.000	0.001	0.000	0.000	0.000	0.000	0.000	0.000	0.000	0.000	0.000	0.000	0.000	0.000	0.000	0.000	0.000	0.000	0.000
Zr	0.006	0.013	0.015	0.011	0.016	0.012	0.010	0.011	0.008	0.014	0.011	0.066	0.004	0.007	0.012	0.018	0.061	0.055	0.056	0.043	0.043	0.032	0.030	0.044
Nb	0.000	0.000	0.000	0.000	0.000	0.000	0.000	0.000	0.001	0.001	0.000	0.001	0.002	0.003	0.002	0.002	0.001	0.002	0.001	0.003	0.001	0.000	0.000	0.001
Y	0.000	0.000	0.000	0.000	0.000	0.000	0.000	0.000	0.000	0.000	0.000	0.000	0.000	0.000	0.000	0.000	0.000	0.000	0.000	0.000	0.000	0.000	0.000	0.000
Yb	0.000	0.000	0.000	0.000	0.001	0.001	0.001	0.000	0.000	0.000	0.000	0.000	0.000	0.000	0.000	0.000	0.000	0.000	0.000	0.000	0.000	0.000	0.000	0.000
Σ Octahedral	4.716	4.875	4.869	4.858	4.773	4.774	4.782	4.610	4.725	4.669	4.748	4.836	4.712	4.638	4.672	4.745	4.572	4.649	4.586	4.604	4.723	4.777	4.753	4.803
Na	2.969	2.812	2.796	2.809	2.867	2.866	2.858	2.739	2.756	2.519	2.801	2.853	2.574	2.688	2.638	2.745	2.783	2.784	2.768	2.579	2.645	2.602	2.796	2.733
K	0.223	0.247	0.256	0.246	0.305	0.312	0.319	0.367	0.321	0.556	0.298	0.256	0.512	0.434	0.438	0.376	0.372	0.372	0.350	0.471	0.474	0.453	0.365	0.369
Ca	0.017	0.066	0.079	0.087	0.055	0.048	0.041	0.022	0.022	0.020	0.014	0.038	0.022	0.043	0.033	0.027	0.021	0.016	0.019	0.288	0.021	0.016	0.016	0.017
Σ Alkalis	3.229	3.125	3.131	3.142	3.227	3.226	3.218	3.128	3.099	3.096	3.133	3.148	3.109	3.165	3.109	3.147	3.175	3.172	3.136	3.337	3.140	3.071	3.177	3.119
F	1.084	0.924	0.922	0.937	0.964	0.975	0.963	1.050	0.900	0.903	1.427	1.371	1.082	1.291	1.058	0.893	1.073	1.157	1.208	1.581	0.883	0.845	1.273	1.244
Cl	0.004	0.001	0.001	0.001	0.001	0.001	0.002	0.000	0.000	0.000	0.000	0.000	0.000	0.000	0.000	0.000	0.000	0.000	0.000	0.000	0.000	0.000	0.000	0.000
OH	0.912	1.074	1.077	1.062	1.034	1.024	1.036	0.950	1.100	1.092	0.573	0.629	0.918	0.709	0.942	1.107	0.927	0.843	0.792	0.419	1.117	1.155	0.727	0.756
Σ OH,F,Cl	2.000	2.000	2.000	2.000	2.000	2.000	2.000	2.000	2.000	2.000	2.000	2.000	2.000	2.000	2.000	2.000	2.000	2.000	2.000	2.000	2.000	2.000	2.000	2.000

Acronyms used are: ed=edge; lt=light; lt=r=lighter; dk=r=darker; dk=dark; nr=near; md=middle; 2nd=second; gr=grain; alt=altered

Mineral formulae were calculated based on 23 atoms of oxygen and 16 cations, with Fe^{3+} calculated by the method of Droop (1987)

Appendix B-1 Electron microprobe analyses of arfvedsonitic amphibole

Unit	Altered Si									SL-8-1				SL-8-1								
Sample #	SL-1-17																					
Description	#4 all	mided	dker	dkcenter	lter	dker	lt	dked	SL-8 nrby	br	br	brnr	br		altl	bt	ed		lted	ed	ed	
File	am92	kp	kp	kp	kp	kp	kp	kp	am93	am93	am93	am93	am93		kp	kp	kp	kp	kp	kp	kp	
Analysis #	110	168	169	170	171	172	173	174	24	30	32	33	34		123	124	125	126	127	128	85.2	
Na_2O	8.82	9.27	8.91	9.06	9.17	8.95	9.19	9.23	9.16	7.97	9.05	9.28	8.99		9.73	9.63	9.77	9.75	9.62	9.81	8.71	
K_2O	1.72	1.10	1.24	1.21	0.98	1.08	0.97	1.13	1.72	2.89	1.49	1.75	1.74		1.51	1.68	1.67	1.65	1.69	1.62	2.23	
CaO	0.11	0.83	1.91	0.60	0.83	0.98	0.88	0.93	0.11	0.07	0.14	0.08	0.11		0.17	0.06	0.08	0.05	0.05	0.17	0.17	
FeO	27.44	26.91	26.24	28.71	28.09	29.18	28.30	27.61	27.53	18.92	29.13	27.17	27.96		25.70	26.39	26.83	26.22	26.28	25.72	27.66	
Fe_2O_3	2.05	7.95	7.18	4.27	6.41	4.98	5.90	6.05	5.31	9.31	3.86	4.58	5.00		7.10	6.26	4.45	5.02	6.22	6.16	2.87	
MgO	0.00	0.17	0.31	0.25	0.27	0.23	0.25	0.20	0.04	0.11	0.07	0.03	0.05		0.00	0.01	0.01	0.02	0.02	0.04	0.01	
MnO	1.31	0.66	0.65	0.74	0.67	0.70	0.66	0.63	0.57	3.38	0.58	0.61	0.56		0.72	0.79	0.75	0.81	0.69	0.76	1.09	
ZnO	0.97	0.20	0.18	0.14	0.16	0.19	0.17	0.24	0.22	3.43	0.31	0.35	0.24		0.29	0.36	0.35	0.52	0.30	0.38	0.98	
Cr_2O_3	0.00	0.00	0.00	0.00	0.01	0.01	0.01	0.00	0.00	0.00	0.00	0.00	0.00		0.00	0.00	0.00	0.00	0.00	0.00	0.01	
V_2O_3	0.00	0.01	0.00	0.00	0.01	0.01	0.00	0.01	0.00	0.00	0.00	0.00	0.00		0.02	0.00	0.00	0.01	0.00	0.01	0.01	
ZrO_2	0.28	0.11	0.09	0.08	0.05	0.08	0.06	0.07	0.15	0.05	0.17	0.18	0.10		0.18	0.11	0.11	0.11	0.10	0.09	0.07	
Nb_2O_3	0.00	0.00	0.00	0.00	0.00	0.00	0.00	0.00	0.00	0.01	0.01	0.00	0.01		0.00	0.00	0.00	0.00	0.00	0.00	0.01	
Y_2O_3	0.00	0.00	0.00	0.00	0.00	0.00	0.00	0.00	0.00	0.00	0.00	0.00	0.00		0.00	0.00	0.00	0.00	0.00	0.00	0.00	
Yb_2O_3	0.00	0.00	0.00	0.01	0.01	0.01	0.01	0.00	0.00	0.00	0.00	0.00	0.00		0.02	0.00	0.01	0.01	0.00	0.01	0.00	
TiO_2	1.15	0.82	1.14	1.47	1.10	0.92	1.13	0.86	0.73	0.60	0.94	0.71	0.69		1.59	1.10	1.38	0.66	0.66	0.66	0.76	
SiO_2	50.33	49.83	49.31	50.22	49.99	50.58	50.21	50.44	50.71	46.93	50.96	51.03	50.58		50.21	51.20	51.84	51.95	51.37	51.67	51.43	
Al_2O_3	0.27	0.71	1.07	1.02	1.00	0.88	1.00	0.95	0.34	3.05	0.33	0.28	0.34		0.29	0.28	0.28	0.30	0.30	0.30	0.19	
F	2.31	1.82	2.66	1.70	1.64	1.73	1.55	1.94	2.60	1.50	2.00	3.17	2.98		2.39	2.41	2.48	2.27	2.13	1.92	1.76	
Cl	0.00	0.02	0.01	0.03	0.01	0.01	0.01	0.02	0.00	0.00	0.00	0.00	0.00		0.00	0.01	0.00	0.01	0.01	0.00	0.00	
H_2O	0.73	1.02	0.62	1.07	1.12	1.08	1.16	0.97	0.63	1.14	0.92	0.36	0.45		0.75	0.75	0.72	0.81	0.88	0.98	1.02	
Total	97.49	101.46	101.51	100.57	101.51	101.58	101.46	101.29	99.82	99.36	99.96	99.59	99.80		100.66	101.03	100.71	100.16	100.31	100.29	98.95	
=O=F	0.97	0.77	1.12	0.71	0.69	0.73	0.65	0.82	1.09	0.63	0.84	1.34	1.25		1.00	1.02	1.05	0.95	0.89	0.81	0.74	
=O=Cl	0.00	0.00	0.00	0.01	0.00	0.00	0.00	0.00	0.00	0.00	0.00	0.00	0.00		0.00	0.00	0.00	0.00	0.00	0.00	0.00	
Total	96.52	100.69	100.39	99.85	100.82	100.85	100.80	100.47	98.73	98.73	99.11	98.25	98.54		99.65	100.01	99.66	99.20	99.41	99.48	98.21	
Si	8.269	7.888	7.823	7.984	7.892	7.985	7.920	7.971	8.151	7.614	8.168	8.224	8.158		7.996	8.109	8.204	8.253	8.167	8.189	8.302	
^{IV}Al	0.000	0.112	0.177	0.016	0.108	0.015	0.080	0.029	0.000	0.386	0.000	0.000	0.000		0.004	0.000	0.000	0.000	0.000	0.000	0.000	
Σ Tetrahedral	8.269	8.000	8.000	8.000	8.000	8.000	8.000	8.000	8.151	8.000	8.168	8.224	8.158		8.000	8.109	8.204	8.253	8.167	8.189	8.302	
^{VI}Al	0.052	0.020	0.023	0.176	0.078	0.148	0.106	0.149	0.064	0.198	0.062	0.054	0.064		0.050	0.052	0.051	0.055	0.057	0.055	0.036	
Ti	0.142	0.098	0.136	0.176	0.131	0.109	0.134	0.102	0.088	0.073	0.113	0.087	0.083		0.191	0.131	0.164	0.079	0.078	0.079	0.092	
Fe^{3+}	0.253	0.948	0.857	0.511	0.761	0.591	0.701	0.719	0.642	1.137	0.466	0.555	0.608		0.851	0.746	0.530	0.601	0.745	0.734	0.348	
Fe^{2+}	3.771	3.562	3.482	3.817	3.708	3.852	3.734	3.650	3.702	2.567	3.905	3.662	3.772		3.422	3.496	3.551	3.484	3.494	3.409	3.734	
Mg	0.000	0.041	0.073	0.060	0.063	0.053	0.058	0.048	0.011	0.027	0.016	0.007	0.013		0.000	0.001	0.001	0.004	0.004	0.009	0.001	
Mn	0.182	0.089	0.087	0.099	0.090	0.093	0.088	0.085	0.078	0.464	0.079	0.083	0.077		0.097	0.106	0.101	0.109	0.093	0.103	0.148	
Zn	0.118	0.023	0.021	0.016	0.019	0.023	0.020	0.028	0.026	0.411	0.036	0.042	0.029		0.034	0.042	0.041	0.060	0.035	0.044	0.116	
Cr	0.000	0.000	0.000	0.000	0.001	0.001	0.001	0.000	0.000	0.000	0.000	0.000	0.000		0.000	0.000	0.000	0.000	0.000	0.000	0.001	
V	0.000	0.001	0.000	0.000	0.001	0.001	0.000	0.001	0.000	0.000	0.000	0.000	0.000		0.002	0.000	0.000	0.001	0.000	0.001	0.001	
Zr	0.023	0.008	0.007	0.006	0.004	0.006	0.005	0.006	0.011	0.004	0.013	0.014	0.008		0.014	0.008	0.008	0.009	0.008	0.007	0.005	
Nb	0.000	0.000	0.000	0.000	0.000	0.000	0.000	0.000	0.000	0.000	0.000	0.000	0.000		0.000	0.000	0.000	0.000	0.000	0.000	0.000	
Y	0.000	0.000	0.000	0.000	0.000	0.000	0.000	0.000	0.000	0.000	0.000	0.000	0.000		0.000	0.000	0.000	0.000	0.000	0.000	0.000	
Yb	0.000	0.000	0.000	0.000	0.001	0.001	0.000	0.000	0.000	0.000	0.000	0.000	0.000		0.001	0.000	0.000	0.000	0.000	0.000	0.000	
Σ Octahedral	4.541	4.790	4.686	4.862	4.856	4.878	4.846	4.787	4.622	4.882	4.691	4.504	4.653		4.662	4.583	4.448	4.401	4.515	4.441	4.483	
Na	2.810	2.845	2.739	2.792	2.806	2.739	2.810	2.829	2.854	2.507	2.813	2.899	2.813		3.003	2.957	2.997	3.002	2.967	3.015	2.727	
K	0.361	0.223	0.250	0.244	0.197	0.218	0.194	0.227	0.354	0.598	0.304	0.360	0.357		0.306	0.340	0.338	0.335	0.342	0.327	0.459	
Ca	0.019	0.141	0.324	0.101	0.141	0.166	0.149	0.157	0.020	0.013	0.024	0.014	0.020		0.029	0.011	0.013	0.009	0.009	0.028	0.019	
Σ Alkalis	3.191	3.210	3.314	3.138	3.144	3.122	3.154	3.213	3.227	3.118	3.142	3.272	3.189		3.338	3.307	3.348	3.346	3.318	3.370	3.215	
F	1.198	0.913	1.336	0.853	0.817	0.863	0.771	0.971	1.320	0.769	1.012	1.617	1.520		1.201	1.209	1.242	1.138	1.069	0.960	0.899	
Cl	0.000	0.004	0.003	0.008	0.002	0.003	0.003	0.004	0.000	0.000	0.000	0.000	0.000		0.001	0.001	0.001	0.002	0.001	0.001	0.001	
OH	0.802	1.083	0.661	1.139	1.181	1.134	1.226	1.025	0.680	1.231	0.988	0.383	0.480		0.798	0.789	0.757	0.860	0.930	1.039	1.100	
Σ OH,F,Cl	2.000	2.000	2.000	2.000	2.000	2.000	2.000	2.000	2.000	2.000	2.000	2.000	2.000		2.000	2.000	2.000	2.000	2.000	2.000	2.000	

Acronyms used are: ed=edge; br=brown; dk=dark; nr=near

Appendix B-1. Electron microprobe analyses of arfvedsonitic amphibole

Unit	Subsolvus - Drill Core																			
Sample #	LB-30-6.87							LB-30-15.80		LB-30-17.22							LB-30-17.50			
Description	30687	30-6	aral		ed	#3ed	mid	ed 30-15.8 o		#1 o 30-1722 o		mid o	ed o	ed o	17.2 o	mid o	ed o	4-30 0	o	o
File	am93	am93	am93	am93	am93	am93	am93	am93	am93	am93	am93	am93	am93	am93	am93	am93	am93	am93	am93	am93
Analysis #	41	55	56	60	61	62	63	64	34	37	32	33	34	35	47	48	49	8	11	12
Na_2O	8.69	8.96	9.01	9.30	8.72	8.85	8.64	8.63	8.70	8.20	8.23	8.42	8.15	8.80	8.86	9.02	8.92	8.28	8.48	8.09
K_2O	1.88	1.65	2.12	1.54	2.11	2.36	2.42	2.59	2.31	2.76	2.87	2.64	3.11	2.01	2.49	2.10	1.93	2.54	2.40	3.00
CaO	0.14	0.28	0.09	0.28	0.16	0.11	0.19	0.18	0.15	0.11	0.12	0.12	0.12	0.10	0.09	0.10	0.12	0.16	0.17	0.14
FeO	26.91	27.36	26.71	26.48	27.86	26.38	26.43	26.12	26.27	26.64	25.87	26.50	25.18	26.67	24.53	25.79	26.74	27.66	27.52	27.02
Fe_2O_3	4.08	5.25	6.68	7.78	3.91	5.24	6.11	5.81	4.57	4.42	5.93	4.57	3.69	1.79	4.98	4.53	3.62	4.39	3.40	3.94
MgO	0.05	0.16	0.30	0.46	0.04	0.08	0.04	0.06	0.03	0.01	0.03	0.03	0.03	0.03	0.02	0.00	0.03	0.00	0.02	0.01
MnO	1.15	1.10	0.69	0.65	1.20	1.21	1.25	1.18	1.48	1.71	1.80	1.73	2.06	1.87	1.66	1.35	1.31	1.36	1.41	1.42
ZnO	1.22	0.97	0.33	0.28	1.38	1.25	1.31	1.22	0.88	1.18	1.41	1.23	2.37	2.13	1.81	1.20	0.95	1.21	1.22	1.21
Cr_2O_3	0.00	0.00	0.00	0.00	0.00	0.00	0.00	0.00	0.00	0.00	0.00	0.00	0.00	0.00	0.00	0.00	0.00	0.00	0.00	0.00
V_2O_3	0.00	0.00	0.00	0.00	0.00	0.00	0.00	0.00	0.00	0.00	0.00	0.00	0.00	0.00	0.00	0.00	0.00	0.00	0.00	0.00
ZrO_2	0.13	0.10	0.17	0.10	0.09	0.09	0.04	0.01	0.05	0.08	0.00	0.05	0.02	0.14	0.03	0.06	0.12	0.06	0.00	0.10
Nb_2O_5	0.00	0.00	0.02	0.00	0.02	0.02	0.02	0.00	0.00	0.01	0.06	0.05	0.06	0.00	0.04	0.00	0.02	0.04	0.02	0.01
Y_2O_3	0.00	0.00	0.00	0.00	0.00	0.00	0.00	0.00	0.00	0.00	0.00	0.00	0.00	0.00	0.00	0.00	0.00	0.00	0.00	0.00
Yb_2O_3	0.00	0.00	0.00	0.00	0.00	0.00	0.00	0.00	0.00	0.00	0.00	0.00	0.00	0.00	0.00	0.00	0.00	0.00	0.00	0.00
TiO_2	1.06	0.90	0.94	0.81	1.15	1.31	0.90	0.73	0.65	0.30	0.32	0.46	0.29	1.28	0.46	0.85	1.06	0.48	0.51	0.61
SiO_2	49.98	50.76	50.67	50.54	51.29	50.97	50.79	51.00	50.83	50.94	50.86	51.25	51.59	51.41	51.32	51.00	50.67	51.06	51.51	50.99
Al_2O_3	0.31	0.39	0.28	0.36	0.21	0.25	0.23	0.22	0.20	0.16	0.22	0.26	0.25	0.43	0.20	0.22	0.25	0.18	0.18	0.16
F	1.63	1.65	2.25	2.06	1.76	1.61	1.69	1.78	2.25	2.08	1.92	2.14	2.17	2.27	2.12	2.16	2.48	1.82	2.03	1.82
Cl	0.00	0.00	0.00	0.00	0.00	0.00	0.00	0.00	0.00	0.00	0.00	0.00	0.00	0.00	0.00	0.00	0.00	0.00	0.00	0.00
H_2O	1.07	1.10	0.82	0.92	1.05	1.12	1.08	1.03	0.79	0.87	0.96	0.85	0.83	0.79	0.86	0.84	0.67	1.00	0.90	0.99
Total	98.28	100.63	101.07	101.56	100.95	100.85	101.14	100.55	99.16	99.47	100.59	100.31	99.93	99.72	99.47	99.21	98.88	100.25	99.77	99.53
=O=F	0.68	0.69	0.95	0.87	0.74	0.68	0.71	0.75	0.95	0.87	0.81	0.90	0.92	0.96	0.89	0.91	1.04	0.77	0.86	0.76
=O=Cl	0.00	0.00	0.00	0.00	0.00	0.00	0.00	0.00	0.00	0.00	0.00	0.00	0.00	0.00	0.00	0.00	0.00	0.00	0.00	0.00
Total	97.60	99.94	100.12	100.69	100.21	100.17	100.43	99.80	98.22	98.59	99.78	99.41	99.01	98.77	98.58	98.30	97.84	99.48	98.91	98.77
Si	8.150	8.085	8.051	7.979	8.160	8.102	8.078	8.141	8.221	8.243	8.151	8.217	8.303	8.263	8.258	8.224	8.218	8.200	8.284	8.237
^{IV}Al	0.000	0.000	0.000	0.021	0.000	0.000	0.000	0.000	0.000	0.000	0.000	0.000	0.000	0.000	0.000	0.000	0.000	0.000	0.000	0.000
Σ Tetrahedral	8.150	8.085	8.051	8.000	8.160	8.102	8.078	8.141	8.221	8.243	8.151	8.217	8.303	8.263	8.258	8.224	8.218	8.200	8.284	8.237
^{VI}Al	0.059	0.073	0.052	0.046	0.040	0.047	0.044	0.041	0.038	0.031	0.042	0.049	0.047	0.081	0.037	0.042	0.047	0.034	0.034	0.031
Ti	0.129	0.108	0.112	0.096	0.138	0.156	0.108	0.088	0.079	0.036	0.039	0.055	0.035	0.154	0.056	0.103	0.130	0.058	0.061	0.075
Fe^{3+}	0.501	0.629	0.798	0.924	0.468	0.626	0.732	0.698	0.556	0.538	0.715	0.551	0.447	0.217	0.603	0.550	0.442	0.531	0.411	0.479
Fe^{2+}	3.669	3.644	3.550	3.497	3.706	3.507	3.516	3.487	3.554	3.606	3.467	3.554	3.390	3.585	3.302	3.479	3.627	3.715	3.701	3.650
Mg	0.013	0.038	0.071	0.108	0.010	0.019	0.009	0.014	0.008	0.003	0.008	0.006	0.008	0.007	0.005	0.001	0.006	0.001	0.004	0.004
Mn	0.158	0.149	0.092	0.086	0.162	0.162	0.169	0.160	0.203	0.234	0.244	0.235	0.280	0.255	0.227	0.184	0.179	0.186	0.192	0.195
Zn	0.147	0.114	0.039	0.033	0.162	0.147	0.153	0.143	0.105	0.141	0.166	0.146	0.282	0.253	0.215	0.143	0.113	0.144	0.145	0.145
Cr	0.000	0.000	0.000	0.000	0.000	0.000	0.000	0.000	0.000	0.000	0.000	0.000	0.000	0.000	0.000	0.000	0.000	0.000	0.000	0.000
V	0.000	0.000	0.000	0.000	0.000	0.000	0.000	0.000	0.000	0.000	0.000	0.000	0.000	0.000	0.000	0.000	0.000	0.000	0.000	0.000
Zr	0.011	0.007	0.014	0.008	0.007	0.007	0.003	0.001	0.004	0.006	0.000	0.004	0.001	0.011	0.002	0.005	0.010	0.005	0.000	0.008
Nb	0.000	0.000	0.001	0.000	0.001	0.001	0.001	0.000	0.000	0.000	0.002	0.002	0.003	0.000	0.002	0.000	0.001	0.002	0.001	0.001
Y	0.000	0.000	0.000	0.000	0.000	0.000	0.000	0.000	0.000	0.000	0.000	0.000	0.000	0.000	0.000	0.000	0.000	0.000	0.000	0.000
Yb	0.000	0.000	0.000	0.000	0.000	0.000	0.000	0.000	0.000	0.000	0.000	0.000	0.000	0.000	0.000	0.000	0.000	0.000	0.000	0.000
Σ Octahedral	4.688	4.763	4.728	4.797	4.694	4.673	4.734	4.631	4.548	4.596	4.683	4.603	4.494	4.563	4.448	4.505	4.555	4.676	4.550	4.586
Na	2.747	2.769	2.777	2.845	2.691	2.728	2.664	2.671	2.729	2.572	2.557	2.619	2.543	2.744	2.766	2.821	2.806	2.577	2.645	2.533
K	0.392	0.335	0.429	0.311	0.428	0.479	0.491	0.526	0.476	0.569	0.587	0.540	0.638	0.412	0.512	0.432	0.400	0.520	0.493	0.618
Ca	0.024	0.048	0.015	0.047	0.027	0.019	0.032	0.031	0.026	0.020	0.021	0.021	0.021	0.018	0.016	0.017	0.022	0.027	0.029	0.024
Σ Alkalis	3.163	3.152	3.221	3.203	3.146	3.225	3.187	3.228	3.231	3.161	3.165	3.180	3.203	3.174	3.294	3.271	3.227	3.124	3.166	3.176
F	0.839	0.831	1.130	1.026	0.883	0.811	0.849	0.900	1.148	1.063	0.972	1.086	1.107	1.154	1.079	1.099	1.271	0.923	1.033	0.928
Cl	0.000	0.000	0.000	0.000	0.000	0.000	0.000	0.000	0.000	0.000	0.000	0.000	0.000	0.000	0.000	0.000	0.000	0.000	0.000	0.000
OH	1.161	1.169	0.870	0.974	1.117	1.189	1.151	1.100	0.852	0.937	1.028	0.914	0.893	0.846	0.921	0.901	0.729	1.077	0.967	1.072
Σ OH,F,Cl	2.000	2.000	2.000	2.000	2.000	2.000	2.000	2.000	2.000	2.000	2.000	2.000	2.000	2.000	2.000	2.000	2.000	2.000	2.000	2.000

Acronyms used are: edsedge; litlight; litrslighter; dkrsdarker; dksdark; nrsnear; midsmiddle; 2ndsssecond; grsgrain; altsaltered

Mineral formulae were calculated based on 23 atoms of oxygen and 16 cations, with Fe^{3+} calculated by the method of Droop (1987)

Appendix B-1: Electron microprobe analyses of arfvedsonitic amphibole

Unit	Sulsoivus - Drill Core																
Sample #	LB-60-9.26	LB-60-11.67					#2	mid	ed	#3ed	SL-84-212						
Description	60-926	#2	6011.67								ed	SL84212	SL84212		alt		
File	am93	am93	am93	am93	am93	am93	am93	am93	am93	am93	am93	am92	am92	am93	am93	am93	am93
Analysis #	66	70	21	23	26	27	28	29	30	32	34	41	26	3	9	15	16
Na_2O	8.87	8.94	9.77	8.86	8.26	8.55	8.42	8.43	8.99	8.40	9.17	8.73	8.89	8.69	7.76	9.07	8.57
K_2O	2.25	2.05	2.15	1.80	1.96	2.02	2.55	2.50	2.35	2.68	2.16	1.84	1.65	2.01	1.47	1.89	2.47
CaO	0.09	0.10	0.11	0.30	0.13	0.09	0.18	0.14	0.17	0.21	0.09	0.18	0.18	0.14	1.18	0.08	0.23
FeO	26.73	27.20	23.37	27.40	29.75	28.94	26.68	26.77	24.10	25.74	25.44	28.22	28.21	29.24	26.05	26.92	27.72
Fe_2O_3	4.26	4.77	8.40	4.20	1.00	2.00	4.49	5.43	7.56	6.27	6.13	4.21	4.33	1.43	0.00	4.25	3.17
MgO	0.00	0.00	0.10	0.13	0.10	0.07	0.08	0.07	0.09	0.09	0.10	0.05	0.03	0.03	5.31	0.01	0.01
MnO	1.51	1.17	0.86	1.03	1.04	1.08	1.19	1.18	1.09	1.19	0.93	0.88	0.85	0.81	0.68	0.90	1.02
ZnO	1.21	0.67	0.60	0.86	1.07	1.27	1.35	1.20	1.35	1.42	0.93	0.35	0.48	0.69	0.68	0.71	0.77
Cr_2O_3	0.00	0.00	0.00	0.00	0.00	0.00	0.00	0.00	0.00	0.00	0.00	0.00	0.00	0.00	0.00	0.00	0.00
V_2O_3	0.00	0.00	0.00	0.00	0.00	0.00	0.00	0.00	0.00	0.00	0.00	0.00	0.00	0.00	0.00	0.00	0.00
ZrO_2	0.05	0.39	0.12	0.10	0.10	0.10	0.05	0.09	0.07	0.02	0.09	0.13	0.02	0.12	0.12	0.12	0.12
Nb_2O_5	0.06	0.01	0.00	0.00	0.01	0.05	0.04	0.04	0.02	0.03	0.01	0.08	0.05	0.00	0.00	0.01	0.02
Y_2O_3	0.00	0.00	0.00	0.00	0.00	0.00	0.00	0.00	0.00	0.00	0.00	0.00	0.00	0.00	0.00	0.00	0.00
Yb_2O_3	0.00	0.00	0.00	0.00	0.00	0.00	0.00	0.00	0.00	0.00	0.00	0.00	0.00	0.00	0.00	0.00	0.00
TiO_2	0.72	1.20	1.27	1.48	1.27	1.51	0.57	0.66	0.70	0.47	1.42	0.86	0.94	1.24	0.48	0.75	1.03
SiO_2	51.61	50.66	50.71	50.30	50.60	50.93	50.92	50.60	50.24	50.54	50.45	50.33	50.46	51.32	52.98	50.88	51.16
Al_2O_3	0.26	0.21	0.31	0.39	0.28	0.26	0.15	0.19	0.19	0.16	0.28	0.25	0.25	0.30	0.34	0.34	0.19
F	2.05	2.12	2.42	2.05	2.23	1.97	2.14	2.23	1.92	1.97	2.54	2.12	2.06	2.22	1.97	1.74	1.90
Cl	0.00	0.00	0.00	0.00	0.00	0.00	0.00	0.00	0.00	0.00	0.00	0.00	0.00	0.00	0.00	0.00	0.00
H_2O	0.91	0.87	0.75	0.89	0.78	0.93	0.84	0.81	0.95	0.93	0.67	0.84	0.88	0.80	0.99	1.03	0.96
Total	100.58	100.35	100.92	99.80	98.60	99.78	99.65	100.33	99.80	100.14	100.42	99.06	99.26	99.05	100.02	98.71	99.33
=O=F	0.86	0.89	1.02	0.86	0.94	0.83	0.90	0.94	0.81	0.83	1.07	0.89	0.87	0.94	0.83	0.73	0.80
=O=Cl	0.00	0.00	0.00	0.00	0.00	0.00	0.00	0.00	0.00	0.00	0.00	0.00	0.00	0.00	0.00	0.00	0.00
Total	99.71	99.46	99.91	98.94	97.66	98.95	98.75	99.39	98.99	99.31	99.35	98.17	98.39	98.12	99.19	97.98	98.53
Si	8.225	8.114	8.028	8.088	8.257	8.202	8.218	8.135	8.076	8.129	8.069	8.162	8.157	8.293	8.248	8.223	8.247
^{IV}Al	0.000	0.000	0.000	0.000	0.000	0.000	0.000	0.000	0.000	0.000	0.000	0.000	0.000	0.000	0.000	0.000	0.000
Σ Tetrahedral	8.225	8.114	8.028	8.088	8.257	8.202	8.218	8.135	8.076	8.129	8.069	8.162	8.157	8.293	8.248	8.223	8.247
^{VI}Al	0.050	0.040	0.057	0.074	0.054	0.049	0.029	0.036	0.035	0.031	0.052	0.048	0.047	0.058	0.062	0.065	0.037
Ti	0.086	0.145	0.151	0.179	0.156	0.183	0.069	0.079	0.084	0.057	0.171	0.105	0.115	0.151	0.056	0.091	0.124
Fe^{3+}	0.511	0.575	1.000	0.508	0.123	0.243	0.546	0.657	0.914	0.759	0.738	0.514	0.527	0.174	0.000	0.517	0.385
Fe^{2+}	3.562	3.643	3.094	3.684	4.060	3.898	3.601	3.599	3.240	3.462	3.402	3.827	3.814	3.952	3.388	3.638	3.738
Mg	0.001	0.000	0.023	0.031	0.024	0.017	0.019	0.017	0.022	0.022	0.024	0.012	0.007	0.008	1.232	0.002	0.002
Mn	0.203	0.158	0.115	0.140	0.144	0.148	0.162	0.160	0.149	0.163	0.126	0.120	0.116	0.112	0.090	0.123	0.139
Zn	0.142	0.079	0.071	0.102	0.129	0.151	0.161	0.143	0.160	0.169	0.110	0.042	0.057	0.082	0.078	0.084	0.091
Cr	0.000	0.000	0.000	0.000	0.000	0.000	0.000	0.000	0.000	0.000	0.000	0.000	0.000	0.000	0.000	0.000	0.000
V	0.000	0.000	0.000	0.000	0.000	0.000	0.000	0.000	0.000	0.000	0.000	0.000	0.000	0.000	0.000	0.000	0.000
Zr	0.004	0.031	0.009	0.008	0.008	0.008	0.004	0.007	0.005	0.002	0.007	0.010	0.001	0.009	0.009	0.010	0.009
Nb	0.003	0.001	0.000	0.000	0.001	0.002	0.002	0.002	0.001	0.001	0.001	0.004	0.002	0.000	0.000	0.000	0.001
Y	0.000	0.000	0.000	0.000	0.000	0.000	0.000	0.000	0.000	0.000	0.000	0.000	0.000	0.000	0.000	0.000	0.000
Yb	0.000	0.000	0.000	0.000	0.000	0.000	0.000	0.000	0.000	0.000	0.000	0.000	0.000	0.000	0.000	0.000	0.000
Σ Octahedral	4.562	4.672	4.521	4.726	4.700	4.700	4.591	4.700	4.612	4.666	4.631	4.681	4.686	4.545	4.916	4.532	4.527
Na	2.741	2.778	2.999	2.764	2.613	2.669	2.634	2.628	2.802	2.619	2.845	2.746	2.786	2.723	2.343	2.842	2.679
K	0.457	0.419	0.435	0.370	0.408	0.415	0.526	0.512	0.481	0.551	0.441	0.380	0.341	0.415	0.292	0.389	0.508
Ca	0.015	0.018	0.018	0.052	0.023	0.015	0.032	0.025	0.029	0.016	0.015	0.031	0.030	0.025	0.197	0.014	0.039
Σ Alkalis	3.213	3.214	3.451	3.185	3.044	3.099	3.191	3.165	3.313	3.205	3.301	3.157	3.157	3.162	2.832	3.245	3.226
F	1.034	1.074	1.210	1.043	1.150	1.005	1.091	1.132	0.976	1.003	1.283	1.088	1.054	1.136	0.968	0.891	0.969
Cl	0.000	0.000	0.000	0.000	0.000	0.000	0.000	0.000	0.000	0.000	0.000	0.000	0.000	0.000	0.000	0.000	0.000
OH	0.966	0.926	0.790	0.957	0.850	0.995	0.909	0.868	1.024	0.997	0.717	0.912	0.946	0.864	1.032	1.109	1.031
Σ OH,F,Cl	2.000	2.000	2.000	2.000	2.000	2.000	2.000	2.000	2.000	2.000	2.000	2.000	2.000	2.000	2.000	2.000	2.000

Acronyms used are: ed=edge; lt=light; lt=a=lighter; dk=darker; dk=dark; nr=near; md=middle; 2nd=second; gr=grain; alt=altered

Mineral formulae were calculated based on 23 atoms of oxygen and 16 cations, with Fe^{3+} calculated by the method of Droop (1987)

Appendix B-1: Electron microprobe analyses of arfvedsonitic amphibole

Unit	Subsolvus - Drill Core														
Sample #	SL-178-99.1	178-176.3				SL-178-211.6									
Description	9911 o	1763 o	mid o	ed o	#1 o	o 78 -211.6				#1		dk	lt	mid	ed
File	am93	am93	am93	am93	am93	am93	am93	am93	am93	am93	am93	am93	am93	am93	am93
Analysis #	73	27	28	29	30	32	14	16	17	21	22	23	24	25	26
Na_2O	8.71	9.09	9.12	8.55	8.79	9.00	8.28	8.46	8.21	8.79	8.65	9.22	8.78	9.07	8.98
K_2O	2.40	2.13	2.01	2.28	2.12	1.87	2.72	2.77	2.63	2.26	2.07	1.83	1.95	1.61	1.67
CaO	0.03	0.08	0.05	0.12	0.03	0.05	0.24	0.20	0.22	0.07	0.11	0.08	0.08	0.08	0.05
FeO	25.63	26.01	26.56	27.63	26.46	27.12	27.13	25.91	27.98	27.14	27.73	26.67	28.25	28.32	26.84
Fe_2O_3	6.72	3.86	5.40	3.58	4.21	5.36	4.82	6.40	3.77	4.33	4.97	5.47	3.50	3.81	5.42
MgO	0.12	0.03	0.06	0.03	0.05	0.08	0.05	0.05	0.05	0.07	0.07	0.06	0.08	0.06	0.08
MnO	1.40	0.73	1.11	1.31	0.95	0.89	1.19	1.13	1.21	0.97	0.88	0.72	0.83	0.70	0.97
ZnO	1.27	1.92	0.88	1.26	1.59	0.59	1.02	0.92	1.07	0.66	0.66	0.47	0.39	0.38	0.80
Cr_2O_3	0.00	0.00	0.00	0.00	0.00	0.00	0.00	0.00	0.00	0.00	0.00	0.00	0.00	0.00	0.00
V_2O_3	0.00	0.00	0.00	0.00	0.00	0.00	0.00	0.00	0.00	0.00	0.00	0.00	0.00	0.00	0.00
ZrO_2	0.06	0.11	0.04	0.03	0.09	0.11	0.02	0.06	0.01	0.11	0.15	0.35	1.16	0.13	0.09
Nb_2O_5	0.00	0.00	0.02	0.06	0.01	0.00	0.07	0.05	0.04	0.00	0.00	0.02	0.00	0.00	0.01
Y_2O_3	0.00	0.00	0.00	0.00	0.00	0.00	0.00	0.00	0.00	0.00	0.00	0.00	0.00	0.00	0.00
Yb_2O_3	0.00	0.00	0.00	0.00	0.00	0.00	0.00	0.00	0.00	0.00	0.00	0.00	0.00	0.00	0.00
TiO_2	0.63	1.23	0.73	0.87	0.91	0.69	0.44	0.38	0.43	1.11	0.79	1.23	0.98	1.65	0.88
SiO_2	50.66	51.16	51.30	51.16	50.63	50.73	51.00	50.69	51.29	50.74	50.41	50.30	50.20	50.30	50.06
Al_2O_3	0.23	0.26	0.29	0.22	0.27	0.30	0.18	0.18	0.19	0.24	0.29	0.30	0.30	0.42	0.31
F	1.50	1.61	2.35	1.80	2.07	2.23	1.65	1.93	1.75	2.48	1.60	1.69	1.52	1.48	1.68
Cl	0.00	0.00	0.00	0.00	0.00	0.00	0.00	0.00	0.00	0.00	0.00	0.00	0.00	0.00	0.00
H_2O	1.17	1.10	0.77	1.01	0.87	0.81	1.08	0.95	1.03	0.68	1.10	1.06	1.13	1.16	1.06
Total	100.53	99.31	100.69	99.91	99.04	99.84	99.89	100.08	99.88	99.66	99.49	99.48	99.18	99.18	98.90
=O=F	0.63	0.68	0.99	0.76	0.87	0.94	0.69	0.81	0.74	1.05	0.67	0.71	0.64	0.62	0.71
=O=Cl	0.00	0.00	0.00	0.00	0.00	0.00	0.00	0.00	0.00	0.00	0.00	0.00	0.00	0.00	0.00
Total	99.90	98.64	99.70	99.15	98.17	98.90	99.19	99.27	99.14	98.61	98.82	98.77	98.54	98.56	98.19
Si	8.087	8.218	8.170	8.218	8.199	8.150	8.201	8.145	8.248	8.177	8.128	8.087	8.126	8.100	8.107
^{IV}Al	0.000	0.000	0.000	0.000	0.000	0.000	0.000	0.000	0.000	0.000	0.000	0.000	0.000	0.000	0.000
Σ Tetrahedral	8.087	8.218	8.170	8.218	8.199	8.150	8.201	8.145	8.248	8.177	8.128	8.087	8.126	8.100	8.107
^{VI}Al	0.043	0.049	0.055	0.041	0.051	0.057	0.034	0.033	0.037	0.046	0.055	0.058	0.058	0.080	0.059
Ti	0.076	0.148	0.087	0.105	0.111	0.084	0.053	0.046	0.052	0.134	0.096	0.149	0.120	0.200	0.108
Fe^{3+}	0.807	0.466	0.647	0.433	0.513	0.648	0.583	0.773	0.456	0.525	0.604	0.661	0.427	0.462	0.660
Fe^{2+}	3.423	3.495	3.537	3.712	3.583	3.643	3.648	3.482	3.764	3.658	3.739	3.587	3.825	3.814	3.636
Mg	0.028	0.008	0.014	0.007	0.012	0.019	0.012	0.012	0.011	0.017	0.018	0.014	0.020	0.014	0.019
Mn	0.189	0.099	0.150	0.178	0.130	0.122	0.161	0.154	0.164	0.133	0.120	0.098	0.114	0.096	0.133
Zn	0.150	0.228	0.104	0.150	0.190	0.070	0.121	0.109	0.127	0.079	0.079	0.056	0.047	0.045	0.096
Cr	0.000	0.000	0.000	0.000	0.000	0.000	0.000	0.000	0.000	0.000	0.000	0.000	0.000	0.000	0.000
V	0.000	0.000	0.000	0.000	0.000	0.000	0.000	0.000	0.000	0.000	0.000	0.000	0.000	0.000	0.000
Zr	0.005	0.009	0.003	0.002	0.007	0.008	0.002	0.005	0.001	0.009	0.012	0.028	0.092	0.010	0.007
Nb	0.000	0.000	0.001	0.002	0.000	0.000	0.003	0.001	0.002	0.000	0.000	0.001	0.000	0.000	0.001
Y	0.000	0.000	0.000	0.000	0.000	0.000	0.000	0.000	0.000	0.000	0.000	0.000	0.000	0.000	0.000
Yb	0.000	0.000	0.000	0.000	0.000	0.000	0.000	0.000	0.000	0.000	0.000	0.000	0.000	0.000	0.000
Σ Octahedral	4.720	4.502	4.598	4.630	4.597	4.651	4.618	4.616	4.613	4.601	4.722	4.651	4.701	4.722	4.719
Na	2.698	2.830	2.817	2.664	2.760	2.805	2.580	2.636	2.560	2.746	2.705	2.873	2.756	2.833	2.820
K	0.489	0.436	0.407	0.467	0.439	0.384	0.558	0.568	0.539	0.464	0.426	0.375	0.403	0.332	0.346
Ca	0.005	0.013	0.008	0.021	0.006	0.009	0.042	0.034	0.039	0.012	0.019	0.014	0.014	0.013	0.008
Σ Alkalis	3.192	3.279	3.233	3.152	3.204	3.199	3.180	3.239	3.138	3.223	3.150	3.262	3.173	3.177	3.174
F	0.757	0.818	1.186	0.912	1.060	1.133	0.838	0.982	0.891	1.266	0.814	0.860	0.779	0.754	0.858
Cl	0.000	0.000	0.000	0.000	0.000	0.000	0.000	0.000	0.000	0.000	0.000	0.000	0.000	0.000	0.000
OH	1.243	1.182	0.814	1.088	0.940	0.867	1.162	1.018	1.109	0.734	1.186	1.140	1.221	1.246	1.142
Σ OH,F,Cl	2.000	2.000	2.000	2.000	2.000	2.000	2.000	2.000	2.000	2.000	2.000	2.000	2.000	2.000	2.000

Acronyms used are: ed=edge; lt=light; lt=r=lighter; dk=r=darker; dk=dark; mid=middle; 2nd=second; gr=grain; alt=altered

Mineral formulae were calculated based on 23 atoms of oxygen and 16 cations, with Fe^{3+} calculated

Appendix B-1 Electron microprobe analyses of arfvedsonitic amphibole

Unit	Subsolvus - Drill Core																									
Sample #	SL-182-10.18									SL-182-19.40					SL-182-31.06							SL-182-40.08				
Description	10.18		mid		ed	#2ed				ed	19.40				ed	ed	31.06	2 am	bi	gr	gr 0.08 am	am	#2l	bram	#3ed	mid
File	am93	am93	am93	am93	am93	am93	am93	am93	am93	am93	am93	am93	am93	am93	am93	am93	1/1/95	1/1/95	1/1/95	1/1/95	1/1/95	am93	am93	am93	am93	am93
Analysis #	41	42	43	44	45	46	47	48	49	50	52	53	54	55	56	70	72	75	76	77	65	67	69	70	71	72
Na_2O	8.56	8.94	8.85	8.94	8.06	8.95	9.11	8.98	8.99	8.10	8.31	8.90	9.32	8.06	8.08	9.42	9.06	9.54	9.37	9.43	9.13	9.02	9.19	9.09	8.52	8.65
K_2O	2.24	1.53	1.66	1.61	2.96	2.11	1.61	1.69	1.62	2.80	2.90	1.60	1.54	2.89	2.88	1.45	2.00	1.25	1.52	1.40	1.68	1.70	1.86	1.72	2.28	1.93
CaO	0.19	0.37	0.28	0.36	0.23	0.11	0.34	0.11	0.28	0.22	0.23	0.14	0.16	0.23	0.24	0.61	0.06	0.70	0.16	0.22	0.25	0.23	0.16	0.24	0.10	0.16
FeO	27.92	29.39	29.38	29.42	26.66	26.92	28.32	28.81	28.92	27.56	27.44	30.40	27.74	27.70	27.42	25.79	28.13	27.35	27.56	27.86	26.91	27.12	26.49	27.51	27.42	27.76
Fe_2O_3	3.40	3.42	3.35	2.85	4.54	4.06	5.05	4.89	4.71	4.33	4.47	0.87	4.38	4.19	4.38	5.60	3.61	4.40	5.56	5.10	5.82	2.97	6.34	4.42	2.07	2.21
MgO	0.05	0.19	0.21	0.21	0.05	0.05	0.23	0.14	0.20	0.05	0.06	0.17	0.19	0.07	0.07	0.03	0.06	0.29	0.17	0.17	0.22	0.14	0.09	0.28	0.04	0.06
MnO	1.10	0.76	0.70	0.71	1.03	1.02	0.71	0.66	0.68	1.08	1.11	0.72	0.81	1.14	1.08	1.41	1.08	0.86	0.92	0.70	0.62	0.89	0.69	0.63	1.14	1.17
ZnO	1.19	0.36	0.36	0.30	1.45	1.39	0.28	0.29	0.35	1.47	1.51	0.56	0.65	1.31	1.47	1.06	0.73	0.40	0.54	0.25	0.29	0.88	0.35	0.46	1.35	1.48
Cr_2O_3	0.00	0.00	0.00	0.00	0.00	0.00	0.00	0.00	0.00	0.00	0.00	0.00	0.00	0.00	0.00	0.01	0.00	0.00	0.00	0.00	0.00	0.00	0.00	0.00	0.00	0.00
V_2O_3	0.00	0.00	0.00	0.00	0.00	0.00	0.00	0.00	0.00	0.00	0.00	0.00	0.00	0.00	0.00	0.03	0.00	0.00	0.00	0.02	0.00	0.00	0.00	0.00	0.00	0.00
ZrO_2	0.07	0.12	0.14	0.12	0.06	0.13	0.07	0.11	0.10	0.02	0.01	0.38	0.17	0.04	0.03	0.07	0.06	0.13	0.12	0.10	0.17	0.14	0.16	0.13	0.07	0.18
Nb_2O_5	0.03	0.05	0.00	0.00	0.01	0.02	0.02	0.00	0.00	0.09	0.04	0.02	0.04	0.06	0.00	0.00	0.00	0.00	0.00	0.00	0.00	0.00	0.02	0.00	0.02	0.01
Y_2O_3	0.00	0.00	0.00	0.00	0.00	0.00	0.00	0.00	0.00	0.00	0.00	0.00	0.00	0.00	0.00	0.00	0.00	0.00	0.00	0.00	0.00	0.00	0.00	0.00	0.00	0.00
Yb_2O_3	0.00	0.00	0.00	0.00	0.00	0.00	0.00	0.00	0.00	0.00	0.00	0.00	0.00	0.00	0.00	0.00	0.00	0.00	0.00	0.00	0.00	0.00	0.00	0.00	0.00	0.00
TiO_2	0.96	1.08	1.27	1.18	0.51	0.98	1.11	0.88	1.20	0.42	0.66	2.15	1.28	0.59	0.68	1.16	1.41	1.13	0.83	0.93	0.91	1.01	1.12	1.00	1.29	0.97
SiO_2	51.14	51.25	51.01	51.39	50.63	51.36	51.10	51.07	51.03	51.08	51.81	51.11	51.21	51.11	50.99	50.94	51.66	51.64	51.48	51.35	50.32	50.74	50.26	50.91	50.64	50.89
Al_2O_3	0.19	0.37	0.41	0.42	0.18	0.23	0.37	0.29	0.37	0.17	0.18	0.41	0.35	0.19	0.16	0.52	0.27	0.43	0.32	0.40	0.36	0.37	0.32	0.36	0.27	0.32
F	2.21	2.32	1.76	2.26	1.85	2.24	2.25	2.69	2.54	1.69	2.03	1.86	2.07	1.79	1.74	2.01	2.31	2.20	1.68	2.14	2.10	1.85	2.50	2.26	1.54	1.71
Cl	0.00	0.00	0.00	0.00	0.00	0.00	0.00	0.00	0.00	0.00	0.00	0.00	0.00	0.00	0.00	0.02	0.01	0.02	0.02	0.02	0.00	0.00	0.00	0.00	0.00	0.00
H_2O	0.82	0.78	1.04	0.81	0.97	0.81	0.83	0.61	0.69	1.06	0.93	0.99	0.91	1.02	1.04	0.94	0.79	0.85	1.10	0.87	0.87	0.97	0.68	0.80	1.10	1.04
Total	100.08	100.93	100.42	100.58	99.19	100.40	101.38	101.25	101.67	100.13	101.67	100.29	100.82	100.37	100.26	101.08	101.26	101.19	101.35	100.96	99.64	98.04	100.22	99.81	97.86	98.53
=O=F	0.93	0.98	0.74	0.95	0.78	0.94	0.95	1.13	1.07	0.71	0.86	0.78	0.87	0.75	0.73	0.85	0.97	0.93	0.71	0.90	0.88	0.78	1.05	0.95	0.65	0.72
=O=Cl	0.00	0.00	0.00	0.00	0.00	0.00	0.00	0.00	0.00	0.00	0.00	0.00	0.00	0.00	0.00	0.00	0.00	0.00	0.00	0.01	0.00	0.00	0.00	0.00	0.00	0.00
Total	99.15	99.95	99.68	99.63	98.41	99.45	100.44	100.12	100.60	99.42	100.82	99.51	99.95	99.62	99.52	100.23	100.29	100.26	100.64	100.06	98.76	97.27	99.17	98.86	97.21	97.81
Si	8.216	8.152	8.134	8.182	8.212	8.206	8.086	8.123	8.078	8.213	8.204	8.160	8.127	8.201	8.189	8.064	8.180	8.138	8.117	8.129	8.086	8.246	8.056	8.157	8.267	8.263
^{IV}Al	0.000	0.000	0.000	0.000	0.000	0.000	0.000	0.000	0.000	0.000	0.000	0.000	0.000	0.000	0.000	0.000	0.000	0.000	0.000	0.000	0.000	0.000	0.000	0.000	0.000	0.000
Σ Tetrahedral	8.216	8.152	8.134	8.182	8.212	8.206	8.086	8.123	8.078	8.213	8.204	8.160	8.127	8.201	8.189	8.064	8.180	8.138	8.117	8.129	8.086	8.246	8.056	8.157	8.267	8.263
^{VI}Al	0.035	0.070	0.077	0.078	0.035	0.043	0.069	0.054	0.068	0.033	0.033	0.078	0.065	0.036	0.030	0.097	0.051	0.080	0.060	0.074	0.069	0.071	0.060	0.069	0.052	0.060
Ti	0.116	0.130	0.152	0.142	0.062	0.118	0.132	0.105	0.143	0.050	0.079	0.259	0.153	0.071	0.083	0.139	0.168	0.134	0.098	0.111	0.110	0.124	0.135	0.120	0.158	0.119
Fe^{3+}	0.411	0.410	0.402	0.342	0.554	0.488	0.601	0.585	0.561	0.524	0.532	0.105	0.523	0.506	0.529	0.667	0.430	0.521	0.660	0.608	0.704	0.363	0.765	0.533	0.254	0.270
Fe^{2+}	3.751	3.910	3.918	3.917	3.616	3.597	3.748	3.832	3.828	3.705	3.634	4.060	3.682	3.717	3.683	3.415	3.725	3.604	3.635	3.689	3.616	3.686	3.551	3.687	3.743	3.770
Mg	0.013	0.044	0.049	0.049	0.013	0.012	0.053	0.034	0.048	0.012	0.014	0.039	0.044	0.016	0.017	0.008	0.013	0.067	0.040	0.041	0.052	0.034	0.023	0.068	0.010	0.014
Mn	0.150	0.102	0.095	0.096	0.142	0.138	0.095	0.090	0.091	0.146	0.149	0.098	0.108	0.155	0.147	0.189	0.144	0.115	0.123	0.093	0.084	0.123	0.093	0.085	0.158	0.160
Zn	0.142	0.043	0.042	0.036	0.173	0.164	0.033	0.034	0.041	0.174	0.177	0.066	0.076	0.155	0.174	0.124	0.082	0.047	0.063	0.030	0.035	0.106	0.041	0.055	0.163	0.177
Cr	0.000	0.000	0.000	0.000	0.000	0.000	0.000	0.000	0.000	0.000	0.000	0.000	0.000	0.000	0.000	0.001	0.000	0.000	0.000	0.000	0.000	0.000	0.000	0.000	0.000	0.000
V	0.000	0.000	0.000	0.000	0.000	0.000	0.000	0.000	0.000	0.000	0.000	0.000	0.000	0.000	0.000	0.003	0.000	0.000	0.000	0.002	0.000	0.000	0.000	0.000	0.000	0.000
Zr	0.006	0.009	0.011	0.009	0.005	0.010	0.006	0.009	0.007	0.002	0.001	0.030	0.013	0.003	0.002	0.006	0.005	0.010	0.009	0.008	0.013	0.011	0.013	0.010	0.005	0.014
Nb	0.001	0.002	0.000	0.000	0.000	0.001	0.001	0.000	0.000	0.004	0.002	0.001	0.002	0.002	0.000	0.000	0.000	0.000	0.000	0.000	0.000	0.000	0.001	0.000	0.001	0.000
Y	0.000	0.000	0.000	0.000	0.000	0.000	0.000	0.000	0.000	0.000	0.000	0.000	0.000	0.000	0.000	0.000	0.000	0.000	0.000	0.000	0.000	0.000	0.000	0.000	0.000	0.000
Yb	0.000	0.000	0.000	0.000	0.000	0.000	0.000	0.000	0.000	0.000	0.000	0.000	0.000	0.000	0.000	0.000	0.000	0.000	0.000	0.000	0.000	0.000	0.000	0.000	0.000	0.000
Σ Octahedral	4.625	4.719	4.746	4.669	4.600	4.573	4.737	4.743	4.788	4.651	4.620	4.735	4.667	4.661	4.665	4.648	4.623	4.578	4.688	4.655	4.683	4.518	4.682	4.627	4.545	4.586
Na	2.666	2.756	2.735	2.759	2.535	2.771	2.794	2.770	2.759	2.524	2.553	2.756	2.867	2.507	2.515	2.892	2.783	2.916	2.863	2.896	2.845	2.843	2.856	2.825	2.695	2.722
K	0.460	0.310	0.337	0.328	0.613	0.431	0.325	0.343	0.328	0.574	0.585	0.325	0.312	0.592	0.591	0.293	0.405	0.250	0.305	0.283	0.345	0.352	0.379	0.351	0.475	0.401
Ca	0.013	0.062	0.048	0.062	0.039	0.019	0.058	0.021	0.047	0.038	0.018	0.024	0.028	0.039	0.040	0.104	0.010	0.118	0.027	0.037	0.043	0.041	0.027	0.041	0.018	0.028
Σ Alkalis	3.159	3.129	3.120	3.149	3.188	3.222	3.177	3.135	3.134	3.136	3.176	3.105	3.207	3.138	3.146	3.288	3.197	3.284	3.195	3.216	3.232	3.236	3.262	3.217	3.188	3.151
F	1.123	1.169	0.889	1.138	0.948	1.132	1.127	1.351	1.273	0.858	1.017	0.941	1.041	0.909	0.884	1.006	1.158	1.096	0.836	1.072	1.067	0.950	1.269	1.147	0.797	0.876
Cl	0.000	0.000	0.000	0.000	0.000	0.000	0.000	0.000	0.000	0.000	0.000	0.000	0.000	0.000	0.000	0.005	0.002	0.006	0.004	0.006	0.000	0.000	0.000	0.000	0.000	0.000
OH	0.877	0.831	1.111	0.862	1.052	0.868	0.873	0.649	0.727	1.142	0.983	1.059	0.959	1.091	1.116	0.989	0.840	0.898	1.160	0.922	0.933	1.050	0.731	0.853	1.203	1.124
Σ OH,F,Cl	2.000	2.000	2.000	2.000	2.000	2.000	2.000	2.000	2.000	2.000	2.000	2.000	2.000	2.000	2.000	2.000	2.000	2.000	2.000	2.000	2.000	2.000	2.000	2.000	2.000	2.000

Acronyms used are: ed=edge; lt=light; ltr=lighter; dkr=darker; dk=dark; nr=near; mid=middle; 2nd=second; gr=grain; alt=altered
Mineral formulae were calculated based on 23 atoms of oxygen and 16 cations, with Fe^{3+} calculated by the method of Droop (1987)

Appendix B-1. Electron microprobe analyses of arfvedsonitic amphibole

Unit	Subsolvus - Drill Core							SL-182-47.85			SL-182-50.60								SL-182-54.90				SL-182-59.4				
Sample #	-40.98	-40.77																									
Description	rim	40.77			ed	mid	amar	-47.85 o	arpy o	#2am	5060 o		o 3-50.6 o		yel o	o	o	5490 o	ed	ed	mid	59.40 o	o	o	#3ed	mid	ed
File	am93	am93	am93	am93	am93	am93	am93	am93	am93	am93	am93	am93	am93	am93	am93	am93	am93	1/1/95	1/1/95	1/1/95	1/1/95	am93	am93	am93	am93	am93	am93
Analysis #	73	14	15	16	17	18	21	12	13	17	67	70	7	9	10	12	92	94	96	97	46	47	58	61	62	63	
Na_2O	8.20	8.31	9.10	8.40	8.88	8.30	8.83	8.38	8.67	8.57	8.20	8.50	8.99	9.42	8.97	8.74	8.47	8.54	8.53	8.60	8.86	9.19	8.49	8.59	8.98	8.57	
K_2O	2.84	2.87	1.61	2.76	2.15	2.86	1.87	2.78	2.58	2.94	2.69	2.43	1.75	1.46	1.85	2.05	2.61	2.71	2.72	2.26	2.18	2.12	2.55	2.79	2.21	2.51	
CaO	0.22	0.51	0.26	0.20	0.13	0.22	0.18	0.20	0.24	0.04	0.16	0.15	0.08	0.34	0.06	0.08	0.02	0.12	0.07	0.16	0.14	0.21	0.23	0.19	0.06	0.16	
FeO	25.84	24.95	26.99	26.47	25.83	26.83	27.27	26.07	25.22	26.30	27.28	27.20	27.46	27.16	28.83	29.80	25.53	26.03	22.83	27.45	27.23	25.07	26.54	24.83	27.28	25.88	
Fe_2O_3	5.49	7.24	5.83	5.91	6.25	5.71	5.03	4.33	4.80	3.17	2.57	2.05	3.45	4.17	1.77	0.33	2.21	3.22	2.91	3.12	3.05	5.98	4.15	5.72	2.48	3.87	
MgO	0.03	0.07	0.17	0.11	0.06	0.12	0.07	0.00	0.00	0.01	0.00	0.01	0.08	0.10	0.08	0.04	0.05	0.02	0.04	0.02	0.02	0.01	0.00	0.00	0.02	0.01	
MnO	1.16	1.22	0.97	1.09	1.16	1.15	1.10	1.65	1.63	1.27	1.66	1.63	1.27	0.69	0.83	0.98	2.75	1.96	4.46	1.62	1.23	1.17	1.51	1.47	1.07	1.35	
ZnO	1.46	1.62	0.76	1.09	1.53	1.02	1.26	1.25	1.51	1.12	1.27	1.17	0.79	0.44	0.51	0.44	1.82	1.31	1.75	0.99	0.84	0.70	1.00	1.05	0.68	1.27	
Cr_2O_3	0.00	0.00	0.00	0.00	0.00	0.00	0.00	0.00	0.00	0.00	0.00	0.00	0.00	0.00	0.00	0.00	0.01	0.01	0.00	0.00	0.00	0.00	0.00	0.00	0.00	0.00	
V_2O_3	0.00	0.00	0.00	0.00	0.00	0.00	0.00	0.00	0.00	0.00	0.00	0.00	0.00	0.00	0.00	0.00	0.00	0.00	0.00	0.00	0.00	0.00	0.00	0.00	0.00	0.00	
ZrO_2	0.00	0.01	0.18	0.18	0.10	0.19	0.14	0.04	0.04	0.04	0.06	0.08	0.31	0.19	0.72	0.56	0.06	0.00	0.04	0.05	0.05	0.05	0.06	0.06	1.47	0.06	
Nb_2O_5	0.00	0.01	0.00	0.02	0.00	0.02	0.00	0.06	0.06	0.03	0.00	0.04	0.00	0.01	0.00	0.04	0.00	0.00	0.00	0.00	0.00	0.00	0.05	0.05	0.00	0.04	
Y_2O_3	0.00	0.00	0.00	0.00	0.00	0.00	0.00	0.00	0.00	0.00	0.00	0.00	0.00	0.00	0.00	0.00	0.00	0.00	0.00	0.00	0.00	0.00	0.00	0.00	0.00	0.00	
Yb_2O_3	0.00	0.00	0.00	0.00	0.00	0.00	0.00	0.00	0.00	0.00	0.00	0.00	0.00	0.00	0.00	0.00	0.00	0.00	0.00	0.00	0.00	0.00	0.00	0.00	0.00	0.00	
TiO_2	0.69	0.50	1.25	1.15	1.14	1.10	1.12	0.47	0.56	0.62	0.50	0.72	0.78	0.79	0.99	2.90	0.54	0.39	0.34	0.61	0.95	0.86	0.53	0.39	0.92	0.53	
SiO_2	50.15	50.40	50.30	50.42	50.43	50.58	50.54	51.12	51.14	51.77	51.27	51.41	51.02	51.23	51.37	50.44	51.80	51.86	51.85	51.47	51.36	50.70	51.07	50.70	50.99	50.83	
Al_2O_3	0.16	0.16	0.45	0.16	0.29	0.15	0.33	0.18	0.20	0.18	0.20	0.24	0.30	0.31	0.30	0.30	0.23	0.18	0.18	0.20	0.25	0.22	0.19	0.16	0.23	0.20	
F	1.74	1.81	1.72	1.69	1.74	1.68	1.74	2.27	2.44	2.65	2.25	2.37	2.30	2.83	2.42	1.66	2.91	2.26	2.33	1.83	2.38	2.26	2.13	2.02	2.05	2.03	
Cl	0.00	0.00	0.00	0.00	0.00	0.00	0.00	0.00	0.00	0.00	0.00	0.00	0.00	0.00	0.00	0.00	0.00	0.01	0.00	0.00	0.00	0.00	0.00	0.00	0.00	0.00	
H_2O	1.02	1.01	1.07	1.07	1.05	1.08	1.05	0.78	0.71	0.60	0.78	0.72	0.77	0.52	0.71	1.08	0.47	0.79	0.75	0.99	0.73	0.79	0.85	0.89	0.88	0.88	
Total	99.00	100.69	100.65	100.72	100.72	101.02	100.52	99.57	99.80	99.31	98.89	98.72	99.36	99.67	99.41	99.44	99.46	99.40	99.00	99.37	99.26	99.34	99.34	98.91	99.33	98.18	
=O=F	0.73	0.76	0.72	0.71	0.73	0.71	0.73	0.95	1.03	1.11	0.95	1.00	0.97	1.19	1.02	0.70	1.23	0.95	0.98	0.77	1.00	0.95	0.90	0.85	0.86	0.86	
=O=Cl	0.00	0.00	0.00	0.00	0.00	0.00	0.00	0.00	0.00	0.00	0.00	0.00	0.00	0.00	0.00	0.00	0.00	0.00	0.00	0.00	0.00	0.00	0.00	0.00	0.00	0.00	
Total	98.27	99.93	99.93	100.01	99.99	100.31	99.79	98.61	98.77	98.19	97.94	97.73	98.39	98.47	98.39	98.74	98.23	98.44	98.02	98.60	98.26	98.39	98.44	98.05	98.47	97.33	
Si	8.150	8.070	8.014	8.060	8.047	8.069	8.079	8.253	8.232	8.352	8.328	8.344	8.228	8.223	8.279	8.128	8.370	8.352	8.379	8.290	8.280	8.162	8.251	8.217	8.233	8.287	
^{IV}Al	0.000	0.000	0.000	0.000	0.000	0.000	0.000	0.000	0.000	0.000	0.000	0.000	0.000	0.000	0.000	0.000	0.000	0.000	0.000	0.000	0.000	0.000	0.000	0.000	0.000	0.000	
Σ Tetrahedral	8.150	8.070	8.014	8.060	8.047	8.069	8.079	8.253	8.232	8.352	8.328	8.344	8.228	8.223	8.279	8.128	8.370	8.352	8.379	8.290	8.280	8.162	8.251	8.217	8.233	8.287	
^{VI}Al	0.031	0.030	0.085	0.031	0.054	0.028	0.062	0.034	0.039	0.034	0.038	0.046	0.058	0.058	0.057	0.058	0.043	0.034	0.035	0.037	0.047	0.042	0.036	0.030	0.044	0.038	
Ti	0.085	0.060	0.149	0.138	0.137	0.132	0.135	0.057	0.068	0.075	0.061	0.088	0.095	0.096	0.120	0.351	0.065	0.047	0.041	0.074	0.115	0.104	0.064	0.048	0.112	0.064	
Fe^{3+}	0.671	0.873	0.699	0.711	0.750	0.686	0.606	0.527	0.581	0.384	0.314	0.250	0.419	0.503	0.215	0.041	0.269	0.390	0.354	0.378	0.370	0.725	0.505	0.698	0.302	0.475	
Fe^{2+}	3.511	3.341	3.596	3.539	3.447	3.579	3.646	3.520	3.396	3.548	3.705	3.692	3.704	3.645	3.886	4.016	3.449	3.506	3.085	3.698	3.671	3.375	3.586	3.365	3.683	3.529	
Mg	0.008	0.016	0.040	0.027	0.013	0.029	0.016	0.001	0.001	0.003	0.001	0.002	0.020	0.023	0.020	0.010	0.011	0.004	0.008	0.004	0.004	0.003	0.000	0.000	0.006	0.002	
Mn	0.159	0.165	0.132	0.148	0.156	0.156	0.148	0.225	0.222	0.174	0.229	0.225	0.173	0.094	0.113	0.134	0.377	0.268	0.638	0.220	0.168	0.160	0.207	0.201	0.146	0.187	
Zn	0.175	0.192	0.089	0.129	0.180	0.120	0.148	0.149	0.180	0.133	0.153	0.141	0.095	0.052	0.061	0.052	0.217	0.155	0.209	0.118	0.100	0.083	0.119	0.126	0.081	0.153	
Cr	0.000	0.000	0.000	0.000	0.000	0.000	0.000	0.000	0.000	0.000	0.000	0.000	0.000	0.000	0.000	0.000	0.001	0.001	0.000	0.000	0.000	0.000	0.000	0.000	0.000	0.000	
V	0.000	0.000	0.000	0.000	0.000	0.000	0.000	0.000	0.000	0.000	0.000	0.000	0.000	0.000	0.000	0.000	0.000	0.000	0.000	0.000	0.000	0.000	0.000	0.000	0.000	0.000	
Zr	0.000	0.001	0.014	0.014	0.007	0.015	0.011	0.003	0.003	0.004	0.005	0.006	0.024	0.015	0.057	0.044	0.005	0.000	0.003	0.004	0.004	0.004	0.004	0.004	0.116	0.004	
Nb	0.000	0.000	0.000	0.001	0.000	0.001	0.000	0.003	0.003	0.002	0.000	0.002	0.000	0.000	0.000	0.002	0.000	0.000	0.000	0.000	0.000	0.000	0.002	0.002	0.000	0.002	
Y	0.000	0.000	0.000	0.000	0.000	0.000	0.000	0.000	0.000	0.000	0.000	0.000	0.000	0.000	0.000	0.000	0.000	0.000	0.000	0.000	0.000	0.000	0.000	0.000	0.000	0.000	
Yb	0.000	0.000	0.000	0.000	0.000	0.000	0.000	0.000	0.000	0.000	0.000	0.000	0.000	0.000	0.000	0.000	0.000	0.000	0.000	0.000	0.000	0.000	0.000	0.000	0.000	0.000	
Σ Octahedral	4.641	4.678	4.803	4.738	4.745	4.746	4.772	4.518	4.492	4.357	4.505	4.452	4.587	4.488	4.528	4.707	4.436	4.406	4.374	4.533	4.480	4.496	4.524	4.475	4.490	4.454	
Na	2.582	2.580	2.811	2.604	2.748	2.566	2.736	2.623	2.706	2.680	2.582	2.674	2.810	2.932	2.802	2.729	2.654	2.666	2.673	2.685	2.769	2.870	2.660	2.699	2.811	2.708	
K	0.589	0.586	0.328	0.563	0.438	0.581	0.382	0.572	0.529	0.604	0.556	0.503	0.361	0.298	0.380	0.421	0.537	0.556	0.562	0.465	0.447	0.436	0.525	0.576	0.456	0.522	
Ca	0.038	0.087	0.044	0.034	0.022	0.038	0.030	0.034	0.041	0.007	0.028	0.027	0.013	0.059	0.011	0.014	0.003	0.020	0.011	0.028	0.024	0.037	0.019	0.033	0.010	0.028	
Σ Alkalis	3.210	3.253	3.183	3.202	3.208	3.186	3.148	3.229	3.276	3.291	3.167	3.205	3.184	3.289	3.193	3.165	3.194	3.243	3.247	3.177	3.240	3.343	3.225	3.308	3.277	3.258	
F	0.894	0.917	0.864	0.853	0.878	0.847	0.880	1.158	1.241	1.350	1.156	1.218	1.172	1.438	1.236	0.843	1.488	1.153	1.188	0.931	1.213	1.148	1.088	1.037	1.046	1.047	
Cl	0.000	0.000	0.000	0.000	0.000	0.000	0.000	0.000	0.000	0.000	0.000	0.000	0.000	0.000	0.000	0.000	0.000	0.002	0.000	0.001	0.000	0.000	0.000	0.000	0.000	0.000	
OH	1.106	1.083	1.136	1.147	1.122	1.153	1.120	0.842	0.759	0.650	0.844	0.782	0.828	0.562	0.764	1.157	0.512	0.846	0.812	1.068	0.787	0.852	0.912	0.963	0.954	0.953	
Σ OH,F,Cl	2.000	2.000	2.000	2.000	2.000	2.000	2.000	2.000	2.000	2.000	2.000	2.000	2.000	2.000	2.000	2.000	2.000	2.000	2.000	2.000	2.000	2.000	2.000	2.000	2.000	2.000	

Acronyms used are: ed=edge; lt=light; lter=lighter; dker=darker; dk=dark; nr=near; mid=middle; 2nd=second; gr=grain; alt=altered; yel=yellow

Mineral formulae were calculated based on 23 atoms of oxygen and 16 cations, with Fe^{3+} calculated by the method of Droop (1987)

Appendix B-1: Electron microprobe analyses of arfvedsonitic amphibole

Unit	Subsolvus - Drill Core																											
Sample #	SL-182-71.0						SL-182-74.73												SL-182-77.20							SL-182-84.96		
Description	71.0	mid	ed	#2	mid	ed	74.73					ed	#2	ed	mid	#3	mid	77.2 nr							nr 4	84.96 mid 1ed		midbl
File	am93	am93	am93	am93	am93	am93	am93	am93	am93	am93	am93	am93	am93	am93	am93	am93	am93	am93	am93	am93	am93	am93	am93	am93	am93	1/1/95	1/1/95	1/1/95
Analysis #	59	60	61	64	65	66	22	23	24	25	26	27	29	30	31	33	34	40	41	42	43	44	45	53	54	55		
Na_2O	7.07	8.22	8.28	7.85	7.64	8.13	8.64	9.25	9.23	8.99	9.28	8.90	8.89	8.47	9.28	8.20	8.54	8.09	6.88	8.43	8.36	8.72	8.54	9.24	9.18	9.41		
K_2O	2.18	2.33	2.75	2.53	2.63	2.71	2.42	2.12	1.77	1.98	1.96	2.26	2.28	2.90	1.91	2.72	2.75	2.26	2.05	2.95	2.97	2.18	2.84	1.37	1.24	1.44		
CaO	1.35	0.13	0.25	0.55	0.87	0.42	0.17	0.08	0.08	0.09	0.07	0.19	0.15	0.21	0.07	0.21	0.20	0.27	0.10	0.15	0.10	0.09	0.03	0.31	0.52	0.33		
FeO	27.81	29.68	26.80	29.84	29.16	28.07	26.36	26.59	27.37	27.42	27.76	25.95	25.77	25.27	26.34	27.60	25.16	29.62	26.80	23.97	22.20	26.66	23.69	28.84	28.25	27.86		
Fe_2O_3	0.00	1.55	2.74	0.00	0.86	2.13	5.47	5.54	4.56	1.96	4.15	5.38	5.44	6.96	4.15	3.85	6.92	2.01	4.19	6.44	7.72	4.20	6.81	4.53	4.72	5.45		
MgO	0.17	0.02	0.02	0.37	0.44	0.19	0.06	0.06	0.03	0.04	0.08	0.03	0.03	0.03	0.04	0.03	0.01	0.14	0.05	0.07	0.09	0.04	0.07	0.18	0.52	0.31		
MnO	1.31	1.39	2.06	1.52	1.42	1.59	1.42	0.81	1.07	1.52	0.76	1.39	1.51	1.51	1.45	1.47	1.45	1.19	1.09	1.75	1.98	1.29	1.82	0.78	0.70	0.65		
ZnO	0.74	0.98	1.66	1.21	1.20	1.30	1.15	0.48	0.70	1.09	0.40	1.03	1.23	1.23	1.27	1.21	1.17	1.08	1.07	2.12	2.67	1.56	2.35	0.34	0.28	0.24		
Cr_2O_3	0.00	0.00	0.00	0.00	0.00	0.00	0.00	0.00	0.00	0.00	0.00	0.00	0.00	0.00	0.00	0.00	0.00	0.00	0.00	0.00	0.00	0.00	0.00	0.02	0.01	0.00		
V_2O_3	0.00	0.00	0.00	0.00	0.00	0.00	0.00	0.00	0.00	0.00	0.00	0.00	0.00	0.00	0.00	0.00	0.00	0.00	0.00	0.00	0.00	0.00	0.00	0.00	0.00	0.01		
ZrO_2	0.02	0.09	0.05	0.08	0.05	0.06	0.01	0.11	0.14	1.75	0.43	0.10	0.09	0.03	0.08	0.06	0.06	0.22	0.86	0.03	0.00	0.03	0.01	0.12	0.13	0.10		
Nb_2O_5	0.04	0.03	0.01	0.04	0.02	0.00	0.12	0.02	0.05	0.00	0.04	0.07	0.02	0.00	0.00	0.01	0.05	0.03	0.00	0.00	0.00	0.01	0.00	0.00	0.00	0.00		
Y_2O_3	0.00	0.00	0.00	0.00	0.00	0.00	0.00	0.00	0.00	0.00	0.00	0.00	0.00	0.00	0.00	0.00	0.00	0.00	0.00	0.00	0.00	0.00	0.00	0.00	0.00	0.00		
Yb_2O_3	0.00	0.00	0.00	0.00	0.00	0.00	0.00	0.00	0.00	0.00	0.00	0.00	0.00	0.00	0.00	0.00	0.00	0.00	0.00	0.00	0.00	0.00	0.00	0.00	0.00	0.00		
TiO_2	0.95	0.86	0.40	0.50	0.43	0.55	0.79	1.38	1.26	1.72	2.53	0.74	0.73	0.39	2.32	0.50	0.46	0.80	1.00	0.83	0.24	0.95	0.19	1.14	1.34	0.98		
SiO_2	51.55	51.59	52.00	52.67	51.66	52.01	50.89	51.02	51.14	50.48	50.56	51.03	51.12	50.97	50.81	51.35	50.62	51.07	50.40	50.48	49.94	50.91	50.97	51.34	50.79	51.50		
Al_2O_3	0.22	0.23	0.16	0.21	0.20	0.21	0.23	0.28	0.29	0.34	0.34	0.22	0.23	0.16	0.36	0.17	0.17	0.21	0.29	0.17	0.15	0.26	0.15	0.41	0.49	0.41		
F	2.03	2.17	2.37	2.10	1.96	2.05	1.86	2.57	1.97	1.83	2.03	2.02	2.15	2.27	1.98	2.03	1.97	1.67	1.83	1.91	2.15	1.94	2.09	1.74	1.83	2.48		
Cl	0.00	0.00	0.00	0.00	0.00	0.00	0.00	0.00	0.00	0.00	0.00	0.00	0.00	0.00	0.00	0.00	0.00	0.00	0.00	0.00	0.00	0.00	0.00	0.01	0.02	0.02		
H_2O	0.83	0.84	0.75	0.88	0.93	0.90	1.00	0.67	0.95	1.00	0.93	0.92	0.86	0.80	0.95	0.91	0.94	1.07	0.99	0.96	0.83	0.94	0.88	1.07	1.02	0.73		
Total	96.29	100.12	100.30	100.35	99.46	100.32	100.55	100.98	100.60	100.21	101.30	100.23	100.50	101.20	101.01	100.33	100.47	99.70	99.60	100.26	99.38	99.77	100.44	101.43	101.03	101.91		
=O=F	0.85	0.91	1.00	0.88	0.83	0.86	0.78	1.08	0.83	0.77	0.86	0.85	0.91	0.96	0.83	0.85	0.83	0.70	0.77	0.81	0.90	0.82	0.88	0.73	0.77	1.04		
=O=Cl	0.00	0.00	0.00	0.00	0.00	0.00	0.00	0.00	0.00	0.00	0.00	0.00	0.00	0.00	0.00	0.00	0.00	0.00	0.00	0.00	0.00	0.00	0.00	0.00	0.00	0.00		
Total	95.44	99.21	99.30	99.47	98.64	99.45	99.76	99.89	99.77	99.44	100.44	99.38	99.59	100.24	100.18	99.47	99.64	99.00	98.83	99.45	98.48	98.95	99.56	100.69	100.26	100.87		
Si	8.621	8.292	8.334	8.420	8.339	8.319	8.132	8.107	8.139	8.106	8.007	8.165	8.165	8.122	8.056	8.239	8.111	8.240	8.129	8.107	8.108	8.188	8.169	8.097	8.036	8.094		
^{IV}Al	0.000	0.000	0.000	0.000	0.000	0.000	0.000	0.000	0.000	0.000	0.000	0.000	0.000	0.000	0.000	0.000	0.000	0.000	0.000	0.000	0.000	0.000	0.000	0.000	0.000	0.000		
Σ Tetrahedral	8.621	8.292	8.334	8.420	8.339	8.319	8.132	8.107	8.139	8.106	8.007	8.165	8.165	8.122	8.056	8.239	8.111	8.240	8.129	8.107	8.108	8.188	8.169	8.097	8.036	8.094		
^{VI}Al	0.044	0.044	0.030	0.039	0.038	0.039	0.043	0.052	0.054	0.064	0.063	0.041	0.043	0.030	0.067	0.033	0.033	0.039	0.055	0.032	0.029	0.049	0.027	0.077	0.091	0.077		
Ti	0.120	0.104	0.048	0.060	0.052	0.066	0.095	0.165	0.150	0.208	0.301	0.090	0.087	0.046	0.277	0.061	0.056	0.097	0.121	0.100	0.029	0.114	0.022	0.135	0.159	0.116		
Fe^{3+}	0.000	0.187	0.330	0.000	0.104	0.257	0.658	0.662	0.547	0.237	0.495	0.648	0.653	0.835	0.495	0.465	0.834	0.244	0.509	0.779	0.943	0.508	0.822	0.538	0.562	0.644		
Fe^{2+}	3.825	3.990	3.593	3.984	3.936	3.754	3.523	3.533	3.643	3.683	3.676	3.473	3.442	3.368	3.493	3.704	3.372	3.996	3.614	3.219	3.015	3.586	3.175	3.804	3.738	3.663		
Mg	0.043	0.005	0.004	0.088	0.105	0.045	0.015	0.013	0.008	0.010	0.020	0.007	0.007	0.007	0.010	0.006	0.004	0.034	0.013	0.017	0.021	0.009	0.018	0.042	0.121	0.072		
Mn	0.185	0.189	0.280	0.206	0.194	0.216	0.192	0.110	0.145	0.206	0.102	0.189	0.204	0.204	0.194	0.200	0.196	0.162	0.150	0.238	0.272	0.176	0.246	0.104	0.094	0.087		
Zn	0.092	0.117	0.196	0.143	0.143	0.153	0.136	0.056	0.082	0.129	0.047	0.122	0.145	0.145	0.148	0.144	0.138	0.128	0.128	0.252	0.320	0.185	0.278	0.040	0.033	0.028		
Cr	0.000	0.000	0.000	0.000	0.000	0.000	0.000	0.000	0.000	0.000	0.000	0.000	0.000	0.000	0.000	0.000	0.000	0.000	0.000	0.000	0.000	0.000	0.000	0.002	0.001	0.000		
V	0.000	0.000	0.000	0.000	0.000	0.000	0.000	0.000	0.000	0.000	0.000	0.000	0.000	0.000	0.000	0.000	0.000	0.000	0.000	0.000	0.000	0.000	0.000	0.000	0.000	0.001		
Zr	0.002	0.007	0.004	0.006	0.004	0.005	0.006	0.008	0.011	0.137	0.033	0.008	0.007	0.002	0.006	0.005	0.005	0.017	0.068	0.002	0.000	0.002	0.001	0.009	0.010	0.007		
Nb	0.002	0.001	0.000	0.002	0.001	0.000	0.001	0.001	0.002	0.000	0.002	0.003	0.001	0.000	0.000	0.001	0.002	0.001	0.000	0.000	0.000	0.000	0.000	0.000	0.000	0.000		
Y	0.000	0.000	0.000	0.000	0.000	0.000	0.000	0.000	0.000	0.000	0.000	0.000	0.000	0.000	0.000	0.000	0.000	0.000	0.000	0.000	0.000	0.000	0.000	0.000	0.000	0.000		
Yb	0.000	0.000	0.000	0.000	0.000	0.000	0.000	0.000	0.000	0.000	0.000	0.000	0.000	0.000	0.000	0.000	0.000	0.000	0.000	0.000	0.000	0.000	0.000	0.000	0.000	0.000		
Σ Octahedral	4.313	4.644	4.486	4.529	4.576	4.536	4.668	4.602	4.641	4.674	4.737	4.580	4.590	4.637	4.691	4.618	4.639	4.719	4.657	4.638	4.628	4.630	4.590	4.751	4.810	4.694		
Na	2.293	2.563	2.573	2.435	2.392	2.522	2.678	2.849	2.848	2.799	2.849	2.762	2.754	2.615	2.854	2.551	2.654	2.530	2.775	2.624	2.632	2.719	2.653	2.824	2.816	2.868		
K	0.466	0.478	0.562	0.516	0.542	0.553	0.493	0.430	0.359	0.405	0.395	0.462	0.465	0.590	0.387	0.557	0.562	0.464	0.423	0.605	0.615	0.448	0.582	0.275	0.250	0.289		
Ca	0.242	0.023	0.043	0.094	0.151	0.071	0.029	0.013	0.014	0.015	0.011	0.032	0.026	0.036	0.011	0.036	0.035	0.047	0.017	0.026	0.018	0.015	0.006	0.053	0.088	0.056		
Σ Alkalis	3.001	3.064	3.179	3.045	3.085	3.146	3.199	3.292	3.220	3.219	3.256	3.255	3.245	3.241	3.252	3.144	3.250	3.041	3.215	3.255	3.264	3.182	3.240	3.152	3.154	3.212		
F	1.074	1.101	1.199	1.062	1.001	1.038	0.938	1.293	0.993	0.931	1.019	1.021	1.088	1.145	0.991	1.029	0.999	0.852	0.935	0.971	1.101	0.987	1.059	0.866	0.915	1.231		
Cl	0.000	0.000	0.000	0.000	0.000	0.000	0.000	0.000	0.000	0.000	0.000	0.000	0.000	0.000	0.000	0.000	0.000	0.000	0.000	0.000	0.000	0.000	0.000	0.004	0.004	0.005		
OH	0.926	0.899	0.801	0.938	0.999	0.962	1.062	0.707	1.007	1.069	0.981	0.979	0.912	0.855	1.009	0.971	1.001	1.148	1.065	1.029	0.899	1.013	0.941	1.130	1.080	0.765		
Σ OH,F,Cl	2.000	2.000	2.000	2.000	2.000	2.000	2.000	2.000	2.000	2.000	2.000	2.000	2.000	2.000	2.000	2.000	2.000	2.000	2.000	2.000	2.000	2.000	2.000	2.000	2.000	2.000		

Acronyms used are: ed=edge; lt=light; lter=lighter; dk=darker; dkmd=dark; nr=near; md=middle; 2nd=second; gr=grain; alt=altered

Mineral formulae were calculated based on 23 atoms of oxygen and 16 cations, with Fe^{3+} calculated by the method of Droop (1987)

Appendix B-1: Electron microprobe analyses of arfvedsonitic amphibole

Unit	Subsolvus - Drill Core																										
Sample #	SL-182-84.96											SL-182-86.50															
Description	edbl	gr	blmid	2		2aded	mid	ed	3 mid	ed	2ndcore	86 dked	lter	eddker	lter	ed		lt	dker	med		lt	dker	lt	ed	
File	1/1/95	1/1/95	1/1/95	1/1/95	1/1/95	1/1/95	1/1/95	1/1/95	1/1/95	1/1/95	1/1/95	kp	kp	kp	kp	kp	kp	kp	kp	kp	kp	kp	kp	kp	kp	kp	kp
Analysis #	56	57	58	59	62	63	64	65	67	68	69	129	130	131	132	133	134	135	136	137	138	139	140	141	142	143	
Na_2O	9.40	9.45	9.18	9.14	8.66	8.88	9.15	9.14	8.61	8.95	9.16	9.53	9.46	9.16	9.14	9.13	9.41	9.07	8.90	9.34	8.94	9.07	9.30	9.27	9.25	9.29	
K_2O	1.48	1.24	1.36	1.65	2.16	2.06	1.40	1.66	2.58	2.05	2.09	1.82	1.36	2.55	1.08	1.23	1.35	1.07	2.54	1.39	1.29	1.23	1.66	1.21	1.32	1.48	
CaO	0.26	0.58	0.23	0.24	0.16	0.13	0.40	0.13	0.19	0.06	0.10	0.11	0.36	0.00	1.27	1.03	0.34	1.54	0.00	0.41	0.66	0.93	0.25	0.69	0.72	0.26	
FeO	27.50	27.69	28.19	27.17	27.33	27.39	28.04	27.22	26.13	27.20	26.65	27.17	28.04	24.43	27.32	27.26	27.20	26.69	24.96	27.16	28.54	27.27	26.36	26.81	26.11	27.94	
Fe_2O_3	5.44	4.32	4.76	4.40	4.03	4.09	3.51	3.76	6.31	3.88	4.98	4.02	4.36	6.86	6.32	6.09	6.26	7.27	8.19	5.19	4.89	6.57	7.39	7.32	7.01	4.41	
MgO	0.17	0.43	0.32	0.05	0.06	0.06	0.07	0.05	0.05	0.06	0.08	0.09	0.09	0.19	0.13	0.14	0.27	0.24	0.28	0.13	0.18	0.17	0.23	0.19	0.18	0.06	
MnO	0.78	0.76	0.65	1.20	1.51	1.22	1.19	1.19	1.26	1.30	1.22	0.80	0.68	1.29	0.67	0.67	0.64	0.67	1.00	0.90	0.74	0.68	0.65	0.68	0.74	0.67	
ZnO	0.41	0.31	0.24	1.24	1.65	1.10	1.28	1.55	1.25	1.33	0.95	0.40	0.28	0.74	0.26	0.27	0.20	0.22	0.39	0.35	0.28	0.22	0.20	0.25	0.25	0.29	
Cr_2O_3	0.00	0.01	0.00	0.00	0.00	0.01	0.01	0.00	0.00	0.00	0.00	0.00	0.00	0.00	0.00	0.00	0.01	0.00	0.00	0.00	0.00	0.00	0.00	0.00	0.00	0.00	
V_2O_3	0.02	0.00	0.00	0.03	0.01	0.00	0.01	0.00	0.04	0.00	0.01	0.01	0.01	0.01	0.00	0.01	0.00	0.01	0.00	0.01	0.00	0.00	0.00	0.01	0.01	0.01	
ZrO_2	0.15	0.14	0.14	0.14	0.13	0.06	0.12	0.13	0.01	0.13	0.10	0.09	0.24	0.01	0.09	0.10	0.07	0.08	0.03	0.23	0.08	0.07	0.05	0.05	0.11	0.26	
Nb_2O_5	0.00	0.00	0.00	0.00	0.00	0.00	0.00	0.00	0.00	0.00	0.00	0.00	0.00	0.00	0.00	0.00	0.00	0.00	0.00	0.00	0.00	0.00	0.00	0.00	0.00	0.00	
Y_2O_3	0.00	0.00	0.00	0.00	0.00	0.00	0.00	0.00	0.00	0.00	0.00	0.00	0.00	0.00	0.00	0.00	0.00	0.00	0.00	0.00	0.00	0.00	0.00	0.00	0.00	0.00	
Yb_2O_3	0.00	0.00	0.00	0.00	0.00	0.00	0.00	0.00	0.00	0.00	0.00	0.01	0.00	0.00	0.03	0.01	0.00	0.00	0.00	0.01	0.01	0.02	0.01	0.00	0.04	0.00	
TiO_2	1.09	1.21	0.95	1.24	0.98	0.94	1.09	1.08	0.64	1.48	0.99	1.67	1.26	0.37	0.80	0.81	0.77	0.72	0.22	1.22	0.77	0.76	0.80	0.85	0.82	1.56	
SiO_2	51.18	51.46	50.90	51.06	51.32	51.40	51.50	51.40	51.01	51.16	51.64	51.62	51.22	51.52	50.14	50.20	50.81	49.76	50.70	50.60	50.47	49.96	50.43	49.98	49.75	50.51	
Al_2O_3	0.38	0.44	0.38	0.42	0.27	0.23	0.43	0.35	0.15	0.30	0.24	0.28	0.42	0.22	0.69	0.75	1.12	0.92	0.20	0.41	0.72	0.75	0.70	0.73	0.81	0.35	
F	2.28	2.32	2.55	2.01	1.61	1.91	1.72	1.83	1.78	1.94	2.24	2.09	2.01	2.49	2.12	2.15	1.69	2.22	2.15	2.06	1.78	2.04	1.68	1.84	1.98	1.97	
Cl	0.01	0.02	0.02	0.01	0.01	0.01	0.02	0.02	0.01	0.02	0.00	0.01	0.01	0.01	0.02	0.02	0.01	0.02	0.00	0.01	0.01	0.02	0.00	0.02	0.02	0.01	
H_2O	0.81	0.79	0.67	0.93	1.12	0.97	1.07	1.01	1.04	0.96	0.83	0.90	0.93	0.70	0.88	0.86	1.10	0.83	0.86	0.90	1.03	0.91	1.10	1.01	0.93	0.94	
Total	101.35	101.16	100.72	100.94	101.00	100.45	101.00	100.53	101.04	100.80	101.27	100.61	100.73	100.53	100.95	100.73	101.24	101.34	100.39	100.33	100.38	100.68	100.81	100.90	100.03	100.01	
=O=F	0.96	0.98	1.07	0.85	0.68	0.80	0.72	0.77	0.75	0.82	0.94	0.88	0.85	1.05	0.89	0.90	0.71	0.93	0.91	0.87	0.75	0.86	0.71	0.78	0.83	0.83	
=O=Cl	0.00	0.00	0.00	0.00	0.00	0.00	0.00	0.00	0.00	0.00	0.00	0.00	0.00	0.00	0.00	0.00	0.00	0.01	0.00	0.00	0.00	0.00	0.00	0.00	0.00	0.00	
Total	100.39	100.18	99.64	100.09	100.32	99.64	100.27	99.75	100.29	99.98	100.33	99.73	99.88	99.49	100.06	99.82	100.53	100.40	99.49	99.46	99.63	99.82	100.11	100.12	99.20	99.18	
Si	8.089	8.119	8.109	8.112	8.160	8.198	8.158	8.183	8.118	8.141	8.171	8.175	8.123	8.195	7.972	7.993	8.000	7.890	8.097	8.071	8.054	7.965	7.991	7.939	7.962	8.085	
^{IV}Al	0.000	0.000	0.000	0.000	0.000	0.000	0.000	0.000	0.000	0.000	0.000	0.000	0.000	0.000	0.028	0.007	0.000	0.110	0.000	0.000	0.000	0.035	0.009	0.061	0.038	0.000	
Σ Tetrahedral	8.089	8.119	8.109	8.112	8.160	8.198	8.158	8.183	8.118	8.141	8.171	8.175	8.123	8.195	8.000	8.000	8.000	8.000	8.097	8.071	8.054	8.000	8.000	8.000	8.000	8.085	
^{VI}Al	0.071	0.082	0.071	0.078	0.051	0.042	0.080	0.066	0.028	0.057	0.045	0.052	0.079	0.041	0.101	0.133	0.208	0.062	0.037	0.077	0.136	0.106	0.123	0.076	0.116	0.065	
Ti	0.130	0.144	0.114	0.149	0.117	0.113	0.129	0.129	0.077	0.177	0.118	0.199	0.150	0.044	0.096	0.097	0.091	0.086	0.026	0.147	0.092	0.091	0.095	0.101	0.098	0.188	
Fe^{3+}	0.646	0.513	0.571	0.526	0.482	0.491	0.418	0.450	0.755	0.465	0.593	0.479	0.521	0.821	0.757	0.730	0.742	0.867	0.984	0.623	0.587	0.789	0.882	0.875	0.844	0.531	
Fe^{2+}	3.635	3.654	3.783	3.610	3.634	3.654	3.715	3.624	3.478	3.620	3.526	3.599	3.719	3.249	3.633	3.631	3.581	3.539	3.334	3.624	3.810	3.636	3.494	3.562	3.495	3.739	
Mg	0.040	0.100	0.075	0.013	0.013	0.014	0.017	0.013	0.012	0.014	0.018	0.021	0.020	0.044	0.032	0.034	0.063	0.056	0.067	0.032	0.042	0.040	0.054	0.045	0.043	0.015	
Mn	0.104	0.102	0.087	0.162	0.204	0.164	0.160	0.161	0.169	0.175	0.163	0.108	0.092	0.173	0.090	0.091	0.086	0.090	0.135	0.121	0.099	0.092	0.087	0.091	0.100	0.091	
Zn	0.047	0.036	0.028	0.146	0.194	0.129	0.150	0.183	0.146	0.156	0.111	0.046	0.032	0.087	0.030	0.032	0.023	0.026	0.046	0.042	0.033	0.026	0.024	0.029	0.030	0.034	
Cr	0.000	0.001	0.000	0.000	0.000	0.001	0.001	0.001	0.000	0.000	0.000	0.001	0.000	0.000	0.000	0.000	0.001	0.000	0.000	0.000	0.000	0.000	0.000	0.000	0.000	0.000	
V	0.002	0.000	0.000	0.003	0.001	0.000	0.001	0.000	0.004	0.000	0.001	0.001	0.001	0.001	0.000	0.001	0.000	0.001	0.000	0.001	0.000	0.000	0.000	0.001	0.001	0.001	
Zr	0.011	0.010	0.011	0.011	0.010	0.005	0.009	0.010	0.001	0.010	0.007	0.007	0.018	0.001	0.007	0.008	0.005	0.006	0.002	0.018	0.006	0.005	0.004	0.004	0.009	0.020	
Nb	0.000	0.000	0.000	0.000	0.000	0.000	0.000	0.000	0.000	0.000	0.000	0.000	0.000	0.000	0.000	0.000	0.000	0.000	0.000	0.000	0.000	0.000	0.000	0.000	0.000	0.000	
Y	0.000	0.000	0.000	0.000	0.000	0.000	0.000	0.000	0.000	0.000	0.000	0.000	0.000	0.000	0.000	0.000	0.000	0.000	0.000	0.000	0.000	0.000	0.000	0.000	0.000	0.000	
Yb	0.000	0.000	0.000	0.000	0.000	0.000	0.000	0.000	0.000	0.000	0.000	0.000	0.000	0.000	0.001	0.001	0.000	0.000	0.000	0.000	0.000	0.001	0.000	0.000	0.002	0.000	
Σ Octahedral	4.687	4.642	4.741	4.697	4.705	4.614	4.681	4.635	4.671	4.673	4.582	4.512	4.632	4.461	4.746	4.757	4.799	4.733	4.630	4.685	4.806	4.787	4.763	4.783	4.738	4.686	
Na	2.881	2.891	2.835	2.816	2.669	2.747	2.812	2.822	2.656	2.761	2.809	2.927	2.908	2.825	2.817	2.819	2.871	2.788	2.755	2.890	2.765	2.805	2.859	2.854	2.869	2.883	
K	0.299	0.250	0.275	0.334	0.438	0.419	0.282	0.338	0.523	0.415	0.422	0.367	0.275	0.518	0.220	0.250	0.271	0.217	0.518	0.284	0.262	0.249	0.336	0.246	0.269	0.302	
Ca	0.044	0.098	0.040	0.041	0.028	0.022	0.067	0.022	0.033	0.011	0.017	0.019	0.062	0.000	0.217	0.175	0.058	0.262	0.000	0.071	0.113	0.159	0.042	0.117	0.124	0.045	
Σ Alkali	3.224	3.240	3.150	3.191	3.135	3.188	3.161	3.182	3.211	3.187	3.247	3.313	3.245	3.343	3.254	3.243	3.201	3.267	3.272	3.244	3.140	3.213	3.237	3.217	3.262	3.229	
F	1.138	1.160	1.285	1.010	0.808	0.964	0.860	0.923	0.897	0.975	1.120	1.049	1.007	1.250	1.065	1.080	0.839	1.111	1.087	1.039	0.899	1.030	0.841	0.925	1.002	0.997	
Cl	0.003	0.005	0.004	0.003	0.003	0.003	0.006	0.004	0.003	0.004	0.001	0.002	0.003	0.001	0.005	0.005	0.002	0.006	0.001	0.002	0.003	0.005	0.001	0.004	0.004	0.002	
OH	0.859	0.836	0.711	0.987	1.189	1.034	1.134	1.073	1.100	1.021	0.879	0.950	0.990	0.749	0.930	0.915	1.159	0.883	0.912	0.959	1.098	0.966	1.159	1.071	0.994	1.000	
Σ OH,F,Cl	2.000	2.000	2.000	2.000	2.000	2.000	2.000	2.000	2.000	2.000	2.000	2.000	2.000	2.000	2.000	2.000	2.000	2.000	2.000	2.000	2.000	2.000	2.000	2.000	2.000	2.000	

Acronyms used are: edmedge; ltxlight; lterxlighter; dkersdarker; dkxdark; nrxnear; mdxmiddle; 2ndxsecond; grxgrain; altxaltered
Mineral formulae were calculated based on 23 atoms of oxygen and 16 cations, with Fe^{3+} calculated by the method of Droop (1987)

Appendix B-1. Electron microprobe analyses of arfvedsonitic amphibole

Unit	Suhsolvus - Drill Core																	
Sample #	SL-182-86.50		SL-182-86.76															
Description		ed	8676 gr	ledgr	gred	mid	bl				2 ed		3	2ndgr	mid	4		
File	kp	kp	1/1/95	1/1/95	1/1/95	1/1/95	1/1/95	1/1/95	1/1/95	1/1/95	1/1/95	1/1/95	1/1/95	1/1/95	1/1/95	1/1/95	1/1/95	1/1/95
Analysis #	144	145	35	36	37	38	39	40	41	42	43	47	48	49	50	51	52	
Na_2O	9.33	9.44	9.25	9.34	9.11	9.20	9.21	9.37	9.26	9.48	8.35	8.85	9.14	8.58	9.21	9.17	8.92	
K_2O	1.51	1.49	1.40	1.19	1.71	1.40	1.53	1.41	1.28	1.28	2.74	2.20	1.70	2.76	1.72	1.42	1.56	
CaO	0.28	0.29	0.34	0.22	0.17	0.20	0.10	0.15	0.20	0.18	0.23	0.14	0.17	0.23	0.25	0.42	0.29	
FeO	27.55	26.88	28.14	28.62	28.42	28.41	28.32	28.72	29.59	28.23	26.05	27.59	27.21	25.99	27.31	27.91	28.88	
Fe_2O_3	5.63	6.22	4.79	4.19	2.95	5.39	5.70	5.24	4.35	5.18	4.84	4.02	4.21	5.68	3.63	4.26	2.54	
MgO	0.06	0.07	0.23	0.44	0.09	0.40	0.10	0.10	0.11	0.14	0.08	0.06	0.05	0.05	0.07	0.14	0.08	
MnO	0.66	0.65	0.76	0.66	0.95	0.65	0.58	0.56	0.55	0.68	1.64	1.22	1.14	1.20	1.13	0.93	1.12	
ZnO	0.24	0.27	0.38	0.16	0.75	0.23	0.24	0.23	0.16	0.33	1.74	1.09	1.18	1.23	1.24	0.52	1.11	
Cr_2O_3	0.00	0.00	0.00	0.00	0.00	0.00	0.01	0.00	0.01	0.00	0.00	0.02	0.01	0.00	0.01	0.00	0.02	
V_2O_3	0.01	0.01	0.00	0.00	0.01	0.00	0.00	0.00	0.02	0.00	0.00	0.00	0.02	0.00	0.00	0.01	0.00	
ZrO_2	0.26	0.27	0.16	0.66	0.16	0.07	0.13	0.17	0.11	0.11	0.00	0.09	0.15	0.03	0.12	0.18	0.14	
Nb_2O_5	0.00	0.00	0.00	0.00	0.00	0.00	0.00	0.00	0.00	0.00	0.00	0.00	0.00	0.00	0.00	0.00	0.00	
Y_2O_3	0.00	0.00	0.00	0.00	0.00	0.00	0.00	0.00	0.00	0.00	0.00	0.00	0.00	0.00	0.00	0.00	0.00	
Yb_2O_3	0.01	0.01	0.00	0.00	0.00	0.00	0.00	0.00	0.00	0.00	0.00	0.00	0.00	0.00	0.00	0.00	0.00	
TiO_2	1.54	1.56	1.11	1.26	1.28	0.95	0.67	0.82	0.84	0.71	0.58	0.92	0.58	0.69	1.20	1.26	1.06	
SiO_2	50.35	50.19	51.07	50.87	51.53	51.13	51.07	51.50	51.53	51.60	51.24	51.74	51.55	51.19	51.61	50.78	51.54	
Al_2O_3	0.35	0.36	0.41	0.40	0.32	0.35	0.35	0.38	0.43	0.40	0.17	0.20	0.34	0.16	0.36	0.43	0.34	
F	1.90	1.93	1.97	2.42	2.38	2.11	2.55	1.96	2.23	2.45	2.01	2.12	1.80	1.86	1.93	1.67	1.68	
Cl	0.01	0.01	0.01	0.02	0.01	0.01	0.01	0.01	0.01	0.02	0.01	0.01	0.01	0.00	0.02	0.02	0.01	
H_2O	0.98	0.97	0.96	0.74	0.75	0.89	0.67	0.97	0.84	0.73	0.92	0.88	1.01	1.00	0.97	1.08	1.08	
Total	100.66	100.59	100.97	101.18	100.59	101.39	101.25	101.58	101.52	101.52	100.59	101.14	100.26	100.62	100.77	100.20	100.36	
=O=F	0.80	0.81	0.83	1.02	1.00	0.89	1.07	0.82	0.94	1.03	0.85	0.89	0.76	0.78	0.81	0.70	0.71	
=O=Cl	0.00	0.00	0.00	0.00	0.00	0.00	0.00	0.00	0.00	0.00	0.00	0.00	0.00	0.00	0.00	0.00	0.00	
Total	99.86	99.78	100.14	100.16	99.59	100.50	100.18	100.75	100.58	100.49	99.74	100.25	99.50	99.84	99.95	99.49	99.66	
Si	8.018	7.995	8.094	8.067	8.207	8.079	8.109	8.117	8.138	8.141	8.197	8.208	8.217	8.166	8.187	8.101	8.215	
^{IV}Al	0.000	0.005	0.000	0.000	0.000	0.000	0.000	0.000	0.000	0.000	0.000	0.000	0.000	0.000	0.000	0.000	0.000	
Σ Tetrahedral	8.018	8.000	8.094	8.067	8.207	8.079	8.109	8.117	8.138	8.141	8.197	8.208	8.217	8.166	8.187	8.101	8.215	
^{VI}Al	0.065	0.062	0.077	0.076	0.060	0.065	0.066	0.071	0.080	0.075	0.031	0.037	0.064	0.029	0.066	0.081	0.063	
Ti	0.185	0.187	0.132	0.150	0.153	0.113	0.080	0.097	0.100	0.084	0.070	0.109	0.070	0.083	0.143	0.151	0.127	
Fe^{3+}	0.675	0.745	0.572	0.500	0.354	0.641	0.682	0.622	0.517	0.615	0.583	0.480	0.505	0.682	0.434	0.511	0.305	
Fe^{2+}	3.669	3.581	3.730	3.796	3.786	3.755	3.761	3.786	3.909	3.726	3.485	3.660	3.628	3.468	3.623	3.724	3.850	
Mg	0.014	0.016	0.054	0.103	0.022	0.094	0.022	0.023	0.027	0.034	0.020	0.013	0.012	0.011	0.017	0.033	0.020	
Mn	0.090	0.087	0.101	0.089	0.128	0.086	0.078	0.074	0.074	0.091	0.222	0.164	0.153	0.161	0.152	0.126	0.151	
Zn	0.028	0.031	0.044	0.019	0.088	0.027	0.028	0.027	0.019	0.019	0.205	0.127	0.138	0.144	0.145	0.061	0.131	
Cr	0.000	0.000	0.000	0.000	0.000	0.000	0.001	0.000	0.001	0.000	0.000	0.002	0.001	0.000	0.001	0.000	0.002	
V	0.001	0.001	0.000	0.000	0.001	0.000	0.000	0.000	0.002	0.000	0.000	0.000	0.002	0.000	0.000	0.001	0.000	
Zr	0.020	0.021	0.012	0.051	0.012	0.005	0.010	0.013	0.008	0.009	0.000	0.007	0.011	0.002	0.009	0.014	0.010	
Nb	0.000	0.000	0.000	0.000	0.000	0.000	0.000	0.000	0.000	0.000	0.000	0.000	0.000	0.000	0.000	0.000	0.000	
Y	0.000	0.000	0.000	0.000	0.000	0.000	0.000	0.000	0.000	0.000	0.000	0.000	0.000	0.000	0.000	0.000	0.000	
Yb	0.000	0.000	0.000	0.000	0.000	0.000	0.000	0.000	0.000	0.000	0.000	0.000	0.000	0.000	0.000	0.000	0.000	
Σ Octahedral	4.748	4.732	4.723	4.784	4.605	4.787	4.728	4.712	4.736	4.672	4.616	4.600	4.585	4.581	4.590	4.702	4.659	
Na	2.881	2.916	2.842	2.871	2.813	2.818	2.836	2.862	2.835	2.900	2.590	2.723	2.823	2.652	2.833	2.836	2.758	
K	0.307	0.303	0.283	0.240	0.346	0.282	0.311	0.283	0.257	0.258	0.559	0.445	0.346	0.562	0.347	0.289	0.318	
Ca	0.047	0.049	0.058	0.038	0.029	0.034	0.017	0.026	0.033	0.030	0.019	0.024	0.028	0.038	0.042	0.072	0.049	
Σ Alkalis	3.234	3.268	3.183	3.150	3.188	3.134	3.163	3.171	3.126	3.187	3.187	3.192	3.198	3.252	3.223	3.197	3.125	
F	0.958	0.970	0.986	1.213	1.198	1.056	1.282	0.976	1.114	1.224	1.018	1.065	0.905	0.938	0.968	0.845	0.844	
Cl	0.002	0.001	0.003	0.005	0.002	0.002	0.003	0.002	0.003	0.005	0.002	0.001	0.001	0.004	0.004	0.005	0.004	
OH	1.040	1.028	1.011	0.783	0.799	0.942	0.715	1.022	0.883	0.771	0.979	0.934	1.094	1.061	1.028	1.150	1.152	
Σ OH,F,Cl	2.000	2.000	2.000	2.000	2.000	2.000	2.000	2.000	2.000	2.000	2.000	2.000	2.000	2.000	2.000	2.000	2.000	

Acronyms used are: edsedge; ltslight; dkdark; nrnnear; mdsmiddle; 2ndzoncond; grngrain; altsaltered
Mineral formulae were calculated based on 23 atoms of oxygen and 16 cations, with Fe^{3+} calculated

Appendix B-1: Electron microprobe analyses of arfvedsonitic amphibole

Unit	Lindinosite																								
Sample #	SL-BS-1																								
Description	SLBS1	mid	dk	mid	ed	gr#2	mid	mid	ed	ed								#3ed	bs 1ed	mid	mid	ed	2 ed	mid	ed	3 ed	mid
File	am92	am92	am92	am92	am92	am92	am92	am92	am92	am92	am92	am92	am92	am92	am92	am92	am92	am92	kp	kp	kp	kp	kp	kp	kp	kp	kp
Analysis #	1	2	3	4	5	6	7	8	10	11	12	13	14	15	16	17	18	19	52	53	54	55	56	57	58	59	60
Na_2O	8.37	8.61	8.76	8.64	8.66	8.42	8.19	8.19	7.93	8.38	8.30	8.63	8.56	8.46	8.52	8.33	8.66	8.32	9.20	9.12	9.43	9.13	9.36	9.34	9.13	9.50	9.31
K_2O	2.84	2.60	2.61	2.80	2.93	2.82	2.89	2.90	3.08	2.75	2.88	2.61	2.76	3.07	2.63	2.85	2.07	3.08	2.73	2.32	2.31	2.21	2.29	2.35	2.39	2.39	2.28
CaO	0.07	0.06	0.07	0.06	0.12	0.06	0.02	0.05	0.07	0.27	0.06	0.07	0.08	0.12	0.05	0.04	0.04	0.06	0.07	0.13	0.05	0.05	0.04	0.04	0.06	0.06	0.05
FeO	24.10	23.33	21.60	23.30	22.19	23.34	25.02	24.83	25.39	23.68	24.01	23.78	23.67	22.85	24.21	24.35	24.95	23.47	24.06	24.65	23.83	24.97	24.63	24.39	24.89	23.87	25.15
Fe_2O_3	6.50	7.95	9.82	8.24	8.67	8.01	6.29	6.16	5.10	7.31	6.84	7.55	7.39	9.14	7.56	7.46	6.42	7.94	7.42	6.92	8.03	6.29	7.32	7.32	6.23	7.30	6.28
MgO	0.00	0.00	0.06	0.01	0.00	0.02	0.00	0.02	0.02	0.40	0.00	0.00	0.01	0.03	0.00	0.01	0.00	0.01	0.01	0.21	0.02	0.00	0.01	0.00	0.06	0.01	0.01
MnO	1.61	1.81	1.89	1.84	1.51	1.86	1.72	1.75	1.84	1.98	1.75	1.80	1.86	1.55	1.96	1.95	1.73	1.50	1.37	1.93	1.95	1.96	1.98	1.90	1.72	1.63	1.78
ZnO	1.47	1.22	1.12	1.06	1.54	1.17	1.23	1.39	1.53	1.06	1.21	1.12	1.44	1.46	1.14	1.07	1.26	1.46	1.32	0.93	0.89	0.91	0.91	0.86	1.13	1.12	0.89
Cr_2O_3	0.00	0.00	0.00	0.00	0.00	0.00	0.00	0.00	0.00	0.00	0.00	0.00	0.00	0.00	0.00	0.00	0.00	0.00	0.00	0.00	0.00	0.00	0.01	0.00	0.01	0.00	0.00
V_2O_3	0.00	0.00	0.00	0.00	0.00	0.00	0.00	0.00	0.00	0.00	0.00	0.00	0.00	0.00	0.00	0.00	0.00	0.00	0.06	0.06	0.00	0.00	0.02	0.00	0.03	0.00	0.02
ZrO_2	0.19	0.01	0.02	0.02	0.01	0.00	0.03	0.01	0.02	0.02	0.14	0.08	0.01	0.00	0.03	0.05	0.04	0.04	0.00	0.04	0.09	0.00	0.12	0.13	0.23	0.19	0.22
Nb_2O_5	0.04	0.03	0.09	0.04	0.02	0.10	0.06	0.12	0.07	0.08	0.05	0.09	0.04	0.03	0.03	0.07	0.08	0.06	0.05	0.04	0.04	0.04	0.03	0.03	0.03	0.01	0.05
Y_2O_3	0.00	0.00	0.00	0.00	0.00	0.00	0.00	0.00	0.00	0.00	0.00	0.00	0.00	0.00	0.00	0.00	0.00	0.00	0.00	0.00	0.00	0.00	0.00	0.00	0.00	0.00	0.00
Yb_2O_3	0.00	0.00	0.00	0.00	0.00	0.00	0.00	0.00	0.00	0.00	0.00	0.00	0.00	0.00	0.00	0.00	0.00	0.00	0.00	0.01	0.00	0.00	0.01	0.00	0.02	0.00	0.00
TiO_2	0.53	0.42	0.37	0.45	0.32	0.38	0.42	0.37	0.30	0.35	0.48	0.58	0.32	0.43	0.43	0.47	0.36	0.30	0.39	0.37	0.42	0.63	0.42	0.44	0.51	0.66	0.47
SiO_2	49.64	49.44	48.74	49.85	49.63	49.31	49.85	49.92	50.14	49.97	49.39	49.63	50.16	49.60	49.86	49.71	49.64	49.63	51.97	51.65	51.67	51.24	51.99	51.79	51.62	51.86	51.98
Al_2O_3	0.15	0.16	0.16	0.16	0.14	0.17	0.14	0.16	0.16	0.15	0.18	0.14	0.15	0.14	0.16	0.17	0.15	0.14	0.13	0.15	0.15	0.16	0.15	0.16	0.14	0.17	0.16
F	1.92	1.99	2.07	1.89	1.80	1.90	1.98	2.06	2.03	1.95	1.86	1.79	1.81	1.68	1.82	1.91	1.94	1.81	1.37	1.70	1.51	1.79	1.94	1.92	1.82	1.33	1.77
Cl	0.00	0.00	0.00	0.00	0.00	0.00	0.00	0.00	0.00	0.00	0.00	0.00	0.00	0.00	0.00	0.00	0.00	0.00	0.01	0.00	0.01	0.01	0.00	0.00	0.01	0.01	0.00
H_2O	0.92	0.89	0.85	0.96	0.99	0.93	0.90	0.86	0.87	0.93	0.94	0.99	0.99	1.06	0.99	0.94	0.91	0.98	1.25	1.09	1.19	1.03	0.99	0.99	1.03	1.28	1.06
Total	98.35	98.51	98.21	99.31	98.52	98.48	98.73	98.76	98.54	99.29	98.07	98.87	99.27	99.59	99.37	99.38	98.26	98.80	101.42	101.32	101.59	100.43	102.23	101.69	101.03	101.39	101.49
=O=F	0.81	0.84	0.87	0.80	0.76	0.80	0.83	0.87	0.85	0.82	0.78	0.75	0.76	0.71	0.77	0.81	0.82	0.76	0.58	0.71	0.63	0.75	0.82	0.81	0.76	0.56	0.75
=O=Cl	0.00	0.00	0.00	0.00	0.00	0.00	0.00	0.00	0.00	0.00	0.00	0.00	0.00	0.00	0.00	0.00	0.00	0.00	0.00	0.00	0.00	0.00	0.00	0.00	0.00	0.00	0.00
Total	97.54	97.68	97.34	98.52	97.76	97.68	97.89	97.89	97.68	98.46	97.29	98.11	98.51	98.89	98.60	98.58	97.44	98.04	100.84	100.60	100.96	99.67	101.41	100.88	100.27	100.83	100.74
Si	8.127	8.076	7.991	8.070	8.087	8.066	8.141	8.152	8.208	8.088	8.109	8.073	8.122	8.020	8.078	8.068	8.129	8.091	8.173	8.149	8.119	8.163	8.142	8.148	8.177	8.146	8.186
^{IV}Al	0.000	0.000	0.009	0.000	0.000	0.000	0.000	0.000	0.000	0.000	0.000	0.000	0.000	0.000	0.000	0.000	0.000	0.000	0.000	0.000	0.000	0.000	0.000	0.000	0.000	0.000	0.000
Σ Tetrahedral	8.127	8.076	8.000	8.070	8.087	8.066	8.141	8.152	8.208	8.088	8.109	8.073	8.122	8.020	8.078	8.068	8.129	8.091	8.173	8.149	8.119	8.163	8.142	8.148	8.177	8.146	8.186
^{VI}Al	0.029	0.031	0.023	0.031	0.026	0.033	0.026	0.030	0.031	0.029	0.034	0.028	0.029	0.026	0.031	0.032	0.030	0.027	0.025	0.029	0.028	0.030	0.027	0.029	0.026	0.031	0.030
Ti	0.065	0.052	0.045	0.054	0.039	0.046	0.051	0.045	0.036	0.043	0.059	0.071	0.039	0.052	0.052	0.058	0.044	0.037	0.046	0.044	0.050	0.076	0.050	0.053	0.060	0.078	0.055
Fe^{3+}	0.801	0.977	1.211	1.003	1.063	0.986	0.773	0.757	0.628	0.891	0.845	0.924	0.900	1.112	0.922	0.911	0.791	0.974	0.878	0.822	0.950	0.754	0.863	0.867	0.743	0.863	0.745
Fe^{2+}	3.300	3.186	2.962	3.155	3.024	3.193	3.418	3.391	3.476	3.206	3.296	3.235	3.206	3.090	3.280	3.305	3.417	3.200	3.165	3.252	3.132	3.327	3.226	3.209	3.297	3.136	3.312
Mg	0.000	0.000	0.014	0.002	0.000	0.005	0.000	0.004	0.004	0.096	0.000	0.000	0.002	0.007	0.000	0.002	0.000	0.002	0.001	0.049	0.004	0.000	0.002	0.001	0.014	0.002	0.002
Mn	0.223	0.250	0.263	0.252	0.208	0.257	0.238	0.242	0.255	0.271	0.243	0.248	0.256	0.212	0.269	0.269	0.240	0.207	0.183	0.258	0.260	0.264	0.262	0.253	0.231	0.217	0.238
Zn	0.178	0.147	0.135	0.127	0.186	0.141	0.148	0.168	0.185	0.127	0.146	0.135	0.172	0.175	0.136	0.129	0.152	0.176	0.153	0.108	0.104	0.107	0.105	0.100	0.132	0.130	0.103
Cr	0.000	0.000	0.000	0.000	0.000	0.000	0.000	0.000	0.000	0.000	0.000	0.000	0.000	0.000	0.000	0.000	0.000	0.000	0.000	0.000	0.000	0.000	0.001	0.000	0.001	0.000	0.000
V	0.000	0.000	0.000	0.000	0.000	0.000	0.000	0.000	0.000	0.000	0.000	0.000	0.000	0.000	0.000	0.000	0.000	0.000	0.006	0.007	0.000	0.000	0.002	0.000	0.003	0.000	0.002
Zr	0.015	0.001	0.001	0.001	0.000	0.000	0.002	0.001	0.001	0.002	0.011	0.007	0.001	0.000	0.002	0.004	0.003	0.003	0.000	0.003	0.007	0.000	0.009	0.010	0.018	0.015	0.017
Nb	0.002	0.001	0.004	0.002	0.001	0.005	0.003	0.005	0.003	0.003	0.002	0.004	0.002	0.001	0.001	0.003	0.004	0.002	0.002	0.002	0.002	0.002	0.001	0.001	0.001	0.001	0.002
Y	0.000	0.000	0.000	0.000	0.000	0.000	0.000	0.000	0.000	0.000	0.000	0.000	0.000	0.000	0.000	0.000	0.000	0.000	0.000	0.000	0.000	0.000	0.000	0.000	0.000	0.000	0.000
Yb	0.000	0.000	0.000	0.000	0.000	0.000	0.000	0.000	0.000	0.000	0.000	0.000	0.000	0.000	0.000	0.000	0.000	0.000	0.000	0.000	0.000	0.000	0.000	0.000	0.001	0.000	0.000
Σ Octahedral	4.612	4.646	4.658	4.628	4.548	4.666	4.659	4.642	4.620	4.668	4.636	4.651	4.607	4.675	4.694	4.712	4.682	4.629	4.460	4.574	4.536	4.560	4.551	4.523	4.527	4.472	4.507
Na	2.656	2.726	2.784	2.712	2.737	2.670	2.594	2.593	2.517	2.629	2.641	2.723	2.687	2.653	2.676	2.622	2.750	2.630	2.807	2.790	2.873	2.819	2.842	2.849	2.803	2.894	2.841
K	0.593	0.542	0.545	0.579	0.608	0.589	0.602	0.604	0.642	0.568	0.602	0.541	0.570	0.632	0.544	0.590	0.433	0.640	0.548	0.466	0.463	0.450	0.458	0.472	0.483	0.478	0.458
Ca	0.013	0.010	0.012	0.011	0.020	0.010	0.004	0.009	0.013	0.047	0.011	0.012	0.014	0.020	0.008	0.007	0.006	0.010	0.012	0.021	0.009	0.009	0.007	0.007	0.010	0.009	0.008
Σ Alkalis	3.262	3.279	3.342	3.302	3.365	3.268	3.200	3.206	3.172	3.243	3.255	3.276	3.272	3.305	3.228	3.219	3.189	3.280	3.367	3.277	3.345	3.277	3.307	3.329	3.296	3.382	3.307
F	0.992	1.027	1.075	0.967	0.927	0.981	1.022	1.062	1.049	0.999	0.965	0.922	0.925	0.857	0.932	0.982	1.004	0.933	0.682	0.846	0.748	0.900	0.959	0.955	0.910	0.658	0.882
Cl	0.000	0.000	0.000	0.000	0.000	0.000	0.000	0.000	0.000	0.000	0.000	0.000	0.000	0.000	0.000	0.000	0.000	0.000	0.003	0.001	0.001	0.004	0.001	0.001	0.002	0.003	0.001
OH	1.008	0.973	0.925	1.033	1.073	1.019	0.978	0.938	0.951	1.001	1.035	1.078	1.075	1.143	1.068	1.018	0.996	1.067	1.315	1.153	1.251	1.097	1.040	1.044	1.088	1.338	1.117
Σ OH,F,Cl	2.000	2.000	2.000	2.000	2.000	2.000	2.000	2.000	2.000	2.000	2.000	2.000	2.000	2.000	2.000	2.000	2.000	2.000	2.000	2.000	2.000	2.000	2.000	2.000	2.000	2.000	2.000

Acronyms used are: edsedge; litlight; literalighter; dkr=darker; dk=dark; nr=near; mi=middle; 2nd=second; gr=grain; alt=altered
Mineral formulae were calculated based on 23 atoms of oxygen and 16 cations, with Fe^{3+} calculated by the method of Droop (1987)

Appendix B-1. Electron microprobe analyses of arfvedsonitic amphibole

Unit	Lindinosite																					
Sample #	SL-BS-1						SL-BS-chip															
Description	ed	4 ed	mid	ed	5 ed	ed	BS-C	mid	ed	BS-C ed	mid	ed	ed	SLBS	mid	ed		#3ed				ed
File	kp	kp	kp	kp	kp	kp	am93	am93	am93	am93	am93	am93	am93	am93	am93	am93	am93	am93	am93	am93	am93	am93
Analysis #	61	62	63	64	65	66	36	37	38	46	47	48	58	59	60	61	62	63	64	65	66	
Na_2O	9.20	9.20	9.14	9.04	8.84	8.91	8.33	8.21	8.45	8.65	8.73	8.25	8.44	8.06	8.57	7.68	8.16	8.33	8.33	8.39	8.02	
K_2O	2.29	2.21	2.24	2.19	2.37	2.56	2.82	2.57	2.89	2.56	2.60	3.13	2.97	3.28	2.70	2.38	3.10	3.05	2.80	2.91	3.25	
CaO	0.06	0.05	0.05	0.05	0.03	0.10	0.15	0.14	0.13	0.21	0.09	0.10	0.05	0.17	0.13	0.57	0.16	0.12	0.08	0.05	0.14	
FeO	25.30	25.43	24.98	24.88	25.33	24.33	25.67	23.82	25.55	24.55	25.15	25.75	25.28	25.23	24.73	25.46	25.23	24.55	25.58	24.95	25.15	
Fe_2O_3	6.11	5.77	6.73	6.38	6.35	7.61	5.95	6.67	5.77	6.29	6.88	6.46	7.56	6.52	6.97	2.20	6.63	8.09	6.31	7.58	6.56	
MgO	0.04	0.00	0.00	0.10	0.00	0.00	0.12	0.11	0.00	0.22	0.00	0.00	0.00	0.00	0.00	1.48	0.05	0.01	0.00	0.00	0.53	
MnO	1.90	1.89	1.92	1.76	1.91	1.78	1.48	1.81	1.43	2.01	1.91	1.56	1.72	1.30	1.98	1.55	1.58	1.10	1.49	1.72	0.91	
ZnO	0.93	0.91	0.91	1.00	0.85	0.93	1.72	1.22	1.64	1.39	1.10	1.53	1.26	1.74	1.33	2.32	1.82	1.84	1.72	1.30	1.94	
Cr_2O_3	0.00	0.00	0.00	0.00	0.00	0.01	0.00	0.00	0.00	0.00	0.00	0.00	0.00	0.00	0.00	0.00	0.00	0.00	0.00	0.00	0.00	
V_2O_3	0.02	0.03	0.00	0.01	0.01	0.00	0.00	0.00	0.00	0.00	0.00	0.00	0.00	0.00	0.00	0.00	0.00	0.00	0.00	0.00	0.00	
ZrO_2	0.02	0.03	0.04	0.12	0.02	0.03	0.00	0.00	0.00	0.11	0.10	0.00	0.00	0.00	0.04	0.03	0.00	0.00	0.04	0.21	0.06	
Nb_2O_5	0.03	0.03	0.03	0.05	0.06	0.04	0.03	0.04	0.02	0.05	0.03	0.00	0.06	0.04	0.08	0.06	0.02	0.03	0.01	0.04	0.06	
Y_2O_3	0.00	0.00	0.00	0.00	0.00	0.00	0.00	0.00	0.00	0.00	0.00	0.00	0.00	0.00	0.00	0.00	0.00	0.00	0.00	0.00	0.00	
Yb_2O_3	0.00	0.01	0.00	0.00	0.00	0.01	0.00	0.00	0.00	0.00	0.00	0.00	0.00	0.00	0.00	0.00	0.00	0.00	0.00	0.00	0.00	
TiO_2	0.81	0.79	0.61	0.45	0.43	0.37	0.39	0.62	0.47	0.84	0.57	0.43	0.43	0.30	0.43	0.33	0.31	0.35	0.39	0.45	0.26	
SiO_2	51.76	51.64	51.31	50.98	50.91	50.88	50.98	48.21	51.18	50.63	50.98	51.15	50.93	50.60	50.71	50.48	50.84	50.30	50.68	50.33	50.84	
Al_2O_3	0.16	0.17	0.14	0.16	0.16	0.16	0.21	2.90	0.24	0.33	0.26	0.30	0.19	0.15	0.15	0.16	0.14	0.14	0.15	0.12	0.13	
F	1.78	1.56	1.59	1.48	1.69	1.61	1.91	1.69	1.86	1.93	2.04	1.83	1.83	1.81	1.97	1.63	1.80	1.99	2.05	2.05	1.75	
Cl	0.00	0.00	0.00	0.01	0.00	0.01	0.00	0.00	0.00	0.00	0.00	0.00	0.00	0.00	0.00	0.00	0.00	0.00	0.00	0.00	0.00	
H_2O	1.06	1.15	1.14	1.17	1.07	1.11	0.97	1.05	0.99	0.96	0.92	1.02	1.02	1.00	0.94	1.06	1.02	0.93	0.89	0.90	1.04	
Total	101.45	100.87	100.82	99.82	100.03	100.44	100.73	99.05	100.63	100.72	101.37	101.52	101.75	100.19	100.74	97.38	100.87	100.84	100.52	100.99	100.64	
=O=F	0.75	0.66	0.67	0.62	0.71	0.68	0.81	0.71	0.78	0.81	0.86	0.77	0.77	0.76	0.83	0.69	0.76	0.84	0.86	0.86	0.74	
=O=Cl	0.00	0.00	0.00	0.00	0.00	0.00	0.00	0.00	0.00	0.00	0.00	0.00	0.00	0.00	0.00	0.00	0.00	0.00	0.00	0.00	0.00	
Total	100.70	100.21	100.15	99.19	99.32	99.76	99.93	98.34	99.84	99.91	100.51	100.75	100.97	99.43	99.91	96.70	100.11	100.01	99.66	100.13	99.90	
Si	8.158	8.174	8.140	8.161	8.158	8.118	8.151	7.792	8.175	8.077	8.095	8.120	8.074	8.145	8.110	8.271	8.130	8.060	8.137	8.058	8.130	
^{IV}Al	0.000	0.000	0.000	0.000	0.000	0.000	0.000	0.208	0.000	0.000	0.000	0.000	0.000	0.000	0.000	0.000	0.000	0.000	0.000	0.000	0.000	
Σ Tetrahedral	8.158	8.174	8.140	8.161	8.158	8.118	8.151	8.000	8.175	8.077	8.095	8.120	8.074	8.145	8.110	8.271	8.130	8.060	8.137	8.058	8.130	
^{VI}Al	0.030	0.032	0.027	0.030	0.030	0.030	0.039	0.344	0.045	0.062	0.049	0.056	0.036	0.029	0.029	0.031	0.027	0.027	0.029	0.024	0.024	
Ti	0.096	0.094	0.072	0.054	0.052	0.044	0.047	0.075	0.057	0.101	0.068	0.052	0.051	0.036	0.051	0.041	0.038	0.042	0.047	0.054	0.031	
Fe^{3+}	0.725	0.687	0.803	0.769	0.766	0.913	0.716	0.811	0.694	0.756	0.821	0.772	0.902	0.790	0.839	0.271	0.798	0.976	0.762	0.913	0.789	
Fe^{2+}	3.335	3.367	3.315	3.331	3.395	3.246	3.452	3.221	3.414	3.275	3.340	3.419	3.352	3.397	3.308	3.488	3.374	3.290	3.434	3.341	3.363	
Mg	0.009	0.000	0.000	0.025	0.000	0.000	0.029	0.026	0.000	0.052	0.000	0.000	0.001	0.001	0.001	0.361	0.013	0.003	0.000	0.000	0.127	
Mn	0.254	0.253	0.258	0.239	0.260	0.240	0.201	0.248	0.193	0.271	0.257	0.210	0.230	0.177	0.269	0.215	0.214	0.150	0.202	0.233	0.124	
Zn	0.108	0.106	0.107	0.118	0.100	0.109	0.203	0.145	0.194	0.164	0.129	0.180	0.148	0.207	0.157	0.280	0.215	0.218	0.204	0.153	0.229	
Cr	0.000	0.000	0.000	0.000	0.000	0.001	0.000	0.000	0.000	0.000	0.000	0.000	0.000	0.000	0.000	0.000	0.000	0.000	0.000	0.000	0.000	
V	0.002	0.003	0.000	0.001	0.001	0.000	0.000	0.000	0.000	0.000	0.000	0.000	0.000	0.000	0.000	0.000	0.000	0.000	0.000	0.000	0.000	
Zr	0.001	0.002	0.003	0.009	0.002	0.002	0.000	0.000	0.000	0.009	0.008	0.000	0.000	0.000	0.003	0.002	0.000	0.000	0.003	0.016	0.005	
Nb	0.001	0.001	0.001	0.002	0.003	0.002	0.001	0.002	0.001	0.002	0.001	0.000	0.002	0.002	0.003	0.003	0.001	0.001	0.001	0.002	0.002	
Y	0.000	0.000	0.000	0.000	0.000	0.000	0.000	0.000	0.000	0.000	0.000	0.000	0.000	0.000	0.000	0.000	0.000	0.000	0.000	0.000	0.000	
Yb	0.000	0.000	0.000	0.000	0.000	0.001	0.000	0.000	0.000	0.000	0.000	0.000	0.000	0.000	0.000	0.000	0.000	0.000	0.000	0.000	0.000	
Σ Octahedral	4.561	4.548	4.587	4.577	4.609	4.588	4.668	4.873	4.598	4.691	4.674	4.689	4.722	4.638	4.661	4.692	4.678	4.707	4.682	4.735	4.695	
Na	2.811	2.823	2.812	2.806	2.745	2.756	2.581	2.574	2.617	2.675	2.689	2.538	2.594	2.514	2.656	2.440	2.531	2.588	2.593	2.603	2.488	
K	0.460	0.446	0.453	0.447	0.484	0.521	0.574	0.529	0.588	0.522	0.526	0.635	0.601	0.673	0.551	0.497	0.632	0.624	0.573	0.594	0.664	
Ca	0.010	0.008	0.008	0.009	0.005	0.017	0.026	0.024	0.022	0.035	0.016	0.018	0.009	0.029	0.023	0.101	0.028	0.020	0.014	0.009	0.023	
Σ Alkalis	3.281	3.278	3.273	3.262	3.234	3.294	3.181	3.127	3.227	3.232	3.231	3.190	3.204	3.216	3.229	3.038	3.191	3.232	3.181	3.207	3.175	
F	0.887	0.781	0.796	0.749	0.855	0.811	0.968	0.865	0.941	0.975	1.022	0.917	0.920	0.922	0.995	0.845	0.908	1.009	1.041	1.038	0.885	
Cl	0.001	0.000	0.000	0.002	0.000	0.003	0.000	0.000	0.000	0.000	0.000	0.000	0.000	0.000	0.000	0.000	0.000	0.000	0.000	0.000	0.000	
OH	1.112	1.219	1.204	1.249	1.145	1.186	1.032	1.135	1.059	1.025	0.978	1.083	1.080	1.078	1.005	1.155	1.092	0.991	0.959	0.962	1.115	
Σ OH,F,Cl	2.000	2.000	2.000	2.000	2.000	2.000	2.000	2.000	2.000	2.000	2.000	2.000	2.000	2.000	2.000	2.000	2.000	2.000	2.000	2.000	2.000	

Acronyms used are: ed=edge; lt=light; lter=lighter; dk=dark; dker=darker; dkst=dark; nr=near; mid=middle, 2nd=second; gr=grain; alt=altered
Mineral formulae were calculated based on 23 atoms of oxygen and 16 cations, with Fe^{3+} calculated by the method of Droop (1987)

Appendix B-2 Electron-microprobe analyses of aegirine

Type	Type-1 (Green)															
Unit	Hypersolvus															
Sample #	49-C-2			57-A-1							57-A-3					
Description			dkgr	#2 gr	113	115	dk	dk	dk	dk		ygr	#2	br gr	125	dk gr
File	am93	am93	am93	am93	am93	am93	icp	icp	icp	icp	am93	am93	am93	am93	am93	am93
#	26	27	32	68	70	71					113	72	73	75	77	78
Analysis #	29	30	35	81	83	85	88	90	92	93	140	89	90	92	94	98
Na_2O	13.58	13.55	13.29	13.92	13.75	14.02	13.41	13.25	13.62	13.69	13.38	13.61	13.85	13.59	13.83	13.68
K_2O	0.00	0.00	0.00	0.00	0.00	0.01	0.00	0.00	0.00	0.00	0.01	0.02	0.01	0.02	0.01	0.01
CaO	0.02	0.07	0.25	0.06	0.01	0.12	0.15	0.19	0.16	0.18	0.14	0.18	0.16	0.15	0.14	0.13
Fe_2O_3	28.20	29.18	27.87	31.76	32.48	33.18	30.99	27.54	27.09	30.93	26.78	27.78	32.02	31.51	30.80	26.51
FeO	3.27	3.47	3.41	0.64	1.05	0.06	2.30	4.16	3.41	1.37	3.93	2.71	1.44	1.98	1.49	3.44
MgO	0.01	0.00	0.02	0.04	0.02	0.02	0.03	0.00	0.00	0.00	0.03	0.04	0.01	0.03	0.02	0.02
MnO	0.19	0.08	0.24	0.21	0.08	0.11	0.11	0.22	0.20	0.18	0.30	0.23	0.10	0.15	0.23	0.26
ZnO	0.00	0.00	0.05	0.00	0.00	0.00	0.00	0.00	0.00	0.00	0.01	0.02	0.00	0.01	0.01	0.00
Nb_2O_5	0.00	0.01	0.01	0.00	0.02	0.03	0.00	0.00	0.00	0.00	0.02	0.08	0.00	0.03	0.00	0.02
V_2O_3	0.03	0.05	0.02	0.01	0.00	0.06	0.00	0.00	0.01	0.01	0.00	0.12	0.00	0.03	0.00	0.00
Cr_2O_3							0.01	0.00	0.00	0.01						
Yb_2O_3							0.01	0.02	0.00	0.00						
ZrO_2	0.12	0.12	0.91	0.27	0.18	0.12	0.10	0.27	0.21	0.30	0.28	0.29	0.12	0.41	0.35	2.57
TiO_2	2.44	1.67	1.62	1.38	0.99	0.82	1.01	1.92	3.43	1.67	2.25	2.72	1.57	1.23	1.55	2.22
Al_2O_3	0.48	0.41	0.18	0.30	0.11	0.33	0.28	0.28	0.29	0.33	0.54	0.54	0.27	0.32	0.34	0.54
SiO_2	52.06	52.50	51.60	51.48	51.15	51.65	51.34	52.07	51.78	51.12	52.31	51.67	51.80	51.46	51.94	51.95
F							0.00	0.00	0.00	0.00						
Cl							0.00	0.00	0.00	0.00						
Total	100.40	101.11	99.46	100.07	99.84	100.54	99.73	99.93	100.21	99.78	99.98	100.02	101.36	100.92	100.71	101.35
-O=F	0.00	0.00	0.00	0.00	0.00	0.00	0.00	0.00	0.00	0.00	0.00	0.00	0.00	0.00	0.00	0.00
-O=Cl	0.00	0.00	0.00	0.00	0.00	0.00	0.00	0.00	0.00	0.00	0.00	0.00	0.00	0.00	0.00	0.00
Total	100.40	101.11	99.46	100.07	99.84	100.54	99.73	99.92	100.21	99.78	99.98	100.02	101.36	100.92	100.71	101.35
Structural formula calculated based on 6 atoms of oxygen and 4 cations																
Na	1.003	0.995	0.995	1.031	1.023	1.033	1.000	0.985	1.008	1.018	0.992	1.009	1.015	1.003	1.019	1.008
K	0.000	0.000	0.000	0.000	0.000	0.000	0.000	0.000	0.000	0.000	0.001	0.001	0.001	0.001	0.000	0.000
Ca	0.001	0.003	0.010	0.003	0.000	0.005	0.006	0.008	0.007	0.007	0.006	0.007	0.006	0.006	0.006	0.005
Fe^{3+}	0.808	0.832	0.810	0.913	0.938	0.949	0.897	0.795	0.778	0.893	0.770	0.799	0.911	0.903	0.881	0.758
Fe^{2+}	0.104	0.110	0.110	0.021	0.034	0.002	0.074	0.134	0.109	0.044	0.126	0.087	0.045	0.063	0.047	0.109
Mg	0.000	0.000	0.001	0.002	0.001	0.001	0.001	0.000	0.000	0.000	0.001	0.002	0.000	0.001	0.001	0.001
Mn	0.006	0.003	0.008	0.007	0.002	0.003	0.003	0.007	0.006	0.006	0.010	0.008	0.003	0.005	0.007	0.008
Zn	0.000	0.000	0.001	0.000	0.000	0.000	0.000	0.000	0.000	0.000	0.000	0.000	0.000	0.000	0.000	0.000
Nb	0.000	0.000	0.000	0.000	0.000	0.000	0.000	0.000	0.000	0.000	0.000	0.001	0.000	0.000	0.000	0.000
V	0.001	0.002	0.000	0.000	0.000	0.002	0.000	0.000	0.000	0.000	0.000	0.004	0.000	0.001	0.000	0.000
Cr	0.000	0.000	0.000	0.000	0.000	0.000	0.000	0.000	0.000	0.000	0.000	0.000	0.000	0.000	0.000	0.000
Yb	0.000	0.000	0.000	0.000	0.000	0.000	0.000	0.000	0.000	0.000	0.000	0.000	0.000	0.000	0.000	0.000
Zr	0.002	0.002	0.017	0.005	0.003	0.002	0.002	0.005	0.004	0.006	0.005	0.005	0.002	0.008	0.006	0.048
Ti	0.070	0.047	0.047	0.040	0.029	0.023	0.029	0.055	0.099	0.048	0.065	0.078	0.045	0.035	0.044	0.064
Al	0.022	0.018	0.008	0.013	0.005	0.015	0.013	0.013	0.013	0.015	0.024	0.025	0.012	0.015	0.015	0.024
Si	1.983	1.988	1.992	1.966	1.964	1.963	1.974	1.998	1.976	1.962	2.000	1.975	1.958	1.959	1.973	1.974
F	0.000	0.000	0.000	0.000	0.000	0.000	0.000	0.000	0.000	0.000	0.000	0.000	0.000	0.000	0.000	0.000
Cl	0.000	0.000	0.000	0.000	0.000	0.000	0.000	0.000	0.000	0.000	0.000	0.000	0.000	0.000	0.000	0.000

Absent oxides were not analyzed.

Appendix B-2 Electron-microprobe analyses of aegirine

Type	Type-1 (Green)														
Unit	Hypersolvus			Fresh Subsolvus											
Sample #	57-A-3			37-D-1	38-B-3										
Description	#4lt	dk	dk	#2 gr		br gr	nr aen	dk	#2nr	ltgr	#3vg	ltgr	lt	dker	ed
File	am93	am93	am93	am93	am93	am93	am93	am93	am93	am93	am93	am93	am93	am93	lcp
#	79	80	81	96	52	53	54	55	56	57	58	59	60	61	
Analysis #	99	100	101	119	64	65	66	67	68	69	70	71	72	73	95
Na_2O	13.58	13.43	13.56	13.42	13.60	13.79	13.57	13.74	13.56	13.58	13.62	13.74	13.67	13.68	13.64
K_2O	0.02	0.01	0.01	0.02	0.00	0.00	0.01	0.00	0.01	0.00	0.02	0.00	0.01	0.00	0.00
CaO	0.18	0.16	0.18	0.28	0.17	0.28	0.01	0.14	0.13	0.10	0.14	0.06	0.05	0.02	0.16
Fe_2O_3	30.24	28.02	25.98	32.05	27.49	26.77	22.78	29.31	28.87	29.46	27.41	30.70	31.78	27.97	27.70
FeO	2.23	3.16	3.24	1.09	3.63	3.04	5.31	2.44	2.83	2.94	3.46	1.95	1.37	3.15	3.17
MgO	0.09	0.00	0.01	0.01	0.02	0.00	0.00	0.00	0.01	0.01	0.00	0.00	0.04	0.01	0.01
MnO	0.13	0.27	0.25	0.29	0.27	0.41	0.43	0.28	0.29	0.21	0.22	0.17	0.06	0.13	0.21
ZnO	0.00	0.01	0.05	0.12	0.03	0.16	0.11	0.00	0.03	0.00	0.00	0.00	0.00	0.00	0.00
Nb_2O_5	0.03	0.15	0.07	0.05	0.00	0.02	0.16	0.00	0.00	0.03	0.02	0.00	0.00	0.04	0.00
V_2O_3	0.02	0.00	0.02	0.00	0.02	0.00	0.00	0.00	0.00	0.07	0.02	0.00	0.00	0.00	0.02
Cr_2O_3															0.00
Yb_2O_3															0.00
ZrO_2	0.14	0.56	0.36	0.06	0.23	0.24	0.54	0.24	0.16	0.10	0.26	0.13	0.03	0.13	0.30
TiO_2	1.05	2.40	3.33	0.61	2.86	4.17	4.99	2.69	2.23	1.97	2.77	1.75	0.32	2.60	3.09
Al_2O_3	0.31	0.28	0.44	0.40	0.46	0.22	0.36	0.30	0.21	0.27	0.31	0.37	0.47	0.60	0.44
SiO_2	52.18	51.28	51.59	50.89	52.43	52.03	52.35	51.77	51.87	52.04	52.30	51.76	51.91	52.16	51.83
F															0.00
Cl															0.00
Total	100.19	99.73	99.08	99.28	101.21	101.14	100.62	100.91	100.18	100.77	100.55	100.63	99.71	100.49	100.56
-O=F	0.00	0.00	0.00	0.00	0.00	0.00	0.00	0.00	0.00	0.00	0.00	0.00	0.00	0.00	0.00
-O=Cl	0.00	0.00	0.00	0.00	0.00	0.00	0.00	0.00	0.00	0.00	0.00	0.00	0.00	0.00	0.00
Total	100.19	99.73	99.08	99.28	101.21	101.14	100.62	100.91	100.18	100.77	100.55	100.63	99.71	100.49	100.56
	Structural formula calculated based on 6 atoms of oxygen and 4 cations														
Na	1.005	1.002	1.013	1.005	0.997	1.011	1.000	1.011	1.005	1.001	1.004	1.013	1.015	1.008	1.006
K	0.001	0.000	0.000	0.001	0.000	0.000	0.001	0.000	0.000	0.000	0.001	0.000	0.000	0.000	0.000
Ca	0.007	0.007	0.007	0.012	0.007	0.011	0.001	0.006	0.005	0.004	0.006	0.002	0.002	0.001	0.006
Fe^{3+}	0.868	0.811	0.753	0.931	0.782	0.762	0.652	0.837	0.830	0.843	0.784	0.879	0.916	0.800	0.793
Fe^{2+}	0.071	0.102	0.105	0.035	0.115	0.096	0.169	0.078	0.091	0.093	0.110	0.062	0.044	0.100	0.101
Mg	0.005	0.000	0.000	0.001	0.001	0.000	0.000	0.000	0.000	0.001	0.000	0.000	0.002	0.000	0.001
Mn	0.004	0.009	0.008	0.010	0.009	0.013	0.014	0.009	0.009	0.007	0.007	0.005	0.002	0.004	0.007
Zn	0.000	0.000	0.001	0.003	0.001	0.004	0.003	0.000	0.001	0.000	0.000	0.000	0.000	0.000	0.000
Nb	0.001	0.003	0.001	0.001	0.000	0.000	0.003	0.000	0.000	0.000	0.000	0.000	0.000	0.001	0.000
V	0.001	0.000	0.001	0.000	0.001	0.000	0.000	0.000	0.000	0.002	0.001	0.000	0.000	0.000	0.001
Cr	0.000	0.000	0.000	0.000	0.000	0.000	0.000	0.000	0.000	0.000	0.000	0.000	0.000	0.000	0.000
Yb	0.000	0.000	0.000	0.000	0.000	0.000	0.000	0.000	0.000	0.000	0.000	0.000	0.000	0.000	0.000
Zr	0.003	0.011	0.007	0.001	0.004	0.004	0.010	0.004	0.003	0.002	0.005	0.002	0.000	0.002	0.006
Ti	0.030	0.070	0.097	0.018	0.081	0.119	0.143	0.077	0.064	0.056	0.079	0.050	0.009	0.074	0.088
Al	0.014	0.013	0.020	0.018	0.020	0.010	0.016	0.013	0.009	0.012	0.014	0.017	0.021	0.027	0.020
Si	1.991	1.973	1.987	1.965	1.982	1.968	1.990	1.965	1.982	1.978	1.989	1.969	1.988	1.982	1.972
F	0.000	0.000	0.000	0.000	0.000	0.000	0.000	0.000	0.000	0.000	0.000	0.000	0.000	0.000	0.000
Cl	0.000	0.000	0.000	0.000	0.000	0.000	0.000	0.000	0.000	0.000	0.000	0.000	0.000	0.000	0.000

Absent oxides were not analyzed.

Appendix B-2 Electron-microprobe analyses of aegirine

Type	Type-1 (Green)				
Unit	Near Hypersolvus-Subsolvus Contact				
Sample #	46-A-3				46-I-3
Description	yel gr	#2gr	dker	#1nr	2 btae
File	am93	am93	am93	am93	lep
#	108	109	110	111	
Analysis #	132	133	134	137	36
Na_2O	13.56	13.45	13.43	13.38	13.75
K_2O	0.00	0.01	0.01	0.04	0.00
CaO	0.08	0.10	0.08	0.08	0.35
Fe_2O_3	25.20	27.36	25.66	27.22	29.61
FeO	4.23	3.97	4.71	3.46	2.13
MgO	0.01	0.00	0.01	0.03	0.00
MnO	0.39	0.31	0.31	0.14	0.25
ZnO	0.10	0.04	0.03	0.00	0.00
Nb_2O_5	0.01	0.04	0.00	0.00	0.00
V_2O_5	0.03	0.02	0.00	0.04	0.00
Cr_2O_3					0.00
Yb_2O_3					0.03
ZrO_2	0.12	0.16	0.09	0.17	0.98
TiO_2	3.32	2.08	3.56	1.29	1.60
Al_2O_3	0.41	0.35	0.33	0.35	0.13
SiO_2	52.74	52.67	52.34	52.51	52.16
F					0.00
Cl					0.00
Total	100.20	100.56	100.54	98.71	101.00
-O=F	0.00	0.00	0.00	0.00	0.00
-O=Cl	0.00	0.00	0.00	0.00	0.00
Total	100.20	100.56	100.54	98.71	101.00
	Structural formula calculated based on 6 atoms of oxygen and 4 cations				
Na	1.001	0.992	0.991	1.001	1.012
K	0.000	0.000	0.000	0.002	0.000
Ca	0.003	0.004	0.003	0.003	0.014
Fe^{3+}	0.722	0.783	0.735	0.791	0.846
Fe^{2+}	0.135	0.126	0.150	0.112	0.068
Mg	0.001	0.000	0.000	0.002	0.000
Mn	0.013	0.010	0.010	0.005	0.008
Zn	0.003	0.001	0.001	0.000	0.000
Nb	0.000	0.001	0.000	0.000	0.000
V	0.001	0.001	0.000	0.001	0.000
Cr	0.000	0.000	0.000	0.000	0.000
Yb	0.000	0.000	0.000	0.000	0.000
Zr	0.002	0.003	0.002	0.003	0.018
Ti	0.095	0.060	0.102	0.037	0.046
Al	0.019	0.016	0.015	0.016	0.006
Si	2.007	2.003	1.992	2.027	1.981
F	0.000	0.000	0.000	0.000	0.000
Cl	0.000	0.000	0.000	0.000	0.000

Appendix B-2. Electron-microprobe analyses of aegirine

Type	Type-2 (Yellow)															
Unit	Hypersolvus								Near Hypersolvus-Subsolvus Contact							
Sample #	49-C-2		57-A-1								46-A-3			46-I-3		
Description		mid					mid		lipyx	lipyx		yell	yenr	brholey	better	sideam
File	am93	am93	am93	am93	am93	am93	am93	am93	lcp	lcp	am93	am93	am93	Jan-95	Jan-95	Jan-95
#	30	33	62	63	64	65	66	67			105	106	107			
Analysis #	33	36	74	75	76	77	78	79	87	91	129	130	131	139	141	145
Na_2O	13.26	13.57	13.63	13.37	13.42	13.39	13.33	13.13	13.26	13.26	13.59	13.34	13.11	12.98	13.43	13.56
K_2O	0.01	0.00	0.01	0.00	0.00	0.01	0.01	0.00	0.00	0.00	0.00	0.00	0.01	0.00	0.00	0.00
CaO	0.09	0.21	0.00	0.01	0.00	0.18	0.15	0.24	0.31	0.14	0.06	0.08	0.12	0.32	0.10	0.20
Fe_2O_3	28.67	30.28	32.42	31.36	31.02	30.03	28.56	27.89	29.26	28.38	27.30	28.16	28.53	28.95	29.41	30.73
FeO	4.34	2.33	1.51	2.97	2.49	3.23	3.44	3.73	2.79	3.57	3.78	3.88	3.78	3.66	3.27	1.92
MgO	0.01	0.02	0.07	0.00	0.04	0.01	0.00	0.00	0.01	0.01	0.03	0.03	0.02	0.11	0.02	0.01
MnO	0.08	0.07	0.32	0.11	0.14	0.11	0.22	0.26	0.24	0.20	0.42	0.12	0.47			
ZnO	0.00	0.03	0.02	0.00	0.00	0.00	0.02	0.00	0.00	0.00	0.09	0.05	0.00	0.25	0.13	0.20
Nb_2O_5	0.00	0.03	0.00	0.00	0.00	0.00	0.03	0.00	0.00	0.00	0.00	0.00	0.02			
V_2O_3	0.02	0.00	0.01	0.03	0.00	0.02	0.03	0.00	0.01	0.02	0.00	0.04	0.00	0.00	0.02	0.02
Cr_2O_3									0.00	0.01				0.00	0.00	0.00
Yb_2O_3									0.02	0.00						
ZrO_2	0.12	0.14	0.15	0.12	0.09	0.17	0.42	1.14	0.74	0.56	0.08	0.09	1.02	0.62	0.69	0.45
TiO_2	0.81	1.15	0.81	0.82	0.99	0.98	1.77	1.63	1.22	1.47	3.03	1.31	0.81	0.87	0.87	0.93
Al_2O_3	0.31	0.49	0.40	0.23	0.25	0.29	0.23	0.15	0.14	0.20	0.41	0.28	0.16	0.26	0.09	0.10
SiO_2	52.86	52.00	51.59	51.64	51.46	52.19	51.64	51.08	51.17	51.65	52.52	52.55	51.73	51.34	52.20	51.64
F									0.00	0.00				0.00	0.00	0.00
Cl									0.00	0.00				0.01	0.01	0.00
Total	100.57	100.33	100.93	100.67	99.89	100.63	99.85	99.25	99.15	99.45	101.31	99.92	99.77	99.36	100.23	99.77
-O=F	0.00	0.00	0.00	0.00	0.00	0.00	0.00	0.00	0.00	0.00	0.00	0.00	0.00	0.00	0.00	0.00
-O=Cl	0.00	0.00	0.00	0.00	0.00	0.00	0.00	0.00	0.00	0.00	0.00	0.00	0.00	0.00	0.00	0.00
Total	100.57	100.33	100.93	100.67	99.89	100.63	99.85	99.25	99.15	99.45	101.31	99.92	99.77	99.36	100.23	99.77
	Structural formula calculated based on 6 atoms of oxygen and 4 cations															
Na	0.979	1.003	1.005	0.990	0.999	0.989	0.993	0.988	0.996	0.992	0.995	0.990	0.981	0.974	0.997	1.010
K	0.001	0.000	0.000	0.000	0.000	0.000	0.000	0.000	0.000	0.000	0.000	0.000	0.000	0.000	0.000	0.000
Ca	0.004	0.009	0.000	0.000	0.000	0.007	0.006	0.010	0.013	0.006	0.002	0.003	0.005	0.013	0.004	0.008
Fe^{3+}	0.822	0.869	0.927	0.901	0.897	0.861	0.826	0.814	0.853	0.824	0.776	0.811	0.828	0.844	0.848	0.888
Fe^{2+}	0.138	0.074	0.048	0.095	0.080	0.103	0.111	0.121	0.090	0.115	0.120	0.124	0.122	0.119	0.105	0.062
Mg	0.000	0.001	0.004	0.000	0.002	0.001	0.000	0.000	0.001	0.000	0.002	0.002	0.001	0.006	0.001	0.001
Mn	0.003	0.002	0.010	0.003	0.004	0.003	0.007	0.009	0.008	0.007	0.014	0.004	0.015	0.000	0.000	0.000
Zn	0.000	0.001	0.000	0.000	0.000	0.000	0.000	0.000	0.000	0.000	0.002	0.001	0.000	0.007	0.004	0.006
Nb	0.000	0.000	0.000	0.000	0.000	0.000	0.001	0.000	0.000	0.000	0.000	0.000	0.000	0.000	0.000	0.000
V	0.000	0.000	0.000	0.001	0.000	0.001	0.001	0.000	0.000	0.001	0.000	0.001	0.000	0.000	0.001	0.001
Cr	0.000	0.000	0.000	0.000	0.000	0.000	0.000	0.000	0.000	0.000	0.000	0.000	0.000	0.000	0.000	0.000
Yb	0.000	0.000	0.000	0.000	0.000	0.000	0.000	0.000	0.000	0.000	0.000	0.000	0.000	0.000	0.000	0.000
Zr	0.002	0.003	0.003	0.002	0.002	0.003	0.008	0.022	0.014	0.010	0.002	0.002	0.019	0.012	0.013	0.008
Ti	0.023	0.033	0.023	0.024	0.029	0.028	0.051	0.047	0.036	0.043	0.086	0.038	0.023	0.025	0.025	0.027
Al	0.014	0.022	0.018	0.010	0.011	0.013	0.010	0.007	0.006	0.009	0.018	0.013	0.007	0.012	0.004	0.005
Si	2.014	1.983	1.961	1.972	1.976	1.989	1.985	1.982	1.983	1.993	1.984	2.012	1.996	1.988	1.999	1.984
F	0.000	0.000	0.000	0.000	0.000	0.000	0.000	0.000	0.000	0.000	0.000	0.000	0.000	0.000	0.000	0.000
Cl	0.000	0.000	0.000	0.000	0.000	0.000	0.000	0.000	0.000	0.000	0.000	0.000	0.000	0.001	0.000	0.000

Absent oxides were not analyzed.

Appendix B-2 Electron-microprobe analyses of aegirine

Type	Type-2 (Yellow)											
Unit	Near Hypersolvus-Subsolvus Contact											
Sample #	46-I-3								46-I-3.2	46-I-3		
Description	br	3 gr			holey	holey	holey	holey			nram	ed
File #	Jan-95	Jan-95	Jan-95	Jan-95	Jan-95	Jan-95	Jan-95	Jan-95	icpadd	icp	icp	icp
Analysis #	147	148	149	150	152	153	155	157	68	21	22	27
Na_2O	13.33	13.32	13.56	13.52	13.69	13.74	13.32	13.73	14.17	13.61	13.86	13.47
K_2O	0.00	0.00	0.00	0.00	0.00	0.00	0.00	0.00	0.00	0.00	0.00	0.00
CaO	0.14	0.21	0.11	0.12	0.05	0.12	0.31	0.16	0.11	0.16	0.09	0.65
Fe_2O_3	29.62	29.43	30.89	31.81	32.05	32.12	29.47	30.99	32.45	30.41	32.22	30.87
FeO	3.44	2.84	2.31	2.37	2.08	1.59	3.39	1.60	0.00	1.40	0.65	1.92
MgO	0.00	0.00	0.00	0.00	0.00	0.00	0.04	0.00	0.00	0.00	0.01	0.05
MnO									0.51	0.32	0.60	0.36
ZnO	0.10	0.06	0.12	0.09	0.18	0.08	0.21	0.18	0.14	0.00	0.00	0.00
Nb_2O_5									0.01	0.00	0.00	0.05
V_2O_3	0.01	0.02	0.01	0.00	0.01	0.01	0.00	0.01	0.01	0.00	0.00	0.00
Cr_2O_3	0.01	0.01	0.00	0.00	0.01	0.00	0.01	0.01	0.00	0.00	0.01	0.01
Yb_2O_3									0.04	0.02	0.00	0.02
ZrO_2	0.37	0.75	0.28	0.02	0.03	0.16	0.56	0.64	0.69	1.25	0.63	0.60
TiO_2	0.77	1.20	0.59	0.34	0.37	0.56	0.86	0.89	0.93	0.41	0.94	0.95
Al_2O_3	0.18	0.21	0.27	0.15	0.12	0.09	0.23	0.11	0.15	0.08	0.14	0.17
SiO_2	52.16	51.17	52.09	52.18	52.52	52.11	52.27	51.86	51.97	51.46	51.68	51.84
F	0.00	0.00	0.00	0.00	0.00	0.00	0.00	0.00	0.00	0.00	0.00	0.00
Cl	0.00	0.00	0.00	0.00	0.00	0.00	0.00	0.02	0.01	0.00	0.01	0.01
Total	100.13	99.21	100.22	100.60	101.11	100.59	100.66	100.19	101.17	99.10	100.83	100.97
-O=F	0.00	0.00	0.00	0.00	0.00	0.00	0.00	0.00	0.00	0.00	0.00	0.00
-O=Cl	0.00	0.00	0.00	0.00	0.00	0.00	0.00	0.00	0.00	0.00	0.00	0.00
Total	100.13	99.21	100.22	100.60	101.11	100.59	100.66	100.18	101.17	99.10	100.83	100.97
	Structural formula calculated based on 6 atoms of oxygen and 4 cations											
Na	0.990	1.000	1.005	0.999	1.006	1.014	0.985	1.019	1.039	1.021	1.022	0.994
K	0.000	0.000	0.000	0.000	0.000	0.000	0.000	0.000	0.000	0.000	0.000	0.000
Ca	0.006	0.009	0.004	0.005	0.002	0.005	0.013	0.006	0.004	0.007	0.004	0.027
Fe^{3+}	0.854	0.857	0.888	0.912	0.914	0.920	0.846	0.892	0.924	0.886	0.923	0.884
Fe^{2+}	0.110	0.092	0.074	0.076	0.066	0.051	0.108	0.051	0.000	0.045	0.028	0.061
Mg	0.000	0.000	0.000	0.000	0.000	0.000	0.002	0.000	0.000	0.000	0.000	0.003
Mn	0.000	0.000	0.000	0.000	0.000	0.000	0.000	0.000	0.016	0.010	0.019	0.011
Zn	0.003	0.002	0.003	0.003	0.005	0.002	0.006	0.005	0.004	0.000	0.000	0.000
Nb	0.000	0.000	0.000	0.000	0.000	0.000	0.000	0.000	0.000	0.000	0.000	0.001
V	0.000	0.001	0.000	0.000	0.000	0.000	0.000	0.000	0.000	0.000	0.000	0.000
Cr	0.000	0.000	0.000	0.000	0.000	0.000	0.000	0.000	0.000	0.000	0.000	0.000
Yb	0.000	0.000	0.000	0.000	0.000	0.000	0.000	0.000	0.000	0.000	0.000	0.000
Zr	0.007	0.014	0.005	0.000	0.001	0.003	0.010	0.012	0.013	0.024	0.012	0.011
Ti	0.022	0.035	0.017	0.010	0.011	0.016	0.025	0.026	0.026	0.012	0.027	0.027
Al	0.008	0.009	0.012	0.007	0.005	0.004	0.010	0.005	0.007	0.003	0.006	0.007
Si	1.999	1.981	1.991	1.989	1.990	1.984	1.994	1.984	1.966	1.992	1.966	1.973
F	0.000	0.000	0.000	0.000	0.000	0.000	0.000	0.000	0.000	0.000	0.000	0.000
Cl	0.000	0.000	0.000	0.000	0.000	0.000	0.000	0.001	0.001	0.000	0.000	0.001

Absent oxides were not analyzed.

Appendix B-2 Electron-microprobe analyses of aegirine

Type	Type-2 (Yellow)							
Unit	Fresh Subsolvus							
Sample #	37-D-1							
Description		161	Rye	166	edge	mid	ed	other
File	am93	am93	am93	am93	am93	am93	am93	am93
#	94	95	97	98	99	101	102	103
Analysis #	117	118	120	122	123	125	126	127
Na_2O	13.69	13.33	13.45	13.48	13.45	13.36	13.45	13.50
K_2O	0.01	0.02	0.01	0.00	0.01	0.00	0.01	0.01
CaO	0.01	0.07	0.03	0.12	0.06	0.03	0.01	0.09
Fe_2O_3	32.73	31.50	31.37	29.73	30.64	29.96	30.93	30.09
FeO	1.00	2.04	1.49	2.49	2.44	2.79	2.12	2.32
MgO	0.03	0.03	0.02	0.03	0.02	0.02	0.04	0.03
MnO	0.09	0.05	0.44	0.18	0.07	0.06	0.05	0.04
ZnO	0.03	0.08	0.31	0.00	0.00	0.00	0.00	0.00
Nb_2O_5	0.00	0.00	0.05	0.13	0.00	0.02	0.01	0.02
V_2O_3	0.00	0.00	0.00	0.02	0.00	0.01	0.00	0.01
Cr_2O_3								
Yb_2O_3								
ZrO_2	0.10	0.07	0.06	0.07	0.04	0.05	0.06	0.12
TiO_2	0.79	0.69	0.73	0.84	0.45	0.70	0.51	0.58
Al_2O_3	0.40	0.36	0.17	0.97	0.50	0.21	0.52	0.28
SiO_2	51.17	50.95	51.36	52.04	52.02	51.75	51.57	52.05
F								
Cl								
Total	100.06	99.17	99.49	100.10	99.69	98.96	99.28	99.14
-O=F	0.00	0.00	0.00	0.00	0.00	0.00	0.00	0.00
-O=Cl	0.00	0.00	0.00	0.00	0.00	0.00	0.00	0.00
Total	100.06	99.17	99.49	100.10	99.69	98.96	99.28	99.14
Structural formula calculated based on 6 atoms of oxygen and 4 cations								
Na	1.016	1.000	1.005	0.997	1.001	1.001	1.005	1.009
K	0.001	0.001	0.001	0.000	0.000	0.000	0.000	0.001
Ca	0.000	0.003	0.001	0.005	0.002	0.001	0.000	0.004
Fe^{3+}	0.943	0.917	0.910	0.853	0.884	0.872	0.897	0.872
Fe^{2+}	0.032	0.066	0.048	0.079	0.078	0.090	0.068	0.075
Mg	0.002	0.002	0.001	0.002	0.001	0.001	0.002	0.002
Mn	0.003	0.002	0.014	0.006	0.002	0.002	0.002	0.001
Zn	0.001	0.002	0.009	0.000	0.000	0.000	0.000	0.000
Nb	0.000	0.000	0.001	0.002	0.000	0.000	0.000	0.000
V	0.000	0.000	0.000	0.001	0.000	0.000	0.000	0.000
Cr	0.000	0.000	0.000	0.000	0.000	0.000	0.000	0.000
Yb	0.000	0.000	0.000	0.000	0.000	0.000	0.000	0.000
Zr	0.002	0.001	0.001	0.001	0.001	0.001	0.001	0.002
Ti	0.023	0.020	0.021	0.024	0.013	0.020	0.015	0.017
Al	0.018	0.017	0.008	0.043	0.022	0.010	0.024	0.013
Si	1.959	1.971	1.980	1.985	1.995	2.001	1.986	2.005
F	0.000	0.000	0.000	0.000	0.000	0.000	0.000	0.000
Cl	0.000	0.000	0.000	0.000	0.000	0.000	0.000	0.000

Absent oxides were not analyzed.

Appendix B-2 Electron-microprobe analyses of aegirine

Type	Type-2 (Yellow)															
Unit	Altered Subsolvus															
Sample #	27-A-2								27-B-1				34-C-1	36-B-3		
Description	#2	nr ox	152	#3 ed	154	yel mid		#1	alt	alt	alt	moreox	alt	alt	alt	alt
File	am93	am93	am93	am93	am93	am93	am93	am93	Jun-95	Jun-95	Jun-95	Jun-95	Jun-95	lcpadd	lcpadd	lcpadd
#	84	85	86	87	88	90	91	93								
Analysis #	107	108	109	110	111	113	114	116	31	32	33	34	84	242	243	261
Na_2O	13.62	13.49	13.56	13.59	13.62	13.81	13.63	13.71	13.45	13.73	13.51	13.14	12.55	13.37	13.32	13.65
K_2O	0.01	0.00	0.00	0.00	0.01	0.01	0.00	0.01	0.00	0.00	0.00	0.00	0.00	0.00	0.00	0.00
CaO	0.01	0.02	0.01	0.01	0.03	0.00	0.02	0.00	0.11	0.10	0.10	0.08	0.86	0.11	0.29	0.13
Fe_2O_3	31.04	31.47	31.43	32.09	31.58	32.12	31.59	32.56	30.24	32.18	30.98	31.80	29.48	33.30	31.68	33.39
FeO	2.61	2.88	2.43	2.21	2.18	1.44	1.80	1.79	2.66	1.07	1.92	2.81	4.03	1.37	0.88	0.60
MgO	0.01	0.01	0.04	0.00	0.04	0.03	0.02	0.00	0.12	0.05	0.20	0.14	0.08	0.06	0.08	0.01
MnO	0.05	0.05	0.14	0.06	0.05	0.02	0.23	0.03						0.55	0.92	0.60
ZnO	0.00	0.00	0.00	0.00	0.06	0.00	0.00	0.00	0.25	0.17	0.21	0.09	0.53	0.00	0.06	0.08
Nb_2O_5	0.00	0.03	0.01	0.02	0.00	0.03	0.05	0.00						0.07	0.00	0.00
V_2O_3	0.02	0.01	0.03	0.00	0.01	0.01	0.04	0.00	0.02	0.00	0.00	0.01	0.00	0.00	0.00	0.00
Cr_2O_3									0.00	0.01	0.00	0.00	0.00	0.00	0.00	0.00
Yb_2O_3														0.01	0.03	0.00
ZrO_2	0.12	0.13	0.10	0.11	0.17	0.08	0.09	0.15	0.11	0.11	0.06	0.09	0.13	0.09	0.27	0.11
TiO_2	1.33	0.72	0.77	0.68	0.65	0.72	0.80	0.61	0.65	0.65	0.71	0.75	1.09	0.65	0.75	0.69
Al_2O_3	0.27	0.31	0.22	0.34	0.29	0.46	0.36	0.20	0.33	0.35	0.72	0.43	0.27	0.33	0.75	0.36
SiO_2	51.98	52.06	52.04	51.83	52.14	52.06	51.77	51.91	52.36	51.66	51.96	50.88	50.71	50.64	50.77	51.17
F									0.00	0.03	0.00	0.00	0.00	0.02	0.01	0.00
Cl									0.01	0.01	0.01	0.01	0.02	0.00	0.02	0.01
Total	101.07	101.19	100.76	100.93	100.82	100.78	100.39	100.97	100.30	100.11	100.36	100.24	99.74	100.57	99.83	100.79
-O=F	0.00	0.00	0.00	0.00	0.00	0.00	0.00	0.00	0.00	0.01	0.00	0.00	0.00	0.01	0.00	0.00
-O=Cl	0.00	0.00	0.00	0.00	0.00	0.00	0.00	0.00	0.00	0.00	0.00	0.00	0.00	0.00	0.00	0.00
Total	101.07	101.19	100.76	100.93	100.82	100.78	100.39	100.97	100.29	100.08	100.36	100.24	99.73	100.55	99.81	100.79
						Structural formula calculated based on 6 atoms of oxygen and 4 cations										
Na	1.002	0.993	1.000	1.002	1.004	1.016	1.008	1.010	0.995	1.017	0.998	0.979	0.943	0.993	0.993	1.008
K	0.000	0.000	0.000	0.000	0.000	0.000	0.000	0.000	0.000	0.000	0.000	0.000	0.000	0.000	0.000	0.000
Ca	0.000	0.001	0.000	0.000	0.001	0.000	0.001	0.000	0.005	0.004	0.004	0.003	0.036	0.004	0.012	0.005
Fe^{3+}	0.886	0.899	0.900	0.918	0.903	0.917	0.907	0.931	0.868	0.926	0.888	0.919	0.860	0.960	0.917	0.957
Fe^{2+}	0.083	0.091	0.077	0.070	0.069	0.046	0.057	0.057	0.085	0.034	0.061	0.090	0.131	0.044	0.028	0.019
Mg	0.001	0.001	0.002	0.000	0.002	0.001	0.001	0.000	0.007	0.003	0.011	0.008	0.005	0.003	0.004	0.001
Mn	0.002	0.002	0.005	0.002	0.001	0.001	0.007	0.001	0.000	0.000	0.000	0.000	0.000	0.018	0.030	0.019
Zn	0.000	0.000	0.000	0.000	0.002	0.000	0.000	0.000	0.007	0.005	0.006	0.003	0.015	0.000	0.002	0.002
Nb	0.000	0.001	0.000	0.000	0.000	0.000	0.001	0.000	0.000	0.000	0.000	0.000	0.000	0.001	0.000	0.000
V	0.000	0.000	0.001	0.000	0.000	0.000	0.001	0.000	0.001	0.000	0.000	0.000	0.000	0.000	0.000	0.000
Cr	0.000	0.000	0.000	0.000	0.000	0.000	0.000	0.000	0.000	0.000	0.000	0.000	0.000	0.000	0.000	0.000
Yb	0.000	0.000	0.000	0.000	0.000	0.000	0.000	0.000	0.000	0.000	0.000	0.000	0.000	0.000	0.000	0.000
Zr	0.002	0.002	0.002	0.002	0.003	0.001	0.002	0.003	0.002	0.002	0.001	0.002	0.002	0.002	0.005	0.002
Ti	0.038	0.021	0.022	0.019	0.019	0.021	0.023	0.017	0.019	0.019	0.020	0.022	0.032	0.019	0.022	0.020
Al	0.012	0.014	0.010	0.015	0.013	0.021	0.016	0.009	0.015	0.016	0.033	0.020	0.012	0.015	0.034	0.016
Si	1.973	1.976	1.981	1.971	1.982	1.975	1.975	1.972	1.998	1.975	1.979	1.954	1.965	1.941	1.953	1.950
F	0.000	0.000	0.000	0.000	0.000	0.000	0.000	0.000	0.000	0.004	0.000	0.000	0.000	0.003	0.001	0.000
Cl	0.000	0.000	0.000	0.000	0.000	0.000	0.000	0.000	0.000	0.000	0.000	0.001	0.001	0.000	0.001	0.000

Absent oxides were not analyzed.

Appendix B-2. Electron-microprobe analyses of aegirine

Type	Type-2 (Yellow)														
Unit	Altered Subsolvus														
Sample #	36-B-3										SL-8-1				
Description	alt	alt	dkalt	alt	4dk	4dk	alt	dker	alt	alt	gr	yel		near	#2 near
File	lcpadd	lcpadd	lcpadd	lcpadd	lcpadd	lcpadd	lcpadd	lcpadd	lcpadd	lcpadd	am93	am93	am93	am93	am93	am93
#											12	13	14	15	16	17
Analysis #	267	268	275	283	284	285	286	288	293	294	14	15	16	17	19	20
Na_2O	13.85	13.87	12.93	13.77	13.43	13.05	13.47	13.08	13.61	13.43	14.00	13.67	13.66	13.85	13.85	13.77
K_2O	0.00	0.00	0.00	0.00	0.00	0.00	0.00	0.00	0.00	0.00	0.00	0.00	0.03	0.02	0.01	0.00
CaO	0.08	0.19	0.81	0.09	0.23	0.79	0.13	0.48	0.18	0.07	0.06	0.10	0.04	0.01	0.02	0.06
Fe_2O_3	34.53	34.06	32.59	34.28	34.41	34.15	34.32	33.49	34.48	33.80	32.34	32.10	32.28	31.84	31.62	32.19
FeO	0.00	0.00	1.88	0.12	0.56	0.99	0.77	1.89	0.47	1.00	0.60	1.70	1.56	1.27	1.01	1.31
MgO	0.02	0.03	0.15	0.01	0.05	0.05	0.08	0.08	0.08	0.02	0.01	0.02	0.00	0.00	0.05	0.01
MnO	0.62	0.72	0.80	0.59	0.81	0.75	0.55	0.62	0.54	0.55	0.11	0.07	0.13	0.11	0.21	0.08
ZnO	0.00	0.02	0.17	0.00	0.18	0.12	0.00	0.05	0.03	0.00	0.04	0.00	0.00	0.00	0.05	0.00
Nb_2O_5	0.03	0.00	0.00	0.00	0.00	0.00	0.00	0.00	0.00	0.00	0.03	0.00	0.03	0.00	0.03	0.02
V_2O_3	0.01	0.01	0.00	0.00	0.00	0.01	0.00	0.01	0.01	0.01	0.02	0.01	0.03	0.01	0.02	0.00
Cr_2O_3	0.00	0.00	0.00	0.00	0.00	0.00	0.00	0.00	0.00	0.00						
Yb_2O_3	0.00	0.01	0.00	0.00	0.00	0.01	0.00	0.00	0.00	0.00						
ZrO_2	0.13	0.11	0.10	0.11	0.22	0.28	0.13	0.09	0.09	0.14	0.11	0.04	0.07	0.14	0.14	0.07
TiO_2	0.68	0.70	0.71	0.68	0.75	0.63	0.94	0.92	0.63	0.71	0.71	0.29	0.54	0.69	0.72	0.83
Al_2O_3	0.42	0.33	0.30	0.31	0.21	0.33	0.28	0.31	0.32	0.46	0.40	0.37	0.25	0.23	0.34	0.21
SiO_2	50.53	50.76	50.73	51.02	50.43	49.93	50.25	50.34	50.87	50.39	52.13	52.17	51.80	52.17	52.12	51.75
F	0.00	0.00	0.00	0.00	0.00	0.00	0.00	0.00	0.00	0.00						
Cl	0.01	0.02	0.02	0.01	0.00	0.00	0.00	0.02	0.00	0.01						
Total	100.93	100.83	101.17	100.98	101.29	101.09	100.92	101.37	101.30	100.58	100.55	100.53	100.39	100.34	100.19	100.30
-O=F	0.00	0.00	0.00	0.00	0.00	0.00	0.00	0.00	0.00	0.00	0.00	0.00	0.00	0.00	0.00	0.00
-O=Cl	0.00	0.00	0.00	0.00	0.00	0.00	0.00	0.00	0.00	0.00	0.00	0.00	0.00	0.00	0.00	0.00
Total	100.93	100.82	101.16	100.97	101.28	101.08	100.92	101.36	101.30	100.58	100.55	100.53	100.39	100.34	100.19	100.30
Structural formula calculated based on 6 atoms of oxygen and 4 cations																
Na	1.022	1.023	0.957	1.016	0.993	0.969	0.998	0.968	1.003	0.997	1.030	1.008	1.011	1.023	1.023	1.019
K	0.000	0.000	0.000	0.000	0.000	0.000	0.000	0.000	0.000	0.000	0.000	0.000	0.001	0.001	0.001	0.000
Ca	0.003	0.008	0.033	0.004	0.009	0.032	0.005	0.020	0.007	0.003	0.002	0.004	0.001	0.000	0.001	0.003
Fe^{3+}	0.989	0.975	0.937	0.981	0.988	0.984	0.987	0.962	0.986	0.974	0.924	0.919	0.927	0.912	0.907	0.934
Fe^{2+}	0.000	0.000	0.060	0.004	0.018	0.032	0.024	0.060	0.015	0.032	0.019	0.054	0.050	0.040	0.032	0.042
Mg	0.001	0.002	0.009	0.001	0.003	0.003	0.004	0.005	0.004	0.001	0.001	0.001	0.000	0.000	0.003	0.000
Mn	0.020	0.023	0.026	0.019	0.026	0.024	0.018	0.020	0.018	0.018	0.003	0.002	0.004	0.004	0.007	0.003
Zn	0.000	0.001	0.005	0.000	0.005	0.003	0.000	0.001	0.001	0.000	0.001	0.000	0.000	0.000	0.001	0.000
Nb	0.001	0.000	0.000	0.000	0.000	0.000	0.000	0.000	0.000	0.000	0.000	0.000	0.001	0.000	0.001	0.000
V	0.000	0.000	0.000	0.000	0.000	0.000	0.000	0.000	0.000	0.000	0.001	0.000	0.001	0.000	0.001	0.000
Cr	0.000	0.000	0.000	0.000	0.000	0.000	0.000	0.000	0.000	0.000	0.000	0.000	0.000	0.000	0.000	0.000
Yb	0.000	0.000	0.000	0.000	0.000	0.000	0.000	0.000	0.000	0.000	0.000	0.000	0.000	0.000	0.000	0.000
Zr	0.002	0.002	0.002	0.002	0.004	0.005	0.002	0.002	0.002	0.003	0.002	0.001	0.001	0.003	0.003	0.001
Ti	0.020	0.020	0.020	0.019	0.022	0.018	0.027	0.027	0.018	0.020	0.020	0.008	0.015	0.020	0.021	0.024
Al	0.019	0.015	0.013	0.014	0.010	0.015	0.013	0.014	0.014	0.021	0.018	0.017	0.011	0.010	0.015	0.010
Si	1.923	1.931	1.938	1.941	1.923	1.913	1.920	1.922	1.933	1.930	1.978	1.985	1.977	1.987	1.986	1.974
F	0.000	0.000	0.000	0.000	0.000	0.000	0.000	0.000	0.000	0.000	0.000	0.000	0.000	0.000	0.000	0.000
Cl	0.000	0.001	0.001	0.001	0.000	0.000	0.000	0.001	0.000	0.001	0.000	0.000	0.000	0.000	0.000	0.000

Absent oxides were not analyzed.

Appendix B-2 Electron-microprobe analyses of aegirine

Type	Type-2 (Yellow)									
Unit	Altered Subsolvus									
Sample #	SL-8-1									
Description		wedg	nr ed	lt	dk	dk	#2 ed	mid	ed	mid
File	am93	am93	am93	lcp	lcp	lcp	lcp	lcp	lcp	lcp
#	18	19	20							
Analysis #	21	22	23	79	80	81	82	83	84	86
Na_2O	13.66	13.69	13.83	11.59	13.67	13.67	13.87	13.58	13.53	13.10
K_2O	0.01	0.01	0.01	0.00	0.00	0.00	0.00	0.00	0.00	0.00
CaO	0.10	0.11	0.12	3.41	0.07	0.00	0.10	0.03	0.07	0.03
Fe_2O_3	31.50	31.41	32.32	28.37	31.99	32.18	33.20	31.34	31.17	30.56
FeO	1.98	1.53	0.64	3.16	1.77	1.24	0.71	2.40	2.41	2.73
MgO	0.02	0.00	0.00	0.12	0.00	0.03	0.00	0.01	0.00	0.04
MnO	0.17	0.11	0.13	0.92	0.08	0.37	0.09	0.10	0.14	0.18
ZnO	0.00	0.01	0.03	0.91	0.00	0.00	0.00	0.00	0.00	0.00
Nb_2O_5	0.03	0.00	0.04	0.01	0.12	0.00	0.00	0.00	0.00	0.00
V_2O_3	0.02	0.03	0.00	0.00	0.00	0.00	0.00	0.00	0.00	0.01
Cr_2O_3				0.00	0.00	0.00	0.00	0.00	0.00	0.00
Yb_2O_3				0.00	0.01	0.00	0.01	0.01	0.00	0.02
ZrO_2	0.12	0.04	0.05	0.00	0.03	0.07	0.06	0.11	0.05	0.06
TiO_2	0.74	0.54	0.74	0.02	0.31	0.59	0.54	0.77	0.54	0.76
Al_2O_3	0.20	0.29	0.51	0.35	0.50	0.35	0.30	0.20	0.36	0.52
SiO_2	52.18	52.04	51.60	51.13	52.08	51.72	51.75	52.08	52.20	50.70
F				0.00	0.00	0.00	0.00	0.00	0.00	0.00
Cl				0.00	0.00	0.00	0.00	0.00	0.00	0.00
Total	100.73	99.80	100.03	99.99	100.62	100.23	100.63	100.62	100.48	98.70
-O=F	0.00	0.00	0.00	0.00	0.00	0.00	0.00	0.00	0.00	0.00
-O=Cl	0.00	0.00	0.00	0.00	0.00	0.00	0.00	0.00	0.00	0.00
Total	100.73	99.80	100.03	99.99	100.62	100.23	100.63	100.62	100.48	98.70
Structural formula calculated based on 6 atoms of oxygen and 4 cations										
Na	1.007	1.016	1.024	0.870	1.008	1.013	1.022	1.003	1.000	0.988
K	0.000	0.000	0.000	0.000	0.000	0.000	0.000	0.000	0.000	0.000
Ca	0.004	0.004	0.005	0.141	0.003	0.000	0.004	0.001	0.003	0.001
Fe^{3+}	0.901	0.905	0.929	0.827	0.916	0.925	0.950	0.898	0.894	0.894
Fe^{2+}	0.063	0.049	0.021	0.102	0.056	0.040	0.023	0.076	0.077	0.089
Mg	0.001	0.000	0.000	0.007	0.000	0.002	0.000	0.001	0.000	0.002
Mn	0.005	0.003	0.004	0.030	0.002	0.012	0.003	0.003	0.004	0.006
Zn	0.000	0.000	0.001	0.026	0.000	0.000	0.000	0.000	0.000	0.000
Nb	0.000	0.000	0.001	0.000	0.002	0.000	0.000	0.000	0.000	0.000
V	0.001	0.001	0.000	0.000	0.000	0.000	0.000	0.000	0.000	0.000
Cr	0.000	0.000	0.000	0.000	0.000	0.000	0.000	0.000	0.000	0.000
Yb	0.000	0.000	0.000	0.000	0.000	0.000	0.000	0.000	0.000	0.000
Zr	0.002	0.001	0.001	0.000	0.000	0.001	0.001	0.002	0.001	0.001
Ti	0.021	0.015	0.021	0.001	0.009	0.017	0.015	0.022	0.015	0.022
Al	0.009	0.013	0.023	0.016	0.022	0.016	0.013	0.009	0.016	0.024
Si	1.984	1.992	1.970	1.980	1.981	1.975	1.968	1.984	1.989	1.972
F	0.000	0.000	0.000	0.000	0.000	0.000	0.000	0.000	0.000	0.000
Cl	0.000	0.000	0.000	0.000	0.000	0.000	0.000	0.000	0.000	0.000

Absent oxides were not analyzed.

Appendix B-2 Electron-microprobe analyses of aegirine

Type	Type-2 (Yellow)															
Unit	Subsolvus - Drill Core															
Sample #	SL-182-40.08		SL-182-47.80								SL-182-54.90					
Description	40	ed			mid	ed	#2ed				alt	3 ed	mid	alt	br	un
File	am93	am93	am93	am93	am93	am93	am93	am93	am93	am93	Jan-95	Jan-95	Jan-95	Jan-95	Jan-95	Jan-95
#	48	51	40	41	42	43	44	45	46	47						
Analysis #	57	60	49	50	51	52	53	54	55	56	91	99	100	101	102	103
Na_2O	13.63	13.69	13.21	13.74	13.71	13.63	13.57	13.52	13.65	13.72	12.39	13.61	13.63	12.04	13.70	13.77
K_2O	0.01	0.01	0.01	0.00	0.00	0.01	0.01	0.00	0.00	0.00	0.00	0.00	0.00	0.00	0.00	0.01
CaO	0.06	0.05	0.03	0.00	0.03	0.03	0.14	0.05	0.03	0.04	0.99	0.11	0.02	1.69	0.09	0.01
Fe_2O_3	32.50	32.57	29.85	33.14	32.38	31.77	32.78	31.26	30.63	31.73	33.09	29.40	31.18	28.87	30.23	31.08
FeO	0.86	0.91	2.13	0.91	1.20	0.81	0.73	2.12	2.19	1.69	2.68	2.51	2.00	4.59	1.97	2.24
MgO	0.06	0.05	0.00	0.02	0.01	0.02	0.00	0.00	0.02	0.01	0.07	0.00	0.03	0.07	0.04	0.04
MnO	0.60	0.40	0.81	0.28	0.46	0.75	0.34	0.14	0.21	0.19						
ZnO	0.25	0.20	0.45	0.00	0.00	0.22	0.10	0.00	0.03	0.04	0.33	0.09	0.04	0.37	0.08	0.00
Nb_2O_5	0.04	0.06	0.10	0.00	0.08	0.02	0.04	0.01	0.01	0.00						
V_2O_3	0.00	0.00	0.00	0.00	0.00	0.06	0.00	0.00	0.03	0.00	0.00	0.03	0.00	0.02	0.00	0.00
Cr_2O_3											0.00	0.00	0.00	0.00	0.00	0.01
Yb_2O_3																
ZrO_2	0.03	0.02	0.04	0.05	0.14	0.09	0.01	0.08	0.06	0.13	0.19	0.11	0.10	0.07	0.69	0.11
TiO_2	0.58	0.63	0.61	0.53	0.62	0.52	0.48	0.64	1.25	0.94	1.09	1.20	0.60	1.03	0.74	0.75
Al_2O_3	0.15	0.18	0.39	0.15	0.16	0.17	0.24	0.39	0.33	0.14	0.23	0.25	0.25	0.19	0.39	0.24
SiO_2	51.68	51.69	51.59	51.52	51.74	51.78	51.02	51.77	52.05	51.93	48.33	52.27	52.01	50.09	52.14	52.68
F											0.00	0.00	0.00	0.00	0.00	0.00
Cl											0.01	0.01	0.01	0.04	0.01	0.00
Total	100.46	100.46	99.21	100.34	100.53	99.87	99.46	99.97	100.48	100.55	99.40	99.58	99.86	99.06	100.06	100.93
-O=F	0.00	0.00	0.00	0.00	0.00	0.00	0.00	0.00	0.00	0.00	0.00	0.00	0.00	0.00	0.00	0.00
-O=Cl	0.00	0.00	0.00	0.00	0.00	0.00	0.00	0.00	0.00	0.00	0.00	0.00	0.00	0.01	0.00	0.00
Total	100.46	100.46	99.21	100.34	100.53	99.87	99.46	99.97	100.48	100.55	99.39	99.58	99.85	99.04	100.05	100.93
Structural formula calculated based on 6 atoms of oxygen and 4 cations																
Na	1.009	1.013	0.990	1.018	1.014	1.013	1.014	1.004	1.008	1.013	0.941	1.012	1.012	0.913	1.015	1.011
K	0.000	0.000	0.000	0.000	0.000	0.000	0.000	0.000	0.000	0.000	0.000	0.000	0.000	0.000	0.000	0.000
Ca	0.002	0.002	0.001	0.000	0.001	0.001	0.006	0.002	0.001	0.002	0.042	0.004	0.001	0.071	0.003	0.000
Fe^{3+}	0.934	0.935	0.868	0.953	0.929	0.916	0.951	0.901	0.878	0.910	0.976	0.848	0.899	0.850	0.870	0.886
Fe^{2+}	0.028	0.029	0.069	0.029	0.038	0.026	0.024	0.068	0.070	0.054	0.088	0.080	0.064	0.150	0.063	0.071
Mg	0.003	0.003	0.000	0.001	0.001	0.001	0.000	0.000	0.001	0.000	0.004	0.000	0.001	0.004	0.002	0.002
Mn	0.019	0.013	0.027	0.009	0.015	0.024	0.011	0.004	0.007	0.006	0.000	0.000	0.000	0.000	0.000	0.000
Zn	0.007	0.006	0.013	0.000	0.000	0.006	0.003	0.000	0.001	0.001	0.009	0.002	0.001	0.011	0.002	0.000
Nb	0.001	0.001	0.002	0.000	0.001	0.000	0.001	0.000	0.000	0.000	0.000	0.000	0.000	0.000	0.000	0.000
V	0.000	0.000	0.000	0.000	0.000	0.002	0.000	0.000	0.001	0.000	0.000	0.001	0.000	0.001	0.000	0.000
Cr	0.000	0.000	0.000	0.000	0.000	0.000	0.000	0.000	0.000	0.000	0.000	0.000	0.000	0.000	0.000	0.000
Yb	0.000	0.000	0.000	0.000	0.000	0.000	0.000	0.000	0.000	0.000	0.000	0.000	0.000	0.000	0.000	0.000
Zr	0.001	0.000	0.001	0.001	0.003	0.002	0.000	0.001	0.001	0.002	0.004	0.002	0.002	0.001	0.013	0.002
Ti	0.017	0.018	0.018	0.015	0.018	0.015	0.014	0.018	0.036	0.027	0.032	0.035	0.017	0.030	0.021	0.021
Al	0.007	0.008	0.018	0.007	0.007	0.008	0.011	0.018	0.015	0.006	0.011	0.011	0.011	0.009	0.018	0.011
Si	1.973	1.972	1.994	1.968	1.973	1.985	1.966	1.983	1.982	1.978	1.894	2.004	1.992	1.960	1.993	1.995
F	0.000	0.000	0.000	0.000	0.000	0.000	0.000	0.000	0.000	0.000	0.000	0.000	0.000	0.000	0.000	0.000
Cl	0.000	0.000	0.000	0.000	0.000	0.000	0.000	0.000	0.000	0.000	0.001	0.000	0.000	0.003	0.000	0.000

Absent oxides were not analyzed.

Appendix B-2 Electron-microprobe analyses of aegirine

Type	Type-2 (Yellow)						
Unit	Subsolvus - Drill Core						
Sample #	SL-182-54.90 SL-182-84.96						
Description	am	poor	poor	3		ed	mld
File #	Jan-95	Jan-95	Jan-95	Jan-95	Jan-95	Jan-95	Jan-95
Analysis #	104	60	61	66	44	45	46
Na_2O	13 65	13 45	13 49	13 62	13 47	13 65	13 42
K_2O	0 00	0 00	0 00	0 00	0 00	0 00	0 00
CaO	0 00	0 09	0 15	0 16	0 23	0 20	0 29
Fe_2O_3	30 95	30 61	29 53	29 96	30 24	30 46	31 11
FeO	2 26	2 92	3 61	3 06	2 76	2 62	2 82
MgO	0 04	0 00	0 00	0 00	0 01	0 01	0 01
MnO							
ZnO	0 02	0 00	0 03	0 03	0 02	0 04	0 00
Nb_2O_5							
V_2O_3	0 00	0 02	0 00	0 01	0 00	0 02	0 01
Cr_2O_3	0 00	0 00	0 00	0 01	0 00	0 00	0 00
Yb_2O_3							
ZrO_2	0 09	0 01	0 07	0 07	0 06	0 12	0 01
TiO_2	0 75	0 59	1 01	0 90	0 82	0 90	0 45
Al_2O_3	0 24	0 25	0 43	0 50	0 55	0 34	0 17
SiO_2	52 24	52 28	52 90	52 96	52 25	52 69	52 33
F	0 00	0 00	0 00	0 00	0 00	0 00	0 00
Cl	0 00	0 00	0 01	0 00	0 01	0 01	0 01
Total	100 23	100 24	101 22	101 28	100 42	101 05	100 62
-O=F	0 00	0 00	0 00	0 00	0 00	0 00	0 00
-O=Cl	0 00	0 00	0 00	0 00	0 00	0 00	0 00
Total	100 23	100 24	101 22	101 28	100 42	101 05	100 61
	Structural formula calculated based on 6 atoms of oxygen and 4 cations						
Na	1 010	0 996	0 989	0 996	0 995	1 002	0 991
K	0 000	0 000	0 000	0 000	0 000	0 000	0 000
Ca	0 000	0 004	0 006	0 006	0 009	0 008	0 012
Fe^{3+}	0 889	0 880	0 840	0 851	0 867	0 868	0 892
Fe^{2+}	0 072	0 093	0 114	0 096	0 088	0 083	0 090
Mg	0 002	0 000	0 000	0 000	0 001	0 000	0 001
Mn	0 000	0 000	0 000	0 000	0 000	0 000	0 000
Zn	0 001	0 000	0 001	0 001	0 001	0 001	0 000
Nb	0 000	0 000	0 000	0 000	0 000	0 000	0 000
V	0 000	0 001	0 000	0 000	0 000	0 001	0 000
Cr	0 000	0 000	0 000	0 000	0 000	0 000	0 000
Yb	0 000	0 000	0 000	0 000	0 000	0 000	0 000
Zr	0 002	0 000	0 001	0 001	0 001	0 002	0 000
Ti	0 022	0 017	0 029	0 026	0 024	0 026	0 013
Al	0 011	0 011	0 019	0 022	0 024	0 015	0 008
Si	1 993	1 997	2 000	1 999	1 990	1 994	1 994
F	0 000	0 000	0 000	0 000	0 000	0 000	0 000
Cl	0 000	0 000	0 000	0 000	0 001	0 001	0 001

Absent oxides were not analyzed.

Appendix B-2 Electron-microprobe analyses of aegirine

Type	Type-3 (Yellow-green)										
Unit	Lindinaite						Ore Zone				
Sample #	SL-BS-1						SL-1-20				
Description		area		brgr		yell		ph	ph	ph	near
File	am93	am93	am93	am93	am93	am93	am93	am93	am93	am93	am93
#	4	5	6	7	8	9	21	22	23	24	25
Analysis #	4	6	7	8	9	10	24	25	26	27	28
Na_2O	13.48	13.83	13.87	14.03	13.76	13.85	13.54	13.79	13.80	13.82	13.68
K_2O	0.00	0.01	0.01	0.00	0.01	0.01	0.00	0.00	0.00	0.00	0.01
CaO	0.22	0.06	0.08	0.13	0.16	0.15	0.11	0.10	0.13	0.15	0.18
Fe_2O_3	30.98	33.45	33.85	34.32	33.11	32.99	31.84	32.46	31.89	30.24	31.55
FeO	2.39	0.67	0.58	0.00	1.27	0.93	1.75	0.68	0.64	0.85	1.21
MgO	0.00	0.00	0.02	0.00	0.00	0.01	0.00	0.00	0.03	0.01	0.00
MnO	0.52	0.54	0.21	0.04	0.07	0.16	0.18	0.40	0.53	0.55	0.54
ZnO	0.11	0.04	0.11	0.04	0.04	0.18	0.03	0.17	0.24	0.26	0.20
Nb_2O_5	0.18	0.05	0.00	0.00	0.05	0.00	0.06	0.03	0.05	0.03	0.08
V_2O_3	0.01	0.00	0.00	0.00	0.01	0.03	0.03	0.00	0.00	0.00	0.00
Cr_2O_3											
Yb_2O_3											
ZrO_2	0.10	0.02	0.00	0.02	0.04	0.01	0.08	0.11	0.16	0.18	0.40
TiO_2	0.46	0.28	0.29	0.31	0.25	0.71	0.44	1.09	1.33	1.46	0.71
Al_2O_3	0.44	0.12	0.18	0.39	0.24	0.25	0.20	0.20	0.25	0.37	0.27
SiO_2	52.43	52.09	51.98	51.86	52.07	52.09	51.68	51.46	51.56	51.97	51.94
F											
Cl											
Total	101.30	101.15	101.18	101.16	101.08	101.37	99.95	100.48	100.60	99.87	100.77
-O=F	0.00	0.00	0.00	0.00	0.00	0.00	0.00	0.00	0.00	0.00	0.00
-O=Cl	0.00	0.00	0.00	0.00	0.00	0.00	0.00	0.00	0.00	0.00	0.00
Total	101.30	101.15	101.18	101.16	101.08	101.37	99.95	100.48	100.60	99.87	100.77
	Structural formula calculated based on 6 atoms of oxygen and 4 cations										
Na	0.989	1.016	1.018	1.029	1.011	1.014	1.007	1.020	1.019	1.024	1.009
K	0.000	0.000	0.001	0.000	0.000	0.001	0.000	0.000	0.000	0.000	0.000
Ca	0.009	0.003	0.003	0.005	0.007	0.006	0.005	0.004	0.005	0.006	0.007
Fe^{2+}	0.883	0.954	0.965	0.976	0.945	0.938	0.919	0.932	0.914	0.870	0.904
Fe^{3+}	0.076	0.021	0.018	0.000	0.040	0.029	0.056	0.022	0.020	0.027	0.038
Mg	0.000	0.000	0.001	0.000	0.000	0.001	0.000	0.000	0.001	0.000	0.000
Mn	0.017	0.017	0.007	0.001	0.002	0.005	0.006	0.013	0.017	0.018	0.018
Zn	0.003	0.001	0.003	0.001	0.001	0.005	0.001	0.005	0.007	0.007	0.006
Nb	0.003	0.001	0.000	0.000	0.001	0.000	0.001	0.001	0.001	0.000	0.001
V	0.000	0.000	0.000	0.000	0.000	0.001	0.001	0.000	0.000	0.000	0.000
Cr	0.000	0.000	0.000	0.000	0.000	0.000	0.000	0.000	0.000	0.000	0.000
Yb	0.000	0.000	0.000	0.000	0.000	0.000	0.000	0.000	0.000	0.000	0.000
Zr	0.002	0.000	0.000	0.000	0.001	0.000	0.002	0.002	0.003	0.003	0.007
Ti	0.013	0.008	0.008	0.009	0.007	0.020	0.013	0.031	0.038	0.042	0.020
Al	0.020	0.005	0.008	0.018	0.011	0.011	0.009	0.009	0.011	0.017	0.012
Si	1.986	1.974	1.968	1.960	1.974	1.968	1.981	1.962	1.963	1.986	1.977
F	0.000	0.000	0.000	0.000	0.000	0.000	0.000	0.000	0.000	0.000	0.000
Cl	0.000	0.000	0.000	0.000	0.000	0.000	0.000	0.000	0.000	0.000	0.000

Absent oxides were not analyzed

Appendix B-2 Electron-microprobe analyses of aegirine

Type	The Rest										
Unit	Altered Subsolvus			Fresh Subsolvus				Hypersolvus	Altered Subsolvus		
Sample #	27-A-2			38-B-3				48-A-7	36-B-3		
Description	gr	dkgr	gr	core	mid	mid	ed	aeg	alt	3 dk	dkalt
File	am93	am93	am93	lcp	lcp	lcp	lcp	lcp	lcpadd	lcpadd	lcpadd
#	83	89	92								
Analysis #	104	112	115	94	96	97	98	14	295	271	273
Na_2O	13.15	13.73	13.70	13.96	13.61	13.86	13.81	13.61	12.15	12.41	12.92
K_2O	0.00	0.00	0.01	0.00	0.00	0.00	0.00	0.00	0.00	0.00	0.00
CaO	0.01	0.00	0.04	0.05	0.06	0.10	0.02	0.02	2.06	1.62	1.07
Fe_2O_3	29.33	32.84	32.11	32.76	29.90	31.78	30.88	31.45	31.69	31.82	33.12
FeO	3.84	1.37	1.51	0.72	2.56	1.42	1.76	2.66	2.37	2.40	1.34
MgO	0.01	0.03	0.03	0.01	0.01	0.02	0.00	0.02	0.17	0.06	0.10
MnO	0.02	0.03	0.25	0.08	0.20	0.09	0.22	0.05	1.14	0.88	0.60
ZnO	0.00	0.01	0.09	0.00	0.00	0.00	0.00	0.00	0.33	0.51	0.06
Nb_2O_5	0.00	0.00	0.01	0.00	0.00	0.00	0.00	0.00	0.03	0.03	0.00
V_2O_3	0.03	0.00	0.00	0.00	0.01	0.00	0.02	0.02	0.01	0.00	0.00
Cr_2O_3				0.00	0.00	0.00	0.00	0.01	0.01	0.00	0.00
Yb_2O_3				0.01	0.01	0.00	0.00	0.01	0.00	0.00	0.00
ZrO_2	0.16	0.06	0.11	0.18	0.19	0.13	0.18	0.05	0.08	0.11	0.07
TiO_2	0.73	0.60	0.66	1.07	1.68	1.15	1.59	0.62	0.89	0.65	0.60
Al_2O_3	0.26	0.39	0.24	0.35	0.37	0.40	0.28	0.33	0.22	0.20	0.40
SiO_2	51.78	51.68	52.02	51.70	51.93	52.05	51.93	52.51	49.84	50.31	50.20
F				0.00	0.00	0.00	0.00	0.00	0.00	0.00	0.00
Cl				0.00	0.00	0.00	0.00	0.00	0.01	0.02	0.02
Total	99.30	100.75	100.78	100.90	100.53	101.00	100.69	101.35	100.98	101.01	100.50
-O=F	0.00	0.00	0.00	0.00	0.00	0.00	0.00	0.00	0.00	0.00	0.00
-O=Cl	0.00	0.00	0.00	0.00	0.00	0.00	0.00	0.00	0.00	0.00	0.00
Total	99.30	100.75	100.78	100.90	100.53	101.00	100.69	101.35	100.97	101.01	100.49
	Structural formula calculated based on 6 atoms of oxygen and 4 cations										
Na	0.985	1.012	1.010	1.027	1.005	1.017	1.018	0.998	0.907	0.925	0.963
K	0.000	0.000	0.001	0.000	0.000	0.000	0.000	0.000	0.000	0.000	0.000
Ca	0.001	0.000	0.001	0.002	0.002	0.004	0.001	0.001	0.085	0.067	0.044
Fe^{3+}	0.853	0.940	0.919	0.935	0.857	0.906	0.883	0.895	0.919	0.921	0.958
Fe^{2+}	0.124	0.044	0.048	0.023	0.082	0.045	0.056	0.084	0.076	0.077	0.043
Mg	0.000	0.001	0.002	0.000	0.001	0.001	0.000	0.001	0.010	0.003	0.006
Mn	0.001	0.001	0.008	0.003	0.006	0.003	0.007	0.002	0.037	0.029	0.019
Zn	0.000	0.000	0.002	0.000	0.000	0.000	0.000	0.000	0.009	0.015	0.002
Nb	0.000	0.000	0.000	0.000	0.000	0.000	0.000	0.000	0.000	0.000	0.000
V	0.001	0.000	0.000	0.000	0.000	0.000	0.001	0.001	0.000	0.000	0.000
Cr	0.000	0.000	0.000	0.000	0.000	0.000	0.000	0.000	0.000	0.000	0.000
Yb	0.000	0.000	0.000	0.000	0.000	0.000	0.000	0.000	0.000	0.000	0.000
Zr	0.003	0.001	0.002	0.003	0.004	0.002	0.003	0.001	0.001	0.002	0.001
Ti	0.021	0.017	0.019	0.031	0.048	0.033	0.045	0.018	0.026	0.019	0.017
Al	0.012	0.018	0.011	0.016	0.016	0.018	0.012	0.015	0.010	0.009	0.018
Si	2.000	1.965	1.977	1.960	1.978	1.971	1.974	1.986	1.919	1.934	1.929
F	0.000	0.000	0.000	0.000	0.000	0.000	0.000	0.000	0.000	0.000	0.000
Cl	0.000	0.000	0.000	0.000	0.000	0.000	0.000	0.000	0.001	0.001	0.001

Absent oxides were not analyzed.

Appendix B-2 Electron-microprobe analyses of aegirine

Type	Average Green	Average Yellow			Average Subsolvus			Average Yellow-Green
Unit			Hypersolvus	Near Contact	All	Drill Core	Altered	
Sample #								
Description								
File #								
Analysis #								
Na_2O		13 60	13 48	13 36	13 52	13 49	13 48	13 50	13.77
K_2O		0 01	0 00	0 00	0 00	0 00	0 00	0 00	0 00
CaO		0 13	0 18	0 13	0 17	0 19	0 19	0 19	0 13
Fe_2O_3		28 78	31 28	29 79	30 30	31 72	31 10	32 01	32 42
FeO		2 77	2 05	3 04	2 44	1 82	2 15	1 66	1 00
MgO		0 01	0 03	0 02	0 02	0 03	0 02	0 04	0 01
MnO		0 22	0 30	0 17	0 40	0 32	0 42	0 29	0 34
ZnO		0 02	0 08	0 01	0 10	0 08	0 10	0 07	0 13
Nb_2O_5		0 02	0 02	0 01	0 01	0 02	0 04	0 02	0 05
V_2O_3		0 02	0 01	0 01	0 01	0 01	0 01	0 01	0 01
Cr_2O_3		0 00	0 00	0 00	0 00	0 00	0 00	0 00	
Yb_2O_3		0 01	0 01	0 01	0 02	0 01		0 01	
ZrO_2		0 32	0 20	0 36	0 50	0 10	0 10	0 10	0 10
TiO_2		2 14	0 79	1 16	0 92	0 71	0 77	0 68	0 67
Al_2O_3		0 35	0 30	0 27	0 18	0 33	0 28	0 36	0 26
SiO_2		51 91	51 67	51 73	51 96	51 58	51 82	51 47	51 92
F		0 00	0 00	0 00	0 00	0 00	0 00	0 00	
Cl		0 00	0 01	0 00	0 01	0 01	0 01	0 01	
Total		100 32	100 30	100 07	100 29	100.34	100 23	100 39	100 81
-O=F		0 00	0 00	0 00	0 00	0 00	0 00	0 00	0 00
-O=Cl		0 00	0 00	0 00	0 00	0 00	0 00	0 00	0 00
Total		100 32	100 30	100 07	100 28	100 33	100 23	100 38	100 81
				Structural formula calculated based on 6 atoms of oxygen and 4 cations					
Na		1.006	1 000	0.993	1 002	1 000	0 999	1 000	1 014
K		0 000	0 000	0 000	0 000	0 000	0 000	0 000	0 000
Ca		0 006	0 008	0 005	0 007	0 008	0 008	0 008	0 005
Fe^{3+}		0 826	0.900	0 860	0 872	0 912	0 895	0 920	0 927
Fe^{2+}		0 088	0 066	0 098	0 078	0 058	0 069	0 053	0 032
Mg		0 001	0 002	0 001	0 001	0 002	0 001	0 002	0 000
Mn		0 007	0 007	0 006	0 005	0 008	0 006	0 009	0 011
Zn		0 001	0 002	0 000	0 003	0 002	0 003	0 002	0 004
Nb		0 000	0 000	0 000	0 000	0 000	0 000	0 000	0 001
V		0 001	0 000	0 000	0 000	0 000	0 000	0 000	0 000
Cr		0 000	0 000	0 000	0 000	0 000	0 000	0 000	0 000
Yb		0 000	0 000	0 000	0 000	0 000	0 000	0 000	0.000
Zr		0 006	0 004	0 007	0 009	0 002	0 002	0 002	0 002
Ti		0 061	0 023	0 034	0 027	0 020	0 022	0 020	0 019
Al		0 016	0 013	0 012	0 008	0 015	0 012	0 016	0 012
Si		1 980	1.976	1 984	1 987	1 972	1 982	1 967	1 973
F		0 000	0 000	0 000	0 000	0 000	0 000	0 000	0 000
Cl		0 000	0 000	0 000	0 000	0 000	0 000	0 000	0 000

Absent oxides were not analyzed.

Appendix B-3 Electron-microprobe analyses of selected titanium minerals

Mineral	Astrophyllite														
Sample#	38-A-3											38-B-381			
Description	gr#1														
File Name	jrastal.tr	jrastal.tr	jrastal.tr	jrastal.tr	jrastal.tr	jrastal.tr	jrastal.tr	jrastal.tr	jrastal.tr	jrastal.tr	jrastal.tr	Mar26/93	Mar26/93	Mar26/93	Mar26/93	Mar26/93
Analysis #	1	5	7	19	21	22	24	25	27	29	30	1	5	7	19	21
Na_2O	3.17	3.06	3.24	2.90	3.14	3.43	3.29	3.18	3.26	4.19	3.22	0.02	3.06	3.24	2.90	3.14
K_2O	4.24	4.29	4.19	2.26	4.55	2.70	4.58	4.66	4.50	1.79	4.38	5.10	5.16	5.05	2.72	5.48
CaO	0.14	0.08	0.09	0.07	0.20	0.13	0.35	0.25	0.11	0.08	0.36	0.14	0.08	0.09	0.07	0.20
MgO	0.03	0.05	0.03	0.09	0.01	0.01	0.00	0.01	0.00	0.01	0.01	0.03	0.05	0.03	0.09	0.01
FeO	32.90	31.65	31.90	34.01	34.69	35.59	34.38	34.73	35.69	36.05	36.05	32.90	31.65	31.90	34.01	34.69
MnO	4.29	5.13	4.98	1.27	1.99	1.89	1.87	1.78	1.54	1.41	1.49	4.29	5.13	4.98	1.27	1.99
ZnO	0.23	0.25	0.21	0.40	0.54	0.45	0.38	0.42	0.45	0.30	0.36	0.29	0.25	0.21	0.40	0.54
Y_2O_3																
SnO_2																
PbO																
BaO																
V_2O_3																
SrO																
TiO_2	11.90	10.09	11.96	11.34	12.06	10.52	11.03	11.21	12.13	10.01	11.95	11.90	10.09	11.96	11.34	12.06
ZrO_2	0.02	1.61	0.08	0.10	0.04	0.07	0.02	0.02	0.01	0.00	0.05	0.02	1.61	0.08	0.10	0.04
Nb_2O_5	0.10	1.09	0.33	0.22	0.09	0.33	1.65	1.61	0.09	0.07	0.03	0.10	1.09	0.33	0.22	0.09
SiO_2	35.25	35.18	35.67	35.99	36.28	39.30	36.01	35.98	35.88	41.88	35.67	35.25	35.17	35.67	35.98	36.28
Al_2O_3	0.08	0.16	0.06	0.36	0.05	0.07	0.06	0.06	0.04	0.19	0.34	0.08	0.16	0.06	0.36	0.05
F	1.34	1.27	0.93	0.91	0.93	1.30	1.03	1.07	1.04	0.92	1.02	1.34	1.27	0.93	0.91	0.93
Cl	0.01	0.00	0.00	0.02	0.01	0.00	0.00	0.01	0.00	0.00	0.01	0.01	0.00	0.00	0.02	3.01
Total	90.54	90.83	90.41	87.02	91.42	92.36	91.34	91.80	91.48	92.69	91.72	91.49	94.76	94.51	90.38	98.50
						Structural formula calculated based on 31 atoms of oxygen										
Na	1.483	1.439	1.515	1.383	1.454	1.533	1.528	1.471	1.508	1.828	1.491	0.011	1.433	1.509	1.380	1.405
K	1.304	1.327	1.298	0.709	1.384	0.794	1.398	1.417	1.370	0.515	1.334	1.602	1.591	1.545	0.852	1.611
Ca	0.037	0.021	0.024	0.017	0.052	0.033	0.090	0.063	0.028	0.019	0.092	0.038	0.021	0.024	0.017	0.050
Mg	0.010	0.016	0.011	0.032	0.004	0.004	0.001	0.004	0.000	0.002	0.002	0.010	0.016	0.011	0.031	0.003
Fe^{2+}	6.641	6.421	6.432	7.000	6.924	6.873	6.879	6.931	7.133	6.786	7.197	6.770	6.393	6.405	6.984	6.691
Mn	0.877	1.055	1.016	0.265	0.401	0.369	0.378	0.360	0.311	0.269	0.301	0.895	1.050	1.012	0.264	0.388
Zn	0.041	0.044	0.037	0.073	0.094	0.077	0.067	0.074	0.080	0.049	0.064	0.052	0.044	0.037	0.073	0.091
Y	0.000	0.000	0.000	0.000	0.000	0.000	0.000	0.000	0.000	0.000	0.000	0.000	0.000	0.000	0.000	0.000
Sn	0.000	0.000	0.000	0.000	0.000	0.000	0.000	0.000	0.000	0.000	0.000	0.000	0.000	0.000	0.000	0.000
Pb	0.000	0.000	0.000	0.000	0.000	0.000	0.000	0.000	0.000	0.000	0.000	0.000	0.000	0.000	0.000	0.000
Ba	0.000	0.000	0.000	0.000	0.000	0.000	0.000	0.000	0.000	0.000	0.000	0.000	0.000	0.000	0.000	0.000
V	0.000	0.000	0.000	0.000	0.000	0.000	0.000	0.000	0.000	0.000	0.000	0.000	0.000	0.000	0.000	0.000
Sr	0.000	0.000	0.000	0.000	0.000	0.000	0.000	0.000	0.000	0.000	0.000	0.000	0.000	0.000	0.000	0.000
Ti	2.161	1.840	2.168	2.099	2.164	1.828	1.984	2.011	2.180	1.693	2.145	2.203	1.832	2.159	2.094	2.091
Zr	0.003	0.190	0.009	0.012	0.005	0.008	0.002	0.003	0.001	0.000	0.006	0.003	0.189	0.009	0.012	0.005
Nb	0.011	0.119	0.036	0.024	0.010	0.035	0.179	0.173	0.010	0.007	0.004	0.012	0.119	0.036	0.025	0.010
Si	8.509	8.533	8.600	8.856	8.658	9.073	8.614	8.585	8.574	9.424	8.513	8.674	8.496	8.563	8.835	8.366
Al	0.024	0.045	0.017	0.105	0.013	0.018	0.017	0.017	0.011	0.049	0.096	0.024	0.045	0.016	0.105	0.013
F	1.019	0.977	0.709	0.707	0.701	0.946	0.778	0.809	0.788	0.653	0.769	1.039	0.972	0.706	0.705	0.678
Cl	0.003	0.001	0.000	0.007	0.002	0.001	0.000	0.003	0.000	0.000	0.005	0.003	0.001	0.000	0.007	1.174
Σ Cations	21.100	21.052	21.152	20.575	21.163	20.645	21.136	21.107	21.207	20.641	21.246	20.294	21.230	21.325	20.672	20.724

Appendix B-3 Electron-microprobe analyses of selected titanium minerals

Mineral	Astrophyllite															
Sample#	38-B-3#1						46-B-3			48-F-1						
Description																
File Name	Mar26/93	Mar26/93	Mar26/93	Mar26/93	Mar26/93	Mar26/93	1/1/95	1/1/95	1/1/95	3/1/93	3/1/93	3/1/93	1/1/95	1/1/95	1/1/95	1/1/95
Analysis #	22	24	25	27	29	30	82	83	86	83	84	85	35	36	37	38
Na_2O	3.43	3.29	3.18	3.26	4.19	3.22	3.66	2.22	3.72	3.34	3.19	3.40	3.52	3.61	3.51	3.69
K_2O	3.25	5.52	5.61	5.42	2.16	5.28	5.34	2.43	4.50	5.34	5.63	5.48	5.57	5.63	4.87	5.41
CaO	0.13	0.35	0.25	0.11	0.08	0.36	0.17	3.72	0.12	0.46	0.30	0.58	0.19	0.12	0.20	0.03
MgO	0.01	0.00	0.01	0.00	0.01	0.00	0.03	0.10	0.10	0.05	0.05	0.06	0.01	0.01	0.01	0.03
FeO	35.59	34.38	34.73	35.69	36.05	36.05	31.06	32.15	34.68	33.58	32.99	35.09	36.28	36.16	34.45	36.52
MnO	1.89	1.86	1.78	1.54	1.41	1.49	4.91	0.34	1.88	1.32	1.37	1.43	1.29	1.38	1.36	0.69
ZnO	0.46	0.38	0.42	0.45	0.30	0.36	0.52	1.08	0.78	0.28	0.30	0.30	0.37	0.44	0.37	0.10
Y_2O_3							0.00	0.00	0.00				0.00	0.00	0.00	0.00
SnO_2							0.47	0.00	0.00				0.00	0.00	0.00	0.00
PbO							0.05	1.16	0.08				0.10	0.03	0.09	0.02
BaO							0.18	0.20	0.04				0.11	0.14	0.12	0.05
V_2O_3																
SrO							0.00	0.00	0.00				0.00	0.00	0.00	0.00
TiO_2	10.52	11.03	11.21	12.13	10.00	11.95	9.64	9.67	11.71	10.92	11.08	11.38	12.05	11.77	10.51	11.26
ZrO_2	0.07	0.02	0.02	0.01	0.00	0.05	0.89	0.40	0.08	0.42	0.17	0.10	0.00	0.00	0.05	0.30
Nb_2O_5	0.33	1.65	1.61	0.10	0.07	0.03	1.95	0.70	0.02	0.43	0.97	0.22	0.00	0.00	1.91	0.39
SiO_2	39.29	36.00	32.98	35.88	41.88	35.66	36.12	33.24	36.33	34.74	34.90	35.01	36.40	36.49	35.99	36.22
Al_2O_3	0.07	0.06	0.06	0.04	0.19	0.34	0.18	0.37	0.02	0.07	0.07	0.04	0.05	0.17	0.13	0.07
F	1.30	1.03	1.07	1.04	0.92	1.02	0.62	3.97	0.72	1.46	0.29	1.33	1.15	1.17	1.09	1.22
Cl	0.00	0.00	0.01	0.00	0.00	0.01	0.00	0.03	0.00	0.00	0.01	0.00	0.01	0.01	0.00	0.02
Total	96.34	95.57	92.93	95.65	97.24	95.83	95.53	90.09	94.47	92.41	91.31	94.44	96.60	96.63	94.21	95.50
							Structural formula calculated based on 31 atoms of oxygen									
Na	1.530	1.521	1.535	1.501	1.823	1.485	1.698	1.056	1.724	1.592	1.543	1.593	1.602	1.641	1.634	1.696
K	0.954	1.677	1.781	1.644	0.619	1.600	1.632	0.759	1.373	1.674	1.789	1.689	1.667	1.686	1.490	1.636
Ca	0.032	0.089	0.066	0.028	0.018	0.091	0.043	0.979	0.030	0.122	0.080	0.150	0.049	0.029	0.052	0.007
Mg	0.004	0.001	0.004	0.000	0.002	0.001	0.011	0.036	0.036	0.020	0.017	0.021	0.005	0.003	0.004	0.009
Fe^{2+}	6.855	6.847	7.231	7.101	6.775	7.166	6.220	6.598	6.933	6.897	6.874	7.092	7.122	7.093	6.908	7.238
Mn	0.368	0.376	0.375	0.310	0.268	0.300	0.995	0.071	0.381	0.275	0.289	0.292	0.256	0.275	0.277	0.139
Zn	0.077	0.066	0.077	0.079	0.049	0.064	0.093	0.195	0.137	0.050	0.055	0.054	0.064	0.077	0.066	0.018
Y	0.000	0.000	0.000	0.000	0.000	0.000	0.000	0.000	0.000	0.000	0.000	0.000	0.000	0.000	0.000	0.000
Sn	0.000	0.000	0.000	0.000	0.000	0.000	0.050	0.000	0.000	0.000	0.000	0.000	0.000	0.000	0.000	0.000
Pb	0.000	0.000	0.000	0.000	0.000	0.000	0.003	0.076	0.005	0.000	0.000	0.000	0.006	0.002	0.006	0.001
Ba	0.000	0.000	0.000	0.000	0.000	0.000	0.017	0.019	0.004	0.000	0.000	0.000	0.010	0.013	0.011	0.005
V	0.000	0.000	0.000	0.000	0.000	0.000	0.000	0.000	0.000	0.000	0.000	0.000	0.000	0.000	0.000	0.000
Sr	0.000	0.000	0.000	0.000	0.000	0.000	0.000	0.000	0.000	0.000	0.000	0.000	0.000	0.000	0.000	0.000
Ti	1.823	1.976	2.098	2.170	1.690	2.136	1.735	1.783	2.104	2.017	2.076	2.068	2.126	2.076	1.896	2.006
Zr	0.008	0.002	0.003	0.001	0.000	0.006	0.104	0.048	0.009	0.050	0.020	0.012	0.000	0.000	0.006	0.035
Nb	0.035	0.178	0.181	0.010	0.007	0.004	0.212	0.078	0.002	0.047	0.109	0.024	0.000	0.000	0.207	0.042
Si	9.050	8.574	8.210	8.535	9.409	8.476	8.648	8.156	8.685	8.533	8.694	8.459	8.543	8.559	8.630	8.583
Al	0.018	0.017	0.017	0.011	0.049	0.095	0.052	0.106	0.007	0.019	0.021	0.013	0.012	0.048	0.036	0.019
F	0.943	0.774	0.844	0.785	0.652	0.766	0.467	3.077	0.542	1.132	0.229	1.017	0.851	0.866	0.824	0.917
Cl	0.001	0.000	0.003	0.000	0.000	0.005	0.000	0.012	0.001	0.000	0.003	0.001	0.003	0.003	0.000	0.008
Σ Cations	20.754	21.323	21.576	21.390	20.710	21.424	21.514	19.960	21.429	21.296	21.567	21.469	21.463	21.501	21.223	21.434

Appendix B-3 Electron-microprobe analyses of selected titanium minerals

Mineral	Astrophyllite															
Sample#	48-F-1			48-F-1.2						48-F-2 spray		49-A-1	49-C-1			
Description																
File Name	1/1/95	1/1/95	1/1/95	1/1/95	1/1/95	1/1/95	1/1/95	1/1/95	1/1/95	Mar30/93	Mar30/93	1/1/95	Mar-93	Mar-93	Mar-93	Mar-93
Analysis #	56	61	67	17	18	19	20	23	26	5	6	75	67	68	69	70
Na_2O	3.17	3.37	3.54	2.59	2.86	2.57	2.71	3.01	3.73	3.14	2.87	2.32	3.08	1.76	3.03	3.18
K_2O	1.30	5.68	5.62	6.19	6.15	6.07	6.00	5.93	5.89	2.92	5.84	1.61	4.57	2.04	5.84	5.47
CaO	0.14	0.47	0.19	0.75	0.67	0.69	0.62	0.58	0.44	0.12	0.74	0.21	0.21	0.91	0.40	0.27
MgO	0.01	0.01	0.00	0.10	0.12	0.12	0.10	0.10	0.05	0.01	0.04	0.04	0.03	0.07	0.05	0.02
FeO	34.67	35.38	35.22	36.99	36.58	36.84	36.65	36.20	33.25	33.01	35.35	30.21	33.86	27.03	33.98	35.50
MnO	1.78	1.58	1.60	0.82	0.86	0.85	0.89	1.06	1.39	1.60	1.47	2.89	2.05	1.81	1.64	1.74
ZnO	0.66	0.46	0.43	0.06	0.08	0.07	0.08	0.05	0.25	0.06	0.05	0.99	0.39	0.27	0.16	0.11
Y_2O_3	0.00	0.00	0.00	0.00	0.00	0.00	0.00	0.00	0.00			0.00				
SnO_2	0.00	0.00	0.00	0.00	0.00	0.00	0.00	0.00	0.00			0.00				
PbO	0.53	0.17	0.61	0.00	0.00	0.04	0.00	0.02	0.07			1.30				
BaO	0.10	0.09	0.17	0.35	0.37	0.53	0.43	0.31	0.12			0.52				
V_2O_3										0.05	0.04					
SrO	0.00	0.00	0.00	0.00	0.00	0.00	0.00	0.00	0.00			0.00				
TiO_2	11.30	12.01	11.97	11.33	11.73	11.43	11.69	11.78	10.51	8.97	11.22	9.09	9.44	10.13	10.20	12.32
ZrO_2	0.17	0.00	0.05	0.00	0.17	0.11	0.04	0.03	0.65	1.04	0.66	1.59	1.65	0.30	1.25	0.05
Nb_2O_5	0.07	0.00	0.00	0.00	0.00	0.00	0.00	0.00	1.49	1.88	0.17	0.64	1.41	1.44	1.30	0.01
SiO_2	37.12	36.09	35.99	35.33	35.78	35.34	35.17	35.86	35.53	38.21	34.86	36.77	35.03	33.23	35.48	36.02
Al_2O_3	0.30	0.14	0.06	1.60	0.95	1.30	1.16	0.74	0.09	1.59	0.42	0.64	0.31	0.30	0.18	0.15
F	0.93	0.80	0.73	0.85	0.89	1.00	0.74	1.09	1.13			1.14	1.22	3.29	1.42	1.20
Cl	0.01	0.01	0.00	0.00	0.00	0.01	0.01	0.00	0.00			0.05	0.00	0.25	0.00	0.00
Total	92.08	95.91	95.86	96.60	96.82	96.52	95.98	96.30	94.11	92.61	93.74	89.50	93.26	82.83	94.93	96.03
							Structural formula calculated based on 31 atoms of oxygen									
Na	1.474	1.548	1.634	1.186	1.304	1.177	1.250	1.375	1.745	1.450	1.366	1.113	1.460	0.889	1.410	1.455
K	0.398	1.719	1.709	1.863	1.847	1.830	1.822	1.784	1.811	0.889	1.828	0.507	1.426	0.678	1.791	1.647
Ca	0.037	0.118	0.049	0.190	0.168	0.174	0.159	0.146	0.113	0.030	0.195	0.056	0.054	0.254	0.102	0.069
Mg	0.003	0.005	0.000	0.036	0.043	0.041	0.034	0.035	0.019	0.005	0.014	0.015	0.011	0.028	0.017	0.008
Fe^{2+}	6.965	7.017	7.022	7.304	7.195	7.281	7.292	7.134	6.704	6.584	7.249	6.250	6.924	5.892	6.830	7.013
Mn	0.363	0.317	0.323	0.164	0.171	0.170	0.180	0.211	0.283	0.323	0.306	0.606	0.425	0.401	0.334	0.348
Zn	0.117	0.081	0.075	0.011	0.013	0.012	0.014	0.009	0.044	0.011	0.010	0.181	0.070	0.053	0.028	0.019
Y	0.000	0.000	0.000	0.000	0.000	0.000	0.000	0.000	0.000	0.000	0.000	0.000	0.000	0.000	0.000	0.000
Sn	0.000	0.000	0.000	0.000	0.000	0.000	0.000	0.000	0.000	0.000	0.000	0.000	0.000	0.000	0.000	0.000
Pb	0.034	0.011	0.039	0.000	0.000	0.003	0.000	0.001	0.004	0.000	0.000	0.086	0.000	0.000	0.000	0.000
Ba	0.028	0.008	0.016	0.033	0.034	0.049	0.040	0.029	0.012	0.000	0.000	0.051	0.000	0.000	0.000	0.000
V	0.000	0.000	0.000	0.000	0.000	0.000	0.000	0.000	0.000	0.009	0.007	0.000	0.000	0.000	0.000	0.000
Sr	0.000	0.000	0.000	0.000	0.000	0.000	0.000	0.000	0.000	0.000	0.000	0.000	0.000	0.000	0.000	0.000
Ti	2.042	2.142	2.145	2.011	2.074	2.032	2.091	2.087	1.906	1.608	2.069	1.690	1.736	1.986	1.844	2.189
Zr	0.020	0.000	0.006	0.000	0.020	0.012	0.005	0.003	0.077	0.121	0.079	0.192	0.197	0.038	0.146	0.015
Nb	0.007	0.000	0.000	0.000	0.000	0.000	0.000	0.000	0.163	0.203	0.018	0.072	0.156	0.170	0.141	0.001
Si	8.917	8.559	8.579	8.340	8.416	8.351	8.369	8.449	8.567	9.113	8.547	9.095	8.567	8.662	8.526	8.510
Al	0.084	0.039	0.017	0.446	0.264	0.361	0.326	0.206	0.025	0.447	0.123	0.185	0.090	0.093	0.051	0.041
F	0.710	0.599	0.553	0.631	0.661	0.749	0.560	0.809	0.863	0.000	0.000	0.895	0.946	2.710	1.080	0.894
Cl	0.004	0.004	0.001	0.002	0.000	0.002	0.004	0.000	0.000	0.000	0.000	0.019	0.001	0.110	0.002	0.000
Σ Cations	20.490	21.563	21.612	21.584	21.550	21.493	21.581	21.469	21.472	20.794	21.810	20.099	21.116	19.143	21.220	21.307

Appendix B-3: Electron-microprobe analyses of selected titanium minerals

Mineral	Astrophyllite														
Sample#	49-C-1													58-F-1	
Description	ed	mid	ed	mid	#5In	ed	mid	ed	green	mid	ed			#3	ed
File Name	Mar-93	Mar-93	Mar-93	Mar-93	Mar-93	Mar-93	Mar-93	Mar-93	Mar-93	Mar-93	Mar-93	1/1/95	1/1/95	1/1/95	Mar-93	Mar-93
Analysis #	71	72	73	74	75	76	77	78	79	80	81	90	91	92	101	102
Na_2O	3.36	3.70	3.55	3.15	2.61	3.11	3.01	3.07	3.14	3.14	3.45	2.87	3.03	3.03	3.15	3.10
K_2O	3.74	2.44	0.80	5.50	4.97	1.68	5.62	5.51	4.79	5.07	0.84	3.25	3.08	3.41	5.54	5.41
CaO	0.21	1.57	0.31	0.22	0.44	1.71	0.32	0.29	0.32	0.53	0.50	0.44	0.37	0.38	0.31	0.18
MgO	0.01	0.02	0.01	0.04	0.08	0.08	0.05	0.05	0.06	0.03	0.02	0.06	0.06	0.07	0.08	0.07
FeO	35.18	34.45	35.52	34.96	28.95	34.90	34.01	34.82	34.13	34.40	34.80	35.94	35.72	35.39	34.45	35.08
MnO	1.79	1.40	1.68	1.54	1.28	1.62	1.44	1.58	1.63	1.53	1.89	1.08	1.08	1.10	1.60	1.64
ZnO	0.11	0.16	0.19	0.11	0.21	0.28	0.20	0.20	0.11	0.15	0.10	0.20	0.17	0.17	0.27	0.25
Y_2O_3												0.00	0.00	0.00		
SnO_2												0.00	0.00	0.00		
PbO												0.14	0.19	0.15		
BaO												0.12	0.10	0.16		
V_2O_3																
SrO												0.00	0.00	0.00		
TiO_2	10.46	11.47	11.02	10.71	9.51	10.19	10.40	10.57	10.34	11.08	11.41	11.52	11.48	11.51	12.01	11.58
ZrO_2	1.00	0.00	0.64	0.91	0.41	1.23	0.98	1.39	0.92	0.78	0.01	0.12	0.23	0.16	0.08	0.06
Nb_2O_5	0.93	0.02	0.71	1.33	0.87	1.21	1.16	0.95	0.86	0.23	0.47	0.00	0.00	0.00	0.07	0.04
SiO_2	35.72	36.19	35.06	35.06	32.56	34.47	34.82	34.80	34.88	35.06	35.44	36.55	36.38	36.25	35.19	35.26
Al_2O_3	0.18	0.08	0.24	0.10	0.36	0.14	0.17	0.18	0.16	0.15	0.18	0.37	0.31	0.27	0.08	0.10
F	1.27	2.80	1.16	1.11	1.28	1.30	1.17	1.18	1.37	1.43	1.34	1.12	0.90	1.24	1.48	1.48
Cl	0.00	0.02	0.03	0.00	0.01	0.04	0.01	0.01	0.01	0.00	0.03	0.00	0.01	0.01	0.01	0.00
Total	93.97	94.31	90.91	94.74	83.52	91.96	93.34	94.57	92.71	93.57	90.48	93.31	92.70	92.77	94.31	94.26
						Structural formula calculated based on 31 atoms of oxygen										
Na	1.568	1.685	1.691	1.476	1.357	1.481	1.426	1.441	1.491	1.476	1.637	1.329	1.411	1.411	1.468	1.449
K	1.150	0.733	0.251	1.694	1.701	0.525	1.753	1.704	1.496	1.569	0.263	0.991	0.945	1.044	1.701	1.662
Ca	0.054	0.396	0.081	0.057	0.127	0.449	0.083	0.075	0.084	0.137	0.130	0.112	0.096	0.099	0.079	0.047
Mg	0.005	0.008	0.002	0.014	0.032	0.030	0.018	0.019	0.022	0.010	0.007	0.021	0.020	0.025	0.029	0.027
Fe^{2+}	7.084	6.771	7.294	7.064	6.497	7.163	6.959	7.059	6.995	6.982	7.126	7.174	7.189	7.108	6.931	7.073
Mn	0.365	0.278	0.350	0.316	0.290	0.336	0.299	0.323	0.338	0.315	0.392	0.217	0.221	0.224	0.326	0.335
Zn	0.020	0.027	0.034	0.019	0.042	0.051	0.035	0.035	0.020	0.027	0.017	0.035	0.030	0.031	0.048	0.045
Y	0.000	0.000	0.000	0.000	0.000	0.000	0.000	0.000	0.000	0.000	0.000	0.000	0.000	0.000	0.000	0.000
Sn	0.000	0.000	0.000	0.000	0.000	0.000	0.000	0.000	0.000	0.000	0.000	0.000	0.000	0.000	0.000	0.000
Pb	0.000	0.000	0.000	0.000	0.000	0.000	0.000	0.000	0.000	0.000	0.000	0.009	0.012	0.010	0.000	0.000
Ba	0.000	0.000	0.000	0.000	0.000	0.000	0.000	0.000	0.000	0.000	0.000	0.011	0.009	0.015	0.000	0.000
V	0.000	0.000	0.000	0.000	0.000	0.000	0.000	0.000	0.000	0.000	0.000	0.000	0.000	0.000	0.000	0.000
Sr	0.000	0.000	0.000	0.000	0.000	0.000	0.000	0.000	0.000	0.000	0.000	0.000	0.000	0.000	0.000	0.000
Ti	1.895	2.028	2.035	1.946	1.919	1.881	1.913	1.928	1.906	2.022	2.101	2.068	2.078	2.078	2.172	2.099
Zr	0.118	0.000	0.077	0.108	0.053	0.147	0.117	0.164	0.110	0.092	0.001	0.014	0.027	0.018	0.009	0.007
Nb	0.101	0.002	0.078	0.146	0.106	0.135	0.128	0.104	0.095	0.025	0.052	0.000	0.000	0.000	0.008	0.004
Si	8.601	8.504	8.607	8.471	8.736	8.460	8.517	8.436	8.547	8.509	8.677	8.725	8.754	8.704	8.466	8.499
Al	0.050	0.022	0.069	0.028	0.113	0.041	0.050	0.052	0.045	0.042	0.053	0.105	0.087	0.076	0.022	0.028
F	0.966	2.080	0.904	0.846	1.083	1.007	0.906	0.902	1.059	1.098	1.038	0.844	0.682	0.940	1.128	1.131
Cl	0.000	0.007	0.010	0.002	0.006	0.017	0.004	0.003	0.003	0.000	0.011	0.001	0.003	0.004	0.003	0.000
Σ Cations	21.009	20.454	20.568	21.337	20.973	20.697	21.298	21.339	21.150	21.205	20.456	20.811	20.879	20.842	21.259	21.276

The acronyms are: ed=edge; mid=middle

Appendix B-3 Electron-microprobe analyses of selected titanium minerals

Mineral	Astrophyllite																	
Sample#	LB-9-2.12							LB-9-7.47										
Description																		
File Name	Mar-93	Mar-93	1/1/95	1/1/95	1/1/95	1/1/95	1/1/95	1/1/95	1/1/95	1/1/95	1/1/95	1/1/95	1/1/95	1/1/95	1/1/95	1/1/95	1/1/95	1/1/95
Analysis #	105	109	101	103	106	108	110	113	119	121	122	123	124	125	126	127	131	135
Na_2O	3.38	3.22	3.64	3.63	3.45	3.71	3.61	3.32	2.00	3.67	3.87	3.66	3.81	3.64	3.86	3.85	3.70	3.71
K_2O	5.49	4.05	4.64	5.60	5.63	5.44	4.20	5.73	1.66	5.69	5.69	5.72	5.22	5.47	4.86	5.15	5.83	5.69
CaO	0.07	0.09	0.14	0.27	0.29	0.21	0.15	0.29	0.64	0.29	0.36	0.43	0.19	0.14	0.22	0.15	0.20	0.34
MgO	0.16	0.03	0.07	0.02	0.01	0.00	0.06	0.04	0.93	0.04	0.04	0.05	0.14	0.14	0.16	0.13	0.04	0.04
FeO	35.93	35.32	35.45	35.92	36.10	36.06	36.16	35.48	24.49	34.21	33.67	33.59	35.74	35.83	35.69	35.77	35.87	34.59
MnO	1.21	1.64	1.58	1.28	1.27	1.21	1.10	1.65	1.23	1.62	1.74	1.83	1.13	1.13	1.07	1.18	1.28	1.60
ZnO	0.25	0.40	0.31	0.25	0.26	0.20	0.28	0.30	0.28	0.29	0.30	0.29	0.33	0.33	0.31	0.32	0.27	0.31
Y_2O_3			0.00	0.00	0.00	0.00	0.00	0.00	0.93	0.00	0.00	0.00	0.00	0.00	0.00	0.00	0.00	0.00
SnO_2			0.07	0.00	0.00	0.00	0.00	0.00	0.00	0.10	0.06	0.03	0.00	0.00	0.00	0.00	0.00	0.03
PbO			0.07	0.11	0.04	0.07	0.12	0.14	5.66	0.09	0.11	0.12	0.18	0.20	0.24	0.10	0.07	0.12
BaO			0.14	0.18	0.23	0.10	0.13	0.37	0.66	0.25	0.29	0.32	0.11	0.08	0.15	0.12	0.14	0.20
V_2O_3																		
SrO			0.00	0.00	0.00	0.00	0.00	0.00	0.00	0.00	0.00	0.00	0.00	0.00	0.00	0.00	0.00	0.00
TiO_2	11.39	11.38	11.62	11.82	11.89	11.70	11.52	11.66	9.46	11.00	9.95	9.63	11.86	12.01	12.06	11.91	11.79	10.53
ZrO_2	0.46	0.20	0.07	0.07	0.15	0.42	0.28	0.07	3.08	0.30	0.37	0.92	0.02	0.04	0.05	0.04	0.11	1.05
Nb_2O_5	0.10	0.21	0.00	0.00	0.00	0.00	0.00	0.00	1.02	0.70	2.35	2.43	0.00	0.00	0.00	0.00	0.09	1.11
SiO_2	35.14	34.73	36.90	36.80	36.65	36.63	37.36	36.20	36.13	36.40	35.93	35.38	36.63	36.58	36.57	36.64	36.38	36.39
Al_2O_3	0.02	0.11	0.06	0.05	0.13	0.06	0.20	0.24	0.30	0.08	0.18	0.32	0.05	0.03	0.02	0.05	0.01	0.07
F	1.24	1.12	0.76	1.23	0.88	0.71	1.07	0.78	0.63	0.65	0.64	1.00	1.11	0.95	0.76	1.02	1.02	0.77
Cl	0.00	0.06	0.01	0.01	0.01	0.00	0.01	0.01	0.17	0.00	0.00	0.00	0.00	0.01	0.01	0.00	0.01	0.01
Total	94.83	92.55	95.18	96.72	96.60	96.21	95.79	95.93	88.96	95.11	95.29	95.30	96.04	96.17	95.70	96.01	96.36	96.23
								Structural formula calculated based on 31 atoms of oxygen										
Na	1.581	1.530	1.671	1.645	1.573	1.697	1.638	1.530	0.986	1.702	1.802	1.703	1.739	1.663	1.766	1.754	1.690	1.706
K	1.690	1.266	1.402	1.670	1.686	1.637	1.253	1.737	0.539	1.735	1.741	1.754	1.565	1.641	1.465	1.545	1.752	1.720
Ca	0.019	0.024	0.035	0.068	0.072	0.052	0.037	0.073	0.175	0.075	0.093	0.110	0.047	0.036	0.055	0.039	0.049	0.086
Mg	0.057	0.010	0.024	0.007	0.005	0.000	0.022	0.014	0.353	0.014	0.015	0.016	0.049	0.048	0.057	0.047	0.013	0.013
Fe^{2+}	7.242	7.245	7.020	7.023	7.090	7.117	7.073	7.044	5.211	6.836	6.755	6.748	7.029	7.055	7.052	7.037	7.071	6.860
Mn	0.247	0.342	0.318	0.253	0.252	0.243	0.218	0.331	0.265	0.329	0.354	0.373	0.226	0.226	0.214	0.236	0.255	0.320
Zn	0.044	0.072	0.055	0.044	0.045	0.035	0.048	0.052	0.053	0.050	0.053	0.051	0.057	0.058	0.054	0.055	0.046	0.055
Y	0.000	0.000	0.000	0.000	0.000	0.000	0.000	0.000	0.125	0.000	0.000	0.000	0.000	0.000	0.000	0.000	0.000	0.000
Sn	0.000	0.000	0.007	0.000	0.000	0.000	0.000	0.000	0.000	0.011	0.006	0.004	0.000	0.000	0.000	0.000	0.000	0.003
Pb	0.000	0.000	0.004	0.007	0.002	0.005	0.008	0.009	0.387	0.006	0.007	0.008	0.012	0.013	0.015	0.006	0.004	0.008
Ba	0.000	0.000	0.013	0.017	0.021	0.009	0.012	0.034	0.066	0.023	0.027	0.030	0.010	0.007	0.014	0.011	0.012	0.019
V	0.000	0.000	0.000	0.000	0.000	0.000	0.000	0.000	0.000	0.000	0.000	0.000	0.000	0.000	0.000	0.000	0.000	0.000
Sr	0.000	0.000	0.000	0.000	0.000	0.000	0.000	0.000	0.000	0.000	0.000	0.000	0.000	0.000	0.000	0.000	0.000	0.000
Ti	2.065	2.099	2.068	2.079	2.100	2.078	2.026	2.081	1.810	1.976	1.795	1.740	2.097	2.127	2.142	2.106	2.091	1.878
Zr	0.054	0.024	0.008	0.008	0.017	0.048	0.032	0.008	0.382	0.035	0.044	0.108	0.003	0.004	0.006	0.005	0.013	0.122
Nb	0.011	0.024	0.000	0.000	0.000	0.000	0.000	0.000	0.117	0.076	0.255	0.264	0.000	0.000	0.000	0.000	0.009	0.119
Si	8.469	8.519	8.737	8.602	8.608	8.646	8.739	8.595	9.190	8.698	8.620	8.500	8.612	8.610	8.642	8.618	8.576	8.629
Al	0.006	0.031	0.016	0.013	0.036	0.016	0.054	0.067	0.091	0.023	0.051	0.090	0.013	0.008	0.006	0.014	0.003	0.019
F	0.941	0.866	0.569	0.906	0.654	0.528	0.789	0.586	0.504	0.489	0.482	0.757	0.822	0.708	0.569	0.757	0.758	0.578
Cl	0.001	0.023	0.002	0.003	0.002	0.000	0.004	0.002	0.071	0.000	0.000	0.000	0.001	0.002	0.004	0.000	0.004	0.002
Σ Cations	21.483	21.186	21.378	21.436	21.507	21.582	21.161	21.575	19.750	21.589	21.619	21.498	21.457	21.496	21.489	21.475	21.586	21.557

Appendix B-3. Electron-microprobe analyses of selected titanium minerals

Mineral	Aenigmatite													
Sample#	48-F-1				58-D-1					LB-9-2.12				
Description				lst	red	red	red	red	red					
File Name	1/1/95	1/1/95	1/1/95	1/1/95	95mncor	95mncor	95mncor	95mncor	95mncor	1/1/95	1/1/95	1/1/95	1/1/95	1/1/95
Point #	47	49	50	68	3	6	9	12	13	99	107	109	116	117
Na_2O	7.76	7.71	7.74	7.92	7.78	7.72	7.71	7.62	7.76	7.67	7.74	7.63	7.89	7.71
K_2O	0.02	0.03	0.00	0.03	0.00	0.00	0.00	0.00	0.00	0.02	0.01	0.02	0.02	0.02
CaO	0.00	0.22	0.23	0.00	0.00	0.00	0.00	0.00	0.00	0.14	0.02	0.20	0.02	0.03
MgO	0.01	0.00	0.01	0.01	0.02	0.01	0.01	0.00	0.00	0.03	0.01	0.03	0.00	0.00
FeO	36.41	35.58	36.73	36.98	38.82	38.97	38.18	32.12	38.72	37.15	38.90	37.08	37.25	38.63
Fe_2O_3	3.80	5.71	5.09	3.58	2.51	2.19	2.89	8.17	3.36	4.31	2.40	4.19	3.70	2.12
MnO	1.05	0.96	0.97	1.07	1.29	1.31	1.43	0.66	1.29	1.03	1.00	1.17	1.21	1.24
ZnO	0.11	0.12	0.17	0.20	0.09	0.09	0.12	0.06	0.09	0.12	0.13	0.14	0.10	0.14
ZrO_2	0.00	0.01	0.01	0.00	0.04	0.00	0.05	0.02	0.03	0.02	0.00	0.05	0.02	0.01
Nb_2O_5	0.00	0.00	0.00	0.00						0.00	0.00	0.00	0.00	0.00
PbO	0.02	0.00	0.00	0.02						0.04	0.00	0.00	0.02	0.02
BaO	0.01	0.03	0.04	0.04						0.03	0.04	0.03	0.07	0.03
V_2O_3					0.02	0.04	0.02	0.03	0.04					
TiO_2	9.94	7.92	8.04	9.16	9.80	9.62	9.65	1.92	10.10	8.70	9.24	8.80	8.91	9.18
SiO_2	40.15	40.83	41.62	41.74	42.05	42.16	41.56	41.97	41.56	41.28	42.35	41.15	41.94	42.35
Al_2O_3	0.11	0.46	0.45	0.06	0.34	0.10	0.34	0.32	0.42	0.42	0.00	0.60	0.26	0.03
F	0.00	0.00	0.00	0.00	0.00	0.00	0.00	0.00	0.00	0.00	0.00	0.00	0.00	0.00
Total	99.38	99.59	101.10	100.81	102.75	102.21	101.96	92.89	103.36	100.94	101.84	101.07	101.41	101.50
					Structural formula calculated based on 20 atoms of oxygen and 14 cations									
Na	2.162	2.134	2.113	2.171	2.100	2.094	2.097	2.211	2.085	2.102	2.106	2.088	2.149	2.105
K	0.004	0.005	0.001	0.005	0.000	0.000	0.000	0.000	0.000	0.003	0.002	0.004	0.004	0.004
Ca	0.000	0.034	0.034	0.000	0.000	0.000	0.000	0.000	0.000	0.021	0.003	0.031	0.003	0.004
Mg	0.001	0.000	0.002	0.003	0.004	0.003	0.001	0.000	0.000	0.007	0.001	0.007	0.000	0.000
Fe^{3+}	4.378	4.245	4.324	4.371	4.519	4.562	4.481	4.019	4.489	4.392	4.566	4.379	4.378	4.549
Fe^{2+}	0.449	0.700	0.606	0.413	0.278	0.242	0.325	1.120	0.377	0.505	0.267	0.490	0.426	0.236
Mn	0.128	0.116	0.115	0.129	0.152	0.155	0.170	0.084	0.151	0.123	0.119	0.140	0.143	0.148
Zn	0.011	0.013	0.017	0.021	0.009	0.009	0.012	0.006	0.009	0.013	0.014	0.014	0.011	0.014
Zr	0.000	0.001	0.001	0.000	0.003	0.000	0.004	0.002	0.002	0.001	0.000	0.003	0.001	0.001
Nb	0.000	0.000	0.000	0.000	0.000	0.000	0.000	0.000	0.000	0.000	0.000	0.000	0.000	0.000
Y	0.000	0.000	0.000	0.000	0.000	0.000	0.000	0.000	0.000	0.000	0.000	0.000	0.000	0.000
Sn	0.000	0.000	0.000	0.000	0.000	0.000	0.000	0.000	0.000	0.000	0.000	0.000	0.000	0.000
Pb	0.001	0.000	0.000	0.001	0.000	0.000	0.000	0.000	0.000	0.002	0.000	0.000	0.001	0.001
Ba	0.001	0.002	0.002	0.002	0.000	0.000	0.000	0.000	0.000	0.002	0.002	0.001	0.004	0.002
V	0.000	0.000	0.000	0.000	0.003	0.004	0.002	0.004	0.004	0.000	0.000	0.000	0.000	0.000
Sr	0.000	0.000	0.000	0.000	0.000	0.000	0.000	0.000	0.000	0.000	0.000	0.000	0.000	0.000
Cr	0.000	0.000	0.000	0.000	0.000	0.000	0.000	0.000	0.000	0.000	0.000	0.000	0.000	0.000
Ti	1.075	0.849	0.851	0.974	1.026	1.012	1.018	0.216	1.052	0.924	0.976	0.934	0.942	0.972
Si	5.771	5.825	5.859	5.900	5.852	5.902	5.832	6.281	5.760	5.836	5.944	5.810	5.895	5.961
Al	0.019	0.077	0.075	0.010	0.055	0.016	0.057	0.057	0.069	0.069	0.000	0.100	0.043	0.004
F	0.000	0.000	0.000	0.000	0.000	0.000	0.000	0.000	0.000	0.000	0.000	0.000	0.000	0.000

Fe^{3+} was calculated using the method of Droop (1987)

Appendix B-3 Electron-microprobe analyses of selected titanium minerals

Mineral	Neptunite															
Sample#	38-A-3							38-B-381								48-F-1
Description	2 acnig?	11 acnl?	17 astro?	18 astro?	20 astro?	26 nrpyx	32 ast-dipy									acn?
File Name	jrastsl.tr	jrastsl.tr	jrastsl.tr	jrastsl.tr	jrastsl.tr	jrastsl.tr	jrastsl.tr	Mar26/93	Mar26/93	Mar26/93	Mar26/93	Mar26/93	Mar26/93	Mar26/93	Mar26/93	Mar-93
Point #	2	11	17	18	20	26	32	2	11	16	17	18	20	26	32	92
Na_2O	6.73	5.68	7.68	7.16	6.33	6.70	6.52	6.73	5.68	9.45	7.68	7.16	6.33	6.70	6.52	6.93
K_2O	4.25	4.23	3.92	3.91	4.23	4.18	4.09	5.12	5.10	4.66	4.72	4.70	5.10	5.03	4.92	5.13
CaO	0.00	0.00	0.01	0.01	0.02	0.00	0.01	0.00	0.00	0.02	0.01	0.01	0.02	0.00	0.01	0.01
MgO	0.08	0.08	0.03	0.01	0.04	0.15	0.06	0.08	0.08	0.02	0.03	0.01	0.04	0.15	0.06	0.01
FeO	16.34	18.21	17.95	21.95	18.13	17.75	18.63	16.34	18.21	20.26	17.95	21.95	18.13	17.75	18.63	18.19
MnO	0.05	0.14	0.54	0.54	0.38	0.17	0.28	0.05	0.14	0.59	0.54	0.54	0.38	0.17	0.28	0.39
ZnO	0.04	0.00	0.11	0.11	0.06	0.00	0.09	0.04	0.00	0.05	0.11	0.11	0.06	0.00	0.09	0.11
ZrO_2	0.00	0.01	0.02	0.00	0.03	0.01	0.02	0.00	0.01	0.10	0.02	0.00	0.03	0.01	0.02	0.01
Nb_2O_5	0.04	0.05	0.00	0.04	0.11	0.04	0.12	0.04	0.05	0.00	0.00	0.04	0.11	0.04	0.13	0.00
Y_2O_3																
SnO_2																
PbO																
BaO																
V_2O_3																
SrO																
Cr_2O_3																
TiO_2	16.38	16.09	15.00	13.43	16.39	16.10	15.48	16.38	16.09	15.10	15.00	13.43	16.39	16.10	15.48	15.21
SiO_2	51.66	51.92	52.90	52.09	48.49	52.09	51.18	51.66	51.92	52.32	52.89	52.09	48.49	52.09	51.17	51.95
Al_2O_3	0.09	0.12	0.11	0.15	0.06	0.08	0.11	0.09	0.12	0.15	0.11	0.15	0.06	0.08	0.11	0.18
F	0.34	0.28	0.20	0.70	0.33	0.35	0.37	0.34	0.28	0.16	0.20	0.70	0.33	0.35	0.37	0.34
Cl	0.00	0.01	0.01	0.00	0.00	0.00	0.00	0.00	0.01	0.00	0.01	0.00	0.00	0.00	0.00	0.03
Total	89.26	91.14	90.78	92.93	88.26	90.91	90.43	96.86	97.69	102.88	99.26	100.88	95.46	98.46	97.79	98.47
Structural formulae calculated based on 24 atoms of oxygen and 16 cations assuming 1 cation of Li																
Na	2.030	1.719	2.238	2.079	1.955	1.991	1.959	2.007	1.700	2.600	2.215	2.058	1.932	1.969	1.938	2.030
K	0.844	0.843	0.752	0.746	0.860	0.817	0.807	1.005	1.004	0.843	0.896	0.890	1.024	0.973	0.962	0.989
Ca	0.000	0.000	0.001	0.001	0.004	0.000	0.001	0.000	0.000	0.003	0.001	0.001	0.004	0.000	0.001	0.002
Li	1.000	1.000	1.000	1.000	1.000	1.000	1.000	1.000	1.000	1.000	1.000	1.000	1.000	1.000	1.000	1.000
Mg	0.018	0.019	0.006	0.002	0.009	0.034	0.014	0.018	0.018	0.004	0.006	0.002	0.008	0.034	0.014	0.002
Fe^{2+}	1.390	2.007	0.742	1.034	1.225	1.394	1.386	1.012	1.616	0.000	0.422	0.717	0.850	1.032	1.029	0.735
Fe^{3+}	0.736	0.371	1.515	1.714	1.189	0.881	1.026	1.090	0.734	2.405	1.812	2.004	1.536	1.219	1.357	1.565
Mn	0.006	0.019	0.069	0.068	0.051	0.022	0.036	0.006	0.019	0.071	0.068	0.068	0.050	0.021	0.036	0.050
Zn	0.004	0.000	0.012	0.012	0.007	0.000	0.011	0.004	0.000	0.006	0.012	0.012	0.007	0.000	0.011	0.012
Zr	0.000	0.001	0.001	0.000	0.002	0.001	0.001	0.000	0.001	0.007	0.001	0.000	0.002	0.001	0.001	0.001
Nb	0.003	0.004	0.000	0.003	0.008	0.003	0.009	0.003	0.004	0.000	0.000	0.002	0.008	0.003	0.009	0.000
Y	0.000	0.000	0.000	0.000	0.000	0.000	0.000	0.000	0.000	0.000	0.000	0.000	0.000	0.000	0.000	0.000
Sn	0.000	0.000	0.000	0.000	0.000	0.000	0.000	0.000	0.000	0.000	0.000	0.000	0.000	0.000	0.000	0.000
Pb	0.000	0.000	0.000	0.000	0.000	0.000	0.000	0.000	0.000	0.000	0.000	0.000	0.000	0.000	0.000	0.000
Ba	0.000	0.000	0.000	0.000	0.000	0.000	0.000	0.000	0.000	0.000	0.000	0.000	0.000	0.000	0.000	0.000
V	0.000	0.000	0.000	0.000	0.000	0.000	0.000	0.000	0.000	0.000	0.000	0.000	0.000	0.000	0.000	0.000
Sr	0.000	0.000	0.000	0.000	0.000	0.000	0.000	0.000	0.000	0.000	0.000	0.000	0.000	0.000	0.000	0.000
Cr	0.000	0.000	0.000	0.000	0.000	0.000	0.000	0.000	0.000	0.000	0.000	0.000	0.000	0.000	0.000	0.000
Ti	1.916	1.889	1.696	1.513	1.962	1.856	1.803	1.894	1.867	1.612	1.678	1.498	1.939	1.836	1.783	1.729
Si	8.037	8.106	7.950	7.801	7.719	7.987	7.926	7.945	8.014	7.425	7.869	7.722	7.629	7.899	7.839	7.854
Al	0.016	0.023	0.019	0.027	0.011	0.014	0.020	0.016	0.023	0.025	0.019	0.027	0.011	0.014	0.020	0.032
F	0.167	0.139	0.093	0.331	0.167	0.172	0.181	0.165	0.137	0.070	0.092	0.328	0.165	0.170	0.179	0.161
Cl	0.001	0.001	0.002	0.000	0.001	0.001	0.001	0.001	0.001	0.000	0.002	0.000	0.001	0.001	0.001	0.008

Appendix B-3. Electron-microprobe analyses of selected titanium minerals

Mineral	Neptunite															
Sample#	48-F-1												58-D-1	58-F-1		
Description														dkrd	rd	#4rd
File Name	1/1/95	1/1/95	1/1/95	1/1/95	1/1/95	1/1/95	1/1/95	1/1/95	1/1/95	1/1/95	1/1/95	1/1/95	lateJan95	Mar-93	Mar-93	Mar-93
Point #	39	40	41	42	55	57	58	60	65	66	70	71	10	98	100	104
Na_2O	7.70	7.24	7.78	7.08	7.17	7.37	7.78	7.29	7.81	7.23	7.84	7.39	7.14	6.89	6.57	6.59
K_2O	4.19	5.35	4.05	5.39	5.39	5.19	4.32	5.32	4.28	5.24	4.35	5.35	4.25	4.27	5.41	5.23
CaO	0.02	0.00	0.02	0.00	0.01	0.01	0.01	0.00	0.02	0.00	0.00	0.00	0.00	0.03	0.00	0.00
MgO	0.01	0.01	0.02	0.02	0.00	0.01	0.00	0.01	0.01	0.00	0.01	0.01	0.06	0.08	0.03	0.03
FeO	21.51	16.44	21.61	16.18	16.56	17.42	21.14	16.33	22.08	17.30	20.70	15.90	22.64	23.27	17.45	16.46
MnO	0.64	0.51	0.59	0.47	0.37	0.48	0.57	0.31	0.64	0.40	0.72	0.39	0.64	0.70	0.42	0.40
ZnO	0.21	0.13	0.18	0.00	0.00	0.00	0.14	0.00	0.11	0.00	0.17	0.05	0.11	0.18	0.10	0.10
ZrO_2	0.00	0.00	0.02	0.00	0.00	0.00	0.00	0.00	0.03	0.01	0.02	0.09	0.02	0.01	0.00	0.00
Nb_2O_5	0.00	0.00	0.00	0.00	0.00	0.00	0.00	0.00	0.00	0.00	0.00	0.00		0.01	0.03	0.04
Y_2O_3	0.00	0.00	0.00	0.00	0.00	0.00	0.00	0.00	0.00	0.00	0.00	0.00				
SnO_2	0.00	0.00	0.00	0.00	0.00	0.00	0.00	0.00	0.00	0.00	0.00	0.10				
PbO	0.07	0.01	0.03	0.00	0.00	0.04	0.00	0.02	0.00	0.00	0.00	0.00				
BaO	0.06	0.07	0.03	0.05	0.07	0.03	0.04	0.01	0.07	0.05	0.05	0.05				
V_2O_3													0.09			
SrO	0.00	0.00	0.00	0.00	0.00	0.00	0.00	0.00	0.00	0.00	0.00	0.00				
Cr_2O_3													0.00			
TiO_2	12.04	15.54	12.23	15.51	15.63	14.86	12.61	16.09	11.59	14.85	12.67	15.86	12.62	11.14	15.69	15.88
SiO_2	50.91	52.03	50.68	51.62	52.55	51.93	51.38	52.28	50.35	51.65	50.53	52.07	49.71	50.08	51.45	51.14
Al_2O_3	0.15	0.11	0.18	0.15	0.13	0.22	0.16	0.09	0.17	0.11	0.13	0.13	0.29	0.08	0.13	0.07
F	0.76	0.23	0.78	0.24	0.28	0.38	0.62	0.16	0.82	0.36	0.66	0.13	0.85	1.11	0.36	0.24
Cl	0.01	0.00	0.00	0.00	0.01	0.01	0.00	0.00	0.00	0.00	0.01	0.00	0.01	0.00	0.00	0.00
Total	97.95	97.59	97.86	96.61	98.04	97.78	98.51	97.84	97.63	97.07	97.56	97.46	98.42	97.84	97.65	96.19
	Structural formulae calculated based on 24 atoms of oxygen and 16 cations assuming 1 cation of Li															
Na	2.257	2.127	2.283	2.101	2.097	2.158	2.263	2.134	2.294	2.135	2.301	2.168	2.107	2.051	1.948	1.980
K	0.809	1.034	0.783	1.051	1.037	1.001	0.827	1.024	0.827	1.019	0.841	1.032	0.826	0.836	1.055	1.034
Ca	0.002	0.000	0.003	0.000	0.001	0.002	0.001	0.001	0.003	0.000	0.000	0.000	0.000	0.006	0.000	0.000
Li	1.000	1.000	1.000	1.000	1.000	1.000	1.000	1.000	1.000	1.000	1.000	1.000	1.000	1.000	1.000	1.000
Mg	0.002	0.002	0.004	0.004	0.001	0.001	0.000	0.002	0.001	0.001	0.001	0.002	0.014	0.018	0.007	0.007
Fe^{2+}	0.372	0.431	0.385	0.499	0.589	0.430	0.332	0.504	0.212	0.474	0.200	0.374	0.631	0.803	0.838	0.848
Fe^{3+}	2.349	1.651	2.350	1.571	1.500	1.771	2.322	1.557	2.584	1.730	2.422	1.639	2.251	2.184	1.393	1.284
Mn	0.082	0.065	0.076	0.061	0.047	0.061	0.072	0.039	0.082	0.052	0.093	0.050	0.082	0.090	0.055	0.053
Zn	0.024	0.015	0.020	0.000	0.000	0.000	0.015	0.000	0.012	0.000	0.019	0.006	0.013	0.020	0.011	0.011
Zr	0.000	0.000	0.001	0.000	0.000	0.000	0.000	0.000	0.002	0.001	0.001	0.007	0.001	0.001	0.000	0.000
Nb	0.000	0.000	0.000	0.000	0.000	0.000	0.000	0.000	0.000	0.000	0.000	0.000	0.000	0.001	0.002	0.003
Y	0.000	0.000	0.000	0.000	0.000	0.000	0.000	0.000	0.000	0.000	0.000	0.000	0.000	0.000	0.000	0.000
Sn	0.000	0.000	0.000	0.000	0.000	0.000	0.000	0.000	0.000	0.000	0.000	0.007	0.000	0.000	0.000	0.000
Pb	0.003	0.000	0.001	0.000	0.000	0.002	0.000	0.001	0.000	0.000	0.000	0.000	0.000	0.000	0.000	0.000
Ba	0.003	0.004	0.002	0.003	0.004	0.002	0.003	0.001	0.004	0.003	0.003	0.003	0.000	0.000	0.000	0.000
V	0.000	0.000	0.000	0.000	0.000	0.000	0.000	0.000	0.000	0.000	0.000	0.000	0.011	0.000	0.000	0.000
Sr	0.000	0.000	0.000	0.000	0.000	0.000	0.000	0.000	0.000	0.000	0.000	0.000	0.000	0.000	0.000	0.000
Cr	0.000	0.000	0.000	0.000	0.000	0.000	0.000	0.000	0.000	0.000	0.000	0.000	0.000	0.000	0.000	0.000
Ti	1.370	1.770	1.392	1.785	1.773	1.688	1.424	1.827	1.321	1.701	1.443	1.805	1.445	1.286	1.803	1.849
Si	7.699	7.880	7.669	7.898	7.928	7.845	7.712	7.894	7.626	7.866	7.653	7.883	7.567	7.689	7.864	7.919
Al	0.027	0.020	0.031	0.027	0.023	0.039	0.028	0.016	0.030	0.020	0.022	0.023	0.053	0.015	0.023	0.013
F	0.364	0.110	0.371	0.114	0.135	0.181	0.296	0.075	0.391	0.174	0.314	0.063	0.408	0.539	0.174	0.118
Cl	0.002	0.001	0.001	0.001	0.001	0.001	0.001	0.001	0.000	0.001	0.001	0.001	0.002	0.000	0.001	0.001

Appendix B-3. Electron-microprobe analyses of selected titanium minerals

Mineral	Neptunite											
Sample#	58-F-1		LB-9-2.12				LB-9-7.47					
Description	rd	dkrd										
File Name	Mar-93	Mar-93	1/1/95	1/1/95	1/1/95	1/1/95	1/1/95	1/1/95	1/1/95	1/1/95	1/1/95	1/1/95
Point #	106	110	94	96	98	105	120	128	129	130	136	137
Na_2O	6.55	6.63	7.60	7.72	7.52	7.18	6.96	7.14	7.33	7.69	7.74	7.25
K_2O	5.33	5.35	4.30	4.41	4.30	5.34	5.28	5.42	4.78	4.23	4.25	5.20
CaO	0.00	0.00	0.03	0.04	0.03	0.00	0.01	0.02	0.04	0.03	0.00	0.00
MgO	0.02	0.03	0.05	0.06	0.05	0.02	0.02	0.00	0.08	0.06	0.07	0.06
FeO	17.33	16.16	22.67	24.30	22.22	16.95	17.31	15.76	20.72	24.36	21.77	17.58
MnO	0.48	0.38	0.77	0.73	0.68	0.38	0.69	0.47	0.53	0.72	0.69	0.37
ZnO	0.12	0.09	0.17	0.15	0.15	0.06	0.05	0.03	0.10	0.18	0.16	0.07
ZrO_2	0.01	0.00	0.03	0.01	0.00	0.00	0.03	0.02	0.04	0.02	0.01	0.00
Nb_2O_5	0.03	0.00	0.00	0.00	0.00	0.00	0.00	0.00	0.00	0.00	0.00	0.00
Y_2O_3			0.00	0.00	0.00	0.00	0.00	0.00	0.00	0.00	0.00	0.00
SnO_2			0.00	0.00	0.00	0.00	0.00	0.00	0.00	0.00	0.00	0.00
PbO			0.01	0.03	0.03	0.00	0.15	0.00	0.02	0.02	0.00	0.00
BaO			0.14	0.17	0.13	0.12	0.05	0.08	0.06	0.13	0.12	0.09
V_2O_3												
SrO			0.00	0.00	0.00	0.00	0.00	0.00	0.00	0.00	0.00	0.00
Cr_2O_3												
TiO_2	15.60	16.42	11.35	10.40	11.80	15.26	14.67	16.30	13.21	10.58	12.19	14.79
SiO_2	50.98	51.06	50.96	51.06	50.75	52.66	51.52	52.04	51.37	50.46	51.14	52.15
Al_2O_3	0.06	0.05	0.12	0.09	0.13	0.18	0.09	0.10	0.10	0.15	0.10	0.11
F	0.33	0.18	0.79	1.00	0.76	0.31	0.36	0.07	0.65	1.11	0.69	0.46
Cl	0.01	0.01	0.01	0.00	0.00	0.00	0.01	0.00	0.00	0.00	0.00	0.00
Total	96.84	96.36	98.66	99.74	98.21	98.32	97.06	97.42	98.76	99.28	98.64	97.92
			Structural formulae calculated based on 24 atoms of oxygen and 16 cations assuming 1 cation of Li									
Na	1.956	1.985	2.214	2.226	2.204	2.094	2.062	2.102	2.135	2.232	2.253	2.125
K	1.048	1.055	0.825	0.837	0.828	1.025	1.030	1.048	0.917	0.808	0.813	1.002
Ca	0.000	0.001	0.005	0.006	0.005	0.000	0.002	0.004	0.006	0.005	0.000	0.000
Li	1.000	1.000	1.000	1.000	1.000	1.000	1.000	1.000	1.000	1.000	1.000	1.000
Mg	0.004	0.007	0.011	0.012	0.011	0.003	0.004	0.000	0.019	0.014	0.016	0.013
Fe^{3+}	0.818	0.792	0.316	0.226	0.372	0.569	0.541	0.480	0.469	0.313	0.311	0.550
Fe^{2+}	1.416	1.296	2.535	2.797	2.436	1.564	1.673	1.520	2.137	2.736	2.422	1.672
Mn	0.062	0.049	0.098	0.091	0.087	0.049	0.089	0.060	0.068	0.091	0.088	0.047
Zn	0.013	0.010	0.018	0.017	0.016	0.007	0.006	0.004	0.011	0.020	0.017	0.007
Zr	0.001	0.000	0.002	0.001	0.000	0.000	0.002	0.001	0.003	0.002	0.001	0.000
Nb	0.002	0.000	0.000	0.000	0.000	0.000	0.000	0.000	0.000	0.000	0.000	0.000
Y	0.000	0.000	0.000	0.000	0.000	0.000	0.000	0.000	0.000	0.000	0.000	0.000
Sn	0.000	0.000	0.000	0.000	0.000	0.000	0.000	0.000	0.000	0.000	0.000	0.000
Pb	0.000	0.000	0.001	0.001	0.001	0.000	0.006	0.000	0.001	0.001	0.000	0.000
Ba	0.000	0.000	0.008	0.010	0.008	0.007	0.003	0.004	0.004	0.008	0.007	0.005
V	0.000	0.000	0.000	0.000	0.000	0.000	0.000	0.000	0.000	0.000	0.000	0.000
Sr	0.000	0.000	0.000	0.000	0.000	0.000	0.000	0.000	0.000	0.000	0.000	0.000
Cr	0.000	0.000	0.000	0.000	0.000	0.000	0.000	0.000	0.000	0.000	0.000	0.000
Ti	1.809	1.907	1.284	1.163	1.341	1.727	1.687	1.861	1.493	1.191	1.377	1.681
Si	7.859	7.888	7.662	7.596	7.668	7.923	7.877	7.898	7.722	7.553	7.677	7.880
Al	0.010	0.010	0.021	0.016	0.022	0.032	0.017	0.018	0.018	0.026	0.018	0.019
F	0.161	0.088	0.375	0.470	0.361	0.146	0.176	0.035	0.309	0.525	0.329	0.218
Cl	0.001	0.002	0.002	0.000	0.000	0.000	0.002	0.001	0.001	0.000	0.000	0.000

Appendix B-3: Electron-microprobe analyses of selected titanium minerals

Mineral	Baferrisdite		
Sample#	48-F-1	49-C-2	LJB-9-7.47
Description			
File Name	1/1/95	1/1/95	1/1/95
Point #	29	87	112
Na_2O	0.58	0.78	0.17
K_2O	0.49	0.77	0.12
CaO	0.15	0.30	0.01
MgO	0.00	0.04	0.01
FeO	15.99	9.74	25.57
MnO	0.80	0.38	1.75
ZnO	0.41	0.05	0.23
ZrO_2	0.05	0.11	0.03
Nb_2O_5	1.35	1.87	0.00
Y_2O_3	0.00	0.00	0.00
SnO_2	0.13	0.00	0.00
PbO	0.16	0.16	0.05
BaO	27.10	29.33	30.31
SrO	0.00	0.00	0.00
TiO_2	18.35	30.02	15.65
SiO_2	28.77	22.56	24.29
Al_2O_3	0.13	0.06	0.02
F	2.83	0.47	4.13
Cl	0.01	1.63	0.01
Total	96.11	97.68	100.60
Structural formulae calculated based on 9 atoms of oxygen			
Na	0.085	0.116	0.026
K	0.048	0.076	0.012
Ca	0.012	0.025	0.001
Mg	0.000	0.005	0.001
Fe^{2+}(Total)	1.018	0.625	1.675
Mn	0.052	0.025	0.116
Zn	0.023	0.003	0.013
Zr	0.002	0.004	0.001
Nb	0.047	0.065	0.000
Y	0.000	0.000	0.000
Sn	0.005	0.000	0.000
Pb	0.003	0.003	0.001
Ba	0.808	0.882	0.930
V	0.000	0.000	0.000
Sr	0.000	0.000	0.000
Cr	0.000	0.000	0.000
Ti	1.050	1.733	0.922
Si	2.188	1.732	1.902
Al	0.011	0.005	0.002
F	0.682	0.114	1.022
Cl	0.001	0.211	0.001
Σ Cations	5.351	5.297	5.601

Appendix B-3 Electron-microprobe analyses of selected titanium minerals

Mineral	Ilmenite						
Sample#	Hypersolvus						
Description	Core am	Core am	Core am	Core am	Core am	Core am	Core am
File Name							
Point #	1	2	3	4	5	6	7
FeO	43 65	46 31	46 00	46 08	41 70	41 96	41 62
MnO	1 72	1 82	1 75	2 16	4 90	5 12	5 12
TiO_2	50 58	50 46	50 62	50 95	50 50	51 04	51 81
Total	95 94	98 59	98 36	99 18	97 10	98 12	98 54
	Structural formula calculated based on 3 atoms of oxygen						
Fe	0 960	1 000	0 994	0 988	0 910	0 906	0 892
Mn	0 038	0 040	0 038	0 050	0 108	0 112	0 111
Ti	1 001	0 980	0 984	0 983	0 991	0 991	0 999
ΣCations	1 999	2 020	2 016	2 021	2 009	2 009	2 002

Appendix B-4: Bulk ICP-MS analysis of arfvedsonitic amphibole

	Sample#			
ppm	**48-A-7**	**46-I-3**[1]	**SL-4-15**	**SL-BS-1**[2]
Li	1545	2254	3100	2165
V	0	2	0	0
Cr	0	6	0	0
Zn	3114	7101	3289	10214
Rb	38	63	51	81
Sr	7	4	1	16
Y	38	85	20	181
Zr	1000	3207	903	638
Nb	126	325	91	1369
Ba	677	5	13	15
La	46	4	8	105
Ce	125	17	20	297
Pr	10	2	2	26
Nd	34	8	6	68
Sm	6	3	1	15
Eu	0	0	0	1
Gd	5	3	1	17
Tb	1	1	0	6
Dy	5	10	2	44
Ho	2	4	1	9
Er	11	26	8	26
Tm	4	11	3	5
Yb	43	119	36	32
Lu	10	21	9	4
Hf	50	163	43	25
Th	3	4	4	39
U	5	2	1	291
Ta	2	7	1	75
Sn	114	917	175	736
Σ REE	301	230	98	655

[1] may contain inclusions of aegirine
[2] contains minute inclusions of pyrochlore

Appendix B-5: LAM-ICP-MS analyses

Unit	Hypersolvus							
Sample#	LB-9-2.12	LB-9-5.33	49-C-2					
HighZ[1]			M7 - U2	M7 - U3	M7 - U4	M7 - U5	M7 - U3	M6-U5
Low Z[2]	J21B-U1	J21B-U2	M21B-U9	M20A-U8	M20B-U8	M20B-U9	M20B-U7	M20B-U7
Analysis#	182	185	90	90	90	90	91	91
SiO_2	48.72	51.30	51.40	51.40	51.40	51.40	50.91	50.91
Al_2O_3	1.04	0.20	0.32	0.32	0.32	0.32	0.44	0.44
TiO_2	0.81	0.80	1.24	1.24	1.24	1.24	1.10	1.10
FeO	35.08	31.84	32.11	32.11	32.11	32.11	33.39	33.39
MgO	0.34	0.01	0.03	0.03	0.03	0.03	0.05	0.05
MnO	0.77	1.21	0.72	0.72	0.72	0.72	0.65	0.65
ZnO	0.19	0.64	0.33	0.33	0.33	0.33	0.25	0.25
Cr_2O_3	0.00	0.00	0.00	0.00	0.00	0.00	0.00	0.00
V_2O_3	0.00	0.00	0.00	0.00	0.00	0.00	0.01	0.01
Nb_2O_5	0.00	0.00	0.00	0.00	0.00	0.00	0.00	0.00
ZrO_2	0.11	0.12	0.08	0.08	0.08	0.08	0.14	0.14
Y_2O_3	0.00	0.00	0.00	0.00	0.00	0.00	0.00	0.00
Yb_2O_3	0.00	0.01	0.00	0.00	0.00	0.00	0.00	0.00
Na_2O	8.10	9.12	9.56	9.56	9.56	9.56	9.51	9.51
K_2O	0.72	2.05	1.65	1.65	1.65	1.65	1.32	1.32
CaO	2.28	0.17	0.06	0.06	0.06	0.06	0.30	0.30
F	1.48	1.80	1.95	1.95	1.95	1.95	1.96	1.96
Cl	0.03	0.00	0.01	0.01	0.01	0.01	0.01	0.01
Total	99.03	98.51	98.62	98.62	98.62	98.62	99.22	99.22
Isotope								
^{6}Li	244.11	1461.80	1846.68	1503.89	2052.84	2376.83	1451.77	1451.77
^{9}Be	22.77	15.51	9.84	12.06	10.64	10.66	12.12	12.12
^{11}B	4.43	7.78	2.74	2.56	3.22	2.60	2.63	2.63
^{51}V			1.15	1.15	1.15	1.15	0.95	2.08
^{52}Cr			0.00	0.00	0.00	0.00	0.00	0.00
^{55}Mn			0.49	0.49	0.49	0.49	0.47	0.47
^{66}Zn			3027.77	3027.77	3027.77	3027.77	2862.49	2177.77
^{85}Rb			35.16	35.16	35.16	35.16	33.77	25.68
^{88}Sr			2.41	2.41	2.41	2.41	3.90	2.64
^{89}Y			41.18	41.18	41.18	41.18	38.37	41.72
^{90}Zr			1460.01	1460.01	1460.01	1460.01	1375.17	904.12
^{93}Nb			87.65	87.65	87.65	87.65	87.35	67.76
^{138}Ba			0.91	0.91	0.91	0.91	0.85	0.67
^{139}La			11.74	11.74	11.74	11.74	11.56	14.64
^{140}Ce			32.33	32.33	32.33	32.33	33.45	48.65
^{141}Pr			4.62	4.62	4.62	4.62	5.11	7.79
^{146}Nd			20.31	20.31	20.31	20.31	20.11	30.50
^{147}Sm			4.29	4.29	4.29	4.29	4.43	6.81
^{151}Eu			0.35	0.35	0.35	0.35	0.33	0.44
^{157}Gd			3.88	3.88	3.88	3.88	3.98	4.53
^{159}Tb			0.62	0.62	0.62	0.62	0.58	0.79
^{162}Dy			5.87	5.87	5.87	5.87	6.05	6.42
^{165}Ho			2.12	2.12	2.12	2.12	2.02	2.17
^{166}Er			13.31	13.31	13.31	13.31	13.75	12.54
^{169}Tm			4.75	4.75	4.75	4.75	4.63	3.91
^{174}Yb			55.97	55.97	55.97	55.97	54.93	46.49
^{175}Lu			13.88	13.88	13.88	13.88	12.93	11.79
^{178}Hf			58.75	58.75	58.75	58.75	51.00	29.40
^{232}Th			0.92	0.92	0.92	0.92	0.54	0.01
^{238}U			0.13	0.13	0.13	0.13	0.59	0.00
Σ REE			174.05	174.05	174.05	174.05	173.87	197.49
La/Lu			0.85	0.85	0.85	0.85	0.89	1.24
Nb/Zr			0.06	0.06	0.06	0.06	0.06	0.07
Th/U			7.26	7.26	7.26	7.26	0.91	0.00

[1] High atomic number; [2] low atomic number

Acronyms refer to: m=march; j=june;s=september; a,b,c=run on that day; u=unknown analysis number based on electron-microprobe data; ltgr=light green; lt=light; dk=dark med=medium; av=average; int=intermediate; alt=alteration; py=pyroxene; am=amphibole; ~ approximately; no value indicates no analysis performed, n.d. indicates element not analyzed

Appendix B-5: LAM-ICP-MS analyses

Unit	Hypersolvus							
Sample#	49-C-2							
HighZ[1]			M7 - U4	M7 - U5	11sea - u3	11sea - u2	11sea - u2	11sea - u2
Low Z[2]	M20B-U5	M20B-U6	M20B-U4	M20A-U4	M20A-U4	M20A-U9	M20A-U10	M20B-U3
Analysis#	92	92	93	-94	-93	95	95	95
SiO_2	50.53	50.53	50.50	50.15	50.50	50.13	50.13	50.13
Al_2O_3	0.59	0.59	0.55	0.51	0.55	0.50	0.50	0.50
TiO_2	1.06	1.06	1.05	1.04	1.05	1.05	1.05	1.05
FeO	33.76	33.76	34.09	34.33	34.09	34.70	34.70	34.70
MgO	0.20	0.20	0.14	0.18	0.14	0.16	0.16	0.16
MnO	0.66	0.66	0.65	0.67	0.65	0.66	0.66	0.66
ZnO	0.22	0.22	0.21	0.19	0.21	0.24	0.24	0.24
Cr_2O_3	0.00	0.00	0.00	0.00	0.00	0.00	0.00	0.00
V_2O_3	0.01	0.01	0.01	0.02	0.01	0.00	0.00	0.00
Nb_2O_5	0.00	0.00	0.00	0.00	0.00	0.00	0.00	0.00
ZrO_2	0.11	0.11	0.13	0.14	0.13	0.12	0.12	0.12
Y_2O_3	0.00	0.00	0.00	0.00	0.00	0.00	0.00	0.00
Yb_2O_3	0.00	0.00	0.02	0.02	0.02	0.00	0.00	0.00
Na_2O	9.25	9.25	9.17	9.15	9.17	8.82	8.82	8.82
K_2O	1.14	1.14	1.18	1.07	1.18	1.06	1.06	1.06
CaO	0.60	0.60	0.56	0.55	0.56	0.55	0.55	0.55
F	1.88	1.88	1.94	1.99	1.94	1.97	1.97	1.97
Cl	0.01	0.01	0.01	0.01	0.01	0.01	0.01	0.01
Total	99.23	99.23	99.40	99.17	99.40	99.14	99.14	99.14
Isotope								
^{6}Li	1353.52	1505.76	1259.39	1370.53	1370.53	1372.77	1433.19	1315.18
^{9}Be	12.08	14.06	10.95	10.37	10.37	11.52	12.09	11.61
^{11}B	2.20	2.73	2.29	2.43	2.43	2.38	2.00	2.09
^{51}V			1.35	1.55	0.99	1.72	1.72	1.72
^{52}Cr			0.09	0.21	0.27	0.39	0.39	0.39
^{55}Mn			0.47	0.47	0.45	0.50	0.50	0.50
^{66}Zn			2893.95	2846.70	2900.99	2754.67	2754.67	2754.67
^{85}Rb			25.93	24.66	51.02	25.02	25.02	25.02
^{88}Sr			3.28	2.38	4.57	2.39	2.39	2.39
^{89}Y			47.46	40.90	148.52	43.35	43.35	43.35
^{90}Zr			1087.46	1062.12	1076.63	1007.24	1007.24	1007.24
^{93}Nb			85.44	63.26	71.50	64.13	64.13	64.13
^{138}Ba			0.94	0.66	1.64	0.75	0.75	0.75
^{139}La			23.57	14.81	40.64	13.26	13.26	13.26
^{140}Ce			66.14	44.65	90.23	43.07	43.07	43.07
^{141}Pr			9.65	7.26	13.94	6.87	6.87	6.87
^{146}Nd			36.87	29.99	65.57	28.29	28.29	28.29
^{147}Sm			7.15	6.47	15.57	6.57	6.57	6.57
^{151}Eu			0.43	0.28	0.88	0.26	0.26	0.26
^{157}Gd			5.59	5.12	16.43	3.87	3.87	3.87
^{159}Tb			1.03	0.74	2.68	0.83	0.83	0.83
^{162}Dy			7.51	6.89	16.46	6.63	6.63	6.63
^{165}Ho			2.48	2.14	3.98	2.09	2.09	2.09
^{166}Er			13.97	11.57	15.92	13.43	13.43	13.43
^{169}Tm			4.49	3.57	4.00	4.02	4.02	4.02
^{174}Yb			53.21	43.52	43.05	48.23	48.23	48.23
^{175}Lu			12.76	10.57	10.14	11.90	11.90	11.90
^{178}Hf			43.76	47.03	39.28	32.48	32.48	32.48
^{232}Th			0.06	0.72	0.84	0.02	0.02	0.02
^{238}U			0.02	0.08	0.18	0.04	0.04	0.04
Σ REE			244.85	187.58	339.47	189.31	189.31	189.31
La/Lu			1.85	1.40	4.01	1.11	1.11	1.11
Nb/Zr			0.08	0.06	0.07	0.06	0.06	0.06
Th/U			3.12	9.14	4.77	0.44	0.44	0.44

[1] High atomic number; [2] low atomic number

Acronyms refer to: m=march; j=june;s=september; a,b,c=run on that day; u=unknown analysis number based on electron-microprobe data; ltgr=light green; lt=light; dk=dark med=medium; av=average; int=intermediate; alt=alteration; py=pyroxene; am=amphibole; ~ approximately; no value indicates no analysis performed, n.d. indicates element not analyzed

Appendix B-5: LAM-ICP-MS analyses

Unit	Hypersolvus							
Sample#	49-C-2				57-A-1			
High Z[1]	M6-U3	m6-U4			18sea-u6	18sea-u7	18sea-u8	18sea-u9
Low Z[2]	M20A-U3	M20B-U2	M20A-U5	M20A-U7				
Analysis#	97	97	102	103	87ltpy	89 am	90dkpy	92dkpy
SiO_2	50.38	50.38	50.27	50.40	51.17	50.79	52.07	51.78
Al_2O_3	0.55	0.55	0.61	0.54	0.14	0.47	0.28	0.29
TiO_2	1.02	1.02	1.09	1.10	1.22	1.29	1.92	3.43
FeO	34.59	34.59	34.08	33.79	29.11	30.60	28.95	27.79
MgO	0.19	0.19	0.15	0.16	0.01	0.23	0.00	0.00
MnO	0.66	0.66	0.67	0.66	0.24	1.51	0.22	0.20
ZnO	0.20	0.20	0.20	0.15	0.00	0.63	0.00	0.00
Cr_2O_3	0.00	0.00	0.00	0.00	0.00	0.01	0.00	0.00
V_2O_3	0.01	0.01	0.00	0.01	0.01	0.01	0.00	0.01
Nb_2O_5	0.00	0.00	0.00	0.00	0.00	0.00	0.00	0.00
ZrO_2	0.13	0.13	0.14	0.11	0.74	0.14	0.27	0.21
Y_2O_3	0.00	0.00	0.00	0.00	0.00	0.00	0.00	0.00
Yb_2O_3	0.01	0.01	0.01	0.01	0.02	0.00	0.02	0.00
Na_2O	8.96	8.96	9.17	9.33	13.26	8.94	13.25	13.62
K_2O	1.06	1.06	1.15	1.00	0.00	1.40	0.00	0.00
CaO	0.61	0.61	0.60	0.59	0.31	0.26	0.19	0.16
F	1.90	1.90	1.95	1.91	0.00	1.89	0.00	0.00
Cl	0.02	0.02	0.01	0.01	0.00	0.01	0.00	0.00
Total	99.47	99.47	99.28	98.97	96.22	97.38	97.17	97.50
Isotope								
^{6}Li	1323.73	1244.78	1431.70	1486.30				
^{9}Be	10.94	11.62	11.35	16.02				
^{11}B	2.76	2.35	2.64	3.85				
^{51}V	2.48	1.88			5.25	3.53	1.07	0.09
^{52}Cr	0.00	0.00			2.56	1.44	0.96	0.57
^{55}Mn	0.49	0.48			0.35	0.83	0.18	0.17
^{66}Zn	2088.10	1885.66			2267.02	5109.27	1860.10	1867.92
^{85}Rb	23.34	24.28			299.93	132.09	24.38	13.95
^{88}Sr	3.70	2.65			22.51	34.81	1.97	1.56
^{89}Y	46.64	47.38			1048.73	281.07	90.11	68.82
^{90}Zr	1030.89	1008.17			5038.46	617.80	2534.13	2573.57
^{93}Nb	81.31	75.88			209.70	144.36	17.64	60.90
^{138}Ba	0.98	0.79			65.57	36.60	1.87	2.00
^{139}La	20.99	15.90			3060.29	3379.09	91.60	83.35
^{140}Ce	60.86	52.95			4580.64	5335.56	216.66	170.50
^{141}Pr	9.37	8.55			546.48	711.74	23.47	19.34
^{144}Nd	37.10	33.89			1689.25	2448.47	84.57	74.86
^{147}Sm	7.62	7.97			244.75	254.06	19.49	14.12
^{151}Eu	0.52	0.49			5.24	8.15	0.51	0.56
^{157}Gd	4.75	4.68			252.33	203.82	16.86	11.81
^{159}Tb	0.92	0.82			40.25	16.45	3.52	1.98
^{163}Dy	7.27	7.27			238.47	72.03	21.48	12.70
^{165}Ho	2.38	2.27			44.17	10.78	4.20	2.85
^{166}Er	14.02	13.94			125.60	31.25	17.27	12.87
^{169}Tm	4.06	4.70			18.67	6.21	5.14	3.86
^{174}Yb	49.87	55.17			140.08	62.65	71.08	53.01
^{175}Lu	11.92	13.41			28.52	14.34	20.46	14.25
^{178}Hf	37.30	33.95			223.13	22.62	84.47	96.36
^{232}Th	0.04	0.04			234.77	421.51	15.56	43.04
^{238}U	0.00	0.00			7.50	3.32	0.79	2.20
Σ REE	231.64	221.99			11014.74	12554.61	596.30	476.06
La/Lu	1.76	1.19			107.31	235.66	4.48	5.85
Nb/Zr	0.08	0.08			0.04	0.23	0.01	0.02
Th/U	393.00	0.00			31.30	126.86	19.57	19.59

[1] High atomic number; [2] low atomic number

Acronyms refer to: m=march; j=june;s=september; a,b,c=run on that day; u=unknown analysis number based on electron-microprobe data; ltgr=light green; lt=light; dk=dark med=medium; av=average; int=intermediate; alt=alteration; py=pyroxene; am=amphibole; ~ approximately; no value indicates no analysis performed, n.d. indicates element not analyzed

Appendix B-5: LAM-ICP-MS analyses

Unit	Hypersolvus							
Sample#	57-A-1	48-F-3		48-F-3#2		48-A-7		
HighZ[1]	19sea-u10	11sea - u6	11sea - u7			08sea-u8	08sea-u9	08sea-u10
Low Z[2]		M21A-U9	J21A-U7	M21B-U10	J21A-U7	M21A-U10	M21A-U3	M21A-U5
Analysis#	91lit.py	203	200	202	201	154	156	159
SiO_2	51.65	50.29	50.14	50.83	50.50	50.30	50.53	50.67
Al_2O_3	0.20	0.46	0.46	0.33	0.61	0.41	0.41	0.42
TiO_2	1.47	0.81	0.91	1.15	1.23	0.96	0.93	0.97
FeO	29.11	33.36	33.75	33.19	32.84	33.65	33.84	33.64
MgO	0.01	0.18	0.20	0.21	0.16	0.01	0.01	0.01
MnO	0.20	0.84	0.87	0.86	0.83	0.59	0.60	0.60
ZnO	0.00	0.27	0.28	0.29	0.23	0.23	0.22	0.22
Cr_2O_3	0.01	0.00	0.00	0.00	0.01	0.00	0.00	0.00
V_2O_3	0.02	0.00	0.00	0.01	0.00	0.00	0.00	0.01
Nb_2O_5	0.00	0.01	0.00	0.00	0.00	0.00	0.00	0.00
ZrO_2	0.56	0.02	0.22	0.06	0.07	0.16	0.21	0.15
Y_2O_3	0.00	0.00	0.00	0.00	0.00	0.00	0.00	0.00
Yb_2O_3	0.00	0.02	0.01	0.03	0.01	0.01	0.01	0.00
Na_2O	13.26	9.23	9.35	9.21	9.25	9.35	9.59	9.58
K_2O	0.00	1.65	1.25	2.02	2.10	1.24	1.24	1.39
CaO	0.14	0.33	0.63	0.19	0.17	0.18	0.18	0.16
F	0.00	1.59	1.56	1.56	1.71	2.12	2.09	1.76
Cl	0.00	0.01	0.01	0.00	0.00	0.01	0.01	0.01
Total	96.61	98.38	98.98	99.29	99.00	98.31	98.98	98.84
Isotope								
^{6}Li		1055.44	770.27	821.22	1137.71	1452.32	1467.68	1650.36
^{9}Be		110.82	60.21	51.68	74.33	8.77	9.69	9.23
^{11}B		32.61	16.74	12.07	10.06	2.43	2.53	2.59
^{51}V	0.52	2.28	0.69			0.00	0.36	0.00
^{52}Cr	0.44	15.19	5.92			1.53	1.52	2.14
^{55}Mn	0.15	0.59	0.51			0.40	0.40	0.39
^{66}Zn	1310.50	2204.58	3158.85			2495.28	2578.85	2544.72
^{85}Rb	30.78	28.67	15.81			27.52	31.89	38.95
^{88}Sr	2.05	28.17	87.58			1.62	1.66	1.68
^{89}Y	170.97	1059.47	3011.66			29.06	29.27	31.41
^{90}Zr	5582.05	626.16	644.50			1522.79	1830.82	1544.90
^{93}Nb	54.02	107.09	132.53			67.87	78.20	70.52
^{138}Ba	1.84	17.35	12.58			0.46	0.63	1.11
^{139}La	34.88	86.77	232.25			4.18	4.44	4.57
^{140}Ce	41.70	232.71	618.54			14.44	15.25	14.43
^{141}Pr	17.15	46.26	108.55			2.33	2.32	2.32
^{146}Nd	105.84	206.89	555.85			9.82	9.28	9.35
^{147}Sm	37.59	76.11	197.41			1.67	2.07	2.22
^{151}Eu	1.54	5.52	13.73			0.04	0.13	0.11
^{157}Gd	33.12	86.80	252.14			1.54	1.46	1.39
^{159}Tb	6.42	23.47	59.26			0.36	0.37	0.36
^{163}Dy	35.02	185.65	449.32			3.98	3.93	4.03
^{165}Ho	6.95	45.14	105.13			1.60	1.60	1.56
^{166}Er	25.84	173.99	363.97			10.73	10.73	10.82
^{169}Tm	6.61	32.35	56.45			3.69	3.62	3.52
^{174}Yb	82.21	256.19	339.76			44.98	44.96	42.05
^{175}Lu	21.22	38.16	42.31			11.20	11.22	10.38
^{178}Hf	251.97	21.30	29.93			107.74	94.25	75.54
^{232}Th	73.90	28.75	21.47			0.08	0.24	2.73
^{238}U	3.13	1.33	0.81			0.52	0.49	0.00
Σ REE	456.10	1496.00	3394.67			110.56	111.39	107.11
La/Lu	1.64	2.27	5.49			0.37	0.40	0.44
Nb/Zr	0.01	0.17	0.21			0.04	0.04	0.05
Th/U	23.61	21.67	26.53			0.15	0.50	0.00

[1] High atomic number; [2] low atomic number

Acronyms refer to: m=march; j=june;s=september; a,b,c=run on that day; u=unknown analysis number based on electron-microprobe data; ltgr=light green; lt=light; dk=dark med=medium; av=average; int=intermediate; alt=alteration; py=pyroxene; am=amphibole; ~ approximately; no value indicates no analysis performed, n.d. indicates element not analyzed

Appendix B-5: LAM-ICP-MS analyses

Unit	Hypersolvus						
Sample#	48-A-7						
HighZ[1]			11seb-u4		11seb-u2	11seb-u3	11seb-u5
Low Z[2]	M21B-U2	M21B-U4		S6B-U10	S6B-U9	S6B-U8	S6B-U8
Analysis#	155	158	am 13	am 2	py 16	py 15	py 15
SiO_2	50.32	50.71	51.33	51.17	52.51	52.87	52.87
Al_2O_3	0.40	0.42	0.47	0.42	0.27	0.36	0.36
TiO_2	0.96	0.95	0.95	0.88	1.07	2.01	2.01
FeO	33.57	33.78	32.68	33.39	30.48	29.39	29.39
MgO	0.01	0.01	0.18	0.21	0.00	0.01	0.01
MnO	0.60	0.62	0.67	0.65	0.09	0.17	0.17
ZnO	0.18	0.21	0.11	0.05	0.00	0.00	0.00
Cr_2O_3	0.00	0.00	0.00	0.00	0.01	0.00	0.00
V_2O_3	0.00	0.02	0.00	0.00	0.01	0.01	0.01
Nb_2O_5	0.00	0.00	0.00	0.00	0.00	0.00	0.00
ZrO_2	0.17	0.19	0.12	0.12	0.13	0.10	0.10
Y_2O_3	0.00	0.00	0.00	0.00	0.00	0.00	0.00
Yb_2O_3	0.00	0.00	0.00	0.00	0.02	0.00	0.00
Na_2O	9.65	9.42	9.17	9.60	13.89	13.76	13.76
K_2O	1.23	1.33	1.62	1.23	0.00	0.00	0.00
CaO	0.16	0.17	0.40	0.34	0.04	0.02	0.02
F	2.09	1.93	2.03	1.83	0.00	0.00	0.00
Cl	0.01	0.01	0.01	0.01	0.00	0.00	0.00
Total	98.47	98.95	98.88	99.14	98.51	98.70	98.70
Isotope							
^{6}Li	1488.10	1333.69		2158.00	1385.00	614.00	614.00
^{9}Be	9.03	10.28		18.00	12.00	12.00	12.00
^{11}B	2.39	2.67		3.00	4.00	5.00	5.00
^{51}V			3.16		2.21	1.04	1.35
^{53}Cr			1.43		3.04	1.16	1.10
^{55}Mn			0.44		0.51	0.28	0.15
^{66}Zn			3007.97		2815.36	1935.50	1133.30
^{85}Rb			22.50		16.39	16.83	2.64
^{88}Sr			58.55		24.66	6.04	44.72
^{89}Y			2752.92		2224.63	120.23	14516.68
^{90}Zr			1080.16		913.08	1389.90	697.16
^{93}Nb			79.23		135.81	106.58	97.67
^{138}Ba			12.79		14.05	8.90	29.52
^{139}La			1089.73		451.63	158.51	3424.76
^{140}Ce			2025.81		803.75	257.25	6526.80
^{141}Pr			292.44		105.16	27.09	936.58
^{146}Nd			1379.17		480.88	103.12	3942.61
^{147}Sm			319.54		132.66	18.49	1140.84
^{151}Eu			17.42		7.88	0.84	68.64
^{157}Gd			354.84		152.64	15.71	1486.74
^{159}Tb			53.48		30.28	2.36	396.89
^{163}Dy			292.56		213.89	15.71	2655.68
^{165}Ho			55.50		46.08	4.10	470.70
^{166}Er			144.17		146.69	17.91	1014.22
^{169}Tm			17.16		22.37	5.07	86.72
^{174}Yb			107.62		159.73	60.27	307.30
^{175}Lu			17.94		24.34	14.25	29.98
^{178}Hf			45.32		38.61	52.97	23.45
^{232}Th			5.77		52.34	34.16	100.15
^{238}U			0.47		3.15	1.88	2.17
Σ REE			6167.40		2777.97	700.68	22488.48
La/Lu			60.73		18.56	11.12	114.24
Nb/Zr			0.07		0.15	0.08	0.14
Th/U			12.21		16.62	18.22	46.18

[1] High atomic number; [2] low atomic number

Acronyms refer to: m=march; j=june;s=september; a,b,c=run on that day; u=unknown analysis number based on electron-microprobe data; py=pyroxene; am=amphibole; no value indicates no analysis performed, n.d. indicates element not analyzed

Appendix B-5: LAM-ICP-MS analyses

Unit	Fresh Subsolvus							
Sample#	38-B-3		38B3#2					46-I-3
HighZ[1]	18seb-u9	18seb-u10	11sea - u8	11sea - u8				08sea-u3
Low Z[2]			M21A-U6	M21A-U8	M21A-U5	M21A-U7	M21A-U9	M20C-U1
Analysis#	95Tipy	- 97ltgr.py	gr#2 110	gr#2 10	109	113	114	153
SiO_2	51.83	52.05	50.57	50.57	50.61	51.16	51.11	50.39
Al_2O_3	0.44	0.40	0.40	0.40	0.41	0.38	0.37	0.16
TiO_2	3.09	1.15	1.12	1.12	1.12	0.92	0.93	0.84
FeO	28.10	30.01	33.34	33.34	33.11	33.06	33.07	31.75
MgO	0.01	0.02	0.15	0.15	0.13	0.09	0.08	0.00
MnO	0.21	0.09	0.66	0.66	0.63	0.61	0.57	1.45
ZnO	0.00	0.00	0.19	0.19	0.24	0.20	0.21	0.70
Cr_2O_3	0.00	0.00	0.00	0.00	0.00	0.00	0.00	0.00
V_2O_3	0.02	0.00	0.02	0.02	0.02	0.01	0.01	0.01
Nb_2O_5	0.00	0.00	0.00	0.00	0.00	0.00	0.00	0.01
ZrO_2	0.30	0.13	0.16	0.16	0.13	0.13	0.12	0.50
Y_2O_3	0.00	0.00	0.00	0.00	0.00	0.00	0.00	0.00
Yb_2O_3	0.00	0.00	0.00	0.00	0.01	0.00	0.01	0.02
Na_2O	13.64	13.96	9.53	9.53	9.50	9.56	9.82	9.16
K_2O	0.00	0.00	1.30	1.30	1.30	1.26	1.22	2.24
CaO	0.16	0.10	0.35	0.35	0.32	0.13	0.13	0.19
F	0.00	0.00	2.04	2.04	1.64	1.79	2.10	1.85
Cl	0.00	0.00	0.01	0.01	0.01	0.01	0.01	0.00
Total	97.79	97.82	98.97	98.97	98.50	98.56	98.87	98.47
Isotope								
^{6}Li			1301.00	1562.23	1552.42	1322.91	1890.59	1691.63
^{9}Be			102.19	9.82	7.84	20.41	8.02	15.00
^{11}B			21.53	3.18	2.71	5.68	3.01	4.44
^{51}V	0.25	0.00	1.17	1.17				0.23
^{52}Cr	0.00	0.00	1.28	1.28				3.08
^{55}Mn	0.26	0.08	0.44	0.44				0.98
^{66}Zn	666.64	245.57	2333.57	2333.57				7241.61
^{85}Rb	1.97	308.05	28.11	28.11				69.91
^{88}Sr	19.12	4.32	2.99	2.99				2.17
^{89}Y	156.63	43.61	34.87	34.87				62.57
^{90}Zr	1103.48	813.15	1367.53	1367.53				4538.29
^{93}Nb	212.71	83.99	74.94	74.94				272.15
^{138}Ba	3.33	9.39	1.03	1.03				1.69
^{139}La	10.05	4.75	9.39	9.39				1.69
^{140}Ce	21.21	11.47	24.65	24.65				7.10
^{141}Pr	4.66	1.87	4.15	4.15				1.10
^{146}Nd	24.76	10.06	16.16	16.16				4.17
^{147}Sm	12.59	3.91	2.31	2.31				1.06
^{151}Eu	0.92	0.23	0.23	0.23				0.08
^{157}Gd	17.20	4.64	2.13	2.13				0.80
^{159}Tb	3.33	0.97	0.50	0.50				0.32
^{162}Dy	22.98	6.10	5.05	5.05				6.08
^{165}Ho	5.03	1.35	1.87	1.87				3.35
^{166}Er	16.65	5.34	12.66	12.66				26.90
^{169}Tm	3.20	1.45	4.16	4.16				8.99
^{174}Yb	41.84	22.25	48.43	48.43				99.05
^{175}Lu	11.89	5.98	11.91	11.91				19.66
^{178}Hf	52.77	33.77	51.26	51.26				182.09
^{232}Th	61.31	17.04	0.10	0.10				0.05
^{238}U	15.94	4.11	0.05	0.05				0.02
Σ REE	196.31	80.39	143.59	143.59				180.34
La/Lu	0.84	0.79	0.79	0.79				0.09
Nb/Zr	0.19	0.10	0.05	0.05				0.06
Th/U	3.85	4.15	1.89	1.89				1.89

[1] High atomic number; [2] low atomic number

Acronyms refer to: m=march; j=june;s=september; a,b,c=run on that day; u=unknown analysis number based on electron-microprobe data; ltgr=light green; lt=light; dk=dark med=medium; av=average; int=intermediate; alt=alteration; py=pyroxene; am=amphibole; ~ approximately; no value indicates no analysis performed, n.d. indicates element not analyzed

Appendix B-5: LAM-ICP-MS analyses

Unit	Altered pegmatite							
Sample#	46-I-3							
HighZ[1]	08sea-u4	08sea-u5	08sea-u6	08sea-u7	08sea-u7	11sea - u4	11sea - u5	11seb-u6
Low Z[2]	M20C-U2						M20B-U10	S6B-U4
Analysis#	150	148	147	146	146	149	-150	py 20
SiO_2	50.83	50.56	50.45	50.51	50.51	51.01	50.83	52.14
Al_2O_3	0.14	0.16	0.16	0.16	0.16	0.16	0.14	0.17
TiO_2	0.82	0.83	0.80	0.83	0.83	0.83	0.82	0.63
FeO	31.70	31.79	31.74	31.66	31.66	31.66	31.70	30.63
MgO	0.00	0.00	0.01	0.00	0.00	0.00	0.00	0.00
MnO	1.47	1.47	1.44	1.44	1.44	1.43	1.47	0.59
ZnO	0.68	0.66	0.70	0.66	0.66	0.66	0.68	0.04
Cr_2O_3	0.00	0.01	0.00	0.00	0.00	0.00	0.00	0.00
V_2O_3	0.00	0.00	0.00	0.00	0.00	0.00	0.00	0.01
Nb_2O_5	0.01	0.00	0.01	0.02	0.02	0.00	0.01	0.04
ZrO_2	0.53	0.51	0.48	0.47	0.47	0.51	0.53	0.07
Y_2O_3	0.00	0.00	0.00	0.00	0.00	0.00	0.00	0.00
Yb_2O_3	0.01	0.00	0.00	0.01	0.01	0.01	0.01	0.01
Na_2O	9.14	9.12	8.96	8.94	8.94	9.03	9.14	13.94
K_2O	2.33	2.29	2.23	2.26	2.26	2.27	2.33	0.00
CaO	0.17	0.19	0.21	0.18	0.18	0.17	0.17	0.13
F	1.93	1.83	1.94	1.81	1.81	1.89	1.93	0.00
Cl	0.00	0.00	0.00	0.00	0.00	0.00	0.00	0.01
Total	98.95	98.65	98.30	98.19	98.19	98.85	98.95	98.41
Isotope								
^{6}Li	1628.11			1656.95	1683.77		1686.12	18.00
^{9}Be	16.88			14.73	15.26		15.08	36.00
^{11}B	4.58			4.71	4.45		4.59	30.00
^{51}V	4.42	0.00	0.37	0.00	0.00	0.00	0.00	0.63
^{52}Cr	7.04	2.56	0.70	1.38	1.38	0.12	0.10	1.26
^{55}Mn	0.95	0.93	0.92	0.90	0.90	1.02	0.99	0.12
^{66}Zn	7681.84	8931.95	9285.00	9440.14	9440.14	8656.34	10076.41	1728.04
^{85}Rb	78.58	74.50	71.83	74.03	74.03	78.46	84.74	48.77
^{88}Sr	4.37	1.83	2.04	2.22	2.22	1.93	1.77	13.63
^{89}Y	60.37	53.08	62.44	60.22	60.22	60.22	55.72	187.49
^{90}Zr	4204.13	3777.10	4248.30	4122.11	4122.11	4178.87	3854.32	4191.08
^{93}Nb	273.89	246.96	265.40	258.41	258.41	267.70	252.86	1117.87
^{138}Ba	5.34	1.38	1.59	1.53	1.53	1.60	1.40	37.84
^{139}La	5.08	1.35	1.63	1.78	1.78	1.73	1.60	25.98
^{140}Ce	9.22	6.32	6.64	6.57	6.57	7.14	6.61	90.49
^{141}Pr	3.15	1.05	1.02	0.91	0.91	1.16	1.02	7.28
^{146}Nd	20.32	3.39	3.71	3.54	3.54	4.30	3.62	26.87
^{147}Sm	18.42	0.84	1.14	0.96	0.96	1.25	0.90	15.65
^{151}Eu	4.47	0.04	0.06	0.03	0.03	-0.04	0.01	0.79
^{157}Gd	22.26	0.67	0.72	0.83	0.83	0.54	0.69	19.73
^{159}Tb	3.21	0.26	0.28	0.34	0.34	0.29	0.31	7.13
^{163}Dy	13.85	4.78	5.81	5.43	5.43	5.65	5.37	53.14
^{165}Ho	5.09	2.76	3.28	3.07	3.07	3.05	2.90	10.89
^{166}Er	30.25	22.70	25.90	25.06	25.06	25.23	23.34	38.60
^{169}Tm	10.19	7.78	8.78	8.74	8.74	8.38	7.81	9.53
^{174}Yb	95.45	86.07	98.04	94.67	94.67	94.56	88.55	113.24
^{175}Lu	20.41	16.83	19.26	18.93	18.93	18.89	16.92	23.19
^{178}Hf	169.79	154.40	174.39	171.83	171.83	172.35	156.59	147.90
^{232}Th	2.16	0.01	0.04	0.04	0.04	0.03	0.03	32.67
^{238}U	2.24	0.02	0.00	0.00	0.00	0.04	0.04	23.77
Σ REE	261.38	154.83	176.27	170.87	170.87	172.14	159.66	442.51
La/Lu	0.25	0.08	0.08	0.09	0.09	0.09	0.09	1.12
Nb/Zr	0.07	0.07	0.06	0.06	0.06	0.06	0.07	0.27
Th/U	0.97	0.48	0.00	0.00	0.00	0.73	0.65	1.37

[1] High atomic number; [2] low atomic number

Acronyms refer to: m=march; j=june;s=september; a,b,c=run on that day; u=unknown analysis number based on electron-microprobe data; ltgr=light green; lt=light; dk=dark med=medium; av=average; int=intermediate; alt=alteration; py=pyroxene; am=amphibole; ~ approximately; no value indicates no analysis performed, n.d. indicates element not analyzed

Appendix B-5: LAM-ICP-MS analyses

Unit	Altered pegmatite							
Sample#	46-I-3						54-A-1	
HighZ[1]	11seb-u7	11seb-u8	11seb-u9	11seb-u10			08seb u5	08seb u7
Low Z[2]	S6B-U5	S6B-U6	S6B-U3	S6B-U7	S6B-U1	S6b-U2		
Analysis#	ambleb 22	amnrpy 23	pynram 26	am 24	am-25	amnrpy 25	145	198
SiO_2	51.68	51.20	52.49	50.87	51.20	51.20	50.19	50.50
Al_2O_3	0.14	0.15	0.10	0.15	0.15	0.15	0.36	0.49
TiO_2	0.94	0.95	0.91	0.94	0.93	0.93	1.56	0.68
FeO	29.64	31.40	30.17	31.82	31.96	31.96	32.48	33.71
MgO	0.01	0.00	0.01	0.00	0.00	0.00	0.07	0.23
MnO	0.60	1.43	0.29	1.45	1.44	1.44	0.65	0.51
ZnO	0.00	0.50	0.00	0.50	0.54	0.54	0.27	0.20
Cr_2O_3	0.01	0.00	0.00	0.00	0.01	0.01	0.00	0.00
V_2O_3	0.00	0.01	0.00	0.01	0.00	0.00	0.01	0.01
Nb_2O_5	0.00	0.01	0.00	0.02	0.00	0.00	0.00	0.00
ZrO_2	0.63	0.60	0.50	0.56	0.61	0.61	0.27	0.10
Y_2O_3	0.00	0.00	0.00	0.00	0.00	0.00	0.00	0.00
Yb_2O_3	0.00	0.02	0.02	0.01	0.03	0.03	0.01	0.02
Na_2O	13.86	9.10	14.02	8.94	9.01	9.01	9.44	9.46
K_2O	0.00	2.13	0.00	2.20	2.14	2.14	1.49	1.15
CaO	0.09	0.21	0.15	0.20	0.20	0.20	0.29	0.23
F	0.00	1.80	0.00	1.74	1.90	1.90	1.93	1.97
Cl	0.01	0.00	0.00	0.00	0.00	0.00	0.01	0.02
Total	97.60	98.74	98.67	98.67	99.33	99.33	98.19	98.44
Isotope								
^{6}Li	17.00	1937.00	233.00	1955.00	1866.00	1762.00		
^{9}Be	49.00	22.00	82.00	18.00	20.00	20.00		
^{11}B	129.00	23.00	38.00	8.00	7.00	6.00		
^{51}V	0.00	0.00	0.00	0.00			7.94	8.06
^{52}Cr	0.45	0.36	0.54	0.76			7.85	9.17
^{55}Mn	0.37	1.09	0.19	1.02			0.38	0.35
^{66}Zn	2677.06	6861.12	1727.83	7208.95			1704.19	1656.04
^{85}Rb	127.39	56.37	49.17	56.24			46.96	26.17
^{88}Sr	9.38	2.03	12.26	1.92			7.84	11.42
^{89}Y	103.64	99.47	176.94	89.00			79.06	303.96
^{90}Zr	4281.54	6625.80	5268.36	5770.23			1177.74	895.80
^{93}Nb	485.23	368.99	1156.81	349.89			87.78	81.09
^{138}Ba	23.20	5.57	24.52	1.54			1.81	6.72
^{139}La	20.13	3.92	26.27	2.21			15.80	30.85
^{140}Ce	67.24	14.89	87.40	8.37			38.04	85.86
^{141}Pr	3.80	2.65	6.57	1.47			4.75	9.95
^{144}Nd	14.15	10.65	24.11	6.41			26.89	56.93
^{147}Sm	6.25	3.52	14.84	2.04			9.78	26.60
^{151}Eu	0.45	0.29	0.94	0.20			1.65	1.60
^{157}Gd	8.89	2.64	18.25	2.04			13.24	37.44
^{159}Tb	2.99	0.83	6.57	0.56			1.97	7.14
^{162}Dy	22.77	9.70	50.02	8.05			11.23	44.69
^{165}Ho	5.88	5.04	11.06	4.60			2.75	9.64
^{166}Er	25.30	44.77	48.95	40.89			11.23	27.57
^{169}Tm	8.49	15.76	15.95	14.56			2.91	4.66
^{174}Yb	115.73	180.14	196.97	171.58			36.23	40.56
^{175}Lu	29.95	37.04	40.50	35.03			8.29	8.34
^{178}Hf	187.74	242.98	210.67	219.65			42.54	33.33
^{232}Th	10.34	0.60	15.91	0.22			1.18	4.46
^{238}U	10.61	1.56	21.01	0.41			0.00	0.76
Σ REE	332.03	331.83	548.40	298.02			184.74	391.83
La/Lu	0.67	0.11	0.65	0.06			1.91	3.70
Nb/Zr	0.11	0.06	0.22	0.06			0.07	0.09
Th/U	0.97	0.38	0.76	0.54			0.00	5.88

[1] High atomic number; [2] low atomic number

Acronyms refer to: m=march; j=june;s=september; a,b,c=run on that day; u=unknown analysis number based on electron-microprobe data; ltgr=light green; lt=light; dk=dark med=medium; av=average; int=intermediate; alt=alteration; py=pyroxene; am=amphibole; ~ approximately; no value indicates no analysis performed, n.d. indicates element not analyzed

Appendix B-5: LAM-ICP-MS analyses

Unit	Altered Subsolvus							
Sample#	54A1#2				63-B-1			63-B-1#1
HighZ[1]					08seb u8	08seb u9	08seb u10	11sea - u10
Low Z[2]	J21B-U7	J21B-U8	J21B-U9	J21B-U10	M20C-U5	M20C-U7	M20C-U8	M21B-U7
Analysis#	195	197	194	~196	~ 190	191	192	~188
SiO_2	51.27	51.13	51.18	51.19	50.39	50.55	50.64	50.21
Al_2O_3	0.29	0.47	0.45	0.45	0.30	0.30	0.29	0.39
TiO_2	0.97	0.72	0.74	0.76	1.61	1.92	1.89	1.08
FeO	33.24	33.58	33.30	33.11	32.82	32.86	32.51	34.00
MgO	0.19	0.26	0.29	0.32	0.19	0.09	0.16	0.19
MnO	0.54	0.50	0.53	0.53	0.80	0.87	0.88	0.84
ZnO	0.19	0.16	0.17	0.17	0.30	0.35	0.42	0.32
Cr_2O_3	0.00	0.00	0.00	0.00	0.00	0.00	0.00	0.00
V_2O_3	0.01	0.00	0.00	0.01	0.01	0.00	0.01	0.00
Nb_2O_5	0.00	0.00	0.00	0.00	0.00	0.00	0.00	0.00
ZrO_2	0.12	0.10	0.09	0.09	0.21	0.15	0.13	0.20
Y_2O_3	0.00	0.00	0.00	0.00	0.00	0.00	0.00	0.00
Yb_2O_3	0.01	0.01	0.00	0.00	0.03	0.01	0.02	0.01
Na_2O	9.42	9.69	9.47	9.68	9.34	9.38	9.34	9.10
K_2O	1.76	1.14	1.17	1.13	1.51	1.55	1.58	1.27
CaO	0.09	0.24	0.22	0.23	0.32	0.29	0.24	0.47
F	1.99	1.83	2.04	1.90	1.93	1.96	1.93	1.84
Cl	0.00	0.01	0.01	0.01	0.01	0.00	0.01	0.00
Total	99.26	99.06	98.79	98.78	98.94	99.46	99.23	99.14
Isotope								
^{6}Li	1347.44	1235.89	1331.17	1506.79	967.13	1085.86	1179.65	756.28
^{9}Be	7.75	24.43	7.55	12.81	26.80	26.02	774.59	24.42
^{11}B	6.07	10.57	7.58	6.55	3.27	3.89	3.50	3.87
^{51}V					0.15	0.00	4.79	0.00
^{52}Cr					0.92	0.59	60.58	0.79
^{55}Mn					0.58	0.57	0.50	0.56
^{66}Zn					3712.00	4857.90	5440.61	3170.70
^{85}Rb					26.98	28.29	26.51	27.30
^{88}Sr					4.18	3.45	2.65	5.07
^{89}Y					64.38	57.88	50.23	69.68
^{90}Zr					1575.93	1299.25	1181.55	1728.80
^{93}Nb					129.97	151.65	142.82	156.87
^{138}Ba					5.35	4.78	4.56	1.83
^{139}La					5.77	4.72	4.05	15.20
^{140}Ce					19.98	17.49	15.17	48.34
^{141}Pr					3.02	2.63	2.27	8.29
^{146}Nd					11.09	9.58	7.79	32.56
^{147}Sm					2.87	2.67	2.30	8.13
^{151}Eu					0.20	0.11	0.11	0.51
^{157}Gd					2.19	2.09	1.77	5.65
^{159}Tb					0.72	0.67	0.55	1.21
^{162}Dy					8.61	7.82	6.56	11.85
^{165}Ho					4.00	3.83	3.28	4.51
^{166}Er					33.23	31.77	27.92	31.12
^{169}Tm					11.73	11.70	10.33	10.30
^{174}Yb					143.35	147.84	130.57	121.52
^{175}Lu					35.25	35.49	32.31	28.34
^{178}Hf					54.95	44.72	40.97	73.04
^{232}Th					0.00	0.00	0.00	0.01
^{238}U					0.00	0.00	0.00	0.00
Σ REE					282.01	278.41	244.97	327.54
La/Lu					0.16	0.13	0.13	0.54
Nb/Zr					0.08	0.12	0.12	0.09
Th/U					0.00	0.00	0.00	0.00

[1] High atomic number; [2] low atomic number

Acronyms refer to: m=march; j=june;s=september; a,b,c=run on that day; u=unknown analysis number based on electron-microprobe data; ltgr=light green; lt=light; dk=dark med=medium; av=average; int=intermediate; alt=alteration; py=pyroxene; am=amphibole; ~ approximately; no value indicates no analysis performed, n.d. indicates element not analyzed

Appendix B-5: LAM-ICP-MS analyses

Unit	Altered Subsolvus							
Sample#	63-B-1#1		63-B-3a#3					
HighZ[1]								
Low Z[2]	M21B-U8	M21B-U6	S6A-U1	S6A-U2	S6A-U3	S6A-U4	S6A-U5	S6A-U9
Analysis#	187	185	alt 283	alt 274	am+alt 271	am+alt-279	Am+alt-276	am 246
SiO_2	50.16	51.30	51.02	51.28	50.31	51.85	51.98	51.15
Al_2O_3	0.39	0.20	0.31	0.22	0.20	0.23	0.44	0.39
TiO_2	1.42	0.80	0.68	0.75	0.65	0.77	0.98	1.52
FeO	33.71	31.84	30.96	30.82	31.03	32.21	32.80	32.13
MgO	0.20	0.01	0.01	0.05	0.06	0.11	0.18	0.03
MnO	0.73	1.21	0.59	0.86	0.88	1.05	0.55	0.69
ZnO	0.24	0.64	0.00	0.30	0.51	0.61	0.09	0.00
Cr_2O_3	0.00	0.00	0.00	0.00	0.00	0.00	0.00	0.01
V_2O_3	0.00	0.00	0.00	0.00	0.00	0.00	0.01	0.02
Nb_2O_5	0.00	0.00	0.00	0.00	0.03	0.00	0.00	0.00
ZrO_2	0.17	0.12	0.11	0.17	0.11	0.15	0.57	0.02
Y_2O_3	0.00	0.00	0.00	0.00	0.00	0.00	0.00	0.00
Yb_2O_3	0.00	0.01	0.00	0.00	0.00	0.00	0.00	0.00
Na_2O	9.13	9.12	13.77	13.54	12.41	8.99	9.74	9.49
K_2O	1.22	2.05	0.00	0.00	0.00	2.27	1.14	1.57
CaO	0.39	0.17	0.09	0.19	1.62	0.19	0.20	0.08
F	1.84	1.80	0.00	0.00	0.00	1.24	2.33	0.43
Cl	0.01	0.00	0.01	0.01	0.02	0.00	0.01	0.01
Total	98.84	98.51	97.54	98.19	97.82	99.15	100.03	97.33
Isotope								
^{6}Li	770.86	735.50	30.00	62.00	1221.00	464.00	505.00	1824.00
^{9}Be	26.44	28.72	18.00	326.00	10.00	30.00	87.00	18.00
^{11}B	3.29	3.16	90.00	477.00	58.00	141.00	113.00	6.00
^{51}V								
^{52}Cr								
^{55}Mn								
^{66}Zn								
^{85}Rb								
^{88}Sr								
^{89}Y								
^{90}Zr								
^{93}Nb								
^{138}Ba								
^{139}La								
^{140}Ce								
^{141}Pr								
^{146}Nd								
^{147}Sm								
^{151}Eu								
^{157}Gd								
^{159}Tb								
^{162}Dy								
^{165}Ho								
^{166}Er								
^{169}Tm								
^{174}Yb								
^{175}Lu								
^{178}Hf								
^{232}Th								
^{238}U								
Σ REE								
La/Lu								
Nb/Zr								
Th/U								

[1] High atomic number; [2] low atomic number

Acronyms refer to: m=march; j=june;s=september; a,b,c=run on that day; u=unknown analysis number based on electron-microprobe data; ltgr=light green; lt=light; dk=dark med=medium; av=average; int=intermediate; alt=alteration; py=pyroxene; am=amphibole; ~ approximately; no value indicates no analysis performed, n.d. indicates element not analyzed

Appendix B-5: LAM-ICP-MS analyses

Unit	Altered Subsolvus							
Sample#	63-B-3a#3	63-B-3c#3		63-B-3c#3	SL-182-86.3		Grain#2	SL-1-17
HighZ[1]								11sea - u9
Low Z[2]	S6A-U10	S6A-U6	S6A-U8	S6A-U7	J21A-U1	J21A-U2	J21A-U3	J21B-U3
Analysis#	ed 257	263	alt 267	int 259	135	137	138	- 169
SiO_2	52.02	48.93	50.53	50.01	49.76	50.60	50.47	49.31
Al_2O_3	0.29	0.95	0.42	0.36	0.92	0.41	0.72	1.07
TiO_2	1.39	1.01	0.68	0.83	0.72	1.22	0.77	1.14
FeO	30.24	33.70	31.07	30.48	33.23	31.83	32.94	32.70
MgO	0.02	0.27	0.02	0.11	0.24	0.13	0.18	0.31
MnO	0.91	0.55	0.62	0.79	0.67	0.90	0.74	0.65
ZnO	0.81	0.07	0.00	0.51	0.22	0.35	0.28	0.18
Cr_2O_3	0.00	0.00	0.00	0.00	0.00	0.00	0.00	0.00
V_2O_3	0.00	0.00	0.01	0.00	0.01	0.01	0.00	0.00
Nb_2O_5	0.00	0.03	0.03	0.01	0.00	0.00	0.00	0.00
ZrO_2	0.12	0.09	0.13	0.11	0.08	0.23	0.08	0.09
Y_2O_3	0.00	0.00	0.00	0.00	0.00	0.00	0.00	0.00
Yb_2O_3	0.00	0.01	0.00	0.01	0.00	0.01	0.01	0.00
Na_2O	9.75	10.06	13.85	12.28	9.07	9.34	8.94	8.91
K_2O	1.77	0.77	10.00	0.00	1.07	1.39	1.29	1.24
CaO	0.09	1.11	0.08	2.00	1.54	0.41	0.66	1.91
F	2.26	1.16	0.00	0.00	2.22	2.06	1.78	2.66
Cl	0.01	0.02	0.01	0.01	0.02	0.01	0.01	0.01
Total	98.71	98.25	97.47	97.49	98.84	98.04	98.11	99.05
Isotope								
^{6}Li	880.00	137.00	135.00	1225.00	1273.06	2052.04	1795.73	1189.28
^{9}Be	21.00	28.00	98.00	37.00	23.91	36.09	33.71	25.78
^{11}B	8.00	47.00	144.00	7.00	4.87	9.89	5.92	3.86
^{51}V								2.11
^{52}Cr								0.46
^{55}Mn								0.44
^{66}Zn								1998.83
^{85}Rb								17.10
^{88}Sr								6.42
^{89}Y								64.87
^{90}Zr								941.85
^{93}Nb								1893.24
^{138}Ba								25.25
^{139}La								30.09
^{140}Ce								95.83
^{141}Pr								14.13
^{144}Nd								55.11
^{147}Sm								14.20
^{151}Eu								0.90
^{157}Gd								11.31
^{159}Tb								2.13
^{162}Dy								14.89
^{165}Ho								3.60
^{166}Er								18.70
^{169}Tm								5.38
^{174}Yb								61.39
^{175}Lu								14.53
^{178}Hf								31.63
^{232}Th								164.71
^{238}U								45.74
Σ REE								342.17
La/Lu								2.07
Nb/Zr								2.01
Th/U								3.60

[1] High atomic number; [2] low atomic number

Acronyms refer to: m=march; j=june;s=september; a,b,c=run on that day; u=unknown analysis number based on electron-microprobe data; ltgr=light green; lt=light; dk=dark med=medium; av=average; int=intermediate; alt=alteration; py=pyroxene; am=amphibole; ~ approximately; no value indicates no analysis performed, n.d. indicates element not analyzed

Appendix B-5: LAM-ICP-MS analyses

Unit	Subsolvus altered							
Sample#	SL-1-17		SL-4-15			SL-8-1		
HighZ[1]			18sea-u2	18sea-u3	18seb-u3	08seb u2	08seb u3	08seb u4
Low Z[2]	J21B-U3	J21B-U5					M20C-U10	
Analysis#	-168	170	68.00	70.00	71.00	123.00	py	123.00
SiO_2	49.83	50.22	51.02	50.82	50.55	50.21		50.21
Al_2O_3	0.71	1.02	0.29	0.31	0.33	0.29		0.29
TiO_2	0.82	1.47	0.98	0.95	0.96	1.59		1.59
FeO	34.07	32.56	33.39	33.65	33.49	32.09		32.09
MgO	0.17	0.25	0.09	0.11	0.10	0.00		0.00
MnO	0.66	0.74	0.62	0.61	0.60	0.72		0.72
ZnO	0.20	0.14	0.04	0.17	0.06	0.29		0.29
Cr_2O_3	0.00	0.00	0.00	0.00	0.00	0.00		0.00
V_2O_3	0.01	0.00	0.01	0.00	0.00	0.02		0.02
Nb_2O_5	0.00	0.00	0.00	0.00	0.00	0.00		0.00
ZrO_2	0.11	0.08	0.14	0.14	0.15	0.18		0.18
Y_2O_3	0.00	0.00	0.00	0.00	0.00	0.00		0.00
Yb_2O_3	0.00	0.01	0.02	0.00	0.00	0.02		0.02
Na_2O	9.27	9.06	9.01	8.98	9.33	9.73		9.73
K_2O	1.10	1.21	1.76	1.71	1.44	1.51		1.51
CaO	0.83	0.60	0.09	0.10	0.12	0.17		0.17
F	1.82	1.70	2.38	2.34	2.38	2.39		2.39
Cl	0.02	0.03	0.01	0.00	0.00	0.00		0.00
Total	98.86	98.35	98.84	98.90	98.51	98.19		98.19
Isotope								
^{6}Li	1018.74	1674.46					42.03	
^{9}Be	20.96	36.40					18.53	
^{11}B	3.86	7.94					4.48	
^{51}V			0.06	0.00	6.58	1.05	0.00	0.00
^{52}Cr			1.16	0.85	19.73	19.33	1.62	9.03
^{55}Mn			0.45	0.42	0.49	0.45	0.08	0.51
^{66}Zn			2915.77	2225.21	1499.36	9750.15	1979.97	6761.34
^{85}Rb			54.74	51.01	33.42	32.27	47.37	35.08
^{88}Sr			0.81	0.85	0.95	11.68	2.77	10.75
^{89}Y			13.89	14.66	21.03	825.05	108.42	356.14
^{90}Zr			1122.79	1184.91	1276.19	769.85	849.64	758.10
^{93}Nb			51.75	54.31	54.87	118.96	216.67	245.66
^{138}Ba			0.54	0.62	1.40	12.62	6.43	15.13
^{139}La			0.60	0.78	9.90	359.10	25.41	134.17
^{140}Ce			2.45	2.77	22.33	709.43	64.80	264.35
^{141}Pr			0.35	0.47	2.68	151.72	12.27	56.56
^{144}Nd			1.34	1.48	9.08	695.40	58.56	282.76
^{147}Sm			0.47	0.37	2.90	187.59	18.34	77.46
^{151}Eu			0.01	0.01	0.10	8.11	0.94	2.99
^{157}Gd			0.19	0.13	1.07	167.79	17.96	73.50
^{159}Tb			0.10	0.11	0.34	29.71	3.77	12.30
^{163}Dy			1.29	1.48	3.60	172.31	24.29	74.67
^{165}Ho			0.82	0.74	1.19	35.17	5.07	14.52
^{166}Er			5.59	5.55	7.38	97.67	16.24	45.50
^{169}Tm			2.13	2.13	2.86	13.85	3.11	6.36
^{174}Yb			26.32	25.36	38.50	80.32	27.72	47.58
^{175}Lu			6.67	6.71	7.97	12.10	5.32	8.69
^{178}Hf			38.41	40.63	46.98	36.65	38.74	36.34
^{232}Th			0.03	0.00	1.45	19.70	5.26	13.43
^{238}U			0.02	0.00	0.61	0.00	0.58	0.00
Σ REE			48.33	48.11	109.91	2720.27	283.81	1101.43
La/Lu			0.09	0.12	1.24	29.69	4.77	15.45
Nb/Zr			0.05	0.05	0.04	0.15	0.26	0 32
Th/U			1.45	0.00	2.39	0.00	9.10	0.00

[1] High atomic number; [2] low atomic number

Acronyms refer to: m=march; j=june;s=september; a,b,c=run on that day; u=unknown analysis number based on electron-microprobe data; ltgr=light green; lt=light; dk=dark med=medium; av=average; int=intermediate; alt=alteration; py=pyroxene; am=amphibole; ~ approximately; no value indicates no analysis performed, n.d. indicates element not analyzed

Appendix B-5: LAM-ICP-MS analyses

Unit	Altered Subsolvus							
Sample#	SL-8-1					SL-8-1		
High Z[1]						18seb-u6	18seb-u7	18seb-u8
Low Z[2]	M20C-U9	J21A-U4	M21A-U2	M21A-U3	M21A-U4			
Analysis#	124	124	128	int-127	alt -126	82py	83py+am	85am
SiO_2	51.20	51.20	51.67	51.37	51.95	51.75	52.08	51.43
Al_2O_3	0.28	0.28	0.30	0.30	0.30	0.30	0.20	0.19
TiO_2	1.10	1.10	0.66	0.66	0.66	0.54	0.77	0.76
FeO	32.02	32.02	31.26	31.88	30.75	30.59	30.60	30.24
MgO	0.01	0.01	0.04	0.02	0.02	0.00	0.01	0.01
MnO	0.79	0.79	0.76	0.69	0.81	0.09	0.10	1.09
ZnO	0.36	0.36	0.38	0.30	0.52	0.00	0.00	0.98
Cr_2O_3	0.00	0.00	0.00	0.00	0.00	0.00	0.00	0.01
V_2O_3	0.00	0.00	0.01	0.00	0.01	0.00	0.00	0.01
Nb_2O_5	0.00	0.00	0.00	0.00	0.00	0.00	0.00	0.01
ZrO_2	0.11	0.11	0.09	0.10	0.11	0.06	0.11	0.07
Y_2O_3	0.00	0.00	0.00	0.00	0.00	0.00	0.00	0.00
Yb_2O_3	0.00	0.00	0.01	0.00	0.01	0.01	0.01	0.00
Na_2O	9.63	9.63	9.81	9.62	9.75	13.87	13.58	8.71
K_2O	1.68	1.68	1.62	1.69	1.65	0.00	0.00	2.23
CaO	0.06	0.06	0.17	0.05	0.05	0.10	0.03	0.17
F	2.41	2.41	1.92	2.13	2.27	0.00	0.00	1.76
Cl	0.01	0.01	0.00	0.01	0.01	0.00	0.00	0.00
Total	98.64	98.64	97.88	97.91	97.89	97.30	97.49	96.90
Isotope								
^{6}Li	1410.14	1694.96	1357.05	1737.56	427.36			
^{9}Be	12.94	15.81	8.98	7.69	5.90			
^{11}B	12.18	16.58	25.51	22.04	76.47			
^{51}V						0.02	0.27	0.00
^{52}Cr						0.00	0.00	0.00
^{55}Mn						0.08	0.08	0.55
^{66}Zn						1006.34	622.83	9258.57
^{85}Rb						10.89	31.15	40.60
^{88}Sr						0.34	1.54	6.79
^{89}Y						13.61	66.17	136.83
^{90}Zr						1017.17	1431.61	760.21
^{93}Nb						42.41	238.06	286.55
^{138}Ba						2.54	5.31	11.37
^{139}La						1.92	6.09	19.40
^{140}Ce						3.66	13.34	31.05
^{141}Pr						1.19	2.49	11.52
^{146}Nd						5.28	12.22	62.39
^{147}Sm						2.44	6.89	26.21
^{151}Eu						0.02	0.35	1.22
^{157}Gd						2.26	6.54	25.07
^{159}Tb						0.54	1.67	5.31
^{162}Dy						2.75	13.53	32.18
^{165}Ho						0.68	2.91	6.49
^{166}Er						2.13	10.69	20.37
^{169}Tm						0.65	2.31	3.72
^{174}Yb						7.40	25.74	33.18
^{175}Lu						1.97	6.24	6.65
^{178}Hf						47.50	73.51	30.05
^{232}Th						1.14	5.85	9.98
^{238}U						0.80	1.77	0.71
Σ REE						32.89	111.01	284.76
La/Lu						0.98	0.98	2.92
Nb/Zr						0.04	0.17	0.38
Th/U						1.43	3.30	14.00

[1] High atomic number; [2] low atomic number

Acronyms refer to: m=march; j=june;s=september; a,b,c=run on that day; u=unknown analysis number based on electron-microprobe data; ltgr=light green; lt=light; dk=dark med=medium; av=average; int=intermediate; alt=alteration; py=pyroxene; am=amphibole; ~ approximately; no value indicates no analysis performed, n.d. indicates element not analyzed

Appendix B-5: LAM-ICP-MS analyses

Unit	Lindinosite	
Sample#	Bob's Sample	
HighZ[1]	M6-U6	M6-U7
Low Z[2]		
Analysis#	BS - av	BS - av
SiO_2	51.55	51.55
Al_2O_3	0.16	0.16
TiO_2	0.52	0.52
FeO	30.84	30.84
MgO	0.03	0.03
MnO	1.83	1.83
ZnO	0.96	0.96
Cr_2O_3	0.00	0.00
V_2O_3	0.02	0.02
Nb_2O_5	0.04	0.04
ZrO_2	0.09	0.09
Y_2O_3	0.00	0.00
Yb_2O_3	0.00	0.00
Na_2O	9.19	9.19
K_2O	2.34	2.34
CaO	0.06	0.06
F	1.66	1.66
Cl	0.01	0.01
Total	98.58	98.58
Isotope		
^{6}Li		
^{9}Be		
^{11}B		
^{51}V	2.09	1.77
^{52}Cr	15.19	12.27
^{55}Mn	1.24	1.28
^{66}Zn	8028.19	7142.77
^{85}Rb	90.05	75.19
^{88}Sr	4.75	10.18
^{89}Y	82.45	185.51
^{90}Zr	458.21	569.70
^{93}Nb	531.16	896.83
^{138}Ba	9.53	18.06
^{139}La	17.17	56.12
^{140}Ce	35.98	109.82
^{141}Pr	4.65	14.96
^{144}Nd	15.18	40.09
^{147}Sm	6.94	14.52
^{151}Eu	0.55	1.31
^{157}Gd	8.01	18.47
^{159}Tb	3.04	6.20
^{163}Dy	22.00	51.98
^{165}Ho	5.08	10.19
^{166}Er	16.00	32.94
^{169}Tm	2.63	5.50
^{174}Yb	21.06	39.87
^{175}Lu	2.46	4.48
^{178}Hf	16.60	23.55
^{232}Th	35.56	34.15
^{238}U	128.15	184.38
ΣREE	160.76	406.46
La/Lu	6.97	12.53
Nb/Zr	1.16	1.57
Th/U	0.28	0.19

av=average

Appendix B-6: Setup conditions for LAM-ICP-MS analysis.

Parameter	Range of values Low[1]	High[2]
Extraction lens (V)	0.09-1.12	0.80-1.30
Collector lens (V)	7.84-7.94	7.93-8.97
Nebulizer flow rate (L/m)	1.102-1.194	1.117-1.190
Cooling gas-flow rate (L/m)	14.0-14.3	14.0-14.2
Auxiliary gas-flow rate (L/m)	0.90-2.00	0.90-0.95
Acquisition mode	Peak jumping	Peak jumping
Measuring point/peak (points) (separated by 1/200 AMU)	3	3
Dwell-time per point (ms)	10.24	10.24
Pre-ablate time (s)	20 or 30	30
Acquisition time (s)	30	60
Number of repeats	3	3
Number of completed sweeps	86 or 94	55 or 58

[1] Low atomic number elements (see text).

[2] High atomic number elements.

AMU = atomic mass unit.

Appendix B-7: Calculated Lower Limit of Detection (LLD) of LAM-ICP-MS analyses.

Element	Isotope	Average LLD *
Li	6	11.17
Be	9	21.62
B	11	81.42
V	51	111.63
Cr	52	113.37
Zn	66	111.19
Rb	85	59.02
Sr	88	43.20
Y	89	51.84
Zr	90	50.43
Nb	93	30.68
Ba	138	15.06
La	139	15.29
Ce	140	12.19
Pr	141	11.11
Nd	146	12.13
Sm	147	12.07
Eu	151	10.80
Gd	157	12.10
Tb	159	10.52
Dy	162	11.12
Ho	165	11.55
Er	166	10.19
Tm	169	8.99
Yb	174	8.48
Lu	175	9.40
Hf	178	10.74
Th	232	11.23
U	238	10.35

* Based on 3 repeats (in ppm).

Appendix B-8: Low Z elemental contents of arfvedsonitic amphibole.

Atomic absorption spectrometry analyses

Sample #	Li (ppm)
46-I-3	1,545
54-A-1	2,254
SL-BS-1	2,165

Ion-probe analyses courtesy of F.C. Hawthorne.

Sample #	Li (ppm)	Be (ppm)	B (ppm)
48-A-7	1,350	11	1
49-C-2	976	12	1
54-A-1	1,140	5	1
46-I-3	1,347	18	3
63-B-3	1,324	16	2
SL-1-17	1,460	20	2
SL-BS-1	1,420	90	2

Appendix B-9: X-ray Powder Diffraction Data.

Mineral	**Arfvedsonitic Amphibole**					**Type-2 Aegirine**	
Unit	**H**	**46-I-3**	**S alt**	**S alt**	**BS**	**S alt**	**S alt**
Sample #	**49-C-2**	**46-I-3**	**63-B**	**63-B-4**	**SL-BS-1**	**63-B**	**63-B-4**
a (Å)	9.899	9.883	9.879	9.864	9.909	9.667	9.671
b (Å)	18.047	18.029	18.044	18.021	18.036	8.803	8.784
c (Å)	5.3187	5.3120	5.3081	5.3150	5.3158	5.2974	5.2997
α (°)	90.00	90.00	90.00	90.00	90.00	90.00	90.00
β (°)	103.76	103.78	103.65	103.60	103.72	107.40	107.43
γ (°)	90.00	90.00	90.00	90.00	90.00	90.00	90.00
Volume (Å^3)	922.92	919.30	919.53	918.30	922.90	430.15	429.88
Errors							
a (Å)	0.002	0.001	0.005	0.005	0.001	0.002	0.001
b (Å)	0.004	0.002	0.004	0.010	0.002	0.002	0.002
c (Å)	0.0009	0.0005	0.0018	0.0022	0.0004	0.0011	0.0007
α (°)	0.00	0.00	0.00	0.00	0.00	0.00	0.00
β (°)	0.02	0.01	0.05	0.05	0.01	0.02	0.02
γ (°)	0.00	0.00	0.00	0.00	0.00	0.00	0.00
Volume (Å^3)	0.23	0.12	0.53	0.57	0.11	0.11	0.07

* Data determined from a powder X-ray diffraction pattern using a Guinier-Hagg focusing camera. The cell parameters were refined using the program of Appleman & Evans (1973), as modified by Garvey (1986).

Appleman, D.E. & Evans, H.T., Jr. (1973): Job 9214: indexing and least-squares refinement of powder diffraction data. U.S. Geological Survey, Computer Contributions, 20, (NTIS Doc. PB2-16188).

Garvey, R. (1986): LSUCRIPC, least squares unit-cell refinement with indexing on personal computer. Powder Diffraction, 1, 114.

Appendix B-10: AEM analyses of minerals from the hypersolvus granite

Mineral	Aegirine												
Spectrum#	1	21	25	27	28	31	38	4	6	24	8	15	17
Label	pyx	small	in amph	at ed. amph	incl.	elong.	at ed.	pyx	pyx	by incl.	by prev.	pyx	pyx
K_2O	0.00	0.13	0.11	0.15	0.73	0.08	0.34	0.00	0.00	0.09	0.05	0.17	0.02
Rb_2O	0.04	0.44	0.08	0.00	0.00	0.00	3.82	0.07	0.15	0.58	0.10	0.00	0.22
Na_2O	17.39	16.37	15.98	17.90	17.79	13.35	12.73	10.84	12.90	16.68	14.41	14.15	14.23
CaO	0.19	0.01	0.00	0.07	0.05	0.22	0.40	0.16	0.14	0.18	0.03	0.06	0.00
MgO	0.19	0.00	0.00	0.00	0.05	0.63	0.40	0.09	0.35	1.84	0.02	0.19	0.30
FeO	41.68	40.92	39.25	38.11	36.11	43.41	41.35	43.92	41.70	38.09	39.32	38.59	40.18
MnO	0.06	0.07	0.09	0.09	0.90	0.18	0.58	0.17	0.18	0.20	0.30	0.21	0.17
ZnO	0.80	0.57	0.67	0.00	3.96	0.00	3.52	0.00	0.16	0.00	0.75	0.33	0.10
ZrO_2	0.86	2.63	0.23	0.00	0.00	0.00	3.62	0.32	0.43	0.00	0.61	2.10	0.00
TiO_2	0.81	0.70	0.52	0.19	0.28	0.70	0.00	0.73	0.63	0.32	0.20	0.22	0.01
Al_2O_3	1.03	0.46	1.30	0.61	1.13	1.05	0.00	0.02	0.00	0.00	0.00	0.01	0.12
SiO_2	36.96	37.69	41.77	42.88	38.98	40.38	33.22	43.69	43.37	42.02	44.22	43.96	44.65
Total*	100.00	100.00	100.00	100.00	100.00	100.00	100.00	100.00	100.00	100.00	100.00	100.00	100.00
# Oxygen[1]	6	6	6	6	6	6	6	6	6	6	6	6	6
K	0.000	0.005	0.004	0.005	0.028	0.003	0.015	0.000	0.000	0.003	0.002	0.006	0.001
Rb	0.001	0.008	0.001	0.000	0.000	0.000	0.075	0.001	0.003	0.010	0.002	0.000	0.004
Na	1.169	1.103	1.008	1.120	1.169	0.857	0.933	0.677	0.807	1.051	0.895	0.883	0.877
Ca	0.007	0.001	0.000	0.003	0.002	0.008	0.017	0.006	0.005	0.006	0.001	0.002	0.000
Mg	0.012	0.000	0.000	0.000	0.003	0.038	0.028	0.005	0.021	0.110	0.001	0.011	0.017
Fe	1.153	1.135	1.020	0.981	0.976	1.147	1.247	1.129	1.074	0.988	1.006	0.991	1.019
Mn	0.002	0.002	0.002	0.002	0.025	0.005	0.018	0.005	0.005	0.005	0.008	0.005	0.004
Zn	0.019	0.014	0.015	0.000	0.091	0.000	0.091	0.000	0.003	0.000	0.016	0.007	0.002
Zr	0.015	0.045	0.004	0.000	0.000	0.000	0.067	0.005	0.007	0.000	0.010	0.033	0.000
Ti	0.026	0.023	0.016	0.006	0.009	0.022	0.000	0.022	0.019	0.010	0.006	0.007	0.000
Al	0.059	0.026	0.070	0.032	0.063	0.058	0.000	0.001	0.000	0.000	0.000	0.001	0.006
Si	2.033	2.079	2.158	2.196	2.096	2.121	1.992	2.233	2.221	2.167	2.248	2.245	2.252
ΣCations	4.496	4.440	4.298	4.345	4.462	4.258	4.482	4.083	4.164	4.350	4.194	4.192	4.183

* The total is set to 100.00 due to the fact that the analyses were performed by EDS, while assuming that all Fe present was as Fe^{2+}

[1] Number of atoms of oxygen used in the calculation of the mineral formulae

The acronyms used are: pyx=pyroxene, prev.=previous, amph=amphibole; ast=astrophyllite; phyllo=phyllosilicate
opp.=opposite; rt=right; ed=edge; incl.=inclusion; 2nd=second; gr=grain
The numbers in the label section refer to the corresponding HRTEM image

Appendix B-10: AEM analyses of minerals from the hypersolvus granite

Mineral	Aegirine												
Spectrum#	23	24	25	26	29	30	31	32	33	34	35	5	6
Label	pyx	pyx	pyx	pyx	pyx with phyllo		(6015-23)	bit away ther nr feld		further	between	amph	-4892
K_2O	0.00	0.01	0.19	0.00	0.06	0.30	0.13	0.39	0.08	0.00	0.26	2.59	1.97
Rb_2O	0.49	0.05	0.00	0.13	0.10	0.26	0.53	0.86	0.36	0.46	0.16	0.00	0.20
Na_2O	14.72	15.84	16.13	15.91	14.77	14.07	16.37	15.94	16.06	16.75	17.13	13.35	12.82
CaO	0.26	0.12	0.06	0.11	0.07	0.00	0.51	0.27	0.54	0.02	0.46	0.00	0.22
MgO	0.00	0.07	0.03	0.00	0.02	0.07	0.12	0.05	0.08	0.10	0.00	1.02	0.14
FeO	40.25	41.79	41.50	43.65	42.39	40.94	37.32	38.86	39.55	38.32	38.73	36.44	38.94
MnO	0.16	0.01	0.25	0.00	0.13	0.19	0.01	0.03	0.00	0.24	0.00	3.66	0.64
ZnO	0.00	0.27	0.39	0.00	0.44	0.06	0.15	0.00	0.44	0.00	0.00	4.59	3.20
ZrO_2	0.99	0.09	0.13	0.00	0.17	0.70	0.00	1.86	1.24	1.25	1.74	0.29	0.79
TiO_2	0.26	0.19	0.31	0.11	0.13	0.21	0.60	0.76	0.75	2.58	1.77	0.25	0.90
Al_2O_3	0.19	0.18	0.00	0.00	0.20	0.24	0.11	0.19	0.11	0.13	0.26	1.02	1.12
SiO_2	42.68	41.38	41.00	40.08	41.53	42.96	44.13	40.79	40.78	40.15	39.48	36.78	39.06
Total*	100.00	100.00	100.00	100.00	100.00	100.00	100.00	100.00	100.00	100.00	100.00	100.00	100.00
# Oxygen[1]	6	6	6	6	6	6	6	6	6	6	6	23	23
K	0.000	0.000	0.007	0.000	0.002	0.011	0.005	0.015	0.003	0.000	0.010	0.397	0.292
Rb	0.008	0.001	0.000	0.002	0.002	0.004	0.009	0.015	0.006	0.008	0.003	0.000	0.014
Na	0.931	1.016	1.041	1.041	0.947	0.886	1.011	1.031	1.037	1.079	1.117	3.474	3.235
Ca	0.009	0.004	0.002	0.004	0.002	0.000	0.018	0.010	0.020	0.001	0.017	0.000	0.031
Mg	0.000	0.004	0.002	0.000	0.001	0.004	0.007	0.003	0.005	0.006	0.000	0.252	0.033
Fe	1.048	1.103	1.103	1.175	1.119	1.062	0.949	1.035	1.051	1.016	1.040	3.904	4.045
Mn	0.004	0.000	0.007	0.000	0.004	0.005	0.000	0.001	0.000	0.007	0.000	0.399	0.068
Zn	0.000	0.006	0.009	0.000	0.010	0.001	0.003	0.000	0.010	0.000	0.000	0.420	0.284
Zr	0.016	0.001	0.002	0.000	0.003	0.011	0.000	0.030	0.020	0.020	0.029	0.019	0.050
Ti	0.008	0.006	0.010	0.004	0.004	0.006	0.018	0.024	0.023	0.080	0.055	0.031	0.109
Al	0.010	0.010	0.000	0.000	0.011	0.013	0.006	0.011	0.006	0.007	0.015	0.226	0.241
Si	2.209	2.172	2.166	2.146	2.180	2.215	2.231	2.160	2.156	2.116	2.108	7.835	8.066
ΣCations	4.243	4.325	4.349	4.371	4.285	4.220	4.256	4.334	4.338	4.340	4.393	16.957	16.468

* The total is set to 100.00 due to the fact that the analyses were performed by EDS, while assuming that all Fe present was as Fe^{2+}

[1] Number of atoms of oxygen used in the calculation of the mineral formulae

The acronyms used are: pyx=pyroxene, prev.=previous, amph=amphibole; ast=astrophyllite; phyllo=phyllosilicate
opp.=opposite; rt=right; ed=edge; incl.=inclusion; 2nd=second; gr=grain; nr=near
The numbers in the label section refer to the corresponding HRTEM image

Appendix B-10: AEM analyses of minerals from the hypersolvus granite

Mineral	Arfvedsonitic amphibole							
Spectrum#	15	22	24	26	29	30	14	17
Label	(4945-8)	by pyx	opp. side	right side	amph	amph	by ast	300sec
K_2O	2.37	2.12	2.43	1.49	1.71	2.13	3.31	3.34
Rb_2O	2.33	0.08	0.29	0.15	0.00	0.00	0.07	1.67
Na_2O	5.30	14.27	13.58	14.29	12.35	12.70	3.83	4.02
CaO	0.64	0.37	0.18	0.21	0.24	0.29	0.12	0.00
MgO	0.27	0.00	0.40	0.00	0.29	0.04	1.82	1.96
FeO	33.78	40.93	37.46	43.54	42.76	41.30	42.65	38.58
MnO	9.99	1.17	1.96	1.17	0.88	0.85	2.66	2.32
ZnO	4.75	2.24	3.13	0.06	1.18	1.16	3.21	0.00
ZrO_2	1.53	0.27	0.00	0.00	1.00	0.15	1.35	1.03
TiO_2	9.42	0.82	0.44	0.74	1.06	0.84	0.44	0.16
Al_2O_3	0.71	1.17	1.00	0.77	0.89	1.43	0.00	0.46
SiO_2	28.92	36.57	39.14	37.59	37.64	39.11	40.54	46.46
Total*	100.00	100.00	100.00	100.00	100.00	100.00	100.00	100.00
# Oxygen[1]	23	23	23	23	23	23	23	23
K	0.390	0.325	0.361	0.225	0.258	0.314	0.488	0.456
Rb	0.176	0.006	0.020	0.010	0.000	0.000	0.005	0.104
Na	1.487	3.715	3.426	3.675	3.174	3.188	0.961	0.932
Ca	0.103	0.055	0.026	0.031	0.036	0.041	0.017	0.000
Mg	0.073	0.000	0.095	0.000	0.070	0.009	0.432	0.429
Fe	3.899	4.387	3.890	4.610	4.523	4.267	4.408	3.682
Mn	1.172	0.128	0.207	0.126	0.095	0.089	0.280	0.225
Zn	0.468	0.205	0.278	0.005	0.107	0.103	0.284	0.000
Zr	0.108	0.018	0.000	0.000	0.065	0.009	0.086	0.060
Ti	1.267	0.102	0.053	0.091	0.131	0.101	0.052	0.018
Al	0.169	0.259	0.215	0.169	0.194	0.307	0.000	0.091
Si	6.638	7.794	8.082	7.916	7.918	8.035	8.330	8.817
ΣCations	15.949	16.994	16.651	16.859	16.570	16.463	15.342	14.814

* The total is set to 100.00 due to the fact that the analyses were performed by EDS, while assuming that all Fe present was as Fe^{2+}

[1] Number of atoms of oxygen used in the calculation of the mineral formulae

The acronyms used are: pyx=pyroxene, prev.=previous, amph=amphibole; ast=astrophyllite; phyllo=phyllosilicate
opp.=opposite; rt=right; ed=edge; incl.=inclusion; 2nd=second; gr=grain
The numbers in the label section refer to the corresponding HRTEM image

Appendix B-10: AEM analyses of minerals from the hypersolvus granite

Mineral	Arfvedsonitic Amphibole							
Spectrum#	18	19	12	27	28	38	39	40
Label	300 sec	by ast	amph	amph	amph	by prev.	by prev.	by prev.
K_2O	2.66	3.66	1.59	1.71	1.23	1.77	2.51	1.93
Rb_2O	0.27	0.91	0.00	0.14	0.00	0.44	0.01	0.17
Na_2O	6.43	9.99	9.75	10.36	10.21	10.91	11.49	10.69
CaO	0.00	0.04	0.33	0.40	0.41	0.46	0.03	0.16
MgO	1.17	3.64	0.71	0.63	0.79	0.02	0.01	0.21
FeO	39.57	35.91	44.49	42.85	42.79	43.68	43.43	42.08
MnO	2.09	1.86	1.30	1.34	1.46	1.25	1.76	0.94
ZnO	0.00	1.46	0.00	1.95	1.51	0.60	1.31	1.01
ZrO_2	2.46	0.33	0.89	0.88	1.20	1.13	0.00	0.27
TiO_2	0.29	0.42	1.01	0.87	0.99	0.21	0.00	0.85
Al_2O_3	0.41	0.00	0.12	0.14	0.29	0.01	0.56	0.22
SiO_2	44.65	41.77	39.81	38.76	39.12	39.53	38.88	41.45
Total*	100.00	100.00	100.00	100.00	100.00	100.00	100.00	100.00
# Oxygen[1]	23	23	23	23	23	23	23	23
K	0.372	0.523	0.235	0.256	0.183	0.264	0.378	0.280
Rb	0.017	0.060	0.000	0.009	0.000	0.030	0.001	0.012
Na	1.527	2.426	2.448	2.644	2.585	2.778	2.939	2.634
Ca	0.000	0.006	0.047	0.058	0.060	0.067	0.004	0.023
Mg	0.262	0.835	0.170	0.151	0.190	0.004	0.003	0.048
Fe	3.868	3.590	4.599	4.503	4.458	4.580	4.571	4.268
Mn	0.207	0.189	0.137	0.143	0.154	0.133	0.188	0.097
Zn	0.000	0.125	0.000	0.175	0.134	0.054	0.118	0.088
Zr	0.147	0.020	0.056	0.057	0.076	0.073	0.000	0.017
Ti	0.034	0.049	0.122	0.107	0.120	0.026	0.000	0.101
Al	0.082	0.000	0.025	0.030	0.062	0.001	0.122	0.047
Si	8.679	8.302	8.184	8.098	8.105	8.242	8.137	8.359
ΣCations	15.196	16.124	16.023	16.230	16.128	16.252	16.460	15.974

* The total is set to 100.00 due to the fact that the analyses were performed by EDS, while assuming that all Fe present was as Fe^{2+}

[1] Number of atoms of oxygen used in the calculation of the mineral formulae

The acronyms used are: pyx=pyroxene, prev.=previous, amph=amphibole; ast=astrophyllite; phyllo=phyllosilicate

opp.=opposite; rt=right; ed=edge; incl.=inclusion; 2nd=second; gr=grain

The numbers in the label section refer to the corresponding HRTEM image

Appendix B-10: AEM analyses of minerals from the hypersolvus granite

Mineral	Combinations							
Spectrum#	5	6	22	24	26	28	29	30
Label	amph	4892	amph	amph	rt side	amph incl.	amph	amph
K_2O	2.59	1.97	2.12	2.43	1.49	0.73	1.71	2.13
Rb_2O	0.00	0.20	0.08	0.29	0.15	0.00	0.00	0.00
Na_2O	13.35	12.82	14.27	13.58	14.29	17.79	12.35	12.70
CaO	0.00	0.22	0.37	0.18	0.21	0.05	0.24	0.29
MgO	1.02	0.14	0.00	0.40	0.00	0.05	0.29	0.04
FeO	36.44	38.94	40.93	37.46	43.54	36.11	42.76	41.30
MnO	3.66	0.64	1.17	1.96	1.17	0.90	0.88	0.85
ZnO	4.59	3.20	2.24	3.13	0.06	3.96	1.18	1.16
ZrO_2	0.29	0.79	0.27	0.00	0.00	0.00	1.00	0.15
TiO_2	0.25	0.90	0.82	0.44	0.74	0.28	1.06	0.84
Al_2O_3	1.02	1.12	1.17	1.00	0.77	1.13	0.89	1.43
SiO_2	36.78	39.06	36.57	39.14	37.59	38.98	37.64	39.11
Total*	100.00	100.00	100.00	100.00	100.00	100.00	100.00	100.00
# Oxygen[1]	6	6	6	6	6	6	6	6
K	0.104	0.076	0.085	0.094	0.059	0.028	0.067	0.082
Rb	0.000	0.004	0.001	0.005	0.003	0.000	0.000	0.000
Na	0.906	0.844	0.969	0.894	0.959	1.169	0.828	0.832
Ca	0.000	0.008	0.014	0.007	0.008	0.002	0.009	0.011
Mg	0.066	0.009	0.000	0.025	0.000	0.003	0.018	0.002
Fe	1.018	1.055	1.145	1.015	1.203	0.976	1.180	1.113
Mn	0.104	0.018	0.033	0.054	0.033	0.025	0.025	0.023
Zn	0.110	0.074	0.054	0.072	0.001	0.091	0.028	0.027
Zr	0.005	0.013	0.005	0.000	0.000	0.000	0.017	0.002
Ti	0.008	0.028	0.027	0.014	0.024	0.009	0.034	0.026
Al	0.059	0.063	0.068	0.056	0.044	0.063	0.051	0.080
Si	2.044	2.104	2.033	2.108	2.065	2.096	2.066	2.096
ΣCations	4.424	4.296	4.433	4.344	4.398	4.462	4.323	4.295

* The total is set to 100.00 due to the fact that the analyses were performed by EDS, while assuming that all Fe present was as Fe^{2+}

[1] Number of atoms of oxygen used in the calculation of the mineral formulae

The acronyms used are: pyx=pyroxene, prev.=previous, amph=amphibole; ast=astrophyllite; phyllo=phyllosilicate
opp.=opposite; rt=right; ed=edge; incl.=inclusion; 2nd=second; gr=grain; nr=near
The numbers in the label section refer to the corresponding HRTEM image

Appendix B-10: AEM analyses of minerals from the hypersolvus granite

Mineral	Combinations						
Spectrum#	38	40	6	31	32	33	34
Label	pyx at ed	amph inside	pyx + ast	opp (6015-23)	bit away	further nr feld	further
K_2O	0.34	0.00	2.34	0.13	0.39	0.08	0.00
Rb_2O	3.82	0.63	1.98	0.53	0.86	0.36	0.46
Na_2O	12.73	11.06	6.94	16.37	15.94	16.06	16.75
CaO	0.40	0.00	0.06	0.51	0.27	0.54	0.02
MgO	0.40	2.41	0.19	0.12	0.05	0.08	0.10
FeO	41.35	42.45	36.43	37.32	38.86	39.55	38.32
MnO	0.58	0.72	6.05	0.01	0.03	0.00	0.24
ZnO	3.52	3.75	7.59	0.15	0.00	0.44	0.00
ZrO_2	3.62	0.00	2.99	0.00	1.86	1.24	1.25
TiO_2	0.00	0.01	7.51	0.60	0.76	0.75	2.58
Al_2O_3	0.00	0.00	0.04	0.11	0.19	0.11	0.13
SiO_2	33.22	38.97	27.87	44.13	40.79	40.78	40.15
Total*	100.00	100.00	100.00	100.00	100.00	100.00	100.00
# Oxygen[1]	6	6	6	6	6	6	6
K	0.015	0.000	0.105	0.005	0.015	0.003	0.000
Rb	0.075	0.011	0.041	0.009	0.015	0.006	0.008
Na	0.933	0.730	0.529	1.011	1.031	1.037	1.079
Ca	0.017	0.000	0.003	0.018	0.010	0.020	0.001
Mg	0.028	0.150	0.014	0.007	0.003	0.005	0.006
Fe	1.247	1.154	1.143	0.949	1.035	1.051	1.016
Mn	0.018	0.020	0.193	0.000	0.001	0.000	0.007
Zn	0.091	0.087	0.203	0.003	0.000	0.010	0.000
Zr	0.067	0.000	0.057	0.000	0.030	0.020	0.020
Ti	0.000	0.000	0.275	0.018	0.024	0.023	0.080
Al	0.000	0.000	0.003	0.006	0.011	0.006	0.007
Si	1.992	2.106	1.738	2.231	2.160	2.156	2.116
ΣCations	4.482	4.259	4.303	4.256	4.334	4.338	4.340

* The total is set to 100.00 due to the fact that the analyses were performed by EDS, while assuming that all Fe present was as Fe^{2+}

[1] Number of atoms of oxygen used in the calculation of the mineral formulae

The acronyms used are: pyx=pyroxene, prev.=previous, amph=amphibole; ast=astrophyllite; phyllo=phyllosilicate
opp.=opposite; rt=right; ed=edge; incl.=inclusion; 2nd=second; gr=grain; nr=near
The numbers in the label section refer to the corresponding HRTEM image

Appendix B-10: AEM analyses of minerals from the hypersolvus granite

Mineral	Astrophyllite												
Spectrum#	8	9	15	16	3	7	8	9	10	11	12	13	15
Label	ast	ast	(4945-8)	ast	ast	ast	thinner	nr atn opp	ast	ast	ast	ast	ast at top
K_2O	3.34	3.23	2.37	2.36	6.87	6.85	6.54	7.49	6.52	6.54	6.68	6.61	6.57
Rb_2O	2.30	2.68	2.33	2.20	1.08	0.29	0.51	1.03	1.46	0.78	0.75	0.66	0.71
Na_2O	6.57	7.12	5.30	5.87	3.39	0.00	0.00	0.00	0.00	0.00	3.12	4.47	3.97
CaO	0.36	0.52	0.64	0.28	0.09	0.14	0.29	0.34	0.15	0.12	0.13	0.12	0.14
MgO	0.00	0.24	0.27	0.21	0.33	0.46	1.01	0.32	0.39	0.51	0.50	0.12	0.54
FeO	35.85	33.08	33.78	35.20	33.64	32.55	35.06	35.68	32.11	33.25	33.78	32.48	34.91
MnO	9.36	7.90	9.99	6.67	10.69	10.64	9.90	11.41	9.94	9.70	10.02	10.06	10.69
ZnO	4.33	4.43	4.75	6.51	4.01	8.59	4.48	1.45	7.83	7.28	4.26	9.18	8.39
ZrO_2	1.79	2.01	1.53	1.90	0.00	2.94	0.90	4.51	5.92	6.54	5.36	2.51	2.02
TiO_2	8.30	8.57	9.42	8.60	9.76	9.19	10.25	9.31	7.95	8.73	8.58	8.68	7.44
Al_2O_3	0.58	1.14	0.71	0.86	0.09	0.16	0.00	0.00	0.04	0.08	0.00	0.00	0.10
SiO_2	27.23	29.07	28.92	29.33	30.04	28.18	31.06	28.46	27.69	26.48	26.82	25.09	24.52
Total*	100.00	100.00	100.00	100.00	100.00	100.00	100.00	100.00	100.00	100.00	100.00	100.00	100.00
# Oxygen[1]	31	31	31	31	31	31	31	31	31	31	31	31	31
K	0.769	0.718	0.526	0.525	1.513	1.573	1.415	1.714	1.534	1.559	1.574	1.598	1.610
Rb	0.243	0.272	0.237	0.224	0.109	0.030	0.050	0.108	0.157	0.085	0.081	0.073	0.079
Na	2.576	2.691	2.004	2.218	1.270	0.000	0.000	0.000	0.000	0.000	1.249	1.837	1.655
Ca	0.081	0.112	0.138	0.061	0.020	0.031	0.061	0.076	0.034	0.027	0.031	0.029	0.032
Mg	0.000	0.087	0.098	0.074	0.117	0.171	0.352	0.119	0.150	0.194	0.188	0.047	0.212
Fe	5.789	5.146	5.255	5.478	5.186	5.232	5.311	5.718	5.293	5.550	5.572	5.498	5.987
Mn	1.537	1.249	1.580	1.056	1.675	1.738	1.524	1.859	1.666	1.645	1.680	1.731	1.864
Zn	0.598	0.589	0.631	0.866	0.528	1.179	0.579	0.198	1.102	1.039	0.600	1.327	1.229
Zr	0.176	0.192	0.145	0.181	0.000	0.289	0.083	0.443	0.598	0.668	0.542	0.260	0.212
Ti	1.562	1.555	1.708	1.561	1.755	1.723	1.810	1.740	1.528	1.699	1.650	1.714	1.488
Al	0.195	0.367	0.228	0.276	0.030	0.055	0.000	0.000	0.013	0.026	0.000	0.000	0.035
Si	8.744	8.993	8.947	9.077	9.210	9.007	9.355	9.071	9.078	8.787	8.797	8.445	8.361
ΣCations	22.269	21.973	21.496	21.596	21.412	21.029	20.542	21.046	21.154	21.280	21.963	22.559	22.766

* The total is set to 100.00 due to the fact that the analyses were performed by EDS, while assuming that all Fe present was as Fe^{2+}

[1] Number of atoms of oxygen used in the calculation of the mineral formulae

The acronyms used are: pyx=pyroxene, prev.=previous, amph=amphibole; ast=astrophyllite; phyllo=phyllosilicate
opp.=opposite; rt=right; ed=edge; incl.=inclusion; 2nd=second; gr=grain
The numbers in the label section refer to the corresponding HRTEM image

Appendix B-10: AEM analyses of minerals from the hypersolvus granite

Mineral	Astrophyllite												
Spectrum#	16	21	26	27	28	30	31	32	33	1	2	3	4
Label	ast at top ear shaped		amazing	amazing	amazing1	to center	to center	to center	to center	First gr	2nd gr	2nd gr	by gr
K_2O	5.62	2.72	1.96	2.82	1.02	2.04	3.30	3.53	1.58	1.88	1.84	3.01	2.23
Rb_2O	0.00	6.39	0.79	3.69	2.71	1.61	2.84	3.73	1.91	1.40	2.27	2.46	1.76
Na_2O	4.05	2.64	1.31	5.69	6.75	6.62	4.17	1.40	6.45	6.11	5.57	5.61	7.77
CaO	0.14	0.41	0.48	0.30	0.52	0.26	0.50	0.69	0.42	0.46	0.49	0.31	0.03
MgO	0.70	1.53	0.47	0.25	0.46	0.64	0.36	0.24	1.04	2.19	0.90	0.01	0.03
FeO	32.04	39.31	40.11	34.78	39.11	37.64	40.03	40.88	41.45	34.33	37.48	37.76	38.61
MnO	11.01	6.20	5.59	7.63	2.69	6.19	8.03	6.67	2.56	4.21	4.60	6.33	6.57
ZnO	8.32	0.00	4.80	3.96	3.19	8.27	0.52	7.19	3.56	12.20	3.11	5.21	4.60
ZrO_2	3.13	0.00	2.61	3.63	1.26	0.00	2.09	0.36	1.45	0.00	7.22	2.15	2.02
TiO_2	8.75	8.84	5.83	7.95	4.56	6.74	8.57	8.46	4.76	7.17	7.20	8.44	6.66
Al_2O_3	0.00	0.89	0.01	0.01	0.17	0.01	0.00	0.01	0.37	1.10	0.49	0.03	0.02
SiO_2	26.24	31.07	36.05	29.28	37.58	29.99	29.61	26.84	34.46	28.95	28.84	28.68	29.68
Total*	100.00	100.00	100.00	100.00	100.00	100.00	100.00	100.00	100.00	100.00	100.00	100.00	100.00
# Oxygen[1]	31	31	31	31	31	31	31	31	31	31	31	31	31
K	1.326	0.584	0.405	0.639	0.207	0.456	0.735	0.828	0.331	0.417	0.419	0.683	0.503
Rb	0.000	0.628	0.075	0.382	0.251	0.164	0.290	0.401	0.183	0.142	0.236	0.256	0.181
Na	1.625	0.964	0.462	2.192	2.327	2.511	1.581	0.560	2.308	2.303	2.157	2.170	2.981
Ca	0.032	0.086	0.096	0.067	0.102	0.056	0.108	0.157	0.085	0.100	0.110	0.068	0.007
Mg	0.266	0.527	0.156	0.090	0.149	0.231	0.128	0.091	0.352	0.781	0.328	0.002	0.010
Fe	5.291	5.916	5.817	5.515	5.551	5.882	6.255	6.715	6.105	5.330	5.973	6.008	6.094
Mn	1.849	0.948	0.825	1.230	0.388	0.983	1.276	1.113	0.384	0.665	0.744	1.024	1.055
Zn	1.173	0.000	0.595	0.537	0.386	1.104	0.069	1.009	0.447	1.618	0.423	0.708	0.621
Zr	0.316	0.000	0.232	0.353	0.109	0.000	0.200	0.036	0.131	0.000	0.704	0.210	0.195
Ti	1.684	1.552	0.985	1.470	0.754	1.227	1.561	1.621	0.817	1.298	1.338	1.567	1.226
Al	0.000	0.279	0.003	0.002	0.049	0.004	0.000	0.003	0.114	0.354	0.161	0.008	0.006
Si	8.614	9.299	10.397	9.234	10.607	9.318	9.198	8.768	10.094	8.939	9.138	9.076	9.316
ΣCations	22.177	20.784	20.049	21.711	20.881	21.935	21.400	21.303	21.352	21.946	21.731	21.780	22.196

* The total is set to 100.00 due to the fact that the analyses were performed by EDS, while assuming that all Fe present was as Fe^{2+}

[1] Number of atoms of oxygen used in the calculation of the mineral formulae

The acronyms used are: pyx=pyroxene, prev.=previous, amph=amphibole; ast=astrophyllite; phyllo=phyllosilicate opp.=opposite; rt=right; ed=edge; incl.=inclusion; 2nd=second; gr=grain

The numbers in the label section refer to the corresponding HRTEM image

Appendix B-10: AEM analyses of minerals from the hypersolvus granite

Mineral	Astrophyllite						
Spectrum#	5	6	9	14	18	19	
Label	by gr	ast	2nd gr	ast	incl.	incl.	
K_2O	2.52	2.34	2.89	2.85	5.06	5.32	3.95
Rb_2O	1.99	1.98	0.00	1.39	1.54	2.21	1.79
Na_2O	3.84	6.94	7.03	6.26	4.85	5.29	4.32
CaO	0.40	0.06	0.64	0.26	0.18	0.35	0.32
MgO	0.21	0.19	0.53	0.53	0.00	0.10	0.48
FeO	38.91	36.43	31.99	43.94	35.90	34.69	36.15
MnO	8.94	6.05	17.69	0.15	7.49	7.77	7.92
ZnO	6.46	7.59	0.00	1.12	7.18	7.07	5.31
ZrO_2	0.66	2.99	1.70	3.31	1.69	1.84	2.38
TiO_2	9.69	7.51	2.78	8.37	7.32	7.33	7.87
Al_2O_3	0.03	0.04	0.16	0.00	0.44	0.73	0.26
SiO_2	26.36	27.87	34.59	31.83	28.35	27.29	29.26
Total*	100.00	100.00	100.00	100.00	100.00	100.00	100.00
# Oxygen[1]	31	31	31	31	31	31	31
K	0.587	0.542	0.614	0.615	1.164	1.239	0.904
Rb	0.212	0.210	0.000	0.137	0.162	0.235	0.184
Na	1.519	2.733	2.543	2.296	1.894	2.097	1.648
Ca	0.091	0.014	0.133	0.054	0.041	0.081	0.070
Mg	0.080	0.070	0.182	0.184	0.000	0.036	0.171
Fe	6.340	5.903	4.763	6.635	5.778	5.658	5.705
Mn	1.480	0.997	2.677	0.023	1.225	1.289	1.281
Zn	0.899	1.050	0.000	0.144	0.987	0.985	0.726
Zr	0.065	0.296	0.155	0.306	0.167	0.184	0.233
Ti	1.841	1.420	0.482	1.474	1.373	1.394	1.456
Al	0.011	0.015	0.049	0.000	0.148	0.247	0.084
Si	8.541	8.979	10.237	9.557	9.072	8.853	9.160
ΣCations	21.666	22.231	21.835	21.425	22.010	22.298	21.619

[1] Number of atoms of oxygen used in the calculation of the mineral formulae

The acronyms used are: incl.=inclusion; gr=grain

Appendix B-10: AEM analyses of minerals from the hypersolvus granite

Mineral	Phyllosilicates									
Spectrum#	12	13	23	10	11	13	16	20	21	22
Label	(4938-9)	(4935-7)	shaped	phyllo	phyllo	phyllo	phyllo	thin	thin	thin
K_2O	7.76	7.40	1.91	2.65	3.42	2.50	1.35	2.09	1.54	1.92
Rb_2O	0.65	2.21	0.83	0.00	0.00	1.36	0.10	0.06	0.22	1.07
Na_2O	6.06	3.13	0.96	6.64	4.78	6.88	8.48	5.29	5.60	4.96
CaO	0.00	0.00	0.14	0.00	0.66	0.78	0.58	0.67	0.69	0.93
MgO	16.02	18.09	9.12	0.50	0.28	0.34	0.37	0.47	0.19	0.46
FeO	11.88	9.90	10.62	50.23	45.24	42.23	41.31	44.38	45.39	44.66
MnO	0.68	0.50	2.01	5.97	0.54	1.65	0.01	2.32	2.43	3.14
ZnO	0.00	0.00	36.04	2.44	0.00	0.00	2.23	2.38	1.44	0.00
ZrO_2	0.66	0.42	4.96	0.90	3.11	1.69	1.02	0.66	0.79	0.48
TiO_2	1.40	0.62	2.35	0.86	0.16	0.09	1.14	0.59	0.33	1.04
Al_2O_3	2.34	2.34	1.98	0.00	0.06	0.23	0.54	0.49	0.39	0.01
SiO_2	52.55	55.37	29.09	29.82	41.76	42.24	42.87	40.61	40.99	41.34
Total*	100.00	100.00	100.00	100.00	100.00	100.00	100.00	100.00	100.00	100.00
# Oxygen[1]	28	28	28	28	28	28	28	28	28	28
K	1.098	1.015	0.385	0.555	0.610	0.441	0.234	0.374	0.275	0.341
Rb	0.042	0.139	0.076	0.000	0.000	0.110	0.008	0.005	0.018	0.087
Na	1.459	0.730	0.329	2.368	1.450	2.065	2.491	1.611	1.701	1.496
Ca	0.000	0.000	0.028	0.000	0.114	0.134	0.098	0.116	0.121	0.161
Mg	3.645	3.989	2.962	0.169	0.080	0.097	0.102	0.134	0.055	0.131
Fe	1.177	0.951	1.502	7.379	5.651	5.214	4.993	5.559	5.674	5.548
Mn	0.068	0.049	0.288	0.892	0.068	0.207	0.001	0.295	0.308	0.396
Zn	0.000	0.000	4.354	0.307	0.000	0.000	0.230	0.255	0.154	0.000
Zr	0.040	0.025	0.429	0.080	0.238	0.128	0.075	0.051	0.060	0.036
Ti	0.162	0.069	0.387	0.147	0.024	0.013	0.161	0.087	0.049	0.150
Al	0.480	0.464	0.579	0.000	0.015	0.060	0.136	0.127	0.101	0.002
Si	10.353	10.570	8.180	8.709	10.374	10.371	10.303	10.115	10.187	10.209
ΣCations	18.524	18.001	19.500	20.606	18.625	18.839	18.831	18.728	18.702	18.558

[1] Number of atoms of oxygen used in the calculation of the mineral formulae

The acronyms used are: phyllo=phyllosilicate

The numbers in the label section refer to the corresponding HRTEM image

Appendix B-10: AEM analyses of minerals from the hypersolvus granite

Mineral	Inclusions						
Spectrum#	2	4	10	11	1	2	5
Label	albite	albite	fluoride	fluoride	fluoride	fluoride	fluoride
K_2O	0.78	0.46	0.02	0.00	0.51	0.14	0.01
Rb_2O	0.37	0.00	0.05	2.24	1.42	0.69	0.72
Na_2O	7.74	16.43	0.54	2.20	0.59	2.00	0.00
CaO	0.00	1.64	94.58	86.46	19.59	23.32	23.97
MgO	0.14	0.16	0.00	0.00	0.41	0.14	0.11
FeO	8.54	4.48	2.95	6.64	12.20	12.25	14.15
MnO	0.35	0.15	0.34	0.02	0.00	0.00	0.00
ZnO	0.00	0.53	0.00	0.00	3.90	2.46	0.04
ZrO_2	0.53	0.13	0.30	0.23	1.32	2.44	5.65
TiO_2	0.12	0.09	0.08	0.26	1.63	1.93	2.45
Al_2O_3	19.62	18.53	0.20	0.55	0.56	0.00	0.00
SiO_2	61.80	57.39	0.92	1.40	57.86	54.63	52.90
Total*	100.00	100.00	100.00	100.00	100.00	100.00	100.00
# Oxygen[1]	8	8	3	3	6	6	6
K	0.027	0.017	0.001	0.000	0.015	0.004	0.000
Rb	0.006	0.000	0.001	0.032	0.020	0.010	0.010
Na	0.460	1.016	0.028	0.115	0.030	0.106	0.000
Ca	0.000	0.058	2.815	2.595	0.580	0.713	0.748
Mg	0.008	0.009	0.000	0.000	0.020	0.007	0.006
Fe	0.209	0.114	0.063	0.143	0.259	0.269	0.317
Mn	0.009	0.004	0.007	0.000	0.000	0.000	0.000
Zn	0.000	0.012	0.000	0.000	0.071	0.046	0.001
Zr	0.008	0.002	0.004	0.003	0.017	0.033	0.078
Ti	0.003	0.003	0.002	0.006	0.040	0.049	0.064
Al	0.994	0.977	0.009	0.024	0.025	0.000	0.000
Si	3.009	2.907	0.039	0.060	2.446	2.384	2.356
ΣCations	4.734	5.119	2.969	2.979	3.524	3.622	3.580

[1] Number of atoms of oxygen used in the calculation of the formulae

Appendix B-11: AEM analyses of minerals from the subsolvus granite

Mineral	Amphibole	Hematite		Aegirine						
Spectrum#	9	2.6	10	2.1	2	3	8	11	12	2.2
Label	at tip	beside	by py	in py			at tip	(6473)	(6478)	
Na_2O	9.41	8.67	1.70	2.20	13.50	12.90	14.90	15.64	15.38	14.11
MgO	0.70	0.18	0.00	0.42	0.64	0.54	0.01	0.04	0.02	0.12
Al_2O_3	0.34	0.09	0.14	0.00	0.01	0.04	0.02	0.04	0.01	0.00
SiO_2	40.39	38.73	3.54	5.37	38.26	38.73	36.58	39.52	43.99	37.62
K_2O	0.15	1.84	0.55	0.00	0.40	0.06	0.08	0.02	0.12	0.08
CaO	4.77	0.18	0.04	0.00	0.92	1.31	0.44	0.26	0.55	0.38
TiO_2	0.76	0.01	0.87	0.91	0.85	0.77	0.34	0.53	0.59	0.47
MnO	2.23	0.57	0.37	1.00	1.47	1.65	0.78	1.00	1.38	0.90
FeO	38.81	45.87	90.35	82.67	41.99	40.95	41.84	41.44	37.27	43.79
ZnO	0.02	3.57	0.19	1.06	1.47	2.77	3.06	0.00	0.00	1.01
ZrO_2	0.60	0.30	1.89	5.26	0.42	0.28	0.76	1.07	0.53	1.03
Rb_2O	1.81	0.00	0.36	1.11	0.08	0.00	1.19	0.45	0.17	0.48
Total*	100.00	100.00	100.00	100.00	100.00	100.00	100.00	100.00	100.00	100.00
# Oxygen[1]	23	23	3	3	6	6	6	6	6	6
Na	2.327	2.237	0.112	0.138	0.900	0.855	1.026	1.029	0.954	0.956
Mg	0.164	0.044	0.000	0.025	0.040	0.034	0.001	0.003	0.001	0.008
Al	0.072	0.019	0.008	0.000	0.000	0.002	0.001	0.002	0.001	0.000
Si	8.177	8.181	0.190	0.277	2.088	2.101	2.063	2.130	2.233	2.085
K	0.022	0.279	0.021	0.000	0.016	0.002	0.003	0.001	0.005	0.003
Ca	0.677	0.027	0.002	0.000	0.035	0.050	0.018	0.010	0.019	0.015
Tl	0.090	0.001	0.027	0.027	0.027	0.024	0.011	0.017	0.017	0.015
Mn	0.231	0.062	0.010	0.026	0.041	0.046	0.023	0.028	0.036	0.025
Fe	3.951	4.874	2.435	2.145	1.152	1.117	1.186	1.123	0.952	1.221
Zn	0.002	0.324	0.004	0.024	0.034	0.064	0.074	0.000	0.000	0.024
Zr	0.038	0.019	0.031	0.084	0.007	0.005	0.013	0.018	0.008	0.018
Rb	0.121	0.000	0.006	0.019	0.001	0.000	0.022	0.008	0.003	0.009
Σ Cations	15.872	16.066	2.846	2.765	4.343	4.302	4.441	4.368	4.229	4.379

* The total is set to 100.00 due to the fact that the analyses were performed by EDS, with all Fe as Fe^{2+}

[1] Number of atoms of oxygen used in the calculation of the mineral formulae

The acronyms are: py=pyroxene; numbers in brackets are of the associated HRTEM image

Appendix B-11: AEM analyses of minerals from the subsolvus granite

Mineral	Phyllosilicate								
Spectrum#	7	6	2.3	2.5	5	14	15	2.4	16
Label	chlorite	chlorite	clay	clay	clay	clay	clay	clay	clay
Na_2O	1.84	0.80	0.44	0.79	3.08	9.49	10.60	2.49	6.96
MgO	27.41	27.41	36.84	27.20	10.49	1.15	0.54	11.32	6.91
Al_2O_3	10.55	11.43	12.40	11.76	9.36	7.09	5.21	7.85	8.47
SiO_2	34.89	34.59	39.07	31.09	31.27	31.98	28.37	29.16	28.46
K_2O	0.37	0.48	0.00	0.11	0.56	0.68	0.78	0.31	0.98
CaO	0.74	1.27	0.19	0.31	1.90	2.83	3.60	1.35	1.58
TiO_2	0.03	0.21	0.00	0.45	0.22	0.59	3.74	0.25	0.27
MnO	0.48	0.53	0.00	1.17	0.18	0.02	0.04	0.55	0.24
FeO	19.21	17.89	3.59	22.67	40.19	45.94	41.52	43.52	44.48
ZnO	3.18	2.54	5.38	4.23	0.97	0.16	5.02	1.48	0.00
ZrO_2	0.46	2.77	1.78	0.00	0.00	0.00	0.58	1.72	1.65
Rb_2O	0.83	0.07	0.30	0.22	1.78	0.08	0.00	0.00	0.00
Total*	100.00	100.00	100.00	100.00	100.00	100.00	100.00	100.00	100.00
# Oxygen[1]	14	14	14	14	11	11	11	11	11
Na	0.240	0.104	0.052	0.106	0.362	1.178	1.392	0.304	0.872
Mg	3.373	3.365	4.102	3.461	1.167	0.135	0.068	1.310	0.820
Al	1.170	1.264	1.245	1.349	0.938	0.750	0.582	0.818	0.905
Si	3.717	3.676	3.766	3.424	3.011	3.249	3.047	2.919	2.921
K	0.028	0.037	0.000	0.009	0.039	0.049	0.060	0.023	0.072
Ca	0.055	0.095	0.013	0.024	0.128	0.202	0.271	0.095	0.113
Ti	0.002	0.013	0.000	0.029	0.013	0.035	0.236	0.015	0.017
Mn	0.026	0.029	0.000	0.066	0.009	0.001	0.002	0.028	0.013
Fe	1.029	0.956	0.174	1.256	1.946	2.347	2.243	2.192	2.296
Zn	0.146	0.116	0.223	0.200	0.040	0.007	0.232	0.064	0.000
Zr	0.015	0.091	0.053	0.000	0.000	0.000	0.019	0.053	0.052
Rb	0.029	0.003	0.009	0.008	0.056	0.003	0.000	0.000	0.000
Σ Cations	9.831	9.749	9.637	9.930	7.708	7.955	8.152	7.820	8.082

[1] Number of atoms of oxygen used in the calculation of the mineral formulae

The acronyms are: py=pyroxene; numbers in brackets are of the associated HRTEM image

Appendix B-12: Range of relative errors of AEM analyses

Oxide	Average range of the Relative Errors*
Na_2O	0.00-0.10
K_2O	0.00-0.40
Rb_2O	0.00-0.35
CaO	0.00-0.40
MgO	0.00-0.68
FeO	0.01-0.04
MnO	0.00-0.50
ZnO	0.00-0.17
ZrO_2	0.00-0.25
TiO_2	0.00-0.15
Al_2O_3	0.00-0.30
SiO_2	0.01-0.03

* Relative errors were calculated from the peak intensity.

Appendix B-13: Method of calculation of the amount released

The surface area of the Strange Lake complex is 36 km^2, so the radius is 3.385 km.

Assuming that the complex is cone shaped and 10 km in depth:

Its volume is $0.33333\pi r^2h = 119.99\ km^3 = 1.1999 \times 10^{11}\ m^3$

Assuming that the average density of rock is 2.8 g/cm^3.

Thus, the weight of rock in the complex = Density•volume = $2800\ kg/m^3 \bullet 1.1999 \times 10^{11}\ m^3$

$= 3.3597 \times 10^{14}\ kg$

To calculate the amount of trace elements released:

Assume: a) That the complex is ½ hypersolvus and ½ subsolvus granite.

b) Let the volume of amphibole in the complex be 7%.

c) Only 40% of the amphibole is converted to aegirine in subsolvus granite and none in the hypersolvus granite.

This gives the least amount released:

= weight•conversion factor•amount complex•% amphibole•amount converted

$= 3.3597 \times 10^{14}\ kg \bullet 100\ g/kg \bullet 0.5 \bullet 0.07 \bullet 0.40$

$= 4.70 \times 10^{14}\ g$

For the sake of comparison, the ore body contains 52,000,000,000 kg of ore at:

2.93% ZrO_2, 0.31% Y_2O_3, 0.38% Nb_2O_5, 0.54% REE and 0.08% BeO.

In grams this is:

$1.524 \times 10^{11}\ ZrO_2$ or 1.1×10^{11} Zr

$1.612 \times 10^{10}\ Y_2O_3$ or 1.3×10^{10} Y

$1.976 \times 10^{10}\ Nb_2O_5$ or 1.4×10^{13} Nb

2.808×10^{10} REE or 2.8×10^{10} REE

4.160×10^{9} BeO or 1.5×10^{9} Be

Appendix B-14: Electron-microprobe analyses of brown winchitic amphibole

Sample #	SL-8-1				
Description	bram	alt	bram	bram	bram
K_2O	2.89	2.21	1.49	1.75	1.74
CaO	0.07	0.11	0.14	0.08	0.11
Nb_2O_5	0.01	0.00	0.01	0.00	0.01
ZrO_2	0.05	0.05	0.17	0.18	0.10
Na_2O	7.97	7.09	9.05	9.28	8.99
MgO	0.11	0.33	0.07	0.03	0.05
Al_2O_3	3.05	0.41	0.33	0.28	0.34
F	1.50	1.83	2.00	3.17	2.98
SiO_2	46.93	51.71	50.96	51.03	50.58
FeO	27.30	29.08	32.61	31.29	32.46
MnO	3.38	1.55	0.58	0.61	0.56
TiO_2	0.60	0.63	0.94	0.71	0.69
ZnO	3.43	1.64	0.31	0.35	0.24
Total	97.29	96.63	98.64	98.77	98.85

bram=brown amphibole; alt=alteration

Appendix B-15: Electron-microprobe analyses of phyllosilicates

Mineral	**Smectite**	**Chlorite-smectite**							
Sample #	**SL-8-1**	**LB-30-15.70**	**LB-30-15.70**			**LB-30-11.7**			
Description			**ltgr**	**dkgr**		**dkalt**	**bralt**	**alt**	**alt**
K_2O	0.08	0.27	0.06	0.04	0.03	0.77	0.40	0.59	1.87
CaO	0.43	2.01	0.92	0.71	0.78	1.40	1.63	1.54	1.03
Nb_2O_5	0.00	0.01	0.00	0.02	0.00	0.03	0.00	0.00	1.90
ZrO_2	0.00	0.40	0.00	0.01	0.02	0.00	0.02	0.03	0.36
Na_2O	3.83	0.27	0.25	0.23	0.26	0.13	0.14	0.14	0.10
MgO	0.00	16.07	17.44	16.58	16.07	16.66	16.40	15.93	12.41
Al_2O_3	21.76	6.86	8.39	8.26	8.05	10.21	9.13	9.21	8.36
F	0.00	0.48	0.10	0.07	0.02	0.41	0.26	0.37	0.69
SiO_2	73.81	41.33	34.73	32.32	33.14	43.67	41.46	42.36	39.89
FeO	0.03	13.08	14.33	15.41	16.95	12.89	11.85	12.31	6.75
MnO	0.00	0.14	3.03	3.66	3.61	0.55	0.55	0.49	0.23
TiO_2	0.00	0.00	0.01	0.01	0.02	0.07	0.09	0.09	0.30
ZnO	0.03	0.78	6.31	6.87	7.06	2.36	2.32	2.22	2.46
Total	99.96	81.70	85.55	84.18	86.00	89.15	84.25	85.27	76.35

Appendix B-15: Electron-microprobe analyses of phyllosilicates

Mineral	**Smectite**	**Chlorite-smectite**							
Sample #	**SL-8-1**	**LB-30-15.70**	**LB-30-15.70**			**LB-30-11.7**			
Description			**ltgr**	**dkgr**		**dkalt**	**bralt**	**alt**	**alt**
Na	0.976	0.096	0.091	0.086	0.098	0.041	0.050	0.050	0.039
K	0.013	0.065	0.014	0.011	0.007	0.167	0.092	0.135	0.469
Ca	0.061	0.400	0.188	0.151	0.163	0.257	0.316	0.295	0.217
Mg	0.000	4.463	4.962	4.896	4.675	4.249	4.419	4.238	3.637
Fe	0.003	2.039	2.289	2.553	2.766	1.845	1.791	1.838	1.110
Mn	0.000	0.022	0.490	0.614	0.597	0.080	0.084	0.074	0.038
Zn	0.003	0.107	0.889	1.006	1.017	0.298	0.309	0.293	0.357
Nb	0.000	0.001	0.000	0.002	0.000	0.002	0.000	0.000	0.169
Zr	0.000	0.037	0.000	0.001	0.002	0.000	0.001	0.002	0.035
Ti	0.000	0.000	0.002	0.001	0.003	0.009	0.012	0.012	0.045
Si	9.693	7.704	6.632	6.404	6.468	7.472	7.495	7.565	7.842
Al	3.369	1.508	1.890	1.930	1.852	2.060	1.945	1.939	1.938
F	0.000	0.283	0.057	0.041	0.012	0.222	0.151	0.208	0.430
Total	13.141	16.346	17.355	17.568	17.549	16.438	16.465	16.391	15.857

Formulae calculated based on 25 atoms of oxygen.

Appendix B-15: Electron-microprobe analyses of phyllosilicates

Mineral	**Smectite**	**Chlorite-smectite**							
Sample #	**SL-8-1**	**LB-30-15.70**	**LB-30-15.70**			**LB-30-11.7**			
Description			**ltgr**	**dkgr**		**dkalt**	**bralt**	**alt**	**alt**
K	0.014	0.072	0.016	0.012	0.008	0.187	0.104	0.151	0.525
Na	1.093	0.108	0.102	0.097	0.110	0.046	0.056	0.055	0.043
Ca	0.068	0.448	0.210	0.169	0.182	0.288	0.354	0.330	0.243
Σ Interlayer	1.175	0.629	0.328	0.278	0.300	0.522	0.513	0.537	0.811
Mg	0.000	4.998	5.557	5.483	5.236	4.758	4.949	4.747	4.074
Fe	0.003	2.283	2.564	2.859	3.098	2.066	2.006	2.058	1.243
Mn	0.000	0.025	0.549	0.688	0.668	0.089	0.094	0.083	0.043
Zn	0.003	0.119	0.996	1.126	1.139	0.334	0.347	0.328	0.400
Nb	0.000	0.001	0.000	0.002	0.000	0.002	0.000	0.000	0.189
Zr	0.000	0.041	0.000	0.001	0.002	0.000	0.001	0.003	0.039
Ti	0.000	0.000	0.002	0.002	0.004	0.010	0.013	0.013	0.050
Al	3.773	1.689	1.544	1.334	1.317	2.307	2.178	2.171	2.170
Σ Octahedral	3.780	9.158	11.211	11.495	11.465	9.567	9.589	9.403	8.208
Al	0.000	0.000	0.573	0.828	0.756	0.000	0.000	0.000	0.000
Si	10.856	8.629	7.427	7.172	7.244	8.368	8.394	8.473	8.784
Σ Tetrahedral	10.856	8.629	8.000	8.000	8.000	8.368	8.394	8.473	8.784
OH	16.000	15.683	15.936	15.954	15.986	15.752	15.831	15.767	15.519
F	0.000	0.317	0.064	0.046	0.014	0.248	0.169	0.233	0.481
Al	3.773	1.689	2.116	2.162	2.074	2.307	2.178	2.171	2.170
^{VI}Al	3.773	1.689	1.544	1.334	1.317	2.307	2.178	2.171	2.170
^{IV}Al	0.000	0.000	0.573	0.828	0.756	0.000	0.000	0.000	0.000

Formulae calculated based on 28 atoms of oxygen.

Appendix B-15: Electron-microprobe analyses of phyllosilicates

Mineral	Smectite	Chlorite-smectite							
Sample #	SL-8-1	LB-30-15.70	LB-30-15.70			LB-30-11.7			
Description			ltgr	dkgr		dkalt	bralt	alt	alt
K	0.011	0.057	0.016	0.012	0.008	0.147	0.081	0.119	0.413
Na	0.859	0.085	0.102	0.097	0.110	0.036	0.044	0.044	0.034
Ca	0.053	0.352	0.210	0.169	0.182	0.226	0.278	0.260	0.191
Σ Interlayer	0.923	0.494	0.328	0.278	0.300	0.410	0.403	0.422	0.637
Mg	0.000	3.927	5.557	5.483	5.236	3.739	3.889	3.730	3.201
Fe	0.003	1.794	2.564	2.859	3.098	1.624	1.576	1.617	0.977
Mn	0.000	0.020	0.549	0.688	0.668	0.070	0.074	0.065	0.034
Zn	0.002	0.094	0.996	1.126	1.139	0.262	0.272	0.258	0.314
Nb	0.000	0.001	0.000	0.002	0.000	0.002	0.000	0.000	0.149
Zr	0.000	0.032	0.000	0.001	0.002	0.000	0.001	0.002	0.030
Ti	0.000	0.000	0.002	0.002	0.004	0.008	0.011	0.010	0.039
Al	0.000	1.220	0.573	0.828	0.756	1.425	1.405	1.343	1.099
Σ Octahedral	0.005	7.088	10.240	10.989	10.904	7.129	7.228	7.025	5.843
Al	2.964	0.107	1.544	1.334	1.317	0.388	0.307	0.363	0.606
Si	8.530	6.780	7.427	7.172	7.244	6.575	6.595	6.657	6.901
Σ Tetrahedral	11.494	6.887	8.971	8.507	8.561	6.963	6.902	7.021	7.508
OH	4.000	3.751	3.936	3.954	3.986	3.805	3.867	3.817	3.622
F	0.000	0.249	0.064	0.046	0.014	0.195	0.133	0.183	0.378
Al	2.964	1.327	2.116	2.162	2.074	1.813	1.711	1.706	1.705
^{IV}Al	2.964	0.107	1.544	1.334	1.317	0.388	0.307	0.363	0.606
^{VI}Al	0.000	1.220	0.573	0.828	0.756	1.425	1.405	1.343	1.099

Formulae calculated based on 22 atoms of oxygen.
ltgr=light green; dkgr=dark green; dkalt=dark altered'; bralt=brown altered; alt=altered.

Appendix B-16: AEM analyses of winchitic amphibole.

Sample#	lb301070													
Analysis#	1	6	8	10	11	12	13	6	10	11	14	15	17	18
Na_2O	8.96	0.41	0.75	5.78	6.91	9.99	9.04	2.90	3.90	4.30	3.10	2.30	3.60	3.50
K_2O	2.93	0.33	0.22	2.91	3.49	3.07	2.82	0.70	0.40	0.00	0.00	0.70	0.00	0.00
CaO	0.71	7.17	3.97	0.88	0.47	0.47	1.07	11.90	10.80	15.10	14.20	9.80	11.20	12.90
FeO	39.04	37.52	33.71	44.31	42.25	39.05	38.04	25.10	9.70	10.80	8.90	22.80	12.10	12.10
MgO	0.01	7.91	12.47	0.07	0.02	0.12	0.37	6.30	20.20	11.00	15.60	9.10	15.00	16.00
MnO	2.11	1.26	0.72	2.35	2.13	1.93	2.03	8.80	5.30	16.20	11.50	11.80	12.40	11.10
ZnO	2.23	1.81	2.75	3.12	2.07	2.49	2.74	0.00	0.00	0.00	0.00	0.00	0.00	0.00
ZrO_2	2.90	0.73	0.00	3.40	4.18	3.40	3.33	0.00	0.00	0.00	0.00	0.00	0.00	0.00
Rb_2O	0.28	0.19	0.29	0.19	0.00	0.03	1.33	0.00	0.00	0.00	0.00	0.00	0.00	0.00
TiO_2	1.53	0.32	0.17	1.74	1.73	1.64	1.49	1.40	0.60	0.40	0.40	0.40	0.40	0.80
SiO_2	39.26	36.50	37.31	35.26	36.54	37.70	37.75	40.60	49.00	42.20	46.10	40.50	45.30	43.70
Al_2O_3	0.05	5.87	7.63	0.01	0.20	0.11	0.00	2.40	0.00	0.00	0.20	2.50	0.00	0.00
Total*	100.00	100.00	100.00	100.00	100.00	100.00	100.00	100.00	100.00	100.00	100.00	100.00	100.00	100.00
Na	3.046	0.132	0.235	2.040	2.404	3.433	3.119	0.915	1.106	1.327	0.911	0.723	1.073	1.046
K	0.654	0.069	0.045	0.675	0.799	0.694	0.640	0.145	0.075	0.000	0.000	0.145	0.000	0.000
Ca	0.133	1.276	0.685	0.172	0.090	0.089	0.204	2.074	1.693	2.575	2.305	1.703	1.844	2.131
Fe	5.722	5.211	4.534	6.744	6.336	5.784	5.662	3.415	1.187	1.438	1.128	3.092	1.555	1.560
Mg	0.003	1.958	2.988	0.018	0.006	0.032	0.099	1.527	4.404	2.609	3.522	2.199	3.435	3.676
Mn	0.313	0.177	0.098	0.362	0.324	0.289	0.305	1.213	0.657	2.184	1.476	1.621	1.614	1.450
Zn	0.289	0.221	0.327	0.420	0.275	0.325	0.360	0.000	0.000	0.000	0.000	0.000	0.000	0.000
Zr	0.248	0.059	0.000	0.302	0.365	0.294	0.289	0.000	0.000	0.000	0.000	0.000	0.000	0.000
Rb	0.032	0.020	0.030	0.022	0.000	0.003	0.152	0.000	0.000	0.000	0.000	0.000	0.000	0.000
Ti	0.201	0.040	0.021	0.238	0.233	0.218	0.200	0.171	0.066	0.048	0.046	0.049	0.046	0.093
Al	0.011	1.149	1.447	0.002	0.042	0.022	0.000	0.460	0.000	0.000	0.036	0.478	0.000	0.000
Si	6.880	6.062	6.001	6.417	6.554	6.678	6.719	6.604	7.168	6.717	6.984	6.568	6.961	6.737
Σ Cations	17.531	16.375	16.410	17.411	17.428	17.863	17.748	16.524	16.356	16.899	16.407	16.578	16.529	16.693

*Total = 100.00 as these are EDS analyses.
Mineral formulae calculated based on 23 atoms of oxygen.

Appendix B-16: AEM analyses of winchitic amphibole.

Sample#														
Analysis#	**19**	**20**	**22**	**24**	**27**	**31**	**32**	**33**	**34**	**35**	**36**	**37**	**40**	**41**
Na_2O	3.20	2.80	2.70	1.40	2.90	11.00	1.40	1.30	1.70	1.10	1.50	8.60	5.80	11.70
K_2O	0.10	0.30	0.00	0.00	0.00	2.90	0.00	0.00	0.00	0.00	0.10	2.80	1.10	2.90
CaO	14.00	16.20	15.50	16.30	15.50	1.10	17.50	17.80	17.20	16.40	15.90	0.80	12.10	4.70
FeO	12.10	14.50	16.00	16.20	18.30	39.50	20.10	19.90	20.40	19.40	16.30	43.20	20.70	29.30
MgO	13.40	7.80	10.50	11.80	12.20	0.00	10.80	10.00	11.10	12.10	6.80	0.10	9.90	3.80
MnO	12.80	20.30	11.10	9.30	7.80	3.20	7.80	8.50	7.30	6.80	18.20	3.60	5.40	5.20
ZnO	0.00	0.00	0.00	0.00	0.00	0.00	0.00	0.00	0.00	0.00	0.00	0.00	0.00	0.00
ZrO_2	0.00	0.00	0.00	0.00	0.00	0.00	0.00	0.00	0.00	0.00	0.00	0.00	0.00	0.00
Rb_2O	0.00	0.00	0.00	0.00	0.00	0.00	0.00	0.00	0.00	0.00	0.00	0.00	0.00	0.00
TiO_2	0.40	0.30	0.60	0.90	0.10	2.00	0.30	0.10	0.20	0.20	0.30	2.00	0.60	0.50
SiO_2	44.00	37.80	43.40	43.90	43.00	40.10	42.20	42.10	42.10	43.80	40.80	38.80	44.40	41.70
Al_2O_3	0.00	0.10	0.10	0.10	0.10	0.10	0.00	0.20	0.00	0.10	0.10	0.00	0.00	0.00
Total*	100.00	100.00	100.00	100.00	100.00	100.00	100.00	100.00	100.00	100.00	100.00	100.00	100.00	100.00
Na	0.966	0.909	0.827	0.424	0.887	3.693	0.432	0.403	0.525	0.334	0.478	2.930	1.776	3.810
K	0.020	0.064	0.000	0.000	0.000	0.641	0.000	0.000	0.000	0.000	0.021	0.628	0.222	0.621
Ca	2.336	2.905	2.625	2.730	2.619	0.204	2.985	3.051	2.936	2.754	2.800	0.151	2.048	0.846
Fe	1.576	2.029	2.115	2.117	2.414	5.720	2.676	2.662	2.718	2.543	2.240	6.347	2.734	4.115
Mg	3.110	1.945	2.473	2.748	2.867	0.000	2.562	2.384	2.636	2.827	1.665	0.026	2.330	0.951
Mn	1.688	2.878	1.486	1.231	1.042	0.469	1.052	1.152	0.985	0.903	2.533	0.536	0.722	0.740
Zn	0.000	0.000	0.000	0.000	0.000	0.000	0.000	0.000	0.000	0.000	0.000	0.000	0.000	0.000
Zr	0.000	0.000	0.000	0.000	0.000	0.000	0.000	0.000	0.000	0.000	0.000	0.000	0.000	0.000
Rb	0.000	0.000	0.000	0.000	0.000	0.000	0.000	0.000	0.000	0.000	0.000	0.000	0.000	0.000
Ti	0.047	0.038	0.071	0.106	0.012	0.260	0.036	0.012	0.024	0.024	0.037	0.264	0.071	0.063
Al	0.000	0.020	0.019	0.018	0.019	0.020	0.000	0.038	0.000	0.018	0.019	0.000	0.000	0.000
Si	6.852	6.326	6.859	6.861	6.781	6.944	6.718	6.734	6.707	6.865	6.704	6.817	7.012	7.003
Σ Cations	16.595	17.113	16.474	16.236	16.641	17.952	16.462	16.436	16.531	16.269	16.498	17.698	16.915	18.149

*Total = 100.00 as these are EDS analyses.
Mineral formulae calculated based on 23 atoms of oxygen.

Appendix B-16: AEM analyses of winchitic amphibole.

Sample#	lb30158											lb301722		
Analysis#	1	3	4	5	6	7	8	9	10	11	12	1	2	3
Na_2O	1.05	0.24	3.14	0.22	2.12	2.61	1.49	0.46	0.51	2.26	2.63	2.04	6.45	5.97
K_2O	5.63	5.58	0.93	4.02	0.50	1.12	1.00	17.37	18.17	1.04	1.02	0.31	1.95	1.80
CaO	1.07	0.14	2.25	0.49	2.69	4.85	3.26	0.26	0.00	2.56	2.64	9.71	1.92	1.66
FeO	2.30	6.13	1.61	1.67	1.73	2.33	2.66	0.00	2.95	8.40	2.23	27.44	48.42	51.11
MgO	7.29	0.37	27.20	0.22	21.05	25.49	16.34	0.30	0.21	23.38	20.27	9.11	0.22	0.24
MnO	0.26	0.00	0.24	0.10	0.31	0.62	0.58	0.00	0.00	0.63	0.12	2.07	0.90	1.25
ZnO	5.89	2.59	3.11	0.00	11.10	0.00	18.63	0.00	0.00	11.25	11.17	6.99	1.04	0.72
ZrO_2	0.61	1.32	3.09	5.43	8.10	4.97	2.29	2.66	1.49	1.19	1.57	0.57	0.52	0.13
Rb_2O	0.49	1.46	0.61	0.00	0.80	2.39	0.96	0.46	0.25	0.22	2.70	0.11	0.00	0.15
TiO_2	2.05	0.01	0.16	3.82	0.14	0.03	0.05	0.61	0.00	0.00	0.00	1.20	2.01	1.88
SiO_2	61.07	67.76	52.91	71.20	47.20	51.16	49.10	64.38	64.25	44.86	50.04	38.72	36.37	34.94
Al_2O_3	12.29	14.41	4.75	12.83	4.25	4.42	3.64	13.50	12.16	4.21	5.61	1.74	0.21	0.15
Total*	100.00	100.00	100.00	100.00	100.00	100.00	100.00	100.00	100.00	100.00	100.00	100.00	100.00	100.00
Na	0.275	0.061	0.834	0.055	0.603	0.708	0.433	0.121	0.136	0.651	0.738	0.656	2.239	2.104
K	0.966	0.939	0.162	0.650	0.094	0.199	0.192	3.024	3.204	0.198	0.189	0.066	0.445	0.417
Ca	0.154	0.019	0.330	0.066	0.423	0.726	0.523	0.037	0.000	0.407	0.409	1.722	0.368	0.323
Fe	0.258	0.677	0.184	0.177	0.212	0.273	0.333	0.000	0.341	1.044	0.270	3.799	7.247	7.768
Mg	1.463	0.073	5.547	0.042	4.601	5.304	3.645	0.061	0.043	5.180	4.374	2.247	0.057	0.065
Mn	0.030	0.000	0.028	0.011	0.039	0.074	0.074	0.000	0.000	0.080	0.014	0.290	0.136	0.193
Zn	0.586	0.252	0.314	0.000	1.202	0.000	2.059	0.000	0.000	1.235	1.194	0.854	0.137	0.097
Zr	0.040	0.085	0.206	0.336	0.579	0.338	0.167	0.177	0.101	0.086	0.111	0.046	0.046	0.012
Rb	0.042	0.124	0.053	0.000	0.076	0.214	0.092	0.041	0.023	0.021	0.251	0.012	0.000	0.018
Ti	0.207	0.001	0.017	0.365	0.015	0.003	0.006	0.063	0.000	0.000	0.000	0.149	0.270	0.257
Al	1.952	2.241	0.766	1.920	0.736	0.728	0.643	2.172	1.982	0.737	0.957	0.340	0.044	0.031
Si	8.222	8.942	7.239	9.035	6.922	7.144	7.349	8.786	8.880	6.670	7.245	6.419	6.508	6.351
Σ Cations	14.197	13.414	15.680	12.657	15.502	15.711	15.515	14.482	14.710	16.311	15.754	16.592	17.497	17.634

*Total = 100.00 as these are EDS analyses.
Mineral formulae calculated based on 23 atoms of oxygen.

Appendix B-16: AEM analyses of winchitic amphibole.

Sample#												
Analysis#	4	5	8	10	11	14	15	16	17	18	19	20
Na_2O	6.71	1.57	0.78	6.55	6.94	7.22	7.67	11.68	10.35	10.34	11.21	10.89
K_2O	1.78	0.63	0.50	0.74	1.53	1.14	1.27	1.71	1.77	1.70	1.70	1.82
CaO	1.39	5.92	2.88	1.93	3.60	3.49	2.87	1.63	1.20	1.21	1.20	1.03
FeO	49.96	19.21	20.01	46.46	42.05	30.45	32.99	41.77	42.93	43.04	43.17	42.67
MgO	0.27	17.78	22.40	2.12	2.76	10.37	8.31	0.45	0.18	0.38	0.14	0.28
MnO	1.06	0.79	0.59	1.46	1.42	0.82	0.99	1.11	1.09	1.09	1.21	1.07
ZnO	0.97	4.59	4.70	1.28	1.14	1.91	1.62	1.36	1.40	0.86	1.15	0.95
ZrO_2	0.40	0.23	0.68	1.91	0.44	0.00	0.15	0.69	0.00	0.47	0.51	0.85
Rb_2O	0.17	0.10	0.13	0.31	0.08	0.00	0.24	0.00	0.18	0.14	0.13	0.07
TiO_2	1.49	0.97	0.43	1.96	1.78	1.08	1.10	1.68	1.42	1.44	1.33	1.57
SiO_2	35.31	43.91	39.00	34.86	38.19	40.87	40.19	37.57	39.38	39.02	38.27	38.45
Al_2O_3	0.49	4.31	7.91	0.41	0.07	2.64	2.59	0.35	0.10	0.31	0.00	0.36
Total*	100.00	100.00	100.00	100.00	100.00	100.00	100.00	100.00	100.00	100.00	100.00	100.00
Na	2.353	0.460	0.229	2.274	2.336	2.260	2.442	3.986	3.505	3.498	3.831	3.699
K	0.412	0.121	0.096	0.170	0.340	0.235	0.265	0.384	0.394	0.379	0.382	0.408
Ca	0.270	0.960	0.467	0.371	0.670	0.603	0.504	0.308	0.225	0.226	0.226	0.193
Fe	7.561	2.430	2.539	6.958	6.103	4.109	4.527	6.149	6.270	6.282	6.363	6.252
Mg	0.074	4.008	5.064	0.565	0.713	2.495	2.033	0.119	0.047	0.100	0.037	0.073
Mn	0.162	0.101	0.076	0.222	0.209	0.112	0.138	0.166	0.161	0.161	0.180	0.159
Zn	0.129	0.512	0.526	0.170	0.147	0.228	0.196	0.176	0.180	0.111	0.149	0.123
Zr	0.035	0.017	0.050	0.167	0.037	0.000	0.012	0.060	0.000	0.040	0.043	0.073
Rb	0.020	0.010	0.013	0.036	0.008	0.000	0.025	0.000	0.021	0.016	0.014	0.007
Ti	0.202	0.110	0.049	0.264	0.233	0.131	0.136	0.222	0.187	0.189	0.176	0.207
Al	0.104	0.769	1.416	0.086	0.014	0.503	0.501	0.072	0.020	0.065	0.000	0.074
Si	6.390	6.643	5.918	6.242	6.628	6.594	6.594	6.613	6.877	6.810	6.746	6.736
Σ Cations	17.712	16.141	16.443	17.524	17.437	17.271	17.374	18.254	17.886	17.875	18.148	18.004

*Total = 100.00 as these are EDS analyses.
Mineral formulae calculated based on 23 atoms of oxygen.

Appendix B-17: AEM analyses of biopyriboles

Mineral	Arfvedsonitic amphibole									
Analysis#	2	18	19	6	7	8	9	10	12	13
Description	bottom	only amph	near area	tip		(6831 or 3)	rich (area2)	above it	below it	below it
SiO_2	35.64	36.77	29.74	32.60	30.91	23.77	30.20	29.73	30.68	30.02
Al_2O_3	0.00	0.04	0.06	0.00	0.06	0.62	0.57	0.05	0.24	0.13
TiO_2	0.95	0.96	1.01	1.03	0.64	0.19	0.10	1.22	0.64	0.53
FeO	44.65	45.47	53.92	54.26	54.12	62.63	52.46	52.71	56.42	54.48
MgO	0.01	0.04	0.00	0.01	0.12	0.02	0.60	0.11	0.04	0.03
MnO	2.00	2.05	2.49	1.09	0.98	0.48	0.70	0.88	0.87	1.63
ZnO	3.14	2.71	3.32	1.00	1.43	2.80	2.00	1.51	1.49	1.55
ZrO_2	2.35	1.67	2.00	1.85	4.33	2.52	0.51	2.75	3.22	2.47
CaO	0.27	0.28	0.37	0.39	0.31	1.32	6.49	0.36	0.37	0.91
Rb_2O	0.09	0.05	0.00	0.22	0.24	0.00	0.00	0.89	0.01	0.30
K_2O	3.10	3.06	3.30	0.03	0.01	0.00	0.01	0.03	0.00	0.03
Na_2O	7.80	6.89	3.79	7.51	6.85	5.66	6.36	9.77	6.02	7.92
Total*	100.00	100.00	100.00	100.00	100.00	100.00	100.00	100.00	100.00	100.00
Atoms of oxygen	23	23	23	6	6	6	6	6	6	6
Si	7.878	7.986	7.204	1.952	1.913	1.642	1.843	1.857	1.899	1.874
Al	0.000	0.009	0.016	0.000	0.004	0.044	0.036	0.003	0.016	0.008
Ti	0.123	0.122	0.143	0.036	0.023	0.008	0.004	0.045	0.023	0.020
Fe	4.964	4.967	6.569	1.634	1.685	2.176	1.610	1.656	1.757	1.710
Mg	0.003	0.010	0.000	0.001	0.009	0.002	0.042	0.008	0.003	0.002
Mn	0.226	0.228	0.309	0.033	0.031	0.017	0.022	0.028	0.027	0.052
Zn	0.298	0.253	0.345	0.026	0.038	0.083	0.052	0.040	0.040	0.042
Zr	0.160	0.112	0.149	0.034	0.082	0.054	0.010	0.053	0.061	0.048
Ca	0.042	0.042	0.063	0.016	0.014	0.064	0.278	0.016	0.016	0.040
Rb	0.006	0.004	0.000	0.004	0.005	0.000	0.000	0.018	0.000	0.006
K	0.493	0.477	0.573	0.001	0.000	0.000	0.001	0.001	0.000	0.001
Na	2.106	1.830	1.121	0.550	0.518	0.478	0.474	0.745	0.455	0.604
ΣCations	16.298	16.040	16.492	4.287	4.321	4.567	4.372	4.470	4.298	4.405

* Assuming that all Fe present was as Fe^{2+}

Appendix B-17: AEM analyses of biopyriboles

Mineral	Biopyribole					Aegirine			
Analysis#	3	4	5	11	14	15	16	17	20
Description	first area	to rt	area at tip	other area	middle	opp(6867-74)	defects	no defects	
SiO_2	27.05	28.56	30.13	27.66	25.87	40.42	38.76	39.83	42.06
Al_2O_3	0.36	0.00	0.22	0.52	0.95	0.18	0.46	0.05	0.01
TiO_2	0.27	0.51	0.29	0.23	0.48	0.61	0.57	1.03	1.03
FeO	54.99	51.73	54.23	54.90	55.12	39.77	43.27	43.44	40.75
MgO	0.49	0.42	0.62	0.59	0.68	0.19	0.13	0.08	0.04
MnO	1.47	2.26	0.03	1.07	1.25	0.97	0.25	0.65	0.93
ZnO	4.41	0.85	2.72	4.05	5.13	1.33	1.30	0.47	0.85
ZrO_2	0.44	1.62	0.12	0.47	0.00	0.77	1.64	0.88	1.27
CaO	4.29	7.98	4.36	5.50	3.92	0.39	2.19	0.20	0.10
Rb_2O	0.00	0.00	0.14	0.00	0.00	0.00	0.10	0.00	0.12
K_2O	0.06	0.08	0.00	0.17	0.00	0.03	0.02	0.00	0.00
Na_2O	6.19	5.99	7.13	4.84	6.59	15.35	11.31	13.38	12.84
Total*	100.00	100.00	100.00	100.00	100.00	100.00	100.00	100.00	100.00
Atoms of oxygen	34	34	34	34	34	6	6	6	6
Si	9.912	10.166	10.495	10.006	9.569	2.146	2.105	2.134	2.193
Al	0.136	0.000	0.081	0.195	0.366	0.010	0.026	0.003	0.001
Ti	0.058	0.107	0.060	0.049	0.105	0.019	0.018	0.032	0.032
Fe	10.134	9.260	9.499	9.986	10.254	1.062	1.182	1.171	1.069
Mg	0.209	0.173	0.248	0.247	0.292	0.011	0.008	0.005	0.002
Mn	0.275	0.411	0.006	0.198	0.237	0.026	0.007	0.018	0.025
Zn	0.694	0.130	0.408	0.630	0.816	0.030	0.030	0.011	0.019
Zr	0.049	0.177	0.012	0.052	0.000	0.013	0.027	0.014	0.020
Ca	1.101	1.990	1.065	1.394	1.016	0.014	0.083	0.008	0.004
Rb	0.000	0.000	0.016	0.000	0.000	0.000	0.002	0.000	0.002
K	0.015	0.020	0.000	0.043	0.000	0.001	0.001	0.000	0.000
Na	2.770	2.605	3.034	2.138	2.976	0.996	0.750	0.876	0.818
ΣCations	25.354	25.039	24.922	24.938	25.631	4.328	4.240	4.270	4.184

* Assuming that all Fe present was as Fe^{2+}

Appendix B-18: AEM analyses of related minerals.

Mineral	Titanite							
Sample#	LB-30-10.70		LB-30-15.70					
Label					(5010-12)	(5013-4)	(5018-21)	(5047-51)
Na_2O	0.30	0.10	0.52	0.09	0.45	1.33	0.21	0.46
MgO	0.50	0.00	0.00	0.02	1.23	0.11	0.07	0.00
Al_2O_3	1.60	0.80	1.68	2.44	1.24	0.10	1.92	2.54
SiO_2	26.20	24.00	24.83	26.17	23.94	23.27	25.19	26.04
K_2O	0.00	0.00	0.01	0.00	0.00	0.01	0.00	0.00
CaO	35.70	37.90	36.05	35.43	33.11	36.57	36.52	34.68
TiO_2	31.60	33.90	32.25	32.59	32.35	32.45	30.33	32.17
MnO	0.00	0.10	0.23	0.07	0.81	0.16	0.05	0.18
FeO	4.10	3.30	4.08	3.20	5.00	5.30	5.10	3.53
ZnO	0.00	0.00	0.33	0.00	1.87	0.70	0.62	0.40
ZrO_2	0.00	0.00	0.00	0.00	0.00	0.00	0.00	0.00
Rb_2O	0.00	0.00	0.00	0.00	0.00	0.00	0.00	0.00
Total	100.00	100.00	100.00	100.00	100.00	100.00	100.00	100.00
# Oxygen	5	5	5	5	5	5	5	5
Na	0.013	0.007	0.027	0.004	0.023	0.071	0.011	0.024
Mg	0.025	0.000	0.000	0.001	0.061	0.006	0.003	0.000
Al	0.070	0.035	0.074	0.105	0.055	0.005	0.085	0.110
Si	1.094	1.022	1.052	1.082	1.029	1.017	1.071	1.081
K	0.000	0.000	0.000	0.000	0.000	0.000	0.000	0.000
Ca	1.044	1.132	1.070	1.027	0.997	1.120	1.088	1.009
Ti	0.773	0.848	0.801	0.790	0.815	0.832	0.756	0.783
Mn	0.000	0.002	0.005	0.001	0.018	0.004	0.001	0.004
Fe	0.086	0.070	0.087	0.066	0.108	0.117	0.109	0.074
Zn			0.006	0.000	0.035	0.013	0.011	0.007
Zr			0.000	0.000	0.000	0.000	0.000	0.000
Rb			0.000	0.000	0.000	0.000	0.000	0.000
ΣCations	3.105	3.116	3.123	3.077	3.141	3.184	3.136	3.092

*Total=100.00 as these are EDS analyses
#Oxygen is the number of atoms of oxygen

Appendix B-18: AEM analyses of related minerals.

Mineral	Titanite							
Sample#	LB-30-15.70					LB-30-17.22		
Label	(5052-6)	(5128-30)			(6094-5)	(6094-5)		
Na_2O	0.27	0.80	0.25	0.59	0.50	0.57	0.39	0.27
MgO	0.07	0.14	0.04	0.02	0.00	0.27	0.20	0.10
Al_2O_3	3.00	2.12	1.88	1.99	1.34	1.57	1.57	1.27
SiO_2	26.18	26.53	23.17	25.96	20.74	26.10	25.53	25.74
K_2O	0.00	0.00	0.04	0.00	0.17	0.06	0.00	0.00
CaO	37.14	35.03	38.12	35.62	28.97	33.63	34.32	34.34
TiO_2	29.20	30.88	32.97	31.19	43.39	23.61	29.99	30.49
MnO	0.04	0.21	0.21	0.23	0.37	0.63	0.19	0.15
FeO	3.59	3.66	2.95	3.48	0.02	7.60	6.07	5.82
ZnO	0.52	0.64	0.37	0.93	0.50	1.88	0.67	0.50
ZrO_2	0.00	0.00	0.00	0.00	2.71	3.57	1.06	1.20
Rb_2O	0.00	0.00	0.00	0.00	1.28	0.53	0.00	0.12
Total	100.00	100.00	100.00	100.00	100.00	100.00	100.00	100.00
# Oxygen	5	5	5	5	5	5	5	5
Na	0.014	0.041	0.013	0.030	0.026	0.031	0.021	0.014
Mg	0.003	0.007	0.002	0.001	0.000	0.014	0.010	0.005
Al	0.131	0.092	0.084	0.087	0.060	0.073	0.070	0.057
Si	1.095	1.105	0.994	1.089	0.888	1.157	1.091	1.098
K	0.000	0.000	0.001	0.000	0.005	0.002	0.000	0.000
Ca	1.088	1.023	1.145	1.047	0.869	1.045	1.028	1.027
Ti	0.716	0.754	0.829	0.767	1.089	0.614	0.752	0.763
Mn	0.001	0.004	0.005	0.005	0.008	0.014	0.004	0.003
Fe	0.076	0.077	0.064	0.073	0.000	0.169	0.131	0.125
Zn	0.009	0.011	0.007	0.017	0.009	0.036	0.012	0.009
Zr	0.000	0.000	0.000	0.000	0.036	0.049	0.014	0.016
Rb	0.000	0.000	0.000	0.000	0.018	0.008	0.000	0.002
ΣCations	3.131	3.114	3.143	3.115	3.009	3.209	3.132	3.118

*Total=100.00 as these are EDS analyses
#Oxygen is the number of atoms of oxygen

Appendix B-18: AEM analyses of related minerals.

Mineral	Titanite		Hematite			
Sample#	LB-30-17.22		25-E-2			LB-30-15.80
Label	cs		(6763-4)	by py	in py	
Na_2O	0.40	0.61	0.51	1.70	2.20	4.64
MgO	0.47	0.34	0.39	0.00	0.40	0.39
Al_2O_3	2.19	1.33	1.63	0.10	0.00	1.41
SiO_2	31.78	26.55	25.91	3.60	5.40	4.84
K_2O	0.08	0.01	0.00	0.60	0.00	0.11
CaO	39.44	33.22	33.95	0.00	0.00	1.27
TiO_2	15.61	28.91	30.23	0.90	0.90	0.79
MnO	0.00	0.06	0.16	0.40	1.00	0.19
FeO	8.81	6.56	5.94	92.60	82.70	84.91
ZnO	1.22	0.33	0.27	0.00	1.10	1.46
ZrO_2	0.00	1.73	0.89	0.00	5.30	0.00
Rb_2O	0.00	0.35	0.13	0.00	1.10	0.00
Total	100.00	100.00	100.00	99.90	100.10	100.00
# Oxygen	5	5	5	3	3	3
Na	0.020	0.032	0.026	0.113	0.138	0.281
Mg	0.023	0.017	0.019	0.000	0.025	0.022
Al	0.096	0.059	0.072	0.008	0.000	0.073
Si	1.339	1.132	1.099	0.019	0.277	0.240
K	0.002	0.000	0.000	0.021	0.000	0.004
Ca	1.164	0.993	1.009	0.002	0.000	0.044
Ti	0.386	0.723	0.752	0.028	0.027	0.023
Mn	0.000	0.001	0.003	0.010	0.026	0.005
Fe	0.187	0.141	0.127	2.469	2.145	2.120
Zn	0.022	0.006	0.005		0.024	0.031
Zr	0.000	0.023	0.012		0.084	0.000
Rb	0.000	0.005	0.002		0.019	0.000
ΣCations	3.239	3.131	3.126	2.843	2.765	2.843

*Total=100.00 as these are EDS analyses
#Oxygen is the number of atoms of oxygen

Appendix B-18: AEM analyses of related minerals.

Mineral	Arfvedsonitic amphibole							
Sample#	LB-30-10.70						LB-30-15.80	
Label	(6706-9)				(6720-3)	(6720-3)	nr ed	(5166-8)
Na_2O	9.50	10.80	6.20	7.40	10.60	9.80	10.10	13.72
MgO	0.00	1.20	0.10	0.00	0.10	0.40	0.00	0.23
Al_2O_3	0.10	0.80	0.00	0.20	0.10	0.00	0.05	0.00
SiO_2	41.50	42.50	37.80	39.00	40.00	40.70	36.91	38.43
K_2O	3.10	1.00	3.10	3.70	3.30	3.00	2.70	3.26
CaO	0.70	3.20	0.90	0.50	0.50	1.20	1.04	0.65
TiO_2	1.60	0.70	1.90	1.80	1.70	1.60	1.88	0.37
MnO	2.20	2.90	2.50	2.30	2.10	2.20	2.97	4.53
FeO	41.30	36.80	47.40	45.00	41.50	41.10	36.43	31.40
ZnO	0.00	0.00	0.00	0.00	0.00	0.00	7.92	7.41
ZrO_2	0.00	0.00	0.00	0.00	0.00	0.00	0.00	0.00
Rb_2O	0.00	0.00	0.00	0.00	0.00	0.00	0.00	0.00
Total	100.00	99.90	99.90	99.90	99.90	100.00	100.00	100.00
# Oxygen	23	23	23	23	23	23	23	23
Na	2.329	2.590	1.605	1.873	2.656	2.423	2.647	3.542
Mg	0.003	0.272	0.017	0.005	0.031	0.094	0.000	0.055
Al	0.011	0.158	0.003	0.046	0.024	0.000	0.011	0.000
Si	8.352	8.300	8.007	8.117	8.193	8.252	7.919	8.121
K	0.447	0.134	0.474	0.557	0.480	0.444	0.416	0.495
Ca	0.105	0.442	0.140	0.073	0.071	0.164	0.156	0.097
Ti	0.190	0.086	0.231	0.224	0.209	0.192	0.236	0.045
Mn	0.229	0.294	0.273	0.241	0.215	0.227	0.326	0.489
Fe	4.173	3.622	5.050	4.713	4.275	4.193	3.931	3.336
Zn							0.730	0.673
Zr							0.000	0.000
Rb							0.000	0.000
ΣCations	15.840	15.897	15.800	15.850	16.154	15.990	16.372	16.853

*Total=100.00 as these are EDS analyses
#Oxygen is the number of atoms of oxygen

Appendix B-18: AEM analyses of related minerals.

Mineral	Arfvedsonitic amphibole							
Sample#	LB-30-15.80				LB-30-17.22			
Label	(5166-8)				at pt	(6765-8)	further	furthest
Na_2O	14.13	11.43	10.88	9.89	7.92	6.45	5.97	6.71
MgO	0.00	0.17	0.30	0.09	0.00	0.22	0.24	0.27
Al_2O_3	0.01	0.08	0.00	0.00	0.00	0.21	0.15	0.49
SiO_2	37.66	33.65	37.01	37.52	28.54	36.37	34.94	35.31
K_2O	3.14	3.76	3.88	3.71	2.70	1.95	1.80	1.78
CaO	0.58	0.56	1.85	1.44	0.93	1.92	1.66	1.39
TiO_2	0.59	0.46	2.94	3.10	1.21	2.01	1.88	1.49
MnO	4.24	2.27	3.13	1.96	2.34	0.90	1.25	1.06
FeO	31.88	30.03	32.46	32.30	34.20	48.42	51.11	49.96
ZnO	7.77	14.62	4.44	5.19	21.45	1.04	0.72	0.97
ZrO_2	0.00	2.51	3.12	4.37	0.71	0.52	0.13	0.40
Rb_2O	0.00	0.46	0.00	0.44	0.00	0.00	0.15	0.17
Total	100.00	100.00	100.00	100.00	100.00	100.00	100.00	100.00
# Oxygen	23	23	23	23	23	23	23	23
Na	3.684	3.200	2.831	2.569	2.398	1.694	1.601	1.788
Mg	0.000	0.046	0.075	0.021	0.000	0.053	0.061	0.069
Al	0.003	0.019	0.000	0.000	0.000	0.046	0.033	0.111
Si	8.040	7.713	7.886	7.981	7.074	7.812	7.670	7.704
K	0.482	0.619	0.593	0.567	0.480	0.301	0.283	0.280
Ca	0.086	0.089	0.276	0.215	0.162	0.289	0.255	0.213
Ti	0.074	0.061	0.367	0.387	0.176	0.253	0.242	0.190
Mn	0.463	0.266	0.341	0.213	0.297	0.099	0.140	0.118
Fe	3.422	3.462	3.479	3.455	4.264	5.231	5.641	5.481
Zn	0.713	1.439	0.406	0.475	2.285	0.096	0.068	0.091
Zr	0.000	0.177	0.204	0.286	0.054	0.035	0.009	0.027
Rb	0.000	0.035	0.000	0.031	0.000	0.000	0.011	0.012
ΣCations	16.967	17.126	16.459	16.201	17.189	15.909	16.014	16.083

*Total=100.00 as these are EDS analyses
#Oxygen is the number of atoms of oxygen

Appendix B-18: AEM analyses of related minerals.

Mineral	**Arfvedsonitic amphibole**				
Sample#	**LB-30-17.22**				
Label		**def.(6749-53)**	**few(6744-8)**	**further**	**furthest**
Na_2O	11.68	10.35	10.34	11.21	10.89
MgO	0.45	0.18	0.38	0.14	0.28
Al_2O_3	0.35	0.10	0.31	0.00	0.36
SiO_2	37.57	39.38	39.02	38.27	38.45
K_2O	1.71	1.77	1.70	1.70	1.82
CaO	1.63	1.20	1.21	1.20	1.03
TiO_2	1.68	1.42	1.44	1.33	1.57
MnO	1.11	1.09	1.09	1.21	1.07
FeO	41.77	42.93	43.04	43.17	42.67
ZnO	1.36	1.40	0.86	1.15	0.95
ZrO_2	0.69	0.00	0.47	0.51	0.85
Rb_2O	0.00	0.18	0.14	0.13	0.07
Total	100.00	100.00	100.00	100.00	100.00
# Oxygen	23	23	23	23	23
Na	2.998	2.611	2.612	2.875	2.773
Mg	0.110	0.043	0.092	0.034	0.067
Al	0.076	0.021	0.068	0.000	0.077
Si	7.896	8.131	8.071	8.033	8.014
K	0.258	0.262	0.253	0.256	0.273
Ca	0.240	0.174	0.175	0.176	0.150
Ti	0.207	0.172	0.174	0.163	0.192
Mn	0.120	0.115	0.115	0.130	0.114
Fe	4.415	4.458	4.477	4.557	4.473
Zn	0.123	0.124	0.077	0.104	0.085
Zr	0.045	0.000	0.030	0.033	0.055
Rb	0.000	0.013	0.009	0.009	0.004
ΣCations	16.487	16.123	16.153	16.369	16.278

*Total=100.00 as these are EDS analyses
#Oxygen is the number of atoms of oxygen

Appendix B-19: AEM analyses of phyllosilicates.

Sample#	25-E-2				SL-8-1									
Spectrum#	5	6	3	4	5	11	12	13	14	15	16	17	18	19
Description	chl 6454-8	chl thick	clay	clay 6529-33	by prev.									
K_2O	0.48	0.37	0.00	0.31	0.11	0.35	0.77	0.94	0.57	1.59	0.98	0.59	0.65	0.88
Na_2O	0.80	1.84	0.44	2.49	0.79	1.41	1.40	1.38	1.47	1.50	1.28	0.91	0.66	1.47
CaO	1.27	0.74	0.19	1.35	0.31	0.49	0.80	0.51	0.87	0.50	0.60	0.61	0.68	0.63
MgO	27.41	27.41	36.84	11.32	27.20	32.56	34.33	27.89	24.32	29.57	31.58	26.89	35.97	30.91
FeO	17.89	19.21	0.00	43.52	22.67	7.10	6.46	7.00	8.30	11.81	4.53	7.19	3.71	4.79
MnO	0.53	0.48	0.00	0.55	1.17	0.43	0.43	0.31	0.36	0.35	0.45	0.08	0.36	0.42
ZnO	2.54	3.18	5.38	1.48	4.23	5.52	4.34	4.22	3.41	5.24	4.96	5.35	5.79	5.50
ZrO_2	2.77	0.46	1.78	1.72	0.00	0.26	1.44	0.93	1.58	0.00	0.60	0.57	0.94	0.23
Rb_2O	0.07	0.83	0.30	0.00	0.22	0.00	0.84	0.45	0.00	1.63	0.48	0.66	0.25	1.90
TiO_2	0.21	0.03	0.00	0.25	0.45	0.01	0.06	0.15	0.34	0.13	0.00	0.33	0.18	0.00
Al_2O_3	11.43	10.55	12.40	7.85	11.76	12.17	10.50	14.00	14.53	11.40	10.75	9.60	11.14	12.66
SiO_2	34.59	34.89	39.07	29.16	31.09	39.69	38.62	42.22	44.25	36.29	43.78	47.23	39.68	40.60
Total	100.00	100.00	96.41	100.00	100.00	100.00	100.00	100.00	100.00	100.00	100.00	100.00	100.00	100.00
# Oxygens	25	25	25	25	25	25	25	25	25	25	25	25	25	25
K	0.066	0.051	0.000	0.051	0.015	0.044	0.098	0.116	0.070	0.211	0.119	0.072	0.081	0.109
Na	0.186	0.428	0.094	0.691	0.189	0.300	0.303	0.288	0.305	0.339	0.265	0.187	0.140	0.313
Ca	0.169	0.099	0.023	0.215	0.043	0.060	0.099	0.061	0.103	0.064	0.072	0.072	0.082	0.077
Mg	6.009	6.024	7.326	2.977	6.180	6.550	7.025	5.511	4.755	6.305	6.190	5.233	7.188	6.198
Fe	1.707	1.838	0.311	4.981	2.242	0.622	0.576	0.602	0.707	1.096	0.387	0.609	0.322	0.418
Mn	0.052	0.047	0.000	0.064	0.118	0.039	0.039	0.027	0.031	0.033	0.039	0.007	0.032	0.037
Zn	0.207	0.260	0.398	0.145	0.358	0.413	0.330	0.310	0.248	0.416	0.361	0.387	0.430	0.410
Zr	0.162	0.027	0.095	0.121	0.000	0.014	0.079	0.049	0.082	0.000	0.031	0.029	0.050	0.012
Rb	0.004	0.052	0.017	0.000	0.014	0.000	0.049	0.025	0.000	0.099	0.027	0.036	0.014	0.108
Ti	0.024	0.003	0.000	0.033	0.052	0.001	0.006	0.015	0.034	0.014	0.000	0.032	0.018	0.000
Al	2.258	2.089	2.222	1.860	2.408	2.206	1.937	2.492	2.560	2.190	1.899	1.683	2.006	2.288
Si	6.565	6.637	6.726	6.635	6.114	6.910	6.842	7.222	7.490	6.700	7.427	7.954	6.863	7.048
ΣCations	17.408	17.555	17.210	17.773	17.732	17.158	17.384	16.718	16.384	17.466	16.816	16.301	17.227	17.019

Appendix B-19: AEM analyses of phyllosilicates.

Sample#	SL-8-1		LB-30-15.70										
Spectrum#	20	22	1	1	3	4	6	7	8	9	10	11	12
Description			Chlorite	poly 6659-62	poly	unk	unk	6673-4	6673-4	poly	poly unk at bot. (6676-7)		6698-700
K_2O	0.12	0.76	0.42	5.63	5.58	0.93	0.50	1.12	1.00	17.37	18.17	1.04	1.02
Na_2O	0.20	0.93	0.00	1.05	0.24	3.14	2.12	2.61	1.49	0.46	0.51	2.26	2.63
CaO	0.41	1.01	0.00	1.07	0.14	2.25	2.69	4.85	3.26	0.26	0.00	2.56	2.64
MgO	34.41	28.86	6.46	7.29	0.37	27.20	21.05	25.49	16.34	0.30	0.21	23.38	20.27
FeO	7.68	5.50	45.44	2.30	6.13	1.61	1.73	2.33	2.66	0.00	2.95	8.40	2.23
MnO	0.68	0.19	0.00	0.26	0.00	0.24	0.31	0.62	0.58	0.00	0.00	0.63	0.12
ZnO	5.30	3.79	2.19	5.89	2.59	3.11	11.10	0.00	18.63	0.00	0.00	11.25	11.17
ZrO_2	0.00	0.41	3.01	0.61	1.32	3.09	8.10	4.97	2.29	2.66	1.49	1.19	1.57
Rb_2O	0.00	0.00	1.67	0.49	1.46	0.61	0.80	2.39	0.96	0.46	0.25	0.22	2.70
TiO_2	0.00	0.14	0.30	2.05	0.01	0.16	0.14	0.03	0.05	0.61	0.00	0.00	0.00
Al_2O_3	8.65	15.02	18.32	12.29	14.41	4.75	4.25	4.42	3.64	13.50	12.16	4.21	5.61
SiO_2	42.54	43.38	22.20	61.07	67.76	52.91	47.20	51.16	49.10	64.38	64.25	44.86	50.04
Total	100.00	100.00	100.00	100.00	100.00	100.00	100.00	100.00	100.00	100.00	100.00	100.00	100.00
# Oxygens	25	25	25	25	25	25	25	25	25	25	25	25	25
K	0.014	0.091	0.071	0.632	0.604	0.109	0.066	0.136	0.132	1.967	2.084	0.137	0.128
Na	0.042	0.190	0.000	0.202	0.044	0.631	0.471	0.540	0.332	0.088	0.099	0.505	0.560
Ca	0.050	0.118	0.000	0.117	0.014	0.259	0.343	0.575	0.417	0.028	0.000	0.328	0.322
Mg	6.840	5.560	1.755	1.319	0.065	5.165	4.424	4.976	3.444	0.055	0.038	4.941	4.082
Fe	0.664	0.461	5.378	0.181	0.465	0.133	0.158	0.198	0.244	0.000	0.237	0.773	0.196
Mn	0.060	0.016	0.000	0.021	0.000	0.020	0.029	0.054	0.054	0.000	0.000	0.059	0.010
Zn	0.392	0.272	0.222	0.396	0.168	0.220	0.867	0.000	1.460	0.000	0.000	0.884	0.836
Zr	0.000	0.021	0.218	0.029	0.061	0.156	0.454	0.259	0.129	0.129	0.073	0.067	0.084
Rb	0.000	0.000	0.129	0.025	0.072	0.033	0.048	0.133	0.057	0.024	0.013	0.013	0.155
Ti	0.000	0.014	0.042	0.188	0.001	0.016	0.015	0.003	0.005	0.056	0.000	0.000	0.000
Al	1.550	2.608	4.487	2.003	2.261	0.812	0.806	0.778	0.692	2.216	2.022	0.801	1.017
Si	7.320	7.236	5.224	9.557	10.219	8.696	8.586	8.647	8.957	10.150	10.257	8.206	8.722
ΣCations	16.934	16.587	17.526	14.670	13.974	16.252	16.265	16.298	15.923	14.713	14.824	16.714	16.113

Appendix B-19: AEM analyses of phyllosilicates.

Sample#	25-E-2				SL-8-1									
Spectrum#	5	6	3	4	5	11	12	13	14	15	16	17	18	19
Description	chl 6454-8	chl thick	clay	clay 6529-33	by prev.									
# Oxygens	22	22	22	22	22	22	22	22	22	22	22	22	22	22
K	0.058	0.045	0.000	0.045	0.014	0.039	0.087	0.102	0.061	0.186	0.105	0.063	0.071	0.096
Na	0.163	0.377	0.082	0.608	0.166	0.264	0.267	0.253	0.268	0.298	0.233	0.164	0.124	0.275
Ca	0.148	0.087	0.020	0.189	0.038	0.052	0.087	0.053	0.090	0.056	0.063	0.063	0.072	0.067
Mg	5.288	5.301	6.446	2.620	5.438	5.764	6.182	4.849	4.185	5.548	5.447	4.605	6.326	5.454
Fe	1.502	1.617	0.274	4.383	1.973	0.547	0.507	0.530	0.622	0.964	0.340	0.536	0.284	0.368
Mn	0.046	0.041	0.000	0.056	0.103	0.034	0.034	0.024	0.027	0.029	0.034	0.006	0.028	0.033
Zn	0.183	0.229	0.350	0.128	0.315	0.363	0.291	0.273	0.218	0.366	0.318	0.340	0.379	0.361
Zr	0.142	0.024	0.083	0.106	0.000	0.012	0.069	0.043	0.072	0.000	0.028	0.026	0.044	0.011
Rb	0.004	0.046	0.015	0.000	0.012	0.000	0.043	0.022	0.000	0.087	0.023	0.032	0.013	0.095
Ti	0.021	0.003	0.000	0.029	0.046	0.001	0.005	0.014	0.030	0.012	0.000	0.029	0.016	0.000
Al	1.987	1.839	1.955	1.636	2.119	1.941	1.704	2.193	2.253	1.928	1.671	1.481	1.765	2.014
Si	5.777	5.840	5.919	5.839	5.380	6.081	6.021	6.355	6.591	5.896	6.535	7.000	6.039	6.202
ΣCations	15.319	15.448	15.145	15.640	15.604	15.099	15.298	14.712	14.418	15.370	14.798	14.345	15.160	14.977
# Oxygens	28	28	28	28	28	28	28	28	28	28	28	28	28	28
K	0.074	0.057	0.000	0.057	0.017	0.050	0.110	0.129	0.078	0.237	0.134	0.080	0.091	0.122
Na	0.208	0.480	0.105	0.774	0.211	0.336	0.340	0.323	0.341	0.380	0.297	0.209	0.157	0.350
Ca	0.189	0.111	0.026	0.241	0.048	0.067	0.111	0.068	0.115	0.072	0.080	0.081	0.092	0.086
Mg	6.730	6.747	8.205	3.334	6.921	7.336	7.869	6.172	5.326	7.061	6.932	5.861	8.051	6.942
Fe	1.912	2.058	0.348	5.578	2.511	0.696	0.645	0.675	0.791	1.227	0.433	0.682	0.361	0.468
Mn	0.058	0.052	0.000	0.072	0.132	0.043	0.044	0.031	0.035	0.037	0.044	0.008	0.035	0.042
Zn	0.232	0.291	0.445	0.162	0.401	0.462	0.370	0.347	0.278	0.466	0.405	0.433	0.482	0.459
Zr	0.181	0.030	0.106	0.135	0.000	0.015	0.088	0.055	0.092	0.000	0.035	0.033	0.056	0.014
Rb	0.005	0.058	0.019	0.000	0.016	0.000	0.054	0.028	0.000	0.110	0.030	0.041	0.016	0.121
Ti	0.027	0.004	0.000	0.037	0.059	0.001	0.007	0.017	0.038	0.016	0.000	0.036	0.020	0.000
Al	2.529	2.340	2.488	2.083	2.697	2.471	2.169	2.791	2.867	2.453	2.126	1.884	2.247	2.563
Si	7.353	7.433	7.533	7.431	6.847	7.740	7.664	8.089	8.388	7.504	8.318	8.909	7.686	7.893
ΣCations	19.497	19.661	19.275	19.906	19.860	19.217	19.470	18.724	18.350	19.562	18.834	18.257	19.294	19.061

The total is set to 100.00 due to the fact that the analyses were performed by EDS, while assuming that all Fe present was Fe^{2+}
The numbers in the description refer to the corresponding TEM image.
chl=chlorite; poly=polylithionite; prev.=previous; unk=unknown; bot.=bottom

Appendix B-19: AEM analyses of phyllosilicates.

Sample#	SL-8-1		LB-30-15.70										
Spectrum#	20	22	1	1	3	4	6	7	8	9	10	11	12
Description			Chlorite	poly 6659-62	poly	unk	unk	6673-4	6673-4	poly	poly unk at bot. (6676-7)		6698-700
# Oxygens	22	22	22	22	22	22	22	22	22	22	22	22	22
K	0.013	0.080	0.062	0.556	0.531	0.096	0.058	0.119	0.116	1.731	1.834	0.121	0.113
Na	0.037	0.167	0.000	0.177	0.039	0.556	0.414	0.475	0.292	0.078	0.087	0.444	0.493
Ca	0.044	0.104	0.000	0.103	0.013	0.228	0.302	0.506	0.367	0.025	0.000	0.288	0.283
Mg	6.019	4.893	1.545	1.160	0.057	4.545	3.893	4.379	3.031	0.048	0.034	4.348	3.592
Fe	0.585	0.406	4.732	0.159	0.409	0.117	0.139	0.175	0.215	0.000	0.208	0.680	0.172
Mn	0.053	0.014	0.000	0.018	0.000	0.018	0.026	0.047	0.048	0.000	0.000	0.052	0.009
Zn	0.345	0.239	0.195	0.349	0.148	0.193	0.763	0.000	1.285	0.000	0.000	0.778	0.736
Zr	0.000	0.019	0.192	0.026	0.054	0.138	0.399	0.228	0.113	0.113	0.065	0.059	0.074
Rb	0.000	0.000	0.113	0.022	0.064	0.029	0.042	0.117	0.050	0.021	0.012	0.012	0.136
Ti	0.000	0.012	0.037	0.165	0.000	0.014	0.013	0.003	0.005	0.050	0.000	0.000	0.000
Al	1.364	2.295	3.949	1.763	1.990	0.715	0.709	0.685	0.609	1.950	1.779	0.705	0.895
Si	6.441	6.367	4.597	8.410	8.992	7.653	7.555	7.609	7.883	8.932	9.026	7.221	7.675
ΣCations	14.901	14.597	15.423	12.910	12.297	14.302	14.314	14.343	14.013	12.948	13.045	14.708	14.180
# Oxygens	28	28	28	28	28	28	28	28	28	28	28	28	28
K	0.016	0.102	0.079	0.708	0.676	0.122	0.074	0.152	0.147	2.203	2.334	0.153	0.143
Na	0.048	0.213	0.000	0.226	0.049	0.707	0.527	0.605	0.372	0.099	0.111	0.565	0.627
Ca	0.056	0.132	0.000	0.131	0.016	0.290	0.384	0.644	0.467	0.032	0.000	0.367	0.361
Mg	7.661	6.227	1.966	1.477	0.072	5.785	4.954	5.574	3.857	0.061	0.043	5.534	4.571
Fe	0.744	0.516	6.023	0.202	0.521	0.149	0.177	0.222	0.273	0.000	0.265	0.866	0.219
Mn	0.067	0.018	0.000	0.024	0.000	0.023	0.033	0.060	0.061	0.000	0.000	0.066	0.012
Zn	0.439	0.304	0.248	0.444	0.188	0.246	0.971	0.000	1.635	0.000	0.000	0.990	0.937
Zr	0.000	0.024	0.244	0.033	0.069	0.175	0.508	0.290	0.144	0.144	0.082	0.075	0.095
Rb	0.000	0.000	0.144	0.028	0.081	0.037	0.054	0.149	0.064	0.027	0.015	0.015	0.173
Ti	0.000	0.016	0.047	0.211	0.001	0.018	0.016	0.004	0.006	0.063	0.000	0.000	0.000
Al	1.736	2.921	5.026	2.243	2.533	0.910	0.902	0.872	0.775	2.481	2.264	0.897	1.139
Si	8.198	8.104	5.851	10.704	11.445	9.740	9.616	9.684	10.032	11.368	11.488	9.191	9.769
ΣCations	18.966	18.577	19.629	16.431	15.651	18.202	18.217	18.254	17.834	16.479	16.602	18.720	18.047

The total is set to 100.00 due to the fact that the analyses were performed by EDS, while assuming that all Fe present was Fe^{2+}

The numbers in the description refer to the corresponding TEM image.

chl=chlorite; poly=polylithionite; prev.=previous; unk=unknown; bot.=bottom

IMAGE EVALUATION
TEST TARGET (QA-3)

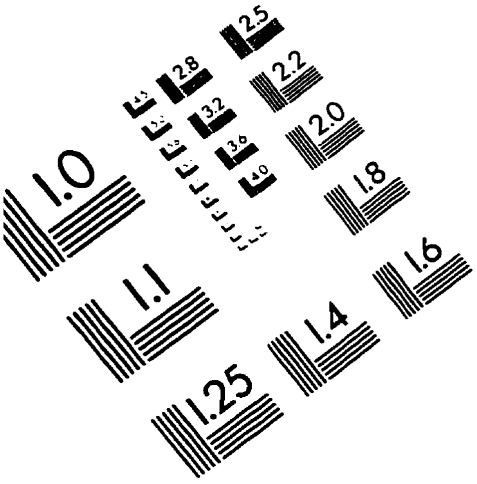

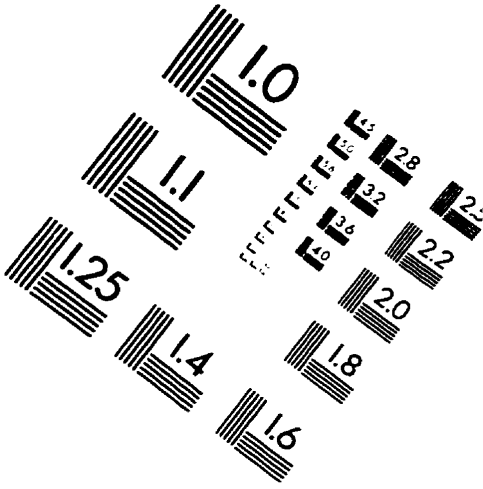

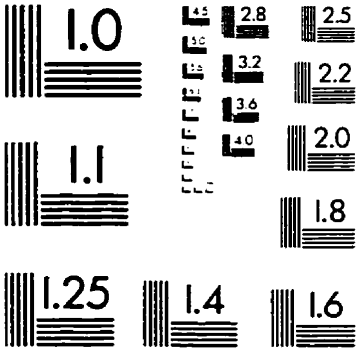

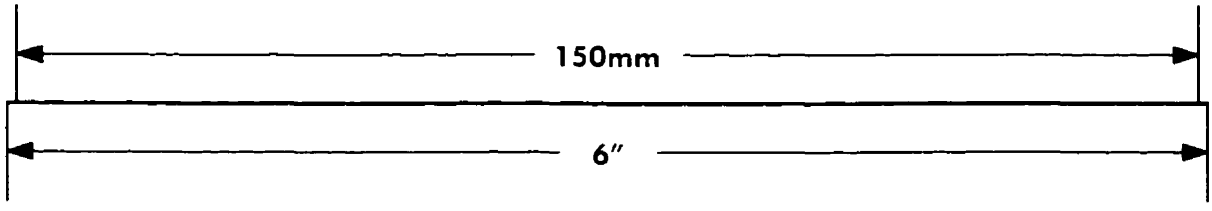

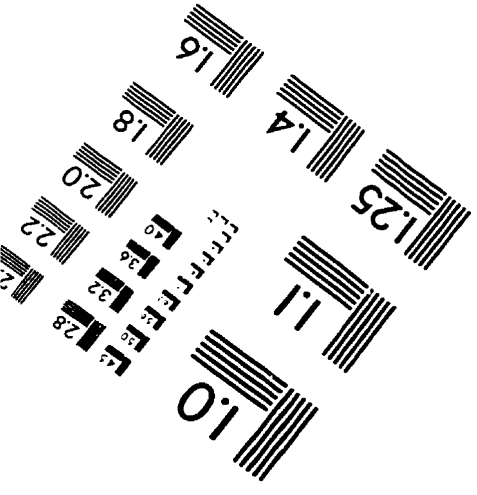

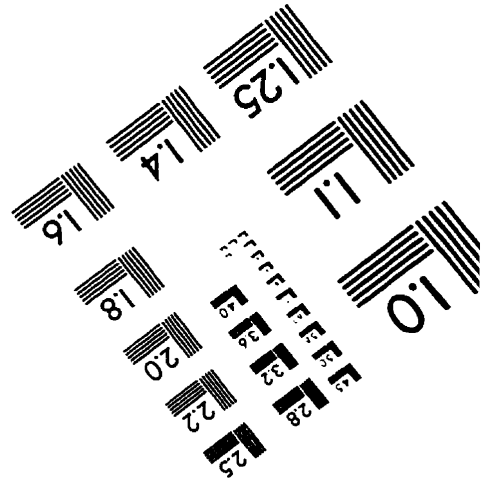

APPLIED IMAGE, Inc
1653 East Main Street
Rochester, NY 14609 USA
Phone: 716/482-0300
Fax: 716/288-5989

© 1993, Applied Image, Inc., All Rights Reserved